

รายงานวิจัยฉบับสมบูรณ์

โครงการภูมิคุ้มกันของกุ้งกับการควบคุมโรค
Shrimp Immunity and Implication for Disease Control

โดย

ศาสตราจารย์ ดร. อัญชลี ทัศนาขจร และคณะ

สิงหาคม 2561

สัญญาเลขที่ RTA5880004

รายงานวิจัยฉบับสมบูรณ์

โครงการภูมิคุ้มกันของกุ้งกับการควบคุมโรค
Shrimp Immunity and Implication for Disease Control

ผู้วิจัย	**สังกัด**
ศ.ดร. อัญชลี ทัศนาขจร	จุฬาลงกรณ์มหาวิทยาลัย
ศ.ดร.วิเชียร ริมพณิชยกิจ	จุฬาลงกรณ์มหาวิทยาลัย
ผศ.ดร.กุลยา สมบูรณ์วิวัฒน์	จุฬาลงกรณ์มหาวิทยาลัย
ผศ.ดร.เกื้อการุณย์ ครูส่ง	จุฬาลงกรณ์มหาวิทยาลัย
ดร. เปรมฤทัย สุพรรณกูล	ศูนย์พันธุวิศวกรรมและเทคโนโลยีชีวภาพแห่งชาติ
ดร. ปิติ อ่ำพายัพ	ศูนย์พันธุวิศวกรรมและเทคโนโลยีชีวภาพแห่งชาติ
ดร. วลัยพร เจริญทรัพย์ศรี	ศูนย์พันธุวิศวกรรมและเทคโนโลยีชีวภาพแห่งชาติ
ดร. ภคกุล สังข์สุริยะ	ศูนย์พันธุวิศวกรรมและเทคโนโลยีชีวภาพแห่งชาติ
น.ส. สุรีรัตน์ แซ่ตั้ง	ศูนย์พันธุวิศวกรรมและเทคโนโลยีชีวภาพแห่งชาติ
ผศ.ดร. ราตรี วงศ์ปัญญา	มหาวิทยาลัยเกษตรศาสตร์
อ.ดร. ศิรินิตย์ ธารธาดา	มหาวิทยาลัยเกษตรศาสตร์
อ.ดร. สุเชาน์ ดอนพุดซา	มหาวิทยาลัยศรีนครินทรวิโรฒ
อ.ดร. ศิริขวัญ พลประทีป	มหาวิทยาลัยศรีนครินทรวิโรฒ

สนับสนุนโดยสำนักงานกองทุนสนับสนุนการวิจัย
(ความเห็นในรายงานนี้เป็นของผู้วิจัย สกว. ไม่จำเป็นต้องเห็นด้วยเสมอไป)

บทคัดย่อ

โรคระบาดเป็นปัญหาสำคัญของการเลี้ยงกุ้งทั่วโลก ซึ่งมีสาเหตุหลักมาจากไวรัสและแบคทีเรีย เช่น โรคตัวแดงดวงขาว และโรคที่เกิดจากเชื้อแบคทีเรียกลุ่มวิบริโอ งานวิจัยนี้สนใจศึกษาภูมิคุ้มกันของกุ้งที่ตอบสนองต่อเชื้อแบคทีเรีย *Vibrio parahaemolyticus* สายพันธุ์ที่มีการสร้างโปรตีนสารพิษ (VP$_{AHPND}$) ซึ่งเป็นสาเหตุของการระบาดของโรคตายด่วน หรือ early mortality syndrome (EMS) หรือเรียกอีกชื่อหนึ่งว่า Acute hepatopancreatic necrosis syndrome (AHPND) และการตอบสนองต่อไวรัส โดยเฉพาะไวรัสจุดขาว หรือ white spot syndrome virus (WSS) ซึ่งเป็นสาเหตุของโรคระบาดที่รุนแรงในการเพาะเลี้ยงกุ้ง

จากงานวิจัยเราพบแนวทางสำคัญที่ทำให้กุ้งต้านโรค AHPND คือการกระตุ้นด้วยความร้อน หรือการให้กุ้งได้รับโปรตีนฮีทช็อค (Heat shock proteins; HSPs) เพิ่มขึ้น โดยอุณหภูมิที่เหมาะสม คืออุณหภูมิสูงสุดที่ช่วยกระตุ้น แต่ไม่ทำให้ตาย (Non-lethal heat shock; NLHS) ซึ่งกุ้งจะสามารถต้านเชื้อ VP$_{AHPND}$ ได้ โดยสภาวะ NLHS ที่พบ คือ สภาวะที่ให้ความร้อนต่อเนื่อง (Chronic NLHS) โดยการย้ายกุ้งจากอุณหภูมิ 28°C ไปที่อุณหภูมิ 38°C ทันทีเป็นเวลา 5 นาทีทุกวันเป็นเวลา 7 วัน หรือการให้กุ้งได้รับโปรตีน *Lv*HSP70 ในปริมาณที่เหมาะสม จะทำให้กุ้งสามารถทนการติดเชื้อ VP$_{AHPND}$ ได้เพิ่มขึ้น โดยมีอัตราการรอดเพิ่มขึ้นจาก 20% เป็น 60-70% โดย *Lv*HSP70 จะไปกระตุ้นยีนที่สำคัญในระบบภูมิคุ้มกัน ทำให้กุ้งมีความต้านทานโรคสูงขึ้น และการศึกษา Transcriptome พบว่ายีนสำคัญที่ตอบสนองต่อความเครียดจากความร้อนในกุ้งที่ติดเชื้อ VP$_{AHPND}$เป็นกลุ่มยีนที่อยู่ในวิถี Toll วิถี IMD และระบบ Phenoloxidase ซึ่งเป็นวิถีการส่งสัญญาณที่สำคัญในระบบภูมิคุ้มกันของกุ้ง ซึ่งสอดคล้องกับงานวิจัยหลายชิ้นที่ระบุว่าสัตว์น้ำที่ถูกกระตุ้นด้วยความร้อนจะมีความ สามารถในการต้านทานแบคทีเรียและไวรัสเพิ่มขึ้น นอกจากนี้เราได้ศึกษาบทบาทของโปรตีนที่ตอบสนองต่อเชื้อ กลุ่มแรกคือ pattern recognition receptors (PRRs) ซึ่งทำหน้าที่จดจำองค์ประกอบของผนังเซลล์ของจุลชีพ ส่งสัญญาณผ่านวิถีการส่งสัญญาณ เพื่อกระตุ้นระบบภูมิคุ้มกันในการต้านเชื้อ โดยพบการตอบสนองต่อไวรัส WSSV ในกุ้งกุลาดำ ผ่าน STING-dependent cytosolic DNA sensing pathway และพบปฏิสัมพันธ์ของไวรัสต่อระบบฟีนอลออกสิเดสในกุ้ง และการส่งสัญญานใน 2 วิถีหลัก คือ วิถี Toll และวิถี IMD มีโปรตีนที่มีความสำคัญ ได้แก่ Spätzle และ Relish ตามลำดับ โดยวิถีส่งสัญญาณทั้ง 2 เกี่ยวข้องกับควบคุมการสร้างเปปไทด์ต้านจุลชีพที่แตกต่างกัน ส่วนโปรตีนในกระบวนการ clathrin-mediated endocytosis ที่มีบทบาทสำคัญเมื่อกุ้งติดเชื้อ WSSV และ ไวรัสหัวเหลือง (YHV) และยังคาดว่ากระบวนการนี้มีความสัมพันธ์กับวิถีการส่งสัญญาณ JAK/STAT ซึ่งเป็น antiviral pathway ที่สำคัญ องค์ความรู้จากงานวิจัยนี้จะนำมาประมวลเพื่อหาแนวทางการป้องกันและควบคุมโรคระบาดในกุ้ง ซึ่งมีความสำคัญยิ่งต่อความยั่งยืนของอุตสาหกรรมการเลี้ยงกุ้ง

คำสำคัญ เปปไทด์ต้านจุลชีพ กุ้งต้านทานโรค โปรตีนฮีทช็อค ภาวะเครียดจากความร้อน ยีนในระบบภูมิคุ้มกัน ภูมิคุ้มกันของกุ้ง โรคกุ้ง วิถีส่งสัญญาณ

Abstract

Diseases which are caused mainly by virus and bacteria, are the major concern of shrimp aquaculture worldwide. In this study, we investigate the immune responses of shrimp to major pathogens, particularly to a specific strain of *Vibrio parahaemolyticus* carrying toxin producing plasmid which caused a disease called acute hepatopancreatic necrosis disease (AHPND) and to white spot syndrome virus (WSSV) which is the most severe viral disease in shrimp.

We found that either exposure of shrimp to chronic non-lethal heat shock (NLHS) (from 28°C to 38°C for 5 min every day for 7 days) or direct injection of recombinant heat shock protein 70 (rHSP70) could enhance the resistance of shrimp to VP_{AHPND}. The survival rate of shrimp was increased from 20% in the control non-heated shrimp to 60-70% in the experimental groups and this was due to the induction of shrimp immunity. Subsequently, transcriptome analysis identified a number of heat stress responsive genes followed VP_{AHPND} infection. These genes are involved in Toll and Imd pathways and the prophenoloxidase (proPO) system which are the major immune pathways in shrimp. These results are concordant with the previous studies which reported that NLHS could enhance disease tolerance in aquatic animals. Moreover, we investigate the role of pattern recognition proteins (PRPs) which recognize pathogens and sending signal to the signal transduction pathways to activate the synthesis of several immune-related molecules. In WSSV-infected shrimp, we found DDX41 is a viral sensing PRP and that STING-dependent cytosolic DNA sensing pathway plays a crucial role in viral response. In the proPO system, we found the interaction between *Pm*LGBP and several WSSV proteins as an important anti-melanization mechanism which occurs upon WSSV infection. Furthermore, the two signalling pathways, Toll and IMD pathways, were studied for their role in shrimp immunity. The function of Spätzle และ Relish were revealed by gene silencing which resulted in a decrease of transcription level of several antimicrobial peptides (AMPs). These suggested that the synthesis of shrimp AMPs is specifically regulated under Toll and/or IMD pathways. We also show that clathrin-mediated endocytosis is involved in yellow head virus (YHV) and WSSV infections in shrimp *Penaeus monodon* and it might interact with JAK/STAT pathway, the crucial antiviral pathway. The knowledge from this study will be used in establishing a new strategy for disease control which will lead to a sustainable shrimp aquaculture.

Keywords Antimicrobial peptide, Disease resistant shrimp, Heat shock protein, Heat stress, Immune-related genes, Shrimp immunity, Shrimp disease, Signal transduction pathway

Executive summary

อุตสาหกรรมการเลี้ยงกุ้งมีความสำคัญต่อเศรษฐกิจของประเทศไทย โดยนำรายได้เข้าประเทศปีละหลายหมื่นล้านบาท อย่างไรก็ตามการเลี้ยงกุ้งยังคงได้รับผลกระทบอย่างต่อเนื่องจากโรคระบาดซึ่งมีสาเหตุหลักมาจากไวรัสและแบคทีเรีย เช่น โรคตัวแดงดวงขาว และโรคที่เกิดจากเชื้อแบคทีเรียจำพวกวิบริโอ ในปี 2556 ผลผลิตกุ้งของประเทศไทยได้ลดลงกว่า 50% เนื่องจากมีการของระบาดการระบาดของโรคตายด่วน หรือ early mortality syndrome (EMS) หรือเรียกอีกชื่อหนึ่งว่า Acute hepatopancreatic necrosis syndrome (AHPND) ซึ่งมีสาเหตุจากการติดเชื้อแบคทีเรีย *Vibrio parahaemolyticus* สายพันธุ์ที่มีการสร้างโปรตีนสารพิษ (VP_{AHPND}) งานวิจัยเพื่อหาแนวทางการป้องกันและควบคุมโรคระบาดในกุ้งจึงมีความสำคัญต่อความยั่งยืนของอุตสาหกรรมการเลี้ยงกุ้ง

มีงานวิจัยหลายชิ้นที่แสดงให้เห็นว่าสัตว์น้ำที่ถูกกระตุ้นด้วยความร้อนจะเพิ่มความสามารถในการต้านทานแบคทีเรียและไวรัสได้ ในอาร์ทีเมียการเพิ่มขึ้นของ Heat shock protein (HSPs) กระตุ้นให้เกิดการป้องกันการติดเชื้อ *Vibrio campbellii* ได้ ซึ่งแสดงให้เห็นว่า HSPs สำคัญต่อการป้องกันการติดเชื้อ และคาดว่า HSP เกี่ยวข้องกับการกระตุ้นระบบภูมิคุ้มกัน แต่กลไกของการกระตุ้นยังไม่เป็นที่ชัดเจน อย่างไรก็ตามการได้มีการเสนอว่าการนำกุ้งมากระตุ้นให้เกิดความเครียดด้วยความร้อนเป็นวิธีที่จะช่วยให้กุ้งต้านทานต่อโรค VP_{AHPND} ได้ดีขึ้น ในการศึกษานี้เราจึงจะทดสอบว่าความร้อนช่วย กระตุ้นระบบภูมิคุ้มกันของกุ้ง และช่วยให้กุ้งทนต่อโรค VP_{AHPND} มากขึ้นหรือไม่ และจะระบุและศึกษาหน้าที่ของยีนที่มีการแสดงออกเปลี่ยนไปเมื่อกุ้งได้รับการกระตุ้นด้วยความร้อนเพื่อศึกษาระบบภูมิคุ้มกันของกุ้งที่ตอบสนองต่อการติดเชื้อ VP_{AHPND} ในสภาวะที่ถูกกระตุ้นด้วยความร้อน

นอกจากนี้เรายังสนใจถึงบทบาทของโปรตีนที่ตอบสนองต่อเชื้อก่อโรค โดยโปรตีนกลุ่มแรก คือ pattern recognition receptors (PRRs) ซึ่งทำหน้าที่จดจำองค์ประกอบของผนังเซลล์ของจุลชีพ ซึ่งเกี่ยวข้องกับการกระตุ้นระบบการส่งสัญญาณเพื่อสร้างโปรตีนต่างๆ ที่ทำหน้าที่ในระบบภูมิคุ้มกัน ปัจจุบันนี้มีการศึกษา PRRs หลายชนิดในกุ้ง แต่ยังไม่มีการศึกษ PRRs ที่จดจำไวรัส โดยเฉพาะโปรตีนที่จับกับไวรัสตัวแดงดวงขาว และกระตุ้นให้ระบบภูมิคุ้มกันตอบสนองต่อการติดเชื้อไวรัส นอกจากนี้จะศึกษาวิถีการส่งสัญญานแบบ Toll และ Imd และหน้าที่ในการควบคุมการสร้างเปปไทด์ต้านจุลชีพ และจะศึกษาวิธีการนำสารเข้าสู่เซลล์โดยคลาทริน (Clathrin-mediated endocytosis) และวิถีสื่อสัญญาณ JAK/STAT ในกุ้งกุลาดำ และศึกษาโปรตีนต่างๆ ที่มีส่วนเกี่ยวข้องกับวิถีนี้ องค์ความรู้ที่ได้จากการศึกษานี้จะเป็นประโยชน์ในการนำไปใช้ควบคุมการแพร่ระบาดของโรคในการเพาะเลี้ยงกุ้งได้อย่างมีประสิทธิภาพ โดยสรุปผลงานในโครงการต่างๆมีดังต่อไปนี้

โครงการที่ 1 ศึกษาและค้นหาลักษณะสมบัติของโปรตีนที่ควบคุมการป้องกันสภาวะเครียดจากความร้อนในกุ้งขาวและการควบคุมการติดเชื้อ *Vibrio parahaemolyticus*

โรคตายด่วน (Early mortality syndrome) หรือ Acute hepatopancreatic necrosis syndrome (AHPND) เป็นโรคติดเชื้อจากแบคทีเรีย *Vibrio parahaemolyticus* สายพันธุ์ที่มีการสร้างโปรตีนสารพิษ (Toxin) โรคนี้เป็นปัญหาสำคัญที่ส่งผลกระทบต่ออุตสาหกรรมการเลี้ยงกุ้งของประเทศไทย การหาแนวทางในการควบคุมและป้องกันการเกิดโรคจึงเป็นวิธีที่จะช่วยแก้ไขปัญหาดังกล่าว จากการศึกษาวิจัยที่ผ่านมาในสัตว์น้ำ พบว่าการให้ความร้อนในสภาวะกดดัน (heat stress) จะทำให้สัตว์มีความต้านทานต่อโรคเพิ่มขึ้น โดยความร้อนจะกระตุ้นการทำงานของโปรตีนฮีดช็อค (Heat shock protein; HSP) ซึ่งจะส่งผลกระตุ้นระบบภูมิคุ้มกัน ทำให้สามารถต้านทานการติดเชื้อไวรัสและแบคทีเรียได้มากขึ้น งานวิจัยนี้จึงมีวัตถุประสงค์ดังต่อไปนี้

(1) ระบุชนิดและลักษณะสมบัติของ Heat shock proteins (HSPs) และศึกษาบทบาทต่อการกระตุ้นวิถีในระบบภูมิคุ้มกันและการทนต่อความร้อน
(2) ระบุชนิดและหน้าที่ของยีนที่ตอบสนองต่อเชื้อ VP_{AHPND} ภายใต้สภาวะความเครียดจากความร้อน
(3) การค้นหาและระบุชนิดของยีนที่ตอบสนองต่อเชื้อ VP_{AHPND}

ผลการดำเนินงาน

งานวิจัยนี้ค้นพบว่าเมื่อกุ้งขาวถูกกระตุ้นด้วยความร้อน ในสภาวะที่ทำให้เกิดความกดดันแต่ไม่ทำให้กุ้งตาย หรือที่เรียกว่า non-lethal heat shock (NLHS) กุ้งจะสามารถต้านเชื้อ VP_{AHPND} ได้ โดยสภาวะ NLHS ที่พบ คือ สภาวะที่ให้ความร้อนต่อเนื่อง (Chronic NLHS) โดยการย้ายกุ้งจากอุณหภูมิ 28°C ไปที่อุณหภูมิ 38°C ทันทีเป็นเวลา 5 นาทีทุกวันเป็นเวลา 7 วัน ทำให้กุ้งสามารถทนการติดเชื้อ VP_{AHPND} ได้มากกว่ากลุ่มกุ้งควบคุมที่ไม่ได้กดดันด้วยความร้อน โดยมีอัตราการรอดเพิ่มขึ้นจาก 20% เป็น 60% และสามารถป้องกันการติดเชื้อได้ยาวนานถึง 30 วัน ภายหลังการให้ความร้อน และพบว่าโปรตีนสำคัญที่มีส่วนทำให้กุ้งมีความต้านทานโรคเพิ่มขึ้น คือ *Lv*HSP70 และ *Lv*HSP90 และการฉีดโปรตีน *Lv*HSP70 เข้าไปในกุ้งโดยตรงให้ผลเช่นเดียวกัน โดย *Lv*HSP70 จะไปกระตุ้นยีนที่สำคัญในระบบภูมิคุ้มกัน ทำให้กุ้งมีความต้านทานโรคสูงขึ้น และการศึกษา Transcriptome พบว่ายีนสำคัญที่ตอบสนองต่อความเครียดจากความร้อนในกุ้งที่ติดเชื้อ VP_{AHPND} เป็นกลุ่มยีนที่อยู่ในวิถี Toll วิถี IMD และระบบ Phenoloxidase ซึ่งเป็นวิถีการส่งสัญญาณที่สำคัญในระบบ

โครงการนี้ได้ตีพิมพ์ผลงานในวารสารวิชาการนานาชาติจำนวน 3 บทความ และอยู่ระหว่างการจัดเตรียมต้นฉบับ 2 บทความ โดยรายละเอียดของผลงานวิจัยมีดังนี้

ส่วนที่ (1) ระบุชนิดและลักษณะสมบัติของ Heat shock proteins (HSPs) และศึกษาบทบาทต่อการกระตุ้นวิถีในระบบภูมิคุ้มกัน

งานวิจัยนี้พบว่า *Lv*HSP70 และ *Lv*HSP90 มีความสำคัญในการตอบสนองต่อการกระตุ้นด้วยความร้อน โดยพบว่ากุ้งที่กดดันด้วยความร้อนมีการแสดงออกของ *Lv*HSP70 และ *Lv*HSP90 เพิ่มมากกว่ากลุ่มที่ไม่ได้กดดันด้วยความร้อน และส่งผลให้กุ้งต้านทานต่อการติดเชื้อ VP_{AHPND} ได้ และการฉีดโปรตีนเข้าสู่ตัวกุ้งโดยตรงมีผลให้กุ้งต้านโรคได้เช่นเดียวกับการกระตุ้นด้วยความร้อน โดยพบว่า r*Lv*HSP70 สามารถเข้าสู่เซลล์เม็ดเลือดกุ้งได้ส่งผลให้กุ้งมีความต้านทานต่อการติดเชื้อ VP_{AHPND} โดยไปกระตุ้นยีนในระบบภูมิคุ้มกันของกุ้ง คือ *LvMyD88*, *LvIKK*ε, *LvIKK*β, *LvCrustin1*, *LvPEN2, LvPEN4, LvproPO1, LvproPO2* และ *LvTG1* ให้มีการแสดงออกเพิ่มมากขึ้น นอกจากนี้ยังได้โคลนและศึกษาหน้าที่ของ *Pm*HSF1 ในการควบคุมการทำงานของ HSPs พบว่าในกุ้งที่ถูกกดดันด้วยความร้อนมีการแสดงออกของโปรตีน *Pm*HSF1 เพิ่มมากขึ้น และพบว่าเมื่อยับยั้งการแสดงออกของยีน HSF1 ส่งผลต่อการแสดงออกของยีน PmHSPs และยีนสำคัญในระบบภูมิคุ้มกันของกุ้ง ดังนั้นจึงคาดว่า *Pm*HSF1 ทำหน้าที่เป็น transcription factor ที่ควบคุมการแสดงออกของยีนที่เกี่ยวข้องกับการต้านโรค

ส่วนที่ (2) การค้นหาและระบุชนิดของยีนที่ตอบสนองต่อเชื้อVP_{AHPND} ภายใต้สภาวะความเครียดจากความร้อน

จากผลการวิเคราะห์การแสดงออกของยีนในเซลล์เม็ดเลือดของกุ้งที่ถูกทำให้เครียดด้วยความร้อนและติดเชื้อ VP_{AHPND} ด้วยเทคนิค Next Generation Sequencing (NGS) พบยีนที่ตอบสนองต่อความเครียดจากความร้อนในกุ้งที่ติดเชื้อ VP_{AHPND} ในวิถี Toll วิถี IMD และระบบ Phenoloxidase ซึ่งเป็นวิถีการส่งสัญญาณที่สำคัญในระบบภูมิคุ้มกัน และเมื่อตรวจสอบการแสดงออกของยีนดังกล่าวด้วยเทคนิค qRT-PCR พบว่ายีน *Toll1, Toll2, MyD88* และ *Cactus* ในวิถี Toll ยีน *IMD, IKK*β และ *IKK*ε ในวิถี IMD ยีน *Dome* และ *STAT* ในวิถี JAK/STAT ยีน *PO1* และ *PO2* ในระบบ phonoloxidase มีการแสดงออกเพิ่มขึ้น 1.5 – 3 เท่า เมื่อกุ้งติดเชื้อ VP_{AHPND} ในขณะที่เมื่อกุ้งได้รับความเครียดด้วยความร้อนการแสดงออกของยีนในวิถี Toll ได้แก่ ยีน *Toll1, Toll2, MyD88* และ *TRAF6* มีการแสดงออกลดลง 1.5 – 3 เท่า และยีน *Cactus* มีการแสดงออกเพิ่มขึ้น 1.5 – 3 เท่า ยีน *IMD, IKK*β และ *IKK*ε ในวิถี IMD ยีน *Dome* และ *STAT* ในวิถี JAK/STAT ยีน *PO1* และ *PO2* ในระบบ phonoloxidase มีการแสดงออกเพิ่มขึ้น 1.5 – 8 เท่า จากผลการทดลองดังกล่าว อาจกล่าวได้ว่า วิถี Toll IMD JAK/STAT และระบบ phenoloxidase ถูกกระตุ้นให้มีการแสดงออกมากขึ้นเมื่อกุ้งติดเชื้อ VP_{AHPND} ในขณะที่เมื่อกุ้งได้รับความเครียดจากความร้อนวิถี IMD JAK/STAT และระบบ phenoloxidase ถูกกระตุ้นให้มีการแสดงออกมากขึ้น และวิถี Toll มีการแสดงออกของยีนลดลง

ส่วนที่ (3) การค้นหาและระบุชนิดของยีนที่ตอบสนองต่อเชื้อ VP_{AHPND}

ทำการค้นหายีนจากเซลล์เม็ดเลือดของกุ้งขาวที่มีการแสดงออกตอบสนองต่อเชื้อ **VP_{AHPND}** ด้วยเทคนิค Next generation sequencing (NGS) พบว่า เมื่อเปรียบเทียบยีนที่แสดงออกที่เวลา 0 ชั่วโมงหลังการทำให้ติดเชื้อ (hpi) กับที่เวลา 3 และ 6 hpi ได้ยีนที่มีการแสดงออกเปลี่ยนแปลงไปจำนวน 359 ยีน และเมื่อเปรียบเทียบกับที่เวลา 48 hpi ได้ยีนที่มีการแสดงออกเปลี่ยนแปลงไปจำนวน 429 ยีน และได้ยืนยันการแสดงออกของยีนที่สนใจจำนวน 9 ยีน ด้วยเทคนิค Quantitiative Realtime RT-PCR ทั้งในสภาวะที่กุ้งติดเชื้อ VP_{AHPND} และในสภาวะที่ถูกกระตุ้นด้วย VP_{AHPND} toxin พบว่ายีน LvALF เป็นยีนที่มีการแสดงออกตอบสนองต่อ toxin และเมื่อทำการยับยั้งการแสดงออกของยีน *Lv*ALF ในกุ้ง พบว่าทำให้อัตราการตายของกุ้งที่ได้รับ VP_{AHPND} toxin เพิ่มขึ้นอย่างมีนัยสำคัญ จึงทำการวิเคราะห์โครงสร้างสามมิติของ *Lv*ALF และ VP_{AHPND} toxin เพื่อศึกษาการจับกันของโปรตีนทั้งสอบ โดยวิธีทางคอมพิวเตอร์ จากการวิเคราะห์พบว่า *Lv*ALF น่าจะจับกับ VP_{AHPND} toxin ได้โดยอาศัยบริเวณ LPS-binding domain

ผลงานวิจัย

1. Junprung W, Supungul P, Tassanakajon A. (2017). HSP70 and HSP90 are involved in shrimp *Penaeus vannamei* tolerance to AHPND-causing strain of *Vibrio parahaemolyticus* after non-lethal heat shock. Fish & Shellfish Immunology. 60:237-246.
2. Maralit BA, Jaree P, Boonchuen P, Tassanakajon A, Somboonwiwat K (2018). Differentially expressed genes in hemocytes of *Litopenaeus vannamei* challenged with *Vibrio parahaemolyticus* AHPND (VP_{AHPND}) and VP_{AHPND} toxin. Fish Shellfish Immunol., 81:284-296.
3. Sornchuera P, Junprung W, Yingsunthonwattana W, Tassanakajonab A (2018). Heat shock factor 1 regulates heat shock proteins and immune-related genes in *Penaeus monodon* under thermal stress. Dev Comp Immunol. 2018, 88:19-27.
4. Boonchuen P, Jaree P, Tassanakajon A, Somboonwiwat K. Effect of heat stress and *Vibrio parahaemolyticus* AHPND (VP_{AHPND}) challenge on *Litopenaeus vannamei* hemocyte transcriptome. (manuscript in preparation)
5. Junprung W, Supungul P, Tassanakajon A. *Litopenaeus vannamei* heat shock protein 70 (*Lv*HSP70) enhances resistance to AHPND-causing strain of *Vibrio parahaemolyticus* by activating shrimp immunity (manuscript in preparation).

โครงการที่ 2 Pattern recognition receptors และปฏิสัมพันธ์กับไวรัสตัวแดงดวงขาวในกุ้ง

Pattern recognition receptors (PRRs) เป็นกลุ่มโปรตีนจดจำที่ทำหน้าที่จับกับส่วนประกอบของผนังเซลล์จุลชีพและกระตุ้นระบบภูมิคุ้มกันเพื่อการต้านทานเชื้อก่อโรค อย่างไรก็ตาม องค์ความรู้ PRRs ในกุ้งที่ตอบสนองหรือเกิดปฏิสัมพันธ์กับไวรัสตัวแดงดวงขาว (White spot syndrome virus; WSSV) ยังมีอยู่อย่างจำกัด โครงการวิจัยนี้จึงมีวัตถุประสงค์เพื่อค้นหาและศึกษาบทบาทของโปรตีนจดจำ PRRs ในการกระตุ้นวิถีการส่งสัญญาณและกระตุ้นระบบภูมิคุ้มกันเพื่อการต้านเชื้อไวรัส WSSV ในกุ้งกุลาดำ *Penaeus monodon* งานวิจัยนี้คณะผู้วิจัยได้มุ่งเน้นค้นหาและศึกษาบทบาทของยีนใน 3 กลุ่มหลัก ได้แก่

(1) PRRs ใน STING-dependent cytosolic DNA sensing pathway และยีนที่เกี่ยวข้อง

(2) PRRs ในกลุ่ม Lectins

(3) PRRs ในระบบโพรฟีนอลออกซิเดสต่อการต้านเชื้อไวรัส WSSV ในกุ้งกุลาดำ

ผลการดำเนินงาน

งานวิจัยนี้ได้ค้นหาและศึกษาบทบาทของโปรตีนในกลุ่ม PRRs ในการกระตุ้นวิถีการส่งสัญญาณและกระตุ้นระบบภูมิคุ้มกันเพื่อการต้านเชื้อไวรัส WSSV ในกุ้งกุลาดำ โครงการนี้ได้ตีพิมพ์ผลงานในวารสารวิชาการนานาชาติ

จำนวน 3 บทความ อยู่ในระหว่างแก้ไขต้นฉบับ 1 บทความ และอยู่ระหว่างการจัดเตรียมต้นฉบับ 3 บทความ โดยรายละเอียดของผลงานวิจัยมีดังนี้

ส่วนที่ (1) การค้นหาและศึกษายีน PRRs ใน STING-dependent cytosolic DNA sensing pathway และยีนที่เกี่ยวข้องในกุ้ง

คณะผู้วิจัยประสบความสำเร็จในการค้นหาและศึกษาหน้าที่ของยีน *Pm*DDX41 ในกุ้งกุลาดำ โดยพบว่ายีน *Pm*DDX41 มีระดับการแสดงออกเพิ่มสูงขึ้นภายหลังจากการติดเชื้อไวรัส WSSV เมื่อยับยั้งการแสดงออกของยีน *Pm*DDX41 ด้วยเทคนิค RNAi และฉีดด้วยเชื้อไวรัส WSSV พบว่ากุ้งมีอัตราการตายสะสมเพิ่มสูงขึ้น และการยับยั้งการแสดงออกของยีน *Pm*DDX41 ยังส่งผลทำให้ยีนในระบบภูมิคุ้มกัน ได้แก่ *Pm*IKK**β**, *Pm*IKK**ε**, *Pm*Relish, *Pm*Cactus, *Pm*Dorsal, *Pm*PEN3, *Pm*PEN5 และ ALF*Pm*6 มีระดับการแสดงออกลดต่ำลง แสดงให้เห็นว่า *Pm*DDX41 เป็นยีนสำคัญในระบบภูมิคุ้มกันที่ทำหน้าที่ต้านเชื้อไวรัสในกุ้งโดยอาจส่งสัญญาณผ่านทาง DNA-sensing pathway (*Dev Comp Immunol. 2018, 81:291-302*) นอกจากนี้ โครงการวิจัยนี้ยังได้ค้นพบและศึกษาหน้าที่ของยีนใน STING-dependent cytosolic DNA sensing pathway ของกุ้งกุลาดำเพิ่มเติม โดยได้ค้นพบยีนที่สมบูรณ์ของ *Pm*STING และ *Pm*IRF และยังพบว่าทั้งยีน *Pm*STING และ *Pm*IRF มีระดับการแสดงออกเพิ่มสูงขึ้นภายหลังจากการติดเชื้อไวรัส WSSV เมื่อยับยั้งการแสดงออกของยีน *Pm*STING และ *Pm*IRF ด้วยเทคนิค RNAi และฉีดด้วยเชื้อไวรัส WSSV พบว่ากุ้งที่ถูกยับยั้งยีนมีอัตราการตายสะสมเพิ่มสูงขึ้น ผลจากการศึกษาแสดงให้เห็นว่า *Pm*STING และ *Pm*IRF มีบทบาทสำคัญในระบบภูมิคุ้มกันต้านเชื้อไวรัส WSSV ในกุ้งกุลาดำ (*Manuscript in preparation*)

ส่วนที่ (2) การค้นหาและศึกษายีน PRRs ในกลุ่ม Lectins ในกุ้ง

คณะผู้วิจัยประสบความสำเร็จในการค้นหาและศึกษาหน้าที่ของยีน PRRs ในกลุ่ม Lectins ในกุ้ง โดยค้นพบยีนที่สมบูรณ์ของเลคตินชนิดซี *Pm*CLec ในกุ้งกุลาดำ เมื่อยับยั้งการแสดงออกของยีน *Pm*CLec ด้วยเทคนิค RNAi ในกุ้งที่ติดเชื้อแบคทีเรีย *Vibrio harveyi* พบว่ากุ้งมีอัตราการตายสะสมเพิ่มสูงขึ้น และพบว่ารีคอมบิแนนท์โปรตีนของ *Pm*CLec สามารถจับและทำให้เกิดการเกาะกลุ่มของแบคทีเรีย *Staphylococcus haemolyticus*, *S. aureus* และ *Escherichia coli* แสดงให้เห็นว่า *Pm*CLec เป็นโปรตีนจดจำเชื้อโรค PRR ที่มีบทบาทสำคัญในระบบภูมิคุ้มกันของกุ้ง (*Fish Shellfish Immunol. 2017, 60:103-113*) นอกจากนี้คณะผู้วิจัยยังค้นพบยีนที่สมบูรณ์ของเลคตินชนิดฟิโคลิน (*Pm*Ficolin) และ Mannose binding protein (*Pm*MBP) โดยพบว่า *Pm*Ficolin มีการแสดงออกเพิ่มสูงขึ้นภายหลังจากการติดเชื้อ *V. harveyi* เมื่อทำการผลิตรีคอมบิแนนท์โปรตีนเพื่อศึกษาหน้าที่ของโปรตีน พบว่ารีคอมบิแนนท์โปรตีนของ *Pm*Ficolin สามารถจับและทำให้เกิดการเกาะกลุ่มของเชื้อ *E. coli*, *Bacillus megaterium* และ *S. aureus* ขณะที่ยีน *Pm*MBP มีการแสดงออกเพิ่มสูงขึ้นภายหลังการติดเชื้อ *V. harveyi* และ WSSV และรีคอมบิแนนท์โปรตีนของ *Pm*MBP สามารถจับและทำให้เกิดการเกาะกลุ่มของเชื้อ *B. megaterium*, *S. aureus*, *S. haemolyticus*, *E. coli*, *V. parahaemolyticus*, *V. harveyi*, *Saccharomyces cerevisiae* และ *Pichia pastoris* ผลจากการศึกษาแสดงให้เห็นว่า *Pm*Ficolin และ *Pm*MBP เป็นโปรตีนจดจำเชื้อโรค PRRs ที่มีบทบาทสำคัญในระบบภูมิคุ้มกันของกุ้งกุลาดำ (*Manuscript in preparation*)

ส่วนที่ (3) การศึกษาปฏิสัมพันธ์ระหว่างโปรตีน PRRs ในระบบโพรฟีนอลออกซิเดสและโปรตีนจากไวรัสตัวแดงดวงขาว

คณะผู้วิจัยประสบความสำเร็จในการค้นหาปฏิสัมพันธ์และศึกษาหน้าที่ของโปรตีน PRRs ในระบบโพรฟีนอลออกซิเดสของกุ้งกุลาดำและโปรตีนจากไวรัส WSSV โดยค้นพบว่า WSSV164 เป็นยีนจากไวรัสที่มีการแสดงออกเพิ่มสูงขึ้นในกุ้งที่ถูกยับยั้งการแสดงออกของยีน *Pm*proPO1 และ *Pm*proPO2 ที่ติดเชื้อไวรัส WSSV เมื่อค้นหาปฏิสัมพันธ์ระหว่างโปรตีน *Pm*proPO1 หรือ *Pm*proPO2 กับโปรตีนจากไวรัส WSSV ด้วยเทคนิค yeast two-hybrid และ co-immunoprecipitation พบว่าโปรตีน WSSV164 สามารถจับได้กับโปรตีน *Pm*proPO1 และ *Pm*proPO2 เมื่อศึกษาบทบาทของโปรตีน WSSV164 ในการควบคุมระบบโพรฟีนอลออกซิเดสโดยการยับยั้งการ

แสดงออกของยีน WSSV164 ในกุ้งกุลาดำที่ติดเชื้อไวรัส WSSV ด้วยเทคนิค RNAi พบว่าการยับยั้งยีน WSSV164 ส่งผลทำให้กุ้งที่ติดเชื้อไวรัสมีกิจกรรมของเอนไซม์ฟีนอลออกซิเดสในน้ำเลือดเพิ่มสูงขึ้น และเมื่อทำการบ่มรีคอมบิแนนท์โปรตีนของ WSSV164 กับโปรตีนจากน้ำเลือดกุ้งและรีคอมบิแนนท์โปรตีนของ *Pm*proPO1 และ *Pm*proPO2 พบว่าโปรตีน WSSV164 สามารถยับยั้งกิจกรรมของเอนไซม์ฟีนอลออกซิเดสได้แบบ dose-dependent จากผลการทดลองแสดงให้เห็นว่าโพรฟีนอลออกซิเดสมีบทบาทสำคัญในการต้านเชื้อไวรัสตัวแดงดวงขาว และไวรัสตัวแดงดวงขาวสามารถก่อโรคผ่านกลไกการเกิดปฏิสัมพันธ์ของโปรตีน WSSV164 กับโปรตีน *Pm*proPO1 และ *Pm*proPO2 และยับยั้งการกระตุ้นระบบโพรฟีนอลออกซิเดสในกุ้ง (*Dev Comp Immunol. 2018, 86:109-117*) นอกจากนี้ คณะผู้วิจัยยังได้ศึกษาปฏิสัมพันธ์ระหว่างโปรตีน *Pm*LGBP ซึ่งเป็น PRR ในระบบโพรฟีนอลออกซิเดสและโปรตีนจากไวรัส WSSV ด้วยเทคนิค yeast two-hybrid และ co-immunoprecipitation โดยพบว่าโปรตีน WSSV004, WSSV362, WSSV456, WSSV458 และ WSSV471 สามารถจับได้กับโปรตีน *Pm*LGBP เมื่อยับยั้งการแสดงออกของยีน WSSV471 ในกุ้งกุลาดำที่ติดเชื้อไวรัส WSSV พบว่าส่งผลทำให้กิจกรรมของเอนไซม์ฟีนอลออกซิเดสในน้ำเลือดของกุ้งที่ติดเชื้อไวรัสเพิ่มสูงขึ้น นอกจากนี้ เมื่อศึกษาปฏิสัมพันธ์ระหว่างโปรตีน *Pm*LGBP และ PRRs ชนิดอื่นในระบบโพรฟีนอลออกซิเดสของกุ้งกุลาดำด้วยเทคนิค yeast two-hybrid พบว่าโปรตีน *Pm*LGBP สามารถจับได้กับ *Pm*MasSPH1 และ *Pm*ClipSP2 ผลจากการศึกษาแสดงให้เห็นว่า *Pm*LGBP อาจกระตุ้นการทำงานของระบบโพรฟีนอลออกซิเดสผ่านการเกิดปฏิสัมพันธ์กับ *Pm*MasSPH1 และ *Pm*ClipSP2 และไวรัสตัวแดงดวงขาวสามารถยับยั้งกลไกการทำงานของโปรตีน *Pm*LGBP ในการกระตุ้นระบบโพรฟีนอลออกซิเดสผ่านการเกิดปฏิสัมพันธ์กับโปรตีนของไวรัส (*Manuscript in preparation*)

ผลงานวิจัย

1. Wongpanya, R., Sengprasert, P., Amparyup, P., Tassanakajon, A. A novel C-type lectin in the black tiger shrimp *Penaeus monodon* functions as a pattern recognition receptor by binding and causing bacterial agglutination. Fish Shellfish Immunol. 2017, 60:103-113.
2. Soponpong, S., Amparyup, P., Tassanakajon, A. A cytosolic sensor, *Pm*DDX41, mediates antiviral immune response in black tiger shrimp *Penaeus monodon*. Dev Comp Immunol. 2018, 81:291-302.
3. Sangsuriya, P., Charoensapsri, W., Sutthangkul, J., Senapin, S., Hirono, I., Tassanakajon, A., Amparyup, P. A novel white spot syndrome virus protein WSSV164 controls prophenoloxidases, *Pm*proPOs in shrimp melanization cascade. Dev Comp Immunol. 2018, 86:109-117.
4. Chomwong, S., Charoensapsri, W., Amparyup, P., Tassanakajon, A. Two host gut-derived lactic acid bacteria activate the proPO system and increase resistance to an AHPND-causing strain of *Vibrio parahaemolyticus* in the shrimp *Litopenaeus vannamei*. Dev Comp Immunol. (Revised)
5. Charoensapsri, W., Chomwong, S., Soponpong, S., Jearaphunt, M., Wongpanya, R., Tassanakajon, A., Amparyup, P. *Pm*STING- and *Pm*IRF-mediated signaling are crucial for the innate antiviral defense against white spot syndrome virus infection in black tiger shrimp *Penaeus monodon*. (Manuscript in preparation).
6. Sangsuriya, P., Charoensapsri, W., Tassanakajon, A., Amparyup, P. Molecular interaction of pathogen recognition proteins in shrimp prophenoloxidase system with white spot syndrome virus proteins. (Manuscript in preparation)
7. Wongpanya, R., Amparyup, P., Tassanakajon, A. Fuctional characterization of *Pm*Ficolin and *Pm*MBP in the black tiger shrimp *Penaeus monodon*. (Manuscript in preparation)

โครงการที่ 3 สื่อสัญญาณตอบสนองต่อการติดเชื้อในกุ้งกุลาดำ

การส่งสัญญานเพื่อตอบสนองต่อการติดเชื้อประกอบด้วย 2 วิถีหลัก คือ วิถี Toll และวิถี Imd โปรตีนที่มีความสำคัญในการส่งสัญญานใน 2 วิถีนี้ได้แก่ Spätzle และ Relish โดยที่ Spätzle เป็นโปรตีนที่อยู่นอกเซลล์ทำหน้าที่ส่งสัญญานว่ามีการติดเชื้อให้กับ Toll receptor ขณะที่ Relish จะทำหน้าที่เป็น transcription factor ภายในเซลล์ที่กระตุ้นให้เกิดการสร้างโปรตีนต้านจุลชีพในวิถี Imd งานวิจัยนี้สนใจศึกษาโปรตีนที่ทำหน้าที่สื่อสัญญานทั้ง 2 สองชนิดนี้ รวมถึง Krüppel-like factors (KLFs) ซึ่งเป็น transcription factor ในวิถีของการเจริญเติบโต การพัฒนา การแบ่งเซลล์ ซึ่งจากงานวิจัยที่ผ่านมาพบว่า KLF มีการตอบสนองต่อการติดเชื้อไวรัสสูงมาก จึงน่าจะมีความสำคัญในการสื่อสัญญาณ นอกจากโปรตีนที่เกี่ยวข้องกับการส่งสัญญานแล้วโครงการนี้ได้ศึกษาโปรตีนที่เกี่ยวข้องกับการต้านจุลชีพในวิถีดังกล่าว ซึ่งได้แก่ SWD ตัวยับยั้งซีรีนโพรทีเนส Alpha-2-macroglobulin และ ครัสทิน งานวิจัยจึงนี้มีวัตถุประสงค์ในการทำวิจัย 2 ส่วนหลัก ดังต่อไปนี้

(1) ศึกษาโปรตีนที่ทำหน้าที่สื่อสัญญาน

(2) ศึกษาโปรตีนที่เกี่ยวข้องกับการต้านจุลชีพ

ผลการดำเนินงาน

งานวิจัยนี้ได้ค้นหาและศึกษาบทบาทของโปรตีนที่ทำหน้าที่สื่อสัญญานและโปรตีนต่างๆ ที่เกี่ยวข้องกับการต้านจุลชีพในกุ้ง โครงการนี้ได้ตีพิมพ์ผลงานในวารสารวิชาการนานาชาติจำนวน 6 บทความ และอยู่ระหว่างการจัดเตรียมต้นฉบับ 2 บทความ โดยรายละเอียดของผลงานวิจัยมีดังนี้ โดยรายละเอียดของผลงานวิจัยมีดังนี้

ส่วนที่ (1) โปรตีนที่ทำหน้าที่สื่อสัญญาน

การศึกษาหน้าที่ของโปรตีน PmRelish ในการตอบสนองต่อการติดเชื้อ YHV

จากการศึกษาหน้าที่ของยีน *PmRelish* ด้วยเทคนิค RNA interference (RNAi) และ suppression subtractive hybridization (SSH) พบว่า cDNA โคลน จำนวน 252 โคลน จากห้องสมุด forward ที่บ่งชี้ถึงยีนที่ตอบสนองต่อการติดเชื้อ YHV และอยู่ภายใต้การควบคุมของโปรตีน *Pm*Relish และ 99 โคลน จากห้องสมุด reverse ที่แสดงถึงยีนที่ตอบสนองต่อการติดเชื้อ YHV และนำโคลนทั้งหมดมาหาลำดับที่คล้ายคลึงกันด้วยโปรแกรม BLAST พบยีนที่เกี่ยวข้องกับการป้องกันและธำรงสมดุลอย่างมากจากห้องสมุดทั้ง 2 ชนิด เช่น โปรตีนต้านจุลชีพ และตัวยับยั้งโปรตีเนส จากรูปแบบการแสดงออกของยีนเพปไทด์ต้านจุลชีพในสภาวะที่กุ้งติดเชื้อ *V. harveyi* และถูกยับยั้งการแสดงออกของยีน *Pm*Relish พบว่า *penaeidin5* และ *penaeidin3* อยู่ภายใต้การควบคุมของ *Pm*Relish ในวิถี Imd แต่ *ALFPm3* และ*crustinPm1* อยู่นอกเหนือจากการควบคุมของ *Pm*Relish ในวิถี Imd (*Fish Shellfish Immunol. 2015, 47:572-581*)

การศึกษาโปรตีน PmSpätzle

เราพบว่ากุ้งกุลาดำมีโปรตีน *Pm*Spätzle อยู่ 3 ชนิด คือ *Pm*Spz1, 2 และ 3 จากการศึกษา *Pm*Spz1 พบว่า *PmSpz1* แสดงออกในเนื้อเยื่อต่าง ๆ ของกุ้ง เช่น เม็ดเลือด กระเพาะ เหงือก เฮพาโทแพนเครส อวัยวะต่อมน้ำเหลือง ก้านตา กล้ามเนื้อ ลำไส้ และหัวใจ การติดเชื้อ WSSV ทำให้การแสดงออกของ *PmSpz1* สูงขึ้น Western blot analysis แสดงให้เห็นว่า *Pm*Spz1 อยู่ในรูปที่ active รอเวลาที่จะกระตุ้นวิถี Toll เมื่อฉีดกุ้งด้วยโปรตีนรีคอมบิแนนท์ r*Pm*Spz1 กุ้งจะต้านทานการติดเชื้อ WSSV ได้ดี เมื่อฉีดโปรตีน *Pm*Spz1 ที่ active ไปในกุ้งปกติ จะมีการกระตุ้นการแสดงออกของ *crustinPm1*, *crustinPm7*, *ALFPm3*, *penaeidin3* แต่ไม่กระตุ้นการแสดงออกของ *penaeidin5* แสดงให้เห็นว่า ยีนที่แสดงออกอยู่ภายใต้การควบคุมในวิถี Toll (*Fish Shellfish Immunol. 2017, 65:88-95*)

การศึกษาหน้าที่ของ Krüppel-like factors (KLFs)

จากการเปรียบเทียบการแสดงออกของยีน KLF (Krüppel-like factor) พบมีการแสดงออกแตกต่างกันระหว่างกุ้งสายพันธุ์ต้านทานและไม่ต้านทานไวรัสทอร่า เมื่อศึกษาปฏิสัมพันธ์ของ KLF ด้วยเทคนิค Yeast two hybrid พบปฏิสัมพนัธ์กับ non-structural protein ของไวรัสทอร่า ได้แก่ โปรตีน BIR-like sequence, Helicase

และ RNA-dependent RNA polymerase และ structural protein ของไวรัสทอร่า ได้แก่ VP2 และ VP3 ของไวรัสทอร่า ชี้ให้เห็นว่า KLF เกี่ยวข้องกับการต้านทานไวรัส นอกจากนี้ยังพบความแตกต่างระดับจีโนมิกส์ระหว่างกุ้งทั้งสองสายพันธุ์ที่ intron1 และ 2 ซึ่งนำไปพัฒนาเป็นดีเอ็นเอเครื่องหมายช่วยในการคัดพันธุ์ระหว่างกุ้งทั้งสองสายพันธุ์ต่อไป (*Manuscript in preparation*)

ส่วนที่ (2) โปรตีนที่เกี่ยวข้องกับการต้านจุลชีพ
ยีนที่ตอบสนองต่อการติดเชื้อ YHV ในกุ้งกุลาดำ

จากฐานข้อมูล Suppression Subtractive Hybridization (SSH) ของกุ้งกุลาดำที่ถูกกระตุ้นด้วยเชื้อไวรัสหัวเหลือง พบว่า ยีน SWDPm2 และ SPIPm2 ตอบสนองต่อการติดเชื้อไวรัสหัวเหลืองและเกี่ยวข้องกับระบบการส่งสัญญาณผ่านวิถี Imd ของกุ้งกุลาดำ โดยพบยีน SWDPm2 ถึง 11 โคลน และยีน SPIPm2 จำนวน 7 โคลน จากจำนวนโคลนที่นำมาวิเคราะห์ 252 และ 99 โคลน ตามลำดับ ดังนั้นเราจึงสนใจศึกษาถึงบทบาทหน้าที่ของ SWDPm2 และ SPIPm2 ในการตอบสนองต่อการติดเชื้อไวรัสหัวเหลืองในกุ้งกุลาดำ

อย่างไรก็ตามเนื่องจากมีข้อจำกัดในการหาตัวอย่างกุ้งกุลาดำ จึงได้ทำการศึกษาโปรตีน SWD ในกุ้งขาว และศึกษาหน้าที่ของโปรตีน *Lv*SWD ในการต่อต้านการติดเชื้อ *Vibrio parahaemolyticus* เนื่องจากพบว่ายีน *Lv*SWD แสดงออกมากที่เซลล์เม็ดเลือดกุ้ง และตอบสนองต่อการติดเชื้อ VP_{AHPND} จากการศึกษาพบว่าโปรตีนรีคอมบิแนนท์ *Lv*SWD (r*Lv*SWD) และ *Lv*SWD-WAP (r*Lv*SWD-WAP) สามารถยับยั้งการทำงานของ subtilisin เฉพาะ r*Lv*SWD ที่สามารถยับยั้งการเจริญเติบโตของเชื้อ *B.* megaterium และ VP_{AHPND} ได้ที่ค่า MIC เท่ากับ 30 μM และเมื่อศึกษาความสามารถในการฆ่าเชื้อด้วยวิธี MBC พบว่า r*Lv*SWD เป็น bactericidal ต่อเชื้อ VP_{AHPND} และส่งผลต่ออัตราการตายของกุ้งระยะ (post-larval) ที่ 50% เท่ากับ 78 ชั่วโมง ซึ่งแตกต่างจากกุ้งระยะที่ไม่ได้รับ r*Lv*SWD จะมีอัตราการตายที่ 50% เท่ากับ 36 ชั่วโมง แสดงว่าสามารถนำ r*Lv*SWD ไปประยุกต์ใช้ในการควบคุมโรคติดเชื้อในกุ้งได้ (*Fish Shellfish Immunol. 2017, 68:341-348*)

จากการศึกษาหน้าที่ของตัวยับยั้งซีรีนโปรตีเนส SPI*Pm2* พบว่า ยีน *SPIPm2* แสดงออกมากที่เซลล์เม็ดเลือดกุ้งและตอบสนองต่อการติดเชื้อ YHV อย่างมาก เมื่อยับยั้งการแสดงออกของยีน *SPIPm2* ด้วย RNAi พบว่า การหายไปของยีน *SPIPm2* ส่งผลกระทบต่อระดับการแสดงออกของยีนในระบบภูมิคุ้มกันหลายยีน เช่น ยีนอะพอบโทซิส แทรนสคริปชันแฟคเตอร์ และเพปไทด์ต้านจุลชีพ และทำให้ปริมาณเม็ดเลือดในระบบหมุนเวียนเลือดกุ้งลดลงอย่างมาก รวมทั้งทำให้กุ้งอ่อนแอต่อการติดเชื้อ YHV จากผลการศึกษาแอกทิวิตีของเอนไซม์ caspase-3 และ caspase-7 ในเม็ดเลือดกุ้งที่ถูกยับยั้งการแสดงออกของยีน *SPIPm2* พบว่า กุ้งมีแอกทิวิตี 5.32 เมื่อเทียบกับกลุ่มควบคุม แสดงว่าตัวยับยั้งซีรีนโปรตีเนส SPI*Pm2* เกี่ยวข้องกับการธำรงสมดุลของเม็ดเลือดกุ้ง (*Fish Shellfish Immunol. 2018, 79:18-27*)

นอกจากตัวยับยั้งซีรีนโปรตีเนส SPI*Pm2* แล้วได้ศึกษาการแสดงออกของตัวยับยั้งซีรีนโปรตีเนส *SPIPm5* ในเนื้อเยื่อกุ้ง พบว่า มีการแสดงออกของ *SPIPm5* ในเนื้อเยื่อต่าง ๆ เช่น เม็ดเลือด กระเพาะ เหงือก อวัยวะต่อมน้ำเหลือง กล้ามเนื้อ ลำไส้ และหัวใจ แต่แสดงออกน้อยในเฮพาโทแพนเครสและก้านตา การแสดงออกเพิ่มมากขึ้นจากการกระตุ้นด้วยความเครียดจากอุณหภูมิที่เพิ่มขึ้น การติดเชื้อ WSSV และ YHV การฉีดโปรตีนรีคอมบิแนนท์ rSPI*Pm5* ไปในกุ้งปกติไม่มีผลต่อการแสดงออกของยีนอื่น ๆ ที่เกี่ยวข้องกับภูมิคุ้มกัน คือ *crustinPm1*, *penaeidin3*, *penaeidin5*, *Hsp70*, *SPIPm2* และ *SPIPm5* โปรตีน SPI*Pm5* สามารถยับยั้งการทำงานของ proPO ในเลือด การฉีดโปรตีน rSPI*Pm5* ช่วยให้กุ้งที่ติดเชื้อ WSSV YHV *Vibrio harveyi V. parahaemolyticus* และกุ้งที่ทำให้เกิดความเครียดโดยเพิ่มอุณหภูมิมีชีวิตอยู่รอดได้นานขึ้น การทนต่อการติดเชื้อน่าจะเป็นผลจากการยับยั้งการเพิ่มจำนวนของไวรัสและแบคทีเรีย ที่กระตุ้นจาก rSPI*Pm5* แต่ไม่ใช่จากการแสดงออกของเพปไทด์ต้านจุลชีพ ดังนั้น SPI*Pm5* จึงทำหน้าที่สำคัญใน innate immunity ของกุ้ง (*Fish Shellfish Immunol. 2018, 77:147-155*)

ผลของ Alpha-2-macroglobulin ต่อระบบ prophenoloxidase

โปรตีน alpha-2-macroglobulin (A2M) ซึ่งพบมากในเลือดกุ้งและมีการแสดงออกมากขึ้นเมื่อกุ้งติดเชื้อจุลชีพ ได้ทำการศึกษาหน้าที่ของ *Lv*A2M จาก *Litopenaeus vannamei* ต่อระบบ prophenoloxidase (proPO) พบว่า โปรตีนรีคอมบิแนนท์ r*Lv*A2M สามารถยับยั้ง trypsin และการทำงานของ PO ในน้ำเลือดของกุ้ง การยับยั้งการแสดงออกของ *Lv*A2M ทำให้การทำงานของ PO สูงขึ้น แม้ว่าการแสดงออกของ proPO-activating enzyme (PPAE) และ prophenoloxidase (proPO) ลดลง ในกุ้งที่ติดเชื้อ *Vibrio parahaemolyticus* การทำงานของ *Lv*A2M จะลดลง ขณะที่การทำงานของ PO เพิ่มขึ้น แสดงว่า *Lv*A2M สามารถควบคุมระบบ proPO (*Fish Shellfish Immunol. 2017, 62:68-74*)

การศึกษาบทบาทของครัสตินในกุ้งขาวต่อเชื้อก่อโรคตายด่วน

ครัสติน โปรตีนต้านจุลชีพที่มีส่วนของบริเวณ cysteine-rich และ single whey acidic protein (WAP) ครัสตินที่พบในกุ้งขาว *Litopenaeus vannamei* พบทั้งหมด 4 ประเภท คือ Type II-a, Type II-b, Type III และ Type IV ในงานวิจัยนี้ได้ศึกษาการแสดงออกของยีนต่อการติดเชื้อวิบริโอ พาราฮีโมไลติคัส (ชนิดที่ก่อโรค AHPND) ของ Type II-a และยีน Crus-like*Lv*, SWD77 และ DWD*Lv* เพื่อเป็นตัวแทนของ Type II-b, Type III และ Type IV ตามลำดับ พบว่าการแสดงออกของ Type II-a และยีน Crus-like*Lv* นั้นสูงขึ้น ในขณะที่การแสดงออกของยีน SWD77 และ DWD*Lv* มีแนวโน้มว่ามีการแสดงออกสูงขึ้น งานวิจัยนี้ได้เลือกที่จะศึกษาสมบัติของ DWD*Lv* ดังนั้นโปรตีนรีคอมบิแนนท์ของ DWD*Lv* จึงถูกผลิตโดยอาศัยระบบของ *Escherichia coli* และนำไปทำให้บริสุทธิ์ด้วยวิธีโครมาโทกราฟีแบบจำเพาะด้วยนิกเกิล โปรตีนที่ได้แสดงสมบัติการยับยั้งโพรทีเอสที่หลั่งจากเชื้อ *Bacillus subtilis* และ *Vibrio parahaemolyticus* AHPND (*Manuscript in preparation*)

ผลงานวิจัย

1. Visetnan S, Supungul P, Tang S, Hirono I, Tassanakajon A, Rimphanitchayakit V. (2015). YHV-responsive gene expression under the influence of *Pm*Relish. Fish & Shellfish Immunology. 47(1):572-581.
2. Boonrawd S, Mani R, Ponprateep S, Supungul P, Masrinoul P, Tassanakajon A, Rimphanitchayakit V. (2017). Characterization of *Pm*Spätzle 1 from the black tiger shrimp *Peneaus monodon*. Fish & Shellfish Immunology. 65:88-95.
3. Visetnan S, Supungul P, Tassanakajon A, Donpudsa S, Rimphanitchayakit V. (2017). A single WAP domain-containing protein from *Litopenaeus vannamei* possesses antiproteinase activity against subtilisin and antimicrobial activity against AHPND-inducing *Vibrio parahaemolyticus*. Fish & Shellfish Immunology. 68:341-348.
4. Visetnan S, Tassanakajon A, Donpudsa S, Rimphanitchayakit V. (2018). Silencing of a Kazal-type serine proteinase inhibitor SPIPm2 from Penaeus monodon affects YHV susceptibility and hemocyte homeostasis. Fish & Shellfish Immunology. 79:18-27.
5. Boonrawd S, Supungul P, Tassanakajon A, Rimphanitchayakit V. (2018). Antimicrobial activity of a serine proteinase inhibitor SPI*Pm*5 from the black tiger shrimp *Penaeus monodon*. Fish & Shellfish Immunology. 77:147-155
6. Ponprateep S, Vatanavicharn T, Lo CF, Tassanakajon A, Rimphanitchayakit V. (2017). Alpha-2-macroglobulin is a modulator of prophenoloxidase system in pacific white shrimp *Litopenaeus vannamai*. Fish & Shellfish Immunology. 62:68-74.
7. Supungul, P., Tang, S., Tassanakajon, A., Rimphanitchayakit, V.Kruppel like factor gene with its variation related to TSV-resistance of Penaeus vannamei. (Manuscript in preparation).

8. Sakunwattana C., Tassanakajon A., Tharntada S. A double WAP domain-containing protein (DWD) from *Litopenaeus vannamei* with proteinase-inhibition activity (Manuscript in preparation)

โครงการที่ 4 การนำสารเข้าสู่เซลล์โดยคลาทรินและวิถีสื่อสัญญาณ JAK/STAT ในกุ้งกุลาดำ

จากการศึกษาของ Jatuyosporn et al, 2014 พบว่า clathrin coat assembly protein17 (AP17) ซึ่งเป็นโปรตีนที่เกี่ยวข้องกับการนำสารเข้าสู่เซลล์โดยใช้คลาทริน มีความเกี่ยวข้องโดยตรงต่อการติดไวรัสหัวเหลือง (yellow head virus, YHV) ในกุ้งกุลาดำผ่านกระบวนการ clathrin-mediated endocytosis ในงานวิจัยนี้ กลุ่มวิจัยจึงสนใจ ที่จะศึกษาโปรตีนในกระบวนการ clathrin-mediated endocytosis ซึ่งประกอบไปด้วย clathrin coat assembly protein (AP) หลาย subunit โดยสนใจ clathrin AP subunit beta (AP2B) และ mu (AP2M) ซึ่งคาดว่าจะเป็น AP ที่จับกับโปรตีนตัวรับ (receptor) เพื่อนำไปตรวจหาโปรตีนตัวรับที่เกี่ยวข้องกับ กระบวนการ clathrin mediated endocytosis ต่อไป งานวิจัยก่อนหน้านี้ใน *Drosophila* พบว่า กระบวนการ clathrin mediated endocytosis มีความเกี่ยวข้องโดยตรง กับวิถีการส่งสัญญาณ JAK/STAT ซึ่งเป็น antiviral pathway (Devergne, et al., 2007) ในงานวิจัยนี้จึงมีวัตถุประสงค์หลักในการทำวิจัยดังต่อไปนี้

(1) ระบุโปรตีนที่เกี่ยวข้องกับกระบวนการ clathrin-mediated endocytosis เมื่อกุ้งกุลาดำติด YHV

(2) ศึกษาการแสดงออกของยีนในวิถีการส่งสัญญาณ JAK/STAT เมื่อกุ้งกุลาดำติด YHV

ผลการดำเนินงาน

ทำการค้นหาและโคลนยีน AP2B และ AP2M พบว่า ทั้งสองยีนมีขนาด 2,826 bp และ 1,299 bp ตามลำดับ จากนั้นได้ทำการแสดงออกยีนเพื่อผลิตโปรตีนรีคอมบิแนนท์ AP2B และ AP2M ใน *E. coli* BL21 (DE3) ซึ่งพบการแสดงออกของโปรตีนใน inclusion bodies จึงได้ทำให้บริสุทธิ์โดยใช้ Ni-NTA resin ในภาวะ denaturation แล้วทำการ refolding โปรตีนรีคอมบิแนนท์ AP2B มีขนาด 104 kDa และมี pI = 5.17 ส่วนโปรตีนรีคอมบิแนนท์ AP2M มีขนาด 49 kDa และมี pI = 9.55 ทำการศึกษาการแสดงออกของยีน AP2B พบว่ามีการแสดงออกในทุกอวัยวะ (เม็ดเลือด ก้านตา epipodite เหงือก หัวใจ lymphoid organ กระเพาะ ลำไส้ ตับ และกล้ามเนื้อ) เมื่อกุ้งกุลาดำติดไวรัสหัวเหลือง (YHV) เมื่อทำการ knockdown ยีน AP2B พบว่ากุ้งที่ติด YHV มีการตายช้าลง จึงคาดว่าโปรตีนนี้มีบทบาทสำคัญในการติดเชื้อ YHV

ในส่วนของการศึกษาวิถีการส่งสัญญาณ JAK/STAT ได้ศึกษาการแสดงออกของยีน *Pm*DOME, *Pm*JAK และ *Pm*STAT พบว่ามีการแสดงออกในทุกอวัยวะ (เม็ดเลือด ก้านตา epipodite เหงือก หัวใจ lymphoid organ กระเพาะ ลำไส้ ตับ และกล้ามเนื้อ) และมีการแสดงออกเพิ่มขึ้น เมื่อกุ้งติด YHV แสดงให้เห็นว่า เมื่อกุ้งกุลาดำติด YHV มีการตอบสนองผ่านวิถีการส่งสัญญาณ JAK/STAT

ผลงานวิจัย

1. Jatuyosporn, T., Laohawutthichai, P., Sunpungkul, P., Tassanakajon, A. and Krusong, K. Clathrin coat assembly protein 2 subunit β (*Pm*AP2B) and its role during YHV infection in the black tiger shrimp *Penaeus monodon* (Manuscript in preparation)

โครงการที่ 5 โปรตีนในระบบภูมิคุ้มกันอื่นๆ

นอกจากกลุ่มโปรตีนสำคัญในโครงการที่ 1-4 เรายังได้ศึกษาโปรตีนในระบบภูมิคุ้มกันอื่นๆ ที่มีบทบาทสำคัญในการต้านเชื้อแบคทีเรียและไวรัสในกุ้ง โดยงานวิจัยนี้คณะผู้วิจัยได้มุ่งเน้นการศึกษาเชิงลึกในระดับกลไกการทำงานของโปรตีนในการตอบสนองต่อเชื้อ

ผลการดำเนินงาน

ได้ค้นพบกลไกการทำงานของโปรตีนหลายชนิดในระบบภูมิคุ้มกันของกุ้ง และการปฏิสัมพันธ์ของโปรตีนกับเชื้อ โครงการนี้ได้ตีพิมพ์ผลงานในวารสารวิชาการนานาชาติจำนวน 12 บทความ

ผลงานวิจัย

1. Apitanyasai K, Noonin C, Tassanakajon A, Söderhäll I, Söderhäll K. (2016). Characterization of a hemocyte homeostasis-associated-like protein (HHAP) in the freshwater crayfish *Pacifastacus leniusculus.* Fish & Shellfish Immunology. 58:429-435.
2. Arayamethakorn S, Supungul P, Tassanakajon A, Krusong K. (2017). Characterization of molecular properties and regulatory pathways of Crustin*Pm*1 and Crustin*Pm*7 from the black tiger shrimp *Penaeus monodon*. Dev Comp Immunol. 67:18-29
3. Methatham T, Boonchuen P, Jaree P, Tassanakajon A, Somboonwiwat K. (2017). Antiviral action of the antimicrobial peptide ALF*Pm*3 from *Penaeus monodon* against white spot syndrome virus. Dev Comp Immunol. 69:23-32.
4. Monwan W, Amparyup P, Tassanakajon A. (2017). A snake-like serine proteinase (*Pm*Snake) activates prophenoloxidase-activating system in black tiger shrimp *Penaeus monodon*. Dev Comp Immunol. 67:229-238.
5. Khorattanakulchai N, Amparyup P, Tassanakajon A. (2017). Binding of *Pm*ClipSP2 to microbial cell wall components and activation of the proPO-activating system in the black tiger shrimp *Penaeus monodon*. Dev Comp Immunol. 77:38-45.
6. Noothuan N, Amparyup P, Tassanakajon A. (2017). Melanization inhibition protein of *Penaeus monodon* acts as a negative regulator of the prophenoloxidase-activating system. Dev Comp Immunol. 72:97-102.
7. Sutthangkul J, Amparyup P, Eum JH, Strand MR, Tassanakajon A. (2017). Anti-melanization mechanism of the white spot syndrome viralprotein, WSSV453, via interaction with shrimp proPO-activatingenzyme, *Pm*proPPAE2. J Gen Virol. 98(4):769-778.
8. Kamsaeng P, Tassanakajon A, Somboonwiwat K. (2017). Regulation of antilipopolysaccharide factors, ALF*Pm*3 and ALF*Pm*6, in *Penaeus monodon*. Sci Rep. 7(1):12694.
9. Jaturontakul K, Jatuyosporn T, Laohawutthichai P, Kim SY, Mori T, Supungul P1, Hakoshima T, Tassanakajon A, Krusong K. (2017). Molecular Characterization of Viral Responsive Protein 15 and Its Possible Role in Nuclear Export of Virus in Black Tiger Shrimp Penaeus monodon. Sci Rep. 26;7(1):6523
10. Apitanyasai K, Amparyup P, Charoensapsri W, Sangsuriya P, Tassanakajon A. (2018). Shrimp hemocyte homeostasis-associated protein (*Pm*HHAP) interacts with WSSV134 to control apoptosis in white spot syndromevirus infection. Fish & Shellfish Immunology. 76:174-182.
11. Tummamunkong P, Jaree P, Tassanakajon A, Somboonwiwat K. (2018). WSSV-responsive gene expression under the influence of *Pm*VRP15 suppression. Fish & Shellfish Immunology. 72:86-94.
12. Tassanakajon A, Rimphanitchayakit V, Visetnan S, Amparyup P, Somboonwiwat K, Charoensapsri W, Tang S. (2018). Shrimp humoral responses against pathogens: antimicrobialpeptides and melanization. Dev Comp Immunol. 80:81-93.

ผลงานจากงานวิจัย

1. ผลงานตีพิมพ์ในวารสารวิชาการนานาชาติ

มีการตีพิมพ์เผยแพร่ผลงานวิจัยในวารสารระดับนานาชาติ 23 เรื่อง และตีพิมพ์บทความประเภท review article 1 เรื่อง รวมเป็น 24 เรื่อง มีผลงานวิจัยที่อยู่ระหว่างแก้ไข (revised) 1 เรื่อง และอยู่ระหว่างจัดเตรียมบทความอีก 8 เรื่อง

1.1 Visetnan S, Supungul P, Tang S, Hirono I, Tassanakajon A, Rimphanitchayakit V. (2015). YHV-responsive gene expression under the influence of *Pm*Relish. Fish & Shellfish Immunology. 47(1):572-581.

1.2 Apitanyasai K, Noonin C, Tassanakajon A, Söderhäll I, Söderhäll K. (2016). Characterization of a hemocyte homeostasis-associated-like protein (HHAP) in the freshwater crayfish Pacifastacus leniusculus. Fish & Shellfish Immunology. 58:429-435.

1.3 Arayamethakorn S, Supungul P, Tassanakajon A, Krusong K. (2017). Characterization of molecular properties and regulatory pathways of Crustin*Pm*1 and Crustin*Pm*7 from the black tiger shrimp *Penaeus monodon*. Dev Comp Immunol. 67:18-29

1.4 Boonrawd S, Mani R, Ponprateep S, Supungul P, Masrinoul P, Tassanakajon A, Rimphanitchayakit V. (2017). Characterization of *Pm*Spätzle 1 from the black tiger shrimp Peneaus monodon. Fish & Shellfish Immunology. 65:88-95.

1.5 Jaturontakul K, Jatuyosporn T, Laohawutthichai P, Kim SY, Mori T, Supungul P1, Hakoshima T, Tassanakajon A, Krusong K. (2017). Molecular Characterization of Viral Responsive Protein 15 and Its Possible Role in Nuclear Export of Virus in Black Tiger Shrimp *Penaeus monodon*.Sci Rep. 26;7(1):6523

1.6 Junprung W, Supungul P, Tassanakajon A. (2017). HSP70 and HSP90 are involved in shrimp Penaeus vannamei tolerance to AHPND-causing strain of *Vibrio parahaemolyticus* afternon-lethal heat shock. Fish & Shellfish Immunology. 60:237-246.

1.7 Kamsaeng P, Tassanakajon A, Somboonwiwat K. (2017). Regulation of antilipopolysaccharide factors, ALF*Pm*3 and ALF*Pm*6, in *Penaeus monodon*. Sci Rep. 7(1):12694.

1.8 Khorattanakulchai N, Amparyup P, Tassanakajon A. (2017). Binding of *Pm*ClipSP2 to microbial cell wall components and activation of the proPO-activating system in the black tiger shrimp *Penaeus monodon*. Dev Comp Immunol. 77:38-45.

1.9 Methatham T, Boonchuen P, Jaree P, Tassanakajon A, Somboonwiwat K. (2017). Antiviral action of the antimicrobial peptide ALF*Pm*3 from *Penaeus monodon* against white spot syndrome virus. Dev Comp Immunol. 69:23-32.

1.10 Monwan W, Amparyup P, Tassanakajon A. (2017). A snake-like serine proteinase (*Pm*Snake) activatesprophenoloxidase-activating system in black tiger shrimp *Penaeus monodon*. Dev Comp Immunol. 67:229-238.

1.11 Noothuan N, Amparyup P, Tassanakajon A. (2017). Melanization inhibition protein of *Penaeus monodon* acts as a negative regulator of the prophenoloxidase-activating system. Dev Comp Immunol. 72:97-102.

1.12 Ponprateep S, Vatanavicharn T, Lo CF, Tassanakajon A, Rimphanitchayakit V. (2017). Alpha-2-macroglobulin is a modulator of prophenoloxidase system in pacific white shrimp Litopenaeus vannamai. Fish & Shellfish Immunology. 62:68-74.

1.13 Sutthangkul J, Amparyup P, Eum JH, Strand MR, Tassanakajon A. (2017). Anti-melanization mechanism of the white spot syndrome viral protein, WSSV453, via interaction with shrimp proPO-activatingenzyme, *Pm*proPPAE2. J Gen Virol. 98(4):769-778.

1.14 Visetnan S, Supungul P, Tassanakajon A, Donpudsa S, Rimphanitchayakit V. (2017). A single WAP domain-containing protein from *Litopenaeus vannamei* possesses antiproteinase activity against subtilisin and antimicrobial activity against AHPND-inducing *Vibrio parahaemolyticus*. Fish & Shellfish Immunology. 68:341-348.

1.15 Wongpanya R, Sengprasert P, Amparyup P, Tassanakajon A. (2017). A novel C-type lectin in the black tiger shrimp *Penaeus monodon* functions as a pattern recognition receptor by binding and causing bacterial agglutination. Fish & Shellfish Immunology. 60:103-113.

1.16 Apitanyasai K, Amparyup P, Charoensapsri W, Sangsuriya P, Tassanakajon A. (2018). Shrimp hemocyte homeostasis-associated protein (*Pm*HHAP) interacts with WSSV134 to control apoptosis in white spot syndromevirus infection. Fish & Shellfish Immunology. 76:174-182.

1.17 Boonrawd S, Supungul P, Tassanakajon A, Rimphanitchayakit V. (2018). Antimicrobial activity of a serine proteinase inhibitor SPI*Pm*5 from the black tiger shrimp *Penaeus monodon*. Fish & Shellfish Immunology. 77:147-155

1.18 Maralit BA, Jaree P, Boonchuen P, Tassanakajon A, Somboonwiwat K. (2018). Differentially expressed genes in hemocytes of *Litopenaeus vannamei* challenged with *Vibrio parahaemolyticus* AHPND (VPAHPND) and VPAHPND toxin. Fish & Shellfish Immunology. 81:284-296.

1.19 Sangsuriya P, Charoensapsri W, Sutthangkul J, Senapin S, Hirono I, Tassanakajon A, Amparyup P. (2018). A novel white spot syndrome virus protein WSSV164 controls prophenoloxidases, *Pm*proPOs in shrimp melanization cascade. Dev Comp Immunol. 86:109-117.

1.20 Soponpong S, Amparyup P, Tassanakajon A. (2018). A cytosolic sensor, *Pm*DDX41, mediates antiviral immune response in black tiger shrimp *Penaeus monodon*. Dev Comp Immunol. 81:291-302.

1.21 Sornchuera P, Junprung W, Yingsunthonwattana W, Tassanakajonab A. (2018). Heat shock factor 1 regulates heat shock proteins and immune-related genes in *Penaeus monodon* under thermal stress. Dev Comp Immunol.88:19-27.

1.22 Tassanakajon A, Rimphanitchayakit V, Visetnan S, Amparyup P, Somboonwiwat K, Charoensapsri W, Tang S. (2018). Shrimp humoral responses against pathogens: antimicrobial peptides and melanization. Dev Comp Immunol. 80:81-93. **(Review Article)**

1.23 Tummamunkong P, Jaree P, Tassanakajon A, Somboonwiwat K. (2018). WSSV-responsive gene expression under the influence of *Pm*VRP15 suppression. Fish & Shellfish Immunology. 72:86-94.

1.24 Visetnan S, Tassanakajon A, Donpudsa S, Rimphanitchayakit V. (2018). Silencing of a Kazal-type serine proteinase inhibitor SPI*Pm*2 from *Penaeus monodon* affects YHV susceptibility and hemocyte homeostasis. Fish & Shellfish Immunology. 79:18-27.

1.25 Chomwong S, Charoensapsri W, Amparyup P, Tassanakajon A. Two host gut-derived lactic acid bacteria activate the proPO system and increase resistance to an AHPND-causing strain of *Vibrio parahaemolyticus* in the shrimp *Litopenaeus vannamei*. Dev Comp Immunol. **(Revised)**

1.26 Boonchuen P, Jaree P, Tassanakajon A, Somboonwiwat K. Effect of heat stress and *Vibrio parahaemolyticus* AHPND (VPAHPND) challenge on *Litopenaeus vannamei* hemocyte transcriptome. (Manuscript in preparation).

1.27 Charoensapsri W, Chomwong S, Soponpong S, Jearaphunt M, Wongpanya R, Tassanakajon A, Amparyup P. *Pm*STING- and *Pm*IRF-mediated signaling are crucial for the innate antiviral defense against white spot syndrome virus infection in black tiger shrimp *Penaeus monodon*.(Manuscript in preparation).

1.28 Jatuyosporn T, Laohawutthichai P, Sunpungkul P, Tassanakajon A, Krusong K. Clathrin coat assembly protein 2 subunit b (*Pm*AP2B) and its role during YHV infection in the black tiger shrimp *Penaeus monodon*. (Manuscript in preparation).

1.29 Junprung W, Supungul P, Tassanakajon A. *Litopenaeus vannamei* heat shock protein 70 (*Lv*HSP70) enhances resistance to AHPND-causing strain of *Vibrio parahaemolyticus* by activating shrimp immunity. (Manuscript in preparation).

1.30 Sakunwattana C., Tassanakajon A., Tharntada S. A double WAP domain-containing protein (DWD) from *Litopenaeus vannamei* with proteinase-inhibition activity. (Manuscript in preparation).

1.31 Sangsuriya P, Charoensapsri W, Tassanakajon A, Amparyup, P. Molecular interaction of pathogen recognition proteins in shrimp prophenoloxidase system with white spot syndrome virus proteins. (Manuscript in preparation).

1.32 Supungul, P., Tang, S., Tassanakajon, A., Rimphanitchayakit, V.Kruppel like factor gene with its variation related to TSV-resistance of Penaeus vannamei. (Manuscript in preparation).

1.33 Wongpanya R, Amparyup P, Tassanakajon A. Fuctional characterization of *Pm*Ficolin and *Pm*MBP in the black tiger shrimp *Penaeus monodon*. (Manuscript in preparation).

2. การได้รับเชิญไปเป็นวิทยากร

2.1 ศ.ดร. อัญชลี ทัศนาขจร ได้รับเชิญให้ไปบรรยายในงานประชุมวิชาการต่างๆ ดังนี้

2.1.1 ได้รับเชิญให้เป็น Invited Spearker ในงานประชุมวิชาการวิทยาศาสตร์และเทคโนโลยีแห่งประเทศไทย ครั้งที่ 41 (วทท.41) ซึ่งจัดขึ้นระหว่างวันที่ 6-8 พฤศจิกายน 2558 ที่ จังหวัดนครราชสีมา บรรยายในหัวข้อ “Regulation and function of melanization in shrimp Peneaus monodon”

2.1.2 ได้รับเชิญให้เป็น Plenary Spearker ในงานประชุมวิชาการวิชาการนานาชาติ Asia-Pacific Marine Biotechnology Conference 2017 ซึ่งจัดขึ้นระหว่างวันที่ 22-24 พฤษภาคม 2560 ที่ รัฐฮาวาย ประเทศสหรัฐอเมริกา บรรยายในหัวข้อ “Innate immunity and disease resistance in shrimp”

2.1.3 ได้รับเชิญให้เป็น Plenary Spearker ในงานประชุมวิชาการ The 29th Annual Meeting of the Thai Society for Biotechnology and International Conference (TSB2017) ซึ่งจัดขึ้นระหว่างวันที่ 23-25 พฤศจิกายน 2560 ที่ โรงแรม Swissôtel Le Concorde กรุงเทพมหานคร บรรยายในหัวข้อ “From immunity to disease resistance: Bringing basic research to shrimp farming”

2.1.4 ได้รับเชิญให้เป็น Invited Spearker ในงานประชุมวิชาการ FAO Regional Meeting on Agricultural Biotechnologies in Sustainable Food Systems and Nutrition in Asia-Pacific ซึ่งจัดขึ้นระหว่างวันที่ 11-13 กันยายน 2560 ที่ กรุงกัวลาลัมเปอร์ ประเทศมาเลเซีย บรรยายในหัวข้อ “Personal reflections on the status and challenges regarding use of agricultural biotechnologies in the fishery sector”

2.1.5 ได้รับเชิญให้เป็น Invited Spearker ในงานประชุมวิชาการ FAO Regional Meeting on Agricultural Biotechnologies in Sustainable Food Systems and Nutrition in Asia-Pacific ซึ่งจัดขึ้นระหว่างวันที่ 11-13 กันยายน 2561 ที่ กรุงกัวลาลัมเปอร์ ประเทศมาเลเซีย บรรยายในหัวข้อ“The role of genomics in shrimp improvement”

2.1.6 ได้รับเชิญให้เป็น Invited Spearker ในงานประชุมวิชาการ International Mini-symposium on Frontier Aquaculture Science ซึ่งจัดขึ้นในวันที่ 9 ธันวาคม 2560 ที่ National Cheng Kung University ประเทศไต้หวัน บรรยายในหัวข้อ “From immunity to disease resistance: Bringing basic research to shrimp farming”

2.2 ผศ.ดร. กุลยา สมบูรณ์วิวัฒน์ ได้รับเชิญให้ไปบรรยายในงานประชุมวิชาการต่างๆ ดังนี้

2.2.1 ได้รับเชิญให้เป็น Invited Spearker ในงานประชุมวิชาการ International Mini-symposium on Frontier Aquaculture Science ซึ่งจัดขึ้นในวันที่ 9 ธันวาคม 2560 ที่ National Cheng Kung University ประเทศไต้หวัน บรรยายในหัวข้อ “The shrimp antimicrobial peptide antilipopolysaccharide factor (ALF): Basic and protential applications”

2.2.2 ได้รับเชิญให้เป็น Invited Spearker ในงานประชุมวิชาการวิทยาศาสตร์และเทคโนโลยีแห่งประเทศไทย ครั้งที่ 43 (วทท.43) ซึ่งจัดขึ้นระหว่างวันที่ 17-19 ธันวาคม 2560 ที่ จุฬาลงกรณ์มหาวิทยาลัย กรุงเทพมหานคร บรรยายในหัวข้อ “The shrimp antimicrobial peptide antilipopolysaccharide factor (ALF): Basic and protential applications”

3. การเสนอผลงานในที่ประชุมวิชาการ

มีผลงานนำเสนอในที่ประชุมวิชาการรวมทั้งสิ้น 41 เรื่อง โดยแบ่งเป็นผลงานที่นำเสนอในที่ประชุมวิชาการระดับนานาชาติ 28 เรื่อง และผลงานที่นำเสนอในที่ประชุมวิชาการระดับชาติ 13 เรื่อง

3.1 การเสนอผลงานในที่ประชุมระดับนานาชาติ

มีผลงานนำเสนอในที่ประชุมวิชาการระดับนานาชาติรวม 28 เรื่อง โดยแบ่งเป็นประเภทบรรยาย 15 เรื่อง และโปสเตอร์ 13 เรื่อง ประกอบด้วยรายงานการประชุมวิชาการ (Proceeding) 1 เรื่อง และบทคัดย่อจำนวน 27 เรื่อง ดังนี้

3.1.1 ประเภทบรรยาย

3.1.1.1 Chomwong S, Amparyup P, Charoensapsri W, Tassanakajon A. (2016). Isolation and investigation of the immunomodulatory functions of lactic acid bacteria from shrimp gut. The 28th Annual Meeting of the Thai Society for Biotechnology and International Conference. 28–30 November 2016. The Empress Hotel, Chiang Mai, Thailand. **(Proceeding)**

3.1.1.2 Boonchuen P, Methatham T, Tassanakajon A, Somboonwiwat K. (2015). Antiviral action of antilipopolysaccharide factor isoform 3 on white spot syndrome virus. 20th Biological Sciences Graduate Congress (BSGC). 9–11 December 2015. Chulalongkorn Univeristy, Bangkok, Thailand.

3.1.1.3 Boonchuen P, Jaree P, Somboonwiwat K. (2016). Differential expression of mRNAs from *Penaeus vannamei* upon *Vibrio parahaemolyticus* AHPND infection. 21st Biological Sciences Graduate Congress (BSGC). 15–16 December 2016. University Of Malaya, Malaysia.

3.1.1.4 Junprung W, Supungul P, Tassanakajon, A. (2016). Shrimp *Penaeus vannamei* tolerance to AHPND–causing strain of *Vibrio parahaemolyticus* by non–lethal heat shock is mediated by HSP70 and HSP90. 21st Biological Sciences Graduate Congress (BSGC). 15–16 December 2016. University Of Malaya, Malaysia.

3.1.1.5 Sangsuriya P, Charoensapsri W, Chomwong S, Senapin S, Tassanakajon A, amparyup P. (2016). Control of prophenoloxidase system and its role in antiviral immunity in shrimp. Asian–Pacific Aquaculture 2016. 26–29 April 2016. Grand City, Surabaya, Indonesia.

3.1.1.6 Junprung W, Supungul P, Tassanakajon A. (2016). Heat shock proteins (*Lv*HSPs) from *Penaeus vannamei* and theirs roles in protection against *Vibrio parahaemolyticus* causing acute hepatopancreatic necrosis disease (AHPND). BMB 2016 "The 5th International Biochemistry and Molecular Biology Conference 2016". 26–27 May 2016. Songkla, Thailand.

3.1.1.7 Apitanyasai K, Charoensapsri W, Amparyup P, Noonin C, Söderhäll I, Söderhäll K, Tassanakajon A. (2017). Role of hemocyte homeostasis–associated protein (HHAP) in two species of crustaceans. Asia–Pacific Marine Biotechnology Conference 2017. 22–24 May 2017. University of Hawaii Mãnoa, Hawaii, USA.

3.1.1.8 Junprung W, Supungul P, Tassanakajon A. (2017). Heat shock proteins play roles in protection against AHPND–causing strain of *Vibrio parahaemolyticus* by induction of shrimp immune system. Asia–Pacific Marine Biotechnology Conference 2018. 22–24 May 2017. University of Hawaii Mãnoa, Hawaii, USA.

3.1.1.9 Kamsaeng P, Tassanakajon A, Somboonwiwat K. (2017). Two major *Penaeus monodon* antilipopolysaccharide factor isoforms (ALF*Pm*s) are regulated by Toll and IMD pathways. Asia–Pacific Marine Biotechnology Conference 2017. 22–24 May 2017. University of Hawaii Mãnoa, Hawaii, USA.

3.1.1.10 Somboonwiwat K, Maralit BA, Jaree P, Boonchuen P, Luangtrakul W, Tassanakajon T. (2017). Efffect of chronic heat stress response on hemocyte transcriptome of *Penaeus vannamei* challenged with *Vibrio parahaemolyticus* AHPND. The 10th

Symposium on Diseases in Asian Aquaculture (DAA10). 28 August–1 September 2017. The Anvaya Beach Resort, Kuta, Bali, Indonesia.

3.1.1.11 Boonchuen P. (2017). Identification of miRNAs from *Penaeus vannamei* in response to *Vibrio parahaemolyticus* AHPND infection and heat stress. The 22nd Biological Sciences Graduate Congress (BSGC2017). 19–21 December 2017. University Town, NUS, Singapore.

3.1.1.12 Jatuyosporn T. (2017). Molecular characterization of viral responsive protein 15 and its possible role in nuclear export of viras in black tiger shrimp *Penaeus monodon*. The 22nd Biological Sciences Graduate Congress (BSGC2017). 20–21 December 2017. University Town, NUS, Singapore.

3.1.1.13 Soponpong S, Amparyup P, Tassanakajon A. (2017). Functional characterization of cytosolic DDX41 sensor in mediating antiviral immune response in black tiger shrimp *Penaeus monodon*. The 29th Annual Meeting of the Thai Society for Biotechnology and International Conference (TSB2017).. 23–25 November 2017. Swissôtel Le Concorde, Bangkok, Thailand.

3.1.1.14 Sangsuriya P , Charoensapsri W, Senapin S, Tassanakajon A, Amparyup P. (2017). Molecular interaction of pathogen recognition proteins in shrimp prophenoloxidase system with white spot syndrome virus proteins. The 5th Biotechnology International Congress (BIC 2017). 6–8 September 2017. BITEC, Bangkok, Thailand.

3.1.1.15 Luangtrakul W, Boonchuen P, Jaree P, Tassanakajon A, Somboonwiwat K. (2018). The possible role of two aminopeptidase N proteins from *Penaeus vannamei* hemocyte as receptor of *Vibrio parahaemolyticus* AHPND toxin. The 6th International Conference on Biochemistry and Molecular Biology (BMB). 20–22 June 2018. Rayong, Thailand.

3.1.2 ประเภทโปสเตอร์

3.1.2.1 Khorattanakulchai N, Amparyup P, Tassanakajon A. (2016). Role of clip domain serine proteinase 2, *Pm*ClipSP2, in activation of prophenoloxidas–activating system in black tiger shrimp *Penaeus monodon*. 21st Biological Sciences Graduate Congress (BSGC). 15–16 December 2016. University Of Malaya, Malaysia.

3.1.2.2 Soponpong S, Amparyup P, Tassanakajon, A. (2016). Functional Characterization of Cytosolic Sensor, DDX41 in mediating antiviral immune response in shrimp *Penaeus*

monodon. 21st Biological Sciences Graduate Congress (BSGC). 15–16 December 2016. University Of Malaya, Malaysia.

3.1.2.3 Tummamunkong P, Jaree P, Tassanakajon A, Somboonwiwat K. (2017). *Penaeus monodon* viral responsive protein 15 (*Pm*VRP15) involved in regulation of hemocyte homostasis. The 10th Symposium on Diseases in Asian Aquaculture (DAA10). 28 August–1 September 2017. The Anvaya Beach Resort, Kuta, Bali, Indonesia.

3.1.2.4 Boonchuen P, Methatham T, Jaree P, Tassanakajon A, Somboonwiwat K. (2017). Hemocyanin of *Litopenaeus vannamei* agglutinates *Vibrio parahaemolyticus* AHPND (VPAHPND) and neutralizes VPAHPND toxin. The 10th Symposium on Diseases in Asian Aquaculture (DAA10). 28 August–1 September 2017. The Anvaya Beach Resort, Kuta, Bali, Indonesia.

3.1.2.5 Wongdontri C. (2017). Expression and purification of Kunitz ttype serine protease inhibitor from hemocyte of black tiger shrimp Penaeus mondon. The 22nd Biological Sciences Graduate Congress (BSGC2017). 21–21 December 2017. University Town, NUS, Singapore.

3.1.2.6 Luangtrakul W. (2017). Identification of shrimp PIWI–interacting RNAs (piRNAs) that involved in pathogen infections. The 22nd Biological Sciences Graduate Congress (BSGC2017). 22–21 December 2017. University Town, NUS, Singapore.

3.1.2.7 Apichatayanon T. (2017). Mutagenesis of recombinant crustin*Pm*1 from black tiger shrimp *Penaeus monodon* and its binding properties. The 22nd Biological Sciences Graduate Congress (BSGC2017). 23–21 December 2017. University Town, NUS, Singapore.

3.1.2.8 Nhnhkorn Z. (2017). Functional characterizationof IKK in *Penaeus monodon* antiviral signaling pathway. The 22nd Biological Sciences Graduate Congress (BSGC2017). 24–21 December 2017. University Town, NUS, Singapore.

3.1.2.9 Laohawutthichai P. (2017). Preliminary crystallization of the recombinant viral responsive protein 15 (*Pm*VRP15) from the black tiger shrimp *Penaeus monodon*. The 22nd Biological Sciences Graduate Congress (BSGC2017). 25–21 December 2017. University Town, NUS, Singapore.

3.1.2.10 Nhnhkorn Z, Amparyup P, Tassanakajon A. (2017). Functional characterization of IKK in *Penaeus monodon* antiviral signaling pathway. The 29th Annual Meeting of the

Thai Society for Biotechnology and International Conference (TSB2017). 23–25 November 2018. Swissôtel Le Concorde, Bangkok, Thailand.

3.1.2.11 Boonchuen P, Somboonwiwat K. (2018). Identification of miRNAs from *Penaeus vannamei* in response to *Vibrio parahaemolyticus* AHPND infection. The 6th International Conference on Biochemistry and Molecular Biology (BMB). 20–22 June 2018. Rayong, Thailand.

3.1.2.12 Wanvimonsuk S, Nonejuie P, Somboonwiwat, K. (2018). Identification of ALF*Pm*3–resistant genes from acute hepatopancreatic necrosis disease (AHPND)–causing *Vibrio parahaemolyticus*. The 6th International Conference on Biochemistry and Molecular Biology (BMB). 20–22 June 2018. Rayong, Thailand.

3.1.2.13 Wongdontri C, Somboonwiwat K. (2018). Characterization of shrimp miRNAs involved in pathogen–challenged responses. The 6th International Conference on Biochemistry and Molecular Biology (BMB). 20–22 June 2018. Rayong, Thailand.

3.2 การเสนอผลงานในที่ประชุมระดับชาติ

มีผลงานนำเสนอในที่ประชุมวิชาการระดับชาติ 13 เรื่อง โดยแบ่งเป็นประเภทบรรยาย 8 เรื่อง และ โปสเตอร์ 5 เรื่อง ซึ่งประกอบด้วยรายงานการประชุมวิชาการ (Proceeding) 2 เรื่อง และบทคัดย่อจำนวน 11 เรื่อง ดังนี้

3.2.1 ประเภทบรรยาย

3.2.1.1 Phumkumarn N, Wongpanya R. (2017). Expression and characterization of mannose binding protein from black tiger shrimp, *Penaeus monodon*. The 14th KU–KPS Conference. 7–8 December 2017. Kasetsart University Kamphaeng Saen Campus, Nakhon Pathom, Thailand. **(Proceeding)**

3.2.1.2 Phumkumarn N, Wongpanya R. (2017). Identification and characterization of mannose binding protein in black tiger shrimp, *Penaeus monodon*. The 55th Kasetsart University Annual Conferenc. 31 January–3 February 2017. Kasetsart University, Bangkok, Thailand. **(Proceeding)**

3.2.1.3 Kamsaeng P, Tassanakajon A, Somboonwiwat K. (2015). Antibacterial activity and gene regulation of antilipopolysaccharide factor from black tiger shrimp *Penaeus monodon*. The 41st Congress on Science and Technology of Thailand (STT41). 6–8 November 2015. Nakhonratchasima, Thailand.

3.2.1.4 Somboonwiwat K, Kaewkascholkul N, Somboonviwat K, Hirono I, Tassanakajon A. (2015). Identification and characterization of miRNAs that involved in wssv infection

in *Penaeus monodon*. The 41st Congress on Science and Technology of Thailand (STT41). 6–8 November 2015. Nakhonratchasima, Thailand.

3.2.1.5 Jaree P, Tassanakajon A, Somboonwiwat K. (2015). Characterization of mir–315 function in shrimp, *Penaeus monodon*, antiviral immunity. The 41st Congress on Science and Technology of Thailand (STT41). 6–8 November 2015. Nakhonratchasima, Thailand.

3.2.1.6 Tummanunkong P, Jaree P, Kawai T, Tassanakajon A. Somboonwiwat K. (2017). An Interferon regulatory factor negatively regulates *Penaeus monodon* viral responsive protein 15 gen. The 43rd Congress on Science and Technology of Thailand (STT43). 17–19 December 2017. Chulalongkorn University, Bangkok, Thailand.

3.2.1.7 Junprung W, Supungul P, Bossier P, Tassanakajon A. (2017). Heat shock proteins play roles in protection against AHPND causing strain of *Vibrio parahaemolyticus* by induction . ATPER2017. 30 September–1 October 2017. The Royal Thai Embassy Vienna, Austria.

3.2.1.8 Junprung W, Supungul P, Tassanakajon A. (2017). Heat shock proteins play roles in protection against AHPND–causing strain of *Vibrio parahaemolyticus* by induction of shrimp immune system. RGJ–Ph.D. Congress 18. 8–10 June 2017. Richnond Stylish Convention Hotel Nonthaburi, Thailand.

3.2.2 ประเภทโปสเตอร์

3.2.2.1 Wongdontri C, Somboonwiwat K. (2017). Expression and purification of Kunitz–type serine protease inhibitor from hemocyte of WSSV–infected *Penaeus monodon*. The 43rd Congress on Science and Technology of Thailand (STT43). 17–19 December 2017. Chulalongkorn University, Bangkok, Thailand.

3.2.2.2 Kanoksinwuttipong N, Wongdontri C, Somboonwiwat K. (2017). Expression analysis of miRNAs involved in pathogen challenge in shrimp. The 43rd Congress on Science and Technology of Thailand (STT43). 17–19 December 2017. Chulalongkorn University, Bangkok, Thailand.

3.2.2.3 Apichatayanon T, Tassanakajon A, Krusong K. (2017). Preliminary crystallization of recombinant crustin*Pm*1 from the black tiger shrimp *Penaeus monodon*. The 43rd Congress on Science and Technology of Thailand (STT43). 17–19 December 2017. Chulalongkorn University, Bangkok, Thailand.

3.2.2.4 Laohawutthichai P, Tassanakajon A, Krusong K. (2017). Crystallization of the recombinant viral responsive protein (15*Pm*VRP15) from the black tiger shrimp *Penaeus monodon*. The 43rd Congress on Science and Technology of Thailand (STT43). 17–19 December 2017. Chulalongkorn University, Bangkok, Thailand.

3.2.2.5 Charoensapsri W, Chomwong S, Tassanakajon A, Amparyup P. (2018). Function of interferon regulatory factor (*Pm*IRF) in antiviral immunity against white spot syndrome virus in black tiger shrimp *Penaeus monodon*. The 6th Marine Science Conference. 18–20 June 2018. Bangsaen Heritage Hotel, Chon Buri, Thailand.

4. รางวัล

4.1 รางวัลจากหน่วยงานต่างๆ

อาจารย์และนักวิจัยได้รับรางวัลจากหน่วยงานต่างๆ ดังนี้

4.1.1 ศ. ดร. วิเชียร ริมพณิชยกิจ ได้รับการโปรดเกล้าฯ ให้ดำรงตำแหน่งศาสตราจารย์

4.1.2 ผศ.ดร. กุลยา สมบูรณ์วิวัฒน์ ได้รับรางวัล ดุษฎีบัณฑิต คปก. ดีเด่น ปี 2558 สาขาวิทยาศาสตร์ชีวภาพ จาก สำนักงานกองทุนสนับสนุนการวิจัย รับรางวัลวันที่ 17 ธันวาคม 2558

4.1.3 ผศ.ดร. กุลยา สมบูรณ์วิวัฒน์ ได้รับรางวัล Young Protein Scientist of Thailand Award ปี 2561 จากผลงานทางด้าน “Molecular Mechanism of Immune-Related Proteins in Shrimp Immunity” จากสมาคมโปรตีนแห่งประเทศไทย รับรางวัลวันที่ 9 สิงหาคม 2561

4.1.4 ดร. ภัทรันดา จารีย์ ได้รับรางวัล ผลงานวิจัยดีเด่นสำหรับนิสิตระดับปริญญาเอก จากผลงานวิทยานิพนธ์เรื่อง “ลักษณะสมบัติเชิงหน้าที่ของโปรตีนในระบบภูมิคุ้มกันจากกุ้งกุลาดำ *Penaeus monodon* ในการตอบสนองต่อการติดเชื้อโรค” จาก กองทุนรัชดาภิเษกสมโภช ประจำปี 2559

4.1.5 ดร. สุวัฒนา วิเศษนันท์ ได้รับรางวัล ผลงานวิจัยดีเด่นสำหรับนิสิตระดับปริญญาเอก จากผลงานวิทยานิพนธ์เรื่อง “ลักษณะสมบัติเชิงหน้าที่ของโปรตีนรีลิชจากกุ้งกุลาดำ *Penaeus monodon*” จาก กองทุนรัชดาภิเษกสมโภช ประจำปี 2559

4.1.6 ดร. ปิติ อ่ำพายัพ ได้รับรางวัล Thailand Frontier Researcher Award 2016 จาก Thomson Reuters รับรางวัลวันที่ 25 สิงหาคม 2559

4.1.7 ดร.วลัยพร เจริญทรัพย์ศรี ได้รับรางวัล Carolina MacGillavry Collaborative Research Award ประจำปี 2016 ภายใต้ชุดโครงการ Climate change and pathogenicity with emphasized on *Vibrio parahaemolyticus* causing acute hepatopancreatic necrosis disease (AHPND) in shrimp. (หัวหน้าชุดโครงการ และหัวหน้าโครงการย่อย) จาก the Royal Netherlands Academy of Arts and Sciences

4.1.8 ดร.ภคกุล สังข์สุริยะ ได้รับรางวัล Carolina MacGillavry Collaborative Research Award ประจำปี 2016 ภายใต้ชุดโครงการ Climate change and pathogenicity with emphasized on *Vibrio parahaemolyticus* causing acute hepatopancreatic necrosis disease (AHPND) in shrimp. (หัวหน้าโครงการย่อย) จาก the Royal Netherlands Academy of Arts and Sciences

4.2 รางวัลจากการเสนอผลงานในที่ประชุมวิชาการต่างๆ

นิสิต และนักวิจัย ได้รับรางวัลจากการเสนอผลงานในที่ประชุมวิชาการต่างๆ ดังนี้

4.2.1 ประเภทบรรยาย

4.2.1.1 นาย วิศรุต จันทร์ปรุง ได้รับรางวัล Outstanding Oral Presentation Award ในงานประชุม BMB 2016 "The 5th International Biochemistry and Molecular Biology Conference 2016" จากผลงานวิจัยเรื่อง "Heat shock proteins (*Lv*HSPs) from *Penaeus vannamei* and theirs roles in protection against *Vibrio parahaemolyticus* causing acute hepatopancreatic necrosis disease (AHPND)" รับรางวัลวันที่ 27 พฤษภาคม 2559

4.2.1.2 นาย ภาคภูมิ บุญชื่น ได้รับรางวัล Third Place Award for Oral Presentation ในงานประชุม 21st Biological Sciences Graduate Congress (BSGC) จากผลงานวิจัยเรื่อง "Differential expression of mRNAs from *Penaeus vannamei* upon *Vibrio parahaemolyticus* AHPND infection" รับรางวัลวันที่ 17 ธันวาคม 2559

4.2.1.3 นาย วิศรุต จันทร์ปรุง ได้รับรางวัล Outstanding oral presentation ในงานประชุม RGJ-Ph.D. Congress จากผลงานวิจัยเรื่อง "Heat shock proteins play roles in protection against AHPND-causing strain of *Vibrio parahaemolyticus* by induction of shrimp immune system" รับรางวัลวันที่ 10 มิถุนายน 2560

4.2.1.4 นางสาว ศุภมน เจนวรรธนะกุล ได้รับรางวัล รองชนะเลิศ ประเภทบรรยาย ในการประกวดโครงงานวิทยาศาสตร์ การประชุมวิชาการ (The Science Forum 2018) ครั้งที่ 26 ประจำปี 2561 จากผลงานวิจัยเรื่อง "Role of *Litopenaeus vannamei* heat shock protein 70 (*Lv*HSP70) in response to white spot syndrome virus infection" รับรางวัลวันที่ 6 มิถุนายน 2561

4.2.2 ประเภทโปสเตอร์

4.2.2.1 นางสาว สุดารัตน์ ชมวงค์ ได้รับรางวัล Gold Popular Vote Poster ในงานประชุม The 28th Annual Meeting of the Thai Society for Biotechnology and International Conference

จากผลงานวิจัยเรื่อง "Isolation and investigation of the immunomodulatory functions of lactic acid bacteria from shrimp gut" รับรางวัลวันที่ 30 พฤศจิกายน 2559

4.2.2.2 นาย ภาคภูมิ บุญชื่น ได้รับรางวัล 2nd Winner Poster Presentation ในงานประชุม The 10th Symposium on Diseases in Asian Aquaculture (DAA10) จากผลงานวิจัยเรื่อง “Hemocyanin of *Litopenaeus vannamei* agglutinates *Vibrio parahaemolyticus* AHPND (VPAHPND) and neutralizes VPAHPND toxin” รับรางวัลวันที่ 1 กันยายน 2560

4.2.2.3 นาย สิทธิพงษ์ ณ นคร ได้รับรางวัล Best Poster Presentation Awards at TSB 2017 ในงานประชุม The 29th Annual Meeting of the Thai Society for Biotechnology and International Conference (TSB2017) จากผลงานวิจัยเรื่อง "Functional characterization of IKK in *Penaeus monodon* antiviral signaling pathway" รับรางวัลวันที่ 25 พฤศจิกายน 2560

4.2.2.4 ดร. วลัยพร เจริญทรัพย์ศรี ได้รับรางวัล นำเสนอผลงานวิชาการ ระดับดี ประเภทโปสเตอร์ ในงานประชุม The 6th Marine Science Conference จากผลงานวิจัยเรื่อง "Function of interferon regulatory factor (*Pm*IRF) in antiviral immunity against white spot syndrome virus in black tiger shrimp *Penaeus monodon*" รับรางวัลวันที่ 20 มิถุนายน 2561

4.2.2.5 นายภาคภูมิ บุญชื่น ได้รับรางวัล Outstanding poster presentation ในงานประชุม The 6th International Conference on Biochemistry and Molecular Biology (BMB) จากผลงานวิจัยเรื่อง "Identification of miRNAs from *Penaeus vannamei* in response to Vibrio parahaemolyticus AHPND infection" รับรางวัลวันที่ 22 มิถุนายน 2561

4.2.2.6 นางสาว ฉันทกา วงษ์ดนตรี ได้รับรางวัล Outstanding poster presentation ในงานประชุม The 6th International Conference on Biochemistry and Molecular Biology (BMB) จากผลงานวิจัยเรื่อง “Characterization of shrimp miRNAs involved in pathogen-challenged responses” รับรางวัลวันที่ 22 มิถุนายน 2561

5. ความก้าวหน้าในการสร้างทีมวิจัย

มีการสนับสนุนให้นักวิจัยรุ่นกลางขอทุนวิจัย โดย ผศ.ดร. กุลยา สมบูรณ์วิวัฒน์ได้ขอทุน องค์ความรู้ใหม่ที่เป็นพื้นฐานต่อการพัฒนา สำนักงานกองทุนสนับสนุนการวิจัยและมีการดึงนักวิจัยรุ่นใหม่ คือ ดร. ศิรินิตย์ ธารธาดา อาจารย์ประจำภาควิชาเทคนิคการสัตวแพทย์ คณะเทคนิคการสัตวแพทย์ มหาวิทยาลัยเกษตรศาสตร์ ให้เข้ามาในกลุ่มเพื่อสร้างทีม และได้รับนักวิจัยหลังปริญญาเอกเพื่อทำงานวิจัยภายในโครงการ 5 คน คือ ดร. สุวัฒนา วิเศษนันท์ ดร. ภัทรันดา จารีย์ Dr. Benedict Maralit ดร.พรพรรณ สอนเชื้อ และ ดร. อาจารีย์ เจียวก๊ก นอกจากนี้ได้มีนิสิตปริญญาเอกและปริญญาโทที่ช่วยในงานวิจัยดังนี้

นิสิตสำเร็จการศึกษา ระดับปริญญาเอก 1 คน

1. นางสาว กัณฑมาศ อภิธันยาศัย สาขาวิชา ชีวเคมีและชีววิทยาโมเลกุล ภาควิชาชีวเคมี คณะวิทยาศาสตร์ จุฬาลงกรณ์มหาวิทยาลัย

นิสิตสำเร็จการศึกษา ระดับปริญญาโท 3 คน

1. นางสาว สุดารัตน์ ชมวงค์ สาขาวิชา เทคโนโลยีชีวภาพ คณะวิทยาศาสตร์ จุฬาลงกรณ์มหาวิทยาลัย
2. นาย ประวิทย์ อังคะณา สาขาวิชา พันธุวิศวกรรม โครงการสหวิทยาการระดับบัณฑิตศึกษา มหาวิทยาลัยเกษตรศาสตร์
3. นางสาว นพรัตน์ พุ่มกุมาร สาขาวิชา พันธุวิศวกรรม โครงการสหวิทยาการระดับบัณฑิตศึกษา มหาวิทยาลัยเกษตรศาสตร์

นิสิตระดับปริญญาเอก สาขาวิชา ชีวเคมีและชีววิทยาโมเลกุล ภาควิชาชีวเคมี คณะวิทยาศาสตร์ จุฬาลงกรณ์มหาวิทยาลัย

1. นาย ฐปนรรค์ จตุยศพร
2. นาย ภาคภูมิ บุญชื่น
3. นาย วิศรุต จันทร์ปรุง
4. นางสาว ภาสุนีย์ เลาหวุฒิชัย
5. นางสาว สุธินี โสภณพงษ์

นิสิตระดับปริญญาเอก สาขาวิชา เทคโนโลยีชีวภาพ คณะวิทยาศาสตร์ จุฬาลงกรณ์มหาวิทยาลัย

1. นาย สิทธิชัย บุญรอด

นิสิตระดับปริญญาโท สาขาวิชา ชีวเคมีและชีววิทยาโมเลกุล ภาควิชาชีวเคมี คณะวิทยาศาสตร์ จุฬาลงกรณ์มหาวิทยาลัย

1. นาย สิทธิพงษ์ ณ นคร
2. นางสาว ฉันทกา วงษ์ดนตรี
3. นาย ธัชชีวา อภิชาตยานนท์
4. นางสาว วรันธร เหลืองตระกูล

6. การนำผลจากโครงการไปใช้ประโยชน์

- อยู่ในระหว่างทดสอบการนำโปรตีน ALF*Pm*3 ไปใช้ในการควบคุมโรค
- มีการรับทำวิจัยร่วมกับภาคเอกชน คือ บริษัท Toray Inductries Inc. ประเทศญี่ปุ่น ในโครงการวิจัยเรื่อง The effects of dietary polyphenols on enhancing immune systems of juvenile Pacific white shrimp *Litopenaeus vannamei*

- มีการนำองค์ความรู้ด้านภูมิคุ้มกันของกุ้งไปช่วยสร้างกระบวนการประเมินสุขภาพกุ้ง โดยร่วมมือกับบริษัทเอกชน คือ บริษัท TORAY industries และบริษัท INVE รับจ้างวิจัยเพื่อประเมินสุขภาพกุ้ง
- ร่วมมือกับบริษัท BASF New Business ผ่านสถาบันทรัพย์สินทางปัญญาของจุฬาฯ เพื่อขอนำโปรตีนรีคอมบิแนนท์ antilipopolysaccharide factor (ALFPm3) ที่โคลนได้จากกุ้งกุลาดำ ไปทำการทดสอบและประเมินความเป็นไปได้ในทางการค้า

รายชื่อกลุ่มวิจัย

ชื่อ-นามสกุล	เริ่มเข้าร่วมโครงการ			ปัจจุบัน		
	ตำแหน่งวิชาการ	สังกัด	ตำแหน่งในโครงการ	ตำแหน่งวิชาการ	สังกัด	สถานภาพปัจจุบัน
1. นาง อัญชลี ทัศนาขจร	ศาสตราจารย์	ภาควิชาชีวเคมี คณะวิทยาศาสตร์ จุฬาลงกรณ์มหาวิทยาลัย	หัวหน้าโครงการ	ศาสตราจารย์	ภาควิชาชีวเคมี คณะวิทยาศาสตร์ จุฬาลงกรณ์มหาวิทยาลัย	ยังอยู่ในโครงการ
2. นาย วิเชียร ริมพณิชยกิจ	รองศาสตราจารย์		ผู้ร่วมโครงการ	ศาสตราจารย์		
3. นางสาว กุลยา สมบูรณ์วิวัฒน์	ผู้ช่วยศาสตราจารย์			ผู้ช่วยศาสตราจารย์		
4. นางสาว เกื้อการุณย์ ครูส่ง	ผู้ช่วยศาสตราจารย์			ผู้ช่วยศาสตราจารย์		
5. นาง เปรมฤทัย สุพรรณกูล	นักวิจัย	หน่วยวิจัยเทคโนโลยีชีวภาพสัตว์ ห้องปฏิบัติการอณูพันธุศาสตร์และ เทคโนโลยีชีวภาพสัตว์น้ำ ศูนย์พันธุวิศวกรรมและเทคโนโลยีชีวภาพแห่งชาติ		นักวิจัย	หน่วยวิจัยเทคโนโลยีชีวภาพสัตว์ ห้องปฏิบัติการอณูพันธุศาสตร์และ เทคโนโลยีชีวภาพสัตว์น้ำ ศูนย์พันธุวิศวกรรมและเทคโนโลยีชีวภาพแห่งชาติ	
6. นาย ปิติ อ่ำพายัพ	นักวิจัยอาวุโส			นักวิจัยอาวุโส		
7. นางสาว ภคกุล สังข์สุริยะ	นักวิจัย			นักวิจัย		
8. นางสาว สุรีรัตน์ แซ่ตั้ง	ผู้ช่วยนักวิจัยอาวุโส			ผู้ช่วยนักวิจัยอาวุโส		
9. นางสาว วลัยพร เจริญทรัพย์ศรี	นักวิจัย	หน่วยเครือข่าย ห้องปฏิบัติการเทคโนโลยีชีวภาพกุ้ง ศูนย์พันธุวิศวกรรมและเทคโนโลยีชีวภาพแห่งชาติ		นักวิจัย	หน่วยเครือข่าย ห้องปฏิบัติการเทคโนโลยีชีวภาพกุ้ง ศูนย์พันธุวิศวกรรมและเทคโนโลยีชีวภาพแห่งชาติ	
10. นาง ราตรี วงศ์ปัญญา	ผู้ช่วยศาสตราจารย์	ภาควิชาชีวเคมี คณะวิทยาศาสตร์ มหาวิทยาลัยเกษตรศาสตร์		ผู้ช่วยศาสตราจารย์	ภาควิชาชีวเคมี คณะวิทยาศาสตร์ มหาวิทยาลัยเกษตรศาสตร์	
11. นางสาว ศิรินิตย์ ธารธาดา	อาจารย์	ภาควิชาเทคนิคการสัตวแพทย์ คณะเทคนิคการสัตวแพทย์ มหาวิทยาลัยเกษตรศาสตร์		อาจารย์	ภาควิชาเทคนิคการสัตวแพทย์ คณะเทคนิคการสัตวแพทย์ มหาวิทยาลัยเกษตรศาสตร์	
12. นาย สุเชาน์ ดอนพุดซา	อาจารย์	ภาควิชาเคมี คณะวิทยาศาสตร์ มหาวิทยาลัยศรีนครินทรวิโรฒ		อาจารย์	ภาควิชาเคมี คณะวิทยาศาสตร์ มหาวิทยาลัยศรีนครินทรวิโรฒ	
13. นาง ศิริขวัญ พลประทีป	อาจารย์			อาจารย์		
14. นางสาว กัณฑมาศ อภิธันยาศัย	-	ภาควิชาชีวเคมี คณะวิทยาศาสตร์ จุฬาลงกรณ์มหาวิทยาลัย	นักศึกษาปริญญาเอก	-	ภาควิชาชีวเคมี คณะวิทยาศาสตร์ จุฬาลงกรณ์มหาวิทยาลัย	สำเร็จการศึกษา
15. นาย ฐปนรรค์ จตุยศพร						ยังไม่สำเร็จการศึกษา
16. นาย ภาคภูมิ บุญชื่น						
17. นาย วิศรุต จันทร์ปรุง						
18. นางสาว ภาสุนีย์ เลาหวุฒิชัย						
19. นางสาว สุทธินี โสภณพงษ์						
20. นาย สิทธิชัย บุญรอด	-	สาขาวิชา เทคโนโลยีชีวภาพ คณะวิทยาศาสตร์ จุฬาลงกรณ์มหาวิทยาลัย	นักศึกษาปริญญาเอก	-	สาขาวิชา เทคโนโลยีชีวภาพ คณะวิทยาศาสตร์ จุฬาลงกรณ์มหาวิทยาลัย	ยังไม่สำเร็จการศึกษา
21. นาย สิทธิพงษ์ ณ นคร		ภาควิชาชีวเคมี คณะวิทยาศาสตร์ จุฬาลงกรณ์มหาวิทยาลัย	นักศึกษาปริญญาโท		ภาควิชาชีวเคมี คณะวิทยาศาสตร์ จุฬาลงกรณ์มหาวิทยาลัย	
22. นางสาว ฉันทกา วงษ์ดนตรี						
23. นาย ธัชชีวา อภิชาตยานนท์						
24. นางสาว วรันธร เหลืองตระกูล						
25. นางสาว สุดารัตน์ ชมวงค์		สาขาวิชา เทคโนโลยีชีวภาพ คณะวิทยาศาสตร์ จุฬาลงกรณ์มหาวิทยาลัย			สาขาวิชา เทคโนโลยีชีวภาพ คณะวิทยาศาสตร์ จุฬาลงกรณ์มหาวิทยาลัย	สำเร็จการศึกษา
26. นาย ประวิทย์ อังคะณา		สาขาวิชา พันธุวิศวกรรม โครงการสหวิทยาการระดับบัณฑิตศึกษา มหาวิทยาลัยเกษตรศาสตร์			สาขาวิชา พันธุวิศวกรรม โครงการสหวิทยาการระดับบัณฑิตศึกษา มหาวิทยาลัยเกษตรศาสตร์	
27. นางสาว นพรัตน์ พุ่มกุมาร						

Fish & Shellfish Immunology 47 (2015) 572–581

Contents lists available at ScienceDirect

Fish & Shellfish Immunology

journal homepage: www.elsevier.com/locate/fsi

Full length article

YHV-responsive gene expression under the influence of *Pm*Relish regulation

Suwattana Visetnan [a], Premruethai Supungul [a, b], Sureerat Tang [a, b], Ikuo Hirono [c], Anchalee Tassanakajon [a], Vichien Rimphanitchayakit [a, *]

[a] *Center of Excellence for Molecular Biology and Genomics of Shrimp, Department of Biochemistry, Faculty of Science, Chulalongkorn University, Phyathai Road, Bangkok 10330, Thailand*

[b] *National Center for Genetic Engineering and Biotechnology (BIOTEC), National Science and Technology Development Agency (NSTDA), Pathum Thani 10120, Thailand*

[c] *Laboratory of Genome Science, Tokyo University of Marine Science and Technology, Konan 4-5-7, Minato, Tokyo 108-8477, Japan*

ARTICLE INFO

Article history:
Received 15 July 2015
Received in revised form
28 September 2015
Accepted 29 September 2015
Available online 3 October 2015

Keywords:
Relish
Suppression subtractive hybridization
Yellow head virus
Penaeus monodon
Antimicrobial proteins

ABSTRACT

In animals, infection by Gram-negative bacteria and certain viruses activates the Imd signaling pathway wherein the a NF-κB transcription factor, Relish, is a key regulatory protein for the synthesis of antimicrobial proteins. Infection by yellow head virus (YHV) activates the Imd pathway. To investigate the expression of genes involved in YHV infection and under the influence of *Pm*Relish regulation, RNA interference and suppression subtractive hybridization (SSH) are employed. The genes in forward library expressed in shrimp after YHV infection and under the activity of *Pm*Relish were obtained by subtracting the cDNAs from YHV-infected and *PmRelish*-knockdown shrimp with cDNAs from YHV-infected shrimp. Opposite subtraction gave a reverse library whereby an alternative set of genes under YHV infection and no *PmRelish* expression were obtained. Nucleotide sequences of 252 and 99 cDNA clones from the forward and reverse libraries, respectively, were obtained and annotated through blast search against the GenBank sequences. Genes involved in defense and homeostasis were abundant in both libraries, 31% and 23% in the forward and reverse libraries, respectively. They were predominantly antimicrobial proteins, proteinases and proteinase inhibitors. The expression of antimicrobial protein genes, *ALFPm3*, *crustinPm1*, *penaeidin3* and *penaeidin5* were tested under *PmRelish* silencing and Gram-negative bacterium *Vibrio harveyi* infection. Together with the results using YHV infection previously reported, the expression of *penaeidin5* and also *penaeidin3* but not *ALFPm3* and *crustinPm1* were under the regulation of *Pm*Relish in the Imd pathway.

© 2015 Elsevier Ltd. All rights reserved.

1. Introduction

Humans and animals alike are prone to be infected by disease-producing entities, the pathogens, which lead to sickness and sometimes death. However, nature has provided them means of immunity to defense against these pathogens. Besides the adaptive immunity found in vertebrate animals, innate immunity is the basic defense against pathogens in all animals. Once infected by the pathogens, the innate immunity recognizes certain characteristics of the pathogens though pattern recognition proteins. The interaction between pattern recognition proteins and pathogens leads to triggers in probably several signaling pathways to prepare the animals for the pathogenic invasion and for several cellular responses, such as defense responses, stress responses, inflammation, cell proliferation, etc. [1–3].

In terms of defense responses, there are two main defense signaling pathways, the Toll and Imd pathways, that respond to different types of pathogens. The Toll pathway is activated by Gram-positive bacteria and fungi whereas the Imd pathway is activated by Gram-negative bacteria. The invasion triggers these two pathways through the binding of activated pattern recognition proteins or other downstream activated carrier proteins to the cell membrane receptors. The receptors are activated and relayed the signal into the cytoplasm through a series of protein components. The cytoplasmic inactive NF-κB transcription factors are activated and translocate into the nucleus to regulate the expression of

* Corresponding author.
E-mail address: kpvr2@yahoo.com (V. Rimphanitchayakit).

http://dx.doi.org/10.1016/j.fsi.2015.09.053
1050-4648/© 2015 Elsevier Ltd. All rights reserved.

antimicrobial protein genes. The antimicrobial proteins are synthesized and secreted into the circulation to counter attack and directly kill the pathogens. It is presumed that different antimicrobial proteins are expressed in the two signaling pathway responses [2–4].

In shrimp and other crustaceans, it is certain that Toll and Imd signaling pathways exist for the related protein components of the pathways, such as the Toll receptors from *Penaeus monodon* and *Litopenaeus vannamei* [5,6], MyD88 from *Fenneropenaeus chinensis* [7], Cactus from *F. chinensis* [8], and Dorsal from *L. vannamei* [9] in Toll pathway, the IMDs from *L. vannamei* and *F. chinensis* [10,11] and Relish from *L. vannamei* and *F. chinensis* [12,13] in Imd pathways, have been identified. The two pathways are responsive to bacterial infection for the pathway protein members are up-regulated in response to bacterial infection. The response to white spot syndrome virus (WSSV) infection has been reported. The LvTolls, LvDorsal and LvRelish from Pacific white shrimp, the FcIMD from Chinese white shrimp and the PcIMD from crayfish are up-regulated after WSSV infection [6,11,14]. Moreover, the WSSV replication seems to partly rely on the activation of LvDorsal and LvRelish or, in other words, the WSSV gains certain benefit in their multiplication from the Toll and Imd pathways [14].

We have shown previously that the expression of *Pm*Relish, a NF-κB transcription factor in the Imd pathway from the black tiger shrimp, was up-regulated upon *Vibrio harveyi*, YHV and WSSV challenges [15]. The up-regulation is relatively stronger with bacterial infection than viral infection. Furthermore, the shrimp are more susceptible to YHV if the defense response from the Imd pathway is absence. Therefore, the Imd pathway is responsive to the YHV infection. In this study, we further explore the consequence of YHV infection in shrimp to fish out genes that are under the influence of the Imd pathway using suppression subtractive hybridization (SSH) technique. The expression of some genes identified from the SSH libraries is tested to confirm that it is under the effect of *Pm*Relish activation by YHV. The expression of some antimicrobial proteins is also investigated under infection by Gram-negative bacterium, a bacterium that activate the Imd pathway, to determine whether the expression is under the *Pm*Relish regulation.

2. Materials and methods

2.1. Shrimp and pathogen challenge

Healthy shrimp, *Penaeus monodon*, with body weight of 7–10 g for gene silencing experiment and 10–15 g for other experiments were purchased from a local farm and maintained in aerated water with a salinity of 15 ppt for at least 7 days before use.

The Yellow Head Virus (YHV) and *V. harveyi* 639 solutions were prepared as previously described [16]. Appropriate dilution of YHV in the volume of 20 μl was injected into each shrimp in the abdominal muscle. This amount of YHV caused a cumulative mortality of 50% at about 3 days after injection. The *V. harveyi* 639 suspension of 20 μl in 0.85% NaCl (normal saline) having 2×10^4 CFU was used for injection into each shrimp.

2.2. Silencing of PmRelish using dsRNA interference

To investigate the response of shrimp under *PmRelish* silencing on YHV infection, the double-stranded RNA (dsRNA)-mediated gene knock-down of *PmRelish* gene was employed by using the T7 RiboMAX™ Express RNAi System (Promega). The *PmRelish* dsRNA and *GFP* dsRNA as a control dsRNA were prepared as described in our previous study [15]. The specific primers KD_PmRelish_T7F/KD_PmRelish_R and KD_PmRelish_F/KD_PmRelish_T7R (Table 1) were used for the synthesis of upper and lower RNA strands, respectively. The *GFP* dsRNA was produced using primers KD_GFP_T7F/KD_GFP_R and KD_GFP_F/KD_GFP_T7R (Table 1).

Briefly, a plasmid clone containing either *PmRelish* gene or *GFP* gene was used as a template in the PCR amplification reactions. The 25-μl reaction contained 1 μl plasmid DNA template, 1 × PCR buffer, 0.2 mM each dNTP, 0.4 μM each primer and 1.5 unit RBC *Tag* DNA polymerase (RBC Bioscience). The reaction was pre-denatured at 94 °C for 2 min, followed by 36 cycles of 94 °C for 30 s, 58 °C for *GFP* or 60 °C for *PmRelish* for 30 s and 72 °C for 30 s, and the final extension step at 72 °C for 10 min. The PCR products were analyzed with 2% agarose gel electrophoresis.

Then, 1 μg of each PCR products was used as templates for in vitro transcription using T7 RiboMAX™ Express Large Scale RNA Production Systems (Promega) according to the manufacturer's recommendation. Equal amount of the two complementary RNA strands were annealed. The quality and amount of RNAs were verified by 1.5% agarose gel electrophoresis and measured spectrophotometrically, respectively.

The dsRNAs were tested for their efficacy on gene silencing. Four groups of six shrimp were given injection of 20 μl of normal saline (NaCl control group), normal saline (YHV group), *GFP* dsRNA (5 μg/g shrimp) (*GFP* dsRNA-YHV group) and *PmRelish* dsRNA (5 μg/g shrimp) (*PmRelish* dsRNA-YHV group). After 24 h, shrimp in NaCl control group were injected again with the same solutions and shrimp in the other three groups were injected again with the same solutions plus YHV. The hemocytes were collected at 3 and 6 h after the second injection. Total RNA was extracted by a FavorPrep™ Blood/Cultured Cell Total RNA Purification Mini Kit (Favorgen). One microgram of total RNA was used for the synthesis of first strand cDNA using SMARTer™ PCR cDNA Synthesis Kit (Clontech) according to the manufacturer's instructions.

The RT-PCR was performed to evaluate the silencing of target *PmRelish* gene transcript in NaCl control group, *GFP* dsRNA-YHV group and *PmRelish* dsRNA-YHV group using the specific primers PmRelish_RT_F and PmRelish_RT_R (Table 1) and the PCR condition as described above. The PCR products were analyzed by 2.5% agarose gel electrophoresis. The expression level of silenced gene was reported relative to that of *EF-1α*.

2.3. Construction of cDNA libraries using suppression subtractive hybridization

To do the suppression subtractive hybridization (SSH), the combined 3-h and 6-h cDNAs from *GFP* dsRNA-YHV group and *PmRelish* dsRNA-YHV group were used. The SSH was performed in two direction, forward and reverse using the PCR-select™ cDNA Subtraction Kit (Clontech) according to the manufacturer's instructions. For the forward subtraction, cDNAs of *PmRelish* dsRNA-YHV group were used as driver to subtract from those of tester, *GFP* dsRNA-YHV group. For the reverse subtraction, cDNAs of *GFP* dsRNA-YHV group were used as driver to subtract from those of tester *PmRelish* dsRNA-YHV group. The efficiency of SSH was analyzed using elongation factor-1α (*EF-1α*) gene.

The subtracted mixture was nested PCR-amplified and cloned into a pGEM-T easy vector (Promega), transformed into *Escherichia coli* StrataClone™ SoloPack® competent cells (Algilent). After plating, the positive clones were randomly selected and purified by FavorPrep Plasmid DNA Extraction Mini Kit (Flavogen). The SSH positive clones were sequenced using M13 forward primer by Macrogen Inc., South Korea.

2.4. Bioinformatic analysis of genes derived from the SSH libraries

The gene sequences obtained from SSH experiment were

Table 1
Primers used in this study.

Primer	Sequence (5′–3′)	Product size (bp)	Usage
PmRelish_RT_F	TCTCCAGGTGAGCACTCAGTTGGC	223	RT-PCR and qRT-PCR of *PmRelish*
PmRelish_RT_R	GCTGTAGCTGTTGCTGTTGTTGAG		
EF-1α_F	GGTGCTGGACAAGCTGAAGGC	150	Internal control gene
EF-1α_R	CGTTCCGGTGATCATGTTCTTGA		
KD_PmRelish_T7F	GGATCCTAATACGACTCACTATAGGCTCGTGGTCAGGAAGACTCAAT	434	Preparation of *Pm*Relish dsRNA
KD_PmRelish_R	GACTGGAGATGGAGACTGAATG		
KD_PmRelish_F	CTCGTGGTCAGGAAGACTCAAT		
KD_PmRelish_T7R	GGATCCTAATACGACTCACTATAGGGACTGGAGATGGAGACTGAATG		
KD_GFP_T7F	GGATCCTAATACGACTCACTATAGGATGGTGAGCAAGGGGGAGGA	720	Preparation of GFP dsRNA
KD_GFP_R	TTACTTGTACAGCTCGTCCA		
KD_GFP_F	ATGGTGAGCAAGGGGGAGGA		
KD_GFP_T7R	GGATCCTAATACGACTCACTATAGGTTACTTGTACAGCTCGTCCA		
ALFPm3_F	CCCACAGTGCCAGGCTCAA	202	Expression analyses of antimicrobial peptide genes
ALFPm3_R	TGCTGGCTTCTCCTCTGATG		
CrustinPm1_F	CTGCTGCGAGTCAAGGTATG	118	
CrustinPm1_R	AGGTACTGGCTGCTCTA CTG		
Penaeidin3_F	GGCTTAGCCCCTTACA	353	
Penaeidin3_R	GACCCATACCTACAAATAAC		
Penaeidin5_F	ATCCCGACCTATTAGTACTC	133	
Penaeidin5_R	TTATCCTTTCAATGCAGAACAA		
Kunitz_F	GCCATGGGCCTACTCCGCCCA	212	Expression analyses of genes obtained from the SSH libraries
Kunitz_R	GCTCGAGTCGGCCGCAGAC		
Transglutaminase_F	ACGACGACTGGGACATAAGG	237	
Transglutaminase_R	CATACTCCTGGCGCATTTTT		
SWDPm2_F	CGGCATCATCACCACGTGCGAG	212	
SWDPm2_R	TCAGTAACCTTTCCAGGGAGAC		
HHAP_F	GCAACAGGAGAACCTGTGGATA	243	
HHAP_R	GGTTCCAGAATCGCCTCCTATA		
SPIPm2_F	ATGCAACCACGTCTGTACTG	192	
SPIPm2_R	CTGCAAGGTTCCACATCT		

processed by removing the unwanted vector and primer sequences using the NCBI VecScreen and, then, analyzed against the NCBI GenBank database with the BLASTN and BLASTX programs (http://www.ncbi.nlm.nih.gor/BLAST/) for clone annotation. The significant matches were accepted at *E*-values lower than 1×10^{-7}.

Genes were categorized into 9 groups: defense and homeostasis; transport; gene expression, regulation and protein synthesis; cell cycle/DNA synthesis, repair and replication; energy and metabolism; signaling and communication; miscellaneous functions; hypothetical proteins; and unknown proteins. The numbers of genes were recorded.

2.5. Validation of the expression in response to YHV infection under the PmRelish knockdown and un-knockdown conditions

The genes in SSH experiment were selected for qRT-PCR to verify that their expression is under the YHV infection and modulated by *Pm*Relish. Seven responsive genes from the forward SSH library: *Kunitz* (a Kunitz-type serine proteinase inhibitor gene), *penaeidin*3, *penaeidin*5, *transglutaminase, SWDPm2* (single whey acidic protein domain-containing protein isoform 2), and two alternative responsive genes from the reverse library: *HHAP* (hemocyte homeostasis-associated protein), *SPIPm2* (Kazal-type serine proteinase inhibitor isoform 2) (Tables 2 and 3) were selected. The shrimp *EF-1α* gene was used as an internal control.

The cDNAs from NaCl control, YHV, *GFP* dsRNA-YHV and *PmRelish* dsRNA-YHV groups were used in qRT-PCR. The real-time PCR was performed using an appropriate amount of cDNAs for each gene with the specific oligonucleotide primers (Table 1) in an iCycler iQ™ Real-Time Detection system using iQ™ SYBR Green Supermix (Bio-Rad) with the following conditions: 95 °C for 9 min, 40 cycles of 95 °C for 30 s, 58 °C for 30 s and 72 °C for 45 s.

Each qRT-PCR reaction was done in triplicate. The standard curves for seven responsive genes and *EF-1α* was generated by running triplicate reactions of five different cDNA concentrations prepared by 2-fold serial dilution [15]. The efficiencies for *Kunitz*, *penaeidin3*, *penaeidin5*, *transglutaminase*, *SWDPm2*, *HHAP*, *SPIPm2* and *EF-1α* were 101.2, 99.6, 99.6, 99.2, 98.7, 101.5, 101.6 and 99.8%, respectively. Relative expression was calculated using a mathematic model of Pfaffl (2001) [17]. The data for *penaeidin3* and *penaeidin5* had been reported previously and were again presented here for comparison [15]. Data were analyzed for statistically significance using one-way ANOVA followed by Duncan's new multiple ranges test and presented as means ± standard deviations. Values were considered statistically significant at $P < 0.05$.

2.6. Effect of PmRelish gene silencing on the transcription of antimicrobial proteins under V. harveyi 639 infection

The expression levels of four antimicrobial proteins: *ALFPm*3, *crustinPm1*, *penaeidin*3 and *penaeidin*5, were examined in the *PmRelish* silencing and *V. harveyi* 639 infected shrimp. Shrimp were divided into two groups of six shrimp, a *PmRelish* knockdown group and a *GFP* control group. They were first injected with 20 μl of *PmRelish* dsRNA (5 μg/g shrimp) and *GFP* dsRNA (5 μg/g shrimp), respectively. After 24 h of primary injection, the shrimp were given a second injection of the same solutions plus *V. harveyi* 639.

The hemocytes were collected at 3 and 6 h after second injection. The transcription levels of four antimicrobial peptides were analyzed by real-time RT-PCR as described above using specific primer pairs (Table 1). The *EF-1α* was used as an internal control. The experiments were performed in triplicate for statistical analysis.

The standard curves for *ALFPm*3, *crustinPm*1, *penaeidin*3, *penaeidin*5 and *EF-1α* were generated as described above. The PCR efficiencies were 99.4, 99.4, 99.6, 99.6 and 99.8%, respectively. The calculation of relative expression level was also performed as described above. Data were analyzed for statistically significance

Table 2
Forward library.

Highest homology	Accession no.	*E* Value	Closet species	Assigned accession no	No. of clones
Defense & homeostasis					
Antimicrobial proteins					
Crustin*Pm*1	ABW82154	8.00E-42	*Penaeus monodon*	JZ892866–8	3
Crustin*Pm*4	ACQ66005	3.00E-03	*Penaeus monodon*	JZ892869–71	3
Cysteine-rich protein 1-like	XP967808	8.00E-27	*Tribolium castaneum*	JZ892872	1
Lysozyme	AAN16375	5.93E-91	*Penaeus monodon*	JZ892873–5	3
Penaeidin3	ACH70378	3.45E-16	*Penaeus monodon*	JZ892876–8	3
Penaeidin5	ACQ66008	5.00E-16	*Penaeus monodon*	JZ892879–83	5
Single whey acidic protein domain-containing protein 2 (SWD*Pm*2)	ACF28465	6.49E-38	*Penaeus monodon*	JZ892884–94	11
Stylicine 2	ABW24769	1.62E-27	*Litopenaeus stylirostris*	JZ892895	1
Pattern recognition protein					
QM protein	ACV72062	2.00E-78	*Penaeus monodon*	JZ892896-7	2
Proteinases & their inhibitors					
Clip domain serine protease	ACP19733	6.90E-13	*Eriocheir sinensis*	JZ892898-9	2
Kazal-type proteinase inhibitor (SPI*Pm5*)	ACB47427	4.00E-43	*Penaeus monodon*	JZ892900–1	2
Kunitz-type serine protease inhibitor	AGU16239	5.14E-42	*Fenneropenaeus chinensis*	JZ892902–16	15
Mas-like protein	AAT42131	9.64E-105	*Penaeus monodon*	JZ892917-8	2
Masquerade-like serine proteinase-like protein 2	ABO33174	2.64E-59	*Penaeus monodon*	JZ892919	1
Serine protease snake-like	XP008547524	3.00E-14	*Microplitis demolitor*	JZ892920	1
Serine proteinase inhibitor (Serpin)	CAA57964	7.00E-23	*Pacifastacus leniusculus*	JZ892921-2	2
Chaperones					
Glutathione-dependent prostaglandin D synthase	AFJ11393	1.00E-23	*Penaeus monodon*	JZ892923	1
Heat shock protein 70	AAW71958	2.45E-66	*Fenneropenaeus chinensis*	JZ892924–6	3
Mitochondrial import inner membrane translocase subunit Tim9	XP008192294	1.00E-28	*Tribolium castaneum*	JZ892927–9	3
Clotting protein					
Transglutaminase	AAL78166	5.45E-82	*Penaeus monodon*	JZ892930–9	10
Other defense and homeostasis proteins					
CD82 antigen-like isoform X2	XP012263853	5.00E-27	*Athalia rosae*	JZ892940	1
DEAD(Asp-Glu-Ala-Asp) box polypeptide 5	ADB44900	1.00E-20	*Macrobrachium nipponense*	JZ892941	1
Prophenoloxidase 2-like protein	AIE45536	1.00E-136	*Penaeus monodon*	JZ892942-3	2
Cell cycle/DNA synthesis, repair & replication					
Apoptosis					
Caspase 3	AEW91437	3.00E-54	*Penaeus monodon*	JZ892944	1
Caspase 3c	AET34920	5.00E-30	*Macrobrachium rosenbergii*	JZ892945	1
Cell cycle					
E3 ubiquitin-protein ligase Nedd-4 isoform X3	XP012260927	6.00E-10	*Tribolium castaneum*	JZ892946	1
Oncoprotein nm23	AFL02665	2.00E-53	*Penaeus monodon*	JZ892947	1
Ubiquitin-conjugating enzyme E2 c	AFU93453	2.00E-100	*Litopenaeus vannamei*	JZ892948	1
DNA replication					
Proliferating cell nuclear antigen	AEJ89927	2.00E-41	*Litopenaeus vannamei*	JZ892949	1
Gene expression, regulation & protein synthesis					
Transcription					
H/ACA ribonucleoprotein complex subunit 2-like protein	XP012345208	2.00E-90	*Apis florea*	JZ892950	1
Protein spinster-like	XP005987471	1.00E-07	*Latimeria chalumnae*	JZ892951	1
U5 small nuclear ribonucleoprotein 200 kDa helicase-like protein	XP008933667	6.00E-94	*Merops nubicus*	JZ892952	1
Protein synthesis					
39S ribosomal protein L2	KFM83087	6.00E-27	*Stegodyphus mimosarum*	[a]	1
60S ribosomal protein L27	ACY66537	8.00E-29	*Scylla paramamosain*	JZ892953	1
Aspartyl-tRNA synthetase	XP002423869	1.00E-74	*Pediculus humanus corporis*	JZ892954	1
Elongation factor 1-alpha	BAH28836	1.00E-129	*Marsupenaeus japonicus*	JZ892955	1
Elongation factor 2	ABR01223	7.00E-25	*Penaeus monodon*	JZ892956	1
Eukaryotic translation initiation factor 3 subunit D-like	XP011432044	9.00E-69	*Crassostrea gigas*	JZ892957	1
Eukaryotic translation initiation factor 4 gamma 2-like	XP003396125	2.00E-90	*Bombus terrestris*	JZ892958	1
Poly A binding protein, cytoplasmic 1 a	ACO51197	2.90E-30	*Hypophthalmichthys nobilis*	JZ892959	1
Ribonuclease P/MRP 30 subunit	XP004349060	6.00E-14	*Capsaspora owczarzaki*	JZ892960	1
Ribosomal protein L4	ADD21621	1.00E-51	*Mya truncata*	JZ892961-2	2
Ribosomal protein L7	ACQ91224	6.00E-12	*Penaeus monodon*	JZ892963	1
Ribosomal protein P1	ACR54112	1.00E-28	*Palaemon varians*	JZ892964-5	2
Transport					
Beta actin	ACZ60616	4.00E-101	*Panulirus argus*	JZ892966–71	6
Tubulin-alpha	AGV09111	4.42E-28	*Torbia viridissima*	JZ892972	1
Energy & metabolism					
ADP/ATP translocase II	AEK78307	1.83E-71	*Litopenaeus vannamei*	JZ892973	1
Cytochrome c oxidase subunit iii	NP038293	3.00E-61	*Penaeus monodon*	[a]	4
Glutamate dehydrogenase	ACC95446	3.61E-42	*Litopenaeus vannamei*	JZ892974	1
Mitochondrial ATP synthase gamma subunit precursor	AEB40302	1.00E-62	*Litopenaeus vannamei*	[a]	1
NADH dehydrogenase subunit 1	NP038300	4.37E-48	*Penaeus monodon*	[a]	1
Propionyl-CoA carboxylase beta chain	KDQ71473	1.00E-38	*Zootermopsis nevadensis*	JZ892975	1
Saposin- isoform a	ADK94870	2.00E-67	*Penaeus monodon*	JZ892976	1
Signaling & communication					
Extracellular signal-regulated kinase 1/2	ADT80930	4.13E-97	*Penaeus monodon*	JZ892977	1
Miscellaneous functions					
Adaptin, alpha/gamma/epsilon	XP001649235	9.00E-22	*Aedes aegypti*	JZ892978	1

(*continued on next page*)

Table 2 (*continued*)

Highest homology	Accession no.	*E* Value	Closet species	Assigned accession no	No. of clones
O-sialoglycoprotein endopeptidase	XP002434405	8.00E-43	*Ixodes scapularis*	JZ892979	1
SocE	EDX54372	7.00E-20	*Bacillus cereus*	JZ892980	1
Hypothetical proteins					78
Unknown proteins					52
Total					252

[a] Clones excluded by GenBank.

Table 3
Reverse library.

Highest homology	Accession no.	*E* Value	Closet species	Assigned accession no	No. of clones
Defense & homeostasis					
Antimicrobial proteins					
Anti-lipopolysaccharide factor (ALF*Pm*3)	ACC86067	2.34E-62	*Penaeus monodon*	JZ893103	1
Single whey acidic protein domain-containing protein 1 (SWD*Pm*1)	ACF28464	3.00E-28	*Penaeus monodon*	JZ893104	1
Homeostasis					
Hemocyte homeostasis-associated protein (*Pm*HHAP)	ADN43412	4.00E-60	*Penaeus monodon*	JZ893105-6	2
Proteinases & their inhibitors					
Kazal-type proteinase inhibitor (SPI*Pm*2)	AAP92779	1.00E-140	*Penaeus monodon*	JZ893107–13	7
Viral responsive protein					
*Pm*VRP15	AHN10846	2.00E-22	*Penaeus monodon*	JZ893114–8	5
Chaperones					
Heat shock protein 70	ABF83607	2.00E-135	*Marsupenaeus japonicus*	JZ893119-20	2
Sacsin-like	XP006822247	1.00E-19	*Saccoglossus kowalevskii*	JZ893121-22	2
Other defense and homeostasis proteins					
Cyclophilin a	ABV90639	3.00E-104	*Penaeus monodon*	JZ893123–25	3
Gene expression, regulation & protein synthesis					
Peptidyl-prolyl cis-trans isomerase 5	XP004535714	1.00E-63	*Ceratitis capitata*	JZ893126	1
Protein disulfide isomerase	ACN89260	2.00E-104	*Litopenaeus vannamei*	JZ893127	1
Ribosomal protein S23e	ACY66586	9.00E-90	*Scylla paramamosain*	JZ893128	1
Zinc finger protein 84	KFM83369	2.00E-17	*Stegodyphus mimosarum*	JZ893129	1
Transport					
Beta-actin	AAF82308	2.00E-56	*Metridium senile*	JZ893130	1
Tubulin beta-1 chain	ABL75455	2.00E-37	*Homarus americanus*	JZ893131	1
Energy & metabolism					
Cytochrome c oxidase subunit VIIA putative	ACY66414	1.00E-12	*Scylla paramamosain*	[a]	1
Signaling & communication					
Ubiquitin-activating enzyme E1	AFK65746	5.00E-54	*Eriocheir sinensis*	JZ893132	1
Miscellaneous functions					
26S proteasome non-ATPase regulatory subunit 2	XP_967560	3.00E-30	*Tribolium castaneum*	JZ893134-5	2
Granulins-like isoform X2	XP009862363	7.00E-45	*Ciona intestinalis*	JZ893135	1
Protein bcn92	P82116	8.00E-21	*Drosophila subobscura*	JZ893136	1
Protein Dom3Z	KFM80607	5.00E-11	*Stegodyphus mimosarum*	JZ893137	1
Hypothetical proteins	CAM36311	4.00E-11	*Thermobia domestica*		25
Unknown proteins					38
Total					99

[a] Clones excluded by GenBank.

using one-way ANOVA followed by Duncan's new multiple ranges test and presented as means ± standard deviations. Statistical significance was accepted at $P < 0.05$.

3. Results

3.1. Suppression subtractive hybridization

Previously, we used the dsRNA-mediated gene knockdown to study the effect on antimicrobial protein synthesis of *PmRelish* suppression in YHV-infected shrimp [15]. To be able to pick up more genes involved in YHV infection that were under the influence of *Pm*Relish activity, the suppression subtractive hybridization (SSH) technique was used. Since the *Pm*Relish is a cytoplasmic protein responding to a signal of infection and its expression is increased by YHV infection and peaked at 12 h afterwards, the appropriate time to search for YHV responsive genes would be within this 12-h period [15]. The 3-h and 6-h time points after YHV infection were chosen for the SSH experiment.

There are two possible subtraction we can make, the forward subtraction and reverse subtraction. The forward direction subtracts the cDNAs of the *PmRelish* dsRNA-YHV shrimp from those of the *GFP* dsRNA-YHV shrimp. The remaining cloneable cDNAs are the YHV responsive genes under the influence or regulation of *Pm*Relish. The reverse subtraction does the opposite. Logically, the reverse subtraction should not give any cloneable genes. However, without the activity of *Pm*Relish in the knockdown shrimp, it is deemed possible for the shrimp to adapt alternative conditions by expressing other alternative defense genes for their survival upon YHV infection.

The cDNAs were prepared from *GFP*-injected and *PmRelish* knockdown shrimp infected with YHV for 3 h and 6 h and checked for the silencing of *PmRelish* by RT-PCR. As compared to the cDNAs isolated from NaCl control and *GFP* dsRNA-YHV shrimp, it was found that the *PmRelish* gene expression was suppressed in *PmRelish* dsRNA-YHV shrimp at both time points (Fig. 1).

The suppression subtractive hybridization was performed using the combined cDNAs from the two time points. The SSH efficiency was shown to be excellent with *EF-1α* (data not shown). The remaining cloneable cDNAs after subtraction were cloned into a

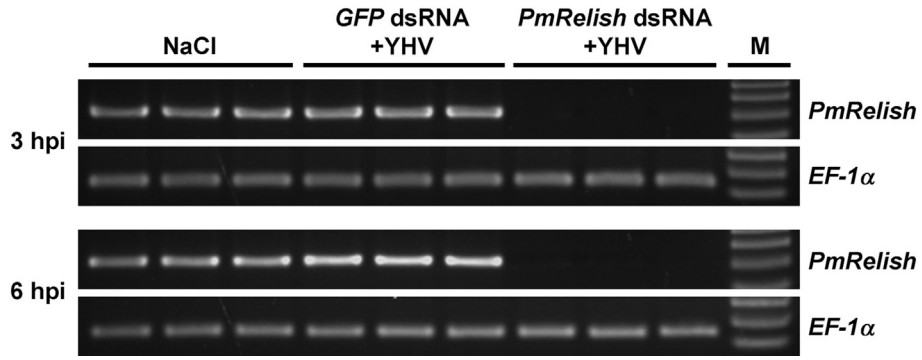


Fig. 1. Silencing of *PmRelish* by dsRNA interference. Shrimp were doubly injected with normal saline (NaCl), *GFP* dsRNA and *PmRelish* dsRNA. YHV was included in the second injection of *GFP* dsRNA and *PmRelish* dsRNA. At 3 h and 6 h after the second injection (hpi), hemolymph was collected and processed for RT-PCR analysis of *PmRelish* expression. The expression of *EF-1α* was used as an internal control. M is a DNA size marker.

plasmid vector. Since we were interested in the forward subtraction than the reverse subtraction, we selected randomly about 350 clones from forward library but only 126 clones from reverse library. The plasmid clones were subjected to nucleotide sequencing. Only 252 and 99 good quality sequences were obtained from the forward and reverse libraries, respectively. The sequences were blast searched for sequence homology against the NCBI GenBank database with BLASTN and BLASTX programs. Significant matches (E-values $< 1 \times 10^{-7}$) were obtained with 122 (48.4%) and 36 (36%) cDNA sequences for annotatable known genes representing 57 and 20 different genes, and the remaining 130 (51.6%) and 63 (64%) cDNA sequences were hypothetical plus unknown genes in the forward and reverse libraries, respectively (Tables 2, 3 and Fig. 2).

The genes were categorized according to their putative functions into groups which were defense and homeostasis, transport, regulation and gene expression, cell cycle, energy and metabolism, signaling and communication, and miscellaneous functions (Tables 2 and 3). The numbers of genes involved in defense and homeostasis were abundant in both libraries, 78 (31%) and 23 (23%) copies in the forward and reverse libraries, respectively. The genes in this group were antimicrobial proteins, proteinases and their inhibitors, chaperones, clotting protein, and other defense and homeostasis proteins. A few of these genes that were abundant and/or interesting antimicrobial proteins were selected for further

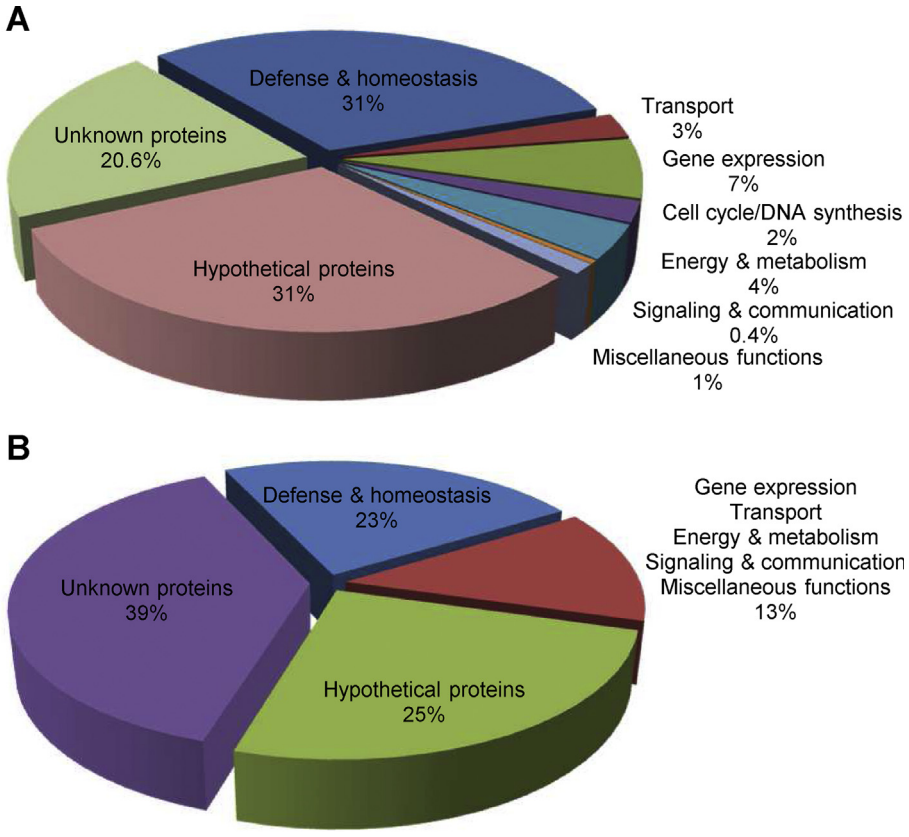


Fig. 2. Percentage proportions of gene groups identified from SSH libraries. A total of 252 and 99 sequences of clones from forward (A) and reverse (B) SSH libraries, respectively, were obtained from sequencing, annotated and categorized into nine groups of genes. Owing to a low number of sequencing clones, not all gene groups were identified in the reverse library.

studied to validate the SSH technique.

3.2. Differential expression of genes from SSH libraries

Since it was the subtraction of cDNAs of *PmRelish* dsRNA-YHV shrimp from those cDNA of *GFP* dsRNA-YHV shrimp, the genes in the forward library were genes that were up-regulated by YHV infection and also under the regulation or influence of *Pm*Relish (Table 2). On the contrary, without the response from the Imd pathway in the *PmRelish* dsRNA-YHV shrimp, the shrimp might adopt alternative means to defense and survive the YHV infection. This resulted in up-regulated genes identified in the reverse libraries (Table 3). To validate that the genes were up-regulated by YHV infection and might be under or not under the modulation of *Pm*Relish, seven responsive genes from the forward SSH library: *Kunitz* (a Kunitz-type serine proteinase inhibitor gene), *penaeidin3*, *penaeidin5*, *transglutaminase*, *SWDPm2* (single whey acidic protein domain-containing protein isoform 2), and two alternative responsive genes from the reverse library: *HHAP* (hemocyte homeostasis-associated protein), *SPIPm2* (Kazal-type serine proteinase inhibitor isoform 2) were selected and tested by real-time RT-PCR. The shrimp elongation factor-1α gene (*EF-1α*) was used as an internal control.

It was expected that the three genes, *Kunitz*, *penaeidin3* and *penaeidin5* would be up-regulated by YHV infection but would not be responsive to the infection under *PmRelish* silencing. Agreeing well with the expectation, the three genes were up-regulated similarly in YHV-injected shrimp and *GFP* dsRNA-YHV shrimp and did not respond to the YHV infection if the *PmRelish* was silenced (Fig. 3).

The transglutaminase gene was one of the major transcript detected in the group of defense and homeostasis in the forward library. However, its expression profile in response to YHV infection was different from those of *Kunitz*, *penaeidin3* and *penaeidin5* in that the expression of *transglutaminase* was up-regulated at 3 h and, then, decreased at 6 h. Strangely enough, the expression of transglutaminase in *PmRelish* dsRNA-YHV shrimp was down-regulated at 3 h but increased dramatically at 6 h (Fig. 3).

The *SWDPm2* was also detected as the major transcript in the forward library. The expression was up-regulated slightly in YHV-infected and *GFP* dsRNA-YHV shrimp. In *PmRelish* dsRNA-YHV shrimp, it was down-regulated at 3 h and, then, up-regulated substantially at 6 h after YHV infection (Fig. 3). Logically, considering from the up-regulation of this gene in *PmRelish* dsRNA-YHV shrimp, it should be detected more in the reverse library than the forward library.

The *HHAP* and *SPIPm2* were alternative genes up-regulated in response to YHV infection without the *Pm*Relish regulation or the Imd pathway response. The expression of *HHAP* was extremely high in YHV-infected and *GFP* dsRNA-YHV shrimp. The expression was decreased substantially below basal level at 6 h in *PmRelish* dsRNA-YHV shrimp (Fig. 3). The expression profile of *HHAP* was similar to those of *Kunitz*, *penaeidin3* and *penaeidin5* in the forward library but the *HHAP* transcript was not detected at all in the forward library.

In contrast, the expression of *SPIPm2* was not up-regulated at 3 h and 6 h after YHV infection in YHV-injected and *GFP* dsRNA-YHV shrimp. However, when the *PmRelish* gene was silenced, the expression was increased in response to YHV infection. Thus, the synthesis of SPI*Pm2* protein was increased as one of the alternative proteins in the defense against the YHV if the Imd pathway was blocked (Fig. 3).

3.3. Antimicrobial proteins under the regulation of PmRelish

A few genes of antimicrobial proteins were identified in the SSH libraries: *crustinPm1*, *penaeidin3*, *penaeidin5* in the forward library and antilipopolysaccharide *ALFPm3* in the reverse library. To check whether they were under or not under the regulation of *PmRelish*, we undertook another *PmRelish* silencing experiment. A Gram-negative bacterium, *V. harveyi*, was used instead of YHV for it was well known that the Gram-negative bacteria stimulated the Imd pathway. If the expression of an antimicrobial protein was under the regulation of the Imd pathway, it should be up-regulated in response to both *V. harveyi* and YHV infection, and was not responsive under *PmRelish* silencing. The expression of the four genes has already been tested with YHV infection [15]. In this report, they were tested with *V. harveyi*.

The *PmRelish* knockdown shrimp along with their controls, GFP dsRNA injected shrimp, were injected with *V. harveyi* 639. The shrimp hemocytes were collected at 3 h and 6 h after *V. harveyi* infection. The cDNAs were prepared and the expression of four

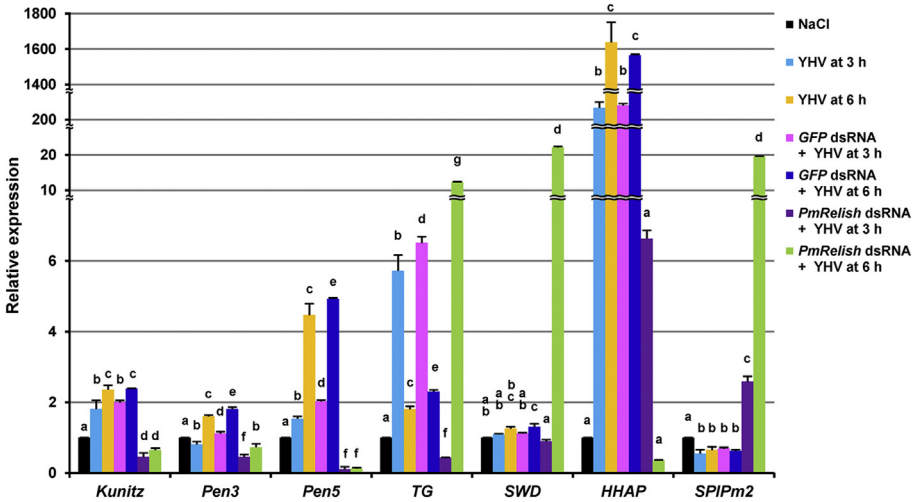


Fig. 3. Expression of selected genes from SSH libraries in YHV-infected, GFP dsRNA-YHV and PmRelish dsRNA-YHV shrimp. The *Kunitz*, *penaeidin3* (*Pen3*), *penaeidin5* (*Pen5*), *transglutaminase* (*TG*) and *SWDPm2* (*SWD*) were from the forward library whereas the *HHAP* and *SPIPm2* were from the reverse libraries. The cDNAs from the shrimp were analyzed for the transcription level of each gene. The expression was calculated relative to that of the control shrimp injected with normal saline (NaCl) either at 3 h or 6 h. The experiment was done in triplicate. Data are presented as means ± standard deviations. Different letters indicate significant differences between data at 3 h and 6 h accepted at $P < 0.05$.

antimicrobial proteins were analyzed by qRT-PCR. It was found that, at 3 h after *V. harveyi* infection, the expression of all four antimicrobial proteins was severely decreased (Fig. 4). The expression resumed at 6 h after *V. harveyi* infection. The expression of *ALFPm3* and *crustinPm1* was up-regulated whereas that of *penaeidin3* and *penaeidin5* was still at the subnormal level. Considering these results along with those reported previously with YHV infection [15], it indicated that the *penaeidin3* and *penaeidin5* were under the regulation of *Pm*Relish. In contrast, the expression of *ALFPm3* and *crustinPm1* was not regulated by the Imd pathway although the *crustinPm1* was detected in forward library.

4. Discussion

In order to reveal the whole scheme of gene expression under certain condition such as infection by pathogens, the SSH technique has been employed in several studied. Prapavorarat et al. (2010) used SSH to identify genes expressed in response to 24 h–72 h yellow head virus infection in the black tiger shrimp [18]. Wang et al. (2013) used the same technique to screen for the genes regulated by FcRelish in 1-h *Vibrio anguillarium*-infected shrimp [19]. Herein, the same technique is used to look for a group of genes that are involved in YHV infection under the regulation of Imd signaling pathway.

When the shrimp are infected by YHV, it is thought that several genes are modulated either up-regulated or down regulated to prepare the shrimp for their defense against the virus, the stress from the disease, tissue damages from the infection, the multiplication of virus, etc. The expression of regular housekeeping genes may not be changed. One pathway that is responsive to YHV infection is the Imd pathway [15]. The Relish is a key NF-κB transcription factor of the Imd pathway that regulates the synthesis of defense genes, particularly the antimicrobial proteins. If Relish is knocked down by RNAi technique, the Imd response would be forfeited. To fish out the genes that are up-regulated against YHV infection under the Imd regulation in the forward library, the expressed cDNAs from YHV infected shrimp are subtracted with those from YHV-infected and Relish-silenced shrimp. In the reverse situation, if there is no Imd pathway response, there should be an alternative gene expression to respond to the infection in addition to the Imd pathway-independent responses already exist. The reverse subtraction may provide us with alternative genes that are expressed for the shrimp to withstand the infection for sometimes. Nevertheless, it should be noted that the shrimp are more susceptible to the YHV if the *PmRelish* expression is silenced [15].

Another important factor is the duration of infection. For the shrimp to defense themselves from infection, the Imd response should be immediate. After infection, the expression of *PmRelish* is increased gradually from the subnormal level and peaked at 12 h [15]. It suggests that the constitutive level of *Pm*Relish protein has

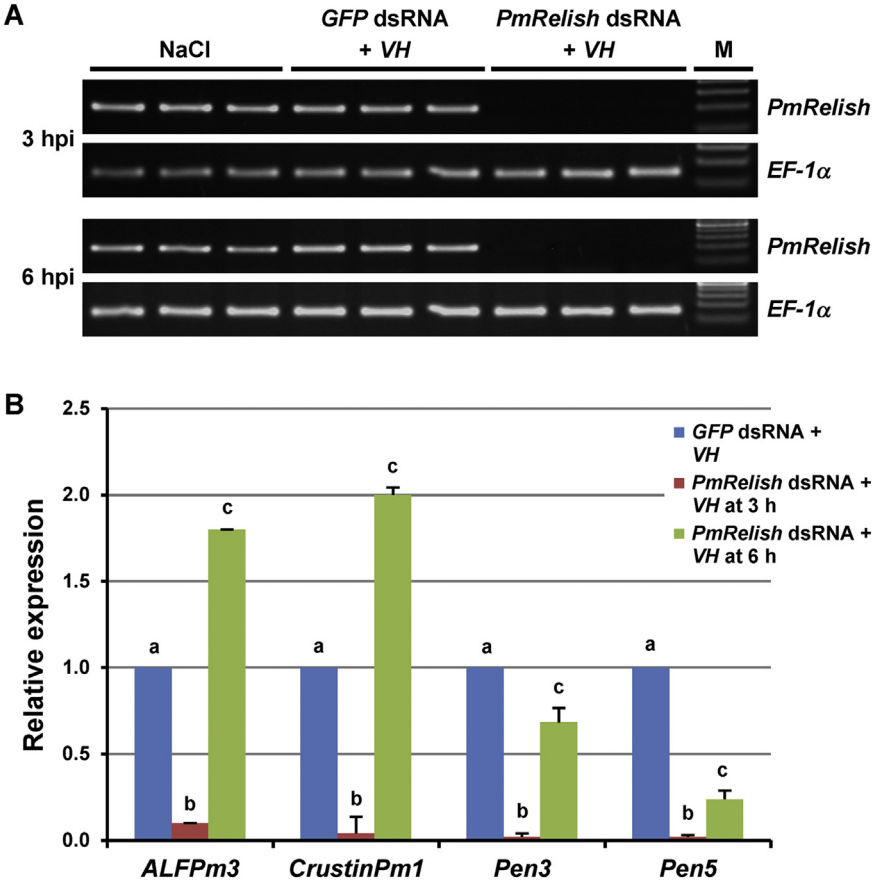


Fig. 4. The effect *PmRelish* silencing on the expression of *ALFPm3*, *crustinPm1*, *penaeidin3* and *penaeidin5*. The *PmRelish* gene is silenced by dsRNA interference like in Fig. 1 but *V. harveyi* (*VH*) was included in the second injection of *GFP* dsRNA and *PmRelish* dsRNA. The hemolymph was collected at 3 h and 6 h after the second injection (hpi), and processed for RT-PCR analysis of the expression of *PmRelish* by RT-PCR (A) and antimicrobial protein genes: *ALFPm3*, *crustinPm1*, *penaeidin3* (*Pen3*) and *penaeidin5* (*Pen5*), by qRT-PCR (B). The expression of *EF-1α* was used as an internal control. M is a DNA size marker. The expression was calculated relative to that of the control shrimp injected with *GFP* dsRNA and *V. harveyi*. The experiment was done in triplicate. The expression of antimicrobial protein genes in the control shrimp was presented for comparison. Data are presented as means ± standard deviations. Different letters indicate significant differences between data at 3 h and 6 h accepted at $P < 0.05$.

been used in the early hours within 12-h period and requires replenishment through gene expression. Therefore, we believe that the Imd pathway actually responds quite early after the infection. We, thus, choose to collect the shrimp blood samples at 3 h and 6 h after infection in this experiment.

After the SSH and sequencing were done, we obtained as many as 252 clones from the forward library and 99 clones of alternate responsive genes from the reverse library. The forward library is far more interesting for it contains the YHV responsive genes expressed under the influence of *Pm*Relish regulation. The results from the mining of sequencing data and classification of annotatable genes seem to confirm our expectation that the Imd pathway responds early in YHV infection. At 3–6 h after infection, the genes in defense and homeostasis are abundantly expressed as major expressed genes, and are accounted for 31% and 23% of all cDNAs sequenced in forward and reverse libraries, respectively. Majority of the genes in defense and homeostasis belong to the subgroup antimicrobial proteins and subgroup proteinases and their inhibitors. Ones should bear in mind the possibility that some genes in the forward library are not under fully the direct regulation of *Pm*Relish but may be under complex gene regulation processes.

A few genes were tested by qRT-PCR to validate the SSH technique. The *Kunitz*, *penaeidin3*, *penaeidin5*, *transglutaminase* and *SWDPm2* from the forward library and the *HHAP* and *SPIPm2* from the reverse library are chosen for they are particularly high abundant and/or interesting genes. The *Kunitz*, *penaeidin3*, *penaeidin5*, *transglutaminase* and *SWDPm2* exhibit expression profiles more or less as expected; in particular, the *Kunitz*, *penaeidin3* and *penaeidin5*. Their expression was up-regulated by YHV infection. Once the *PmRelish* gene is knocked down, the expression is decreased. On the contrary, the *SPIPm2* from the reverse library is somewhat down-regulated by the YHV infection but up-regulated substantially after the silencing of *PmRelish* gene.

When the expression profiles of *transglutaminase*, *SWDPm2* and *HHAP* are considered in details, we can say that they may be partly under the influence of *Pm*Relish regulation at early hours of infection, 3–6 h post infection in our experiment. Different from *Kunitz*, *penaeidin3* and *penaeidin5*, the *transglutaminase* gene is highly up-regulated at 3 h and subsided afterwards. Without the *Pm*Relish in silencing shrimp, the expression is down-regulated at 3 h and, then, highly increased at 6 h. As in the fly, the expression of *transglutaminase* may be increased under the activation of Imd signaling pathway for it is needed to regulate the said pathway via its crosslinking activity on specific transcription factors, *Pm*Relish in this case [20]. Like that of *transglutaminase* gene, the expression of *SWDPm2* is highly increased at 6 h in *PmRelish* silencing shrimp, up from the more or less basal level expression.

It has been shown that the *HHAP* gene is highly up-regulated upon white spot syndrome virus infection and is important for maintaining the level of circulating hemocytes in shrimp. Silencing of *HHAP* results in a significant decrease in the number of circulating hemocytes, deformation of the hemocytes and, finally, 100% shrimp mortality [21]. In this study, the YHV infection also results in high up-regulation of *HHAP* but the expression is reduced to subnormal level in *PmRelish* silenced shrimp. The expression profile is similar to those of *Kunitz*, *penaeidin3* and *penaeidin5* genes. It is not known why the *HHAP* gene is only detected in the reverse library. Moreover, Prapavorarat et al. (2010) did not find *HHAP* gene in their forward SSH libraries either [18]. What we know is that there is an increase in the number of apoptotic hemocytes at 12 h after YHV infection which means a reduction in hemocytes [15,22]. At 3–6 h after YHV infection, it is possible that the *HHAP* gene is expressed at high rate for the shrimp to protect the hemocyte cellular integrity.

The Toll and Imd pathways are known to regulate AMP synthesis in response to infection [2]. In this work, a few AMP genes supposedly under and not under the Imd regulation are identified from the SSH libraries; relatively abundant expression are *crustinPm1*, *crustinPm4*, *penaeidin3*, *penaeidin5*, *SWDPm2* from the forward library and *ALFPm3*, *SWDPm1* from the reverse library. The expression profiles of *ALFPm3*, *crustinPm1*, *penaeidin3* and *penaeidin5* determined using Gram-negative bacterium *V. harveyi* as an inducer of the Imd pathway indicate that the expression of *penaeidin5* is under the *Pm*Relish regulation in agreement with previous report using YHV as an inducer of Imd pathway [15]. From its low expression level under *PmRelish* silencing, *penaeidin3* is very likely under the *Pm*Relish regulation as well. The expression of *ALFPm3* and *crustinPm1* is not under the regulation of *Pm*Relish.

Acknowledgments

This project was supported by the 90th Anniversary of Chulalongkorn University Fund, the NRCT-JSPS ASIAN CORE Program in Fishery Science, the Japan International Cooperation Agency (JICA) and the TRF Senior Research Scholar (No. RTA5880004), Thailand Research Fund. We thank Chulalongkorn University for the 60/40 Support for Tuition Fee to Suwattana Visetnan and the support under the Ratchadaphisek Somphot Endowment to the Center of Excellence for Molecular Biology and Genomics of Shrimp.

References

[1] J.A. Hoffmann, J.M. Reichhart, *Drosophila* innate immunity: an evolutionary perspective, Nat. Immunol. 3 (2) (2002) 121–126.
[2] A. Tassanakajon, K. Somboonwiwat, P. Supungul, S. Tang, Discovery of immune molecules and their crucial functions in shrimp immunity, Fish. Shellfish Immunol. 34 (4) (2013) 954–967.
[3] F. Li, J. Xiang, Recent advances in researches on the innate immunity of shrimp in China, Dev. Comp. Immunol. 39 (1–2) (2013) 11–26.
[4] T. Tanji, Y.T. Ip, Regulators of the Toll and Imd pathways in the *Drosophila* innate immune response, Trends Immunol. 26 (4) (2005) 193–198.
[5] J.A. Arts, F.H. Cornelissen, T. Cijsouw, T. Hermsen, H.F. Savelkoul, R.J. Stet, Molecular cloning and expression of a Toll receptor in the giant tiger shrimp, *Penaeus monodon*, Fish. Shellfish Immunol. 23 (3) (2007) 504–513.
[6] P.H. Wang, J.P. Liang, Z.H. Gu, D.H. Wan, S.P. Weng, X.Q. Yu, J.G. He, Molecular cloning, characterization and expression analysis of two novel Tolls (LvToll2 and LvToll3) and three putative Spätzle-like Toll ligands (LvSpz1-3) from *Litopenaeus vannamei*, Dev. Comp. Immunol. 36 (2) (2012) 359–371.
[7] R. Wen, F. Li, Z. Sun, S. Li, J. Xiang, Shrimp MyD88 responsive to bacteria and white spot syndrome virus, Fish. Shellfish Immunol. 34 (2) (2013) 574–581.
[8] D. Wang, F. Li, S. Li, Y. Chi, R. Wen, N. Feng, J. Xiang, An IκB homologue (FcCactus) in Chinese shrimp *Fenneropenaeus chinensis*, Dev. Comp. Immunol. 39 (4) (2013) 352–362.
[9] X.D. Huang, Z.X. Yin, X.T. Jia, J.P. Liang, H.S. Ai, L.S. Yang, X. Liu, P.H. Wang, S.D. Li, S.P. Weng, X.Q. Yu, J.G. He, Identification and functional study of a shrimp Dorsal homologue, Dev. Comp. Immunol. 34 (2) (2010) 107–113.
[10] P.H. Wang, Z.H. Gu, X.D. Huang, B.D. Liu, X.X. Deng, H.S. Ai, J. Wang, Z.X. Yin, S.P. Weng, X.Q. Yu, J.G. He, An immune deficiency homolog from the white shrimp, *Litopenaeus vannamei*, activates antimicrobial peptide genes, Mol. Immunol. 46 (8–9) (2009) 1897–1904.
[11] J.F. Lan, J. Zhou, X.W. Zhang, Z.H. Wang, X.F. Zhao, Q. Ren, J.X. Wang, Characterization of an immune deficiency homolog (IMD) in shrimp (*Fenneropenaeus chinensis*) and crayfish (*Procambarus clarkii*), Dev. Comp. Immunol. 41 (4) (2013) 608–617.
[12] X.D. Huang, Z.X. Yin, J.X. Liao, P.H. Wang, L.S. Yang, H.S. Ai, Z.H. Gu, X.T. Jia, S.P. Weng, X.Q. Yu, J.G. He, Identification and functional study of a shrimp Relish homologue, Fish. Shellfish Immunol. 27 (2) (2009) 230–238.
[13] F. Li, H. Yan, D. Wang, T.A. Priya, S. Li, B. Wang, J. Zhang, J. Xiang, Identification of a novel relish homolog in Chinese shrimp *Fenneropenaeus chinensis* and its function in regulating the transcription of antimicrobial peptides, Dev. Comp. Immunol. 33 (10) (2009) 1093–1101.
[14] W. Qiu, S. Zhang, Y.G. Chen, P.H. Wang, X.P. Xu, C.Z. Li, Y.H. Chen, W.Z. Fan, H. Yan, S.P. Weng, S. FrancisChan, J.G. He, *Litopenaeus vannamei* NF-κB is required for WSSV replication, Dev. Comp. Immunol. 45 (1) (2014) 156–162.
[15] S. Visetnan, P. Supungul, I. Hirono, A. Tassanakajon, V. Rimphanitchayakit, Activation of *Pm*Relish from *Penaeus monodon* by yellow head virus, Fish. Shellfish Immunol. 42 (2) (2015) 335–344.
[16] S. Pongsomboon, S. Tang, S. Boonda, T. Aoki, I. Hirono, A. Tassanakajon, A cDNA microarray approach for analyzing transcriptional changes in *Penaeus monodon* after infection by pathogens, Fish. Shellfish Immunol. 30 (1) (2011) 439–446.

[17] M.W. Pfaffl, A new mathematical model for relative quantification in real-time RT-PCR, Nucleic Acids Res. 29 (9) (2001) e45.
[18] A. Prapavorarat, S. Pongsomboon, A. Tassanakajon, Identification of genes expressed in response to yellow head virus infection in the black tiger shrimp, *Penaeus monodon*, by suppression subtractive hybridization, Dev. Comp. Immunol. 34 (6) (2010) 611–617.
[19] D. Wang, S. Li, F. Li, Screening of genes regulated by Relish in Chinese shrimp *Fenneropenaeus chinensis*, Dev. Comp. Immunol. 41 (2) (2013) 209–216.
[20] T. Shibata, S. Sekihara, T. Fujikawa, R. Miyaji, K. Maki, T. Ishihara, T. Koshiba, S. Kawabata, Transglutaminase-catalyzed protein-protein cross-linking suppresses the activity of the NF-κB-like transcription factor relish, Sci. Signal 6 (285) (2013) ra61.
[21] A. Prapavorarat, T. Vatanavicharn, K. Söderhäll, A. Tassanakajon, A novel viral responsive protein is involved in hemocyte homeostasis in the black tiger shrimp, *Penaeus monodon*, J. Biol. Chem. 285 (28) (2010) 21467–21477.
[22] K. Khanobdee, C. Soowannayan, T.W. Flegel, S. Ubol, B. Withyachumnarnkul, Evidence for apoptosis correlated with mortality in the giant black tiger shrimp *Penaeus monodon* infected with yellow head virus, Dis. Aquat. Organ 48 (2) (2002) 79–90.

Fish & Shellfish Immunology 58 (2016) 429–435

Contents lists available at ScienceDirect

Fish & Shellfish Immunology

journal homepage: www.elsevier.com/locate/fsi

Full length article

Characterization of a hemocyte homeostasis-associated-like protein (HHAP) in the freshwater crayfish *Pacifastacus leniusculus*

Kantamas Apitanyasai [a, b], Chadanat Noonin [a], Anchalee Tassanakajon [b], Irene Söderhäll [a], Kenneth Söderhäll [a, *]

[a] Department of Comparative of Physiology, Uppsala University, Uppsala, Sweden
[b] Center of Excellence for Molecular Biology and Genomics of Shrimp, Department of Biochemistry, Faculty of Science, Chulalongkorn University, 254 Phayathai Road, Bangkok 10330, Thailand

ARTICLE INFO

Article history:
Received 7 June 2016
Received in revised form
19 September 2016
Accepted 20 September 2016
Available online 20 September 2016

Keywords:
Pacifastacus leniusculus
Hemocyte homeostasis
RNA interference
Intestine
Aeromonas hydrophila

ABSTRACT

Hemocyte homeostasis-associated-like protein (HHAP) in the freshwater crayfish *Pacifastacus leniusculus* has a distinct role from that of its homolog *Pm*HHAP in the shrimp *Penaeus monodon*. Knockdown of *Pl*HHAP *in vitro* using double-stranded RNA (dsRNA) had no effect on the cell morphology of hematopoietic tissue (HPT) cells. The total hemocyte number and caspase activity were unchanged after *Pl*HHAP knockdown *in vivo*, in contrast to the results found in shrimp. Moreover, suppression of *Pl*HHAP both *in vitro* and *in vivo* did not change the mRNA levels of some genes involved in hematopoiesis and hemocyte homeostasis. Interestingly, bacterial count and scanning electron microscope revealed that depletion of *Pl*HHAP in intestine by RNAi resulted in higher number of bacteria in the crayfish intestine. Together, these results suggest that *Pl*HHAP is not involved in hemocyte homeostasis in the crayfish *P. leniusculus* but appears to affect the bacterial number in the intestine through an unknown mechanism. Since *Pl*HHAP has different functions from *Pm*HHAP, we therefore named it HHAP-like protein.
© 2016 Published by Elsevier Ltd.

1. Introduction

Crustacean defense systems rely on innate immunity, and the major immune-responsive cells are the hemocytes [7,8,10,17,21,24,25]. Hemocyte production or hematopoiesis occurs in hematopoietic tissues (HPTs), and the maturing hemocytes are then released into the circulatory system [2,22]. Hemocyte number and type vary after pathogen infection, injury or stress [6,8,18,21], and this variability is essential to maintaining the number of hemocytes in circulation.

In recent years, several genes involved in hematopoiesis and hemocyte homeostasis have been characterized in crustaceans [15,16,19,20,22,23]. In crustaceans, the cytokine astakine was first discovered in *Pacifastacus leniusculus* and in the shrimp *Penaeus monodon* [23]. Astakine is important for the proliferation and differentiation of cells in hematopoietic tissue [5,14,23]. Recently, an astakine-like factor was reported to be involved in hemocyte proliferation in the pacific oyster, *Crassostrea gigas* [11] and a Runt homolog and CBFβ were reported to play a role in production of hemocytes in the scallop, *Chlamys farreri* [28]. A cysteine-rich protein called crustacean hematopoietic factor (CHF) has been shown to be essential for hemocyte homeostasis in crayfish [16]. RNAi experiments have shown that loss of CHF leads to an increase in HPT cell apoptosis and a decrease in hemocyte numbers in the circulatory system [16]. Recently, two β-thymosin proteins (β-thymosin 1 and β-thymosin 2) have been shown to regulate hemocyte homeostasis in crayfish [20]. Both β-thymosins can interact with the β-subunit of ATP synthase on the HPT cell surface and are also involved in the migration and release of hemocytes from HPT. Injection of a β-thymosin 2 recombinant protein results in an increase in the number of hemocytes in circulation [20].

A hemocyte homeostasis-associated protein (HHAP) has been identified as a viral-responsive protein and an anti-apoptotic protein in the black tiger shrimp *Penaeus monodon* [1,19]. Silencing of *Pm*HHAP has been found to lead to a significant decrease in the total hemocyte number, clear changes in hemocyte morphology and 100% shrimp mortality within 30 h, [19]. Knockdown of *Pm*HHAP also causes hemocytes to undergo apoptosis [1]. In addition, the *Pm*HHAP protein has been found to bind to the P20 domain of *P. monodon* caspase (PmCasp) and to reduce the caspase

* Corresponding author.
E-mail address: Kenneth.Soderhall@ebc.uu.se (K. Söderhäll).

http://dx.doi.org/10.1016/j.fsi.2016.09.038
1050-4648/© 2016 Published by Elsevier Ltd.

activity in recombinant *Pm*Casp-treated hemocytes [1]. Furthermore, it has been shown that HHAP in *Litopenaeus vannamei* binds to a laminin receptor (Lamr), and knockdown of Lamr leads to downregulation of *Lv*HHAP and a reduction in hemocyte number. Therefore, HHAP has been suggested to participate in hemocyte homeostasis in shrimp [3].

Interestingly, HHAP has also been identified in the freshwater crayfish *Pacifastacus leniusculus* [19]. The *Pm*HHAP and *Pl*HHAP proteins share 47% identity and has eight conserved cysteine residues. In the present study, we first examined the role of *Pl*HHAP in hemocyte homeostasis and hematopoiesis since this role of HHAP has been reported in shrimp. We found that, in contrast to shrimp, silencing of *Pl*HHAP by dsRNA had no effect on the morphology of the HPT cells *in vitro* or the transcription of genes involved in hemocyte homeostasis both *in vitro* and *in vivo* in crayfish. Moreover, suppression of *Pl*HHAP did not change the hemocyte number, and we did not observe any signs of apoptosis. Because of high expression of *Pl*HHAP in intestine, we then examined its potential role in intestine. We found that silencing of *Pl*HHAP altered the amount of bacteria in the crayfish intestine. Our data suggest that *Pl*HHAP does not have the same role as the shrimp *Pm*HHAP and that it is not involved in hemocyte homeostasis in crayfish, as it is in shrimp. Instead, it affects the bacterial number in the intestine. According to the functional differences, we named the *Pl*HHAP a "HHAP-like protein".

2. Materials and methods

2.1. Animals

Freshwater crayfish (*Pacifastacus leniusculus*) were obtained from Lake Erken, Sweden. Crayfish were maintained in tanks with aerated water at 10 °C. Only healthy animals were used in the experiments.

2.2. Analysis of *Pl*HHAP transcript expression in crayfish tissues

The tissue-specific expression of *Pl*HHAP was qualitatively assayed by reverse transcription-PCR (RT-PCR). Total RNA was extracted from the muscles, anterior proliferation centers (APCs) in HPT, brains, hematopoietic tissues, hemocytes, eyestalks, hepatopancreas, gills, intestines, hearts, nerves and abdominal nerves of crayfish with TRIzol Reagent (Invitrogen). After RNase-free DNase I (Biolabs) treatment, equal amounts of total RNA were used for cDNA synthesis with ThermoScript (Invitrogen) according to the manufacturer's instructions. Then, *Pl*HHAP transcript levels in each tissue were analyzed using gene-specific primers (Table 1). The 40S ribosomal protein was used as an internal control. The PCR thermal cycling conditions consisted of 98 °C for 1 min, followed by 30 cycles for *Pl*HHAP or 25 cycles for 40S at 98 °C for 30 s, 58 °C for 30 s and 72 °C for 30 s, plus a final extension step at 72 °C for 5 min. The PCR products were analyzed on a 1.5% agarose gel stained with GelRed and visualized by UV-transillumination.

2.3. Hematopoietic tissue (HPT) cell culture

The HPT cells were isolated from freshwater crayfish as described previously with minor modifications [23]. Briefly, the hematopoietic tissue was dissected from the dorsal side of the stomach, washed with crayfish phosphate buffered saline (CPBS) (10 mM Na_2HPO_4, 10 mM KH_2PO_4, 150 mM NaCl, 10 mM $CaCl_2$ and 10 mM $MnCl_2$, pH 6.8), and then incubated in 700 μl of 0.1% collagenase Type I and Type IV (Sigma) in CPBS at room temperature (RT) for 30 min. The digested HPT was then centrifuged at 800 × g for 5 min at RT to remove the collagenase solution. The cell pellets were washed twice with CPBS, and the undigested tissue was removed. The isolated HPT cells were resuspended in L-15 medium (Sigma-Aldrich) supplemented with 1 μM phenylthiourea, 60 μg/ml penicillin, 50 μg/ml streptomycin, 50 μg/ml gentamicin and 2 mM L-glutamine. The cells were subsequently seeded in 96-well plates at a density of 4×10^4 cells/100 μl/well. The cells were supplemented with 2% of cell-free crayfish plasma and incubated at 16 °C. One-third of the medium was changed every other day.

2.4. Preparation of double-stranded RNAs (dsRNAs) for RNA interference (RNAi) experiments

The dsRNA specific to the *Pl*HHAP (GenBank: HQ130432.1) gene

Table 1
Nucleotide sequence of the primers used.

Primer	Sequence (5′-3′)	GenBank accession number
RT-PCR		
*Pl*HHAP-F	AGTGCAGTTTAGGAACACAT	HQ130432
*Pl*HHAP-R	ACACATACATTCTTGCAGTC	HQ130432
CHF-F	ATGCGGAGCAGCTACCGCTTGAGGTG	GQ497446
CHF-R	GGCCGACATGTGAATGAG	GQ497446
Astakine1-F	GGCTATGGCTGGCTCTTGTAA	AY787656
Astakine1-R	AGGTGGCTGAAGGTCGGGTA	AY787656
Astakine2-F	ATGGTGTTAGTGTTGATGTGTGGC	EF568370
Astakine2-R	GGGACTCAGCGGAGATTTTGC	EF568370
IGFBP7-F	GCAGAAGAGGTCTCTGGTAAGG	
IGFBP7-R	CCCGCATAATACATGATCTGCTCC	
VP28-F	TCACTCTTTCGGTCGTGTCG	AF502435
VP28-R	CCACACACAAAGGTGCCAAC	AF502435
40S-R	GACGAATGGCATACACCTGAGAGG	CF542417
40S-F	CAGGACTCTGCAGTTCAAGCTGATG	CF542417
qRT-PCR		
q*Pl*HHAP-F	CCATACCAGGGCAAGAGGAG	HQ130432
q*Pl*HHAP-R	CCACAGAACTGCCCTATTTG	HQ130432
q40S-F	GACGAATGGCATACACCTGAGAGG	CF542417
q40S-F	CAGGACTCTGCAGTTCAAGCTGATG	CF542417
Gene silencing		
*Pl*HHAPi-F	TAATACGACTCACTATAGGGCCATACCAGGGCAAGAGGAG	HQ130432
*Pl*HHAPi-R	TAATACGACTCACTATAGGGCCACAGAACTGCCCTATTTG	HQ130432
GFPi-F	TAATACGACTCACTATAGGGCGACGTAAACGGCCACAAGT	U55761
GFPi-R	TAATACGACTCACTATAGGGTTCTTGTACAGCTCGTCCATGC	U55761

transcript was amplified using gene-specific primers (Table 1). In addition, a GFP fragment from the pd2EGFP-1 vector (Clontech) was amplified and used to prepare the dsRNA of GFP, which served as a negative control. The size of *Pl*HHAP dsRNA was 233 nucleotides and covered the region of nucleotides 83–315 and the size of GFP dsRNA was 657 nucleotides. The PCR was performed at 98 °C for 1 min, followed by 30 cycles of 98 °C for 30 s, 64 °C for 30 s and 72 °C for 30 s, and then a final extension at 72 °C for 5 min. To generate the dsRNA, 1 μg of purified PCR product was used as a template for *in vitro* transcription using a MEGAscript kit (Ambion), and the *in vitro* transcription reaction was performed according to the manufacturer's instruction. Briefly, the purified PCR product was incubated with 4 ribonucleotides (ATP, CTP, GTP and UTP) and RNA polymerase enzyme at 37 °C overnight. After treating with DNase to remove the DNA template, nuclease-free water (30 μl) and 30 μl LiCl precipitation solution were added and incubated at −20 °C for more than 30 min. The supernatant was removed carefully after centrifugation at 4 °C and the dsRNA pellets were washed with 70% ethanol. Then the dsRNA was resuspended in RNase-free water and 1 μl of dsRNAs was subjected to 1.5% agarose gel electrophoresis in order to check if a discrete band could be observed.

2.5. RNA interference (RNAi) experiments

For the *in vitro* RNAi experiments, dsRNA was transfected into HPT cells as described previously, with minor modifications [13]. Briefly, 1 μg of dsRNA was mixed with 3 μl calf histone H2A (1 mg/ml of histone type II-A from calf thymus in modified L-15 medium) (Sigma-Aldrich) and incubated for 10 min at RT. Then, a mixture of dsRNA and H2A was combined with 20 μl of cell culture medium and added to one well of HPT cell culture (96-well plates) before incubation at 16 °C. One-third of the total volume of the medium was changed every other day during incubation. To determine the

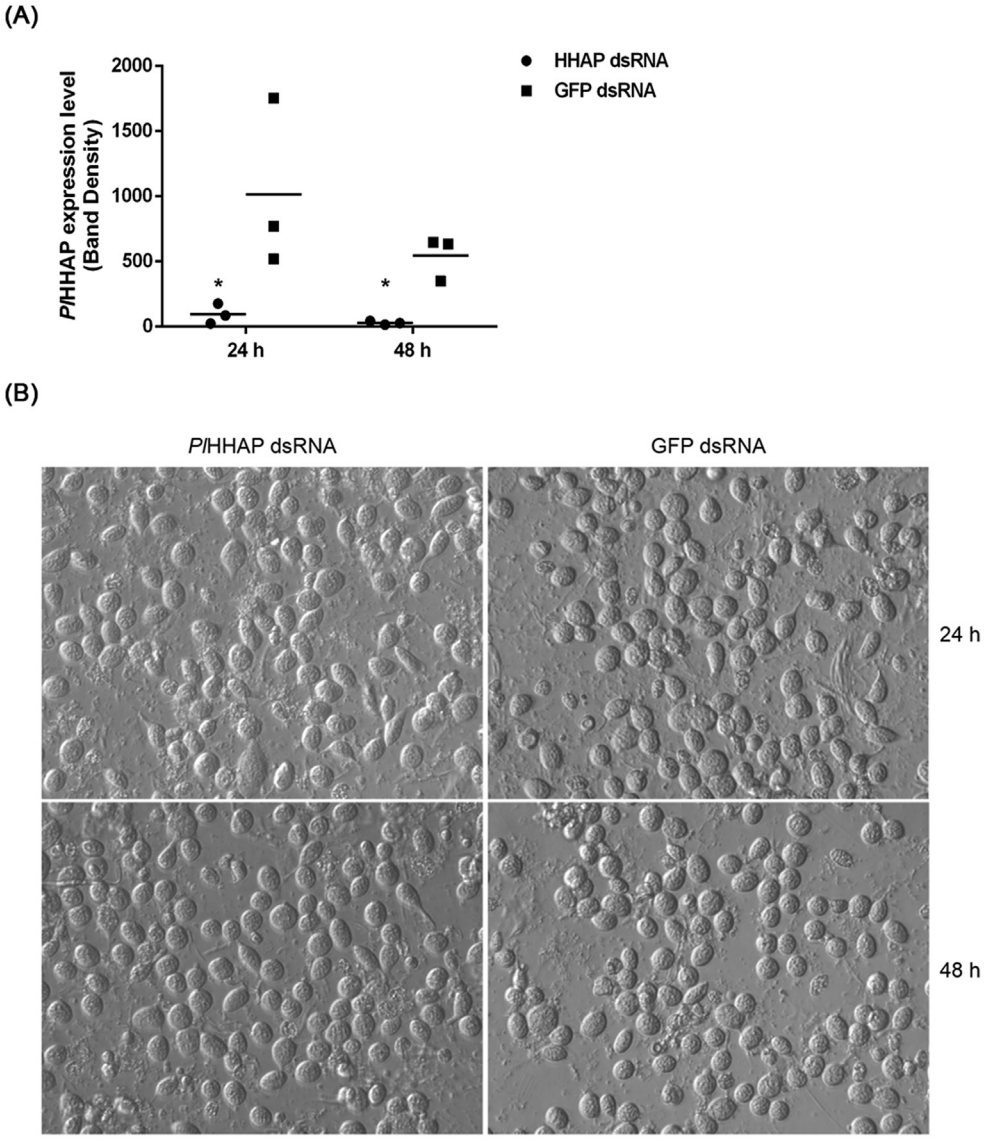


Fig. 1. *In vitro* RNAi of *Pl*HHAP. (A) Semi-quantitative RT-PCR analysis of *Pl*HHAP mRNA levels at 24 and 48 h post dsRNA treatment in *in vitro* HPT cell culture. Band density of *Pl*HHAP from agarose gel electrophoresis was determined. – represents the mean of each group, which was derived from three individual crayfish. ● represents the mRNA expression of *Pl*HHAP from each individual *Pl*HHAP knockdown crayfish, and ■ represents the mRNA expression of *Pl*HHAP from each individual GFP control crayfish. Significant differences compared with the control are indicated by an asterisk ($P < 0.05$). (B) Morphology of the HPT cells after treatment with *Pl*HHAP dsRNA and GFP dsRNA control at 24 and 48 h.

efficiency of the *Pl*HHAP gene transcript silencing, total RNA was extracted from the HPT cells at 24 and 48 h and subjected to semi-quantitative RT-PCR analysis (500 ng RNA were used for cDNA synthesis). In addition, the cell morphology of the HPT cells was observed every day for 5 days after transfection.

For the *in vivo* RNAi treatments, small intermolt crayfish (18–25 g fresh weight) were divided into two groups with three crayfish in each group. Briefly, 100 μl of crayfish saline solution containing 100 μg of *Pl*HHAP or GFP dsRNA was injected into the base of a walking leg of each crayfish. Hemocytes of individual crayfish were collected at 24 h post-injection (hpi), and total RNA was extracted from each crayfish and analyzed by semi-quantitative RT-PCR (500 ng RNA were used for cDNA synthesis) as described above. To silence gene expression in crayfish intestines, dsRNA was injected twice, and the second injection was performed 24 h after the first injection. The intestine was collected for RNA extraction and RT-PCR at 24 h after the second injection (500 ng RNA were used for cDNA synthesis).

2.6. Effects of PlHHAP depletion on the mRNA levels of genes involved in hematopoiesis and hemocyte homeostasis

To determine the effect of *Pl*HHAP silencing on the mRNA level of genes involved in hematopoiesis and hemocyte homeostasis, semi-quantitative RT-PCR analysis was performed using gene-specific primers for CHF (GenBank: GQ497446), astakine1 (GenBank: AY787656), astakine2 (GenBank: EF568370) and IGFBP (Table 1). Amplification of the 40S ribosomal transcript served as the internal control.

2.7. Total hemocyte count (THC) after silencing of PlHHAP

Crayfish were separated into two groups with 5 crayfish per group. Hemolymph samples were taken from each crayfish to determine the total hemocyte number before injection of dsRNA (0 h). Subsequently, the crayfish were injected with *Pl*HHAP dsRNA or GFP dsRNA at the base of a walking leg. After 24 h of dsRNA injection, hemolymph samples were taken from each crayfish, and the total hemocyte number was determined. The hemocyte number after injection of each crayfish was then divided by the hemocyte number before injection, and the value is reported as the hemocyte index.

2.8. Apoptosis analysis in hemocytes of the PlHHAP-silenced animals

To determine the effects of *Pl*HHAP on hemocyte apoptosis in the *Pl*HHAP knockdown animals, RNAi experiments were performed as described above. Hemocyte apoptosis was analyzed using the Caspase-Glo 3/7 Assay Kit (Promega) according to the manufacturer's instructions. Briefly, hemocytes were collected from each crayfish and suspended in 500 μl of CPBS. The same amount of cell suspension from each crayfish was seeded in a white 96-well plate, and 100 μl of Caspase-Glo reagent was then added to each well, gently mixed with the cells and incubated for 1 h at RT. The luminescence of each sample was measured in a plate-reading

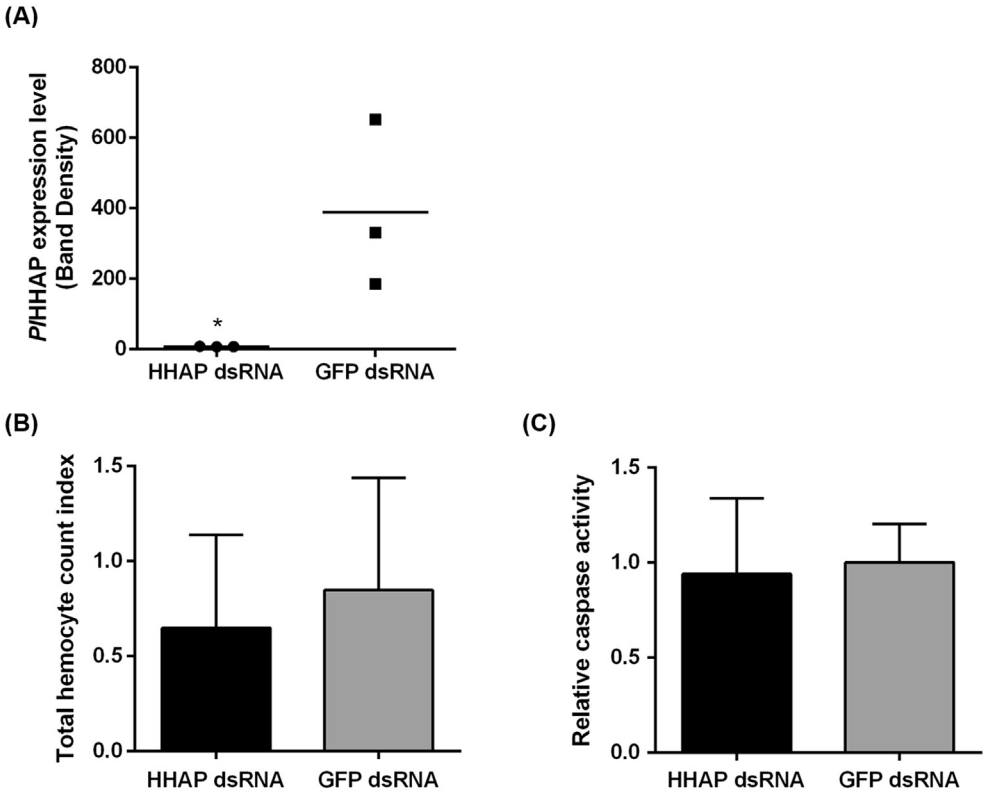


Fig. 2. Effects of RNAi-mediated suppression of *Pl*HHAP in crayfish hemocytes. (A) The efficiency of dsRNA-mediated *Pl*HHAP gene knockdown was examined in hemocytes at 24 h post-dsRNA injection using semi-quantitative RT-PCR analysis. Band density of *Pl*HHAP from agarose gel electrophoresis was determined. Each dot represents expression in each individual crayfish. – represents the mean of each group which derived from three individual animals. Significant differences compared with the control are indicated by an asterisk ($P < 0.05$). (B) Total hemocyte number (THC) was determined 24 h post-injection of *Pl*HHAP or GFP dsRNA. THC was determined before and after injection, and the change in THC was calculated. Five animals were used in each experimental group. Each column represents the mean of five separate animals, and error bars represent SD values. (C) Caspase 3/7 activity in the hemocytes of *Pl*HHAP-silenced crayfish 24 h post-dsRNA injection. Each column represents the mean of five independent animals, and error bars represent SD values.

luminometer.

2.9. Determination of bacterial number in the intestine of PlHHAP-silenced animals

To elucidate the effect of *Pl*HHAP knockdown on bacterial number in crayfish intestines, RNAi experiments were performed, and the bacterial counts were then assayed. Twenty-four hours after the second dsRNA injection, the intestine was collected from each crayfish and homogenized in 0.15 M NaCl. The intestinal lysate was then serially diluted, and 10 μl of each dilution was deposited on a LB agar plate and incubated overnight at 37 °C. The bacterial colonies were reported in colony-forming units (CFU) per ml. Five crayfish were used in each group in this experiment.

2.10. Scanning electron microscopy (SEM) of crayfish intestines

The intestines of crayfish injected with *Pl*HHAP dsRNA or GFP dsRNA were collected individually 24 h after the second dsRNA injection. The tissues were immediately fixed in 0.1 M phosphate buffer, pH 7.4, containing 3% (v/v) glutaraldehyde at 4 °C in the darkness overnight. The samples were washed twice with 0.1 M phosphate buffer for 15 min each, then once with distilled water for 15 min. Then, each intestine was dehydrated for 15 min each in an ethanol series: 30%, 50%, 70%, 95%, followed by 2 times for 15 min in absolute ethanol. Next, the samples were dried using a critical point dryer and then mounted on stubs. During mounting, the samples were split longitudinally to expose the intestinal lumen, and the mounted samples were coated with gold through ion sputtering. The specimens were examined with a scanning electron microscope. The images from the SEM were analyzed by blind tests. The images without labeling were given to 4 blinded independent analysts, who assessed each image.

2.11. Statistical analysis

Statistical analysis was performed using a one-way ANOVA (analysis of variance) followed by Duncan's test, whereas two treatments were compared by a Student's paired *t*-test. The cutoff for significance was $P < 0.05$, and the results are presented as the mean ± standard deviation (SD).

3. Results and discussion

3.1. Effects of PlHHAP gene silencing on HPT cell morphology in vitro

*Pm*HHAP has been reported to play an important role in hemocyte homeostasis in shrimp; thus, *Pl*HHAP may also be involved in hemocyte homeostasis in crayfish. To investigate this possibility, *in vitro* RNAi of *Pl*HHAP in crayfish HPT cells was conducted. HPT cells were treated with either *Pl*HHAP dsRNA or GFP dsRNA as controls. Semi-quantitative RT-PCR analysis showed that the *Pl*HHAP mRNA level was specifically and significantly decreased in *Pl*HHAP dsRNA-treated HPT cells compared with that in GFP dsRNA-treated HPT cells (Fig. 1A). However, there were no significant changes in the morphology of HPT cells after 24 and 48 h of *Pl*HHAP dsRNA treatment (Fig. 1B), and the cell morphology remained unchanged 5 days after dsRNA treatment (data not shown).

In recent years, the genes involved in hematopoiesis and hemocyte homeostasis in a few crustaceans have been studied. In *P. leniusculus*, two isoforms of astakine, astakine 1 and astakine 2, have been shown to play a role in hematopoiesis. Astakine 1 is essential for the proliferation and differentiation of the semi-granular cells, and astakine 2 appears to be responsible for granular cell differentiation [14,23]. Moreover, astakine has been found in shrimp, *P. monodon*, in which it promotes proliferation of cells in HPT [5,9,12]. Additionally, a crustacean hematopoietic factor (CHF) in *P. leniusculus* is involved in hemocyte homeostasis by preventing cell apoptosis [16]. The shrimp *Pm*HHAP is essential for survival and plays important roles in hemocyte homeostasis of shrimp [19]. Thus, we investigated the effect on gene expression of hematopoiesis and hemocyte homeostasis-related genes after *Pl*HHAP knockdown. The results showed that silencing of the *Pl*HHAP gene had no significant effect on the expression levels of any of the tested genes (data not shown). Because suppression of *Pl*HHAP had no effect on cell morphology or gene transcription, *Pl*HHAP is not important in hematopoiesis in crayfish.

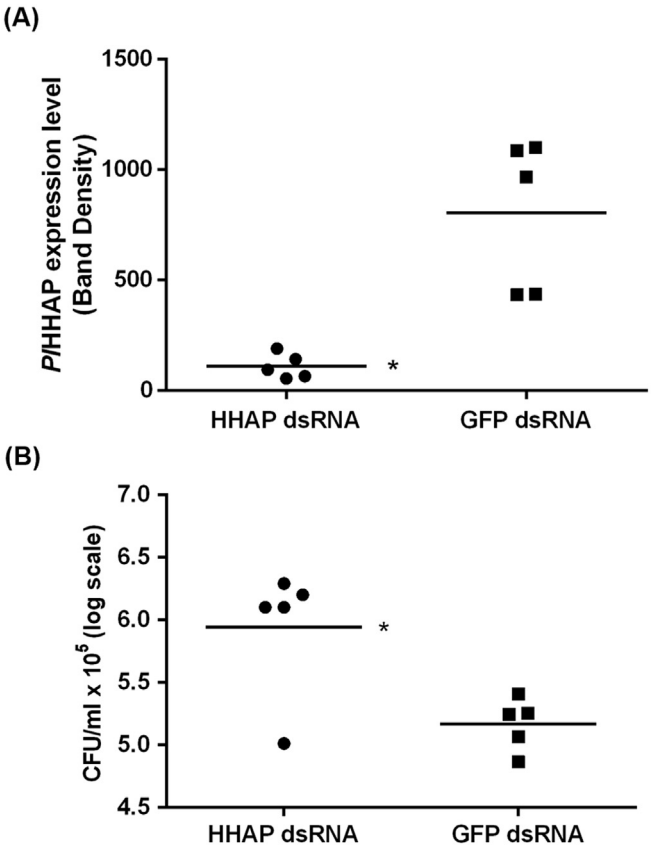


Fig. 3. Depletion of *Pl*HHAP resulted in a higher number of bacteria in the crayfish intestines. (A) Semi-quantitative RT-PCR analysis of *Pl*HHAP mRNA levels at 24 h post-second dsRNA injection in crayfish intestines. Band density of *Pl*HHAP from agarose gel electrophoresis was determined. Each dot represents expression of each individual crayfish. – represents the mean of each group which derived from five individual animals. Significant differences compared with the control are indicated by an asterisk ($P < 0.05$). (B) The bacterial colony-forming units (CFUs) in the intestine of knockdown crayfish were determined 24 h after the second injection of dsRNA using a total plate count method. – represents the mean of each group, which was derived from five crayfish. ● represents CFU in the intestines from each individual *Pl*HHAP knockdown crayfish, and ■ represents CFU in the intestines from each individual GFP control crayfish. *$P < 0.05$, significant difference compared to the control.

3.2. Effects of PlHHAP gene silencing on total hemocyte number and hemocyte apoptosis in crayfish in vivo

To determine whether *Pl*HHAP is essential for crayfish survival, dsRNA-mediated gene silencing was performed *in vivo*. The efficiency of *Pl*HHAP gene silencing was evaluated, and the results showed that the transcript levels of *Pl*HHAP in hemocytes were significantly decreased in the *Pl*HHAP knockdown group compared

with that in the control GFP knockdown group (Fig. 2A). Interestingly, suppression of *Pl*HHAP did not cause any mortality in the crayfish, even ten days post-dsRNA infection, in contrast to the findings in shrimp, which died within 30 h post-dsRNA injection [19]. Then, the mRNA levels of genes involved in hemocyte homeostasis and hematopoiesis were further analyzed in the hemocytes of *Pl*HHAP knockdown crayfish compared with GFP control crayfish. Silencing of the *Pl*HHAP gene had no significant effect on the transcripts of the tested genes, including CHF, astakine1, astakine2 and insulin-like growth factor-binding protein7 (IGFBP7) (data not shown).

Furthermore, we also found that silencing of *Pl*HHAP had no effect on the number of circulating hemocytes compared with the total hemocyte index of GFP dsRNA-injected crayfish (Fig. 2B). This result is in contrast to the findings in shrimp, in which THC decreases dramatically in HHAP-silenced shrimp. In addition, after knockdown of *Pl*HHAP *in vivo*, the caspase activity in the hemocytes of *Pl*HHAP-silenced crayfish remained unchanged compared with that in GFP-silenced crayfish (Fig. 2C). This result again contrasts with the effects of HHAP depletion in shrimp, which results in increased apoptosis in shrimp hemocytes [1]. All data from the RNAi experiments indicate that, unlike *Pm*HHAP in shrimp, *Pl*HHAP is not involved in hemocyte homeostasis in crayfish.

3.3. Depletion of *Pl*HHAP gene expression caused higher amounts of bacteria in crayfish intestines

Tissue distribution results showed that *Pl*HHAP is highly expressed in the crayfish intestine and gills, whereas the shrimp HHAP is highly expressed in shrimp HPT [19]. Moreover, we also checked the expression of *Pl*HHAP in different parts of intestine and found that *Pl*HHAP was highly expressed in foregut and then hindgut but not in midgut. This differential expression is similar to the expression pattern of *P. leniusculus* thiolester containing protein

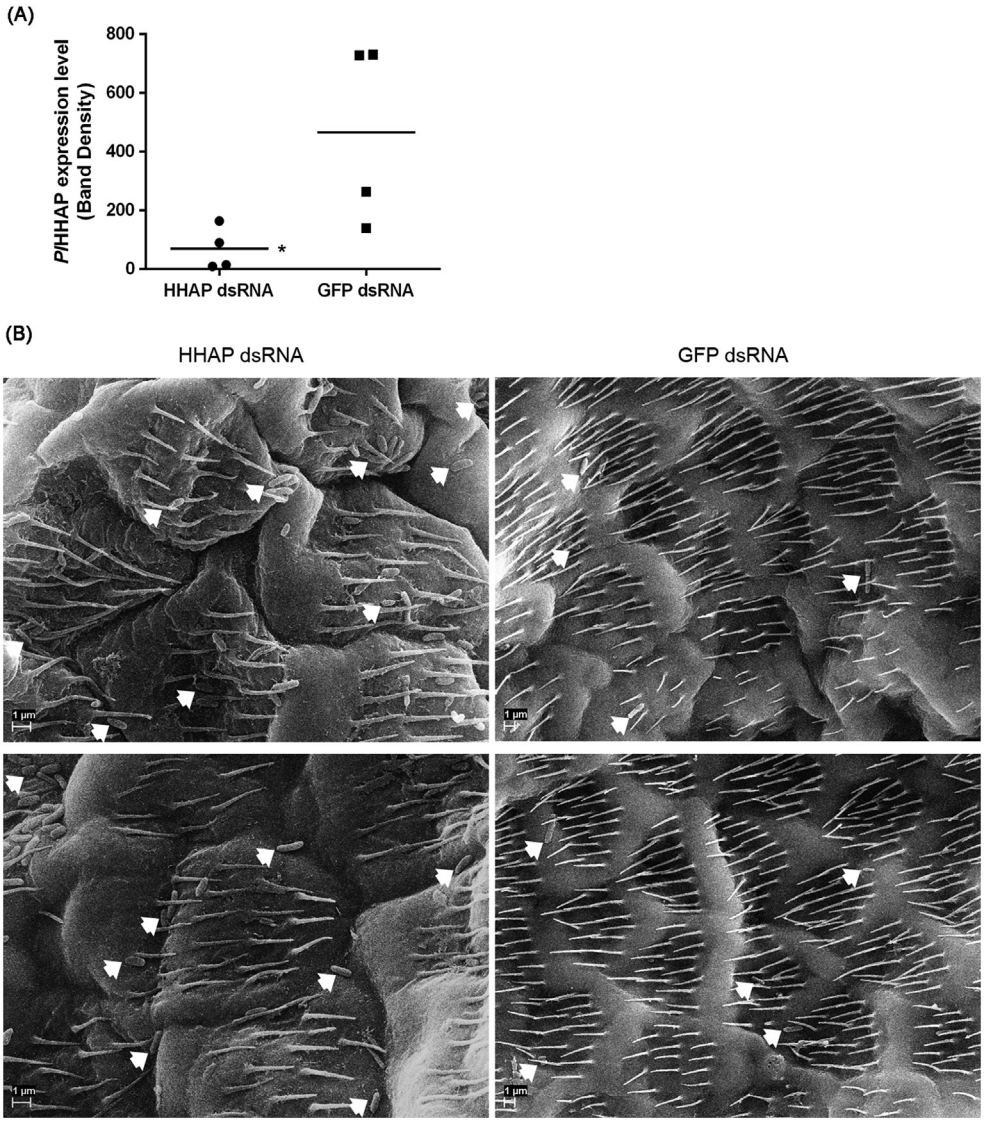


Fig. 4. Representative scanning electron microscopy (SEM) images of the luminal surface of the intestines of crayfish after *Pl*HHAP knockdown. (A) Semi-quantitative RT-PCR analysis of *Pl*HHAP transcript levels 24 h post-second dsRNA injection in the crayfish intestine. The controls were injected with GFP dsRNA. Band density of *Pl*HHAP from agarose gel electrophoresis was determined. Each dot represents expression of each individual crayfish. – represents mean of each group which derived from four individual animals. Significant differences compared with the control are indicated by an asterisk ($P < 0.05$). (B) SEM images of the intestine from *Pl*HHAP knockdown crayfish compared to the GFP-injected control crayfish. Bacteria are visible in the intestines of each group (white arrow). Micrographs are representatives of two fields of view per sample, and four independent intestines from individual crayfish were used in this experiment.

(*Pl*TEP) in crayfish gastrointestinal tract [27]. *Pl*TEP was reported to play a role in defending against intestinal bacterial infection in crayfish [27]. Accordingly, we hypothesized that *Pl*HHAP might have similar function with *Pl*TEP in affecting the intestinal bacterial number. Therefore, we tried to identify a possible function for this protein in the intestine. First, we knocked down expression of *Pl*HHAP *in vivo* and assessed the expression of *Pl*HHAP at 24 h post-dsRNA injection. The gene expression of *Pl*HHAP in the intestine was not significantly decreased compared with that of the control. Then, we increased the dose of dsRNA by injecting dsRNA twice and collected intestines from individual crayfish to examine *Pl*HHAP mRNA level 24 h after the second dsRNA injection. The results showed that *Pl*HHAP was significantly decreased 24 h post-second dsRNA injection (Fig. 3A). Then, the bacterial count in the intestinal lysate was performed after silencing of *Pl*HHAP. The bacterial colonies were observed 24 h post-second dsRNA injection, and the results showed that the mean bacterial CFUs in intestines from the *Pl*HHAP knockdown crayfish were significantly higher than those of the control crayfish injected with GFP dsRNA (Fig. 3B). We also visualized the normal flora inside the intestines from the knockdown *Pl*HHAP and control GFP groups by using scanning electron microscopy (SEM). The small pieces of the intestines that were processed for SEM were separated to assess the efficiency of the *Pl*HHAP knockdown, and the expression of *Pl*HHAP mRNA was lower than that of the control (Fig. 4A). Silencing of *Pl*HHAP resulted in a large number of bacterial cells at the luminal surface of the intestine, and several of the cells were clustered together, but others were spread throughout the intestine (Fig. 4B). However, a few bacterial cells were found in some areas of the luminal surface of the intestine from the GFP control (Fig. 4B). On the basis of the bacterial counts and the SEM results in the intestine, silencing of *Pl*HHAP affected the number of bacteria in the crayfish intestine, but the underlying mechanism is unknown.

In conclusion, we investigated possible functions of *Pl*HHAP in the crayfish *Pacifastacus leniusculus*. We found that *Pl*HHAP was not responsive to the WSSV infection in crayfish hemocytes (data not shown), whereas in shrimp, HHAP is upregulated after a WSSV or yellow head virus (YHV) infection [4,19,26]. Although we tried to study the function of *Pl*HHAP in hemocyte homeostasis in crayfish, our results revealed that *Pl*HHAP was not important for animal survival and did not play a role in hemocyte homeostasis, in contrast to the function of *Pm*HHAP [1,19]. Instead, we showed that depletion of *Pl*HHAP affected the number of bacteria in the crayfish intestine. This discovery indicates that HHAP-like protein from crayfish *P. leniusculus* has a role in affecting the intestinal microflora or bacterial number in the intestine.

Acknowledgments

This work was supported by the Thailand Research Fund (Grant No. RTA588004). K.A. is the recipient of a student fellowship from the Royal Golden Jubilee Ph.D. Program, Joint Funding of the Thailand Research Fund and Chulalongkorn University. The Swedish Science Research Council also funded the research. (2012–2418).

References

[1] K. Apitanyasai, P. Amparyup, W. Charoensapsri, S. Senapin, T. Tassanakajon, Role of *Penaeus monodon* hemocyte homeostasis associated protein (*Pm*HHAP) in regulation of caspase-mediated apoptosis, Dev. Comp. Immunol. 53 (2015) 234–243.
[2] O. Chaga, M. Lignell, K. Söderhäll, The hematopoietic cells of the freshwater crayfish, *Pacifastacus leniusculus*, Anim. Biol. 4 (1995) 59–70.
[3] W. Charoensapsri, P. Sangsuriya, T. Lertwimol, W. Gangnonngiw, K. Phiwsaiya, S. Senapin, Laminin receptor protein is implicated in hemocyte homeostasis for the whiteleg shrimp *Penaeus (Litopenaeus) vannamei*, Dev. Comp. Immunol. 51 (2015) 39–47.
[4] P. Goncalves, C. Guertler, E. Bachère, C.R. de Souza, R.D. Rosa, L.M. Perazzolo, Molecular signatures at imminent death: hemocyte gene expression profiling of shrimp succumbing to viral and fungal infections, Dev. Comp. Immunol. 42 (2014) 294–301.
[5] C.Y. Hsiao, Y.L. Song, A long form of shrimp astakine transcript: molecular cloning, characterization and functional elucidation in promoting hematopoiesis, Fish. Shellfish Immonol. 28 (2010) 77–86.
[6] P. Jiravanichpaisal, E. Bangyeekhun, K. Söderhäll, I. Söderhäll, Experimental infection of white spot syndrome virus in freshwater crayfish *Pacifastacus leniusculus*, Dis. Aquat. Organ 47 (2001) 151–157.
[7] P. Jiravanichpaisal, B.L. Lee, K. Söderhäll, Cell-mediated immunity in arthropods: hematopoiesis, coagulation, melanization and opsonization, Immunobiology 211 (2006) 213–236.
[8] M. Johansson, P. Keyser, K. Sritunyalucksana, K. Söderhäll, Crustacean haemocytes and haematopoiesis, Aquaculture 191 (2000) 45–52.
[9] M. Inada, T. Yui, T. Kono, T. Yoshida, M. Sakai, T. Itami, An ancient cytokine gene from kuruma shrimp Marsupenaeus japonicus: astakine is important in the innate immunity, Fish. Shellfish Immonol. 34 (2013) 1712.
[10] S.Y. Lee, K. Söderhäll, Early events in crustacean innate immunity, Fish. Shellfish Immunol. 12 (2002) 421–437.
[11] Y. Li, S. Jiang, M. Li, L. Xin, L. Wang, H. Wang, L. Qiu, L. Song, A cytokine-like factor astakine accelerates the hemocyte production in pacific oyster *Crassostrea gigas*, Dev. Comp. Immunol. 55 (2016) 179–187.
[12] G.F. Liang, Y. Liang, Q. Xue, J.F. Lu, J.J. Cheng, J. Huang, Astakine LvAST binds to the β subunit of F1-ATP synthase and likely plays a role in white shrimp Litopeneaus vannamei defense against white spot syndrome virus, Fish. Shellfish Immunol. 43 (2015) 75–81.
[13] H. Liu, I. Söderhäll, Histone H2A as a transfection agent in crayfish hematopoietic tissue cells, Dev. Comp. Immunol. 31 (2007) 340–346.
[14] X. Lin, M. Novotny, K. Söderhäll, I. Söderhäll, Ancient cytokines, the role of astakines as hematopoietic growth factors, J. Biol. Chem. 285 (2010) 28577–28586.
[15] X. Lin, I. Söderhäll, Crustacean hematopoiesis and the astakine cytokines, Blood 117 (2011a) 6417–6424.
[16] X. Lin, K. Söderhäll, I. Söderhäll, Invertebrate hematopoiesis: an astakine-dependent novel hematopoietic factor, J. Immunol. 186 (2011b) 2073–2079.
[17] G.G. Martin, B.L. Graves, Fine structure and classification of shrimp hemocytes, J. Morphol. 185 (1985) 339–348.
[18] M. Persson, L. Cerenius, K. Söderhäll, The influence of haemocyte number on the resistance of the freshwater crayfish, *Pacifastacus leniusculus* Dana, to the parasitic fungus Aphan omyces ast aci, J. Fish. Dis. 10 (1987) 471–477.
[19] A. Prapavorarat, T. Vatanavicharn, K. Söderhäll, A. Tassanakajon, A novel viral responsive protein is involved in hemocyte homeostasis in the black tiger shrimp, *Penaeus monodon*, J. Biol. Chem. 285 (2010) 21467–21477.
[20] N. Saelee, C. Noonin, B. Nupan, K. Junkunlo, A. Phongdara, X. Lin, K. Söderhäll, I. Söderhäll, β-thymosins and hemocyte homeostasis in a crustacean, PLoS ONE 8 (2013) e60974.
[21] V.J. Smith, K. Söderhäll, β-1,3 glucan activation of crustacean hemocytes in vitro and in vivo, Biol. Bull. 164 (1983) 299–314.
[22] I. Söderhäll, E. Bangyeekhun, S. Mayo, K. Söderhäll, Hemocyte production and maturation in an invertebrate animal; proliferation and gene expression in hematopoietic stem cells of *Pacifastacus leniusculus*, Dev. Comp. Immunol. 27 (2003) 661–672.
[23] I. Söderhäll, Y.A. Kim, P. Jiravanichpaisal, S.Y. Lee, K. Söderhäll, An ancient role for a prokineticin domain in invertebrate hematopoiesis, J. Immunol. 174 (2005) 6153–6160.
[24] A. Tassanakajon, K. Somboonwiwat, P. Supungul, S. Tang, Discovery of immune molecules and their crucial functions in shrimp immunity, Fish. Shellfish Immunol. 34 (2013) 954–967.
[25] L. Vazquez, J. Alpuche, G. Maldonado, C. Aqundis, A. Pereyra-Morales, E. Zenteno, Immunity mechanisms in crustaceans, Innate Immun. 15 (2009) 179–188.
[26] S. Visetnan, P. Supungul, S. Tang, I. Hirono, A. Tassanakajon, V. Rimphanitchayakit, YHV-responsive gene expression under the influence of *Pm*Relish regulation, Fish. Shellfish Immunol. 47 (2015) 572–581.
[27] C. Wu, C. Noonin, P. Jiravanichpaial, I. Söderhäll, K. Söderhäll, An insect TEP in a crustacean is specific for cuticular tissues and involved in intestinal defense, Insect. Biochem. Mol. Biol. 42 (2012) 71–80.
[28] F. Yue, Z. Zhou, L. Wang, R. Sun, Q. Jiang, Q. Yi, T. Zhang, L. Song, The essential roles of core binding factors CfRunt and CfCBFβ in hemocyte production of scallop *Chlamys farreri*, Dev. Comp. Immunol. 44 (2014) 291–302.

Developmental and Comparative Immunology 67 (2017) 18–29

Contents lists available at ScienceDirect

Developmental and Comparative Immunology

journal homepage: www.elsevier.com/locate/dci

Characterization of molecular properties and regulatory pathways of Crustin*Pm*1 and Crustin*Pm*7 from the black tiger shrimp *Penaeus monodon*

Sopacha Arayamethakorn [a], Premruethai Supungul [a, b], Anchalee Tassanakajon [a], Kuakarun Krusong [a, *]

[a] *Center of Excellence for Molecular Biology and Genomics of Shrimp, Department of Biochemistry, Faculty of Science, Chulalongkorn University, Bangkok 10330, Thailand*

[b] *National Center for Genetic Engineering and Biotechnology (BIOTEC), National Science and Technology Development Agency (NSTDA), Pathumthani, 12120, Thailand*

ARTICLE INFO

Article history:
Received 5 August 2016
Received in revised form
31 October 2016
Accepted 31 October 2016
Available online 2 November 2016

Keywords:
Antimicrobial peptides
Crustin
Imd pathway
Penaeus monodon
Toll pathway

ABSTRACT

Crustin*Pm*1 and crustin*Pm*7 are the two most abundant isoforms of crustins identified from the hemocytes of the black tiger shrimp, *Penaeus monodon*. Crustin*Pm*1 inhibits only Gram-positive bacteria, while crustin*Pm*7 acts against both Gram-positive and Gram-negative bacteria. This work aims to characterize the molecular properties of recombinant crustin*Pm*1 and crustin*Pm*7, and the regulatory pathways of these two crustins. Circular dichroism spectroscopy revealed that crustin*Pm*1 contained 40.81% alpha-helix and 22.34% beta-sheet, whereas crustin*Pm*7 is made up of 32.86% alpha-helix and 27.53% beta-sheet. Crustin*Pm*1 and crustin*Pm*7 bound to phosphatidic acid (PA) with positive cooperativity of Hill slope (H) > 2, indicating that at least two molecules of crustins bind with one PA molecule. It is worth noting that both crustins bound to PA with significantly higher affinity than to lipoteichoic acid (LTA) and lipopolysaccharide (LPS). We speculate that crustin might also achieve antimicrobial activity by targeting PA, a signaling lipid. Regulatory pathways of crustin*Pm*1 and crustin*Pm*7 were investigated by knockdown of *Pm*Relish and *Pm*MyD88. This study demonstrated that crustin*Pm*1 is mediated through the Toll signaling pathway, while crustin*Pm*7 is regulated via both Toll and Imd pathways.

© 2016 Elsevier Ltd. All rights reserved.

1. Introduction

Crustin is a cationic cysteine-rich antimicrobial peptide that contains a signal peptide at the amino terminus and a single whey acidic protein (WAP) domain at the carboxyl terminus. It is mainly found in the plasma and hemocyte granules of shrimps. From the previous review, crustins are classified into three subgroups based on the structure of the central region (Smith et al., 2008). Type I crustin, found in crabs, lobsters, and crayfish, contains a cysteine-rich region and the WAP domain, which is an incomplete four-disulphide core (4-DSC). Type II crustins possess a long glycine-rich region between the signal sequence and cysteine-rich region, followed by the WAP domain. Type II crustins are mainly present in shrimps, and the glycine-rich domain is often arranged as repeat VGGGLG motifs that vary in number from 5 to 8 (Amparyup et al., 2008b; Donpudsa et al., 2014; Supungul et al., 2004, 2008; Vargas-Albores et al., 2004; Zhang et al., 2007). However, some Type II crustins, e.g. crustin-like or crustin*Pm7* from *P. monodon*, contain 22 glycine residues, and do not show the same VGGGLG repeat (Amparyup et al., 2008b). Type III crustins contain a proline-arginine rich domain and the WAP domain. Type III crustins are commonly known as single-whey acidic domain (SWD) proteins and are reported in several shrimp species (Amparyup et al., 2008a; Jia et al., 2008; Jimenez-Vega et al., 2004; Rojtinnakorn et al., 2002).

The WAP domain has diverse functions, including proteinase inhibition (Sallenave, 2000) and antimicrobial activity (Shugars, 1999; Wiedow et al., 1998). Synthesized Type I crustin from *Marsupenaeus japonicas*, *Mj*Cru I-1, containing the WAP domain, but not a cysteine-rich domain showed antibacterial and agglutinative activities (Liu et al., 2015). In contrast, Type II crustin*Pm*1 from *Penaeus monodon* containing the WAP domain, but not glycine-rich

Abbreviations: AMPs, antimicrobial peptides; *Pm*, *Penaeus monodon*.

* Corresponding author.
E-mail address: Kuakarun.K@chula.ac.th (K. Krusong).

http://dx.doi.org/10.1016/j.dci.2016.10.015
0145-305X/© 2016 Elsevier Ltd. All rights reserved.

and cysteine-rich domains, showed no antibacterial activity against *Staphylococcus aureus* (Suthianthong et al., 2012). However, deletion mutants of crustin*Pm*1 where either the glycine-rich or the cysteine-rich domains were deleted exhibited some antibacterial activity. This emphasized the important of the *N*-terminal glycine-rich and cysteine-rich regions on the antimicrobial activity of crustin*Pm*1.

Crustin acts against microbial pathogens via both antibacterial and agglutinative activities (Arockiaraj et al., 2013; Krusong et al., 2012). In addition, *Mj*Cru I-1 promotes hemocyte phagocytosis (Liu et al., 2015). Our previous study showed that crustin*Pm*1 and crustin*Pm*7 bound to bacterial cell wall components with high affinities, potentially leading to bacterial agglutination and disruption of the physiochemical properties of the bacterial surface (Krusong et al., 2012).

This work aims to characterize the molecular properties and regulatory pathways of crustin*Pm*1 and crustin*Pm*7, the two most abundant isoforms found in the hemocytes of *P. monodon*. Although, both crustins bind to Gram-positive and Gram-negative bacterial cells, only crustin*Pm*7 exhibits antimicrobial activity against both Gram-positive and Gram-negative bacteria (Amparyup et al., 2008b; Krusong et al., 2012; Supungul et al., 2008). We hypothesized that expression of crustin*Pm*1 and crustin*Pm*7 may be regulated by different pathways. In *Drosophila melanogaster,* two separated intracellular signal transduction pathways, Toll and immune deficiency (Imd), are responsible for controlling the antibacterial and antifungal responses (Lemaitre et al., 1995, 1996). The Toll and Imd pathways were stimulated by recognition of pathogen associated molecules, such as peptidoglycans, to induce antimicrobial responses. These two pathways are homologous to the mammalian Toll-like receptor (TLR) and tumor necrosis factor receptor (TNFR) signaling pathways, respectively, and are essential for Drosophila to survive infection. Toll pathway is involved in fungal and Gram-positive bacterial infections, while the signaling cascade of Imd pathway is stimulated by Gram-negative bacterial infections but not fungal infections. The genetic requirements of the signaling components in these two pathways are independent (Lemaitre et al., 1995). In shrimp, several components of the Toll and Imd pathways have been identified such as *Fenneropenaeus chinensis* FcSpätzle (Shi et al., 2009), *Litopenaeus vannamei Lv*IMD (Wang et al., 2009), *Lv*Dorsal (Huang et al., 2010), *Pm*Toll (Assavalapsakul and Panyim, 2012), *Pm*MyD88 (Deepika et al., 2014), and *Pm*Relish (Visetnan et al., 2015).

In this work, recombinant crustin*Pm*1 and crustin*Pm*7 were produced in *Pichia pastoris* and used for molecular characterization. Assays to test binding affinities of the two crustin isoforms to bacterial cell wall components and lipids were performed. To investigate the regulatory pathways of crustin*Pm*1 and crustin*Pm*7, expression levels of several genes in shrimp immunity were measured by quantitative real time RT-PCR after Gram-positive (*S. aureus*) and Gram-negative (*Vibrio harveyi*) bacteria challenges. The role of these immune pathways on expression levels of crustin*Pm*1 and crustin*Pm*7 were confirmed by RNA interference experiments.

2. Materials and methods

2.1. Plasmid construction, expression and purification of recombinant crustinPm1 and crustinPm7

Both recombinant crustin*Pm*1 and crustin*Pm*7 were expressed in *P. pastoris.* Recombinant *P. pastoris* with crustin*Pm*1 gene was a gift from Dr. Premruethai Supungul. Plasmid carrying crustin*Pm*7 was constructed by insertion of crustin*Pm*7 gene into pPIC9K, a yeast transfer vector under AOX1 promoter, via *Eco*R I and *Nco* I sites. In brief, specific primers (forward: 5′GATGAATTCCATCATCAT CATCATCACCAGGATAAAGGCAATGCCGA3′, which introduced an *Eco*R I site and an *N*-terminal 6 × His-Tag at 5′ end, and reverse: 5′ CTGCGGCCGCCTATCCC TGAGAACCTGCCA 3′, which introduced a *Not* I site at 3′ end) were used to amplify the crustin*Pm*7 gene (Genbank accession no. EF654658) from cDNA of unchallenged shrimp. PCR reactions were performed as follows: 94 °C for 2 min, 30 cycles of 94 °C for 30 s, 55 °C for 30 s, and 72 °C for 1 min. The amplified crustin*Pm*7 gene fragment (426 bp) was ligated into pPIC9K vector (Invitrogen), and the ligation mixture transformed into the *Escherichia coli* strain XL-1 Blue competent (Stratagene). *E. coli* harboring pPIC9K-crustin*Pm*7 were verified by sequencing (Macrogen Inc., Korea) and the recombinant plasmid was linearized by *Sac* I. Approximately, 5–10 μg of linearized DNA was transformed into *P. pastoris* strain GS115 competent and the His^+ GS115 transformants were subjected to screening for Mut^+ (Methanol utilization plus) and Mut^S (Methanol utilization slow) phenotypes. Colonies containing crustin*Pm*7 gene were confirmed by direct PCR amplification.

Recombinant crustin*Pm*1 and crustin*Pm*7 was expressed in *P. pastoris* strain GS115 and tranformants that displayed the highest expression were selected by Geneticin®. A single colony of *P. pastoris* harbouring either crustin*Pm*1 or crustin*Pm*7 gene was grown in 5 ml of Buffered Glycerol-complex Medium (BMGY) media at 30 °C with 280 rpm shaking overnight. The culture was then diluted 1:100 in a 100 ml of fresh BMGY and grown at 30 °C with 280 rpm shaking until the OD_{600} reached 4. Cells were then harvested by centrifugation at 8000×*g* for 10 min, the cell pellet was resuspended in 1/5 of the original volume of Buffered Methanol-complex Medium (BMMY), and incubated at 30 °C with shaking. Expression of crustin*Pm*1 and crustin*Pm*7 was induced by addition of 100% methanol to a final concentration of 0.5% every 24 h for 3 days. The cells were centrifuged and the supernatant was kept for purification.

Crude proteins were filtered, added to a binding buffer (50 mM Tris-HCl pH 7.4, 20 mM imidazole and 300 mM NaCl) and equilibrated with Ni-NTA resin. The resin was then poured into a column and allowed to settle by gravity. The column was washed with binding buffer and the protein was eluted from the column with elution buffer (50 mM Tris-HCl pH 7.4, 150 mM imidazole and 300 mM NaCl). Finally, the purified protein was dialyzed in 10 mM MES, pH 5.8, and analyzed by 15% Sodium Dodecyl Sulfate Polyacrylamide Gel Electrophoresis (SDS-PAGE) and Western blot using anti-His monoclonal antibody (GE Healthcare). The concentration of purified protein was determined by Pierce® BCA Protein Assay Kit (Thermo scientific).

2.2. Antimicrobial activity assay

The antimicrobial activity of purified rcrustin*Pm*1 and rcrustin*Pm*7 was determined using Gram-positive (*S. aureus and Micrococcus luteus)* and Gram-negative bacteria (*E. coli 363 and V. harveyi)* as described in Krusong et al., 2012. Active proteins were then used in circular dichroism, lipid-protein interaction and binding experiments.

2.3. Circular Dichroism (CD)

The secondary structure of rcrustin*Pm*1 and rcrusti*Pm*7 was determined by a JASCO J-715 CD Spectropolarimeter, using a 1-mm-pathlenght quartz cell. (1S)-(+)-Camphor-10-sulfonic acid (CSA) was used for CD calibration. Purified rcrustin*Pm*1 and rcrustin*Pm*7 were diluted to 0.8 mg/ml in 10 mM Tris-HCl, pH 7.4 and scanned from wavelength of 190–240 nm using a bandwidth of 2 nm and a response time of 2 s with 50 nm/min scanning speed. The CD

spectra were converted to molar ellipticity in units of degree cm^2 $dmol^{-1}$ using Eq. (1):

$$[\theta] = \theta/(10 \times n \times C_p \times l) \quad (1)$$

Where θ is the ellipticity in millidegrees, n is the number of amino acid residues, C_p is the peptide molar concentration (M) and l is the cell path length (cm). The percentage of helical and β-sheet content of protein was analyzed using K2D3 (http://www.cbdm-01.zdv.uni-mainz.de/~andrade/k2d3/) (Louis-Jeune et al., 2011).

2.4. Lipid-protein interaction

Binding of rcrustin*Pm*1 and rcrustin*Pm*7 to various lipid components was determined using PIP Strips™ (Echelon). First, the strip membrane that contains dots of lipid was blocked with 3% BSA in PBS-T (PBS containing 0.1% (v/v) Tween™-20) for 1 h with gentle shaking, followed by addition of 0.5 μg/ml of rcrustin*Pm*1 or rcrustin*Pm*7 onto the membrane. After 1 h incubation at room temperature, the membrane was washed 3 times with PBS-T and incubated with anti-His monoclonal antibody in PBS-T 1:3000 (v/v) for 3 h. After washing, the membrane was incubated with peroxidase-conjugated secondary antibody against IgG (Abnova) in PBS-T 1:10,000 (v/v) for 1 h and the color change of the reaction was observed using 3,3′,5,5′-Tetramethylbenzidine (TMB) and H_2O_2.

2.5. Enzyme-linked immunosorbent assay (ELISA)

After lipid strip test, ELISA was carried out to quantitatively measure the binding of rcrustin*Pm*1 and rcrustin*Pm*7 to PA, LPS and LTA. Microtiter plate was coated with 100 μl/well of 30 μg/ml PA, LPS or LTA at 37 °C for 1 h and washed twice with PBS-T. The plate was blocked with 5% BSA in PBS-T and incubated with 100 μl of various concentrations of rcrustin*Pm*1 or rcrustin*Pm*7 for 1 h. The plate was washed twice with PBS-T before adding anti-His monoclonal antibody in PBS-T 1:3000 (v/v). After 2 h incubation, the plate was washed and incubated with alkaline phosphatase-conjugated secondary antibody against IgG in PBS-T 1:10,000 (v/v) dilution. One hundred microliter of substrate solution (*p*-nitrophenylphosphate) was added and the reaction was stopped by addition of 0.4 N NaOH. An absorbance at 405 nm was measured using SpectraMax M5 Multi-Mode Microplate Reader (Molecular Devices, Sunnyvale, CA, USA). The dissociation constants (K_d) and the maximum binding (B_{max}) parameters were calculated with GraphPad Prism version 6.0 for Windows (GraphPad Software, San Diego, CA, USA), using nonlinearly fitting as one site – Specific binding with Hill slope model (Eq. (2)):

$$Y = \left(B_{max}[X]^h\right) \Big/ \left((K_d)^h + [X]^h\right) \quad (2)$$

Where Y is the recorded absorbance, B_{max} is the maximum specific binding (absorbance), *[X]* is the protein concentration, h is the Hillslope and K_d is the apparent dissociation constant.

2.6. Effect of bacterial cell wall components on crustinPm1, crustinPm7, PmRelish, PmSpätzle, dorsal and PmMyD88 gene expression

2.6.1. Shrimp

Healthy black tiger shrimp of about 6–10 g body weight were obtained from the local farm at Suratthani province, Southern Thailand, and accommodated in laboratory aquaria at a temperature of 28 ± 4 °C and a salinity of 20 ppt for at least 5 days before use in experiments.

2.6.2. Preparation of heat-killed S. aureus and V. harveyi

A single colony of *S. aureus* was inoculated into LB broth containing 1% NaCl and cultured at 37 °C with 250 rpm shaking for 16–18 h. The overnight culture was then diluted 1:100 into a fresh LB broth and grown until OD_{600} reached 0.6, which given bacterial cell density of 10^8 CFU/ml by plate count method. The cell culture was heat-killed at 80 °C for 30 min and resuspended in 0.85% (w/v) NaCl in a ratio of 1:100, to obtain a final cell density of 10^6 CFU/ml.

For *V. harveyi* preparation, the bacteria were grown overnight on Thiosulfate Citrate Bile Salt Sucrose (TCBS) plate at 30 °C. Subsequently, a single colony of *V. harveyi* was inoculated in Tryptic Soy Broth (TSB) containing 2% NaCl and grown at 30 °C with 250 rpm shaking for 16–18 h. After that, the culture was diluted 1:100 into a fresh TSB and grown until OD_{600} reached 0.6, in which the bacterial cell density was 10^8 CFU/ml. The cell culture was heat-killed at 60 °C for 2 h and resuspended in 0.85% (w/v) NaCl in a ratio of 1:100, given a final cell density of 10^6 CFU/ml.

2.6.3. Gene expression in unchallenged and heat-killed bacteria challenged shrimp hemocytes

In this study, heat-killed *S. aureus* (Gram-positive bacteria) and *V. harveyi* (Gram-negative bacteria) were used to investigate the effect of bacterial cell wall components on the expression of crustin*Pm*1, crustin*Pm*7 and other genes in the Imd (*Pm*Relish) and Toll pathways (*Pm*Spätzle, Dorsal and *Pm*MyD88). Shrimp were divided into 2 groups (control and heat-killed bacteria challenged groups). Control shrimp were injected with 150 mM NaCl while challenged shrimp were injected with 50 μl of 10^6 CFU/ml bacteria. Hemocytes of nine individuals at each time point (3, 6, 12, 24 and 48 h post-injection, hpi) were collected by centrifugation at 800×*g* for 10 min at 4 °C and used for total RNA extraction by FavorPrep™ Tissue Total RNA Mini Kit (Favorgen). cDNA was synthesized by ImProm-II™ Reverse Transcription Kit (Promega).

Quantitative real-time PCR (qRT-PCR) was performed using iCycler-iQ™ Real-Time detection system (BIO-RAD) and the SsoFast™ EvaGreen® Supermix (BIO-RAD). Gene-specific primers used in this experiment are listed in Table 1. Elongation factor 1-α (EF1α) was used as an internal control to correct RNA loading variation. The qRT-PCR was run using a standard cycling program as follows: 1 cycle of 95 °C for 30 s, followed by 40 cycles of 95 °C for 15 s and 55 °C for 30 s, and performed in triplicate.

Comparative C_T method was used to compare gene expression in the two different samples (control and challenged shrimp) (Livak and Schmittgen, 2001). The fold change of gene expression was calculated as follows:

$$\text{Fold change} = 2^{-\Delta\Delta CT}$$

$$\Delta\Delta C_T = [(C_T \text{ of target gene} - C_T \text{ internal control}) \text{ challenge} - (C_T \text{ of target gene} - C_T \text{ internal control}) \text{ control}]$$

Statistical analysis was performed using a one-way ANOVA followed by a post-hoc test (Duncan's new multiple range test). Expression levels were considered to be significantly different when $P < 0.05$.

2.7. Knockdown of PmRelish and PmMyD88 gene by dsRNA-mediated RNA interference and quantitative determination of crustinPm1 and crustinPm7 transcript levels

Recombinant *Pm*Relish, *Pm*MyD88 and GFP plasmids were used as templates for *Pm*Relish (Rel) dsRNA, *Pm*MyD88 (MyD) dsRNA

Table 1
Nucleotide sequences of the primers.

Genes	Primers	Primer sequences (5′–3′)
Real-time PCR		
EF1- α	EF1α-F	5′-GGTGCTGGACAAGCTGAAGGC-3′
	EF1α-R	5′-CGTTCCGGTGATCATGTTCTTGATG-3′
crustin*Pm*1		
	*Pm*Crus1-F	5′-CTGCTGCGAGTCAAGGTATG-3′
	*Pm*Crus1-R	5′-AGGTACTGGCTGCTCTACTG-3′
crustin*Pm*7		
	*Pm*Crus7-F	5′-GGCATGGTGGCGTTGTTCCT-3′
	*Pm*Crus7-R	5′-TGTCGGAGCCGAAGCAGTCA-3′
*Pm*Relish		
	Relish-F	5′-TCTCCAGGTGAGCACTCAGTTGGC-3′
	Relish-R	5′-GCTGTAGCTGTTGCTGTTGTTGAG-3′
*Pm*Spätzle		
	Spätzle-F	5′-TAAGCAAGGAGCAGGAAGAG-3′
	Spätzle-R	5′-TGGCATACACCACATCTGAG-3′
Dorsal		
	Dorsal-F	5′-TCACTGTTGACCCACCTTAC-3′
	Dorsal-R	5′-GGAAAGGGTCCACTCTAATC-3′
*Pm*MyD88		
	MyD88-F	5′-GTGCACCAGAGTCATTGTAG-3′
	MyD88-R	5′-GGGAGTGGCAGAAACTTATC-3′
Gene silencing		
GFP	GFP1-T7-F	5′-TAATACGACTCACTATAGGATGGTGAGCAAGGGCGAGGA-3′
	GFP1-R	5′-TTACTTGTACAGCTCGTCCA-3′
	GFP2- F	5′-ATGGTGAGCAAGGGCGAGGA-3′
	GFP2-T7-R	5′-TAATACGACTCACTATAGGTTACTTGTACAGCTCGTCCA-3′
*Pm*Relish		
	Rel-T7-F	5′-GGATCCTAATACGACTCACTATAGGCTCGTGGTCAGGAAGACTCAAT-3′
	Rel-R	5′-GACTGGAGATGGAGACTGAATG
	Rel-F	5′-CTCGTGGTCAGGAAGACTCAAT-3′
	Rel-T7-R	5′-GGATCCTAATACGACTCACTATAGGGACTGGAGATGGAGACTGAATG-3′
*Pm*MyD88		
	MyD-T7-F	5′-TAATACGACTCACTATAGGCCTCAGCAAAGGTCTTGAAC-3′
	MyD-R	5′-CAGTCCACCAATTAGGTCTC-3′
	MyD-F	5′-CCTCAGCAAAGGTCTTGAAC-3′
	MyD-T7-R	5′-TAATACGACTCACTATAGGCAGTCCACCAATTAGGTCTC-3′

and GFP dsRNA synthesis, respectively. Two sets of primers specific to each gene were used to introduce T7 RNA polymerase promoters (underline) at the 5′-end of the PCR products (Table 1). The two PCR products (as sense and antisense DNA) were separately amplified by the following conditions: 94 °C for 2 min, followed by 36 cycles of 94 °C for 30s, 60 °C for *Pm*Relish, 55 °C for *Pm*MyD88 or 58 °C for GFP for 30s and 72 °C for 30s, and a final extension at 72 °C for 10 min. The two PCR product templates were used to produce two complementary single-stranded RNAs by the T7 RiboMAX™ System (Promega) and the complementary single-stranded RNAs were then mixed, incubated at 70 °C for 10 min, and then slowly cooled to room temperature to form a dsRNA. Synthesized *Pm*Relish dsRNA, *Pm*MyD88 dsRNA and GFP dsRNA were analyzed by 1.8% agarose gel electrophoresis and concentrations of the dsRNAs were determined by measuring absorbance at 260 nm.

In knockdown experiments, shrimps of approximately 2–5 g were divided into four groups (nine individuals per group) and injected with either (i) *Pm*Relish dsRNA (5 μg per g shrimp) or (ii) *Pm*MyD88 dsRNA (7.5 μg per g shrimp) or (iii) GFP dsRNA (control group) or (iv) 150 mM NaCl (control group). All hemolymph samples in each group were collected at 24 h post-dsRNA injection (hpi) for RNA extraction and cDNA synthesis. RT-PCR was conducted to determine *Pm*Relish, *Pm*MyD88, and EF1α gene expression levels. RT-PCR was carried out as followed: 1 cycle of 94 °C for 3 min, followed by 30 cycles of 94 °C for 30 s, 50 °C for 30 s and 72 °C for 30 s.

Shrimps were divided into two groups for heat-killed *S. aureus* and *V. harveyi* challenge. Each group contained nine individuals that were pre-injected with 20 μl of either (i) 150 mM NaCl, (ii) GFP dsRNA (5 μg or 7.5 μg per g shrimp), or (iii) *Pm*Relish dsRNA (5 μg per g shrimp) or (iv) *Pm*MyD88 dsRNA (7.5 μg per g shrimp). After 24 h, inactivated *S. aureus* and *V. harveyi* (10^6 CFU/ml) mixed with either 150 mM NaCl, GFP dsRNA (5 μg or 7.5 μg per g shrimp), *Pm*Relish dsRNA (5 μg per g shrimp) or *Pm*MyD88 dsRNA (7.5 μg per g shrimp) were injected intramuscularly to shrimp. The hemolymph was taken from each individual at 12 and 24 hpi. Total RNA was extracted and used for cDNA synthesis. Transcription levels of crustin*Pm*1 and crustin*Pm*7 in each sample were analyzed by real-time PCR.

Statistical analysis was carried out from triplicate experiments using a One-Way ANOVA and Post Hoc test in SPSS version 21 software. The result differences were considered significant at $P < 0.05$ (*) and $P < 0.01$ (**).

3. Results

3.1. Expression and purification of the recombinant crustinPm1 and crustinPm7 in Pichia pastoris expression system and antimicrobial activity test

Previously, crustin*Pm*1 and crustin*Pm*7 were identified and the recombinant proteins were produced in the *E. coli* expression system (Amparyup et al., 2008b; Supungul et al., 2008). Both crustin*Pm*1 and crustin*Pm*7 were purified under a denaturing condition, which could possibly lead to protein misfolding during refolding process. As a result, some batches of recombinant crustin*Pm*1 and crustin*Pm*7 produced in *E. coli* exhibited no antimicrobial activity. This work aimed to express both crustin*Pm*1 and crustin*Pm*7 in the *P. pastoris* expression system and purify the recombinant proteins under a native condition.

Both pPIC9K-crustin*Pm*1 and pPICK9K-crustin*Pm*7 recombinant plasmids were successfully constructed (data not shown). The recombinant crustin*Pm*1 and crustin*Pm*7 were efficiently produced in *P. pastoris* strain GS115 in soluble form and then purified under native condition using a Ni-NTA affinity chromatography. As shown in Fig. 1., two major protein bands appeared just below 15 kDa, which were closed to the estimated size of rcrustin*Pm*1 (14.7 kDa) and rcrustin*Pm*7 (12.8 kDa). They were confirmed as rcrustin*Pm*1 and rcrustin*Pm*7 by Western immunoblotting using anti-His monoclonal antibody. In addition, a minor protein band of approximately 30 kDa was observed in rcrustin*Pm*7 fraction. This band was presumably a dimer form of rcrustin*Pm*7, which may form through the disulfide cross-link (the protein has 12 cysteine residues).

To ensure rcrustin*Pm*1 and rcrustin*Pm*7 are in their active form, the proteins were assayed for their antimicrobial activities. The minimal inhibitory concentration (MIC) value was reported as a range between the highest concentration of the protein where bacterial growth was observed and the lowest concentration that kills 100% of bacteria. The result showed that purified rcrustin*Pm*1 exhibited strong antibacterial activity against Gram-positive bacteria, *S. aureus* (MIC 3.5–5 μM) and *M. luteus* (MIC 20–50 μM), but not Gram-negative bacteria, *E. coli* 363 (MIC 50–80 μM) and *V. harveyi*. Meanwhile, rcrustin*Pm*7 was active against both Gram-positive and Gram-negative bacteria, with MIC values ranging from 2 to 10 μM. The MIC values determined in these experiments were similar to those in previous studies (Amparyup et al., 2008b; Supungul et al., 2008).

3.2. CD measurement

Fig. 2 showed CD spectra for rcrustin*Pm*1 and rcrustin*Pm*7. The result suggested that crustin*Pm*1 contained 40.81% alpha-helix and 22.34% beta-sheet, whereas crustin*Pm*7 possessed 32.86% alpha-helix and 27.53% beta-sheet.

3.3. Lipid and cell wall components binding assay

3.3.1. Lipid-protein interaction

To investigate the binding ability of rcrustin*Pm*1 and rcrustin*Pm*7 to lipid components, PIP strips™ (Echelon), containing15 different biologically active lipids at 100 pmol, was used. Fig. 3

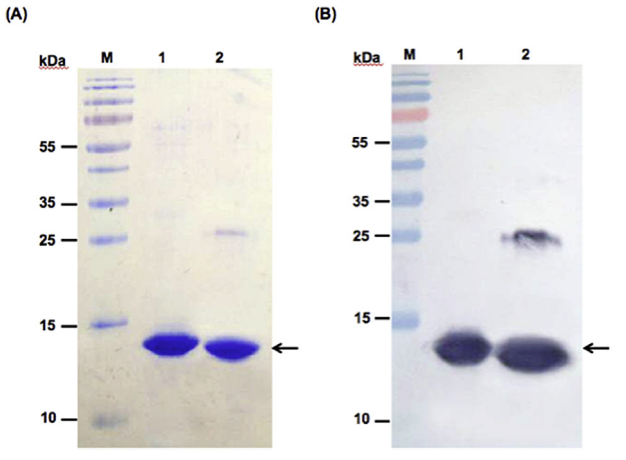
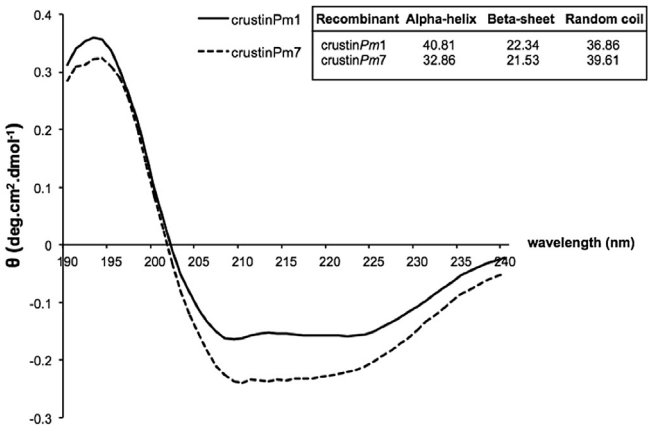


Fig. 1. SDS-PAGE (A) and Western blot (B) of purified rcrustin*Pm*1 and rcrustin*Pm*7 produced in *P. pastoris* expression system.
The expected bands of the rcrustin*Pm*1 and rcrustin*Pm*7 are indicated by the arrow. Lane M: Prestained protein marker; Lane 1: purified rcrustin*Pm*1; Lane 2: purified rcrustin*Pm*7.



Recombinant	Alpha-helix	Beta-sheet	Random coil
crustin*Pm*1	40.81	22.34	36.86
crustin*Pm*7	32.86	21.53	39.61

Fig. 2. CD spectra of rcrustin*Pm*1 and rcrustin*Pm*7.

shows the color change of lipid spots to purple, while blank spots remained blue. PA spots developed a dark purple color within a few minute, suggesting that rcrustin*Pm*1 and rcrustin*Pm*7 rapidly bound to PA. As shown in Fig. 3, both rcrustin*Pm*1 and rcrustin*Pm*7 bound to PA with higher affinity than to other lipids.

3.3.2. Binding properties of rcrustinPm1 and rcrustinPm7 to PA, LTA and LPS

Quantitative bindings of rcrustin*Pm*1 and rcrustin*Pm*7 to PA, LTA and LPS were carried out by Enzyme-linked immunosorbent assay (ELISA). PA is a part of common phospholipids that are major constituents of prokaryote cell membranes. LTA is a major constituent of the cell wall of Gram-positive bacteria, while LPS is a main component of the outer membrane of Gram-negative bacteria.

Both rcrustin*Pm*1 and rcrustin*Pm*7 bound to PA, LTA and LPS in a concentration dependent manner (Fig. 4). Both proteins bound to PA at least 10 times more tightly, than to LTA or LPS. As shown in Fig. 4A, rcrustin*Pm*1 bound to PA, LTA, and LPS with an apparent dissociation constant (K_d) value of 8.672×10^{-8} M with Hill slope (H) of 2.153 for PA, a K_d of 1.146×10^{-7} M with H of 2.153 for LTA and a K_d of 4.131×10^{-6} M with H of 2.771 for LPS. Meanwhile, rcrustin*Pm*7 showed a K_d of 9.719×10^{-8} M with H of 2.276 for PA, a K_d of 1.499×10^{-7} M with H of 2.141 for LTA and a K_d of 1.658×10^{-7} M with H of 2.169 for LPS (Fig. 4B). Hill slope (H) > 2 indicated positive cooperativity, in which at least two molecules of crustin bind with one molecule of PA, LTA or LPS.

3.4. Effect of bacterial cell wall components injection on genes expression

It was obvious that crustins play an important role against bacterial infection in *P. monodon* (Amparyup et al., 2008b; Supungul et al., 2008). In order to investigate a pathway that regulates crustin*Pm*1 and crustin*Pm*7 gene expression, shrimp were injected with heat-killed *S. aureus* and *V.* harveyi and the expression of genes in the shrimp immune system, including crustin*Pm*1, crustin*Pm*7, *Pm*Relish, *Pm*Spätzle, *Pm*MyD88 and Dorsal, were measured. *Pm*Relish belongs to the Imd pathway, while *Pm*Spätzle, *Pm*MyD88 and Dorsal are part of the Toll pathway.

The expression profiles of crustin*Pm*1 in shrimp after stimulation by heat-inactivated *S. aureus* and *V. harveyi* are shown in Fig. 5A. At 3 and 6 hpi, the expression levels of crustin*Pm*1 in shrimp stimulated by *S. aureus* and *V. harveyi* were either significantly down-regulated or unchanged, compared with the NaCl group at the same sampling point. Crustin*Pm*1 expression in the

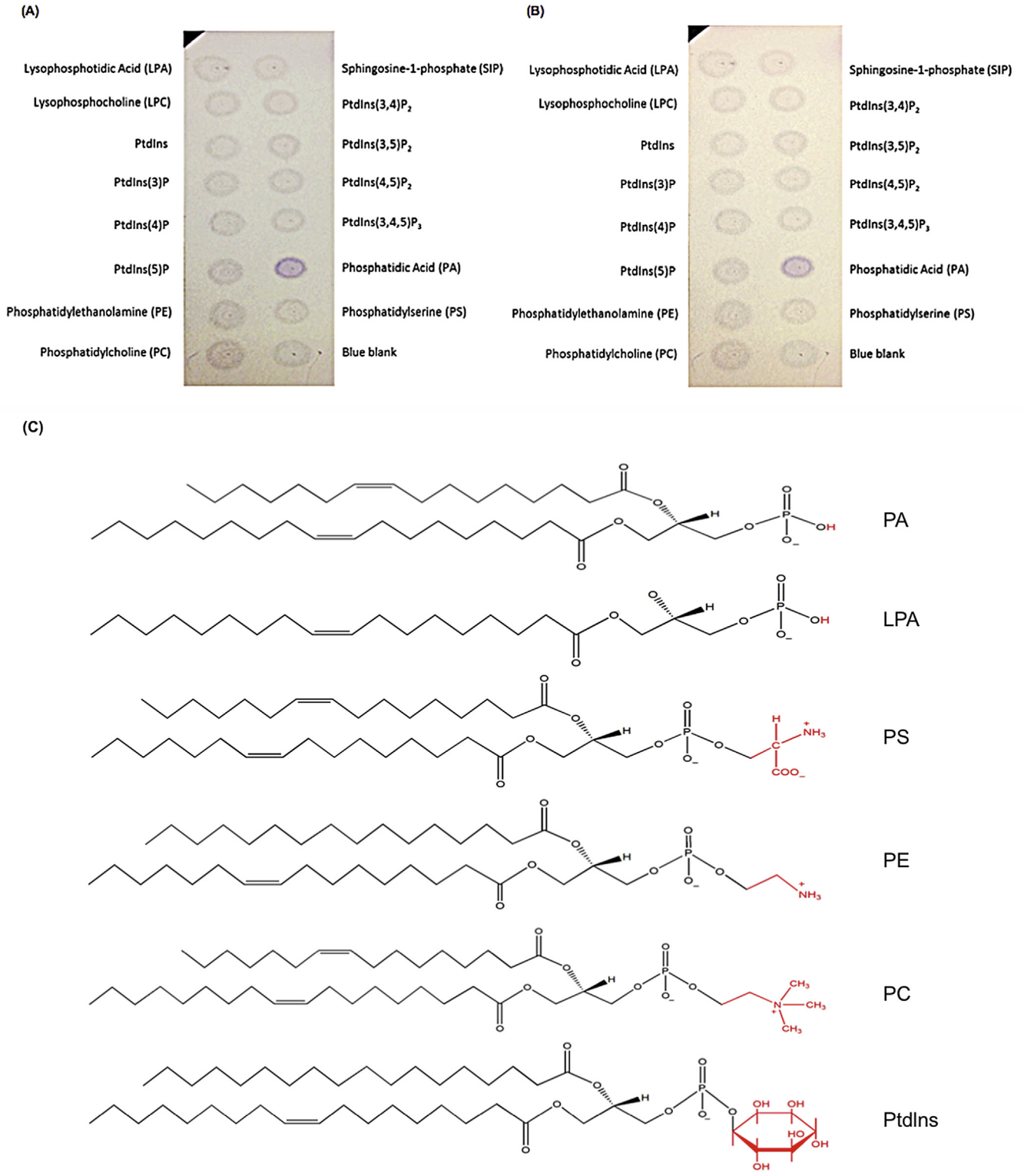


Fig. 3. The rcrustin*Pm*1 (A) and rcrustin*Pm*7 (B) were incubated with lipid strips and the bound proteins were probed by anti-His tag antibody. The structures of phospholipid PA, PLA, PS, PE, PC and PtdIns are shown in (C). The types of fatty acids esterified to the glycerol-3-phosphate backbone are arbitrarily drawn.

S. aureus-injected group was remarkably up-regulated at 12 and 24 hpi, and decreased at 48 hpi, compared to that of the NaCl-injected group. In contrast, crustin*Pm*1 expression levels in the *V. harveyi*-injected group remained unchanged at 12, 24 and 48 hpi. Clearly, crustin*Pm*1 responded highly to *S. aureus* injection, but not to *V. harveyi*.

Fig. 5B shows the expression profiles of crustin*Pm*7 in shrimp after stimulation by heat-killed *S. aureus* and *V. harveyi*. Similar to the crustin*Pm*1 expression profile, transcription levels of crustin*Pm*7 after stimulation by *S. aureus* and *V. harveyi* were either down-regulated or unchanged at 3 and 6 hpi, compared with that of NaCl group. The transcription levels of crustin*Pm*7 in the *S. aureus*

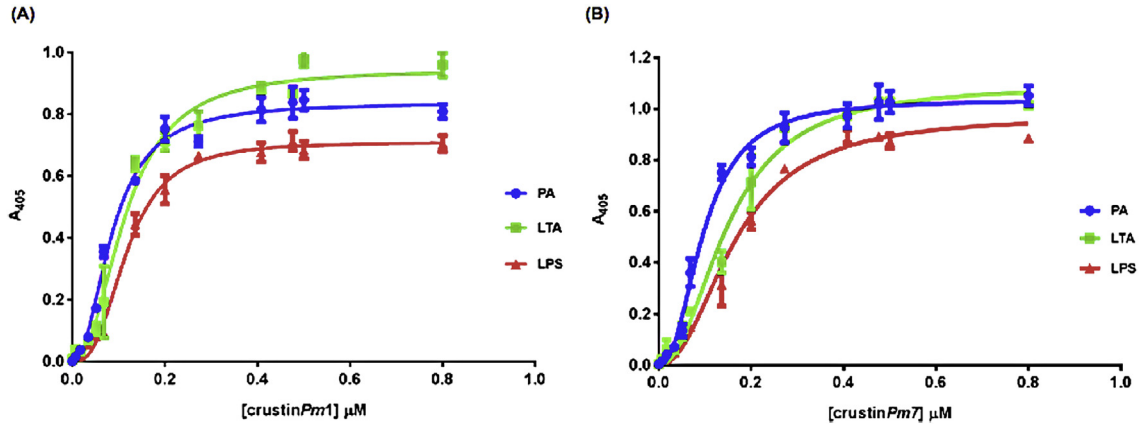


Fig. 4. Quantitative binding of rcrustin*Pm*1 (A) and rcrustin*Pm*7 (B) to PA, LTA, and LPS. The microtiter plates were coated with 3 μg of either PA (blue), LTA (green) or LPS (red) and then incubated with various amounts of rcrustin*Pm*1 and rcrustin*Pm*7. Bound crustin*Pm*s were detected by anti-histidine tag monoclonal antibody. The data are shown with the best fit to a nonlinear fit as one site-specific binding with Hill slope. (A) data for rcrustin*Pm*1, dissociation constant (K_d) values are as followed: PA, $K_d = 8.672 \times 10^{-8}$ M with Hill slope (H) = 2.153; LTA, $K_d = 1.146 \times 10^{-7}$ M with H = 2.241 and; LPS, $K_d = 4.131 \times 10^{-6}$ M with H = 2.771. (B) data for rcrustin*Pm*7, K_d values are as followed: PA, $K_d = 9.719 \times 10^{-8}$ M with Hill slope (H) = 2.276; LTA, $K_d = 1.499 \times 10^{-7}$ M with H = 2.141 and; LPS, $K_d = 1.658 \times 10^{-7}$ M with H = 2.169. (For interpretation of the references to colour in this figure legend, the reader is referred to the web version of this article.)

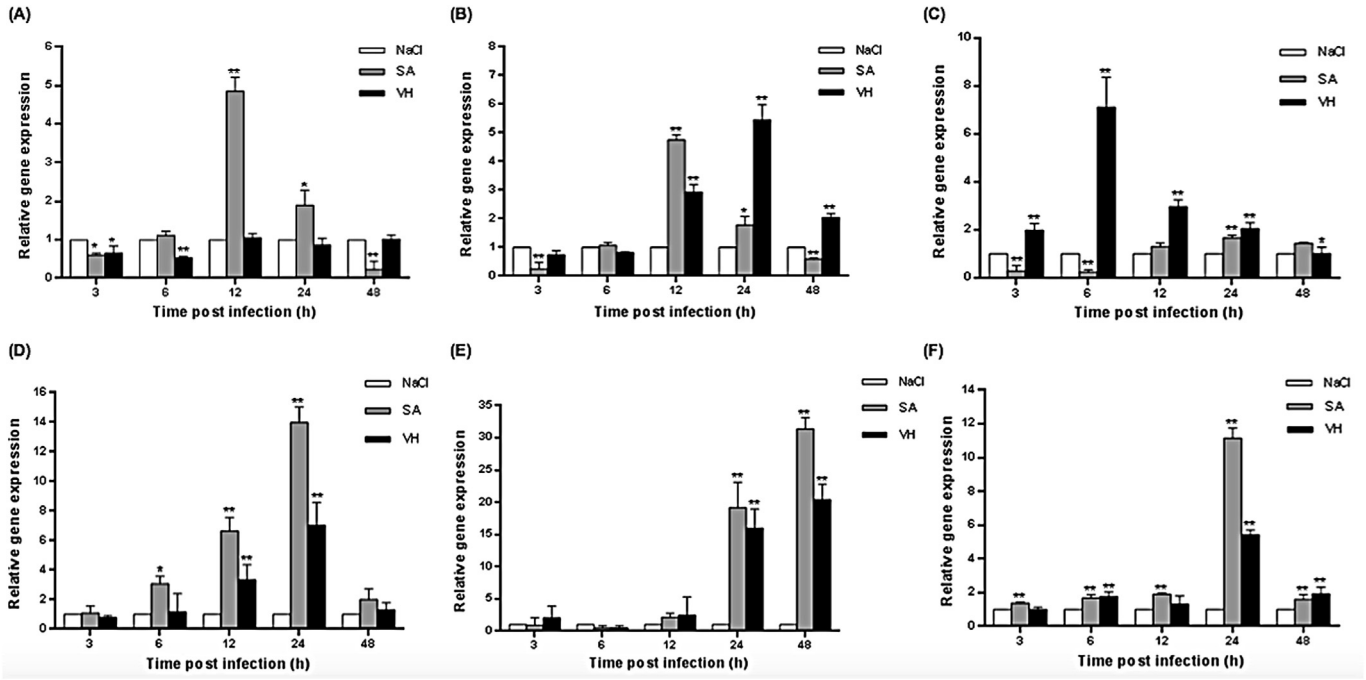


Fig. 5. Expression profiles of crustin*Pm*1 (A), crustin*Pm*7 (B), *Pm*Relish (C), *Pm*Spätzle (D), Dorsal (E) and *Pm*MyD88 (F) in shrimp hemocyte after bacterial challenge at different time points.
The relative expression of crustin*Pm*1 in treated groups, NaCl: experiment group with NaCl; SA: experiment group with *S. aureus* injection; VH: experiment group with *V. harveyi* injection. The mRNA expression levels of target genes were analyzed by Quantitative Real-time RT-PCR. The data were normalized to EF1α gene, which served as an internal control and shown as the mean ± SD. A single asterisk (*) and a double asterisk (**) indicate significant differences of $p < 0.05$ and $p < 0.01$, compared with control group, respectively. Experiments were carried out in triplicate.

group were increased by 4.5- and 1.6-fold at 12 and 24 hpi, respectively, and gradually decreased at 48 hpi. In contrast, crustin*Pm*7 was significantly up-regulated upon *V. harveyi* challenge by 2.9-fold and 5.3-fold at 12 and 24 hpi, respectively, and remained up-regulated by 2-fold at 48 hpi. Unlike crustin*Pm*1, crustin*Pm*7 responded highly to both *S. aureus* and *V. harveyi* injection.

The expression profiles of *Pm*Relish, a candidate gene of the Imd pathway, after *S. aureus* and *V. harveyi* injection are shown in Fig. 5C. *S. aureus* injection seemed to caused small changes in *Pm*Relish expression as the gene was down-regulated at 3 and 6 hpi, showed no significant change at 12 hpi, followed by a small up-regulation (1.8 fold) at 24 hpi and a small drop at 48 hpi. *V. harveyi* injection, however, triggered drastic changes in the *Pm*Relish expression profile. After heat-killed *V. harveyi* challenge, the transcription level of *Pm*Relish was increased by 2 fold at 3 hpi, reached its highest level (7.3 fold) at 6 hpi and remained up-regulated at 12, 24 and 48 hpi. Apparently, *Pm*Relish plays a role in *V. harveyi* infection.

The role of the Toll pathway in bacterial infection was investigated by monitoring expression of the three candidate genes in the

Toll pathway, *Pm*Spätzle, Dorsal and *Pm*MyD88, after heat-inactivated *S. aureus* and *V. harveyi* challenge (Fig. 5D–F). Fig. 5D shows that the expression levels of *Pm*Spätzle were continuously increased after stimulation by both *S. aureus* and *V. harveyi*, and reached their highest level at 24 hpi. At 24 hpi, *Pm*Spätzle was up-regulated by 14.2 and 7.3 fold after *S. aureus* and *V. harveyi* injection, respectively. It is likely that both *S. aureus* and *V. harveyi* injection could trigger *Pm*Spätzle expression.

As shown in Fig. 5E, both heat-killed *S. aureus* and *V. harveyi* injection also altered Dorsal expression level. Dorsal was significantly up-regulated at 24 hpi (>15 fold) and 48 hpi (>20 fold) after *S. aureus* and *V. harveyi* injection. Seemingly, dorsal gene was greatly induced at a late phase of bacterial injection.

Fig. 5F demonstrates that the transcription level of *Pm*MyD88 was significantly up-regulated at 3–48 hpi after bacterial injection. At 24 hpi, *Pm*MyD88 transcript levels were increased by 11 and 5.2 fold upon *S. aureus* and *V. harveyi* injection, respectively. This result suggested that *Pm*MyD88 responded to both *S. aureus* and *V. harveyi* infection.

3.5. Effect of PmRelish knockdown on crustinPm1 and crustinPm7 transcript levels

The Imd and Toll pathways are two distinct signal transduction pathways, involved in AMPs gene expression. Rel/NF-kB transcription factors, Relish, are activated in the signaling cascade of the Imd pathway for antibacterial responses, while Spätzle, Dorsal and MyD88 are required for the Toll pathway to turn on the gene expression of AMPs.

Study of the expression of crustin*Pm*1, crustin*Pm*7, *Pm*Relish, *Pm*Spätzle, Dorsal and *Pm*MyD88 genes after bacterial infection, pointed out that genes in the Imd and the Toll pathways may regulate crustin expression upon bacterial infection. To confirm this, *Pm*Relish and *Pm*MyD88, candidate genes of the Imd and the Toll pathways, were knocked down by RNAi, and subsequent expression levels of crustin*Pm*1 and crustin*Pm*7 were monitored after bacterial injection.

RT-PCR analysis showed that the *Pm*Relish transcript level was significantly decreased in the *Pm*Relish dsRNA knockdown shrimp, whereas injection of GFP dsRNA had no effect on the *Pm*Relish mRNA transcript level, when compared to that in NaCl injection group (Fig. 6A). This indicated that *Pm*Relish dsRNA injection successfully suppressed the expression of *Pm*Relish at 24 hpi.

Next, *Pm*Relish-silenced shrimp were injected with either heat-inactivated Gram-positive bacteria (*S. aureus)* or Gram-negative bacteria (*V. harveyi),* mixed with dsRNA to ensure gene knockdown. It was clear that, after bacterial challenge, *Pm*Relish-silenced shrimp exhibited significantly lower levels of crustin*Pm*7 transcript than control shrimp (Fig. 6B and C). However, *Pm*Relish silencing showed no effect on crustin*Pm*1 expression upon *S. aureus* and *V. harveyi* injection. It is likely that crustin*Pm*7 is regulated by Imd pathway but crustin*Pm*1 is not.

3.6. Effect of PmMyD88 knockdown on crustinPm1 and crustinPm7 transcript levels

As shown in Fig. 7A, *Pm*MyD88 was completely silenced at 24 h after *Pm*MyD88 dsRNA injection. In contrast, injection of either GFP dsRNA or 150 mM NaCl did not affect *Pm*MyD88 transcript levels.

To investigate the role of *Pm*MyD88 on crustin*Pm*1 and crustin*Pm*7 expressions, *Pm*MyD88-silenced shrimp were injected with heat-killed bacteria. Fig. 7B showed that, after *S. aureus* injection, transcription levels of both crustin*Pm*1 and crustin*Pm*7 in *Pm*MyD88-silenced shrimp were significantly lower than in control shrimp. Similar effects were also found in *Pm*MyD88-depleted shrimp injected with *V. harveyi,* of which crustin*Pm*1 and crustin*Pm*7 expressions were reduced by 2–5 folds at 12 and 24 hpi, in comparison with the control group (Fig. 7C). Evidently, knockdown of *Pm*MyD88, a gene in the Toll pathway, reduced both crustin*Pm*1 and crustin*Pm*7 transcripts.

4. Discussion

AMPs are found in the innate immune system of both invertebrates and vertebrates. They act directly against invading microorganisms, including bacteria, fungi, viruses, parasites, and yeast; and some can modulate the activities of the innate and adaptive immune systems. The mechanisms of AMPs may occur through electrostatic bonding between AMPs and the negatively charged surface of bacteria or viruses, leading to interruption of the cell function (Bahar and Ren, 2013; Hancock et al., 2006).

In previous studies, rcrustin*Pm*1 has been reported to act effectively against Gram-positive bacteria only while rcrustin*Pm*7 inhibits both Gram-positive and Gram-negative bacteria (Amparyup et al., 2008b; Supungul et al., 2008). Nevertheless, both isoforms can bind to Gram-positive and Gram-negative bacteria, and exhibit tight binding to LTA and LPS, the major cell wall components of Gram-positive and Gram-negative bacteria, respectively (Krusong et al., 2012). It is likely that crustins operate through bacterial agglutination and disruption of membrane integrity, resulting in bacterial killing.

This work aims to further investigate the molecular properties and regulatory pathways of crustin*Pm*1 and crustin*Pm*7. In this work, rcrustin*Pm*1 and rcrustin*Pm*7 were produced in *P. pastoris* expression system, in order to avoid protein misfolding during the purification process. Both crustin*Pm*1 and crustin*Pm*7 produced in this study exhibited antimicrobial activity with MIC values similar to those reported in Supungul et al., 2008 and Amparyup et al., 2008b.

CD analysis revealed the proportion of alpha-helix and beta-sheet of both crustin*Pm*1 and crustin*Pm*7. These alpha-helix and beta-sheet conformations are postulated to be a part of the WAP domain at the *C*-terminus of crustins, while random coils (approximately 35–40%) are possibly located at the *N*-terminus. WAP domains contribute to various biological functions such as protease inhibitors or antimicrobial properties. Previously, in mammals, secretory leukocyte proteinase inhibitor contains two WAP domains; one of which, at the *N*-terminus, possesses antimicrobial activity while another WAP domain, at the *C*-terminus, contains proteinase inhibitory activity (Fitch et al., 2006; Moreau et al., 2008). The WAP domain of crustin*Pm*1 alone, however, exhibited no antibacterial activity (Suthianthong et al., 2012). In contrast, truncated crustin*Pm* 1 mutants with either glycine-rich or cysteine-rich domains deletion showed some antibacterial activity. It is possible that the *N*-terminal glycine-rich and cysteine-rich domains play an important role in initiate electrostatic interactions with the negatively charged cell membrane and may insert into the membrane interior.

To further investigate binding of crustin*Pm*1 and crustin*Pm*7 to lipids and cell wall components, PIP strips™ (Echelon) were used for initial screening. Among 15 different bioactive lipids on PIP strips™, rcrustin*Pm*1 and rcrustin*Pm*7 appeared to bind best to PA, a diacyl-glycerophospholipid, consisting of two fatty acids and a phosphate group covalently linked to a glycerol backbone. PA is a precursor for the biosynthesis of membrane phospholipids. It also interacts with various proteins, and activates enzyme catalytic activities and/or recruits these proteins to membranes. As a result, PA mediates a wide variety of cellular activities such as vesicular trafficking, cytoskeletal organization, secretion, cell proliferation and survival (Liu et al., 2013).

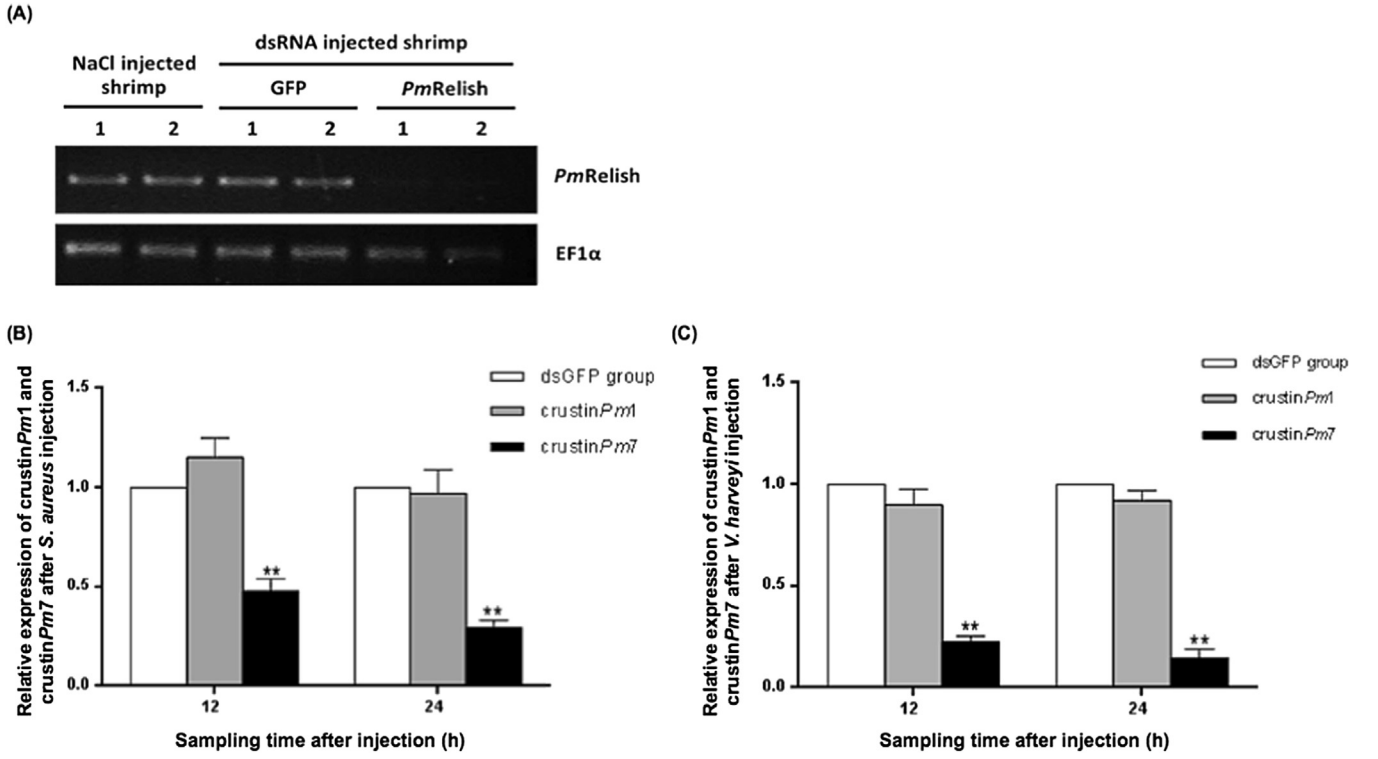


Fig. 6. Effect of *Pm*Relish silencing on crustin*Pm*1 and crustin*Pm*7 transcript levels in shrimp, after heat-inactivated *S. aureus* and *V. harveyi* challenge.
(A) Determination of *Pm*Relish transcript level in *P. monodon* hemocytes after *in vivo* RNAi-mediated gene silencing. Either 150 mM NaCl, GFP dsRNA (5 μg per g shrimp) or *Pm*Relish dsRNA (5 μg per g shrimp) were injected into shrimp. Each lane represents an individual shrimp. The mRNA expression levels of *Pm*Relish were analyzed by RT-PCR using EF1α as an internal control. (B) Relative expression of crustin*Pm*1 and crustin*Pm*7 after *S. aureus* injection in *Pm*Relish-silenced shrimp. (C) Relative expression of crustin*Pm*1 and crustin*Pm*7 after *V. harveyi* challenged in *Pm*Relish-depleted shrimp. Shrimp were divided into three groups and injected with 150 mM NaCl, GFP dsRNA (5 μg per g shrimp) or *Pm*Relish dsRNA (5 μg per g shrimp) before bacterial injection. The hemocytes were collected at 12 and 24 h after bacterial challenge and used for determination of crustin*Pm*1 and crustin*Pm*7 expressions by Quantitative Real-time RT-PCR. Gene expression level of knockdown shrimp was normalized to that of control group. The data are shown as the mean ± standard deviation. A single asterisk (*) indicates significant differences from control group ($p < 0.05$) and a double asterisk (**) represents significant differences from control group ($p < 0.01$). Experiments were carried out in triplicate.

Clearly, crustin*Pm*1 and crustin*Pm*7 bound to PA with much higher affinity than to other lipids. As seen in Fig. 3C, phosphatidylinositol (PtdIns), phosphatidylserine (PS), phosphatidylethanolamine (PE) and phosphatidylcholine (PC) differ from PA as they have hydrophilic head groups, attached to the basic phospholipid structure. These head groups have positive charges, which may not interact well with crustin, a cationic antimicrobial peptide. In addition, crustins bound poorly to lysophosphatidic acid (LPA), with a lack of fatty acid chain attached to C-2 of the glycerol backbone. This result suggested that the phosphate group and two fatty acids of PA may play a part in crustin binding. It is also possible that types of fatty acids esterified to the glycerol-3-phosphate backbone of the phospholipids may also influence crustin binding.

Quantitative binding assays of crustins and the cell wall components were carried out by ELISA. Binding properties of rcrustin*Pm*1 and rcrustin*Pm*7 produced in *P. pastoris* to LTA and LPS are similar to those in previous report, in which both recombinant crustins were expressed in *E. coli* (Krusong et al., 2012). Both rcrustin*Pm*1 and rcrustin*Pm*7 bound to PA, LTA and LPS in a sigmoidal manner and fit well to the Hill slope model with the H values < 2. This indicated that crustins bound to PA, LTA and LPS with a 2:1 stoichiometry in a positive cooperative manner. This binding behavior may be important for bacterial agglutinative activity and membrane-disrupting properties of crustins (Krusong et al., 2012).

Both rcrustin*Pm*1 and rcrustin*Pm*7 bound more tightly to PA than to LPS and LTA. Undoubtably, PA is one of the target molecules for the rcrustin*Pm*1 and rcrustin*Pm*7. PA is a component of the phospholipid membrane, as well as a backbone for the biosynthesis of other membrane phospholipids. PA also functions as a signaling messenger to modulate several proteins, including protein kinases and small G-proteins (McPhail et al., 1999; Zhang and Du, 2009). It is possible that the antimicrobial activity of crustin does not only rely on bacterial agglutinative activity and membrane-disrupting ability but also comes from the inhibition of intracellular proteins. MtDef4, a cysteine-rich defensin from *Medicago truncatula*, mediates its antifungal activity by permeabilizing fungal plasma membrane and entering into the fungal cells. Once in the cells, MtDef4 can bind to PA and affect intracellular targets (Sagaram et al., 2013).

It was evident that crustin*Pm*1 and crustin*Pm*7 possess different antimicrobial activity against Gram-positive and Gram-negative bacteria. Accordingly, we speculate that crustin*Pm*1 and crustin*Pm*7 gene expressions may be regulated by different pathways. In *Drosophila melanogaster*, two distinct intracellular signal transduction pathways, the Imd and Toll pathways, have been reported to control the antibacterial and antifungal responses (Lemaitre et al., 1995, 1996). Binding of pathogen molecules (e.g. peptidoglycan; PGN) to conserved host recognition proteins (e.g. PGRP-LC) transmits the signal to IMD, which controls at least three downstream events, including (i) IKK-dependent cleavage stimulated by TAK1; (ii) Fadd-DREDD interactions; and (iii) activation of the JNK cascade through TAK1. The first and second pathways activate Relish cleavage, resulting in the translocation of the REL domain of Relish to the nucleus, which ultimately regulates the transcriptions of immune-related genes. In addition, the JNK cascade, which

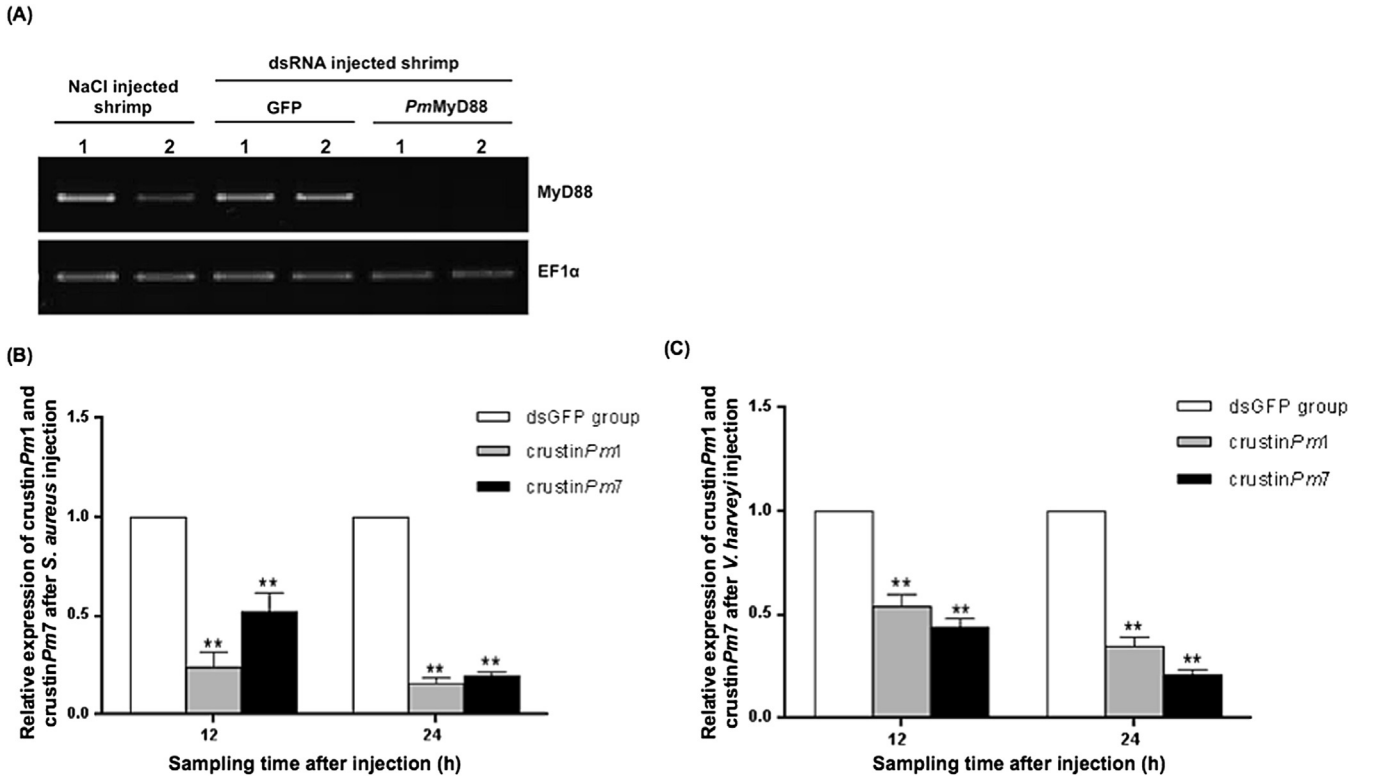


Fig. 7. Effect of *Pm*MyD88 silencing on crustin*Pm*1 and crustin*Pm*7 transcript levels in shrimp, after heat-inactivated *S. aureus* and *V. harveyi* challenge.
(A) Determination of *Pm*MyD88 transcript level in *P. monodon* hemocytes after *in vivo* RNAi-mediated gene silencing. Either 150 mM NaCl, GFP dsRNA (7.5 μg per g shrimp) or *Pm*MyD88 dsRNA (7.5 μg per g shrimp) were injected into shrimp. Each lane represents an individual shrimp. The mRNA expression levels of *Pm*MyD88 were analyzed by RT-PCR using EF1α as an internal control. (B) Relative expression of crustin*Pm*1 and crustin*Pm*7 after *S. aureus* injection in *Pm*MyD88-silenced shrimp. (C) Relative expression of crustin*Pm*1 and crustin*Pm*7 after *V. harveyi* challenged in *Pm*MyD88-depleted shrimp. Shrimp were divided into three groups and injected with 150 mM NaCl, GFP dsRNA (7.5 μg per g shrimp) or *Pm*MyD88 dsRNA (7.5 μg per g shrimp) before bacterial injection. The hemocytes were collected at 12 and 24 h after bacterial challenge and used for determination of crustin*Pm*1 and crustin*Pm*7 expressions by Quantitative Real-time RT-PCR. Gene expression level of knockdown shrimp was normalized to that of control group. The data are shown as the mean ± standard deviation. An asterisk (*) indicates significant differences from control group ($p < 0.05$) and a double asterisk (**) represents significant differences from control group ($p < 0.01$). Experiments were carried out in triplicate.

regulates immediate early response genes, wound healing and melanization, is negatively regulated by Relish. In the Toll pathway, the serine protease cascade initiates the processing of Spätzle, leading to the binding of Spätzle to Toll. Activated Toll then recruits MyD88, Tube, and the kinase Pelle, to form the signaling complex, which later induces the degradation of cytoplasmic Dorsal-Cactus and Dif-Cactus complexes. Consequently, the NF-κB-like transcription factors Dorsal and Dif translocate to the nucleus and activate the expression of AMP genes (Lemaitre, 2004; Tanji and Ip, 2005).

Several potential transcription factor binding sites have been identified at the 5′-upstream region of crustin genes. For example, the 5′-UTR crustin*Pm*7 gene has several putative transcription factor binding motifs such as GATA binding factor, signal transducer and activator of transcription 5 (STAT5), a CAAT enhancer-binding protein β (C/EBPβ), NF-κB and an activator protein 1 (AP1) *cis*-acting element (Amparyup et al., 2008b). In addition, two NF-κB, one complete heat-shock regulatory element (HSE), and five GATA factor binding sites were found upstream of the crustin*Pm*5 gene (Vatanavicharn et al., 2009).

To identify the regulatory pathway of crustin*Pm*1 and crustin*Pm*7 in *P. monodon*, transcription levels of crustin*Pm*1 and crustin*Pm*7, along with genes in the Imd (*Pm*Relish) and Toll pathways (*Pm*Spätzle, *Pm*MyD88 and Dorsal) were measured after shrimp were injected with heat-inactivated Gram-positive and Gram-negative bacteria. In addition, effects of *Pm*Relish and *Pm*MyD88 gene knockdown on crustin*Pm*1 and crustin*Pm*7 expressions upon bacterial infection were examined.

Crustin*Pm*1 gene was up-regulated following injection with *S. aureus* (Gram-positive), but not the Gram-negative bacterium, *V. harveyi*. Crustin*Pm*7, meanwhile, acted in response to both *S. aureus and V. harveyi* injection. This result is in agreement with the fact that crustin*Pm*1 inhibits Gram-positive bacteria only, while crustin*Pm*7 exhibits antimicrobial activity against both Gram-positive and Gram-negative bacteria. It is worth noting that crustin*Pm1* expression reached the highest level at 12 h after *S. aureus* injection, whereas crustin*Pm7* expression peaked at 12 h and 24 h after *S. aureus* and *V. harveyi* challenge, respectively. Crustin response time seemed to depend on strains of bacterial infection. In L. *vannamei*, crustin transcript level was highest at 48 h after *Micrococcus lysodeikticus* infection (Liu et al., 2016).

Heat-killed bacterial injection also stimulated immune-related genes in the Imd (*Pm*Relish) and Toll (*Pm*Spätzle, *Pm*MyD88 and Dorsal) pathways. The transcription level of *Pm*Relish in hemocytes was responsive to both *S. aureus* and *V. harveyi* injection, indicating that *Pm*Relish participates in the immune response against both Gram-positive and Gram-negative bacteria. While *Pm*Relish was highly responsive to *V. harveyi*, its response to *S. aureus* injection was at a much lower level. This suggests that the Imd pathway is a major pathway activated by Gram-negative bacteria in *P. monodon*. Similar results were reported in Drosophila, where the Imd pathway mainly responded to Gram-negative bacteria infection,

while the Toll pathway was triggered by Gram-positive bacteria and fungi (Hoffmann and Reichhart, 2002; Tzou et al., 2002). In the silkworm *Bombyx mori*, both *Bm*Relish1 and *Bm*Relish2 transcripts responded to *E. coli*, but not *S. aureus* (Tanaka et al., 2007). In the Chinese shrimp *F. chinensis*, *Fc*Relish transcript was up-regulated by 4 fold at 1 h after Gram-negative bacterial infection. However, *Fc*Relish was increased by 1.5 fold at 6 h after Gram-positive bacterial infection (Li et al., 2009). These data also indicate that the Imd pathway in *F. chinensis* is mainly responsive to Gram-negative bacteria.

Genes in the Toll pathway, *Pm*Spätzle, *Pm*MyD88 and Dorsal were also up-regulated upon *S. aureus* and *V. harveyi* challenge. This indicates that the Toll pathway is involved in both Gram-positive and Gram-negative bacterial infection in *P. monodon*. When the time point of up-regulation of immune-related genes in the Imd and Toll pathways are considered, it is likely that the Imd pathway is activated in early bacterial infection, whereas the Toll partway is triggered at the late phase of bacterial infection. This corresponds to the fact that, in Drosophila, genes controlled by Imd generally show an acute phase profile, while gene regulated by Toll exhibit a late and sustained expression pattern (Boutros et al., 2002; Lemaitre et al., 1997; Rutschmann et al., 2000).

To investigate the regulatory pathway of rcrustin*Pm*1 and rcrustin*Pm*7, *Pm*Relish gene in the Imd pathway and *Pm*MyD88 gene in the Toll pathway were knocked down. In the chinese shrimp, silencing of *Fc*Relish resulted in changes in the transcription profile of AMPs (Li et al., 2009). The data showed that the transcription level of crustin*Pm*1 in *Pm*Relish-silenced shrimp remained unchange after *S. aureus* and *V. harveyi* injection, when compared with the control group. In contrast, the transcription level of crustin*Pm*7 in *Pm*Relish-silenced shrimp after bacterial infection was significantly lower than that in control shrimp. It can be postulated that the Imd pathway mediates expression of crustin*Pm*7, but not crustin*Pm*1.

Knockdown of *Pm*MyD88 gene in the Toll pathway resulted in a reduction of both crustin*Pm*1 and crustin*Pm*7 transcripts in *Pm*MyD88-silenced shrimp. This suggests that crustin*Pm*1 and crustin*Pm*7 can be modulated by the Toll pathway. Similarly, knockdown of Dorsal of Toll pathway in freshwater prawn *Macrobrachium rosenbergii* resulted in suppression of *Mr*Crustin2 and *Mr*Crustin 4 transcripts (Huang et al., 2016). In addition, silencing of Flightless-I (FliI), a negative regulator of the Toll-like receptor pathway through interaction with MyD88, resulted in an increase of crustin expression in *L. vannamei* (Zhang et al., 2015).

We concluded that crustin*Pm*1 is regulated through the Toll signaling pathway, while crustin*Pm*7 is mediated through both Toll and Imd pathways. In Drosophila, the induction of some antimicrobial peptide genes, such as defensin, mechnikowin, cecropin A1 and attacin, depends on both pathways (Uvell and Engstrom, 2007). In previous reports, suppression of proPO appeared to down regulate the expression of crustin, as well as penaedin and lysozyme (Amparyup et al., 2012; Fagutao et al., 2009). It is likely that expression of crustin is mediated by at least three pathways, including Toll, Imd and proPO.

In conclusion, rcrustin*Pm*1 and rcrusin*Pm*7 bound tightly to PA, LTA and LPS in a positive cooperative manner. It is possible that the antimicrobial activity of crustin does not only come from bacterial agglutination and membrane-disruption but also through targeting with PA, a lipid signaling messenger. In *P. monodon*, it was evident that the Imd pathway mainly acts against Gram-negative bacteria, while the Toll pathway is responsible for both Gram-positive and Gram-negative bacterial infection. Gene expression profiles and knockdown experiments revealed that crustin*Pm*1 was regulated through the Toll signaling pathway, while crustin*Pm*7 was mediated through both the Toll and Imd pathways.

Acknowledgements

We thank Professor Dr. Vichien Rimphanitchayakit for *Pm*Spätzl sequence information, Associate Professor Dr. Chartchai Krittanai for access to Circular Dichrosim Spectrometer and Dr. Krupa O'Neill for critical reading of this manuscript. This work was supported by the 90th Anniversary of Chulalongkorn University Fund (Ratchadaphiseksomphot Endowment Fund), The Thailand Research Fund through the TRF Senior Research Scholar RTA5880004 and IRG 5780008. KK has been partially supported by Structural and Computational Biology Research Group (GSTAR 59-012-23-001), Special Task Force for Activating Research (STAR), Faculty of Science, Chulalongkorn University.

References

Amparyup, P., Donpudsa, S., Tassanakajon, A., 2008a. Shrimp single WAP domain (SWD)-containing protein exhibits proteinase inhibitory and antimicrobial activities. Dev. Comp. Immunol. 32, 1497–1509.
Amparyup, P., Kondo, H., Hirono, I., Aoki, T., Tassanakajon, A., 2008b. Molecular cloning, genomic organization and recombinant expression of a crustin-like antimicrobial peptide from black tiger shrimp *Penaeus monodon*. Mol. Immunol. 45, 1085–1093.
Amparyup, P., Sutthangkul, J., Charoensapsri, W., Tassanakajon, A., 2012. Pattern recognition protein binds to lipopolysaccharide and beta-1,3-glucan and activates shrimp prophenoloxidase system. J. Biol. Chem. 287, 10060–10069.
Arockiaraj, J., Gnanam, A.J., Muthukrishnan, D., Gudimella, R., Milton, J., Singh, A., Muthupandian, S., Kasi, M., Bhassu, S., 2013. Crustin, a WAP domain containing antimicrobial peptide from freshwater prawn *Macrobrachium rosenbergii*: immune characterization. Fish. Shellfish Immunol. 34, 109–118.
Assavalapsakul, W., Panyim, S., 2012. Molecular cloning and tissue distribution of the Toll receptor in the black tiger shrimp, *Penaeus monodon*. Genet. Mol. Res. GMR 11, 484–493.
Bahar, A.A., Ren, D., 2013. Antimicrobial peptides. Pharm. (Basel) 6, 1543–1575.
Boutros, M., Agaisse, H., Perrimon, N., 2002. Sequential activation of signaling pathways during innate immune responses in *Drosophila*. Dev. Cell 3, 711–722.
Deepika, A., Sreedharan, K., Paria, A., Makesh, M., Rajendran, K.V., 2014. Toll-pathway in tiger shrimp (*Penaeus monodon*) responds to white spot syndrome virus infection: evidence through molecular characterisation and expression profiles of MyD88, TRAF6 and TLR genes. Fish. Shellfish Immunol. 41, 441–454.
Donpudsa, S., Visetnan, S., Supungul, P., Tang, S., Tassanakajon, A., Rimphanitchayakit, V., 2014. Type I and type II crustins from Penaeus monodon, genetic variation and antimicrobial activity of the most abundant crustinPm4. Dev. Comp. Immunol. 47, 95–103.
Fagutao, F.F., Koyama, T., Kaizu, A., Saito-Taki, T., Kondo, H., Aoki, T., Hirono, I., 2009. Increased bacterial load in shrimp hemolymph in the absence of prophenoloxidase. FEBS J. 276, 5298–5306.
Fitch, P.M., Roghanian, A., Howie, S.E., Sallenave, J.M., 2006. Human neutrophil elastase inhibitors in innate and adaptive immunity. Biochem. Soc. Trans. 34, 279–282.
Hancock, R.E., Brown, K.L., Mookherjee, N., 2006. Host defence peptides from invertebrates–emerging antimicrobial strategies. Immunobiology 211, 315–322.
Hoffmann, J.A., Reichhart, J.M., 2002. Drosophila innate immunity: an evolutionary perspective. Nat. Immunol. 3, 121–126.
Huang, X., Wang, W., Ren, Q., 2016. Dorsal transcription factor is involved in regulating expression of crustin genes during white spot syndrome virus infection. Dev. Comp. Immunol. 63, 18–26.
Huang, X.D., Yin, Z.X., Jia, X.T., Liang, J.P., Ai, H.S., Yang, L.S., Liu, X., Wang, P.H., Li, S.D., Weng, S.P., Yu, X.Q., He, J.G., 2010. Identification and functional study of a shrimp Dorsal homologue. Dev. Comp. Immunol. 34, 107–113.
Jia, Y.P., Wang, Z.H., Wang, Q., Zhao, X.F., Wang, J.X., 2008. A single whey acidic protein domain (SWD)-containing peptide from the fleshy prawn with antimicrobial and proteinase inhibition activities. Aquaculture 284, 246–259.
Jimenez-Vega, F., Yepiz-Plascencia, G., Soderhall, K., Vargas-Albores, F., 2004. A single WAP domain-containing protein from *Litopenaeus vannamei* hemocytes. Biochem. Biophys. Res. Commun. 314, 681–687.
Krusong, K., Poolpipat, P., Supungul, P., Tassanakajon, A., 2012. A comparative study of antimicrobial properties of crustinPm1 and crustin*Pm*7 from the black tiger shrimp *Penaeus monodon*. Dev. Comp. Immunol. 36, 208–215.
Lemaitre, B., 2004. The road to Toll. Nat. Rev. Immunol. 4, 521–527.
Lemaitre, B., Kromer-Metzger, E., Michaut, L., Nicolas, E., Meister, M., Georgel, P., Reichhart, J.M., Hoffmann, J.A., 1995. A recessive mutation, immune deficiency (imd), defines two distinct control pathways in the *Drosophila* host defense. Proc. Natl. Acad. Sci. U. S. A. 92, 9465–9469.
Lemaitre, B., Nicolas, E., Michaut, L., Reichhart, J.M., Hoffmann, J.A., 1996. The dorsoventral regulatory gene cassette Spätzle/Toll/cactus controls the potent antifungal response in *Drosophila* adults. Cell 86, 973–983.
Lemaitre, B., Reichhart, J.M., Hoffmann, J.A., 1997. Drosophila host defense: differential induction of antimicrobial peptide genes after infection by various classes

of microorganisms. Proc. Natl. Acad. Sci. U. S. A. 94, 14614–14619.
Li, F., Yan, H., Wang, D., Priya, T.A., Li, S., Wang, B., Zhang, J., Xiang, J., 2009. Identification of a novel relish homolog in Chinese shrimp *Fenneropenaeus chinensis* and its function in regulating the transcription of antimicrobial peptides. Dev. Comp. Immunol. 33, 1093–1101.
Liu, N., Lan, J.F., Sun, J.J., Jia, W.M., Zhao, X.F., Wang, J.X., 2015. A novel crustin from *Marsupenaeus japonicus* promotes hemocyte phagocytosis. Dev. Comp. Immunol. 49, 313–322.
Liu, Y., Song, L., Sun, Y., Liu, T., Hou, F., Liu, X., 2016. Comparison of immune response in Pacific white shrimp, *Litopenaeus vannamei*, after knock down of Toll and IMD gene in vivo. Dev. Comp. Immunol. 60, 41–52.
Liu, Y., Su, Y., Wang, X., 2013. Phosphatidic acid-mediated signaling. Adv. Exp. Med. Biol. 991, 159–176.
Livak, K.J., Schmittgen, T.D., 2001. Analysis of relative gene expression data using real-time quantitative PCR and the 2(-Delta Delta C(T)) Method. Methods 25, 402–408.
Louis-Jeune, C., Andrade-Navarro, M.A., Perez-Iratxeta, C., 2011. Prediction of protein secondary structure from circular dichroism using theoretically derived spectra. Proteins 80, 374–381.
McPhail, L.C., Waite, K.A., Regier, D.S., Nixon, J.B., Qualliotine-Mann, D., Zhang, W.X., Wallin, R., Sergeant, S., 1999. A novel protein kinase target for the lipid second messenger phosphatidic acid. Biochim. Biophys. Acta 1439, 277–290.
Moreau, T., Baranger, K., Dade, S., Dallet-Choisy, S., Guyot, N., Zani, M.L., 2008. Multifaceted roles of human elafin and secretory leukocyte proteinase inhibitor (SLPI), two serine protease inhibitors of the chelonianin family. Biochimie 90, 284–295.
Rojtinnakorn, J., Hirono, I., Itami, T., Takahashi, Y., Aoki, T., 2002. Gene expression in haemocytes of kuruma prawn, *Penaeus japonicus*, in response to infection with WSSV by EST approach. Fish. Shellfish Immunol. 13, 69–83.
Rutschmann, S., Jung, A.C., Hetru, C., Reichhart, J.M., Hoffmann, J.A., Ferrandon, D., 2000. The Rel protein DIF mediates the antifungal but not the antibacterial host defense in *Drosophila*. Immunity 12, 569–580.
Sagaram, U.S., El-Mounadi, K., Buchko, G.W., Berg, H.R., Kaur, J., Pandurangi, R.S., Smith, T.J., Shah, D.M., 2013. Structural and functional studies of a phosphatidic acid-binding antifungal plant defensin MtDef4: identification of an RGFRRR motif governing fungal cell entry. PLoS One 8, e82485.
Sallenave, J.M., 2000. The role of secretory leukocyte proteinase inhibitor and elafin (elastase-specific inhibitor/skin-derived antileukoprotease) as alarm antiproteinases in inflammatory lung disease. Respir. Res. 1, 87–92.
Shi, X.Z., Zhang, R.R., Jia, Y.P., Zhao, X.F., Yu, X.Q., Wang, J.X., 2009. Identification and molecular characterization of a Spatzle-like protein from Chinese shrimp (*Fenneropenaeus chinensis*). Fish. Shellfish Immunol. 27, 610–617.
Shugars, D.C., 1999. Endogenous mucosal antiviral factors of the oral cavity. J. Infect. Dis. 179 (Suppl. 3), S431–S435.
Smith, V.J., Fernandes, J.M., Kemp, G.D., Hauton, C., 2008. Crustins: enigmatic WAP domain-containing antibacterial proteins from crustaceans. Dev. Comp. Immunol. 32, 758–772.
Supungul, P., Klinbunga, S., Pichyangkura, R., Hirono, I., Aoki, T., Tassanakajon, A., 2004. Antimicrobial peptides discovered in the black tiger shrimp Penaeus monodon using the EST approach. Dis. Aquat. Organ 61, 123–135.
Supungul, P., Tang, S., Maneeruttanarungroj, C., Rimphanitchayakit, V., Hirono, I., Aoki, T., Tassanakajon, A., 2008. Cloning, expression and antimicrobial activity of crustin*Pm*1, a major isoform of crustin, from the black tiger shrimp *Penaeus monodon*. Dev. Comp. Immunol. 32, 61–70.
Suthianthong, P., Donpudsa, S., Supungul, P., Tassanakajon, A., Rimphanitchayakit, V., 2012. The N-terminal glycine-rich and cysteine-rich regions are essential for antimicrobial activity of crustin*Pm*1 from the black tiger shrimp *Penaeus monodon*. Fish. Shellfish Immunol. 33, 977–983.
Tanaka, H., Matsuki, H., Furukawa, S., Sagisaka, A., Kotani, E., Mori, H., Yamakawa, M., 2007. Identification and functional analysis of Relish homologs in the silkworm, *Bombyx mori*. Biochim. Biophys. Acta 1769, 559–568.
Tanji, T., Ip, Y.T., 2005. Regulators of the Toll and Imd pathways in the *Drosophila* innate immune response. Trends Immunol. 26, 193–198.
Tzou, P., De Gregorio, E., Lemaitre, B., 2002. How *Drosophila* combats microbial infection: a model to study innate immunity and host-pathogen interactions. Curr. Opin. Microbiol. 5, 102–110.
Uvell, H., Engstrom, Y., 2007. A multilayered defense against infection: combinatorial control of insect immune genes. Trends Genet. 23, 342–349.
Vargas-Albores, F., Yepiz-Plascencia, G., Jimenez-Vega, F., Avila-Villa, A., 2004. Structural and functional differences of *Litopenaeus vannamei* crustins. Comp. Biochem. Physiol. B Biochem. Mol. Biol. 138, 415–422.
Vatanavicharn, T., Supungul, P., Puanglarp, N., Yingvilasprasert, W., Tassanakajon, A., 2009. Genomic structure, expression pattern and functional characterization of crustin*Pm*5, a unique isoform of crustin from *Penaeus monodon*. Comp. Biochem. Physiol. B Biochem. Mol. Biol. 153, 244–252.
Visetnan, S., Supungul, P., Hirono, I., Tassanakajon, A., Rimphanitchayakit, V., 2015. Activation of *Pm*Relish from *Penaeus monodon* by yellow head virus. Fish. Shellfish Immunol. 42, 335–344.
Wang, P.H., Gu, Z.H., Huang, X.D., Liu, B.D., Deng, X.X., Ai, H.S., Wang, J., Yin, Z.X., Weng, S.P., Yu, X.Q., He, J.G., 2009. An immune deficiency homolog from the white shrimp, Litopenaeus vannamei, activates antimicrobial peptide genes. Mol. Immunol. 46, 1897–1904.
Wiedow, O., Harder, J., Bartels, J., Streit, V., Christophers, E., 1998. Antileukoprotease in human skin: an antibiotic peptide constitutively produced by keratinocytes. Biochem. Biophys. Res. Commun. 248, 904–909.
Zhang, J., Li, F., Wang, Z., Xiang, J., 2007. Cloning and recombinant expression of a crustin-like gene from Chinese shrimp, *Fenneropenaeus chinensis*. J. Biotechnol. 127, 605–614.
Zhang, S., Qiu, W., Chen, Y.G., Yuan, F.H., Li, C.Z., Yan, H., Weng, S.P., He, J.G., 2015. Flightless-I (Flil) is a potential negative regulator of the Toll pathway in *Litopenaeus vannamei*. Fish. Shellfish Immunol. 42, 413–425.
Zhang, Y., Du, G., 2009. Phosphatidic acid signaling regulation of Ras superfamily of small guanosine triphosphatases. Biochim. Biophys. Acta 1791, 850–855.

Fish & Shellfish Immunology 65 (2017) 88–95

Contents lists available at ScienceDirect

Fish & Shellfish Immunology

journal homepage: www.elsevier.com/locate/fsi

Full length article

Characterization of *Pm*Spätzle 1 from the black tiger shrimp *Peneaus monodon*

Sittichai Boonrawd [a], Ravi Mani [b], Sirikwan Ponprateep [c], Premruethai Supungul [d], Promsin Masrinoul [e], Anchalee Tassanakajon [a], Vichien Rimphanitchayakit [a, *]

[a] Center of Excellence for Molecular Biology and Genomics of Shrimp, Department of Biochemistry, Faculty of Science, Chulalongkorn University, Phyathai Road, Bangkok 10330, Thailand
[b] Department of Biotechnology, Sathyabama University, Jeppiaar Nagar, Rajiv Gandhi Road, Chennai, Tamil Nadu 600119, India
[c] Department of Chemistry, Faculty of Science, Srinakharinwirot University, 114 Sukhumvit 23 Road, Bangkok 10110, Thailand
[d] National Center for Genetic Engineering and Biotechnology (BIOTEC), National Science and Technology Development Agency (NSTDA), Pathum Thani 10120, Thailand
[e] Institute of Molecular Biosciences, Mahidol University, 25/25 Phuttamonthon 4 Road, Salaya, Nakhon Pathom 73170, Thailand

ARTICLE INFO

Article history:
Received 12 January 2017
Received in revised form
2 April 2017
Accepted 7 April 2017
Available online 8 April 2017

Keywords:
Penaeus monodon
*Pm*Spätzles
Antimicrobial proteins
White spot syndrome virus
Toll pathway

ABSTRACT

Spätzle is a signaling ligand in innate immune response that signals pathogenic infection via Toll receptor and Toll pathway into the cells for the synthesis of antimicrobial proteins. Herein, three *Pm*Spätzle isoforms were identified in *Penaeus monodon*, namely *Pm*Spz1, 2 and 3. The *Pm*Spz1 was chosen for detailed study. The *PmSpz1* gene was expressed in all nine tissues tested including the hemocytes, stomach, hepatopancreas, gill, lymphoid tissue, eyestalk, muscle, intestine and heart. Its expression was up-regulated upon white spot syndrome virus (WSSV) infection. Western blot analysis of hemolymph showed that the *Pm*Spz1 mostly existed as a cleaved active form awaiting to activate the Toll pathway. Injection of a recombinant *Pm*Spz1 rendered the shrimp less susceptible to the WSSV infection. Injection of a recombinant active form of *Pm*Spz1 into a normal shrimp activated the synthesis of *crustinPm1*, *crustinPm7*, *ALFPm3*, *penaeidin3* but not *penaeidin5* indicating that the expression of all antimicrobial proteins but not *penaeidin5* was under the regulation of Toll pathway.

© 2017 Elsevier Ltd. All rights reserved.

1. Introduction

Penaeid shrimp are economically important marine organisms for aquaculture in several countries including Thailand. However, a massive loss in shrimp production occurs continuously due to shrimp diseases which are mostly bacteria or viruses. Understanding of shrimp immunity is, therefore, important for the prevention of shrimp diseases and management of shrimp aquaculture [1]. Like other arthropods, penaeid shrimp respond to pathogen infections by the innate immunity which consists of cellular and humoral responses. The humoral immune response involves the synthesis of immune proteins such as antimicrobial peptides (AMPs), proteinase inhibitors and cytokine-like proteins [1–3].

Upon microbial infection, two major signaling pathways may be triggered. The Toll pathway responds to Gram-positive bacteria and fungi while the Imd pathway responds to Gram-negative bacteria. In the Toll pathway, an extracellular protein Spätzle is a signaling protein that relays the infection signal through the Toll receptor into the cells. The Spätzle is synthesized as a pro-protein and secreted into the hemolymph. The recognition of microbes by pattern recognition proteins triggers a proteinase cascade which, finally, activates Spätzle. Then, the active Spätzle binds to the cell membrane Toll receptor. The infection signal is transferred into the cytoplasm and, then, nucleus to up-regulate the synthesis of AMPs [2,4–7].

Multiple Spätzle proteins have been identified in arthropods. The *Drosophila melanogaster* genome contains six Spätzle isoforms (*Dm*Spz1-6) [8]. The mosquito, *Aedes aegypti*, has three Spätzle homologs and one of these, Spätzle1C, is able to activate the anti-fungal immune response [9]. Three Spätzle isoforms have been detected in the white shrimp *Litopenaeus vannamei*, *Lv*Spz1, 2 and 3 [10]. The different Spätzles are thought to be involved in responses to different pathogens.

The expression of *Spätzle* gene is found to be responded to the

* Corresponding author.
E-mail address: kpvr2@yahoo.com (V. Rimphanitchayakit).

http://dx.doi.org/10.1016/j.fsi.2017.04.005
1050-4648/© 2017 Elsevier Ltd. All rights reserved.

pathogen infections. In silkworm larvae, the expression of *Bombyx mori Spätzle1*, *BmSpz1*, is up-regulated after injection with *Bacillus subtilis*, *Escherichia coli*, *Micrococcus luteus* and *Saccharomyces cerevisiae* [11]. The *ApSpz* in oak silkworm, *Antheraea pernyi*, is activated after infection with fungus, *Nosema pernyi* and Gram-positive bacteria, *Enterococcus pernyi* [12]. The *MsSpz1* transcript in *Manduca sexta* is increased in the hemocytes after *M. luteus* and microbial elicitor curdlan injections [13]. In shrimp, the expression of *FcSpz* gene from the Chinese shrimp, *Fenneropenaeus chinensis*, is up-regulated in tissues after injection with *Vibrio anguillarum* and WSSV [14]. The expression of *LvSpz1* and *3* genes is increased in gills after challenging with *Vibrio alginolyticus* [10].

Upon activation, the Spätzle is cleaved by either Easter in embryonic patterning or Spätzle activating enzyme in infection letting the C terminal conserved domain bind to the cognate Toll receptor [15,16]. The active domain of Spätzle has been studied on its activity to signal the synthesis of AMPs [4,5]. The active domain Spätzle-C106 of *Drosophila* leads to a strong induction of drosomysin after injection into the flies [16]. The Spätzle-C114 of *F. chinensis* is able to activate the *Crustin2* gene but does not activate the expression of *lysozyme*, *astacidin* and *crustin1* (SWD) genes [14]. The Spätzle-C108 of *M. sexta* induces the synthesis of attacin-1, cecropin-6, moricin, lysozyme and the immunoglobulin domain of hemolin [13].

In this study, three isoforms of *Spätzle* in *Penaeus monodon* were identified. The complete gene sequence of *PmSpz1* was cloned from the hemocyte cDNA. The expression profile of *PmSpz1* was investigated in tissues and in response to WSSV infection. The recombinant *PmSpz1* and its active domain were produced for the studies of its protective effect on the survival rate of WSSV-infected shrimp and the effect on AMP synthesis.

2. Materials and methods

2.1. Shrimp

The black tiger shrimp, *P. monodon*, were purchased from local farm and obtained in 17 ppt sea water. The shrimp were reared at an ambient water temperature of 28–30 °C for a few days before experiments.

2.2. Identification of PmSpz isoforms

Three isoforms of Spätzle genes, namely, *LvSpz1*, *LvSpz2* and *LvSpz3*, were identified from *L. vannamei* [10]. It was interesting to know whether the *P. monodon* also possesses these three Spätzle genes. The forward and reverse primers were designed from the nucleotide sequences of *LvSpz1* (accession no. JN180646), *LvSpz2* (JN180647) and *LvSpz3* (JN180648) for the amplification of gene segments from the cDNA preparation (Table 1).

The hemocytes and gill of normal shrimp were collected for total RNA extraction. The total RNA was extracted with Trizol reagent (Genaeid) following the manufacturer instruction. The cDNAs were synthesized using RevertAid First Strand cDNA Synthesis Kit (Thermo Scientific). The PCR reaction contained 1.25 unit *Taq* DNA polymerase (RBC), 10 μM dNTP mix, 10 μM each forward and reverse primers and appropriately diluted cDNA preparation. The PCR condition started with pre-denaturation at 95 °C for 3 min followed by 30 cycles for *PmSpz* isoforms or 25 cycles for *EF-1α* of denaturation at 95 °C for 1 min, annealing at 55 °C for 30 min and extension at 72 °C for 1 min, and ended with final extension at 72 °C for 10 min. The PCR product were analyzed by agarose gel analysis. The major amplified PCR products were eluted from the agarose gel, purified and subjected to DNA sequencing by commercial service.

2.3. Cloning of PmSpz1 gene

The primers for the amplification of *Pm*Spz1 gene from a cDNA preparation, SPZF and SPZR (Table 1), were designed from *Lv*Spz1 sequence from *L. vannamei* (accession no. JN180646) (Table 1) [10]. The cDNA was prepared as described above from the hemocytes of normal shrimp. The full-length gene was amplified by PCR and analyzed by agarose gel electrophoresis. The PCR product was eluted from the excised agarose gel and sequenced by the commercial service.

Table 1
Sequences of primers used in this study.

Primer	Sequence (5'→3')	Usage
SPZF	GCGACTCTCGTATCTATCCGC	Cloning of *PmSpz1* gene
SPZR	TGGCCAGGGAGTCCTAGATCC	
*Pm*SPZF	GCGCCCATGGGCTCCGTCCAACC	Cloning of *PmSpz1* gene and its active form into the expression vectors
*Pm*SPZR	GCGCAAGCTTTGCTGGAAGATGG	
CTSPZF	ATATCCATGGCGGGTGGTCCTGA	
RTSPZF	CGCTTGGAGACCTGTCTGTT	qRT-PCR and RT-PCR of *PmSpz1* gene
RTSPZR	TAGGGATCGCATGGGTCGTA	
ALF*Pm*3F	ATACTAGAATTCCAAGGGTGGGAGGCTGTGGCA	qRT-PCR of *crustinPm1*, *crustinPm7*, *ALFPm3*, *penaiedin3* and *penaiedin5* genes
ALF*Pm*3R	TATTATGGATCCCTATGAGCTGAGCCACTGGTTGGCCT	
Crustin*Pm*1F	CTGCTGCGAGTCAAGGTATG	
Crustin*Pm*1R	AGGTACTGGCTGCTCTACTG	
Crustin*Pm*7F	GGCATGGTGGCGTTGTTCCT	
Crustin*Pm*7R	TGTCGGAGCCGAAGCAGTCA	
Pen3F	ATGCGTCTCGTGGTCTGCCT	
Pen3R	CCTGTGAATACACGAGGA	
Pen5F	TTGGTCTATGCTTTGCAAGG	
Pen5R	ACAGATAGTTAAAGTGAAAGAC	
*Lv*SPZ1F	TGGGGACTCTCCTTACGA	Amplification of *PmSpz1*, *2* and *3* gene segments
*Lv*SPZ1R	GGGAACAGACAGGTCTCCA	
*Lv*SPZ2F	ACAGCCCACCTGACTGTACC	
*Lv*SPZ2R	ATCGCTACTGACGAGGCAAT	
*Lv*SPZ3F	ACACCCTGGAGGAGGAAACT	
*Lv*SPZ3R	TCTGCAGACACTTGGACTC	
EF-1αF	GGTGCTGGACAAGCTGAAGGC	qRT-PCR internal control gene
EF-1αR	CGTTCCGGTGATCATGTTCTTGATG	

The nucleotide sequence was analyzed for the open reading frame, the deduced amino acid sequence using ORF Finder (https://www.ncbi.nlm.nih.gov/orffinder/) and other bioinformatics information using ExPASy (http://www.expasy.org/proteomics), SignalP 4.1 Server (http://www.cbs.dtu.dk/services/SignalP/) and blastp in BLAST® (https://blast.ncbi.nlm.nih.gov/Blast.cgi).

2.4. Expression of PmSpz1 gene in tissues

Nine tissues, hemocytes, stomach, hepatopancreas, gill, lymphoid organ, muscle, eyestalk, intestine and heart, were collected from the normal shrimp. The total RNAs were extracted and the cDNAs were synthesized as described above. The expression of *PmSpz1* was analyzed by RT-PCR using the primers RTSPZF and RTSPZR under the condition as described above and agarose gel electrophoresis. The expression of *EF-1α* was used as an internal control.

2.5. Expression of PmSpz1 gene in response to WSSV infection

The normal shrimp were separated into two groups. The challenge group was injected with 50 μL of WSSV containing 16,950 copies of WSSV that caused 100% mortality within four days. The control group was injected with 50 μL normal saline (0.85% NaCl). The hemolymph was collected from three individual shrimp at each time point 3, 6, 12, 24 and 48 h for total RNA preparation. The experiment was done in triplicate. The expression of *PmSpz1* was analyzed by qRT-PCR using primers RTSPZF and RTSPZR (Table 1).

The qRT-PCR was carried out in a real-time thermal cycler (Bio-Rad Laboratories, USA) with QPCR Green Master Mix LRox (Biotechrabbit). The reaction mixture (10 μL) consisted of 2 μL of the 1:10 diluted cDNA template, 0.2 μM of each primer and 1 × QPCR Green Master Mix LRox containing DNA polymerase. The PCR amplification started with pre-denaturation at 95 °C for 8 min followed by 40 cycles of denaturation at 95 °C for 30 s, annealing and extension at 60 °C for 30 s. The expression of *EF-1α* was used as an internal control.

The relative expression of *PmSpz1* was calculated using a comparative method described by Pfaffl [17]. The mean data values were derived from triplicate amplifications and expressed as means ± standard deviations. Statistical analysis was done using the One-way ANOVA followed by Duncan's new multiple range test. Data differences were considered statistically significant at $P < 0.05$.

2.6. PmSpz1 in the hemocytes and plasma of WSSV-infected shrimp

Shrimp were injected with 1×10^4 copy/shrimp of purified WSSV. The hemolymph was collected at 0, 12, 24 and 48 h post infection (hpi). The hemolymph was collected from five shrimp hemolymph at each time point with 10% sodium citrate at the ratio of 1:3 and immediately centrifuged at 800 × g for 15 min to separate the hemocytes from the plasma. The hemocytes were re-suspended with PBS and sonicated to break the cells. The total protein concentrations of plasma and hemocyte lysate were determined using Bradford assay [18]. To detect the *Pm*Spz1, 1000 μg protein of plasma and 200 μg protein of hemocyte lysate at each time point were run on a SDS-PAGE. The protein bands were transferred to nitrocellulose membrane for Western blot analysis to detect the *Pm*Spz1. The β-actin was detected as an internal control protein. The *Pm*Spz1 and β-actin were detected with mouse antibody specific to *Pm*Spz1 and anti-actin (Millipore) and, then, with secondary antibody conjugated with horseradish peroxidase. The protein bands were developed using chemiluminescent substrates and detected by X-ray film.

2.7. Protein expression of rPmSpz1 and its active form racPmSpz1

In order to produce the mature recombinant (r)*Pm*Spz1 protein, the *Pm*SPZF and *Pm*SPZR primers were designed from the *PmSpz1* gene sequences (Table 1). The forward and reverse primers were added the restriction sites *Nco*I and *Hin*dIII, respectively, for the cloning into an expression vector pET-28b(+). The mature gene fragment was amplified by PCR from the hemocyte cDNA preparation, separated by agarose gel electrophoresis, gel purified and cleaned up and ligated to pET-28b(+) vector. The resulting pET-28b_PmSpz1 construct was sequenced to ensure the correct sequence and reading frame.

The recombinant active domain of *Pm*Spz1 (rac*Pm*Spz1) was also produced. The protease-cleavage site of *Pm*Spz1 was predicted by comparing the amino acid sequence with those of *M. sexta* (*Ms*_Spz), *B. mori* (*Bm*_Spz) and *D. melanogaster* (*Dm*_Spz). The forward primer with *Nco*I restriction site, CTSPZF, was designed (Table 1). Together with the reverse primer, *Pm*SPZR (Table 1), the active domain of *PmSpz1* was amplified and cloned into an expression vector, pVR500, a derivative of pET-32a(+) [19]. In this construct, pVR500_acPmSpz1, the active domain of *Pm*Spz1 (ac*Pm*Spz1) was produced as fusion protein to the thioredoxin (Trx) tag.

The pET-28b_PmSpz1 and pVR500_acPmSpz1 were transformed into an *E. coli* BL21-CodonPlus (DE3). A transformant from each plasmid was cultured until an OD_{600} reached 0.6 and the protein expression was induced by adding IPTG to the final concentration of 1 mM. The culture was continued for 3 h at 37 °C. The cells were harvested by centrifugation at 2500 g, 4 °C for 15 min, re-suspended in phosphate buffered saline pH 7.4 (PBS) and sonicated with Sonics Vibracell VCX750 to break the cells. The pellet was collected by centrifugation at 2500 g, 4 °C for 15 min, washed once with each respective solution: 2% Triton X-100, 0.5 M NaCl in PBS; 0.5 M NaCl in PBS; PBS, and solubilized with 50 mM sodium carbonate buffer pH 10.0 at room temperature. The insoluble matter was removed by centrifugation. The soluble protein was purified using Ni-NTA agarose column. The purified protein was dialyzed against PBS. The recombinant protein was traced using SDS-PAGE and its concentration was determined by Bradford method [18]. The mouse polyclonal antiserum was raised against the *Pm*Spz1 using 0.5 mg of the purified recombinant *Pm*Spz1 protein.

The Trx tag was removed from the recombinant (r)ac*Pm*Spz1 by enterokinase digestion. The 0.3 mg of fusion protein was incubated with 0.002 μg of enterokinase (New England Biolabs) at room temperature for 3 days. The rac*Pm*Spz1 was re-purified with Ni-NTA column. The progress of the digestion and the final preparation of rac*Pm*Spz1 were analysed by SDS-PAGE. The concentration was determined using the Bradford method [18].

2.8. Effect of racPmSpz1 on the expression of antimicrobial proteins

The shrimp were separated into two groups. The challenge group were injected with 0.3 and 3 nmol of rac*Pm*Spz1 in 100 μL normal saline (0.85% NaCl). The control group were injected with 100 μL normal saline. The hemolymph was collected at 24 h from three individual shrimp for each concentration of rac*Pm*Spz1 tested for total RNA preparation and first strand cDNA synthesis. The expression of AMP genes was investigated by real time RT-PCR using specific primers for *CrustinPm1* and *7*, *Penaeidin3* and *5* and *ALFPm3* (Table 1). The PCR products were analyzed by gel electrophoresis. The expression of *EF-1α* gene was used as an internal control.

The relative expression of AMPs was calculated using a comparative method described by Pfaffl [17]. The mean data values were derived from triplicate samples and expressed as means ±

standard deviations. Statistical analysis was done using the one-way ANOVA followed by Duncan's new multiple range test. Data differences were considered statistically significant at $P < 0.05$.

2.9. Effect of PmSpz1 protein on the survival of WSSV-infected shrimp

In these experiment, the effect of r*Pm*Spz1 protein on the survival of WSSV-injected shrimp was investigated. The normal shrimp were divided into four groups of 10 shrimp each. The WSSV dilution used had an LD_{50} of 2 days. The shrimp were injected with 66 μL equal volume of suspension of 0.3 nmol of r*Pm*Spz1 protein (group 1), 0.3 nmol of r*Pm*Spz1 plus WSSV (group 2), WSSV (group 3) and PBS (group 4) 1. The experiment was conducted in triplicate. The cumulative mortality was observed for 10 days. The survival rates were analyzed with the survival program in GraphPad Prism.

3. Results

3.1. Identification of PmSpz isoforms

From the *P. monodon* EST database [20], a clone of *PmSpz1* with partial sequence was identified. From the GenBank database, two clones of *Spz3* genes from *P. monodon* (accession no. KM225266) and *Fenneropenaeus chinensis* (accession no. EU523114) have been reported (unpublished). In L. *vannamei*, three Spätzle genes, namely *LvSpz1*, *2* and *3*, have been identified [10]. From the said data, it can be speculated that the black tiger shrimp also possesses at least 3 Spätzle genes. Since the protein sequences of *Pm*Spz1 and 3 are highly homologous to those of *L. vannamei* counterparts, primers for PCR were designed from the sequences of the three *LvSpz* genes for the amplification of the equivalent genes in the black tiger shrimp.

The hemocyte cDNA was used for RT-PCR amplification of *PmSpz1* and *3* genes whereas the gill cDNA was for the *PmSpz2* for the *LvSpz2* was highly expressed in gill [10]. All three gene fragments of *PmSpz1*, *2* and *3* were observed (Fig. 1). The DNA fragments were excised, eluted, purified and sequenced. The nucleotide sequences were analyzed with blastX and shown to be equivalent to *LvSpz1*, *2* and *3*. The complete sequence of *PmSpz1* (see below), partial sequences of *PmSpz2* and *3* were deposited into the GenBank with the accession numbers KY053796, KY053798 and KY053797, respectively. The results suggested that the *P. monodon* had at least three isoforms of *Pm*Spz genes. With reference to the expression of *EF-1α*, the *PmSpz1* and *3* were expressed fairly common in the hemocytes. The expression of *PmSpz2* in the hemocytes, however, was hardly detected (data not shown) and only in gill could the expression be detected (Fig. 1).

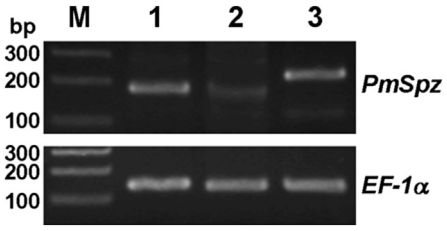


Fig. 1. Identification of three *PmSpz* genes. The *PmSpz* genes were amplified from the cDNA preparation using primers designed from *LvSpz* genes. Lanes M, 1, 2 and 3 are DNA ladder, PCR products from *PmSpz* isoform 1 (*PmSpz1*, hemocytes), *PmSpz* isoform 2 (*PmSpz2*, gill) and *PmSpz* isoform 3 (*PmSpz3*, hemocytes), respectively. The internal control expressed *EF-1α* was used to compare the level of expression.

3.2. PmSpz1 gene and its active domain

The *PmSpz1* was chosen for this study for it was the only *Spz* clone in the *P. monodon* EST database. The complete gene was PCR amplified from the hemocyte cDNA using primers designed from the *LvSpz1* gene. The PCR product was sequenced and the sequence was analysed. It was found that the *PmSpz1* gene consisted of an open reading frame of 714 bp encoding a protein of 237 amino acids. The *Pm*Spz1 protein had a signal peptide of 25 amino acid residues (Fig. 2). The mature *Pm*Spz1 protein had an estimated molecular mass of 23.7 kDa and a p*I* of 5.34. The blastp indicated a Spätzle conserved domains at 116–208 amino acid residues of the mature protein.

By comparing to the Spätzle sequences of *D. melanogaster* Spz1 (*Dm*Spz1), *M. sexta* Spz1A (*Ms*Spz1A) and *B. mori* Spz1 (*Bm*Spz1), six conserved Cys residues at the carboxyl-terminal domain, also known as cysteine knot domain, were observed (Fig. 3). The protease cleavage site was predicted to be C-terminal of His109 equivalent to Arg195, Arg169 and Arg152 of *Dm*Spz1, *Ms*Spz1A and *Bm*Spz1, respectively, and possibly not cleaved by a trypsin-like protease. No basic amino acids, Arg and Lys, were in the vicinity of His109 of *Pm*Spz1.

3.3. Expression of PmSpz1 gene in shrimp tissues and in response to WSSV infection

The *PmSpz1* gene expression was investigated in nine tissues of the normal shrimp: hemocytes, stomach, hepatopancreas, gill, lymphoid organ, eyestalk, muscle, intestine and heart, by RT-PCR. The results revealed that the *PmSpz1* gene was expressed in all tissues tested although it was expressed less in muscle (Fig. 4 A). The hemocytes were used for the studies of the expression of *PmSpz1* gene in response to WSSV infection and the expression of AMP genes.

The expression of *PmSpz1* has been shown to be up-regulated in response to injection with both heat-killed Gram-positive *Staphylococcus aureus* and Gram-negative *Vibrio harveyi* [21]. In this study, the expression in response to WSSV infection was investigated. After WSSV injection, the hemolymph was collected from shrimp at 3, 6, 12, 24 and 48 h and processed for qRT-PCR. In response to infection, the expression of *PmSpz1* gene was up-regulated several folds compared with the control normal saline group as shown in Fig. 4 B.

3.4. Hemolymph PmSpz1 in WSSV-infected shrimp

The Späzle protein is a secretory protein for it has a signal peptide. It is secreted into the hemolymph as an extracellular signaling molecule to capture the infection signal and relay it to the Toll receptor on the cell membrane [16,22,23]. To detect the *Pm*Spz1 in the hemolymph, the shrimp hemocyte lysate and plasma from WSSV-infected shrimp at various time points were prepared and subjected to SDS-PAGE. After Western blotting, the *Pm*Spz1 was detected using *anti-Pm*Spz1 antibody. Much to our surprise, two forms of *Pm*Spz1 corresponding to the *Pm*Spz1 pro-protein and ac*Pm*Spz1 were detected in the plasma and only the ac*Pm*Spz1 in the hemocyte lysate (Fig. 5). The pro-protein was decreased in plasma as the infection progressed. It was also interesting that a large proportion of *Pm*Spz1 were in an active form. The *Pm*Spz1 was also detected in other un-infected samples and the same results that the *Pm*Spz1 was in an active form were obtained (data not shown).

```
  CTCTCATATTGGTAGGTTGGTCATCATAATTCATAAAACAATTTAAATGGTTTTCATCCACCAT   64
ATTGTATTAATGCTATCACTTTGATACAATAACAATAAAAGAAATAATACATAATTGATTTTCTTG 130
TAC ATG TATAATTTTCAGTCGGTCGTTCTGGCTTGTGCCGGAGTCGTTCTGGGCTCCGTCCAACCC 196
   M  Y  N  F  Q  S  V  V  L  A  C  A  G  V  V  L  G  S  V  Q  P

CCAGCATATGGTCATCATCCACAGCCTGCTTACGGTCATCGTGCGCCTGCTTACGGTCATCAGCCT 262
P  A  Y  G  H  H  P  Q  P  A  Y  G  H  R  A  P  A  Y  G  H  Q  P

GCCTACAAGCACGGTTACTGCGATCCAACTGTGGCGCCTTCGTGTGCTACCAACTCAACTCTCTCC 328
A  Y  K  H  G  Y  C  D  P  T  V  A  P  S  C  A  T  N  S  T  L  S

TATTGCTTGGAAGATGCTGAGTATCCCGAGTACGAGATCAAGGGGGCCATCAGTGCTGATCATCTG 394
Y  C  L  E  D  A  E  Y  P  E  Y  E  I  K  G  A  I  S  A  D  H  L

TTCGCCAAGAAGTATGCTGATATCGCCGACCAGTCTGCTGATGATCTGGTAGACATGGTAAGCAAG 460
F  A  K  K  Y  A  D  I  A  D  Q  S  A  D  D  L  V  D  M  V  S  K

GAGCAGGAAGAGGCTTTCGATTACTCTTACTACACAGGGGCATCCACCGGGGACTCTCCTTATGAT 526
E  Q  E  E  A  F  D  Y  S  Y  Y  T  G  A  S  T  G  D  S  P  Y  D

GCCACCCACTGGGGTGGTCCTGAGGGCTACATTTGTCCCTCAGATGTGGTGTATGCCATGCCCAAA 592
A  T  H  W  G  G  P  E  G  Y  I  C  P  S  D  V  V  Y  A  M  P  K

CGTGCCCAAAACGTGGAGGGTAAATGGCGCGTGATTGTCAACGACGTTCACTATTACACCCAGACT 658
R  A  Q  N  V  E  G  K  W  R  V  I  V  N  D  V  H  Y  Y  T  Q  T

GCCCGCTTGGAGACCTGTCTGTTCCCAGAGGCTGCTTGCCGTGCCCTTGCCCCTTGCTATCAGAGT 724
A  R  L  E  T  C  L  F  P  E  A  A  C  R  A  L  A  P  C  Y  Q  S

CACTGTACCCAGAAGTCAGTGTACCACCGCCTCCTGTCGTACGACCCATGCGATCCCTATAAGGGT 790
H  C  T  Q  K  S  V  Y  H  R  L  L  S  Y  D  P  C  D  P  Y  K  G

CTCTTCATCGACATCTACAAGCTGCCTTCTGCCTGCTCCTGCCATCTTCCAGCA TAA TACGCC    853
L  F  I  D  I  Y  K  L  P  S  A  C  S  C  H  L  P  A  *
```

Fig. 2. The cDNA sequence of *PmSpz1* revealing the open-reading frame of *PmSpz1* and its deduced amino acid sequence. The signal peptide is underlined. The start and stop codons are shown in boldface. The asterisk indicates stop codon. The Spätzle conserved domain is shaded green. (For interpretation of the references to colour in this figure legend, the reader is referred to the web version of this article.)

```
PmSpz1   ------------------------------------------------------------  0
DmSpz1   KEYERIIKELFTITNDEGVVLFNTSADSAPFMPIPTQHDDPTQKQKQNQNQSPIPETNRH  60
MsSpz1A  ----YKCKDCFSFASQ------YPSYDSQVY-EQPDRRIAGRS--AQY---EHLRTNERS  44
BmSpz1   ----------------------------YKY-RQNDQQDSPHSHPQKYLAAEPNRMSERS  31

PmSpz1   ------------------------------------------------------------  0
DmSpz1   YHQYHS--LIQP--------DQYFKVQRSPNGKLNLVFNDTFVSLQRTDTEVQSEQPIPP  110
MsSpz1A  LPVYSETQRIQAEERRRHSSRLEEPRQRAENGSYKILNNPPKPCITNR--------RSQI  96
BmSpz1   IHNTDHNQRLQS-----RSSTKIEEASRTENGTFKILNKPFSIH-RRF--------AQTD  77

PmSpz1   -------HHPQPAYGHRAPAYGHQPAYKHGYCDPTVAPSCATNSTLSYCLEDAEYPEYEI  53
DmSpz1   RHPSDTFVFPDSPIAKYRPPQSPARPLRNDTKEHNPCAKDESQHLRNFCTNVDDYPDLS-  169
MsSpz1A  DSSNDRVVFPGPTSE---RSYVPEVP--------------EECKKIGICDSIPNYPEEHV  139
BmSpz1   DSPGDRVVFPGLTSRSGVNPYVPEIP--------------ESCKKMGICDKIPNYPREQV  123
                .*                                  . * .  :**

                                                                    ▼
PmSpz1   KGAISADHLFAKKYADIADQSADDLVDMVSKEQEEAFDYSYYTGASTGDSPYDATHWGGP  113
DmSpz1   -GLTHKLKN---NFA-----------------------KFFSNDL---QPTDVSSRVGGS  199
MsSpz1A  ANIISRLGD---KGK----------------------VLQIDELDVSDTPDIAQRLGPQ  173
BmSpz1   EKIVAKLGE---KTE----------------------FQFDKLDLPSIPDIAQRAGSF  156
                    :                                  .    : : *

                   1                                   2      3
PmSpz1   --EGYICPSDVVYAMPKRAQNVEGKWRVIVNDVHYYTQTARLETCLFPEAACRALA---P  168
DmSpz1   D-ERFLCRSIRKLVYPKKGLRADDTWQLIVNNDE-YKQAIQIEECEGADQPCDFAANFPQ  257
MsSpz1A  EDNMELCSFREKIFYPKAAPDKDGNWFFVVNSKENPVQGYKVEICDRQQLPCAEFASFQQ  233
BmSpz1   EDSYELCDFRVQIMTPLAGQSDDLKWYHVLNFNENPLQGFRVEICNTTSTGCAKFVTMEN  216
             :*        *  .   : .*  ::*  .   *  ::* *   .  *   .

                   4                                  5 6
PmSpz1   CYQSHCTQKSVYHRLLSYDPCDPYKGLFIDIYKLPSACSCHLPA---  212
DmSpz1   SYNPICKQHYTQQTLASIKSDGEL-DVVQNSFKIPSCCKCALKTG--  301
MsSpz1A  GYEARCIQKYVRRTMLALDPKGQM---TDMPLKVPSCCSCVAKLTII  277
BmSpz1   NYNPKCVQKFIFRKMKILSESGEM---IERSMKVPSCCSCVATLLG-  259
          *:  * *:   : :   .  .          *:**.*.*
```

Fig. 3. Amino acid sequence alignment of *Pm*Spz1 protein with the *D. melanogaster* Spz1 (accession no. NM_079802), *M. sexta* Spz1A (GQ249944) and *B. mori* Spz1 (NM_001114594). The six conserved cysteine residues of the cystine knot domain are shaded blue. The proteolytic cleavage sites that activate Spz proteins are indicated by black triangle after the green-shaded amino acids. (For interpretation of the references to colour in this figure legend, the reader is referred to the web version of this article.)

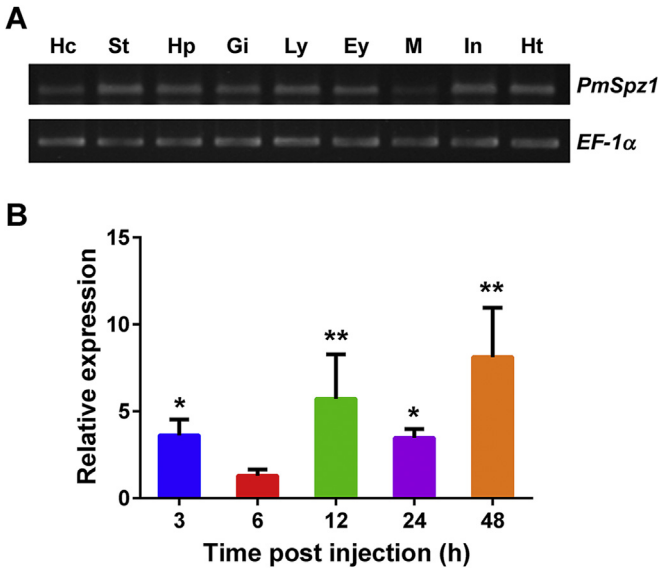


Fig. 4. Expression of *PmSpz1* gene in shrimp tissues and in response to WSSV infection. (A) Nine tissues from shrimp: hemocytes (Hc), stomach (St), hepatopancreas (Hp), gill (Gi), lymphoid organ (Ly), eyestalk (Ey), muscle (M), intestine (In) and heart (Ht) were tested for the expression of *PmSpz1*. (B) Shrimp were infected with WSSV and tested for the expression of *PmSpz1* in the hemocytes at various times. The results are means ± SDs of three independent amplifications. The * and ** indicate significant differences more than 2-fold and 10-fold, respectively, over the normal saline control. For both experiments, the expression of *EF-1α* was used as an internal control.

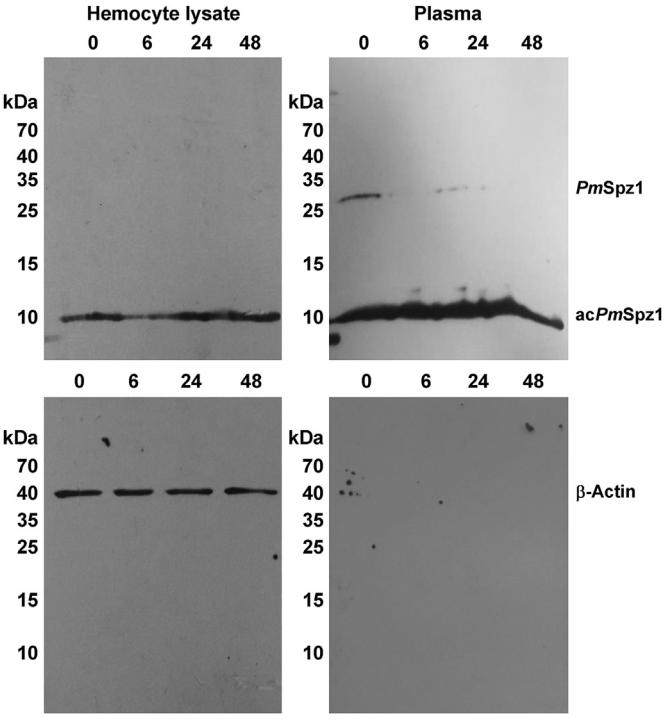


Fig. 5. Western blot analysis of *Pm*Spz1 in hemocyte lysate and plasma from WSSV-infected shrimp. The hemocyte lysate and plasma were prepared from WSSV-infected shrimp at 0, 6, 24 and 48 hpi. They were subjected to SDS-PAGE and Western blotting. The *Pm*Spz1 was detected using *anti-Pm*Spz1 as primary antibody and secondary antibody conjugated with horseradish peroxidase. The protein bands were developed using chemiluminescent substrates and detected by X-ray film. The β-actin was detected as an internal control. Nevertheless, the β-actin was not detected in the plasma.

3.5. Protein expression of PmSpz1 protein and its active domain

To study the activity of *Pm*Spz1 protein, the gene fragments encoding the mature *Pm*Spz1 and its active domain ac*Pm*Spz1 obtained through PCR were cloned into an *E. coli* expression vectors. They are over-produced using a host cell *E. coli* BL21 (DE3) CodonPlus.

The r*Pm*Spz1 was over-expressed as inclusion bodies. It was solubilized in sodium carbonate buffer pH 10.0 and purified by Ni-NTA column. The purification was traced by SDS-PAGE. The purified r*Pm*Spz1 had an estimated size of about 30 kDa although the calculated MW was 26.2 kDa (Fig. 6, lane 1). Nevertheless, the expressed protein was shown to be genuine r*Pm*Spz1 by Western blot analysis using anti-His antibody (data not shown).

The rac*Pm*Spz1 was produced as a fusion protein to Trx tag of 26.0 kDa and also as inclusion bodies. The fusion protein was solubilized and cleaved with enterokinase to completion. The active domain was re-purified by Ni-NTA column (Fig. 6, lane 2). The rac*Pm*Spz1 after removing the Trx tag was 13.3 kDa in size.

3.6. Effect of rPmSpz1 protein on the survival of WSSV-infected shrimp

Since the Spätzle protein is involved in immune response to pathogens, it is interesting to know whether the protein can provide any antimicrobial actions in the shrimp. The shrimp were injected with WSSV along with r*Pm*Spz1 protein and observed their survival compared to those injected with WSSV alone and other injection controls. The results showed that the r*Pm*Spz1 protected the shrimp from the usual WSSV extermination. The shrimp was able to survive more than 40% up to ten days (Fig. 7).

3.7. racPmSpz1 stimulated the expression of some antimicrobial peptide genes

The active domain of Spätzle is known to activate the Toll receptor leading to the Toll signaling into the nucleus to trigger the synthesis of certain AMPs. To test which AMPs were synthesized in this Spätzle activated immune response, the active domain rac*Pm*Spz1 was injected into the shrimp. The cDNAs from the hemocytes at 24 h were tested by qRT-PCR for the expression of five AMP genes, namely *ALFPm3*, *crustinPm1*, *crustinPm7*, *penaeidin3* and *penaeidin5*. The qRT-PCR showed that the gene expression of

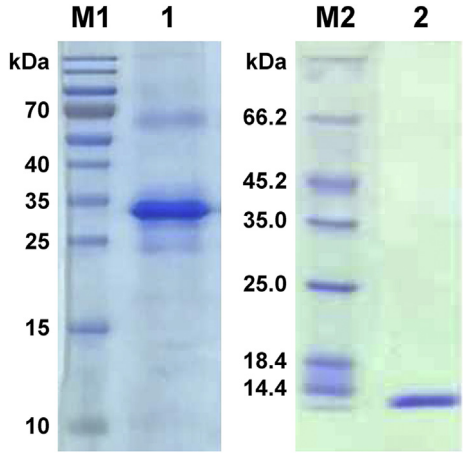


Fig. 6. The purified r*Pm*Spz1 and rac*Pm*Spz1 proteins. The purified r*Pm*Spz1 (lane 1) and rac*Pm*Spz1 (lane 2) was analyzed by SDS-PAGE. Lanes M1 and M2 are two different protein standard markers.

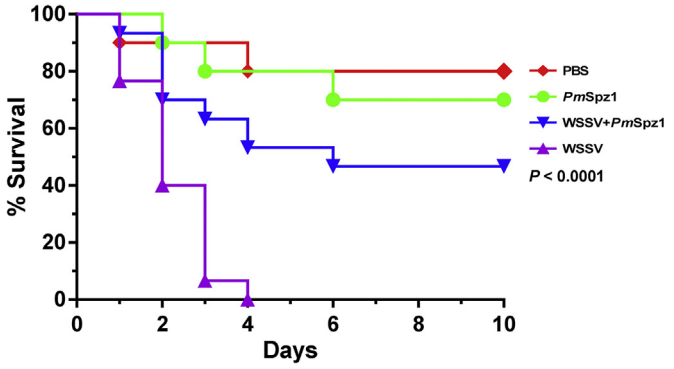


Fig. 7. The Kaplan-Meier survival plots showing the protective effect of r*Pm*Spz1 protein on the WSSV-infected shrimp. Four groups of shrimp were injected with 1 × PBS, r*Pm*Spz1, WSSV + r*Pm*Spz1 and WSSV. Some shrimp died in the PBS and *Pm*Spz1 groups because of moulting and cannibalism. The *P* value calculated by log-rank test in the GraphPad Sigma Plot indicates significant difference.

crustinPm1, *crustinPm7*, *ALFPm3*, and *penaeidin3* but not *penaeidin5* were significantly up-regulated after injecting with 3 nmol of rac*Pm*Spz1 (Fig. 8) although the levels of up-regulation were different. The genes with up-regulated expression were under or partly under the control of Toll pathway.

4. Discussion

A Spätzle protein is a signaling protein involved in the activation of Toll pathway for embryonic dorso-ventral patterning and the biosynthesis of the cognate antimicrobial proteins [7]. The proteins in several organisms have been studied, for example *Drosophila* Spz [16], *M sexta* Spz1A [13], *L. vannamei* *Lv*Spz1, 2 and 3 [10], *F. chinensis* *Fc*Spz [14], etc. In *P. monodon*, there have been a few clones of Spätzle genes identified but have not been studied any further. Therefore, we undertook a study of Spätzles from *P. monodon* and only the *Pm*Spz1, one of the three *Pm*Spzs, was studied in details.

Since there are three Spätzles identified in *L. vannamei* [10], as a close related species, the *P. monodon* was expected to have at least three *PmSpz* genes. By searching through the databases, two *Pm*Spz genes from *Penaeus monodon* EST database and GenBank (accession no. KM225266) were obtained equivalent to the *LvSpz1* and *3*

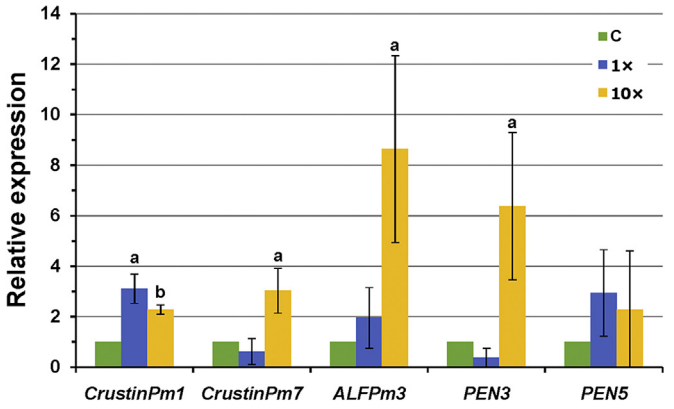


Fig. 8. Expression of the five AMP genes after injecting 0.3 (1 ×) and 3 (10 ×) nmol of the active domain rac*Pm*Spz1 protein. The AMPs tested were *crustinPm1*, crustin*Pm7*, *ALFPm3*, *penaedin3* and *penaeidin5*. The data represent means ± SDs of three independent qPCR amplifications. The expression of *EF-1α* gene was used as an internal control. Letters indicate significant differences above the normal saline control at $P < 0.05$.

genes, respectively. By using PCR primers designed from the *LvSpz2* gene sequence, the *PmSpz2* gene was amplified and identified by DNA sequencing as *PmSpz2* gene fragment. It was concluded that there were at least three *PmSpz* genes in *P. monodon*. The reason that the *PmSpz2* gene had not been identified before was due to the fact that it was expressed at very low level. The *PmSpz1* was supposedly the most abundant one since it was the only clone detected in *Penaeus monodon* EST database. The function of each *Pm*Spz remained to be elucidated.

As an immune protein in Toll signaling pathway, the expression of *PmSpz1* gene would be detected in all shrimp tissues and modulated in response to infection by Gram-positive bacteria and fungi. By RT-PCR analysis of the cDNAs derived from different shrimp tissues, the expression of *PmSpz1* was detected in all shrimp tissues and up-regulated in response to WSSV infection. Arayamethakorn et al. (2017) reported that the *Pm*Spz1 was also up-regulated after challenging with heat-killed *S. aureau* and *V. herveyi* [21]. Shi et al. (2009) also found that the *Fc*Spz, supposedly *Fc*Spz3 as compared to *Lv*Spz3, expressed in all tissues tested and its expression was up-regulated by both WSSV and *Vibrio anguillarum* [14]. In oak silkworm, *Antheraea pernyi*, *Ap*Spz is activated after infection in tissues with fungus, *Nosema pernyi* and Gram-positive bacterium, *Enterococcus pernyi*, but not with the Gram-negative bacterium *E. coli* [12].

It is assumed that the *Pm*Spz1 synthesized in hemocytes is secreted into the blood circulation as a pro-protein and cleaved in response to infection. The *Pm*Spz1 in the hemocytes and plasma of WSSV-infected shrimp was, then, analyzed by Western blot analysis. It was intriguing to find out that the majority of *Pm*Spz1 in the hemocytes and plasma, even at zero-time point of WSSV infection, was an active domain ac*Pm*Spz1. Small amount of the *Pm*Spz1 pro-protein was observed in the plasma. It was not clear why and how the active form of *Pm*Spz1 was found already in the hemolymph. The existence of ac*Pm*Spz1 suggested that the active form in the blood circulation was possibly not ready for Toll activation. To activate the Toll pathway, certain factor(s) derived from pathogen infection might be needed for the active form to bind with the Toll receptor. The finding of essentially active form of *Pm*Spz1 was in contrast to that of *Fc*Spz3 in which the pro-protein was detected in several tissues including hemolymph [14].

To study the *Pm*Spz1 protein, the complete *PmSpz1* gene was cloned, sequenced and analyzed. The *Pm*Spz1 was 237 amino acids in length with 25 amino acid signal peptide. The mature protein was 23.7 kDa in size with a Spätzle conserved domains at its C-terminal amino acid sequence positions 116–208. It is known that the Spätzle protein is cleaved by the serine proteases Easter during dorso-ventral patterning and Spätzle-processing enzyme upon infection to release the active C-terminal domain to relay the signal through the Toll pathway [2,24]. By amino acid sequence comparison with other Spätzle proteins whose cleavage sites were known, a cleavage site for *Pm*Spz1 was identified at the C-terminal of His109. The same cleavage site could be predicted for *Lv*Spz1. The Spätzle proteins in other arthropods are cleaved by trypsin-like enzymes for the cleavage sites are C-terminal to Arg. A proteinase that cleaves *Pm*Spz1 was not a trypsin-like enzyme.

The mature r*Pm*Spz1 protein and its active domain, rac*Pm*Spz1, were over-produced in an *E. coli* expression system for activity studies. The purified r*Pm*Spz1 protein was tested for its function in immune defense by injecting it into the shrimp along with WSSV. It was found that the r*Pm*Spz1 helped prolong the life of shrimp by about 50% up to ten days. The added r*Pm*Spz1 might provide excess Spätzle for the shrimp to response immediately with the WSSV infection. The defense response was possibly the induction of AMP synthesis. Weber et al. (2003) found that injection of the mature form of Spätzle followed by immune challenge activated the

synthesis of drosomycin [16].

However, injection of Spätzle active fragment C-106 readily activates *drosomycin* expression in flies bypassing the immune challenge [16]. The same results were observed with *F. chinensis* and *B. mori*. The recombinant *Fc*Spz C-114 up-regulated the expression of *crustin 2* gene but not *lysozyme*, *astacidin* and *crustin 1* genes in crayfish [14]. The active *Bm*Spz1 but not its pro-protein induced the expression of eight AMP genes, *attacin-2*, *cecropin-A1*, *-B1*, *-D1*, *gloverin-A5*, *-B*, *lebocin-3* and *moricin-A1* [11]. The active rac*Pm*Spz1 was also tested for its activity to up-regulate the synthesis of AMPs. After injecting the rac*Pm*Spz1 into the shrimp, the expression of *crustinPm1*, *crustinPm7*, *ALFPm3*, *penaeidin3* and *penaeidin5* were analyzed. All but *penaeidin5* were under the Toll pathway. The expression results of *penaeidin3* and *5* agreed well with our previous results and suggested that the expression of *penaeidin3* was partly under the regulation of Toll and Imd pathways whereas that of *penaeidin5* was under the control of Imd pathway [25,26]. We also found in those previous studies that the expression of *ALFPm3* was not under the Imd regulation but, in this study, under the Toll pathway. Arayamethakorn et al. (2017) found that the expression of *crustinPm1* was under the regulation of Toll pathway whereas that of *crustinPm7* was under the regulation of both Toll and Imd pathways [21].

Acknowledgements

This project was supported by research grants from the Srinakharinwirot University (028/2558) to S. Ponprateep and the TRF Senior Research Scholar (No. RTA5880004), Thailand Research Fund. We thank the matching fund from the Thailand Research Fund and the Srinakharinwirot University (Grant No. TRG5880147) to S. Ponprateep and the support under the Ratchadapisek Somphot Endowment to the Center of Excellence for Molecular Biology and Genomics of Shrimp. We acknowledge the support of equipment used in this study under the JST-JICA joint program “Science and Technology Research Partnership for Sustainable Development, SATREPS”.

References

[1] A. Tassanakajon, K. Somboonwiwat, P. Supungul, S. Tang, Discovery of immune molecules and their crucial functions in shrimp immunity, Fish. Shellfish Immunol. 34 (2013) 954–967.
[2] F. Li, J. Xiang, Signaling pathways regulating innate immune responses in shrimp, Fish. Shellfish Immunol. 34 (2013) 973–980.
[3] J. Royet, R. Dziarski, Peptidoglycan recognition proteins: pleiotropic sensors and effectors of antimicrobial defences, Nat. Rev. Microbiol. 5 (2007) 264–277.
[4] B.A. Stokes, S. Yadav, U. Shokal, L.C. Smith, L. Eleftherianos, Bacterial and fungal pattern recognition receptors in homologous innate signaling pathways of insects and mammals, Front. Microbiol. 6 (2015) 1–12.
[5] S. Valanne, J.H. Wang, M. Rämet, The *Drosophila* Toll signaling pathway, J. Immunol. 186 (2011) 649–656.
[6] C.J. Arnot, N.J. Gay, M. Gangloff, Molecular mechanism that induces activation of Spätzle, the ligand for the *Drosophila* Toll receptor, J. Biol. Chem. 285 (2010) 19502–19509.
[7] I.H. Jang, N. Chosa, S.H. Kim, H.J. Nam, B. Lemaitre, M. Ochiai, Z. Kambris, S. Brun, C. Hashimoto, M. Ashida, A Spätzle-processing enzyme required for Toll signaling activation in *Drosophila* innate immunity, Dev. Cell 10 (2006) 45–55.
[8] J.S. Parker, K. Mizuguchi, N.J. Gay, A family of proteins related to Spätzle, the toll receptor ligand, are encoded in the *Drosophila* genome, Proteins 45 (2001) 71–80.
[9] S.W. Shin, G. Bian, A.S. Raikhel, A toll receptor and a cytokine, Toll5A and Spz1C, are involved in Toll antifungal immune signalling in the mosquito *Aedes aegypti*, J. Biol. Chem. 281 (2006) 39388–39395.
[10] P.H. Wang, J.P. Liang, Z.H. Gu, D.H. Wan, S.P. Weng, X.Q. Yu, J.G. He, Molecular cloning, characterization and expression analysis of two novel Tolls (*Lv*Toll2 and *Lv*Toll3) and three putative Spätzle-like Toll ligands (*Lv*Spz1-3) from *Litopenaeus vannmei*, Dev. Comp. Immunol. 36 (2012) 359–371.
[11] Y. Wang, T. Cheng, S. Rayaprolu, Z. Zou, Q. Xia, Z. Xiang, Proteolytic activation of pro-Spätzle is required for the induced transcription of antimicrobial peptide gene in lepidopteran insects, Dev. Comp. Immunol. 31 (2007) 1002–1012.
[12] Y. Sun, Y. Jiang, Y. Wang, X. Li, R. Yang, Z. Yu, L. Qin, The Toll signaling pathway in the Chinese oak silkworm, Antheraea pernyi: innate immune responses to different microorganisms, PLOS ONE 11 (2016) e0160200.
[13] C. An, H. Jiang, M.R. Kanost, Proteolytic activation and function of the cytokine Spätzle in innate immune responses of a lepidopteran insect, *Manduca sexta*, FEBS J. 277 (2010) 148–162.
[14] X.Z. Shi, R.R. Zhang, Y.P. Jia, X.F. Zhao, X.Q. Yu, J.X. Wang, Identification and molecular characterization of a Spätzle-like protein from Chinese shrimp (*Fenneropenaeus chinensis*), Fish. Shellfish Immunol. 27 (2009) 610–617.
[15] D.S. Schneider, Y. Jin, D. Morisato, K.V. Anderson, A processed form of the Spätzle protein defines dorsal-ventral polarity in the *Drosophila* embryo, Development 120 (1994) 1243–1250.
[16] A.N. Weber, S.T. Tauszig-Delamasure, J.A. Hoffmann, E. Lelievre, H. Gascan, K.P. Ray, M.A. Morse, J.L. Imler, N.J. Gay, Binding of the *Drosophila* cytokine Spätzle to Toll is direct and establishes signaling, Nat. Immunol. 4 (2003) 794–800.
[17] M.W. Pfaffl, A new mathematical model for relative quantification in real-time RT-PCR, Nucleic Acids Res. 29 (2001) e45.
[18] M.M. Bradford, A rapid and sensitive method for the quantitation of microgram quantities of protein utilizing the principle of protein-dye binding, Anal. Biochem. 72 (1976) 248–254.
[19] S. Donpudsa, A. Tassanakajon, V. Rimphanitchayakit, Domain inhibitory and bacteriostatic activities of the five-domain Kazal-type serine proteinase inhibitor from black tiger shrimp *Penaeus monodon*, Dev. Comp. Immunol. 33 (2009) 481–488.
[20] A. Tassanakajon, S. Klinbunga, N. Paunglarp, V. Rimphanitchayakit, A. Udomkit, S. Jitrapakdee, K. Sritunyalucksana, A. Phongdara, S. Pongsomboon, P. Supungul, S. Tang, K. Kuphanumart, R. Pichyangkura, C. Lursinsap, *Penaeus monodon* gene discovery project: the generation of an EST collection and establishment of a database, Gene 384 (2006) 104–112.
[21] S. Arayamethakorn, P. Supungul, A. Tassanakajon, K. Krusong, Characterization of molecular properties and regulatory pathways of Crustin*Pm*1 and Crustin*Pm*7 from the black tiger shrimp *Penaeus monodon*, Dev. Comp. Immunol. 67 (2017) 18–29.
[22] S. Mulinari, U. Hacker, C. Castillejo-Lopez, Expression and regulation of Spätzle processing enzyme in *Drosophila*, FEBS Lett. 80 (2006) 5406–5410.
[23] A.K.H. Shia, M. Glittenberg, G. Thompson, A.N. Weber, J.M. Reichhart, P. Ligoxygakis, Toll-dependent antimicrobial responses in *Drosophila* larval fat body require Spätzle secreted by haemocytes, J. Cell Sci. 122 (2009) 4505–4515.
[24] D. Ferrandon, J.L. Imler, J.A. Hoffmann, Sensing infection in *Drosophila*: toll and beyond, Semin. Immunol. 16 (2004) 43–53.
[25] S. Visetnan, P. Supungul, I. Hirono, A. Tassanakajon, V. Rimphanitchayakit, Activation of *Pm*Relish from *Penaeus monodon* by yellow head virus, Fish. Shellfish Immunol. 42 (2015) 335–344.
[26] S. Visetnan, P. Supungul, S. Tang, I. Hirono, A. Tassanakajon, V. Rimphanitchayakit, YHV-responsive gene expression under the influence of *Pm*Relish regulation, Fish. Shellfish Immunol. 47 (2015) 572–581.

SCIENTIFIC REPORTS

OPEN

Molecular Characterization of Viral Responsive Protein 15 and Its Possible Role in Nuclear Export of Virus in Black Tiger Shrimp *Penaeus monodon*

Received: 28 March 2017
Accepted: 15 June 2017
Published online: 26 July 2017

Krisadaporn Jaturontakul[1], Thapanan Jatuyosporn[1], Pasunee Laohawutthichai[1], Sun-Yong Kim[2], Tomoyuki Mori[2], Premruethai Supungul[1,3], Toshio Hakoshima[2], Anchalee Tassanakajon[1] & Kuakarun Krusong[1]

A viral responsive protein 15 from *Penaeus monodon* (*Pm*VRP15) has been reported to be important for white spot syndrome virus (WSSV) infection *in vivo*. This work aims to characterize *Pm*VRP15 and investigate its possible role in nuclear import/export of the virus. Circular dichroism spectra showed that *Pm*VRP15 contains high helical contents (82%). Analytical ultracentrifugation suggested that *Pm*VRP15 could possibly form oligomers in solution. A subcellular fractionation study showed that *Pm*VRP15 was found in heavy and light membrane fractions, indicating that *Pm*VRP15 may be associated with endoplasmic reticulum. Double-stranded RNAi-mediated knockdown of *Pm*VRP15 gene expression *in vitro* showed no effect on WSSV copy number in whole hemocyte cells. However, *Pm*VRP15 silencing resulted in an accumulation of WSSV DNA in the nucleus of *Pm*VRP15-silenced hemocytes. Immunofluorescence confocal microscopy showed that *Pm*VRP15 knockdown hemocytes had a much lower level of VP28 (WSSV envelope protein), in comparison to that in the control. It is likely that *Pm*VRP15 may play a role in viral nuclear egress.

White spot syndrome virus (WSSV) is highly infectious and can cause 100% cumulative mortality of farmed shrimps within 3–10 days[1]. In the past decades, shrimp aquaculture industry has been threatened by WSSV, and so far there is no effective treatment for WSSV infection. Understanding the molecular mechanism of WSSV infection will certainly promote the development of potent agents acting against the virus.

WSSV is a bacilliform, non-occluded enveloped virus with the tightly packed nucleocapsid located inside its lipidic, trilaminar membranous envelope[2–5]. The virus replicates and assembles in the host nucleus[6]; and at the late stage of infection, the infected cells are lysed, causing extensive tissue necrosis.

Despite intensive investigations of WSSV infection, the mechanisms of WSSV entry and propagation in shrimp have not yet been fully understood. Several methods including expressed sequenced tag (EST)[7–9], DNA microarray[10–14] and proteomic[15–19], have been used to analyse molecular changes during WSSV infection.

Suppression subtractive hybridization (SSH) of WSSV-challenged *P. monodon* hemocytes identified the novel viral responsive protein 15 (*Pm*VRP15) as one of the most highly up-regulated genes in the acute phase of WSSV infection[20]. Tissue distribution analysis showed that *Pm*VRP15 transcript was mainly expressed in the hemocytes of shrimp, and found in all three types of hemocyte (hyaline, semigranular and granular cells). *Pm*VRP15 knock-down resulted in a significant decrease in viral gene expression and cumulative mortality rate of WSSV-infected shrimp, indicating that *Pm*VRP15 is crucial for WSSV propagation. *Pm*VRP15 was also named as *Pm*ERP15,

[1]Center of Excellence for Molecular Biology and Genomics of Shrimp, Department of Biochemistry, Faculty of Science, Chulalongkorn University, Bangkok, 10330, Thailand. [2]Structural Biology Laboratory, Nara Institute of Science and Technology, 8916-5 Takayama, Ikoma, Nara, 630-0192, Japan. [3]National Center for Genetic Engineering and Biotechnology (BIOTEC), National Science and Technology Development Agency (NSTDA), Pathumthani, 12120, Thailand. Krisadaporn Jaturontakul and Thapanan Jatuyosporn contributed equally to this work. Correspondence and requests for materials should be addressed to K.K. (email: Kuakarun.K@chula.ac.th)

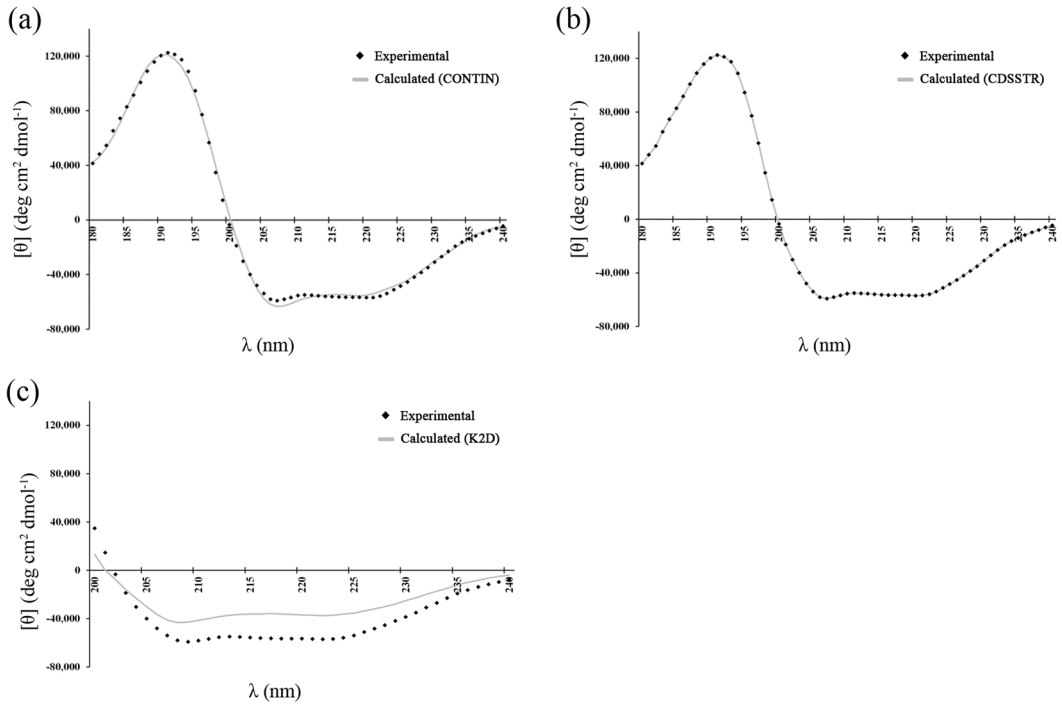


Figure 1. CD spectra of r*Pm*VRP15 analysed by CONTINLL (**a**), CDSSTR (**b**) and K2D (**c**) algorithms via DichroWeb. SMP180 was used as reference dataset. CDSSTR (the best fit) gave calculated secondary structure of 82% α-helix, 4% β-strand, 8% turn and 6% unordered.

an endoplasmic reticulum (ER) stress-induced protein, which was reported to be important for the survival of WSSV infected shrimps[21]. Recently, WSV399 viral tegument protein was identified as *Pm*VRP15 binder[22].

This study examines the molecular characteristics of *Pm*VRP15, a 137-amino acid protein containing a putative transmembrane helix, using biophysical techniques including mass spectrometry, circular dichroism, analytical ultracentrifugation and size-exclusion chromatography. In addition, a possible role of *Pm*VRP15 in nuclear import/export has been investigated by measuring WSSV copy number in nuclear and cytoplasmic fractions.

Results

Expression and purification of recombinant *Pm*VRP15. Recombinant *Pm*VRP15 was expressed in *E. coli* C43 (DE3) and purified by Ni-NTA Sepharose™ 6 Fast Flow and HiTrap SP Fast Flow columns. A major protein band appeared just below 15 kDa, close to the estimated size of r*Pm*VRP15 (15.86 kDa) (See Supplementary Information, Fig. S1). This protein band was confirmed as r*Pm*VRP15 by Western immunoblotting using anti-His monoclonal antibody.

Molecular characterization of recombinant *Pm*VRP15. MALDI-TOF MS analysis showed that the molecular mass of recombinant *Pm*VRP15 was 15,899.9 Da (data not shown), which corresponded to the calculated MW of *Pm*VRP15 protein (15,859.5 Da), using ExPASy server[23]. CD spectra were analysed by K2D, CONTINLL and CDSSTR algorithms via DichroWeb, using a mixed soluble and membrane protein dataset, SMP180, as reference. CDSSTR produced the best fit to the experimental data (NRMSD = 0.001), in comparison to CONTINLL (NRMSD = 0.044) and K2D (NRMSD = 0.336) (Fig. 1). Output from the CDSSTR/SMP180 suggested that r*Pm*VRP15 is an α-helical protein containing 82% α-helix, 4% β-strand, 8% turn and 6% unordered.

Ultracentrifuge sedimentation-velocity analysis of purified r*Pm*VRP15 showed a principal peak at 172 kDa (Fig. 2). Assuming that the molar mass of a single molecule of r*Pm*VRP15 bound to detergent was 39.5 kDa (the first peak in Fig. 2), a major peak of 172 kDa corresponds to a tetramer and that of 349 kDa to an octamer. It is also possible that the first peak is a dimer and the other two are octamer and 16-mer.

Size-exclusion chromatography (SEC) was performed to monitor protein aggregation by Superdex 200 column (GE Healthcare). r*Pm*VRP15 was aggregated in equilibration buffer without DM as the protein eluted in early fractions (data not shown). In contrast, r*Pm*VRP15 seemed to be soluble in equilibration buffer with DM and eluted with an approximate MW of ~200 kDa (Fig. 3), which is consistent with the AUC result. This suggested that it is necessary to include detergent in buffer to maintain r*Pm*VRP15 solubility.

Protein localization of *Pm*VRP15 by subcellular protein fractionation. Intact nuclei, heavy membrane, light membrane and cytosol fractions were extracted from WSSV-infected hemocyte cultures by differential centrifugation. Immunoblot analysis of all fractions using anti-*Pm*VRP15 antibody revealed that *Pm*VRP15 exists in heavy membrane (plasma membrane and rough ER) and light membrane (polysomes, golgi apparatus, smooth ER) fractions (Fig. 4), indicating that *Pm*VRP15 may be an ER-localized protein.

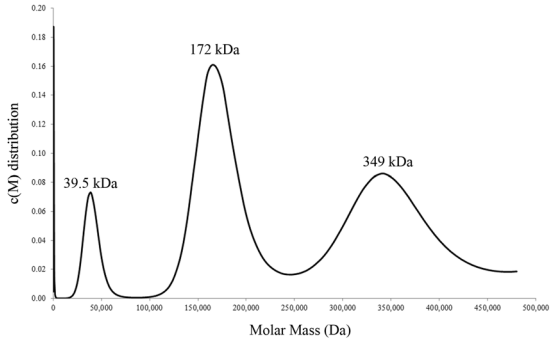


Figure 2. Sedimentation velocity analysis of r*Pm*VRP15. Three peaks of apparent molecular mass of 39.5, 172 and 349 kDa are displayed. The major peak is found at 172 kDa.

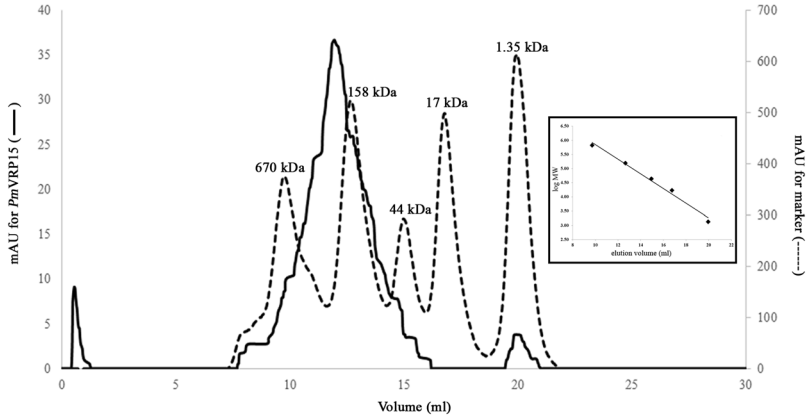


Figure 3. Analytical gel filtration profile of r*Pm*VRP15. Elution profiles of a protein standard mixture and r*Pm*VRP15 are shown in dashed (----) and solid lines (—), respectively. The inset shows a linear relationship between log MW and elution volume.

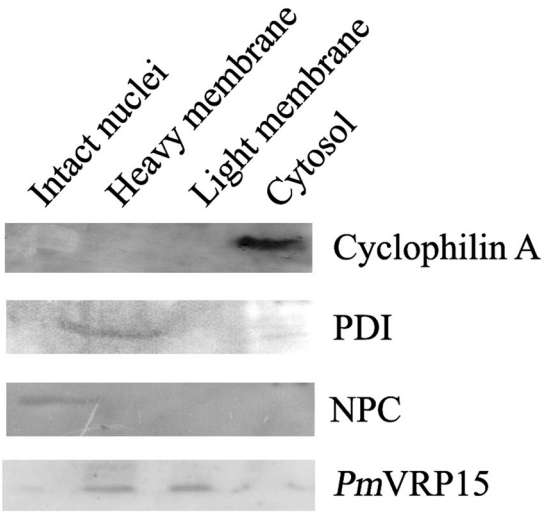


Figure 4. Western blotting analysis of subcellular fractionated WSSV-infected hemocytes. Anti-Cyclophilin A, PDI and NPC antibodies were used as cytosol, ER and nuclear markers, respectively. The blots shown here are cropped from full-length blots in the Supplementary Information.

***Pm*VRP15 mRNA expression in shrimp primary hemocyte culture in response to WSSV.** *Pm*VRP15 expression in unchallenged and WSSV-challenged *P. monodon* primary hemocyte cultures was examined by RT-PCR. Clearly, *Pm*VRP15 transcripts were increased after 12 h post-WSSV infection onwards

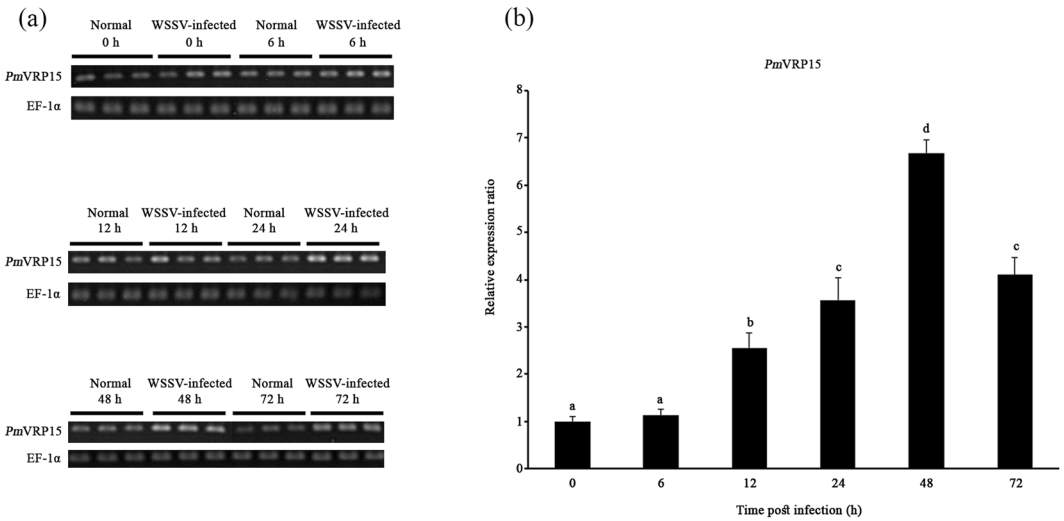


Figure 5. *In vitro Pm*VRP15 mRNA levels in response to WSSV infection. Relative expression ratios of *Pm*VRP15 transcript levels were determined in WSSV-infected *P. monodon* hemocytes, compared to control (non-infected) shrimp and standardized against elongation factor-1 alpha (EF-1α) as an internal reference, at 0, 6, 12, 24, 48 and 72 hpi by (**a**) RT-PCR and (**b**) real time RT-PCR. The statistical significance of the data was evaluated using one-way ANOVA followed by post hoc test (Duncan's new multiple range test). Data differences were considered significant at $P < 0.01$. The gels shown here (**a**) are cropped from full-length gels, included in the Supplementary Information.

(Fig. 5a). Real-time RT-PCR confirmed that *Pm*VRP15 mRNA expression was up-regulated by 2.6-, 3.6-, 6.7- and 4.1- fold at 12, 24, 48 and 72 h post-WSSV infection, respectively (Fig. 5b). These results indicated that *Pm*VRP15 was highly expressed in *P. monodon* primary hemocyte cultures in response to WSSV infection.

Double strand RNAi-mediated silencing of *Pm*VRP15 resulted in an increase of WSSV copy number ratio in nucleus/cytoplasm. In this study, RNA interference (RNAi) technique was used to knockdown *Pm*VRP15 transcript in order to investigate the function of *Pm*VRP15. Figure 6a showed that *Pm*VRP15 dsRNA treatment could silence *Pm*VRP15 expression at 24 h-post incubation. In contrast, addition of either GFP or NaCl into hemocyte cultures did not affect *Pm*VRP15 transcript levels. Primary hemocyte cell cultures were then incubated with either *Pm*VRP15 dsRNA, GFP dsRNA or NaCl prior to WSSV infection; and WSSV copy numbers in whole cells were determined at 12 and 20 hpi. Clearly, WSSV copy numbers of hemocytes treated with either *Pm*VRP15 dsRNA, GFP dsRNA or NaCl at 20 hpi were significantly increased, in comparison to WSSV copy numbers at 12 hpi (Fig. 6b). This suggested that WSSV copy number was multiplied in all groups. Interestingly, *Pm*VRP15-silenicng did not change WSSV copy number in knVRP15 group, compared with those in NaCl-treated and knGFP groups.

In a further study, the hemocytes of *Pm*VRP15 dsRNA, GFP dsRNA or the NaCl treated group were collected at 12 and 20 hpi and fractionated into cytoplasmic and nuclear fractions for quantification of WSSV copy number. Western blotting was carried out, in order to confirm that there was no cross contamination between cytoplasmic and nuclear fractions. Anti-cyclophilin A and anti-NPC antibodies were used as subcellular markers for the cytoplasmic and nuclear fractions, respectively. As shown in Fig. 6c, cyclophilin A was detected in the cytoplasmic fractions only and NPC was present solely in the nuclear fractions. This indicated that the cytoplasmic and nuclear fractions were separated well. Thus, WSSV copy numbers in these two fractions were quantified by Real-time PCR.

Figure 6d showed that *Pm*VPR15-knockdown hemocytes contained WSSV copy number ratio in nucleus and cytoplasm of 1.77 at 12 hpi, while NaCl and GFP treated hemocytes showed WSSV copy number ratio in nucleus and cytoplasm of 0.34 and 0.31, respectively. In addition, WSSV copy number ratio in nucleus and cytoplasm of knVPR15 group was 4.89 at 20 hpi, which was much higher than those in both control groups (1.49 and 1.54). These results demonstrated that although control and knVRP groups contained similar amounts of WSSV copy number, it is obvious that WSSV DNA accumulated in the nucleus of *Pm*VRP15-knockdown hemocytes.

Expression and localization of *Pm*VRP15 in normal and *Pm*VRP15-knockdown hemocytes during WSSV infection. *Pm*VRP15 and VP28 in *Pm*VRP15 dsRNA and GFP dsRNA- treated hemocytes at 48 h post-WSSV infection was examined by confocal laser scanning microscopy using the antibodies specific to *Pm*VRP15 and VP28 coupled with different fluorescence-conjugated secondary antibodies. As shown in Fig. 7, *Pm*VRP15 (in green color) was observed in all three types of hemocytes, including granular cells (GC) semi-granular cells (SGC) and hyaline cells (HC). It also showed that *Pm*VRP15 protein was located around the edge of nucleus. The green fluorescent signal of *Pm*VRP15 was still observed in kn*Pm*VRP15 hemocytes; however, the intensity of the signal was much lower than that observed in the control (knGFP hemocytes). This suggested that *Pm*VRP15 was not completely silenced at 48 hpi, the time point at which *Pm*VRP15 was expressed at

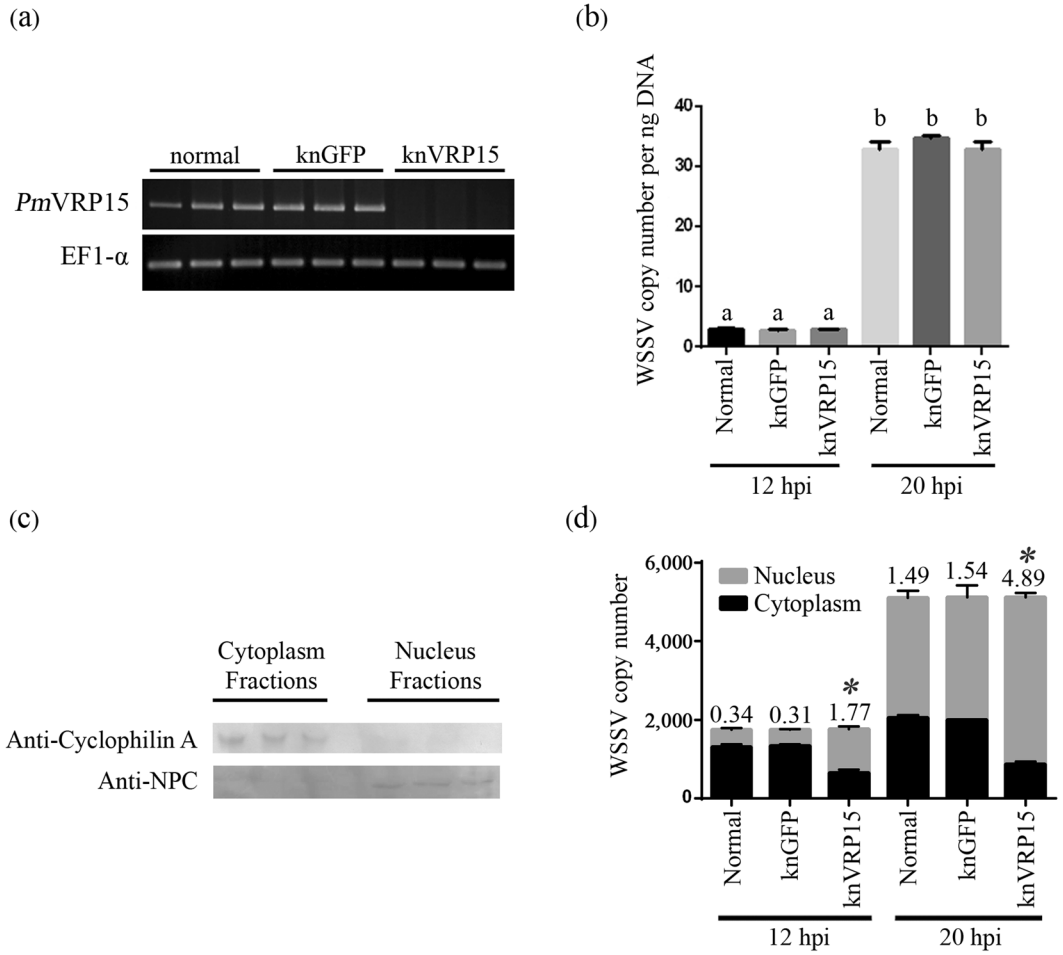


Figure 6. Determination of WSSV copy number in WSSV-infected *P. monodon* hemocytes after *Pm*VRP15-silencing. (**a**) RT-PCR analysis of *Pm*VRP15 transcripts in shrimp hemocytes treated with either NaCl, GFP dsRNA or *Pm*VRP15 at 24 hpi. (**b**) WSSV copy number in WSSV-infected whole hemocytes cells at 12 and 20 hpi. (**c**) Western blotting analysis of cytoplasmic and nuclear fractions of WSSV-infected hemocytes. Anti-Cyclophilin A and NPC antibodies were used as cytosol and nuclear markers, respectively. Western blot detection was carried out using Fast Western Blot Kit, SuperSignal® West Femto kit. (**d**) WSSV copy number in cytoplasmic and nuclear fractions of WSSV-infected hemocytes cells at 12 and 20 hpi. The statistical significance of the data was evaluated using one-way ANOVA followed by post hoc test (Duncan's new multiple range test). Data differences were considered significant at $P < 0.05$. The gel (**a**) and the blot (**b**) are cropped from full-length images, shown in the Supplementary Information.

the highest level (Fig. 5b). Interestingly, hemocytes of kn*Pm*VRP15 showed significantly lower amounts of VP28 than those in knGFP cells. This indicated that knockdown of *Pm*VRP15 resulted in a reduction of VP28 protein.

Discussion

This work aims to characterize the molecular properties of *Pm*VRP15 and investigate its role during WSSV infection. r*Pm*VRP15 was successfully expressed and purified. It is worth noting that r*Pm*VRP15 may be a toxic protein or very unstable since r*Pm*VRP15 was expressed within 1–2 h after IPTG induction only (data not shown). In general, the expression of hydrophobic heterologous proteins (usually membrane proteins) could be toxic to *E. coli*. A previous prediction based on amino acid sequence suggested that r*Pm*VRP15 could be a membrane protein with a single transmembrane helix[20]. As a result, *E. coli* C43 (DE3), which is effective in expressing toxic proteins, was used to express r*Pm*VRP15. In this research, n-decyl-ß-D-maltopyranoside (DM) was used in the purification process. Several studies have shown that DM does not interfere with the bioactivities of target proteins, denature or inactivate target proteins[24]. In nature, proteins bound to cell membranes have hydrophobic sites embedded inside the phospholipid bilayers and hydrophilic sites facing toward the water layer. DM can interact with the hydrophobic sites of proteins, providing a lipid-like environment.

The molecular mass of purified r*Pm*VRP15 determined by MALDI-TOF MS (15,899.9 Da) was in a good agreement with the calculated molecular mass. SEC was performed to monitor protein aggregation. Clearly, r*Pm*VRP15 required detergent to enhance protein solubility. AUC analysis demonstrated that, at 60 μM, r*Pm*VRP15 exists in three forms. The major peak was found at 172 kDa, indicating that most of r*Pm*VRP15 molecules existed

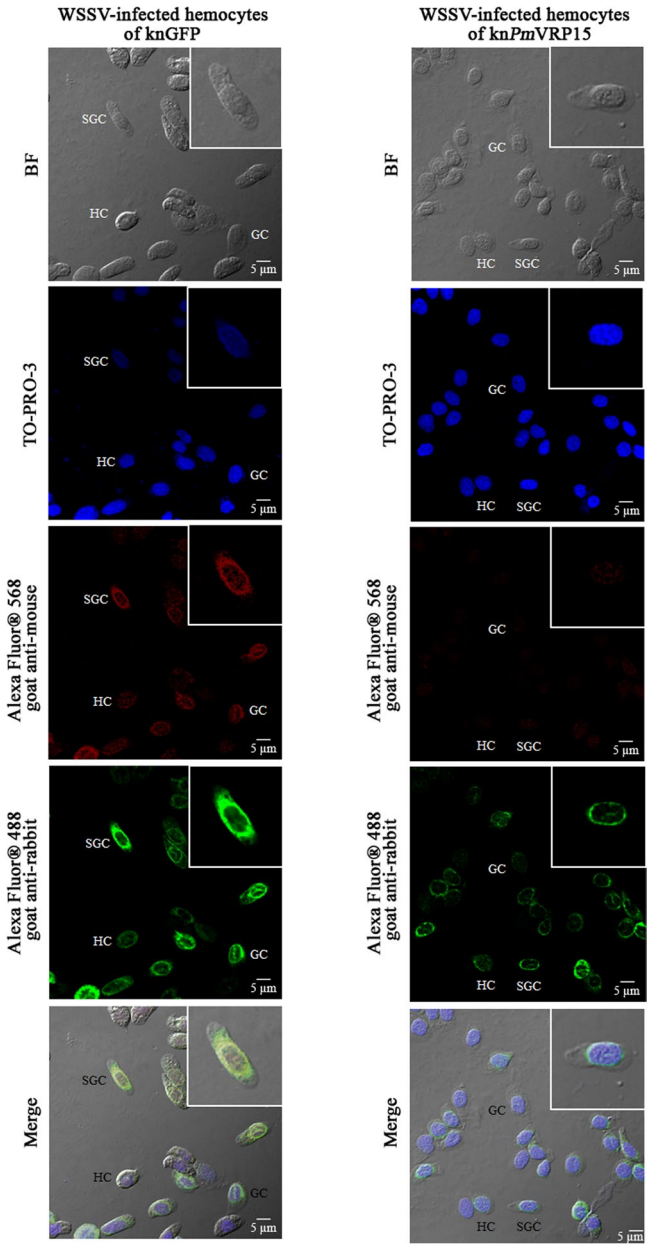


Figure 7. Immunofluorescent staining analysis of *Pm*VRP15 and VP28 in the WSSV-infected *Pm*VRP15-silenced hemocytes by confocal laser scanning microscopy. Hemocytes from *Pm*VRP15-silenced and GFP-silenced shrimp, infected by WSSV were collected at 48 hpi and probed by anti-*Pm*VRP15 and anti-VP28 antibodies. *Pm*VRP15 and VP28 proteins were visualized by secondary antibodies conjugated with Alexa Fluor® 488 (green) and Alexa Fluor® 568 (red), respectively. Nuclei were stained in blue. The GC, SGC and HC are granular, semigranular and hyaline cells, respectively. BFs are bright field images.

in a tetrameric (or octameric) form. The CD spectrum of r*Pm*VRP15 revealed that r*Pm*VRP15 possessed a high content of α-helix, which is consistent with a result of our prediction of the secondary structure elements using a Web Server (data not shown).

Immunofluorescence confocal microscopy showed that *Pm*VRP15 protein was found around the edge of nucleus. A subcellular fractionation study revealed that *Pm*VRP15 was present in heavy membrane (plasma membrane and rough ER) and light membrane (polysomes, golgi apparatus, smooth ER) fractions. A previous study showed that *Pm*ERP15 (or *Pm*VRP15 in this study) was colocalized with an ER enzyme[21]. Taken together, this work confirmed that *Pm*VRP15 is likely to be a membrane-bound protein, which localized at the ER.

Leu *et al.*[21] suggested that *Pm*ERP15 expression was induced due to ER stress exposure[21]. In addition, *Pm*ERP15 silencing increases the mortality of *P. monodon* after WSSV infection. As a result, *Pm*ERP15 was proposed to function in relieving ER stress, and in this regard, the absence of the protein led to the death of the shrimp due to the ER stress caused by WSSV infection. In contrast, Vatanavicharn *et al.*, 2004 demonstrated that

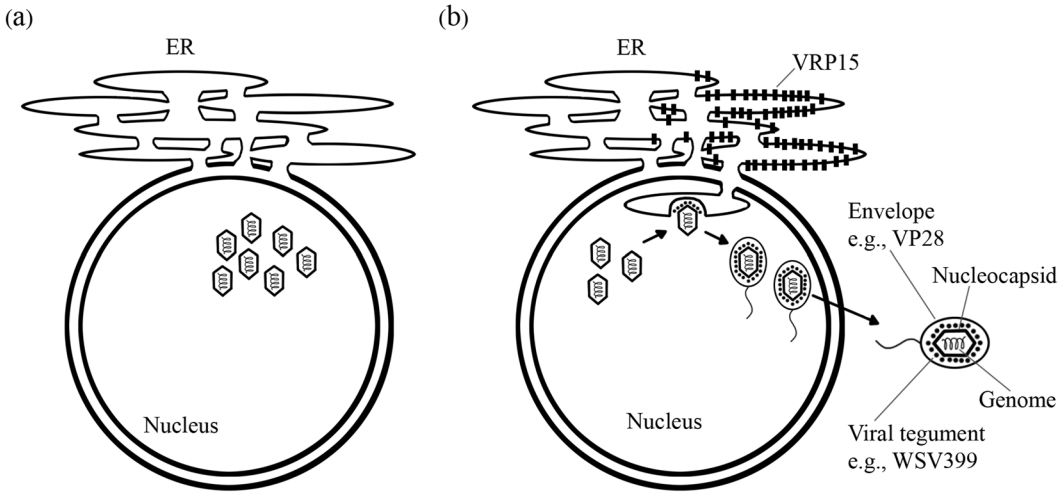


Figure 8. Proposed role of *Pm*VRP15 during WSSV infection. (**a**) In the absence of *Pm*VRP15, replicated WSSV genomes accumulate in the nucleus. (**b**) Overexpressed of *Pm*VRP15 at ER facilitates viral nuclear exit and assembly.

silencing of *Pm*VRP15 reduced the cumulative mortality rate of WSSV-infected shrimps[20]. To reconcile these conflicting data, a further study on role of *Pm*VRP15 during WSSV infection was carried out *in vitro*.

In primary hemocyte cultures, *Pm*VRP15 was up-regulated from 12 h onwards after WSSV infection. The highest level of *Pm*VRP15 expression in primary hemocyte cell cultures was observed at 48 h after WSSV infection, which was in agreement with the *in vivo* study[20]. At 48 hpi, *Pm*VRP15 was increased by 6.7-fold, in comparison to non-infected cells. This suggested that *Pm*VRP15 was induced by WSSV infection.

*In vitro Pm*VRP15-silencing did not affect WSSV copy number in whole hemocyte cells at 12 and 20 hpi. This suggested that *Pm*VRP15 plays no role in WSSV replication. This result was consistent with previously reported *Pm*VRP15 knockdown *in vivo*[21,22]. Interestingly, *Pm*VRP15 knockdown resulted in a significant increase in WSSV copy number ratio in nuclear and cytoplasmic fractions at 12 and 20 hpi. This suggested that silencing of *Pm*VRP15 caused an accumulation of WSSV DNA in nucleus. It was previously reported that WSSV DNA started to be synthesized from 6 hpi and the progeny WSSV were released from 12 hpi and peaked at 18 hpi[25]. It is possible that *Pm*VRP15 plays a role in viral exit from the nucleus, and that when *Pm*VRP15 was absent, the newly synthesized viral genomes accumulated in the nucleus.

Immunofluorescence microscopy showed that *Pm*VRP15 was observed in all three types of hemocytes, including GC, SGC and HC. However, the signal of *Pm*VRP15 in HC was much weaker than those in GC and SGC. This corresponds with the fact that WSSV selectively targets GCs and SGCs[26]. Although *Pm*VRP15-silencing showed that knVRP15 hemocytes contained similar amount of WSSV copy number to those in knGFP hemocytes, it appeared that, by confocal laser scanning microscopy, *Pm*VRP15 knockdown hemocytes had much lower level of VP28 envelope protein than those in knGFP group. This implied that *Pm*VRP15 most likely functions to accommodate viral assembly but not viral replication. Previously, *Pm*VRP15 was reported to interact with WSV399 viral tegument protein, which functions in capsid transport during viral trafficking and assembly[22].

It is evident that several virus families, including both enveloped and nonenveloped DNA and RNA viruses, rearrange the ER-membrane to facilitate viral entry, replication and assembly[27–30]. For example, rotavirus uses ER as the final assembly site, where a viral intermediate, composed of the core shell and the middle layer capsid, migrates into the ER lumen to acquire the final capsid assembly.

It is also common for viruses to use the host machinery for their advantages. For example, WSSV enters crayfish hematopoietic cells via multiple endocytic routes, including clathrin-mediated endocytosis, macropinocytosis and caveolae-mediated endocytosis[31]. In addition, *Pm*Rab7 is used in sorting and endocytic trafficking of WSSV in the host cells[32]. *P. monodon* Krupple-like factor (*Pm*KLFF) is also crucial for WSSV replication by enhancing WSSV immediate-early gene expression[33]. Previously, Li *et al.*[25] proposed that the virus enters the cell via endocytosis and viral particle disassembly begins in the early endosome. The free nucleocapsid then injects the viral genome via a nuclear pore within the nucleus. After the mRNAs of immediate-early genes are produced, they travel into the cytoplasm and are translated into proteins by free ribosomes. The immediate-early proteins activate early and late proteins. The WSSV major envelope protein VP28 is expressed in the rER and migrates to the inner nuclear membrane. The newly synthesized viral genomes are assembled with the virus capsids, forming nucleocapsids which are then bud with VP28. We hypothesized that WSSV hijacks *Pm*VRP15 to facilitate viral nuclear egress and a maturation step, which may take place at ER (Fig. 8).

In conclusion, this work has confirmed that *Pm*VRP15 is a membrane-bound protein and localized at the ER. To our knowledge, this work is the first report to show that *Pm*VRP15 could possibly form an oligomer. In addition, *Pm*VRP15-silecning causes accumulation of viral DNA inside the nucleus, suggesting that *Pm*VRP15 plays a role in viral exit from the nucleus.

Methods

Expression and purification of recombinant *Pm*VRP15. *Escherichia coli* C43 (DE3) harboring pET-22b(+)-*Pm*VRP15 plasmid was grown in LB medium containing 100 µg/ml ampicillin at 37 °C. A final concentration of 1 mM isopropyl-β-D-thio-galactoside (IPTG) was added and the cells were harvested and resuspended in 50 mM Tris-HCl buffer, pH 7.0 containing a Complete protease inhibitor cocktail tablet (Roche). Cells were disrupted by sonication and the supernatant was collected by centrifugation at 8,000 × *g*, 4 °C for 20 min. Membrane fraction was obtained by centrifugation at 100,000 × *g*, 4 °C for 1 h and homogenized in 50 mM Tris-HCl buffer, pH 7.0.

Membrane-bound proteins were solubilized in solubilizing buffer (50 mM Tris-HCl, pH 7, 20 mM Imidazole, 300 mM NaCl, 20% glycerol and 1% n-decyl-ß-d-maltopyranoside, DM) at 4 °C overnight. Recombinant *Pm*VRP15 (r*Pm*VRP15) was purified using Ni-NTA Sepharose™ 6 Fast Flow (GE Healthcare). Crude proteins were incubated with Ni-NTA Sepharose™ 6 FF bead in binding buffer (50 mM Tris-HCl, pH 7, 20 mM Imidazole, 10% glycerol and 0.1% DM), and non-specific proteins were removed by wash buffer (50 mM Tris-HCl, pH 7, 50 mM Imidazole, 5% glycerol and 0.1% DM). Recombinant *Pm*VRP15 protein was eluted with elution buffer (50 mM Tris-HCl, pH 7.0, 300 mM Imidazole, 5% glycerol and 0.1% DM) and analyzed by 15% sodium dodecyl sulphate polyacrylamide gel electrophoresis (SDS-PAGE).

Recombinant *Pm*VRP15 was further purified by HiTrap SP Fast Flow (GE Healthcare) and eluted in 20 mM MES, pH 6.5, 150 mM NaCl, 5% glycerol and 0.1% DM. The concentration of purified r*Pm*VRP15 was determined by Pierce® BCA Protein Assay Kit (Thermo scientific). Western blotting was performed to identify His-tagged *Pm*VRP15 using a primary anti-His antibody (PAB10339 Abnova).

MALDI-TOF Mass spectrometry (MALDI-TOF MS). Mass spectrometric analysis was carried out on a Voyager DE-Pro MALDI-TOF MS instrument (Applied Biosystems) in linear positive mode. After time-delayed extraction, the ions were accelerated to 20 kV for TOF mass spectrometric analysis. A total of 400 laser shots were acquired and signal averaged per mass spectrum.

Circular Dichroism (CD) spectroscopy. Secondary structure of r*Pm*VRP15 was estimated by circular dichroism (CD) spectroscopy using JASCO J-715 CD Spectropolarimeter with temperature controller and a 1 mm optical cuvette. The (+)-10-camphorsulfonic acid (CSA) was used as calibration standard before measuring CD spectrum. Spectra were recorded between 180–320 nm using a bandwidth of 2 nm and a response time of 2 sec with 50 mm/min scanning speed. Each spectrum was the average of three scans and background was subtracted with the spectrum of the buffer solution (blank). The CD spectra of r*Pm*VRP15 (0.42 mg/ml) were analyzed via DichroWeb (http://dichroweb.cryst.bbk.ac.uk)[34,35]. Calculated spectra were obtained using K2D[36] CONTINLL[37,38] and CDSSTR[39–41] algorithms and the SMP180 protein dataset was used as ref. 42.

Analytical ultracentrifugation. Size distribution of r*Pm*VRP15 was analyzed by analytical ultracentrifugation (AUC). Sedimentation velocity experiments were performed on an Optima XL-A analytical ultracentrifuge (Beckman Instruments) with an An-60 Ti rotor. Purified r*Pm*VRP15 (60 µM) was dissolved in 10 mM Tris-HCl, pH 7.5, 100 mM NaCl and 0.03% n-dodecyl β-D maltoside (DDM). The sample and reference buffer were injected into each side of a double-sector centerpiece and centrifuged at 20,000 rpm (Max. RCF = 40,275× g) at 20 °C for 16.5 h. The spectrum was monitored continuously using a time interval of 600 s per scan. The dataset from these multiple scans at 280 nm at different time intervals were then fitted to a continuous c(s) distribution model using the SEDFIT program[43,44]. The partial-specific volume of *Pm*VRP15 was calculated to be 0.73 ml/g, based on the solvent density of 1.035 g/ml and the viscosity of 1.83 cP

Size-exclusion chromatography. Purified r*Pm*VRP15 was loaded onto Superdex 200 column (GE Healthcare), pre-equilibrated with a running buffer (10 mM Tris-HCl, pH 7.5, 150 mM NaCl and 0.087% DM). *Pm*VRP15 was eluted using a running buffer. The column was calibrated using a protein standard mix (Bio-RAD) of thyroglobin (670 kDa), γ-globulin (158 kDa), ovalbumin (44 kDa), myoglobin (17 kDa) and vitamin B12 (1,350 Da). The calibration data fit to a straight line with $r^2 > 0.999$.

Shrimp. Juvenile black tiger shrimp, *P. monodon*, of about 10–15 g bodyweight were obtained from a shrimp farm in Nakhon Si Thammarat Province, Thailand. The animals were acclimated in laboratory tanks at ambient temperature (28 ± 4 °C), and maintained in aerated water with a salinity of 20 ppt for at least 7 days before use.

Preparation of WSSV stock. The gill tissue from WSSV-infected moribund shrimp was collected for purification of viral particles. The purification method was slightly modified from Xie, X. *et al.*[45]. Gill tissue was homogenized in TNE buffer (50 mM Tris-HCl pH 8.5, 400 mM NaCl and 5 mM EDTA) and, then, centrifuged at 3,500 × *g* for 15 min at 4 °C. The supernatant was filtrated with MILLEX®-HP Filter Unit 0.45 µm (Merck Millipore) and centrifuged at 30,000 × *g* for 30 min at 4 °C to pellet the virions. The pellet was rinsed with TM buffer (50 mM Tris-HCl pH 7.5 and 10 mM $MgCl_2$) and centrifuged at 3,500 × *g* for 10 min at 4 °C. The upper loose pellet was removed and the lower pellet resuspended in TM buffer, then centrifuged at 30,000 × *g* for 30 min at 4 °C. The pellet was suspended in TM buffer, aliquoted and stored at −80 °C until use.

Primary Shrimp hemocyte cultures. Hemolymph was drawn from each shrimp using a sterile 1 ml syringe with 500 µl of anti-coagulant solution, pH 5.6 (0.82% (w/v) sodium chloride, 0.55% (w/v) citric acid, 1.98% (w/v) glucose and 0.88% (w/v) sodium citrate). The hemolymph-anticoagulant mixture was immediately centrifuged at 800 × *g* for 10 min at 4 °C to separate the hemocytes from the plasma. The hemocyte pellet was resuspended in 1 ml of L-15 culture medium (2x Leibovitz L-15 medium (Gibco) supplemented with 20% (v/v)

fetal bovine serum (FBS), 1% (w/v) glucose, 0.4% (w/v) sodium chloride, 100 IU/ml penicillin and 100 µg/ml streptomycin; pH 7.6; adjusting the osmotic pressure to 750 ± 15 mOsm/kg with sodium chloride solution).

The number of hemocytes in the cell suspension was counted by a hematocytometer. Cell concentration was adjusted to 10^6 cells per ml per well by L-15 fresh medium to obtain a final volume of 400 µl per well. The 24-well culture plate was incubated at 27 °C for 24 h, prior to being used in experiments.

Subcellular fractionation. The hemocyte cell cultures (4×10^5 cells per well) were incubated with 50 µl of the diluted WSSV solution (~15,000 viral copies/µl) and incubated at 27 °C. Subcellular fractionation by differential centrifugation was carried out as described in Taha, *et al.*[46] with some modifications[46]. At 12 and 20 h post-WSSV infection, the hemocytes were resuspended with lysis buffer containing 10 mM Tris-HCl, pH 7.4, 10 mM NaCl, 0.5 mM $MgCl_2$ and EDTA-free protease inhibitor cocktail (Roche), and cells were counted by hematocytometer. The hemocyte cells were homogenized and centrifuged at 1,200 × *g* for 5 min. Pellets were resuspended in 250 mM sucrose solution containing 10 mM $MgCl_2$ and applied through an 880 mM sucrose cushion containing 0.5 mM $MgCl_2$ by centrifugation at 1,200 × *g* for 10 min, to obtain the intact nuclei fraction. Meanwhile, supernatants of total cell lysate were re-centrifuged at 1,200 × *g* for 5 min and the cytosolic fraction (supernatant) was collected. The cytosolic fractions were further centrifuged at 16,000 × *g* for 10 min to isolate the heavy membrane pellet and the post-nuclear supernatant fraction, containing cytoplasm and light membrane. The post-nuclear fractions were then centrifuged at 100,000 × *g* for 120 min, in order to separate the light membrane pellet from the cytoplasmic supernatant. The total protein concentration of each fraction (intact nuclei, heavy membrane, light membrane and cytoplasm) was determined by BCA protein assay and 10 µg of proteins were loaded onto 15% SDS-PAGE for Western blot analysis. *Pm*VRP15 was probed by purified rabbit anti-*Pm*VRP15 polyclonal IgG antibody diluted 1:1000[20]. Anti-cyclophilin A, anti-PDI and anti-Nuclear Pore Complex (NPC) antibodies were used as a subcellular marker for cytoplasm, heavy membrane and intact nuclei, respectively. Anti-cyclophilin A antibody is a gift from Dr. Sirikwan Ponprateep, Srinakharinwirot University.

***Pm*VRP15 mRNA expression in shrimp primary hemocyte culture in response to WSSV.** A 400 µl of fresh L-15 culture medium, with or without 50 µl of the diluted WSSV solution (~15,000 viral copies/µl), was added to shrimp primary hemocyte culture. Total RNA was extracted from the hemocytes at 0, 6, 12, 24, 48 and 72 h post-WSSV infection using the TRI Reagent® (Molecular Research Center), followed by DNase I, RNase-free (Thermo scientific) treatment. The total RNA was used for single-stranded cDNA synthesis by the First Strand cDNA Synthesis Kit (Thermo Scientific). The transcription level of target genes was identified by RT-PCR using an equal amount of cDNA template with gene-specific primers (See Supplementary Information, Table S1). Elongation factor-1 alpha (EF-1α) was used as an internal control. The PCR reaction was started with 94 °C for 3 min, followed by 33 cycles (for *Pm*VRP15) or 28 cycles (for EF-1α) of 95 °C for 30 sec, 58 °C for 30 sec and 72 °C for 30 sec, and a final extension at 72 °C for 5 min. PCR products were analyzed by 1.5% (w/v) agarose gel electrophoresis and the differential expression level of *Pm*VRP15 was reported as relative to EF-1α.

The expression levels of *Pm*VRP15 and EF-1α gene were further analyzed by quantitative real time RT-PCR (qRT-PCR). *Pm*VRP15 and EF-1α specific primers for qRT-PCR are shown in Supplementary Information, Table S1. The qRT-PCR was performed using the CFX96™ Real-Time PCR Detection System (Bio-Rad). PCR conditions were carried out as follows: 95 °C for 30 sec, followed by 40 cycles of 95 °C for 5 sec, 58 °C for 5 sec and 60 °C for 5 sec. The experiment was done in triplicate. The threshold cycle (C_T) for each sample was analyzed by a mathematical model[47]. The data were shown as means ± standard deviations (SD). Statistical analysis was done using the one-way ANOVA followed by post hoc test (Duncan's new multiple range test). Data differences were considered significant at $^*P < 0.05$, $^{**}P < 0.01$.

Comparative C_T method was used to compare the gene expression in two different samples. The fold change of gene expression was calculated using the following formula.

$$\begin{aligned} \text{Fold change} &= 2^{-\Delta\Delta CT} \\ \Delta\Delta C_T &= [(C_T \text{ gene of interest} - C_T \text{ internal control}) \text{ sample A} \\ &\quad - (C_T \text{ gene ofinterest} - C_T \text{ internal control}) \text{ sample B})] \end{aligned}$$

Silencing of *Pm*VRP15 gene in shrimp primary hemocyte culture. *Pm*VRP15 dsRNA and GFP dsRNA (control) were synthesized using T7 RiboMAX™ Express Large Scale RNA Production System (Promega). Two sets of primers specific to each *Pm*VRP15 and GFP were designed as shown in Supplementary Information, Table S1. One of the specific primer pairs contained the T7 promoter at the 5′ end. The two PCR products were separately amplified by those primer pairs with the following conditions: 94 °C for 3 min, 30 cycles of 94 °C for 30 sec, 57 °C for 30 sec and 72 °C for 30 sec, and then a final extension at 72 °C for 5 min. Subsequently, the two PCR product templates were used to produce two complementary single-stranded RNAs by T7 RiboMAX™ Express Large Scale RNA Production System (Promega). RQ1 RNase-free DNase was added and incubated at 37 °C for 15 min to remove the DNA template. Single-stranded RNAs were then purified by phenol-chloroform extraction. Double-stranded RNAs were produced by mixing equal amounts of each of the complementary single-stranded RNAs, incubated at 70 °C for 10 min, and then slowly cooled down at room temperature. *Pm*VRP15 dsRNA and GFP dsRNA were analyzed by 1% agarose gel electrophoresis and concentrations of both dsRNAs were determined by measuring absorbance at 260 nm.

The hemocyte cell cultures were divided into 3 groups and incubated with either 50 µl of L-15 medium (Group 1) or 50 µl of L-15 medium with 20 µg/well of GFP dsRNA (Group 2) or 50 µl of L-15 medium with 20 µg/well of *Pm*VRP15 dsRNA (Group 3). After 12 h, 50 µl of L-15 medium with or without, GFP dsRNA (10 µg/well) and *Pm*VRP15 dsRNA (10 µg/well) were added along with 50 µl of diluted WSSV solution (~15,000 viral copies/µl)

and incubated at 27 °C. At 24 h post-WSSV infection, hemocyte cells were harvested and total RNA was extracted from hemocytes using the TRI Reagent® (Molecular Research Center) followed by DNase I, RNase-free (Thermo scientific) treatment. Then, single-stranded cDNA was synthesized with the First Strand cDNA Synthesis Kit (Thermo Scientific) and used for analysis of *Pm*VRP15 mRNA expression by RT-PCR with EF-1α as an internal reference. The PCR product was analyzed by 2% (w/v) agarose gel electrophoresis to confirm the silencing of *Pm*VRP15 transcripts.

Quantification of WSSV copy number in whole cells and in the nuclear and cytoplasmic fractions of normal and *Pm*VRP15 gene-silenced hemocytes after WSSV infection. The hemocyte cell cultures were divided into 3 groups and incubated with 50 µl of either L-15 medium, GFP dsRNA (20 µg/well) or *Pm*VRP15 dsRNA (20 µg/well). After 12 h, 50 µl of either L-15 medium, GFP dsRNA (10 µg/well) or *Pm*VRP15 dsRNA (10 µg/well) were added, along with 50 µl of the diluted WSSV solution (~15,000 viral copies/µl) and incubated at 27 °C. At 12 and 20 h post-WSSV infection, the hemocyte cells were collected and used as whole cells or cytoplasmic and nuclear fractions for quantification of WSSV copy numbers.

In brief, cytoplasmic and nuclear fractions were separated by differential centrifugation as shown in Fig. 1. The hemocyte cells were homogenized and centrifuged at 1,200 × *g* for 5 min. Pellets were resuspended, layered onto a sucrose cushion and centrifuged at 1,200 × *g* for 10 min, to obtain the nuclear fraction. Supernatants of total cell lysate were re-centrifuged at 1,200 × *g* for 5 min to collect the cytoplasmic fraction (supernatant). To confirm that there was no cross-contamination between the nuclear and cytoplasmic fractions, 10 µg of proteins from each fraction were applied on SDS-PAGE. Anti-NPC antibody and anti-cyclophilin A antibodies were used as a subcellular markers for the nuclear and cytoplasmic fractions, respectively. Pierce™ Fast Western Blot Kit and SuperSignal™ West Femto were then used for Western blot detection.

The total DNA was extracted from either whole cells or the nuclear and cytoplasmic fractions. WSSV copy number was then determined by Real-time PCR using WSSV1011F/WSSV1079R primers (See Supplementary Information, Table S1). The experiment was carried out in triplicate and WSSV recombinant plasmid (known copy number) was used as the standard for quantification[48].

Visualization of normal and *Pm*VRP15-knockdown hemocyte-infected by WSSV using confocal immunofluorescence microscopy. Shrimp (~10 g body weight) were injected with 25 µl of 150 mM sodium chloride containing either GFP dsRNA (10 µg/g shrimp) or *Pm*VRP15 dsRNA (10 µg/g shrimp). After 24 h, the shrimp were repeatedly injected with either GFP dsRNA (5 µg/g shrimp) or *Pm*VRP15 dsRNA (5 µg/g shrimp), together with 30 µl of the diluted WSSV solution (~4×10^3 viral copies). At 48 h post-WSSV injection, hemolymph was immediately fixed with 4% (w/v) paraformaldehyde in PBS, pH 7.4 (ratio 1:1). Hemocytes were collected by centrifugation at 800 × *g* for 10 min, washed three times with PBS, pH 7.4, then immersed in PBS, pH 7.4, and kept at 4 °C until used.

Hemocytes (1×10^6 cells/mL) were attached onto a microscope slide (Polysine slides, Thermo Scientific) and incubated with 0.1% (v/v) Triton-X 100 in PBS for 5 min. After rinsing the slide in PBS, it was immersed in a blocking solution (10% (v/v) FBS in PBS) for 1 h, followed by washing in PBS. The fixed hemocytes were incubated with a 1:500 dilution of purified rabbit anti-*Pm*VRP15 polyclonal antibody and 1:100 dilution of mouse anti-VP28 polyclonal antibody in PBS, pH 7.4, containing 1% (v/v) FBS. After PBS washing, the fixed hemocytes were incubated with a 1:500 dilution of Alexa Fluor® 488 goat anti-rabbit IgG antibody (Invitrogen) and Alexa Fluor® 568 goat anti-mouse IgG antibody (Invitrogen) in PBS, pH 7.4. The nucleus was then stained with a 1:1500 dilution of TO-PRO-3 iodide (Invitrogen) in PBS, pH 7.4. Coverslips were then coated with Prolong Gold Antifade Reagent (Invitrogen) and kept in the dark at 4 °C until they were visualized under a confocal laser scanning microscope (Olympus).

References

1. Lightner, D. V. *et al.* Risk of spread of penaeid shrimp viruses in the Americas by the international movement of live and frozen shrimp. *Rev. Sci. Tech.* **16**, 146–160 (1997).
2. Chou, H. Y., Huang, C. Y., Wang, C. H., Chiang, H. C. & Lo, C. F. Pathogenicity of a baculovirus infection causing white spot syndrome in cultured penaeid shrimp in Taiwan. *Dis. Aquat. Organ.* **23**, 165–173 (1995).
3. Wang, C. H. *et al.* Purification and genomic analysis of baculovirus associated with white spot syndrome (WSBV) of *Penaeus mondon*. *Dis. Aquat. Organ.* **23**, 239–242 (1995).
4. Wongteerasupaya, C. *et al.* A non-occluded, systemic baculovirus that occurs in cells of ectodermal and mesodermal origen and causes high mortality in the black tier prawn *Penaeus monodon*. *Dis. Aquat. Organ.* **21**, 69–77 (1995).
5. Durand, S., Lightner, D. V., Redman, R. M. & Bonami, J. R. Ultrastructure and morphgenesis of white spot syndrome baculovirus. *Dis. Aquat. Organ.* **29**, 205–211 (1997).
6. Maeda, M., Saitoh, H., Mizuki, E., Itami, T. & Ohba, M. Replication of white spot syndrome virus in ovarian primary cultures from the kuruma shrimp, Marsupenaeus japonicus. *J. Virol. Methods* **116**, 89–94 (2004).
7. Tassanakajon, A. *et al. Penaeus monodon* gene discovery project: the generation of an EST collection and establishment of a database. *Gene* **384**, 104–112 (2006).
8. Leu, J. H. *et al.* Comparative analysis of differentially expressed genes in normal and white spot syndrome virus infected *Penaeus monodon*. *BMC Genomics* **8**, 120 (2007).
9. Rojtinnakorn, J., Hirono, I., Itami, T., Takahashi, Y. & Aoki, T. Gene expression in haemocytes of kuruma prawn, *Penaeus japonicus*, in response to infection with WSSV by EST approach. *Fish. Shellfish. Immunol.* **13**, 69–83 (2002).
10. Dhar, A. K., Dettori, A., Roux, M. M., Klimpel, K. R. & Read, B. Identification of differentially expressed genes in shrimp (*Penaeus stylirostris*) infected with White spot syndrome virus by cDNA microarrays. *Arch. Virol.* **148**, 2381–2396 (2003).
11. Aoki, T. *et al.* Microarray analyses of shrimp immune responses. *Mar. Biotechnol. (NY)* **13**, 629–638 (2011).
12. Wang, B. *et al.* Discovery of the genes in response to white spot syndrome virus (WSSV) infection in *Fenneropenaeus chinensis* through cDNA microarray. *Mar. Biotechnol. (NY)* **8**, 491–500 (2006).
13. Pongsomboon, S. *et al.* A cDNA microarray approach for analyzing transcriptional changes in *Penaeus monodon* after infection by pathogens. *Fish. Shellfish. Immunol.* **30**, 439–446 (2011).

14. Shekhar, M. S., Gomathi, A., Gopikrishna, G. & Ponniah, A. G. Gene expression profiling in gill tissues of White spot syndrome virus infected black tiger shrimp *Penaeus monodon* by DNA microarray. *Virusdisease* **26**, 9–18 (2015).
15. Wang, H. C., Wang, H. C., Kou, G. H., Lo, C. F. & Huang, W. P. Identification of icp11, the most highly expressed gene of shrimp white spot syndrome virus (WSSV). *Dis. Aquat. Organ.* **74**, 179–189 (2007).
16. Wang, H. C. *et al*. Protein expression profiling of the shrimp cellular response to white spot syndrome virus infection. *Dev. Comp. Immunol.* **31**, 672–686 (2007).
17. Li, S., Li, F., Sun, Z., Zhang, X. & Xiang, J. Differentially proteomic analysis of the Chinese shrimp at WSSV latent and acute infection stages by iTRAQ approach. *Fish. Shellfish. Immunol.* **54**, 629–638 (2016).
18. Li, W., Tang, X., Xing, J., Sheng, X. & Zhan, W. Proteomic analysis of differentially expressed proteins in *Fenneropenaeus chinensis* hemocytes upon white spot syndrome virus infection. *PLoS One* **9**, e89962 (2014).
19. Chai, Y. M., Yu, S. S., Zhao, X. F., Zhu, Q. & Wang, J. X. Comparative proteomic profiles of the hepatopancreas in *Fenneropenaeus chinensis* response to white spot syndrome virus. *Fish. Shellfish. Immunol.* **29**, 480–486 (2010).
20. Vatanavicharn, T., Prapavorarat, A., Jaree, P., Somboonwiwat, K. & Tassanakajon, A. *Pm*VRP15, a novel viral responsive protein from the black tiger shrimp, *Penaeus monodon*, promoted white spot syndrome virus replication. *PLoS One* **9**, e91930 (2014).
21. Leu, J. H. *et al*. The novel white spot syndrome virus-induced gene, *Pm*ERP15, encodes an ER stress-responsive protein in black tiger shrimp, *Penaeus monodon*. *Dev. Comp. Immunol.* **49**, 239–248 (2015).
22. Jaree, P. *et al*. WSV399, a viral tegument protein, interacts with the shrimp protein *Pm*VRP15 to facilitate viral trafficking and assembly. *Dev. Comp. Immunol.* **59**, 177–185 (2016).
23. Gasteiger, E. *et al*. *Protein identification and analysis tools on the ExPASy server* (Humana Press, 2005).
24. Prive, G. G. Detergents for the stabilization and crystallization of membrane proteins. *Methods* **41**, 388–397 (2007).
25. Li, W. *et al*. Virus replication cycle of white spot syndrome virus in secondary cell cultures from the lymphoid organ of *Litopenaeus vannamei*. *J. Gen. Virol.* **96**, 2844–2854 (2015).
26. Wang, Y. T. *et al*. White spot syndrome virus (WSSV) infects specific hemocytes of the shrimp *Penaeus merguiensis*. *Dis. Aquat. Organ.* **52**, 249–259 (2002).
27. Stephens, E. B. & Compans, R. W. Assembly of animal viruses at cellular membranes. *Annu. Rev. Microbiol.* **42**, 489–516 (1988).
28. Miller, S. & Krijnse-Locker, J. Modification of intracellular membrane structures for virus replication. *Nature reviews. Microbiology* **6**, 363–374 (2008).
29. den Boon, J. A. & Ahlquist, P. Organelle-like membrane compartmentalization of positive-strand RNA virus replication factories. *Annu. Rev. Microbiol.* **64**, 241–256 (2010).
30. Inoue, T. & Tsai, B. How viruses use the endoplasmic reticulum for entry, replication, and assembly. *Cold Spring Harb. Perspect. Biol.* **5**, a013250 (2013).
31. Chen, R. Y. *et al*. White spot syndrome virus entry is dependent on multiple endocytic routes and strongly facilitated by Cq-GABARAP in a CME-dependent manner. *Sci. Rep.* **6**, 28694 (2016).
32. Sritunyalucksana, K., Wannapapho, W., Lo, C. F. & Flegel, T. W. *Pm*Rab7 is a VP28-binding protein involved in white spot syndrome virus infection in shrimp. *J. Virol.* **80**, 10734–10742 (2006).
33. Chang, L. K. *et al*. Role of *Penaeus monodon* Kruppel-like factor (*Pm*KLF) in infection by white spot syndrome virus. *Dev. Comp. Immunol.* **36**, 121–129 (2012).
34. Whitmore, L. & Wallace, B. A. Protein secondary structure analyses from circular dichroism spectroscopy: methods and reference databases. *Biopolymers* **89**, 392–400 (2008).
35. Whitmore, L. & Wallace, B. A. DICHROWEB, an online server for protein secondary structure analyses from circular dichroism spectroscopic data. *Nucleic Acids Res.* **32**, W668–673 (2004).
36. Andrade, M. A., Chacón, P., Merelo, J. J. & Morán, F. Evaluation of secondary structure of proteins from UV circular dichroism spectra using an unsupervised learning neural network. *Protein Eng.* **6**, 383–390 (1993).
37. Provencher, S. W. & Glockner, J. Estimation of globular protein secondary structure from circular dichroism. *Biochemistry* **20**, 33–37 (1981).
38. Van Stokkum, I. H. M., Spoelder, H. J. W., Bloemendal, M., Van Grondelle, R. & Groen, F. C. A. Estimate of protein secondary structure and error analysis from CD spectra. *Anal. Chem.* **191**, 110–118 (1990).
39. Compton, L. A. & Johnson, W. C. Jr. Analysis of protein circular dichroism spectra for secondary structure using a simple matrix multiplication. *Anal. Biochem.* **155**, 155–167 (1986).
40. Manavalan, P. & Johnson, W. C. Jr. Variable selection method improves the prediction of protein secondary structure from circular dichroism spectra. *Anal. Biochem.* **167**, 76–85 (1987).
41. Sreerama, N. & Woody, R. W. Estimation of protein secondary structure from circular dichroism spectra: comparison of CONTIN, SELCON, and CDSSTR methods with an expanded reference set. *Anal. Biochem.* **287**, 252–260 (2000).
42. Abdul-Gader, A., Miles, A. J. & Wallace, B. A. A reference dataset for the analyses of membrane protein secondary structures and transmembrane residues using circular dichroism spectroscopy. *Bioinformatics* **27**, 1630–1636 (2011).
43. Brown, P. H. & Schuck, P. Macromolecular size-and-shape distributions by sedimentation velocity analytical ultracentrifugation. *Biophys. J.* **90**, 4651–4661 (2006).
44. Schuck, P. Size-distribution analysis of macromolecules by sedimentation velocity ultracentrifugation and lamm equation modeling. *Biophys. J.* **78**, 1606–1619 (2000).
45. Xie, X., Li, H., Xu, L. & Yang, F. A simple and efficient method for purification of intact white spot syndrome virus (WSSV) viral particles. *Virus Res.* **108**, 63–67 (2005).
46. Taha, M. S. *et al*. Subcellular fractionation and localization studies reveal a direct interaction of the fragile X mental retardation protein (FMRP) with nucleolin. *PLoS One* **9**, e91465 (2014).
47. Pfaffl, M. W. A new mathematical model for relative quantification in real-time RT-PCR. *Nucleic Acids Res.* **29**, e45 (2001).
48. Li, S., Zhang, X., Sun, Z., Li, F. & Xiang, J. Transcriptome analysis on Chinese shrimp *Fenneropenaeus chinensis* during WSSV acute infection. *PLoS One* **8**, e58627 (2013).

Acknowledgements

We thank Assoc. Prof. Chartchai Krittanai and his staff at Mahidol University for access to the CD spectrometer, Dr. Sujint Thammasart, D.V.M. at Charoen Pokphand Foods PCL and Mr. Arthit Chalorsrikul, Aquatic Animal Health Research Center CPF for their kind assistance in detection of WSSV copy number and Dr. Krupa O'Neill for critical reading of this manuscript. This work was supported by Thailand Research Fund RSA5580053 (to KK) and the 90th Year Chulalongkorn Scholarship (to KJ and KK). Additional support came from TRF Senior Research Scholar RTA5580004 (to AT) and IRG 5780008 (to KK and AT). KJ was supported by His Majesty the King's 72nd Birthday Anniversary Scholarship. TJ has been fully supported by The 100th Anniversary Chulalongkorn University Fund for Doctoral Scholarship. KK has been partially supported by Structural and Computational Biology Research Group, Special Task Force for Activating Research (STAR), Faculty of Science, Chulalongkorn University.

Author Contributions

K.J. characterized *Pm*VRP15 by MS and CD and also conducted immunolocalization experiment. T.J. conducted subcellular fractionation and nuclear import/export experiments. P.L. provided help in *Pm*VRP15 production and Western blotting. K.K., S.K. and T.M. performed SEC and AUC experiments and analysed SEC and AUC data, under the supervision of T.H., P.S. involved in immunolocalization and RNAi experiments. A.T. and K.K. conceived and supervised the project. K.K. analysed data and wrote the manuscript. All authors reviewed the results and approved the final version of the manuscript.

Additional Information

Supplementary information accompanies this paper at doi:10.1038/s41598-017-06653-7

Competing Interests: The authors declare that they have no competing interests.

Publisher's note: Springer Nature remains neutral with regard to jurisdictional claims in published maps and institutional affiliations.

Open Access This article is licensed under a Creative Commons Attribution 4.0 International License, which permits use, sharing, adaptation, distribution and reproduction in any medium or format, as long as you give appropriate credit to the original author(s) and the source, provide a link to the Creative Commons license, and indicate if changes were made. The images or other third party material in this article are included in the article's Creative Commons license, unless indicated otherwise in a credit line to the material. If material is not included in the article's Creative Commons license and your intended use is not permitted by statutory regulation or exceeds the permitted use, you will need to obtain permission directly from the copyright holder. To view a copy of this license, visit http://creativecommons.org/licenses/by/4.0/.

© The Author(s) 2017

Fish & Shellfish Immunology 60 (2017) 237–246

Contents lists available at ScienceDirect

Fish & Shellfish Immunology

journal homepage: www.elsevier.com/locate/fsi

Full length article

HSP70 and HSP90 are involved in shrimp *Penaeus vannamei* tolerance to AHPND-causing strain of *Vibrio parahaemolyticus* after non-lethal heat shock

Wisarut Junprung [a], Premruethai Supungul [b], Anchalee Tassanakajon [a, *]

[a] Center of Excellence for Molecular Biology and Genomics of Shrimp, Department of Biochemistry, Faculty of Science, Chulalongkorn University, Bangkok 10330, Thailand
[b] National Center for Genetic Engineering and Biotechnology (BIOTEC), National Science and Technology Development Agency (NSTDA), Pathumthani 12120, Thailand

ARTICLE INFO

Article history:
Received 11 August 2016
Received in revised form
18 November 2016
Accepted 19 November 2016
Available online 22 November 2016

Keywords:
Heat shock protein
Penaeus vannamei
Vibrio parahaemolyticus
Acute hepatopancreatic necrosis disease
Chronic heat stress

ABSTRACT

Acute hepatopancreatic necrosis disease (AHPND) caused by *Vibrio parahaemolyticus* carrying toxin-producing plasmid, has led to severe mortalities in farmed penaeid shrimp throughout Asia. Previous studies reported that a non-lethal heat shock (NLHS) could enhance disease tolerance in aquatic animals. Here, we investigate whether the NLHS could enhance the survival of shrimp *Penaeusvannamei* upon challenge with an AHPND-causing strain of *V. Parahaemolyticus* (VP_{AHPND}). Two NLHS conditions, acute and chronic NLHSs, were used. The former abruptly exposed the juveniles shrimp from 28 °C to 38 °C for 30 min only once whereas the latter exposed the shrimp to 38 °C for 5 min every day for 7 days. The treated shrimp were, then, challenged with VP_{AHPND} at day 3, day 7, and day 30 during the recovery time after the treatment. The results showed that the shrimp exposed to either acute or chronic NLHS had higher survival rate (>50%) than that of the non-heated shrimp control (20%) when they were challenged with VP_{AHPND} at day 3 recovery time. However, only those exposed to chronic NLHS showed the VP_{AHPND} protection at day 7 and day 30 recovery times. Furthermore, the qRT-PCR analysis revealed that the expression of heat shock proteins, *LvHSP70*, *LvHSP90* as well as other immune-related genes, *LvproPO* and *LvCrustin*, were induced upon exposure of shrimp to chronic NLHS. Interestingly, gene silencing of *LvHSP70* and *LvHSP90* eliminated the VP_{AHPND} tolerance in the chronic NLHS shrimp and had decreasing PO activity suggesting that these *LvHSPs* played crucial roles in bacterial defense in shrimp. All together, we show for the first time that the NLHS enhance the shrimp tolerance to VP_{AHPND} infection and this is likely mediated by the induction of *LvHSP70*, *LvHSP90* and subsequent activation of the proPO system.
© 2016 Elsevier Ltd. All rights reserved.

1. Introduction

Infectious diseases especially new emerging diseases have contributed to a major loss of shrimp production in recent years [1]. In Thailand, the shrimp production declines nearly 30–70% because of an emerging disease called “early mortality syndrome” (EMS) or acute hepatopancreatic necrosis disease (AHPND) [2]. The disease typically affects the post larvae within 20–30 days after stocking and causes mass mortalities (up to 100%) in farmed shrimp afterwards [3]. The high mortalities occur in both the black tiger shrimp (*P. monodon*) and the white-leg shrimp (*P. vannamei*) [4]. The causative agent of AHPND has been identified as a unique strain of bacterium *Vibrio parahaemolyticus* [5] harboring a 69-kb plasmid that contains two genes coding for *Pir* toxin-like proteins, *pirA* and *pirB* [6]. Experimental data indicated that the virulence of *V. parahaemolyticus* AHPND (VP_{AHPND}) depends on the isolates, and the rate of mortality was dose-dependent [7]. Currently, the detection methods of AHPND are available by means of histological examination [5] and molecular diagnostic methods [6,8,9]. Although, the early diagnosis and detection of AHPND makes it possible for control and prevention of AHPND in farmed shrimp, effective measures to control the disease are urgently required.

Several reports have shown that the exposure of aquatic animals to non-lethal heat shock (NLHS) can induce protection against bacterial and viral infections by the induction of heat shock

* Corresponding author.
E-mail address: anchalee.k@chula.ac.th (A. Tassanakajon).

http://dx.doi.org/10.1016/j.fsi.2016.11.049
1050-4648/© 2016 Elsevier Ltd. All rights reserved.

proteins (HSPs) and subsequently activating the immune system [10,11]. The NLHS of *Artemia franciscana* induces Hsp70 expression and protects the *Artemia* larvae against *V. campbellii* and *V. proteolyticus* [11,12]. The shrimp *Penaeus monodon* exposed to a short hyperthermal heat stress have shown Hsp70 accumulation and tolerance against gill associated virus (GAV) [10]. The priming of Asian green mussel *Perna viridis* with NLHS promotes thermotolerance and increases resistance to *V. alginolyticus* [13]. However, the NLHS of *P. vannamei* did not enhance tolerance against *V. harveyi* despite significantly up regulation of HSP70 [14]. The NLHS also fails to protect platyfish *Xiphophorus maculates* against *Yersinia ruckeri* infection, but protection is enhanced when NLHS is combined with the injection of bacterial Hsps, GroEL and DnaK [15]. Moreover, some evidences show that feeding the *P. vannamei* with food pellets containing *Escherichia coli* over-expressing the heat shock protein Dnak, enhances the Pacific white shrimp tolerance against *V. harveyi* infection [16].

The families of HSPs that function as molecular chaperones, are classified according to their molecular mass in kilodaltons (kDa) such as HSP110, HSP90, HSP70, HSP60, HSP21, and HSP10. In pathological situations, such as necrotic cell death, the HSPs can be released into the extracellular environment with cellular proteins to induce autoimmunity by receptor-mediated activation of the innate immune response [17]. In shrimp, there is evidence that the HSPs are highly expressed in response to pathogen infection. The *Lv*Hsp60 protein from *P. vannamei* is significantly up-regulated in the gills, hepatopancreas and haemocytes after challenged with either Gram-positive and Gram−negative bacteria [18]. On the contrary, the *PmHSP21* mRNA level is significantly decreased after WSSV infection [19]. In addition, the transcriptomic results in RNA-seq analysis of the freshwater prawn *Macrobrachium rosenbergii* show up regulation of the heat shock proteins; HSP21, HSP70, and the small heat shock proteins in response to *V. parahaemolyticus* infection [20].

In this study, we investigate whether the NLHS can induce protection against the strain of VP_{AHPND} in the Pacific white-leg shrimp *P. vannamei*. The juveniles shrimp were exposed to two different procedures of heat treatment, acute and chronic NLHS, before they were challenged thereafter with VP_{AHPND} at day 3, day 7, or day 30 recovery time. The shrimp survival were observed and the gene expression of *LvHSPs* as well as some other immune related genes were analyzed. Furthermore, the RNA interference (RNAi) was conducted to confirm the importance of *LvHSPs* in mediating the NLHS protection against VP_{AHPND}.

2. Materials and methods

2.1. Experimental animals

Juveniles *P. vannamei* (2−3 g body weight) were kindly provided by the Marine Shrimp Broodstock Research Center II (MSBRC-2), Charoen Pokphand Foods PCL in Phetchaburi province, Thailand. The animals were acclimated under constant aeration (>5 ppm) at ambient temperature of 28 ± 1 °C and 20 parts per thousand (ppt) of salinity for one week prior to use. During acclimation, shrimp were fed twice daily with shrimp feed.

2.2. Determination of the NLHS temperature for P. vannamei

To determine the appropriate NLHS temperature, four groups of twenty *P. vannamei* (2−3 g), acclimated at 28 ± 1 °C, were abruptly exposed to heat shock temperatures at 37 °C, 38 °C, 39 °C, or 40 °C in heat shock treatment tank (100 L) for 30 min. The shrimp were, then, transferred immediately after heat shock back to ambient temperature for recovery and shrimp survival was observed at 6 h recovery time by counting the live animals. Shrimp raised at 28 ± 1 °C were used as control. The percent survival was calculated as $N_t/N_0 \times 100$ where N_0 and N_t are initial and final numbers of live shrimp respectively. Experiments were done in triplicate.

2.3. Chronic and acute NLHS of P. vannamei

Juveniles *P. vannamei* (2−3 g body weight) acclimated at 28 ± 1 °C for one week were separated into two groups for two heat shock treatment conditions. In acute NLHS group, shrimp was transferred from 28 ± 1 °C to 38 ± 0.2 °C and incubated for 30 min once whereas those in chronic NLHS group were subjected to 5 min heating at 38 ± 0.2 °C daily for 7 days. The aeration in both conditions was controlled by maintaining the dissolved oxygen (DO) at high ppm (10 ppm). After completed heating, they were transferred immediately back to ambient temperature for recovery prior to sampling for RNA, challenge test and gene specific knockdown. Shrimp in control group were non-heated juveniles shrimp. The details experimental design is shown schematically in Fig. 1.

2.4. Bacterial culture and immersion dose of V. parahaemolyticus

Bacterial isolates of AHPND strain (VP_{AHPND}); Chanthaburi2, and non-AHPND strain ($VP_{non\text{-}AHPND}$); Rayong1, used in the study were confirmed the virulence by immersion and examination of shrimp hepatopancreas using histological method [21]. The bacteria were grown overnight at 30 °C in tryptic soy agar plates (TSA) (Becton, Dickson and Company) supplemented with 1.5% NaCl. The colonies were picked, inoculated into tryptic soy broth (TSB) containing 1.5% NaCl and cultured to stationary phase by incubation 24 h with shaking at 150 rpm at 30 °C. The cell density was determined with spectrophotometer at 600 nm. The OD_{600} of 1.0 was equivalent to approximately 1×10^9 CFU/ml according to total plate count method (data not shown).

Twenty juveniles reared at 28 ± 1 °C were incubated in separate aquaria containing 35 L of filtered seawater with the VP_{AHPND} at the final concentration of 1×10^5, 5×10^5, 1×10^6, and 5×10^6 CFU/ml. Survival was observed every 12 h after challenge for 120 h by counting the swimming animals. Each treatment was performed in triplicate and the percentage of survival was calculated as above. The lowest number of VP_{AHPND} causing 50% mortality after 48 h post infection was used for VP_{AHPND} challenge test after NLHS.

2.5. V. parahaemolyticus protection after NLHS

To study the effects of NLHS on the protection against VP_{AHPND} infection, the challenge test of *P. vannamei* was conducted. Six groups of 20 juveniles each were treated under chronic NLHS. At 3-day-, 7-day-, and 30-day recovery times, they were, then, challenged with 1×10^6 CFU/ml of VP_{AHPND} and $VP_{non\text{-}AHPND}$. The survival was observed every 12 h for 120 h as described above. Moribund shrimp were counted as dead shrimp. Each treatment was performed in triplicate. Non-heat juveniles were used as a control. The details of challenged test is shown schematically in Fig. 1.

2.6. Differential gene expression analysis by qRT-PCR

To examine the effect of NLHS on the expression of *LvHSP* and immune-related genes in shrimp, the hemolymph was collected at various time points: 0, 3, 6, 12, 24, 48, 72, 96, and 120 h, after completed chronic NLHS and at 0 h for non-heat group using 10% (w/v) sodium citrate as an anticoagulant. The hemocytes were separated by centrifugation at 800 × g for 10 min at 4 °C. Total RNA was extracted from the hemocytes using the TRI Reagent

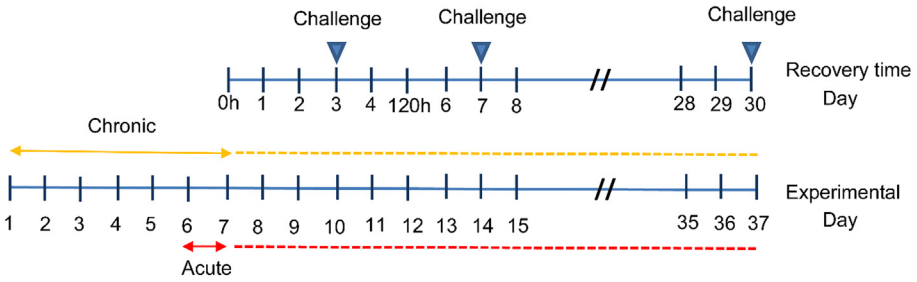


Fig. 1. Schematic of heat treatment and challenge experiments. The chronic NLHS, shrimp were abruptly heated for 5 min every day for 7 days while in acute NLHS, shrimp were heated once for 30 min. After that, shrimp were recovered at ambient temperature. The recovery time started immediately after completed heat treatment and transferred shrimp to ambient temperature (0 h recovery time). The challenge experiments of both groups were conducted in the same period of time at day 3, day 7 and day 30 of recovery time.

(Molecular Research Center) and the contaminating genomic DNA was eliminated by treatment with DNase I (RNase-free) (New England BioLabs). The purity and quantity of the RNA were determined by 2% agarose gel electrophoresis and NanoDrop 2000 spectrophotometer (Thermo Scientific), respectively. The first strand cDNA was synthesized from 500 ng of total RNA using a cDNA synthesis kit (Thermo Scientific).

The qRT-PCR was performed in CFX96 Touch™ Real-Time PCR Detection System (Bio-Rad) using QPCR Green Master Mix Fluorescein (Biotechrabbit) with forward and reverse primers, specific for *LvHSP* genes (*LvHSP10*, *LvHSP21*, *LvHSP60*, *LvHSP70*,and *LvHSP90*) and other immune-related genes (*LvproPO*, *LvA2M*, *LvCrustin*, *LvALF*, and *LvKazal*) (Table 1). The housekeeping gene, *EF1α*, was used as an internal control (Table 1). The cycling parameters started with an initial activation at 95 °C for 5 min followed by 40 cycles of 95 °C for 30 s, gene specific annealing temperatures for 45 s and 72 °C for 30 s. The fluorescent signal intensities were recorded at the end of each cycle. Melting curve analysis was performed from 55 to 95 °C with continuous fluorescent reading every 0.5 °C increments to confirm that only one product was amplified. The cycle threshold (Ct) values and fold difference in quantity for each *LvHSP* and other immune-related genes were recorded by CFX Manager Software (Bio-Rad). Relatively to the expression of *EF1α* transcripts, the relative expression was calculated by the $2^{-\Delta\Delta Ct}$ method. The amplification was done in triplicate for each sample. The statistical significance of any differences was tested by using a one-way ANOVA followed by the Duncan's new multiple range test using the SPSS software.

2.7. In vivo gene knockdown of LvHSP70 and LvHSP90

To investigate the function of *LvHSPs* genes upon chronic NLHS,

Table 1
Nucleotide sequence of the primers used.

Primer name	Sequence (5′-3′)	Purpose
LvHSP10-F	TCGACCGTGTGCTGGTCCAA	qRT-PCR
LvHSP10-R	GTGGTGCCAGCATCAGTTCT	
LvHSP21-F	CACGAGGAGAAGTCTGACAAC	qRT-PCR
LvHSP21-R	GAGAGCGAGGACTTGATGAG	
LvHSP60-F	TGCCAACAACACCAACGAAG	qRT-PCR
LvHSP60-R	GCCAACATAACTCCACGCCT	
LvHSP70-F	CTCCTGCGTGGGTGTGTT	RT-PCR, qRT-PCR
LvHSP70-R	GCGGCGTCACCAATCAGA	
LvHSP90-F	TGGGCTTCTACTCCGCCTACC	RT-PCR, qRT-PCR
LvHSP90-R	ACGGTGAAAGAGCCTCCAGCA	
LvALF-F	GTTATCACGCCCTTTTCTAC	qRT-PCR
LvALF-R	GAAGAATGACCTGTCCAAC	
LvA2M-F	GCACGTAATCAAGATCCG	qRT-PCR
LvA2M-R	CCCATCTCATTAGCACAAAC	
LvCrustin-F	GCTGGCCTCGATAAGTGTTG	qRT-PCR
LvCrustin-R	CATCGGTCGTTCTTCAGATG	
LvKazal-F	CGACAAGACCTGCAATGG	qRT-PCR
LvKazal-R	AAACAGCTGCCTGGAAAC	
LvproPO-F	CGGTGACAAAGTTCCTCTTC	qRT-PCR
LvproPO-R	GCAGGTCGCCGTAGTAAG	
ds*LvHSP70*-F	CGAAGGACGCTGGACACATCT	RNAi
ds*LvHSP70*-R	GGACGATGTCGTGGATCTG	
T7ds*LvHSP70*-F	TAATACGACTCACTATAGGCGAAGGACGCTGGACACATCT	RNAi
T7ds*LvHSP70*-R	TAATACGACTCACTATAGGGGACGATGTCGTGGATCTG	
ds*LvHSP90*-F	AGACCGAGTACCTGGAGGAA	RNAi
ds*LvHSP90*-R	GACGCACGTACAGCTTGATCT	
T7ds*LvHSP90*-F	TAATACGACTCACTATAGGAGACCGAGTACCTGGAGGAA	RNAi
T7ds*LvHSP90*-R	TAATACGACTCACTATAGGGACGCACGTACAGCTTGATCT	
ds*GFP*-F	ATGGTGAGCAAGGGCGAGGA	RNAi
ds*GFP*-R	TTACTTGTACAGCTCGTCCA	
T7ds*GFP*-F	TAATACGACTCACTATAGGATGGTGAGCAAGGGCGAGGA	RNAi
T7ds*GFP*-R	TAATACGACTCACTATAGGTTACTTGTACAGCTCGTCCA	
EF1α-F	CTTGATTGCCACACTGCTCAC	RT-PCR, qRT-PCR
EF1α-R	TCTCCACGCACATAGGCTTG	

gene silencing was performed by using RNA interference. Double-stranded RNAs (dsRNAs) of *LvHSP70, LvHSP90*, and *GFP* genes were generated using *in vitro* T7 RiboMAX™ Express Large Scale RNA Production System (Promega). Two PCR reactions were set up using the gene specific primers flanked by a T7 promoter sequence at the 5′ ends (Table 1) to produce the sense and anti-sense strands DNA templates separately. To produce dsRNA, 1.5 mg of each gel purified PCR products was used as a template for *in vitro* transcription. Then, equal amount of sense and anti-sense single-stranded RNAs were annealed to produce dsRNA. The remaining DNA templates were eliminated with RNase-free DNase I (Promega). The quality of dsRNAs was verified by agarose gel electrophoresis with UV visualization and quantified by using NanoDrop 2000 Spectrophotometer (Thermo Scientific).

Four healthy individual shrimp were injected with gene-specific dsRNA in saline solution (SSS) (5 μg/g shrimp ds*LvHSP70* or 1 μg/g shrimp ds*LvHSP90* or 5 μg/g shrimp ds*GFP*) or SSS. After 24 h, the hemolymph was drawn and the hemocytes were separated by centrifugation at 800 × g for 10 min at 4 °C. Total RNAs and cDNAs were prepared as described above. Semi-quantitative RT-PCR was performed by using *LvHSP70* and *LvHSP90* gene specific primers (Table 1). The PCR products were analyzed by agarose gel electropholesis.

2.8. Effect of in vivo gene knockdown of LvHSP70 and LvHSP90 after NLHS

To study function of *LvHSP70* and *LvHSP90* in bacterial infection, shrimp were subjected to chronic NLHS and after completed heating at two days recovery time, they were divided into three groups of 15 shrimp each. Two groups were injected with gene-specific dsRNA in SSS (5 μg/g shrimp of ds*LvHSP70* and 1 μg/g shrimp of ds*LvHSP90*) and another group was injected with 5 μg/g shrimp of *GFP* dsRNA in SSS serving as the control. After 24 hpi (72 h recovery time), these shrimp were challenged with 1×10^6 CFU/ml of either strain of *V. parahaemolyticus* (VP_{AHPND} and $VP_{non\text{-}AHPND}$) by immersion as previously described. The cumulative mortality of each shrimp group was recorded every 12 h until 120 h post VP_{AHPND} challenge. This experiment was performed in triplicate.

2.9. Effect of LvHSP70 and LvHSP90 gene knockdown upon VP_{AHPND} infection

Shrimp were heated as described above and at 48 h recovery time, two groups of three shrimp were injected with *LvHSP70* and *LvHSP90* dsRNAs as described above. Twenty-four hours after dsRNA injection, they were immersed in water containing VP_{AHPND} as described above. After 24 h post immersion, shrimp stomachs were individually collected and homogenized in 0.85% SSS. The homogenized tissue was serially diluted and dotted onto a thiosulfate citrate bile salts sucrose agar plates (TCBS) (Becton, Dickson and Company) with 3 replicate. The number of bacterial green colonies as CFU/ml was then counted after incubation at 30 °C for 18 h. Controls were non-heated shrimp and NLHS shrimp injected with SSS or *GFP* dsRNA.

Besides bacterial counting, the homogenates were used for genomic DNA extraction by using Genomic DNA Mini Kit (Tissue) (Geneaid Biotech). The DNA concentrations were determined using NanoDrop 2000 Spectrophotometer (Thermo Scientific) and adjusted to a concentration of 50 ng/μl with elution buffer (Geneaid Biotech) for PCR detection of VP_{AHPND}. The AP4 nested PCR method was used for approximately quantification of VP_{AHPND} as previously reported [8]. Both of VP_{AHPND} and $VP_{non\text{-}AHPND}$ cells were used for negative and positive control respectively.

2.10. Effect of LvHSP70 and LvHSP90 gene silencing on the hemolymph PO activity

The PO activity in the gene silenced shrimp was determined in the hemolymph of heat-shocked shrimp injected with dsRNA and non-heated shrimp as described above. The hemolymph PO activity, expressed as the amount of dopachrome formation from the L-3,4-dihydroxyphenylalanine substrate, was measured as previously reported [22]. Briefly, total hemolymph proteins of 200 mg in 85 μl of 10 mM Tris-HCl pH 8.0 were mixed with 15 μl freshly prepared 3 mg/ml L-DOPA in water (Fluka). The absorbance at 490 nm was monitored for 30 min by using Molecular devices Sprectramax 250 Microplate Reader. The PO activity was reported as ΔA_{490}/mg protein/min. The experiment was performed in triplicate of three pooled hemolymph samples, each sample was from three shrimp.

3. Results

3.1. Non-lethal heat shock of P. vannamei

To determine an appropriate NLHS temperature, four groups of 20 juveniles shrimp acclimated at 28 ± 1 °C were abruptly heat-shocked for 30 min at 37, 38, 39, or 40 °C and, then, transferred immediately back to 28 °C. The survival rate was determined at 6 h recovery time. The result showed that the shrimp could survive 100% up to 38 °C and mortality occurred at and above 39 °C with approximately 50% survival (Fig. 2). The maximum abrupt temperature of 38 °C defined as NLHS temperature that could retain 100% survival was used for heat shock treatment in subsequent experiments.

3.2. Effect of NLHS on tolerance to VP_{AHPND}

The LD_{50} dose (1×10^6 CFU/ml) of VP_{AHPND} was determined and used in the challenge experiments. 20 juveniles (2–3 g) *P. vannamei* in each group were exposed to two different NLHS: the acute NLHS, 30 min abrupt heating at 38 °C once and the chronic NLHS, 5 min abrupt heating at 38 °C daily for 7 days. After completed heating at 3-, 7-, and 30-day recovery times, the animals were challenged by immersion with 1×10^6 CFU/ml of VP_{AHPND} in aquatic tanks and the survival was observed every 12 h for 120 h. The results showed that exposing the shrimp to chronic heat stress could enhance shrimp survival from approximately 20-30% survival in the non-heated control groups up to 50–60% in the NLHS groups (Fig. 3A, B, 3C). However, it was found that the acute heat stress could increase

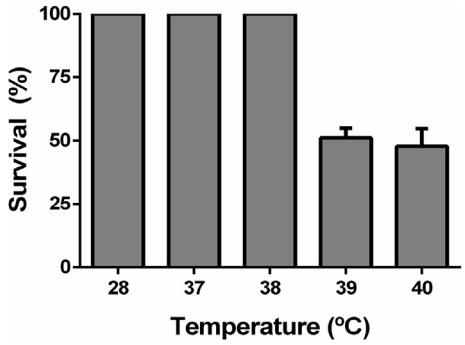


Fig. 2. Determination of a NLHS temperature in *P. vannamei*. Four groups of 20 juveniles *P. vannamei* each acclimated at 28 ± 1 °C were abruptly exposed for 30 min at heat shock temperatures of 37 ± 0.2 °C, 38 ± 0.2 °C, 39 ± 0.2 °C, and 40 ± 0.2 °C and, then, transferred immediately after heat shock back to ambient temperature. One control group was kept at 28 ± 1 °C. Animal survival was observed after 6 h by counting the live animals. The error bars are the SD values from three replicates.

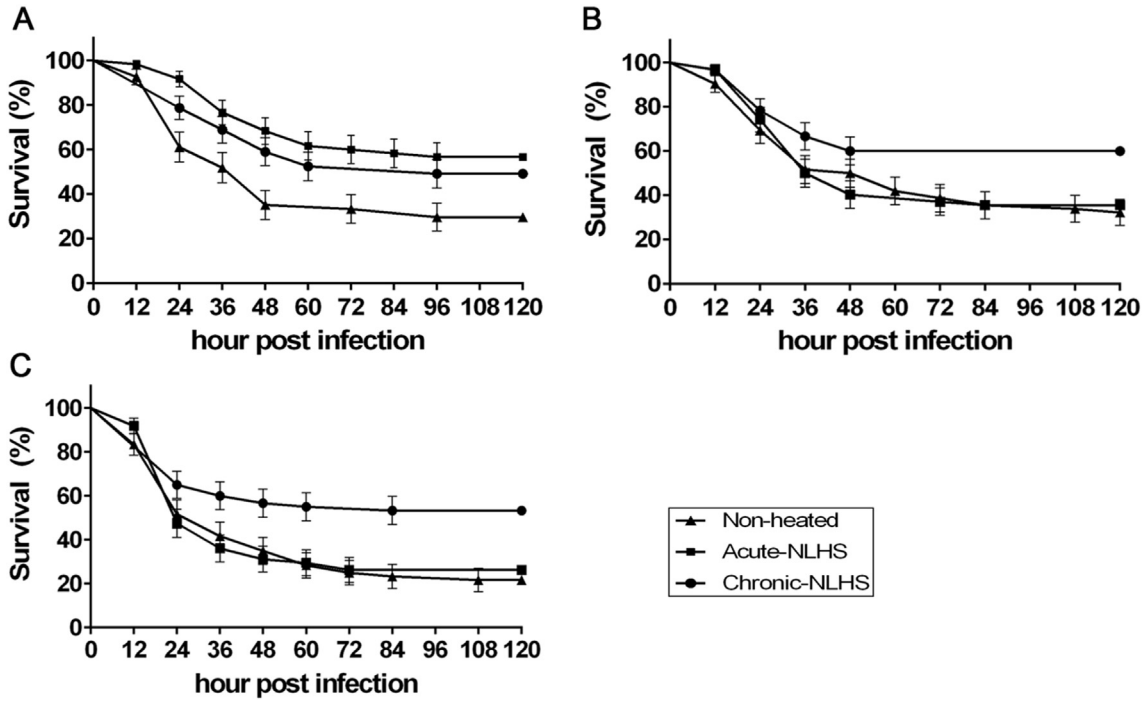


Fig. 3. Chronic NLHS induced bacterial tolerance of *P. vannamei*. Shrimp acclimated at 28 ± 1 °C were exposed to acute NLHS (abrupt heating at 38 ± 0.2 °C for 30 min) or chronic NLHS (abrupt heating at 38 ± 0.2 °C for 5 min daily for 7 days). After completed heating at (A) day 3 (B) day 7 or (C) day 30 recovery times, shrimp were challenged by immersion with 1×10^6 CFU/ml of VP_{AHPND}. Survivors were counted every 12 h for 120 h after challenge. Non-heated group was a control. The error bars are the SD values from three replicates.

shrimp tolerance to bacterial infection only temporary when challenged at day 3 recovery time (Fig. 3A) while no protection was observed when challenged at longer recovery time (Fig. 3B and C). These results clearly showed that the chronic NLHS could induce bacterial tolerance up to 30 days which was much better than the acute NLHS condition.

3.3. NLHS induced expression of LvHSPs and some other immune related genes

According to the challenge test, chronic NLHS could enhance shrimp tolerance to VP_{AHPND} infection which was likely associated with the increasing expression of heat shock proteins and the induction of shrimp innate immunity. Differential gene expression was performed by qRT-PCR to determine the expression profiles of *LvHSP*s and some immune related genes of shrimp exposed to chronic NLHS. The candidate heat shock protein genes: *LvHSP90*, *LvHSP70*, *LvHSP60*, *LvHSP21*, and *LvHSP10*, were selected for the determination of gene expression after chronic heat treatment at various recovery time points after return to ambient temperature to 120 h.

The expression profiles of five *LvHSPs* genes in the hemocytes of *P. vannamei* after chronic NLHS are shown in Fig. 4A. Dramatic up regulation of *LvHSP70* and *LvHSP90* was observed at 0–6 h followed by down regulation of *LvHSP70* at 12–96 h and down regulation of *LvHSP90* at 24 h before returning to basal level. The relative expression ratios of *LvHSP10* and *LvHSP60* were slightly increased at 0–3 h and declined afterwards. Contrary to other *LvHSP*s, the expression of *LvHSP21* was significantly decreased at all time points.

Interestingly, the expression of two immune related genes, *LvCrustin* and *LvproPO*, were significantly up regulated from 0 h to 120 h recovery time. The expression reached the maximum of 12-fold at 48 h recovery time for *LvCrustin* and 14-fold at 72 h recovery time for *LvproPO* (Fig. 4B). On the contrary, the relative expression of *LvALF*, *LvA2M*, and *LvKazal* was insignificantly or not induced after the heat shock treatment. The expression was slightly down regulated for *LvA2M* and *LvKazal*.

3.4. Chronic NLHS could not induce tolerance to VP_{AHPND} in LvHSP70- and LvHSP90-silenced P. vannamei

To understand the functional of *LvHSPs* in bacterial tolerance, RNAi-mediated gene silencing was performed to knockdown the *LvHSP70* and *LvHSP90* transcripts in the shrimp. The *GFP* dsRNA was used as a control. After 24 h of dsRNA injection, total RNA was extracted from hemocytes of knockdown and control shrimp and then subjected to semi-quantitative RT-PCR. Both *LvHSP70* and *LvHSP90* transcripts were successfully suppressed (Fig. 5A) for the expression of both genes was reduced by nearly 90% (Fig. 5B and C). Complete knockdown of the *LvHSP70* and *LvHSP90* transcripts was avoided since it resulted in high mortality of shrimp (data not shown).

In the chronic NLHS experiment, shrimp were exposed to chronic NLHS followed by injection with dsRNAs of *LvHSP70*, *LvHSP90* or *GFP* at day two recovery time. Twenty-four hours after dsRNA injection, the animals were challenged with $VP_{non\text{-}AHPND}$ or VP_{AHPND} and the mortality was observed every 12 hpi till 120 hpi. The results showed that there was higher mortality of *LvHSP70*- and *LvHSP90*-silenced shrimp as compared with the control group injected with *GFP* dsRNA. Insignificant mortality of silenced shrimp was shown in $VP_{non\text{-}AHPND}$ infection suggesting the crucial role of both *LvHSPs* in NLHS-induced bacterial tolerance (Fig. 5D).

3.5. LvHSP70 and LvHSP90 are essential for tolerance to VP_{AHPND} infection

According to the challenge test of *LvHSP70*- and *LvHSP90*-

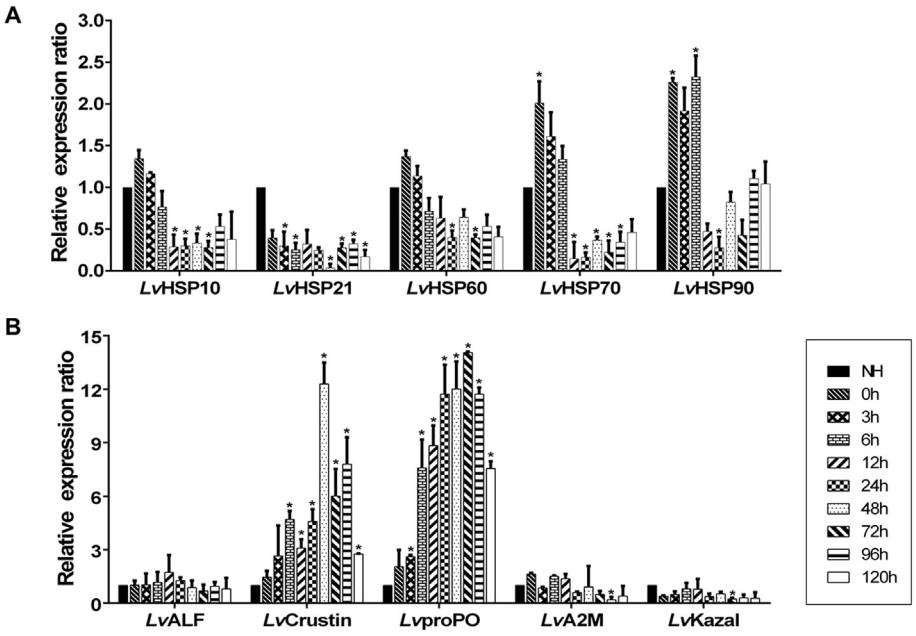


Fig. 4. NLHS induced the expression of *LvHSP*s and immune-related genes. The *LvHSP* mRNAs (A) and other immune-related mRNAs (B) were quantified by qRT-PCR at various recovery times after chronic NLHS (0, 3, 6, 12, 24, 48, 72, 96, and 120 h) compared to the control non-heated shrimp. The *EF1α* was used as an internal control. The error bars are the SD values from three replicates. Asterisks indicate statistically significant different ratios (>2-fold) compared with the control.

silenced shrimp, the animals were no longer resist to VP_{AHPND} infection. We, then, further investigated whether they had higher amount of bacterial infection than the control shrimp injected with *GFP* dsRNA. The amount of VP_{AHPND} in shrimp stomach was counted after specific *LvHSPs* gene knockdown. The results revealed that 24 h after *LvHSPs* gene silencing, the VP_{AHPND} concentration (CFU/ml) was much higher when compared with those of the SSS and *GFP* dsRNA injected groups. As expected, the VP_{AHPND} concentration of the control non-heated shrimp infected with VP_{AHPND} showed higher amounts of bacteria than those exposed to chronic NLHS (SSS and *GFP* dsRNA injected groups) (Fig. 6A).

The AP4 nested PCR method was also performed to confirm the high amount of bacterial infection in the knockdown shrimp. Genomic DNA (50 ng/μl) extracted from the stomach tissue was used as template for PCR. The results showed a lower level of single amplicon band of 230 bp from the 2nd (nested) PCR step in shrimp that were injected with SSS and *GFP* dsRNA (Fig. 6B) indicating a low level of VP_{AHPND} target in the template DNA. However, the *LvHSP70*- and *LvHSP90*-silenced shrimp and non-heated shrimp showed higher band intensity of 230 bp product with additional amplicon bands (Fig. 6B) similar to the positive control of VP_{AHPND} cultured overnight indicating a high level of VP_{AHPND} target in the template DNA. Therefore, the *Lv*HSP70 and *Lv*HSP90 are essential for tolerance to VP_{AHPND} infection.

3.6. *LvHSP70- and LvHSP90-gene silencing reduces the shrimp PO activity upon VP_{AHPND} infection*

Additionally, the treated animals were investigated the hemolymph PO activity after VP_{AHPND} infection. A significant decrease in PO activity was observed in the *LvHSP70*- and *LvHSP90*-silenced shrimp compared with the control shrimp injected with SSS and *GFP* dsRNA (Fig. 7). Thus, the gene knockdown of *LvHSP*s could affect melanization in shrimp upon bacterial infection. Moreover, NLHS shrimp that were injected with SSS and *GFP* dsRNA showed a higher PO activity than the non-heated shrimp (Fig. 7) suggesting that the NLHS could induce proPO activating-system in shrimp.

4. Discussion

The causative agent of AHPND has been reported as a unique strain of the bacterium *V. parahaemolyticus* [7]. The VP_{AHPND} colonizes in shrimp stomach and produces soluble toxins, ToxA (12.7 kDa) and ToxB (50.1 kDa), that enter the hepatopancreas causing cell sloughing, the pathology and finally shrimp mortality [23]. Many isolates of *V. parahaemolyticus* containing toxins have been reported for example three bacterial isolates (1D, 3HP, and 5HP) from a shrimp farm in Thailand that was experiencing massive death within 35 days after stocking [7]. Owing to the widespread infection of VP_{AHPND}, the effective treatment for AHPND is urgently required to counteract the high mortality rate of the cultured shrimp.

Previous reports indicate that the NLHS treatment can enhance the toleration of pathogen infections in aquatic animals such as *Artermia* and Asian green mussel [11–13]. In contrast, the successful NLHS treatments that enhance shrimp tolerance to pathogen infections have not been obtained. In this study, the NLHS of *P. vannamei* at 38 ± 0.2 °C from ambient temperature is demonstrated. The condition is similar to those reported in other aquatic animals to induce animal tolerance upon bacterial infection [11–13].

Abruptly heating the animals in chronic NLHS conditions has only previously been reported in mammals, such as the Rex rabbit (*Oryctolagus cuniculus*) that is exposed to chronic heat stress at 36 °C from an ambient temperature of 26 °C. It is found that both gene and protein expressions of HSP60, HSC70, HSP70 and HSP90 are significantly up-regulated after heat stress. Interestingly, the up-regulation remains until week nine of recovery [24]. Likewise, this study found that the chronic heat stress could induce shrimp tolerance to VP_{AHPND} up to 30 days recovery time. On the other hand, acute heat stress could only induce shrimp tolerance to bacterial infection for a short period of 3-day recovery time.

Heat shock proteins (HSPs) are the best studied heat stress response proteins that are induced in animals after heat treatment. Several reports has shown that the small heat shock protein (sHSPs)

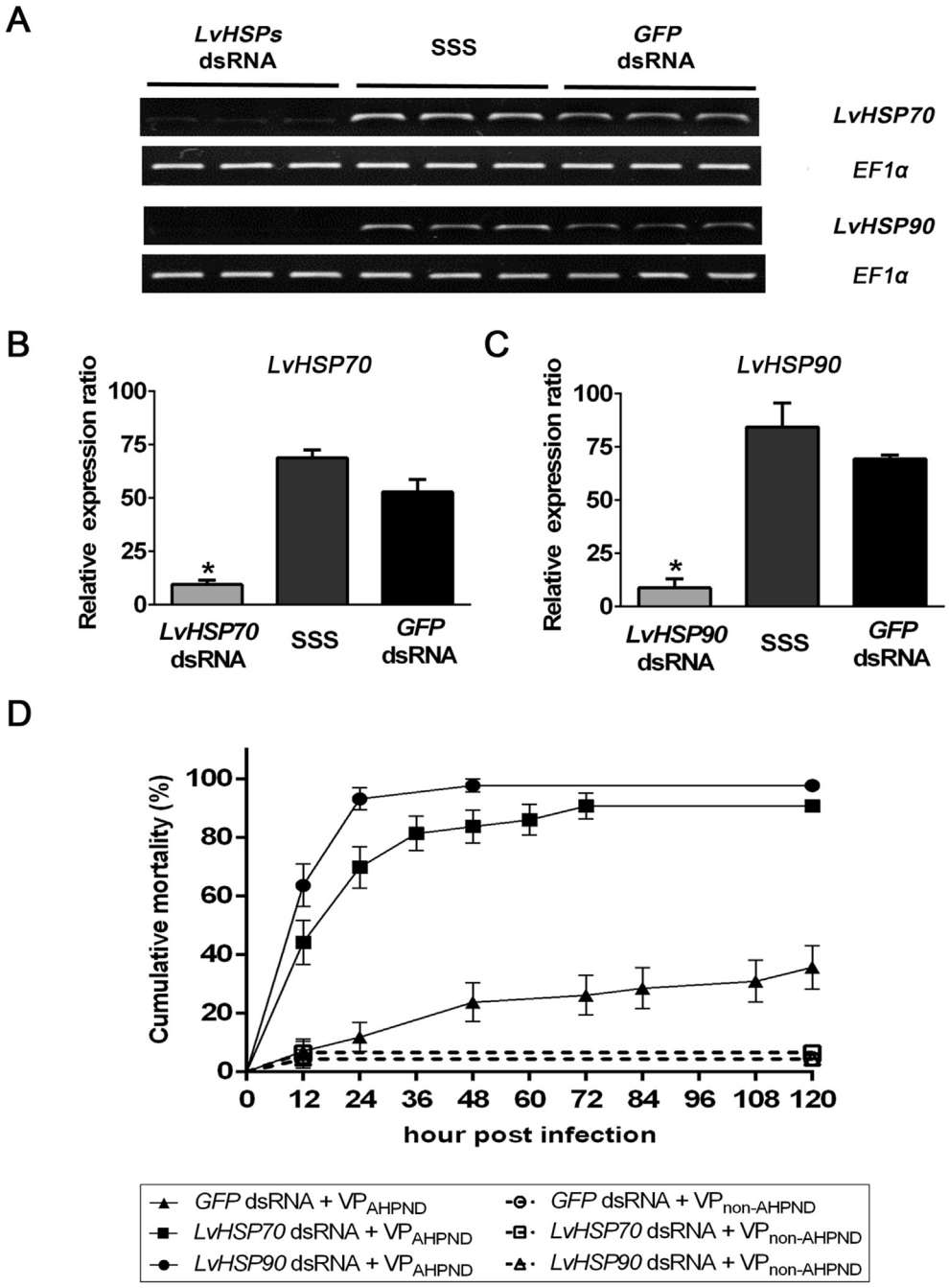


Fig. 5. The *LvHSP* knockdown affects the shrimp tolerance to VP_{AHPND}. Juvenile shrimp were injected with 5 μg/g shrimp of *GFP* dsRNA, 5 μg/g shrimp of *LvHSP70* dsRNA or 1 μg/g shrimp of *LvHSP90* dsRNA. The gene silencing efficiency of *LvHSP70* and *LvHSP90* was analyzed by (A) Semi-quantitative RT-PCR and (B, C) the relative expression analysis. Juvenile shrimp injected with saline solution (SSS) and GFP dsRNA act as controls. (D) Fifteen shrimp exposed to chronic NLHS and dsRNA injection after that were immersed with 1×10^6 CFU/ml of either $VP_{non\text{-}AHPND}$ or VP_{AHPND}. The cumulative mortality was observed every 12 hpi till 120 hpi. This experiment was done in triplicate. The error bars are the SD values from the three replicates. Asterisk indicates statistically significant different ratio compared to SSS and GFP dsRNA injection ($P < 0.05$).

and the major heat shock proteins such as HSP60, HSP70, and HSP90 are synthesized under heat stress to protect the host against pathogens by functioning as molecular chaperones, and they are thought to mediate humoral and cellular innate immune responses [25].

To understand how the chronic NLHS protected the *P. vannamei* from AHPND infection, we further examined the expression of *LvHSP*s and some immune genes after heat treatments. The expression of *LvHSP70* and *LvHSP90* showed a slight increase at 0 h and 3 h recovery times while that of *LvHSP70* and *LvHSP90* were highly up-regulated in the hemocytes during the early phase of recovery times, e.g. 0, 3, and 6 h. A similar result is obtained in heat shock treatment of *P. monodon* that shows highly up regulation of *PmHSP21*, *PmHSP70*, and *PmHSP90* in the hepatopancreas within the first hours after the heat exposure [26]. Moreover, after acute heat stress of shrimp, the mRNA transcript and protein expression of *LvHSP70* are highly increased compared with those of non-heated shrimp [14].

The early up regulation within a few hours after heat stress suggests that the *LvHSP*s might function as a regulator of other

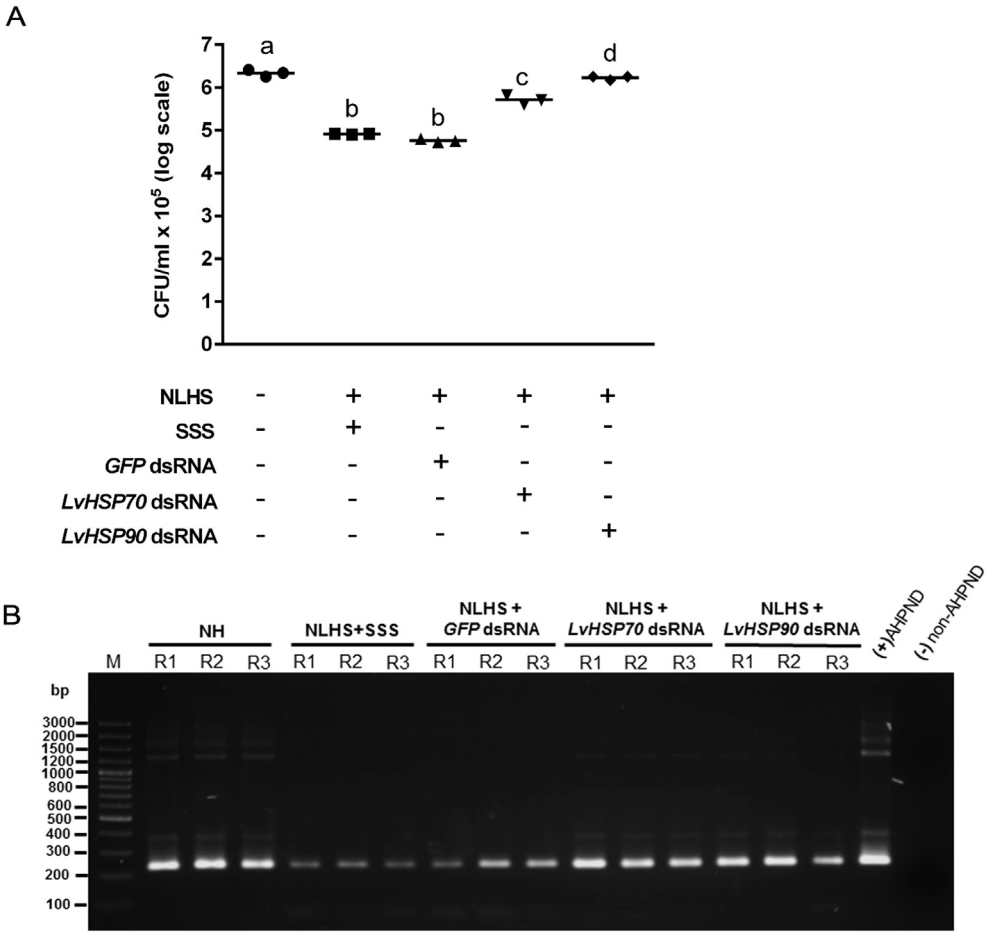


Fig. 6. *LvHSPs* knockdown shrimp were susceptible to VP_{AHPND} infection. (A) Bacteria counting. Three groups of three shrimp each were exposed to chronic NLHS and injected with 5 μg/g shrimp of *GFP* dsRNA, 5 μg/g shrimp of *LvHSP70* dsRNA or 1 μg/g shrimp of *LvHSP90* dsRNA. After 24 h post dsRNA injection, shrimp were immersed with 1×10^6 CFU/ml VP_{AHPND}. After 24 hpi, stomachs were individually collected to determine the amount of VP_{AHPND} by dotting on TCBS agar. After incubating overnight, the total numbers of viable green colonies (CFUs) were evaluated. (B) The PCR detection method. Genomic DNA was extracted from the shrimp stomach tissue samples. The AP4 nested PCR method was performed and analyzed by 1.8% agarose gel electrophoresis. VP_{AHPND} and VP_{AHPND} cultures were used as positive and negative control, respectively. NLHS shrimp injected with SSS or *GFP* dsRNA were used as controls. The alphabets denote statistically significant difference between values obtained for NH and NLHS injected with dsRNA ($P < 0.05$).

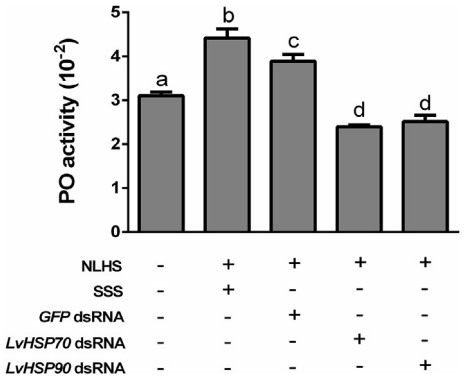


Fig. 7. Reduction of hemolymph PO activity in *LvHSP*-silenced shrimp challenged with VP_{AHPND}. Juvenile L. *vannamei* exposed to NLHS were injected with 5 μg/g shrimp of *GFP* dsRNA, 5 μg/g shrimp of *LvHSP70* dsRNA or 1 μg/g shrimp of *LvHSP90* dsRNA, followed by immersion with 1×10^6 CFU/ml VP_{AHPND}. After 24 hpi, the hemolymph was withdrawn and 200 μg of hemolymph proteins were separately mixed with the PO substrate (3 mg/μl L-DOPA). The PO activity was defined as ΔA_{490}/mg protein/min. The experiment was performed in triplicate of three pooled hemolymph samples, each sample from three shrimp. The data are shown as the means ± SD and the alphabets indicate statistically significant difference between values obtained from NH and NLHS injected with dsRNA ($P < 0.05$).

genes. Here, we observed a dramatic increase of mRNA transcription levels in *LvproPO* and *LvCrustin* beginning at 6 h until 120 h after chronic heat stress. Similar to the previous report in *P. monodon* that the transcript levels of *crustinPm5*, *crustinPm1*, and *crustin-likePm* in epipodite are up-regulated upon heat treatment [27] and in *P. vannamei* that the mRNAs encoding proPO increase significantly after NLHS [14]. Moreover, injection of recombinant Dnak followed by *V. campbellii* challenge of Pacific white shrimp also affects transcription of prophenoloxidase-2 (proPO-2) [28]. The up-regulation of *LvHSP70*, *LvHSP90*, *LvproPO*, and *LvCrustin* found in this study might be related to the function of the two heat shock proteins in regulating the immune related genes such as crustin and proPO. Genomic structure of *crustinPm5* gene reveals the presence of a putative heat-shock regulatory element (HSE) at the 5′ upstream region suggesting that it might be regulated by HSPs but no direct evidence has been shown [27]. In contrast, the *LvHSP21* is down regulated after chronic heat stress whilst the previous experiments in *P. monodon* shows the constitutive expression of *PmHSP21* but inducible immediately after acute heat stress [26,19]. We speculate that this might be due to the difference of heat stress conditions.

Previous studies have reported that the chronic heat stress is involved in inducing apoptosis in the organism during the cell development [29] and *Pm*HSP21 might be related with the host

apoptosis referring to human *HSP27* which is found to have a function in blocking apoptosis [19]. The heat induced synthesis of sHSPs and HSP90 enhances the *C. elegans* immunity to pathogenic *Pseudomonas aeruginosa*. The mechanism might involve heat shock transcription factor-1 and the associated DAF2/DAF-16 pathway which regulates aging and immunity in nematodes [30].

In this study, we successfully knockdown the expression of two HSPs; *LvHSP70* and *LvHSP90*. Following the challenge of the knockdown shrimp with VP_{AHPND}, we found the increase in shrimp mortality which was corresponding with the increase of bacterial counts and high levels of VPAHPND infection detected by AP4 PCR diagnosis method. Previously, the elevation of HSP70 also reduces the bacterial load in *V. campbellii* challenge [31].

Furthermore, hemolymph PO activity of *LvHSP70*- and *LvHSP90*-silenced shrimp was significantly decreased. Since the proPO-activating system plays an important role in bacterial defense in shrimp [22], gene silencing of *LvHSP70* and *LvHSP90* might affect the tolerance to VP_{AHPND} infection by subsequent reduction of PO activity. In this study demonstrate that the up-regulation of HSPs, proPO, and crustin after chronic heat stress enhances the Pacific white shrimp tolerance to VP_{AHPND} and the knockdown of *LvHSPs* results in high cumulative mortality. This finding is also in accordance with the report that feeding *Artemia franciscana* with either *Artemia* Hsp70 or the *E. coli* Hsp70 followed by *V. campbellii* challenge enhances the proPO system at both mRNA and protein activity levels and led to high survival rate of the animals [32]. Moreover, previous studies have reported the correlation of the proPO system and AMP synthesis [33–35]. Gene silencing of shrimp proPOs resulted in a reduction of AMP gene expression [36] which might be related to the overlapping of the proPO system and the toll pathways which regulate the AMP synthesis [34,35]. Thus, the upregulation of immune genes, *LvproPO*, and *LvCrustin*, after chronic NLHS might be likely correlated and together play crucial role in bacterial defense leading to shrimp tolerance to VP_{AHPND}.

In conclusion, we present here for the first time that the NLHS conditions can induce protection against VP_{AHPND} in the Pacific white shrimp *P. vannamei*. The gene expression analysis after chronic NLHS demonstrates that the *LvHSP70*, *LvHSP90*, *LvCrustin*, and *LvproPO* are highly up-regulated suggesting that they might play an important role in bacterial defense. The *LvHSP70*- and *LvHSP90*-silenced shrimp no longer show bacterial protection induced by the NLHS implying that the *Lv*HSP70 and *Lv*HSP90 are the heat stress response proteins that mediate the immunity of shrimp against VP_{AHPND} infection.

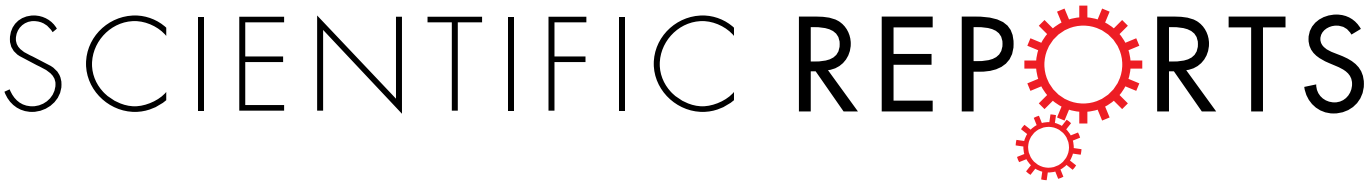
Acknowledgements

We thank Prof. Vichien Rimphanitchayakit for valuable comments on the manuscript. We would also like to thank Marine Shrimp Broodstock Research Center II (MSBRC-2), Charoen Pokphand Foods PCL for providing experimental animals and heat shock treated instrument. This work is supported by Thailand Research Fund to A.T. (TRF Senior Scholar No. RTA5880004). Additional support from TRF (grant no. IRG5780008) to the Department of Biochemistry, Faculty of Science, Chulalongkorn University is acknowledged. Student fellowship to W. J. from the Royal Golden Jubilee Ph.D. program, Thailand Research Fund, is greatly appreciate.

References

[1] H.C. Lai, T.H. Ng, M. Ando, C.T. Lee, I.T. Chen, J.C. Chuang, et al., Pathogenesis of acute hepatopancreatic necrosis disease (AHPND) in shrimp, Fish. Shellfish Immunol. 47 (2015) 1006–1014.
[2] FAO, The State of World Fisheries and Aquaculture 2014, Rome vol. 223, 2014, p. 2014.
[3] P. De Schryver, T. Defoirdt, P. Sorgeloos, Early mortality syndrome outbreaks: a microbial management issue in shrimp farming? PLoS Pathog. 10 (4) (2014) e1003919.
[4] FAO, FAO/MARD Technical Workshop on Early Mortality Syndrome (EMS) or Acute Hepatopancreatic Necrosis Syndrome (AHPNS) of Cultured Shrimp (Under TCP/VIE/3304), 2013, 2013.
[5] L. Tran, L. Nunan, R.M. Redman, L.L. Mohney, C.R. Pantoja, K. Fitzsimmons, et al., Determination of the infectious nature of the agent of acute hepatopancreatic necrosis syndrome affecting penaeid shrimp, Dis. Aquat. Organ 105 (2013) 45–55.
[6] J.E. Han, K.F. Tang, L.H. Tran, D.V. Lightner, Photorhabdus insect-related (Pir) toxin-like genes in a plasmid of *Vibrio parahaemolyticus*, the causative agent of acute hepatopancreatic necrosis disease (AHPND) of shrimp, Dis. Aquat. Organ 113 (2015) 33–40.
[7] J. Joshi, J. Srisala, V.H. Truong, I.T. Chen, B. Nuangsaeng, O. Suthienkul, et al., Variation in *Vibrio parahaemolyticus* isolates from a single Thai shrimp farm experiencing an outbreak of acute hepatopancreatic necrosis disease (AHPND), Aquaculture 428–429 (2014) 297–302.
[8] S. Dangtip, R. Sirikharin, P. Sanguanrut, S. Thitamadee, K. Sritunyalucksana, S. Taengchaiyaphum, et al., AP4 method for two-tube nested PCR detection of AHPND isolates of *Vibrio parahaemolyticus*, Aquac. Rep. 2 (2015) 158–162.
[9] J. Kongrueng, N. Tansila, P. Mitraparp-arthorn, M. Nishibuchi, G.J. Vora, V. Vuddhakul, LAMP assay to detect *Vibrio parahaemolyticus* causing acute hepatopancreatic necrosis disease in shrimp, Aquac. Int. 23 (2015) 1179–1188.
[10] E. De la Vega, M.R. Hall, B.M. Degnan, K.J. Wilson, Short-term hyperthermic treatment of *Penaeus monodon* increases expression of heat shock protein 70 (HSP70) and reduces replication of gill associated virus (GAV), Aquaculture 253 (2006) 82–90.
[11] P. Norouzitallab, K. Baruah, D.M. Muthappa, P. Bossier, Non-lethal heat shock induces HSP70 and HMGB1 protein production sequentially to protect *Artemia franciscana* against *Vibrio campbellii*, Fish. Shellfish Immunol. 42 (2015) 395–399.
[12] Y. Yik Sung, E.J. Van Damme, P. Sorgeloos, P. Bossier, Non-lethal heat shock protects gnotobiotic *Artemia franciscana* larvae against virulent Vibrios, Fish. Shellfish Immunol. 22 (2007) 318–326.
[13] N.A. Aleng, Y.Y. Sung, T.H. MacRae, M.E. Abd Wahid, Non-lethal heat shock of the Asian green mussel, Perna viridis, promotes Hsp70 Synthesis, induces thermotolerance and protects against Vibrio infection, PLoS One 10 (2015) e0135603.
[14] N.H. Loc, T.H. Macrae, N. Musa, M.D. Bin Abdullah, M.E. Abdul Wahid, Y.Y. Sung, Non-lethal heat shock increased Hsp70 and immune protein transcripts but not Vibrio tolerance in the white-leg shrimp, PLoS One 8 (2013) e73199.
[15] J. Ryckaert, F. Pasmans, E. Tobback, L. Duchateau, A. Decostere, F. Haesebrouck, et al., Heat shock proteins protect platyfish (*Xiphophorus maculatus*) from *Yersinia ruckeri* induced mortality, Fish. Shellfish Immunol. 28 (2010) 228–231.
[16] S. Sinnasamy, N.M. Noordin, T.H. MacRae, Abdullah Mlb, P. Bossier, Wahid MEbA, et al., Ingestion of food pellets containing *Escherichia coli* overexpressing the heat-shock protein DnaK protects *Penaeus vannamei* (Boone) against *Vibrio harveyi* (Baumann) infection, J. Fish Dis. 39 (2015) 577–584.
[17] J.G. Routsias, A.G. Tzioufas, The role of chaperone proteins in autoimmunity, Ann. N. Y. Acad. Sci. 1088 (2006) 52–64.
[18] J. Zhou, W.N. Wang, W.Y. He, Y. Zheng, L. Wang, Y. Xin, et al., Expression of HSP60 and HSP70 in white shrimp, *Litopenaeus vannamei* in response to bacterial challenge, J. Invertebr. Pathol. 103 (2010) 170–178.
[19] P.Y. Huang, S.T. Kang, W.Y. Chen, T.C. Hsu, C.F. Lo, K.F. Liu, et al., Identification of the small heat shock protein, HSP21, of shrimp *Penaeus monodon* and the gene expression of HSP21 is inactivated after white spot syndrome virus (WSSV) infection, Fish. Shellfish Immunol. 25 (2008) 250–257.
[20] R. Rao, Y. Bing Zhu, T. Alinejad, S. Tiruvayipati, K. Lin Thong, J. Wang, et al., RNA-seq analysis of *Macrobrachium rosenbergii* hepatopancreas in response to *Vibrio parahaemolyticus* infection, Gut Pathog. 7 (2015) 6.
[21] P. Supungul, P. Jaree, K. Somboonwiwat, W. Junprung, P. Proespraiwong, R. Mavichak, et al., A potential application of shrimp antilipopolysaccharide factor in disease control in aquaculture, Aquac. Res. (2015) 1–13, 10.1111/are.12925.
[22] P. Amparyup, W. Charoensapsri, A. Tassanakajon, Two prophenoloxidases are important for the survival of *Vibrio harveyi* challenged shrimp *Penaeus monodon*, Dev. Comp. Immunol. 33 (2009) 247–256.
[23] R. Sirikharin, S. Taengchaiyaphum, P. Sanguanrut, T.D. Chi, R. Mavichak, P. Proespraiwong, et al., Characterization and PCR detection of binary, Pir-Like toxins from *Vibrio parahaemolyticus* isolates that cause acute hepatopancreatic necrosis disease (AHPND) in shrimp, PLoS One 10 (2015) e0126987.
[24] Y. Pei, Y. Wu, Y. Qin, Effects of chronic heat stress on the expressions of heat shock proteins 60, 70, 90, A2, and HSC70 in the rabbit testis, Cell Stress Chaperones 17 (2012) 81–87.
[25] Y.Y. Sung, T.H. MacRae, Heat shock proteins and disease control in aquatic organisms, J Aquac Res Development S2 (2011) 006.
[26] W. Rungrassamee, R. Leelatanawit, P. Jiravanichpaisal, S. Klinbunga, N. Karoonuthaisiri, Expression and distribution of three heat shock protein genes under heat shock stress and under exposure to *Vibrio harveyi* in *Penaeus monodon*, Dev. Comp. Immunol. 34 (2010) 1082–1089.

[27] T. Vatanavicharn, P. Supungul, N. Puanglarp, W. Yingvilasprasert, A. Tassanakajon, Genomic structure, expression pattern and functional characterization of crustin*Pm*5, a unique isoform of crustin from *Penaeus monodon*, Comp. Biochem. Physiol. B Biochem. Mol. Biol. 153 (2009) 244–252.
[28] L.H. Phuoc, B. Hu, M. Wille, N.T. Hien, V.H. Phuong, N.T. Tinh, et al., Priming the immune system of Penaeid shrimp by bacterial HSP70 (DnaK), J. Fish. Dis. 39 (2016) 555–564.
[29] P. Raina, S. Kaur, Chronic heat-shock treatment driven differentiation induces apoptosis in *Leishmania donovani*, Mol. Cell Biochem. 289 (2006) 83–90.
[30] V. Singh, A. Aballay, Heat-shock transcription factor (HSF)-1 pathway required for *Caenorhabditis elegans* immunity, Proc. Natl. Acad. Sci. U. S. A. 103 (2006) 13092–13097.
[31] Y.Y. Sung, C. Pineda, T.H. MacRae, P. Sorgeloos, P. Bossier, Exposure of gnotobiotic *Artemia franciscana* larvae to abiotic stress promotes heat shock protein 70 synthesis and enhances resistance to pathogenic *Vibrio campbellii*, Cell Stress Chaperones 13 (2008) 59–66.
[32] K. Baruah, J. Ranjan, P. Sorgeloos, T.H. Macrae, P. Bossier, Priming the prophenoloxidase system of *Artemia franciscana* by heat shock proteins protects against *Vibrio campbellii* challenge, Fish. Shellfish Immunol. 31 (2011) 134–141.
[33] P. Amparyup, W. Charoensapsri, A. Tassanakajon, Prophenoloxidase system and its role in shrimp immune responses against major pathogens, Fish. Shellfish Immunol. 34 (2013) 990–1001.
[34] F.F. Fagutao, T. Koyama, A. Kaizu, T. Saito-Taki, H. Kondo, T. Aoki, et al., Increased bacterial load in shrimp hemolymph in the absence of prophenoloxidase, FEBS J. 276 (2009) 5298–5306.
[35] K.B. Roh, C.H. Kim, H. Lee, H.M. Kwon, J.W. Park, J.H. Ryu, et al., Proteolytic cascade for the activation of the insect toll pathway induced by the fungal cell wall component, J. Biol. Chem. 284 (2009) 19474–19481.
[36] P. Amparyup, J. Sutthangkul, W. Charoensapsri, A. Tassanakajon, Pattern recognition protein binds to lipopolysaccharide and beta-1,3-glucan and activates shrimp prophenoloxidase system, J. Biol. Chem. 287 (2012) 10060–10069.



OPEN

Regulation of antilipopolysaccharide factors, ALF*Pm*3 and ALF*Pm*6, in *Penaeus monodon*

Received: 17 May 2017
Accepted: 1 September 2017
Published online: 04 October 2017

Pitchayanan Kamsaeng, Anchalee Tassanakajon & Kunlaya Somboonwiwat

ALF*Pm*6, a member of antimicrobial peptide in the antilipopolysaccharide factor (ALF) family from *Penaeus monodon*, plays important roles in shrimp immunity against pathogens. However, its antimicrobial activity and underlying mechanism have not been reported. The synthetic cyclic ALF*Pm*6#29–52 peptide (cALF*Pm*6#29–52) corresponding to the ALF*Pm*6 LPS-binding domain can agglutinate and exhibited bacterial killing activity toward a Gram-negative bacterium, *Escherichia coli* 363 and Gram-positive bacteria, *Bacillus megaterium*, *Aerococcus viridans*, and *Micrococcus luteus*, with MIC values of 25–50 μM. Specifically, ALF*Pm*6 and ALF*Pm*3, the most abundant ALF isoforms, are different in terms of gene expression patterns upon pathogen infections. Herein, the regulation of ALF*Pm*3 and ALF*Pm*6 gene expression was studied. The 5′-upstream and promoter sequences were identified and the putative transcription factor (TF)-binding sites were predicted. The narrow down assay indicated that the ALF*Pm*3 promoter and partial promoter of the ALF*Pm*6 active regions were located at nucleotide positions (−814/+302) and (−282/+85), respectively. Mutagenesis of selected TF-binding sites revealed that Rel/NF-κB (−280/−270) of ALF*Pm*3 and C/EBPβ (−88/−78) and Sp1 (−249/−238) sites of ALF*Pm*6 were the activator-binding sites. Knockdown of the *Pm*MyD88 and *Pm*Relish genes in *V. harveyi*-infected shrimp suggested that the ALF*Pm*3 gene was regulated by Toll and IMD pathways, while the ALF*Pm*6 gene was regulated by the Toll pathway.

Currently, white spot syndrome virus (WSSV) and bacteria of *Vibrio* species are considered major shrimp pathogens[1–3]. The major virulent strains of Vibrio in shrimp are *Vibrio harveyi*, *Vibrio alginolyticus*, and *Vibrio parahaemolyticus*, causing acute hepatopancreatic necrosis disease (AHPND)[4]. These virulent strains cause extreme losses of shrimp in hatcheries and grow-out farms, thus making the prevention and control of diseases a priority for shrimp production. To overcome these obstacles, knowledge regarding the innate immune system of shrimp is urgently required.

Antimicrobial peptides (AMPs) in the antilipopolysaccharide factor (ALF) family are important effectors in shrimp. ALFs are mostly highly cationic polypeptides of approximately 100 residues with a hydrophobic N-terminal region. ALFs contain a signal peptide at the N-terminus and a LPS-binding domain (LPS-BD). Two conserved cysteine residues between LPS-BD are involved in an intramolecular disulphide bridge. The differences in the LPS-BD sequences contribute to the binding capability of different ALF*Pm* isoforms to different microbial cell wall components[5]. The *P. monodon* ALF major isoform, ALF*Pm*3, exhibits a broad antimicrobial activity spectrum against filamentous fungi, Gram-positive and Gram-negative bacteria including the natural shrimp bacterial pathogens, *V. harveyi* causing vibriosis and *V. parahaemolyticus* AHPND causing early mortality syndrome[6,7]. The recombinant protein of ALF*Pm*3 (rALF*Pm*3) induce membrane permeabilization and cell lysis of bacterial cells[8]. The antiviral properties of rALF*Pm*3 against the major shrimp viral pathogen, WSSV, have been reported. ALF*Pm*3 inhibits WSSV propagation in crayfish hematopoietic cell culture and in shrimp[9]. It has recently been shown that ALF*Pm*3 performs its anti-WSSV activities by binding to the envelope proteins; WSSV189, WSSV395, and WSSV471; nucleocapsid proteins WSSV189; and tegument protein WSSV458[10,11]. Although ALF*Pm*3 is the major ALF isoform responsible for fighting pathogen infection, other ALF*Pm* isoforms such as the ALF*Pm*6 gene have been shown to be up-regulated in *P. monodon* haemocytes in response to yellow head virus infection[12] and are important for the shrimp immune response to *V. harveyi*- and WSSV infections[13]. However, no reports have described

Center of Excellence for Molecular Biology and Genomics of Shrimp, Department of Biochemistry, Faculty of Science, Chulalongkorn University, Phayathai Rd., Bangkok, 10330, Thailand. Correspondence and requests for materials should be addressed to K.S. (email: kunlaya.s@chula.ac.th)

ALF*Pm*6 activity. Moreover, knockdown of the ALF*Pm*3 gene causes rapid mortality, while gene silencing of ALF*Pm*6 has no effect on shrimp mortality but leads to a significant increase in cumulative mortality and a more rapid mortality rate following *V. harveyi* and WSSV infections, respectively[13]. Thus, the ALF*Pm*3 and ALF*Pm*6 genes might be controlled by different signalling pathways.

In *Drosophila*, the Toll and IMD pathways are clearly the two most important signaling pathways controlling antimicrobial peptide (AMP) genes[14–16]. The Toll pathway is mainly involved in defence against fungi, Gram-positive bacteria, and viruses[17–19], while the IMD pathway plays key roles in controlling Gram-negative bacteria and virus infection. In shrimp, Toll-like receptors (TLRs) and Toll signaling proteins such as Sptzle, myeloid differentiation factor 88 (MyD88), and Dorsal also play regulatory roles on AMP genes upon pathogen infection. LvToll2 from *P. vannamei* can significantly activate the promoters of the NF-κB pathway-controlled AMP genes, but not LvToll1 and LvToll3[20]. The up-regulation of Spätzle proteins from *Fenneropenaeus chinensis* (FcSpz) and *P. vannamei* (LvSpz1–3) during *Vibrio* species and WSSV infections affect the expression of certain AMPs[20,21]. The *Fc*MyD88 transcript from *F. chinensis* is up-regulated after bacterial infection[22]. Dual-luciferase reporter assays indicated that the Dorsal from *P. vannamei* (*Lv*Dorsal) could regulate the transcription of the shrimp penaeidin-4 gene[23]. IMD and their signalling proteins in the IMD pathway have been found in shrimp. *Lv*IMD and *Lv*Relish from *P. vannamei* are involved in penaeidin-4 gene regulation[24]. Moreover, LvIMD can activate the expression of *Lv*ALF-AA-K and *Lv*Relish transcripts in bacteria-challenged shrimp[25]. IMD from *F. chinensis* (*Fc*IMD) and *Procambarus clarkii* (*Pc*IMD) is involved in regulating the expression of several AMPs against Gram-negative bacteria in *F. chinensis* such as Crustin*Fc*1, Crustin*Fc*2, ALF*Fc*1, ALF*Fc*2 and Lys*Fc*1, and in *P. clarkii* such as Crustin*Pc*1, Crustin*Pc*3, ALF*Pc*6, ALF*Pc*8, and Lys*Pc*2. These results suggest that although the IMD distribution and expression patterns exhibit some differences, the IMD pathway may have a conserved function for AMP regulation in shrimp and crayfish immunity[26]. *Fc*Relish is necessary for the expression of penaeidin-5 against *Vibrio anguillarium* infection[27]. In *P. monodon*, it has been demonstrated that PmRelish can transcriptionally regulate penaeidin-5, but not ALF*Pm*3 and Crustin*Pm*1, in YHV-infected shrimp[28].

Although the control of AMP and its promoter has been reported in several shrimp, the crucial transcription factor binding sites and promoter active region involved in ALF regulation have not been studied. Moreover, the comparative regulation of each isoform of ALF is unclear. In this study, the synthetic cyclic peptide (cALF*Pm*6#29–52) corresponding to ALF*Pm*6 LPS-BD was tested for antimicrobial activity and bacterial agglutination property. In addition, the difference in the expression levels of the ALF*Pm*3 and ALF*Pm*6 genes was explored by identifying of their promoter active regions and transcription factor binding sites that might play an important role in controlling gene expression. We also determined whether the Toll and IMD pathways were involved in regulating their gene expression.

Results

The synthetic peptide derived from ALF*Pm*6-LPS BD (cALF*Pm*6#29–52) exhibited antibacterial activity. It is known that the antimicrobial activity of ALF depends on the binding of ALF to pathogen cell wall components, which is mediated mainly via a positively charged cluster within the LPS-BD of ALF[29]. In our study, we attemped to produce the recombinant ALF*Pm*6 protein (rALF*Pm*6) in yeast *Pichia pastoris*. However, the rALF*Pm*6 protein was successfully produced but the purification could not be accomplished (data not shown). To access the activity of ALF*Pm*6, the synthetic cyclic peptide, cALF*Pm*6#29–52, corresponding to the LPS-BD of ALF*Pm*6 was examined for antimicrobial activity against various strains of Gram-negative bacteria and Gram-positive bacteria. The bactericidal activity of cALF*Pm*6#29–52 peptide was observed in comparison to the positive control. The cALF*Pm*6#29–52 peptide was able to kill a Gram-negative bacterium, *E. coli* 363, and some Gram-positive bacteria such as *B. megaterium*, *A. viridans*, and *M. luteus* with MBC values ranging from 25–50 μM (Table 1).

The synthetic peptide cALF*Pm*6#29–52 induced bacterial agglutination *in vitro*. There is evidence showing that some antimicrobial proteins and peptides can agglutinate bacteria cells. In this study, cALF*Pm*6#29–52 was tested for bacterial agglutination properties. We showed herein that the synthetic cALF*Pm*6#29–52 induced bacterial agglutination of *E. coli* 363, *B. megaterium*, *A. viridans*, and *M. luteus* at a 25 μM final concentration. At 50 μM, cALF*Pm*6#29–52 could completely inhibit the bacterial growth, and only cell debris could be detected under microscopic observation (Fig. 1). These results suggested that cALF*Pm*6#29–52 not only agglutinates bacteria but also exhibits bactericidal activity against sensitive strains in a dose-dependent manner.

Determination of regulatory elements of ALF*Pm*3 and ALF*Pm*6 genes. The expression profiles of ALF*Pm*3 and ALF*Pm*6 genes upon pathogen infection of shrimp are different[13]. To better understand how both genes are regulated, the sequences and activity of their promoters were identified and characterized.

The 5′-upstream genomic sequences of ALF*Pm*3, with a length of 1,478 bp, and ALF*Pm*6, with a length of 419 bp, were identified by genome walking. The positions of the transcription start site (+1) of the ALF*Pm*3 and ALF*Pm*6 genes were located at nucleotide positions −302 and −85, respectively, 5′-upstream from the start codon (ATG). The TATA box of ALF*Pm*3 and ALF*Pm*6 genes were located from −31 to −23 and from −29 to −24 5′-upstream from the transcription start site (+1), respectively (Fig. 2).

For the ALF*Pm*3 gene, several TF-binding sites such as specificity protein 1 (Sp1), nuclear factor NF-κB binding sites, CCAAT-enhancer-binding proteins beta (C/EBPβ), CCAAT-enhancer-binding proteins alpha (C/EBPα), octamer-1 (OCT-1), hepatocyte nuclear factors-1 (HNF-1), hepatocyte nuclear factors-1C (HNF-1C), D1, cytoplasmic polyadenylation element binding protein (CPE bind) and interferon consensus sequence-binding

Microorganism	MBC value* of cALF*Pm*6#29–52 (μM)
Gram-positive bacteria	
Aerococcus viridans	25–50
Bacillus megaterium	25–50
Micrococcus luteus	25–50
Staphylococus haemolyticus	>100
Gram-negative bacteria	
Enterobacter cloacae	>100
Erwinia carotovora	>100
Escherichia coli 363	25–50
Klebsiella pneumoniae	>100
Vibrio haemolyticus (AHPND)	>100
Non-virulent Vibrio haemolyticus	>100
Vibrio harveyi	>100

Table 1. Range of bactericidal activity of the synthetic peptide ALF*Pm*6 against various strains of microorganisms using liquid growth inhibition assay. *MBC value is expressed as the interval *a*-*b*, where *a* is the highest concentration tested at which microorganisms are growing and *b* the lowest concentration tested to kill particular bacterium.

protein (ICSBP), were predicted (Fig. 2a,c). For the ALF*Pm*6 gene, TF-binding sites including Sp1, C/EBPβ, and ICSBP, were predicted (Fig. 2b,d).

Identification of transcription factor binding sites that regulate ALF*Pm*3 and ALF*Pm*6 gene expression. The regulatory regions on the ALF*Pm*3 and ALF*Pm*6 promoter sequences were identified by the narrow down assay. Following the ALF*Pm*3 promoter activity assay, the promoter active region (−814/+302) was identified. Narrow down of the promoter fragment to −265/+302 showed the lowest activity (Fig. 3a), suggesting that the promoter sequence at position −814 to −266 might contain the activator-binding site. The DNA sequence at position −814 to −266 of the ALF*Pm*3 promoter active region contained many TF-binding sites such as Sp1 at position −719 to −701, ICSBP at position −700 to −691, 21 units of GAAAGAGAGTAAGAG[T/C] tandem repeats at position −693 to −358 and NF-κB at position −280 to −270.

To further investigate the element responsible for ALF*Pm*3 gene regulation, a deletion assay for 21 units of GAAAGAGAGTAAGAG[T/C] tandem repeats and site-directed mutagenesis at the transcription factor binding sites, Sp1 and NF-κB were performed.

The 21 units of GAAAGAGAGTAAGAG[T/C] tandem repeat-deleted construct, del(−693/−358)/p(−1478/+302), was cloned and assayed for promoter activity. The promoter activity of del(−693/−358)/p(−1478/+302) was not significantly different when compared with the control p(−1478/+302) (Fig. 3b). These results suggested that the 21 units of the GAAAGAGAGTAAGAG[T/C] tandem repeat and ICSBP transcription factor binding site were not involved in ALF*Pm*3 gene regulation.

Site-directed mutagenesis was performed to determine whether Sp1 and Rel/NF-κB transcription factor binding sites are involved in regulating the ALF*Pm*3 gene. The −814/−266 ALF*Pm*3 promoter region, was mutated at the transcription factor binding sites of Sp1 (−719/−701) and NF-κB (−280/−270) by rolling PCR using p(−1478/+302) as a template. The mutated plasmids, ΔSp1/p(−1478/+302) and ΔNF-κB/p(−1478/+302), were assayed for the promoter activity in comparison with the wild type plasmid p(−1478/+302). No significant change in promoter activity was observed with ΔSp1/p(−1478/+302). In constrast, mutation at the NF-κB binding site caused a decrease in promoter activity by 46.6% compared with the wild type plasmid (Fig. 3b), suggesting that the NF-κB binding site is an activator binding site on the ALF*Pm*3 promoter.

The promoter activity of each ALF*Pm*6 promoter fragment was determined. Compared to the control, the promoter fragment −282/+85 had the highest promoter activity whereas the promoter fragment −80/+85 showed the lowest promoter activity (Fig. 4a). The ALF*Pm*6 promoter active region (−282/+85) might have the activator-binding site at position −282 to −81. It contained many transcription factor binding sites such as Sp1 at position −249 to −238, ICSBP at position −146 to −135 and C/EBPβ at position −88 to −80.

For the −282/−81 ALF*Pm*6 promoter region, the mutated reporter plasmids at the transcription factor binding sites of Sp1 (−249/−238), ICSBP (−146/−135) and C/EBPβ (−88/−80) were constructed by rolling PCR using p(−419/+85) as a template. In comparison to the wild type plasmid p(−419/+85), the mutated plasmids, ΔICSBP/p(−419/+85), ΔC/EBPβ/p(−419/+85), and ΔSp1/p(−419/+85), showed an approximately 36.8%, 83.1%, and 98.4% decrease in promoter activity, respectively (Fig. 4b). Our results indicated that these binding regions are involved in ALF*Pm*6 gene regulation and might have different binding affinities for transcription factors that resulted in different activation strengths of ALF*Pm*6 gene expression.

Expression of the ALF*Pm*3 and ALF*Pm*6 genes is regulated by Toll and IMD pathways. The above results suggest that ALF*Pm*3 and ALF*Pm*6 genes are regulated by different transcription factors. However, the pathways that control their expression are still unclear. In this study, MyD88 and Relish, which are the representative adapter proteins of the Toll and IMD pathways, respectively, were silenced in *V. harveyi*-challenged

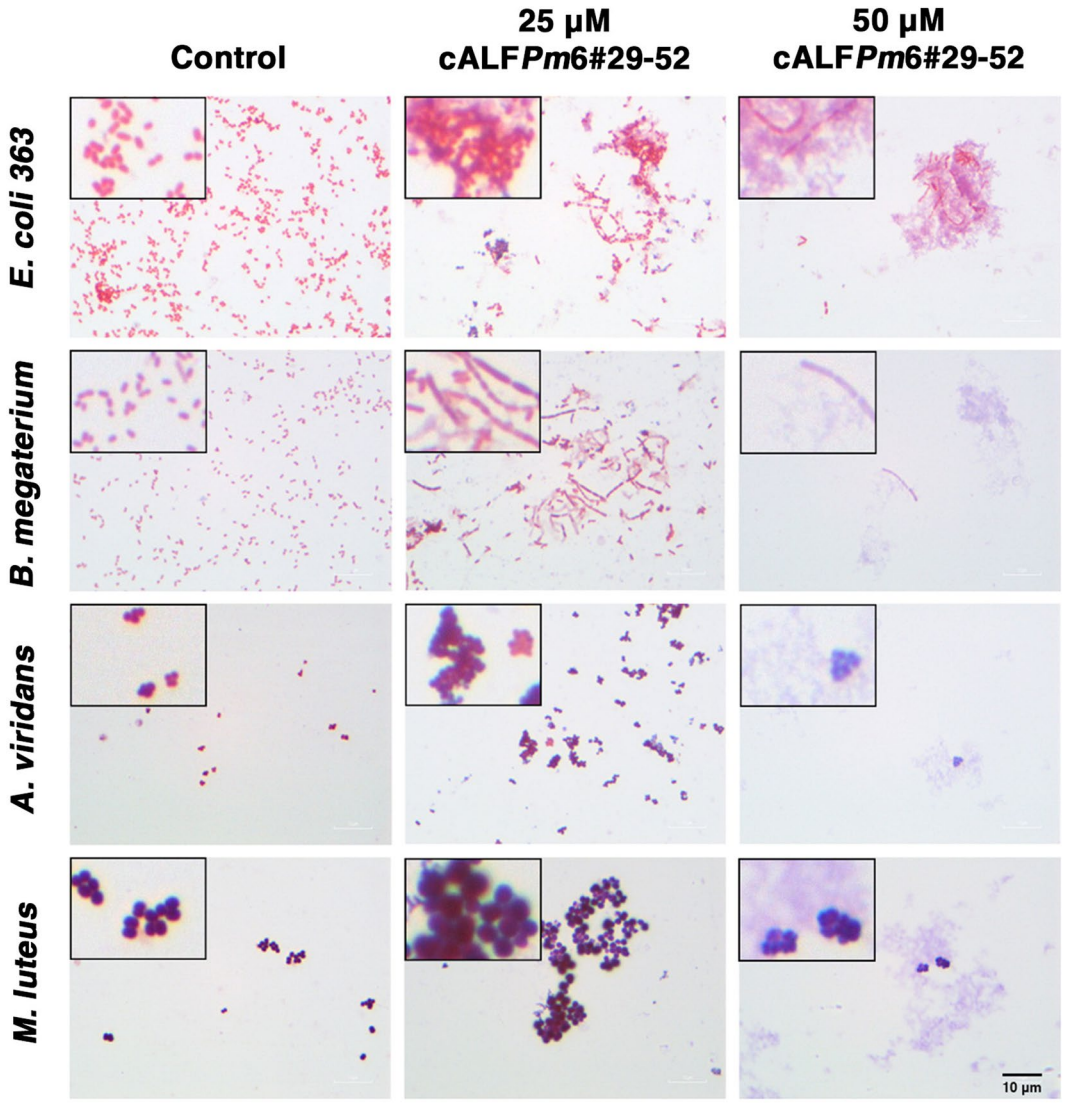


Figure 1. Bacterial agglutination mediated by the synthetic peptide cALF*Pm*6#29–52. *Escherichia coli* 363, *Bacillus megaterium*, *Aerococcus viridans*, or *Micrococcus luteus* was incubated overnight with the synthetic cALF*Pm*6#29–52 at a 25 and 50 μM final concentration. Agglutination was observed a 100X magnification using a light microscope (Olympus CX31). Images were obtained using a Nikon DS-Fi1. The scale bar is 10 μm.

shrimp in order to determine which signalling pathway plays a role in regulating ALF*Pm*3 and ALF*Pm*6 gene expression.

To test the efficiency of MyD88 dsRNA or Relish dsRNA in silencing the gene expression in shrimp, the expression levels of the MyD88 and Relish transcripts, respectively, were determined after injection of 10 μg/g shrimp of the specific dsRNA into shrimp at 0, 24, 48 and 72 h by quantitative real-time PCR (qRT-PCR) using EF1α as an internal control. Normal saline- and GFP dsRNA-injected shrimp were used as negative controls. The result showed that MyD88 gene expression was suppressed at 0–72 h post-MyD88 dsRNA injection. In contrast, expression of the Relish gene was suppressed at 0–48 h post-Relish dsRNA injection and slightly recovered at 72 h post dsRNA-Relish injection (Fig. 5a).

The transcript levels of ALF*Pm*3 and ALF*Pm*6 transcripts in haemocytes of *V. harveyi*-challenged shrimp in the presence of MyD88 and Relish gene knockdown were determined by qRT-PCR. Before ALF*Pm*3 and ALF*Pm*6 expression analysis, the suppression of MyD88 and Relish transcripts in *V. harveyi*-infected shrimp was confirmed by qRT-PCR. Note that in *V. harveyi*-infected shrimp, GFP dsRNA had no effect on Relish and MyD88 mRNA expression levels (Fig. 5b). After challenging MyD88-silenced shrimp with *V. harveyi*, the expression of ALF*Pm*3 transcript sharply decreased at 6 and 24 hpi by 89% and 74.7%, respectively, when normalized to that of dsGFP knockdown shrimp. Knockdown of the Relish gene also resulted in a gradual decrease in ALF*Pm*3 gene expression from 6 hpi (53.9%) to 24 hpi (74.3%) (Fig. 5c). It is likely that ALF*Pm*3 was regulated by both Toll and IMD pathways. ALF*Pm*6 gene expression in MyD88 knockdown shrimp was greatly decreased at 6 hpi (82.9%) and 24 hpi (80.1%) when compared to that of dsGFP knockdown shrimp. In contrast, ALF*Pm*6 gene expression increased by 34.3% at 6 hpi, and no difference was observed at 24 hpi between Relish knockdown shrimp and

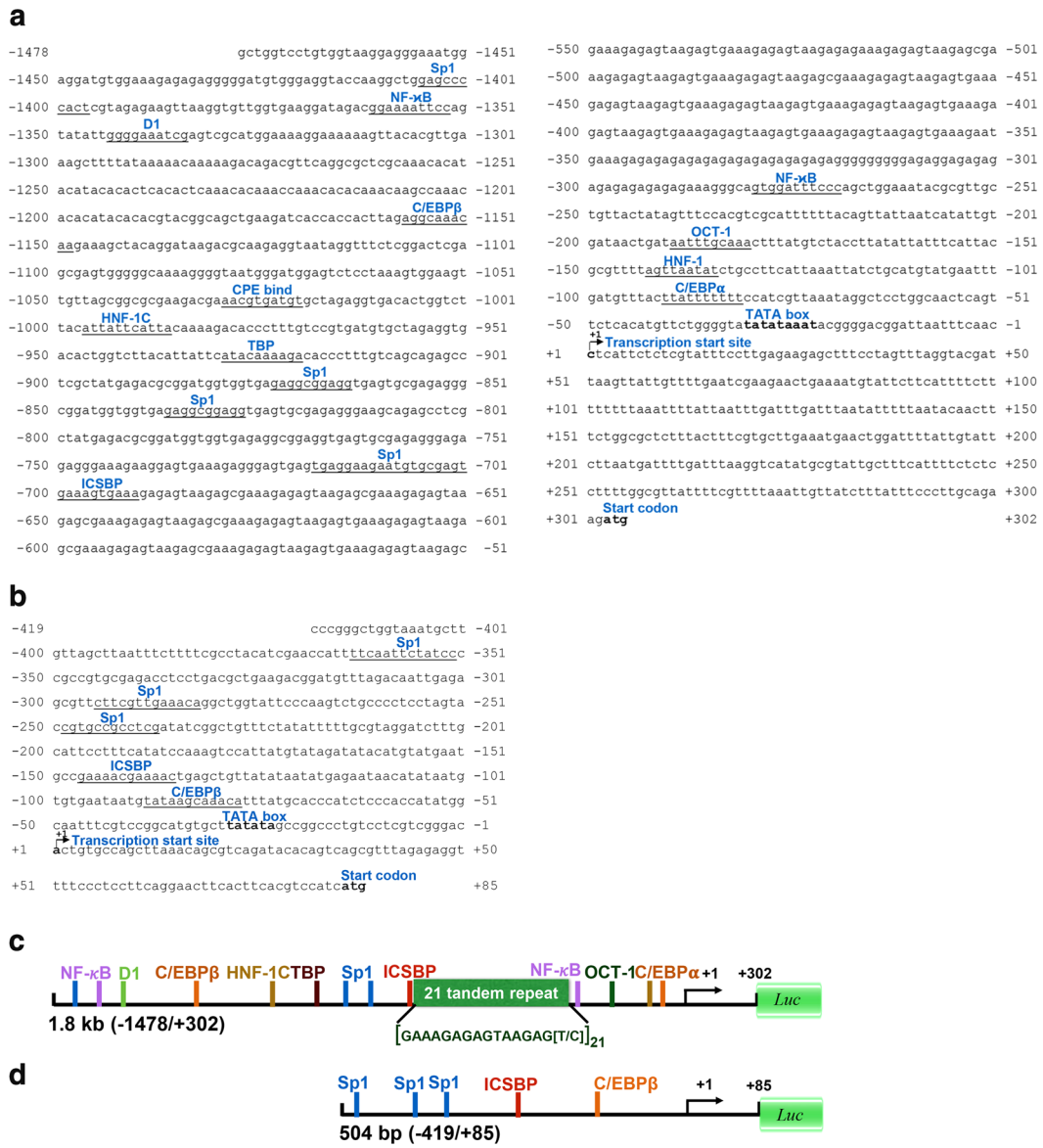


Figure 2. Upstream region and putative transcription factor binding sites of ALF*Pm* gene. The genomic sequence of the 5′-upstream region of the ALF*Pm*3 (**a**) and ALF*Pm*6 (**b**) genes. The putative cis-regulatory elements in the 5′-flanking promoter region are underlined. The transcription start site (+1) is indicated by the arrow labelled +1. The start codon and TATA box are also indicated, and their sequences are bolded. Schematic diagrams of the ALF*Pm*3 (**c**) and ALF*Pm*6 (**d**) promoter constructs used to delineate the TF-binding sites are shown.

dsGFP-challenged shrimp (Fig. 5c). Our results suggested that Toll rather than the IMD pathway might play a greater role in the transcriptional regulation of the ALF*Pm*6 gene.

Discussion

ALF comprises a group of antimicrobial peptides that have been identified and characterized in shrimp and other crustaceans. Six isoforms of ALF have been discovered in *P. monodon*. ALF*Pm*6 is the most recent and the second most abundant isoform identified in the *P. monodon* EST database (http://pmonodon.biotec.or.th)[30]. A previous report has indicated that the ALF*Pm*6 gene is up-regulated upon YHV infection[12]. Moreover, silencing of the ALF*Pm*6 gene revealed that it is essential for shrimp survival and plays protective roles in shrimp against *V. harveyi* and WSSV infections[13]. These findings suggest a potential role for ALF*Pm*6 in the shrimp immunity. However, no reports have characterized ALF*Pm*6. A previous study showed that the synthetic peptide of ALF LPS-BD could interact with LPS *in vitro*[31]. Additionally, the synthetic cycled loop peptide designed based on LPS-BD of *P. monodon*, *Scylla paramamosain*, and *Scylla serrata* showed inhibition effects on the growth of Gram-negative bacteria, such as *V. harveyi*, *Pseudomonas aeruginosa* and *E. coli*, and a Gram-positive bacterium, *M. luteus*[32–34]. In this research, the antimicrobial activity of the synthetic cyclic LPS-BD peptide,

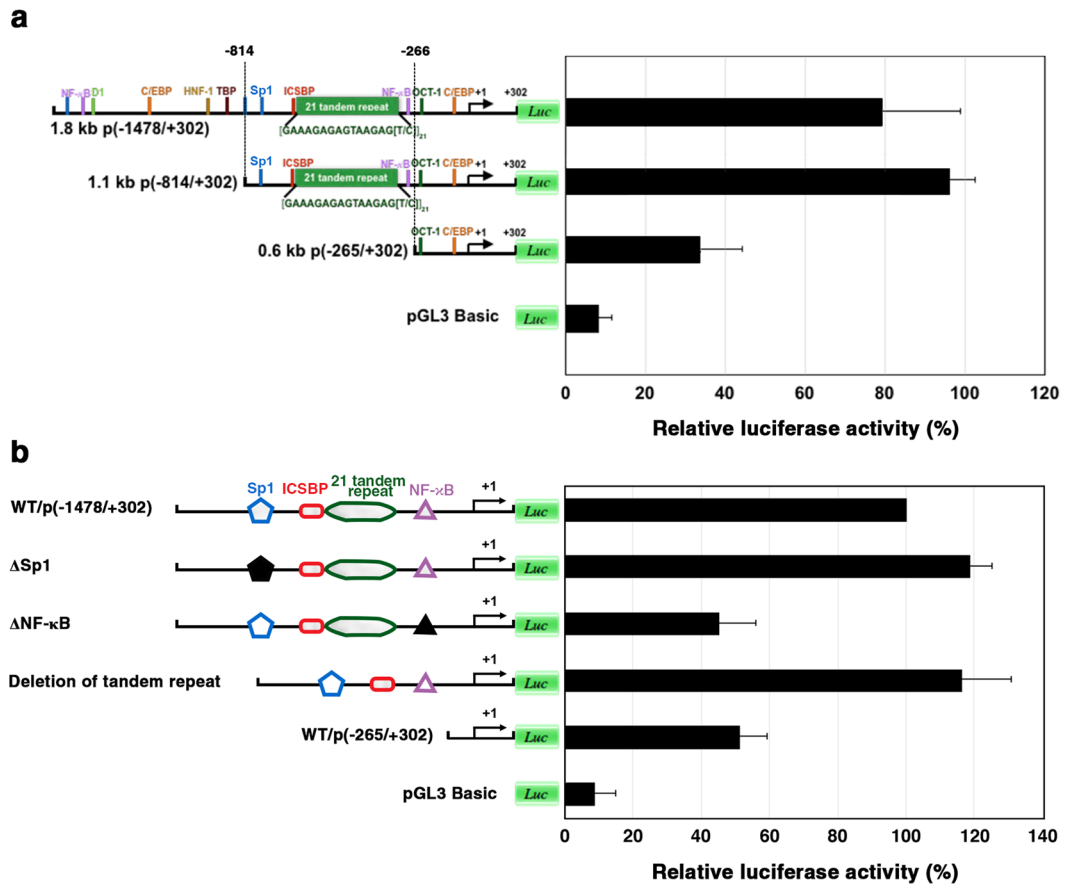


Figure 3. Functional analysis of the ALF*Pm*3 promoter through serial deletion and site-directed mutagenesis experiments. (**a**) Functional mapping of the ALF*Pm*3 promoter deletion. For promoter region −1478 to −265, the reporter vector containing ALF*Pm*3 promoter fragments of (−1478/+302), (−814/+302) and (−265/+302) was constructed. (**b**) Site-directed mutagenesis indicated by closed symbols of the transcription factor binding site Sp1 and NF-κB on the ALF*Pm*3 promoter active region (−814/−266) and deletion of the 21 units of [GAAAGAGAGTAAGAG(T/C)] tandem repeat at position −693 to −358 from the ALF*Pm*3 promoter region. Relative luciferase activity (%) of each construct is shown. Data represent the means ± standard deviations from three independent experiments. The error bars denote standard deviations.

cALFPm6#29–52, exhibited antimicrobial activity against a Gram-negative bacterium, *E. coli* 363 with MBC ranging from 25 to 50 μM and Gram-positive bacteria, including *B. megaterium*, *M. luteus* and *A. viridan*, with MBC ranging from 25 to 50 μM. The cALF*Pm*6#29–52, thus, showed less antimicrobial activity than the synthetic peptide of ALF*Pm*3#35–51, which could act against a broader range of Gram-negative and Gram-positive bacteria[6]. It is noteworthy that the amino acid composition and the total numbers of positively charged amino acid residues (Arg and Lys) of LPS-BD of ALF*Pm*3 and ALF*Pm*6 were different. The LPS-BD of ALF*Pm*3 had 4 Lys and 2 Arg, while ALF*Pm*6 contained 3 Arg and 2 Lys with a net charge of LPS-BD of 6 and 5, respectively. Although the pI values of ALF*Pm*3 (pI = 9.81) and ALF*Pm*6 (pI = 9.96) affect their antimicrobial activities, it could not be responsible for the different antimicrobial activities in each isoform.

Generally, AMPs exhibit antimicrobial activity via several mechanisms. ALF*Pm*3 exhibits the antibacterial activity by binding to bacterial cell wall components and permeabilizing the bacterial membrane to cause a loss of membrane integrity and cell lysis[8]. Several AMPs not only exhibit antibacterial activity but also the agglutination activity. Bacterial agglutination activity has been reported for rcrustin*Pm*1 and rcrustin*Pm*7, a family of antimicrobial peptides from *P. monodon*[35]. In the mud crab, *S. serrata*, haemocyanin can bind to bacterial cells and mediated agglutination through the recognition of bacterial OmpA and Ompx proteins[36]. rEs-DWD1 from the Chinese mitten crab (*Eriocheir sinensis*) causes significant aggregation of *B. subtilis* and *P. pastoris*[22]. The synthetic peptide, GL13NH2, derived from the parotid secretory protein, agglutinates both Gram-negative and Gram-positive bacteria, including the oral pathogen *Aggregatibacter actinomycetemcomitans* and the oral commensal *Streptococcus gordonii*, but it does not showed bactericidal activity. Increasing the calculated net charge of GL13NH2 peptide from +1 to +5 resulted in the loss ability of bacterial agglutination but a gain in bactericidal activity against against *Pseudomonas aeruginosa*, *S. gordonii* and *E. coli*[37]. In the case of cALF*Pm*6#29–52, it could agglutinate *E. coli* 363, *B. megaterium*, *M. luteus* and *A. viridian* and kill those bacteria. Taken together, we can conclude that different isoforms of ALFs have different abilities to kill bacteria via different mechanisms.

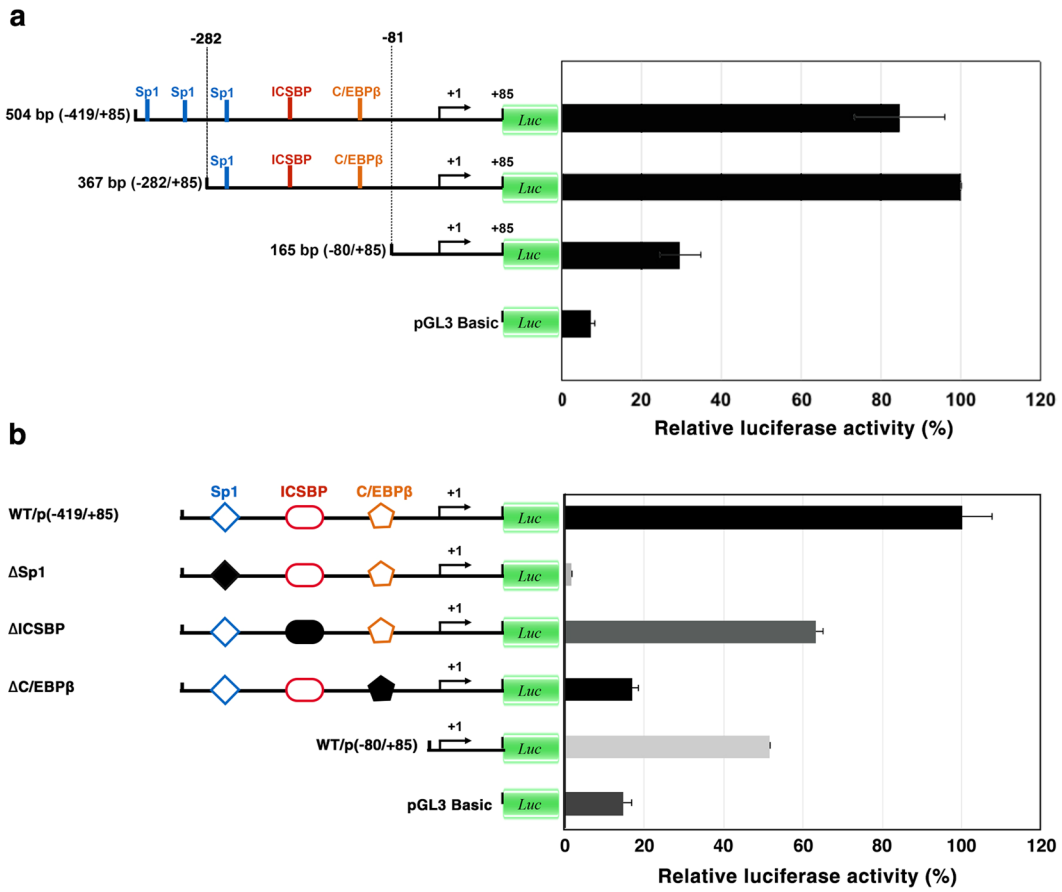


Figure 4. Functional analysis of the partial promoter of ALF*Pm*6 through serial deletion and site-directed mutagenesis experiments. (**a**) Functional mapping of the ALF*Pm*6 promoter sequence deletion from position −419 to −80. The reporter vector containing ALF*Pm*6 promoter fragments (−419/+85), (−282/+85) and (−80/+85) was constructed. (**b**) Site-directed mutagenesis indicated by closed symbols of transcription factor binding site Sp1, ICSBP and C/EBPβ on the ALF*Pm*6 promoter active region (−282/−81). Relative luciferase activity (%) of each construct is shown. Data represent the means ± standard deviations from three independent experiments. The error bars denote the standard deviations.

In addition to the difference in activity, previous studies have also shown that different ALF isoforms are expressed at different levels in response to microbial infection, which could be due to the disparity in gene regulation. Herein, the promoter regions of the ALF*Pm*3 and ALF*Pm*6 genes were characterized. Previously, approximately 600 bp of ALF*Pm*3 5′-upstream sequences from the transcription start site were obtained by the genome walking technique. The putative promoter of ALF*Pm*3 was identified at position −29 of the 5′-upstream sequences. Several transcription factor (TF)-binding sites, including octamer (OCT-1), GATA, CCAAT box and GAAA motifs, were predicted in the 5′-upstream sequences[38]. However, the promoter activity has not been tested. In ALF*Fc* from *F. chinensis*, immune-related TF-binding sites such as one AP4, one NF-κB, one Sp-1, two GAAA, three OCT-1, and three GATA, were identified in the region from −702 to +1. Analysis of the ALF*Fc* promoter activity in insect Sf9 cell lines showed that the putative promoter region from −702 to +33 was induced by lipopolysaccharide or (1,3)-β-D-glucan, but the shorter promoter sequence pALF-318 (from −318 to +33) could only be induced only by (1,3)-β-D-glucan[39]. However, the important TFs controlling ALFs transcription remain uncharacterized.

In this study, the promoter active regions with designated the regulatory regions involved in regulating ALF*Pm*3 and ALF*Pm*6 gene expression were identified using the narrow down technique. From our analysis, we concluded that the ALF*Pm*3 promoter region at the position (−814/−266) contained the activator-binding site. The genomic DNA sequence of the ALF*Pm*3 promoter at position −814 to −266 contained many TF-binding sites such as Sp1, ICSBP, and NF-κB. Tandem repeats of DNA are prevalent and hypervariable in higher eukaryotic genomes. TR's of DNA represent a section of the genome that may be highly evolvable, as repeat numbers can change with frequencies 100–10000 higher than point mutations[40]. The numbers of tandem repeats present in coding regions, promoters, and introns have demonstrated functional roles in modulating protein activity and gene expression and a correlation with disease[41–43]. However, the functional role of intergenic tandem repeats that are found far away from coding regions is unclear. A deletion assay for 21 units of GAAAGAGAGTAAGAG[T/C] tandem repeats and ICSBP suggested that this tandem repeat and ICSBP were not involved in ALF*Pm*3 gene

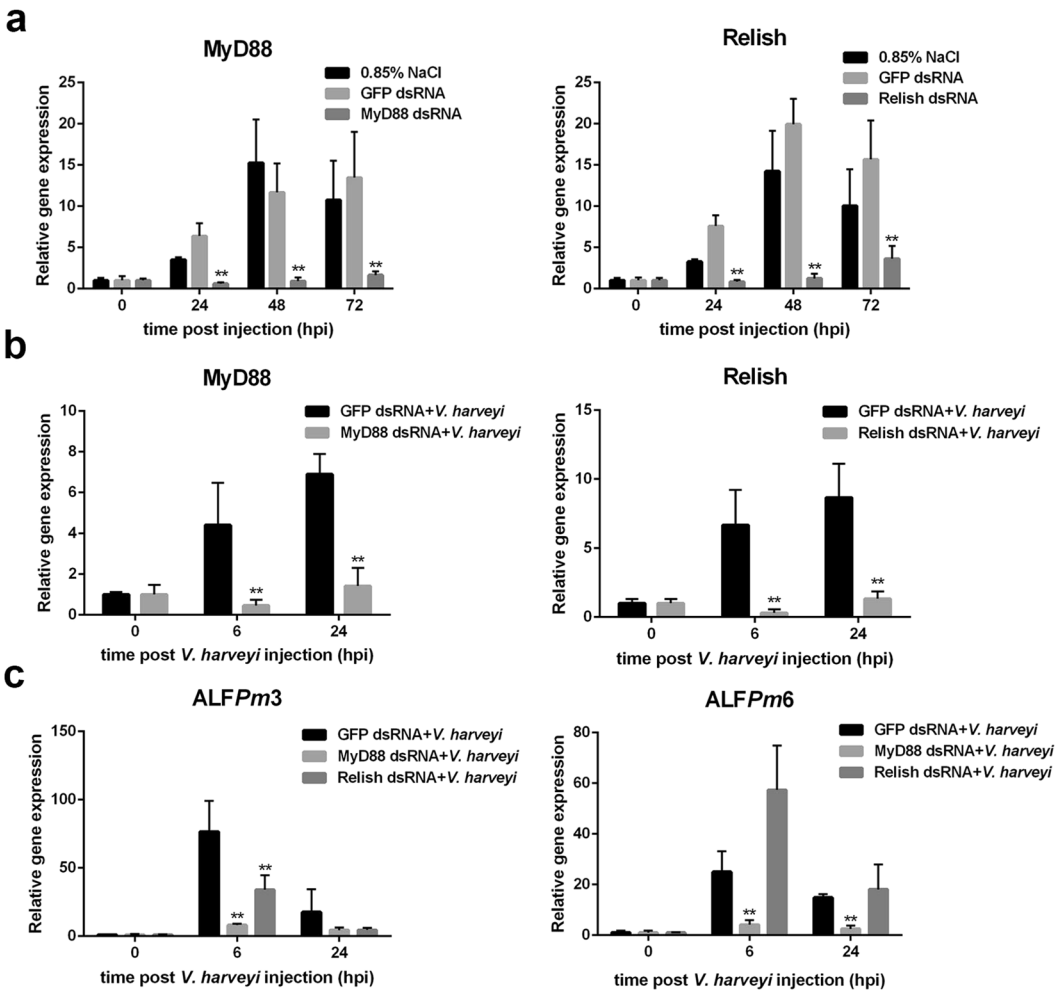


Figure 5. The effect of MyD88 and Relish gene knockdown on ALF*Pm*3 and ALF*Pm*6 transcripts levels upon *V. harveyi* infection. (**a**) Efficiency of MyD88 and Relish gene silencing mediated by dsRNA in shrimp. Control groups were injected with 0.85% NaCl or GFP dsRNA. The experimental groups were shrimp injected with 10 μg/g shrimp MyD88 dsRNA and Relish dsRNA. At 0, 24, 48 and 72 h post-dsRNA injection, haemolymph was collected from 36 individual shrimp and randomly divided into 3 pools (n = 3 in each pool). The transcription levels of MyD88 or Relish were analysed using qRT-PCR. Elongation factor-1α (EF1α) was used as an internal control. (**b**) MyD88 and Relish gene silencing in *V. harveyi*-infected shrimps. The transcriptional level of MyD88 and Relish genes in the haemolymph of MyD88 dsRNA and Relish dsRNA-challenged shrimp, respectively, at 0, 6 and 24 h post-*V. harveyi* infection was determined. The control was shrimp injected with GFP dsRNA. EF1α was used as the internal control gene. (**c**) Silencing of the MyD88 and Relish genes affected the expression of the ALF*Pm*3 and ALF*Pm*6 genes. The expression of the ALF*Pm*3 and ALF*Pm*6 genes in the MyD88 and Relish gene-silenced shrimp upon *V. harveyi* challenge was determined by qRT-PCR. The control was shrimp injected with GFP dsRNA. The ALF*Pm*3 and ALF*Pm*6 gene expression levels were normalized to EF1α. The expression of the ALF*Pm*3 and ALF*Pm*6 genes in the *V. harveyi*-infected group at 6 and 24 hpi was normalized to that of the control group at 0 hpi. The graph shows the means ± standard deviations of 3 independent sets, $^{**}P < 0.01$.

regulation. In contrast, Sp1 and NF-κB might be repressor- and activator-binding sites, respectively, on the ALF*Pm*3 promoter. Rel/NF-κB family genes play a central role in the transcription of innate immune effectors[44]. The NF-κB binding sites were found in different antimicrobial peptide (AMP) genes, including penaeidin, crustin and ALF*Pm*2[38,45,46]. In this study, the NF-κB binding sites of ALF*Pm*3 were also found at nucleotide position −280 to −270 from the transcription start sites. The NF-κB family genes, Relish and Dorsal, could regulate the transcription of shrimp AMP genes such as Pen4, Pen5, crustin, and ALF[20,23,27]. The transcription of other antimicrobial peptides in shrimp including crustin and ALF, was also regulated by Relish[47]. In this study, using site-directed mutagenesis, the NF-κB binding site at position (−280/−270) was identified as the activator-binding site that regulated the ALF*Pm*3 gene regulation.

Compared to the ALF*Pm*3 promoter, the ALF*Pm*6 promoter fragment obtained is relatively short and could probably only part of its regulatory region, although the important regulatory elements could be identified. After deletion of the promoter region at position (−282/−81), the promoter activity was decreased. Based on this result,

we concluded that the ALF*Pm*6 promoter region at the position (−282/−81) contained the activator-binding site. The predicted transcription factor-binding sites identified here were Sp1, C/EBPβ and ICSBP, which were shown to be involved in the positive regulation of ALF*Pm*6 gene by site-directed mutagenesis. Previously, the C/EBPβ binding site was identified as one member of the transcription factor binding motif of the crustin*Pm*7 gene[45]. C/EBPβ is a member of a family of transcription factors involved in important physiological processes, such as cellular proliferation and differentiation, regulation of energy homeostasis, inflammation, and haematopoiesis. Previously, LPS-induced C/EBPβ was shown to specifically bind to the C/EBP response element in the SerpinB2 proximal promoter in mice, and loss of C/EBPβ abrogates constitutive SerpinB2 gene transcription and the response to LPS[48]. C/EBPβ has been reported to physically interact with AP-1 and NF-κB to promote gene expression of inflammatory mediators[49]. Sp1 is a ubiquitous nuclear factor that plays a key role in maintaining the basal transcription of house-keeping genes[50]. According to previous reports, Sp1 and NF-κB are key transcription factors in the regulation of CD40 gene. Sp1 is a key transcription factor controlling the basal expression of CD40. In LPS-stimulated cells, the transcription factor NF-κB up-regulates CD40 expression. In contrast, Sp1 is phosphorylated and its DNA binding activity is reduced after LPS stimulation[51]. Therefore, it can be hypothesized that Sp1 is also involved in ALF*Pm*3 and ALF*Pm*6 gene regulation. However, further investigations are needed. In summary, our studies showed that NF-κB at nucleotide position (−280/−270), C/EBPβ at nucleotide position (−88/−80) and Sp1 at nucleotide position (−249/−238) in the ALF*Pm*3 and ALF*Pm*6 promoter active region, respectively, are necessary for positive regulation.

Toll and IMD pathways are the important NF-κB signalling pathways controlling the expression of antimicrobial peptide genes[14–16]. Previously, the expression profiles of Toll and IMD in bacterial-challenged shrimp were detected and found to be up-regulated at an early stage in haemocytes and hepatopancreas after challenge with *M. lysodeikticu* and *V. anguillarum*. Furthermore, ALF expression was significantly increased in response to *V. anguillarum* and *M. lysodeikticu* challenge[52]. In this study, silencing of the adaptor protein, MyD88, and the transcription factor, Relish, which are key molecules in the Toll and IMD pathways, respectively, was performed to investigate the pathway responsible for controlling the gene expression of each ALF. Instead of down-regulation of the ALF*Pm*6 gene, up-regulation of the ALF*Pm*6 gene was observed at 6 and 24 hpi in Relish knockdown shrimp. These findings suggested that the IMD pathway was not involved in the regulation of ALF*Pm*6 gene expression. However, the positive effect of Relish knockdown on ALF*Pm*6 gene expression remains unclear and necessitates further investigation. It is noteworthy that the transcription levels of ALF*Pm*3 in MyD88- and Relish-silenced shrimp were down-regulated at 6 h post-*V. harveyi* infection. Therefore, ALF*Pm*3 gene expression was probably regulated by both Toll and IMD pathways. A recent study showed that the expression of ALF*Pm*3 was not regulated by *Pm*Relish upon yellow-head virus (YHV) infection. In *V. harveyi*-infected shrimp, it has been reported that the expression of ALF*Pm*3 relies not only on the *Pm*Relish-mediated pathway but also on another un-identified signalling pathway[53].

According to previous reports, some antimicrobial peptides can be activated by both Toll and IMD pathways, such as Defensin and Metchnikowin in Drosophilla[15,44], In *P. vannamei*, RNAi-mediated knockdown of Akirin significantly reduced the expression of NF-κB dependent *Lv*ALF-AA-K, *Lv*crustin-P and *Lv*Pen3 and the transcription factors, Dorsal and Relish post-*V. anguillarum* and *M. lysodeikticu* challenge. These findings suggested that ALF, crustin, and Pen3 might be regulated by both Toll and IMD pathways[54]. Our result together with others implied that Toll and IMD pathways could interact synergistically to induce the independent activation of overlapping target genes. For instance, some target promoters might contain TF-binding sites for both Dif and Relish. Therefore, both pathways could activate them independently, and the response depends on the affinity and number of NF-κB sites[55]. Cooperation regulation is sometime mediated through an interaction of the NF-κB-related transcription factors in the two pathways. As stated previously, ALF*Pm*3 was the most responsive ALF*Pm* isoform during pathogen infections[13]. Our results supported this finding based on the observation that Toll and IMD pathways caused independent activation of ALF*Pm*3 genes and, in turn, enhanced ALF*Pm*3 gene expression.

Overall, in this study, we demonstrated the difference in gene regulation of ALF*Pm* against bacterial infection. ALF*Pm*3 gene expression was regulated by Toll and IMD pathways upon bacterial infection. Promoter analysis implied that ALF*Pm*3 transcription is positively modulated by the Rel/NF-κB transcription factor. Furthermore, ALF*Pm*6 mRNA expression was regulated by the Toll pathway during bacterial challenge. C/EBPβ and Sp1 transcription factors may be the activator that controlling the expression of ALF*Pm*6 (Fig. 6).

Materials and Methods

Peptide synthesis. The amino acid sequences (YCSFNVTPKFKRWQLYFRGRMWCP) corresponding to the cyclic LPS-BD of ALF*Pm*6 (accession number: AER45468) with a flanking amino acid residue at both the N and C terminal ends, in which a disulphide bond was formed between two cysteine residues, was designed and synthesized service by BIO BASIC INC., Canada. The lyophilized cALF*Pm*6#29–52 was resuspended in ultrapure-water and an aliquot was kept at −20 °C until used.

Antimicrobial assay. The bacterial strains including the Gram-negative bacteria *E. coli* 363, *K. pneumoniae*, *E. cloacae*, *V. harveyi*, non-virulent *V. parahaemolyticus*, *V. parahaemolyticus* (AHPND) and *E. carotovora*, and the Gram-positive bacteria *B. megaterium*, *A. viridans*, *M. luteus*, *S. haemolyticus* and *S. aureus*, were used for the antibacterial activity assay.

The liquid growth inhibition assay was performed as previously described[24] to test the antibacterial activity of cALF*Pm*6#29–52 peptide. Briefly, various concentrations of cALF*Pm*6#29–52 peptide (25 μM to 100 μM final concentration) were mixed with the mid-logarithmic growth phase of the bacterial culture in a 96-well plate. Bacteria were grown overnight under vigorous shaking at 30 °C or 37 °C according to the strains. By observation, a bacterial-peptide mixture with high turbidity is considered a the negative result. Only positive results with clear solution as a control were subjected for confirmation of the bacterial killing activity of cALF*Pm*6#29–52

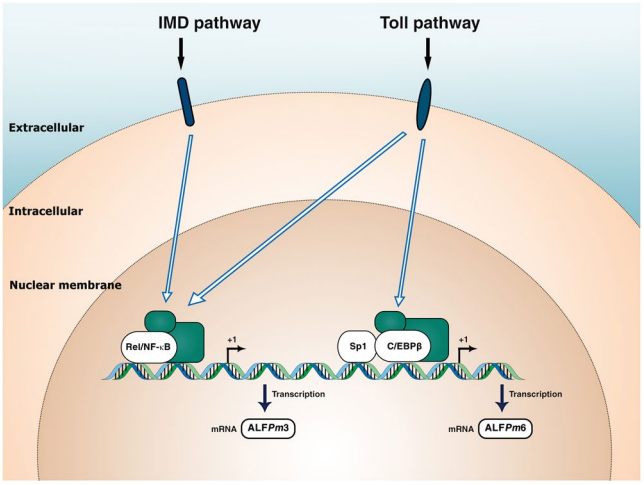


Figure 6. A schematic model of the signalling pathway involved in ALF*Pm*3 and ALF*Pm*6 transcriptional regulation.

peptide. A 20 μl-aliquot of the bacterial culture incubated with the synthetic cALF*Pm*6#29–52 peptide was plated on an LB agar plate and incubated at 30 °C for 16 h. As a positive control, sterile water was used instead of the tested peptide. The number of bacterial colonies that grew on the LB agar plate was determined. The minimum bactericidal concentrations (MBCs) of the synthetic cALF*Pm*6#29–52 peptide was defined as the range between the highest concentration of the peptide where bacterial growth was observed and the lowest concentration of the peptide that killed the bacteria. To further investigate how the peptide inhibited the growth of bacteria, one drop of the above peptide-bacteria mixture was placed on a microscope slide with the bacterial sample and then Gram-stained and observed under a 100X magnification light microscope (Olympus CX31). Images were obtained using a microscope camera (Nikon DS-Fi1).

Determination of the 5′-upstream sequences of the ALF*Pm*3 and ALF*Pm*6 genes. The 5′-upstream sequences of ALF*Pm*3 and ALF*Pm*6 genes were determined using the BD GenomeWalker Universal Kit (Clontech Laboratories, Inc., USA). The restriction enzyme-digested *P. monodon* genomic DNA libraries (E*co*RV, *Dra*I, *Pvu*II and *Stu*I) were used as template. The primary PCR using the outer adaptor primer (AP1) and the first gene-specific primer (GSP1) was amplified. The secondary PCR was performed with the nested adaptor primer (AP2) and a nested gene-specific primer (GSP2). The GSP1 and GSP2 primers designed from the known genomic sequence of ALF*Pm*3 (accession no. EF523562) and ALF*Pm*6 (accession no. JN562340) are shown in Supplementary Table S1. The nested PCR products were cloned into the pGEM-T easy vector (Promega, USA) and analysed by a DNA sequencing service (Macrogen Inc., Korea). The putative start sites and TATA box were predicted using the Promoter 2.0 Prediction Server (www.cbs.dtu.dk) and BDGP (Neural Network Promoter Prediction) (www.fruitfly.org). The putative cis-regulatory elements in the 5′-upstream sequences were predicted by TF search Version 1.3, Match 1.0 and the Alibaba 2 analysis programme (TRANSFAC® Public database) (www.gene-regulation.com). The results were compared with the JASPAR database (jasper.genereg.net) to confirm the putative transcription factor binding sites.

Construction of ALF*Pm* promoter reporter plasmids. To construct the luciferase reporter plasmid harbouring various fragments of promoter sequences, the ALF*Pm*3 and ALF*Pm*6 promoters were randomly narrowed down. ALF*Pm*3 promoter fragments included the nucleotide positions of (−1478/+324), (−814/+324), (−719/+324), (−265/+324), and (−71/+324). For the ALF*Pm*6 promoter, various fragments at nucleotide positions (−419/+85), (−282/+85), (−162/+85), and (−80/+85) were constructed. Primer sequences containing the restriction sites *Nhe*I and *Bgl*II used for promoter fragment amplification are shown in Supplementary Table S1. The PCR cycle was initiated by denaturation at 95 °C for 1 min followed by 35 cycles of 95 °C for 30 sec, 60 °C for 30 sec, and 68 °C for 30 sec, and a final extension at 68 °C for 10 min. The products were purified using Nucleospin® Extract II kit (Macherey-Nagel) and cloned into the pGL3-basic vector (Promega). All recombinant plasmid constructs were purified and sequenced (Macrogen Inc., Korea).

Promoter activity assay. *Drosophila Schneider* 2 (S2) cells were seeded in a 24-well plate and cultured in complete Schneider's Drosophila Medium containing 10% heat-inactivated FBS and antibiotics (50 units penicillin G and 50 μg/ml streptomycin sulphate, Invitrogen) at 27 °C for overnight. The 200 ng of pGL3-Basic (control plasmid) or pGL3 plasmid containing either ALF*Pm*3 or ALF*Pm*6 promoter fragments were co-transfected with 50 ng of the pRL-TK plasmid containing the Renilla luciferase gene into the S2 cells using Effectene® transfection reagent (Qiagen) according to manufacturer's protocol. Cell lysates were collected at 48 h after transfection. Firefly luciferase and Renilla luciferase activities were assayed using the Dual-Luciferase® Reporter Assay System (Promega). Luminescence was detected using a SpectraMax M5 Multi-Mode Microplate Reader (Molecular device). The relative light unit (RLU) was calculated by normalizing the firefly luciferase activity to the Renilla luciferase activity to correct the transfection efficiency. The data were reported as the relative luciferase activity. Independent triplicate experiments were performed for each construct, and the standard deviation was calculated.

Promoter deletion assay and site-directed mutagenesis. The obtained promoter active region was further analysed for the specific transcription factor binding site involved in ALF*Pm* gene regulation. To determine whether the 21 units of GAAAGAGAGTAAGAG[T/C] tandem repeat was involved in regulating ALF*Pm*3 gene expression, the tandem repeat deletion construct, del(−693/−358)/p(−1478/+302), was prepared by rolling PCR using p(−1478/+324) as a template and the primer pair del(−693/−358)/p(−1478/+324)F and del(−693/−358)/p(−1478/+324)R (Table S1). The PCR condition were 94 °C for 2 min, followed by 35 cycles of 98 °C for 10 s, 60 °C for 30 s, and 68 °C for 7 min, using KOD Taq polymerase (TOYOBO). A site-directed mutagenesis technique was performed to identify the putative binding site for the transcription factor that regulates ALF*Pm* genes. For ALF*Pm*3, the promoter transcription factor binding sites of Sp1 (−719/−701) and NF-κB (−280/−270) were mutated using p(−1478/+324) as a template. For the ALF*Pm*6 promoter region, mutation of the transcription factor binding sites of Sp1 (−249/−238), ICSBP (−147/−136) and C/EBPβ (−78/−88) were performed using p(−419/+85) as a template. The mutated constructs of these transcription factor-binding sites were prepared by rolling PCR. The conserved nucleotides of the interested TF-binding site were identified by JASPAR (an open-access database for eukaryotic TF-binding profiles) and their specific primers with mutated nucleotides were designed (Supplementary Table S1). The PCR conditions were 94 °C for 2 min, followed by 35 cycles of 98 °C for 10 s, 60 °C for 30 s, and 68 °C for 7 min, using KOD Taq polymerase (TOYOBO). For each construct, the PCR product was ligated and transformed into *E. coli* strain XL-1 blue by electroporation. The recominant plasmids were extracted using the High-speed plasmid mini kit (Geneaid). The mutated-transcription factor-binding sites were confirmed by DNA sequencing (Macrogen Inc., Korea). The promoter activity of the mutant was measured and compared with wild type using the Dual-Luciferase® Reporter Assay (Promega).

Silencing efficiency of MyD88 dsRNA and Relish dsRNA. The dsRNA specific to MyD88, Relish and GFP were prepared according the T7 RiboMAX™ Express RNAi System (Promega) kit's instructions. DNA template containing the T7 promoter sequence at the 5′-end was generated by PCR using the specific primer, T7-MyD88-F, MyD88-R, MyD88-F, T7-MyD88-R, T7-Relish-F, Relish-R, Relish-F, T7-Relish-R, and T7-GFP-F, GFP-R, GFP-F, T7-GFP-R (Supplementary Table S1) to produce sense and antisense RNA strands separately. The single-stranded RNA was annealed to generate dsRNA. After purification, the dsRNA was quantified and stored at −80 °C until use.

For the dsRNA-mediated gene silencing experiments, 144 shrimps were randomly divided into four groups (n = 36 in each group). The experimental group (3–5 g shrimp) was treated with MyD88 dsRNA or Relish dsRNA (10 μg/g shrimp), while the control groups were injected with GFP dsRNA and 0.85% NaCl, respectively. To test the silencing efficiency, the haemolymph of 9 individuals from each treatment was collected at 0, 24, 48, and 72 h post-dsRNA injection (hpi), and total RNA was extracted. Three sets of pooled samples were prepared, each comprising 3 different individuals. The first-strand cDNA was synthesized from 1 μg of total RNA using the RevertAidTM First Strand cDNA Synthesis Kit (Thermo Scientific). Either MyD88 or Relish gene expression was analysed by quantitative real-time RT-PCR using the gene-specific primer pair, PmMyD88-RT_F, PmMyD88-RT_R, PmRelish-RT_F and PmRelish-RT_F, respectively (Supplementary Table S1). The elongation factor-1α (EF1α) gene was used as an internal control. The relative expression of MyD88 and Relish was calculated using a comparative method described by Pfaffl[56]. The data are shown as the means ± standard deviations. Statistical analysis was performed using the one-way ANOVA followed by Duncan's new multiple range test. Data differences were considered statistically significant at $P < 0.01$.

MyD88 dsRNA and Relish dsRNA-mediated gene knockdown in *V. harveyi*-infected shrimp. To investigate the effect of MyD88 and Relish gene knockdown on the ALF*Pm*3 and ALF*Pm*6 transcript levels upon *V. harveyi* infection, shrimp were injected with 10 μg/g shrimp of the MyD88 dsRNA, Relish dsRNA or GFP dsRNA. After the first dsRNA injection for 12 h, shrimp were challenged with 10^6 CFU/ml of *V. harveyi* mixed with 10 μg/g shrimp dsRNA. At 0, 6 and 24 h post-*V. harveyi* infection, shrimp haemolymph was collected and used for total RNA extraction and cDNA synthesis. Transcript levels of ALF*Pm*3 and ALF*Pm*6 genes in each sample were analysed by quantitative real-time RT-PCR using the specific primers, qRT-ALFPm3_F/R, qRT-ALFPm6_F/R, respectively. The relative expression of ALF*Pm*3 and ALF*Pm*6 was calculated using a comparative method described by Pfaffl[56]. The data are shown as the means ± standard deviations. The statistical analysis was performed using the one-way ANOVA followed by Duncan's new multiple range test. Data differences were considered statistically significant at $P < 0.01$.

References

1. Flegel, T. Update on viral accommodation, a model for host-viral interaction in shrimp and other arthropods. *Dev. Comp. Immunol.* **31**, 217–231 (2007).
2. Lightner, D. *et al*. Historic emergence, impact and current status of shrimp pathogens in the Americas. *J. Invertebr. Pathol.* **110**, 174–183 (2012).
3. Saulnier, D. *et al*. Rapid and sensitive PCR detection of *Vibrio penaeicida*, the putative etiological agent of syndrome 93 in New Caledonia. *Dis. Aquat. Organ.* **49**, 109–115 (2000).
4. Tran, L. *et al*. Determination of the infectious nature of the agent of acute hepatopancreatic necrosis syndrome affecting penaeid shrimp. *Dis. Aquat. Organ.* **105**, 45–55 (2013).
5. Tassanakajon, A., Amparyup, P., Somboonwiwat, K. & Supungul, P. Cationic antimicrobial peptides in penaeid shrimp. *Mar. Biotechnol.* **12**, 487–505 (2010).
6. Somboonwiwat, K. *et al*. Recombinant expression and anti-microbial activity of anti-lipopolysaccharide factor (ALF) from the black tiger shrimp *Penaeus monodon*. *Dev. Comp. Immunol.* **29**, 841–851 (2005).
7. Supungul, P. *et al*. A potential application of shrimp antilipopolysaccharide factor in disease control in aquaculture. *Aquac. Res.* **48,** 809–821 (2017).

8. Jaree, P., Tassanakajon, A. & Somboonwiwat, K. Effect of the anti-lipopolysaccharide factor isoform 3 (ALF*Pm*3) from *Penaeus monodon* on *Vibrio harveyi* cells. *Dev. Comp. Immunol.* **38**, 554–560 (2012).
9. Tharntada, S. *et al*. Role of anti-lipopolysaccharide factor from the black tiger shrimp, *Penaeus monodon*, in protection from white spot syndrome virus infection. *J. Gen. Virol.* **90**, 1491–1498 (2009).
10. Methatham, T., Boonchuen, P., Jaree, P., Tassanakajon, A. & Somboonwiwat, K. Antiviral action of the antimicrobial peptide ALF*Pm*3 from *Penaeus monodon* against white spot syndrome virus. *Dev. Comp. Immunol.* **69**, 23–32 (2017).
11. Suraprasit, S. *et al*. Anti-lipopolysaccharide factor isoform 3 from *Penaeus monodon* (ALF*Pm*3) exhibits antiviral activity by interacting with WSSV structural proteins. *Antiviral Res.* **110**, 142–150 (2014).
12. Prapavorarat, A., Pongsomboon, S. & Tassanakajon, A. Identification of genes expressed in response to yellow head virus infection in the black tiger shrimp, *Penaeus monodon*, by suppression subtractive hybridization. *Dev. Comp. Immunol.* **34**, 611–617 (2010).
13. Ponprateep, S., Tharntada, S., Somboonwiwat, K. & Tassanakajon, A. Gene silencing reveals a crucial role for anti-lipopolysaccharide factors from *Penaeus monodon* in the protection against microbial infections. *Fish Shellfish Immunol.* **32**, 26–34 (2012).
14. Leclerc, V. & Reichhart, J.-M. The immune response of *Drosophila melanogaster*. *Immunol. Rev.* **198**, 59–71 (2004).
15. Lemaitre, B. & Hoffmann, J. The host defense of *Drosophila melanogaster*. *Annu. Rev. Immunol.* **25**, 697–743 (2007).
16. Tanji, T. & Ip, Y. T. Regulators of the Toll and Imd pathways in the *Drosophila* innate immune response. *Trends Immunol.* **26**, 193–198 (2005).
17. Lemaitre, B., Nicolas, E., Michaut, L., Reichhart, J.-M. & Hoffmann, J. A. The dorsoventral regulatory gene cassette *spätzle/Toll/cactus* controls the potent antifungal response in Drosophila adults. *Cell.* **86**, 973–983 (1996).
18. Rutschmann, S. *et al*. Role of Drosophila IKKγ in a Toll-independent antibacterial immune response. *Nat. Immunol.* **1**, 342–347 (2000).
19. Xi, Z., Ramirez, J. L. & Dimopoulos, G. The *Aedes aegypti* Toll pathway controls dengue virus infection. *PLoS Pathog.* **4**, e1000098 (2008).
20. Wang, P.-H. *et al*. Molecular cloning, characterization and expression analysis of two novel Tolls (Lv'Toll2 and *Lv*Toll3) and three putative Spätzle-like toll ligands (LVSpz1–3) from *Litopenaeus vannamei*. *Dev. Comp. Immunol.* **36**, 359–371 (2012).
21. Shi, X.-Z. *et al*. Identification and molecular characterization of a Spätzle-like protein from Chinese shrimp (*Fenneropenaeus chinensis*). *Fish Shellfish Immunol.* **27**, 610–617 (2009).
22. Wen, R., Li, F., Sun, Z., Li, S., & Xiang, J. Shrimp MyD88 responsive to bacteria and white spot syndrome virus. *Fish Shellfish Immunol.* **34,** 574–581 (2013).
23. Huang, X.-D. *et al*. Identification and functional study of a shrimp Dorsal homologue. *Dev. Comp. Immunol.* **34**, 107–113 (2010).
24. Wang, P.-H. *et al*. An immune deficiency homolog from the white shrimp, *Litopenaeus vannamei*, activates antimicrobial peptide genes. *Mol. Immunol.* **46**, 1897–1904 (2009).
25. Hou, F. *et al*. RNAi knock-down of shrimp *Litopenaeus vannamei* Toll gene and immune deficiency gene reveals their difference in regulating antimicrobial peptides transcription. *Dev. Comp. Immunol.* **44**, 255–260 (2014).
26. Lan, J.-F. *et al*. Characterization of an immune deficiency homolog (IMD) in shrimp (*Fenneropenaeus chinensis*) and crayfish (*Procambarus clarkii*). *Dev. Comp. Immunol.* **41**, 608–617 (2013).
27. Li, F. *et al*. Identification of a novel relish homolog in chinese shrimp *Fenneropenaeus chinensis* and its function in regulating the transcription of antimicrobial peptides. *Dev. Comp. Immunol.* **33**, 1093–1101 (2009).
28. Visetnan, S., Supungul, P., Hirono, I., Tassanakajon, A. & Rimphanitchayakit, V. Activation of *Pm*Relish from *Penaeus monodon* by yellow head virus. *Fish Shellfish Immunol.* **42**, 335–344 (2015).
29. Tassanakajon, A., Somboonwiwat, K. & Amparyup, P. Sequence diversity and evolution of antimicrobial peptides in invertebrates. *Dev. Comp. Immunol.* **48**, 324–341 (2015).
30. Tassanakajon, A. *et al*. *Penaeus monodon* gene discovery project: the generation of an est collection and establishment of a database. *Gene.* **384**, 104–112 (2006).
31. Nagoshi, H. *et al*. Cloning and characterization of a LPS-regulatory gene having an LPS binding domain in kuruma prawn *Marsupenaeus japonicus*. *Mol. Immunol.* **43**, 2061–2069 (2006).
32. Imjongjirak, C., Amparyup, P., Tassanakajon, A. & Sittipraneed, S. Antilipopolysaccharide factor (ALF) of mud crab *Scylla paramamosain*: molecular cloning, genomic organization and the antimicrobial activity of its synthetic LPS binding domain. *Mol. Immunol.* **44**, 3195–3203 (2007).
33. Pan, C.-Y. *et al*. Shrimp (*Penaeus monodon*) anti-lipopolysaccharide factor reduces the lethality of *Pseudomonas aeruginosa* sepsis in mice. *Int. Immunopharmacol.* **7**, 687–700 (2007).
34. Sharma, S., Yedery, R., Patgaonkar, M., Selvaakumar, C. & Reddy, K. Antibacterial activity of a synthetic peptide that mimics the LPS binding domain of indian mud crab, *Scylla serrata* anti-lipopolysaccharide factor (*Ss*alf) also involved in the modulation of vaginal immune functions through NF-κB signaling. *Microb. Pathog.* **50**, 179–191 (2011).
35. Krusong, K., Poolpipat, P., Supungul, P. & Tassanakajon, A. A comparative study of antimicrobial properties of crustin*Pm*1 and crustin*Pm*7 from the black tiger shrimp *Penaeus monodon*. *Dev. Comp. Immunol.* **36**, 208–215 (2012).
36. Yan, F. *et al*. Identification and agglutination properties of hemocyanin from the mud crab (*Scylla serrata*). *Fish Shellfish Immunol.* **91**, 207–220 (2011).
37. Abdolhosseini, M., Nandula, S. R., Song, J., Hirt, H. & Gorr, S.-U. Lysine substitutions convert a bacterial-agglutinating peptide into a bactericidal peptide that retains anti-lipopolysaccharide activity and low hemolytic activity. *Peptides.* **35**, 231–238 (2012).
38. Tharntada, S., Somboonwiwat, K., Rimphanitchayakit, V. & Tassanakajon, A. Anti-lipopolysaccharide factors from the black tiger shrimp, *Penaeus monodon*, are encoded by two genomic loci. *Fish Shellfish immunol.* **24**, 46–54 (2008).
39. Tang, T. *et al*. Functional analysis of *Fenneropenaeus chinensis* anti-lipopolysaccharide factor promoter regulated by lipopolysaccharide and (1,3)-β-D-glucan. *Fish Shellfish Immunol.* **38**, 348–353 (2014).
40. Lynch, M. *et al*. A genome-wide view of the spectrum of spontaneous mutations in yeast. *Proc. Natl. Acad. Sci. USA* **105**, 9272–9277 (2008).
41. Hannan, A. J. Tandem repeat polymorphisms: modulators of disease susceptibility and candidates for 'missing heritability'. *Trends Genet.* **26**, 59–65 (2010).
42. Verstrepen, K. J., Jansen, A., Lewitter, F. & Fink, G. R. Intragenic tandem repeats generate functional variability. *Nat. Genet.* **37**, 986–990 (2005).
43. Vinces, M. D., Legendre, M., Caldara, M., Hagihara, M. & Verstrepen, K. J. Unstable tandem repeats in promoters confer transcriptional evolvability. *Science.* **324**, 1213–1216 (2009).
44. Hoffmann, A., Levchenko, A., Scott, M. L. & Baltimore, D. The iκB-NF-κ*B* signaling module: temporal control and selective gene activation. *Science.* **298**, 1241–1245 (2002).
45. Amparyup, P., Kondo, H., Hirono, I., Aoki, T. & Tassanakajon, A. Molecular cloning, genomic organization and recombinant expression of a crustin-like antimicrobial peptide from black tiger shrimp *Penaeus monodon*. *Mol. Immunol.* **45**, 1085–1093 (2008).
46. O'Leary, N. A. & Gross, P. S. Genomic structure and transcriptional regulation of the penaeidin gene family from *Litopenaeus vannamei*. *Gene.* **371**, 75–83 (2006).
47. Wang, D., Li, S. & Li, F. Screening of genes regulated by relish in chinese shrimp *Fenneropenaeus chinensis*. *Dev. Comp. Immunol.* **41**, 209–216 (2013).
48. Udofa, E. A. *et al*. The transcription factor C/EBP-β mediates constitutive and LPS-inducible transcription of murine SerpinB2. *PloS one.* **8**, e57855 (2013).

49. Tsukada, J., Yoshida, Y., Kominato, Y. & Auron, P. E. The ccaat/enhancer (C/EBP) family of basic-leucine zipper (bZIP) transcription factors is a multifaceted highly-regulated system for gene regulation. *Cytokine.* **54**, 6–19 (2011).
50. Samson, S. & Wong, N. Role of Sp1 in insulin regulation of gene expression. *J. Mol, Endocrinol.* **29**, 265–279 (2002).
51. Tone, M., Tone, Y., Babik, J. M., Lin, C.-Y. & Waldmann, H. The role of Sp1 and NF-κB in regulating CD40 gene expression. *J. Biol. Chem.* **277**, 8890–8897 (2002).
52. Liu, Y. *et al.* Comparison of immune response in Pacific white shrimp, *Litopenaeus vannamei*, after knock down of Toll and IMD gene *in vivo*. *Dev. Comp. Immunol.* **60**, 41–52 (2016).
53. Visetnan, S. *et al.* YHV-responsive gene expression under the influence of *Pm*Relish regulation. *Fish Shellfish immunol.* **47**, 572–581 (2015).
54. Hou, F. *et al.* Identification and functional studies of Akirin, a potential positive nuclear factor of NF-κB signaling pathways in the Pacific white shrimp, *Litopenaeus vannamei*. *Dev. Comp. Immunol.* **41**, 703–714 (2013).
55. Tanji, T., Hu, X., Weber, A. N. & Ip, Y. T. Toll and IMD pathways synergistically activate an innate immune response in *Drosophila melanogaster*. *Mol. Cell. Biol.* **27**, 4578–4588 (2007).
56. Pfaffl, M. W. A new mathematical model for relative quantification in real-time RT–PCR. *Nucleic Acids Res.* **29**, e45 (2001).

Acknowledgements

This work was supported by research grants from Chulalongkorn University under the 90th Anniversary of Chulalongkorn University Fund (Ratchadaphiseksomphot Endowment Fund). This research was also partially supported by the Thailand Research Fund (TRF) (RTA5880004 and IRG5780008) and the project "Development of Aquaculture Technology for Food Security and Food Safety in the Next Generation" under JST-JICA joint program "Science and Technology Research Partnership for Sustainable Development, SATREPS". We thank Dr. Benedict A. Maralit for comments on the manuscript.

Author Contributions

Conceived and designed the experiments: K.S. Performed the experiments and analysed the results: P.K. Supervised the experiments: K.S., A.T. Wrote the paper: K.S., P.K. All authors reviewed the manuscript.

Additional Information

Supplementary information accompanies this paper at https://doi.org/10.1038/s41598-017-12137-5.

Competing Interests: The authors declare that they have no competing interests.

Publisher's note: Springer Nature remains neutral with regard to jurisdictional claims in published maps and institutional affiliations.

Open Access This article is licensed under a Creative Commons Attribution 4.0 International License, which permits use, sharing, adaptation, distribution and reproduction in any medium or format, as long as you give appropriate credit to the original author(s) and the source, provide a link to the Creative Commons license, and indicate if changes were made. The images or other third party material in this article are included in the article's Creative Commons license, unless indicated otherwise in a credit line to the material. If material is not included in the article's Creative Commons license and your intended use is not permitted by statutory regulation or exceeds the permitted use, you will need to obtain permission directly from the copyright holder. To view a copy of this license, visit http://creativecommons.org/licenses/by/4.0/.

© The Author(s) 2017

Developmental and Comparative Immunology 77 (2017) 38–45

Contents lists available at ScienceDirect

Developmental and Comparative Immunology

journal homepage: www.elsevier.com/locate/dci

Short communication

Binding of *Pm*ClipSP2 to microbial cell wall components and activation of the proPO-activating system in the black tiger shrimp *Penaeus monodon*

Narach Khorattanakulchai [a], Piti Amparyup [b], Anchalee Tassanakajon [a, *]

[a] Center of Excellence for Molecular Biology and Genomics of Shrimp, Department of Biochemistry, Faculty of Science, Chulalongkorn University, Phyathai Road, Bangkok 10330, Thailand

[b] National Center for Genetic Engineering and Biotechnology (BIOTEC), National Science and Technology Development Agency (NSTDA), 113 Paholyothin Road, Klong1, Klong Luang, Pathumthani 12120, Thailand

ARTICLE INFO

Article history:
Received 21 June 2017
Received in revised form
18 July 2017
Accepted 19 July 2017
Available online 20 July 2017

Keywords:
Shrimp immunity
proPO-activating system
Clip domain serine proteinase
Bacterial binding
Penaeus monodon

ABSTRACT

Clip domain serine proteinases (ClipSPs) play an important role in the prophenoloxidase-activating (proPO) system. In the shrimp *Penaeus monodon*, the ClipSP *Pm*ClipSP2 has been previously shown to bind to microbial polysaccharides (LPS and β-1,3-glucan) and likely activates the proPO system. To reveal the binding site of the *Pm*ClipSP2 protein, the N-terminal clip domain (Clip-*Pm*ClipSP) and C-terminal SP domain (SP-*Pm*ClipSP2) were separately cloned. The recombinant proteins were then assayed for their binding properties and involvement in proPO activation. According to the ELISA-based binding assay, rSP-*Pm*ClipSP2, but not rClip-*Pm*ClipSP, can bind immobilized LPS and β-1,3-glucan as well as significantly activate PO activity. The binding site at the SP domain is proposed to have a pattern sequence (X-[PFY]-X-[AFILV]-[AFY]-[AITV]-X-[ILV]-X(5)-W-[IL]-X) that is located at the C-terminal region of the SP domain of *Pm*ClipSP2. Deletion of the pattern sequence abolished binding to LPS and β-1,3-glucan. Conversely, a recombinant protein containing the pattern sequence (rPT-*Pm*ClipSP2-TRX) had the ability to bind to cell wall components, confirming that the pattern sequence at the C-terminus of *Pm*ClipSP2 is responsible for binding to microbes, subsequently leading to activation of the proPO cascade.

© 2017 Elsevier Ltd. All rights reserved.

1. Introduction

A major innate immunity in invertebrates is melanization, which is mediated by the prophenoloxidase (proPO)-activating system. Melanization protects the hosts from pathogenic infections and is essential for the clearance of various microbial pathogens (Amparyup et al., 2013a; Cerenius and Söderhäll, 2004; Kanost and Gorman, 2008). Phenoloxidase (PO), the key enzyme of the proPO-system, catalyzes the non-enzymatic conversion of phenolic substances to quinones, leading to the production of cytotoxic intermediates and melanin. Melanin encapsulates and kills pathogens (Christensen et al., 2005; Nappi et al., 1991). However, the melanization reaction needs to be tightly controlled; otherwise, excessive quinone as well as other intermediates produced during the procession of the proPO-system would be harmful to the host cells (Cerenius et al., 2008; Nappi and Christensen, 2005).

Melanization is initially triggered by the pattern-recognition proteins (PRPs) that recognize molecular patterns found in microbial pathogens, known as pathogen-associated molecular patterns (PAMPs), leading to the activation of the clip domain serine proteinase (ClipSP) cascade. The terminal ClipSP, named the proPO-activating enzyme (PPAE), cleaves and activates proPO into active PO, which then oxidizes the phenolic substrates, resulting in melanin formation (Amparyup et al., 2013a; Cerenius et al., 2008; Söderhäll et al., 2013). Previously, several proPO-system components were identified and characterized in *Penaeus monodon*, including two proPOs (*Pm*proPO1 and *Pm*proPO2), two PPAEs (*Pm*PPAE1 and *Pm*PPAE2) and a few ClipSPs (see a review by Amparyup et al., 2013a). The *P. monodon* LPS and β-1,3-glucan binding protein (*Pm*LGBP) has been characterized as a PRP for LPS and β-1,3-glucan in the activation of the proPO-system (Amparyup et al., 2012). Moreover, the proPO-system has been shown to be an essential shrimp immune response against highly pathogenic microorganisms, the bacterium *Vibrio harveyi*, fungus *Fusarium solani*

* Corresponding author.
E-mail address: anchalee.k@chula.ac.th (A. Tassanakajon).

http://dx.doi.org/10.1016/j.dci.2017.07.016
0145-305X/© 2017 Elsevier Ltd. All rights reserved.

as well as the white spot syndrome virus (WSSV) (Amparyup et al., 2009; Charoensapsri et al., 2009, 2011; Sutthangkul et al., 2015).

ClipSPs, found in the hemolymph of insects and crustaceans, are composed of one or more amino-terminal clip domains followed by a linker sequence and a carboxyl-terminal serine protease (SP) domain (Jiang and Kanost, 2000; Kanost and Jiang, 2015; Veillard et al., 2016). Microbial infections stimulate the activation of zymogens of ClipSPs in hemolymph by specific cleavage at the amino terminus of the protease domain, creating an active enzyme, in which the clip domain and SP domain remain connected by a disulfide bond. Several ClipSPs have been shown to participate in the proPO activation and Toll signaling pathway in insects and crustaceans (Amparyup et al., 2012; Gorman et al., 2007; Jang et al., 2006). In the shrimp *P. monodon*, two ClipSPs, *Pm*PPAE1 and *Pm*PPAE2, are involved in the proPO-system and likely function as terminal SPs that convert proPO to PO (Amparyup et al., 2009; Charoensapsri et al., 2009, 2011; Sutthangkul et al., 2017). A homolog of ClipSP, named *Pm*ClipSP1, has been identified as a component of the shrimp antibacterial defense system, but it is not involved in the activation of the *P. monodon* proPO-system (Amparyup et al., 2010). On the other hand, *Pm*ClipSP2 and *Pm*Snake have been demonstrated to be the crucial serine proteinases in the activation of the proPO-system (Amparyup et al., 2013b; Monwan et al., 2017). Interestingly, a recombinant protein of *Pm*ClipSP2 binds to both immobilized LPS and laminarin (β-1,3-glucan) and activates the proPO-system (Amparyup et al., 2013b). Thus, *Pm*ClipSP2 might also act as a PRP of the *P. monodon* proPO-system and is likely an initial ClipSP in the serine proteinase cascade. Here, we further investigated the binding ability of *Pm*ClipSP2 to bacterial LPS and β-1,3-glucan to determine which domain is responsible for the binding. Recombinant proteins of each domain, as well as those containing specific regions were expressed and investigated for their binding to PAMPs and the ability to activate the shrimp proPO system.

2. Materials and methods

2.1. Shrimp samples

Juvenile *Penaeus monodon* (8-10 g) were obtained from the Marine Shrimp Broodstock Research Center II (MSBRC-2), Charoen Pokphand Foods PCL in Phetchaburi province, Thailand. The animals were acclimated under constant aeration (>5 ppm) and 20 parts per thousand (ppt) of salinity for one week prior to use. The shrimp were fed once/day in a closed container, and hemolymph was withdrawn for hemocyte collection.

2.2. Expression of recombinant (r) proteins

The recombinant *Pm*ClipSP2, Clip-*Pm*ClipSP2 and SP-*Pm*ClipSP2 were constructed as described previously (Amparyup et al., 2013b). SP-*Pm*ClipSP2 DLT was constructed by deletion of the pattern sequence (349_369delFPGVYTSVSHYRSWVEETLRP; underlined); the PT-*Pm*ClipSP-TRX was constructed from the pattern sequence (FPGVYTSVSHYRSWVE) with the thioredoxin fusion tag (TRX-tag), using specific primers (Table 1), and thioredoxin (rTRX) was expressed from the pET32a + vector (Novagen). Recombinant protein expression was induced with 1 mM IPTG (Thermo Scientific) for 6 h at 37 °C and 250 rpm in a shaking incubator (Innova 4000, New Brunswick) and then was purified and refolded as described previously (Amparyup et al., 2008). The protein preparation was then concentrated using Vivaspin 20 MWCO 10 000 (GE Healthcare) for r*Pm*ClipSP2, rSP-*Pm*ClipSP2, rSP-*Pm*ClipSP2 DLT, rPT-*Pm*ClipSP-TRX and rTRX and Vivaspin 20 MWCO 3000 for rClip-*Pm*ClipSP2. The protein concentration was determined by the Bradford assay, and the samples were stored at -80 °C. To examine the recombinant protein expression and their apparent purification, the protein preparations were resolved per lane on duplicate SDS-PAGE gels, one of which was stained with Coomassie Brilliant Blue to visualize the protein bands, while the other was electrotransferred to an Amersham Protran Premium 0.45-μm PVDF membrane (GE Healthcare) for Western blot detection of recombinant proteins using the mouse anti-His tag monoclonal antibody (GenScript) as described previously (Amparyup et al., 2012).

2.3. ELISA-based binding assay of recombinant proteins

LPS (*Escherichia coli* 0111:B4) and laminarin (β-1,3-glucan from *Laminaria digitata*) were purchased from SIGMA. The binding of recombinant proteins to PAMPs was performed as described previously (Amparyup et al., 2012) with some modifications. Briefly, 2 μg of LPS or laminarin was coated overnight in 96-well microtiter plates (Costar) at 37 °C. After incubating for 1 h at 60 °C, the wells were blocked with phosphate-buffered saline (PBS, pH 7.4) containing 0.5% (w/v) BSA (Sigma Aldrich) for 3 h and then were washed 3 times with PBS containing 0.1% (v/v) Tween 20 (PBST), before incubation with 100 μl of each recombinant protein (0-10 μM in PBS) at 4 °C for overnight. The wells were then washed with PBST, and the bound protein was detected immunochemically using a mouse anti-His tag monoclonal antibody followed by incubation with alkaline phosphatase-conjugated goat anti-mouse IgG (Jackson ImmunoResearch Inc.) as a secondary antibody. Binding was detected by the alkaline phosphatase reaction as described previously (Amparyup et al., 2012). All assays were performed in triplicate, and wells with the addition of PBS without any recombinant protein were used as the negative control. Statistical tests were performed using GraphPad Prism® 6 software (GraphPad Software, Inc.), where the data were fitted with a one-site binding model and the K_d value was determined from the nonlinear curve fitting as $A = A_{max}[L]/(K_d + [L])$, where A is the absorbance, which is proportional to the bound concentration, A_{max} is the maximum binding, and [L] is the concentration of the recombinant proteins.

2.4. Activation of the PO activity by recombinant proteins

The PO activity assay was performed as described previously (Amparyup et al., 2012) with some modifications. In brief, 30 μg of hemocyte lysate supernatant (HLS) protein from a healthy shrimp in cacodylate buffer (10 mM sodium cacodylate and 10 mM calcium chloride) was incubated in the presence or absence of 20 μg of LPS or laminarin and 10 μM of recombinant proteins in a 100-μl

Table 1
Nucleotide sequences of the primers used.

Primer	Sequence (5′-3′)	Purpose
SP-*Pm*ClipSP2 DLT-F	CATGCCATGGGAAGAGTGGTAGGAGGCGAAGA	Recombinant protein
SP-*Pm*ClipSP2 DLT-R	CCGCTCGAGTCCTTTCTGGCCGCAACTCGT	
PT-*Pm*ClipSP2-F	CATGCCATGGGATTCCCTGGCGTCTATACCG	
PT-*Pm*ClipSP2-R	CCGCTCGAGCTCGACCCAGGACCTATAAT	

reaction. Subsequently, 20 μl of L-3,4-dihydroxyphenylalanine (L-DOPA) (3 mg/ml) was added to each reaction and was incubated at 25 °C for 30 min, and then the absorbance at 490 nm was measured using a spectrophotometer (SpectraMax M5 Molecular Device); one unit of PO activity was defined as ΔA490/mg total protein/min. Each experiment was performed in triplicate. The data were analyzed using one-way analysis of variance (ANOVA) with GraphPad Prism® 6.0, and statistical significance was accepted at $P < 0.05$.

3. Results

3.1. Recombinant proteins (rPmClipSP2, rClip-PmClipSP2, rSP-PmClipSP2, rSP-PmClipSP2 DLT rPT-PmClipSP2-TRX and rTRX) are successfully expressed in E. coli

From a previous study, *Pm*ClipSP2 (GenBank: ACP19561.1) acts as a pattern-recognition-protein (PRP) of the shrimp proPO-activating system by binding to both LPS and β-1,3-glucan, activating PO activity (Amparyup et al., 2013b). To elucidate the binding properties and PO activation of each domain of *Pm*ClipSP2, recombinant (r)*Pm*ClipSP2 proteins were expressed in the *E. coli* system. Six clones (containing full length, r*Pm*ClipSP2; clip domain, rClip-*Pm*ClipSP2; serine proteinase domain, rSP-*Pm*ClipSP2; serine proteinase domain with deletion the pattern sequence, rSP-*Pm*ClipSP2 DLT; the pattern sequence of *Pm*ClipSP2 fused with thioredoxin, rPT-*Pm*ClipSP2-TRX and thioredoxin, rTRX) that have the 6× His-tag at the C-terminus were constructed (Fig. 2A). The recombinant proteins were expressed in *E. coli* Rosetta (DE3)-pLysS cells (Novagen) and were purified by Ni-affinity chromatography. Thereafter, they were analyzed and confirmed using SDS-PAGE and immunoblotting with mouse anti-His antibody, respectively. The major bands of r*Pm*ClipSP2, rClip-*Pm*ClipSP2, rSP-*Pm*ClipSP2, rSP-*Pm*ClipSP2 DLT, rPT-*Pm*ClipSP2-TRX and rTRX were indicated, and the theoretical molecular mass of recombinant proteins were 38.4 kDa, 9.4 kDa, 30.2 kDa, 27.9 kDa, 20.3 kDa and 20.4 kDa, respectively (Fig. 2B and C). These recombinant proteins were used in the binding assay with microbial cell wall components by ELISA and PO activation in the hemocyte lysate supernatant (HLS) of *P. monodon*.

3.2. SP domain of PmClipSP2 binds to both LPS and β-1,3-glucan

From the previous study (Amparyup et al., 2013b), r*Pm*ClipSP2 bound to both LPS and β-1,3-glucan. In this study, we further determined which domain of *Pm*ClipSP2 binds to LPS and laminarin (as a representative of β-1,3-glucan) by performing an ELISA-based binding assay with 0-10 μM of recombinant proteins. The results clearly showed that r*Pm*ClipSP2 and rSP-*Pm*ClipSP2 bound to both immobilized LPS and β-1,3-glucan (Fig. 3A and B). By contrast, rClip-*Pm*ClipSP2 did not bind to either LPS or β-1,3-glucan. Analysis of the binding interactions revealed that rSP-*Pm*ClipSP2 bound to LPS with a 1.3-fold higher affinity (dissociation constant (K_d) of 1.54×10^{-6} M) than r*Pm*ClipSP2 (K_d of 2.00×10^{-6} M) and β-1,3-glucan with a 1.1-fold higher affinity (K_d of 1.96×10^{-6} M) than r*Pm*ClipSP2 (K_d of 2.13×10^{-6} M). The high-affinity binding of both LPS and β-1,3-glucan were dose dependent. This result indicates that *Pm*ClipSP2 uses the C-terminal SP domain to bind both LPS and β-1,3-glucan.

3.3. Activation of the proPO system by rPmClipSP2, rClip-PmClipSP2 and rSP-PmClipSP2 in the presence of LPS

More recently, it was reported that *Pm*ClipSP2 may act as a PRP by binding to both LPS and β-1,3-glucan and then activating the shrimp proPO system (Amparyup et al., 2013b). In the present study, we investigated which domain of *Pm*ClipSP2 could trigger the proPO activation cascade in *P. monodon*. Incubation of the purified recombinant proteins (10 μM) and HLS (30 μg) of *P. monodon* shrimp with or without LPS or β-1,3-glucan (20 μg), followed by measurement of the PO activity using L-DOPA (60 μg) as the substrate, revealed that the PO activity was significantly increased by the addition of r*Pm*ClipSP2 and rSP-*Pm*ClipSP2, but not rClip-*Pm*ClipSP2, in the presence of both LPS and β-1,3-glucan (Fig. 4A and B). These *in vitro* results are in accordance with the notion that r*Pm*ClipSP2 interacts with both LPS and β-1,3-glucan and induces the proPO activation system in *P. monodon* shrimp using the SP domain.

3.4. The pattern sequence within the SP domain of PmClipSP2 is an important binding site to LPS and β-1,3-glucan

From the above results, we found that the C-terminal SP domain of *Pm*ClipSP2 interacts with PAMPs and activates the proPO system. Sequence analysis of this binding region identified the sequences (FPGVYTSVSHYRSWVE; except for the amino acid change from I/L to V (underlined)) that match with the pattern sequence (X-[PFY]-X-[AFILV]-[AFY]-[AITV]-X-[ILV]-X(5)-W-[IL]-X (Kasetty et al., 2011)) (Fig. 1B) that was reported to function in the antibacterial and LPS binding activities in the C-terminal-derived peptide from human thrombin and S1 family proteinase (Kasetty et al., 2011; Papareddy et al., 2010). This region may be responsible for binding to LPS and β-1,3-glucan; thus, we constructed a recombinant SP domain protein that contains a deletion of the pattern sequence (rSP-*Pm*ClipSP2 DLT) and tested whether this deletion affects the binding ability of the SP domain of *Pm*ClipSP2. The results of ELISA showed that rSP-*Pm*ClipSP2 DLT did not bind to both LPS and β-1,3-glucan, while rSP-*Pm*ClipSP2 as a control could bind in a dose-dependent manner (Fig. 5A and B). To further confirm this result, we produced a recombinant protein that contains the pattern sequence. However, due to the short sequence, the recombinant protein was fused with thioredoxin (TRX), creating rPT-*Pm*ClipSP2-TRX, and the fusion protein was tested for its binding ability by ELISA using rTRX as a control (Fig. 5C and D). The result revealed that rPT-*Pm*ClipSP2-TRX bound to both LPS and β-1,3-glucan in a dose-dependent manner with higher affinity (K_d of 7.24×10^{-7} M for LPS and 9.82×10^{-7} M for β-1,3-glucan) than rTRX (K_d of 2.29×10^{-6} M for LPS and 1.12×10^{-6} M for β-1,3-glucan). These results confirm that the pattern sequence of *Pm*ClipSP2 is the binding site for microbial cell wall components.

4. Discussion

Proteins in the proPO-activating system (PRPs, proPOs, proteinases and inhibitors), which are involved in the melanization cascade, have been characterized, and their functions have been studied in several invertebrate species (Amparyup et al., 2013a; Cerenius et al., 2008; Cerenius and Söderhäll, 2004; Kanost and Gorman, 2008). The proPO system in crustaceans is reported to play a key role in the immune response against pathogenic bacteria and fungi (Amparyup et al., 2009, 2013a; Charoensapsri et al., 2009, 2011; Fagutao et al., 2009; Jang et al., 2011; Liu et al., 2007). Additionally, the recognition of pathogen cell wall components by PRPs is a critical step in the activation of the proPO system. Current evidence in insects suggests that certain SPs act as PRPs and are required for the activation of the melanization cascade to recognize the microorganisms (Ji et al., 2004; Wang and Jiang, 2006). The SP domain of ClipSPs is classified as the trypsin-like SP family, which has been identified in both vertebrates and invertebrates. This proteinase family has biological functions, which have been widely

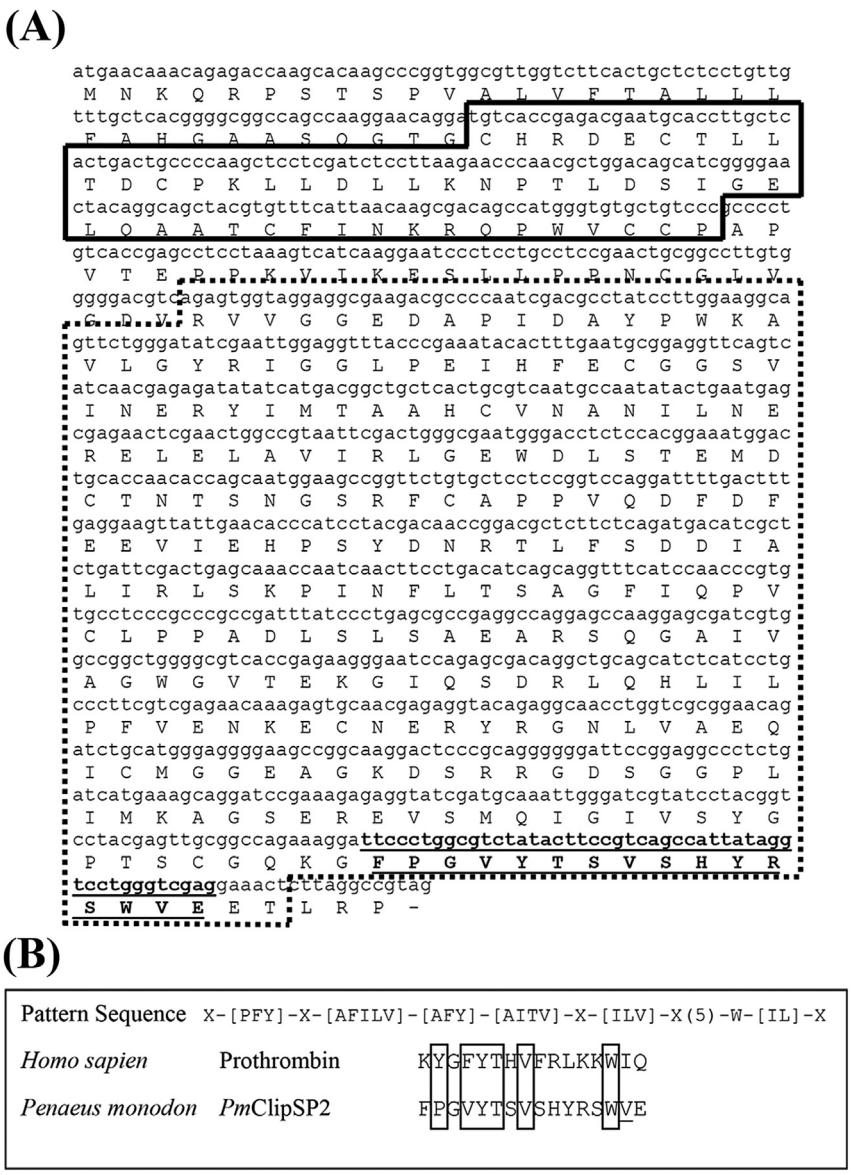


Fig. 1. Conserved domains of *Pm*ClipSP2. (A) The nucleotide and deduced amino acid sequences of *Pm*ClipSP2 (clip domain, black line box; SP domain, dashed line box and the pattern sequence, bold and underlined). (B) The pattern sequence from human prothrombin compared with *Pm*ClipSP2. Matched residues are shown with boxes, and mismatched residues are underlined.

characterized and have been found to be involved in immunity and homeostasis (Jang et al., 2008; Jiang and Kanost, 2000).

In our previous study, *Pm*ClipSP2 was identified from *P. monodon*, and its important functions were reported. Sequence analysis of *Pm*ClipSP2 showed an N-terminus clip domain and a C-terminus SP domain and is a member of the ClipSP family (Jang et al., 2008; Jiang and Kanost, 2000). *Pm*ClipSP2 was found to be expressed mainly in hemocytes, which corresponds to the expression of the other known proPO-associated transcripts in *P. monodon* (*Pm*proPO1, *Pm*proPO2, *Pm*PPAE1, *Pm*PPAE2 and *Pm*LGBP) that are mainly detected in the hemocytes (Amparyup et al., 2009, 2012; Charoensapsri et al., 2009, 2011). *Pm*ClipSP2-knockdown shrimp showed a significant reduction of PO activity and increased susceptibility to *V. harveyi* infection. Interestingly, it has been demonstrated that recombinant *Pm*ClipSP2 binds to LPS and β-1,3-glucan and activates PO activity, suggesting that *Pm*ClipSP2 might act as a PRP and activate the shrimp proPO system. In addition, it has been shown that it may also play an essential role in hemocyte homeostasis by scavenging LPS and neutralizing its toxicity (Amparyup et al., 2013b).

In this study, we further investigated the binding domain of *Pm*ClipSP2 to bacterial cell wall components by separately expressing *Pm*ClipSP2 (N-terminal clip domain, rClip-*Pm*ClipSP2 and C-terminal serine proteinase domain, rSP-*Pm*ClipSP2) and examining the binding properties with LPS and β-1,3-glucan and PO activation in HLS. The results demonstrated that rSP-*Pm*ClipSP2 bound to both LPS and β-1,3-glucan (Fig. 3) with high affinity (K_d of 1.54×10^{-6} M and K_d of 1.96×10^{-6} M, respectively), but the clip domain did not bind. Moreover, the SP domain could activate the proPO system in HLS of *P. monodon* in the presence of LPS (Fig. 4). Thus, the SP domain of *Pm*ClipSP2 plays a recognition role with LPS and β-1,3-glucan and induces the proPO system. However, the

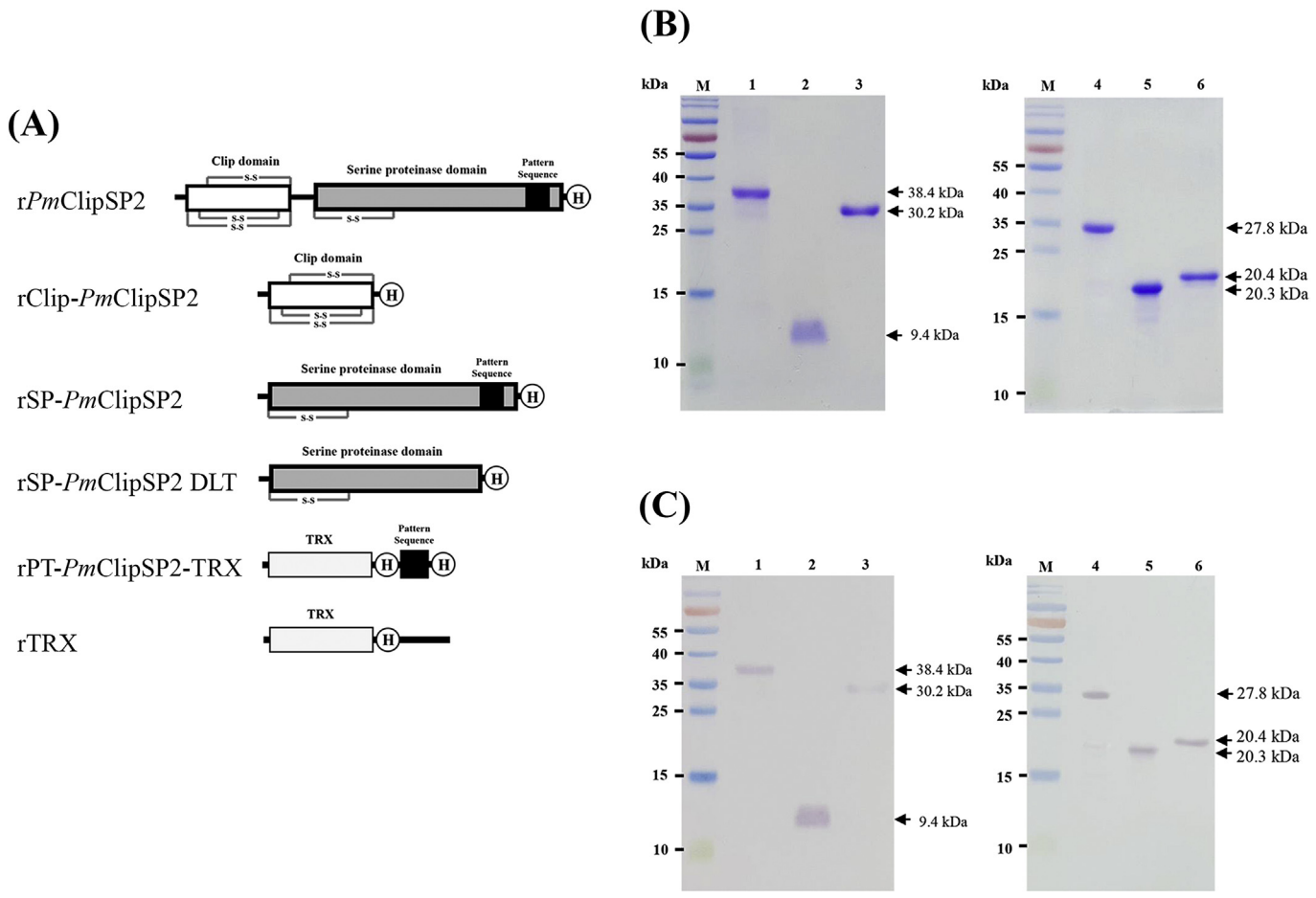


Fig. 2. SDS-PAGE and Western blot analysis of purified recombinant proteins expressed in *E. coli*. (A) Schematic diagram showing recombinant proteins r*Pm*ClipSP2, rClip-*Pm*ClipSP2, rSP-*Pm*ClipSP2 DLT, rPT-*Pm*ClipSP2-TRX and rTRX. (B) The 50 pmol of purified r*Pm*ClipSP2 (lane 1), rClip-*Pm*ClipSP2 (lane 2), rSP-*Pm*ClipSP2 (lane 3), rSP-*Pm*ClipSP2 DLT (lane 4), rPT-*Pm*ClipSP2-TRX (lane 5) and rTRX (lane 6) were subjected to 12.5% SDS-PAGE. (C) Western blot analysis with mouse anti-His tag antibody as the primary antibody and goat anti-mouse-conjugated AP antibody as the secondary antibody for detection. Lane M is the protein marker. Arrows indicate the protein bands with the apparent molecular weights marked on the right.

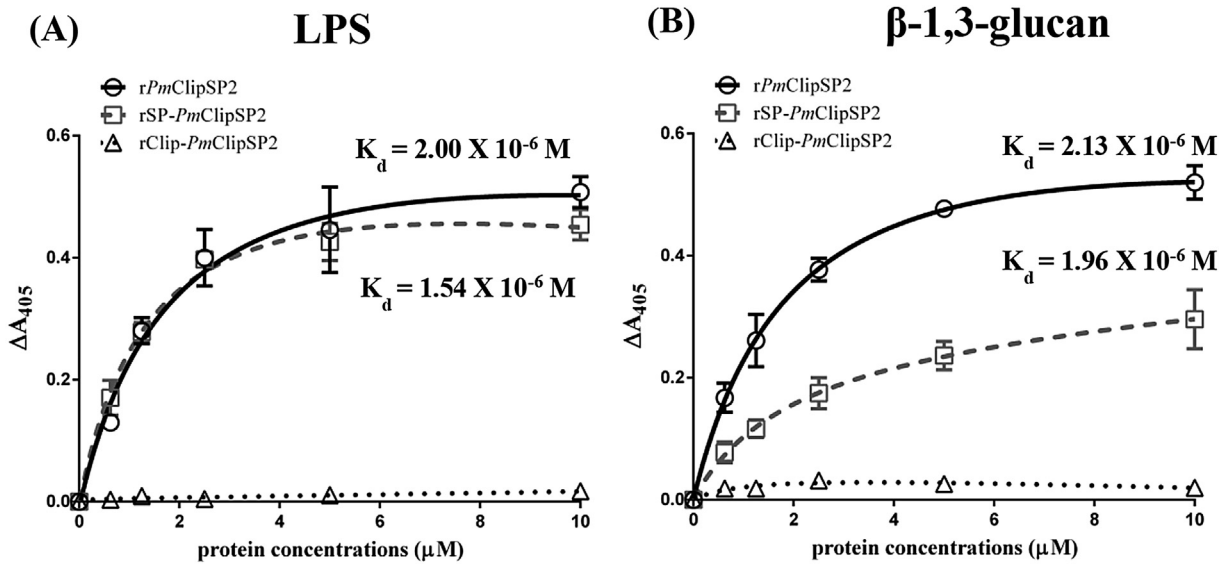


Fig. 3. Binding ability of r*Pm*ClipSP2 (⊖), rSP-*Pm*ClipSP2 (▭) and rClip-*Pm*ClipSP2 (△) to immobilize LPS (A) and β-1,3-glucan (B). The binding activity was examined using ELISA, which used the dose-dependent binding of recombinant proteins (0-10 μM), followed by probing with mouse anti-His tag antibody as the primary antibody and goat anti-mouse-conjugated AP antibody as the secondary antibody for detection and ρ-nitrophenyl phosphate as the substrate. Solid lines illustrate the fitted curves. The data are shown as the dissociation constant (K_d) near the line and the mean ± 1 SEM, derived from triplicate experiments.

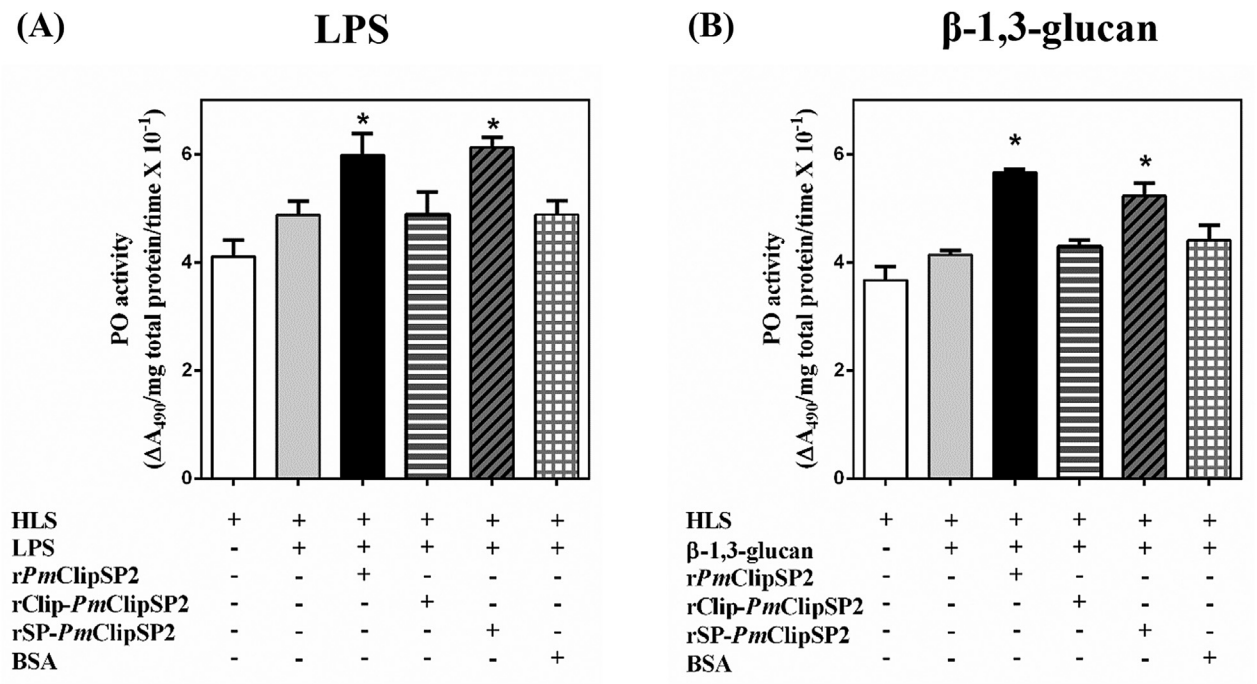


Fig. 4. ***In vitro*** **PO activity assay showing the ability of recombinant proteins to activate the proPO-system.** Hemocyte lysate supernatant (HLS) (30 μg) was incubated with 10 μM of each of the recombinant proteins (r*Pm*ClipSP2 (■) rClip-*Pm*ClipSP2 (▭) and rSP-*Pm*ClipSP2 (▨)) in the presence of 20 μg of pre-incubated LPS or β-1,3-glucan. Controls (▭) were evaluated as above except without the recombinant proteins, and BSA (▭) was used as the negative control. The PO activity was measured by spectrophotometer; after 30 min, L-DOPA was used as the substrate. The data are shown as the mean ± 1 SEM, derived from triplicate experiments. Means with an asterisk are significantly different ($P < 0.05$).

substrate for *Pm*ClipSP2 is still unknown and is not yet clear from available data how binding of this proteinase to microbial surfaces might lead to proPO activation.

In the horseshoe crab coagulation cascade, factor C, an SP zymogen, acts as a PRP for pathogens. The tripeptide motif (-Arg36-Trp37-Arg38-), which is located at the N-terminal Cys-rich region, of factor C interacts with LPS in the lipid A portion (Ariki et al., 2004; Koshiba et al., 2007). However, the N-terminal clip domain of *Pm*ClipSP2 does not contain this motif.

The involvement of SPs in the recognition processes of the horseshoe crab (*Limulus polyphemus and Tachypleus tridentatus*) coagulation cascade system (factor C and factor G) and the tobacco hornworm (*Manduca sexta*) proPO cascade system (HP14), which interact with the microbial cell wall components, have also been reported (Ariki et al., 2004; Ji et al., 2004; Takaki et al., 2002; Theopold et al., 2004; Wang and Jiang, 2006). However, *Pm*ClipSP2 displays only a single predicted N-terminal clip and a C-terminal SP domain with no extra domains, such as those found in factor C, factor G and HP14, which contain additional individual domains involved in the immune recognition of pathogens. Recently, C-terminal peptides from the SP domain of human thrombin, a key enzyme in the coagulation cascade, as well as numerous S1 family members, were reported to bind to LPS and display bactericidal and anti-inflammatory functions, suggesting a new role of thrombin in regulating host defense peptides (Kasetty et al., 2011; Papareddy et al., 2010). Interestingly, a similar C-terminal sequence pattern to that of thrombin and the S1 family (X-[PFY]-X-[AFILV]-[AFY]-[AITV]-X-[ILV]-X(5)-W-[IL]-X (Kasetty et al., 2011)), which exhibits important functions in the antibacterial and LPS binding activities, was also found in the C-terminal region of *Pm*ClipSP2 (FPGVYTSVSHYRSWVE, except for the amino acid change from I/L to V (underlined)). Therefore, we expressed the recombinant proteins, one containing the SP domain with a deletion of the pattern sequence (rSP-*Pm*ClipSP2 DLT) and another fusion protein containing the pattern sequence with TRX-tag (rPT-*Pm*ClipSP2-TRX). The ELISA-based binding result revealed that the pattern sequence participates in the binding property of *Pm*ClipSP2, as rPT-*Pm*ClipSP2-TRX bound to both LPS and β-1,3-glucan but not rSP-*Pm*ClipSP2 DLT (Fig. 5). These results demonstrated that the pattern sequence of *Pm*ClipSP2 was responsible for binding to microbial cell wall components. Nevertheless, the pattern sequence did not exhibit antimicrobial activity (data not shown).

In conclusion, *Pm*ClipSP2 acts as a PRP by binding to LPS and β-1,3-glucan via the C-terminal pattern sequence of the SP domain. This finding increases our understanding of the mechanisms of *Pm*ClipSP2 in melanization and suggest that *Pm*ClipSP2 is involved in the early step of the proPO system that is triggered upon recognition and binding to microbes and stimulates the cascade of serine proteinase, leading to melanin formation.

Acknowledgments

This work was supported by research grants from the Thailand Research Fund to AT (TRF Senior Scholar No. RTA5880004), the Thailand Research Fund and Thailand National Center for Genetic Engineering and Biotechnology (BIOTEC) to PA (Grant No. BRG5880016). Additional support from TRF (Grant No. IRG5780008) to the Department of Biochemistry, Faculty of Science, Chulalongkorn University is acknowledged. NK is the recipient of a student fellowship from Chulalongkorn University Graduate Scholarship to Commemorate the 72nd Anniversary of His Majesty King Bhumibol Adulyadej, the 90th Anniversary of Chulalongkorn University Fund (Ratchadaphiseksomphot Endowment Fund) and from the Young Scientist and Technologist Programme (YSTP), NSTDA SP-56-BT01.

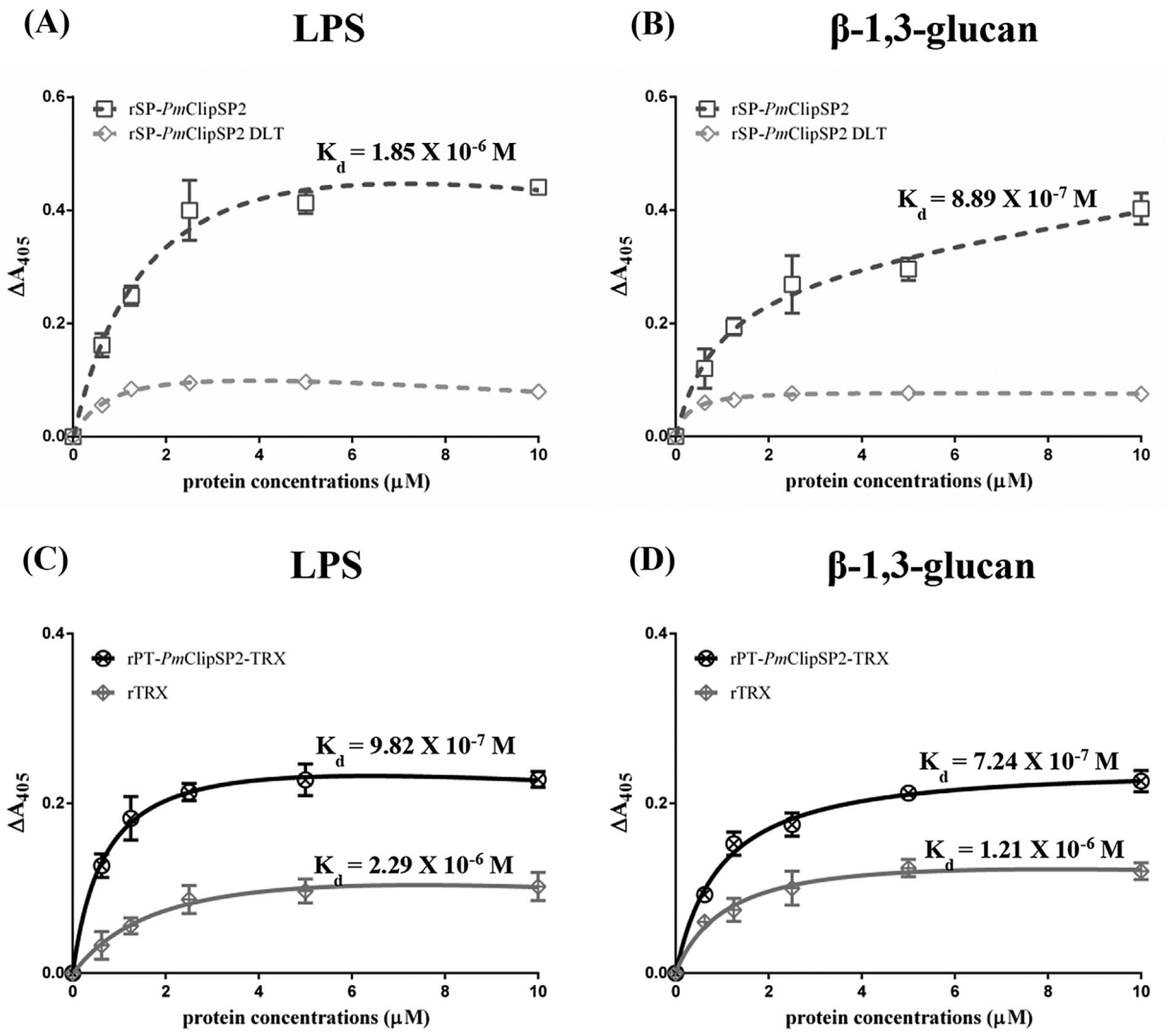


Fig. 5. Binding ability of rSP-*Pm*ClipSP2 (▭), rSP-*Pm*ClipSP2 DLT (◇), rPT-*Pm*ClipSP2-TRX (⊕) and rTRX (◈) to immobilize LPS (A, C) and β-1,3-glucan (B, D). Binding activity was examined using ELISA, which used the dose-dependent binding of recombinant proteins (0-10 μM), probing with mouse anti-His tag antibody as the primary antibody and goat anti-mouse-conjugated AP antibody as the secondary antibody for detection and ρ-nitrophenyl phosphate as the substrate. Solid lines illustrate the fitted curves. Data are shown as the dissociation constant (K_d) above the line and the mean ± 1 SEM, derived from triplicate experiments.

References

Amparyup, P., Charoensapsri, W., Tassanakajon, A., 2009. Two prophenoloxidases are important for the survival of *Vibrio harveyi* challenged shrimp *Penaeus monodon*. Dev. Comp. Immunol. 33, 247–256.

Amparyup, P., Charoensapsri, W., Tassanakajon, A., 2013a. Prophenoloxidase system and its role in shrimp immune responses against major pathogens. Fish. Shellfish Immunol. 34, 990–1001.

Amparyup, P., Kondo, H., Hirono, I., Aoki, T., Tassanakajon, A., 2008. Molecular cloning, genomic organization and recombinant expression of a crustin-like antimicrobial peptide from black tiger shrimp *Penaeus monodon*. Mol. Immunol. 45, 1085–1093.

Amparyup, P., Promrungreang, K., Charoensapsri, W., Sutthangkul, J., Tassanakajon, A., 2013b. A serine proteinase *Pm*ClipSP2 contributes to prophenoloxidase system and plays a protective role in shrimp defense by scavenging lipopolysaccharide. Dev. Comp. Immunol. 41, 597–607.

Amparyup, P., Sutthangkul, J., Charoensapsri, W., Tassanakajon, A., 2012. Pattern recognition protein binds to lipopolysaccharide and β-1,3-glucan and activates shrimp prophenoloxidase system. J. Biol. Chem. 287, 10060–10069.

Amparyup, P., Wiriyaukaradecha, K., Charoensapsri, W., Tassanakajon, A., 2010. A clip domain serine proteinase plays a role in antibacterial defense but is not required for prophenoloxidase activation in shrimp. Dev. Comp. Immunol. 34, 168–176.

Ariki, S., Koori, K., Osaki, T., Motoyama, K., Inamori, K., Kawabata, S., 2004. A serine protease zymogen functions as a pattern-recognition receptor for lipopolysaccharides. Proc. Natl. Acad. Sci. U. S. A. 101, 953–958.

Cerenius, L., Lee, B.L., Söderhäll, K., 2008. The proPO-system: pros and cons for its role in invertebrate immunity. Trends Immunol. 29, 263–271.

Cerenius, L., Söderhäll, K., 2004. The prophenoloxidase-activating system in invertebrates. Immunol. Rev. 198, 116–126.

Charoensapsri, W., Amparyup, P., Hirono, I., Aoki, T., Tassanakajon, A., 2009. Gene silencing of a prophenoloxidase activating enzyme in the shrimp, *Penaeus monodon*, increases susceptibility to *Vibrio harveyi* infection. Dev. Comp. Immunol. 33, 811–820.

Charoensapsri, W., Amparyup, P., Hirono, I., Aoki, T., Tassanakajon, A., 2011. *Pm*PPAE2, a new class of crustacean prophenoloxidase (proPO)-activating enzyme and its role in PO activation. Dev. Comp. Immunol. 35, 115–124.

Christensen, B.M., Li, J., Chen, C.C., Nappi, A.J., 2005. Melanization immune responses in mosquito vectors. Trends Parasitol. 21, 192–199.

Fagutao, F.F., Koyama, T., Kaizu, A., Saito-Taki, T., Kondo, H., Aoki, T., Hirono, I., 2009. Increased bacterial load in shrimp hemolymph in the absence of prophenoloxidase. FEBS J. 276, 5298–5306.

Gorman, M.J., Wang, Y., Jiang, H., Kanost, M.R., 2007. *Manduca sexta* hemolymph proteinase 21 activates prophenoloxidase-activating proteinase 3 in an insect innate immune response proteinase cascade. J. Biol. Chem. 282, 11742–11749.

Jang, I.H., Chosa, N., Kim, S.H., Nam, H.J., Lemaitre, B., Ochiai, M., Kambris, Z., Brun, S., Hashimoto, C., Ashida, M., Brey, P.T., Lee, W.J., 2006. A Spätzle-processing enzyme required for toll signaling activation in *Drosophila* innate immunity. Dev. Cell 10, 45–55.

Jang, I.H., Nam, H.J., Lee, W.J., 2008. CLIP-domain serine proteases in *Drosophila* innate immunity. BMB Rep. 41, 102–107.

Jang, I.K., Pang, Z., Yu, J., Kim, S.K., Seo, H.C., Cho, Y.R., 2011. Selectively enhanced expression of prophenoloxidase activating enzyme 1 (PPAE1) at a bacteria

clearance site in the white shrimp, *Litopenaeus vannamei*. BMC Immunol. 12, 70.
Ji, C., Wang, Y., Guo, X., Hartson, S., Jiang, H., 2004. A pattern recognition serine proteinase triggers the prophenoloxidase activation cascade in the tobacco hornworm, *Manduca sexta*. J. Biol. Chem. 279, 34101–34106.
Jiang, H., Kanost, M.R., 2000. The clip-domain family of serine proteinases in arthropods. Insect Biochem. Mol. Biol. 30, 95–105.
Kanost, M.R., Gorman, M.J., 2008. Phenoloxidase in insect immunity. In: Beckage, N.E. (Ed.), Insect Immunology. Academic Press, San Diego, pp. 69–96.
Kanost, M.R., Jiang, H., 2015. Clip-domain serine proteases as immune factors in insect hemolymph. Curr. Opin. Insect Sci. 11, 47–55.
Kasetty, G., Papareddy, P., Kalle, M., Rydengard, V., Walse, B., Svensson, B., Morgelin, M., Malmsten, M., Schmidtchen, A., 2011. The C-terminal sequence of several human serine proteases encodes host defense functions. J. Innate Immun. 3, 471–482.
Koshiba, T., Hashii, T., Kawabata, S., 2007. A structural perspective on the interaction between lipopolysaccharide and factor C, a receptor involved in recognition of Gram-negative bacteria. J. Biol. Chem. 282, 3962–3967.
Liu, H., Jiravanichpaisal, P., Cerenius, L., Lee, B.L., Söderhäll, I., Söderhäll, K., 2007. Phenoloxidase is an important component of the defense against *Aeromonas hydrophila* infection in a crustacean, *Pacifastacus leniusculus*. J. Biol. Chem. 282, 33593–33598.
Monwan, W., Amparyup, P., Tassanakajon, A., 2017. A snake-like serine proteinase (*Pm*Snake) activates prophenoloxidase-activating system in black tiger shrimp *Penaeus monodon*. Dev. Comp. Immunol. 67, 229–238.
Nappi, A.J., Carton, Y., Frey, F., 1991. Parasite-induced enhancement of hemolymph tyrosinase activity in a selected immune reactive strain of *Drosophila melanogaster*. Arch. Insect Biochem. Physiol. 18, 159–168.
Nappi, A.J., Christensen, B.M., 2005. Melanogenesis and associated cytotoxic reactions: applications to insect innate immunity. Insect Biochem. Mol. Biol. 35, 443–459.
Papareddy, P., Rydengard, V., Pasupuleti, M., Walse, B., Morgelin, M., Chalupka, A., Malmsten, M., Schmidtchen, A., 2010. Proteolysis of human thrombin generates novel host defense peptides. PLoS Pathog. 6, e1000857.
Söderhäll, K., Tassanakajon, A., Ampyrup, P., 2013. Prophenoloxidase-activating enzyme. In: Rawlings, N.D., Salvesen, G. (Eds.), Handbook of Proteolytic Enzymes. Academic Press, San Diego 3, pp. 3068–3074.
Sutthangkul, J., Amparyup, P., Charoensapsri, W., Senapin, S., Phiwsaiya, K., Tassanakajon, A., 2015. Suppression of shrimp melanization during white spot syndrome virus infection. J. Biol. Chem. 290, 6470–6481.
Sutthangkul, J., Amparyup, P., Eum, J.H., Strand, M.R., Tassanakajon, A., 2017. Antimelanization mechanism of the white spot syndrome viral protein, WSSV453, via interaction with shrimp proPO-activating enzyme, *Pm*proPPAE2. J. Gen. Virol. 98, 769–778.
Takaki, Y., Seki, N., Kawabata Si, S., Iwanaga, S., Muta, T., 2002. Duplicated binding sites for (1–>3)-β-D-glucan in the horseshoe crab coagulation factor G: implications for a molecular basis of the pattern recognition in innate immunity. J. Biol. Chem. 277, 14281–14287.
Theopold, U., Schmidt, O., Söderhäll, K., Dushay, M.S., 2004. Coagulation in arthropods: defence, wound closure and healing. Trends Immunol. 25, 289–294.
Veillard, F., Troxler, L., Reichhart, J.M., 2016. Drosophila melanogaster clip-domain serine proteases: structure, function and regulation. Biochimie 122, 255–269.
Wang, Y., Jiang, H., 2006. Interaction of β-1,3-glucan with its recognition protein activates hemolymph proteinase 14, an initiation enzyme of the prophenoloxidase activation system in *Manduca sexta*. J. Biol. Chem. 281, 9271–9278.

Developmental and Comparative Immunology 69 (2017) 23–32

Contents lists available at ScienceDirect

Developmental and Comparative Immunology

journal homepage: www.elsevier.com/locate/dci

Antiviral action of the antimicrobial peptide ALF*Pm*3 from *Penaeus monodon* against white spot syndrome virus

Thanachai Methatham [1], Pakpoom Boonchuen [1], Phattarunda Jaree, Anchalee Tassanakajon, Kunlaya Somboonwiwat*

Center of Excellence for Molecular Biology and Genomics of Shrimp, Department of Biochemistry, Faculty of Science, Chulalongkorn University, Phayathai Rd., Bangkok, 10330, Thailand

ARTICLE INFO

Article history:
Received 22 October 2016
Received in revised form
29 November 2016
Accepted 30 November 2016
Available online 2 December 2016

Keywords:
ALF*Pm*3
WSSV
Penaeus monodon
Antiviral activity
Host-viral interaction

ABSTRACT

The anti-lipopolysaccharide factor isoform 3 (ALF*Pm*3), the antimicrobial peptide from *Penaeus monodon*, possesses antibacterial and antiviral activities. Although the mechanism of action of ALF*Pm*3 against bacteria has been revealed but its antiviral mechanism is still unclear. To further study how the ALF*Pm*3 exhibits antiviral activity against the enveloped virus, white spot syndrome virus (WSSV), the ALF*Pm*3-interacting proteins from WSSV were sought and identified five ALF*Pm*3-interacting proteins, WSSV186, WSSV189, WSSV395, WSSV458, and WSSV471. Only the interaction between ALF*Pm*3 and WSSV189, however, has been confirmed to be involved in anti-WSSV activity of ALF*Pm*3. Herein, the interactions between ALF*Pm*3 and rWSSV186, rWSSV395, rWSSV458, or rWSSV471 were further analyzed and confirmed by *in vitro* pull-down assay. Western blot analysis and immunoelectron microscopy showed that the uncharacterized proteins, WSSV186 and WSSV471, were nucleocapsid and envelope proteins, respectively. The decrease of shrimp survival after injection the shrimp with mixtures of each rWSSV protein, rALF*Pm*3 and WSSV as compared to those injected with rALF*Pm*3-neutralizing WSSV was clearly observed indicating that all rWSSV proteins could interfere with the neutralization effect of rALF*Pm*3 on WSSV similar to that reported previously for WSSV189. Morphological change on WSSV after incubation with rALF*Pm*3 was observed by TEM. The lysed WSSV virions were clearly observed where both viral envelope and nucleocapsid were dismantled. The results lead to the conclusion that the ALF*Pm*3 displays direct effect on the viral structural proteins resulting in destabilization and breaking up of WSSV virions.
© 2016 Elsevier Ltd. All rights reserved.

1. Introduction

Anti-lipopolysaccharide factors (ALFs) are antimicrobial peptides with broad antimicrobial activities toward Gram-positive and Gram-negative bacteria, filamentous fungi and viruses (Tassanakajon et al., 2015). The ALFs are amphipathic peptides that contain a LPS-binding domain (LPS-BD) within a conserved disulfide bridge. This stable disulfide loop harbors either a highly conserved cluster of positively charged (Lys and Arg) residues or negatively charged (Glu and Asp) and hydrophobic residues (Li et al., 2008; Somboonwiwat et al., 2005; Yang et al., 2009). The LPS-BD contributes mainly to the ALF antimicrobial activity.

In *Penaeus monodon,* six different isoforms of ALF (ALF*Pm*1-6) have previously been reported (Ponprateep et al., 2012; Tassanakajon et al., 2006), of which the major isoform is ALF*Pm*3. Recombinant ALF*Pm*3 (rALF*Pm*3) exhibits a broad antimicrobial activity spectrum with antifungal property against filamentous fungi, and antibacterial activities against both Gram-positive and Gram-negative bacteria with a high potency against the natural shrimp pathogens, *Vibrio harveyi* and *Vibrio parahaemolyticus* AHPND causing early mortality syndrome (Somboonwiwat et al., 2005; Supungul et al., 2015). In addition, the antiviral property of ALF against the major shrimp viral pathogen, White Spot Syndrome Virus (WSSV), was first reported in the freshwater crayfish *Pacifastacus leniusculus* (Liu et al., 2006). Subsequently, the rALF*Pm*3 has been shown to inhibit WSSV propagation in crayfish hematopoietic cell culture and in shrimp (Tharntada et al., 2009). Moreover, silencing of the ALF*Pm*3 gene in normal shrimp increased the cumulative mortality to 86% in 7 days. The bacterial counts after 2

* Corresponding author.
E-mail address: kunlaya.s@chula.ac.th (K. Somboonwiwat).
[1] Thanachai Methatham and Pakpoom Boonchuen contributed equally to this article.

http://dx.doi.org/10.1016/j.dci.2016.11.023
0145-305X/© 2016 Elsevier Ltd. All rights reserved.

days of dsRNA-ALF*Pm*3 injection grew by 12- and 50- fold when compared with those of the control in the haemolymph and hepatopancreas, respectively (Ponprateep et al., 2012). It has been reported that the ALF*Pm*3 effectively kills bacteria through bacterial membrane permeabilization (Jaree et al., 2012). How the ALF*Pm*3 displays anti-WSSV activity, however, is still a mystery.

Innate immunity in shrimp has been studied intensively to understand the response to viral infection in shrimp and several WSSV-binding proteins have been identified in shrimp (Sritunyalucksana et al., 2013). Viral-binding proteins are categorized into two types based on the interaction with the virus, specific interaction and non-specific interaction. Several host WSSV-binding proteins with specific interactions have been reported such as PmRab7, PlgC1qR, WSSV-binding protein (WBP), and PmFKBP46. The endosomal protein from the hemocytes of *P. monodon*, PmRab7, was identified as VP28-binding protein (Sritunyalucksana et al., 2006). The PmRab7 gene silencing resulted in the decrease in WSSV replication suggesting that the PmRab7 functions as an important regulator of intracellular trafficking (Ongvarrasopone et al., 2008). The PlgC1qR, a receptor for globular head domain of complement component C1q, can bind to VP15, VP26, and VP28 of WSSV and possibly plays a role in controlling antiviral mechanism (Watthanasurorot et al., 2010). Interaction between VP26, a major tegument protein of WSSV, with shrimp cytoskeletal protein β-actin and 3 kDa WSSV-binding protein (WBP) is identified and its important role in WSSV infection is also revealed (Liu et al., 2011; Xie and Yang, 2005; Youtong et al., 2011). The interaction between a major nucleocapsid protein of WSSV like VP15 with PmFKBP46 has been described and thought to be involved in genome packaging during virion assembly (Sangsuriya et al., 2011). On the other hand, the non-specific interacting proteins like hemocyanin can bind to WSSV virions and act as antiviral factors of *P. monodon* (Zhang et al., 2004).

Previously, yeast-two hybrid screening was performed to elucidate the anti-WSSV action of ALF*Pm*3 (Suraprasit et al., 2014). Several WSSV proteins such as WSSV186, WSSV189, WSSV395, WSSV458, and WSSV471 could interact with ALF*Pm*3 but only WSSV189 was characterized, leaving the other WSSV proteins for further studies. The identified ALF*Pm*3-interacting proteins such as WSSV186 and WSSV471 were further characterized by Western blot analysis and immunoelectron microscopy (IEM). The aim of this study, therefore, is to elucidate how the ALF*Pm*3 acts on WSSV. The protein-protein interaction between the viral proteins, WSSV186, WSSV395, WSSV458, and WSSV471, and ALF*Pm*3 was confirmed using *in vitro* pull-down assay. The WSSV-neutralizing activity of the rALF*Pm*3 after pre-incubation of each WSSV protein with ALF*Pm*3 was tested in order to further prove the genuine interaction between the ALF*Pm*3 and these WSSV proteins. In addition, the demolishing of the WSSV virion by rALF*Pm*3 was also studied by IEM.

2. Materials and methods

2.1. Shrimp and WSSV challenge

The *P. monodon* (average weight of 4–6 g) were purchased from a local shrimp farm in Chachoengsao province, Thailand. The shrimp were acclimatized in the laboratory aquaria at 28 ± 4 °C and a salinity of 15 ppt for at least 2 weeks before use in each experiment.

The WSSV stock for the experimental infection was prepared according to the method described by Xie and Yang, 2005 and diluted with the TN buffer (20 mM Tris-HCl pH 7.4 and 400 mM NaCl). One microliter of WSSV stock was serially diluted with the TN buffer to 1×10^{-9} dilution. Fifty microliters of the diluted WSSV was injected into the second abdominal segment of the shrimp. This dosage resulted in 100% shrimp mortality within 5 days (data not shown).

2.2. Expression and purification of recombinant proteins

In this research, four recombinant ALF*Pm*3-interacting proteins from WSSV, WSSV186 (rWSSV186), WSSV395 (rWSSV395), WSSV458 (rWSSV458), and WSSV471 (rWSSV471) were expressed in the *Escherichia coli* expression system and purified as described in supplementary data. The purified rALF*Pm*3 protein was prepared according to the method described by Suraprasit et al., 2014.

To produce the WSSV proteins tagged with 6 × His-tag (rWSSV186, rWSSV395, rWSSV458, and rWSSV471), each recombinant clone was constructed. Expression and purification of each rWSSV protein with hexahistidine (His6) at its N-terminus were carried out under native conditions as previously described (Suraprasit et al., 2014). The rWSSV186 and rWSSV395 proteins were dialyzed and further purified using DEAE Sepharose fast flow (GE Healthcare). The fractions containing the expected recombinant WSSV proteins were pooled. The purified proteins were finally dialyzed against 20 mM Tris-HCl pH 7.4. Five hundred micrograms of purified rWSSV186 and rWSSV471 proteins were used to immunize a mouse for polyclonal antibody production at the Biomedical Technology Research Unit, Chiang Mai University, Thailand.

2.3. In vitro pull-down assay

In vitro pull-down assays were modified on the basis of described protocols (Suraprasit et al., 2014). For one *in vitro* reaction, 300 μg of rWSSV395 protein was incubated with DEAE Sepharose fast flow (GE Healthcare) at 4 °C for 1 h with gentle rocking motion on a rotating platform with the DEAE beads pre-equilibrated with the wash solution (50 mM Tris-HCl, pH 7.4 containing 200 mM NaCl). Excess rWSSV395 was removed by centrifugation. Then, 30 μg of the rALF*Pm*3 protein, the prey protein, was incubated in rWSSV395 bound-DEAE beads at 4 °C for 1 h with gentle rocking motion. The unbound rALF*Pm*3 was removed from the column by centrifugation. The protein-protein complex of rALF*Pm*3 and rWSSV395 was eluted by adding 150 μl of the elution buffer (50 mM Tris-HCl, pH 7.4 containing 500 mM NaCl) and incubated with gentle rocking motion at 4 °C for 1 h. Following centrifugation, the protein-protein complex fraction was collected. For other *in vitro* reactions, each rWSSV (rWSSV186, rWSSV458, and rWSSV471) was tested using Ni Sepharose 6 Fast Flow bead (GE Healthcare). The Ni beads were equilibrated with wash solution (50 mM Tris-HCl, pH 7.2 and 150 mM NaCl containing 40 mM imidazole). After immobilization of rWSSV proteins and rALF*Pm*3 incubation, as described above, the protein-protein complexes of rALF*Pm*3 and rWSSVs were eluted by adding 150 μl elution buffer (50 mM Tris-HCl, pH 7.2 and 150 mM NaCl containing 500 mM imidazole).

To check the ALF*Pm*3-WSSV interaction, Western blot analysis was performed using polyclonal anti-WSSV antisera for rWSSV186, rWSSV458, and rWSSV471 and anti-His antibody (EMD Millipore) for rWSSV395 as a primary antibody and horseradish peroxidase-conjugated goat anti-mouse IgG (EMD Millipore) as a secondary antibody at the dilution of 1:5000 and 1:10,000, respectively. For rALF*Pm*3 detection, the polyclonal anti-rALF*Pm*3 antiserum was used as a primary antibody and alkaline phosphatase-conjugated goat anti-rabbit IgG (EMD Millipore) as a secondary antibody at the dilution of 1:10,000 and 1:10,000, respectively. The bait control column used was the DEAE beads or Ni beads incubated under the same condition as above except that the rALF*Pm*3 incubation was

omitted. The prey control column used was similar to the experiment for the protein-protein complex assay but each rWSSV protein was omitted.

2.4. Localization of structural proteins on WSSV virion

The purified WSSV used for the localization experiments were provided by Dr. Han Ching Wang, National Cheng Kung University, Tainan, Taiwan. It was prepared from crayfish, *Procambarus clarkii*, as described by Xie and Yang, 2005.

To localize the WSSV proteins, intact WSSV virions were fractionated into envelope and nucleocapsid parts by treatment with Triton X-100 (Tsai et al., 2004). Ten micrograms of purified WSSV virions and protein fraction of envelope and nucleocapsid were separated on 12.5% SDS-PAGE. The WSSV186 and WSSV471 proteins were detected by Western blot analysis. The membrane was incubated with purified polyclonal mouse anti-WSSV186 (1:5000) and -WSSV471 (1:5000) antibodies as primary antibodies at 4 °C overnight. Then, it was incubated with horseradish peroxidase-conjugated goat anti-mouse IgG, the secondary antibody, at the dilution of 1:5000 for 1 h at room temperature. Western Lightning® Plus-ECL (Perkin Elmer, Inc.) was applied for protein detection by chemiluminescence.

2.5. Immunoelectron microscopy (IEM)

Ten microliter aliquots of purified WSSV virion suspension prepared from *P. clarkii* were adsorbed to the Formvar-supported, carbon-coated nickel grids (300 mesh) for 5 min at room temperature, and the excess solution was removed. The grids were blocked with the blocking buffer (5% bovine serum albumin, 5% normal goat serum, 0.1% cold-water fish skin gelatin (Aurion), 10 mM phosphate buffer pH 7.4 and 150 mM NaCl) for 30 min (Suraprasit et al., 2014).

Prior to incubation with the primary antibody, the grids were incubated with incubation buffer (0.1% Aurion BSA-c, 15 mM NaN_3, 10 mM phosphate buffer pH 7.4 and 150 mM NaCl) for 5 min. Either the purified mouse anti-WSSV186 polyclonal antibody or the purified mouse anti-WSSV471 polyclonal antibody diluted 1:40 in the incubation buffer were added and incubated for 2 h at room temperature. As a control, an additional grid containing WSSV virions was incubated with a dilution of preimmune mouse serum. After three washes with the incubation buffer, the grids were incubated for 1 h at room temperature with a goat anti-mouse secondary antibody conjugated with 18-nm-diameter gold particles (1:100 dilution in the incubation buffer). The grids were then washed three times with incubation buffer, then with distilled water to remove the excess salt, and stained with 1% phosphotungstic acid pH 7.2 for 4 min. Specimens were examined with a transmission electron microscope (JEOL JEM-1400 electron microscope).

2.6. Topology prediction and 3D models

The amino acid sequences for WSSV186 (accession no. AAL89054), WSSV189 (accession no. AAL89057), WSSV395 (accession no. AAL89263), WSSV458 (accession no. AAL89326), and WSSV471 (accession no. AAL89339) were downloaded from GenBank (http://ncbi.nlm.nih.gov). The web-versions of four different topology prediction methods were used to model the five structural proteins: SOSUI (http://harrier.nagahama-i-bio.ac.jp/sosui/), TMHMM (http://www.cbs.dtu.dk/services/TMHMM-2.0/), TMpred (http://www.ch.embnet.org/software/TMPRED_form.html), and DAS (http://www.sbc.su.se/~miklos/DAS/). Based on the interaction data between WSSV proteins from Sangsuriya et al., 2014, graphics of the 3D model of the viral protein complex were drawn.

2.7. Neutralizing activity

In these experiments, 10 shrimp of 3–5 g body weight were used for each group. For the WSSV-infected control group, 50 μl purified WSSV in TN buffer with a final concentration of 1×10^{-9} was injected into the second abdominal segment of the shrimp. Control shrimp were injected with TN buffer only. The test groups were incubated with mixtures of rWSSV proteins and rALF*Pm*3 at 1:1 M ratio for 10 min and then incubated with an equal concentration of WSSV for another 30 min before being injected into the shrimp. In order to prove that the rWSSV proteins used here have no effect on WSSV infection, shrimp were injected with purified WSSV pre-incubated with the same concentrations of rWSSV proteins used in the test groups for 30 min.

The glutathione-S-transferase (GST) protein was used in place of rWSSV proteins as a control protein for the test group. The survival of shrimp was observed every 12 h post WSSV infection for the duration of 10 days. The experiment was performed in triplicate. The flowchart showing the experimental groups are shown in Fig. 1.

2.8. Transmission electron microscopy (TEM)

The effect of rALF*Pm*3 treatment on WSSV virions was observed using transmission electron microscope (TEM). Ten microliter aliquots of purified WSSV virion suspension were incubated with 0, 1, 10, 100, and 250 nM rALF*Pm*3 on carbon-coated cobalt grids (300 mesh) for 10 min at room temperature. The grids were stained with 1% phosphotungstic acid (PTA) pH 7.2. Samples grids were examined with a TEM (JEOL JEM-1400 electron microscope). The GST protein at a final concentration of 250 nM was used as a control.

3. Results

3.1. Expression and purification of recombinant WSSV proteins (rWSSV) and the recombinant ALFPm3 protein (rALFPm3)

To confirm the interaction between rALF*Pm*3 and rWSSV proteins, the recombinant proteins including rWSSV186, rWSSV395, rWSSV458, and rWSSV471 were produced in *E. coli* expression system. The crude proteins were purified using Ni-NTA for rWSSV458 and WSSV471 and both Ni-NTA and DEAE for rWSSV186 and rWSSV395. The results showed that the purified rWSSV186 (Fig. 2A), rWSSV395 (Fig. 2B), rWSSV458 (Fig. 2C), and rWSSV471 (Fig. 2D) proteins were detected with the expected size of about 58, 38, 26, and 20 kDa, respectively.

On the other hand, the rALF*Pm*3 was produced from *Pichia pastoris* expression system, purified and shown to have the expected size of about 11.3 kDa (data not shown). Antibacterial activity against *Escherichia coli* 363 and *Bacillus megaterium* of the purified-rALF*Pm*3 protein was tested and shown to have the minimum inhibitory concentration (MIC) values of 0.095–0.19 and 0.19–0.39 μM, respectively (data not shown). The purified ALF*Pm*3 protein was used for the *in vitro* pull-down assay and the study on the binding effect of rWSSV proteins on WSSV-neutralizing activity of rALF*Pm*3.

3.2. Protein-protein interaction assay between rWSSV proteins and rALFPm3 by in vitro pull-down assay

The interaction of ALF*Pm*3 with five WSSV proteins including WSSV186, WSSV189, WSSV395, WSSV458, and WSSV471 was identified by yeast two-hybrid screening (Suraprasit et al., 2014). However, the protein-protein interaction was confirmed for only the WSSV189. In this experiment, the protein-protein interaction between the rest of WSSV proteins and ALF*Pm*3 was further

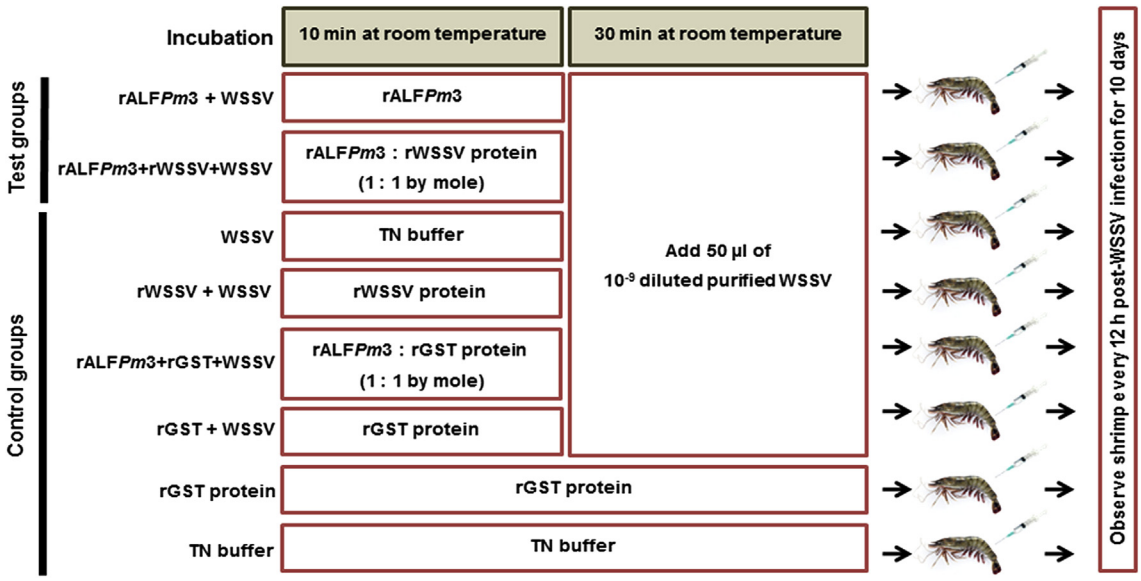


Fig. 1. The experimental design for neutralization activity assay. Eight groups of shrimp were injected with pre-incubated solutions under the conditions described. The rALF*Pm*3, rALF*Pm*3-rWSSV (1:1 by mole), TN buffer, rWSSV, rALF*Pm*3-rGST (1:1 by mole), or rGST mixture were incubated at room temperature for 10 min then 50 µl of 1×10^{-9} diluted WSSV was added to the protein mixtures and incubated at room temperature for 30 min except only the rGST or TN buffer control that was incubated at room temperature for 40 min. After pre-incubating, the mixtures were injected into the tested shrimp groups, 10 shrimp per group. The survival rate was observed every 12 h after WSSV infection for 10 days.

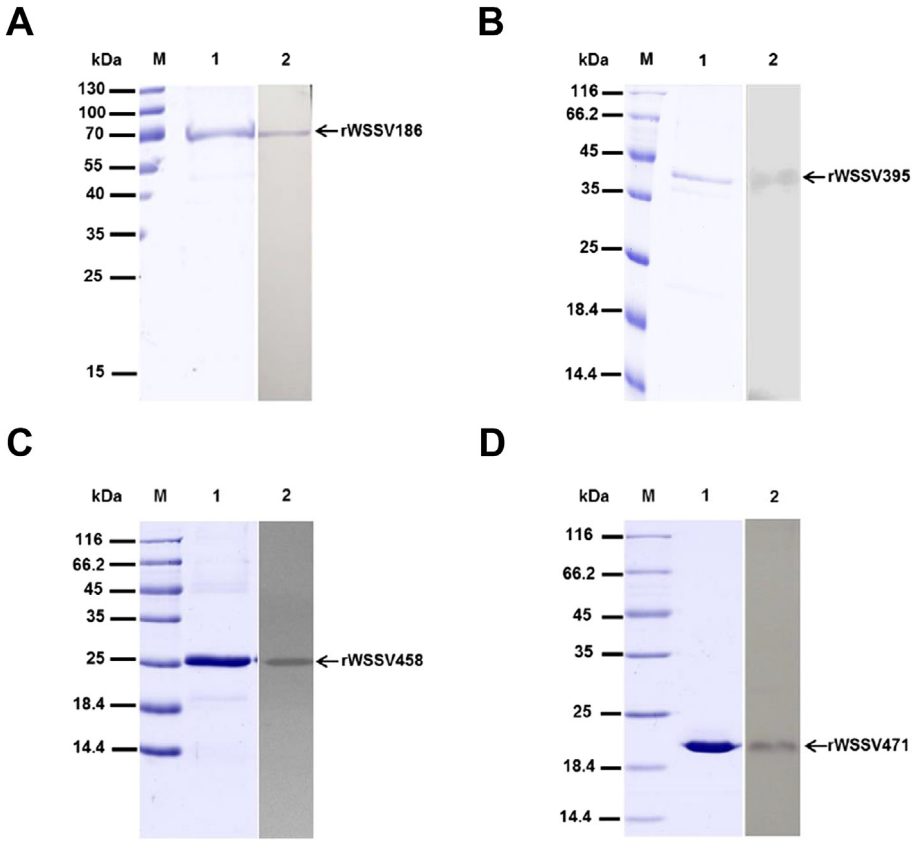


Fig. 2. SDS-PAGE and Western blot analysis of the purified recombinant WSSV proteins. The purified rWSSV proteins including rWSSV186 (A), rWSSV395 (B), rWSSV458 (C), and rWSSV471 (D) were separated by 15% coomassie blue stained- SDS–PAGE (Lane 1) and analyzed by Western blot analysis (Lane 2) using the polyclonal anti-His antibody as a primary antibody and the goat anti-mouse IgG antibody conjugated with alkaline phosphatase as secondary antibody. Lane M is the protein molecular weight marker.

confirmed by using *in vitro* pull-down assay. As shown in Fig. 3, the Ni-NTA bead or DEAE bead effectively pulled-down the protein-protein complexes of rWSSV proteins with rALF*Pm*3 including rWSSV186 (Fig. 3A), rWSSV395 (Fig. 3B), rWSSV458 (Fig. 3C), and rWSSV471 (Fig. 3D). The results indicated that all the rWSSV proteins could specifically bind to rALF*Pm*3 *in vitro*.

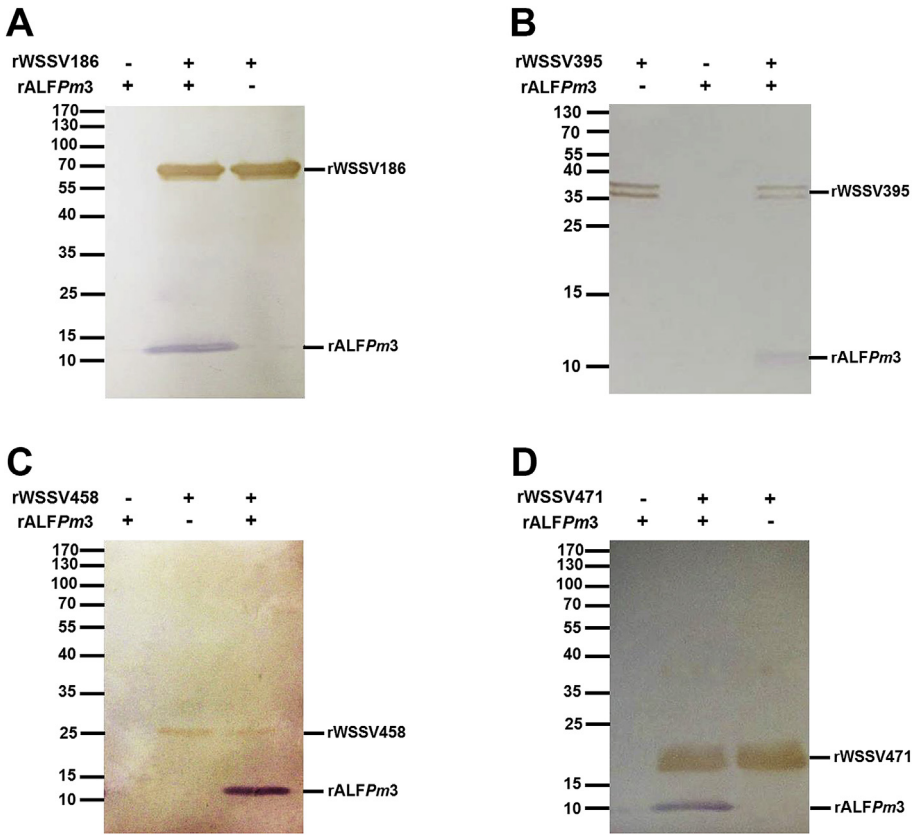


Fig. 3. *In vitro* pull-down assay of protein-protein interaction between the WSSV proteins and rALF*Pm*3. The rWSSV186 (A), rWSSV395 (B), rWSSV458 (C), or rWSSV471 (D) was assayed for their binding to the rALF*Pm*3. The protein-protein complexes were separated by 15% SDS-PAGE and analyzed by Western blotting using anti-His antibody for rWSSV395 and antibody specific to rWSSV186, rWSSV458, rWSSV471, and rALF*Pm*3.

3.3. Localization of WSSV186 and WSSV471 on WSSV

Among the ALF*Pm*3-interacting proteins, WSSV189 and WSSV395 are characterized as envelope proteins, and WSSV458 is known as a tegument protein (Jaree et al., 2016; Suraprasit et al., 2014; Zhu et al., 2006). Previously, WSSV186 and WSSV471 were identified as WSSV structural proteins (Tsai et al., 2004); however, the locations of these proteins were still unknown. Here, the localization of WSSV186 and WSSV471 proteins were investigated on the intact virions, envelope and nucleocapsid protein fractions of WSSV by Western blot analysis using purified WSSV186- and WSSV471- polyclonal antibodies. The VP28, the known envelope protein, was used as a marker for WSSV fractionation.

The result revealed that the WSSV186 protein was detected on the intact WSSV and nucleocapsid fraction. The WSSV471 protein was detected on the intact WSSV and envelope fraction (Fig. 4A). Moreover, the immumoelectron microscopy technique was performed to confirm the locations of these WSSV proteins. The electron micrograph showed that the position of gold particle-labeled-WSSV186 protein was located on the nucleocapsid part of WSSV. The position of gold particle-labeled-WSSV471 protein was located on the envelope part of WSSV (Fig. 4B). Therefore, we conclude here that the WSSV186 is a nucleocapsid protein whereas the WSSV471 is an envelope protein.

3.4. Binding effect of the rWSSV186, rWSSV395, rWSSV458, and rWSSV471 proteins on the WSSV-neutralizing activity of rALFPm3 protein

To test the significance of the WSSV protein-ALF*Pm*3 interaction, the WSSV proteins were tested against the neutralization activity of ALF*Pm*3 on WSSV. Herein, each rWSSV-rALF*Pm*3 protein mixture was injected along with WSSV into the shrimp. Then, the survival of shrimp was observed (Fig. 6).

For the shrimp injected with only TN buffer, no shrimp died during the observation period of 10 days. The WSSV pre-incubated with rWSSV186, rWSSV395, rWSSV458, or rWSSV471 also killed the shrimp like injected with WSSV alone. This indicated that all exogenous rWSSV proteins had no effect on WSSV infectivity. In this experiment, recombinant GST protein was used as control. Injection of GST with either WSSV alone or rALF*Pm*3-WSSV mixture, did not affect to the WSSV infectivity and rALF*Pm*3 activity (Fig. 6E).

In WSSV-infected shrimp, the percentage of shrimp survival decreased to 0% within 5 days. On the other hand, WSSV neutralized with rALF*Pm*3 group, shrimp survived about 20% after day 10 of WSSV infection. In the experimental groups, pre-incubation of rWSSV186 (Fig. 6A), rWSSV395 (Fig. 6B), rWSSV458 (Fig. 6C), and rWSSV471 (Fig. 6D) with the rALF*Pm*3 diminished the WSSV-neutralizing activity of the rALF*Pm*3 protein; a 0% survival was observed in 7–9 days.

3.5. Effect of rALFPm3 treatment on WSSV virions

To investigate the effect of rALF*Pm*3 treatment on WSSV virions, the WSSV was incubated with various concentrations of rALF*Pm*3 protein (1, 10, 100, and 250 nM) and then examined under TEM. Treating the WSSV with the rALF*Pm*3 resulted in the breakage of the envelope of WSSV virions (Fig. 7). The higher the concentration of rALF*Pm*3 used, the more extensive the level of WSSV virion

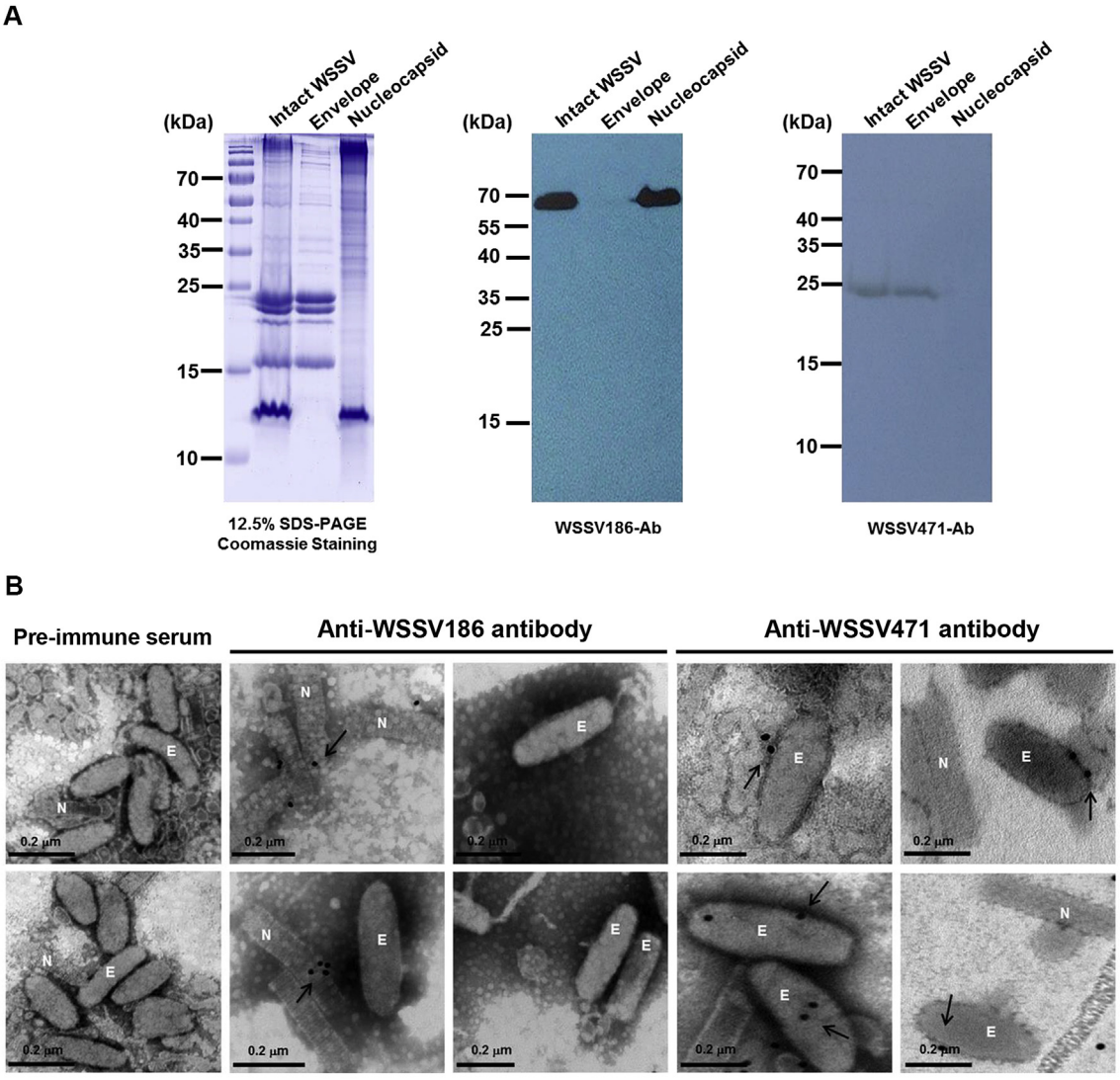


Fig. 4. Localization of WSSV186 and WSSV471 on WSSV virions. Triton X-100 treatment was used to fractionate the WSSV virions into envelope and nucleocapsid protein fractions. Both fractions were separated on 12.5% coomassie blue stained- SDS–PAGE and Western blotting using the purified polyclonal antibody specific to WSSV186 and WSSV471 (A). In addition, IEM was performed using the purified anti-WSSV186 or anti-WSSV471 antibody as a primary antibody and a gold-labeled secondary antibody to detect WSSV186 or WSSV471 on the WSSV virions. As compared to the control using pre-immune serum where the gold particle was undetectable, the positive signals were observed on the nucleocapsid for WSSV186 and envelope for WSSV471 of the virions as indicated by black arrows (B). Letters E and N indicate intact virions and nucleocapsid, respectively.

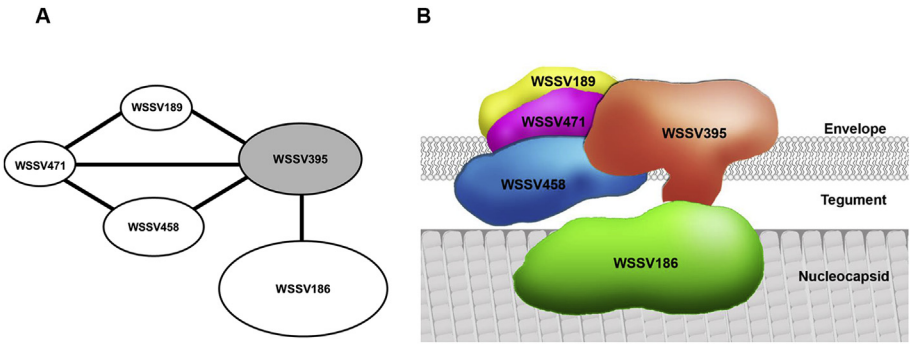


Fig. 5. Matrix diagram and 3D model of the ALF*Pm*3-interacting WSSV protein complex. Base on the data from the WSSV proteins interaction map reported previously (Sangsuriya et al., 2014), the matrix diagram (A) and its side view of the 3D model (B), are illustrated the ALF*Pm*3-interacting WSSV proteins.

damage was observed. As compared to the control, the envelope of WSSV virions was tattered and the WSSV became naked; only nucleocapsid was observed. Furthermore, the morphology of nucleocapsid was changed and bloated. The results indicated that the rALF*Pm*3 fought against WSSV by binding to the structural proteins on the WSSV envelope and nucleocapsid leading to the

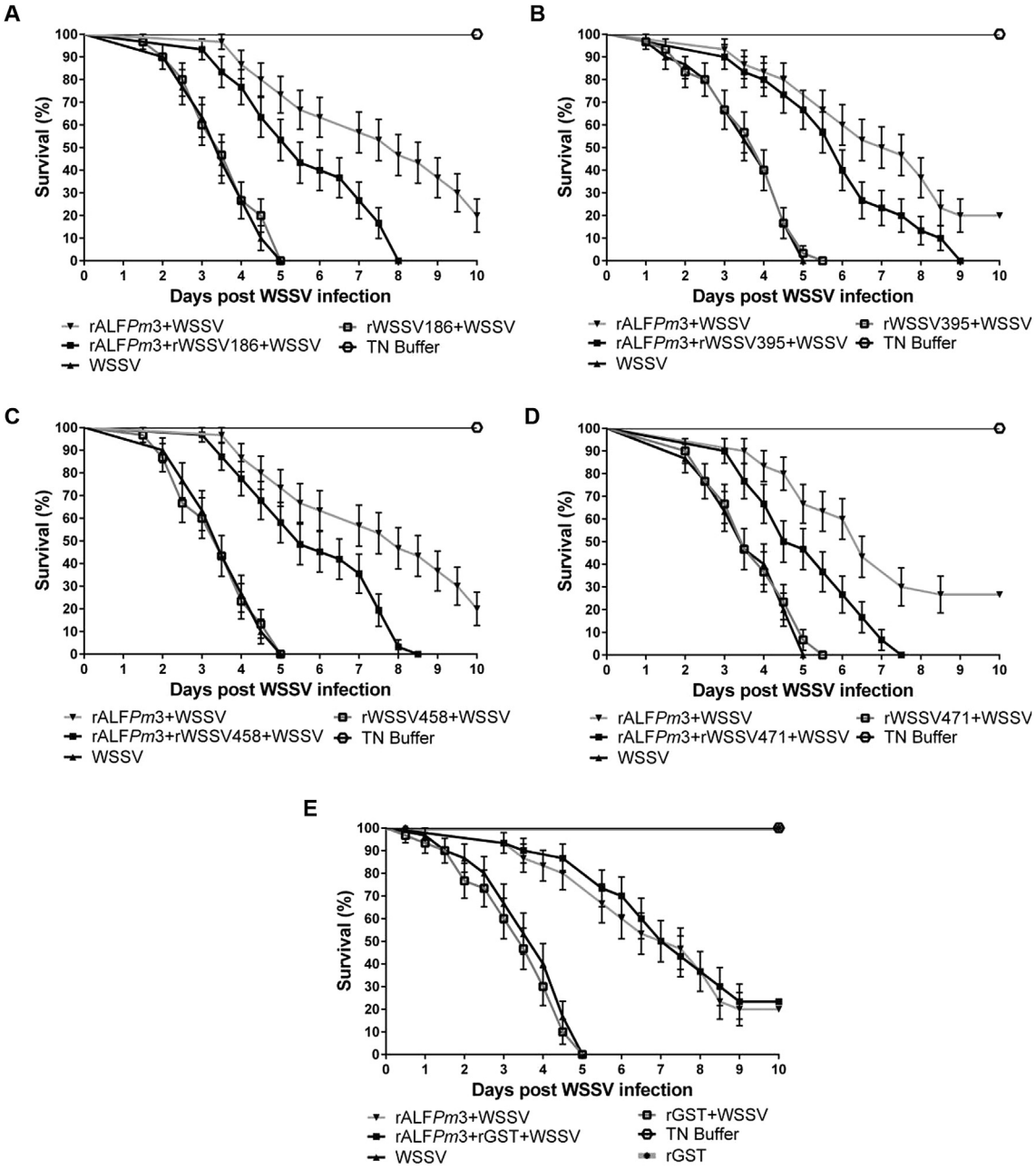


Fig. 6. Effect of the rWSSV proteins on the WSSV-neutralizing activity of rALF*Pm*3 protein. The rWSSV proteins are rWSSV186 (A), rWSSV395 (B), rWSSV458 (C), and rWSSV471 (D). Survival rates of the shrimp groups after challenged with TN buffer, WSSV pre-incubated with rWSSV proteins, WSSV only, WSSV pre-incubated with a mixture of rALF*Pm*3 and rWSSV proteins, and WSSV pre-incubated with rALF*Pm*3 were observed every 12 h post-WSSV infection for 10 days. The rGST protein was used instead of rWSSV proteins in a control group (E).

instability of envelope and nucleocapsid structures and breaking up the WSSV virions.

4. Discussion

The antimicrobial protein ALF*Pm*3 displays broad activity against bacteria, fungi and viruses especially the marine pathogens *V. harveyi* (Somboonwiwat et al., 2005), *V. parahaemolyticus* AHPND causing early mortality syndrome (Supungul et al., 2015) and WSSV (Tharntada et al., 2009). While the mode of action of ALF*Pm*3 on *V. harveyi* has been known through bacterial membrane permeabilization as shown by damaged morphological structure of bacterial cells after rALF*Pm*3 treatment (Jaree et al., 2012), that of ALF*Pm*3 on WSSV still needs to be explored. Previously, the yeast two-hybrid experiment showed that ALF*Pm*3 interacts with five WSSV proteins namely WSSV186, WSSV189, WSSV395, WSSV458, and WSSV471. Our previous study has confirmed that ALF*Pm*3 interacts with WSSV189 providing a clue to our understanding of how ALF*Pm*3 acts on WSSV (Suraprasit et al., 2014). The genuine interactions between ALF*Pm*3 and all WSSV-interacting proteins, however, need to be confirmed to elucidate the antiviral mechanisms of ALF*Pm*3. In this study, the recombinant proteins of WSSV186, WSSV395, WSSV458, and WSSV471 were successfully produced and purified. The interactions between ALF*Pm*3 and these WSSV proteins were investigated by the pull-down assay. It was found that all five WSSV proteins, WSSV186, WSSV189, WSSV395,

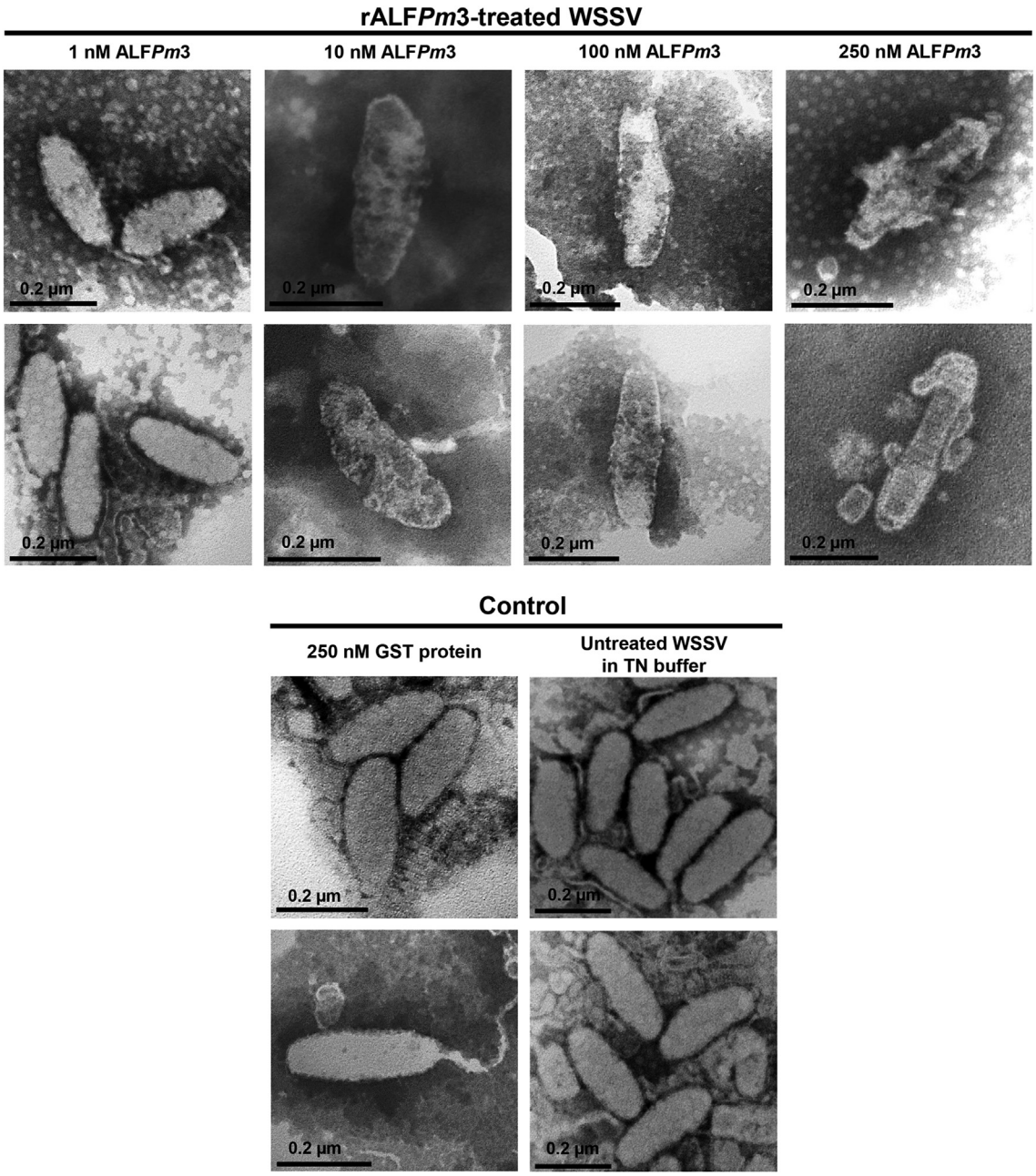


Fig. 7. Effect of rALF*Pm*3 treatment on WSSV virions. The purified-WSSV was incubated with 0, 1, 10, 100, or 250 nM rALF*Pm*3 or 250 nM rGST as a control on the cobalt grids. The 1% PTA was used for staining the viral particles. The morphology of WSSV virions was observed by transmission electron microscopy.

WSSV458, and WSSV471 interact specifically with ALF*Pm*3.

About 40 WSSV proteins have been previously characterized. Most of these proteins are structural proteins in the envelope, tegument and nucleocapsid. Some WSSV proteins that act as non-structural proteins are involved in transcriptional regulation, virus proliferation and regulation of DNA replication (Escobedo-Bonilla et al., 2008). In 2004, liquid chromatography–nano-electrospray ionization tandem mass spectrometry (LC-nanoESI-MS/MS) was performed to identify WSSV proteins (Tsai et al., 2004). They found 39 structural proteins of WSSV including WSSV395. A shotgun proteomic study of WSSV revealed that the WSSV186 and WSSV189 are WSSV structural proteins (Li et al., 2007). Western blot analysis and immunoelectron microscopy showed that WSSV395 and WSSV189 are envelope proteins and WSSV458 is a tegument protein of WSSV (Jaree et al., 2016; Suraprasit et al., 2014; Zhu et al., 2006). Herein, we showed that WSSV186 and WSSV471 are located at the nucleocapsid and envelope parts of WSSV, respectively. All five WSSV proteins that interact with ALF*Pm*3 are, therefore, structural proteins of WSSV.

Interactions between the structural proteins are typically found in enveloped viruses. The viral proteins might form complexes that have specific roles in host-viral interactions or the infectivity of viruses. The membrane-associated model of WSSV structural protein complex, called an infectome, has already been identified, where VP24 acts as a core protein that is conjugated with other WSSV structural proteins. This infectome is believed to play a role in cell recognition and might be involved in viral entry mechanism (Chang et al., 2010). In case of host-viral protein interaction, the

relationship between shrimp chitin binding protein (CBP) and the envelope protein complex including VP24, VP28, VP31, VP32 VP39B, VP53A, and VP56, was recently investigated and shown that CBP plays an important role in virus attachment (Huang et al., 2014). According to our findings and data from the protein-protein interaction network of WSSV constructed by Sangsuriya et al., 2014, it is possible that these five ALF*Pm*3-interacting proteins interact with each other forming a complex that is the target molecule of ALF*Pm*3. Therefore, the proposed model of the ALF*Pm*3-interacting protein complex composing of the envelope core protein, WSSV395, and other envelope, tegument, and nucleocapsid proteins was constructed (Fig. 5). Further research, however, is required to confirm this tentative model.

To date, no data have demonstrated a clear relationship between the structural groups of an antimicrobial peptide (AMP) and its mode of action, the degree of activity, or the host range. The structure, size, charge, hydrophobicity, amphipathicity, and solubility are all crucial for the antimicrobial activities and target specificity of AMPs (Bahar and Ren, 2013). The 3D structure of ALF*Pm*3 contains three α-helices packed against four strands of β-sheet. By comparative molecular modeling, the hypothetical LPS-binding domain consists of six positively charged amino acid residues (four Lys and two Arg) (Yang et al., 2009). So far, none of 3D-structure of ALF*Pm*3-interacting WSSV proteins has been reported, whilst analysis of all WSSV proteins showed that only primary structure of WSSV189 and WSSV471 proteins contains a series of aspartate and glutamate negatively charged residues (Asp^{103}-Ile^{104}-Glu^{105}-Asp^{106}-Asp^{107}) (Suraprasit et al., 2014) and (Glu^{27}-Glu^{28}-Glu^{29}-Glu^{30}), respectively. We hypothesized that, if the negatively charged residues of WSSV189 and WSSV471 located on the protein surface, the ALF*Pm*3 would interact with them via electrostatic interaction. However, how ALF*Pm*3 interacts with each WSSV protein-interacting partner should be further investigated.

The cationic antiviral peptides have several mechanisms that can prevent viral infection including blocking of viral entry into the cell, suppression of cell fusion, suppression of viral gene expression, inhibition of peptide chain elongation, binding of peptides to viral proteins causing inhibition of adsorption or virus-cell fusion, and activation of an immune modulatory pathway (Mulder et al., 2013). Our results indicated that each of ALF*Pm*3 interacting WSSV protein hindered the neutralizing ALF*Pm*3 antiviral activity resulting in lower shrimp survival. Moreover, the neutralization activity assay showed the independent interaction between ALF*Pm*3 and each WSSV protein. TEM micrographs also showed that the purified-WSSV virions incubated with ALF*Pm*3 have undergone a morphological change on their envelope and nucleocapside parts. Hence, we concluded that the ALF*Pm*3 directly interacts with a complex of structural proteins on the WSSV virions and prevents the WSSV infection in shrimp.

In conclusion, ALF*Pm*3 exhibits antiviral activity against WSSV by binding to the complex of WSSV structural proteins and causes severe damages on the integrity of WSSV virions, which in turn reduces the infectivity of WSSV. Consequently, ALF*Pm*3 is a highly potent immune molecule in the defense against WSSV infection, and can potentially be applied for disease control in aquaculture.

Acknowledgements

We acknowledged Dr. Han Ching Wang who kindly provided us the intact WSSV. We thank Prof. Dr. Vichien Rimphanitchayakit for useful comments on the manuscript. This work was supported by research grant from Chulalongkorn University under the 90th Anniversary of Chulalongkorn University Fund (Ratchadaphiseksomphot Endowment Fund) to TM. This research was also partially supported by the project "Development of Aquaculture Technology for Food Security and Food Safety in the Next Generation" under JST-JICA joint program "Science and Technology Research Partnership for Sustainable Development, SATREPS" and the Thailand Research Fund (TRF)(TRF Senior Scholar No. RTA5880004 and IRG5780008).

Appendix A. Supplementary data

Supplementary data related to this article can be found at http://dx.doi.org/10.1016/j.dci.2016.11.023.

References

Bahar, A.A., Ren, D., 2013. Antimicrobial peptides. Pharmaceuticals 6, 1543–1575.
Chang, Y.S., Liu, W.J., Lee, C.C., Chou, T.L., Lee, Y.T., Wu, T.S., Huang, J.Y., Huang, W.T., Lee, T.L., Kou, G.H., Wang, A.H., Lo, C.F., 2010. A 3D model of the membrane protein complex formed by the white spot syndrome virus structural proteins. PLoS ONE 5, e10718.
Escobedo-Bonilla, C.M., Alday-Sanz, V., Wille, M., Sorgeloos, P., Pensaert, M.B., Nauwynck, H.J., 2008. A review on the morphology, molecular characterization, morphogenesis and pathogenesis of white spot syndrome virus. J. Fish. Dis. 31, 1–18.
Huang, P.Y., Leu, J.H., Chen, L.L., 2014. A newly identified protein complex that mediates white spot syndrome virus infection via chitin-binding protein. J. Gen. Virol. 95, 1799–1808.
Jaree, P., Senapin, S., Hirono, I., Lo, C.F., Tassanakajon, A., Somboonwiwat, K., 2016. WSV399, a viral tegument protein, interacts with the shrimp protein *Pm*VRP15 to facilitate viral trafficking and assembly. Dev. Comp. Immunol. 59, 177–185.
Jaree, P., Tassanakajon, A., Somboonwiwat, K., 2012. Effect of the anti-lipopolysaccharide factor isoform 3 (ALF*Pm*3) from *Penaeus monodon* on *Vibrio harveyi* cells. Dev. Comp. Immunol. 38, 554–560.
Li, C., Zhao, J., Song, L., Mu, C., Zhang, H., Gai, Y., Qiu, L., Yu, Y., Ni, D., Xing, K., 2008. Molecular cloning, genomic organization and functional analysis of an anti-lipopolysaccharide factor from Chinese mitten crab *Eriocheir sinensis*. Dev. Comp. Immunol. 32, 784–794.
Li, Z., Lin, Q., Chen, J., Wu, J.L., Lim, T.K., Loh, S.S., Tang, X., Hew, C.L., 2007. Shotgun identification of the structural proteome of shrimp white spot syndrome virus and iTRAQ differentiation of envelope and nucleocapsid subproteomes. Mol. Cell. Proteomics 6, 1609–1620.
Liu, B., Tang, X., Zhan, W., 2011. Interaction between white spot syndrome virus VP26 and hemocyte membrane of shrimp, *Fenneropenaeus chinensis*. Aquaculture 314, 13–17.
Liu, H., Jiravanichpaisal, P., Söderhäll, I., Cerenius, L., Söderhäll, K., 2006. Anti-lipopolysaccharide factor interferes with white spot syndrome virus replication in vitro and in vivo in the crayfish *Pacifastacus leniusculus*. J. Virol. 80, 10365–10371.
Mulder, K.C., Lima, L.A., Miranda, V.J., Dias, S.C., Franco, O.L., 2013. Current scenario of peptide-based drugs: the key roles of cationic antitumor and antiviral peptides. Front. Microbiol. 4, 321.
Ongvarrasopone, C., Chanasakulniyom, M., Sritunyalucksana, K., Panyim, S., 2008. Suppression of PmRab7 by dsRNA inhibits WSSV or YHV infection in shrimp. Mar. Biotechnol. (NY) 10, 374–381.
Ponprateep, S., Tharntada, S., Somboonwiwat, K., Tassanakajon, A., 2012. Gene silencing reveals a crucial role for anti-lipopolysaccharide factors from *Penaeus monodon* in the protection against microbial infections. Fish. Shellfish Immunol. 32, 26–34.
Sangsuriya, P., Huang, J.Y., Chu, Y.F., Phiwsaiya, K., Leekitcharoenphon, P., Meemetta, W., Senapin, S., Huang, W.P., Withyachumnarnkul, B., Flegel, T.W., Lo, C.F., 2014. Construction and application of a protein interaction map for white spot syndrome virus (WSSV). Mol. Cell. Proteomics 13, 269–282.
Sangsuriya, P., Senapin, S., Huang, W.P., Lo, C.F., Flegel, T.W., 2011. Co-interactive DNA-binding between a novel, immunophilin-like shrimp protein and VP15 nucleocapsid protein of white spot syndrome virus. PloS ONE 6, e25420.
Somboonwiwat, K., Marcos, M., Tassanakajon, A., Klinbunga, S., Aumelas, A., Romestand, B., Gueguen, Y., Boze, H., Moulin, G., Bachère, E., 2005. Recombinant expression and anti-microbial activity of anti-lipopolysaccharide factor (ALF) from the black tiger shrimp *Penaeus monodon*. Dev. Comp. Immunol. 29, 841–851.
Sritunyalucksana, K., Utairungsee, T., Sirikharin, R., Srisala, J., 2013. Reprint of: virus-binding proteins and their roles in shrimp innate immunity. Fish. Shellfish Immunol. 34, 1018–1024.
Sritunyalucksana, K., Wannapapho, W., Lo, C.F., Flegel, T.W., 2006. PmRab7 is a VP28-binding protein involved in white spot syndrome virus infection in shrimp. J. Virol. 80, 10734–10742.
Supungul, P., Jaree, P., Somboonwiwat, K., Junprung, W., Proespraiwong, P., Mavichak, R., Tassanakajon, A., 2015. A potential application of shrimp anti-lipopolysaccharide factor in disease control in aquaculture. Aquac. Res. http://dx.doi.org/10.1111/are.12925.
Suraprasit, S., Methatham, T., Jaree, P., Phiwsaiya, K., Senapin, S., Hirono, I., Lo, C.F., Tassanakajon, A., Somboonwiwat, K., 2014. Anti-lipopolysaccharide factor isoform 3 from *Penaeus monodon* (ALF*Pm*3) exhibits antiviral activity by

interacting with WSSV structural proteins. Antivir. Res. 110, 142–150.
Tassanakajon, A., Klinbunga, S., Paunglarp, N., Rimphanitchayakit, V., Udomkit, A., Jitrapakdee, S., Sritunyalucksana, K., Phongdara, A., Pongsomboon, S., Supungul, P., Tang, S., Kuphanumart, K., Pichyangkura, R., Lursinsap, C., 2006. *Penaeus monodon* gene discovery project: the generation of an EST collection and establishment of a database. Gene 384, 104–112.
Tassanakajon, A., Somboonwiwat, K., Amparyup, P., 2015. Sequence diversity and evolution of antimicrobial peptides in invertebrates. Dev. Comp. Immunol. 48, 324–341.
Tharntada, S., Ponprateep, S., Somboonwiwat, K., Liu, H., Söderhäll, I., Söderhäll, K., Tassanakajon, A., 2009. Role of anti-lipopolysaccharide factor from the black tiger shrimp, *Penaeus monodon*, in protection from white spot syndrome virus infection. J. Gen. Virol. 90, 1491–1498.
Tsai, J.M., Wang, H.C., Leu, J.H., Hsiao, H.H., Wang, A.H., Kou, G.H., Lo, C.F., 2004. Genomic and proteomic analysis of thirty-nine structural proteins of shrimp white spot syndrome virus. J. Virol. 78, 11360–11370.
Watthanasurorot, A., Jiravanichpaisal, P., Söderhäll, I., Söderhäll, K., 2010. A gC1qR prevents white spot syndrome virus replication in the freshwater crayfish *Pacifastacus leniusculus*. J. Virol. 84, 10844–10851.
Xie, X., Yang, F., 2005. Interaction of white spot syndrome virus VP26 protein with actin. Virology 336, 93–99.
Yang, Y., Boze, H., Chemardin, P., Padilla, A., Moulin, G., Tassanakajon, A., Pugniere, M., Roquet, F., Destoumieux-Garzon, D., Gueguen, Y., Bachère, E., Aumelas, A., 2009. NMR structure of *r*ALF-*Pm3*, an anti-lipopolysaccharide factor from shrimp: model of the possible lipid A-binding site. Biopolymers 91, 207–220.
Youtong, W., Deachamag, P., Phongdara, A., Chotigeat, W., 2011. WSSV: VP26 binding protein and its biological activity. Fish. Shellfish Immunol. 30, 77–83.
Zhang, X., Huang, C., Qin, Q., 2004. Antiviral properties of hemocyanin isolated from shrimp *Penaeus monodon*. Antivir. Res. 61, 93–99.
Zhu, Y.B., Li, H.Y., Yang, F., 2006. Identification of an envelope protein (VP39) gene from shrimp white spot syndrome virus. Arch. Virol. 151, 71–82.

Developmental and Comparative Immunology 67 (2017) 229–238

Contents lists available at ScienceDirect

Developmental and Comparative Immunology

journal homepage: www.elsevier.com/locate/dci

A snake-like serine proteinase (*Pm*Snake) activates prophenoloxidase-activating system in black tiger shrimp *Penaeus monodon*

Warunthorn Monwan [a], Piti Amparyup [a, b], Anchalee Tassanakajon [a, *]

[a] Center of Excellence for Molecular Biology and Genomics of Shrimp, Department of Biochemistry, Faculty of Science, Chulalongkorn University, 254 Phayathai Road, Bangkok 10330, Thailand

[b] National Center for Genetic Engineering and Biotechnology (BIOTEC), National Science and Technology Development Agency (NSTDA), 113 Paholyothin Road, Klong1, Klong Luang, Pathumthani 12120, Thailand

ARTICLE INFO

Article history:
Received 29 July 2016
Received in revised form
26 September 2016
Accepted 26 September 2016
Available online 28 September 2016

Keywords:
Shrimp
Peneaus monodon
Prophenoloxidase
Snake-like serine proteinase

ABSTRACT

Clip domain serine proteinases (ClipSPs) play critical roles in the activation of proteolytic cascade in invertebrate immune systems including the prophenoloxidase (proPO) activating system. In this study, we characterized a snake-like serine protease, namely *Pm*Snake, from the shrimp *Penaeus monodon* which has previously been identified based on the subtractive cDNA library of proPO double-stranded RNA (dsRNA)-treated hemocytes. An open reading frame of *Pm*Snake contains 1068 bp encoding a predicted protein of 355 amino acid residues with a putative signal peptide of 22 amino acids and two conserved domains (N-terminal clip domain and C-terminal trypsin-like serine proteinase domain). Sequence analysis revealed that *Pm*Snake was closest to the *Ae*Snake from ant *Acromyrmex echinatior* (53% similarity), but was quite relatively distant from other shrimp *Pm*clipSPs. *Pm*Snake transcript was mainly expressed in shrimp hemocytes and up-regulated after systemic *Vibrio harveyi* infection indicating that it is an immune-responsive gene. Suppression of *Pm*Snake expression by dsRNA interference reduced both transcript and protein levels leading to a reduction of the hemolymph phenoloxidase (PO) activity (36%), compared to the control, suggesting that the *Pm*Snake functions as a clip-SP in shrimp proPO system. Western blot analysis using anti-*Pm*Snake showed that the *Pm*Snake was detected in hemocytes but not in cell-free plasma. *In vitro* PO activity and serine proteinase activity assays showed that adding r*Pm*Snake into the shrimp hemolymph could increase PO activity as well as serine proteinase activity suggesting that the r*Pm*Snake activates the proPO system via serine proteinase cascade.

© 2016 Elsevier Ltd. All rights reserved.

1. Introduction

The innate immunity is the first line of defense against microbial infections (Hoebe et al., 2004). Invertebrates, which lack immunoglobulin in the adaptive immunity, instead they have innate immune defenses to detect and respond to the microbial surfaces like lipopolysaccharide (LPS), β-1,3-glucan and peptidoglycan (PGN) (Iwanaga and Lee, 2005). One of the most effective humoral defenses is the melanization which is activated by the prophenoloxidase system leading to the synthesis of melanin and reactive intermediate compounds to accumulate or entrap the pathogen (Amparyup et al., 2013a; Cerenius and Söderhäll, 2004). The system requires many steps of non-enzymatic and enzymatic processes that catalyzed or activated the proPO cascade especially the complex cascade of Clip-domain serine proteinases (Clip-SPs). The final enzyme of the cascade namely the proPO-activating enzymes (PPAEs) convert the zymogen proPOs to the functionally active phenoloxidases (POs) which subsequently catalyze the formation of quinone reactive intermediates for melanin synthesis at the injury site or around invading microorganisms (Amparyup et al., 2012; Cerenius and Söderhäll, 2004; Nappi and Christensen, 2005).

Clip domain serine proteinases (Clip-SPs) consist of one or more clip domain(s) at the N-terminus and a SP domain at the C-terminus (Jiang and Kanost, 2000). The biochemical pathway and several associated proteins involved in the shrimp *P. monodon* proPO system activation have been characterized (see review by (Amparyup et al., 2013a)). Two proPOs, *Pm*proPO1 and *Pm*proPO2, as well as *Pm*ClipSP2, *Pm*PPAE1 and *Pm*PPAE2 have been shown to be involved in the shrimp proPO system (Amparyup et al., 2009,

* Corresponding author.
E-mail address: anchalee.k@chula.ac.th (A. Tassanakajon).

http://dx.doi.org/10.1016/j.dci.2016.09.016
0145-305X/© 2016 Elsevier Ltd. All rights reserved.

2013b; Charoensapsri et al., 2009, 2011). However, the activation steps of clip-SPs in the proteinase cascade of the shrimp proPO system have not been clarified. *Pm*ClipSP2 has been demonstrated to act as a pattern recognition protein and likely activate *P. monodon* proPO system (Amparyup et al., 2013b). Thus it is probably an initial proteinase of the serine proteinase cascade while *Pm*PPAE1 and *Pm*PPAE2 were proposed to be the final proteinases in the cascade (Charoensapsri et al., 2009, 2011).

Recently, snake-like serine proteinase (*PmSnake*) gene was identified from the cDNA library of suppression subtractive hybridization of the proPO dsRNA treated hemocytes (Sangsuriya et al., 2016). The *PmSnake* gene shares similarity to *Hemolymph Proteinase 21* (*HP21*) that is involve in the proPO system in tobacco hornworm *Manduca sexta* (Gorman et al., 2007b). Comparing the proPO activation mechanism in shrimp *P. monodon* and insect *M. sexta* (Gorman et al., 2007b), the shrimp *Pm*ClipSP2 and *M. sexta* HP14 function as pattern recognition receptors for recognition of the bacteria or fungal cell wall components. The *M. sexta* HP14 converts proHP21 to active HP21 which in turn activates the melanization cascade. In shrimp, however, the downstream SPs of *Pm*ClipSP2 are still unknown. Thus, the purpose of this study is to investigate the function of snake-like serine proteinase in the shrimp proPO system. Gene expression analysis of *PmSnake* after *Vibrio harveyi* challenge was performed. Its function was investigated by using RNA interference (RNAi) technique and *in vitro* activity assay of the recombinant protein. The results provide a better understanding of shrimp innate immunity, particularly the regulation of the shrimp proPO system through the activation of serine proteinases.

2. Materials and methods

2.1. Shrimp samples

Juvenile healthy shrimp *P. monodon* (2–5 g) were obtained from local farms in southern and eastern parts of Thailand. Shrimp were maintained in the laboratory tanks with seawater, salinity 15–20 ppt, for at least 7 days before proceeding in the experiments. For the temporal expression analysis of bacterial challenge shrimp, shrimp were divided into 2 groups; *V. harveyi*–injected shrimp and NaCl-injected shrimp (control). Shrimp were injected with 2×10^5 CFU of *V. harveyi* strain 639 in 0.85% (w/v) NaCl. Hemolymph from three individual shrimp per time point was collected at 0, 6, 24, 48 and 72 h after injection for each experiment group using 10% (w/v) trisodium citrate as an anticoagulant. Three independent experiments were performed. Hemocytes were separated by centrifugation at 800 × g for 10 min at 4 °C, and then immediately frozen in liquid nitrogen and stored as such until used. Control shrimp were treated in the same manner except they were injected with an equivalent volume of 0.85% (w/v) NaCl solution.

2.2. Rapid amplification of cDNA ends (RACE)

RACE was performed to obtain the open reading frame sequence of *PmSnake* gene by using gene specific primers designed according to the sequence of *PmSnake* fragment. The 3′ and 5′ RACE fragments were amplified by using SMART™ RACE cDNA amplification kit (Clontech, USA) following the manufacturer's instructions. The PCR amplification was carried out as previously described (Amparyup et al., 2007) using the Advantage 2 DNA polymerase (Clontech, USA). The generated DNA fragments were purified, cloned and commercially sequenced (Macrogen Inc., Korea).

2.3. Sequence analysis and primer design

Nucleotide sequence of the *PmSnake* cDNA was analyzed with the GENETYX 7.0.3 program (GENETYX Corporation). The Blastx program of GeneBank was used to compare the sequence with those sequences in the database. The deduced amino acid sequence and the putative signal peptide were predicted by the simple modular architecture research tool (SMART) version 4.0. The ClustalW2 multiple sequence alignment program was used to align the sequences of *Pm*Snake with *Manduca sexta* hemolymph proteinase 21 (*Ms*HP21) and other serine proteinases of shrimp. The MEGA 6.0 program was used to construct the phylogenetic tree.

All primers were designed based on the nucleotide sequence of *PmSnake* cDNA by using Primer Premier 5 Software (Premier Biosoft) and SECentral program (Scientific & Education Software). The primers for control gene EF1-α were the same as those in the previous research (Amparyup et al., 2013b) (Table 1).

2.4. Total RNA preparation and cDNA synthesis

Hemocytes and tissue samples were homogenized in GeneZol (Geneaid) reagent and total RNA was extracted according to the manufacturer's instructions and treated with RQ1 RNase-free DNase (Promega) to remove any contaminating DNA. Equal amount of total RNA from three shrimp were pooled and subjected to first-strand cDNA synthesis using Revert Aid First Strand cDNA Synthesis kit (Thermo scientific) and the cDNA was stored at −20 °C for further use.

2.5. Tissue distribution analysis

To investigate the tissue-specific expression of *PmSnake* transcript, various tissues of the healthy shrimp (hemocytes, hepatopancreas, hematopoietic tissue, gills, heart, muscle, foregut, midgut/hindgut and lymphoid organ) were collected and stored immediately in liquid nitrogen. Hemocytes were prepared as described above and stored in liquid nitrogen.

2.6. Semi-quantitative reverse transcriptase-PCR (RT-PCR) analysis

Semi-quantitative RT-PCR was performed by using gene-specific primers for *Pm*SnakeRT Snake-F/R (Table 1). The gene expression level of each tissue was normalized relative to that of the elongation factor 1-α (EF1-α) gene (Table 1). The EF1-α gene was amplified in a separate tube and served as an internal control. The PCR thermal cycling conditions were 94 °C for 1 min, 30 cycles of 94 °C for 30 s, 55 °C for 30 s and 72 °C for 30 s, and then a final extension at 72 °C for 5 min. The PCR product was analyzed by 1.8% agarose gel electrophoresis and visualized by UV-transillumination.

2.7. Quantitative real-time RT-PCR analysis

A real-time RT-PCR analysis was performed by SsoFast™ Evagreen® Supermix (Bio-Rad) detection by using RTSnake-F/R primers (Table 1). The thermal profile for SsoFast™ Evagreen® Supermix real-time PCR was 95 °C for 8 min followed by 40 cycles of denaturation (95 °C for 30 s), annealing (58 °C for 30 s) and extension (72 °C for 30 s). The specificity of PCR was verified by measuring the melting curve of the PCR product at the end of the reaction. The reaction was incubated at 95 °C for 5 min and subsequently 55 °C for 5 min, followed by heating for 10 s starting at 55 °C with 0.5 °C increments. The amount of target transcript was analyzed relative to an internal standard, (EF1-α) in the same

Table 1
Nucleotide sequences of the primers.

Primer	Sequence (5′–3′)	Purpose
T7Snake-F	GGATCCTAATACGACTCACTATAGGTTTCTATCGCAACGCTCCAC	RNAi
T7Snake-R	GGATCCTAATACGACTCACTATAGGTCGATGCAATGGGCGGCTGT	RNAi
Snake-F	TTTCTATCGCAACGCTCCAC	RNAi
Snake-R	TCGATGCAATGGGCGGCTGT	RNAi
*Pm*Snake-F	GAGCTCTCCATGGTCCAGGGGACGGGCGAGCAGTG	Recombinant Protein
*Pm*Snake-R	CTCGAGCTAATGATGATGATGATGCACATTTTCTTTGAGCCAAAC	Recombinant Protein
RTSnake-F	TCGCAAACCTTCCAAGTTCTGA	RT-PCR
RTSnake-R	GACAGGCAGGCAACACGCTC	RT-PCR
GFPT7-F	TAATACGACTCACTATAGGATGGTGAGCAAGGGCGAGGA	RNAi
GFPT7-R	TAATACGACTCACTATAGGTTACTTGTACAGCTCGTCCA	RNAi
GFP-F	ATGGTGAGCAAGGGCGAGGA	RNAi
GFP-R	TTACTTGTACAGCTCGTCCA	RNAi
PPAE1-F	TGGGGCGAAGGCAGGGCACAAGGCGCAG	RT-PCR
PPAE1-R	CTCTTCTTCAAGCTCACCACTTCTATCT	RT-PCR
PPAE2-F	GCGGCGGTCACGCTCCTTGTTC	RT-PCR
PPAE2-R	ACTCTCGGGGGCACGCTTGTTG	RT-PCR
SP1-F	TGAGAGCACAAATAGTGGAGGGGTA	RT-PCR
SP1-R	TGGAGGCAGGCACACAGGCAAC	RT-PCR
SP2-F	GGCGTTGGTCTTCACTGCTCTC	RT-PCR
SP2-R	CAGAACTGCCTTCCAAGGATAG	RT-PCR
PO1-F	GGTCTTCCCCTCCCGCTTCG	RT-PCR
PO1-R	GCCGCAGGTCCTTTGGCAGC	RT-PCR
PO2-F	GCCAAGGGGAACGGGTGATG	RT-PCR
PO2-R	TCCCTCATGGCGGTCGAGGT	RT-PCR
Pen3-F	GGTCTTCCTGGCCTCCTTCG	RT-PCR
Pen3-R	TTTGCATCACAACAACGTCCTA	RT-PCR
EF1-α-F	GGTGCTGGACAAGCTGAAGGC	RT-PCR
EF1-α-R	CGTTCCGGTGATCATGTTCTTGATG	RT-PCR

sample of *V. harveyi*-injected shrimp hemocytes. The Ct value of *V. harveyi*-injected sample at each time point was normalized with that of saline-injected sample. All real-time PCR analysis was performed in triplicate. A mathematical model of Pfaffl was used to determine the relative expression ratio (Pfaffl, 2001).

2.8. In vivo gene silencing

Double-stranded RNA (dsRNA) of *PmSnake* was generated *in vitro* using T7 RiboMAX™ Express Large Scale RNA Production System (Promega). The DNA fragment for preparation of *PmSnake* dsRNA was amplified by PCR from a full-length *PmSnake*-containing plasmid using gene specific primers (Table 1). The primers for dsRNA synthesis consist of the same gene specific sequences but flanked at the 5′ end by a T7 promoter sequence. Two separate PCRs were set up, one with T7Snake-F and Snake-R (Table 1) for the sense strand template, the other with Snake-F and T7Snake-R (Table 1) for the anti-sense strand template. The GFP gene as a negative control was amplified with pEGFP-1 vector by using GFPT7-F and GFP-R (Table 1) for the sense strand template, and GFP-F and GFPT7-R (Table 1) for the anti-sense strand template. The T7 RiboMAX™ Express Large Scale RNA Production System was used to generate single stranded RNAs. Equal amount of single stranded RNAs was annealed to produce dsRNA. The quality of dsRNAs were verified by 1.5% agarose gel electrophoresis and quantified by using UV visualization and UV spectrophotometer, respectively.

Shrimp with an average wet weight of 3 g were divided into 3 groups of 6 shrimp individuals each. Two groups of shrimp were injected through the fourth abdominal segment with either *PmSnake* or GFP dsRNA (2.5 μg of dsRNA in 150 mM NaCl per 1 g of a shrimp in 25 μl). The saline control group was injected with 25 μl of 150 mM NaCl. After 24 h of the first injection, injection of dsRNAs was repeated together with 10 μg each of *Escherichia coli* 0111:B4 lipopolysaccharide (LPS) (Sigma) and laminarin (β-1,3-glucan) (Sigma) to stimulate the immune response.

2.9. Hemolymph PO activity of PmSnake-silenced shrimp

The hemolymph was collected 48 h after the second dsRNA injection without using anti-coagulant and subjected to a phenoloxidase (PO) assay. Total protein concentration was measured using a Bradford assay kit (Bio-Rad). Briefly, shrimp hemolymph protein (2 mg) in 435 μl of 10 mM Tris–HCl pH 8.0 was mixed with 65 μl of 3 mg/ml dopamine (Sigma) in water. The reaction was incubated at room temperature for 30 min and stopped by adding 500 μl of 10% (v/v) acetic acid. The PO activity was monitored by spectrophotometry at 470 nm to follow the enzyme reaction, from dopamine quinone to melanochrome. The PO activity was recorded as A_{470}/mg total protein/min against control. The experiment was repeated at least three times.

2.10. Recombinant PmSnake protein

Gene specific primers: *Pm*Snake-F with 5′ NcoI site and *Pm*Snake-R with 5′ 6His tag and XhoI site (Table 1), were designed to PCR amplify the mature *PmSnake* gene. The mature *PmSnake* gene was cloned into the pET-28b (+) vector. The recombinant plasmid pET28b-*Pm*Snake was transformed into an *E. coli* strain BL21. A colony of transformant was grown in LB medium containing 50 μg/ml kanamycin. The expression of recombinant *Pm*Snake protein (r*Pm*Snake) was induced by adding IPTG to the final concentration of 1 mM and analyzed by 12.5% SDS-PAGE. The r*Pm*Snake was found to be in the inclusion bodies. The protein was solubilized by 8 M Urea and purified by using Ni-NTA affinity column (GE Healthcare). The purified r*Pm*Snake was dialyzed against 20 mM Tris-HCl pH 8.0 and concentrated with VivaSpin (GE Healthcare). The purified r*Pm*Snake was used to immunize a rabbit in order to generate anti-*Pm*Snake polyclonal antiserum at the Biomedical Technology Research Unit, Chiangmai University,

Chiangmai, Thailand.

2.11. Hemocyte lysate preparation

Hemolymph was collected from healthy shrimp using 10% trisodium citrate as an anticoagulant. The hemocytes was separated by centrifugation at 800 × g for 10 min at 4 °C, washed with CAC buffer (10 mM sodium cacodylate) twice, homogenized and centrifuged to separate the hemocyte lysate supernatant (HLS) at 25,000 × g at 4 °C for 20 min. The protein concentration was determined by Bradford assay.

2.12. PO activation assay

Hemolymph was collected from the healthy shrimp and its protein content was determined. Aliquots of 25 μl of hemolymph (250 μg) were added into wells of a 96 well plate Costar Clear. Aliquots of 25 μl of 10 μM r*Pm*Snake and 25 μl of activators, LPS and β-1,3-glucan, were added. The plate was incubated at room temperature for 10 min. Then, 25 μl of 3 mg/ml L-DOPA was added into each reaction well. The PO activity was monitored at A_{490} by using microplate reader SpectraMaxM5 (Molecular Devices) every 5 min for 30 min. The BSA was used as a negative control. The experiment was repeated three times. The PO activity was reported as A_{490}/mg total protein/min against the control.

2.13. Proteinase activity assay

Hemolymph was prepared from the healthy shrimp as above. Aliquots of 25 μl of hemolymph (250 μg) were added into wells of a 96 well plate Costar Clear. Aliquots of 25 μl of 10 μM r*Pm*Snake and an activator LPS (50 μg) were added. The reactions were incubated at room temperature for 10 min. Then, 25 μl of 100 μM of B2133 (N-Benzoyl-Pro-Phe-Arg-*p*-nitroanilide hydrochloride) was added in each reaction. The A_{405} was measured by using spectrophotometry. The experiment was repeated three times.

2.14. Immunofluorescence detection of PmSnake

The expression of *Pm*Snake in hemocytes was analyzed by using the purified polyclonal antibody specific to *Pm*Snake. The hemolymph was collected and fixed in 4% paraformaldehyde (ratio 1:1) for 10 min at room temperature. Hemocytes were separated by centrifugation at 800 × g at 4 °C for 10 min. The hemocytes were resuspended with 1 × PBS pH 7.4, counted by hemocytometer and centrifuged 110 cells/slide at 1000 × g at 4 °C for 10 min onto the poly-L-lysine slides (Thermo Scientific). The cells were washed with 1 × PBS pH 7.4 three times, permeabilized by 1% Triton X-100 in 1 × PBS pH 7.4 for 5 min at room temperature and washed three times with 1 × PBS pH 7.4 for 5 min.

The cells were blocked with 10% fetal bovine serum (FBS) in 1 × PBS pH 7.4 at room temperature for 1 h. The cells were probed with 1:1000 dilution of the purified rabbit polyclonal antibody specific to *Pm*Snake at room temperature for 3 h. The negative control was incubated with 1% FBS in 1 × PBS pH 7.4. The slides were washed and probed with secondary antibody, 1:1000 dilution of goat anti-rabbit antibody conjugated with Alexa Fluor 488 in 1% FBS in 1 × PBS pH 7.4 at room temperature for 1 h. Cells were also stained for the nuclear DNA by incubating with TO-PRO-3 iodide (Thermo Fisher Scientific) before mounting with medium Prolong Gold antifade reagent. The fluorescent staining was observed under FV1000 confocal laser scanning microscope (Olympus).

3. Results

3.1. Sequence analysis of PmSnake

A cDNA encoding an incomplete sequence of snake-like serine proteinase (*PmSnake*) gene was identified from the suppression subtractive hybridization cDNA library of proPO dsRNA-treated hemocytes (Sangsuriya et al., 2016). A complete open reading frame of *PmSnake* was then identified using 5′ and 3′ RACE. It contains 1068 bp encoding a predicted protein of 355 amino acid residues with a theoretical isoelectric point of 7.82 and a predicted molecular weight of 38.57 kDa. The database searching using the Blastx algorithm revealed that the *PmSnake* shared high similarity to snake proteases in insects such as *Ae*Snake in *Acromyrmex echinatior* (53% similarity), *Tc*Snake in *Trachymyrmex cornetzi* (51% similarity), *Bm*Snake in *Bombyx mori* (52% similarity) and *Ms*HP21 in *Manduca sexta* (52% similarity).

The *Ms*HP21 was found to be involved in prophenoloxidase activating system in *Manduca sexta* by functioning as a clip domain serine protease in this cascade (Gorman et al., 2007a, 2007b). Based on the SMART analysis program, *Pm*Snake belongs to a trypsin-like serine proteinase family. It contains a putative signal peptide of 22 amino acid residues with six cysteine residues forming three disulfide linkages of clip-domain at the N-terminal region and a conserved catalytic triad (Histidine187, Aspartate198 and Serine299) at the C-terminal region of serine proteinase domain.

3.2. Multiple sequence alignment and phylogenetic analysis

The multiple sequence alignment of deduced amino acid sequence of *Pm*Snake with other clip-domain serine proteinases: *Pm*ClipSP1 (ACP19562.1), *Pm*ClipSP2 (ACP19561.1), *Pm*PPAE2 (ACP19559.1) in *P. monodon* and *Ms*HP21, a Hemolymph proteinase 21 in *M. sexta* (AAV91019.1), using ClustalW2 revealed the six conserved cysteine residues in the clip-domain region and the conserved catalytic traid as well as the cysteine residues in the SP domain (Fig. 1).

Phylogenetic analysis of *Pm*Snake with other arthropods Clip-SPs and Clip-SPHs by the NJ distance based method categorized the arthropod clip-SPs and clip-SPHs into two distinct and separate major groups. Interestingly, *Pm*Snake clusters in the same clade with those of the insect clip-SPs. It was closest to the *Ae*Snake from ant *Acromyrmex echinatior* but was quite relatively distant from other *Pm*ClipSPs. The results indicated that the *Pm*Snake is closely related to insect snake-like serine proteinases. In addition, the phylogenetic tree also indicated that the *Pm*Snake was more closely related to clip-SPs than clip-SPHs (Fig. 2).

3.3. Tissue-specific expression of PmSnake in P. monodon

Tissue-specific expression of *PmSnake* transcripts was examined in various tissues of the healthy shrimp by semi-quantitative RT-PCR analysis using EF1-α as an internal control gene. The results showed that the *Pm*Snake was expressed in many shrimp tissues, mainly in hemocytes, gill, forgut, midgut/hindgut and lymphoid organ with the highest expression in hemocytes (Fig. 3A).

3.4. Temporal gene expression analysis in bacterial challenged P. monodon

To investigate the involvement of *Pm*Snake in immune response to bacteria, the transcription levels of *Pm*Snake were determined in *P. monodon* after systemic *V. harveyi* challenge at 0, 6, 24, 48 and 72 h post infection (hpi) by quantitative real-time RT-PCR analysis. After *V. harveyi* challenge, the transcription level of *Pm*Snake gene

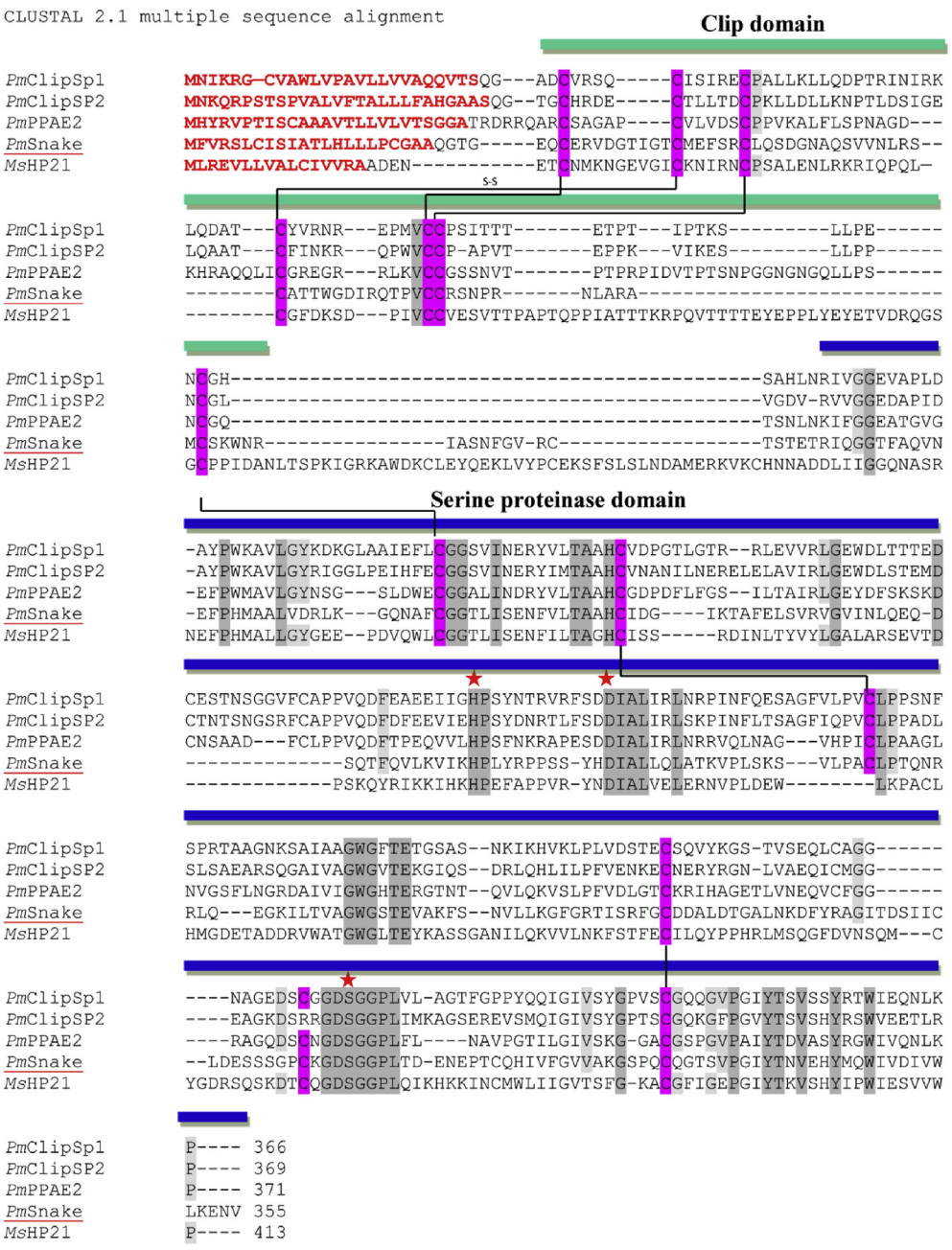


Fig. 1. Amino acid sequence alignment using ClustalW2 of *Pm*Snake with other Clip-SPs from *P. monodon* and the hemolymph proteinase 21 from *M. sexta* (*Ms*HP21). The signal peptides are shown in red. Grey indicates conserved residues. Pink highlights indicate conserved cysteine residues. The disulfide linkages are shown by black solid lines. The amino acid residues corresponding to the catalytic triad of serine proteinases are marked by red stars. (For interpretation of the references to colour in this figure legend, the reader is referred to the web version of this article.)

was gradually increased to 1.9-fold at 6 hpi and reached the highest expression level of 8.0-fold at 48 hpi. At 72 hpi, the expression level of *Pm*Snake gene was dramatically decreased to 0.4-fold (Fig. 3B).

3.5. Gene silencing of PmSnake

To investigate the function of *Pm*Snake, gene silencing technique was employed to evaluate the effect of *PmSnake* gene silencing. Shrimp (2–5 g) were injected with 2.5 μg/g of *Pm*Snake dsRNA and double injected after 24 h with the same amount of dsRNA. The control groups were injected with GFP dsRNA and 150 mM NaCl. At 48 h after the second injection, the hemolymph was collected for total RNA preparation and cDNA synthesis and analyzed by semi-quantitative RT-PCR technique using EF1-α as an internal control. It was found that the expression of *Pm*Snake was efficiently suppressed (Fig. 4A).

To check whether the knockdown of *PmSnake* had any effect on the transcription of other Clip-SPs and proPOs genes, the quantitative real-time RT-PCR was used to analyze the expression of *Pm*PPAE1, *Pm*PPAE2, *Pm*proPO1 and *Pm*proPO2. The results showed that the *Pm*Snake knockdown was specific and had no effect on the expression of above said genes (data not shown). Furthermore, we determined whether the *Pm*Snake dsRNA could also mediate suppression of *Pm*Snake at the protein level by the Western blot analysis. The hemocyte lysates were prepared from each group of the knockdown shrimp and control shrimp. The rabbit polyclonal

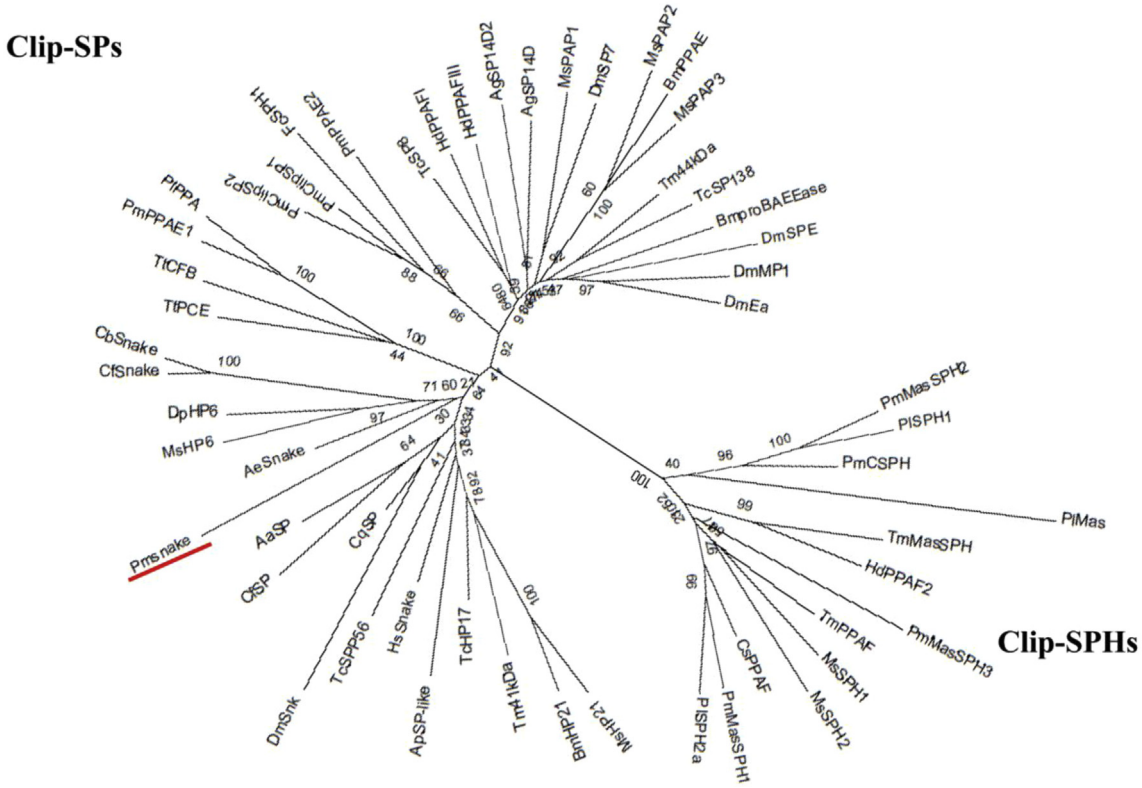


Fig. 2. Bootstrapped unrooted neighbor-joining tree of the serine proteinase domain of Clip-SPs, Clip-SPHs and Snake from various arthropods: *Penaeus monodon* snake-like serine proteinase (*Pm*Snake), prophenoloxidase-activating enzyme 1 (*Pm*PPAE1; ACP19558.1), prophenoloxidase-activating enzyme 2 (*Pm*PPAE2; ACP19559.1), clip domain serine proteinase 1 (*Pm*ClipSP1; ACP19562.1), clip domain serine proteinase 2 (*Pm*ClipSP2; ACP19561.1), prophenoloxidase activating factor Mas-like SPH1 (*Pm*MasSPH1; ABE03741.1), masquerade-like serine proteinase-like protein 2 Mas-like SPH2 (*Pm*MasSPH2; ACP19560.1), masquerade-like serine proteinase-like protein 3 Mas-like SPH3 (*Pm*MasSPH3; ACP19563.1), Mas-like protein (*Pm*CSPH; AAT42131.1); *Fenneropenaeus chinensis* serine proteinase SPH (*Fc*SPH1; ABC33918.1); *Pacifastacus leniusculus* serine protease PPA (*Pl*PPA; CAB63112.1), masquerade-like protein Mas-like protein (*Pl*Mas; CAA72032.2), serine proteinase-like protein 1 SPH1 (*Pl*SPH1; AAX55746.1), serine proteinase-like 2a SPH2a (*Pl*SPH2a; ACB41379.1); *Callinectes sapidus* phenoloxidase activating factor PPAF (*Cs*PPAF; AAS60227.1); *Anopheles gambiae* serine protease 14D (*Ag*SP14D; ACN38198.1), serine protease 14D2 (*Ag*Sp14D2; AAD38335.1); *Drosophila melanogaster* melanization protease 1 (*Dm*MP1; NP_649450.3), Spatzle-processing enzyme (*Dm*SPE; NP_651168.1), snake (*Dm*Snk; NP_524338.2), easter (*Dm*Ea; NP_524362.2), serine protease 7 (*Dm*SP7; NP_649734.2); *Bombyx mori* prophenoloxidase activating enzyme precursor PPAE (*Bm*PPAE; NP_001036832.1), BzArgOEtase precursor SP zymogen (*Bm*proBAEEase; NP_001036844.1); *Holotrichia diomphalia* pro-phenoloxidase activating enzyme-Iprecursor PPAF-I (HdPPAFI; BAA34642.1), prophenoloxidase activating factor PPAF-II (*Hd*PPAFII; CAC12665.1), prophenoloxidase activating factor-III PPAF-III (*Hd*PPAFIII; BAC15604.1); *Manduca sexta* prophenoloxidase-activating proteinase-1 PAP1 (*Ms*PAP1; AAX18636.1), prophenoloxidase-activating proteinase-2 PAP2 (*Ms*PAP2; AAL76085.1), prophenoloxidase-activating proteinase-3 precursor PAP3 (*Ms*PAP3; AAO74570.1), serine proteinase-like protein 1 SPH1 (*Ms*SPH1; AAM69352.2), serine proteinase-like protein 2 SPH2 (*Ms*SPH2; AF518768_1), hemolymph proteinase 6 (*Ms*HP6; AAV91004.1), hemolymph proteinase 21 (*Ms*HP21; AAV91019.1); *Tenebrio molitor* prophenoloxidase activating factor PPAF (*Tm*PPAF; CAC12696.1), masquerade-like serine proteinase homologue Mas-like SPH (*Tm*MasSPH; BAC15605.1), 41 kDa zymogen (*Tm*41 kDa; BAG14261.1), 44 kDa zymogen (*Tm*44 kDa; BAG14262.2); *Tachypleus tridentatus* proclotting enzyme (*Tt*PCE; AAA30094.1) and coagulation factor B precursor (*Tt*CFB; BAA03528.1); *Acromyrmex echinatior* Serine protease snake (*Ae*Snake; EGI60137.1); *Bombyx mori* serine protease HP21 precursor (*Bm*HP21; NP_001243984.1), *Danaus plexippus* hemolymph proteinase 6 (*Dp*HP6; EHJ76340.1); *Aedes aegypti* serine protease snake (*Aa*SP; XP_001649319.1); *Tribolium castaneum* serine protease P56 (*Tc*SPP56; EEZ99345.1), serine protease H17 (TcHP17; EEZ99231.1); *Ctenocephalides felis* trypsin-like serine protease (*Cf*SP; AAD21841.1); *Camponotus floridanus* Serine protease snake (*Cf*Snake; EFN63907.1); *Acyrthosiphon pisum* serine protease-like precursor (*Ap*SP-like; NP_001155379.1); *Tribolium castaneum* serine protease P138 (*Tc*SP138; EFA07560.1); *Harpegnathos saltator* Serine protease snake (*Hs*Snake; EFN87035.1); *Culex quinquefasciatus* serine protease (CqSP; XP_001845292.1). Bootstrap values indicate the percentage of times that the particular node occurred in 1000 trees generated by bootstrapping the original deduced protein sequences.

anti-*Pm*Snake and mouse anti-actin were used to detect the proteins. The immunoblotting results indicated that the *Pm*Snake dsRNA also suppressed the *Pm*Snake at the protein level (Fig. 4B).

3.6. Hemolymph PO activity of PmSnake-silenced shrimp

The hemolymph of *Pm*Snake silenced-shrimp and control shrimp were collected at 48 h after the second dsRNA injection. The PO activity was monitored by measuring the A_{470} and recorded as A_{470}/mg total protein/min. It was found that the hemolymph PO activity of *Pm*Snake-silenced shrimp was decreased by 36% when compared to the control GFP dsRNA groups and NaCl-injected group. This result suggested that the *Pm*Snake is involved in the regulation of the proPO system in shrimp (Fig. 4C).

3.7. Recombinant PmSnake protein expression

By using appropriately designed primers, the mature *PmSnake* gene was amplified and cloned into an expression vector pET-28b (+) at the *Nco*I and *Xho*I sites. The amplified gene contained a 6 His tag at its 3′ end which helped facilitate the purification of the protein product. The r*Pm*Snake protein was over-produced as an inclusion bodies. The protein was solubilized and purified (Fig. 5A). The purified r*Pm*Snake was used to immunize a rabbit for the preparation of rabbit anti-*Pm*Snake. The anti-*Pm*Snake was tested against the r*Pm*Snake and found to be specific (data not shown).

3.8. Detection of endogenous PmSnake protein in the hemocytes

To verify that the *Pm*Snake protein was present in the shrimp

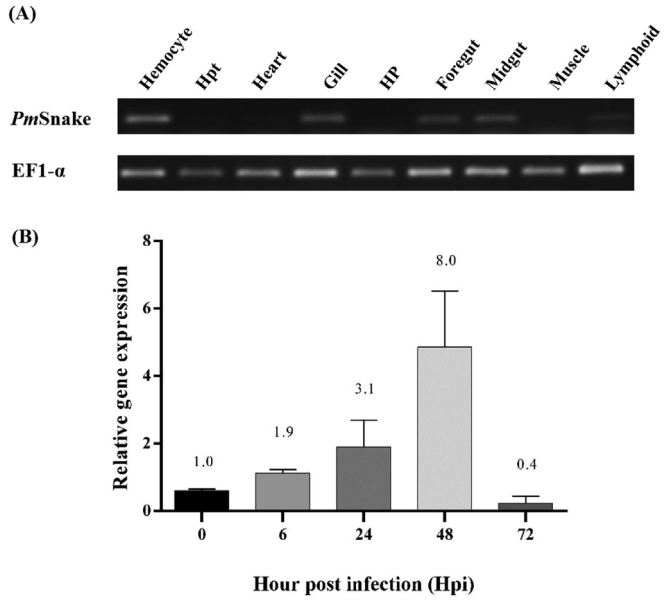


Fig. 3. Gene expression analysis of *PmSnake* (A) The semi-quantitative RT-PCR analysis of *PmSnake* transcript of healthy shrimp *P. monodon* in hemocyte (HC), hematopoietic tissue (HPT), heart (H), gill (G), hepatopancreas (HP), foregut (FG), midgut/hindgut (MG), muscle (M) and lymphoid organ (L). The EF1-α is used as an internal control. (B) The real-time RT-PCR analysis of *PmSnake* transcript in the shrimp hemocytes after *V. harveyi* injection analyzed at the various time points. Relative expression is calculated according to the Pfaffl (Pfaffl, 2001) using the EF1-α as an internal reference gene. Data are derived from triplicate samples per assay and three independent assays and shown as means ± SEM.

hemocytes, 20 μg of *P. monodon* hemocyte lysate supernatant and 100 μg of cell free plasma were run on 12.5% SDS-PAGE. The natural *Pm*Snake protein was analyzed by Western blotting and it was detected in the hemocyte lysate supernatant but not in the plasma (Fig. 5B and C).

Since the *Pm*Snake protein was detected in the hemocytes, it was interesting to know which types of the hemocytes actually produced the protein. Immunofluorescence and confocal microscopy were then employed for this study. The hemocytes were processed for the detection of endogenous *Pm*Snake. The nucleus was stained blue with TO-PRO-3 iodide dye whilst the *Pm*Snake was visualized green of Alexa Fluor 488 dye (Fig. 6). The results revealed that the *Pm*Snake was expressed in all three types of shrimp hemocytes.

3.9. PO activation and serine proteinase activity of rPmSnake protein

As a serine proteinase and possibly involved in the activation of proPO system, the r*Pm*Snake was tested for its serine proteinase activity and its role in PO activation. The r*Pm*Snake was incubated with L-DOPA and B2133 N-Benzoyl-Pro-Phe-Arg-*p*-nitroanilide hydrochloride as substrates of PO activation and serine proteinase, respectively. It was found that the r*Pm*Snake could increase the total hemolymph PO activity by 36% (Fig. 7A) and it significantly increased the proteinase activity as compared to that of control BSA protein and trypsin as negative and positive controls, respectively (Fig. 7B).

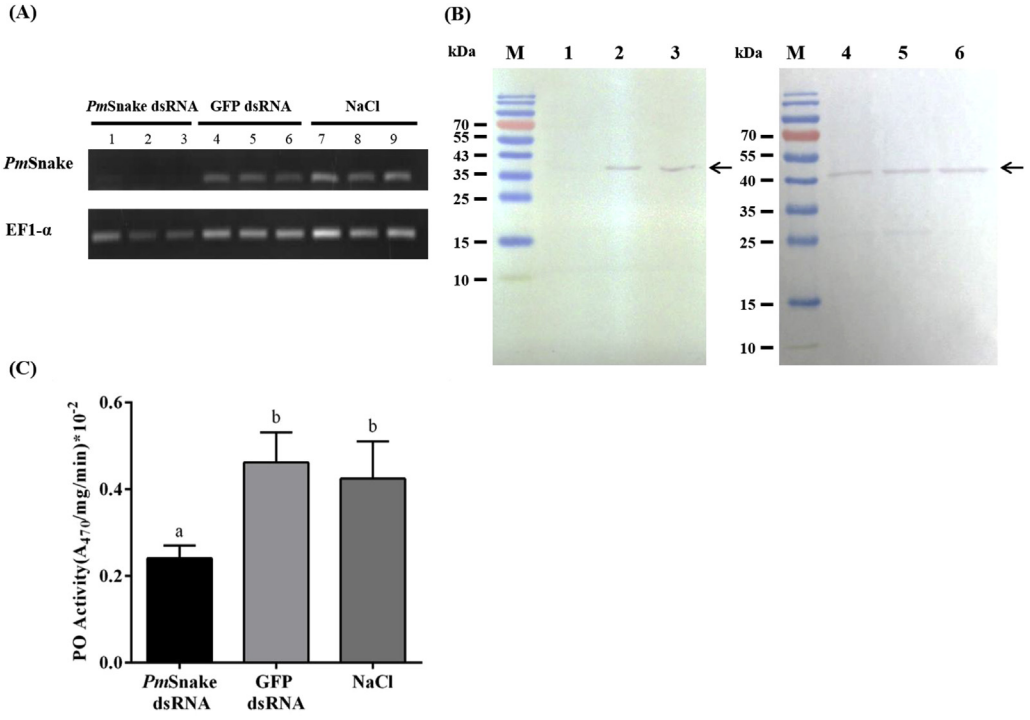


Fig. 4. Gene-silencing of *PmSnake* in the *P. monodon* hemocytes and total hemolymph PO activity (A) Lanes 1–3: shrimp were injected with *PmSnake* dsRNA, Lanes 4–6: shrimp were injected with GFP dsRNA, and Lanes 7–9: shrimp were injected with 150 mM NaCl. The EF1-α was used as an internal control. (B) The dsRNA-mediated gene silencing of *Pm*Snake protein was determined by Western blot analysis. Shrimp injected with GFP dsRNA in 150 mM NaCl or with 150 mM NaCl alone were served as controls. The β-actin was used as a loading control for Western blot analysis. A lane for each condition is the result from individual shrimp. Arrows indicate the *Pm*Snake protein. Lanes 1 and 4 are *PmSnake* dsRNA knockdown shrimp. Lanes 2 and 5 are GFP dsRNA-injected shrimp. Lanes 3 and 6 are saline-injected control. M is MW marker. (C) The PO activity was measured by spectrophotometry at 470 nm and recorded as A_{470}/mg total protein/min. Experiments were repeated three times. The data from three independently replicated experiments are shown as the means ± standard deviation. Different lower case letters indicate significance at $p < 0.05$.

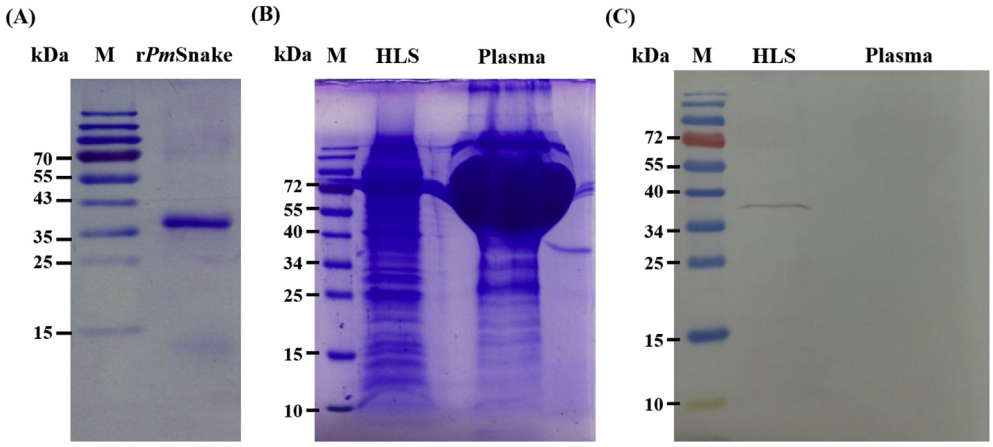


Fig. 5. The SDS-PAGE and Western blot analysis of the *Pm*Snake protein. (A) The 12.5% SDS-PAGE analysis of purified r*Pm*Snake by using Ni-NTA chromatography. Lane M is MW protein marker and r*Pm*Snake protein (B) the 12.5% SDS-PAGE analysis of hemocyte lysate and cell-free plasma (C) the immunoblotting using anti-*Pm*Snake as primary antibody. Lane M is MW protein marker.

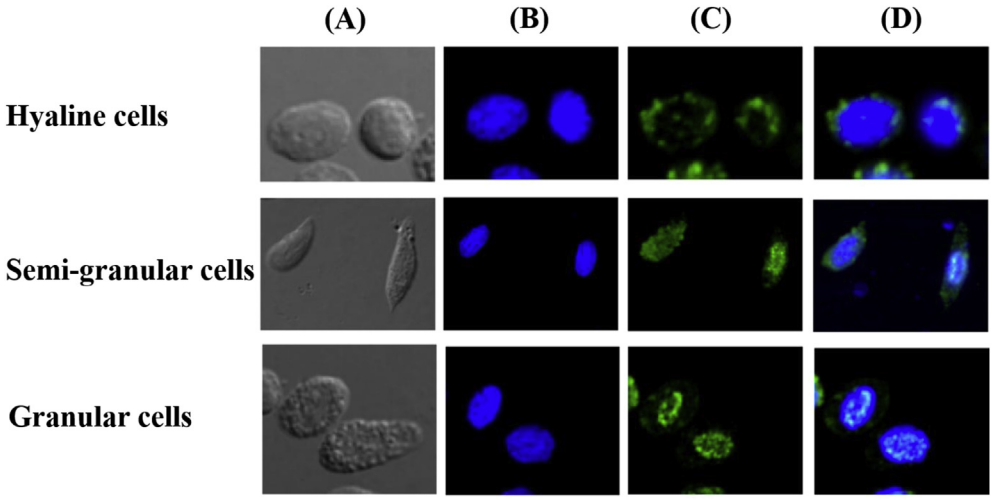


Fig. 6. Immunofluorescence detection of *Pm*Snake-producing hemocytes. The *Pm*Snake protein was expressed in different type of hemocytes (hyaline, granular and semi-granular). The *Pm*Snake was observed in green and nucleus in blue color. (A) Bright field (B) TO-PRO-3 iodide (C) Anti-*Pm*Snake antibody (D) Merge. (For interpretation of the references to colour in this figure legend, the reader is referred to the web version of this article.)

4. Discussion

Clip-SPs play critical roles in innate immunity of arthropods (Jiang and Kanost, 2000) including the proclotting enzyme from the horseshoe crab *Tachypleus tridentatus* was identified first Clip-domain serine protease (Muta et al., 1990; Smith and Delotto, 1992), the two serine proteases, snake and easter, the Clip-SPs from the fly *Drosophila melanogaster* which are involved in the pathway establishing the dorsal-ventral axis of a developing embryo (Anderson, 1998; Morisalo and Anderson, 1995). Clip-SPs were also reported to be involved in the proPO system in the shrimp *Penaeus monodon* (Charoensapsri et al., 2009) tobacco hornworm *Manduca sexta* (Gupta et al., 2005; Jiang and Kanost, 2000; Jiang et al., 1998), large beetle *Holotrichia diomphalia* (Kwon et al., 2000; Lee et al., 1998a, 1998b), silkworm *Bombyx mori* (Satoh et al., 1999) and fly *Drosophila melanogaster* (Jiang and Kanost, 2000). Clip-SPs are composed of two domains, the clip-domain at N-terminal region and C-terminal region of serine proteinase domain with conserved catalytic sites (His, Asp and Ser) that are always found in serine proteinases (SPs). A number of Clip-SPs and Clip-SPHs have been identified in *P. monodon* and found to be involved in the proPO cascade. The Clip-SPs in the cascade are *Pm*ClipSP2 (Amparyup et al., 2013b), *Pm*PPAE1 (Charoensapsri et al., 2009), *Pm*PPAE2 (Charoensapsri et al., 2011) and the Clip-SPHs are *Pm*MasSPH1 (Amparyup et al., 2007; Jitvaropas et al., 2009), *Pm*MasSPH2 (Jearaphunt et al., 2015), *Pm*MasSPH3 (Amparyup et al., unpublished data). Recently, snake-like serine proteinase (*Pm*Snake) gene was identified from the suppression subtractive cDNA library of proPO dsRNA-treated hemocytes of *P. monodon* (Sangsuriya et al., 2016). In this study, we characterized the function of *Pm*Snake in shrimp innate immunity. From the sequence analysis, the *Pm*Snake is a clip-SP which is closely related to the arthropod Clip-SPs including snake-like hemolymph proteinase 21 (*Ms*HP21) in *M. sexta* (52% similarity). The *Ms*HP21 has been reported to participate in the serine proteinase cascade of the insect proPO activation system.

The multiple amino acid sequence alignments of *Pm*Snake with other Clip-SPs in *P. monodon* and *M. sexta* showed the conserved six cysteine residues that form three disulfide linkages of clip-domain at the N-terminal region and the conserved catalytic site (His, Asp

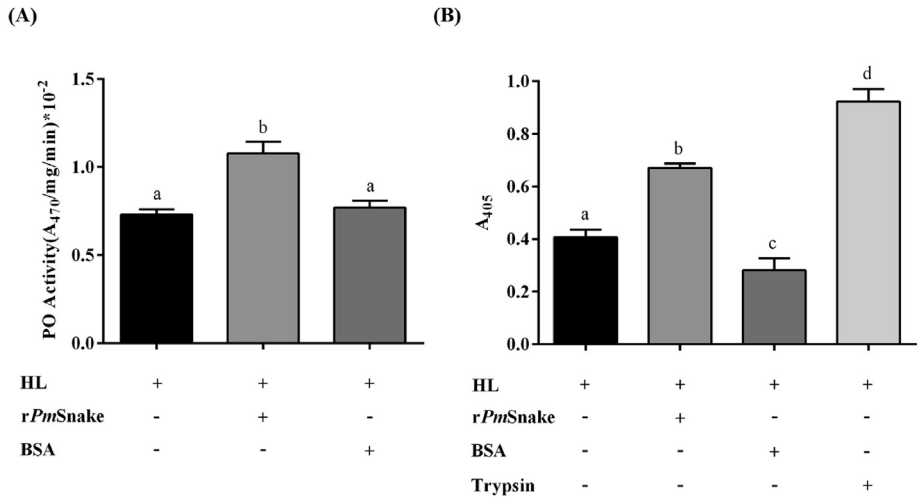


Fig. 7. The *in vitro* PO activation and proteinase activity of r*Pm*Snake protein. (A) *In vitro* PO activation, the L-dopa as substrate was used to detect PO activity at A_{490} nm and reported as PO activity (A_{490}/mg total protein/min). (B) *In vitro* proteinase activity, hemolymph were incubated with r*Pm*Snake (10 μM) and LPS as an activator. The BSA protein (10 μM) and trypsin (2.5 μM) were used as negative and positive controls, respectively. Experiments were repeated three times. The results are from three independently replicated experiments and shown as means ± standard deviations. Different lower case letters indicate significant at $p < 0.05$.

and Ser) at the C-terminal region of serine proteinase domain. The *Pm*Snake is, therefore, a member of the clip-SPs. The Clip domain has been reported to form secondary structure similar to the antibacterial proteins (Jiang et al., 1998) and the SP domain is essential for proteolytic activity. It is likely then that the *Pm*Snake plays a role in shrimp immunity.

The *PmSnake* is expressed in various shrimp tissues and the highest expression is in hemocytes. This expression is similar to those of the other known proPO-associated transcripts in *P. monodon* such as *PmClipSP2* (Amparyup et al., 2013b), *PmClipSP1* (Amparyup et al., 2010), *PmPPAE1* (Charoensapsri et al., 2009) and *PmPPAE2* (Charoensapsri et al., 2011), and also *PPAE* in *P. leniusculus* (Wang et al., 2001) that are primarily detected in the hemocytes. However, the *PmSnake* was also expressed in other tissues such as gill, lymphoid organ and digestive tissues (Fig. 3A) whereas the genes in the proPO system (*PmPPAE1*, *PmPPAE2* and *PmClipSP2*) were not expressed in the digestive tissues (Charoensapsri et al., 2009, 2011; Amparyup et al., 2013b) suggesting that the *Pm*Snake might have multiple functions beside an immune responsive protein. The Clip-SPs have been participated in arthropods in embryonic development and defense responses, including hemolymph coagulation, melanotic encapsulation, induction of antimicrobial peptide synthesis and activation of cytokines (Jiang and Kanost, 2000; Kanost et al., 2001).

Injection of *V. harveyi* into *P. monodon* results in an increased expression of *PmSnake* at 6 and 24 hpi and the expression is increased up to 8 fold at 48 hpi, but rapidly declined at 72 hpi (Fig. 3B). Comparing to other *P. monodon* Clip-SPs, *PmPPAE1* transcript level is decreased at 24 h after bacterial challenge followed by a significant increase at 48 h after infection (Charoensapsri et al., 2009). The *PmClipSP2* mRNA level is increased at 3 h and continuously decreased at 24 h and 48 h after infection (Amparyup et al., 2013b). The *PmClipSP1* transcript level is increased at 3 h, decreased at 6 h and 48 h (Amparyup et al., 2010). In L. *vannamei*, *LvPPAE1* transcription is down-regulated in the hemocytes and up-regulated in the gill after *V. harveyi* challenge (Jiménez-Vega et al., 2005). In the crayfish *P. leniusculus*, the *PPAE1* expression is not affected following infection (Liu et al., 2007). In insect, the *M. sexta PPAE* (*PAP-1*) is expressed at high levels in an integument and less abundantly in the fat body of naive larvae. Nevertheless, the expression levels of *PAP-1* and the two other *PPAE* transcripts (*PAP-2* and *PAP-3*) are up-regulated following bacterial infection (Jiang et al., 2003a, 2003b). The mRNA levels of HP21 in *M. sexta* is increased in the larval fat body and/or hemocytes after a bacterial injection, suggesting that this enzyme plays certain roles in defense responses (Zou and Jiang, 2005; Zou et al., 2005). The different temporal gene expression patterns of these genes might be due to the variation of the particular gene in response to the pathogen or it might be due to different doses of bacteria or sizes of the animals used in challenge experiments. Nonetheless, the alteration of mRNA expression of genes involved in the proPO system was observed suggesting that they play crucial role in bacterial response.

In this study, the *Pm*Snake was tested for its involvement in proPO system by using dsRNA interference. Suppression of *PmSnake* by dsRNA injection results in a significant reduction of the hemolymph PO activity (36%) supporting that *Pm*Snake might participate in the activation of shrimp proPO system. Previously, the function of Clip-SPs in *P. monodon*, *Pm*ClipSP1 (Amparyup et al., 2010); *Pm*PPAE1 (Charoensapsri et al., 2009); *Pm*PPAE2 (Charoensapsri et al., 2011); *Pm*ClipSP2 (Amparyup et al., 2013b) was investigated and the results reveal that the Clip-SPs except *Pm*ClipSP1 play roles in shrimp immunity and are involved in the activation of the proPO cascade.

To further investigate the function of *Pm*Snake *in vitro*, the r*Pm*Snake was produced and used in the activation of the PO activity in shrimp hemolymph. The total hemolymph PO activity is significantly increased when the r*Pm*Snake is added. The *Pm*Snake is, therefore, involved in the proPO activation. In *P. monodon*, r*Pm*ClipSP2 exhibits the ability to activate the proPO system *in vitro* (Amparyup et al., 2013b). In addition, the r*Pm*Snake exhibits proteinase activity when added into the shrimp hemolymph which supports the notion that the r*Pm*Snake participates in proPO activating system in *P. monodon* shrimp via the serine proteinase cascade.

In arthropods, melanization is mediated by a serine proteinase cascade which regulates the conversion of proPO to active PO (Söderhäll and Cerenius, 1998). The mechanism of prophenoloxidase activation in *M. sexta* reveals that the proHP21 is cleaved by the HP14 and then the active HP21 activates the final serine proteinase in the cascade, proPAP3, which in turn activates the conversion of proPO to PO. The proHP21 is activated by a

conformational change that occurs when proHP21 binds to HP14 and proPAP3 (Gorman et al., 2007a, 2007b). Although, *Pm*Snake exhibits the high similarity to the insect proHP21, the mechanism by which this protein activates the *P. monodon* proPO system remains unknown and needs further investigation.

Acknowledgements

We thank Prof. Vichien Rimphanichayakit for valuable comments on the manuscript. This work was supported by research grants from the Thailand Research Fund to AT (TRF Senior Scholar No. 5880004), the Thailand Research Fund and Thailand National Center for Genetic Engineering and Biotechnology (BIOTEC) to PA (Grant No. BRG5880016). Additional support from TRF (grant no. IRG5780008) to the Department of Biochemistry, Faculty of Science, Chulalongkorn University is acknowledged. W.M. is the recipient of Chulalongkorn University Graduate Scholarship to Commemorate the 72nd Anniversary of His Majesty King Bhumibol Adulyadej.

References

Amparyup, P., Charoensapsri, W., Tassanakajon, A., 2009. Two prophenoloxidases are important for the survival of *Vibrio harveyi* challenged shrimp *Penaeus monodon*. Dev. Comp. Immunol. 33, 247–256.

Amparyup, P., Charoensapsri, W., Tassanakajon, A., 2013a. Prophenoloxidase system and its role in shrimp immune responses against major pathogens. Fish. Shellfish. Immunol. 34, 990–1001.

Amparyup, P., Jitvaropas, R., Pulsook, N., Tassanakajon, A., 2007. Molecular cloning, characterization and expression of a masquerade-like serine proteinase homologue from black tiger shrimp *Penaeus monodon*. Fish. Shellfish. Immunol. 22, 535–546.

Amparyup, P., Promrungreang, K., Charoensapsri, W., Sutthangkul, J., Tassanakajon, A., 2013b. A serine proteinase *Pm*ClipSP2 contributes to prophenoloxidase system and plays a protective role in shrimp defense by scavenging lipopolysaccharide. Dev. Comp. Immunol. 41, 597–607.

Amparyup, P., Sutthangkul, J., Charoensapsri, W., Tassanakajon, A., 2012. Pattern recognition protein binds to lipopolysaccharide and beta-1,3-glucan and activates shrimp prophenoloxidase system. J. Biol. Chem. 287, 10060–10069.

Amparyup, P., Wiriyaukaradecha, K., Charoensapsri, W., Tassanakajon, A., 2010. A clip domain serine proteinase plays a role in antibacterial defense but is not required for prophenoloxidase activation in shrimp. Dev. Comp. Immunol. 34, 168–176.

Anderson, K.V., 1998. Pinning down positional information: dorsal-ventral polarity in the Drosophila embryo. Cell 95, 439–442.

Cerenius, L., Söderhäll, K., 2004. The prophenoloxidase-activating system in invertebrates. Immunol. Rev. 198, 116–126.

Charoensapsri, W., Amparyup, P., Hirono, I., Aoki, T., Tassanakajon, A., 2009. Gene silencing of a prophenoloxidase activating enzyme in the shrimp, *Penaeus monodon*, increases susceptibility to *Vibrio harveyi* infection. Dev. Comp. Immunol. 33, 811–820.

Charoensapsri, W., Amparyup, P., Hirono, I., Aoki, T., Tassanakajon, A., 2011. *Pm*PPAE2, a new class of crustacean prophenoloxidase (proPO)-activating enzyme and its role in PO activation. Dev. Comp. Immunol. 35, 115–124.

Gorman, M.J., An, C., Kanost, M.R., 2007a. Characterization of tyrosine hydroxylase from *Manduca sexta*. Insect. Biochem. Mol. Biol. 37, 1327–1337.

Gorman, M.J., Wang, Y., Jiang, H., Kanost, M.R., 2007b. *Manduca sexta* hemolymph proteinase 21 activates prophenoloxidase-activating proteinase 3 in an insect innate immune response proteinase cascade. J. Biol. Chem. 282, 11742–11749.

Gupta, S., Wang, Y., Jiang, H., 2005. *Manduca sexta* prophenoloxidase (proPO) activation requires proPO-activating proteinase (PAP) and serine proteinase homologs (SPHs) simultaneously. Insect. Biochem. Mol. Biol. 35, 241–248.

Hoebe, K., Janssen, E., Beutler, B., 2004. The interface between innate and adaptive immunity. Nat. Immunol. 5, 971–974.

Iwanaga, S., Lee, B.L., 2005. Recent advances in the innate immunity of invertebrate animals. J. Biochem. Mol. Biol. 38, 128–150.

Jearaphunt, M., Amparyup, P., Sangsuriya, P., Charoensapsri, W., Senapin, S., Tassanakajon, A., 2015. Shrimp serine proteinase homologues *Pm*MasSPH-1 and -2 play a role in the activation of the prophenoloxidase system. PLoS One 10, e0121073.

Jiang, H., Kanost, M.R., 2000. The clip-domain family of serine proteinases in arthropods. Insect. Biochem. Mol. Biol. 30, 95–105.

Jiang, H., Wang, Y., Kanost, M.R., 1998. Pro-phenol oxidase activating proteinase from an insect, Manduca sexta: a bacteria-inducible protein similar to *Drosophila easter*. Proc. Natl. Acad. Sci. U. S. A. 95, 12220–12225.

Jiang, H., Wang, Y., Yu, X.Q., Kanost, M.R., 2003a. Prophenoloxidase-activating proteinase-2 from hemolymph of *Manduca sexta*. A bacteria-inducible serine proteinase containing two clip domains. J. Biol. Chem. 278, 3552–3561.

Jiang, H., Wang, Y., Yu, X.Q., Zhu, Y., Kanost, M., 2003b. Prophenoloxidase-activating proteinase-3 (PAP-3) from *Manduca sexta* hemolymph: a clip-domain serine proteinase regulated by serpin-1J and serine proteinase homologs. Insect. Biochem. Mol. Biol. 33, 1049–1060.

Jiménez-Vega, F., Vargas-Albores, F., Söderhäll, K., 2005. Characterization of a serine proteinase from *Penaeus vannamei* haemocytes. Fish. Shellfish Immunol. 18, 101–108.

Jitvaropas, R., Amparyup, P., Gross, P.S., Tassanakajon, A., 2009. Functional characterization of a masquerade-like serine proteinase homologue from the black tiger shrimp *Penaeus monodon*. Comp. Biochem. Physiol. B. Biochem. Mol. Biol. 153, 236–243.

Kanost, M.R., Jiang, H., Wang, Y., Yu, X.Q., Ma, C., Zhu, Y., 2001. Hemolymph proteinases in immune responses of *Manduca sexta*. Adv. Exp. Med. Biol. 484, 319–328.

Kwon, T.H., Kim, M.S., Choi, H.W., Joo, C.H., Cho, M.Y., Lee, B.L., 2000. A masquerade-like serine proteinase homologue is necessary for phenoloxidase activity in the coleopteran insect, *Holotrichia diomphalia* larvae. Eur. J. Biochem. 267, 6188–6196.

Lee, S.Y., Cho, M.Y., Hyun, J.H., Lee, K.M., Homma, K.I., Natori, S., Kawabata, S.I., Iwanaga, S., Lee, B.L., 1998a. Molecular cloning of cDNA for pro-phenol-oxidase-activating factor I, a serine protease is induced by lipopolysaccharide or 1,3-beta-glucan in coleopteran insect, *Holotrichia diomphalia* larvae. Eur. J. Biochem. 257, 615–621.

Lee, S.Y., Kwon, T.H., Hyun, J.H., Choi, J.S., Kawabata, S.I., Iwanaga, S., Lee, B.L., 1998b. In vitro activation of pro-phenol-oxidase by two kinds of pro-phenol-oxidase-activating factors isolated from hemolymph of coleopteran, *Holotrichia diomphalia* larvae. Eur. J. Biochem. 254, 50–57.

Liu, H., Jiravanichpaisal, P., Cerenius, L., Lee, B.L., Söderhäll, I., Söderhäll, K., 2007. Phenoloxidase is an important component of the defense against *Aeromonas hydrophila* infection in a crustacean, *Pacifastacus leniusculus*. J. Biol. Chem. 282, 33593–33598.

Morisalo, D., Anderson, K.V., 1995. Signaling pathways that establish the dorsal-ventral pattern of the *Drosophila* embryo. Annu. Rev. Genet. 29, 371–399.

Muta, T., Hashimoto, R., Miyata, T., Nishimura, H., Toh, Y., Iwanaga, S., 1990. Proclotting enzyme from horseshoe crab hemocytes. cDNA cloning, disulfide locations, and subcellular localization. J. Biol. Chem. 265, 22426–22433.

Nappi, A., Christensen, B., 2005. Melanogenesis and associated cytotoxic reactions: applications to insect innate immunity. Insect. Biochem. Mol. Biol. 35, 443–459.

Pfaffl, M.W., 2001. A new mathematical model for relative quantification in real-time RT-PCR. Nucleic Acids Res. 29, 2004–2007.

Sangsuriya, P., Charoensapsri, W., Chomwong, S., Senapin, S., Tassanakajon, A., Amparyup, P., 2016. A shrimp pacifastin light chain-like inhibitor: molecular identification and role in the control of the prophenoloxidase system. Dev. Comp. Immunol. 54, 32–45.

Satoh, D., Horii, A., Ochiai, M., Ashida, M., 1999. Prophenoloxidase-activating Enzyme of the Silkworm, *Bombyx mori* purification, characterization, and cDNA cloning. J. Biol. Chem. 274, 7441–7453.

Smith, C.L., Delotto, R., 1992. A common domain within the proenzyme regions of the *Drosophila snake* and *easter* proteins and *Tachypleus* proclotting enzyme defines a new subfamily of serine proteases. Protein. Sci. 1, 1225–1226.

Söderhäll, K., Cerenius, L., 1998. Role of the prophenoloxidase-activating system in invertebrate immunity. Curr. Opin. Immunol. 10, 23–28.

Wang, R., Lee, S.Y., Cerenius, L., Söderhäll, K., 2001. Properties of the prophenoloxidase activating enzyme of the freshwater crayfish, *Pacifastacus leniusculus*. Eur. J. Biochem. 268, 895–902.

Zou, Z., Jiang, H., 2005. Gene structure and expression profile of *Manduca sexta* prophenoloxidase-activating proteinase-3 (PAP-3), an immune protein containing two clip domains. Insect. Mol. Biol. 14, 433–442.

Zou, Z., Wang, Y., Jiang, H., 2005. *Manduca sexta* prophenoloxidase activating proteinase-1 (PAP-1) gene: organization, expression, and regulation by immune and hormonal signals. Insect. Biochem. Mol. Biol. 35, 627–636.

Developmental and Comparative Immunology 72 (2017) 97–102

Contents lists available at ScienceDirect

Developmental and Comparative Immunology

journal homepage: www.elsevier.com/locate/dci

Short communication

Melanization inhibition protein of *Penaeus monodon* acts as a negative regulator of the prophenoloxidase-activating system

Nattaphop Noothuan [a], Piti Amparyup [a, b], Anchalee Tassanakajon [a, *]

[a] Center of Excellence for Molecular Biology and Genomics of Shrimp, Department of Biochemistry, Faculty of Science, Chulalongkorn University, 254 Phayathai Road, Bangkok 10330, Thailand
[b] National Center for Genetic Engineering and Biotechnology (BIOTEC), National Science and Technology Development Agency (NSTDA), 113 Paholyothin Road, Klong 1, Klong Luang, Pathumthani 12120, Thailand

ARTICLE INFO

Article history:
Received 6 January 2017
Received in revised form
18 February 2017
Accepted 18 February 2017
Available online 21 February 2017

Keywords:
Melanization
proPO system
Shrimp immunity
Melanization inhibition protein

ABSTRACT

Melanization mediated by the prophenoloxidase-activating system (proPO) is an important immune response in invertebrates. However, in addition to melanin, the proPO system produces reactive intermediates that are not only harmful to the invading microbes but also to the host cells. Thus, the proPO system must be tightly regulated by several inhibitors. Previously, a melanization inhibition protein from the black tiger shrimp *Penaeus monodon*, *Pm*MIP, has been identified and preliminarily characterized. In this study, we investigate the function of *Pm*MIP in the regulation of the proPO system in shrimp. When challenged with the bacterium *Vibrio harveyi*, the expression of *Pm*MIP transcripts in gills was down-regulated dramatically at 24 h but recovered after 48 h post infection (hpi), while the *Pm*MIP protein level in shrimp plasma was decreased at 6 hpi but recovered at 24 hpi. Double-stranded RNA-mediated gene silencing of *Pm*MIP suppressed both *Pm*MIP transcriptional and translational levels and resulted in increased hemolymph phenoloxidase and proteinase activities compared to controls injected with GFP dsRNA or NaCl. Furthermore, the recombinant *Pm*MIP protein successfully expressed in *Escherichia coli* was able to inhibit hemolymph PO activity by 50%. These results suggested that *Pm*MIP was involved in the proPO system by acting as a negative regulator and interfering with hemolymph proteinase activity.
© 2017 Elsevier Ltd. All rights reserved.

1. Introduction

The prophenoloxidase (proPO) system is a major innate immune response in invertebrates (especially arthropods) that produces reactive intermediates and melanin to fight pathogens (Söderhäll and Cerenius, 1998; Cerenius and Söderhäll, 2004; Cerenius et al., 2008; Amparyup et al., 2013). The system is activated by pattern recognition proteins (PRPs) that recognize microbial cell wall components such as lipopolysaccharide, β-glucan, and peptidoglycan which results in activation of the serine proteinase cascade. The final enzyme in the cascade, prophenoloxidase activating-enzyme (PPAE), converts the key enzyme proPO from its zymogen form to active PO. Then, PO catalyzes the phenolic compounds yielding reactive intermediate quinones and melanin for elimination and encapsulation of the invading microorganism (Sritunyalucksana and Söderhäll, 2000; Cerenius and Söderhäll, 2004; Iwanaga and Lee, 2005; Kanost and Gorman, 2008; Cerenius et al., 2008). However, the production of reactive intermediates and quinone can be dangerous to host cells. Hence, this system needs to be strictly regulated by several inhibitors such as pacifastin (Liang et al., 1997) and serpins (Kanost, 1999).

Many serpins have been characterized in insects as inhibitors of proPO activation through inhibition of serine proteinase (SP) in the cascade (Jiang et al., 1997; Levashina et al., 1999; Gan et al., 2001; De Gregorio et al., 2002; Ligoxygakis et al., 2002; Zhu et al., 2003; Wang and Jiang, 2004; Tong and Kanost, 2005). Few serpins have been reported in shrimp; for example, *Pm*SERPIN8 and *Pm*SERPIN3 from the black tiger shrimp *Penaeus monodon* inhibited PO activity and proteinase activity (Somnuk et al., 2012; Wetsaphan et al., 2013). Pacifastin has been reported in the crayfish *Pacifastacus leniusculus* to inhibit *Pl*PPAE1 (Liang et al., 1997). Recently, a pacifastin light chain-like inhibitor has been studied in *P. monodon* and shown to function as a negative regulator of the proPO system (Sangsuriya et al., 2016). In addition, panulirin, a new class of peptidase inhibitor, was identified in the lobster *Panulirus argus* to inhibit the melanization response to lipopolysaccharides

* Corresponding author.
E-mail address: anchalee.k@chula.ac.th (A. Tassanakajon).

http://dx.doi.org/10.1016/j.dci.2017.02.014
0145-305X/© 2017 Elsevier Ltd. All rights reserved.

(Perdomo-Morales et al., 2013). Some components were also reported to interfere with proPO activation such as mannose-binding lectin (*Pl*-MBL) and caspase (Wu et al., 2013; Jearaphunt et al., 2014).

The inhibitor of the melanin reaction, melanization inhibition protein (MIP), was originally identified in the beetle *Tenebrio molitor*. Injection of *Candida albicans* into *T. molitor* larvae resulted in decreased *Tm*MIP protein in melanin-induced hemolymph. *Tm*MIP gene silencing induced melanin synthesis and r*Tm*MIP had an inhibitory effect on melanin synthesis (Zhao et al., 2005). In crustaceans, *Pl*MIP protein from the freshwater crayfish *P. leniusculus*, which contains a fibrinogen related domain (FReD), also showed interference with the melanization reaction from quinone compounds to melanin and delayed LPS-induced proteinase activity. *Pl*MIP was degraded when melanization was induced (Söderhäll et al., 2009). In shrimp, *Pm*MIP from *P. monodon* was identified and exhibited approximately 80% amino acid sequence similarity to the crayfish *Pl*MIP. mRNA expression of *Pm*MIP was observed in several shrimp tissues and *Pm*MIP protein responded to heat-killed *Vibrio harveyi* injection (Angthong et al., 2010). However, the function of *Pm*MIP in the regulation of the proPO system in shrimp has not yet been studied.

In this study, *Pm*MIP was further characterized for the temporal expression profile in response to *V. harveyi* infection and for its function in the proPO system using RNA interference (RNAi). The recombinant *Pm*MIP protein was produced and assayed for its inhibitory activity as a negative regulator of the shrimp proPO system.

2. Methods

2.1. Sample preparation

Shrimp *P. monodon* (3–5 g) were purchased from the Shrimp Genetic Improvement Center (BIOTEC, Surat Thani province, Thailand) and reared at 20 ppt of salinity for 3 days before use. *V. harveyi* 639 was cultured in tryptic soy broth (TSB) containing 2% (w/v) NaCl at 250 rpm with shaking at 30 °C overnight. The overnight culture was inoculated in TSB containing 2% (w/v) NaCl until OD_{600} reached 0.5 (1 $OD_{600} = 1 \times 10^6$ colony forming units, cfu). The culture was diluted 10-fold in 150 mM NaCl for experiments.

2.2. RNA extraction and cDNA synthesis

Total RNA was extracted from tissues by TRI REAGENT® (Molecular Research Center) according to the manufacturer's protocol. cDNA was synthesized using the Reverse Transcriptase System kit (Promega). Total RNA and cDNA were kept at −80 °C and −20 °C until use.

2.3. SDS-PAGE and western blot analysis

For determination of endogenous *Pm*MIP protein in shrimp, hemolymph from each group of shrimp was collected in 10% (w/v) sodium citrate. Then, hemolymph was centrifuged at 800×*g* 4 °C for 10 min to separate plasma from hemocytes. Fifty micrograms of plasma were mixed with 5X reducing SDS loading dye and heated at 100 °C for 10 min. The lysates were subjected to 12.5% SDS-PAGE. One gel was stained with Coomassie blue and the other was used to perform western blot analysis. For western blot analysis, the gel was electro-blotted onto a nitrocellulose membrane. Then, the membrane was blocked with 5% (w/v) skim milk in phosphate-buffered saline and 0.05% (v/v) Tween 20 (PBST) for 1 h. After three PBST washes, the membrane was incubated with rabbit anti-*Pm*MIP polyclonal antibody (1:2000 diluted in 1% (w/v) skim milk in PBST) for 3 h. The membrane was then washed four times and incubated with anti-rabbit IgG alkaline phosphatase-conjugated antibody (diluted 1:10,000 in 1% (w/v) skim milk in PBST) for 1 h. After secondary antibody incubation, the membrane was washed four times. For detection, 5-bromo-4-chloro-3-indolyphosphate/nitro blue tetrazolium (BCIP/NBT) was used as a substrate and the reaction was stopped by 0.02 mM ethylenediaminetetraacetic acid (EDTA).

2.4. Analysis of PmMIP gene and protein expression levels in response to bacterial V. harveyi challenge

To investigate expression levels of the *Pm*MIP gene after *V. harveyi* challenge, shrimp were injected with 20 μl of diluted *V. harveyi* culture (2×10^5 cfu). Gills were collected at 0, 6, 24, 48, and 72 h after bacterial injection. Total RNA was extracted and pooled from three shrimp to synthesize cDNA. SsoFast™ EvaGreen® Supermix was used for real time RT-PCR with specific *Pm*MIP gene primers and EF1α primers as an internal control (Table 1). The cycling conditions were 95 °C for 8 min (1 cycle), 95 °C for 10 s, 58 °C for 15 s, 72 °C for 30 s (39 cycles), 95 °C for 30 s (1 cycle), 55 °C for 1 min (1 cycle), and 55 °C for 10 s (1 cycle). Standard curves were performed using 5-fold diluted cDNA (1500 ng–2.4 ng of total RNA). Each time point was measured in triplicate using the CFX96 Touch™ real-time PCR detection system. The Ct value at each time point was normalized with the saline-injected samples. The mathematical model of Pfaffl (2001) was used to determine the relative expression ratio. For detection of *Pm*MIP protein after bacterial challenge, hemolymph from each time point was collected and analyzed as described above.

2.5. In vivo gene knockdown of PmMIP

To produce a *Pm*MIP template for dsRNA synthesis, the DNA fragment was amplified by PCR from a full-length *Pm*MIP containing plasmid using sense and anti-sense primers which included T7 promoter sequence at the 5' ends (Table 1). Additionally, a GFP fragment was generated from pEGFP-1 plasmid (Clontech) using specific primers (Table 1). The *Pm*MIP and GFP dsRNAs were synthesized using *Pm*MIP and GFP DNA templates and the T7 RiboMAX™ Express Large Scale RNA production system (Promega). For gene silencing, shrimp were injected with 2.5 μg of dsRNA dissolved in 150 mM NaCl/g of shrimp. After 24 h post first injection, shrimp were injected again with dsRNA (or 150 mM NaCl) containing 3 μg of lipopolysaccharide (LPS) from *E. coli* 0111:B4 (Sigma) and 3 μg of laminarin (Sigma). Shrimp were reared for a further 48 h post injection and then used for experiments. GFP dsRNA and 150 mM NaCl were used as controls. *Pm*MIP transcripts and protein were analyzed by semi-quantitative RT-PCR and western blot, respectively.

2.6. Semi-quantitative RT-PCR analysis

The efficiency of *Pm*MIP knockdown was analyzed by semi-quantitative RT-PCR using gene specific primers for the *Pm*MIP gene (Table 1). The gill cDNA from each group (*Pm*MIP dsRNA, GFP dsRNA, and 150 mM NaCl) was diluted 10-fold and 1 μl was used for PCR. The PCR analysis was performed at 94 °C for 1 min, followed by 30 cycles of 94 °C for 30 s, 55 °C for 30 s, and 72 °C for 1 min, with an extension at 72 °C for 10 min. The PCR products were analyzed by 1.8% (w/v) agarose gel electrophoresis. EF1α was used as the internal control.

Table 1
Nucleotide sequence of primers.

Primer	Nucleotide sequence	Purpose(s)
MIPT7-F	5′GGATCCTAATACGACTCACTATAGGTGTGGCAATGCTGTGGGCTG3′	RNAi
MIPT7-R	5′GGATCCTAATACGACTCACTATAGGCTCGCAGCGGACCTTCTTAG3′	RNAi
MIP-F	5′TGTGGCAATGCTGTGGGCTG3′	RNAi
MIP-R	5′CTCGCAGCGGACCTTCTTAG3′	RNAi
GFPT7-F	5′TAATACGACTCACTATAGGATGGTGAGCAAGGGCGAGGA3′	RNAi
GFPT7-R	5′TAATACGACTCACTATAGGTTACTTGTACAGCTCGTCCA3′	RNAi
GFP-F	5′ATGGTGAGCAAGGGCGAGGA3′	RNAi
GFP-R	5′TTACTTGTACAGCTCGTCCA3′	RNAi
EF1α-F	5′GGTGCTGGACAAGCTGAAGGC3′	RNAi and real time RT-PCR
EF1α-R	5′CGTTCCGGTGATCATGTTCTTGATG3′	RNAi and real time RT-PCR
MIP_RT-F	5′TTAGCCGTAGGGCAACATTC3′	Real time RT-PCR
MIP_RT-R	5′GCACGAGGGCTTGTACATCT3′	Real time RT-PCR
MIP_NcoI-F	5′CATGCCATGGGTAACGAGCCCCTTAGCCGTAG3′	Cloning and recombinant protein expression
MIP_EcoRIHis-R	5′GGGAATTCCTA*ATGATGATGATGATGATG*ATATCTCGGCCTGATGAGCA3′	Cloning and recombinant protein expression

Underline is T7 promoter.
Italic is six residues of histidine.

2.7. PO activity assay of PmMIP knockdown

The PO activity assay was modified from the method of Amparyup et al. (2009). The hemolymph was withdrawn without any anticoagulant from the ventral sinus of shrimp after the second injection of *Pm*MIP dsRNA, GFP dsRNA (control) and NaCl (control). Protein concentration of hemolymph was determined by the Bradford assay kit (Bio-Rad). In brief, two micrograms of total hemolymph protein in 435 μl of 10 mM Tris-HCl pH 8.0 was incubated with 65 μl of freshly prepared L-3,4-dihydroxyphenylalanine (L-DOPA) (3 mg/ml in water) at room temperature (25 ∘C) for 30 min. Then, the reaction was stopped by adding 500 μl of 10% (v/v) acetic acid. The PO activity was monitored by spectrophotometry at 490 nm and reported as ΔA_{490}/mg total protein/min. Each experimental group was performed in triplicate and data were analyzed using one-way analysis of variance (ANOVA).

2.8. Proteinase activity assay of PmMIP knockdown

The proteinase activity assay was modified from the method described by Söderhäll et al. (2009). Hemolymph from knockdown shrimp was withdrawn using 10 mM Tris-HCl pH 8.0 as an anticoagulant solution. Two hundred and twenty-five micrograms of total hemolymph protein were used in a total volume of 25 μl adjusted with 10 mM Tris-HCl pH 8.0. The protein concentrations were measured by Bradford assay. Next, the reactions were added to 71 μl of proteinase buffer (100 mM Tris-HCl pH 8.0, 100 mM NaCl, and 5 mM $CaCl_2$). Then, 4 μl of 5 mM proteinase substrate B9385, Boc-Val-Pro-Arg-7-amido-4-methylcoumarin hydrochloride were added into each well. Each reaction was incubated in a 96-well plate at room temperature (25 ∘C) for 15 min and then stopped by adding 10% (v/v) acetic acid. The reactions were spectrophotometrically monitored for fluorescence by emission at 460 nm under excitation at 380 nm. Each experimental group was performed in triplicate and data were analyzed using one-way analysis of variance (ANOVA).

2.9. Construction and expression of recombinant (r) PmMIP protein

The mature *Pm*MIP gene was first cloned into the TA cloning vector. The *Pm*MIP gene was amplified from gill cDNA by PCR with Phusion® High-Fidelity DNA polymerase using specific *Pm*MIP gene primers flanked by *Nco*I and *Eco*RI restriction sites and a 6x His tagged sequence (Table 1). Then, the *Pm*MIP DNA fragment was sub-cloned into pET28b and modified pET43.1a as expression vectors and transformed into *E. coli* Rosetta (DE3)-pLysS and *E. coli* BL21 (DE3)-pLysS, respectively. Recombinant protein was over expressed under 0.5 M isopropyl β-D-1-thiogalactopyranoside (IPTG) induction for 6 h at 37 °C shaking at 250 rpm. Then, r*Pm*MIP was purified by Ni-NTA affinity chromatography, dialyzed against 20 mM Tris-HCl pH 8.0, and concentrated though an Amicon (Millipore). The purified proteins were aliquotted and kept at −80 °C until needed. The purified r*Pm*MIP protein from the pET28b vector was used for polyclonal antibody production in a rabbit at the Biomedical Technology Research Unit, Chiangmai University, Thailand while the purified r*Pm*MIP from the pET43.1a vector was used for activity assays.

2.10. PO inhibitory activity assay

To study the function of purified r*Pm*MIP in the proPO system, the activity was assayed with r*Pm*MIP. The PO inhibitory activity assay was modified from the method of Söderhäll et al. (2009). Briefly, hemolymph from normal shrimp was collected in 10 mM Tris-HCl pH 8.0. Two hundred micrograms of total hemolymph protein were adjusted to a volume of 25 μl in 10 mM Tris-HCl pH 8.0 and incubated with 25 μl of r*Pm*MIP (10 μg) containing 20 mM $CaCl_2$ for 10 min. The sample was then incubated with 25 μl of 2 mg/ml LPS. After that, the reaction was incubated with 25 μl of 3 mg/ml L-DOPA as the substrate. The PO activity was measured at 490 nm and defined as ΔA_{490}/mg total protein/min. For the control, rNus expressed from pET43.1a vector and 20 mM Tris-HCl pH 8.0 were used instead of r*Pm*MIP. All reactions were repeated in triplicate.

3. Results and discussion

3.1. Expression analysis of PmMIP transcript and protein after V. harveyi infection

*Pm*MIP was previously identified and gene expression was characterized in black tiger shrimp (Angthong et al., 2010), however, the function of *Pm*MIP has not been studied. To determine the function of *Pm*MIP in shrimp defense, the *Pm*MIP gene and protein expression levels were analyzed after shrimp were challenged with the bacterium *V. harveyi*. Total RNA extracted from gills was used for cDNA template synthesis. The temporal gene expression of *Pm*MIP transcripts was analyzed by real-time quantitative RT-PCR at 0, 6,

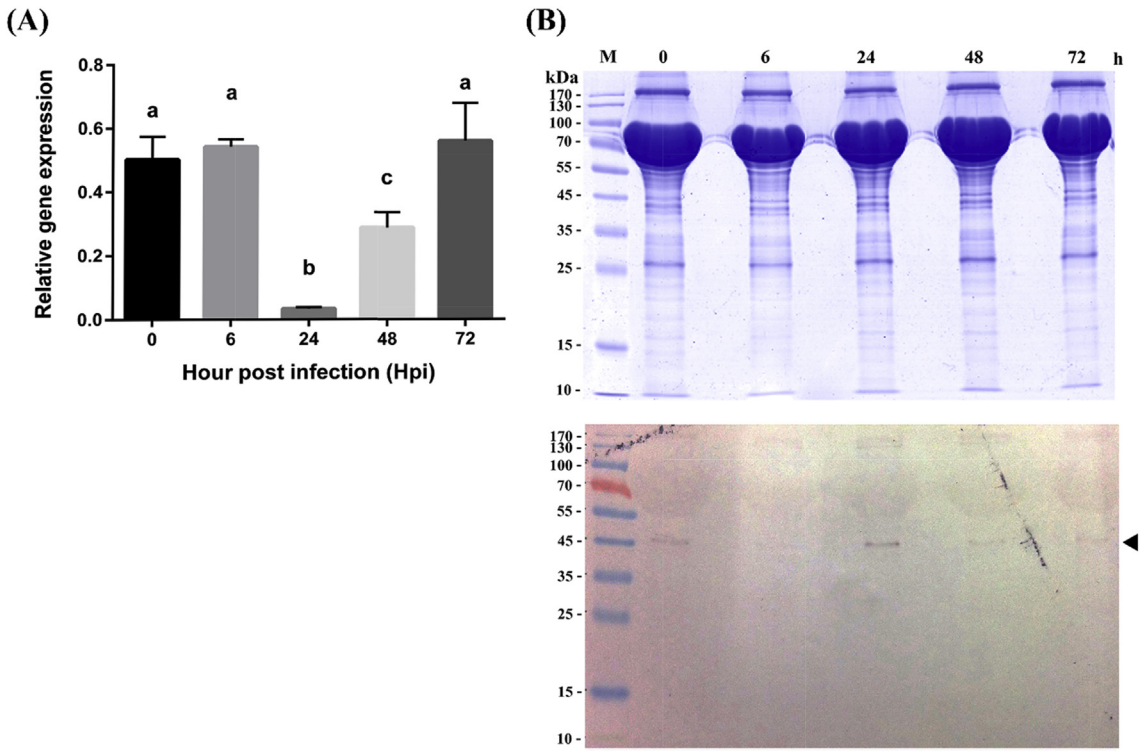


Fig. 1. Expression analysis of *Pm*MIP in *V. harveyi* challenged *P. monodon*. (A) Relative expression of the *Pm*MIP transcript in gills by quantitative real time RT-PCR. Relative expression levels of mRNA were calculated according to Pfaffl (2001) using EF1α as the internal reference gene. The average relative expressions were representative of three independent repeats ± 1S.D. (error bars). Significant difference is indicated by a lowercase letter ($p < 0.05$). (B) *Pm*MIP protein expression profile in cell-free plasma. Samples at various time points (0, 6, 24, 48, and 72 h after injection) were subjected to 12.5% SDS-PAGE with Coomassie blue staining (upper) and western blot (lower) using anti *Pm*MIP antibody. Lane M, PageRuler™ Prestained Protein Ladder. (For interpretation of the references to colour in this figure legend, the reader is referred to the web version of this article.)

24, 48, and 72 h post injection (hpi). The *Pm*MIP transcript was dramatically decreased approximately 7-fold from 0.5 at 0 hpi to 0.07 at 24 hpi, was recovered at 48 hpi and was back to normal levels at 72 hpi (Fig. 1A), suggesting that the *Pm*MIP gene was an immune responsive gene against *V. harveyi* infection. Furthermore, the protein expression level was analyzed in shrimp plasma by western blot using an anti-*Pm*MIP polyclonal antibody. The results showed that *Pm*MIP protein was observed at 0 hpi but disappeared at 6 hpi, then was recovered at 24 hpi (Fig. 1B). This was in accordance with previous studies that reported that *Tm*MIP expression in the beetle *T. molitor* decreased in response to *Candida albicans* and that *Pl*MIP in the crayfish *P. leniusculus* was also absent at 16 h after infection by the bacterium *Hafnia alvei* (Zhao et al., 2005; Söderhäll et al., 2009). Our data are in contrast to the report by Angthong et al. (2010) that found *Pm*MIP transcript was increased at 6 h but disappeared at 24 h and later recovered at 48 and 72 h after being challenged with heat-killed *V. harveyi* (Angthong et al., 2010). It is noteworthy that the previous study used heat-killed bacteria whereas in this study, shrimp were injected with infectious bacteria which might have resulted in the differences in the expression profiles. The responses of *Pm*MIP mRNA and *Pm*MIP protein suggested that it was an immune-related molecule against microbial infection. Decreased *Pm*MIP mRNA expression suggested that the mRNA needed to be down-regulated to control the protein expression. Furthermore, the *Pm*MIP protein had disappeared from shrimp plasma in the early phase of infection to allow the melanization reaction to occur effectively and later had returned back to basal levels to control excessive reactions that would also harmful to the infected shrimp.

3.2. Suppression of PmMIP in shrimp by RNA interference-mediated gene silencing (RNAi)

To study the function of *Pm*MIP in the inhibition of the shrimp proPO system, the *Pm*MIP transcript was silenced by dsRNA-mediated gene knockdown. Shrimp were injected twice with dsRNA against *Pm*MIP or GFP dsRNA or NaCl solution as control groups. Forty-eight hours after the second injection, shrimp hemolymph was collected and gene transcripts were analyzed. The results showed that *Pm*MIP transcripts were suppressed in *Pm*MIP knockdown shrimp when compared to the control GFP dsRNA and NaCl injected shrimp (Fig. 2A). Furthermore, to determine whether *Pm*MIP dsRNA could suppress expression at the protein level, the plasma protein from dsRNA-treated shrimp was analyzed by western blot. It was found that *Pm*MIP protein expression in the plasma protein of dsRNA-treated shrimp was also decreased (Fig. 2B).

3.3. PO activity and proteinase activity in PmMIP knockdown shrimp

To investigate the involvement of *Pm*MIP in the shrimp proPO system, the total hemolymph PO activity of *Pm*MIP knockdown shrimp was measured using L-DOPA as a substrate. The hemolymph PO activity of *Pm*MIP-treated group was significantly increased (55%) when compared to the controls injected with GFP dsRNA or NaCl (Fig. 2C). These results indicated that *Pm*MIP is involved in the proPO system and acts as a negative regulator. To further elucidate the role of *Pm*MIP in melanization inhibition, hemolymph

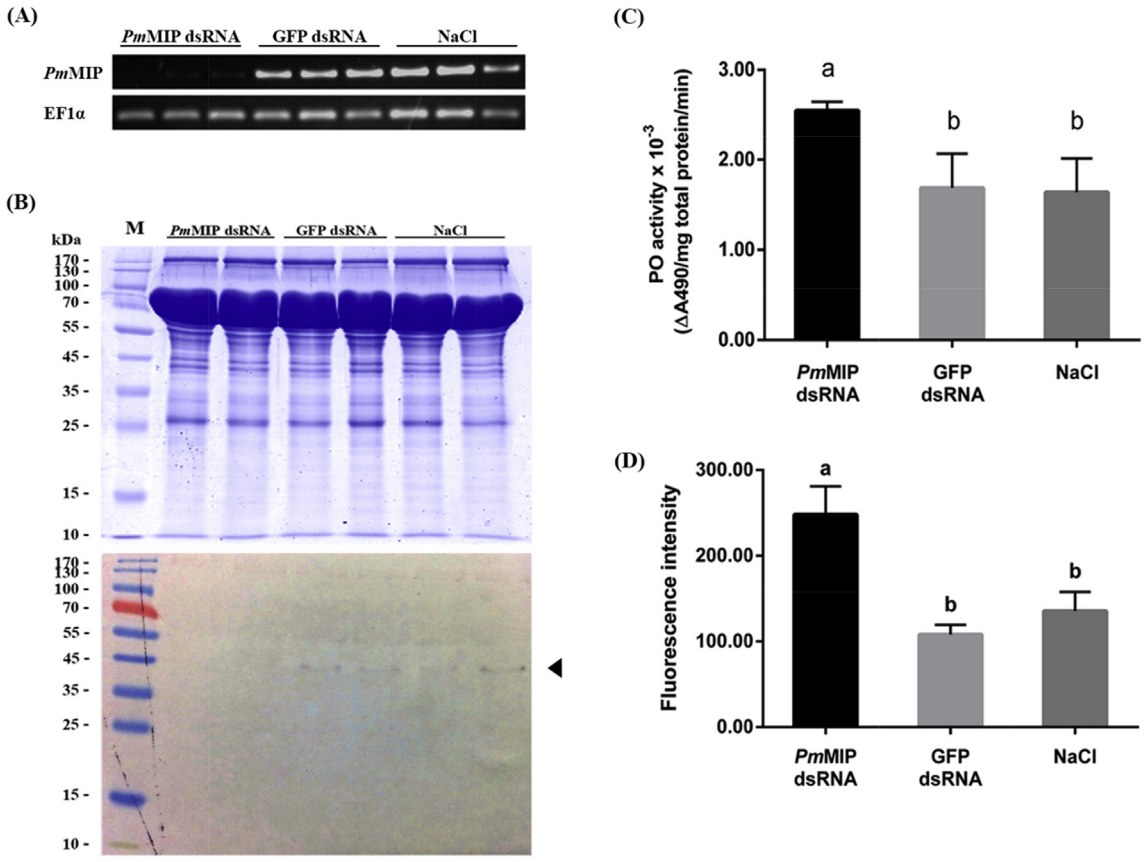


Fig. 2. Gene silencing of *Pm*MIP in shrimp by RNA interference. Shrimp were injected twice with 2.5 μg/g *Pm*MIP dsRNA, GFP dsRNA or NaCl. (A) Efficiency of dsRNA-mediated *Pm*MIP knockdown by semi-quantitative RT-PCR. EF1α was used as the internal reference gene. (B) *Pm*MIP protein expression analysis in the plasma by SDS-PAGE with Coomassie blue staining (upper) and western blot (lower). Lane M, PageRuler™ Prestained Protein Ladder. Each gel lane represents the results from individual shrimp. (C) Hemolymph PO activity in *Pm*MIP knockdown shrimp. Hemolymph were collected at 48 h after the second injection. The total hemolymph PO activity was defined as ΔA_{490}/mg total protein/min. (D) Hemolymph proteinase activity assay in *Pm*MIP knockdown shrimp. The total hemolymph proteinase activity was measured for the fluorescence using proteinase substrate, B9385, with an emission wavelength at 460 nm under the excitation at 380 nm. The data are shown as the mean ± 1S.D. (error bars) and are derived from three independently replicated experiments. Means with a different lowercase letter (above each bar) are significantly different ($p < 0.05$). (For interpretation of the references to colour in this figure legend, the reader is referred to the web version of this article.)

proteinase activity assay was also determined in the *Pm*MIP knockdown shrimp. The proteinase activity was measured by the emission at 460 nm under the excitation at 380 nm using the fluorescence peptide B9385 as substrate. A significant increase in proteinase activity was observed in hemolymph of the *Pm*MIP knockdown group compared with the controls (Fig. 2D). The increased proteinase activity suggested that *Pm*MIP might interfere with the proteinase activation leading to melanization inhibition. Accordingly, r*Pl*MIP protein could inhibit the proteinase activity using the crayfish PPAE substrate S-2222 (Zhao et al., 2005).

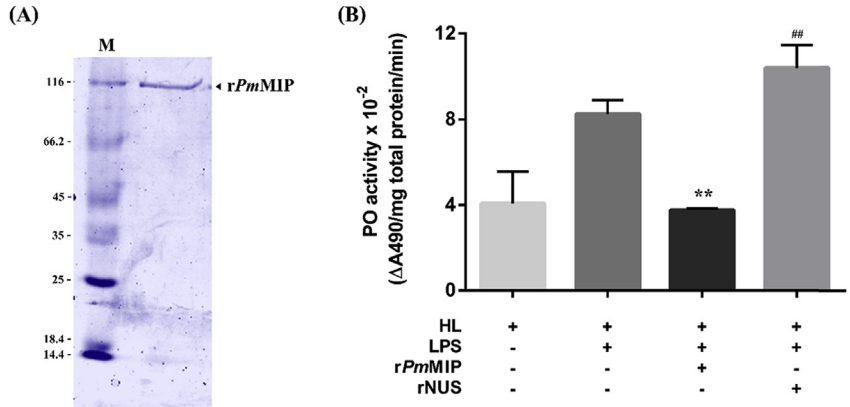


Fig. 3. Purified r*Pm*MIP and Inhibition of hemolymph PO activity by r*Pm*MIP *in vitro*. (A) Purified r*Pm*MIP was expressed under IPTG induction and purified by Ni-NTA column chromatography. (B) The total hemolymph (HL) was incubated with r*Pm*MIP, LPS, and L-DOPA as the substrate. rNus was used as a protein control. The data are shown as the mean ± 1S.D. (error bars) and are derived from three independently replicated experiments. Means with the different asterisk and sharp (above bar) are significantly different ($p < 0.05$) compared with the control group adding buffer.

However, in *T. molitor*, r*Tm*MIP protein could not inhibit the proteinase activity using trypsin substrate (Söderhäll et al., 2009). The mechanism by which the MIP protein inhibits proteinase activity is unclear and need to be further elucidated.

3.4. Inhibition of PO activity in shrimp hemolymph

To study inhibition activity, r*Pm*MIP protein was produced in the *E. coli* system and purified by Ni-NTA affinity chromatography which contains the NUS tag at the N-terminus and the His tag at the C-terminus (Fig. 3A). Hemolymph from normal shrimp was incubated with r*Pm*MIP, LPS, and L-DOPA and monitored at 490 nm. The results showed that the addition of r*Pm*MIP significantly decreased the PO activity. Meanwhile, rNUS significantly increased the hemolymph PO activity (Fig. 3B). This indicated that *Pm*MIP might be an inhibitor of the shrimp proPO system. Previous findings showed that r*Tm*MIP could inhibit melanin synthesis *in vitro* in the presence of β-1,3-glucan and that r*Pl*MIP could inhibit the PO activity when pre-incubated with hemolymph prior to the LPS-PGN addition (Zhao et al., 2005; Söderhäll et al., 2009). Furthermore, *Pm*MIP was reported to contain FReD with an Asp-rich region (Angthong et al., 2010) which might be necessary for the protein. The importance of Asp-rich regions and putative calcium binding sites in crayfish *Pl*MIP was investigated by deleting the four Asp amino acids in r*Pl*MIP and testing the effect of calcium on PO activity. The results showed decreased inhibitory activity when the four Asp amino acids were deleted, but the addition of calcium had no effect on the inhibitory activity of r*Pl*MIP. These data suggested that the Asp-rich region was involved in inhibitory activity by a different ligand (Söderhäll et al., 2009).

Acknowledgments

This work was supported by research grants from the Thailand Research Fund to AT (TRF Senior Scholar No. RTA5880004), the Thailand Research Fund and Thailand National Center for Genetic Engineering and Biotechnology (BIOTEC) to PA (Grant No. BRG5880016). Additional support from TRF (Grant No. IRG5780008) to the Department of Biochemistry, Faculty of Science, Chulalongkorn University is acknowledged. NN is the recipient of a student fellowship from Chulalongkorn University Graduate Scholarship to Commemorate the 72nd Anniversary of His Majesty King Bhumibol Adulyadej and the 90th Anniversary of Chulalongkorn University Fund (Ratchadaphiseksomphot Endowment Fund). We acknowledge Chulalongkorn University for the support to the Center of Excellence for Molecular Biology and Genomics of Shrimp.

References

Amparyup, P., Charoensapsri, W., Tassanakajon, A., 2013. Prophenoloxidase system and its role in shrimp immune responses against major pathogens. Fish. Shellfish Immunol. 34, 990–1001.
Amparyup, P., Charoensapsri, W., Tassanakajon, A., 2009. Two prophenoloxidases are important for the survival of *Vibrio harveyi* challenged shrimp *Penaeus monodon*. Dev. Comp. Immunol. 33, 247–256.
Angthong, P., Watthanasurorot, A., Klinbunga, S., Ruangdej, U., Söderhäll, I., Jiravanichpaisal, P., 2010. Cloning and characterization of a melanization inhibition protein (*Pm*MIP) of the black tiger shrimp, *Penaeus monodon*. Fish. Shellfish Immunol. 29, 464–468.
Cerenius, L., Lee, B.L., Söderhäll, K., 2008. The proPO-system: pros and cons for its role in invertebrate immunity. Trends Immunol. 29, 263–271.
Cerenius, L., Söderhäll, K., 2004. The prophenoloxidase-activating system in invertebrates. Immunol. Rev. 198, 116–126.
De Gregorio, E., Han, S.J., Lee, W.J., Baek, M.J., Osaki, T., Kawabata, S.I., Lee, B.L., Iwanaga, S., Lemaitre, B., Brey, P.T., 2002. An immune-responsive Serpin regulates the melanization cascade in *Drosophila*. Dev. Cell. 3, 581–592.
Gan, H., Wang, Y., Jiang, H., Mita, K., Kanost, M.R., 2001. A bacteria-induced, intracellular serpin in granular hemocytes of *Manduca sexta*. Insect Biochem. Molec. Biol. 31, 887–898.
Iwanaga, S., Lee, B.L., 2005. Recent advances in the innate immunity of invertebrate animals. J. Biol. Mol. 38, 128–150.
Jearaphunt, M., Noonin, C., Jiravanichpaisal, P., Nakamura, S., Tassanakajon, A., Söderhäll, I., Söderhäll, K., 2014. Caspase-1-like regulation of the proPO-system and role of ppA and Caspase-1-like cleaved peptides from proPO in innate immunity. PLoS Pathog. 10, e1004059.
Jiang, H., Wang, Y., Ma, C., Kanost, M.R., 1997. Subunit composition of pro-phenol oxidase from *Manduca sexta*: molecular cloning of subunit ProPO-P1. Insect Biochem. Molec. Biol. 27, 835–850.
Kanost, M.R., 1999. Serine proteinase inhibitors in arthropod immunity. Dev. Comp. Immunol. 23, 291–301.
Kanost, M.R., Gorman, M.J., 2008. Phenoloxidase in insect immunity. In: Beckage, N.E. (Ed.), Insect Immunology. Academic Press, San Diego, pp. 69–96.
Levashina, E.A., Langley, E., Green, C., Gubb, D., Ashburner, M., Hoffmann, J.A., Reichhart, J.M., 1999. Constitutive activation of toll-mediated antifungal defense in serpin-deficient *Drosophila*. Science 285, 1917–1919.
Liang, Z., Sottrup-Jensen, L., Aspan, A., Hall, M., Söderhäll, K., 1997. Pacifastin, a novel 155-kDa heterodimeric proteinase inhibitor containing a unique transferrin chain. Proc. Natl. Acad. Sci. U. S. A. 94, 6682–6687.
Ligoxygakis, P., Pelte, N., Ji, C., Leclerc, V., Duvic, B., Belvin, M., Jiang, H., Hoffmann, J.A., Reichhart, J.M., 2002. A serpin mutant links Toll activation to melanization in the host defence of *Drosophila*. EMBO J. 21, 6330–6337.
Perdomo-Morales, R., Montero-Alejo, V., Corzo, G., Besada, V., Vega-Hurtado, Y., González-González, Y., Perera, E., Porto-Verdecia, M., 2013. The trypsin inhibitor panulirin regulates the prophenoloxidase-activating system in the spiny lobster *Panulirus argus*. J. Biol. Chem. 288, 31867–31879.
Pfaffl, M.W., 2001. A new mathematical model for relative quantification in real-time RT-PCR. Nucleic Acids Res. 29, e45.
Sangsuriya, P., Charoensapsri, W., Chomwong, S., Senapin, S., Tassanakajon, A., Amparyup, P., 2016. A shrimp pacifastin light chain-like inhibitor: molecular identification and role in the control of the prophenoloxidase system. Dev. Comp. Immunol. 54, 32–45.
Söderhäll, I., Wu, C., Novotny, M., Lee, B.L., Söderhäll, K., 2009. A novel protein acts as a negative regulator of prophenoloxidase activation and melanization in the freshwater crayfish *Pacifastacus leniusculus*. J. Biol. Chem. 284, 6301–6310.
Söderhäll, K., Cerenius, L., 1998. Role of the prophenoloxidase-activating system in invertebrate immunity. Curr. Opin. Immunol. 10, 23–28.
Somnuk, S., Tassanakajon, A., Rimphanitchayakit, V., 2012. Gene expression and characterization of a serine proteinase inhibitor *Pm*SERPIN8 from the black tiger shrimp *Penaeus monodon*. Fish. Shellfish. Immunol. 33, 332–341.
Sritunyalucksana, K., Söderhäll, K., 2000. The proPO and clotting system in crustaceans. Aquaculture 191, 53–69.
Tong, Y., Kanost, M.R., 2005. *Manduca sexta* serpin-4 and serpin-5 inhibit the prophenoloxidase activation pathway: cDNA cloning, protein expression, and characterization. J. Biol. Chem. 280, 14923–14931.
Wang, Y., Jiang, H., 2004. Purification and characterization of *Manduca sexta* serpin-6: a serine proteinase inhibitor that selectively inhibits prophenoloxidase-activating proteinase-3. Insect Biochem. Molec. Biol. 34, 387–395.
Wetsaphan, N., Rimphanitchayakit, V., Tassanakajon, A., Somboonwiwat, K., 2013. *Pm*SERPIN3 from black tiger shrimp *Penaeus monodon* is capable of controlling the proPO system. Dev. Comp. Immunol. 41, 110–119.
Wu, C., Charoensapsri, W., Nakamura, S., Tassanakajon, A., Söderhäll, I., Söderhäll, K., 2013. An MBL-like protein may interfere with the activation of the proPO-system, an important innate immune reaction in invertebrates. Immunobiology 218, 159–168.
Zhao, M., Söderhäll, I., Park, J.W., Ma, Y.G., Osaki, T., Ha, N.C., Wu, C.F., Söderhäll, K., Lee, B.L., 2005. A novel 43-kDa protein as a negative regulatory component of phenoloxidase-induced melanin synthesis. J. Biol. Chem. 280, 24744–24751.
Zhu, Y., Wang, Y., Gorman, M.J., Jiang, H., Kanost, M.R., 2003. *Manduca sexta* serpin-3 regulates prophenoloxidase activation in response to infection by inhibiting prophenoloxidase-activating proteinases. J. Biol. Chem. 278, 46556–46564.

Fish & Shellfish Immunology 62 (2017) 68–74

Contents lists available at ScienceDirect

Fish & Shellfish Immunology

journal homepage: www.elsevier.com/locate/fsi

Full length article

Alpha-2-macroglobulin is a modulator of prophenoloxidase system in pacific white shrimp *Litopenaeus vannamai*

Sirikwan Ponprateep [a, *], Tipachai Vatanavicharn [b], Chu Fang Lo [c], Anchalee Tassanakajon [d], Vichien Rimphanitchayakit [d, **]

[a] Department of Chemistry, Faculty of Science, Srinakharinwirot University, 114 Sukhumvit 23 Road, Bangkok 10110, Thailand
[b] Applied Analytical Chemistry Research Unit, Department of Chemistry, Faculty of Science, King Mongkut's Institute of Technology Ladkrabang, Chalongkrung Road, Bangkok 10520, Thailand
[c] Institute of Bioinformatics and Biosignal Transduction, College of Bioscience and Biotechnology, National Cheng Kung University, Tainan 701, Taiwan
[d] Center of Excellence for Molecular Biology and Genomics of Shrimp, Department of Biochemistry, Faculty of Science, Chulalongkorn University, Phyathai Road, Bangkok 10330, Thailand

ARTICLE INFO

Article history:
Received 20 October 2016
Received in revised form
16 December 2016
Accepted 22 December 2016
Available online 24 December 2016

Keywords:
Alpha-2-macroglobulin
Prophenoloxidase system
Vibrio parahaemolyticus AHPND
Litopenaeus vannamei
Proteinase inhibitor

ABSTRACT

The shrimp multifunctional protein alpha-2-macroglobulin (A2M) is abundantly expressed in plasma, highly up-regulated upon microbial infection and involved in several immune pathways such as blood clotting system, phagocytosis and melanization. Herein, the function of *Lv*A2M from *Litopenaeus vannamei* on the prophenoloxidase (proPO) system is reported. The recombinant (r)*Lv*A2M produced strongly and specifically inhibited trypsin and the PO activity in shrimp plasma in a dose-dependent manner. Silencing of *Lv*A2M led to an increase in the PO activity in shrimp plasma although the expression of proPO-associated genes, proPO-activating enzyme (*PPAE*) and prophenoloxidase (*proPO*) but not the proPO-activating factor (*PPAF*) was down-regulated. In *Vibrio parahaemolyticus* AHPND-infected shrimp, the *Lv*A2M activity was suppressed in an early phase of infection while the PO activity was increased. Thus, the proPO-activating system was regulated by the *Lv*A2M.

© 2016 Elsevier Ltd. All rights reserved.

1. Introduction

In crustacean, the innate immune system responds against the pathogenic microorganism. Therein, the humoral defense mechanisms in the hemolymph such as the blood clotting, activation of signaling pathways and melanization, are activated by the serine proteinase cascades [1]. The host pattern recognition of bacterial endotoxin upon infection triggers the serine proteinase cascades resulting in an activation of a series of serine proteinase zymogens and defense mechanisms to accomplish the final task of killing the pathogenic invaders [2,3]. The active proteinases are hazardous to the tissues and needed to be controlled. This immunomodulatory role is played by several serine proteinase inhibitors (SPIs) in the blood circulation system in order to maintain the host homeostasis. The well-known serine proteinase inhibitors are Kazal-type SPIs, Kunitz-type SPIs, Bowman-Birk inhibitors, alpha-2-macroglobulin (A2M), serpins, and pacifastin [4,5].

For the melanization, the formation of melanin leads to the formation of toxic intermediary compounds via the activation of prophenoloxidase (proPO) system which not only destroy the invading microorganisms but also impose serious injury to the host cells [6]. To achieve the appropriate balance in the melanin synthesis, several serine proteinase inhibitors with reported inhibitory effect on the serine proteinases in the plasma come into play. For example, pacifastin from the hemolymph of crayfish *Pacifastacus leniusculus* inhibits the proPO-activating enzyme [7,8]. The proPO activation in the tobacco hornworm, *Manduca sexta*, is regulated by serine proteinase inhibitors (serpins) [9,10].

In crayfish, *Pacifastacus leniusculus*, a high-molecular weight proteinase inhibitor, alpha-2-macroglobulin-like protein, detected in crayfish plasma has been reported to inhibit trypsin and chymotrypsin, and decrease the phenol oxidase activity in the crayfish plasma [8,11]. In shrimp, only a few reports about the negative regulation of proPO activating system have been published. The recombinant LvSerpin from *Litopenaeus vannamei* [12]

* Corresponding author.
** Corresponding author.
E-mail addresses: sirikwanp@g.swu.ac.th (S. Ponprateep), kpvr2@yahoo.com (V. Rimphanitchayakit).

http://dx.doi.org/10.1016/j.fsi.2016.12.028
1050-4648/© 2016 Elsevier Ltd. All rights reserved.

and *Pm*SERPIN8 [13] are able to inhibit the shrimp proPO activating system.

The alpha-2-macroglobulin (A2M), one of the most abundant and multifunctional protein, is a broad range serine proteinase inhibitor [14]. It is involved in several immune responses in invertebrates such as phagocytosis [15], blood clotting system [16], proPO activating system [17]. Although the A2M has been reported its presence in shrimp such as *Marsupenaeus japonicus* [18], *Penaeus monodon* [19], *Litopenaeus vannamei* [20], *Macrobrachium rosenbergii* [21], *Fenneropenaeus chinensis* [22], *Farfantepenaeus paulensis* [23], and *Fenneropenaeus indicus* [24], its biological function on proPO activation has not yet been clearly elucidated. Most studies show the up-regulation of A2M gene transcript upon microbial infection as an important clue for its involvement in shrimp immune responses.

In this report, we have investigated the function of A2M on proPO activating system and its inhibitory activity on commercial serine proteinases. The recombinant A2M was produced using an *E. coli* system and tested for its activity on the proPO activating system in shrimp plasma. Moreover, the effect of A2M gene knockdown on proPO activity was elucidated and the expression of proPO-associated genes was determined in the A2M knockdown shrimp.

2. Materials and methods

2.1. Shrimp and Vibrio parahaemolyticus AHPND

The Pacific white shrimp were kindly provided by Charoen Pokphand Group (CP), Phetchaburi Province, Thailand. The shrimp were acclimatized in sea water with salinity of 15 ppt at ambient temperature for a few days before used.

Vibrio parahaemolyticus AHPND (VP_{AHPND}) was cultured in Tryptic Soy Broth (TSB) containing 3% NaCl at 30 °C for an overnight. The starter culture was inoculated in TSB at a dilution of 1:100 and cultured at 30 °C until the OD_{600} reached 1.7–2.0 equivalent to a bacterial density of approximately 1×10^9 colony forming units per mL (CFU/mL). The culture was diluted to 1×10^6 CFU/mL for immersion experiment.

2.2. Expression and purification of recombinant LvA2M

To construct an expression plasmid encoding the mature *Lv*A2M protein, a pair of PCR primers were designed according to the *LvA2M* cDNA sequence (accession no. DQ988330) [20]; an A2M_LV_Forward primer with 5′ BamHI site and an A2M_LV_Reverse primer with 5′ NotI site (Table 1). The mature *LvA2M* gene was PCR amplified from the shrimp cDNA preparation. The PCR product of 4451 bp was cleaved with NotI and BamHI and cloned in-frame into the NotI and BamHI sites of an expression vector pET-28b(+) derivative, pVR600 (Baucheun et al., unpublished result) [13]. The recombinant plasmid was sequenced to confirm the correctness of *LvA2M* gene sequence. The r*Lv*A2M expression plasmid obtained was named pVR600-*Lv*A2M.

To produce the recombinant *Lv*A2M (r*Lv*A2M), the pVR600-*Lv*A2M was transformed into an *E. coli* BL21(DE3). A single colony was cultured as starter in LB broth plus kanamycin at 37 °C overnight, inoculated into a new LB broth plus kanamycin and cultured until an OD_{600} reached 0.6. The gene expression was induced by adding IPTG to the final concentration of 1 mM and the culture was continued for another 4 h. The cells were collected by centrifugation at 8000 × g for 5 min. The cell pellet was suspended in 50 mM Tris-HCl pH 8.0 and sonicated to break the bacterial cells. The *Lv*A2M protein expressed as inclusion bodies was collected from the cell lysate by centrifugation at 8000 × g for 15 min, dissolved in 10 mM NaOH for 1 h. The crude protein was dialyzed against 50 mM Tris-HCl pH 8.0 and then subjected to 8% SDS-PAGE. The protein band, approximately 180 kDa, was cut from the acrylamide gel and eluted from the gel by crushing and soaking in 50 mM Tris-HCl pH 8.0. The supernatant was collected by centrifugation at 12000 × g for 5 min and then filtrated using PVDF membrane pore size 0.45 μm. The *Lv*A2M was concentrated using ultrafiltration and determined the protein concentration using Bradford assay (Bio-Rad) [25]. The purified *Lv*A2M was subjected to 8% SDS-PAGE to check for the protein purity.

2.3. Proteinase inhibitory activity of rLvA2M

The proteinase inhibitory activity of r*Lv*A2M was assayed against subtilisin (*Bacillus licheniformis*, Sigma), α-chymotrypsin (type II bovine pancreas, Sigma), trypsin (bovine pancreas, Sigma), and elastase (porcine pancreas, Pacific Science) following a method of Hergenhahn et al. (1987) [8]. The reaction mixture consisted of a chromogenic substrate in 50 mM Tris-HCl pH 8.0. The 146.8 and 293.6 μM of *N*-benzoyl–Phe–Val–Arg–*p*-nitroanilide (Sigma) were used as substrate for trypsin and subtilisin, respectively. The 147.3 μM of *N*-succinyl–Ala–Ala–Pro–Phe–*p*-nitroanilide (Sigma) was used as substrate for chymotrypsin and 443.1 μM of *N*-succinyl–Ala–Ala–Ala–*p*-nitroanilide (Sigma) was used as substrate for elastase.

The reaction mixtures were incubated with the molar ratios of r*Lv*A2M to proteinase at 0, 1.56, 3.125, 6.25, 12.5, 25 and 50 for 15 min. The reaction was terminated by adding 50 μL of 50% acetic acid and, then, measured the absorbance of *p*-nitroaniline at 405 nm. The proteinase inhibitory activity of r*Lv*A2M was calculated and presented graphically as the percentages of remaining activity against the molar ratios of r*Lv*A2M to proteinase.

2.4. Effect of rLvA2M on proPO activating system in shrimp plasma

To determine the inhibitory activity of r*Lv*A2M on proPO activating system in shrimp plasma, the hemolymph was collected from five shrimp into phosphate buffered saline (PBS) at the ratio of 1:3. The mixture was centrifuged at 800 × g for 15 min to separate the shrimp plasma. The total protein in shrimp plasma was determined by using the Bradford assay.

In the assay of proPO activating system or PO activity, 150 μg of shrimp plasma protein was pre-incubated with 0.433 μM final concentration of r*Lv*A2M or phenylthiourea (PTU) as a positive control and 10 μL of 5 mg/ml lipopolysaccharides (LPS). The mixture was incubated for 15 min at 30 °C. The reaction volume was adjusted to 90 μL with 50 mM Tris-HCl pH 8.0. Then, 25 μL of 3 mg/mL of the chromogenic substrate, L-3,4-dihydroxyphenylalanine (L-DOPA), was added at time zero to start the reaction. The increase in A_{490} was measured for 60 min in a microplate reader. The experiment was done in triplicate.

To determine the dose-dependence effect of r*Lv*A2M on proPO inhibition, the PO activity was measured as above in the presence of various concentrations of r*Lv*A2M. The r*Lv*A2M was added to the final concentrations of 0, 0.216, 0.433 and 0.866 μM. The experiment was done in triplicate.

2.5. Gene silencing of LvA2M

For dsRNA interference experiment, the gene-specific primers for *LvA2M* gene and green fluorescent protein gene (*GFP*) (Table 1) were used to amplify the said genes in the recombinant plasmids, pVR600-*Lv*A2M and pEGFP-1, using PCR technique. Then, one μg of each DNA template was used for in vitro transcription using the T7 RiboMAX™ Express Large Scale RNA Production System (Promega)

Table 1
Primers used to this study.

Primer	Sequence (5'-3')	Usage
A2M_LV_Forward	ACTGGGATCCATACGTCGTCACGACTCCG	Amplification of *Lv*A2M gene encoding mature protein
A2M_LV_Reverse	TATTATAGCGGCCGCGTCGCACCCTTCGACGTA	
Actin_F	GAACCTCTCGTTGCCGATGGTG	Internal control for RT-PCR
Actin_R	GAAGCTGTGCTACGTGGCTCTG	
proPO_Lv_Forward	CATAGAACACGGCCCTGAG	Real-time RT-PCR
proPO_Lv_Reverse	AATGTCGTACCTGGCGATAAT	
PPAE_Lv_Forward	CACGGGCAACAGGAGAAAC	
PPAE_Lv_Reverse	CGGCAGATTTGGAATGAGGA	
PPAF_Lv_Forward	GCAAGAGGAACTCGCAAGGCTTC	
PPAF_Lv_Reverse	CGGCTGTGAGAACGATGGATGGA	
EF-1α_Lv_Forward	CTTGATTGCCACACTGCTCAC	
EF-1α_Lv_Reverse	TCTCCACGCACATAGGCTTG	
KD_GFP_T7F	GGATCCTAATACGACTCACTATAGGATGGTGAGCAAGGGGGAGGA	dsRNA knockdown
KD_GFP_T7R	GGATCCTAATACGACTCACTATAGGTTACTTGTACAGCTCGTCCA	
KD_GFP_F	ATGGTGAGCAAGGGGGAGGA	
KD_GFP_R	TTACTTGTACAGCTCGTCCA	
KD_A2M_T7F	GGATCCTAATACGACTCACTATAGGCCATGGAGGGGCAGGGATGC	
KD_A2M_T7R	GGATCCTAATACGACTCACTATAGGATCGCACCCTTCGAGGTACG	
KD_A2M_F	CCATGGAGGGGCAGGGATGC	
KD_A2M_R	ATCGCACCCTTCGAGGTACG	

following the manufacturer's instructions. The quality and amount of dsRNA were evaluated by agarose gel electrophoresis and determined by UV spectrophotometer, respectively.

To silence the *LvA2M* gene, the healthy juvenile *L. vannamei* shrimp, each with a body weight of 3 g, were divided into three groups of 5 shrimp. Each shrimp was intramuscularly injected into the third abdominal segment with dsRNA. Two groups were injected with 10 μg of dsRNA-*Lv*A2M and dsRNA-GFP control per g shrimp in 30 μL PBS. The third group was injected with 30 μL PBS as another control. After 24 h, the shrimp were injected again with the same dsRNAs or PBS. The shrimp hemolymph was collected at 6 h after the second injection with 3 vol of PBS.

To assess the gene silencing, the hemolymph was collected from individual shrimp and immediately extracted with TRI Reagent for the total RNA according to the manufacturer's protocol. The first-strand cDNA was synthesized from one μg of total RNA using RevertAid First Strand cDNA Synthesis Kit (Thermo Fisher Scientific) as directed by the manufacturer's protocol. The *Lv*A2M transcript in each total RNA sample was examined by semi-quantitative RT-PCR using *Lv*A2M gene specific primer pair (Table 1). The β-actin gene was served as an internal control.

The RT-PCR reaction was done using 2 μL of 1:5 dilution of the first-strand cDNA preparation in a 25 μL PCR reaction which contains 10 × PCR buffer, 100 μM each dNTP, 0.2 μM each specific primer and 1 unit of *Taq* DNA polymerase (RBC). The thermal cycling conditions were 94 °C for 1 min followed by 25 cycles of 94 °C 30 s, 55 °C 30 s, 72 °C 30 s and the final step of 72 °C 5 min. The PCR reactions were analyzed by 1.8% agarose gel electrophoresis.

2.6. Effect of LvA2M gene knockdown on the hemolymph PO activity

Shrimp were injected with dsRNA-*LvA2M*, dsRNA-*GFP* or PBS as described above. The shrimp hemolymph was collected and pooled. The total protein was measured by Bradford assay. The shrimp hemolymph of 150 μg protein was incubated with LPS for 15 min and, then, added the chromogenic substrate L-DOPA. The PTU was used as a positive control. The reactions were measured the A_{490} for 30 min in a microplate reader. The experiment was done in triplicate. The results were subtracted from those of PTU controls and expressed as relative PO activity.

2.7. Effect of LvA2M gene silencing on the expression of proPO-associated genes

The expression of proPO-associated genes, prophenoloxidase *Lv*proPO1 and 2 (GenBank accession no. EF115296 and EU373096, hereinafter mentioned as *Lv*proPO), prophenoloxidase activating enzyme *Lv*PPAE (JX644452) and prophenoloxidase activating factor *Lv*PPAF (JX644454), in response to *Lv*A2M gene silencing was investigated using qRT-PCR. The first-strand cDNA was synthesized from one μg of total RNA as described above. The level of target gene transcripts in each RNA sample was examined by qRT-PCR using primer pairs specific to the proPO-associated genes (Table 1). The expression of *EF-1α* was served as an internal control.

Two microliters of appropriately diluted first-strand cDNA were subjected to qRT-PCR in a 10 μL reaction volume containing 5 μL of 2 × QPCR Green Master Mix (Fluorescein) (Biotechrabbit) and 0.25 μL of 10 μM each specific primer. The thermal cycling conditions were: 94 °C for 3 min, followed by 40 cycles of 94 °C for 30 s, 56 °C for 30 s, 72 °C for 30 s and 72 °C for 5 min. Each sample group was from 3 to 4 individual shrimp. The threshold cycle (Ct) for each sample was analyzed by a mathematical model described by Pfaffl (2001) [26].

2.8. A2M and PO activities in plasma of VP_{AHPND} infected shrimp

To study how the shrimp responded to the VP_{AHPND} infection in terms of *Lv*A2M and PO activities in shrimp plasma, the white shrimp (7–10 g) were immersed in bacterial suspension in sea water containing 1×10^6 CFU/mL of VP_{AHPND}. The shrimp plasma was collected at 0, 3, 6, 12, 24 and 48 h after immersion. Shrimp hemolymph was collected from 9 shrimp at each time point with anticoagulant at the ratio of 1:3 and immediately centrifuged at 800 × g for 15 min to separate the shrimp plasma. Three shrimp plasma were pooled as one group of plasma sample and determined the total protein using Bradford assay.

The *Lv*A2M inhibitory activity in plasma was assayed by incubating 10 μL of 1 mg/mL bovine pancreatic trypsin (Sigma-Aldrich) with 30 μL of shrimp plasma (1000 μg) or 50 mM Tris-HCl pH 8.0 at 37 °C for 15 min. The reaction mixture was, then, incubated with 10 μL of 2 mg/ml soybean trypsin inhibitor (SBTI, Sigma-Aldrich) at 37 °C for 10 min to inhibit free trypsin. The activity of A2M-trapped trypsin was assayed by adding 100 μL of 1 mg/mL BAPNA (*N*-α-

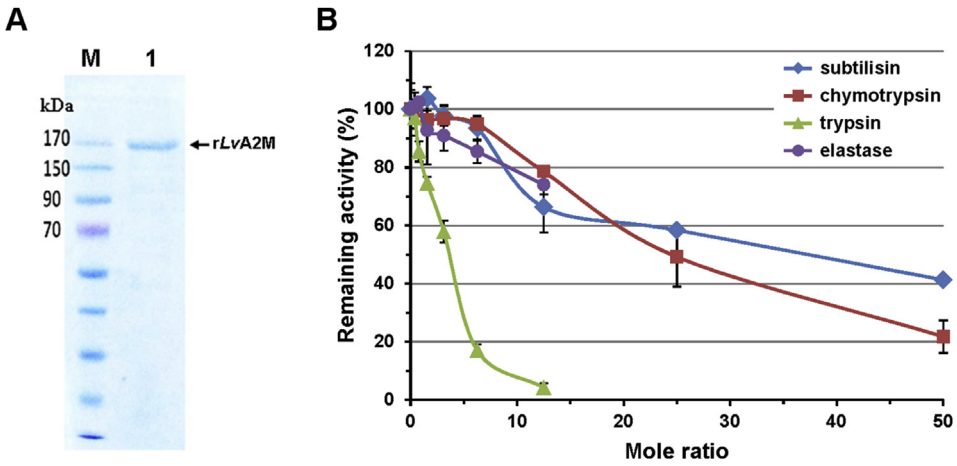


Fig. 1. Proteinase inhibitory assay of r*Lv*A2M. (A) SDS-PAGE analysis of the purified r*Lv*A2M. The "M" is the size marker. (B) The inhibitory activity of r*Lv*A2M against trypsin, α-chymotrypsin, subtilisin and elastase.

benzoyl-DL-arginine *p*-nitroanilide) in 50 mM Tris-HCl pH 8.0, incubating at 37 °C for 1 h and monitoring the hydrolyzed substrate at A_{415} using a microtiter plate reader [27]. The time course activity of A2M was normalized with that of 0-h time-point after VP_{AHPND} immersion and expressed as relative activity of A2M.

The PO activity in shrimp plasma was assayed by pre-incubating 30 μL of shrimp plasma (1000 μg) or 50 mM Tris-HCl pH 8.0 was with 10 μL of 5 mg/mL LPS at 30 °C for 15 min. The reaction volume was adjusted to 60 μL with 50 mM Tris-HCl pH 8.0. Then, 40 μL of 3 mg/ml of L-DOPA was added at time zero to start the reaction. The increase in A_{490} was monitored for 60 min in a microplate reader. Like the *Lv*A2M inhibitory activity, the PO activity at time point 0 was set to 1.

2.9. Statistics

All data were analyzed using SPSS statistics 17.0 and SPSS 11.5 for windows (SPSS Corporation, Chicago, IL). Statistical significance was calculated by paired-samples *t*-test, one-way ANOVA and Scheffe and Duncan's post hoc test. Significant difference was accepted at $P < 0.05$. The data from three replicate experiments are expressed as means ± standard deviations (SDs).

3. Results

3.1. Proteinase inhibitory activity of rLvA2M

To demonstrate the activity of r*Lv*A2M as an inhibitor of serine proteinases and proPO activating system, the r*Lv*A2M was produced using the *E. coli* expression system and purified. The purity was checked using SDS-PAGE as shown in Fig. 1 A. The size of r*Lv*A2M was about 170 kDa.

The r*Lv*A2M was tested for its inhibition against the commercial serine proteinases, trypsin, α-chymotrypsin, subtilisin and elastase. The results showed that the higher the mole ratios of r*Lv*A2M to proteinase, the stronger was the inhibition of proteinase activity (Fig. 1 B). The r*Lv*A2M exhibited specific and strong inhibitory activity against trypsin for the trypsin was inhibited more than 90% at the mole ratio of 10:1. It had much less inhibitory activity against α-chymotrypsin, subtilisin and elastase.

3.2. The rLvA2M inhibited the proPO activating system in a dose-dependence manner

To test the inhibitory effect of r*Lv*A2M on proPO activating activity, the r*Lv*A2M was pre-incubated with the shrimp plasma and LPS. The reaction was monitored after adding the chromogenic substrate, L-DOPA. The results showed that the final concentration of 0.433 μM of r*Lv*A2M inhibited the PO activity about 57% compared with the control without r*Lv*A2M and PTU control (Fig. 2 A).

To elucidate whether the inhibitory activity of r*Lv*A2M against the proPO activating system was dose-dependent, the concentration of r*Lv*A2M was varied. The concentrations of r*Lv*A2M of 0, 0.216, 0.433 and 0.866 μM were used in the proPO activation assay. The result in Fig. 2 B showed the decrease of relative PO activity with the increase of r*Lv*A2M concentrations. These results indicated that the r*Lv*A2M was capable of regulating the proPO activating system in shrimp.

3.3. Effect of LvA2M gene knockdown on proPO activation

From the above result showing that the *Lv*A2M was able to regulate the proPO activating system, it was interesting to find out the level of proPO activating system if the *LvA2M* gene was silenced. The silencing of *LvA2M* gene in shrimp was performed. By injecting the dsRNA-*LvA2M* but not the PBS and dsRNA-*GFP* into the shrimp, the expression of *LvA2M* was abolished at 24 h after injection (Fig. 3 A).

To measure the PO activity in the hemolymph of *LvA2M*-silenced shrimp, the shrimp were doubly injected with dsRNA to ensure the silencing of *LvA2M* gene. The hemolymph was withdrawn for PO activity assay. It was found that the PO activity of the *Lv*A2M-knockdown shrimp was significantly higher than that of the dsRNA-*GFP* control group by more than 50% (Fig. 3 B).

3.4. Effect of LvA2M gene silencing on the expression of proPO-associated genes

The PO activity was increased on *LvA2M* gene knockdown most likely because there was not enough *Lv*A2M to regulate the proPO activation. It was, however, possible that other components of the proPO activating system might be affected. Therefore, the expression of proPO-associated genes was determined using the real time RT-PCR. The *PPAF*, *PPAE* and *proPO* were chosen for this experiment. Under the silencing of *LvA2M*, the expression of *PPAF* gene was found to be increased by 4-fold (Fig. 4 A.) whereas those of *PPAE* and *proPO* were down-regulated (Fig. 4B and C).

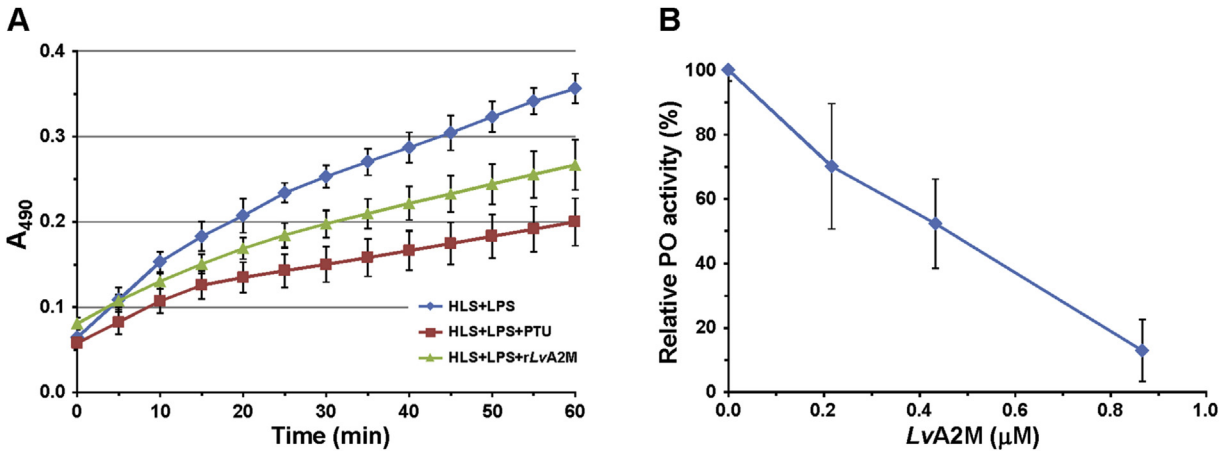


Fig. 2. Inhibition effect of r*Lv*A2M on proPO activation. The r*Lv*A2M was pre-incubated with shrimp plasma and LPS. Then, the reaction was started by adding L-DOPA. (A) A time cause assay of PO activity in the presence of r*Lv*A2M or PTU. (B) Dose-dependent inhibition of PO activity by various concentrations of r*Lv*A2M. The reactions were done in triplicate.

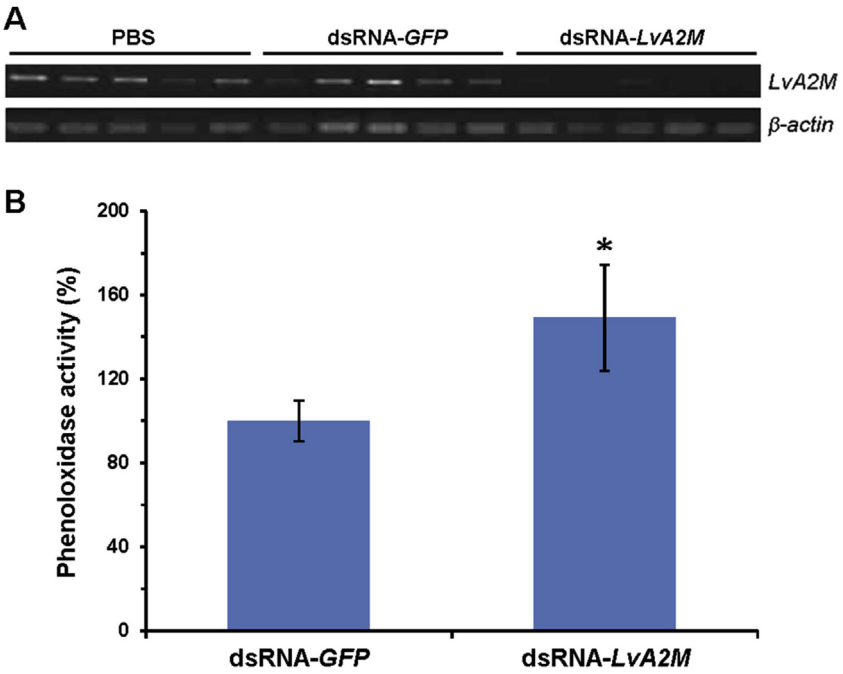


Fig. 3. Effect of *Lv*A2M gene silencing on PO activity in shrimp hemolymph. (A) The silencing of *LvA2M* in *L. vannamei*. The shrimp were doubly injected with 10 μg/g shrimp of PBS, dsRNA-*GFP* and dsRNA-*LvA2M*. The hemolymph was collected for RT-PCR using *β-actin* gene as an internal control. (B) The PO activity assay of the hemolymph samples from (A). The experiment was done in triplicate.

3.5. PO and LvA2M activities in shrimp plasma upon VP_{AHPND} immersion

Since the *Lv*A2M and proPO system co-existed in the blood circulation, it was interesting to examine the activities of *Lv*A2M and PO in the plasma of shrimp after VP_{AHPND} infection. After the early hours of infection, 6 and 12 h, the PO activity was significantly increased and subsided to normal level at 24 and 48 h of infection (Fig. 5 A). Meanwhile, the activity of *Lv*A2M was rapidly and dramatically decreased at 3 h after infection (Fig. 5 B).

4. Discussion

In animal, serine proteinase cascades are involved in humoral immune responses against pathogens. Upon microbial infection, the abundant zymogens in plasma are rapidly activated leading to processes that eliminate the harmful microorganisms. The serine proteinase cascades are found in several immunological pathways, including the coagulation reaction in horseshoe crab [28], the activation of Spätzle-mediated Toll receptor in *Drosophila* [29], the proPO activating system in crayfish [30,31]. The activities of serine proteinases in these cascades not only activate the immune pathways but also impose injury to the host itself [6]. Therefore, the serine proteinases are needed to be controlled. To achieve the immune balance for the host homeostasis, several types of serine proteinase inhibitors found abundantly in plasma come into play. They have a critical role in modulation of proteinase activities.

A multifunctional protein in plasma, namely alpha-2-macroglobulin (A2M), is a broad range serine proteinase inhibitor [14]. Generally, it plays an essential role in protease clearance through the A2M-protease complex from the blood circulation [32,33]. In shrimp, the A2M has been identified from *Marsupenaeus*

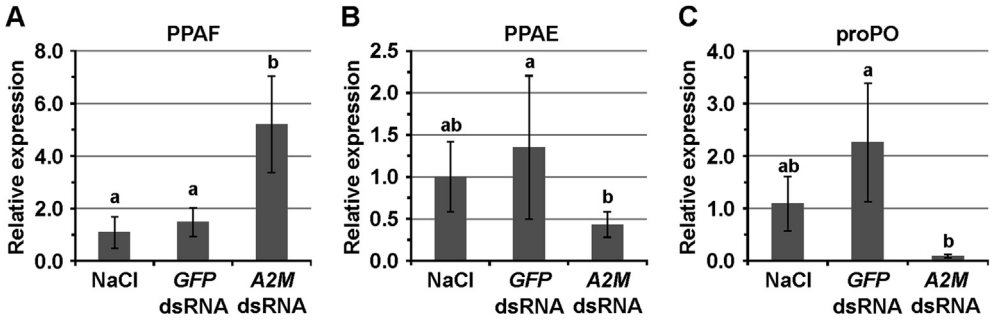


Fig. 4. Effect of *LvA2M* gene knockdown on the expression of proPO-associated genes. The expression of three proPO-associated genes, *PPAF* (A), *PPAE* (B) and *proPO* (C), was determined. The shrimp were doubly injected with 10 μg/g shrimp of dsRNA-*GFP* or dsRNA-*LvA2M*. The PBS was injected instead in the control shrimp. The hemolymph was individually collected for the analysis of gene expression of *PPAF*, *PPAE* and *proPO*. The expression of *EF-1α* gene was used as an internal control.

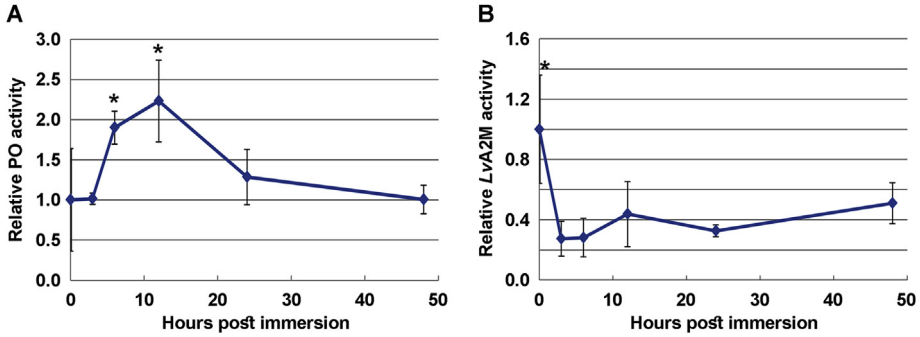


Fig. 5. Relative activities of PO (A) and *Lv*A2M (B) in shrimp plasma upon VP_{AHPND} immersion. The white shrimp were immersed in VP_{AHPND} bacterial suspensions and the shrimp plasma was collected at 0, 3, 6, 12, 24 and 48 h after immersion. The plasma from 3 shrimp was pooled as one group. The activities were normalized with the activities at time 0. The experiment was done in triplicate.

japonicus [18], *Penaeus monodon* [19], *Fenneropenaeus chinensis* [22] and *Litopenaeus vannamei* [20]. The expression of *A2M* gene is highly up-regulated upon bacterial, fungal and viral infection [22–24]. Moreover, the *Pm*A2M protein is involved in fibrinolysis of blood clots in *P. monodon* [34].

In this research, we explored the function of *Lv*A2M in the negative regulation of proPO activating system. The r*Lv*A2M from *L. vannamei* was produced using an *E. coli* system. The molecular weight of r*Lv*A2M obtained was approximately 170 kDa which was approximately the size of other invertebrate A2Ms. To ensure that the preparation was active, the inhibition or trapping spectrum of r*Lv*A2M was determined against different serine proteinases, trypsin, chymotrypsin, elastase and subtilisin. We found that the r*Lv*A2M exhibited strong and specific inhibitory activity against trypsin which was in accordance to the previous report showing that the *Lv*A2M strongly inhibited trypsin [35] but the r*Lv*A2M in our preparation had much less trapping activity for α-chymotrypsin, elastase and subtilisin. The A2M in crayfish also has the inhibitory activity against proteases, trypsin and chymotrypsin [8].

In addition to proteinase inhibitory activity, the crayfish A2M is able to decrease the activity of phenol oxidase in plasma [8]. We also tested the *Lv*A2M against the proPO activating system and found that the PO activity was inhibited by 57%. The inhibition was dose dependent; the more *Lv*A2M added, the lesser was the PO activity. It was, then, likely that the *Lv*A2M was another candidate that negatively regulated the proPO activating system besides other inhibitors such as *Lv*Serpin from *L. vannamei* [12], *Pm*SERPIN8 and *Pm*SERPIN3 from *P. monodon* [13,36]. Nevertheless, the *Lv*A2M also has other potential functions, for example it inhibits the microbial proteinases [34,37].

To support the notion that the *Lv*A2M functioned in regulating the proPO activating system, the expression of *LvA2M* was suppressed. Without the *Lv*A2M inhibitor, the overall PO activity would be increased upon activation. It was found that with suppression of A2M expression, the PO activity was more than 50% higher than the control dsRNA-*GFP* treatment. It was experimented further whether the suppression of *Lv*A2M affected the expression of proPO-associated genes. To activate the proPO system, a key serine proteinase, namely prophenoloxidase activating enzyme (PPAE) is required as well as the prophenoloxidase activating factor (PPAF). The PPAE cleaves the inactive proPO and converts it into an active enzyme PO. The PO, then, catalyzes the first step in melanin synthesis [38,39]. The expression of *PPAF*, *PPAE* and *proPO* was examined in the *Lv*A2M-silenced shrimp. The expression of *PPAF* was up-regulated while that of *PPAE* and *proPO* was significantly down-regulated.

Considering the higher PO activity in the *LvA2M*-silenced shrimp, the down-regulation of *PPAE* and *proPO* gene expression was surprising. With minute amount of *Lv*A2M, the proPO activation was not fully modulated and lesser enzymes could be used to activate the proPO activating system. This presumption is needed to be elucidated further. In contrast to the study on the suppression of *Lv*serpin gene, another supposedly regulator of proPO activation in *L. vannamei*, the suppression leads to higher expression of serine proteinase genes, *PPAE*, *PPAF* and *proPO* in response to *V. anguillarum* infection [12].

The *Lv*A2M and the proPO system are actually present in the hemolymph. If the *Lv*A2M is a regulator of the proPO activating system, it is reasonable to assume that the PO activity is inversely related to the *Lv*A2M inhibitory activity, i.e. if the PO activity is up,

the *Lv*A2M activity would be down. We tested this hypothesis by infecting the shrimp with VP_{AHPND} by immersion and measured the two activities as the infection progressed. The results were as expected; the PO activity was up in the early hours after infection while the *Lv*A2M activity was reduced. The reverse situation was observed in *L. vannamei* rearing at low salinity for the *Lv*A2M activity was increased while the PO activity was decreased [40]. In our case, the causes of reduction in *Lv*A2M activity remains to be elucidated.

In summary, we have shown here unequivocally that the *Lv*A2M functions as one of the regulator of proPO activating system. It limits the extent of proPO activity probably by preventing the trypsin-like proteases from activating the proteinase cascade. Suppression of the *Lv*A2M expression leads to an increase in PO activity upon activation even when the key enzymes in the proPO activating system are down-regulated. Upon VP_{AHPND} infection, the *Lv*A2M activity is decreased while the PO activity is increased.

Acknowledgements

This project was supported by research grants from the Srinakharinwirot University (028/2558) to S. Ponprateep and the TRF Senior Research Scholar (No. RTA5880004), Thailand Research Fund. We thank the matching fund from the Thailand Research Fund and the Srinakharinwirot University (Grant No. TRG5880147) to S. Ponprateep and the support under the Ratchadapisek Somphot Endowment to the Center of Excellence for Molecular Biology and Genomics of Shrimp. We acknowledge the support of equipment used in this study under the JST-JICA joint program “Science and Technology Research Partnership for Sustainable Development, SATREPS”.

References

[1] P. Jiravanichpaisal, B.L. Lee, K. Söderhäll, Cell-mediated immunity in arthropods: hematopoiesis, coagulation, melanization and opsonization, Immunobiology 211 (2006) 213–236.
[2] J.L. Ding, M.A.A. Navas III, B. Ho, Two forms of factor C from the amoebocytes of *Carcinoscorpius rotundicauda*: purification and characterization, Biochim. Biophys. Acta 1202 (1993) 149–156.
[3] P.B. Armstrong, The contribution of proteinase inhibitors to immune defense, Trends Immunol. 22 (2001) 47–52.
[4] M. Laskowski Jr., I. Kato, Protein inhibitors of proteinases, Annu. Rev. Biochem. 49 (1980) 593–626.
[5] M.R. Kanost, Serine proteinase inhibitors in arthropod immunity, Dev. Comp. Immunol. 23 (1999) 291–301.
[6] P.S. Hiemstra, Novel roles of protease inhibitors in infection and inflammation, Biochem. Soc. Trans. 30 (2002) 116–120.
[7] A. Aspán, M. Hall, K. Söderhäll, The effect of endogeneous proteinase inhibitors on the prophenoloxidase activating enzyme, a serine proteinase from crayfish haemocytes, Insect Biochem. 20 (1990) 485–492.
[8] H.G. Hergenhahn, A. Aspán, K. Söderhäll, Purification and characterization of a high-Mr proteinase inhibitor of pro-phenol oxidase activation from crayfish plasma, Biochem. J. 248 (1987) 223–228.
[9] J.M. Christen, Y. Hiromasa, C. An, M.R. Kanost, Identification of plasma proteinase complexes with serpin-3 in *Manduca sexta*, Insect Biochem. Mol. Biol. 42 (2012) 946–955.
[10] C. Suwanchaichinda, R. Ochieng, S. Zhuang, M.R. Kanost, *Manduca sexta* serpin-7, a putative regulator of hemolymph prophenoloxidase activation, Insect Biochem. Mol. Biol. 43 (2013) 555–561.
[11] H.G. Hergenhahn, K. Söderhäll, α2-macroglobulin-like activity in plasma of the crayfish *Pacifastacus leniusculus*, Comp. Biochem. Physiol. B Comp. Biochem. 81 (1985) 833–835.
[12] Y. Liu, F. Hou, S. He, Z. Qian, X. Wang, A. Mao, C. Sun, X. Liu, Identification, characterization and functional analysis of a serine protease inhibitor (Lvserpin) from the Pacific white shrimp, *Litopenaeus vannamei*, Dev. Comp. Immunol. 43 (2014) 35–46.
[13] S. Somnuk, A. Tassanakajon, V. Rimphanitchayakit, Gene expression and characterization of a serine proteinase inhibitor *Pm*SERPIN8 from the black tiger shrimp *Penaeus monodon*, Fish. Shellfish Immunol. 33 (2012) 332–341.
[14] P.B. Armstrong, J.P. Quigley, Alpha2-macroglobulin: an evolutionarily conserved arm of the innate immune system, Dev. Comp. Immunol. 23 (1999) 375–390.
[15] V. Buresova, O. Hajdusek, Z. Franta, D. Sojka, P. Kopacek, IrAM-An alpha2-macroglobulin from the hard tick *Ixodes ricinus*: characterization and function in phagocytosis of a potential pathogen *Chryseobacterium indologenes*, Dev. Comp. Immunol. 33 (2009) 489–498.
[16] M. Hall, K. Söderhäll, Crayfish α-macroglobulin as a substrate for transglutaminases, Comp. Biochem. Phys. B 108 (1994) 65–72.
[17] A. Aspán, M. Hall, K. Söderhäll, The effect of endogeneous proteinase inhibitors on the prophenoloxidase activating enzyme, a serine proteinase from crayfish haemocytes, Insect Biochem. 20 (1990) 485–492.
[18] A. Rattanachai, I. Hirono, T. Ohira, Y. Takahashi, T. Aoki, Molecular cloning and expression analysis of alpha 2-macroglobulin in the kuruma shrimp, *Marsupenaeus japonicus*, Fish. Shellfish Immunol. 16 (2004) 599–611.
[19] Y.C. Lin, B. Vaseeharan, C.F. Ko, T.T. Chiou, J.C. Chen, Molecular cloning and characterisation of a proteinase inhibitor, alpha 2-macroglobulin (alpha2-M) from the haemocytes of tiger shrimp *Penaeus monodon*, Mol. Immunol. 44 (2007) 1065–1074.
[20] Y.C. Lin, B. Vaseeharan, J.C. Chen, Molecular cloning and phylogenetic analysis on alpha2-macroglobulin (alpha2-M) of white shrimp *Litopenaeus vannamei*, Dev. Comp. Immunol. 32 (2008) 317–329.
[21] P.Y. Ho, C.H. Cheng, W. Cheng, Identification and cloning of the alpha2-macroglobulin of giant freshwater prawn *Macrobrachium rosenbergii* and its expression in relation with the molt stage and bacteria injection, Fish. Shellfish Immunol. 26 (2009) 459–466.
[22] H. Ma, B. Wang, J. Zhang, F. Li, J. Xiang, Multiple forms of alpha-2 macroglobulin in shrimp *Fenneropenaeus chinesis* and their transcriptional response to WSSV or *Vibrio* pathogen infection, Dev. Comp. Immunol. 34 (2010) 677–684.
[23] L.M. Perazzolo, E. Bachère, R.D. Rosa, P. Goncalves, E.R. Andreatta, S. Daffre, M.A. Barracco, Alpha2-macroglobulin from an Atlantic shrimp: biochemical characterization, sub-cellular localization and gene expression upon fungal challenge, Fish. Shellfish Immunol. 31 (2011) 938–943.
[24] S. Shanthi, B. Vaseeharan, Alpha 2 macroglobulin gene and their expression in response to GFP tagged *Vibrio parahaemolyticus* and WSSV pathogens in Indian white shrimp, 418–419, Fenneropenaeus indicus, Aquac. (2014) 48–54.
[25] M.M. Bradford, A rapid and sensitive method for the quantitation of microgram quantities of protein utilizing the principle of protein-dye binding, Anal. Biochem. 72 (1976) 248–254.
[26] M.W. Pfaffl, A new mathematical model for relative quantification in real-time RT-PCR, Nucleic Acids Res. 29 (2001) e45.
[27] P.B. Armstrong, M.T. Rossner, J.P. Quigley, An alpha 2-macroglobulinlike activity in the blood of chelicerate and mandibulate arthropods, J. Exp. Zool. 236 (1985) 1–9.
[28] S. Iwanaga, The limulus clotting reaction, Curr. Opin. Immunol. 5 (1993) 74–82.
[29] T. Michel, J.M. Reichhart, J.A. Hoffmann, J. Royet, *Drosophila* Toll is activated by Gram-positive bacteria through a circulating peptidoglycan recognition protein, Nature 414 (2001) 756–759.
[30] K. Söderhäll, A. Aspán, B. Duvic, The proPO-system and associated proteins: role in cellular communication in arthropods, Res. Immunol. 141 (1990) 896–907.
[31] K. Söderhäll, L. Cerenius, Role of the prophenoloxidase-activating system in invertebrate immunity, Curr. Opin. Immunol. 10 (1998) 23–28.
[32] J.P. Quigley, P.B. Armstrong, An endopeptidase inhibitor, similar to mammalian alpha 2-macroglobulin, detected in the hemolymph of an invertebrate, *Limulus Polyphemus*, J. Biol. Chem. 258 (1983) 7903–7906.
[33] J.P. Quigley, P.B. Armstrong, A homologue of alpha 2-macroglobulin purified from the hemolymph of the horseshoe crab *Limulus Polyphemus*, J. Biol. Chem. 260 (1985) 12715–12719.
[34] V. Chaikeeratisak, K. Somboonwiwat, A. Tassanakajon, Shrimp alpha-2-macroglobulin prevents the bacterial escape by inhibiting fibrinolysis of blood clots, PLoS One 7 (2012) e47384.
[35] T. Gollas-Galván, R.R. Sotelo-Mundo, G. Yepiz-Plascencia, C. Vargas-Requena, F. Vargas-Albores, Purification and characterization of alpha 2-macroglobulin from the white shrimp (*Penaeus vannamei*), Comp. Biochem. Physiol. C Toxicol. Pharmacol. 134 (2003) 431–438.
[36] N. Wetsaphan, V. Rimphanitchayakit, A. Tassanakajon, K. Somboonwiwat, *Pm*SERPIN3 from black tiger shrimp *Penaeus monodon* is capable of controlling the proPO system, Dev. Comp. Immunol. 41 (2013) 110–119.
[37] V. Chaikeeratisak, A. Tassanakajon, P.B. Armstrong, Interaction of pathogenic *Vibrio* bacteria with the blood clot of the pacific white shrimp, *Litopenaeus vannamei*, Biol. Bull. 226 (2014) 102–110.
[38] I.H. Jang, H.J. Nam, W.J. Lee, CLIP-domain serine proteases in *Drosophila* innate immunity, BMB Rep. 41 (2008) 102–107.
[39] H. Jiang, M.R. Kanost, The clip-domain family of serine proteinases in arthropods, Insect Biochem. Mol. Biol. 30 (2000) 95–105.
[40] L. Pan, P. Xie, F. Hu, Responses of prophenoloxidase system and related defence parameters of *Litopenaeus vannamei* to low salinity, J. Ocean. Univ. China 9 (2010) 273–278.

JOURNAL OF GENERAL VIROLOGY

RESEARCH ARTICLE

Sutthangkul *et al.*, *Journal of General Virology* 2017;98:769–778

DOI 10.1099/jgv.0.000729

MICROBIOLOGY SOCIETY

Anti-melanization mechanism of the white spot syndrome viral protein, WSSV453, via interaction with shrimp proPO-activating enzyme, *Pm*proPPAE2

Jantiwan Sutthangkul,[1] Piti Amparyup,[2] Jai-Hoon Eum,[3] Michael R. Strand[3,*] and Anchalee Tassanakajon[1,*]

Abstract

Inhibition of the host melanization reaction, activated by the prophenoloxidase activating (proPO) system, is one of the crucial evasion strategies of pathogens. Recently, the shrimp pathogen, white spot syndrome virus (WSSV), was found to inhibit melanization in the shrimp *Penaeus monodon*. The viral protein WSSV453 was previously shown to interact with PO-activating enzyme 2 (*Pm*PPAE2) and reported to be involved in suppressing the shrimp melanization response after WSSV infection. Here, we characterized how WSSV453 inhibits melanization. WSSV453 is a non-structural viral protein, which was first detected in shrimp haemocytes at 6 hours post-infection (hpi) by WSSV and in shrimp plasma at 24 hpi. We produced recombinant proteins for three components of the *P. monodon* proPO system: *Pm*proPPAE2, *Pm*proPO1 and *Pm*proPO2. Functional assays showed that active *Pm*PPAE2 processed *Pm*proPO1 and 2 to produce functional PO. Incubation of WSSV453 with *Pm*proPPAE2 dose-dependently reduced *Pm*PPAE2 activity toward *Pm*PO1 or *Pm*PO2. In contrast, WSSV453 had no effect on activated *Pm*PPAE2. The addition of active *Pm*PPAE2 to WSSV-infected shrimp plasma at day 2 post-infection also rescued PO activity. Taken together, these results indicate that the anti-melanization activity of WSSV is due to WSSV453, which interacts with *Pm*proPPAE2 and interferes with its activation to active *Pm*PPAE2.

INTRODUCTION

The inhibition of immune defences is one strategy pathogens use to successfully infect hosts [1]. In arthropods, melanization is an important innate immune response with functions in pathogen killing, wound healing and cuticle sclerotization [2–4]. Melanization is mediated by the phenoloxidase (PO) cascade, which can be activated by pathogen-associated molecular patterns (PAMPs). This leads to the proteolysis of multiple serine proteinases in the PO cascade. The terminal serine proteinase is called prophenoloxidase-activating proteinase or enzyme (PAP or PPAE), which is responsible for the cleavage of the zymogen prophenoloxidase (proPO) to active PO [4–6]. In the shrimp *Penaeus monodon*, two proPOs (*Pm*proPO1 and 2) were identified and characterized [4]. However, direct evidence showing the relationship between *Pm*proPO1 and 2 is unclear. *Pm*proPO1 shows an amino acid sequence similarity (81 %) to *Pm*proPO2. Suppression of either *Pm*proPO1 or 2 or both genes resulted in a strong PO activity reduction and a very high mortality after *Vibrio harveyi* challenge. Thus, two POs might cooperatively function in the proPO-activating system and probably act as a heteromer [7]. Nevertheless, the role of *Pm*proPO1 and *Pm*proPO2 in shrimp melanization has not yet been clarified. In *Drosophila*, proPOs have been shown to be involved in melanization [8].

PO uses *o*-diphenols and tyrosine as substrates to produce quinones, which are converted to melanin that binds to wound sites or the surface of pathogens [5, 6]. Reactive oxygen and nitrogen intermediates produced during melanization exhibit antibacterial, antifungal and antiviral activities. Melanization can also promote encapsulation, phagocytosis and the formation of nodules [9–12]. Not surprisingly, bacterial and viral pathogens have evolved diverse strategies for overcoming host melanization responses. For example, the pathogenic bacterium *Photorhabdus* produces a small molecule antibiotic, (*E*)-1,3-dihydroxy-2-(isopropyl)-5-

Received 15 November 2016; Accepted 27 January 2017

Author affiliations: [1]Center of Excellence for Molecular Biology and Genomics of Shrimp, Department of Biochemistry, Faculty of Science, Chulalongkorn University, 254 Phayathai Road, Bangkok 10330, Thailand; [2]National Center for Genetic Engineering and Biotechnology (BIOTEC), National Science and Technology Development Agency (NSTDA), 113 Paholyothin Road, Klong1, Klong Luang, Pathumthani 12120, Thailand; [3]Department of Entomology, University of Georgia, Athens, GA 30602, USA.

***Correspondence:** Michael R. Strand, mrstrand@uga.edu; Anchalee Tassanakajon, anchalee.k@chula.ac.th

Keywords: *Peneaus monodon*; prophenoloxidase; melanization; white spot syndrome virus.

Abbreviations: dpi, days post-infection; EAR, *N*-acetyl-Ile-Glu-Ala-Arg *p*-nitroanilide acetate salt; Egf, epidermal growth factor-like motif; Fx, Factor Xa; hpi, hours post-infection; PO, phenoloxidase; PAP, prophenoloxidase-activating proteinase; PPAE, prophenoloxidase-activating enzyme; PTU, phenylthiourea; VPR, Boc-Val-Pro-Arg-7-amido-4-methylcoumarin hydrochloride; WSSV, white spot syndrome virus.

The GenBank accession number for the WSSV453 sequence is AAL89321.1.

000729 © 2017 The Authors

Downloaded from www.microbiologyresearch.org by
IP: 157.[illegible].240.101
On: Tue, 01 Aug 2017 07:33:52

(2-phenylethenyl) benzene, that inhibits PO [13]. The parasitic wasp *Microplitis demolitor* carries *M. demolitor* bracovirus (*Md*BV), which produces two proteins, Egf 1.0 and Egf1.5, that competitively inhibit PAPs [14–16].

White spot syndrome virus (WSSV) is a serious shrimp pathogen that causes high mortality and drastic losses in commercial shrimp production worldwide [17, 18]. The antiviral role of the shrimp melanization response toward WSSV was recently reported in the black tiger shrimp, *Penaeus monodon* [19]. However, WSSV overcomes this by disabling the melanization response of *P. monodon* and several other species of crustaceans. Previous studies report that the proPO genes of *Litopenaeus vannamei* and the crayfish *Procambarus clarkii* were down-regulated after WSSV infection while PO activity was also significantly reduced in *L. vannamei* at 48 h post-infection (hpi) [20–22]. Disabled melanization in WSSV-infected haemocytes was also reported for the freshwater crayfish *Pacifastacus leniusculus* [23]. However, the molecular mechanism by which WSSV inhibits host melanization is unclear. Recently, we proposed that WSSV inhibits melanization in *P. monodon* by disabling the activity of proteinases in the PO cascade [19]. The viral protein WSSV453 was implicated in inhibiting melanization by binding to *P. monodon* proPO-activating enzyme 2 (*Pm*PPAE2) [19]. In turn, *Pm*PPAE1 and 2 were previously proposed to be the terminal clip domain-serine proteinases that activate *Pm*proPO1 and 2 [7, 24, 25]. However, no direct experimental data support these suggestions.

In this study, we report that knockdown of *Pm*proPO1 and of *Pm*proPO2 by RNA interference or WSSV infection disabled melanization and wound healing in *P. monodon*. In addition, we produced functionally active recombinant *Pm*proPPAE2, *Pm*proPO1 and *Pm*proPO2 to clearly demonstrate the anti-melanization mechanism of WSSV453. Our results indicate that WSSV453 interacts with *Pm*proPPAE2 and interferes with its activation to active *Pm*PPAE2 and leads to the reduction of PO activity with both *Pm*proPO1 and *Pm*proPO2.

RESULTS

Melanization disabling in *Pm*proPO1, 2 silenced shrimp and in WSSV-infected shrimp

The first goal of this study was to determine whether RNAi knockdown of *Pm*proPO1, 2 in *P. monodon* negatively affected melanization and wound healing. Shrimp treated with *Pm*proPO1, 2 dsRNA visually showed a reduction in melanization of a wound site compared to GFP-dsRNA-injected shrimp (Fig. 1a). This finding supported that *Pm*proPO1 and 2 contribute to melanization of wound sites. We then examined whether WSSV infection had a similar effect. The results indicated that melanization around a wound produced at 3 hpi was similar to PBS-treated control shrimp, whereas no melanization was observed around a wound produced at 24 hpi (Fig. 1b). This result indicated that melanization of wound sites in *P. monodon* was disabled by 24 hpi with WSSV.

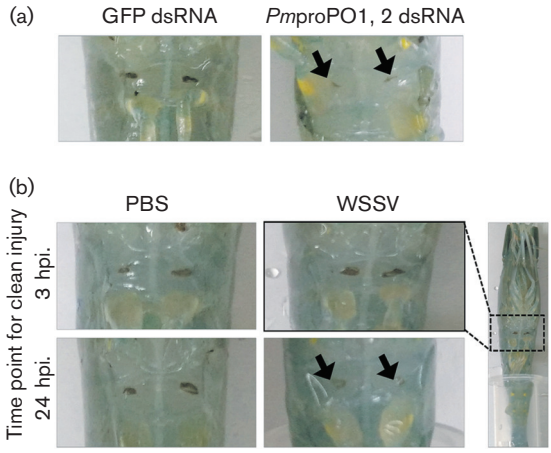


Fig. 1. RNAi knockdown of the *Pm*proPO1, 2 genes and WSSV infection reduce melanization of the wound sites. (a) Juvenile *P. monodon* were injected twice with *Pm*proPO1 and 2 dsRNA (or GFP dsRNA as a control) followed by wounding of an abdominal segment 24 h after the second injection. (b) Shrimp were injected with WSSV (or PBS as a control) and then wounded 3 hpi (early phase of infection) or 24 hpi (late phase of infection). Photos were then taken 24 h after each wounding event.

Production and activation of recombinant *Pm*proPPAE2

In our previous study, we hypothesized that WSSV453 suppresses shrimp melanization by inhibiting *Pm*PPAE2 [19]. To directly examine this, we produced recombinant (r) proteins and used them in functional assays. r*Pm*proPPAE2 and r*Pm*proPPAE2$_{Xa}$ were successfully expressed as zymogens in *Drosophila* S2 cells that were secreted into the medium (Fig. 2a). Each had a molecular mass of 43 kDa, which was also similar to the predicted molecular mass of 42.85 kDa. Incubation of factor Xa with r*Pm*proPPAE2$_{Xa}$ followed by immunoblotting further showed processing to produce a 30 kDa band that corresponded to the predicted mass of active PPAE2. Processing of r*Pm*proPPAE2$_{Xa}$ was detectable at 6 h and complete processing was observed at 16 h (Fig. 2b). The serine proteinase activity of r*Pm*PPAE2$_{Xa}$ was assayed using the substrate B9385 (Boc-Val-Pro-Arg-7-amido-4-methylcoumarin hydrochloride; VPR). Results showed that r*Pm*PPAE2$_{Xa}$ exhibited VPRase activity while unactivated r*Pm*proPPAE2$_{Xa}$ showed no activity (Fig. 2c). In the control group, incubation of factor Xa with culture medium or wild-type r*Pm*proPPAE2 showed neither processing of r*Pm*proPPAE2 nor serine proteinase activity (data not shown).

*Pm*PPAE2 plays a role in *Pm*proPO1, 2 activation

We next examined the role of *Pm*PPAE2 in activation of *Pm*proPO1, 2. Incubation of activated *Pm*PPAE2$_{Xa}$ with *Pm*proPO1, 2 (80 kDa) resulted in cleavage as shown by

Downloaded from www.microbiologyresearch.org by
IP: 157.[illegible].240.101
On: Tue, 01 Aug 2017 07:33:52

the appearance of ~75 kDa bands that corresponded to *Pm*PO1 and 2 (Fig. 3a, b) [7]. In contrast no cleavage was observed in control assays containing BSA (Fig. 3c). *Pm*proPO1 and *Pm*proPO2 also exhibited high PO activity after activation by *Pm*PPAE2$_{Xa}$ but very low activity when incubated with only BSA (Fig. 3c). Moreover, when wild-type r*Pm*proPPAE2 was incubated with factor Xa and *Pm*proPO1, 2 proteins, no activation of *Pm*proPOs was observed (data not shown). These results indicated that *Pm*PPAE2 activates *Pm*proPO1, 2 to produce functional POs.

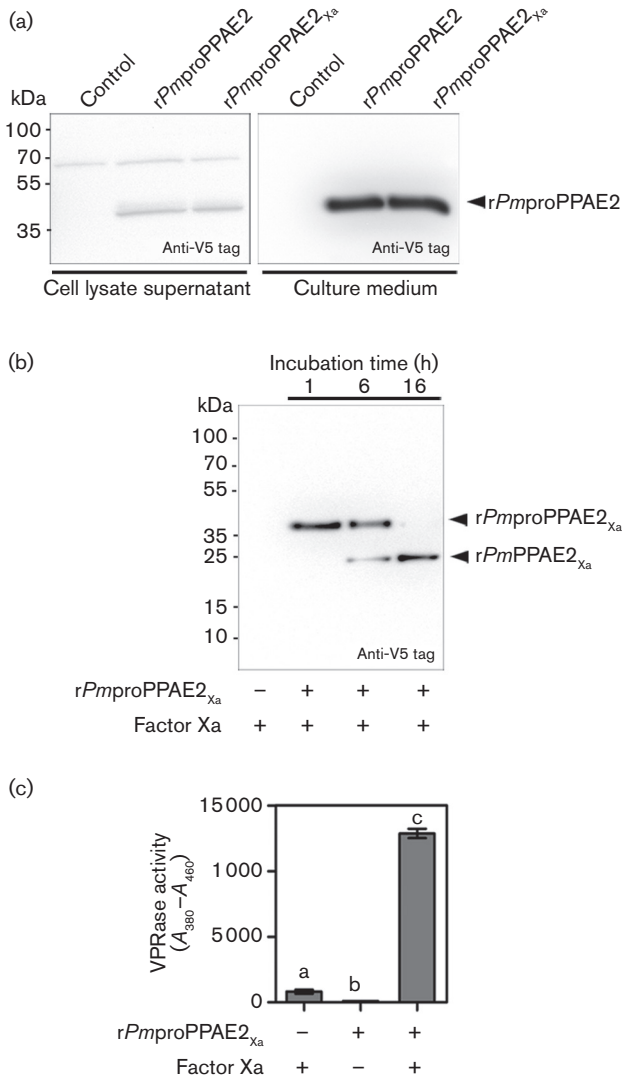


Fig. 2. Production of r*Pm*proPPAE2$_{Xa}$ and its activation by bovine factor Xa. (a) r*Pm*proPPAE2 or mutant *Pm*proPPAE2 (*Pm*proPPAE2$_{Xa}$) were detected by immunoblotting using anti-V5 tag antibody in S2 cell lysate and culture medium 48 h after transfection with pIZT/*Pm*proPPAE2 or pIZT/*Pm*proPPAE2$_{Xa}$ (or without transfection as control). (b) *Pm*proPPAE2$_{Xa}$ processing 1, 6 and 16 h after adding factor Xa was monitored by immunoblotting using an anti-V5 antibody. (c) Catalytic activity of factor Xa-activated *Pm*proPPAE2$_{Xa}$ was detected using VPR as the substrate. The data are shown as the means±SD (error bars) and are derived from three independently replicated experiments, indicating a significant difference (P<0.05) in mean VPRase activity between the three samples.

Characterization of WSSV453 gene/protein in WSSV-infected shrimp

Time course studies indicated that WSSV453 expression was first detectable at 6 hpi (Fig. 4a). Transcript abundance also qualitatively increased by 48 h (Fig. 4a). Sampling of tissues at 48 hpi indicated that WSSV453 was highly expressed in haemocytes and stomach and lower expression was observed in heart, gill, intestine and hepatopancreas (Fig. 4a). Immunoblotting confirmed that WSSV453 protein was present in haemocytes from 6 to 48 hpi and in plasma at 24 and 48 hpi (Fig. 4b). Since WSSV453 has been previously reported as a protein of unknown function [26], we investigated whether it is a structural or non-structural protein. Purified WSSV particles were prepared and subjected to SDS-PAGE and immunoblot analysis using anti-VP28 and anti-WSSV453. WSSV453 was not detected in virions, whereas VP28, a known structural component of WSSV virions [27], was detected (Fig. 4c). These results supported that WSSV453 is a non-structural viral protein.

Effect of WSSV453 on shrimp PO cascade

Recombinant WSSV453 was produced as a fusion protein rWSSV453-NUS and purified as previously reported [19]. Pre-incubation of rWSSV453-NUS with r*Pm*proPPAE2$_{Xa}$ before activation by factor Xa resulted in a significant decrease in PO activity of *rPm*proPO1 and *rPm*proPO2 protein when compared to control treatments [rNUS, phenylthiourea (PTU)] (Fig. 5a). In contrast, pre-incubation of rWSSV453-NUS with *Pm*PPAE2$_{Xa}$ that had already been processed by factor Xa as well as with zymogen or active *rPm*PO1 and *rPm*PO2 did not reduce PO activity (Fig. 5b–d). This outcome indicated that WSSV453 could reduce PO activity by interacting with *Pm*proPPAE2 but not already activated *Pm*PPAE2.

Effect of WSSV453 on shrimp PPAE2 activity

We further elaborated on the preceding results by pre-incubating r*Pm*proPPAE2$_{Xa}$ with increasing amounts of rWSSV453-NUS for 1 h before activating with factor Xa. This showed that rWSSV453-NUS dose-dependently reduced *Pm*PPAE2 activity toward a VPR (B9385) substrate whereas rNUS and BSA did not (Fig. 6a). On the other hand, adding increasing amounts of rWSSV453-NUS to already active r*Pm*PPAE2$_{Xa}$ had no effect on activity when compared to the same controls (Fig. 6b). rWSSV453-NUS also showed no inhibitory activity toward factor Xa (Fig. 6c). This suggested that WSSV453 did not directly inhibit *Pm*PPAE2 activity but might reduce *Pm*PPAE2 activity by interfering with the activation of *Pm*proPPAE2.

Downloaded from www.microbiologyresearch.org by
IP: 157.[illegible].240.101
On: Tue, 01 Aug 2017 07:33:52

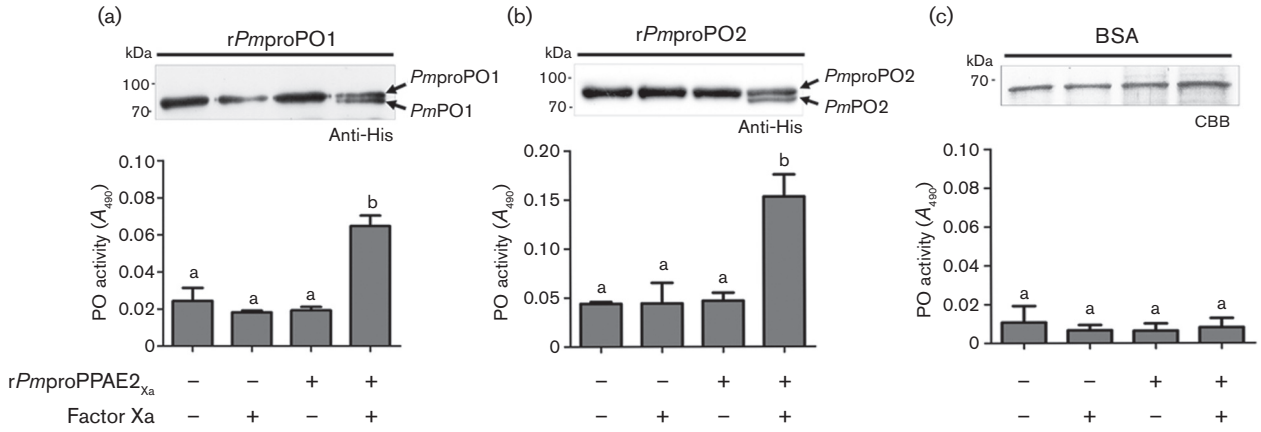


Fig. 3. *Pm*proPPAE2$_{Xa}$ directly cleaves and activates r*Pm*proPO1 and r*Pm*proPO2. (a) r*Pm*proPO1, (b) r*Pm*proPO2 or (c) BSA (control) were incubated with *Pm*proPPAE2$_{Xa}$, factor Xa or both for 30 min, followed by SDS-PAGE, and visualized by staining with Coomassie Brilliant Blue (CBB) or immunoblotting using an anti-His antibody. PO activity for each treatment was detected using L-DOPA as a substrate. The data are shown as the means±SD (error bars) and are derived from three independently replicated experiments. Different letters (above each bar) indicate a significant difference (P<0.05) in the mean PO activity between the four samples.

PO activity of shrimp haemocytes and plasma was changed after WSSV infection

PO activity of WSSV-infected shrimp haemolymph was separately evaluated in haemocytes and plasma at 2 days post-infection (dpi). Results showed that WSSV had no effect on PO activity in haemocytes (Fig. 7a) but reduced PO activity in plasma (Fig. 7b). Adding active r*Pm*PPAE2$_{Xa}$ to haemocytes dramatically increased PO activity in non-infected cells but only slightly increased activity in WSSV-infected cells (Fig. 7c). Interestingly, adding active r*Pm*PPAE2$_{Xa}$ restored PO activity in WSSV-infected plasma (Fig. 7d). This outcome suggested that disabling shrimp melanization via inhibition of *Pm*PPAE2 by WSSV might occur in plasma rather than haemocytes.

DISCUSSION

The PO cascade plays an important role in immune defence and wound healing in arthropods. Melanin accumulation around pathogens or wound sites is often observed [2–5]. The antimicrobial and antiviral effects of compounds generated during melanin synthesis have also been demonstrated [9–12]. It is also known that some pathogens have evolved strategies to suppress melanization [13, 14]. In the case of WSSV, previous studies showed that infection resulted in down-regulation of *Lv*proPO and *Lv*proPPAEs gene expression in*L. vannamei* [20, 22] and reduced melanization of haemocytes in the crayfish *Pacifastacus leniusculus* [23]. However, proPO transcript abundance remained similar in infected *Pacifastacus leniusculus*, which suggested that WSSV might inhibit the proPO system upstream of PO or simply consumed the native substrate of the PO enzyme [23]. In contrast, studies of *Penaeus stylirostris* showed that WSSV infection upregulated expression of lipopolysaccharide and β-1,3-glucan binding protein (LGBP) but also reduced melanization, which suggested that WSSV may activate expression of an inhibitor(s) that blocks the activity of serine protease in the PO cascade or PO itself [28].

Previous results with *P. monodon* showed that *Pm*PPAE2 interacted with a WSSV protein named WSSV453 [19]. Co-immunoprecipitation experiments showed positive binding of WSSV453 with *Pm*PPAE2 protein. Furthermore, the RNAi-mediated gene silencing of WSSV453 and *Pm*PPAE2 suggested that WSSV453 might be involved in suppression of PO activity during WSSV infection via interaction with *Pm*PPAE2 [19]. We began this study by showing that RNAi knockdown of proPO1 and 2 had a similar effect on melanization of wound sites as WSSV infection. Previously, *Pm*proPPAE1 and 2 were characterized as the clip domain-serine proteinases that probably process shrimp proPO [7, 24, 25]. However, we still lacked direct evidence showing that *Pm*PPAE1 and 2 have this activity. We therefore produced in this study the mutant *Pm*proPPAE2 (*Pm*proPPAE2$_{Xa}$) that allowed its activation by bovine factor Xa. We showed that active r*Pm*PPAE2$_{Xa}$ processes both r*Pm*proPO1 and 2 at the predicted site for activation of r*Pm*PO1, 2 (~75 kDa) [7]. This result confirmed that *Pm*PPAE2 processes both *Pm*proPO1 and *Pm*proPO2 and leads to melanization.

WSSV453 has no functional domains predicted by the SMART analysis program that provide insights into activity. We therefore focused on functional assays in this study. We first show that WSSV453 protein is not detectable in WSSV particles. This indicates that WSSV453 is likely to be a non-structural viral protein, which is also consistent with other data in the literature [27, 29]. Previously, one life cycle of WSSV was reported to be around 24 hpi and the time course of WSSV protein synthesis is different for the

Downloaded from www.microbiologyresearch.org by
IP: 157.[illegible].240.101
On: Tue, 01 Aug 2017 07:33:52

different viral proteins [17]. In this study, WSSV453 expression was detected at 6 hpi in virus-infected haemocytes, which corresponded with a previous report that also detected WSSV453 at an early intermediate stage of WSSV infection [30]. Protein expression of WSSV453 in infected shrimp is detected in shrimp haemocytes at 6 hpi and in shrimp plasma at 24 and 48 hpi. Based on the ORF of WSSV453 (GenBank accession number AAL89321.1), the protein has no signal peptide, so how it is released into shrimp plasma remains unclear.

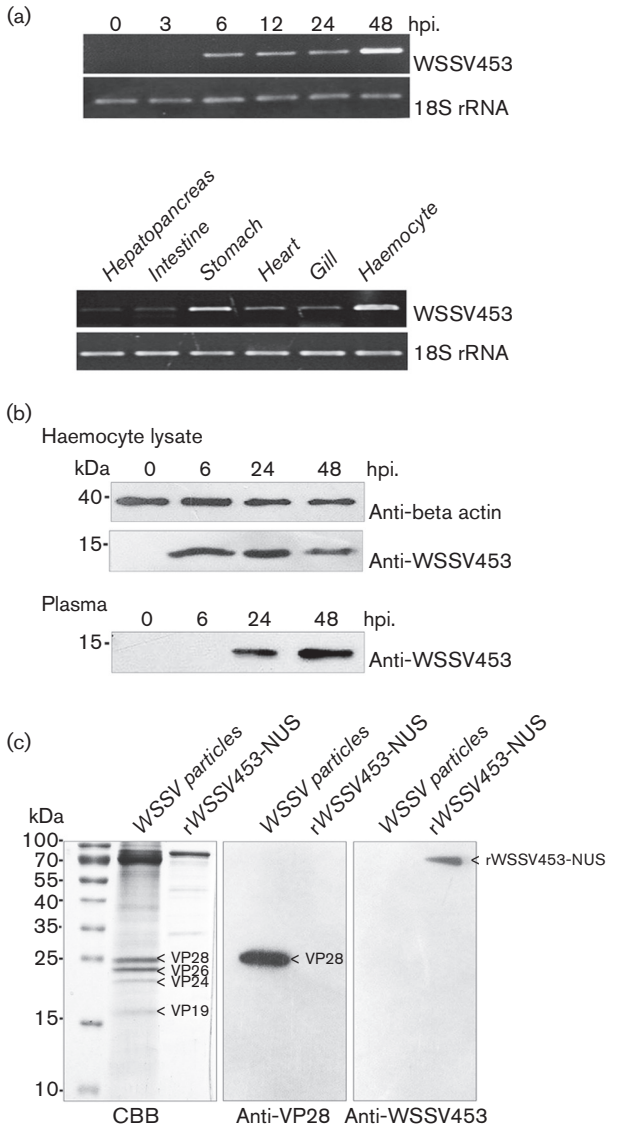


Fig. 4. Characterization of WSSV453 gene and protein expression in WSSV-infected *P. monodon*. (a) Reverse transciptase PCR analysis of WSSV453 in haemolymph collected 0–48 hpi and in hepatopancreas, intestine, stomach, heart, gill and haemocyte samples collected at 48 h p.i. Template for each sample was first-strand cDNA synthesized from total RNA. Gene-specific primers for WSSV453 and the 18S ribosomal gene (18S rRNA) (as an internal control) were then used. PCR was performed and analysed on 1.5 % agarose gels stained with ethidium bromide. (b) WSSV453 protein in haemocyte lysate (30 µg) and plasma (200 µg) of WSSV-infected shrimp at 0, 6, 24 and 48 hpi. Samples were subjected to SDS-PAGE and immunoblotting using anti-WSSV453 antibody and anti-β-actin antibody as control. (c) Purified WSSV particles were subjected to SDS-PAGE and visualized by staining with CBB and immunoblotting using an anti-VP28 antibody and anti-WSSV453 antibody, respectively.

To determine with which step of the PO cascade WSSV453 interferes, we incubated rWSSV453-NUS with r*Pm*proPPAE2$_{Xa}$, r*Pm*proPO1 or r*Pm*proPO2, before or after their activation. Results showed that PO inhibitory activity only occurs with r*Pm*proPPAE2$_{Xa}$. We also show that incubating WSSV453 with *Pm*proPPAE2$_{Xa}$ before addition of factor Xa dose-dependently interferes with *Pm*proPPAE2$_{Xa}$ processing but WSSV453 has no effect on already activated *Pm*PPAE2$_{Xa}$. These results indicate that the order of interaction between WSSV453 and *Pm*proPPAE2 processing is a key factor in reducing *Pm*PPAE2 activity. Moreover, it suggests that rWSSV453-NUS does not inhibit *Pm*PPAE2 enzymatic activity but instead binds to *Pm*proPPAE2, which affects both processing and activation of proPOs leading to a reduction in shrimp melanization.

In comparison, polydnavirus proteins named Egf1.0 and 1.5 from *Microplitis demolitor* Bracovirus (*Md*BV) disable melanization of host insect haemolymph by blocking the processing and amidolytic activity of insect proPO-activating proteinases (pro-PAP1 and 3). Egf1.0 also binds to serine proteinase homologues 1 and 2 (SPH1 and 2) [14–16]. Egf1.0 and Egf1.5 contain cysteine-rich motifs similar to the trypsin inhibitor-like domain of small serine proteinase inhibitors (smapins), but this motif or other serine proteinase inhibitor domains are absent in WSSV453. This suggests that WSSV453 interacts differently with PPAEs/PAPs than Egf proteins. Potentially similar to WSSV453, a viral protein from Dengue Virus named NS1 was recently shown to inhibit protrombin activation by interfering with activation without any specific inhibitor domain [31].

To assess where inhibition of melanization by WSSV occurs, PO activity was separately investigated in haemocytes and plasma of WSSV-infected shrimp. These results showed that at 2 dpi PO activity of WSSV-infected shrimp plasma was reduced whereas activity in haemocytes was not. This supports the suggestion that WSSV453 in plasma might interact with *Pm*proPPAE2, which results in reduced activation of *Pm*proPOs. Supporting this interpretation, adding activated r*Pm*PPAE2$_{Xa}$ to plasma from infected shrimp increased PO activity. The regulation of melanization in invertebrates generally is also mostly in plasma. For example, melanization inhibition proteins (MIPs) from the crayfish *Pacifastacus leniusculus* [32] and *P. monodon* [33] are secreted into plasma. Serine proteinase inhibitor proteins (serpins) in *Manduca sexta* and in *Hyphantria cunea* also function in plasma [34–36]. In conclusion, this study provides novel insights into the function of WSSV453 and its role as an inhibitor of melanization in shrimp.

Downloaded from www.microbiologyresearch.org by
IP: 157.[illegible].240.101
On: Tue, 01 Aug 2017 07:33:52

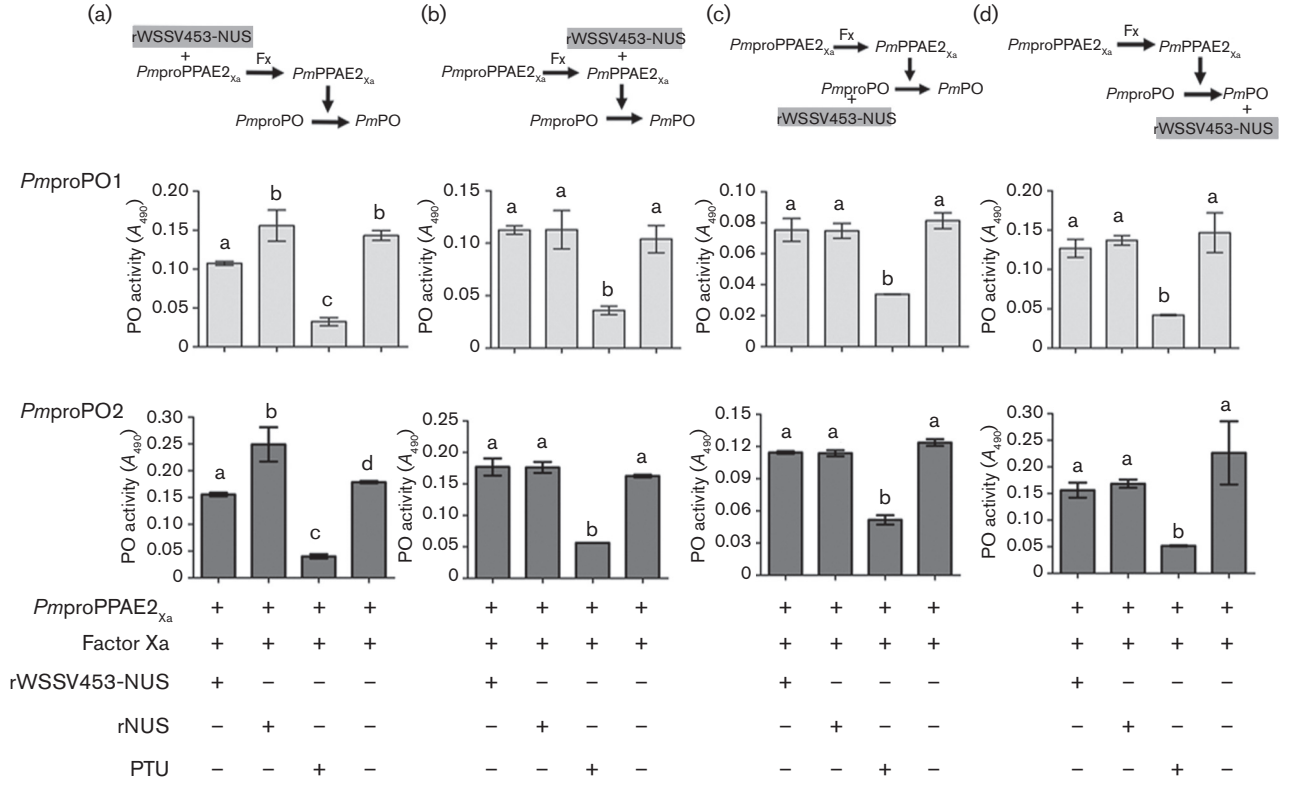


Fig. 5. Effect of WSSV453 on PO activity. (a) rWSSV453-NUS (or rNUS or PTU as control) was pre-incubated with *Pm*proPPAE2$_{Xa}$ for 1 h followed by addition of factor Xa and r*Pm*proPO1 or r*Pm*proPO2. (b) rWSSV453-NUS was pre-incubated with factor Xa-activated *Pm*proPPAE2$_{Xa}$ for 1 h and followed by adding r*Pm*proPO1 or r*Pm*proPO2. (c) rWSSV453-NUS was pre-incubated with r*Pm*proPO1 or r*Pm*proPO2 for 1 h followed by factor Xa-activated *Pm*proPPAE2$_{Xa}$. (d) rWSSV453-NUS was incubated with active r*Pm*proPO1 or active r*Pm*proPO2 for 1 h. Each reaction was incubated in a 96-well plate containing Tris-HCl (pH 8.0) and 5 µM $CuCl_2$. Then, L-DOPA was added as a substrate for determining PO activity at 490 nm. The data shown are means±SD derived from three independently replicated experiments. Different letters (above each bar) indicate a significant difference (P<0.05) in the mean PO activity between the four samples.

METHODS

Animal preparation and purification of intact WSSV viral particles

Specific pathogen-free *P. monodon* were obtained from the Shrimp Genetic Improvement Center, BIOTEC, Thailand. The specific pathogen-free shrimp were screened to be free of major shrimp pathogens including WSSV by PCR diagnosis. Shrimp were kept in laboratory tanks with diluted natural seawater with a salinity of approximately 20 ppt and reared for 7 days before processing. WSSV was isolated as described previously with slight modifications [37]. Briefly, 5 g of gills from WSSV-infected crayfish, *Procambarus clarkii,* were collected and homogenized in 36 ml of TNE buffer (50 mM Tris-HCl, 400 mM NaCl, 5 mM EDTA, pH 8.5) containing a complete protease inhibitor (using complete mini EDTA-free; Roche). After centrifugation at 3500 ***g*** for 5 min at 4 °C, the preparation was filtered through a nylon net (400 mesh). The supernatant was centrifuged at 30 000 ***g*** for 30 min at 4 °C; the supernatant was then carefully discarded, and the lower white pellet was suspended in 1 ml PBS buffer (140 mM NaCl, 2.7 mM KCl, 10 mM Na_2HPO_4, 1.8 mM KH_2PO_4, pH 7.4). Viral genome copy number was determined by real-time quantitative PCR (qPCR) [38]. All shrimp used in experiments weighted ~10 g and were infected with 1×10^5 genome copies of WSSV.

Effect of *Pm*proPOs gene silencing and WSSV infection on shrimp melanization

*Pm*proPO1 and 2 genes were knocked down by injection of complementary dsRNA. In brief, *Pm*proPO1 and *Pm*proPO2 dsRNA were generated using the T7 RiboMAX Express Large Scale RNA Production System (Promega) with the gene-specific primer pairs PO1i T7-F/-R, PO1i- F/-R, PO2iT7-F/-R and PO2i-F/-R [7]. Juvenile shrimp were intramuscularly injected with 25 µl of 150 mM NaCl (sodium saline solution; SSS) containing either (i) *Pm*proPO1 and *Pm*proPO2 dsRNA (5 µg per gram of shrimp, wet body weight), or (ii) GFP dsRNA as control (at the same concentration). At 24 hpi, a second 25 µl injection was administered as before. The cuticle of treated shrimp was pierced 24 h after the second injection using a sterile

Downloaded from www.microbiologyresearch.org by
IP: 157.[illegible].240.101
On: Tue, 01 Aug 2017 07:33:52

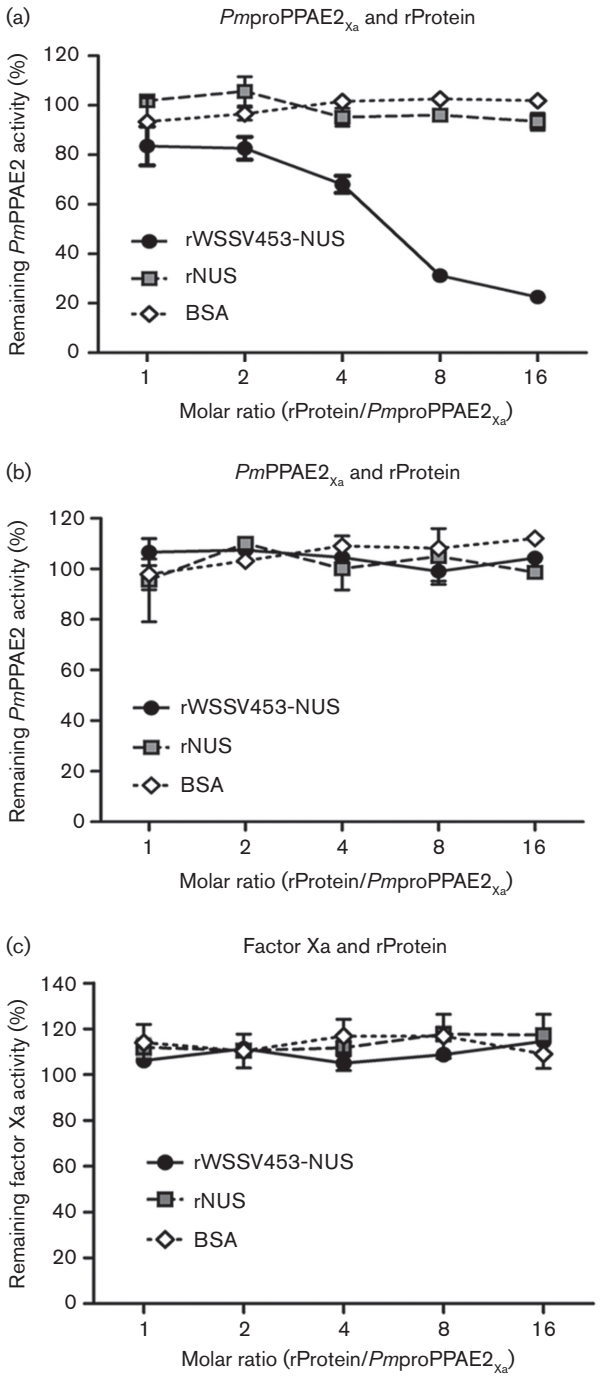


Fig. 6. WSSV453 interferes with *Pm*proPPAE2$_{Xa}$ activation. (a) rWSSV453-NUS, rNUS or BSA was pre-incubated with *Pm*proPPAE2$_{Xa}$ for 1 h at a molar ratio of 1–16 : 1 followed by addition of factor Xa and VPR as a substrate to determine *Pm*PPAE2$_{Xa}$ activity. Results are presented as a percentage relative to when no added protein was present (=100 %). (b) *Pm*PPAE2$_{Xa}$ already activated by pretreatment with factor Xa was incubated with rWSSV453-NUS as described in (a). (c) Effect of rWSSV453-NUS, rNUS or BSA on factor Xa activity using EAR as a substrate. Data shown in (a) to (c) are means±SD from three independently replicated experiments.

needle, while melanization of the wound site was assessed at 24 h. The effect of WSSV infection on injury-mediated melanization of shrimp was also assessed. Shrimp were injected with WSSV or PBS (control) as described above. The cuticle of treated shrimp was pierced at 3 hpi (early phase of infection) or 24 hpi (late phase of infection) followed by assessment of melanization at 24 h after the wounding event. All assays were performed in triplicate. Photos were taken using a Canon PowerShot SX510 HS camera.

SDS-PAGE and immunoblot analysis

Protein samples were run on SDS-PAGE gels, which were either stained with CBB or processed for immunoblotting. In brief, samples were mixed with 2× sample buffer, boiled for 5 min and then loaded on 15 % SDS-PAGE gels. For immunoblotting, proteins were transferred to nitrocellulose (Amersham Hybond ECL Nitrocellulose Membrane; GE Healthcare) after electrophoresis. Membranes were blocked with 5 % non-fat milk powder in PBS at room temperature for 1 h. After washing three times with PBS with 0.05 % Tween 20 (PBS-T), membranes were probed with specific antibodies against WSSV453 (1 : 100), VP28 (1 : 3000), the V5 epitope (1 : 3000; Thermo), β-actin (1 : 3000; Thermo) or polyhistidine tags (1 : 3000; Millipore) at 4 °C overnight. Primary antibodies against V5 epitope, β-actin and polyhistidine were detected with a goat anti-mouse IgG-HRP-conjugated secondary antibody (1 : 10 000; Jackson Immuno Research). The primary antibodies for VP28 and WSSV453 were detected with a goat anti-rabbit IgG-HRP-conjugated secondary antibody (1 : 10 000; Thermo Fisher Scientific). All blots were visualized using the SuperSignal West Pico Chemiluminescent Substrate (Thermo Fisher Scientific). The polyclonal antibody against VP28 was a kind gift from Dr.Paisarn Sithigorngul (Srinakharinwirot University, Thailand). The polyclonal antibody against WSSV453 was prepared against the peptide 'TTSRASPSSVEYKRR' (Genscript).

Preparation of recombinant proteins

rWSSV453, *Pm*proPO1 and *Pm*proPO2 were expressed in *Escherichia coli* while *Pm*proPPAE2 was expressed in *Drosophila* S2 cells. Expression constructs and protein production for *Pm*proPPAE2, mutant *Pm*proPPAE2 (*Pm*proPPAE2$_{Xa}$) and WSSV453-NUS were prepared as reported previously [19]. The expression constructs for *Pm*proPO1 and *Pm*proPO2 were generated by PCR ampliflication of the coding sequences for each using the primers (*Pm*PPO1NdeI-F: 5′CGCCATATGGCCATGGCCGCCAATGACCAGCAGCGT3′/*Pm*PPO1HindIII-R: 5′CCC*AAGCTT*GTTCAATTTCTCGCCCAGAAA3′ and *Pm*PPO2NdeI-F: 5′CGCCATATGGCCATGGCCGAAAAGAATCAGAAGAACCTCC3′/*Pm*PPO2NotI-R: 5′TAAA *GCGGCCGC*GTTCAGCTTCTCTGCCAAGAA3′) and shrimp, *P. monodon*, cDNA as template. The purified *Pm*proPO1, 2 products were digested with the corresponding restriction enzymes and ligated into pET22b (Novagen). Plasmids were transformed into competent *E. coli* JM109 cells and positive recombinant clones were analysed by nucleotide

Downloaded from www.microbiologyresearch.org by
IP: 157.[illegible].240.101
On: Tue, 01 Aug 2017 07:33:52

sequencing. The selected recombinant plasmid (pET22b-*Pm*proPO1, 2) was transformed into *E. coli* BL21 (DE3) pLysS cells (Novagen) and induced with 0.1 mM IPTG. Transformed *E. coli* were cultured at 16 °C for 16 h and harvested by centrifugation at 8000 rpm for 15 min. The pellets were resuspended in 20 mM Tris-HCl (pH 8.0) and disrupted by an ultrasonic oscillator. The r*Pm*proPO1 and r*Pm*proPO2 were found in the soluble fraction and purified by Ni-NTA affinity chromatography according to the manufacturer's protocol for soluble proteins (Qiagen). The concentration of the recombinant proteins was quantified by a Bradford assay while purity and size were assessed by SDS-PAGE and staining with CBB.

In vitro activation of r*Pm*proPPAE2$_{Xa}$ by factor Xa

To investigate the role of *Pm*proPPAE2 in the shrimp PO activation cascade, the predicted activation site of *Pm*proPPAE2 was changed from NLNK to IEGR (*Pm*proPPAE2$_{Xa}$) to allow its activation by bovine factor Xa [19]. The incubation time and concentration between factor Xa and r*Pm*proPPAE2$_{Xa}$ were optimized. Several concentrations (0.02, 0.1 and 0.5 µg) of factor Xa (New England Biolabs; P8010) were incubated with 0.1 µg of r*Pm*proPPAE2$_{Xa}$ at 1, 6 and 16 h at room temperature. Amidase activity of 0.1 µg r*Pm*proPPAE2$_{Xa}$ after activation by 0.5 µg factor Xa for 16 h was assayed by adding to a 96-well plate containing proteinase buffer (100 mM Tris-HCl, 100 mM NaCl, 5 mM $CaCl_2$, pH 7.8), followed by adding VPR (B9385) as substrate. Fluorescence signal was then read using 380 nm excitation and 460 nm emission at 1 h by the plate reader (SpectraMax M5).

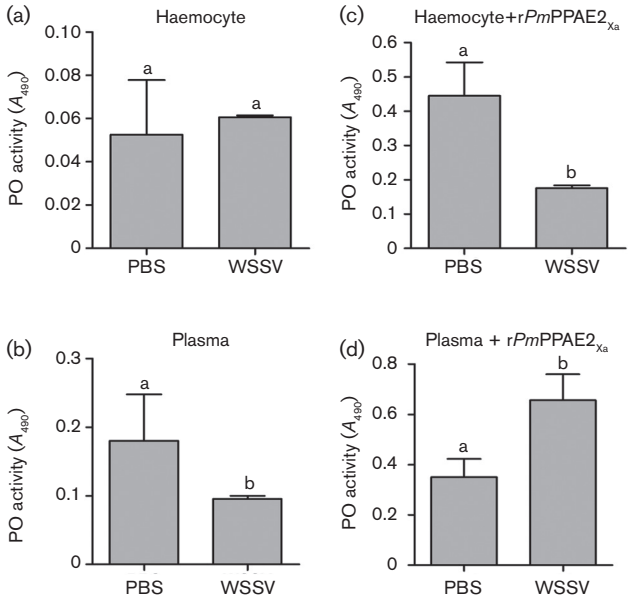


Fig. 7. WSSV infection reduces shrimp PO activity in plasma but not haemocytes. Sub-adult shrimp (~10 g) were infected with WSSV (or PBS as control) followed by collection of haemolymph at 2 dpi. Samples were separated into (a) haemocyte lysate (HLS) and (b) plasma (PL). PO activity in PL (200 µg) and HLS (20 µg) was measured by putting samples in a 96-well plate containing 10 mM Tris-HCl (pH 8.0), adding L-DOPA and measuring absorbance at 490 nm after 30 min. (c and d) *Pm*PPAE2 was added into (c) HLS and (D) PL followed by measurement of PO activity as described for (a) and (b). Data for all treatments are means±SD from three independently replicated experiments. Different letters (above each bar) indicate a significant difference (P<0.05) in the mean PO activity between the two samples.

In vitro activation of r*Pm*proPO1, 2 by active r*Pm*PPAE2$_{Xa}$

Activation of r*Pm*proPO1 and r*Pm*proPO2 by active r*Pm*PPAE2$_{Xa}$ (factor Xa-activated r*Pm*proPPAE2$_{Xa}$) was examined. To obtain active r*Pm*PPAE2$_{Xa}$, r*Pm*proPPAE2$_{Xa}$ (23 nM) was activated by 0.5 µg of factor Xa for 6 h at room temperature. r*Pm*proPO1 (125 nM) or r*Pm*proPO2 (125 nM) were then incubated with active r*Pm*PPAE2$_{Xa}$ (23 nM) for 30 min. proPO cleavage, indicative of activation, was analysed by SDS-PAGE and staining with CBB or immunoblotting using a His-tag primary antibody as described above. *rPm*proPO1 and *rPm*proPO2 activity were accessed after activation by incubating *rPm*proPO1, *rPm*proPO2 or BSA as a control (125 nM) with active r*Pm*PPAE2 (23 nM) in a 96-well plate containing 10 mM Tris-HCl (pH 8.0) and 5 µM $CuCl_2$ (80 µl), for 30 min. L-DOPA (15 µl of 3.0 mg ml^{-1}) was then added as substrate to determine PO activity. PO activity was observed by measuring absorbance at 490 nm at 1 h using a plate reader (SpectraMax M5). Each assay was performed in triplicate and statistical analysis was performed using a one-way ANOVA followed by a *post-hoc* Duncan's test.

WSSV453 gene and protein characterization

Healthy WSSV-susceptible shrimp (size ~10 g) were infected with WSSV, and haemolymph was collected from an abdominal segment at 0, 3, 6, 12, 24 and 48 hpi using a 1 ml sterile syringe without anticoagulant buffer. Shrimp tissues, including hepatopancreas, stomach, intestine, heart, haemocytes and gill, were collected at 48 hpi. Total RNA was isolated from each sample using the RNeasy Mini Kit (Qiagen) followed by cDNA synthesis using the RevertAid first strand cDNA synthesis kit (Thermo Scientific). Gene-specific primers for WSSV453 (WSSV453-F: TAAAG CGATCGCCATGAAGTTGATGGAGTTCCTGAAAGAG/ WSSV453-R: CTTGTTTAAACTTGCCTCCATTTTCTTG TTGGTA) were used and the primer for 18S rRNA (18 S-F: TATACGCTAGTGGAGCTGGAA/18S-R: GGGGAGG TAGTGACGAAAAAT) was used as an internal control. PCR products were analysed on 1.5 % agarose gels stained with ethidium bromide.

To detect WSSV453 protein in WSSV-infected shrimp, haemolymph was collected at 0, 6, 24 and 48 hpi with a 22 gauge needle, fitted to a 1 ml syringe that contained 0.5 ml of anticoagulant consisting of 140 mM NaCl, 30 mM citric acid, 110 mM glucose and 30 mM sodium citrate, pH 5.6. Then, shrimp haemolymph was centrifuged at 800 ***g*** for 10 min at 4 °C. The supernatant was collected as plasma and

Downloaded from www.microbiologyresearch.org by
IP: 157.[illegible].240.101
On: Tue, 01 Aug 2017 07:33:52

the haemocyte pellet was dissolved in 0.2 ml of PBS buffer by sonicating for 10 s as haemocyte lysate. Haemocyte lysate (30 µg) and plasma sample (200 µg) were then analysed by SDS-PAGE and immunoblotting using anti-WSSV453 antibody and anti-β-actin as control as described above. Purified WSSV (10 µg) was prepared as described above and analysed by SDS-PAGE and visualized by staining with CBB and immunoblotting using the anti-WSSV453 antibody or anti-VP28 antibody as a control.

Effect of rWSSV453-NUS on shrimp PO cascade

To understand the inhibition mechanism of WSSV453 on the shrimp proPO system, rWSSV453-NUS (230 nM) was pre-incubated with proPO-associated proteins in four separate reactions: rWSSV453-NUS with r*Pm*proPPAE2$_{Xa}$ before (A) or after (B) activation by factor Xa, and pre-incubation of rWSSV453-NUS with r*Pm*proPO1 or r*Pm*proPO2 before (C) or after (D) activation by active r*Pm*PPAE2$_{Xa}$. r*Pm*proPPAE2$_{Xa}$ (23 nM) was activated by incubation with 0.5 µg factor Xa for 6 h while active r*Pm*POs were produced by incubating r*Pm*proPOs (125 nM) with active r*Pm*PPAE2$_{Xa}$ (23 nM) for 1 h at room temperature. Each reaction was incubated in a 96-well plate containing 10 mM Tris-HCl (pH8.0) and 5 µM $CuCl_2$ (80 µl). L-DOPA (15 µl of 3.0 mg ml^{-1}) was then added as a substrate for determining PO activity by measuring absorbance at 490 nm at 1 h using the plate reader (SpectraMax M5). All experiments were performed in triplicate and statistical analysis was performed using a one-way ANOVA followed by Duncan's test.

Functional study of WSSV453 on *Pm*proPPAE2 and processed *Pm*PPAE2

r*Pm*proPPAE2$_{Xa}$ (2.3 nM) was pre-incubated with rWSSV453-NUS at different molar ratios (0, 2.3, 4.6, 9.2, 18.4 and 36.8 nM) for 1 h before adding 0.05 µg factor Xa. r*Pm*proPPAE2$_{Xa}$ (2.3 nM) was also activated by adding 0.05 µg factor Xa for 6 h followed by addition of rWSSV453-NUS (or rNUS or BSA as controls) at different molar ratios (0, 2.3, 4.6, 9.2, 18.4 and 36.8 nM) for 1 h. The reaction mixtures were incubated in a 96-well plate containing proteinase buffer (80 µl). The substrate VPR (50 µM) was then added to both reactions followed by measurement of fluorescence after 1 h at 380 nm excitation and 460 nm emission using a plate reader (SpectraMax M5). rWSSV453-NUS (0, 2.3, 4.6, 9.2, 18.4 and 36.8 nM) was also incubated with 0.05 µg factor Xa for 1 h in a 96-well plate containing proteinase buffer (80 µl), followed by addition of 50 µM *N*-Acetyl-Ile-Glu-Ala-Arg *p*-nitroanilide acetate salt (A0180; EAR) as a substrate. Factor Xa activity was then measured at 405 nm using a plate reader (SpectraMax M5). All experiments were performed in triplicate and statistical analysis was performed using a one-way ANOVA followed by Duncan's test.

Effect of WSSV infection on PO activity of shrimp plasma and haemocytes

Healthy WSSV-susceptible shrimp (size ~10 g) were injected with WSSV or PBS followed by collection of haemolymph from an abdominal segment at 2 dpi as described above. Haemocyte lysate supernatants and plasma were prepared by collecting haemolymph with a 3 ml syringe and 22 gauge needle that contained ice-cold 10 mM Tris-HCl, pH 8.0. Samples were immediately centrifuged at 1000 ***g*** for 10 min at 4 °C. The supernatant was collected as plasma (PL) and the haemocyte pellet was washed twice with PBS and homogenized in 0.2 ml of ice-cold homogenizer buffer (10 mM sodium cacodylate and 5 mM $CaCl_2$; pH 7.0) and then centrifuged at 25 000 ***g*** for 10 min at 4 °C. The supernatant was collected as haemocyte lysate supernatant (HLS). PO activity of shrimp PL (200 µg) and HLS (20 µg) were determined by adding samples to a 96-well plate containing 10 mM Tris-HCl (pH 8.0; 80 µl) and L-DOPA (15 µl of 3.0 mg ml^{-1}) followed by measurement of absorbance at 490 nm at 30 min using the plate reader (SpectraMax M5). To compare PO activation in infected and normal shrimp, active r*Pm*PPAE2$_{Xa}$ was prepared by incubating r*Pm*proPPAE2$_{Xa}$ (115 nM) with 1 µg factor Xa for 16 h. r*Pm*PPAE2$_{Xa}$ was then added to PL and HLS samples followed by measurement of PO activity as described above. All experiments were performed in triplicate and statistical analysis was performed using a one-way ANOVA followed by Duncan's test.

Funding information
This work was supported by research grants from the Thailand Research Fund to A.T. (RTA5880004, IRG5780008), the Thailand Research Fund and National Center for Genetic Engineering and Biotechnology, National Science and Technology Development Agency to P.A. (Grant No. BRG5880016) and National Research University Project, Office of Higher Education Commission (WCU-017-FW-57). J.S. is the recipient of a student fellowship from the Royal Golden Jubilee PhD Program, Joint Funding of the Thailand Research Fund and Chulalongkorn University and the 90th Anniversary of Chulalongkorn University Fund (Ratchadaphiseksomphot Endowment Fund).

Acknowledgements
We thank Dr.Paisarn Sithigorngul (Srinakharinwirot University, Thailand) for the polyclonal antibody against VP28.

Conflicts of interest
The authors declare that there are no conflicts of interest.

References

1. **Finlay BB, McFadden G.** Anti-immunology: evasion of the host immune system by bacterial and viral pathogens. *Cell* 2006;124:767–782.
2. **Cerenius L, Lee BL, Söderhäll K.** The proPO-system: pros and cons for its role in invertebrate immunity. *Trends Immunol* 2008;29:263–271.
3. **Kanost MR, Gorman MJ.** Phenoloxidases in insect immunity. *Insect Immunology* 2008:69–96.
4. **Amparyup P, Charoensapsri W, Tassanakajon A.** Prophenoloxidase system and its role in shrimp immune responses against major pathogens. *Fish Shellfish Immunol* 2013;34:990–1001.
5. **Söderhäll K, Cerenius L.** Role of the prophenoloxidase-activating system in invertebrate immunity. *Curr Opin Immunol* 1998;10:23–28.
6. **Cerenius L, Kawabata S, Lee BL, Nonaka M, Söderhäll K.** Proteolytic cascades and their involvement in invertebrate immunity. *Trends Biochem Sci* 2010;35:575–583.
7. **Amparyup P, Charoensapsri W, Tassanakajon A.** Two prophenoloxidases are important for the survival of *Vibrio harveyi*

Downloaded from www.microbiologyresearch.org by
IP: 157.[illegible].240.101
On: Tue, 01 Aug 2017 07:33:52

challenged shrimp *Penaeus monodon*. *Dev Comp Immunol* 2009;33: 247–256.

8. **Binggeli O, Neyen C, Poidevin M, Lemaitre B.** Prophenoloxidase activation is required for survival to microbial infections in *Drosophila*. *PLoS Pathog* 2014;10:e1004067.
9. **Nappi AJ, Christensen BM.** Melanogenesis and associated cytotoxic reactions: applications to insect innate immunity. *Insect Biochem Mol Biol* 2005;35:443–459.
10. **Zhao P, Li J, Wang Y, Jiang H.** Broad-spectrum antimicrobial activity of the reactive compounds generated *in vitro* by *Manduca sexta* phenoloxidase. *Insect Biochem Mol Biol* 2007;37:952–959.
11. **Zhao P, Lu Z, Strand MR, Jiang H.** Antiviral, anti-parasitic, and cytotoxic effects of 5,6-dihydroxyindole (DHI), a reactive compound generated by phenoloxidase during insect immune response. *Insect Biochem Mol Biol* 2011;41:645–652.
12. **Charoensapsri W, Amparyup P, Suriyachan C, Tassanakajon A.** Melanization reaction products of shrimp display antimicrobial properties against their major bacterial and fungal pathogens. *Dev Comp Immunol* 2014;47:150–159.
13. **Eleftherianos I, Boundy S, Joyce SA, Aslam S, Marshall JW *et al.*** An antibiotic produced by an insect pathogenic bacterium suppresses host defenses through phenoloxidase inhibition. *Proc Natl Acad Sci USA* 2007;104:2419–2424.
14. **Beck MH, Strand MR.** A novel polydnavirus protein inhibits the insect prophenoloxidase activation pathway. *Proc Natl Acad Sci USA* 2007;104:19267–19272.
15. **Lu Z, Beck MH, Wang Y, Jiang H, Strand MR.** The viral protein Egf1.0 is a dual activity inhibitor of prophenoloxidase-activating proteinases 1 and 3 from *Manduca sexta*. *J Biol Chem* 2008;283: 21325–21333.
16. **Lu Z, Beck MH, Strand MR.** Egf1.5 is a second phenoloxidase cascade inhibitor encoded by *Microplitis demolitor* bracovirus. *Insect Biochem Mol Biol* 2010;40:497–505.
17. **Escobedo-Bonilla CM, Alday-Sanz V, Wille M, Sorgeloos P, Pensaert MB *et al.*** Review on the morphology, molecular characterization, morphogenesis and pathogenesis of white spot syndrome virus. *J Fish Dis* 2008;31:1–18.
18. **Shekhar MS, Ponniah AG.** Recent insights into host-pathogen interaction in white spot syndrome virus infected penaeid shrimp. *J Fish Dis* 2015;38:599–612.
19. **Sutthangkul J, Amparyup P, Charoensapsri W, Senapin S, Phiwsaiya K *et al.*** Suppression of shrimp melanization during white spot syndrome virus infection. *J Biol Chem* 2015;290:6470–6481.
20. **Ai HS, Huang YC, Li SD, Weng SP, Yu XQ *et al.*** Characterization of a prophenoloxidase from hemocytes of the shrimp *Litopenaeus vannamei* that is down-regulated by white spot syndrome virus. *Fish Shellfish Immunol* 2008;25:28–39.
21. **Ai HS, Liao JX, Huang XD, Yin ZX, Weng SP *et al.*** A novel prophenoloxidase 2 exists in shrimp hemocytes. *Dev Comp Immunol* 2009;33:59–68.
22. **Yeh SP, Chen YN, Hsieh SL, Cheng W, Liu CH.** Immune response of white shrimp, *Litopenaeus vannamei*, after a concurrent infection with white spot syndrome virus and infectious hypodermal and hematopoietic necrosis virus. *Fish Shellfish Immunol* 2009;26: 582–588.
23. **Jiravanichpaisal P, Sricharoen S, Söderhäll I, Söderhäll K.** White spot syndrome virus (WSSV) interaction with crayfish haemocytes. *Fish Shellfish Immunol* 2006;20:718–727.
24. **Charoensapsri W, Amparyup P, Hirono I, Aoki T, Tassanakajon A.** Gene silencing of a prophenoloxidase activating enzyme in the shrimp, *Penaeus monodon*, increases susceptibility to *Vibrio harveyi* infection. *Dev Comp Immunol* 2009;33:811–820.
25. **Charoensapsri W, Amparyup P, Hirono I, Aoki T, Tassanakajon A.** *Pm*PPAE2, a new class of crustacean prophenoloxidase (proPO)-activating enzyme and its role in PO activation. *Dev Comp Immunol* 2011;35:115–124.
26. **Lan Y, Xu X, Yang F, Zhang X.** Transcriptional profile of shrimp white spots syndrome virus (WSSV) genes with DNA microarray. *Arch Virol* 2006;151:1723–1733.
27. **Tsai JM, Wang HC, Leu JH, Hsiao HH, Wang AH *et al.*** Genomic and proteomic analysis of thirty-nine structural proteins of shrimp white spot syndrome virus. *J Virol* 2004;78:11360–11370.
28. **Roux MM, Pain A, Klimpel KR, Dhar AK.** The lipopolysaccharide and β-1,3-glucan binding protein gene is upregulated in white spot virus-infected shrimp (*Penaeus stylirostris*). *J Virol* 2002;76: 7140–7149.
29. **Xie X, Xu L, Yang F.** Proteomic analysis of the major envelope and nucleocapsid proteins of white spot syndrome virus. *J Virol* 2006; 80:10615–10623.
30. **Lin X, Söderhäll I.** Crustacean hematopoiesis and the astakine cytokines. *Blood* 2011;117:6417–6424.
31. **Lin SW, Chuang YC, Lin YS, Lei HY, Liu HS *et al.*** Dengue virus nonstructural protein NS1 binds to prothrombin/thrombin and inhibits prothrombin activation. *J Infect* 2012;64:325–334.
32. **Söderhäll I, Wu C, Novotny M, Lee BL, Söderhäll K.** A novel protein acts as a negative regulator of prophenoloxidase activation and melanization in the freshwater crayfish *Pacifastacus leniusculus*. *J Biol Chem* 2009;284:6301–6310.
33. **Angthong P, Watthanasurorot A, Klinbunga S, Ruangdej U, Söderhäll I *et al.*** Cloning and characterization of a melanization inhibition protein (*Pm*MIP) of the black tiger shrimp, *Penaeus monodon*. *Fish Shellfish Immunol* 2010;29:464–468.
34. **Christen JM, Hiromasa Y, An C, Kanost MR.** Identification of plasma proteinase complexes with serpin-3 in *Manduca sexta*. *Insect Biochem Mol Biol* 2012;42:946–955.
35. **An C, Kanost MR.** *Manduca sexta* serpin-5 regulates prophenoloxidase activation and the Toll signaling pathway by inhibiting hemolymph proteinase HP6. *Insect Biochem Mol Biol* 2010;40: 683–689.
36. **Park DS, Shin SW, Hong SD, Park HY.** Immunological detection of serpin in the fall webworm, *Hyphantria cunea* and its inhibitory activity on the prophenoloxidase system. *Mol Cells* 2000;10:186–192.
37. **Xie X, Li H, Xu L, Yang F.** A simple and efficient method for purification of intact white spot syndrome virus (WSSV) viral particles. *Virus Res* 2005;108:63–67.
38. **Li S, Zhang X, Sun Z, Li F, Xiang J.** Transcriptome analysis on Chinese shrimp *Fenneropenaeus chinensis* during WSSV acute infection. *PLoS One* 2013;8:e58627.

Downloaded from www.microbiologyresearch.org by
IP: 157.[illegible].240.101
On: Tue, 01 Aug 2017 07:33:52

Fish & Shellfish Immunology 68 (2017) 341–348

Contents lists available at ScienceDirect

Fish & Shellfish Immunology

journal homepage: www.elsevier.com/locate/fsi

Full length article

A single WAP domain-containing protein from *Litopenaeus vannamei* possesses antiproteinase activity against subtilisin and antimicrobial activity against AHPND-inducing *Vibrio parahaemolyticus*

Suwattana Visetnan [a], Premruethai Supungul [c], Anchalee Tassanakajon [a], Suchao Donpudsa [b, *], Vichien Rimphanitchayakit [a, **]

[a] Center of Excellence for Molecular Biology and Genomics of Shrimp, Department of Biochemistry, Faculty of Science, Chulalongkorn University, Phyathai Road, Bangkok 10330, Thailand
[b] Department of Chemistry, Faculty of Science, Srinakharinwirot University, Bangkok 10110, Thailand
[c] National Center for Genetic Engineering and Biotechnology (BIOTEC), National Science and Technology Development Agency (NSTDA), Pathum Thani 10120, Thailand

ARTICLE INFO

Article history:
Received 25 April 2017
Received in revised form
18 July 2017
Accepted 21 July 2017
Available online 22 July 2017

Keywords:
*Lv*SWD
Crustin
Antimicrobial protein
AHPND-inducing *Vibrio parahaemolyticus*

ABSTRACT

The single WAP domain-containing protein (SWD) is a type III crustin antimicrobial peptide whose function is to defense the host animal against the bacterial infection by means of antimicrobial and antiproteinase activities. A study of SWD from *Litopenaeus vannamei* (*Lv*SWD) is reported herein about its activities and function against bacteria, particularly the AHPND-inducing *Vibrio parahaemolyticus* (VP_{AHPND}) that causes acute hepatopancreatic necrosis disease (AHPND). The *Lv*SWD is mainly synthesized in hemocytes and up-regulated in response to VP_{AHPND} infection. Over-expressed mature recombinant *Lv*SWD (r*Lv*SWD) and its WAP domain (r*Lv*SWD-WAP) are able to strongly inhibit subtilisin but not trypsin, chymotrypsin and elastase. The r*Lv*SWD inhibits subtilisin with the inhibition constant (K_i) of 14.3 nM. However, only r*Lv*SWD exhibited antimicrobial activity against both Gram-positive and Gram-negative bacteria. Unlike the r*Lv*SWD, the r*Lv*SWD-WAP does not possess antimicrobial activity. Therefore, the killing effect of r*Lv*SWD on VP_{AHPND} and *Bacillus megaterium* was studied. The MIC of 30 μM against VP_{AHPND} is bactericidal whereas the MIC against *B. megaterium* is not. With four times the MIC of r*Lv*SWD, the VP_{AHPND}-treated post larval shrimp are able to survive longer with 50% survival rate as long as 78 h as compared to 36 h of the infected shrimp without r*Lv*SWD. The antimicrobial activity of *Lv*SWD against the VP_{AHPND} infection suggests its potential application for disease control in aquaculture.
© 2017 Elsevier Ltd. All rights reserved.

1. Introduction

Shrimp and invertebrates alike have only an innate immunity to defend themselves from pathogenic invasion of bacteria, viruses and fungi. The innate immunity is, thus, very efficient against infection though relatively nonspecific. There are two types of innate immune responses, known as cellular and humoral responses. Upon infection, as the first line of defenses, the hemocytes secrete several humoral molecules for example enzymes and proteins of prophenoloxidase system, proteinases and their inhibitors, and antimicrobial peptides (AMPs), etc., to neutralize and destroy the invading microorganisms as well as activate the cellular components to remove the hazardous pathogens [1–3].

The humoral factors, crustins, are cationic cysteine-rich AMPs containing a whey acidic protein (WAP) domain at their C-terminus. They are found widespread among crustaceans and have important functions in the innate immune system of crustaceans [4–7]. Their WAP domain consists of 50–60 amino acid residues with eight conserved cysteine residues that form four disulfide bridges, called a four-disulfide core structure [8,9]. The proteins containing WAP domain usually have several functions but mostly proteinase inhibition and/or antimicrobial activities [10–12].

Three types of crustins are assigned depending on their domain structures by Smith et al. (2008) as types I, II and III [4]. Type I crustins, also called carcinins, contain a signal sequence, a Cys-rich

* Corresponding author. Tel.: +66 2 6495000 ext. 18201; fax: +66 2 2600128.
** Corresponding author. Tel.: +66 2 2185436; fax: +66 2 2185418.
E-mail addresses: dsuchao@gmail.com (S. Donpudsa), kpvr2@yahoo.com (V. Rimphanitchayakit).

http://dx.doi.org/10.1016/j.fsi.2017.07.046
1050-4648/© 2017 Elsevier Ltd. All rights reserved.

region and a WAP domain. The first carcinin-type crustin is found in the shore crab *Carcinus maenas* [4,13,14]. Type II crustins are mostly found in shrimp and contain an additional Gly-rich region, N-terminally upstream of the Cys-rich region. For the type III crustins, the Gly-rich and Cys-rich regions are absent and replaced by a short N-terminal Pro/Arg-rich sequence [4]. The type III crustins are called single WAP domain-containing protein (SWD). Most crustins possess the antimicrobial activity against Gram-positive bacteria whereas the type III crustins also have proteinase inhibitory activity [15,16].

The expression of several crustins, especially type III crustins, is up-regulated by pathogenic infection in crustaceans such as *Homarus gammarus* [17], *Penaeus monodon* [18], *Procambarus clarkii* [19], *Marsupenaeus japonicus* [20] and *Litopenaeus vannamei* [21]. Interestingly, several SWDs exhibit binding property to the bacterial cells, for example *Pc*-SWD in *Procambarus clarkii* [19], *Mj*SWD in *M. japonicus* [20] and *Lv*-SWDi in *L. vannamei* [21]. Moreover, the SWD*Pm*2 in *P. monodon* has an antimicrobial activity against Gram-positive and the proteinase inhibitory activity against subtilisin [18].

In this study, a type III crustin *Lv*SWD from *L. vannamei* identified by Jiménez-Vega et al. [22] was studied. The tissue expression and the expression in response to VP_{AHPND} infection were investigated. The recombinant proteins were prepared for *in vitro* study of their antimicrobial and antiproteinase activities. In addition, the effect of the Pro/Arg-rich region on the activities of the SWD was also investigated. Importantly, the application of *Lv*SWD against the VP_{AHPND} in post larval shrimp was tested.

2. Materials and methods

2.1. Shrimp and VP_{AHPND}

Healthy white shrimp at post-larval stage (PL30-35) for mortality experiment and shrimp with 2–3 g body weight for other experiments were purchased from local farms and acclimatized in aquaria at an ambient temperature of 29 ± 1 °C and a salinity of 20 ppt for at least one week before use in the experiments.

The VP_{AHPND} (Chanthaburi2) was isolated from Chanthaburi Province in the East of Thailand [23]. TheVP_{AHPND} in a glycerol stock was re-streaked on a Tryptic Soy Agar (TSA) plate containing 3% NaCl, and the plate was incubated at 30 °C overnight. A single colony was inoculated into 2 mL Tryptic Soy Broth (TSB) containing 3% NaCl at 30 °C and shaken at 250 rpm overnight. The starter was subsequently diluted 1:200 in TSB and incubated with vigorous shaking at 30 °C until the OD_{600} reached 1.7–2.0 equivalent to a bacterial density of approximately 1×10^9 colony forming units per ml (CFU/mL). The number of colonies was determined by agar plating. The CFU/mL was adjusted before the bacterium suspension was used in the experiment.

2.2. Tissue distribution

The reverse transcription-polymerase chain reaction (RT-PCR) was carried out to investigate the expression profile of *LvSWD* transcripts in six different tissues including hemocytes, hepatopancreas, lymphoid organ, gill, intestine and heart. The tissues were collected from normal shrimp and were extracted for total RNA preparation using a FavorPrep™ Blood/Cultured Cell Total RNA Purification Mini Kit (Favorgen). One microgram of total RNAs was subjected to cDNA preparation using a cDNA First-strand Synthesis Kit (Fermentas) according to the manufacturer's instruction.

Specific primers for *LvSWD*, LvSWD_F1 and LvSWD_R1, was used (Table 1). The PCR amplification was performed in 25 μL reaction volume containing appropriate amount of first-stand cDNA, 500 mM KCl, 15 mM $MgCl_2$, 100 mM Tris–HCl pH 8.3, 1 mg/mL BSA, 100 mM $(NH_4)_2SO_4$, 0.2 mM each dNTP, 0.4 mM of each primer and 1.5 units *Taq* DNA polymerase (RBC Bioscience). The reaction was denatured at 94 °C for 2 min followed by 25 cycles of 94 °C for 30 s, annealing at 60 °C for *LvSWD* or 52 °C for *EF-1α* for 30 s and extension at 72 °C for 30 s and the final extension step at 72 °C for 10 min. The elongation factor 1-α gene (*EF-1α*) was used as an internal control. The amplified products were analyzed with 2.5% agarose gel electrophoresis.

2.3. Semi-quantitative RT-PCR analysis of LvSWD

The expression of *LvSWD* transcript in hemocytes was determined in shrimp infected with VP_{AHPND} using immersion challenge method [24]. Briefly, shrimp were divided into two groups of 15 shrimp each. The infected group was immersion-challenged with 1×10^9 CFU/mL of VP_{AHPND} in sea water and the control group with equivalent volume of TSB medium containing 3% NaCl in sea water. The shrimp hemocytes were collected from three shrimp each at 6, 12, 24, 48 and 72 h post infection (hpi). The hemocytes were extracted for total RNA preparation which was used as a template for the first strand cDNA synthesis using a RevertAid First Strand cDNA Synthesis Kit (Thermo Fisher Scientific). The cDNA samples were used in RT-PCR to examine the expression of *LvSWD* using the primers LvSWD_F1 and LvSWD_R1 (Table 1) compared with that of an internal control *EF-1α*, and the PCR condition as mentioned above.

The amplification was done in triplicate. The band intensity of the PCR products were analyzed using the GeneTool analysis software. The expression of *LvSWD* was reported relative to that of the *EF-1α*. The data were expressed as means ± standard deviations. The statistical significance of the data was evaluated using one-way ANOVA followed by a post hoc test (Duncan's new multiple range test). Significant differences were accepted at $P < 0.05$.

2.4. Construction of the LvSWD expression plasmids

To express the recombinant mature *Lv*SWD (r*Lv*SWD) and WAP domain protein of *Lv*SWD (r*Lv*SWD-WAP), three primers were designed. Two forward primers with 5′ *Nco*I site (underlined) and 6 × His-tag: LvSWD_F2 for r*Lv*SWD and LvSWD-WAP_F for r*Lv*SWD-WAP, and one reverse primer LvSWD_R2 with 5′ *Xho*I site (underlined) for both constructs (Table 1). The *LvSWD* and *LvSWD-WAP* gene fragments were amplified by PCR using the hemocyte cDNAs from normal shrimp as templates.

The PCR reaction was carried out in a final volume of 50 μL containing 1 × PCR buffer, 0.2 mM dNTP, 0.2 mM each primer, 1 × Advantage 2 Polymerase Mix (Clontech Laboratories) and 1 μL of cDNA. The PCR condition was denaturation at 94 °C for 2 min, 5 cycles of 94 °C for 25 s, 62 °C for 45 s and 72 °C for 3 min, 30 cycles of 94 °C for 25 s, 60 °C for 45 s and 67 °C for 3 min, and the final extension step at 67 °C for 10 min. The two gene fragments were cloned into a derivative of pET-32a(+) expression vector pVR500 [25]. The correct DNA sequences in the expression clones were confirmed by DNA sequencing by Macrogen Inc., South Korea.

2.5. Expression and purification of the recombinant proteins

The recombinant plasmids were transformed into an *Escherichia coli* NiCo21(DE3) for over-production of the r*Lv*SWD and the r*Lv*SWD-WAP proteins. The transformants were cultured in LB broth until the A_{600} reached 0.6. The expression was induced by adding IPTG to the final concentration of 1 mM and the culture was continued for 4 h. The cells were harvested by centrifugation, resuspended in phosphate-buffered saline pH 7.4 (PBS) and

Table 1
Primers used in this study.

Primer	Sequence (5′–3′)	Product size (bp)	Usage
LvSWD_F1	TGGTCAGCGTCAAGGAGGTT	197	RT-PCR of *LvSWD*
LvSWD_R1	GCACTGACTGTCCGACAAG		
EF-1α_F	GGTGCTGGACAAGCTGAAGGC	150	
EF-1α_R	CGTTCCGGTGATCATGTTCTTGA		
LvSWD_F2	TTAACCATGGGCCATCATCATCATCATGTTCCGACGAGACACAGTC	250	Expression of *Lv*SWD
LvSWD-WAP_F	TTAACCATGGGCCATCATCATCATCATCAT TGCCCAGATACGAGCGAC	196	Expression of *Lv*SWD-WAP
LvSWD_R2	ATATCTCGAGTTACCTTCTTCCGTTTCCG	–	Reversed primer for LvSWD_F and LvSWD-WAP_F

sonicated to break the cells. The cell lysate was collected by centrifugation at 5000 rpm for 15 min at 4 °C. The recombinant proteins were purified using a Ni-NTA agarose column, dialyzed against 1 × PBS pH 7.4 and analyzed by sodium dodecyl sulfate polyacrylamide gel electrophoresis (SDS-PAGE) [26]. The concentration of protein was determined by the Bradford method [27]. The recombinant thioredoxin (Trx) was over-expressed by the same above procedure from an expression vector pET-32a(+) and used as a control protein in the experiments described below.

2.6. Serine proteinase inhibition assay

The inhibitory activity of r*Lv*SWD and r*Lv*SWD-WAP upon the serine proteinases, trypsin (bovine pancreas, Sigma), α-chymotrypsin (bovine pancreas, Sigma), subtilisin Carlsberg (*Bacillus licheniformis*, Sigma) and elastase (porcine pancreas, Pacific Science) were investigated using a procedure of Hergenhahn et al. [28].

The reaction mixture consisted of 50 mM Tris–HCl pH 8; 146 μM of *N*-benzoyl–Phe–Val–Arg–*p*-nitroanilide (Sigma) for trypsin, 886 μM of *N*-succinyl–Ala–Ala–Ala–*p*-nitroanilide (Sigma) for elastase and 147 μM of *N*-succinyl–Ala–Ala–Pro–Phe–*p*-nitroanilide for chymotrypsin and subtilisin; and 0.04, 0.04, 0.04 and 0.08 μM of subtilisin, chymotrypsin, trypsin and elastase in a total volume of 100 μL. The final concentrations of r*Lv*SWD and r*Lv*SWD-WAP in the reaction mixtures are listed in Table 2. The reaction was incubated at 30 °C for 15 min and then terminated by adding 50 μL of 50% acetic acid. The absorbance of *p*-nitroaniline formed was measured at 405 nm. The percentages of remaining activity were calculated and plotted against the molar ratios of the inhibitor to proteinase. The Trx was used as the control protein.

2.7. Kinetic of serine proteinase inhibition

The inhibition constant (K_i) assay of r*Lv*SWD was performed following the method described by Visetnan et al. [29]. The experiment was composed of four sets of reactions for 0, 10, 20 and 40 nM of r*Lv*SWD. Each set consisted of 0, 0.38, 0.75, 1.50 and 3.00 mM of *N*-succinyl–Ala–Ala–Pro–Phe–*p*-nitroanilide in the presence of 40 nM of subtilisin. The reactions were performed according to the above procedure. The amount of *p*-nitroaniline was calculated using a millimolar extinction coefficient of 9.96. The activity was calculated as nmole of *p*-nitroaniline/min and was plotted against the concentrations of substrates as substrate saturation curve and a Lineweaver–Burk plot. The apparent K_Ms at different concentrations of inhibitor and V_{max} were determined. The apparent K_Ms were re-plotted against the concentrations of proteinase inhibitor. The latter was constructed for the calculation of K_i.

2.8. Antimicrobial assay

The antimicrobial activity of r*Lv*SWD and r*Lv*SWD-WAP was investigated using liquid growth inhibition test [30]. Three Gram-positive bacteria: *Staphylococcus aureus*, *Bacillus megaterium* and *Micrococcus luteus*, and four Gram-negative bacteria: *E. coli* 363, *V. harveyi* 639, *V. parahaemolyticus* and VP_{AHPND}, were tested. The antimicrobial activity was determined as the minimal inhibitory concentration (MIC), the lowest concentration that caused 100% inhibition of bacterial growth.

The bacterial strains were inoculated into LB medium and grown overnight at 30 or 37 °C according to the strains with shaking as starters. The starters were diluted 1:100 and cultured until the OD_{600} was about 0.2. Bacteria were further diluted with LB medium to an OD_{600} of 0.001. The two-fold serial dilutions of r*Lv*SWD, r*Lv*SWD-WAP and Trx proteins from 50.00 μM to 0.10 μM (0.10, 0.20, 0.39, 0.78, 1.56, 3.13, 6.25, 12.50, 25.00 and 50.00 μM) and other concentrations (10, 20 and 30 μM) were made with 1 × PBS pH 7.4 and 100 μL were added into the wells of a 96-well microtiter plate. Twenty microliters of each inoculate were added to each corresponding wells of a 96-well microtiter plate. The negative control was 100 μL of 1 × PBS pH 7.4 with 20 μL of each inoculate. Cultures were grown at 30 or 37 °C for an overnight under vigorous shaking. The growth of bacteria was evaluated by measuring the OD_{600}. The two-fold serial dilutions of ampicillin and chloramphenicol were used as control.

The minimum bactericidal concentration (MBC) was tested to study the killing effect of r*Lv*SWD on VP_{AHPND} and *B. megaterium*. The MBC is defined as the lowest concentration of r*Lv*SWD needed to kill 99.9% of the inoculums. This is an extension of the MIC procedure to verify whether the MIC is bactericidal concentration by using agar plating. The cultures were taken from the wells of microtiter plates at the MIC with no visible growth and 10-fold serially diluted with 0.85% NaCl. One hundred microliters of each dilution were spread onto the TSA plates containing 3% NaCl and the plates were incubated at 30 °C overnight. The MBC of each

Table 2
The final concentrations of r*Lv*SWD and r*Lv*SWD-WAP in the inhibition assay reactions.

	Concentration of inhibitor (μM) in the reactions			
	Subtilisin reaction	Elastase reaction	Trypsin reaction	Chymotrypsin reaction
r*Lv*SWD	0, 0.006, 0.013, 0.025, 0.050, 0.100, 0.200, 0.400	0, 0.50, 1.00, 2.00, 4.00	0, 0.50, 1.00, 2.00	0, 0.50, 1.00, 2.00
r*Lv*SWD-WAP	0, 0.009, 0.019, 0.038, 0.075, 0.150, 0.300, 0.600	0, 0.60, 1.20, 2.40, 4.80	0, 0.60, 1.20, 2.40	0, 0.60, 1.20, 2.40

cultures were done in triplicate. The microbial growth or no growth was observed. The ampicillin and chloramphenicol were used as the control bactericidal and bacteriostatic antibiotics, respectively.

2.9. Effect of rLvSWD on mortality assay of VP_{AHPND} infection

To test the potential application of r*Lv*SWD in defense against VP_{AHPND}, post-larva shrimp were divided into 8 groups of 10 shrimp. They were immersed in different solutions or bacterial suspensions. Before immersion, the bacterial suspensions, 1×10^9 CFU/mL of VP_{AHPND}, were treated with 120 μM of r*Lv*SWD, 120 μM of r*Lv*SWD-WAP or 120 μM of Trx at room temperature for 1 h. After that, the bacterial suspensions were added directly into an experimental tank containing 150 mL of fresh sea water for 30 min. Then, the two groups of post-larva white shrimp were transferred into the experimental tank. Similarly, shrimp in the five control groups were immersed in 1 × PBS, 120 μM of r*Lv*SWD, 120 μM of r*Lv*SWD-WAP, 120 μM of Trx and 1×10^9 CFU/mL of VP_{AHPND}. The shrimp mortality rate was observed every 3 hpi up to 108 hpi. The VP_{AHPND} used had the LD_{50} of 33 h. This experiment was performed in triplicate. Data were analyzed using GraphPad Sigma Plot, and presented as Kaplan-Meier survival plots with the *P* values calculated by log-rank test.

3. Results

3.1. Tissue distribution of LvSWD

In this study, six tissues: gill, hepatopancreas, heart, intestine, hemocytes and lymphoid organ, were tested by using RT-PCR. The result showed that the *LvSWD* was expressed in all tissues tested, mainly in hemocytes and much less in hepatopancreas and lymphoid organ (Fig. 1).

3.2. Expression of LvSWD in response to VP_{AHPND} challenge

In this experiment, the r*Lv*SWD was tested against the VP_{AHPND} which was a causative agent of AHPND in shrimp [31]. The expression profile of *LvSWD* after VP_{AHPND} challenge was first investigated. The white shrimp were challenged by immersing them into the rearing water with VP_{AHPND}. At suitable time points, the hemolymph was collected from the shrimp and processed for the RT-PCR. It was observed that the expression of *LvSWD* was up-regulated in an early phase of bacterial infection and then returned to non-stimulated level at 24 h. However, at 48 and 72 hpi, the expression of *LvSWD* was dramatically decreased to below the normal levels (Fig. 2).

3.3. Over-expression of LvSWD and LvSWD-WAP

To study the activity of *Lv*SWD and *Lv*SWD-WAP proteins from *L. vannamei*, the *LvSWD* gene sequence from the GenBank database

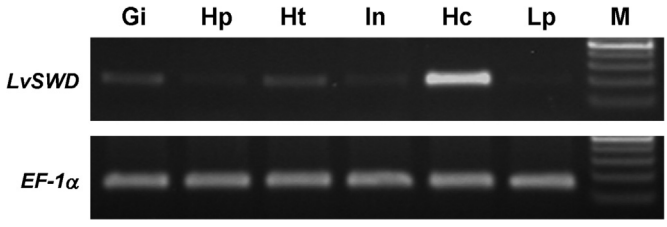


Fig. 1. Expression of *LvSWD* in different tissues of normal white shrimp. The tissues: gill (Gi), hepatopancreas (Hp), heart (Ht), intestine (In), hemocytes (Hc) and lymphoid organ (Lp), were collected from normal white shrimp and processed for RT-PCR analysis of *LvSWD* expression. The *EF-1α* was used as control. M is DNA size marker.

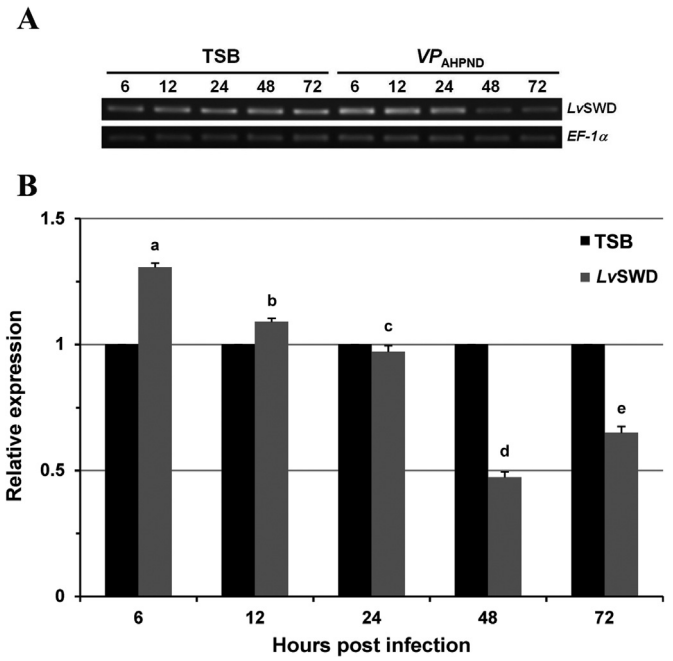


Fig. 2. The relative transcription levels of *LvSWD* in the hemocytes of VP_{AHPND}-infected shrimp. At 6, 12, 24, 48 and 72 h after bacterial infection, the shrimp hemocytes were collected and processed for the RT-PCR analysis of *LvSWD* expression. The immersion by adding TSB was done as a control. The amplified products were analyzed with 2.5% agarose gel electrophoresis (A). The *LvSWD* expression in infected shrimp was calculated relative to that of the control shrimp (B). The expression of *LvSWD* of the control shrimp at each time point was presented for comparison. The *EF-1α* was used as an internal control. Data are presented as means ± standard deviations. The letters indicate significant differences accepted at $P < 0.05$.

(GenBank number AY465833) was retrieved for the design of specific primer pairs [22]. The two gene fragments of the *LvSWD* gene, the *LvSWD* encoding for the mature protein and the *LvSWD-WAP* encoding only the WAP domain, were amplified from the hemocyte cDNAs of normal *L. vannamei* shrimp (Fig. 3). The gene fragments were cloned into a derivative of pET-32a(+) expression vector pVR500 [25] and sequenced to verify the correct sequences. In these constructs, the *LvSWD* and *LvSWD-WAP* sequences were fused 3′ to the thioredoxin gene. From the nucleotide sequences of the expression clones, the predicted molecular weights of r*Lv*SWD and r*Lv*SWD-WAP were 21.2 and 19.1 kDa, respectively.

The r*Lv*SWD and r*Lv*SWD-WAP were over-expressed in an *E. coli* expression system using an *E. coli* NiCo21(DE3). The transformants were cultured and the expression is induced by adding IPTG. The cells were collected by centrifugation and lysed by sonication. SDS-PAGE analysis showed that the two proteins were expressed as soluble proteins of about 22 and 20 kDa (Fig. 4).

3.4. Serine proteinase inhibitory assay and its kinetics

It is known that the type III crustin possesses an antiproteinase activity [18]. Thus, the two recombinant proteins, r*Lv*SWD and r*Lv*SWD-WAP were tested for their serine proteinase inhibitory activity against trypsin, α-chymotrypsin, subtilisin Carlsberg and elastase at various mole ratios of inhibitors to proteinases. The results showed that the r*Lv*SWD and the r*Lv*SWD-WAP exhibited strong inhibition against subtilisin, about 90% inhibition at mole ratio about two (Fig. 5 A). They did not inhibit trypsin, α-chymotrypsin and elastase (data not shown).

The kinetic parameters of subtilisin inhibition by the r*Lv*SWD were further determined. Four different concentrations of the

Signal sequence

```
ATGGTCAGCGTCAAGGAGGTTCTGGTCGTGTTGGTCTTGGTGGCCGCTGTGGCCGTCTCC   60
M  V  S  V  K  E  V  L  V  V  L  V  L  V  A  A  V  A  V  S
```

Pro-Arg rich region

```
CCCGCCGATGCTGTTCCGACGAGACACAGTCGGCCCCGTCCCCAGCCCAGGCCCCGGCCG   120
P  A  D  A  V  P  T  R  H  S  R  P  R  P  Q  P  R  P  R  P

GGCACGTGCCCAGATACGAGCGACGTCATCGGCCCCTGCGTCATCACGGAGAGGAACTGC   180
G  T  C  P  D  T  S  D  V  I  G  P  C  V  I  T  E  R  N  C
```

Whey acidic protein domain (WAP)

```
TTGTCGGACAGTCAGTGCGCACCCGGCCAGAAGTGCTGTCCGATCGGCTGCGGCAGAGAG   240
L  S  D  S  Q  C  A  P  G  Q  K  C  C  P  I  G  C  G  R  E

TGCCTGGCTGTAGGTCCTCCTTACGGAAACGGAAGAAGGTAA   282
C  L  A  V  G  P  P  Y  G  N  G  R  R  *
```

Fig. 3. The DNA sequence of *LvSWD* and its deduced amino acid sequence. The signal peptide is underlined. The Pro-Arg rich region is shaded blue. The WAP domain is double underlined. The latter is cloned as *LvSWD-WAP*. (For interpretation of the references to colour in this figure legend, the reader is referred to the web version of this article.)

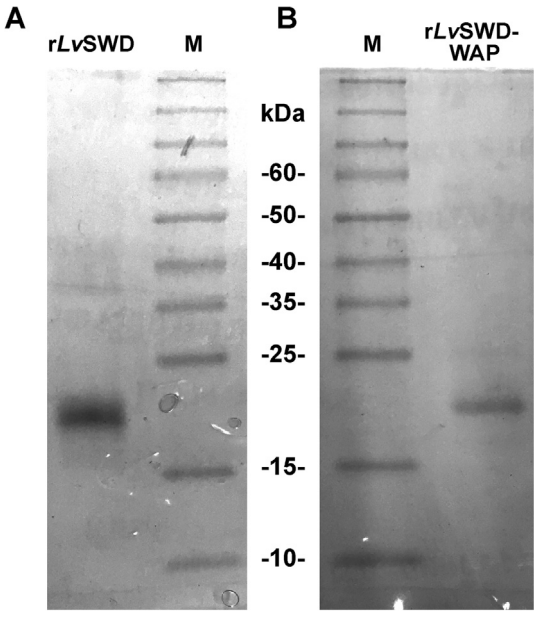


Fig. 4. SDS-PAGE analysis of purified r*Lv*SWD (A) and r*Lv*SWD-WAP (B). The over-expressed proteins were purified by Ni-NTA agarose column and analyzed by SDS-PAGE. Lane M is a protein size marker.

r*Lv*SWD were tested against a fixed concentration of subtilisin in the presence of different substrate concentrations. The Lineweaver-Burk plots were constructed. It was found that the inhibition was a competitive-type inhibition for subtilisin. The V_{max}, K_M and K_i were 5.22 nmol/min, 3.01 mM and 14.3 nM, respectively (Fig. 5 B).

3.5. Antimicrobial activity

It is also known that the type III crustin possesses antimicrobial activity. The antimicrobial activity of r*Lv*SWD or r*Lv*SWD-WAP was investigated by using the liquid growth inhibition test. Both Gram-positive and Gram-negative bacteria were tested. The bacteria were grown in the presence of various serially diluted amounts of the r*Lv*SWD or the r*Lv*SWD-WAP. The highest concentration used that the cells still grew and the lowest concentration that inhibited the growth completely were recorded. As shown in Table 3, the r*Lv*SWD was active against Gram-negative bacteria with the MIC values around 25–50 μM which was a little better than the Gram-positive bacteria with the MIC values 30–50 μM. The VP_{AHPND} seemed to be more sensitive to the r*Lv*SWD; the MIC value was only 20–30 μM.

For r*Lv*SWD-WAP, no antimicrobial activity was observed against both Gram-positive and Gram-negative bacteria (Table 3). This experiment had shown that the antimicrobial activity did not reside in the WAP domain. It could not be ruled out, however, that the N-terminal moiety and the WAP domain were both required for this activity.

The sensitivity of *B. megaterium* and VP_{AHPND} to antibiotics, ampicillin and chloramphenicol, was also tested. The MICs for *B. megaterium* were 90–180 and 6.25–12.50 μM of ampicillin and chloramphenicol, respectively. Those for VP_{AHPND} were 22.5–45.0 and 0.78–1.56 μM, respectively. Interestingly, the antimicrobial activity of r*Lv*SWD upon VP_{AHPND} was comparable to that of ampicillin (Table 3).

3.6. Minimum bactericidal concentration test

The results above indicated that the r*Lv*SWD could inhibit the growth of bacteria, particularly the shrimp pathogen, VP_{AHPND}. The Minimal Bactericidal Concentration (MBC) assay was, therefore, performed to verify whether the MIC of r*Lv*SWD was lethal to the target bacteria *in vitro*. A Gram-positive bacterium, *B. megaterium*, and a Gram-negative shrimp pathogen, VP_{AHPND} were tested. By using agar plate count method following the MIC test results, the cultures at the MIC were plated and examined for the colonies. The results in Fig. 6 revealed that the r*Lv*SWD at MIC killed the VP_{AHPND} (Fig. 6 B) for there were no colony observed but not the *B. megaterium* (Fig. 6 E). As expected from the MIC results in Table 3, the r*Lv*SWD-WAP had no antimicrobial activities and did not kill both *B. megaterium* and VP_{AHPND} (Fig. 6 C and F) as compared to the controls (Fig. 6 A and D). Therefore, the MIC of *Lv*SWD was the MBC for VP_{AHPND}.

Both bacteria were also tested with ampicillin and chloramphenicol as control for bactericidal and bacteriostatic activities (Fig. 6 lower panel).

3.7. Effect of rLvSWD and rLvSWD-WAP on the survival rate of post-larval stage shrimp against VP_{AHPND} infection

Post-larva white shrimp were selected for these experiments for

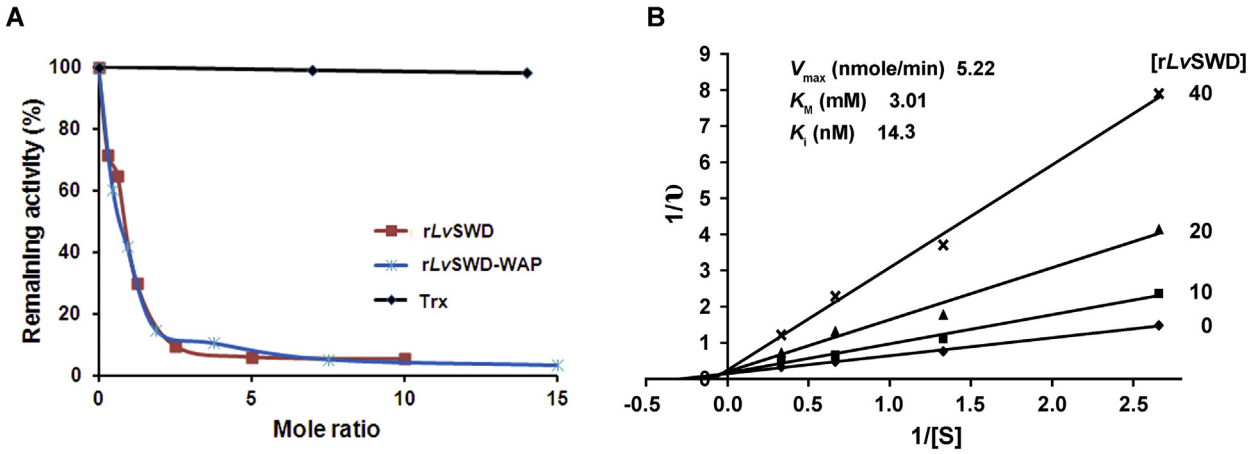


Fig. 5. Proteinase inhibition and kinetic studies. (A) Proteinase inhibition assay of the r*Lv*SWD, the r*Lv*SWD-WAP or the Trx at various mole ratios against subtilisin. (B) The Lineweaver–Burg plot of inhibitory reactions of r*Lv*SWD against subtilisin. The calculated V_{max}, K_M and K_i are shown.

Table 3
Antimicrobial activities of the r*Lv*SWD, r*Lv*SWD-WAP and Trx against Gram-positive and Gram-negative bacteria determined by liquid growth inhibition assay as MIC values. The ampicillin and chloramphenicol were only tested with *B. megaterium* and VP_{AHPND}.

Microorganism	MIC (μM)		
	r*Lv*SWD	r*Lv*SWD-WAP	Trx
Gram-positive bacteria			
Staphylococcus aureus	30–50	na	na
Bacillus megaterium	30–50	na	na
Micrococcus luteus	>50	na	na
Gram-negative bacteria			
Escherichia coli 363	25–50	na	na
Vibrio harveyi 639	25–30	na	na
Vibrio parahaemolyticus	30–50	na	na
VP_{AHPND}	20–30	na	na
	Ampicillin	Chloramphenicol	
Bacillus megaterium	90–180	6.25–12.50	
VP_{AHPND}	22.5–45.0	0.78–1.56	

MIC is expressed as the interval a–b, where "a" is the highest concentration tested at which microorganisms are still growing and "b" is the lowest concentration that causes 100% growth inhibition. The "na" means "not active up to 50 μM".

they were more prone to be infected by VP_{AHPND} than the juvenile shrimp. Knowing that the r*Lv*SWD efficiently inhibited the growth of VP_{AHPND}, we would like to know whether the infection in post-larval shrimp could be alleviated by the application of *Lv*SWD.

In this experiment, the shrimp were immersed into the rearing water containing four times the MIC of r*Lv*SWD or r*Lv*SWD-WAP at the same concentration and VP_{AHPND} and the mortality was recorded. It was observed that without VP_{AHPND} infection, shrimp in the control groups, shrimp immerged in PBS, r*Lv*SWD and r*Lv*SWD-WAP, were not dead. In the presence of VP_{AHPND} with or without the r*Lv*SWD-WAP, the survival rate of infected shrimp at 50% was about 36 h. When the r*Lv*SWD was included along with the VP_{AHPND}, the survival rate was prolonged with the 50% survival rate at about 78 h (Fig. 7). Therefore, the r*Lv*SWD could help the post-larval white shrimp fight the infection and survived longer.

4. Discussion

The *Lv*SWD is a type III crustin from *L. vannamei* which contains a WAP domain at its C-terminal half and a short N-terminal Pro/Arg-rich sequence. Jiménez-Vega et al. (2004) reported that the *LvSWD* was expressed in the hemocytes and its expression was changed in response to *V. alginolyticus* infection suggesting that it had a role in immune response of shrimp [22]. It was later shown that a variant *Lv*SWDi possessed antiproteinase activity against *B. subtilis* secretory proteinases and directly binds to Gram-positive and Gram-negative bacteria [21]. Therefore, its expression was up-regulated after *V. anguillarum* infection [21]. The amino acid identity between *Lv*SWD and *Lv*SWDi was about 81.9%. We further carried out the study of *Lv*SWD. The activities of WAP domain whether they were antimicrobial or antiproteinase or both were investigated as well as the expression of *Lv*SWD in tissues. In this study, we characterized a single WAP domain-containing protein (*Lv*SWD) from the Pacific white shrimp *L. vannamei*. We explored its expression patterns in tissues and upon bacterial infection, its functional characteristics in proteinase inhibition and its bacterial killing activity.

Jiménez-Vega et al. (2004) had shown that the *LvSWD* was mainly expressed in the hemocytes but not hepatopancreas by using Northern blot hybridization [22]. The tissue distribution of *Lv*SWD in healthy white shrimp revealed that the *Lv*SWD was expressed in all tissues tested and mainly expressed in hemocytes and much less expressed in hepatopancreas and lymphoid organ. This expression profile is similar to those of the SWD*Pm*2 from *P. monodon* [18], *Lv*SWD from *L. vannamei* [22] and *Fc*-SWD from *F. chinensis* [32], but is different to that of the *Mj*SWD from *M. japonicus* in which the highest expression is in gill and stomach [20].

The SWDs are presumed to be involved in immune responses against microbial infection by several expression studies. The expression of *LvSWD* from *L. vannamei* is demonstrated by Jimenez-Vaga et al. (2004) to respond to *V. alginolyticus* infection in an early phase (3 and 6 h) of infection [22]. The similar double WAP domain protein gene *PmDWD* in *P. monodon* is up-regulated after *V. harveyi* infection [33]. Like the *Lv*SWD, the *Lv*SWDi from *L. vannamei* is up-regulated after *V. anguillarum* infection [21]. A similar expression profile of *Es-DWD1* has been observed in the Chinese mitten crab *Eriocheir sinensis*. It is up-regulated in hemocytes post-challenge with pathogen-associated molecular patterns (PAMPs) [34]. In addition, the *PmSWD1* and *PmSWD2* transcripts are increased after 6 h of WSSV infection [18]. In our study, the expression of *LvSWD* is significantly increased at 6 h after challenging with a Gram-negative bacteria VP_{AHPND} before returning back to normal expression level at 24 h and down-regulated at 48 and 72 h post infection. This result suggests that, like other WAP-containing proteins mentioned above, the *Lv*SWD is involved in immune responses.

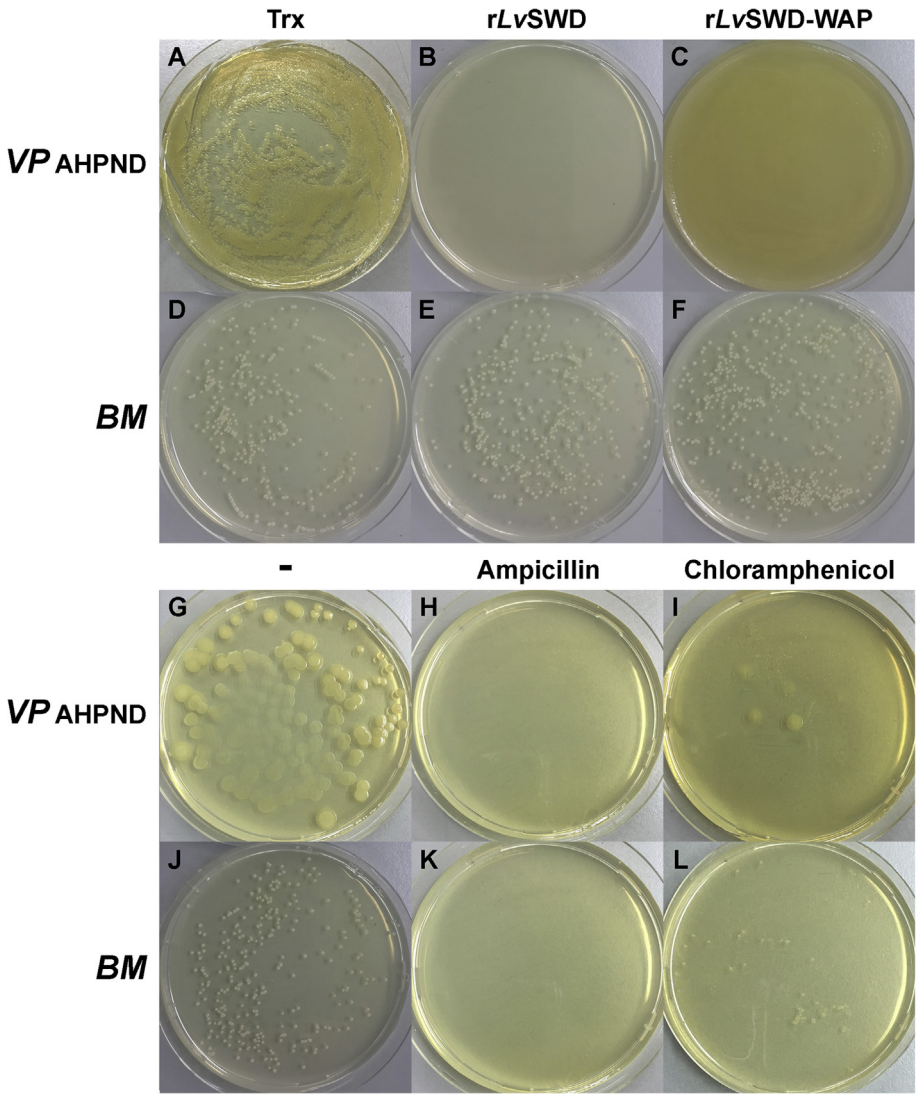


Fig. 6. Minimum bactericidal concentration tests of r*Lv*SWD (B and E) and r*Lv*SWD-WAP (C and F) against *B. megaterium* (*BM*) and VP_{AHPND} examined by agar plate count method (upper panel). The same concentration of Trx protein (A and D) was used as controls. The bacteria in plate C is uncountable for the bacteria covers the whole area of the agar surface. The ampicillin (H and K) and chloramphenicol (I and L) were used as bactericidal and bacteriostatic antibiotics (lower panel). The controls "-" (G and J) were not added r*Lv*SWD and r*Lv*SWD-WAP.

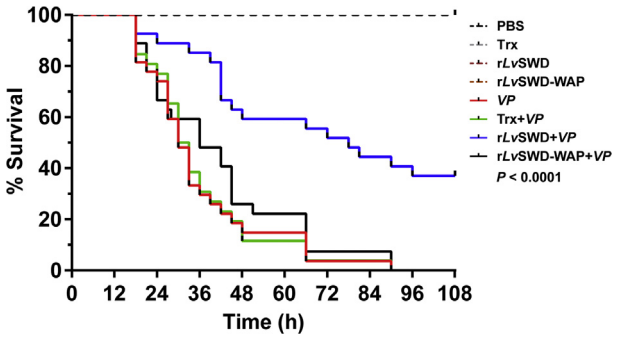


Fig. 7. The Kaplan-Meier survival plots ofVP_{AHPND} -infected shrimp. The post-larva shrimp were infected by immerging in PBS, Trx, r*Lv*SWD with or without VP_{AHPND}, r*Lv*SWD-WAP with or without the bacteria and the mortality was observed. The *P* value indicated was calculated by log-rank test in the GraphPad Sigma Plot.

The antimicrobial activity of type III crustins has been reported in several shrimp species. The *Fc*SWD exhibits antimicrobial activity against Gram-positive and Gram-negative bacteria and fungi [32]. The purified recombinant *Pm*SWD2 possesses antimicrobial activity against both Gram-positive and Gram-negative bacteria [18] whereas the type I crustin*Pm*1 exhibits antimicrobial activity against only Gram-positive bacteria [35]. Another isoform of SWD protein from *L. vannamei*, named *Lv*SWDi, directly binds to Gram-positive and Gram-negative bacteria [21].

The r*Lv*SWD and the r*Lv*SWD-WAP were characterized for antimicrobial and antiproteinase activities. The two recombinant proteins strongly inhibit subtilisin but not trypsin, α-chymotrypsin and elastase. For antimicrobial activity, only the r*Lv*SWD inhibits the growth of Gram-negative bacteria at MIC values of 25–50 μM and displays slightly lower activity against Gram-positive bacteria. The r*Lv*SWD-WAP, however, has no antimicrobial activity against both Gram-positive and Gram-negative bacteria. These activities are similar to those of *Fc*-SWD (for the full-length protein including the signal peptide), m*Fc*-SWD (for the mature protein) and *Fc*-WAPD (for the single WAP domain) from the fleshy prawn *F. chinensis*. The recombinant *Fc*-SWD and the m*Fc*-SWD have antimicrobial activities against Gram-positive and Gram-negative

bacteria and fungi, as well as a strong inhibitory activity against subtilisin A and proteinase K. The *Fc*-WAPD has anti-proteinase activities and negligible antimicrobial activity [32]. The r*Lv*SWD is particularly good in inhibiting the growth of shrimp pathogen VP_{AHPND} and the inhibition is tested by MBC to be bactericidal. On the other hands, the result shows that the r*Lv*SWD has bacteriostatic affect on Gram-positive bacteria.

If the r*Lv*SWD is capable of inhibiting the VP_{AHPND} infectivity, it should be able to reduce the mortality rate of the VP_{AHPND}-infected shrimp. The survival rate assay was carried outusing the post-larval shrimp to investigate the survival of shrimp immerged with a mixture of VP_{AHPND} and r*Lv*SWD protein. Without the r*Lv*SWD protein, the shrimp were more susceptible to VP_{AHPND} infection. The antimicrobial activity of *Lv*SWD against the VP_{AHPND} infection suggests its potential application for disease control in aquaculture. Nevertheless, the mechanism of *Lv*SWD in killing the VP_{AHPND} remains to be investigated further.

Acknowledgments

This project was supported by the Rachadapisek Sompote Fund for Postdoctoral Fellowship Chulalongkorn University to S. Visetnan, and the matching fund from the Thailand Research Fund and the Srinakharinwirot University (Grant No. TRG5880153) to S. Donpudsa. We also thank the TRF Senior Research Scholar (No. RTA5880004), Thailand Research Fund and the support under the Ratchadapisek Somphot Endowment to the Center of Excellence for Molecular Biology and Genomics of Shrimp. We acknowledge the support of equipment used in this study under JST-JICA joint program “Science and Technology Research Partnership for Sustainable Development, SATREPS”.

References

[1] S. Iwanaga, B.L. Lee, Recent advances in the innate immunity of invertebrate animals, J. Biochem. Mol. Biol. 38 (2005) 128–150.
[2] K.S. Zänker, in: Immunology of Invertebrates: Humoral, eLS. John Wiley & Sons Ltd, Chichester, 2010, http://dx.doi.org/10.1002/9780470015902.a0000522.pub2.
[3] A. Tassanakajon, K. Somboonwiwat, P. Supungul, S. Tang, Discovery of immune molecules and their crucial functions in shrimp immunity, Fish. Shellfish Immunol. 34 (2013) 954–967.
[4] V.J. Smith, J.M.O. Fernandes, G.D. Kemp, C. Hauton, Crustins: enigmatic WAP domain-containing antibacterial proteins from crustaceans, Dev. Comp. Immunol. 32 (2008) 758–772.
[5] T.C. Bartlett, B.J. Cuthbertson, E.F. Shepard, R.W. Chapman, P.S. Gross, G.W. Warr, Crustins, homologues of an 11.5-kDa antibacterial peptide, from two species of penaeid shrimp, *Litopenaeus vannamei* and *Litopenaeus setiferus*, Mar. Biotechnol. 4 (2002) 278–293.
[6] P. Jiravanichpaisal, S.Y. Lee, Y.A. Kim, T. Andrén, I. Söderhäll, Antibacterial peptides in hemocytes and hematopoietic tissue from freshwater crayfish *Pacifastacus leniusculus*: characterization and expression pattern, Dev. Comp. Immunol. 31 (2007) 441–455.
[7] A. Tassanakajon, P. Amparyup, K. Somboonwiwat, P. Supungul, Cationic antimicrobial peptides in penaeid shrimp, Mar. Biotechnol. 13 (2011) 639–657.
[8] M.G. Grütter, G. Fendrich, R. Huber, W. Bode, The 2.5 Å X-ray crystal structure of the acid-stable proteinase inhibitor from human mucous secretions analysed in its complex with bovine alpha-chymotrypsin, EMBO J. 7 (1988) 345–351.
[9] M. Tsunemi, Y. Matsuura, S. Sakakibara, Y. Katsube, Crystallization of a complex between an elastase-specific inhibitor elafin and porcine pancreatic elastase, J. Mol. Biol. 232 (1993) 310–311.
[10] J.M. Sallenave, The role of secretory leukocyte proteinase inhibitor and elafin (elastase-specific inhibitor/skin-derived antileukoprotease) as alarm antiproteinases in inflammatory lung disease, Respir. Res. 1 (2000) 87–92.
[11] O. Wiedow, J. Harder, J. Bartels, V. Streit, E. Christophers, Antileukoprotease in human skin: an antibiotic peptide constitutively produced by keratinocytes, Biochem. Biophys. Res. Commun. 248 (1998) 904–909.
[12] D.C. Shugars, Endogenous mucosal antiviral factors of the oral cavity, J. Infect. Dis. 179 (Suppl. 3) (1999) S431–S435.
[13] J.M. Relf, J.R. Chisholm, G.D. Kemp, V.J. Smith, Purification and characterization of a cysteine-rich 11.5-kDa antibacterial protein from the granular haemocytes of the shore crab, *Carcinus maenas*, Eur. J. Biochem. 264 (1999) 350–357.
[14] V. Brockton, J.A. Hammond, V.J. Smith, Gene characterisation, isoforms and recombinant expression of carcinin, an antibacterial protein from the shore crab, *Carcinus maenas*, Mol. Immunol. 44 (2007) 943–949.
[15] V.J. Smith, Phylogeny of whey acidic protein (WAP) four-disulfide core proteins and their role in lower vertebrates and invertebrates, Biochem. Soc. Trans. 39 (2011) 1403–1408.
[16] S. Donpudsa, V. Rimphanitchayakit, A. Tassanakajon, I. Söderhäll, K. Söderhäll, Characterization of two crustin antimicrobial peptides from the freshwater crayfish *Pacifastacus leniusculus*, J. Invertebr. Pathol. 104 (2010) 234–238.
[17] C. Hauton, V. Brockton, V.J. Smith, Cloning of a crustin-like, single whey-acidic-domain, antibacterial peptide from the haemocytes of the European lobster, *Homarus gammarus*, and its response to infection with bacteria, Mol. Immunol. 43 (2006) 1490–1496.
[18] P. Amparyup, S. Donpudsa, A. Tassanakajon, Shrimp single WAP domain (SWD)-containing protein exhibits proteinase inhibitory and antimicrobial activities, Dev. Comp. Immunol. 32 (2008) 1497–1509.
[19] Z.Q. Du, X.C. Li, Z.H. Wang, X.F. Zhao, J.X. Wang, A single WAP domain (SWD)-containing protein with antipathogenic relevance in red swamp crayfish, *Procambarus clarkii*, Fish. Shellfish Immunol. 28 (2010) 134–142.
[20] H.S. Jiang, C. Sun, T. Wang, X.F. Zhao, J.X. Wang, A single whey acidic protein domain containing protein (SWD) inhibits bacteria invasion and dissemination in shrimp *Marsupenaeus japonicus*, Fish. Shellfish Immunol. 35 (2013) 310–318.
[21] Z.Q. Du, J.J. Yuan, D.M. Ren, A novel single WAP domain-containing protein isoform with antibacterial relevance in *Litopenaeus vannamei*, Fish. Shellfish Immunol. 44 (2015) 478–484.
[22] F. Jiménez-Vega, G. Yepiz-Plascencia, K. Söderhäll, F. Vargas-Albores, A single WAP domain-containing protein from *Litopenaeus vannamei* hemocytes, Biochem. Biophys. Res. Commun. 314 (2004) 681–687.
[23] P. Supungul, P. Jaree, K. Somboonwiwat, W. Junprung, P. Proespraiwong, R. Mavichak, A. Tassanakajon, A potential application of shrimp anti-lipopolysaccharide factor in disease control in aquaculture, Aquac. Res. 48 (2017) 809–821.
[24] L. Tran, L. Nunan, R.M. Redman, L.L. Mohney, C.R. Pantoja, K. Fitzsimmons, D.V. Lightner, Determination of the infectious nature of the agent of acute hepatopancreatic necrosis syndrome affecting penaeid shrimp, Dis. Aquat. Organ 105 (2013) 45–55.
[25] S. Donpudsa, A. Tassanakajon, V. Rimphanitchayakit, Domain inhibitory and bacteriostatic activities of the five-domain Kazal-type serine proteinase inhibitor from black tiger shrimp *Penaeus monodon*, Dev. Comp. Immunol. 33 (2009) 481–488.
[26] U.K. Laemmli, Cleavage of structural proteins during the assembly of the head of bacteriophage T4, Nature 227 (1970) 680–685.
[27] M.M. Bradford, A rapid and sensitive method for the quantitation of microgram quantities of protein utilizing the principle of protein-dye binding, Anal. Biochem. 72 (1976) 248–254.
[28] H.G. Hergenhahn, A. Aspan, K. Söderhäll, Purification and characterizationof a high-Mr proteinase inhibitor of pro-phenol oxidase activation from crayfish plasma, Biochem. J. 248 (1987) 223–228.
[29] S. Visetnan, S. Donpudsa, P. Supungul, A. Tassanakajon, V. Rimphanitchayakit, Kazal-type serine proteinase inhibitors from the black tiger shrimp *Penaeus monodon* and the inhibitory activities of SPI*Pm*4 and 5, Fish. Shellfish Immunol. 27 (2009) 266–274.
[30] S.A. Patat, R.B. Carnegie, C. Kingsbury, P.S. Gross, R. Chapman, K.L. Schey, Antimicrobial activity of histones from hemocytes of the Pacific white shrimp, Eur. J. Biochem. 271 (2004) 4825–4833.
[31] R. Sirikharin, S. Taengchaiyaphum, P. Sanguanrut, T.D. Chi, R. Mavichak, P. Proespraiwong, B. Nuangsaeng, S. Thitamadee, T.W. Flegel, K. Sritunyalucksana, Characterization and PCR detection of binary, pir-like toxins from *Vibrio parahaemolyticus* isolates that cause acute hepatopancreatic necrosis disease (AHPND) in shrimp, PLoS One 10 (2015) e0126987.
[32] Y.P. Jia, Y.D. Sun, Z.H. Wang, Q. Wang, X.W. Wang, X.F. Zhao, J.X. Wang, A single whey acidic protein domain (SWD)-containing peptide from fleshy prawn with antimicrobial and proteinase inhibitory activities, Aquaculture 284 (2008) 246–259.
[33] P. Suthianthong, N. Pulsook, P. Supungul, A. Tassanakajon, V. Rimphanitchayakit, A double WAP domain-containing protein *Pm*DWD from the black tiger shrimp *Penaeus monodon* is involved in the controlling of proteinase activities in lymphoid organ, Fish. Shellfish Immunol. 30 (2011) 783–790.
[34] S. Li, X.K. Jin, X.N. Guo, A.Q. Yu, M.H. Wu, S.J. Tan, Y.T. Zhu, W.W. Li, Q. Wang, A double WAP domain-containing protein *Es*-DWD1 from *Eriocheir sinensis* exhibits antimicrobial and proteinase inhibitory activities, PLoS One 8 (2013) e73563.
[35] P. Supungul, S. Tang, C. Maneeruttanarungroj, V. Rimphanitchayakit, I. Hirono, T. Aoki, A. Tassanakajon, Cloning, expression and antimicrobial activity of crustin*Pm*1, a major isoform of crustin, from the black tiger shrimp *Penaeus monodon*, Dev. Comp. Immunol. 32 (2008) 61–70.

Fish & Shellfish Immunology 60 (2017) 103–113

Contents lists available at ScienceDirect

Fish & Shellfish Immunology

journal homepage: www.elsevier.com/locate/fsi

Full length article

A novel C-type lectin in the black tiger shrimp *Penaeus monodon* functions as a pattern recognition receptor by binding and causing bacterial agglutination

Ratree Wongpanya [a, *], Panjana Sengprasert [a], Piti Amparyup [b], Anchalee Tassanakajon [c]

[a] Department of Biochemistry, Faculty of Science, Kasetsart University, 50 Ngamwongwan Road, Bangkok 10900, Thailand
[b] Aquatic Molecular Genetics and Biotechnology Laboratory, Agricultural Biotechnology Research Unit, National Center for Genetic Engineering and Biotechnology (BIOTEC), National Science and Technology Development Agency, Pathum Thani 12120, Thailand
[c] Center of Excellence for Molecular Biology and Genomics of Shrimp, Department of Biochemistry, Faculty of Science, Chulalongkorn University, 254 Phayathai Road, Bangkok 10330, Thailand

ARTICLE INFO

Article history:
Received 17 May 2016
Received in revised form
15 November 2016
Accepted 17 November 2016
Available online 19 November 2016

Keywords:
C-type lectin
Penaeus monodon
Innate immunity
Pattern recognition receptor

ABSTRACT

C-type lectins are pattern recognition proteins that play important roles in innate immunity in invertebrates by mediating the recognition of pathogens. In this study, a novel C-type lectin gene, *Pm*CLec, was cloned and characterized from the black tiger shrimp *Penaeus monodon*. The open reading frame of *Pm*CLec is 657 bp in length. It encodes a predicted protein of 218 amino acids with a calculated molecular mass and an isoelectric point of 24086 Da and 4.67, respectively. Sequence analysis of *Pm*CLec showed similarity to members of the C-type lectin gene superfamily. The deduced protein contains a single carbohydrate recognition domain (CRD) and four conserved cysteine residues (Cys^{58}, Cys^{126}, Cys^{141}, Cys^{149}) that are involved in the formation of disulfide bridges. *Pm*CLec transcripts are expressed in various tiger shrimp tissues, with the highest expression in the lymphoid organ. RNAi-mediated silencing of *Pm*CLec resulted in higher cumulative mortality of knockdown shrimp after *Vibrio harveyi* infection compared to the control groups. Recombinant *Pm*CLec was successfully expressed in the *E. coli* system. In the presence of Ca^{2+}, purified r*Pm*CLec protein binds and agglutinates Gram-positive bacteria (*Staphylococcus aureus*, *S. hemolyticus*), but only slightly binds and agglutinates *E. coli* and could not bind to the Gram-negative bacteria *Bacillus megaterium* and *Vibrio harveyi*. These results suggest that *Pm*CLec functions as a pattern recognition receptor that is implicated in shrimp innate immunity.

© 2016 Elsevier Ltd. All rights reserved.

1. Introduction

Like other invertebrates, shrimp rely on an innate immune system for protecting themselves from various infectious pathogens. This innate immunity consists of two parts, cellular response and humoral defense mechanisms [1–3]. The cellular reaction involves phagocytosis, nodule formation, and encapsulation, whereas the clotting system, antimicrobial peptides, and prophenoloxidase (proPO) system are responsible for the humoral machinery [4]. However, the interaction between pathogen-associated molecular patterns (PAMPs) and pattern recognition receptors (PRRs) is an important stage in the immune response. Different PRRs recognize specific PAMPs and trigger signaling pathways of the immune responses. Among the variety of PRRs, lectins have been identified as potentially important effectors in shrimp immune defense [5]. There are at least seven types of lectins in shrimp consisting of the C-type, L-type, M-type, P-type, fibrinogen-like domain lectins, galectins, and calnexin/calreticulin [6]. However, insight into lectin function in the immune system response is still unclear.

C-type (Ca^{2+}-dependent) lectins are a superfamily of proteins that have one or more carbohydrate recognition domains (CRDs) [7]. Each CRD contains conserved motifs for calcium and carbohydrate binding. Also, the structure of CRDs is stabilized by two or three pairs of disulfide bonds [8]. Invertebrate C-type lectins have been reported to be involved in immune responses, including cell adhesion, activation of prophenoloxidase, nodule formation, phagocytosis and encapsulation [9–11]. In recent years, several C-type lectins have been identified from invertebrates, especially crustaceans. Shrimp C-type lectins have been found to participate

* Corresponding author.
E-mail address: ratree.w@ku.ac.th (R. Wongpanya).

http://dx.doi.org/10.1016/j.fsi.2016.11.042
1050-4648/© 2016 Elsevier Ltd. All rights reserved.

in a series of innate immune responses, including pathogen recognition, microbial agglutination, induction of proPO, promotion of bacterial clearance, microbicidal and anti-viral responses, and enhancement of opsonization, as well as cellular encapsulation [12–17]. In a previous microarray study, we found up-regulation of C-type lectin from *Penaeus monodon* after infection of the shrimp with white spot syndrome virus (WSSV) or *Vibrio harveyi* (Wongpanya et al., 2007). However, the molecular function and mechanism of action of this lectin in the innate immune system of *P. monodon* are still under evaluation. Therefore, the aims of this present study were to clone a novel C-type lectin from the shrimp *Penaeus monodon* and to produce the corresponding recombinant protein using an *Escherichia coli* expression system. Furthermore, functional characterization of the C-type lectin was performed using RNA interference experiments and bacterial binding assays.

2. Methods

2.1. RNA extraction and cDNA synthesis

Juvenile *P. monodon*, 16 g in body weight, were obtained from a local shrimp farm and reared in tanks filled with aerated, circulating sea water for 1 day before the experiments. Hemocytes were collected from healthy, wild-type shrimp in an anti-coagulant solution [10% (w/v) trisodium citrate dehydrate] for RNA extraction. Total RNA was extracted using the TRI reagent (Molecular Research Center, Inc.) as described in the manufacturer's protocol, and then, the resulting RNA was treated with RNase-free DNase I (Promega, USA). This mRNA was used as the template for amplification of full-length cDNA. The cDNAs were synthesized using a SMART cDNA kit according to the manufacturer's instructions (Promega, USA). Based on a cDNA sequence from a *P. monodon* cDNA library, specific PCR primers (*Pm*CLecF and *Pm*CLecR, Table 1) for the novel C-type lectin, named *Pm*CLec, were designed for amplification of the open reading frame. The PCR reaction was carried out as follows: 1 min at 94 °C, then 30 cycles of 94 °C for 1 min, 50 °C for 1 min, 72 °C for 1 min, followed by a final extension at 72 °C for 5 min. The PCR product was separated by agarose gel electrophoresis and subsequently excised and purified. Then, the purified DNA fragment was cloned into a pGEM-T Easy vector (Promega, USA) and sequenced by Macrogen, Korea.

Table 1
Nucleotide sequences of primers used for amplification in this study.

Primers	Sequence (5′-3′)
RAEC-PCR, RT-PCR	
*Pm*CLecF	TGGCTGCTGTTGGTTACAAG
*Pm*CLecR	AGAGCTTCACATGGGGTTTG
*Pm*proPO1-F	GGTCTTCCCCTCCCGCTTCG
*Pm*proPO1-R	GCCGCAGGTCCTTTGGCAGC
*Pm*MasSPH1-F	TACCCTCACCAGGACAGGAACG
*Pm*MasSPH1-R	CTGGAAGAAAGATCCGAGCCGA
*Pm*PPAE1-F	CGTCTGCTTCATTGAGGGAGTG
*Pm*PPAE1-R	GTAGTAGATGGTGCCCCAGCCT
Penaeidin-F	GGTCTTCCTGGCCTCCTTCG
Penaeidin-R	TTTGCATCACAACAACGTCCTA
crustin-F	CTGCTGCGAGTCAAGGTATG
crustin-R	AGGTACTGGCTGCTCTACTG
ALF3-F	TGGTGCTGGTGGTGTCCC
ALF3-R	TGCCAACTGCAGCTGAAC
EF1α-F	GGTGCTGGACAAGCTGAAGGC
EF1α-R	CGTTCCGGTGATCATGTTCTTGATG
RNAi	
lec-F	TTCGGCGCACAGTGACAGAC
lec-R	ATCCTCTCAGCGTCCGATTC
T7lec-F	GGATCCTAATACGACTCACTATAGGGGTCTTGGTGCCCAGCCTTG
T7lec-R	GGATCCTAATACGACTCACTATAGGCGGTGTCCCCCTCTGGTTCA
GFPT7-F	TAATACGACTCACTATAGGATGGTGAGCAAGGGCGAGGA
GFPT7-R	TAATACGACTCACTATAGGTTACTTGTACAGCTCGTCCA
GFP-F	ATGGTGAGCAAGGGCGAGGA
GFP-R	TTACTTGTACAGCTCGTCCA
Recombinant protein expression	
FLec_EcoRI	AGGAATTCCAACTACAGAGGAATTGC
RLec_NotI	ATGCGGCCGCTCTGCATTAGACCATGACTGC

2.2. Sequence analysis

The nucleotide sequence was analyzed using the BLAST program (http://www.ncbi.nlm.nih.gov/blast). The deduced amino acid sequence was analyzed by an Expert Protein Analysis System (http://au.expasy.org/). The potential signal peptide cleavage site was predicted by SignalP 4.1 (http://www.cbs.dtu.dk/services/SignalP/). Multiple sequence alignment was performed with the ClustalW multiple sequence alignment program (http://www.ebi.ac.uk/Tools/clustalw2/). The phylogenetic tree was constructed with MEGA version 6.0 software using the neighbor-joining method based on an amino acid alignment. Domain architecture and conserved cysteine residues that had the potential to form disulfide bonds were identified using ExPASy PROSITE (http://prosite.expasy.org/). A homology model of *Pm*CLec was constructed using SWISS-MODEL (http://swissmodel.expasy.org) and verified by PROCHECK. Finally, molecular docking analysis was carried out using the FlexX program (LeadIT 2.1.8). The model was displayed using PyMoL software.

2.3. Tissue specific expression

The mRNA expression level of *Pm*CLec in various tissues of healthy shrimp was determined using RT-PCR. Total RNA was extracted from hemocytes, gills, hepatopancreas, heart, intestine and lymphoid organs using a RNeasy mini Kit (Qiagen). Then, first-strand cDNAs were synthesized using oligo (dT) primers and an ImProm-IITM Reverse Transcriptase System Kit (Promega) according to the manufacturer's instructions. *Pm*CLec was amplified using specific primers: *Pm*CLecF and *Pm*CLecR (Table 1). An elongation factor 1-α (EF1-α) sequence, serving as an internal control, was amplified with the primers EF1α-F and EF1α-R (Table 1). The PCR conditions were as follows; 95 °C for 5 min; 28 cycles of 95 °C for 1 min, 55 °C for 1 min and 72 °C for 1 min, and a final heating at 72 °C for 5 min. The RT-PCR products were analyzed by agarose gel electrophoresis in 1.2% (w/v) gels.

2.4. Double-stranded RNA (dsRNA) preparation

Double-stranded RNA (dsRNA) was generated as previously described by Amparyup et al. [18]. A DNA fragment of 450 bp was amplified by PCR from the recombinant plasmid containing the *Pm*CLec gene using the gene-specific primers lec-F and lec-R (Table 1). The primers for dsRNA synthesis consist of the same primer sequences but are flanked at the 5′ end by a T7 promoter sequence. Two separate PCR reactions were set up, one with T7lec-F and lec-R for the sense strand template, the other with lec-F and T7lec-R for the anti-sense strand template (Table 1). A DNA fragment (740 bp) encoding green fluorescent protein (GFP) was amplified (negative control) with the pEGFP-1 vector as template using GFPT7-F and GFP-R for the sense strand template and GFP-F and GFPT7-R for the anti-sense strand template (Table 1). The PCR products were purified and used to produce the dsRNA with a T7 RNA polymerase kit (T7 RiboMAX™ Express Large Scale RNA Production Systems, Promega, USA) according to the manufacturer's instruction. The quality and amount of dsRNAs were verified by agarose gel electrophoresis with UV visualization following ethidium bromide staining and UV spectrophotometry, respectively.

2.5. RNA interference (RNAi) treatment of shrimp

Shrimp were injected with either *Pm*CLec-dsRNA or GFP-dsRNA (control) as previously described by Amparyup et al. (2009). Briefly, to assess the sequence-specific knockdown effect of dsRNA, approximately 2.5 μg of dsRNA per 1 g of shrimp body weight in 150 mM NaCl was injected through the lateral area of the fourth abdominal segment using a 0.5-ml insulin syringe with a 29-gauge needle. Injection of 150 mM NaCl alone was performed as an additional control for handling- and injection-induced mortality. 24 h after the first RNAi treatment, the injection of dsRNA or saline was repeated. At 2 days and 5 days after the second RNAi treatment, shrimp hemolymph was collected for total RNA extraction, which was performed using a NucleoSpin1 RNAII kit (MACHEREY-NAGEL) according to the manufacturer's instructions. First-strand cDNA was synthesized from total RNA of *Pm*CLec-silenced shrimp using oligo (dT) primers and the ImProm-II™ Reverse Transcriptase System (Promega, USA) according to the manufacturer's instructions.

2.6. Semi-quantitative RT-PCR analysis

The level of *Pm*CLec gene transcripts in each RNA sample was examined by semi-quantitative RT-PCR using the *Pm*CLecF and *Pm*CLecR primer pair. Other immune genes, including *Pm*MasSPH1, *Pm*proPO1, *Pm*PPAE1, Crustin*Pm*1, ALF*Pm*3 and Penaeidin, were also examined by RT-PCR using their specific primers (Table 1). An EF1-α fragment amplified by EF1α-F and EF1α-R primers was used as an internal control. PCR thermocycling conditions were as follows: 94 °C for 1 min; 25 cycles of 94 °C for 30 s, 55 °C for 30 s and 72 °C for 45 s, and a final heating at 72 °C for 5 min. The PCR products were analyzed by 1.2% (w/v) agarose gel electrophoresis.

2.7. Cumulative mortality assay

For the mortality assay, *P. monodon* shrimp, each of 2 g in size, were injected intramuscularly with 5 μg of *Pm*CLec dsRNA or 30 μl of 150 mM NaCl. The same amount of GFP dsRNA was injected as a sequence-independent dsRNA control. Twenty-four hours after the first injection, 5 μg of dsRNAs or 30 μl 150 mM NaCl was injected along with *V. harveyi* (2×10^5 CFUs). The cumulative mortality rate was recorded twice a day for 7 days post-bacterial challenge. This experiment was performed in triplicate with 10 healthy shrimp per replicate. Statistical analysis was performed using one-way ANOVA.

2.8. Construction of recombinant PmCLec plasmid

The cDNA sequence encoding mature protein was amplified with the specific primers FLec_EcoRI and RLec_NotI (Table 1). *Eco*RI and *Not*I restriction sites were added to the 5′ ends of FLecpET_NotI and RLecpET_EcoRI (after the stop codon), respectively. The purified PCR product was inserted into the pGEM T-easy vector and digested with the restriction enzymes *Eco*RI and *Not*I. The resulting fragment was subcloned into the *Eco*RI/*Not*I site of the pET-32a plasmid (Novagen) to generate pET-32-*Pm*CLec. To ensure in-frame insertion, the recombinant plasmid was sequenced using the Macrogen service (South Korea).

2.9. rPmCLec expression and purification

The full length *Pm*CLec gene was sub-cloned from the plasmid pGEM-*Pm*CLec into the pET32a expression vector. The recombinant plasmid, pET32a-*Pm*CLec, encoded a fusion protein containing an N-terminal TRX fusion and a His_6-tag. This construct was confirmed by sequencing and transformed into chemically competent BL21 Star™ (DE3) *E. coli*. After transformation, bacteria harboring pET32a-*Pm*CLec were selected for r*Pm*CLec expression. Cells were grown in Luria-Bertani (LB) medium supplemented with 50 μg/ml ampicillin and 34 μg/ml chloramphenicol at 37 °C until the $O.D._{600}$ reached 0.6. Protein expression was induced by supplementation with 0.5 mM isopropyl-β-D-thiogalactopyranoside (IPTG) at 30 °C for 5 h. Cells were harvested by centrifugation at 6000 rpm for 30 min at 4 °C. Cells were resuspended in lysis buffer (1 M Tris-HCl pH 8.0, 0.5 M NaCl, 5 mM imidazole, 1 mM PMSF, 2 mM β-mercaptoethanol and 1% Triton X-100) and disrupted by sonication (Sonics Vibracell VCX750). The cell lysate was centrifuged at 10,000 rpm for 30 min at 4 °C. The supernatant was applied onto a 1-ml His-Trap column connected to a FPLC (ÄKTA, GE Healthcare) that was previously equilibrated with five column volumes of buffer A (50 mM Tris-HCl pH 8.0, 0.5 M NaCl and 30 mM imidazole). Bound proteins were then eluted with a step gradient (0%–20%, 20%–40%, 40%–60%, 60%–100%) of buffer B (50 mM Tris-HCl pH 8.0, 0.5 M NaCl and 0.5 M imidazole). The eluted fractions containing r*Pm*CLec were dialyzed against dialysis buffer (50 mM Tris-HCl pH 8.0 and 0.5 M NaCl). The protein concentration was determined by the Bradford assay.

For N-terminal His_6-tagged thioredoxin (TRX) expression, the pET32a plasmid was also transformed into *E. coli* BL21 Star™ (DE3). A single bacterial colony containing the pET32a plasmid was grown in LB medium supplemented with 50 μg/ml ampicillin and 34 μg/ml chloramphenicol at 37 °C until the $O.D._{600}$ reached 0.6. Protein expression was induced by supplementation with 0.5 mM IPTG at 37 °C for 4 h. After collection, the bacterial cells were disrupted by sonication (Sonics Vibracell VCX750) in lysis buffer (1 M Tris-HCl pH 8.0, 0.5 M NaCl, 5 mM imidazole, 1 mM PMSF, 2 mM β-mercaptoethanol and 1% Triton X-100). Soluble protein was applied onto a 1-ml His-Trap column connected to a FPLC (ÄKTA, GE Healthcare) that was previously equilibrated with five column volumes of buffer A (50 mM Tris-HCl pH 8.0, 0.5 M NaCl and 30 mM imidazole). Bound proteins were then eluted with a linear gradient of buffer B (50 mM Tris-HCl pH 8.0, 0.5 M NaCl and 0.5 M imidazole). The eluted fractions containing TRX were dialyzed against dialysis buffer (50 mM Tris-HCl pH 8.0 and 0.5 M NaCl). The protein concentration was determined by the Bradford assay.

2.10. Western blot analysis

Purified r*Pm*CLec or TRX protein was separated on a 12% SDS-PAGE gel and electro-blotted onto a PVDF membrane (Amersham Biosciences) with a constant current of 180 mA for 1.15 h (ATTA system). The membrane was blocked with 3% (w/v) BSA in TBS-T buffer [50 mM Tris-HCl pH 7.4, 150 mM NaCl and 0.2% (v/v) Tween20] for 1 h at room temperature. The membrane was then washed twice with TBS-T buffer. After washing, the membrane was probed with a 1:5000 dilution of the Penta-His™ HRP antibody (Qiagen) in TBS-T buffer for 1 h at room temperature and washed twice with the same buffer. The immunodetection pattern was examined by chemiluminescence using the ECL western blotting reagent (GE Healthcare) and developed on autoradiography film according to the manufacturer's instruction.

2.11. Microbial binding assay

Gram-positive bacteria (*Staphylococcus aureus, S. hemolyticus* and *Bacillus megaterium*), Gram-negative bacteria [*Vibrio harveyi* and *E. coli* (639)], and yeast (*Pichia pastoris*) were grown until reaching an OD_{600} of 0.6 (~10^8 cell/ml). Approximately 2×10^7 cells were pelleted by centrifugation at 10,000 rpm for 10 min before washing in Tris-buffered saline (TBS). Microbes were incubated with 300 μg/ml r*Pm*CLec in TBS containing 20 mM $CaCl_2$ by gentle

A

```
1    tggctgctgttggttacaag

21   ATGACCTCGTTGACAACAAGTCTTTTATTCACCGCTGCTTATCTGGTCTTGGTGCCCAGC
     M  T  S  L  T  T  S  L  L  F  T  A  A  Y  L  V  L  V  P  S
81   CTTGCGGTCTCACAACTACAGAGGAATTGCCCAGACAACTATGTGCTCTTGGCTGACAAA
     L  A  V  S  Q  L  Q  R  N  C  P  D  N  Y  V  L  L  A  D  K
141  TGCTATGGCTTTCGGCGCACAGTGACAGACTGGAATAACGCCCGTGCAACTTGTCTGAAC
     C  Y  G  F  R  R  T  V  T  D  W  N  N  A  R  A  T  C  L  N
201  GAGAATGCTGACCTGACCTCCGTTCTCACGACTCAAGAGTACACGGAGATTCTGGCGCAT
     E  N  A  D  L  T  S  V  L  T  T  Q  E  Y  T  E  I  L  A  H
261  CTGGCTGCTAATTACCCCGGCGTGTACTGGGTTGGAGGTGCCACGAGTAACCAGGGCGCG
     L  A  A  N  Y  P  G  V  Y  W  V  G  G  A  T  S  N  Q  G  A
321  TGGAGGTGGGTGGCTTCGGGCGCGCCCATGAATGAGCAGTGGTGGGGCGGCGACCACACC
     W  R  W  V  A  S  G  A  P  M  N  E  Q  W  W  G  G  D  H  T
281  CCCACTTCACAACGCTGCGCCTACTTCTGCTCCCATACTCGCAAATACTGGAGCAGCACA
     P  T  S  Q  R  C  A  Y  F  C  S  H  T  R  K  Y  W  S  S  T
341  TGCGGGGTGTCCAAGAACTTCATCTGCGAAAAAAGTGCGGAGACCGAAGCCGAATCAGGA
     C  G  V  S  K  N  F  I  C  E  K  S  A  E  T  E  A  E  S  G
401  GAAGAATTTGAACCAGAGGGGGACACCGATCCGGAAAATGAATCGGACGAAGCAGACGCT
     E  E  F  E  P  E  G  D  T  D  P  E  N  E  S  D  E  A  D  A
461  GAGAGGATACCTTCCCTTCCCTCTGTAAGGGCGGAGCTGCGGTCTGGAGTTTCGTCCACC
     E  R  I  P  S  L  P  S  V  R  A  E  L  R  S  G  V  S  S  T
521  ACACAAAACATGGCCTGTCTCGTTTTTCTGTTGAGTTTTTGTGCAGTCATGGTCTAAtac
     T  Q  N  M  A  C  L  V  F  L  L  S  F  C  A  V  M  V  *
581  agatatatgggacttgtgagccagtgactaaaatgccttttcaaaccccatgtg
635  aagctcta
```

B

```
PmClec      --------------------------------MTSLTTSL---LFT-----------------------------------AAYLVLV-PSLAVSQLQRNCPDNYVL-LADKCYGFRRT- 47
AiClec      ------------------------------------------MMFCIG-------------------------------------------LVILAFVQAQASCPHGWTLEGTSCYHIGRE- 36
RpLec       ------------------------------------MKSAIVLLLVV-----------------------------------------ACLAPGINSRACCSDGWIAYKDHCYHIGYGT 42
AfClec5     --------------------------------MFNLYGVLLPVLLLV-----------------------------------------INLRGVQSQNVTCQQDWTAYGGHCYWSVPGL 46
PtClec      MGFVEEALKKMISVDSQLEGEIEKLKENMGVCMSQLSTVM----------------EELGRLKTFSTRLEMLEQTRPEMQNQADQEHDAVWGSAAAYSTCPSPFTRIA-NECFYVSTDE 102
LsClec      ------------------MNPIKSKGTLGIRGHAVLCVLISLLVSAASSEDPEVIEAPKEDVAALKLRLHLLLNSYKEMCKQYSNLAPSCGAPEFNCTECPD-DWLHVGDQCFHLSTD- 99
LcClec      ----------------MMNLIKKKGALGIRGHAVLFVFISLMVSVAADS-------AEGQESYLKLRLDLLKKSYSKLCSEYTNLAQNCSVPVPNCYECPDDKWLLVGDQCLLLETD- 94
Eslect      --------------------------------MTRIACV-----LMVAVA-----------------------------------------GLSAASACHSPYKRVGG-GCFYFSGNI 39
LvLec       --------------------------------MKFLAPVILTALISVA-----------------------------------------SVRSNDCPYPYEPLDDTRRIFLDAYV 42
FcClec1     --------------------------------MKFLAPVILTTLISVAAS---------------------------------------ASVRATECPSPYEPLDETRCIFLDAFV 45

PmLec       VTDWNNARATCLN--ENADLTSVLTTQEYTEILAHLA---ANYPGVYWVGGAT-SNQGAWRWVASGA-----PMNEQWWGGDHTPTSQ-------RCAYF-CSHTRKYWSSTCGVSKNFI 148
AiClec      ELTWTDAQRMCEH-HKNSYLARVETEVEDKAIQ-EMIRAQGHHSHKFWLGATDWTVEGEWQWEPEGS----ASFTYSNWAHHQPNDHG----GNDNCMSMEGESMFHWYDDNCSNKKKYI 146
RpLec       RLTFSAARVYCQS--LGAYLVRLDTFDENTFLK-GFLK--KLMLESTWIGLTDRTHDGIWRWFDTMS-----HATCSDWGPGEPNSHG-----NEDCVNFFVDNDYNWNDSTCHSKYTPL 147
AfClec5     KKSWNDAQSDCQS--RDSNLVKIETAEENSWLE-TIA----TLSDHQWIGATDRDKEGEWRWISDNS-----LVSFTAWGSGEPNNVD----DNEHCGHVYVG--ARWNDLVCSMLFGFI 148
PtClec      MLGWEDARRECGR--LGGDLASPRNLTVLREFL--GSV--QDPPEYVWVGGTK-QDEGTWVWTSGPQAGVPIDMSKSTWNEEVPSGSG-------KCMGLFGQSSYRAYNYDCRERDFFV 208
LsClec      RHGFSTSEQKCEE--KGGHLAILTTREQHEAVEQEGRRI-GGTYTYYWIGLTDAEEEGTWKWVDNST----ITTSFWNTEKGEPDNNVSGGKEGEDCAV-VDSFTKTWYDVPCDFSYPRI 211
LcClec      RNDWLNSSKKCEE--MGAHLAILTTTEQHEAVEKEGRML-GGLYTFYWMGLTDIEKEGEWKWVDNSI----VKNTHWKVGTSEPDNNQSGGEEGEDCAV-VDSYTQSWYDVPCSYLYPRI 206
Eslect      KRNWFGARDYCKSLEQGGSLAIVDDCSLMRPLWNHILFT--YGKSSHWLGASDMHHEGSWTWVDGSP----VAMGMPFWSFNEPNNDG-----QEHCLEFWSAGNGYFNDGQCSRVESFI 148
LvLec       TYTWQDTVDPCKT--HSGEILMIEDCETFALVYDYIKSKDVTQGKHFRLGATDEVEEGTWKFVNNRA----VPQGVPFWGKGEPNSGN-----THNCAIMHASYNHYWYDIQCENKYNPI 151
FcClec1     SYTWQETVDLCKS--HGGEILTIEDCETFALVYDYIRSQDVTKGKHYWLGATDEVEEGTWKFVNNRL----TPMGIPYWGVNEPNNGN-----TYNCAMMHASYNHYWYDAACGSKYNPI 154
                  :  :   *     . :         .              :* :    :* * :                                  *           .  *     :

PmLec       CEKSAETEAESGEEFEPEGDTDPENESDESDAERIPSLPSVRAELRSGVSSTTRNMACLVFLLSFCAVMV 218
AiClec      CETAPSVDMTTVEYLTTKSPSF---QTDV---------------------------------------- 171
RpLec       CEKV------------------------------------------------------------------ 151
AfClec5     CEKEG----------------------------------------------------------------- 153
PtClec      CQYLF----------------------------------------------------------------- 213
LsClec      CQKDATVLP------------------------------------------------------------- 220
LcClec      CQVNAKLLK------------------------------------------------------------- 215
Eslect      CQAPRSKNSWSR---------------------------------------------------------- 160
LvLec       CLKKY----------------------------------------------------------------- 156
FcClec1     CLKNY----------------------------------------------------------------- 159
            *
```

Fig. 1. Sequence analysis of *Pm*CLec. (A) Nucleotide and deduced amino acid sequences of *Pm*CLec. The predicted signal peptide is italicized. The CTLD is shaded in gray. The nucleotides are numbered in the left margin. (B) Alignment of *Pm*CLec with various C-type lectins from other organisms, *Ai*Clec: *Argopecten irradians*, *Rp*Lec: *Ruditapes philippinarum*, *Af*Clec5: *Azumapecten farreri*, *Pt*Clec: *Portunus trituberculatus*, *Ls*Clec: *Lutjanus sanguineus*, *Lc*Clec: *Larimichthys crocea*, *Es*lect: *Eriocheir sinensis*, *Lv*Lec: *Litopenaeus vannamei* and *Fc*CLec1: *Fenneropenaeus chinensis*. Conserved cysteine residues are shaded in red.

rotation for 1 h at room temperature. Microbes incubated with TRX were used as a negative control. After centrifugation, harvested cells were washed three times with 500 μl of TBS. Binding between microbes and recombinant protein was analyzed by 15% SDS-PAGE and was detected by western blot analysis using the Penta-His™ HRP antibody.

2.12. Microbial agglutination assay

The microbial agglutination assay was performed as described by Zhang et al. [19]. Fluorescein isothiocyanate (FITC)-stained Gram-negative bacteria *V. harveyi* and *E. coli* (639); FITC-stained Gram-positive bacteria *B. megaterium, S. aureus* and *S. hemolyticus*; and FITC-labeled yeast *P. pastoris* were suspended in TBS at 2×10^7 cell/ml. A final concentration of 300 μg/ml of r*Pm*CLec in TBS containing 20 mM $CaCl_2$ was then added. To determine whether the agglutination of bacteria required Ca^{2+}, the FITC-labeled bacteria were incubated with r*Pm*CLec (300 μg/ml) in TBS containing 20 mM EGTA. For the negative control, TRX in TBS or TBS only was used. After incubation at room temperature for 1 h, the agglutination activity was observed under a confocal microscope (Nikon).

3. Results

3.1. Characterization and sequence analysis of PmCLec

cDNA encoding a novel C-type lectin of *P. monodon* (*Pm*CLec) had previously been obtained from a cDNA library [20]. To confirm the nucleotide sequence of *Pm*CLec, specific primers were designed to amplify a PCR product that was 657 bp. After cloning and sequencing, the nucleotide and deduced amino acid sequences of *Pm*CLec were analyzed. The open reading frame (ORF) of *Pm*CLec is 657 bp and encodes a protein of 218 amino acid residues that has a 24 aa putative signal peptide (Fig. 1A). The deduced *Pm*CLec amino acid sequence contains four conserved cysteine residues (Cys^{58}, Cys^{126}, Cys^{141}, and Cys^{149}), which could form two disulfide-bonds to stabilize the CRD structure (Fig. 1B), and also contains a single C-type carbohydrate recognition domain (CRD, residues 30 to 150). The deduced mature *Pm*CLec protein (residues 25 to 218) has a predicted molecular mass of 21,561.75 Da, with a theoretical pI of 4.60.

Fig. 2 shows the phylogenetic tree derived from the analysis of the *Pm*CLec deduced amino acid sequence and the sequences of other C-type lectins from shrimp, freshwater crayfish and various species of crab, clam, scallop, tapeworm, viper, roundworm, sea snail and fishes. The *Pm*CLec protein clustered with C-type lectins from other species of shrimp, whereas lectins from vertebrates grouped in a separate cluster.

To predict the tertiary structure of the *Pm*CLec protein, DELTA-BLAST (Domain Enhanced Lookup Time Accelerated BLAST) and SWISS-MODEL were employed. The results showed that *Pm*CLec is closely similar to the C-type lectin DC-SIGNR (1SL6) with an identity of 21%. The modeling-derived structure and the template were visualized with PyMoL, as shown in Fig. 3. The predicted structure of *Pm*CLec contained three β-sheets located between two α-helices.

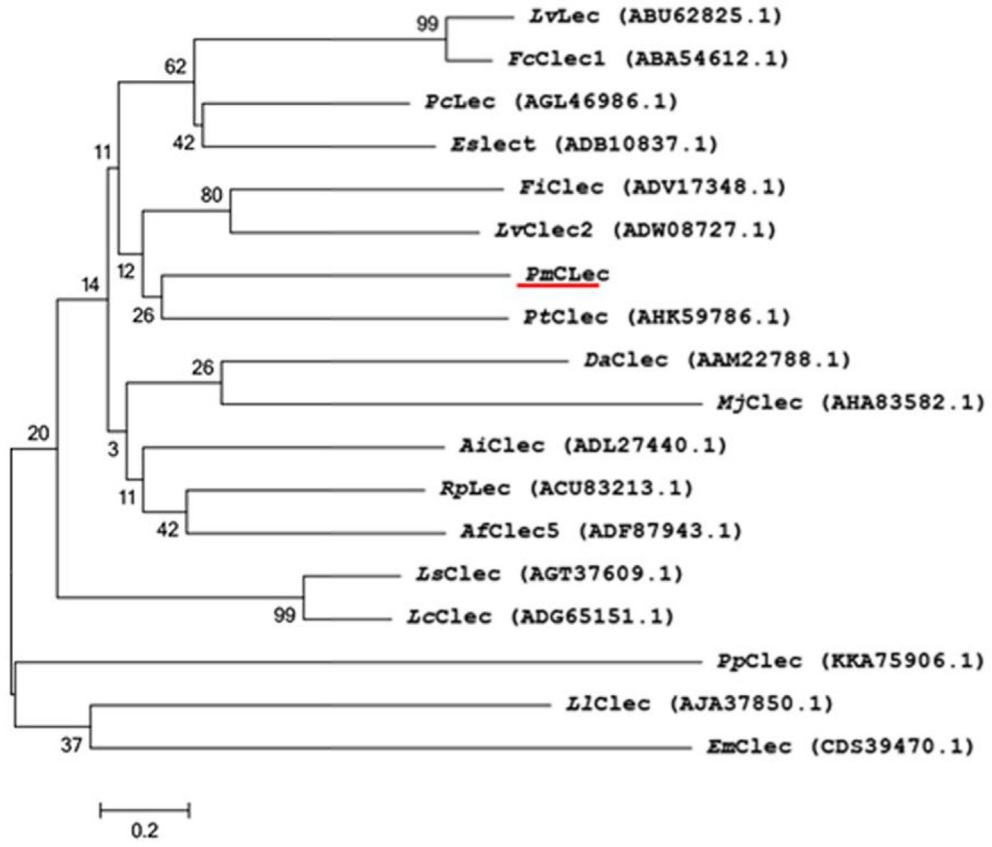


Fig. 2. Phylogenetic analysis of *Pm*CLec and other C-type lectins using MEGA6.0. The GenBank accession numbers are shown in the neighbor-joining tree. The tree is drawn to scale, with branch lengths measured in terms of the number of substitutions per site (next to the branches). *Af*Clec5: a C-type lectin from *Azumapecten farreri*, *Ai*Clec: *Argopecten irradians*, *Da*Clec: *Deinagkistrodon acutus*, *Em*Clec: *Echinococcus multilocularis*, *Es*lect: *Eriocheir sinensis*, *Fc*CLec1: *Fenneropenaeus chinensis*, *Fi*Clec: *F. indicus*, *Lc*Clec: *Larimichthys crocea*, *Ll*Clec: *Littorina littorea*, *Ls*Clec: *Lutjanus sanguineus*, *Lv*Lec: *Litopenaeus vannamei*, *Mj*Clec: *Marsupenaeus japonicas*, *Pc*Lec: *Procambarus clarkii*, *Pp*Clec: *Pristionchus pacificus*, *Pt*Clec: *Portunus trituberculatus* and *Rp*Lec: *Ruditapes philippinarum*.

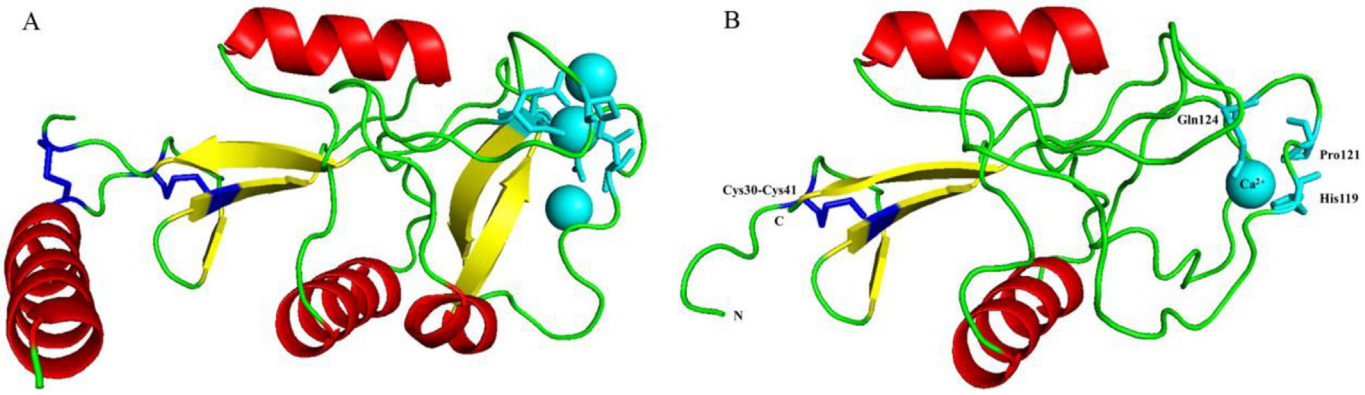


Fig. 3. Homology model of *Pm*CLec. A C-type lectin DC-SIGNR (1SL6) and a *Pm*CLec model are shown in A and B, respectively. Calcium ions are indicated by cyan spheres. (For interpretation of the references to colour in this figure legend, the reader is referred to the web version of this article.)

The model also showed a predicted calcium ion binding site.

The *Pm*CLec amino acid sequence showed no conserved binding motif for any reported sugar moieties. To identify potential *N*-acetylglucosamine (GlcNAc) binding sites of the *Pm*CLec model, an automated molecular docking analysis was performed using the FlexX program (LeadIT 2.1.8) with default parameters. The complex with the best binding energy was visualized using PyMOL and Discovery studio 4.5. The results showed that the *Pm*CLec protein can bind to GlcNAc using His119, Gln124, Tyr128, Trp137, Ser138 and Ser139, with a binding energy of −27 kJ/mol (Fig. 4).

3.2. Tissue specific expression of PmCLec

The transcript levels of *Pm*CLec in various shrimp tissues were characterized by semi-quantitative RT-PCR using EF1-α as an internal control gene. The results showed that the *Pm*CLec gene was expressed in all tested tissues, including the gill, hepatopancreas, hemocytes, heart, intestine, and lymphoid organ (Fig. 5). However, the highest expression level was found in the lymphoid organ, followed by hemocytes and the hepatopancreas.

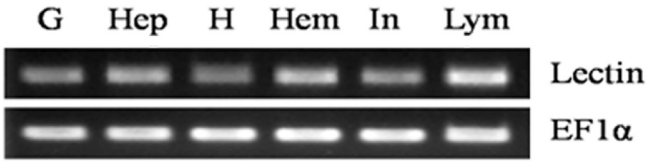


Fig. 5. *Pm*CLec transcript levels in various tissues of *P. monodon* as determined by semi-quantitative RT-PCR. The housekeeping gene EF1-α was used as an internal control. G: gill, Hep: hepatopancreas, H: heart, Hem: hemocytes, In: intestine, and Lym: lymphoid organ.

3.3. PmCLec gene silencing and effect on cumulative mortality

To characterize the potential role of *Pm*CLec in shrimp innate immunity, gene silencing mediated by RNA interference (RNAi) was carried out. Shrimp were injected twice with *Pm*CLec dsRNA, GFP dsRNA or NaCl, the latter two serving as controls. After the dsRNA-mediated knockdown, semi-quantitative RT-PCR was employed to determine the transcription level of the *Pm*CLec gene. The results showed that shrimp receiving *Pm*CLec dsRNA efficiently suppressed *Pm*CLec transcript levels at both days 2 and 5 post-injection, while

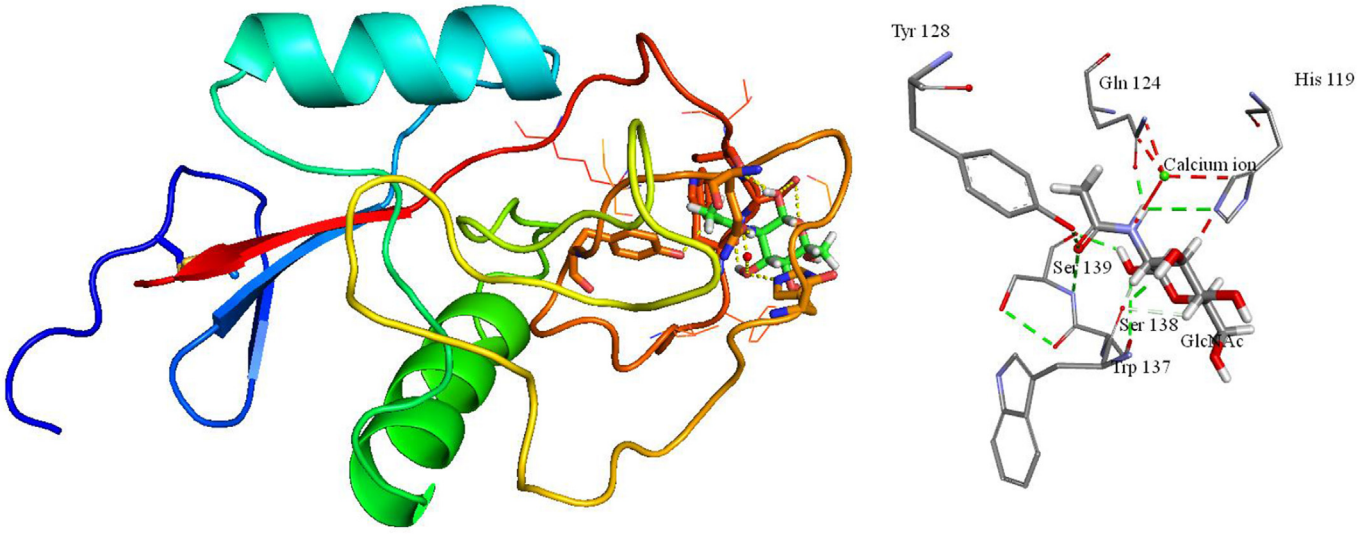


Fig. 4. A predicted *N*-acetylglucosamine (GlcNAc) binding site of the *Pm*CLec model.

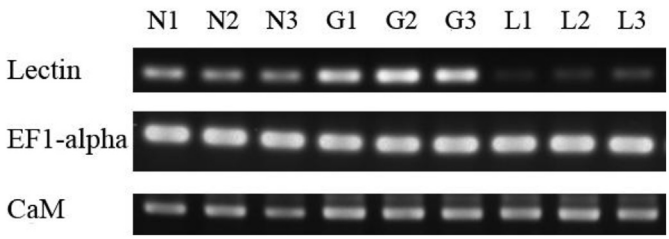


Fig. 6. The efficiency of gene silencing of *Pm*CLec determined by semi-quantitative RT-PCR at 2 days post-injection. The transcript level of *Pm*CLec was determined in shrimp injected with dsRNAs of *Pm*CLec (L1-L3), dsRNAs of GFP (G1-G3) or injected with NaCl (N1-N3). EF1-α and CaM were used as internal controls.

GFP dsRNA or NaCl injection had no effect on *Pm*CLec expression (Fig. 6).

Furthermore, the effect of *Pm*CLec silencing on the cumulative mortality of *V. harveyi*-infected shrimp was also determined. The *Pm*CLec-silenced shrimp were challenged with *V. harveyi* 639 (2×10^5 CFUs). One day after bacterial injection, the *Pm*CLec-silenced shrimp showed a cumulative mortality of 100% compared to 60% and 50% cumulative mortalities in the control shrimp injected with GFP dsRNA and NaCl, respectively (Fig. 7). The increase in mortality rate seen in the *Pm*CLec-silenced shrimp compared to the two control groups was statistically significant, as determined using one-way ANOVA ($p < 0.05$).

To elucidate the effect of silencing the *Pm*CLec gene on other immune-related genes, the expression levels of those genes were examined by semi-quantitative RT-PCR. The result showed that

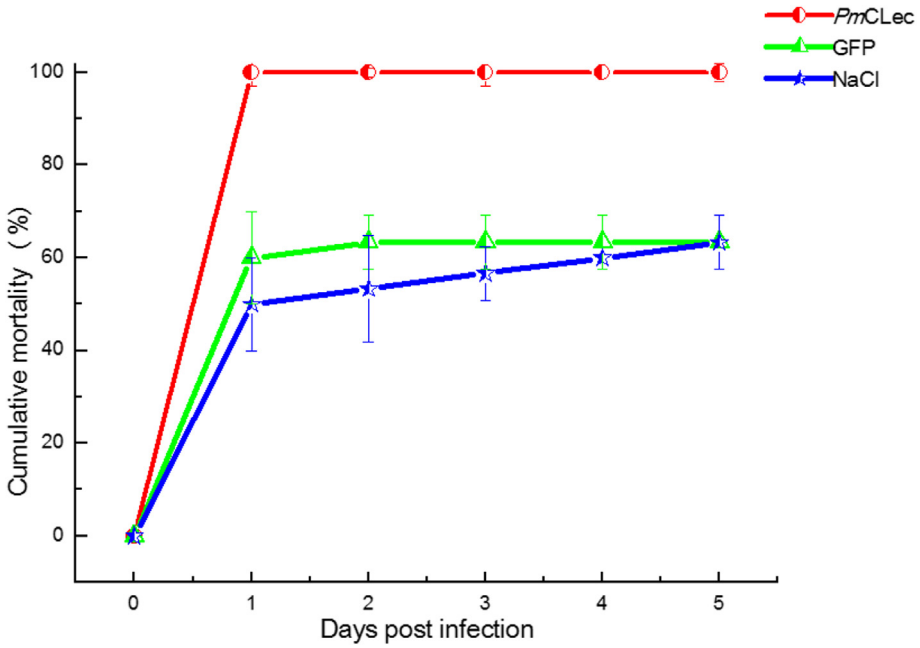


Fig. 7. Cumulative mortality of the *Pm*CLec-silenced shrimp after *V. harveyi* infection. *Pm*CLec: *Pm*CLec dsRNA-injected shrimp, GFP: GFP dsRNA-injected shrimp and NaCl: NaCl-injected shrimp.

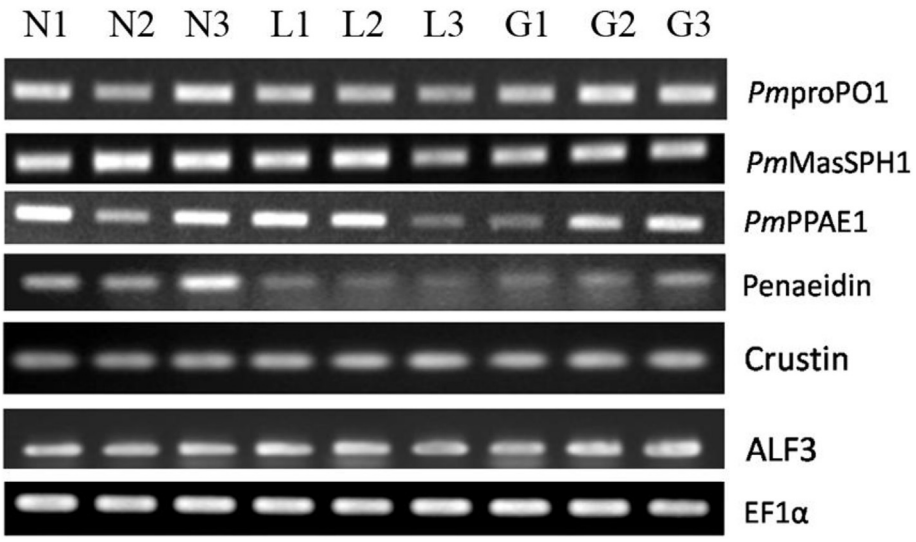


Fig. 8. RT-PCR expression analysis of immune-related genes in dsRNA-injected shrimp, dsRNAs of *Pm*CLec (L1-L3), and dsRNAs of GFP (G1-G3) or NaCl (N1-N3). EF1-α was used as an internal control.

RNAi-mediated *Pm*CLec knockdown did not affect expression of various other immune genes, including prophenoloxidase (*Pm*proPO1), a masquerade-like and serine proteinase homologue (*Pm*MasSPH1), prophenoloxidase activating enzyme (*Pm*PPAE1), penaeidin, crustin and anti-lipopolysaccharide factor (ALF) (Fig. 8).

3.4. Protein purification and characterization

Recombinant *Pm*CLec protein was successfully expressed and purified to a concentration of 0.44 mg/ml. After purification using a His-Trap column, the purified protein was analyzed by SDS-PAGE and western blotting using an anti-His antibody. The analysis showed a single positive band with a corresponding molecular mass of 39.7 kDa, as expected (Fig. 9).

The purified recombinant protein was then characterized in bacterial binding assays, as described in the Materials and Methods. The results showed that the recombinant protein could bind to two types of Gram-positive bacteria, *Staphylococcus aureus* and *S. hemolyticus*. In the case of Gram-negative bacteria, however, the protein could bind slightly to *E. coli* but could not bind to *Bacillus megaterium* and *V. harveyi*. In addition, binding activity was not observed against a yeast, *Pichia partoris* (Fig. 10).

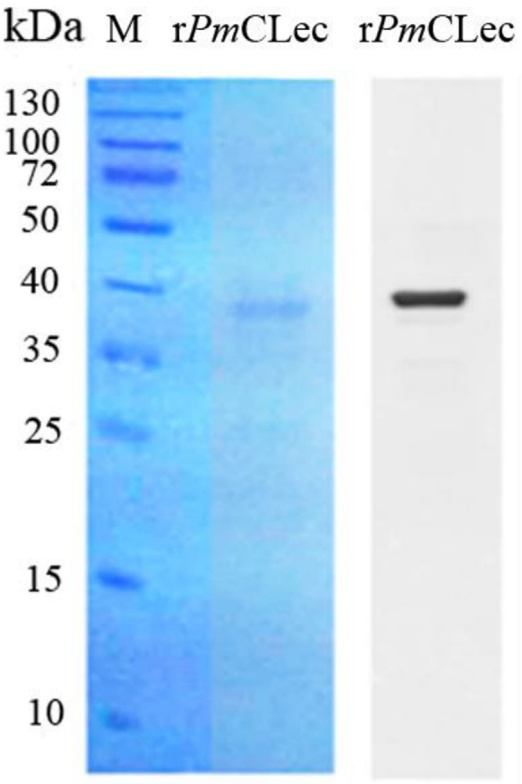


Fig. 9. SDS-PAGE (left) and western blot analysis (right) of purified recombinant *Pm*CLec protein. Purified r*Pm*CLec was analyzed by SDS-PAGE and detected by western blotting using the Penta-His™ HRP antibody.

To determine whether *Pm*CLec could enhance microbial agglutination, all bacteria were cultured and stained with FITC. After incubation with the recombinant protein, bacterial agglutination was observed under a confocal microscope. The results showed that two Gram-positive bacteria, *S. aureus* and *S. hemolyticus,* could be agglutinated by r*Pm*CLec. A small degree of agglutination was found in the case of *E. coli*. As expected, no precipitation was found with other Gram-negative bacteria or with the tested yeast strain. However, the precipitation required calcium ions, as no agglutination was observed in the presence of EGTA (Fig. 11). This result agreed with the bacterial binding assays, which showed that the recombinant protein can bind and precipitate *S. aureus* and *S. hemolyticus*.

4. Discussions

In this study, a C-type lectin (*Pm*CLec) from *P. monodon* was characterized according its role in innate immunity against bacterial infection. According to the cDNA sequence, the predicted *Pm*CLec protein contains a single CRD domain with four conserved cysteine residues. A putative signal peptide was found, suggesting that *Pm*CLec protein might localize on the cell surface or act as a secreted protein. Previous reports showed that C-type lectins can either contain one or two CRDs. C-type lectins with a single CRD domain include LvAV and LvCTL4 in *Litopenaeus vannamei* [15,21] and FcLec4 in *Fenneropenaeus chinesis* [10]. These lectins usually contain a conserved motif in the CRD, such as EPN (Glu-Pro-Asn) or QPD (Gln-Pro-Asp), which are thought to bind mannose and galactose, respectively [22]. However, there is no conserved motif for any specific sugar-binding site in the *Pm*CLec protein. Phylogenetic analysis suggests a close relationship between *Pm*CLec, PtClec, FiClec and LvClec2. In homology modeling, the *Pm*CLec structure was predicted to show the most similarity to the C-type lectin DC-SIGNR. The template structure contains three calcium ions, while the predicted *Pm*CLec model has only one calcium ion. C-type lectins commonly contain four calcium-binding sites, among which site 2 is involved in carbohydrate binding [8]. Recently, Ca^{2+}-binding sites have been reported in the CRDs of many lectins [23,24]. However, there is no such conserved motif in the *Pm*CLec protein. Therefore, molecular modeling for ligand binding of the predicted *Pm*CLec structure with GlcNAc was carried out. The modeling gave a negative value for the binding energy, indicating that protein could bind to GlcNAc, a sugar moiety on peptidoglycan, which represents the basic cell wall component of Gram-positive bacteria.

Tissue distribution analysis showed that the *Pm*CLec transcript was expressed in various shrimp tissues, such as the gill, heart,

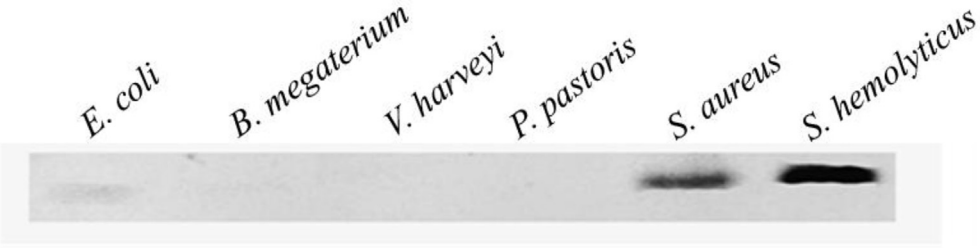


Fig. 10. Bacterial binding assay using western blot analysis. After incubation, the binding between microbes and r*Pm*CLec was analyzed by SDS-PAGE and detected by western blot analysis using the Penta-His™ HRP antibody.

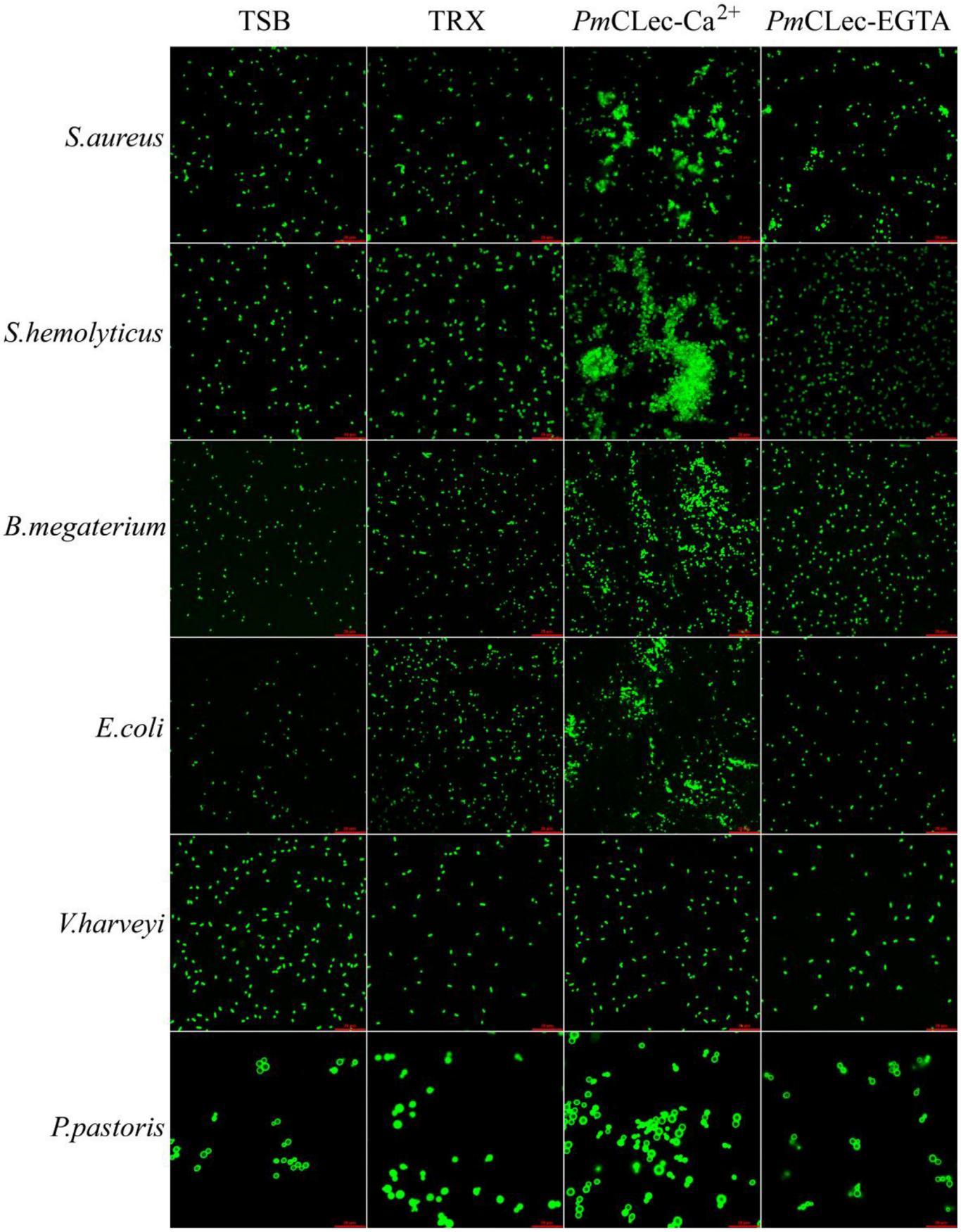


Fig. 11. Microbial agglutination induced by r*Pm*CLec was evaluated with a confocal microscope. FITC-stained *S. aureus*, *S hemolyticus*, *V. harveyi*, *P. pastoris*, *B. megaterium* and *E. coli* were incubated with TBS, TRX, r*Pm*CLec with 20 mM $CaCl_2$ (*Pm*CLec + Ca^{2+}) and r*Pm*CLec with 20 mM EGTA (*Pm*CLec + EGTA). Scale bar indicated 20 μm.

hemocytes, hepatopancreas, intestine, and lymphoid organ. This lectin expression pattern was similar to that of EsLecH in *E. sinensis* [22]. However, the highest expression of *Pm*CLec was found in the lymphoid organ, followed by hemocytes and the hepatopancreas. The lymphoid organ has been characterized as being involved in immune function: several putative immune-related gene transcripts have been observed, including mRNAs for the anti-lipopolysaccharide factor, prophenoloxidase activating factor-III, transglutaminase, proteinases and a protease inhibitor [25]. Hemocytes are also a main site for the production of several immune molecules and are a site where immune reactions take place [26,27]. However, in other shrimps, scallops and crabs, lectins have been reported to be highly expressed in the hepatopancreas [15,21,23,28–30]. This tissue has an important role in metabolism and immunity in crustaceans [21].

To further investigate the crucial role of *Pm*CLec in the shrimp immune response, RNAi-mediated gene silencing was performed. Cumulative mortality after *V. harveyi* injection was significantly higher in *Pm*CLec-silenced shrimp compared to the mortalities of the control groups. These results suggest an involvement of *Pm*CLec in shrimp immunity against bacterial infection. Western blot analysis of bacterial binding assays showed that the recombinant *Pm*CLec protein bound to two Gram-positive bacteria, *S. aureus* and *S. hemolyticus*. In the case of Gram-negative bacteria, however, it was found that the *Pm*CLec protein could bind slightly to *E. coli* but could not bind to *B. megaterium* and *V. harveyi*. In addition, binding activity was not observed against a yeast, *P. partoris*.

Binding to the microbes was calcium-dependent. Moreover, the binding activity of *Pm*CLec induced the agglutination of these bacteria in a concentration-dependent manner. These results are consistent with reports for other C-type lectins that binding to bacteria required calcium ions [17,24]. Additionally, the result was in accord with the computational predictions, even though no specific sugar-binding motif, such as EPN or QPD, could be found in *Pm*Lec. Binding of *Pm*CLec to bacteria might occur via a novel motif that has not been reported. Our previous research also found that the *Pm*CLec transcript was highly responsive to WSSV infection [31]. In the future, it will be desirable to clarify the molecular mechanism of the interaction of *Pm*CLec with a virulent virus, such as WSSV. One future approach under consideration is to perform a protein-protein interaction analysis between the r*Pm*CLec protein and viral proteins. Generally speaking, additional investigations are needed and should be directed towards understanding the specific interaction mechanisms of C-type lectins with various pathogen associated molecular patterns. Further characterization and more molecular information on C-type lectins would lead to a better understanding of the immune defense functions and mechanisms in shrimp.

Acknowledgements

This work was financially supported by the Thailand Research Fund (MRG5280048), Kasetsart University Research and Development Institute (Sci(D)50.53), the Faculty of Science, Kasetsart University and TRF Senior Scholar No. RTA5880004.

References

[1] A. Tassanakajon, K. Somboonwiwat, P. Supungul, S. Tang, Discovery of immune molecules and their crucial functions in shrimp immunity, Fish. Shellfish Immunol. 34 (2013) 954–967.
[2] S.K. Syed Musthaq, J. Kwang, Evolution of specific immunity in shrimp - a vaccination perspective against white spot syndrome virus, Dev. Comp. Immunol. 46 (2014) 279–290.
[3] D. Xu, W. Liu, A. Alvarez, T. Huang, Cellular immune responses against viral pathogens in shrimp, Dev. Comp. Immunol. 47 (2014) 287–297.
[4] W. Charoensapsri, P. Amparyup, I. Hirono, T. Aoki, A. Tassanakajon, PmPPAE2, a new class of crustacean prophenoloxidase (proPO)-activating enzyme and its role in PO activation, Dev. Comp. Immunol. 35 (2011) 115–124.
[5] Y. Zhang, L. Qiu, L. Song, H. Zhang, J. Zhao, L. Wang, Y. Yu, C. Li, F. Li, K. Xing, B. Huang, Cloning and characterization of a novel C-type lectin gene from shrimp Litopenaeus vannamei, Fish. Shellfish Immunol. 26 (2009) 183–192.
[6] X.W. Wang, J.X. Wang, Diversity and multiple functions of lectins in shrimp immunity, Dev. Comp. Immunol. 39 (2013) 27–38.
[7] K. Drickamer, Evolution of Ca(2+)-dependent animal lectins, Prog. Nucleic Acid. Res. Mol. Biol. 45 (1993) 207–232.
[8] A.N. Zelensky, J.E. Gready, The C-type lectin-like domain superfamily, FEBS J. 272 (2005) 6179–6217.
[9] N. Koizumi, M. Imamura, T. Kadotani, K. Yaoi, H. Iwahana, R. Sato, The lipopolysaccharide-binding protein participating in hemocyte nodule formation in the silkworm Bombyx mori is a novel member of the C-type lectin superfamily with two different tandem carbohydrate-recognition domains, FEBS Lett. 443 (1999) 139–143.
[10] X.W. Wang, X.W. Zhang, W.T. Xu, X.F. Zhao, J.X. Wang, A novel C-type lectin (FcLec4) facilitates the clearance of Vibrio anguillarum in vivo in Chinese white shrimp, Dev. Comp. Immunol. 33 (2009) 1039–1047.
[11] X.W. Zhang, W.T. Xu, X.W. Wang, Y. Mu, X.F. Zhao, X.Q. Yu, J.X. Wang, A novel C-type lectin with two CRD domains from Chinese shrimp Fenneropenaeus chinensis functions as a pattern recognition protein, Mol. Immunol. 46 (2009) 1626–1637.
[12] G.J. Yang, X.J. Lu, Q. Chen, J. Chen, Molecular characterization and functional analysis of a novel C-type lectin receptor-like gene from a teleost fish, Plecoglossus altivelis, Fish. Shellfish Immunol. 44 (2015) 603–610.
[13] Y. Xiu, L. Hou, X. Liu, Y. Wang, W. Gu, Q. Meng, W. Wang, Isolation and characterization of two novel C-type lectins from the oriental river prawn, Macrobrachium nipponense, Fish. Shellfish Immunol. 46 (2015) 603–611.
[14] M. Li, C. Li, C. Ma, H. Li, H. Zuo, S. Weng, X. Chen, D. Zeng, J. He, X. Xu, Identification of a C-type lectin with antiviral and antibacterial activity from pacific white shrimp Litopenaeus vannamei, Dev. Comp. Immunol. 46 (2014) 231–240.
[15] H. Li, Y. Chen, M. Li, S. Wang, H. Zuo, X. Xu, S. Weng, J. He, C. Li, A C-type lectin (LvCTL4) from Litopenaeus vannamei is a downstream molecule of the NF-kappaB signaling pathway and participates in antibacterial immune response, Fish. Shellfish Immunol. 43 (2015) 257–263.
[16] X.W. Wang, X.F. Zhao, J.X. Wang, C-type lectin binds to beta-integrin to promote hemocytic phagocytosis in an invertebrate, J. Biol. Chem. 289 (2014) 2405–2414.
[17] H. Li, H. Zhang, S. Jiang, W. Wang, L. Xin, H. Wang, L. Wang, L. Song, A single-CRD C-type lectin from oyster Crassostrea gigas mediates immune recognition and pathogen elimination with a potential role in the activation of complement system, Fish. Shellfish Immunol. 44 (2015) 566–575.
[18] P. Amparyup, W. Charoensapsri, A. Tassanakajon, Two prophenoloxidases are important for the survival of Vibrio harveyi challenged shrimp Penaeus monodon, Dev. Comp. Immunol. 33 (2009) 247–256.
[19] H. Zhang, H. Wang, L. Wang, X. Song, J. Zhao, L. Qiu, L. Li, M. Cong, L. Song, A novel C-type lectin (Cflec-3) from Chlamys farreri with three carbohydrate-recognition domains, Fish. Shellfish Immunol. 26 (2009) 707–715.
[20] A. Tassanakajon, S. Klinbunga, N. Paunglarp, V. Rimphanitchayakit, A. Udomkit, S. Jitrapakdee, K. Sritunyalucksana, A. Phongdara, S. Pongsomboon, P. Supungul, S. Tang, K. Kuphanumart, R. Pichyangkura, C. Lursinsap, Penaeus monodon gene discovery project: the generation of an EST collection and establishment of a database, Gene 384 (2006) 104–112.
[21] S. He, L. Song, Z. Qian, F. Hou, Y. Liu, X. Wang, Z. Peng, C. Sun, X. Liu, Molecular characterization of LvAV in response to white spot syndrome virus infection in the Pacific white shrimp (Litopenaeus vannamei), Dev. Comp. Immunol. 51 (2015) 48–55.
[22] Y.T. Zhu, X. Zhang, S.C. Wang, W.W. Li, Q. Wang, Antimicrobial functions of EsLecH, a C-type lectin, via JNK pathway in the Chinese mitten crab, Eriocheir sinensis, Dev. Comp. Immunol. 61 (2016) 225–235.
[23] L. Wang, D. Zhang, F. Li, M. Wang, M. Huang, H. Zhang, L. Song, A novel C-type lectin from crab Eriocheir sinensis functions as pattern recognition receptor enhancing cellular encapsulation, Fish. Shellfish Immunol. 34 (2013) 832–842.
[24] X.K. Jin, S. Li, X.N. Guo, L. Cheng, M.H. Wu, S.J. Tan, Y.T. Zhu, A.Q. Yu, W.W. Li, Q. Wang, Two antibacterial C-type lectins from crustacean, Eriocheir sinensis, stimulated cellular encapsulation in vitro, Dev. Comp. Immunol. 41 (2013) 544–552.
[25] S. Pongsomboon, R. Wongpanya, S. Tang, A. Chalorsrikul, A. Tassanakajon, Abundantly expressed transcripts in the lymphoid organ of the black tiger shrimp, Penaeus monodon, and their implication in immune function, Fish. Shellfish Immunol. 25 (2008) 485–493.
[26] Y. Duan, P. Liu, J. Li, P. Chen, Immune gene discovery by expressed sequence tag (EST) analysis of hemocytes in the ridgetail white prawn Exopalaemon carinicauda, Fish. Shellfish Immunol. 34 (2013) 173–182.
[27] Y.H. Xu, W.J. Bi, X.W. Wang, Y.R. Zhao, X.F. Zhao, J.X. Wang, Two novel C-type lectins with a low-density lipoprotein receptor class A domain have antiviral function in the shrimp Marsupenaeus japonicus, Dev. Comp. Immunol. 42 (2014) 323–332.
[28] S. Xu, L. Wang, X.W. Wang, Y.R. Zhao, W.J. Bi, X.F. Zhao, J.X. Wang, L-Type lectin from the kuruma shrimp Marsupenaeus japonicus promotes hemocyte phagocytosis, Dev. Comp. Immunol. 44 (2014) 397–405.
[29] P. Kong, L. Wang, H. Zhang, X. Song, Z. Zhou, J. Yang, L. Qiu, L. Song, A novel C-

type lectin from bay scallop Argopecten irradians (AiCTL-7) agglutinating fungi with mannose specificity, Fish. Shellfish Immunol. 30 (2011) 836–844.
[30] Z.Y. Zhao, Z.X. Yin, X.P. Xu, S.P. Weng, X.Y. Rao, Z.X. Dai, Y.W. Luo, G. Yang, Z.S. Li, H.J. Guan, S.D. Li, S.M. Chan, X.Q. Yu, J.G. He, A novel C-type lectin from the shrimp Litopenaeus vannamei possesses anti-white spot syndrome virus activity, J. Virol. 83 (2009) 347–356.
[31] R. Wongpanya, T. Aoki, I. Hirono, M. Yasuike, A. Tassanakajon, Analysis of gene expression in haemocytes of shrimp Penaeus monodon challenged with white spot syndrome virus by cDNA microarray, Sci. Asia 33 (2007) 165–174.

Fish and Shellfish Immunology 76 (2018) 174–182

Contents lists available at ScienceDirect

Fish and Shellfish Immunology

journal homepage: www.elsevier.com/locate/fsi

Full length article

Shrimp hemocyte homeostasis-associated protein (*Pm*HHAP) interacts with WSSV134 to control apoptosis in white spot syndrome virus infection

Kantamas Apitanyasai[a], Piti Amparyup[b], Walaiporn Charoensapsri[b,c], Pakkakul Sangsuriya[b], Anchalee Tassanakajon[a,*]

[a] Center of Excellence for Molecular Biology and Genomics of Shrimp, Department of Biochemistry, Faculty of Science, Chulalongkorn University, Bangkok, Thailand
[b] National Center for Genetic Engineering and Biotechnology (BIOTEC), National Science and Technology Development Agency (NSTDA), Klong Luang, Pathumthani, Thailand
[c] Center of Excellence for Shrimp Molecular Biology and Biotechnology (Centex Shrimp), Faculty of Science, Mahidol University, Bangkok, Thailand

ARTICLE INFO

Keywords:
Shrimp immunity
White spot syndrome virus
Apoptosis
Caspase
Hemocyte homeostasis-associated protein

ABSTRACT

Hemocyte homeostasis-associated protein (*Pm*HHAP) was first identified as a viral-responsive gene, due to a high upregulation in transcription following white spot syndrome virus (WSSV) infection. Functional studies using RNA interference have suggested that *Pm*HHAP is involved in hemocyte homeostasis by controlling apoptosis during WSSV infection. In this study, the role of *Pm*HHAP in host–viral interactions was further investigated. Yeast two-hybrid assay and co-immunoprecipitation revealed that *Pm*HHAP binds to an anti-apoptosis protein, WSSV134. The viral protein WSSV134 is a late protein of WSSV, expressed 24 h post infection (hpi). Gene silencing of WSSV134 in WSSV-infected shrimp resulted in a reduction of the expression level of the viral replication marker genes *VP28*, *wsv477*, and *ie-1*, which suggests that WSSV134 is likely involved in viral propagation. However, co-silencing of *Pm*HHAP and WSSV134 counteracted the effects on WSSV infection, which implies the importance of the host–pathogen interaction between *Pm*HHAP and WSSV134 in WSSV infection. In addition, caspase 3/7 activity was noticeably induced in the *Pm*HHAP and WSSV134 co-silenced shrimp upon WSSV infection. Moreover, *Pm*HHAP and WSSV134 inhibited caspase-induced activation of *Pm*Casp *in vitro* in a non-competitive manner. Taken together, these results suggest that *Pm*HHAP and WSSV134 play a role in the host–pathogen interaction and work concordantly to control apoptosis in WSSV infection.

1. Introduction

White spot syndrome virus (WSSV) is a very serious pathogen, which has caused massive mortality and severe economic losses in shrimp farming throughout the world [1,2]. WSSV has a broad host range [3] and can infect various tissues [4,5]. This virus has an enveloped rod-shaped particle that contains a circular double-stranded DNA of about 300 kb [6–8]. The nucleocapsid is tightly packed within the virion, which is formed from a complex of macromolecules specifically folded and assembled for the protection and delivery of viral genomes [6]. In the process of infection, WSSV invades host cells and then replicates its own components. New virions are then assembled, causing host cell death and disease [2,9]. To date, several proteins of WSSV have been characterized [10].

In shrimp, defenses against invasive microorganisms rely mainly on the innate immune system, including the humoral and cellular mechanisms [11,12]. Immunity appears to play a critical role in antiviral activity in shrimp because it is associated with the ability of infected crustaceans to survive during viral infection [13]. Several immune mechanisms are involved in antiviral immunity, such as immune signaling pathways, RNA interference (RNAi) pathway, nucleic-acid-induced non-specific antiviral immunity, and cell-mediated antiviral mechanisms, including phagocytosis and apoptosis [14]. There have been many studies on the molecular interaction between virus and host, and several proteins from both WSSV and shrimp have been characterized [15,16].

Apoptosis plays a key role in the defense mechanism of animals against viral infection by limiting virus production and decreasing or eliminating the spread of progeny virus in the host [13,17,18]. Many viruses have mechanisms to inhibit host cell apoptosis during infection, prolonging host cell viability until progeny viruses are successfully produced [19]. Some viruses induce apoptosis to facilitate the spread of progeny viruses to neighboring cells at a late stage of infection [20]. Caspases play a key role at various stages of the apoptotic process [21]. WSSV can produce anti-apoptosis proteins in host cells upon infection to regulate apoptosis. AAP-1 (ORF390 or WSSV449) can bind to and is

* Corresponding author.
E-mail address: anchalee.k@chula.ac.th (A. Tassanakajon).

https://doi.org/10.1016/j.fsi.2018.01.043
Received 4 December 2017; Received in revised form 24 January 2018; Accepted 26 January 2018
Available online 01 March 2018
1050-4648/ © 2018 Elsevier Ltd. All rights reserved.

Table 1
Nucleotide sequence of the primers used.

Primer	Sequence (5′-3′)	GenBank accession number
qRT-PCR and semi-quantitative RT-PCR		
*Pm*HHAP-F	5′ GCAACAGGAGAACCTGTGGATA 3′	HQ130431
*Pm*HHAP-R	5′ GGTTCCAGAATCGCCTCCTATA 3′	HQ130431
WSSV134-F	5′ CGAAGCGGAACATACAGTTGAAGG 3′	AAL89002
WSSV134-R	5′ GCTCCTTCGATTTCCGGTAAGTTG 3′	AAL89002
WSSV362-F	5′ GGCACCGAAGAGGACAATAAAG 3′	AAL89230
WSSV362-R	5′ CGCGTAGATACATCATGTTGCC 3′	AAL89230
WSSV395-F	5′ GGACTCCATGGGCTCGTCTAACGGAGATGAG 3′	AAL89263
WSSV395-R	5′ GGTCTACTCGAGAAAAACAAACAGATTGAAA 3′	AAL89263
VP28-F	5′ GGGAACATTCAAGGTGTGGA 3′	DQ979320
VP28-R	5′ GGTGAAGGAGGAGGTGTTGG 3′	DQ979320
ie-1-F	5′ AGCAAGTGGAGGTGCTATGT 3′	AAL33073
ie-1-R	5′ CCATGTCGATCAGTCTCTTC 3′	AAL33073
wsv477-F	5′ GGCCAAGTCATGGAGATCTA 3′	DQ121373
wsv477-R	5′ CCATCCACTTGGTTGCAGTA 3′	DQ121373
EF1α-F	5′ GGTGCTGGACAAGCTGAAGGC 3′	DW042751
EF1α-R	5′ CGTTCCGGTGATCATGTTCTTGATG 3′	DW042751
Gene silencing		
*Pm*HHAPi-F	5′ GCAACAGGAGAACCTGTGGATA 3′	HQ130431
*Pm*HHAPi-R	5′ GGCCTTGTGACGTTCTTCCATT 3′	HQ130431
T7*Pm*HHAPi-F	5′ TAATACGACTCACTATAGGGCAACAGGA GAACCTGTGGATA 3′	HQ130431
T7*Pm*HHAPi-R	5′ TAATACGACTCACTATAGGGGCCTTGTGAC GTTCTTCCATT 3′	HQ130431
WSSV134i-F	5′ GGGAATGTTTCTGCTGCCCTAC 3′	AAL89002
WSSV134i-R	5′ ATAGCCTTGAGCCAGTCCTTTG 3′	AAL89002
T7WSSV134i-F	5′ TAATACGACTCACTATAGGGGGAATGTTTCTGCTGCCCTAC 3′	AAL89002
T7WSSV134i-R	5′ TAATACGACTCACTATAGGATAGCCTTGAGCCAGTCCTTTG 3′	AAL89002
GFP-F	5′ ATGGTGAGCAAGGGCGAGGA 3′	U55761
GFP-R	5′ TTACTTGTACAGCTCGTCCA 3′	U55761
GFPT7-F	5′ TAATACGACTCACTATAGGATGGTGAGCAA GGGCGAGGA 3′	U55761
GFPT7-R	5′ TAATACGACTCACTATAGGTTACTTGTACAG CTCGTCCA 3′	U55761
Cloning and recombinant protein expression		
WSSV395-NcoI	5′ GGACTCCATGGGCTCGTCTAACGGAGATGAG 3′	AAL89263
WSSV395-XhoI	5′ GGTCTACTCGAGAAAAACAAACAGATTGAAA 3′	AAL89263

cleaved by *Penaeus monodon* Caspase (*Pm*Caspase) to inhibit *Pm*Caspase activity [22]. WSSV222 functions as an anti-apoptosis protein in WSSV-infected shrimp via ubiquitin-mediated degradation of the tumor suppressor-like (TSL) protein [23]. Leu et al. (2013) proposed a model for apoptotic interaction between shrimp and WSSV. Briefly, when a host is infected by WSSV, cellular sensors detect the invading virus and trigger the apoptotic signaling pathways to initiate the apoptosis process. Meanwhile, WSSV also activates viral anti-apoptotic proteins to inhibit cell death and complete its own replication [18].

Hemocyte homeostasis-associated protein (HHAP) was initially identified in a previous study as a viral-responsive protein, and it plays an important role in hemocyte homeostasis in *Penaeus monodon* [24]. The silencing of *PmHHAP* led to 100% shrimp mortality within 30 h, which indicates the importance of *Pm*HHAP in shrimp viability [24]. Moreover, the silencing of the *PmHHAP* transcripts leads to a huge decrease in the number of circulating hemocytes and also an increase in hemocyte apoptosis [24,25]. It has also been shown that *Pm*HHAP can bind to the p20 domain of *Pm*Casp and suppress caspase activity, confirming the role of *Pm*HHAP in regulating apoptosis [25]. Recently, HHAP in *Litopenaeus vannamei* was reported to participate in hemocyte homeostasis in shrimp [26]. In the freshwater crayfish *Pacifastacus leniusculus*, *Pl*HHAP plays a role in controlling the number of bacteria in the intestine but is not involved in hemocyte apoptosis [27]. Moreover, *Pl*HHAP does not responded to WSSV infection, in contrast to *Pm*HHAP [27]. Although *Pm*HHAP is dramatically upregulated at both the transcription and protein levels, the mechanism underlying the function of *Pm*HHAP in controlling hemocyte apoptosis upon WSSV infection remains unclear.

In an attempt to study the function of *Pm*HHAP during WSSV infection, the proteins of *Pm*HHAP that interacted with viruses were identified and characterized. Yeast two-hybrid screening and co-immunoprecipitation identified the viral protein WSSV134 (VP36A), which interacts with *Pm*HHAP. The *in vivo* gene silencing of *WSSV134* and the co-silencing of *WSSV134* and *PmHHAP* were performed to investigate the role of these proteins upon WSSV infection. In addition, the effects of the co-silencing of *PmHHAP* and *WSSV134* on caspase 3/7 activity in WSSV-infected shrimp were examined; likewise, the caspase-inhibition kinetics of the two proteins were shown to reveal their role in anti-apoptosis via caspase inhibition. This study demonstrates the importance of the host–pathogen interaction in controlling apoptosis in WSSV infection.

2. Materials and methods

2.1. Experimental shrimp

Specific-pathogen-free (SPF) black tiger shrimp *P. monodon* (3–5 g average weight for the knockdown experiment and 10–15 g for the WSSV challenge) were purchased from a local shrimp farm in Suratthani province, Thailand. The shrimp were maintained in tanks with aerated seawater (20 ppt) at a temperature of 28–32 °C for 7 days before use in the experiment. During acclimation, shrimp were fed shrimp feed twice daily.

2.2. Yeast two-hybrid assay

The yeast two-hybrid assay was carried out using the Matchmaker GAL4 Two-Hybrid System (Clontech) to identify which WSSV proteins

interacted with *Pm*HHAP. The recombinant plasmid pET22b–*PmHHAP* that was obtained was digested with *Nde*I and *Xho*I restriction nucleases. The bait plasmid was generated by cloning the purified *PmHHAP* fragment into the *NdeI/Sal*I site downstream of the GAL4 DNA-binding domain of pGBKT7 (Clontech) to yield the final *PmHHAP*/pGBKT7 construct. The constructs were subsequently sequenced to confirm gene sequences and correct reading frames. Meanwhile, the interacting proteins (prey) from a WSSV DNA library were fused with a GAL4 DNA-activation domain of pGADT7 vector (Clontech). Then the yeast two-hybrid assay was performed by co-transforming *PmHHAP*/pGBKT7 and WSSV DNA library into the yeast cells, *Saccharomyces cerevisiae* strain AH109, using the lithium acetate/dimethyl sulfoxide method [28]. Yeast cells were grown in a low-stringency media lacking leucine and tryptophan, and the binding was tested in a high-stringency medium lacking adenine, histidine, leucine, and tryptophan, supplemented with X-α-gal (Apollo Scientific). Library plasmids from positive colonies were rescued in *Escherichia coli* XL1-blue and then subsequently subjected to DNA sequencing. The nucleotide sequences were compared to the deduced amino acid sequences against the GenBank® database, using the BLASTX program.

2.3. Production and purification of recombinant PmHHAP protein and WSSV proteins

The *E. coli* Rosetta (DE3) strain containing recombinant plasmid pET22b-*PmHHAP* was cultured, then the recombinant protein was produced and purified, as previously described [24]. The gene encoding *WSSV395* was amplified using the Advantage® Polymerase Mix (Clontech) with gene-specific primers (Table 1). The purified polymerase chain reaction (PCR) product was digested with *Nco*I and *Xho*I and then ligated into the pET28b vector (Novagen). Afterwards, the ligation mixture was transformed into competent *E. coli* JM109, and positive clones were analyzed by nucleotide sequencing. The recombinant plasmid pET15b-*WSSV134* was obtained thanks to Dr. Saengchan Senapin. This plasmid and pET28b-*WSSV395* were transformed into an *E. coli* BL21 (DE3). The single colony was grown in Luria-Bertani (LB) medium, and induced with 1 mM IPTG for 4 h. Cells were collected and resuspended in 20 mM Tris-HCl pH 8.0 and then sonicated and purified through Ni-NTA column (GE Healthcare). The protein was analyzed by SDS-PAGE (15% [w/v] acrylamide), followed by Coomassie brilliant blue staining.

2.4. Co-immunoprecipitation

To confirm the interaction between *Pm*HHAP protein and its targets, WSSV proteins, co-immunoprecipitation (Co-IP) was performed. The r*Pm*HHAP protein, rWSSV134 and rWSSV395 were produced in the *E. coli* system as described above. The polyclonal *Pm*HHAP antibody was immobilized and cross-linked with protein A-sepharose CL4B (GE Healthcare) using dimethyl pimelimidate. The cross-linked bead was equilibrated using binding buffer (1 × PBS, pH 7.4, and 1 M NaCl) followed by the addition of 40 μg of r*Pm*HHAP and/or 60 μg of WSSV proteins and then incubation at 4 °C overnight. The protein complex was eluted with 100 mM glycine (pH 2.5) and then the immunoprecipitated complex was separated by SDS-PAGE (18% [w/v] acrylamide) and the protein band was analyzed using Western blot analysis. r*Pm*HHAP and rWSSV134 or rWSSV395 were detected using anti-His tag antibody (1:5,000; Millipore) as primary antibody and goat anti-mouse IgG-AP conjugate (1:10,000; Millipore) as secondary antibody; then the positive bands were detected using NBT/BCIP solution.

2.5. Expression profile of viral genes in WSSV-challenged shrimp hemocytes

The transcription of the viral genes *WSSV134*, *WSSV362*, and *WSSV395* in WSSV-infected shrimp at various time points was investigated using semi-quantitative RT-PCR. Shrimp were injected with 50 μL diluted WSSV solution. Hemocytes were collected from three individual shrimp at 0, 3, 6, 12, 24, and 48 h post infection (hpi) and then subjected to total RNA extraction. The first strand of cDNA was synthesized after treatment with RNase-free DNase I (Biolabs) using the RevertAid First Strand cDNA Synthesis kit (Fermentas). The expression levels of the viral genes *WSSV134*, *WSSV362*, *WSSV395*, *ie-1* (immediate early gene), *wsv477* (early gene), and *VP28* (late gene) were examined using gene-specific primers (Table 1). *EF1-α* was used as an internal control gene. The reaction was pre-denatured at 94 °C for 2 min, which was followed by 35 cycles of denaturation at 94 °C for 30 s, annealing at 60 °C for 30 s or 58 °C for *EF1-α* and extension at 72 °C for 30 s, with final extension at 72 °C for 10 min. The PCR products were analyzed by 1.5% (w/v) agarose gel electrophoresis and visualized under ultraviolet (UV) light after ethidium bromide staining.

2.6. Preparation of double-stranded RNA

Double-stranded RNAs (dsRNA) for *PmHHAP* and *WSSV134* were generated *in vitro* using a T7 RiboMAX™ Express Large Scale RNA Production System (Promega). Briefly, *WSSV134* dsRNA was prepared using recombinant pET15b-WSSV134 plasmid as a template for producing sense and anti-sense DNA template strands separately. The *PmHHAP* dsRNA was prepared using recombinant pET22b-*Pm*HHAP plasmid as a template. DNA templates containing the T7 promoter sequence at the 5′ end were used for *in vitro* transcription according to the instructions provided by the T7 RiboMAX™ Express Large Scale RNA Production Systems (Promega).

2.7. In vivo gene knockdown of WSSV134

The shrimp were divided into two groups of three individuals each. They were intramuscularly injected with 25 μL 150 mM NaCl solution containing 7 μg *WSSV134* dsRNA per 1 g shrimp while the control group was injected with GFP dsRNA (7 μg/g shrimp). Then, 3 h post-dsRNA injection, diluted WSSV solution was injected into the shrimp. Afterwards, hemocytes were collected at 48 hpi and subjected to total RNA extraction, as described above, to determine the efficiency of *WSSV134* gene transcript silencing. RT-PCR was performed to check the transcription of gene using the specific primers for the *WSSV134* gene (Table 1). One microliter of diluted cDNA was used as a template for PCR amplification, a fragment of the *EF1-α* gene was amplified and used as an internal control, and *VP28* was also amplified and used to quantify viral replication in shrimp. The PCR conditions were 94 °C for 2 min, followed by 35 cycles of 94 °C for 30 s, 60 °C (for *WSSV134* and *VP28*) or 58 °C (*EF1-α*) for 30 s, and 72 °C for 30 s, and then a final extension at 72 °C for 5 min. The PCR products were analyzed using 1.5% (w/v) agarose gel electrophoresis and visualized by UV-transillumination.

2.8. Viral propagation after silencing of WSSV134 transcription

To investigate the expression level of representative genes of WSSV after *WSSV134* silencing, the RNAi experiment was performed and the expression level of tested genes was analyzed using quantitative (q)RT-PCR. Two groups of shrimp, experimental and control groups, were injected with 25 μL 150 mM NaCl containing either *WSSV134* dsRNA (7 μg/g shrimp) or *GFP* dsRNA (7 μg/g shrimp). The diluted WSSV solution was injected 3 h after dsRNA injection into each shrimp, and then hemocytes were harvested at 48 h to extract total RNA, as described above. After cDNA was synthesized, qRT-PCR was performed using SsoFast™ EvaGreen® Supermix (Bio-Rad) on a CFX96 touch real-time PCR detection system (Bio-Rad), and each sample was analyzed in triplicate. The specific oligonucleotide primers of the viral genes *ie-1*, *wsv477*, and *VP28* were used to verify the gene expression level, and the *EF1-α* gene served as an internal control and reference standard for verification of the qRT-PCR reaction. The PCR conditions consisted of

95 °C for 8 min, followed by 40 cycles of 95 °C for 10 s, 60 °C for 15 s, and 72 °C for 30 s. The expression levels of the viral genes after knockdown of *WSSV134* were calculated by normalizing the control injected with GFP dsRNA. The results are presented as relative expression ratios of the target genes expressed in hemocytes of *ie-1*, *wsv477*, and *VP28* (mean ± SD of the three replicates).

2.9. Co-silencing of shrimp PmHHAP gene and viral gene WSSV134

The shrimp were divided into four groups of three individuals each. The first group was injected with *WSSV134* dsRNA (7 μg/g shrimp), the second group was injected with *PmHHAP* dsRNA (5 μg/g shrimp), the third group was injected with both *WSSV134* (7 μg/g shrimp) and *PmHHAP* dsRNA (5 μg/g shrimp), and the last group was injected with *GFP* dsRNA (7 μg/g shrimp). At 3 h after dsRNA injection, a diluted WSSV solution was injected into all shrimp groups, which were reared for a further 48 h. In addition, for shrimp that had been subjected to injection with *PmHHAP* dsRNA, it was injected at 24 h after WSSV injection. Afterwards, hemocytes were collected at 48 h after WSSV infection to extract the total RNA, and were used to synthesize the first strand of cDNA, as described above. The efficiency of the gene knockdown was verified via semi-quantitative RT-PCR using the specific primers for the *PmHHAP* gene and *WSSV134* gene (Table 1). The *EF1-α* gene was amplified and used as an internal control gene, and *VP28* was also amplified and used to quantify the viral replication in shrimp. The thermal cycling conditions were 94 °C for 2 min, followed by 35 cycles (30 cycles for *PmHHAP* and 22 cycles for *EF1-α*) at 94 °C for 30 s, 58 °C (*PmHHAP* and *EF1-α*) or 60 °C (*WSSV134* and *VP28*) for 30 s, 72 °C for 30 s, and 72 °C for 5 min. The PCR product was analyzed using 1.5% (w/v) agarose gel electrophoresis and visualized by UV-transillumination. Furthermore, to investigate the effects of gene silencing on the expression levels of the representative genes of WSSV, qRT-PCR was performed as described above.

2.10. Caspase activity assay in hemocytes for co-silencing of PmHHAP and WSSV134 genes

Shrimp were divided into five groups of nine individuals each. The first group was injected with *WSSV134* dsRNA (7 μg/g shrimp), the second group was injected with *PmHHAP* dsRNA (5 μg/g shrimp), the third group was injected with both *WSSV134* (7 μg/g shrimp) and *PmHHAP* dsRNA (5 μg/g shrimp), and the last two groups were injected with *GFP* dsRNA (7 μg/g shrimp) and PBS only (control for apoptosis in normal condition), respectively. Gene knockdown was performed as described above. Hemolymph was withdrawn from each shrimp at 48 h after WSSV challenge; then hemolymph from each of three shrimp per treatment was pooled and subjected to hemocyte lysate supernatant (HLS) preparation. The total levels of proteins in cell suspensions were determined using Bradford Reagent (Bio-Rad). An equal concentration of protein in shrimp hemocytes was used in caspase activity assays using the Caspase-Glo 3/7 Assay Kit (Promega) according to the manufacturer's instructions. Briefly, 100 μL pooled hemocyte-cell suspension was seeded in the 96-well white plate, and then 100 μL Caspase-Glo reagent was added to each well, gently mixed, and incubated for 15 min. The luminescence of each sample was measured with a plate-reading luminometer (Molecular Devices). After subtracting with blank (buffer only), changes in caspase 3/7 activity were determined by comparing the caspase 3/7 activity level of the treated shrimp to that of the PBS control shrimp. The data are reported as the mean ± SD of three replicates.

2.11. In vitro inhibition of caspase activity

To investigate whether *Pm*HHAP and WSSV134 can suppress caspase activation induced by *Pm*Casp, caspase 3/7 activity was detected using Caspase-Glo 3/7 assay (Promega). The recombinant protein of *Pm*HHAP and WSSV134 was prepared as described above, while r*Pm*Casp was produced and purified as described previously [25]. The reactions were prepared in a total volume of 100 μL, containing 7 mM r*Pm*Casp incubated with other proteins, and divided into six groups. The first group was incubated with 10 mM r*Pm*HHAP, the second group was incubated with 10 mM WSSV134, the third group was incubated with 10 mM r*Pm*HHAP together with 10 mM WSSV134, the fourth group was incubated with 10 mM control protein (bovine serum albumin, BSA), and the other groups contained only r*Pm*Casp and PBS buffer, respectively. Caspase-Glo reagents (100 μL) were added and luminescent signals were measured at 0, 30, 60, 90, and 120 min, using a microplate reader (Molecular Devices). The results are expressed as the mean ± SD of three replicates.

2.12. Kinetic assay of caspase activity

Caspase activity was assayed using the colorimetric method with the CaspACE assay system (Promega). Briefly, an incubation mixture containing caspase assay buffer, DMSO, and 100 mM DTT was prepared. r*Pm*Casp was added, followed by the addition of 0.1 mM DEVD-pNA substrate to all wells. After incubation at 37 °C for 3 h, the absorbance was measured at 405 nm to calculate caspase-specific activity. The inhibition experiments were performed by fixing the concentration of r*Pm*Casp, and then the concentrations of substrate, r*Pm*HHAP, and WSSV134 were varied. The reaction mixture consisted of four concentrations of DEVD-pNA substrate (0, 0.025, 0.05, and 0.1 mM) in the presence of a fixed amount of r*Pm*Casp (0.08 mM) and three different concentrations of r*Pm*HHAP and rWSSV134 (0, 0.08, and 0.16 mM). After incubation at 37 °C for 3 h, absorbance was measured at 405 nm to calculate caspase-specific activity and was plotted against the molar ratio of r*Pm*HHAP and rWSSV134.

3. Results

3.1. Interacting proteins of PmHHAP identified by yeast two-hybrid screening

To better understand the role of *Pm*HHAP in preventing hemocyte apoptosis, *Pm*HHAP-interacting proteins were identified from the WSSV library using yeast two-hybrid screening. *Pm*HHAP was used as a bait protein to screen the library, constructed from the open reading frame (ORF) of WSSV genome. Three positive clones were identified and then subjected to DNA sequencing. The obtained sequences were analyzed by searching within the GenBank database using BLASTX. The three positive WSSV ORF clones showed sequence matching to WSSV134 (accession no. AAL89002), WSSV362 (accession no. AAL89230), and WSSV395 (accession no. AAL89263) (Fig. 1A).

3.2. Interactions between rPmHHAP and WSSV proteins by Co-IP

To confirm the interaction between *Pm*HHAP and the identified interacting partners, Co-IP was performed. The recombinant proteins of *Pm*HHAP, WSSV134, and WSSV395 were successfully produced in an *E. coli* system. However, the recombinant protein of WSSV362 was not successfully cloned and constructed. The immunoprecipitated complex was detected by Western blot analysis using anti-His antibody. The r*Pm*HHAP and rWSSV134 and/or rWSSV395 could be detected in the elution step, which indicates that *Pm*HHAP can bind to both WSSV134 and WSSV395 (Fig. 1B and C). Among these proteins, WSSV134 was selected for further study because it functions as an anti-apoptotic protein in WSSV [29], while WSSV 395 has been characterized as an envelope protein with unknown function [30].

3.3. Expression profile of viral genes in WSSV-challenged shrimp hemocytes

The expression levels of viral genes at various time points after

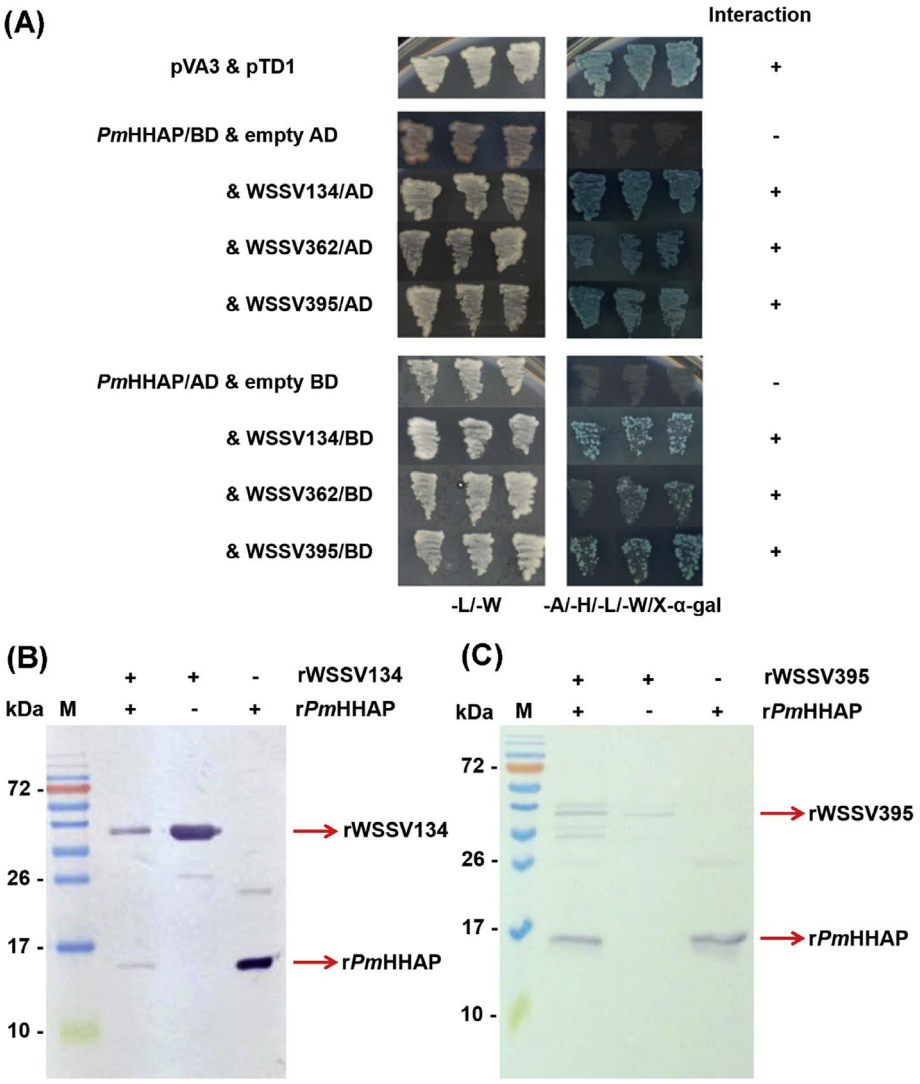


Fig. 1. Yeast two-hybrid screening and co-immunoprecipitation of *Pm*HHAP and WSSV proteins. (A) Protein–protein interactions between *Pm*HHAP and WSSV proteins (WSSV134, WSSV362, and WSSV395), as determined by yeast two-hybrid assays. Interactions (+) are indicated by a blue color; the – symbol indicates no interaction. (B) and (C) The protein–protein interaction between r*Pm*HHAP and rWSSV134 or rWSSV395, respectively, obtained in co-immunoprecipitation assays. The protein complexes were separated by SDS-PAGE and analyzed by Western blot, using anti-His antibody. (For interpretation of the references to color in this figure legend, the reader is referred to the Web version of this article.)

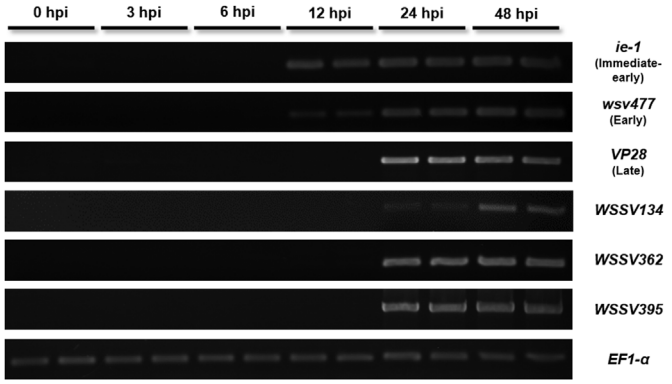


Fig. 2. Expression profile of *WSSV134*, *WSSV362*, and *WSSV395* genes in hemocytes of WSSV-infected shrimp. Hemocytes from both WSSV-infected shrimp and control PBS were collected at 0, 3, 6, 12, 24, and 48 hpi and subjected to transcript analyses by semi-quantitative RT-PCR. The *ie-1* (immediate-early), *wsv477* (early), and *VP28* (late) genes were amplified as positive controls, while the *EF1-α* gene was used as an internal control. Three individual shrimp were analyzed for each group. Representative data for two individuals per group are shown.

WSSV infection were determined by semi-quantitative RT-PCR analysis. The viral genes expressed at different stages of viral replication, *ie-1*, *wsv477*, and *VP28*, were used as marker genes. The hemocytes were collected at 0, 3, 6, 12, 24, and 48 hpi and the gene expression was analyzed by semi-quantitative RT-PCR. *EF1-α* was used as an internal gene control. Transcripts for *WSSV134*, *WSSV362*, and *WSSV395* were detected at 24 and 48 hpi, similar to that of *VP28*. Therefore, *WSSV134*, *WSSV362*, and *WSSV395* were likely late genes, which are transcribed at a late stage of WSSV infection (Fig. 2).

3.4. Effects of RNAi-mediated suppression of WSSV134 on viral propagation

Protein–protein interaction analysis showed that *Pm*HHAP interacts with WSSV134, an anti-apoptosis protein of WSSV [29]. Next, the role of WSSV134 and *Pm*HHAP in hemocyte apoptosis was further investigated using dsRNA-mediated gene silencing. Initially, the efficiency of the gene knockdown of *WSSV134* in WSSV-infected shrimp was determined by semi-quantitative RT-PCR analysis. After injection of dsRNAs (7 μg *WSSV134* dsRNA per gram shrimp and 7 μg *GFP* dsRNA per gram shrimp), followed by WSSV injection, samples were collected after viral infection for 48 hpi, and the transcript levels of *WSSV134*

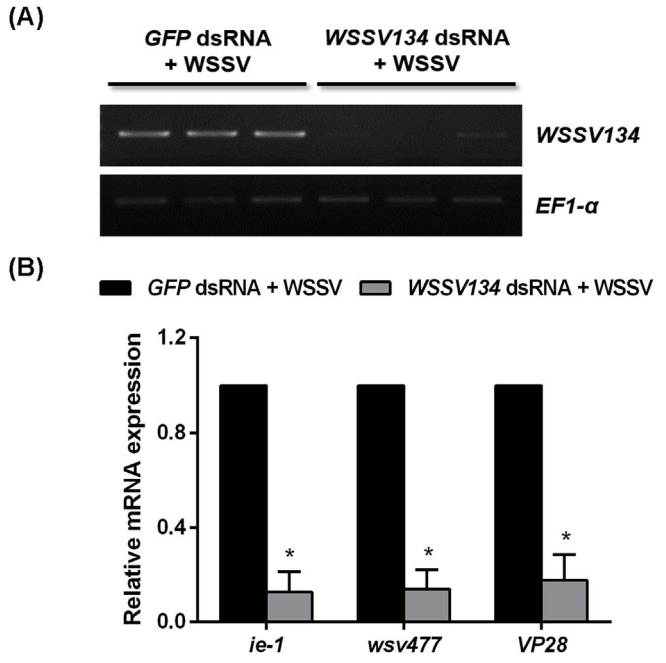


Fig. 3. *In vivo* gene silencing of *WSSV134* by RNA interference (RNAi). (A) The expression level of *WSSV134* was examined using semi-quantitative RT-PCR to check the efficiency of gene knockdown. *EF1-α* served as an internal control gene. Each lane represents the results from three independent shrimp per group. (B) The expression levels of representative WSSV genes for the three stages of WSSV infection, *ie-1* (immediate-early gene), *wsv477* (early gene), and *VP28* (late gene), were determined after *WSSV134* knockdown in WSSV-infected shrimp using qRT-PCR. The data are shown as means ± 1 SD, derived from three independent shrimp. *EF1-α* was used as an internal control gene for normalization with the same cDNA sample. Asterisks indicate statistically significant differences between means (*$P < 0.05$).

were evaluated. The levels of the *WSSV134* transcript were significantly decreased in *WSSV134*-silenced shrimp, whereas the injection of *GFP* dsRNA had no discernible effect on *WSSV134* transcript levels (Fig. 3A).

To investigate the importance of WSSV134 in WSSV infection, the expression of representative WSSV genes after *WSSV134* knockdown in WSSV-infected shrimp, for three stages of WSSV infection, including *ie-1*, *wsv477*, and *VP28*, were determined using qRT-PCR. The silencing of WSSV134 caused a dramatic decrease in the expression of *ie-1*, *wsv477*, and *VP28* compared to the control shrimp (Fig. 3B). This indicates that WSSV134 plays an important role in WSSV infection.

3.5. Co-silencing of PmHHAP and WSSV134 by RNAi

To investigate how *Pm*HHAP and WSSV134 function upon viral infection, specific gene silencing of *PmHHAP* and *WSSV134* or co-silencing of *PmHHAP* and *WSSV134* transcription were performed using RNAi. The efficiency of the gene knockdown was first examined by semi-quantitative RT-PCR analysis. The success of gene silencing is shown in Fig. 4A. The expressions of *ie-1*, *wsv477*, and *VP28* were determined after the *WSSV134* and *PmHHAP* transcripts in WSSV-infected shrimp were silenced using qRT-PCR. As shown in Fig. 4B, silencing of *WSSV134* transcripts caused a significant decrease in the expression level of the *ie-1*, *wsv477*, and *VP28* transcripts, suggesting that WSSV134 might be engaged in WSSV replication. In contrast, such viral transcripts were found to be increased in the *PmHHAP* silenced shrimp, indicating that *Pm*HHAP played positive roles in the antiviral immunity in shrimp. Interestingly, co-silencing of *PmHHAP* and *WSSV134* transcripts resulted in no significant change in the viral gene transcript levels relative to those of the GFP control (Fig. 4B). The finding implies a counteraction of *Pm*HHAP and WSSV134 upon WSSV infection and that these two proteins play important role in host-pathogen interactions.

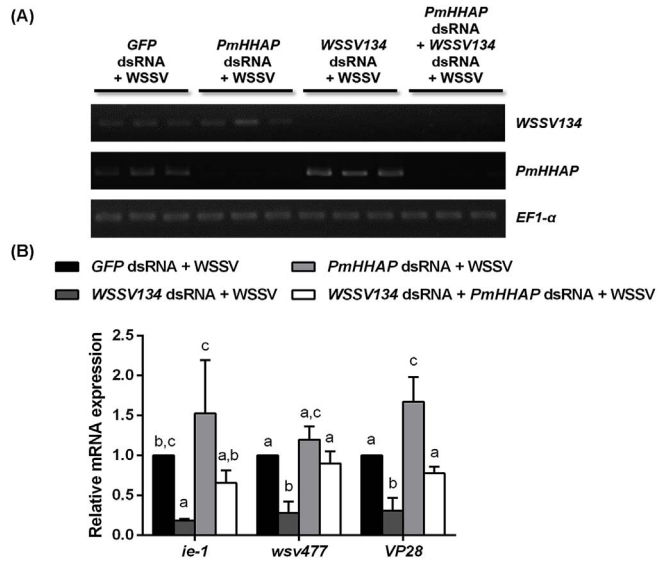


Fig. 4. Co-silencing of *PmHHAP* and *WSSV134* by RNAi. (A) The efficiency of dsRNA-mediated gene knockdown was examined using semi-quantitative RT-PCR. The transcript levels of *PmHHAP* and *WSSV134* are shown. Each condition represents a result from three independent shrimp. *EF1-α* was used as an internal control gene. (B) The expression levels of representative WSSV genes for three stages of WSSV infection, including *ie-1* (immediate-early gene), *wsv477* (early gene), and *VP28* (late gene), were determined using qRT-PCR. The data are shown as means ± 1 SD derived from three independent shrimp. *EF1-α* was used as an internal control gene to normalize the cDNA sample. Different letters indicate significant differences accepted at $P < 0.05$.

3.6. Caspase 3/7 activity in hemocytes of PmHHAP and WSSV134 co-silencing shrimp

To better understand the function of *Pm*HHAP and WSSV134 in hemocyte apoptosis in viral infection, the level of enzyme caspase 3/7 activity was measured in *PmHHAP* and *WSSV134* co-silenced shrimp, relative to that of the controls. After WSSV infection, caspase 3/7 activity was significantly greater in *PmHHAP* and *WSSV134* co-silenced shrimp than in control PBS-injected shrimp (Fig. 5). A significant difference was also observed in the *PmHHAP*- and *WSSV134*-knockdown groups compared to the control *GFP*-knockdown and PBS groups (Fig. 5). Shrimp co-silenced with *PmHHAP* and *WSSV134* had the highest caspase 3/7 activity in hemocytes relative to the *PmHHAP*-

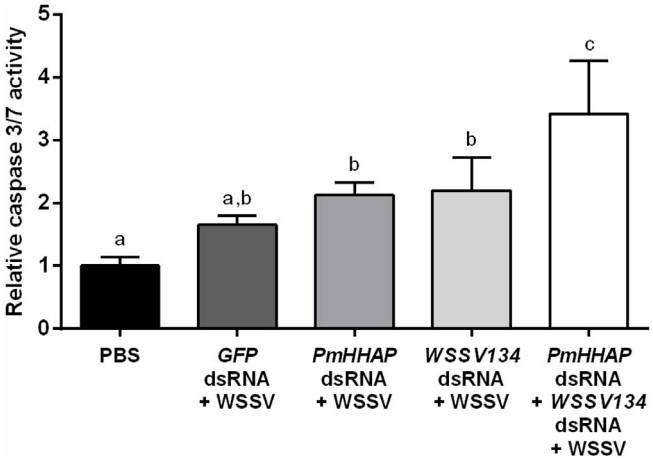


Fig. 5. Caspase activity assay of hemocytes of shrimp co-silenced with *PmHHAP* and *WSSV134*. Shrimp were injected with *PmHHAP* dsRNA, *WSSV134* dsRNA, or *GFP* dsRNA, followed by WSSV injection. The hemocytes were collected 48 h later, and subjected to HLS preparation, and then measured for caspase 3/7 activity. The column represents means ± 1 SD derived from three individual shrimp. Different letters indicate significant differences accepted at $P < 0.05$.

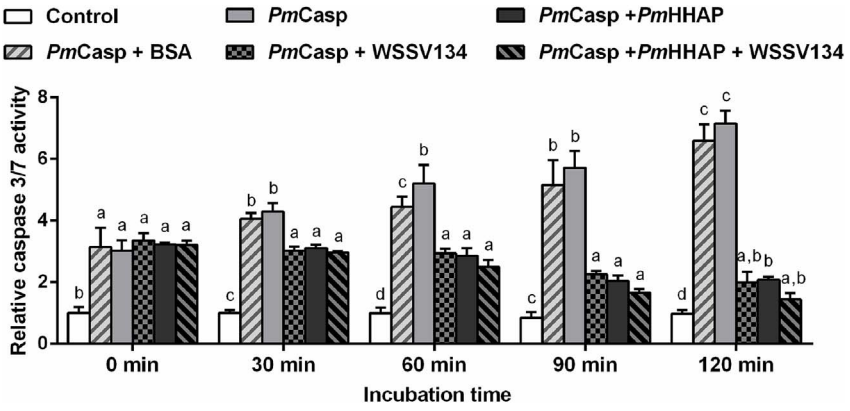


Fig. 6. *In vitro* inhibition of r*Pm*Casp-induced caspase activation by r*Pm*HHAP and rWSSV134. The r*Pm*Casp was incubated with r*Pm*HHAP or rWSSV134 or co-incubated with both r*Pm*HHAP and rWSSV134. The control groups were r*Pm*Casp only and r*Pm*Casp incubated with BSA, and the negative control was PBS buffer. Caspase 3/7 activity was measured at 0, 30, 60, 90, and 120 min. The results are expressed as the mean ± SD of three replicates. Means with different lowercase letters are significantly different ($P < 0.05$).

silenced shrimp, *WSSV134*-silenced shrimp, and other control groups, which suggests that these two proteins may interact and function in controlling hemocyte apoptosis during WSSV infection.

3.7. *In vitro* inhibition of rPmCasp-induced caspase activation by rPmHHAP and rWSSV134

Recently, both *Pm*HHAP and WSSV134 have been found to function as anti-apoptotic proteins via interactions with *Pm*Casp protein [25,29]. To investigate the ability of *Pm*HHAP and WSSV134 to inhibit caspase activity *in vitro*, the recombinant proteins were incubated with r*Pm*Casp, then caspase 3/7 activity was measured at 0, 30, 60, 90, and 120 min. Caspase 3/7 activity was induced in the reaction incubated with r*Pm*Casp in the presence and absence of BSA after 30 min, and it reached its height at 120 min compared to the control group (Fig. 6). However, inhibition of caspase activity was observed when r*Pm*Casp was incubated with either r*Pm*HHAP or WSSV134 or both proteins. No significant differences in caspase 3/7 activity were observed among the groups of r*Pm*Casp incubated with r*Pm*HHAP or rWSSV134 or co-incubated with r*Pm*HHAP and rWSSV134. This suggests that *Pm*HHAP and WSSV134 inhibit caspase activity induced by r*Pm*Casp.

3.8. Non-competitive inhibition of PmCasp by PmHHAP and WSSV134

To determine the kinetics of *Pm*Casp inhibition by *Pm*HHAP and WSSV134, r*Pm*Casp was incubated with various concentrations of the substrate (0, 0.025, 0.05, and 0.1 mM) and r*Pm*HHAP and/or rWSSV134 (0, 0.08, and 0.16 mM). The obtained data were analyzed and a Michaelis–Menten kinetics graph was constructed. r*Pm*HHAP and rWSSV134 inhibited enzyme activity in a concentration-dependent manner (Fig. 7). The Michaelis–Menten constant (K_m) remained constant, but the maximal velocity (V_{max}) decreased, which suggests that both *Pm*HHAP and WSSV134 act as non-competitive inhibitors of *Pm*Casp.

4. Discussion

WSSV is a virulent pathogen that has caused devastating losses to the shrimp industry worldwide [16]. The genome of WSSV is about 300 kbp, with approximately 515 putative ORFs, and it has been isolated in Thailand, Taiwan, China, and Korea [7,8,31]. The WSSV-TH genome, with 184 ORFs, has been assigned a putative function, and the structural proteins of WSSV have been identified [10], but the roles of most WSSV proteins remain to be elucidated. It has been found that WSSV enters its host cell by activating the endocytotic processes [32]. Because WSSV does not have its own transcription machinery, it needs the machinery of its host to promote viral replication [9]. The host has also evolved a mechanism to reduce viral replication. To counteract host cellular responses, viruses have to interact with host proteins to retain an appropriate environment for replication [16]. However, the molecular mechanism of the host–virus interaction is not yet well established.

In shrimp, apoptosis is a powerful antiviral mechanism implicated as the cause of mortality as the terminal result of viral infection [33,34]. The major consequence of apoptosis is the abortion of virus multiplication by the lysis of the infected cell, resulting in a defense mechanism against the virus in the host [19]. In general, WSSV has the ability to avoid apoptosis in infected cells, prolonging the viability of the host cells until its progeny viruses are successfully produced [19,35]. Some viruses induce apoptosis to facilitate the spread of their progeny to neighboring cells in a late stage of infection [20]. Apoptosis has been documented to occur in shrimp during WSSV infections [9]. The suppression of *Pj*Caspase and also *Lv*caspases leads to the inhibition of apoptosis and increases in WSSV replication [36,37]. Several proteins involved in apoptosis in either the host or WSSV have been characterized. The viral proteins VP41B and VP38 are able to bind to *Pj*Caspase promoter and activate or repress *Pj*Caspase promoter activity, respectively [38]. AAP-1 (ORF390 or WSSV449), an anti-apoptosis protein of WSSV, can bind to and inhibit *Pm*Caspase activity [22,36,39]. In contrast to *Pm*Caspase, another effector caspase in *P. monodon*, *Pm*Casp, interacts with other WSSV anti-apoptosis proteins, WSSV134 and WSSV322 [29]. WSSV222 functions as an anti-apoptosis protein in WSSV-infected shrimp via ubiquitin-mediated degradation of the TSL protein and also facilitates the propagation of WSSV [23]. In addition, WSSV-miR-N24 can inhibit apoptosis through downregulation of caspase-8 expression and promote viral replication [40].

Interestingly, in *P. monodon*, a novel protein, namely *Pm*HHAP, is a viral-responsive protein that plays an essential role in shrimp survival and an important role in controlling hemocyte homeostasis [24]. The transcription levels of *Pm*HHAP and its protein are dramatically upregulated upon WSSV infection [24]. The suppression of *PmHHAP* could alter the mRNA expression of specific effector caspase and lead to increases in apoptosis in hemocytes [25]. In addition, *Pm*HHAP may interact with *Pm*Casp via the p20 domain and has the ability to reduce caspase activity in r*Pm*Casp-treated HLS, which indicates the role of *Pm*HHAP in hemocyte homeostasis through the regulation of the apoptotic mechanism [25]. These results indicate that the responses of *Pm*HHAP to WSSV infection would promote the inhibition of apoptosis to prevent massive mortality in shrimp during viral infection.

To gain more insight into the role of *Pm*HHAP responses following WSSV challenge, we characterized the protein–protein interactions between *Pm*HHAP and WSSV. *Pm*HHAP interacted with WSSV134, WSSV362, and WSSV395. Next, we analyzed the transcripts of *WSSV134*, *WSSV362*, and *WSSV395* expressed in a late phase of infection, following a previous study [41]. In previous studies, WSSV134 (VP36A), WSSV362 (VP39A), and WSSV395 (VP39B) have been reported to be structural proteins; WSSV134 and WSSV362 have been reported to be tegument proteins and WSSV395 is an envelope protein

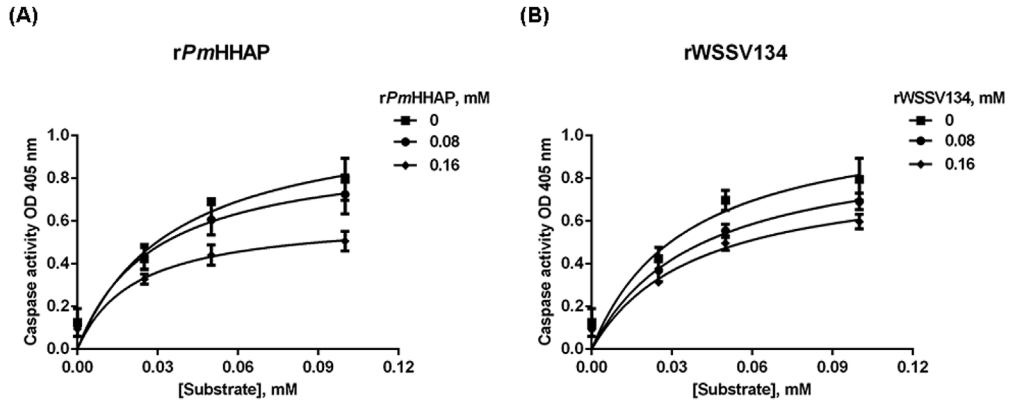


Fig. 7. Inhibition kinetics of caspase activity. (A) r*Pm*Casp was incubated with different concentrations of DEVD-pNA substrate (0, 0.025, 0.05, and 0.1 mM) and various concentrations of r*Pm*HHAP (0, 0.08, and 0.16 mM). (B) Various concentrations of rWSSV134 (0, 0.08, and 0.16 mM). After incubation for 3 h, caspase-specific activity was measured at an absorbance of 405 nm and plotted against the molar ratio of r*Pm*HHAP and rWSSV134.

	r*Pm*HHAP (mM)			rWSSV134 (mM)		
	0	0.08	0.16	0	0.08	0.16
K_m	0.025	0.028	0.022	0.035	0.039	0.038
V_{max}	1.105	0.935	0.619	1.104	0.961	0.842
K_{cat}	110.5	11.69	3.874	110.4	12.12	5.264

[41–44]. WSSV134 has also been identified as a novel anti-apoptosis protein in WSSV, which can bind to the p20 domain of the *Pm*Casp protein and reduces apoptosis induced by *Pm*Casp in Sf-9 cells [29]. Recently, evidence has been found that WSSV134 can inhibit *Pm*Casp in a dose-dependent manner, and that residue D104A is important for inhibiting *Pm*Casp activity [45]. Furthermore, yeast two-hybrid screening has shown that WSSV134 and WSSV395 can interact with WSSV517, but this interaction host not been extensively investigated [43]. Unfortunately, information on WSSV362 remains incomplete. Because WSSV134 is an anti-apoptosis protein that can interact with *Pm*Casp, similar to *Pm*HHAP, this gene was selected for further study.

In this study, suppression of *WSSV134* led to a decrease in the transcription level of the WSSV genes involved in viral replication, including *ie-1*, *wsv477*, and *VP28* [46–48], showing that WSSV134 might play an important role in viral propagation. By contrast, knockdown of *PmHHAP* resulted in increases in the transcription of these three genes, which indicates that *PmHHAP* might be important for shrimp in delaying the initial outbreak of WSSV. However, no significant impact of the transcription level of those genes was found in co-silencing the *PmHHAP* and *WSSV134* genes prior to WSSV infection. In addition, increases in caspase 3/7 activity were observed in the co-silencing of the *PmHHAP* and *WSSV134* genes prior to WSSV infection, which suggests the importance of *Pm*HHAP and WSSV134 in hemocyte apoptosis during viral infection. After WSSV infection, the total level of hemocytes dramatically decreases, whereas the level of apoptosis in hemocytes dramatically increases over time; these factors could contribute to the death of infected shrimp [49–51]. Therefore, it is possible that the responses of *Pm*HHAP during infection control viral-triggered apoptosis and help shrimp survive, while also restricting viral replication and spread. WSSV134 was found to be important for counteracting this cellular response, supporting viral replication, and possibly responding by controlling the extent of the apoptosis to reach optimal viral amplification.

Both *Pm*HHAP and WSSV134 can bind to *Pm*Casp protein via the p20 domain [25,29]. Therefore, we hypothesized that these three proteins might work in concordance to control apoptosis during viral infection. An *in vitro* inhibition assay showed no significant differences in caspase 3/7 activity among the groups of r*Pm*Casp incubated with r*Pm*HHAP and rWSSV134, and co-incubated with r*Pm*HHAP and rWSSV134. Moreover, we found that r*Pm*HHAP and rWSSV134 inhibited enzyme activity in a concentration-dependent manner and might act as non-competitive inhibitors of *Pm*Casp.

Apoptosis is a double-edged sword, such that if it is limited, it can eliminate an invading virus and contribute to a reduction in cumulative mortality in infected shrimp, while on the other hand, if apoptosis is extensive, the infected host will die. Our investigation found that the regulation of the host *Pm*HHAP and expression of the viral protein WSSV134 are very important during WSSV infection. Based on our results, we propose *Pm*HHAP as a control for virus-induced apoptosis, and the absence of this gene could enhance viral replication. WSSV134 was found to have an important role in viral propagation. Taken together, these findings imply that *Pm*HHAP might counteract WSSV134 and control apoptosis triggered by WSSV to protect shrimp from their demise rather than causing shrimp death. However, further research is required to reveal the exact mechanism underlying the interaction between apoptosis in shrimp and WSSV during viral infection.

Acknowledgments

This work was supported by a Thailand Research Fund (TRF) grant to AT (TRF Senior Scholar No. RTA5880004). Additional support from TRF (grant no. IRG5780008) to the Department of Biochemistry, Faculty of Science, Chulalongkorn University is acknowledged. KA is the recipient of a student fellowship from the Royal Golden Jubilee Ph.D. Program, Joint Funding of the Thailand Research Fund and Chulalongkorn University. We would also like to thank Chulalongkorn University for their support of the Center of Excellence for Molecular Biology and Genomics of Shrimp.

References

[1] T.W. Flegel, Major viral diseases of the black tiger prawn (*Penaeus monodon*) in Thailand, World J. Microbiol. Biotechnol. 13 (1997) 433–442.
[2] C. Escobedo-Bonilla, V. Alday-Sanz, M. Wille, P. Sorgeloos, M. Pensaert, H.A. Nauwynck, A review on the morphology, molecular characterization, morphogenesis and pathogenesis of white spot syndrome virus, J. Fish. Dis. 31 (2008) 1–18.
[3] C.F. Lo, J.H. Leu, C.H. Ho, C.H. Chen, S.E. Peng, Y.T. Chen, C.M. Chou, P.Y. Yeh, C.J. Huang, H.Y. Chou, C.H. Wang, G.H. Kou, Detection of baculovirus with white spot syndrome (WSBV) in penaeid shrimps using polymerase chain reaction, Dis. Aquat. Org. 25 (1996) 133–141.
[4] P.S. Chang, C.F. Lo, Y.C. Wang, G.H. Kou, Identification of white spot syndrome associated baculovirus (WSBV) target organs in the shrimp *Penaeus monodon* by in situ hybridization, Dis. Aquat. Org. 27 (1996) 131–139.
[5] C.S. Wang, K.F. Tang, G.H. Kou, S.N. Chen, Light and electron microscopic evidence of white spot disease in the giant tiger shrimp, *Penaeus monodon* (Fabricius), and the kuruma shrimp, *Penaeus japonicus* (Bate), cultured in Taiwan, J. Fish. Dis. 20 (1997) 323–331.
[6] S. Durand, D.V. Lightner, R.M. Redman, J.R. Bonami, Ultrastructure and morphogenesis of white spot syndrome baculovirus (WSSV), Dis. Aquat. Org. 29 (1997)

205–211.
[7] M.C.W. Van Hulten, J. Witteveldt, S. Peters, N. Kloosterboer, R. Tarchini, M. Fiers, H. Sandbrink, R.K. Lankhorst, J.M. Vlak, The white spot syndrome virus DNA genome sequence, Virology 286 (2001) 7–22.
[8] L.L. Chen, H.C. Wang, C.J. Huang, S.E. Peng, Y.G. Chen, S.J. Lin, W.Y. Chen, C.F. Dai, H.T. Yu, C.H. Wang, C.F. Lo, Transcriptional analysis of the DNA polymerase gene of shrimp white spot syndrome virus, Virology 301 (2002) 136–147.
[9] B. Verbruggen, L.K. Bickley, A.R. Van, K.S. Bateman, G.D. Stentiford, E.M. Santos, C.R. Tyler, Molecular mechanisms of white spot syndrome virus infection and perspectives on treatments, Viruses 8 (23) (2016).
[10] J.H. Leu, F. Yang, X. Zhang, X. Xu, G.H. Kou, C.F. Lo, Whispovirus, Curr. Top. Microbiol. Immunol. 328 (2009) 197–227.
[11] P. Jiravanichpaisal, B.L. Lee, K. Söderhäll, Cell-mediated immunity in athropods: hematopoiesis, coagulation, melanization and opsonization, Immunobiology 211 (2006) 213–236.
[12] A. Tassanakajon, K. Somboonwiwat, P. Supungul, S. Tang, Discovery of immune molecules and their crucial functions in shrimp immunity, Fish Shellfish Immunol. 34 (2013) 954–967.
[13] H. Liu, K. Söderhäll, P. Jiravanichpaisan, Antiviral immunity in crustaceans, Fish Shellfish Immunol. 27 (2009) 79–88.
[14] P.H. Wang, T. Huang, X. Zhang, J.G. He, Antiviral defense in shrimp: from innate immunity to viral infection, Antivir. Res. 108 (2014) 129–141.
[15] K. Sritunyalucksana, T. Utairungsee, R. Sirikharin, J. Srisala, Virus-binding proteins and their roles in shrimp innate immunity, Fish Shellfish Immunol. 33 (2012) 1269–1275.
[16] M.S. Shekhar, A.G. Ponniah, Recent insights into host-pathogens interaction in white spot syndrome virus infected penaeid shrimp, J. Fish. Dis. 38 (2015) 599–612.
[17] M. Aubert, K.R. Jerome, Apoptosis prevention as a mechanism of immune evasion, Int. Rev. Immunol. 22 (2003) 361–371.
[18] J.H. Leu, S.J. Lin, J.Y. Huang, T.C. Chen, C.F. Lo, A model for apoptotic interaction between white spot syndrome virus and shrimp, Fish Shellfish Immunol. 34 (2013) 1011–1017.
[19] A.H. Koyama, T. Fukumori, M. Fujita, H. Irie, A. Adachi, Physiological significance of apoptosis in animal virus infection, Microb. Infect. 2 (2000) 1111–1117.
[20] S.M. Best, Viral subversion of apoptotic enzymes: escape from death row, Annu. Rev. Microbiol. 62 (2008) 171–192.
[21] N.A. Thornberry, Caspases: key mediators of apoptosis, Chem. Biol. 5 (1998) R97–R103.
[22] J.H. Leu, H.C. Wang, G.H. Kou, C.F. Lo, *Penaeus monodon* caspase is targeted by a white spot syndrome virus anti-apoptosis protein, Dev. Comp. Immunol. 32 (2008) 476–486.
[23] F. He, S.M. Syed, A.S. Hameed, J. Kwang, Viral ubiquitin ligase WSSV222 is required for efficient white spot syndrome virus replication in shrimp, J. Gen. Virol. 90 (2009) 1483–1490.
[24] A. Prapavorarat, T. Vatanavicharn, K. Söderhäll, A. Tassanakajon, A novel viral responsive protein is involved in hemocyte homeostasis in the black tiger shrimp, *Penaeus monodon*, J. Biol. Chem. 285 (2010) 21467–21477.
[25] K. Apitanyasai, P. Amparyup, W. Charoensapsri, S. Senapin, A. Tassanakajon, Role of *Penaeus monodon* hemocyte homeostasis associated protein (*Pm*HHAP) in regulation of caspase-mediated apoptosis, Dev. Comp. Immunol. 53 (2015) 234–243.
[26] W. Charoensapsri, P. Sangsuriya, T. Lertwimol, W. Gangnonngiw, K. Phiwsaiya, S. Senapin, Laminin receptor protein is implicated in hemocyte homeostasis for the whiteleg shrimp *Penaeus (Litopenaeus) vannamei*, Dev. Comp. Immunol. 51 (2015) 39–47.
[27] K. Apitanyasai, C. Noonin, A. Tassanakajon, I. Söderhäll, K. Söderhäll, Characterization of a hemocyte homeostasis-associated-like protein (HHAP) in the freshwater crayfish *Pacifastacus leniusculus*, Fish Shellfish Immunol. 58 (2016) 429–435.
[28] R.D. Gietz, R.H. Schiestl, A.R. Willems, R.A. Woods, Studies on the transformation of intact yeast cells by the LiAc/SS-DNA/PEG procedure, Yeast 11 (1995) 355–360.
[29] T. Lertwimol, P. Sangsuriya, K. Phiwsaiya, S. Senapin, A. Phongdara, C. Boonchird, T.W. Flegel, Two new anti-apoptotic proteins of white spot syndrome virus that bind to an effector caspase (*Pm*Casp) of the giant tiger shrimp *Penaeus (Penaeus) monodon*, Fish Shellfish Immunol. 38 (2014) 1–6.
[30] Y.B. Zhu, H.Y. Li, F. Yang, Identification of an envelope protein (VP39) gene from shrimp white spot syndrome virus, Arch. Virol. 151 (2006) 71–82.
[31] C.Y. Chai, J. Yoon, Y.S. Lee, Y.B. Kim, T.J. Choi, Analysis of the complete nucleotide sequence of a white spot syndrome virus isolated from pacific white shrimp, J. Microbiol. 51 (2013) 695–699.
[32] J. Huang, F. Li, J. Wu, F. Yang, White spot syndrome virus enters crayfish hematopoietic tissue cells via clathrin-mediated endocytosis, Virology 486 (2015) 35–43.
[33] H. Everett, G. McFadden, Apoptosis: an innate immune response to virus infection, Trends Microbiol. 7 (1999) 160–165.
[34] F. Li, J. Xiang, Signaling pathways regulating innate immune responses in shrimp, Fish Shellfish Immunol. 34 (2013) 973–980.
[35] A.H. Koyama, A. Adachi, H. Irie, Physiological significance of apoptosis during animal virus infection, Int. Rev. Immunol. 22 (2003) 341–359.
[36] L. Wang, B. Zhi, W. Wu, X. Zhang, Requirement for shrimp caspase in apoptosis against virus infection, Dev. Comp. Immunol. 32 (2008) 706–715.
[37] P.H. Wang, D.H. Wan, Y.G. Chen, S.P. Weng, X.Q. Yu, J.G. He, Characterization of four novel caspases from *Litopenaeus vannamei* (*Lv*caspase2–5) and their role in WSSV infection through dsRNA-mediated gene silencing, PLoS One 8 (2013) e80418.
[38] H. Zuo, C. Chen, Y. Gao, J. Lin, C. Jin, W. Wang, Regulation of shrimp *Pj*Caspase promoter activity by WSSV VP38 and VP41B, Fish Shellfish Immunol. 30 (2011) 1188–1191.
[39] J.H. Leu, L.L. Chen, Y.R. Lin, G.H. Kou, C.F. Lo, Molecular mechanism of the interactions between white spot syndrome virus anti-apoptosis protein AAP-1 (WSSV449) and shrimp effector caspase, Dev. Comp. Immunol. 34 (2010) 1068–1074.
[40] T. Huang, Y. Cui, X. Zhang, Involvement of viral microRNA in the regulation of antiviral apoptosis in shrimp, J. Virol. 88 (2014) 2544–2554.
[41] J.M. Tsai, H.C. Wang, J.H. Leu, H.H. Hsiao, A.H. Wang, G.H. Kou, C.F. Lo, Genomic and proteomic analysis of thirty-nine structural proteins of shrimp white spot syndrome virus, J. Virol. 78 (2004) 11360–11370.
[42] Z. Li, Q. Lin, J. Chen, J.L. Wu, T.K. Lim, S.S. Loh, X. Tang, C.L. Hew, Shotgun identification of the structural proteome of shrimp white spot syndrome virus and iTRAQ differentiation of envelope and nucleocapsid subproteomes, Mol. Cell. Proteomics 6 (2007) 1609–1620.
[43] P. Sangsuriya, J.Y. Huang, Y.F. Chu, K. Phiwsaiya, P. Leekitcharoenphon, W. Meemetta, S. Senapin, W.P. Huang, B. Withyachumnarnkul, T.W. Flegel, C.F. Lo, Construction and application of a protein interaction map for white spot syndrome virus (WSSV), Mol. Cell. Proteomics 13 (2014) 269–282.
[44] J.M. Tsai, H.C. Wang, J.H. Leu, A.H. Wang, Y. Zhuang, P.J. Walker, G.H. Kou, C.F. Lo, Identification of the nucleocapsid, tegument, and envelope proteins of the shrimp white spot syndrome virus virion, J. Virol. 80 (2006) 3021–3029.
[45] T. Bowornsakulwong, W. Charoensapsri, T. Rattanarojpong, P. Khunrae, The expression and purification of WSSV134 from white spot syndrome virus and its inhibitory effect on caspase activity from *Penaeus monodon*, Protein. Expr. Purif 130 (2017) 123–128.
[46] M.C.M. Van Hulten, J. Witteveldt, M. Snippe, J.M. Vlak, White spot syndrome virus envelope protein VP28 is involved in the systemic infection of shrimp, Virology 285 (2001) 228–233.
[47] W.J. Liu, Y.S. Chang, C.H. Wang, G.H. Kou, C.F. Lo, Microarray and RT-PCR screening for white spot syndrome virus immediate-early genes in cycloheximide-treated shrimp, Virology 334 (2005) 327–341.
[48] F. Han, J. Xu, X. Zhang, Characterization of an early gene (wsv477) from shrimp white spot syndrome virus (WSSV), Virus Gene. 34 (2007) 193–198.
[49] T.W. Flegel, T. Pasharawipas, Active viral accommodation: a new concept for crustacean response to viral pathogens, in: T.W. Flegel (Ed.), Advances in Shrimp Biotechnology, National Center for Genetic Engineering and Biotechnology, Bangkok, 1998, pp. 245–250.
[50] A.H. Sahtout, M.D. Hassan, M. Shariff, DNA fragmentation, an indicator of apoptosis, in cultured black tiger shrimp *Penaeus monodon* infected with white spot syndrome virus (WSSV), Dis. Aquat. Org. 44 (2001) 155–159.
[51] K. Wongprasert, K. Khanobdee, S.S. Glunukarn, P. Meeratana, B. Withyachumnarnkul, Time-course and levels of apoptosis in various tissues of black tiger shrimp *Penaeus monodon* infected with white-spot syndrome virus, Dis. Aquat. Org. 55 (2003) 3–10.

Fish and Shellfish Immunology 77 (2018) 147–155

Contents lists available at ScienceDirect

Fish and Shellfish Immunology

journal homepage: www.elsevier.com/locate/fsi

Full length article

Antimicrobial activity of a serine proteinase inhibitor SPI*Pm*5 from the black tiger shrimp *Penaeus monodon*

Sittichai Boonrawd[a], Premruethai Supungul[b], Anchalee Tassanakajon[a], Vichien Rimphanitchayakit[a,*]

[a] *Center of Excellence for Molecular Biology and Genomics of Shrimp, Department of Biochemistry, Faculty of Science, Chulalongkorn University, Phyathai Road, Bangkok, 10330, Thailand*

[b] *National Center for Genetic Engineering and Biotechnology (BIOTEC), National Science and Technology Development Agency (NSTDA), Pathum Thani, 10120, Thailand*

ARTICLE INFO

Keywords:
Kazal-type serine proteinase inhibitor
Penaeus monodon
WSSV
YHV
Vibrio parahaemolyticus

ABSTRACT

A two-domain Kazal-type serine proteinase inhibitor, SPI*Pm*5, from *Penaeus monodon* was studied. Its transcript was expressed in all tissues tested including the hemocytes, stomach, gill, lymphoid organ, muscle, intestine and heart albeit less in hepatopancreas and eyestalk. The expression of *SPIPm5* gene was also up-regulated by heat stress, white spot syndrome virus (WSSV) infection and yellow head virus (YHV) infection. Injection of recombinant rSPI*Pm*5 protein into normal shrimp to mimic heat stress condition did not have or had little stimulating effect on the expression of other immune genes: *crustinPm1*, *penaeidin3*, *penaeidin5*, *Hsp70*, *SPIPm2* and *SPIPm5*. Like some other proteinase inhibitors, the rSPI*Pm*5 could inhibit the hemolymph proPO activity. In survival experiments, the rSPI*Pm*5 could prolong the life of WSSV-infected shrimp similar to the effect of heat stress. The rSPI*Pm*5 also helped the YHV-, *Vibrio harveyi*- and *V. parahaemolyticus*-infected shrimp survive longer. The increased endurance against microbial infection was due to the inhibitory effects presumably activated by rSPI*Pm*5 on viral replication and bacterial growth but not the expression of antimicrobial peptides. Therefore, the SPI*Pm*5 plays an important role in shrimp innate immunity against the viral and bacterial infection.

1. Introduction

Invertebrates rely on innate immunity, which are cellular and humoral responses, to defense themselves against pathogenic invaders. The defense responses are phagocytosis, blood coagulation, melanization, etc. The humoral defense involves the soluble components such as antimicrobial peptides (AMPs), proteinase inhibitors and cytokine-like protein [1,2]. The proteinase inhibitors come into play in the innate immune responses because several immune response processes are proteinase-mediated [3]. Several types of proteinase inhibitors are found in living organisms such as serpins, Kunitz-type inhibitors, Kazal-type inhibitors, Bowman-Birk inhibitors, pacifastin, etc. [4].

The Kazal-type serine proteinase inhibitors (KPIs) are characterized by one or more inhibitory domains of about 40–60 amino acid residues. The domain structure is formed by three intra-domain disulfide cross-links among six conserved cysteine residues [5]. The specificity of proteinase inhibition is mainly determined by the P1 amino acid for the side chain of P1 amino acid can fit into a pocket within the active site of a cognate proteinase. The inhibition of proteinase is a competitive-type inhibition [3,5].

In crustacean, the KPIs are implicated in host defenses against the pathogen infection because their expression is changed in response to microbial infection. In Chinese shrimp, *Fenneropenaeus chinensis*, the *FcSPI* genes are up-regulated in response to bacterial and viral infection [6,7]. In freshwater crayfish, *Procambarus clarkii*, the expression of four KPIs, *hcPcSPI1-4*, are changed by microbial infection. The *hcPcSPI1* and *hcPcSPI2* also possess bacteriostatic activity against the *Bacillus subtilis* and *B. thuringiensis* [8,9]. In swimming crab, *Portunus trituberculatus*, one-domain KPI, *PtKPI*, has been identified from the hemocytes. The temporal expression of *PtKPI* is activated against bacterial and fungal challenge [10].

In black tiger shrimp, *Penaeus monodon*, there are at least 9 types of KPIs, SPI*Pm*1-9, identified from the EST database [11]. A five-domain SPI*Pm*2 is the most abundant KPI and involved in defense against pathogens [12,13]. Its domains inhibit subtilisin and elastase and possess bacteriostatic activity against *B. subtilis* [14]. The SPI*Pm*2 is produced mainly by the hemocytes, stored in the cytoplasmic granules and secreted into the circulation upon activation [15]. The expression of SPI*Pm2* is up-regulated after WSSV and YHV infection [16,17]. The two-domain SPI*Pm4* and *5* are identified from the hemocytes of heat-

* Corresponding author.
E-mail address: kpvr2@yahoo.com (V. Rimphanitchayakit).

https://doi.org/10.1016/j.fsi.2018.03.044
Received 7 March 2018; Received in revised form 23 March 2018; Accepted 27 March 2018
Available online 28 March 2018
1050-4648/ © 2018 Elsevier Ltd. All rights reserved.

treated shrimp. They have proteinase inhibitory activity but lack bacteriostatic effect against bacteria. The SPI*Pm*4 inhibits subtilisin whereas the SPI*Pm*5 inhibits subtilisin and elastase. The expression of *SPIPm5* is up-regulated by heat stress [18].

In this study, the possible function of SPI*Pm*5 and its expression in response to pathogen infection were studied in detail. The effects of recombinant SPI*Pm*5 protein on the expression of antimicrobial peptides, on the proPO activating system in hemolymph, on the survival rate of viral and bacterial infected shrimp, on the bacterial counts in hemolymph of infected shrimp and on the AMPs gene expression were elucidated.

2. Materials and methods

2.1. Shrimp

The black tiger shrimp were purchased from a local farm. The shrimp were acclimatized in seawater at ambient temperature of 28 ± 1 °C for a few days before used in the experiment.

2.2. Tissue distribution

Nine tissues were collected from the normal shrimp: hemocytes, stomach, hepatopancreas, gill, lymphoid organ, muscle, eyestalk, intestine and heart. The total RNAs were extracted using Trizol reagent (Geneaid) following the manufacturer instruction. The cDNAs were synthesized with RevertAid First Strand cDNA Synthesis Kit (Thermo Scientific). The expression of *SPIPm5* gene in various tissues was analyzed by RT-PCR. The PCR reaction mixture consisted of 1.25 unit Taq DNA polymerase (RBC), 10 μM dNTP mix, 10 μM each of forward and reverse primers and appropriately 1:10 diluted cDNA template. The PCR started with pre-denaturation at 95 °C for 3 min followed by 30 cycles for *SPIPm5* or 25 cycles for *EF-1α* of denaturation at 95 °C for 1 min, annealing at 55 °C for 30 s and extension at 72 °C for 1 min, and ended with final extension at 72 °C for 10 min. The PCR products were analyzed by agarose gel electrophoresis. The expression of *EF-1α* was used as an internal control.

2.3. SPIPm5 was up-regulated under heat stress

To confirm that the *SPIPm5* was up-regulated after the shrimp were exposed to heat stress [18], the shrimp were heat shocked at 33 °C in seawater for 1 h and reared at ambient temperature. The hemolymph was, then, collected from three shrimp each at 24 and 48 h for total RNA preparation. The expression of *SPIPm5* gene was investigated along with that of *Hsp70* gene by RT-PCR. The hemolymph from shrimp reared at ambient temperature were also collected as a control group. The experiment was done in triplicate. The total RNAs were extracted with Trizol reagent and the cDNAs were synthesized as described above. The expression of *SPIPm5* and *Hsp70* were amplified by RT-PCR using specific primers (Table 1). The gene expression was analyzed by agarose gel electrophoresis. The expression of *EF-1α* was used as an internal control.

2.4. Expression of SPIPm5 gene in response to WSSV and YHV infection

The normal shrimp were divided into three groups of 45 shrimp each. The challenged group was injected with 50 μL of WSSV suspension containing 16,950 copies of WSSV that caused 100% mortality within 4 days. Another challenged group was injected with YHV dilution that killed all the shrimp within 5 days. Normal saline (0.85% NaCl) injection was done for the control group. The hemolymph was collected from 9 shrimp at each time point for each group at 3, 6, 12, 24 and 48 h for total RNA extraction and cDNA synthesis. The experiment was done in triplicate.

Expression of *SPIPm5* was analyzed with qRT-PCR using primers RTSPIPm5F and RTSPIPm5R (Table 1). The qRT-PCR was carried out in a real-time thermal cycler (Bio-Rad Laboratories). The 10-μL reaction mixture consisted of 3 μL of 1:10 diluted cDNA template, 0.2 μM of each primer and 1 × QPCR Green Master Mix LRox (Biotechrabbit) containing DNA polymerase. The PCR amplification started with pre-denaturation at 95 °C for 8 min followed by 40 cycles of denaturation at 95 °C for 30 s, and extension at 60 °C for 3 s. The expression of *EF-1α* was used as an internal control. The relative expression of *SPIPm5* was calculated using a comparative method described by Pfaffl [19]. The mean data values were derived from triplicate amplifications and expressed as means ± standard deviations. Statistical analysis was done using the One-way ANOVA followed by the Duncan's new multiple range test. Data differences were considered statistically significant at $P < 0.05$.

2.5. Expression of rSPIPm5 protein

The recombinant SPI*Pm*5 protein (rSPI*Pm*5) was expressed using an *E. coli* expression system. An expression plasmid, pET28b_SPI*Pm*5 [18], was transformed into an *E. coli* BL21-CodonPlus(DE3). A transformant was cultured in LB broth at 37 °C and induced for the protein expression by 1 mM IPTG. The cells were collected by centrifugation at 2500 g, 4 °C for 20 min. The cell pellet was resuspended in phosphate buffer saline, pH 7.4 (PBS; 137 mM NaCl, 2.7 mM KCl, 10 mM Na_2HPO_4, 2 mM KH_2PO_4) and sonicated with Sonics Vibracell VCX750 to break the cells. The soluble rSPI*Pm*5 in the cell lysate supernatant was purified with Ni-NTA agarose column and eluted with imidazole. The purified protein was dialyzed against PBS. Its purity and its concentration were analyzed by SDS-PAGE [20] and determined by Bradford assay [21], respectively. The purified rSPI*Pm*5 protein was used as an antigen for raising mouse polyclonal antiserum at the Faculty of Agriculture, Kasetsart University, Kamphaeng Saen Campus.

2.6. Effect of rSPIPm5 injection in shrimp

The normal shrimp were divided into two groups of 9 shrimp each. First group was injected with 0.5 nmol of rSPI*Pm*5 in 30 μL of PBS. The control group was injected with 30 μL of PBS. The experiment was done in triplicate. After the rSPI*Pm5* protein injection, the hemolymph was collected at 24 h for total RNA extraction and cDNA synthesis. The gene expression of *crustinPm1, penaeidin3, penaeidin5, SPIPm2, SPIPm5* and *Hsp70* were investigated by RT-PCR using specific primers (Table 1). The PCR products were analyzed by gel electrophoresis. The expression of *EF-1α* gene was used as an internal control.

2.7. Effect of SPIPm5 protein on the proPO activating system in shrimp hemolymph

Inhibitory activity of rSPI*Pm*5 on proPO activating system was investigated using a protocol described by Ponprateep et al. (2017) [22]. The hemolymph was collected from three normal shrimp and mixed with PBS at a ratio of 1:3. The protein content was determined by using Bradford assay [21]. The reactions were done by pre-incubating 200 μg protein of hemolymph with 0, 0.5, 1 and 2 nmol of rSPI*Pm*5. The PBS was used as a control. Then, 10 μL of 5 mg/mL of lipopolysaccharide (LPS) was added and incubated at 30 °C for 15 min. The reaction was adjusted to 150 μL with 50 mM Tris-HCl pH 8.0. Finally, the reaction was added 25 μL of 3 mg/mL L-3,4-dihydroxyphenylalanine (L-DOPA) at time zero to start the reaction. The proPO activity was monitored by measuring the A_{490} for 60 min with a microplate reader. The experiment was done in triplicate.

2.8. Effect of SPIPm5 on the survival of pathogen-infected shrimp

2.8.1. rSPIPm5 injection and heat stress against WSSV infection

The normal shrimp were divided into five groups of 30 shrimp each.

Table 1
Sequences of primers used in this study.

Primers	Sequences (5'→3')	Usage
RTSPIPm5F	ATTCTCTTCGCTGTGGCTGT	qRT-PCR and RT-PCR of *SPIPm5* gene
RTSPIPm5R	TCACAAGACCCATGATGCAC	
PmHsp70F	CTTCGACAACCGCATGGTGA	RT-PCR of heat shock protein 70 [25]
PmHsp70R	GAAGAGGGAGCCGATCTCCA	
RTSPIPm2F	ATGCAACCACGTCTGTACTG	RT-PCR of *SPIPm2* gene [35]
RTSPIPm2R	CTGCAAGGTTCCACATCT	
ALFPm3F	ATACTAGAATTCCAAGGGTGGGAGGCTGTGGCA	RT-PCR of *ALFPm3*, *crustinPm1*, *crustinPm7*, *penaiedin3*, *penaiedin5* and *lysozyme* genes
ALFPm3R	TATTATGGATCCCTATGAGCTGAGCCACTGGTTGGCCT	
CrustinPm1F	CTGCTGCGAGTCAAGGTATG	
CrustinPm1R	AGGTACTGGCTGCTCTACTG	
CrustinPm7F	GGCATGGTGGCGTTGTTCCT	
CrustinPm7R	TGTCGGAGCCGAAGCAGTCA	
LysozymeF	CCGTTACCAAGCCTTACTG	
LysozymeR	TAATCGGTCGCGTAGTCCTC	
Pen3F	ATGCGTCTCGTGGTCTGCCT	
Pen3R	CCTGTGAATACACGAGGA	
Pen5F	TTGGTCTATGCTTTGCAAGGG	
Pen5R	ACAGATAGTTAAAGTGAAAGAC	
VP28F	TCACTCTTTCGGTCGTGTCG	RT-PCR of WSSV (viral late gene) [35]
VP28R	CCACACACAAAGGTGCCAAC	
YHVF	GGTTTTAGGTGACATTAGGGTCT	RT-PCR of YHV gene [26]
YHVR	GATGATTGAAAGGGATTGTCG	
EF-1αF	GGTGCTGGACAAGCTGAAGGC	qRT-PCR and RT-PCR internal control gene
EF-1αR	CGTTCCGGTGATCATGTTCTTGATG	

Three groups were injected with 50 µL of 0.5 nmol rSPI*Pm*5, 0.5 nmol rSPI*Pm*5 plus WSSV and WSSV. Another two groups were injected with WSSV and PBS before they were heat-shocked at 33 °C for 1 h. The shrimp were reared at ambient temperature after heat shock. The WSSV dilution used caused 100% mortality within 4 days. The experiment was conducted in triplicate. The cumulative mortality was observed for 14 days. The survival rates of shrimp were analyzed with the GraphPad Prism.

2.8.2. rSPIPm5 against WSSV and YHV infection

The shrimp were also divided into five groups of 30 shrimp each. They were injected with 50 µL of WSSV, 0.5 nmol rSPI*Pm*5 plus WSSV, YHV, 0.5 nmol rSPI*Pm*5 plus YHV and PBS. The WSSV and YHV dilutions used caused 100% mortality within 4 and 5 days, respectively. The cumulative mortality was observed for 14 days. The survival rates of shrimp were analyzed with the GraphPad Prism.

2.8.3. rSPIPm5 against Vibrio species

The *Vibrio* bacteria from 15% glycerol stocks were grown overnight at 30 °C in tryptic soy agar plates (TSA) (HiMedia Laboratories) supplemented with 1.5% NaCl. The colonies were picked, inoculated into Tryptic soy broth (TSB) contain 1.5% NaCl and cultured at 30 °C with 100 rpm shaking for 24 h. The cell density was determined with spectrophotometer, and the bacteria were grown in TSB until the OD_{600} reached 1 which was equivalent to approximately 3×10^8 CFU/mL. For *V. harveyi*, the bacterial cells from a volume of culture were collected by centrifugation, washed and resuspended with equal volume of 0.85% normal saline. The identity of bacteria was confirmed by PCR analysis with specific primers [23,24].

The normal shrimp were divided into five groups of 30 shrimp each. For two *V. harveyi* groups, the shrimp were injected with 50 µL suspensions of 1×10^6 CFU/mL *V. harveyi* and 0.5 nmol rSPI*Pm*5 plus *V. harveyi*. For two *V. parahaemolyticus* groups, the shrimp were injected with 50 µL PBS and 0.5 nmol rSPI*Pm*5 in 50 µL PBS before they were immersed in seawater containing 1×10^6 CFU/mL *V. parahaemolyticus* [25]. The same volume of PBS was injected into the fifth group of shrimp as a control group. The two *Vibrio* dilutions used caused 100% mortality within 6–7 days. The cumulative mortality was observed for 14 days. The survival rates of shrimp were analyzed with the GraphPad Prism.

2.9. Inhibitory effect of SPIPm5 on viral replication

The normal shrimp were injected with various amounts of 0, 0.5, 2, 8 and 16 nmol of rSPI*Pm*5 plus WSSV or YHV dilutions. The viral dilutions used caused 100% mortality after injection within 4 and 5 days, respectively. The injection of PBS was for a control group. At 24 h after challenging, the hemolymph was collected from 3 shrimp for each amount of rSPI*Pm*5 for total RNA extraction and cDNA synthesis. The expression of viral genes was analyzed by RT-PCR using specific primers (Table 1); the primers for *VP28* gene for the replication of WSSV and *YHV* gene segment between ORF1b and ORF2 of the YHV genome for the replication of YHV [26]. The expression of *EF-1α* gene was used as an internal control. The experiment was done in triplicate.

2.10. Inhibitory effect of SPIPm5 on bacteria in infected shrimp

The normal shrimp were injected with 50 µL of 0, 0.5, 1 and 2 nmol of rSPI*Pm*5 plus 3×10^8 CFU/mL *V. harveyi* or immersion with 3×10^8 CFU/mL *V. parahaemolyticus* in seawater [25]. The bacterial dilution of *V. harveyi* and *V. parahaemolyticus* caused 100% mortality within 4–5 days. The hemolymph from 3 shrimp for each amount of rSPI*Pm*5 injected was collected at 5, 15, 30, 60 and 180 min after infection. The hemolymph was diluted 100-fold with normal saline and 10 µl aliquots of diluted hemolymph were dropped on the TCBS agar plates (HiMedia Laboratories). The control groups were injected with normal saline and their hemolymph was also collected for testing of bystander bacteria. The plates were incubated at 30 °C for 13–14 h. The numbers of colonies of *Vibrio* bacteria were counted [27]. Each experiment was repeated in triplicate. The data shown were means ± standard deviations. Statistical analysis was done using the One-way ANOVA followed by Duncan's new multiple rang test. Data differences were considered statistically significant at $P < 0.05$.

2.11. Effect of SPIPm5 on AMP gene expression in infected shrimp

The inhibitory effect of SPI*Pm*5 on the bacteria may be resulted from the activation of expression of antimicrobial peptides. The shrimp were injected with 50 µL of 0, 0.5, 1 and 2 nmol of rSPI*Pm*5 plus 3×10^8 CFU/mL *V. harveyi* or immersion with 3×10^8 CFU/mL *V. parahaemolyticus* in seawater [25]. The hemolymph were collected from

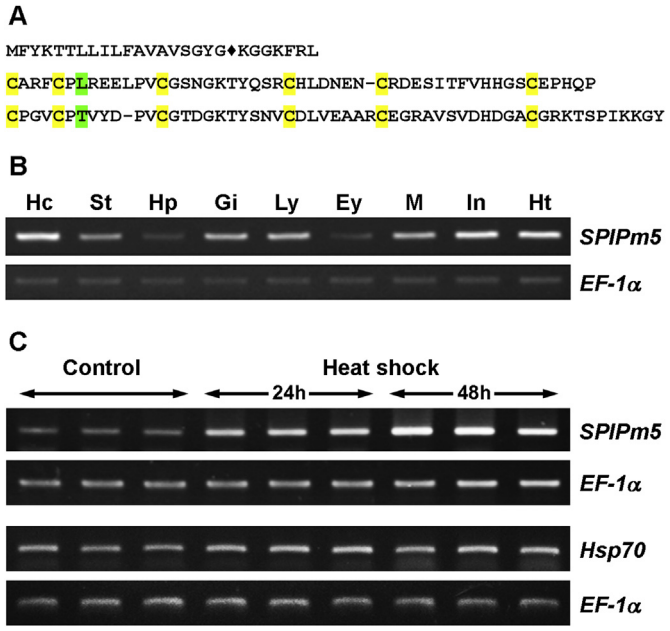


Fig. 1. The SPI*Pm*5 and its gene expression in normal shrimp tissues. (A) The complete amino acid sequence of SPI*Pm*5 showing the two Kazal domains. Black diamond indicates the potential signal peptide cleavage site. Conserved cysteine residues and the P1 amino acids are shaded yellow and green, respectively. (B) Nine tissues: hemocytes (Hc), stomach (St), hepatopancreas (Hp), gill (Gi), lymphoid organ (Ly), eyestalk (Ey), muscle (M), intestine (In) and heart (Ht) were used to detect the gene expression of *SPIPm5*. (C) Expression of *SPIPm5* and *Hsp70* genes under heat stress. The normal shrimp were exposed to heat stress at 33 °C for 1 h and then reared at ambient temperature (28 ± 1 °C). The hemolymph was collected for analysis at 24 and 48 h. The control shrimp were reared normally at ambient temperature. The expression of *SPIPm5* and *Hsp70* genes were detected by RT-PCR. The expression of *EF-1α* gene was used as an internal control. (For interpretation of the references to colour in this figure legend, the reader is referred to the Web version of this article.)

3 shrimp for each rSPI*Pm*5 injected at 1 h for total RNA extraction and cDNA synthesis. The control groups were injected with normal saline. The expression of AMP genes: *ALFPm3*, *crustinPm1*, *crustinPm7*, *penaeidin3*, *penaeidin5* and *lysozyme*, was analysed by RT-PCR using specific primers (Table 1). The PCR products were analysed by agarose gel electrophoresis. The gene expression of *EF-1α* gene was used as an internal control.

3. Results

The SPI*Pm*5 is a two-domain Kazal type serine proteinase inhibitor (KPI) with the P1 residues Leu and Thr capable of inhibiting subtilisin and elastase (Fig. 1 A). The *SPIPm5* gene was identified from the hemocyte cDNA library of heat-stressed shrimp and up-regulated upon heat-treatment as well as YHV infection. It is assumed that the SPI*Pm*5 may have important function in host physiological system involving stresses [18]. Herein, we investigated its activities further.

3.1. Expression of SPIPm5 gene in shrimp tissues

To find out how the *SPIPm5* was expressed in the shrimp. The tissue distribution of *SPIPm5* transcripts were examined by RT-PCR and detected the expression in all nine tissues studied: hemocytes, stomach, hepatopancreas, gill, lymphoid organ, eyestalk, muscle, intestine and heart. The expression was less in hepatopancreas and eyestalk (Fig. 1 B). For further experiments, the hemocytes were used in the studies.

3.2. Up-regulation of SPIPm5 gene expression under heat stress

In this experiment, the normal shrimp were exposed to heat shock temperature at 33 °C for 1 h and reared at ambient temperature afterwards [18]. Under this heat shock condition, whether the *SPIPm5* gene expression was up-regulated was tested. It was found that the expression of *SPIPm5* was increased with time at 24 and 48 h. The expression of *Hsp70*, a positive control [28,29], was also increased slightly at the same time points. Therefore, the heat shock at 33 °C for 1 h induced the expression of *SPIPm5* gene up to 48 h (Fig. 1 C).

3.3. Expression of SPIPm5 gene in response to WSSV and YHV infection

In the hemocyte cDNA libraries from the WSSV and YHV infected shrimp, the *SPIPm5* clones are detected [30,31]. The expression of *SPIPm5* gene in response to the WSSV and YHV infection was examined. The normal shrimp were challenged with WSSV and YHV and the hemolymph was collected at 3, 6, 12, 24 and 48 h after virus injection. The *SPIPm5* gene expression was detected by qRT-PCR. The results in Fig. 3 show that the expression of *SPIPm5* gene was increased significantly at 3 and 12 h after injection for both viruses (Fig. 2).

3.4. rSPIPm5 protein expression

To study the activity of SPI*Pm*5 protein, the rSPI*Pm*5 protein was over-expressed. The soluble recombinant SPI*Pm*5 protein with MW of

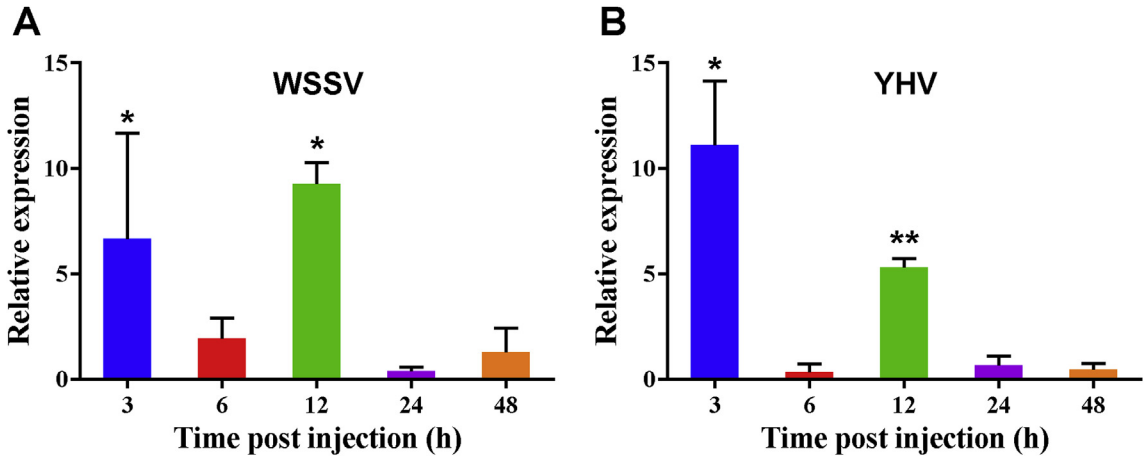


Fig. 2. Expression of *SPIPm5* gene in response to WSSV (A) and YHV (B) infection. The normal shrimp were injected with WSSV and YHV. The expression of *SPIPm5* gene was analyzed by qRT-PCR from hemocytes at various times. The results are means ± SDs of three independent amplifications. The * and ** indicate significant differences ($P < 0.05$) over normal saline control. The expression of *EF-1α* gene was used as an internal control.

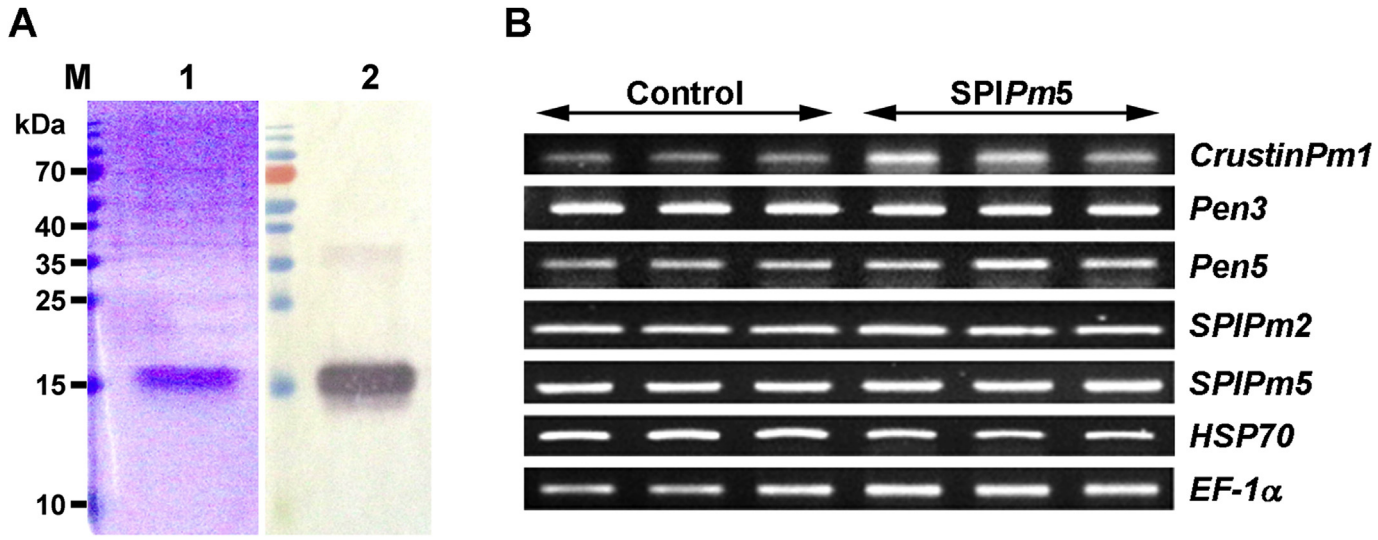


Fig. 3. The purified rSPI*Pm*5 protein and its effect on the expression of other immune genes. (A) The rSPI*Pm*5 was purified through the Nickel-NTA column and analyzed by SDS-PAGE (lane 1) and Western blot analysis (lane 2). Lane M is a protein standard marker. (B) The normal shrimp were injected with 0.5 nmol of rSPI*Pm*5. The hemolymph was collected at 24 h after rSPI*Pm*5 injection. Gene expression of *crustinPm1*, *penaeidin3*, *penaeidin5*, *SPIPm2*, *SPIPm5* and *Hsp70* was analyzed by semi-quantitative RT-PCR. The control shrimp were injected with 1 × PBS. The *EF-1α* was used as an internal control.

17 kDa was purified and the expressed protein was shown to be pure rSPI*Pm*5 by Western blot analysis using the anti-SPI*Pm*5 antibody (Fig. 3 A).

3.5. Effect of rSPIPm5 injection on the expression of other immune-related genes

Upon virus infection, the expression of SPI*Pm*5 was up-regulated. The increase in the SPI*Pm*5 protein in the circulating system may influence the expression of other immune genes in the defense processes against infection. To mimic the similar situation in infected shrimp, the rSPI*Pm*5 was injected into the normal shrimp. The expression of other immune genes: *crustinPm1*, *penaedin3*, *penaedin5*, *SPIPm2*, *SPIPm5* and *Hsp70*, was, then, tested. It was found that the expression of *crustinPm1* but not *penaeidin3* was induced. That of *penaeidin5* was slightly increased (Fig. 3 B). The injection of rSPI*Pm*5 had no effect on the expression of *SPIPm5* and the other KPI, *SPIPm*2. In the contrary, the expression of *Hsp70* was decreased. It suggested that the SPI*Pm*5 could activate the immune system possibly the Toll pathway for the *crustinPm1* and *penaeidin5* were under the Toll pathway.

3.6. Inhibition of rSPIPm5 protein on proPO activity

The proPO activation system is shown to be a potent defense system against microbial infection. In this study, the rSPI*Pm*5 and may affect the hemolymph proPO activity. The rSPI*Pm*5 was, then, tested to see its effect on the hemolymph proPO activity. The result showed that the 0.5 nmol of rSPI*Pm*5 used in this assay had minimal inhibitory effect on the proPO activity. At higher amounts of rSPI*Pm*5, the proPO activity was inhibited (Fig. 4).

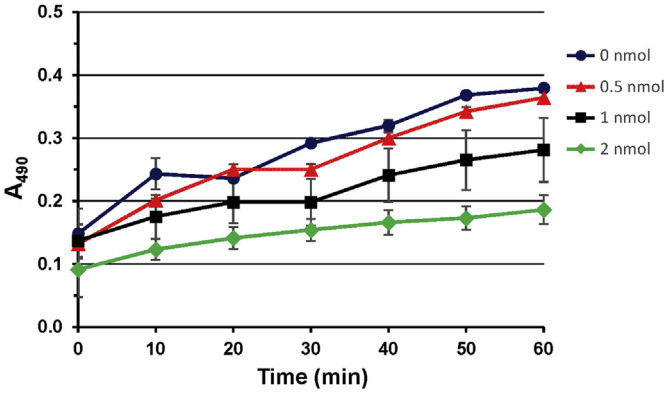


Fig. 4. Inhibition of proPO activity by rSPI*Pm*5. Various amount of rSPI*Pm*5: 0, 0.5, 1 and 2 nmol, were pre-incubated with shrimp hemolymph and LPS. The proPO reaction was started by adding L-DOPA. The progress of reaction was monitored by measuring the A_{490} every 10 min up to 60 min. The experiment was done in triplicate. Results are means ± SDs.

3.7. Mortality assay of microbial-infected shrimp

3.7.1. rSPIPm5 injection and heat stress prolong the lives of WSSV infected shrimp

It is known that the heat stress induces the immune genes in shrimp such as antimicrobial peptides (AMPs), heat shock proteins or prophenoloxidase system [11,25,28]. Since the expression of *SPIPm5* gene is up-regulated by heat shock, the injection of rSPI*Pm*5 seems to mimic the heat shock situation in non-heat-shocked shrimp. Also known is that the heat-shocked shrimp are more tolerant to the infection by WSSV. It is possible that the injection of rSPI*Pm*5 may render the WSSV-infected shrimp live longer. The investigation was carried out. The five normal shrimp groups were treated with PBS injection plus heat shock, WSSV injection plus heat shock, WSSV injection, rSPI*Pm*5 injection and the rSPI*Pm*5 plus WSSV injection. The survival was observed, and the results showed that the rSPI*Pm*5 is able to prolong the survival of WSSV-infected shrimp to about 8 days similar to the effect of heat shock. The mortality of un-infected controls, PBS injection plus heat shock and rSPI*Pm*5 injection, were minimal (Fig. 5 A).

3.7.2. Effect of rSPIPm5 injection on the mortality of WSSV- and YHV-infected shrimp

The results above indicated that the SPI*Pm*5 provided the shrimp with a protective effect against WSSV. The rSPI*Pm*5 was, then, tested against YHV infection compared to the WSSV infection. In this survival experiment, the five groups of shrimp were injected with PBS as a control, WSSV, rSPI*Pm*5 plus WSSV, YHV and rSPI*Pm*5 plus YHV. The mortality was observed. The results showed that the rSPI*Pm*5 could help the infected shrimp survive longer than the infected-control groups from 50% survival rate of 3–4 days to 6 days (Fig. 5 B).

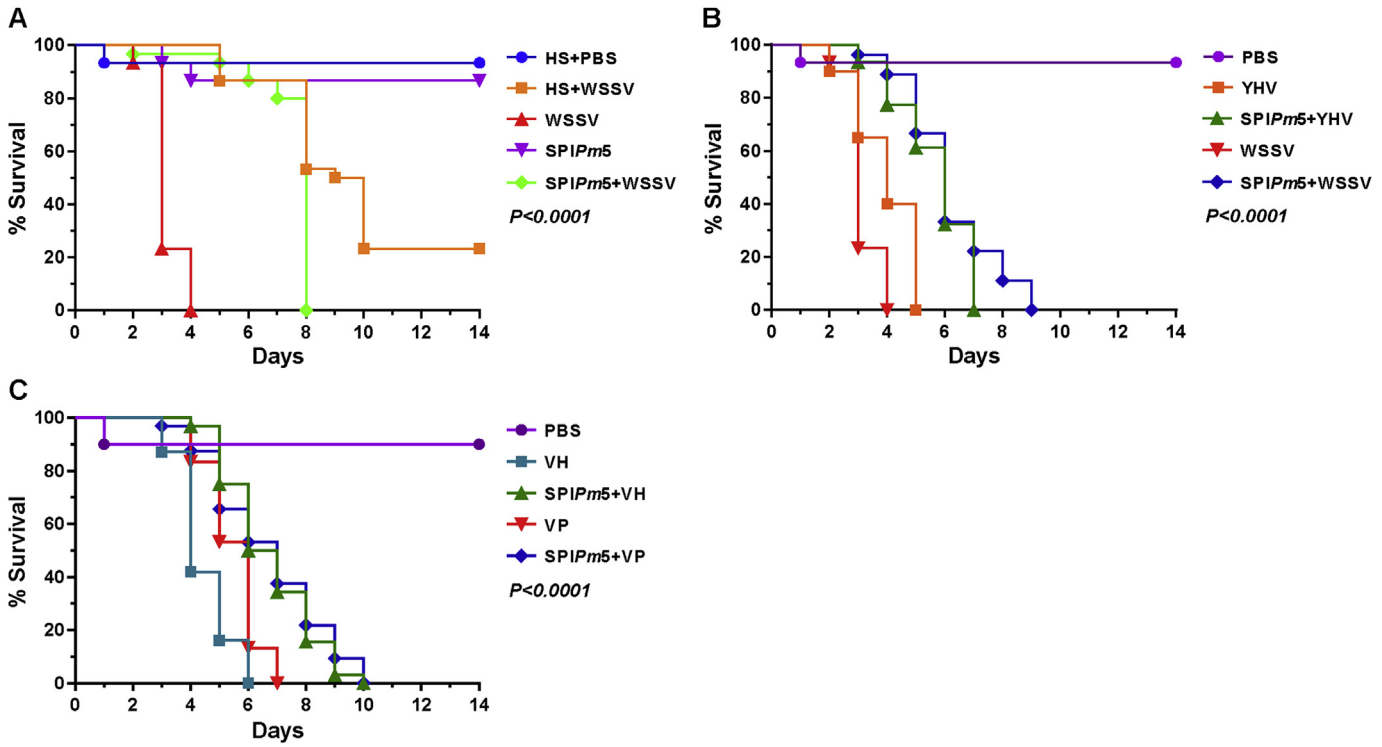


Fig. 5. The Kaplan-Meier survival plots showing the protective effect of rSPI*Pm*5 protein on the pathogen-infected shrimp. The effect of rSPI*Pm*5 was investigated (A) on the WSSV-infected shrimp as compared to heat stress, (B) on the WSSV- and YHV-infected shrimp, and (C) on the *V. parahaemolyticus*- and *V. harveyi*-infected shrimp.

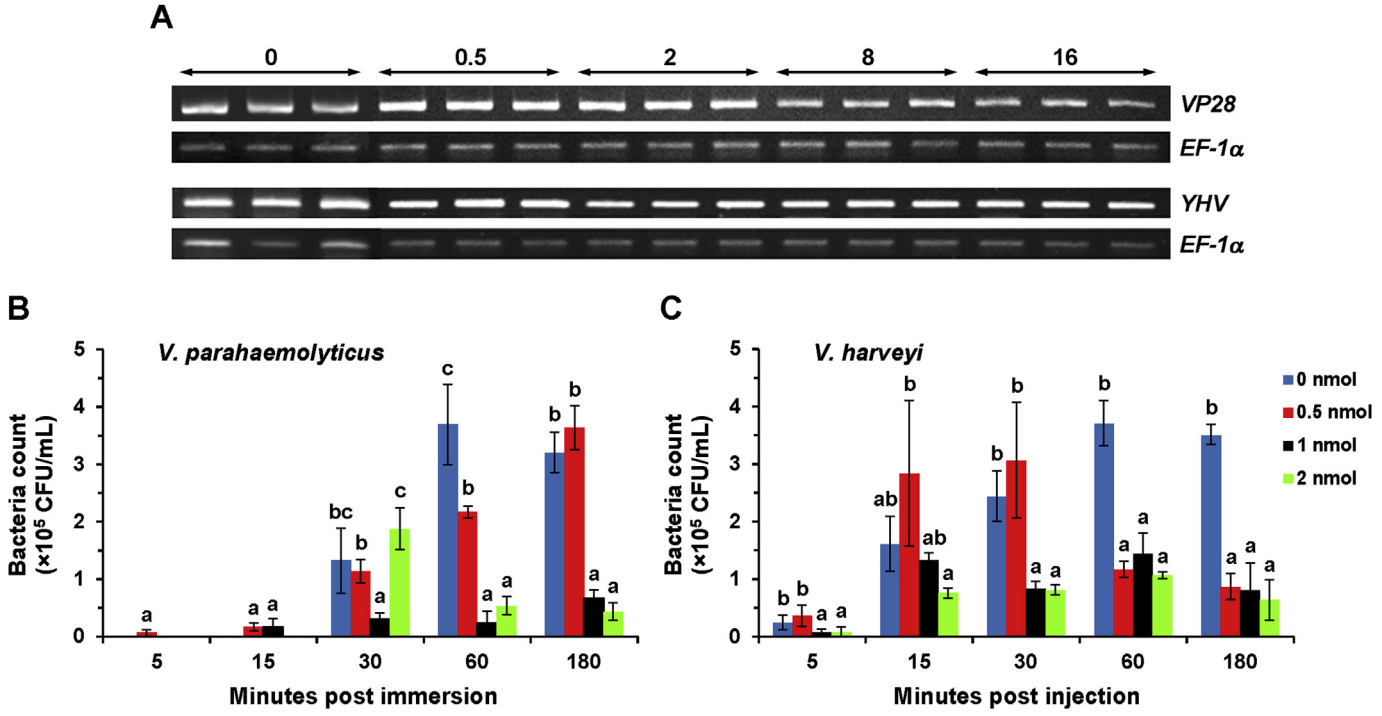


Fig. 6. The inhibitory effect of rSPI*Pm*5 protein on the WSSV, YHV and bacteria. (A) The expression of *VP28* and *YHV* genes. The shrimp were injected with 0, 0.5, 2, 8 and 16 nmol of rSPI*Pm*5 plus WSSV and YHV. The hemolymph was collected at 24 h for the analysis of *VP28* and *YHV* gene expression by RT-PCR. The expression of *EF-1α* gene was used as an internal control. (B and C) The bacterial clearance in *Vibrio*-infected shrimp. The normal shrimp were injected with 0, 0.5, 1 and 2 nmol of rSPI*Pm*5 plus *V. parahaemolyticus* immersion (B) or *V. harveyi* (C). The hemolymph from infected-shrimp were collected at 5, 15, 30, 60 and 180 min after infection for bacterial colony count. The experiment was done in triplicate. The results are means ± SDs. Significant differences are accepted at $P < 0.05$.

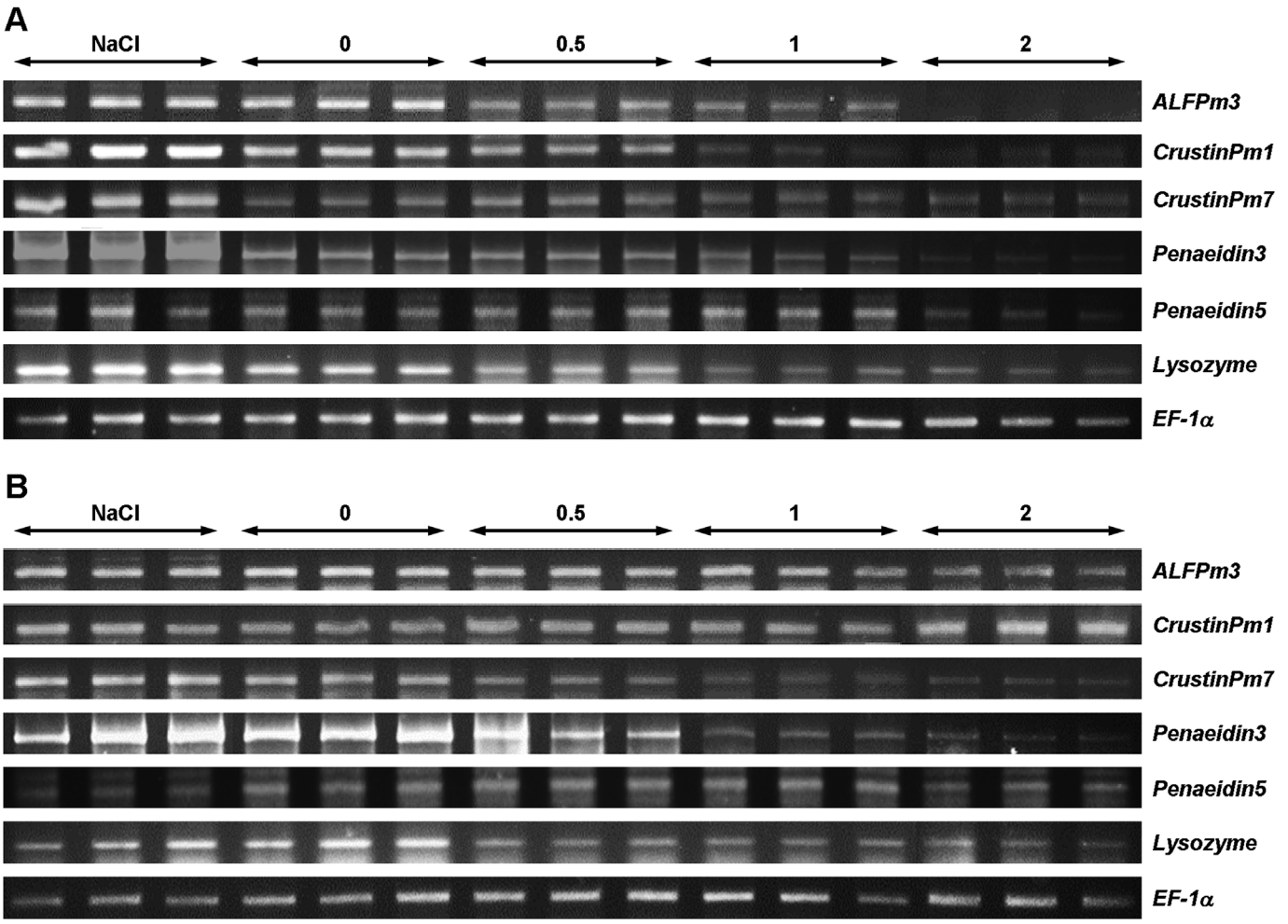


Fig. 7. The AMP gene expression after challenge with the rSPI*Pm*5 plus *V. harveyi* injection (A) and *V. parahaemolyticus* immersion (B). The hemolymph was collected at 1 h. The gene expression of AMPs, *ALFPm3*, *crustinPm1*, *crustinPm7*, *penaeidin3*, *penaeidin5* and *lysozyme*, were investigated by RT-PCR. The expression of *EF-1α* gene was used as an internal control.

3.7.3. Effect of rSPIPm5 injection on the mortality of Vibrio-infected shrimp

Besides the virus infection, the bacterial infection was tested with the rSPI*Pm*5. Two pathogenic strains of shrimp, *Vibrio parahaemolyticus* and *V. harveyi* were used in this experiment. The *V. parahaemolyticus* causes acute hepatopancreatic necrosis disease (AHPND) or early mortality syndrome (EMS) [24,32]. The *V. harveyi* causes luminous vibriosis in shrimp [33]. In this experiment, the five groups of normal shrimp were treated with PBS injection, *V. harveyi* injection, rSPI*Pm*5 plus *V. harveyi* injection, *V. parahaemolyticus* immersion and rSPI*Pm*5 injection plus *V. parahaemolyticus* immersion. The mortality was observed. The results showed that the rSPI*Pm*5 injection helped the shrimp survive a little longer from 50% survival rate of 4–5 days to 6–7 days (Fig. 5 C).

3.8. rSPIPm5 possesses inhibitory effect on the expression of viral genes

The results from mortality indicated that the virus-infected shrimp could resist the onset of viral diseases better. The viruses might be deterred from their normal replication processes. To test this hypothesis, the shrimp were challenged with WSSV and YHV along with various amounts of rSPI*Pm*5 protein. The hemolymph were collected at 24 h after infection. The expression of *VP28* for WSSV and YHV gene were investigated by RT-PCR. The result showed that the expression of *VP28* and *YHV* genes were gradually down-regulated as the amounts of rSPI*Pm*5 injected were increased (Fig. 6 A). The rSPI*Pm*5 showed less inhibitory effect on the expression of *YHV* gene than the *VP28* gene.

3.9. rSPIPm5 reduced the growth of Vibrio species in infected shrimp

The rSPI*Pm*5 protein also delayed the mortality of *Vibrio*-infected shrimp. This might be due to the inhibition of bacterial growth by the rSPI*Pm*5 protein. To test this idea, the *V. parahaemolyticus* and *V. harveyi* were cultured in TSB with 0.5 and 5 nmol of rSPI*Pm*5. The growth was monitored with spectrophotometer by measuring the OD_{600} for 1–4 h. It was found that the rSPI*Pm*5 did not inhibit the growth of both *Vibrio* strains (data not shown). The results indicated that the rSPI*Pm*5 did not act alone in helping the shrimp to fight *Vibrio* infection in mortality assay.

In bacterial clearance assay was, then, employed, the normal shrimp were injected with various amounts of rSPI*Pm*5 plus *V. harveyi* or *V. parahaemolyticus* immersion [25]. The hemolymph were collected at 5, 15, 30, 60 and 180 min after infection. The hemolymph was diluted and aliquots were dropped on TCBS agar. The colonies were counted. The results showed that the numbers of colonies were increased with time but decreased with the higher doses of rSPI*Pm*5. The *V. harveyi* (Fig. 6 C) was more sensitive to the inhibitory effect of rSPI*Pm*5 than *V. parahaemolyticus* (Fig. 6 B) at which results agreed well with those of mortality assay.

3.10. Expression of AMP genes in SPIPm5-and bacteria-injected shrimp

The bacterial clearance assay showed that the growth inhibitory effect of rSPI*Pm*5 after challenging with *V. harveyi* and *V.*

parahaemolyticus was observed as early as 60 min. It was suspected that the clearance might be the result from the activity of AMPs possibly induced their expression by rSPI*Pm*5. To test this possibility, the shrimp were injected with various amounts of rSPI*Pm5* along with *V. harveyi* or immersion with *V. parahaemolyticus*. The hemolymph was collected at 1 h after injection for RT-PCR of AMPs. The results variably showed that the expression of AMP genes: *ALFPm3*, *crustinPm1*, *crustinPm7*, *penaeidin3*, *penaeidin5* and *lysozyme*, was down-regulated compared with the control groups (Fig. 7).

4. Discussion

The Kazal-type serine proteinase inhibitors (KPIs) in crustaceans are implicated in host defenses against pathogenic infection because their expression is responsive to microbial infection. For instances, the *Fc*SPI in Chinese shrimp [6,7], *hc*PcSPI1-4 in freshwater crayfish [8,9], *Pt*KPI in swimming crab [10] *and* SPI*Pm*2 [14] in black tiger shrimp are known for their response to infection and their antimicrobial activities. The SPI*Pm*5 is a two-domain KPI from *P. monodon* that can inhibit subtilisin and elastase. Previous study reveals that its gene expression responds to YHV infection and heat treatment [18,30]. In this study, the *SPIPm5* gene was shown to expression in all shrimp tissues tested. Its expression was up-regulated upon heat stress treatment as compared to that of *Hsp70*, WSSV infection and YHV infection.

Knowing that the expression of *SPIPm5* gene was up-regulated by heat stress, the injection of recombinant rSPI*Pm*5 protein into the shrimp might mimic the heat stress situation and may influence the expression of other immune genes, e.g. AMPs. However, the injected rSPI*Pm*5 had more or less no effect on the expression of *penaeidin3*, *penaeidin5*, *SPIPm2* and *SPIPm5* genes. That of *crustinPm1* was slightly up-regulated and that of Hsp70 was slightly down-regulated. The effect of rSPI*Pm*5 protein on the proPO system, another immune defense system in the hemolymph, was also studied [22]. The proPO activity was inhibited indicating that the SPI*Pm*5 released into the hemolymph from the hemocytes was, in part, controlled the proPO system.

Since the expression of *SPIPm5* gene was induced by WSSV and YHV, it was reasonable to test the influence of rSPI*Pm*5 on the survival of virus-infected shrimp. The heat stress was included for the expression of *SPIPm*2 was increased by heat treatment [11]. All virus-infected shrimp and heat-treated virus-infected shrimp did survive longer compared to the infected-shrimp control. To extend our study, the influence of rSPI*Pm*5 on the survival of *V. harveyi*- and *V. parahaemolyticus*-infected shrimp was investigated. The same results that the bacterial infected shrimp could survive longer were obtained.

The survival experiment led us hypothesized that the replication of viruses and bacterial growth were deterred in the presence of rSPI*Pm*5. The investigation, indeed, showed that the replication of WSSV and YHV was reduced with the increase in the amount of rSPI*Pm*5 injected and the growth of bacteria was reduced in the rSPI*Pm*5-injected shrimp. It should be noted that the rSPI*Pm*2 had no inhibitory effect on the bacterial growth in vitro (data not shown). Thus, the SPI*Pm*5 seems to provide indirectly the shrimp with a protective effect against WSSV, YHV and bacteria.

How the rSPI*Pm*5 functions in the survival experiment was intriguing. One of the innate immune responses against infection is to activate the synthesis of AMPs via the two main signaling pathways, Toll and Imd pathways [31,34]. It is possible that the rSPI*Pm*5 injection may somehow activate the AMP gene expression against microbial infection. It was even more intriguing when it was found that the AMP gene expression were more or less down-regulated in the presence of rSPI*Pm*5. The results indicated that the function of SPI*Pm*5 was not to directly activate the AMP gene expression. Its function against microbial infection in innate immunity remained to be elucidated. Nevertheless, it has been shown here that the SPI*Pm*5 plays an important role in shrimp innate immunity against the microbial infection besides its functions as a proteinase inhibitor [18].

Acknowledgments

This project was supported by the TRF Senior Research Scholar (No. RTA5880004), Thailand Research Fund. We thank also the support under the Ratchadapisek Somphot Endowment to the Center of Excellence for Molecular Biology and Genomics of Shrimp. We acknowledge the support of equipment used in this study under the JST-JICA joint program “Science and Technology Research Partnership for Sustainable Development, SATREPS”

References

[1] L. Cerenius, K. Söderhäll, The prophenoloxidase-activating system in invertebrates, Immunol. Rev. 198 (2004) 116–126.
[2] S. Iwanaga, B.L. Lee, Recent advances in the innate immunity of invertebrate animals, J. Biochem. Mol. Biol. 38 (2005) 128–150.
[3] M. Laskowski Jr., I. Kato, Protein inhibitors of proteinases, Annu. Rev. Biochem. 49 (1980) 593–626.
[4] M.R. Kanost, Serine proteinase inhibitors in arthropod immunity, Dev. Comp. Immunol. 23 (1999) 291–301.
[5] V. Rimphanitchayakit, A. Tassanakajon, Structure and function of invertebrate Kazal-type serine proteinase inhibitors, Dev. Comp. Immunol. 34 (2010) 377–386.
[6] H.J. Kong, H.K. Cho, E.M. Park, G.E. Hong, Y.O. Kim, B.H. Nam, W.J. Kim, S.J. Lee, H.S. Han, I.K. Jang, C.H. Lee, J.H. Cheong, T.J. Choi, Molecular cloning of Kazal-type proteinase inhibitor of the shrimp *Fenneropenaeus chinensis*, Fish Shellfish Immunol. 26 (2009) 109–114.
[7] Z.H. Wang, X.F. Zhao, J.X. Wang, Characterization, kinetics, and possible function of Kazal-type proteinase inhibitors of Chinese white shrimp, *Fenneropenaeus chinensis*, Fish Shellfish Immunol. 26 (2009) 885–897.
[8] X.C. Li, X.W. Wang, Z.H. Wang, X.F. Zhao, J.X. Wang, A three domain Kazal-type serine proteinase inhibitor exhibiting domain inhibitory and bacteriostatic activities from freshwater crayfish *Procambarus clarkii*, Fish Shellfish Immunol. 33 (2009) 1229–1238.
[9] X.C. Li, R.R. Zhang, R.R. Sun, J.F. Lan, X.F. Zhao, J.X. Wang, Three Kazal-type serine proteinase inhibitors from the red swamp crayfish *Procambarus clarkii* and the characterization, function analysis of hcPcSPI2, Fish Shellfish Immunol. 28 (2010) 942–951.
[10] S. Wang, Z. Cui, Y. Liu, Q. Li, C. Song, The first Kazal-type serine proteinase inhibitor in the swimming crab *Portunus trituberculatus* involved in immune response to bacteria and fungi, Aquaculture 356–357 (2012) 55–60.
[11] A. Tassanakajon, S. Klinbunga, N. Paunglarp, V. Rimphanitchayakit, A. Udomkit, S. Jitrapakdee, K. Sritunyalucksana, A. Pongdara, S. Pongsomboon, P. Supungul, S. Tang, K. Kuphanumart, R. Pichyangkura, C. Lursinsap, *Penaeus monodon* gene discovery project: the generation of an EST collection and establishment of a database, Gene 384 (2006) 104–112.
[12] P. Supungul, S. Klinbunga, R. Pichyangkura, S. Jitrapakdee, I. Hirono, T. Aoki, A. Tassanakajon, Identification of immune genes in hemocytes of black tiger shrimp (*Penaeus monodon*), Mar. Biotechnol. 4 (2002) 487–494.
[13] N. Somprasong, V. Rimphanitchayakit, A. Tassanakajon, A five domain Kazal-type serine proteinase inhibitor from black tiger shrimp *Penaeus monodon* and its inhibitory activities, Dev. Comp. Immunol. 30 (2006) 998–1008.
[14] S. Donpudsa, A. Tassanakajon, V. Rimphanitchayakit, Domain inhibitory, bacteriostatic activities of the five-domain Kazal-type serine proteinase inhibitor from black tiger shrimp *Penaeus monodon*, Dev. Comp. Immunol. 33 (2009) 481–488.
[15] S. Ponprateep, A. Tassanakajon, V. Rimphanitchayakit, A Kazal-type serine proteinase inhibitor SPI*Pm*2 from the black tiger shrimp *Penaeus monodon* is capable of neutralization and protection of hemocytes from the white spot syndrome virus, Fish Shellfish Immunol. 31 (2011) 1179–1185.
[16] A. Prapavorarat, S. Pongsomboon, A. Tassanakajon, Identification of genes expressed in response to yellow head virus infection in the black tiger shrimp, *Penaeus monodon*, by suppression subtractive hybridization, Dev. Comp. Immunol. 34 (2010) 611–617.
[17] S. Donpudsa, S. Ponprateep, A. Prapavorarat, S. Visetnan, A. Tassanakajon, V. Rimphanitchayakit, A Kazal-type serine proteinase inhibitor SPI*Pm2* from the black tiger shrimp *Penaeus monodon* is involved in antiviral responses, Dev. Comp. Immunol. 34 (2010) 1101–1108.
[18] S. Visetnan, S. Donpudsa, P. Supungul, A. Tassanakajon, V. Rimphanitchayakit, Kazal-type serine proteinase inhibitors from the black tiger shrimp *Penaeus monodon* and the inhibitory activities of SPI*Pm4* and *5*, Fish Shellfish Immunol. 27 (2011) 266–274.
[19] M.W. Pfaffl, A new mathematical model for relative quantification in real-time RT-PCR, Nucleic Acids Res. 29 (2001) e45.
[20] U.K. Laemmli, Cleavage of structure protein during the assembly of head of bacteriophage T4, Nature 227 (1970) 680–685.
[21] M.M. Bradford, A rapid and sensitive method for the quantification of microgram quantities of protein utilizing the principle of protein-dye binding, Anal. Biochem. 72 (1976) 248–254.
[22] S. Ponprateep, T. Vatanavicharn, C.F. Lo, A. Tassanakajon, V. Rimphanitchayakit, Alpha-2-macroglobulin is a modulator of prophenoloxidase system in pacific white shrimp *Litopenaeus vannamei*, Fish Shellfish Immunol. 62 (2017) 68–74.
[23] B. Maiti, M. Shekar, R. Khushiramani, I. Karunasagar, I. Karunasagar, Evaluation of RAPD-PCR and protein profile analysis to differentiate *Vibrio harveyi* strains

prevalent along the southwest coast of India, J. Genet. 88 (2009) 273–279.
[24] S. Dangtip, R. Sirikharin, P. Sanguanrut, S. Thitamadee, K. Sritunyalucksana, S. Taengchaiyaphum, R. Mavichak, P. Proespraiwong, T.W. Flegel, AP4 method for two-tube nested PCR detection of AHPND isolates of *Vibrio parahaemolyticus*, Aquac. Rep 2 (2015) 158–162.
[25] W. Junprung, P. Supungul, A. Tassanakajon, *HSP70* and *HSP90* are involved in shrimp *Penaeus vannamei* tolerance to AHPND causing strain of *Vibrio parahaemolyticus* after non-lethal heat shock, Fish Shellfish Immunol. 60 (2017) 237–246.
[26] A.R. Ochoa-Meza, C. Ibarra-Gamez, J. Hernandez-Lopez, T. Gollas-Galvan, M.L. Unzueta-Bustamante, Evaluation of a detection system of yellow head disease virus (YHV) using Q-PCR, Arch. Biol. Sci. 65 (2013) 1629–1636.
[27] S. Xu, L. Wang, X.W. Wang, Y.R. Zhao, W.J. Bi, X.F. Zhao, J.X. Wang, L-type lectin from the kuruma shrimp *Marsupenaeus japonicus* promotes hemocyte phagocytosis, Dev. Comp. Immunol. 44 (2014) 397–405.
[28] W. Rungrassamee, R. Leelatanawit, P. Jiravanichpaisal, S. Klinbunga, N. Karoonuthaisiri, Expression and distribution of three heat shock protein genes under heat shock stress and under exposure to *Vibrio harveyi* in *Penaeus monodon*, Dev. Comp. Immunol. 34 (2010) 1082–1089.
[29] D. Cottin, B. Shilito, T. Chertemps, A. Tanguy, N. Leger, J. Ravaux, Identification of differentially expressed genes in the hydrothermal vent shrimp *Rimicaris exoculata* exposed to heat stress, Mar. Genomics 3 (2010) 71–78.
[30] S. Pongsomboon, S. Tang, S. Boonda, T. Aoki, I. Hirono, A. Tassanakajon, A cDNA microarray approach for analysing transcriptional changes in *Penaeus monodon* after infection by pathogens, Fish Shellfish Immunol. 30 (2011) 439–446.
[31] S. Visetnan, P. Supungul, S. Tang, I. Hirono, A. Tassanakajon, V. Rimphanitchayakit, YHV-responsive gene expression under the influence of *Pm*Relish regulation, Fish Shellfish Immunol. 47 (2015) 572–581.
[32] S. Thitamadee, A. Prachumwat, J. Srisala, P. Jaroenlak, P.V. Salachan, K. Sritunyalucksana, T.W. Flegel, O. Itsathiphaisarn, Review of current disease threats for cultivated penaeid shrimp in Asia, Aquaculture 452 (2016) 69–87.
[33] P. Dash, S. Avunje, R.S. Tandel, K.P. Sandeep, A. Panigrahi, Biocontrol of luminous vibriosis in shrimp aquaculture: a review of current approaches and future perspectives, Rev. Fish. Sci. Aquac 25 (2017) 245–255.
[34] S. Arayamethakorn, P. supungul, A. Tassanakajon, K. Krusong, Characterization of molecular properties and regulatory pathways of *crustinPm1* and *crustinPm7* from the black tiger shrimp *Penaeus monodon*, Dev. Comp. Immunol. 67 (2017) 18–29.
[35] S. Ponprateep, K. Phiwsaiya, A. Tassanakajon, V. Rimphanitchayakit, Interaction between Kazal serine proteinase inhibitor SPI*Pm*2 and viral protein WSV477 reduces the replication of white spot syndrome virus, Fish Shellfish Immunol. 35 (2013) 957–964.

Fish and Shellfish Immunology 81 (2018) 284–296

Contents lists available at ScienceDirect

Fish and Shellfish Immunology

journal homepage: www.elsevier.com/locate/fsi

Full length article

Differentially expressed genes in hemocytes of *Litopenaeus vannamei* challenged with *Vibrio parahaemolyticus* AHPND (VP_{AHPND}) and VP_{AHPND} toxin

Benedict A. Maralit[a,1,2], Phattarunda Jaree[a,1], Pakpoom Boonchuen[a], Anchalee Tassanakajon[a,b], Kunlaya Somboonwiwat[a,b,*]

[a] Center of Excellence for Molecular Biology and Genomics of Shrimp, Department of Biochemistry, Faculty of Science, Chulalongkorn University, Thailand
[b] Omics Science and Bioinformatics Center, Faculty of Science, Chulalongkorn University, Thailand

ARTICLE INFO

Keywords:
Shrimp
Transcriptome
Early mortality syndrome
Hemocyte
Immune system

ABSTRACT

While toxin-harboring *Vibrio parahaemolyticus* has been previously established as the causative agent of early mortality syndrome (EMS) or acute hepatopancreatic necrosis disease (AHPND) in shrimp, information on the mechanistic processes that happen in the host during infection is still lacking. Here, we examined the expression responses of the shrimp hemocyte transcriptome to *V. parahaemolyticus* AHPND (VP_{AHPND}) by RNA sequencing (RNA-seq). Using libraries (SRA accession number SRP137285) prepared from shrimp hemocytes under experimental conditions, a reference library was *de novo* assembled for gene expression analysis of VP_{AHPND}-challenged samples at 0, 3/6, and 48 h post infection (hpi). Using the library from 0-hpi as the control, 359 transcripts were found to be differentially expressed in the 3/6-hpi library, while 429 were differentially expressed in the 48-hpi library. The expression patterns reported in the RNA-seq of 9 representative genes such as anti-lipopolysaccharide factor (*Lv*ALF), crustin p (CRU), serpin 3 (SER), C-type lectin 3 (CTL), clottable protein 2 (CLO), mitogen-activated protein kinase kinase 4 (MKK4), P38 mitogen-activated protein kinase (P38), protein kinase A regulatory subunit 1 (PKA) and DNAJ homolog subfamily C member 1-like (DNJ) were validated by qRT-PCR. The expression of these genes was also analyzed in shrimp that were injected with the partially purified VP_{AHPND} toxin. A VP_{AHPND} toxin-responsive gene, *Lv*ALF was identified, and its function was characterized by RNA interference. *Lv*ALF knockdown resulted in significantly rapid increase of shrimp mortality caused by toxin injection. Protein-protein interaction analysis by molecular docking suggested that *Lv*ALF possibly neutralizes VP_{AHPND} toxin through its LPS-binding domain. The data generated in this study provide preliminary insights into the differences in the immune response of shrimp to the bacterial and toxic aspect of VP_{AHPND} as a disease.

1. Introduction

In 2013, the causative agent of acute hepatopancreatic necrosis disease (AHPND), earlier known as early mortality syndrome (EMS), was identified as *Vibrio parahaemolyticus* [49]. Being ubiquitous in the marine environment, *V. parahaemolyticus* is only considered as an opportunistic pathogen [20]. All AHPND-causing strains of *V. parahaemolyticus* (VP_{AHPND}) that are uniquely virulent to shrimp were found to have a large extra-chromosomal plasmid that is absent in non-AHPND strains [14,18,54]. This AHPND-causing plasmid contains 2 toxin genes named as PirA and PirB because they are homologous to the *Photorhabdus* insect-related (Pir) binary toxin [20,40]. Because the ability to cause disease is lost by experimental deletion or the natural absence of plasmid-encoded toxins, the toxins may be considered as the most important factors of AHPND pathogenesis.

In the early stage of VP_{AHPND} infection, sloughing of the hepatopancreas tubule epithelial cells can be observed in histological analysis, while atrophied pale hepatopancreas, the most common sign of AHPND

* Corresponding author. Center of Excellence for Molecular Biology and Genomics of Shrimp, Department of Biochemistry, Faculty of Science, Chulalongkorn University Omics Science and Bioinformatics Center, Faculty of Science, Chulalongkorn University, Thailand.
E-mail address: kunlaya.s@chula.ac.th (K. Somboonwiwat).
[1] These authors contributed equally to this work.
[2] Current Addresses: National Institute of Molecular Biology and Biotechnology, College of Science, University of the Philippines, Diliman, Quezon City, Philippines; and Philippine Genome Center, University of the Philippines, Diliman, Quezon City, Philippines.

https://doi.org/10.1016/j.fsi.2018.06.054
Received 12 April 2018; Received in revised form 26 June 2018; Accepted 29 June 2018
Available online 18 July 2018
1050-4648/ © 2018 Elsevier Ltd. All rights reserved.

in diseased shrimp, can be observed in the later stages of infection, when necrosis of the hepatopancreas tubule epithelial cells and massive hemocyte infiltration occurs [30,45]. Ref. [20] showed that VP_{AHPND} initially colonizes the stomach and secretes toxins at 6 h post infection (hpi), which would then allow both toxin proteins and, subsequently, bacteria to spread from the stomach to the hepatopancreas at 12-hpi. While this information describes the pathogenesis of the AHPND, the mechanistic processes of the shrimp immune system during infection especially the response to VP_{AHPND} toxins is not yet fully understood. Recent transcriptome analysis in hemocyte *Litopenaeus vannamei* challenged with non-AHPND strains of *V. parahaemolyticus* showed differential expression of immune-related genes induced by *Vibrio* infection [37]. Recently, a study showed that the hemocyanin (HMC) gene family was identified from *L. vannamei* hepatopancreas as up-regulated upon VP_{AHPND} infection. Among the hemocyanin isoforms found, hemocyanin subunit L3 (HMCL3) and hemocyanin subunit L4 (HMCL4) were induced in the hepatopancreas as a response to VP_{AHPND} toxin from 1 to 3 h after injection [6].

The aim of the study is to analyze the expression responses of the shrimp hemocyte transcriptome, which is a major immune tissue related to VP_{AHPND} infection, by RNA sequencing (RNA-seq). The effect of partially purified VP_{AHPND} toxin challenge on selected genes was also revealed by qRT-PCR. This provides preliminary insights into the differences in the immune response of shrimp to the bacterial and toxic aspect of AHPND as a disease. Likewise, the study aims to highlight various roles of genes in different stages of AHPND infection.

2. Materials and methods

2.1. Shrimp samples

Shrimp, weighing about 6–8 g, were obtained from a local shrimp farm. They were acclimatized in rearing tanks with ambient temperature of 30 ± 2 °C, water salinity of 20 parts per thousand, and constant aeration. They were fed with commercial pellets 2 times a day and kept in the rearing tanks for 2 weeks before any experiment or tissue collection.

2.2. VP_{AHPND} and VP_{AHPND} toxin challenge

After acclimatization, shrimp were challenged with VP_{AHPND} Thamai isolates by immersion in tanks that were inoculated by a bacterial suspension to a final concentration of 1.5×10^6 CFU/ml as described by Ref. [6]. VP_{AHPND} was grown on TCBS agar. Several colonies were inoculated in tryptic soy broth (TSB) containing 1.5% NaCl and incubated at 30 °C with 250 rpm shaking overnight. This culture was then inoculated to a fresh TSB with 1.5% NaCl medium in a 1:100 ratio and incubated at 30 °C with 250 rpm shaking until an optical density at 600 nm (OD_{600}) of 2 (approximately 10^8 CFU/mL) was achieved. The median lethal dose (LD_{50}) of bacterial inoculants at 48 h was determined in 10 shrimp.

The partially purified VP_{AHPND} toxin, used for knockdown and challenge experiments, was prepared from crude VP_{AHPND} toxin by ammonium sulfate precipitation and dialysis according to [6]. The partially purified VP_{AHPND} toxin was dissolved and dialyzed against 1 × PBS pH of 7.4, quantified by Bradford protein assay, and checked for the presence of PirAB toxin protein using 15% SDS-PAGE before use in any experiment. The partially purified VP_{AHPND} toxin challenge resulting in AHPND in shrimp was confirmed by observation of morphological changes in the hepatopancreas such as paling and atrophy as well as lethargy in surviving shrimp. The partially purified VP_{AHPND} toxin at the dosage that yields 100% mortality in two days which is 0.2 μg/g shrimp was prepared by diluting toxin in 1 × PBS mixed with a red food-grade dye. The red food-grade dye was used to visualize and make sure that injections were administered properly into the shrimp muscle during injection experiments.

2.3. Next generation sequencing and data analysis

For transcriptome analysis, hemocyte collection was done by drawing approximately 500 μl of hemolymph from the ventral sinus of the shrimp using a sterile syringe with an equal volume of filter sterilized and pre-cooled anticoagulant (MAS solution) as described by Ref. [43]. Hemocytes were immediately collected from the suspension by centrifugation in 800 × g for 10 min at 4 °C and kept in liquid nitrogen. Hemocyte from 10 individuals of VP_{AHPND}-challenged shrimp at each time point (0, 3, 6 and 48 h post challenge) was pooled in triplicates. The hemocyte pool for early phase of infection from the 3-h time point was further mixed with the 6-h time point. Total RNA was extracted using Favorgen Tissue Total RNA mini kit (Biotech Corp.).

Total RNA extracts were analyzed in EtBr-stained 1.2% agarose gel and by Agilent 2100 Bioanalyzer using RNA 6000 Pico Kit (Agilent) to determine the integrity and quality. After RNA concentrations were measured by Qubit® RNA HS Assay Kit (ThermoFisher Scientific) on Qubit® 2.0 flourometer, cDNA libraries from 4 μg total RNA were then constructed following the manufacturer's instruction for TruSeq® stranded mRNA LT sample prep kit (Illumina).

The 3 libraries, 0-h library, 3/6-h library and 48-h library, were sequenced using NextSeq 500 High Output v2 Sequencing Kit (Illumina) in a NextSeq 500 desktop sequencer (Illumina) along with 9 other indexed libraries, which were normalized and pooled with a 1% PhiX control spike-in. Using FastQ Toolkit available through the BaseSpace (Illumina) public app repository, adapter trimming and other quality control filtering of raw reads were performed. High quality reads from the 3 hemocyte libraries (SRR6942061, SRR6942062, SRR6942059), and an additional hepatopancreas library (SRR6942060), were assembled together to form a transcriptome reference in Trinity v2.06 software [13]; from which transcript abundance can be based and estimated using RSEM software that is wrapped by scripts included in Trinity. EdgeR software [38] was used to detect differentially expressed transcripts and genes using a dispersion parameter of 0.3.

Leveraging different software for functional annotation, such as BLAST [2]; PFAM [35]; KEGG [16]; Gene ontology [3] and eggNOG [34]; and then running GO-Seq [56]; the Trinotate workflow (http://trinotate.github.io/) was used to analyze gene ontology enrichment for differentially expressed features. UniProt accession numbers from the Trinotate workflow were mapped into Entrez GeneIDs using the UniProt Retrieve/ID mapping tool (http://www.uniprot.org/uploadlists/). The resulting Entrez GeneIDs were then used in KOBAS 2.0 (http://kobas.cbi.pku.edu.cn/home.do) to map KEGG Orthology or conduct enrichment analysis. The identified KEGG orthologies were used as inputs in KEGG Mapper - Search Pathway tool (http://www.kegg.jp/kegg/tool/map_pathway1.html) for mapping to the reference KEGG Pathways and determine distribution. BLAST2GO [10] was used for supplementary annotation. Supplementary tools from galaxy services [1] of National Center for Genome Analysis Support (https://galaxy.ncgas-trinity.indiana.edu/) and Galaxy Queensland (http://galaxy-qld.genome.edu.au/galaxy) such as Fasta tools, Trinity software, BLAST+ were also used.

2.4. Quantitative real-time PCR analysis

A total of 9 representative transcripts from the reference assembly including anti-lipopolysaccharide factor (*Lv*ALF), crustin p (CRU), serpin 3 (SER), C-type lectin 3 (CTL), clottable protein 2 (CLO), mitogen-activated protein kinase kinase 4 (MKK4), P38 mitogen-activated protein kinase (P38), protein kinase A regulatory subunit 1 (PKA) and DNAJ homolog subfamily C member 1-like (DNJ) were analyzed using quantitative real-time PCR (qRT-PCR) to evaluate and confirm the differential expression profiles reported by RNA-Seq analysis. The shrimp EF-1α gene was used as an internal control. Twelve shrimp were challenged with VP_{AHPND} as previously described. Hemocyte of three

Table 1
List of all primer sequences. Primers were designed using Primer3 packaged in Geneious R6. Classifications are based on [47].

Name	Accession	Name	Sequence (5′to3′)	Tm	Target
qRT-PCR Primers					
EF-1α	GU136229.1	EF-1α-F	CGCAAGAGCGACAACTATGA	58.4	171
		EF-1α-R	TGGCTTCAGGATACCAGTCT	57.8	
Antimicrobial peptides					
anti-lipopolysaccharide factor	DQ208702	ALF (197F)	GCTTCACCGTCAAACCTTACATC	60.1	194
		ALF (389R)	CACCGCTTAGCATCTTGTTCG	59.9	
crustin p	AY488496	CRU (292F)	GTTCCAACGACTACAAGTGTGC	60.0	185
		CRU (476R)	CCAAAACATCGGTCGTTCTTCAG	60.4	
Protease and protease inhibitors					
serpin 3	KM280385	SER (857F)	TAAGGGATCAAGACTCAGCATGG	59.9	175
		SER (1031R)	TACCAGCTCCAGTGACTCTTCTA	60.0	
Pattern recognition receptor proteins					
C-type lectin 3	JQ804930	CTL (369F)	GACTTCGTGGGCACTGATTACTA	60.1	172
		CTL (540R)	GCTTGTAGAAGACGTTGTTCAGC	60.4	
Blood clotting system					
clottable protein 2	EU082133	CLO (782F)	TCCCTTTCACTGTCCTTGAGAAC	60.2	223
		CLO (1004R)	GTGGTGATGCTCAGACTGACTAA	60.1	
Signaling transduction					
mitogen-activated protein kinase kinase 4 (MKK4)	KJ023198	MKK (497F)	GGGAGATTGGAAGAGGAGGTTTT	60.0	206
		MKK (702R)	ACAGTCACCCTCCTTGAATATGG	59.8	
P38 mitogen-activated protein kinase	JN035902	P38 (585F)	AGATTGTGAGCTGAAGATCCTCG	60.2	152
		P38 (736R)	AGCCTACTGACCAGATATCCACT	60.1	
protein kinase A regulatory subunit 1	KT203799	PKA (105F)	GCTTGAACCAGTGTCCATAGAGT	60.3	167
		PKA (271R)	CACCAAAGTAGTCTGAAGTCCCA	59.9	
Heat shock proteins					
DNAJ homolog subfamily C member 1-like	XM_014358733	DNJ (436F)	GTCCCTTCAGCTTCATCCAGATA	59.6	161
		DNJ (596R)	AGTATATAGGAGAGCGCCAGTCA	60.2	
Gene Knockdown Primers					
*Lv*ALF-AVR_F	CGTGTCTCTGTGTTGACAAG				56.7
*Lv*ALF-AVR_R	CCTTGTAGTTCAGCTGTAACC				56.3
T7_*Lv*ALF-AVR_F	GGATCCTAATACGACTCACTATAGG-CGTGTCTCTGTGTTGACAAG				68.0
T7_*Lv*ALF-AVR_R	GGATCCTAATACGACTCACTATAGG-CCTTGTAGTTCAGCTGTAACC				68.0
GFP-T7-F	GGATCCTAATACGACTCACTATAGG-ATGGTGAGCAAGGGGGAGGA				68.0
GFP-T7-R	GGATCCTAATACGACTCACTATAGG-TTACTTGTACAGCTCGTCCA				67.0
GFP-F	ATGGTGAGCAAGGGGGAGGA				62.8
GFP-R	TTACTTGTACAGCTCGTCCA				56.2

VP_{AHPND}-infected shrimp was collected at 0-hpi, 3-hpi, 6-hpi, and 48-hpi. Total RNA was isolated using FavorPrep™ Tissue Total RNA Mini Kit (Favorgen Biotech Corp.) and then, first strand cDNA was synthesized using 1 μg total RNA in a reaction containing 1 mM dNTP, 10 units of RNase inhibitor, 0.5 μM oligo-dT (Promega), 1 × RevertUP buffer (BiotechRabbit), and 100 units of RevertUP Reverse Transcriptase (BiotechRabbit).

To study the effect of VP_{AHPND} toxin on the expression of genes under study, shrimp were divided into an experimental and a control group, containing a sample size of 20 individuals. They were intramuscularly injected with 1 × PBS, pH 7.4 and 0.2 μg/g per shrimp of partially purified VP_{AHPND} toxin containing 1% red colored food-grade dye (Winner, Thailand), respectively. Then, the hemocyte of three shrimp from each group was collected at 0, 1, 3, 12, and 24 h post-injection (hpi). Total RNAs and cDNAs were prepared as above.

Gene specific primers (Table 1) were designed from the sequences obtained from RNA-seq data by Primer3 [50] as packaged in Geneious R6 (Biomatters, Ltd). The qRT-PCR reactions, which were composed of 10-fold diluted cDNA template, 1x QPCR Green Master Mix (LRox) (BiotechRabbit) and 0.5 or 0.25 μM forward and reverse primers, were run in CFX96 Touch™ Real-time PCR system (Bio-Rad). Relative expression of each gene was determined and analyzed according to ref. [32] using EF-1α as the control gene. The control was assigned as the 0-hpi group for the bacterial challenge experiment or the 0-h PBS-injected group for the partially purified VP_{AHPND} toxin challenge experiment. Statistical analyses such as one-way ANOVA and Dunnett's multiple comparisons test were conducted in Prism version 6 (GraphPad).

2.5. *LvALF* gene knockdown by RNA interference

The *Lv*ALF dsRNA was prepared using cDNA from *L. vannamei* hemocyte as a template for producing sense and anti-sense DNA templates of *in vitro* transcription. DNA templates (sense and anti-sense strands) containing the T7 promoter sequence at the 5′-end were generated by PCR using *Lv*ALF-T7-F and *Lv*ALF-R primers for the sense strand template, and the other with *Lv*ALF-F and *Lv*ALF-T7-R primers (Table 1). The dsRNA was prepared using T7 RiboMAX™ Express RNAi System (Promega).

L. vannamei samples (approximately 3 g body weight) were divided into three groups of three individuals each. One control group was injected with 10 μg of GFP dsRNA per g of shrimp weight, and another with 0.85% NaCl. The experimental group was injected with 10 μg of *Lv*ALF-dsRNA per gram of shrimp weight. Hemocyte of individual shrimp was collected at 16 h post dsRNA injection and total RNA was extracted, treated with RNase-free DNaseI. An equal amount of DNA-free total RNA from three shrimp was pooled, and 1 μg of pooled total RNA was used for the first strand cDNA synthesis using the RevertAid First Strand cDNA Synthesis kit (Fermentas). *Lv*ALF gene expression was analyzed by RT-PCR using *Lv*ALF-AVR_F/R primers (Table 1) to confirm efficiency of *Lv*ALF gene knockdown. The EF-1α gene was amplified, as an internal control, using the EF-1α-F/R primer pair (Table 1). The PCR conditions were 94 °C for 1 min, followed by 28 cycles (for EF-1α) or 26 cycles (for *Lv*ALF) of 95 °C for 30 s, 58 °C for 30 s, and 72 °C for 30 s, and then a final extension at 72 °C for 5 min. The PCR products were analyzed by 1.5% (w/v) agarose gel electrophoresis.

2.6. Cumulative mortality assay upon VP_{AHPND}-toxin challenge of LvALF-knockdown shrimp

The percentage cumulative mortality was investigated in *Lv*ALF-knockdown shrimp after VP_{AHPND} toxin injection. Twenty *L. vannamei* shrimp of approximately 3 g body weight per group were injected with *Lv*ALF-dsRNA, GFP-dsRNA or 0.85% NaCl as above. Diluted VP_{AHPND} toxin solution at a dosage that causes 100% mortality of shrimp in 2 days post injection was intramuscularly injected into the respective group of shrimp. Mortality was observed every 1 h after VP_{AHPND} toxin injection for 24 h.

2.7. Molecular modeling, model validation and molecular docking

In *L. vannamei*, several sub-isoforms of *Lv*ALF containing single amino acid polymorphisms have been found in the NCBI GenBank database such as *Lv*ALF AV-R (accession no. ABB22832), *Lv*ALF AV-K (accession no. ACT21197), *Lv*ALF AA-K (accession no. ABB22833) and *Lv*ALF VV-R (accession no. ABB22836) (https://www.ncbi.nlm.nih.gov/). To predict the protein-protein interaction of *Lv*ALF and VP_{AHPND} toxin proteins, PirA & PirB, and each of the different *Lv*ALF isoforms were submitted to I-TASSER server [59]; a protein prediction software that is based on model building using multiple-template fragment alignments to build-up predicted-3D structures. The *Lv*ALF model with lowest root-mean-square deviation value (RMSD) was used for further analysis. Stereochemistry of all the models was evaluated by Ramachandran Plot Analysis (http://mordred.bioc.cam.ac.uk/~rapper/rampage.php). The 3D structures of PirA (PDB ID. 3X0T) and PirB (PDB ID. 3X0U) in VP_{AHPND} toxin complex reported by ref. [21] were retrieved from Protein Data Bank (http://www.rcsb.org/). All of ionizable amino acid residues in predicted models were protonated at pH 7.4 by using H++ 1.0 software (http://biophysics.cs.vt.edu/). Molecular docking was performed by web-based service ClusPro [9] to identify the interaction between each *Lv*ALF and VP_{AHPND} toxin proteins. Swiss PDB viewer [5] and VMD [15] were used to perform visualization of 3D models. The coefficient weights of protein binding was calculated from $E = 0.40E_{rep} + (-0.40)E_{att} + 600E_{elec} + 1.00E_{DARS}$ [19].

3. Results

3.1. De novo assembly and annotation

The cDNA libraries from hemocytes of *L. vannamei* challenged with AHPND-causing strain of *V. parahaemolyticus* at 0-hpi, 3/6-hpi, and 48-hpi were sequenced on a high throughput sequencing system, NextSeq 500 (Illumina). The NextSeq 500 run generated a total of 125, 587, 193 raw reads across 3 different libraries which had an average read count of 41 million reads. Quality control and filtering produced 125, 401, 257 clean reads (99.85% retention), which were used in the subsequent Trinity assembly. Assembly statistics are shown in Table 2, where a total of 127,205 transcripts and 104,233 putative genes, with sequence lengths ranging from 201 to 16,976 bp, and an N50 transcript length of 1360 base pairs (bp) have been listed. Sequencing reads were deposited into the Short Read Archive (SRA) of the National Center for Biotechnology Information (NCBI) and can be accessed using accession number SRP137285. All transcripts from the reference assembly were searched against the SwissProt database using BLASTx, which reported that 78% had significant hits (E-value $\leq 10^{-1}$). All sequences with specific hits to the database were graphed and the organisms represented in the library (Fig. 1A) are *Homo sapiens* (12.58%), *Mus musculus* (10.72%), *Drosophila melanogaster* (5.75%), *Arabidopsis thaliana* (4.32%), *Rattus norvegicus* (3.49%), *Bos taurus* (2.59%), etc.

Table 2
Statistics for NGS sequences.

Number of Filtered Reads per Library	
0-hpi library	39,755,956
3/6-hpi library	47,217,902
48-hpi library	38,427,399
Statistics for numbers of transcripts:	
Number of transcripts:	127,205
Total trinity 'genes'	104,233
Number of transcripts ≥ > =1 kb:	22,412
Number of transcripts in N50:	16,467
Number of bases in all transcripts	92,165,807
Number of bases in contigs ≥ > =1 kb	53,012,218
Percent GC:	43.75
Statistics for transcript lengths:	
Min transcript length:	201
Max transcript length:	16,976
Median transcript length:	350
N50 transcript length:	1360

Distribution of 11,952 transcripts with hits to Gene Ontology as leveraged by GO-seq in the Trinity package is shown in Fig. 1B for a total of 52 GO terms in 3 ontologies. Meanwhile, 10,745 KEGG orthologies were assigned to the query sequences, where Metabolic Pathways is the highest assigned KEGG reference pathway (Fig. 1C). A protein BLAST was also done by using predicted coding sequences from the Trinotate protocol and these annotations, along with PFAM information, are shown in Supplementary Table 1.

3.2. Identification of differentially expressed transcripts

A gene was considered differentially expressed when the absolute value of $\log_2$ ratio of that gene in the control (0-hpi) and experimental (3/6-hpi and 48-hpi) libraries is greater than or equal to 1.5 ($|\log_2(a/b)| \geq 1.5$) at a significance of $P \leq 0.001$. Using this criterion in gene expression analysis by edgeR, 815 differentially expressed transcripts were detected in the 0-hpi vs 3/6-hpi libraries at a fold-change of at least 2.8 ($2^{1.5}$). Of these transcripts, 430 are significantly up-regulated in the 3/6-hpi library. 351 (82%) had alignments to Genbank SwissProt sequences as reported by BLASTx. In the 0-hpi vs 48-hpi libraries, 1067 transcripts are at least 2-fold differentially expressed at a significance of $P \leq 0.001$, where 537 transcripts are up-regulated in the 48-hpi library. 446 (83%) of these up-regulated genes had significant alignments to Genbank SwissProt sequences as reported by BLASTx. 202 genes were found to be up-regulated in both 3/6-hpi and 48-hpi libraries. Differentially expressed genes in the 3/6-hpi and 48-hpi library were listed in Supplementary Tables 2 and 3. All the differentially expressed genes were also clustered in a hierarchical heatmap where expression values are reported as (TMM-normalized) FPKM expression values. This heat map is showed in Fig. 2 where major expression clusters are supported by tree percentage values.

3.3. Expression analysis of VP_{AHPND}- and VP_{AHPND} toxin-responsive genes in shrimp hemocyte

In this experiment, pale and atrophied hepatonpancreas was observed in all VP_{AHPND} challenged shrimp that were sampled confirming AHPND pathogenesis. Nine genes were specifically chosen for quantitative real-time PCR analysis to evaluate the expression profiles reported by the RNA-Seq analysis and explore changes in the expression of possibly interesting genes from *in vivo* data. These genes are: crustin p (CRU), anti-lipopolysaccharide factor AV-R isoform (*Lv*ALF), serpin 3 (SER), c-type lectin 3 (CTL), clottable protein 2 (CLO), mitogen-activated kinase kinase 4 (MKK4), p38 mitogen-activated protein kinase

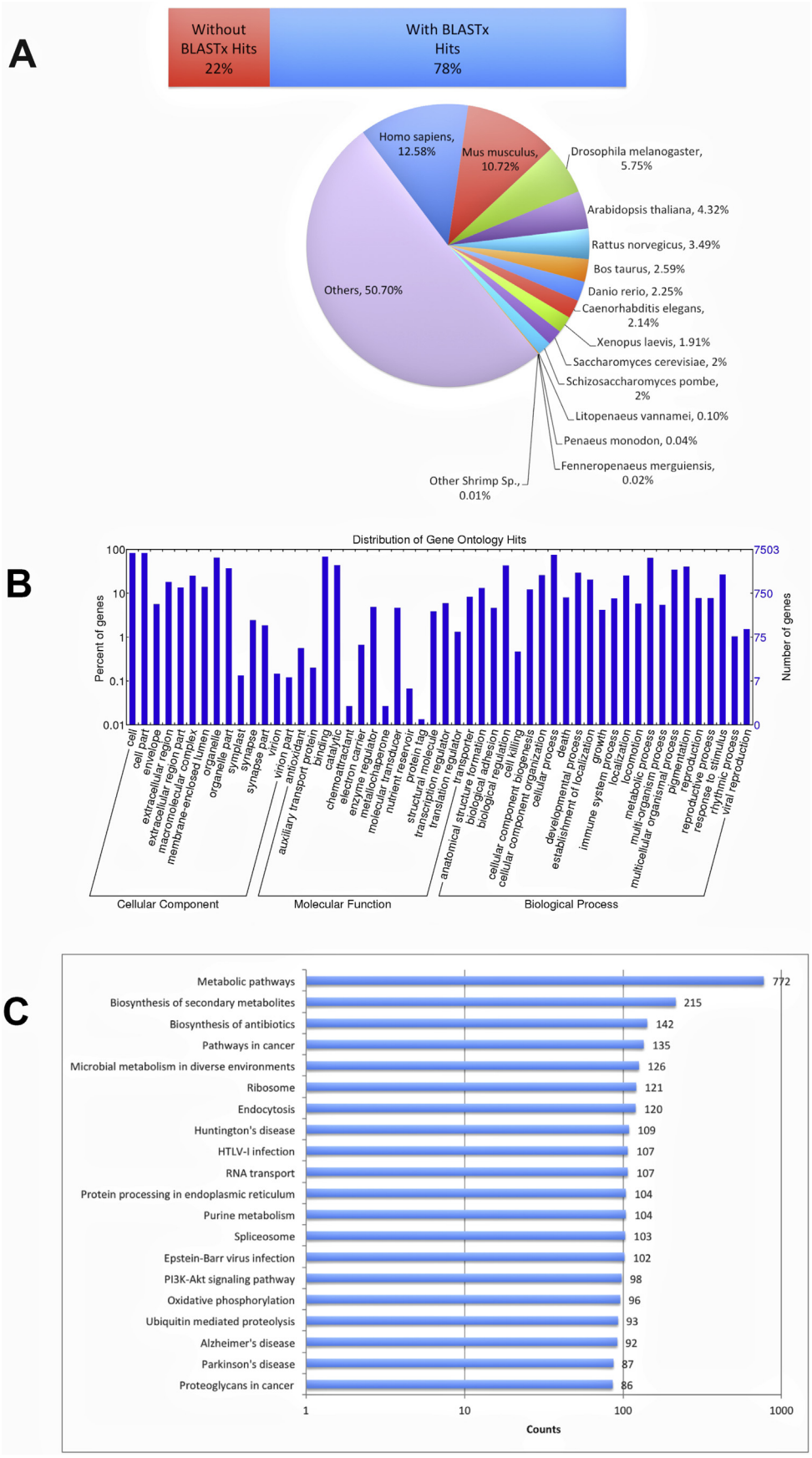


Fig. 1. Annotation of *Litopenaeus vannamei* transcriptome unigenes. A. Percentage of sequences in the transcriptome library aligned against SwissProt Database with E-values of ≤ 10 and organisms represented in the assembly; **B.** Distribution of Gene Ontologies represented in the transcriptome assembly; **C.** Distribution of top 20 KEGG pathways represented in the library.

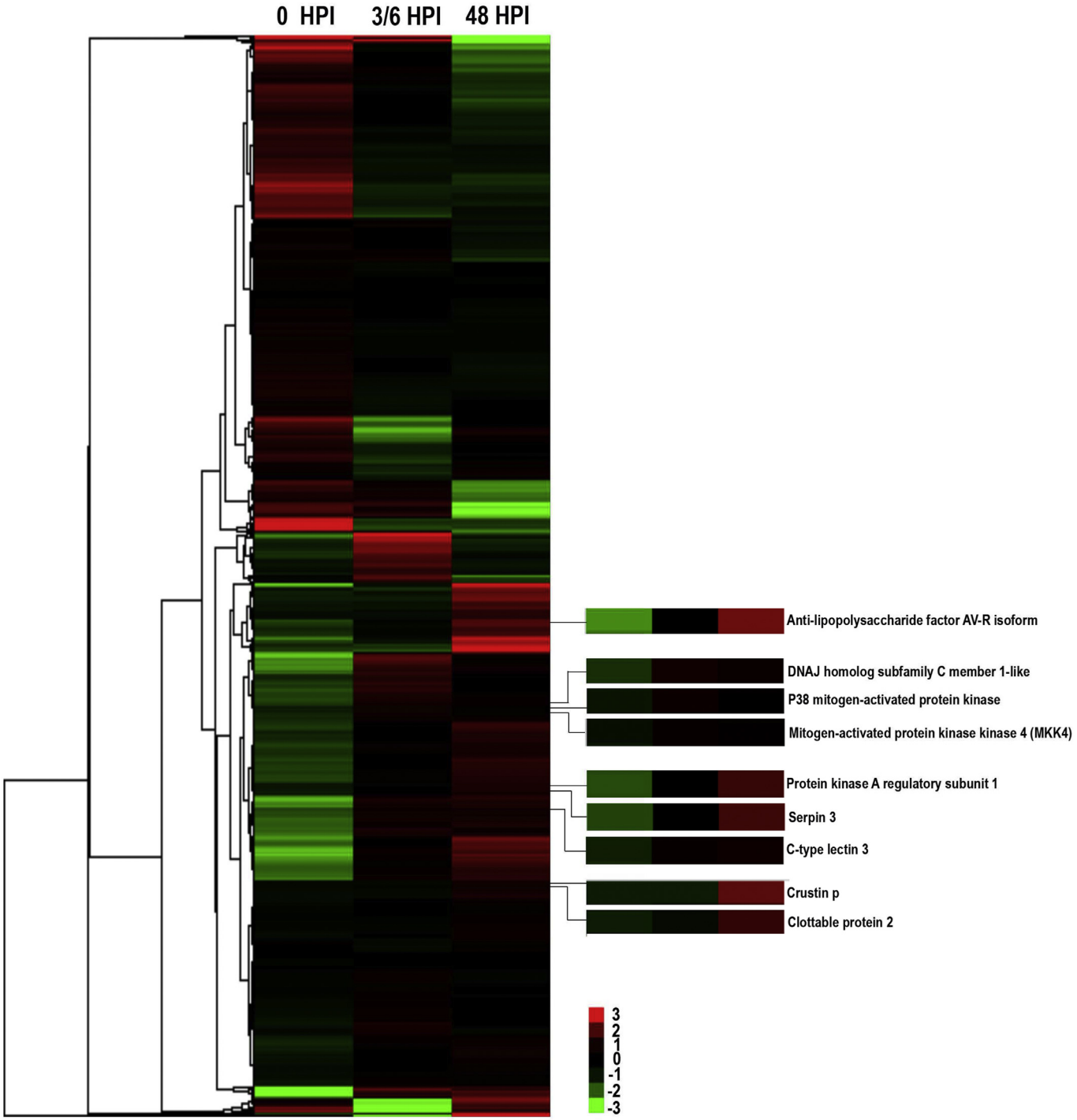


Fig. 2. Hierarchy-clustered heatmap of (TMM-normalized) FPKM expression values for those features that are at least 2-fold differentially expressed and *P*-value < 0.0001.

(P38), protein kinase A regulatory subunit 1 (PKA), and DNAJ homolog subfamily C member 1-like (DNJ). Out of the 9 tested, the expressions of 8 genes were significantly different from that of the 0-h control group in at least one time point after challenge (Fig. 3). Specifically, the expression patterns of 5 genes from RNA-Seq were confirmed to be similar to the qRT-PCR expression profiles in VP_{AHPND}-challenged group. The expression of these same 9 genes was tested in shrimp challenged with partially purified VP_{AHPND} toxin. Using PBS-injected shrimp as the control group, we found that 5 genes were differentially expressed in at least one time point with a cut-off $P < 0.01$ (Fig. 3). Out of these, 3 genes, CRU, SER and p38 were down-regulated while 2 of them, *Lv*ALF and CTL were up-regulated upon VP_{AHPND} toxin challenge. Looking at both bacterial and toxin challenges, the expression levels of *Lv*ALF and CTL were up-regulated, although only that of CTL was statistically significant.

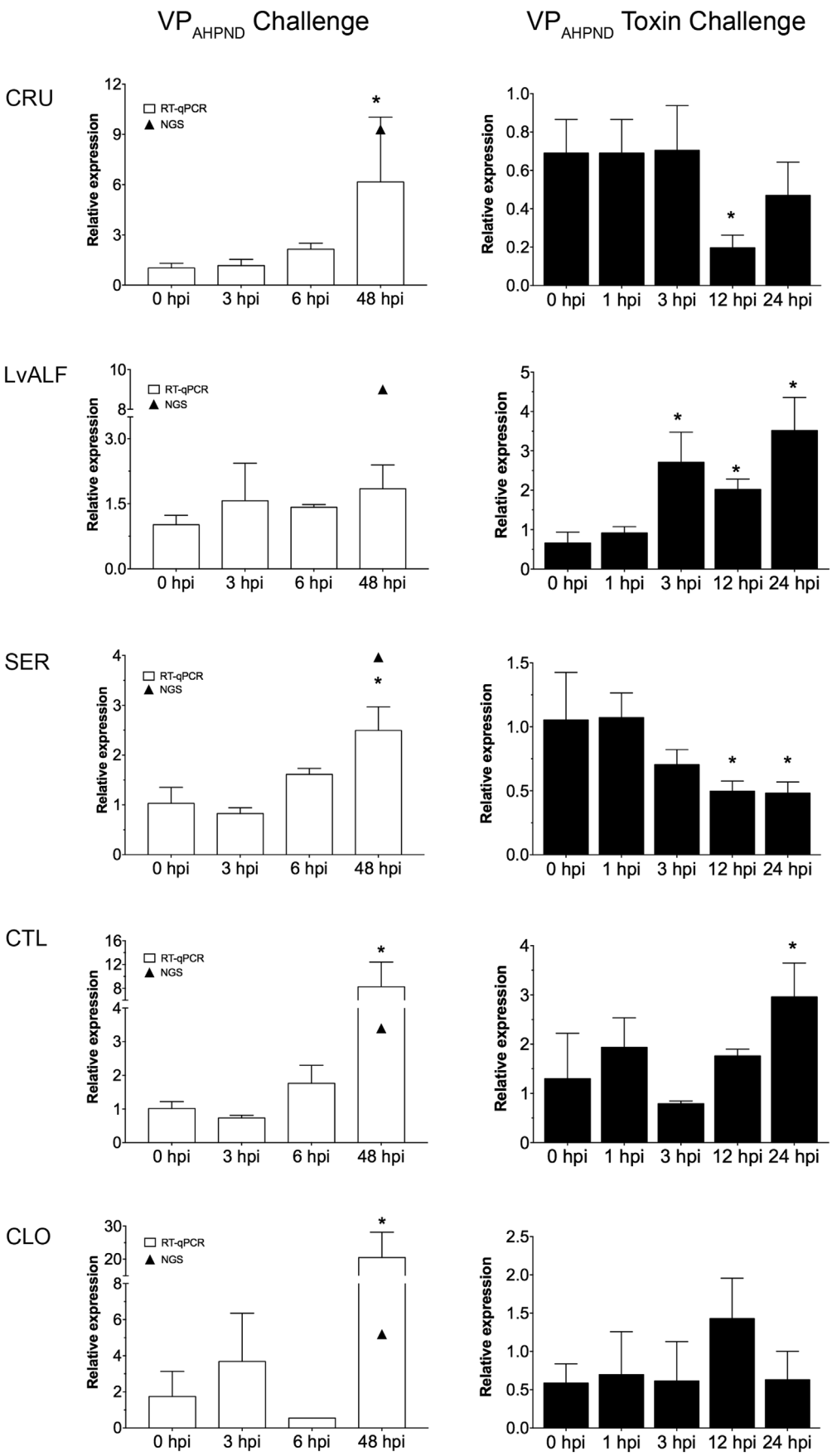

VP AHPND Challenge
VP AHPND Toxin Challenge
CRU
LvALF
SER
CTL
CLO
RT-qPCR
NGS
Relative expression
0 hpi
3 hpi
6 hpi
48 hpi
1 hpi
12 hpi
24 hpi

Fig. 3. Expression analysis of representative up-regulated genes by qPCR. Nine up-regulated genes (CRU –crustin p; *Lv*ALF –anti-lipopolysaccharide factor; SER –serpin 3; CTL –C-type lectin 3; CLO –clottable protein 2; MKK4–mitogen-activated protein kinase kinase 4; P38 –p38 mitogen-activated protein kinase; PKA–protein kinase A regulatory subunit 1; DNJ –DNAJ homolog subfamily C member 1-like) were analyzed for the expression in hemocyte of VP_{AHPND} and VP_{AHPND} toxin -challenged *L. vannamei* at various time points by qPCR using EF-1α as the internal control gene. Asterisks indicate significant difference ($P < 0.05$) from the respective 0 h sampling group based on Dunnett's multiple comparisons test. Triangles indicate expression values with statistical significance from RNA-Seq data analaysis, where expression in 3/6 libraries is plotted in between the 3-hpi and 6-hpi categories of the qPCR counterpart. Absence of these triangles for a gene indicates no significant difference between the specific time point/library and the control.

3.4. Effect of VP_{AHPND} toxin injection on survival of LvALF-knockdown shrimp experiments

According to the expression profiles reported in this study, expression of *Lv*ALF gene was up-regulated upon VP_{AHPND} toxin challenge but showed no significant change upon VP_{AHPND} challenge raising the question on its function during VP_{AHPND} infection. In this experiment, we further explored if *Lv*ALF has an immune role during toxin exposure in shrimp by determination of survival of *Lv*ALF-knockdown shrimp upon toxin challenge. From our observation, all groups that were injected with partially purified VP_{AHPND} toxin reached 80–90% mortality in 24 h, while all control groups without toxin injection survived (Fig. 4B). The test group, where *Lv*ALF gene knockdown was successful (Fig. 4A), reached 100% mortality in as early as 9 h post VP_{AHPND} toxin injection.

3.5. Prediction of LvALF/VP_{AHPND} toxin interaction by molecular modeling and docking

Computational analysis based on the availability of ALF*Pm*3 protein from shrimp *Penaeus monodon* and VP_{AHPND} toxin structures in PDB database was done using molecular docking of shrimp ALFs with the toxin. Due to *Lv*ALF containing several sub-isoforms that arise from amino acid polymorphism, the predicted 3D structure models of each *Lv*ALF protein sub-isoform including *Lv*ALF AV-R, *Lv*ALF AV-K, *Lv*ALF VV-R, and *Lv*ALF AA-K were constructed by web-server I-TASSER software. The results showed that the 3D structure of *Lv*ALF proteins were structurally similar to the NMR structure of ALF*Pm*3 (Fig. 5A). The RMSD value between the Cα atom of the template ALF*Pm*3 and *Lv*ALF AV-R, *Lv*ALF AV-K, *Lv*ALF VV-R, and *Lv*ALF AA-K was 0.73, 0.70, 0.64 and 0.59 Å, respectively. Our analysis showed that 90.8%, 95.8%, 95.0% and 96.7% residues of *Lv*ALF AV-R, *Lv*ALF AV-K, *Lv*ALF VV-R and *Lv*ALF AA-K were in the most favorable region, while 9.2%, 4.2%, 5.0% and 3.3% residues were in the allowed region, respectively. ClusPro web-based software was used to analyze the interaction of *Lv*ALF and VP_{AHPND} toxin protein. Molecular modeling and docking analysis suggests that *Lv*ALF AV-R, *Lv*ALF AV-K, *Lv*ALF VV-R and *Lv*ALF AA-K could interact with the PirB protein of VP_{AHPND} toxin through their LPS-binding sites (Fig. 5B). The coefficient weights of the lowest energy of each interaction were −1176.1, −965.9, −1113.3 and −1162.5, respectively.

4. Discussion

AHPND, or acute hepatopancreatic necrosis disease, is known to be caused by strains of *Vibrio parahaemolyticus*, which accumulates in the stomach and secretes PirA/B in the hepatopancreas [20]. The mechanism by which VP_{AHPND} kills shrimp is currently believed to be caused by the toxin damaging the shrimp stomach epithelium, causing further spread of the toxin proteins together with the bacteria into the hepatopancreas and leading to sloughing of the hepatopancreatic tubule epithelial cells. While this information on the pathogenesis of VP_{AHPND} in the shrimp tissues exists, the mechanistic responses of the shrimp immune system related to the histological events are yet to be understood. Preliminary data in VP_{AHPND} infection studies showed that genes of Toll and IMD pathways and their downstream antimicrobial peptides (AMPs), such as penaeidins, anti-lipopolysaccharide factor, crustin and lysozyme, are overexpressed in the hepatopancreas [55]. Such an observation is expected because the hepatopancreas is one of the major AHPND targets [20]. Meanwhile, data on the expression of the said genes in the stomach and the hemocytes showed that they are suppressed [55]. This is an interesting observation because the hemocytes are also well-known as major immune organs of shrimp [22]. In a recent paper exploring the hemocyte transcriptome of Pacific white shrimp (*L. vannamei*) challenged by *Vibrio parahaemolyticus*, five genes from the humoral immunity such as MNK1/2 MAP kinase interacting serine (MNK), C-type lectin 3 (CTL3), 179 scavenger receptor B1 (SR), gamma-interferon-inducible lysosomal thiol reductase 180 (GILT), and anti-lipopolysaccharide factor-like protein (ALFP) were shown to be significantly up-regulated and important in bacterial clearance [37]. This highlights the diversity of novel genes found shrimp that are crucial during a bacterial infection.

In this study, the gene expression of crustin p is about 6-fold up-regulated while *Lv*ALF did not significantly change based on the qRT-PCR. Crustin molecules are produced and stored in hemocyte granules and thus are easily induced by microbial stimulation. They are then released by degranulation into the hemolymph effectively fighting against a broad spectrum of bacteria [4]. As expected, the bacterial challenge experiment showed gene upregulation and the putative release of crustin, together with other anti-microbial peptides such as serpin 3, clottable protein and c-type lectins (Fig. 3). This mechanism highlights the so-called hallmark of shrimp immunity where different antimicrobial peptides and immune molecules are released to fight off bacteria such as $VP_{AHPND.}$ Meanwhile, it is interesting to note that the differences in expression profiles between the other studies may be due to differences in crustin isoforms [46] as well as anti-lipopolysaccharide factor isoforms [12] or bacterial doses used. In our experiments involving challenge with partially purified VP_{AHPND} toxins, we observed that crustin p expression was significantly lower than the PBS-injected control at 12-hpi (Fig. 3), a similar observation with the study by ref. [55]. In these observations, the toxins might have caused significant cellular stress that affected the expression of some genes in the shrimp immune system such as antimicrobial peptides. Apparently, the marked decrease of antimicrobial peptides like ALF, crustin, lysozyme, and penaeidin in response to stresses such as presence of ammonia in water is common in invertebrates at 6 h post exposure [7,57].

Other well-known innate immunity molecules for bacterial infection such as serpin 3 [24,60]; c-type lectin 3 [27,52]; and clottable protein 2 [28] have agreeing data in both RNA-seq and qRT-PCR analysis, which showed significantly up-regulated expressions during VP_{AHPND} challenge (Fig. 3). These genes are well characterized in other shrimp species as mainly detected in hemocytes, induced by and play critical roles in bacterial infection. More specifically, serpins were found to protect their hosts from infection by pathogens or parasites through inhibiting fungal or bacterial proteinases or regulating endogenous proteinases involved in coagulation, proPO activation, or cytokine activation [17,25,26,44,53]. In *L. vannamei*, two serpins, serpin 3 and serpin 8, have been identified and they were both implicated [25,26] as

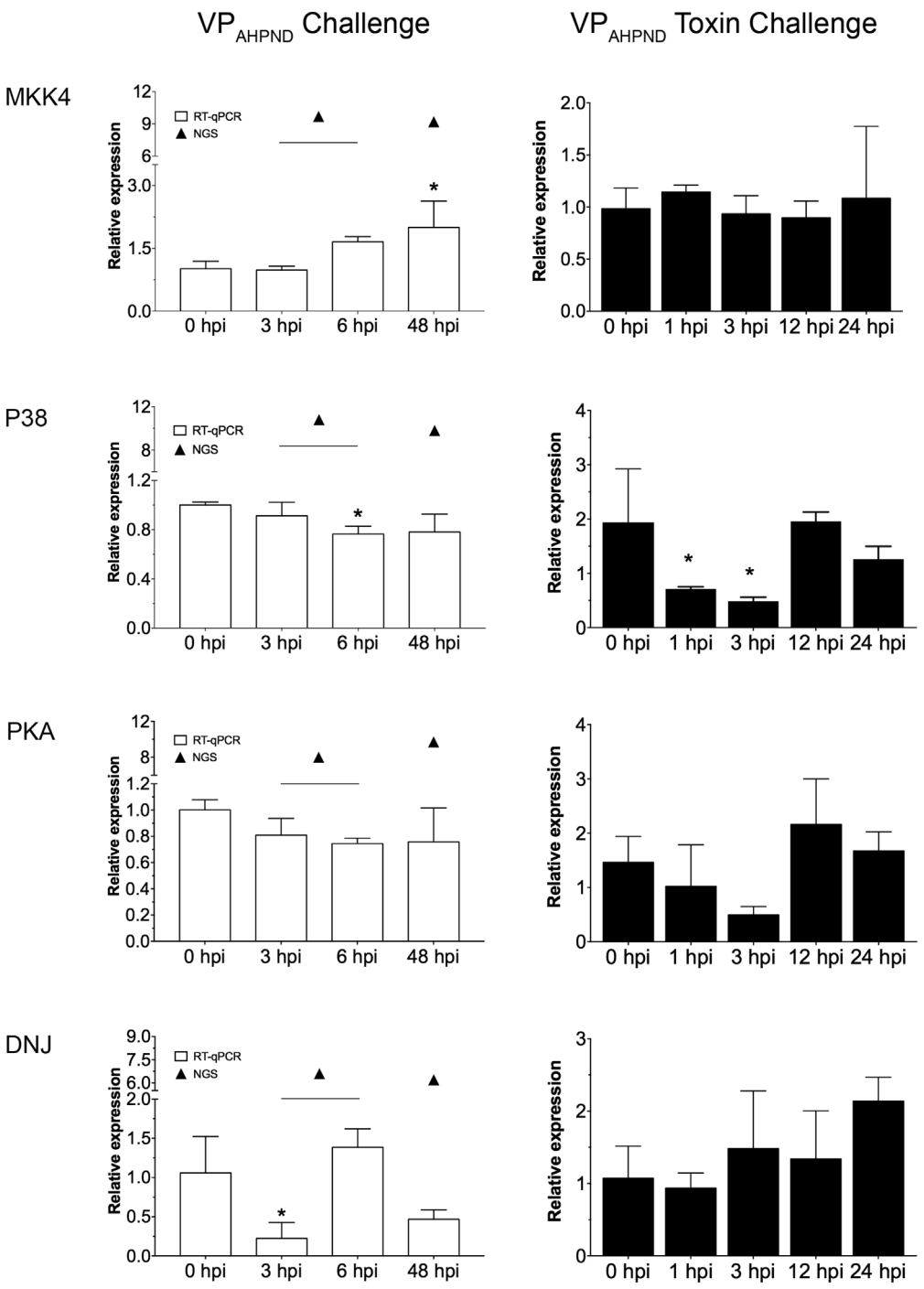


Fig. 3. (*continued*)

important factors during bacterial infection by inhibiting growth of bacteria such as *Vibrio anguillarum*. As the expression of serpin 3 agrees with the expression patterns presented in other studies, this study supports serpin 3 as an important aspect of shrimp immunity during bacterial infection such as VP_{AHPND}.

Likewise, gene upregulation of clottable protein in this study indicates a functional role of the gene during VP_{AHPND} infection. In another study, silencing of clottable protein and its upstream regulator, transglutaminase, showed significantly higher mortalities after bacterial challenge [28].

In qPCR analysis of partial purified VP_{AHPND} toxin-challenged samples, serpin 3 was significantly lower than the control group similar with crustin p. The difference in expression profiles of serpin 3 shows the variability of its response, whether to VP_{AHPND} toxin and bacterial challenges. This phenomenon is also seen in a Chinese shrimp serpin, which is up-regulated after *V. anguillarum* challenge and down-regulated after white spot syndrome virus challenge. Based on this information, a duality of AHPND pathogenesis in terms of the effects of the toxin e.g. cellular stress, or the presence of bacteria on the shrimp immune response may exist.

Meanwhile, up-regulated expression of c-type lectin 3 in both bacteria and toxin -challenged shrimp was observed (Fig. 3). Up-regulation during bacterial challenge was expected because c-type lectins are well-known immune molecules for discrimination of non-self molecules after binding to invading microorganisms [51]. Knockdown of c-type lectin 3 in Pacific white shrimp showing increased bacterial counts in the

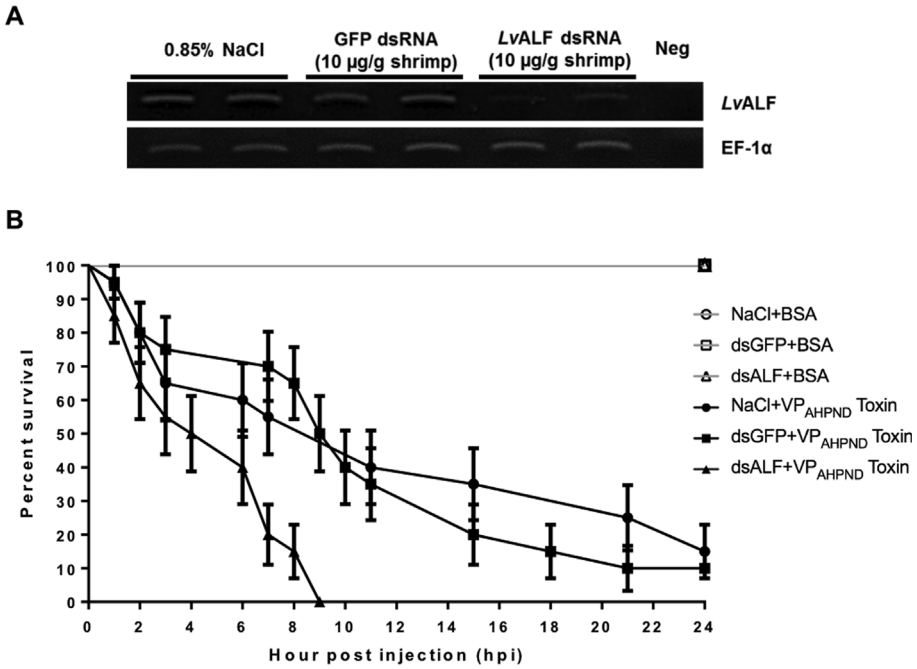


Fig. 4. Survival curve of shrimp during VP_{AHPND} toxin challenge with successful *Lv*ALF gene knockdown. A. Confirmation of *Lv*ALF gene knockdown in *L. vannamei*. Expression level of *Lv*ALF gene in hemocyte of shrimp injected with 0.85% NaCl, 10 µg/g shrimp of GFP dsRNA, and 10 µg/g shrimp of *Lv*ALF dsRNA was determined by semi-quantitative RT-PCR. The 1.5% agarose gel profile was analyzed for the success of *Lv*ALF gene knockdown. Neg is negative control reaction; **B.** Percent survival of shrimp with different injections as indicated by data labels. Standard errors of the survival from 20 individuals are presented as error bars in each time point.

shrimp hemolymph after challenge [37] indicated the crucial role of c-type lectin 3 in bacterial clearance after infection. While the magnitude of the expression of c-type lectin 3 gene is significantly higher in the bacterial challenge experiment than the VP_{AHPND} toxin challenge, up-regulation is detected in both groups, in which the expression profile of bacteria–challenged group is also correctly determined by RNA-Seq data. Aside from binding microorganisms, c-type lectins may induce phagocytosis, prophenoloxidase activating system, respiratory burst, and antiviral immunity [51]. In this study, the described mechanism of c-type lectin in innate immunity is observed in both bacteria and partially purified VP_{AHPND} toxin challenges indicating the important position of lectins in delaying/decreasing morbidity of a wide array of diseases and stress factors in shrimp farms, especially VP_{AHPND} infection.

The shrimp homolog of mitogen-activated protein kinase kinase 4 (MKK4) was also significantly up-regulated in VP_{AHPND}-challenged shrimp (Fig. 3). In the VP_{AHPND} toxin experiment, however, MKK4 expression showed no significant difference from the control. This indicates the possible role of MKK4 in the shrimp immune response for bacteria. In mice, MKK4 becomes activated during cell response to stresses and pro-inflammatory cytokines, which then activates a gene called stress-activated protein kinase-1c (also known as JNK1). The JNK pathway, together with the p38 pathway, are also known as Stress Activated Protein Kinase (SAPK) pathways, since they are activated in response to cellular stress such as irradiation, heat shock, osmotic imbalance, DNA damage, the bacterial product lipopolysaccharide (LPS) as well as inflammatory cytokines [11]. It is possible that the proliferation of bacteria in the gut and in the hepatopancreas caused the up-regulation of the shrimp homolog of MKK4 by signaling cascades activated by LPS. On the other hand, the shrimp homolog of P38 mitogen-activated protein kinase (MAPK) did not show any change in gene expression across all time points in the bacterial challenge. In humans, p38 MAPK, Erk1, and Erk2 phosphorylate and activate MNK1/2 MAP kinase interacting serine (MNK) [36]. The shrimp homolog of MNK1/2 MAP kinase interacting serine (MNK) was associated with bacterial clearance by its up-regulated gene expression during *V. parahaemolyticus* infection and the increased mortality observed in shrimp after its gene knockdown [37]. While the expression of p38 MAPK in this study, along with information from related literature, does not support a conclusive role during bacterial infection, significant changes in p38 MAPK's expression in the 1-h and 3-h time points of this study's toxin-challenge experiments indicate its probable role in the toxin aspect of AHPND pathogenesis. Meanwhile, the difference in expression patterns of MKK4 and p38 MAPK supports the current literature discussing their contrasting involvement in their respective pathways [8]. This then, highlights that the role of p38 MAPK is putatively at the later stages of AHPND when bacteria have already invaded the hepatopancreas and secreted significant amounts of toxin.

Meanwhile, temporal changes in gene expression of the *Lv*ALF in VP_{AHND} challenge were not statistically significant as reported by qPCR. This raises the question on its function in VP_{AHPND} infection because ALFs are known to exhibit antimicrobial activity in shrimp [39,58]. In the VP_{AHPND} toxin-challenged group however, *Lv*ALF was found significantly up-regulated as early as 3 h (Fig. 3). Mapping of the *Lv*ALF AV-R isoform primers for qRT-PCR analysis to different ALF isoforms in *L. vannamei* showed 100% alignment to all the sequences indicating that the expression patterns detected may be the overall response of all *Lv*ALF sub-isoforms mentioned earlier in *L. vannamei*. We thus, consider this possibility and the reason why no significant changes were detected in the bacterial challenge albeit ALFs being well-known antibacterial peptides in *P. monodon* [41]. Although structure prediction of *Lv*ALFs and NMR imaging of ALF*Pm*3 showed similarities in their structures and RMSD values between the Cα atom, previous literature has verified that ALFs are responsive to different pathogen challenges and exhibit multiple antimicrobial and antiviral activities [23,29,48]. It is probable that the various responses of different *Lv*ALF sub-isoforms are masking each other resulting to qRT-PCR not detecting any significant change.

As evidenced by its up-regulation in the toxin injection experiments, *Lv*ALF may have a functional role in preventing cellular toxicity brought by $VP_{AHPND.}$ This role is also supported by knockdown experiments showing that the expression of *Lv*ALF is important in delaying the mortality of shrimp after toxin injection. It is interesting to note that at 9-h post VP_{AHPND} toxin challenge, when the experimental *Lv*ALF knocked-down group reach 100% mortality, shrimp in the VP_{AHPND} toxin-challenged control groups (NaCl + VP_{AHPND} Toxin and dsGFP + VP_{AHPND} Toxin) showed 50% survival, highlighting how decrease/loss of expression of *Lv*ALF aggravates mortality in toxin challenge. This result indicated that *Lv*ALF might play a significant role in protecting shrimp against VP_{AHPND} toxin during infection. In this context, we hypothesize the toxin neutralization mechanism as a function

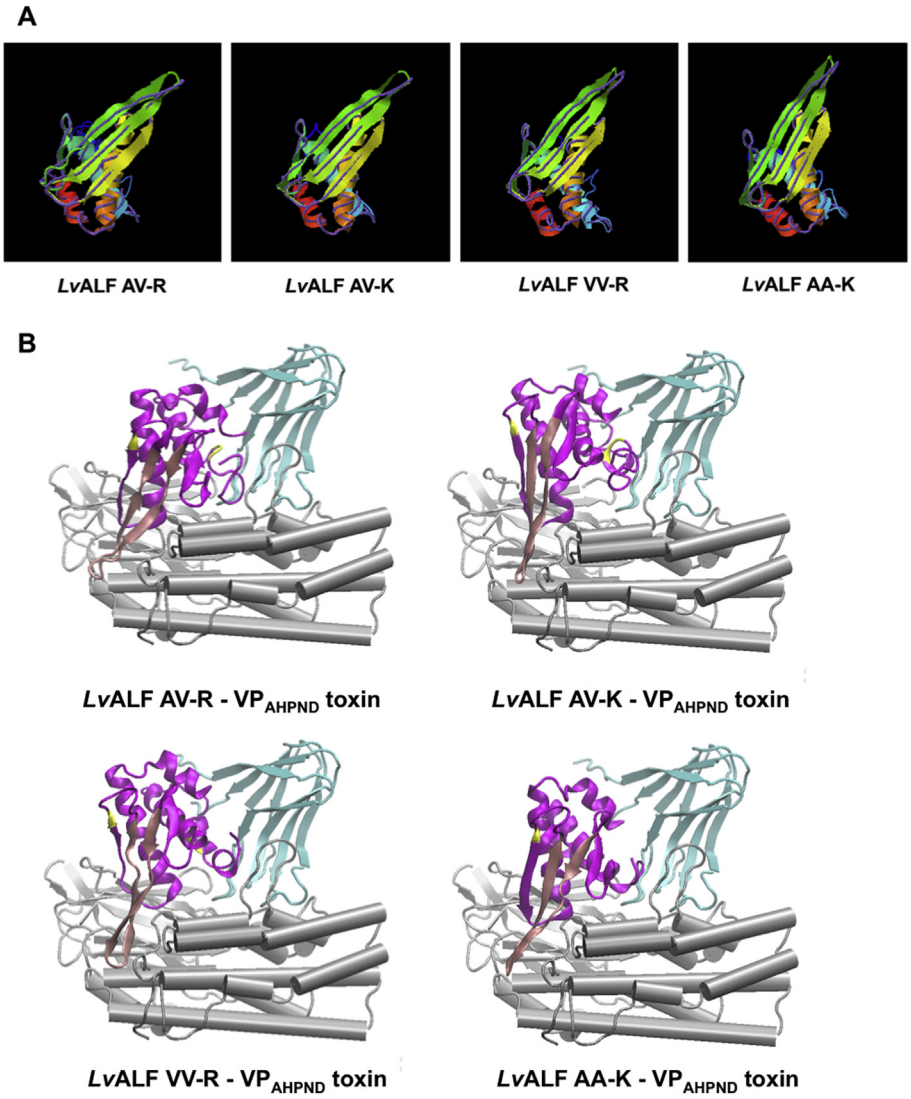


Fig. 5. The molecular modeling and docking analysis for *Lv*ALF and VP_{AHPND} toxin interaction. **A.** The 3D structure alignment of ALF*Pm*3 (line) and *Lv*ALFs (ribbon) including *Lv*ALF AV-R, *Lv*ALF AV-K, *Lv*ALF VV-R and *Lv*ALF AA-K; **B.** Molecular docking of each *Lv*ALF sub-isoform and VP_{AHPND} toxin. The gray color shows PirB protein, blue color shows PirA protein, purple color shows *Lv*ALFs protein, pink color shows LPS-binding site of *Lv*ALFs and yellow color shows the difference amino acid residues of *Lv*ALF isoforms. (For interpretation of the references to color in this figure legend, the reader is referred to the Web version of this article.)

of *Lv*ALF's LPS-binding domain to bind to molecular targets such as the PirA and PirB toxins. After all, this functional domain has been considered a key feature responsible for binding to lipopolysaccharide (LPS) and lipoteichoic acid (LTA) on the bacterial cell membrane [42] and WSSV structural proteins [29]. As seen in the protein model prediction (Fig. 5), the LPS-binding domain protrudes from the surface and is therefore, readily available for binding to any component protein of the VP_{AHPND} toxin. Protein interaction prediction using molecular docking showed low coefficient weights of the lowest energy in a magnitude of −1000 thus suggesting that interaction between *Lv*ALF and VP_{AHPND} toxin is possible through binding of *Lv*ALF's LPS-binding site to the PirB protein of VP_{AHPND} toxin. Toxin neutralization of proteins in shrimp has been recently described [6]; where hemocyanin directly interacts with PirA as reported by protein-protein interaction analysis in ELISA. This mode of shrimp immunity by *Lv*ALF, where the LPS-binding site of *Lv*ALF binds to PirB of the VP_{AHPND} toxin, will be interesting to explore in future studies because a recent report about a natural VP_{AHPND} PirA-B+ mutant that kills shrimp but produces no VP_{AHPND} toxin or AHPND lesions [33] poses the importance of developing new ways to understand and combat the disease not only in terms of exploring the host immune system for battling bacterial infection but also for neutralizing the products bacteria produce.

The shrimp homolog of protein kinase A regulatory subunit 1 showed no significant change in both the bacterial challenge and toxin challenge experiments (Fig. 3). Meanwhile, the DNAJ homolog subfamily C member 1-like was significantly down-regulated in the bacterial challenge at 3-hpi unlike in the toxin challenge, where no significant change was observed (Fig. 3). This quick response in DNAJ at 3-hpi may attribute to bacterial shock as also seen in rock pool shrimp, *Palaemon elegans*, where its down-regulation is attributed to atrophy [31]. While this may be the case, DNAJ's gene expression stabilized later on at 6-hpi and 48-hpi, showing no significant difference from the control.

In summary, we may consider AHPND pathogenesis to be comprised of two aspects. These 2 aspects were clearly observable in the immune mechanisms affected by the VP_{AHPND} bacteria themselves, the partially purified toxin or both. RNA-seq determined a good number of candidate genes that were explored and validated by qPCR, giving good baseline information on the complex immune mechanism induced by what can be considered as two hallmarks of AHPND pathogenesis, bacterial shock and cellular stress by toxin. Three types of immune genes may thus be categorized during VP_{AHPND} infection: genes that are affected by the

VP_{AHPND} bacteria only, such as Serpin 3, clottable protein, and DNAJ homolog; genes that are affected by both VP_{AHPND} bacteria and partially purified toxin, such as crustin p, c-type lectin 3 and P38 MAPK; and genes that are affected by partially purified toxin only, such as *Lv*ALF. There is a possibility for *Lv*ALF's role in toxin neutralization of VP_{AHPND} in Pacific white shrimp highlighting and warranting further studies to characterize its wide range of binding ability.

Acknowledgements

The authors acknowledge the Marine Shrimp Broodstock Research Center II (MSBRC-2), Charoen Pokphand Foods PCL for providing *V. parahaemolyticus* AHPND. This research was supported by Thailand Research Fund (TRF Senior Scholar No. RTA5880004). The authors would also like to thank the support from Chulalongkorn University under the Ratchadaphisek Somphot Endowment to the Center of Excellence for Molecular Biology and Genomics of Shrimp and Outstanding Research Performance Program: Chulalongkorn Academic Advancement into Its 2nd Century Project (CUAASC). The Ratchadaphiseksomphot Endowment Fund for Postdoctoral Fellowship, Chulalongkorn University is also greatly appreciated.

Appendix A. Supplementary data

Supplementary data related to this article can be found at https://doi.org/10.1016/j.fsi.2018.06.054.

References

[1] E. Afgan, D. Baker, M. Van den beek, D. Blankenberg, D. Bouvier, M. Čech, J. Chilton, D. Clements, N. Coraor, C. Eberhard, B. Grüning, A. Guerler, J. Hillman-Jackson, G. Von kuster, E. Rasche, N. Soranzo, N. Turaga, J. Taylor, A. Nekrutenko, J. Goecks, The Galaxy platform for accessible, reproducible and collaborative biomedical analyses: 2016 update, Nucleic Acids Res. 44 (Web Server issue) (2016) W3–W10 http://doi.org/10.1093/nar/gkw343.

[2] S.F. Altschul, W. Gish, W. Miller, E.W. Myers, D.J. Lipman, Basic local alignment search tool, J. Mol. Biol. 215 (1990) 403–410.

[3] M. Ashburner, C.A. Ball, J.A. Blake, D. Botstein, H. Butler, J.M. Cherry, A.P. Davis, K. Dolinski, S.S. Dwight, J.T. Eppig, M.A. Harris, D.P. Hill, L. Issel-Tarver, A. Kasarskis, S. Lewis, J.C. Matese, J.E. Richardson, M. Ringwald, G.M. Rubin, G. Sherlock, Gene ontology: tool for the unification of biology. The Gene Ontology Consortium, Nat. Genet. 25 (2000) 25–29.

[4] D. Banerjee, B. Maiti, S. Girisha, M. Venugopal, I. Karunasagar, A crustin isoform from black tiger shrimp, *Penaeus monodon* exhibits broad spectrum anti-bacterial activity, Aquaculture Rep. 2 (2015) 106–111.

[5] H.M. Berman, J. Westbrook, Z. Feng, G. Gilliland, T.N. Bhat, H. Weissig, I.N. Shindyalov, P.E. Bourne, The protein data bank, 1999, International Tables for Crystallography Volume F: Crystallography of Biological Macromolecules (Pp. 675–684), Springer, Netherlands, 2006.

[6] P. Boonchuen, P. Jaree, A. Tassanakajon, K. Somboonwiwat, Hemocyanin of *Litopenaeus vannamei* agglutinates *Vibrio parahaemolyticus* AHPND (VP_{AHPND}) and neutralizes its toxin, Dev. Comp. Immunol. 84 (2018) 371–381 https://doi.org/10.1016/j.dci.2018.03.010.

[7] Y.-Y. Chen, J.-C. Chen, Y.-C. Lin, S.-T. Yeh, C.-L. Huang, White shrimp *Litopenaeus vannamei* that have received *Gracilaria tenuistipitata* extract show early recovery of immune parameters after ammonia stressing, Mar. Drugs 13 (2015).

[8] P. Cohen, The search for physiological substrates of MAP and SAP kinases in mammalian cells, Trends Cell Biol. 7 (1997) 353–361.

[9] S.R. Comeau, D.W. Gatchell, S. Vajda, C.J. Camacho, ClusPro: an automated docking and discrimination method for the prediction of protein complexes, Bioinformatics 20 (1) (2004) 45–50.

[10] A. Conesa, S. Gotz, J.M. Garcia-Gomez, J. Terol, M. Talon, M. Robles, Blast2GO: a universal tool for annotation, visualization and analysis in functional genomics research, Bioinformatics 21 (2005) 3674–3676.

[11] A. Cuenda, Mitogen-activated protein kinase kinase 4 (MKK4), Int. J. Biochem. Cell Biol. 32 (2000) 581–587.

[12] E. De La Vega, N.A. O'leary, J.E. Shockey, J. Robalino, C. Payne, C.L. Browdy, G.W. Warr, P.S. Gross, Anti-lipopolysaccharide factor in *Litopenaeus vannamei* (*Lv*ALF): a broad spectrum antimicrobial peptide essential for shrimp immunity against bacterial and fungal infection, Mol. Immunol. 45 (2008) 1916–1925.

[13] M.G. Grabherr, B.J. Haas, M. Yassour, J.Z. Levin, D.A. Thompson, I. Amit, X. Adiconis, L. Fan, R. Raychowdhury, Q. Zeng, Z. Chen, E. Mauceli, N. Hacohen, A. Gnirke, N. Rhind, F. Di Palma, B.W. Birren, C. Nusbaum, K. Lindblad-Toh, N. Friedman, A. Regev, Full-length transcriptome assembly from RNA-Seq data without a reference genome, Nat. Biotechnol. 29 (2011) 644–652.

[14] J.E. Han, K.F. Tang, L.H. Tran, D.V. Lightner, Photorhabdus insect-related (Pir) toxin-like genes in a plasmid of *Vibrio parahaemolyticus*, the causative agent of acute hepatopancreatic necrosis disease (AHPND) of shrimp, Dis. Aquat. Org. 113 (2015) 33–40.

[15] W. Humphrey, A. Dalke, K. Schulten, VMD: visual molecular dynamics, J. Mol. Graph. 14 (1) (1996) 33–38.

[16] M. Kanehisa, S. Goto, Y. Sato, M. Furumichi, M. Tanabe, KEGG for integration and interpretation of large-scale molecular data sets, Nucleic Acids Res. 40 (2012) D109–D114.

[17] M.R. Kanost, Serine proteinase inhibitors in arthropod immunity, Dev. Comp. Immunol. 23 (1999) 291–301.

[18] H. Kondo, S. Tinwongger, P. Proespraiwong, R. Mavichak, S. Unajak, R. Nozaki, I. Hirono, Draft genome sequences of six strains of *Vibrio parahaemolyticus* isolated from early mortality syndrome/acute hepatopancreatic necrosis disease shrimp in Thailand, Genome Announc. 2 (2014).

[19] D. Kozakov, D.R. Hall, B. Xia, K.A. Porter, D. Padhorny, C. Yueh, D. Beglov, S. Vajda, The ClusPro web server for protein-protein docking, Nat. Protoc. 12 (2) (2017) 255–278.

[20] H.-C. Lai, T.H. Ng, M. Ando, C.-T. Lee, I.T. Chen, J.-C. Chuang, R. Mavichak, S.-H. Chang, M.-D. Yeh, Y.-A. Chiang, H. Takeyama, H.-O. Hamaguchi, C.-F. Lo, T. Aoki, H.-C. Wang, Pathogenesis of acute hepatopancreatic necrosis disease (AHPND) in shrimp, Fish Shellfish Immunol. 47 (2015) 1006–1014.

[21] C. Lee, I. Chen, Y. Yang, T. Ko, Y. Huang, J. Huang, et al., The opportunistic marine pathogen *Vibrio parahaemolyticus* becomes virulent by acquiring a plasmid that expresses a deadly toxin, Proc. Natl. Acad. Sci. Unit. States Am. 112 (34) (2015) 10798–10803.

[22] J.-H. Leu, S.-H. Chen, Y.-B. Wang, Y.-C. Chen, S.-Y. Su, C.-Y. Lin, J.-M. Ho, C.-F. Lo, A review of the major penaeid shrimp EST studies and the construction of a shrimp transcriptome database based on the ESTs from four penaeid shrimp, Mar. Biotechnol. 13 (2011) 608–621.

[23] S. Li, S. Guo, F. Li, J. Xiang, Functional diversity of anti-lipopolysaccharide factor isoforms in shrimp and their characters related to antiviral activity, Mar. Drugs 13 (2015) 2602–2616.

[24] Y. Liu, F. Li, B. Wang, B. Dong, X. Zhang, J. Xiang, A serpin from Chinese shrimp *Fenneropenaeus chinensis* is responsive to bacteria and WSSV challenge, Fish Shellfish Immunol. 26 (2009) 345–351.

[25] Y. Liu, T. Liu, F. Hou, X. Wang, X. Liu, Lvserpin3 is involved in shrimp innate immunity via the inhibition of bacterial proteases and proteases involved in prophenoloxidase system, Fish Shellfish Immunol. 48 (2016) 128–135 https://doi.org/10.1016/j.fsi.2015.09.039.

[26] Y. Liu, Y. Sun, Q. Wang, F. Hou, X. Liu, Identification and functional characterizations of serpin8, a potential prophenoloxidase-activating protease inhibitor in Pacific white shrimp, *Litopenaeus vannamei*, Fish Shellfish Immunol. 60 (2017) 492–501 https://doi.org/10.1016/j.fsi.2016.11.024.

[27] Z. Luo, J. Zhang, F. Li, X. Zhang, C. Liu, J. Xiang, Identification of a novel C-type lectin from the shrimp *Litopenaeus vannamei* and its role in defense against pathogens infection, Chin. J. Oceanol. Limnol. 29 (2011) 942.

[28] M.B.B. Maningas, H. Kondo, I. Hirono, T. Saito-Taki, T. Aoki, Essential function of transglutaminase and clotting protein in shrimp immunity, Mol. Immunol. 45 (2008) 1269–1275.

[29] T. Methatham, P. Boonchuen, P. Jaree, A. Tassanakajon, K. Somboonwiwat, Antiviral action of the antimicrobial peptide ALF*Pm*3 from *Penaeus monodon* against white spot syndrome virus, Dev. Comp. Immunol. 69 (2017) 23–32.

[30] L. Nunan, D. Lightner, C. Pantoja, S. Gomez-Jimenez, Detection of acute hepatopancreatic necrosis disease (AHPND) in Mexico, Dis. Aquat. Org. 111 (2014) 81–86.

[31] P. Olsvik, B. Lunestad, A. Agnalt, O. Samuelsen, Impact of teflubenzuron on the rockpool shrimp (*Palaemon elegans*), Comp. Biochem. Physiol. C Toxicol. Pharmacol. 201 (2017) 35–43.

[32] M.W. Pfaffl, A new mathematical model for relative quantification in real-time RT-PCR, Nucleic Acids Res. 29 (2001) e45.

[33] K. Phiwsaiya, W. Charoensapsri, S. Taengphu, H. Dong, P. Sangsuriya, G. Nguyen, et al., A natural *Vibrio parahaemolyticus* Δ pirA Vp pirB Vp+ mutant kills shrimp but produces neither Pir Vp toxins nor acute hepatopancreatic necrosis disease lesions, Appl. Environ. Microbiol. 83 (16) (2017) e00680–17.

[34] S. Powell, D. Szklarczyk, K. Trachana, A. Roth, M. Kuhn, J. Muller, R. Arnold, T. Rattei, I. Letunic, T. Doerks, L.J. Jensen, C. Von Mering, P. Bork, eggNOG v3.0: orthologous groups covering 1133 organisms at 41 different taxonomic ranges, Nucleic Acids Res. 40 (2012) D284–D289.

[35] M. Punta, P.C. Coggill, R.Y. Eberhardt, J. Mistry, J. Tate, C. Boursnell, N. Pang, K. Forslund, G. Ceric, J. Clements, A. Heger, L. Holm, E.L.L. Sonnhammer, S.R. Eddy, A. Bateman, R.D. Finn, The Pfam protein families database, Nucleic Acids Res. 40 (2012) D290–D301.

[36] S. Pyronnet, Human eukaryotic translation initiation factor 4G (eIF4G) recruits Mnk1 to phosphorylate eIF4E, EMBO J. 18 (1) (1999) 270–279.

[37] Z. Qin, V. Babu, Q. Wan, M. Zhou, R. Liang, A. Muhammad, et al., Transcriptome analysis of Pacific white shrimp (*Litopenaeus vannamei*) challenged by *Vibrio parahaemolyticus* reveals unique immune-related genes, Fish Shellfish Immunol. 77 (2018) 164–174 https://doi.org/10.1016/j.fsi.2018.03.030.

[38] M.D. Robinson, D.J. Mccarthy, G.K. Smyth, edgeR: a Bioconductor package for differential expression analysis of digital gene expression data, Bioinformatics 26 (2010) 139–140.

[39] R. Rosa, A. Vergnes, J. de Lorgeril, P. Goncalves, L. Perazzolo, L. Sauné, B. Romestand, J. Fievet, Y. Gueguen, E. Bachère, D. Destoumieux-Garzón, Functional divergence in shrimp anti-lipopolysaccharide factors (ALFs): from recognition of cell wall components to antimicrobial activity, PLoS One 8 (7) (2013) e67937.

[40] R. Sirikharin, S. Taengchaiyaphum, P. Sanguanrut, T.D. Chi, R. Mavichak, P. Proespraiwong, B. Nuangsaeng, S. Thitamadee, T.W. Flegel, K. Sritunyalucksana,

Characterization and PCR detection of binary, Pir-like toxins from *Vibrio parahaemolyticus* isolates that cause acute hepatopancreatic necrosis disease (AHPND) in shrimp, PLoS One 10 (2015) e0126987.
[41] K. Somboonwiwat, M. Marcos, A. Tassanakajon, S. Klinbunga, A. Aumelas, B. Romestand, et al., Recombinant expression and anti-microbial activity of anti-lipopolysaccharide factor (ALF) from the black tiger shrimp, Dev. Comp. Immunol. 29 (10) (2005) 841–851.
[42] K. Somboonwiwat, E. Bachere, V. Rimphanitchayakit, A. Tassanakajon, Localization of anti-lipopolysaccharide factor (ALF*Pm*3) in tissues of the black tiger shrimp, *Penaeus monodon*, and characterization of its binding properties, Dev. Comp. Immunol. 32 (2008) 1170–1176.
[43] K. Somboonwiwat, V. Chaikeeratisak, H.C. Wang, C. Fang Lo, A. Tassanakajon, Proteomic analysis of differentially expressed proteins in *Penaeus monodon* hemocytes after *Vibrio harveyi* infection, Proteome Sci. 8 (2010) 39.
[44] S. Somnuk, A. Tassanakajon, V. Rimphanitchayakit, Gene expression and characterization of a serine proteinase inhibitor PmSERPIN8 from the black tiger shrimp *Penaeus monodon*, Fish Shellfish Immunol. 33 (2) (2012) 332–341.
[45] S.A. Soto-Rodriguez, B. Gomez-Gil, R. Lozano-Olvera, M. Betancourt-Lozano, M.S. Morales-Covarrubias, Field and experimental evidence of *Vibrio parahaemolyticus* as the causative agent of acute hepatopancreatic necrosis disease of cultured shrimp (*Litopenaeus vannamei*) in Northwestern Mexico, Appl. Environ. Microbiol. 81 (2015) 1689–1699.
[46] P. Supungul, S. Tang, C. Maneeruttanarungroj, V. Rimphanitchayakit, I. Hirono, T. Aoki, A. Tassanakajon, Cloning, expression and antimicrobial activity of crustin*Pm*1, a major isoform of crustin, from the black tiger shrimp *Penaeus monodon*, Dev. Comp. Immunol. 32 (2008) 61–70.
[47] A. Tassanakajon, K. Somboonwiwat, P. Supungul, S. Tang, Discovery of immune molecules and their crucial functions in shrimp immunity, Fish Shellfish Immunol. 34 (2013) 954–967.
[48] A. Tassanakajon, V. Rimphanitchayakit, S. Visetnan, P. Amparyup, K. Somboonwiwat, W. Charoensapsri, S. Tang, Shrimp humoral responses against pathogens: antimicrobial peptides and melanization, Dev. Comp. Immunol. 80 (2018) 81–93.
[49] L. Tran, L. Nunan, R.M. Redman, L.L. Mohney, C.R. Pantoja, K. Fitzsimmons, D.V. Lightner, Determination of the infectious nature of the agent of acute hepatopancreatic necrosis syndrome affecting penaeid shrimp, Dis. Aquat. Org. 105 (2013) 45–55.
[50] A. Untergasser, I. Cutcutache, T. Koressaar, J. Ye, B.C. Faircloth, M. Remm, S.G. Rozen, Primer3–new capabilities and interfaces, Nucleic Acids Res. 40 (2012) e115.
[51] X.-W. Wang, J.-X. Wang, Diversity and multiple functions of lectins in shrimp immunity, Dev. Comp. Immunol. 39 (2013) 27–38.
[52] X.-W. Wang, J.-D. Xu, X.-F. Zhao, G.R. Vasta, J.-X. Wang, A shrimp C-type lectin inhibits proliferation of the hemolymph microbiota by maintaining the expression of antimicrobial peptides, J. Biol. Chem. 289 (2014) 11779–11790.
[53] N. Wetsaphan, V. Rimphanitchayakit, A. Tassanakajon, K. Somboonwiwat, *Pm*SERPIN3 from black tiger shrimp *Penaeus monodon* is capable of controlling the proPO system, Dev. Comp. Immunol. 41 (2) (2013) 110–119.
[54] Y.T. Yang, I.T. Chen, C.T. Lee, C.Y. Chen, S.S. Lin, L.I. Hor, T.C. Tseng, Y.T. Huang, K. Sritunyalucksana, S. Thitamadee, H.C. Wang, C.F. Lo, Draft genome sequences of four strains of *Vibrio parahaemolyticus*, three of which cause early mortality syndrome/acute hepatopancreatic necrosis disease in shrimp in China and Thailand, Genome Announc. 2 (2014).
[55] M.-D. Yeh, H.-C. Wang, Characterization and involvement of Toll and IMD pathways in AHPND-infected shrimp, Fish Shellfish Immunol. 53 (2016) 62.
[56] M.D. Young, M.J. Wakefield, G.K. Smyth, A. Oshlack, Gene ontology analysis for RNA-Seq: accounting for selection bias, Genome Biol. 11 (2010) R14.
[57] F. Yue, L. Pan, P. Xie, D. Zheng, J. Li, Immune responses and expression of immune-related genes in swimming crab *Portunus trituberculatus* exposed to elevated ambient ammonia-N stress, Comp. Biochem. Physiol. Mol. Integr. Physiol. 157 (2010) 246–251.
[58] W. Zhan, X. Tang, X. Wang, L. He, X. Wei, An anti-lipopolysaccharide factor in *Litopenaeus vannamei* participates in the immune defense against WSSV and *Vibrio anguillarum*, J. Crustac Biol. 35 (5) (2015) 670–675.
[59] Y. Zhang, I-TASSER server for protein 3D structure prediction, BMC Bioinf. 9 (2008) 40.
[60] Y.R. Zhao, Y.H. Xu, H.S. Jiang, S. Xu, X.F. Zhao, J.X. Wang, Antibacterial activity of serine protease inhibitor 1 from kuruma shrimp *Marsupenaeus japonicus*, Dev. Comp. Immunol. 44 (2014) 261–269.

Developmental and Comparative Immunology 86 (2018) 109–117

Contents lists available at ScienceDirect

Developmental and Comparative Immunology

journal homepage: www.elsevier.com/locate/dci

A novel white spot syndrome virus protein WSSV164 controls prophenoloxidases, *Pm*proPOs in shrimp melanization cascade

Pakkakul Sangsuriya [a, b], Walaiporn Charoensapsri [b, c], Jantiwan Sutthangkul [d], Saengchan Senapin [b, c], Ikuo Hirono [e], Anchalee Tassanakajon [d], Piti Amparyup [a, b, *]

[a] *Aquatic Molecular Genetics and Biotechnology Laboratory, National Center for Genetic Engineering and Biotechnology (BIOTEC), National Science and Technology Development Agency (NSTDA), 113 Paholyothin Road, Klong 1, Klong Luang, Pathumthani 12120, Thailand*
[b] *National Center for Genetic Engineering and Biotechnology (BIOTEC), National Science and Technology Development Agency (NSTDA), 113 Paholyothin Road, Klong 1, Klong Luang, Pathumthani 12120, Thailand*
[c] *Center of Excellence for Shrimp Molecular Biology and Biotechnology (Centex Shrimp), Faculty of Science, Mahidol University, Rama VI Road, Bangkok 10400, Thailand*
[d] *Center of Excellence for Molecular Biology and Genomics of Shrimp, Department of Biochemistry, Faculty of Science, Chulalongkorn University, 254 Phayathai Road, Bangkok 10330, Thailand*
[e] *Laboratory of Genome Science, Tokyo University of Marine Science and Technology, Konan 4-5-7, Minato-ku, Tokyo 108-8477, Japan*

ARTICLE INFO

Article history:
Available online 4 May 2018

Keywords:
Shrimp immunity
Penaeus monodon
White spot syndrome virus
Melanization
Prophenoloxidase

ABSTRACT

Melanization, mediated by the prophenoloxidase (proPO)-activating system, is an important innate immune response in invertebrates. The implication of the proPO system in antiviral response and the suppression of host proPO activation by the viral protein have previously been demonstrated in shrimp. However, the molecular mechanism of viral-host interactions in the proPO cascade remains largely unexplored. Here, we characterized the viral protein, namely, WSSV164, which was initially identified from the forward suppression subtractive hybridization (SSH) cDNA library of the *Pm*proPO1/2 co-silenced black tiger shrimp *Penaeus monodon* that was challenged with white spot syndrome virus (WSSV). Using the yeast two-hybrid system, WSSV164 was found to interact with the *Pm*proPO2 protein. The subsequent validation assay by co-immunoprecipitation revealed that WSSV164 directly bound to both *Pm*proPO1 and *Pm*proPO2. The gene silencing experiment was carried out to explore the role of WSSV164 in the control of the proPO pathway in shrimp, and the results showed that suppression of WSSV164 can restore PO activity in WSSV-infected shrimp hemolymph. The recombinant proteins of *Pm*proPO1 and *Pm*proPO2 were produced in Sf-9 cells and were shown to be successfully activated by exogenous trypsin and endogenous serine proteinases from shrimp hemocyte lysate supernatant (HLS), yielding PO activity *in vitro*. Moreover, the activated PO activity in shrimp HLS was dose-dependently reduced by the recombinant WSSV164 protein, suggesting that WSSV164 may interfere with the activation of the proPO system in shrimp. Taken together, these results suggest an alternative infection route of WSSV through the encoded viral protein WSSV164 that binds to the *Pm*proPO1 and *Pm*proPO2 proteins, interfering with the activation of the melanization cascade in shrimp.

© 2018 Elsevier Ltd. All rights reserved.

1. Introduction

Melanization is considered a major innate immune response in invertebrates due to its rapid and effective destruction of invader pathogens (Amparyup et al., 2013a; Cerenius and Söderhäll, 2004; Cerenius et al., 2008; Kanost and Gorman, 2008; Tassanakajon et al., 2018). This process requires multiple steps involving both enzymatic and non-enzymatic reactions. The enzymatic reaction is mediated by the key enzyme phenoloxidase (PO) (Amparyup et al., 2013a; Cerenius and Söderhäll, 2004; Cerenius et al., 2008). Upon microbial recognition, binding of pathogen-associated molecular patterns (PAMPs) with host specific pattern recognition receptors (PRRs) triggered the serine proteinase cascade and resulted in the proteolytic activation of the terminal clip-domain serine

* Corresponding author. Aquatic Molecular Genetics and Biotechnology Laboratory, National Center for Genetic Engineering and Biotechnology (BIOTEC), National Science and Technology Development Agency (NSTDA), 113 Paholyothin Road, Klong 1, Klong Luang, Pathumthani 12120, Thailand.
E-mail address: piti.amp@biotec.or.th (P. Amparyup).

https://doi.org/10.1016/j.dci.2018.05.005
0145-305X/© 2018 Elsevier Ltd. All rights reserved.

proteinases (clip-SPs) and proPO-activating enzymes (PPAEs), which subsequently cleave the zymogen proPO into active PO. PO then catalyzed the conversion of phenolic substances to the corresponding quinone precursors for melanin production (Cerenius and Söderhäll, 2004; Nappi and Christensen, 2005). The melanin directly shields pathogens to limit their growth and spread (Cerenius and Söderhäll, 2004; Cerenius et al., 2008). In addition, the reactive intermediates formed during melanin biosynthesis were cytotoxic and deleterious to both microbial and host cells, and thus the process of melanization and proPO activation must be tightly controlled by certain regulatory molecules (Cerenius et al., 2010; Charoensapsri et al., 2014; Nappi and Christensen, 2005; Zhao et al., 2007, 2011).

There is evidence that the activation of the insect melanization cascade can be suppressed by some viral pathogens. In *Manduca sexta*, host melanization was suppressed by a *Microplitis demolitor* bracovirus (MdBV) carried by the parasitic wasp *M. demolitor*, thereby allowing successful parasitism in the larval insects (Beck and Strand, 2007; Lu et al., 2008, 2010). Furthermore, the reactive compound 5,6-dihydroxyindole (DHI), known as an intermediate substance in proPO cascade, showed antiviral activity against baculoviruses and lambda bacteriophage (Zhao et al., 2011).

White spot syndrome virus (WSSV) is the most devastating causative agent of viral diseases that threaten shrimp aquaculture worldwide. WSSV is a large enveloped virus that possesses a circular double-stranded DNA genome, belonging to its own family *Nimaviridae* and the genus *Whispovirus* (Leu et al., 2009; Sánchez-Paz, 2010). Upon viral infection, a high mortality rate in shrimp has been observed within a few days. Although knowledge of WSSV infection has progressed (Leu et al., 2009; Sánchez-Paz, 2010; Verbruggen et al., 2016), an effective treatment for WSSV has not yet been achieved.

Previously, we identified and characterized several components of the proPO system in shrimp *P. monodon*, including *Pm*proPO1 and 2 (Amparyup et al., 2009), *Pm*PPAE1 and 2 (Charoensapsri et al., 2009, 2011), *Pm*LGBP (Amparyup et al., 2012), *Pm*MasSPH1 and 2 (Amparyup et al., 2007, 2013a; Jearaphunt et al., 2015; Jitvaropas et al., 2009), *Pm*ClipSP2 (Amparyup et al., 2013b; Khorattanakulchai et al., 2017) and *Pm*Snake (Monwan et al., 2017). We also characterized the functions of two negative regulators in the shrimp proPO system, *Pm*Pacifastin-like (Sangsuriya et al., 2016) and *Pm*MIP (Noothuan et al., 2017). Moreover, our previous finding also provided the first evidence that melanization has a significant role in the defense against viral infection in shrimp (Sutthangkul et al., 2015). However, it was found that viruses have evolved evasion strategies to counteract the host immune reaction and establish successful infection. WSSV453 was the first protein identified as a virulence factor to interfere with shrimp melanization by inhibiting the terminal clip-SP, termed *Pm*PPAE2 (Sutthangkul et al., 2015, 2017). Nevertheless, gene silencing of WSSV453 was found to partially recover PO activity after WSSV infection, suggesting that WSSV encodes more than one protein to inhibit the melanization cascade in shrimp.

In this study, we initially used suppression subtractive hybridization (SSH) to identify the potential genes that were differentially expressed in hemocytes of WSSV-challenged *Pm*proPO1/2 co-silenced shrimp *P. monodon*; here, the up-regulated WSSV gene, which was identified as WSSV164, was discovered. Protein-protein interaction studies using a yeast two hybrid assay followed by co-immunoprecipitation (co-IP) assays then demonstrated the binding between WSSV164 and the shrimp *Pm*proPO1 and *Pm*proPO2 proteins. The regulatory mechanism between WSSV and PO-catalyzed melanization was also investigated using RNA interference to mediate gene silencing and biochemically characterize the recombinant *Pm*proPO1 and *Pm*proPO2 with the WSSV164 protein. The result indicated that WSSV164 is a virulence factors encoded by WSSV that is responsible for suppression of shrimp PO activity.

2. Materials and methods

2.1. Experimental shrimp and WSSV preparation

Specific pathogen-free (SPF) *Penaeus monodon* were obtained from the Shrimp Genetic Improvement Center, BIOTEC, Thailand. Shrimp were reared in an aerated tank with seawater at 20 ppt salinity for 7 days before the experiments began. WSSV stock was prepared from the gills of WSSV-infected moribund *P. monodon* as previously described (Sutthangkul et al., 2015). The virus stock with the titer adjusted to the cumulative mortality of approximately 50% within 3 days post infection (LD_{50}) was chosen as the dose for experimental challenge.

2.2. Total RNA preparation and cDNA synthesis

Total RNA was extracted using GENEzol™ Reagent (Geneaid) according to the manufacturer's instructions. First-strand cDNA was synthesized from total RNA and oligo$(dT)_{18}$ primer using a RevertAid™ first strand cDNA synthesis kit (Thermo Scientific) following the manufacturer's instructions. The cDNAs were stored at −80 °C until needed for further experiments.

2.3. In vivo gene silencing of PmproPO1/2 and WSSV challenge

Double-stranded RNAs (dsRNA) for *Pm*proPO1, *Pm*proPO2 and green fluorescent protein (GFP) genes were prepared as described by Amparyup et al. (2009). *In vivo* gene silencing was achieved by intramuscularly injecting shrimp *P. monodon* (5 ± 0.2 g, fresh body weight) with 25 μl of saline buffer (150 mM NaCl) containing *Pm*proPO1 and *Pm*proPO2 dsRNAs (5 μg/g shrimp). Shrimp injected with saline buffer containing GFP dsRNA at the same concentration served as the control group. At 24 h, shrimp were injected again with dsRNAs and WSSV. Hemolymph was then individually collected at 6, 9, 12 and 48 h post-WSSV injection (hpi) in an anticoagulant solution (0.45 M NaCl, 0.1 M glucose, 26 mM citric acid, 30 mM trisodium citrate, 10 mM EDTA, pH 4.6). Hemocyte was subsequently isolated by centrifugation at 800 × *g* for 10 min at 4 °C. Total RNA was extracted using an Illustra™ RNAspin mini kit (GE Healthcare) following the manufacturer's protocol. Verification of *Pm*proPO1 and 2 gene silencing efficiencies were performed by semi-quantitative RT-PCR as described by Amparyup et al. (2009) using the gene specific primer listed in Table 1.

2.4. Suppression subtractive hybridization (SSH) cDNA library construction

To identify the differentially expressed genes in hemocytes of *P. monodon* after the *Pm*proPO1 and 2 transcripts were suppressed under WSSV infections, we constructed four SSH cDNA libraries using a PCR Select™ cDNA Subtraction Kit (Clontech) with some minor modifications, as previously described (Sangsuriya et al., 2016). Briefly, total RNA taken from the *Pm*proPO1/2-silenced and GFP control shrimp were divided into the early (6, 9, and 12 hpi) and late (48 hpi) phases of WSSV infection. One microgram of each total RNA pool were reverse-transcribed into cDNA using a SMARTer™ PCR cDNA synthesis kit (Clontech) according to the manufacturer's instructions. The resulting cDNAs were digested with *Rsa*I and subsequently used as tester and driver for the construction of two forward and two reverse SSH libraries in accordance with the Clontech PCR-Select cDNA subtraction protocols. The subtracted PCR products were cloned into the pGEM®-T easy

Table 1
Primers used in the experiments.

Primer name	Sequence (5′ to 3′)	Purpose
PO1i-F	CACCCTGAGAGCTCCCACTT	RNAi
PO1i-R	GAGATCCTGCAGTGTAACGT	RNAi
PO1iT7-F	GGATCCTAATACGACTCACTATAGGCACCCTGAGAGCTCCCACTT	RNAi
PO1iT7-R	GGATCCTAATACGACTCACTATAGGGAGATCCTGCAGTGTAACGT	RNAi
PO2i-F	CGTCTTCCTCGGCCGCTCCT	RNAi
PO2i-R	CCACGGGGATACCGCTGCCA	RNAi
PO2iT7-F	GGATCCTAATACGACTCACTATAGGCGTCTTCCTCGGCCGCTCCT	RNAi
PO2iT7-R	GGATCCTAATACGACTCACTATAGGCCACGGGGATACCGCTGCCA	RNAi
GFP-F	ATGGTGAGCAAGGGCGAGGA	RNAi
GFP-R	TTACTTGTACAGCTCGTCCA	RNAi
GFPT7-F	TAATACGACTCACTATAGGATGGTGAGCAAGGGCGAGGA	RNAi
GFPT7-R	TAATACGACTCACTATAGGTTACTTGTACAGCTCGTCCA	RNAi
WSSV164-F	CTCGACGACGGGACAGTT	RNAi, RT-PCR
WSSV164-R	TTCACGGCGTTGTTGTTG	RNAi, RT-PCR
WSSV453-F	ATGAAGTTGATGGAGTTCCTG	RT-PCR
WSSV453-R	TTATTGCCTCCATTTTCTTGT	RT-PCR
ICP11-F	ATGGCCACCTTCCAGACT	RT-PCR
ICP11-R	TTCTGTTGTTGGCACAAT	RT-PCR
PO1RT-F	GGTCTTCCCCTCCCGCTTCG	RT-PCR
PO1RT-R	GCCGCAGGTCCTTTGGCAGC	RT-PCR
PO2RT-F	GCCAAGGGGAACGGGTGATG	RT-PCR
PO2RT-R	TCCCTCATGGCGGTCGAGGT	RT-PCR
EF1α-F	GGTGCTGGACAAGCTGAAGGC	RT-PCR
EF1α-R	CGTTCCGGTGATCATGTTCTTGATG	RT-PCR
*Nde*I-PO1-F	TTCCATATGGCCAATGACCAGCAG	Yeast two-hybrid
*Eco*RI-PO1-R	CCGGAATTCTCAGTTCAATTTCTC	Yeast two-hybrid
*Nde*I-PO2-F	TCCATATGGAAAAGAATCAGAAGAACCTCCT	Yeast two-hybrid
*Bam*HI-PO2-R	CGCGGATCCTTAGTTCAGCTTCTC	Yeast two-hybrid
*Hin*dIII-PO1-F	CCAAGCTTACCATGGCCAATGACCAGCA	co-IP assay, Recombinant protein
*Eco*RI-PO1-R2	GGAATTCCCGTTCAATTTCTCGCCCAG	co-IP assay, Recombinant protein
*Hin*dIII-PO2-F	CCAAGCTTACCATGGAAAAGAATCAGAA	co-IP assay, Recombinant protein
*Not*I-PO2-R	GAGCGGCCGCCGTTCAGCTTCTCTGCCAAG	co-IP assay, Recombinant protein
*Bam*HI-WSSV164-F	GCGGATCCAAAATGGGTTCTCACATCAACTCT	co-IP assay, Recombinant protein
*Not*I-WSSV164-R	AGCGGCCGCCCTGGTATCTGATTTCTTG	co-IP assay, Recombinant protein

vector (Promega) and transformed into *Escherichia coli* JM109 (Promega). SSH clones were subjected to plasmid extraction and DNA sequencing (Macrogen Inc., Korea; Tokyo University of Marine Science and Technology, Japan). The homology searches for the obtained sequences were performed using the BLAST algorithms. Protein sequences were characterized using the SMART (http://smart.embl-heidelberg.de/) and Prosite (http://prosite.expasy.org/) programs.

2.5. Yeast two-hybrid analysis

Yeast two-hybrid screens were performed based on the Clontech Matchmaker™ GAL4 Two-Hybrid system. A WSSV DNA library fused with the GAL4 activation domain (AD) of pGADT7 obtained previously was used as prey plasmids (Sangsuriya et al., 2014). Full-length genes encoding *Pm*proPO1 and *Pm*proPO2 (GenBank accession number: AF099741 and FJ025814, respectively) were amplified using the primers *Nde*I-PO1-F/*Eco*RI-PO1-R for *Pm*proPO1 and *Nde*I-PO2-F/*Bam*HI-PO2-R for *Pm*proPO2 (Table 1) and cloned downstream in-frame with the GAL4 DNA binding domain (BD) of pGBKT7 (Clontech). Positive recombinant clones were sequenced in both directions for verification of gene sequences and correct reading frames and then used as bait plasmids.

To screen for the *Pm*proPOs-interacting proteins, each bait plasmid, *Pm*proPO1/BD and *Pm*proPO2/BD, was co-transformed with WSSV164/AD or the WSSV AD library into the *Saccharomyces cerevisiae* strain AH109 using the lithium acetate/dimethyl sulfoxide method (Gietz et al., 1995). The library AD plasmids isolated from the positive colonies were rescued in *E. coli* JM109 and the interactions were reconfirmed by co-transformation of the individual rescued AD and BD plasmids into *S. cerevisiae* strain AH109. Yeast growth with blue color-change on the high stringency medium of synthetic dropout (SD) lacking adenine, histidine, leucine and tryptophan (-A/-H/-L/-W) supplemented with X-α-gal (Apollo Scientific) was counted as a positive interaction. Co-transformation of the murine p53 bait fusion (p53/BD) and SV40 large T-antigen prey fusion (SV40-T/AD) (Clontech) served as a positive control, whereas the empty pGADT7 and bait constructs or p53/BD and WSSV/AD were used as the negative control.

2.6. Co-immunoprecipitation (co-IP) assays

For validation of the yeast two-hybrid results, the cDNA fragments encoding for the *Pm*proPO1, *Pm*proPO2 and WSSV164 proteins were amplified using the primers listed in Table 1. The PCR products were cloned into the heat inducible vectors pDHsp/FLAG or pDHsp/V5 (Leu et al., 2008), and the recombinant plasmids with correct gene inserts and reading frames (as verified by nucleotide sequencing) were subjected to plasmid DNA extraction using the QIAGEN Plasmid Mini Kit. The FLAG-tagged constructs (*Pm*proPO1/FLAG or *Pm*proPO2/FLAG) and V5-tagged construct (WSSV164/V5) were co-transfected pairwise into Sf-9 (*Spodoptera frugiperda*) cells using Cellfectin® II reagent (Life Technologies) according to the manufacturer's protocol. The pairwise co-transfection of shrimp *Pm*HtrA2 (Suwannaboon et al., 2013) and WSSV164 served as the negative control. The expression of the fusion proteins in the co-transfected cells was induced by heat shock at 42 °C for 30 min, and cells were further incubated at 27 °C for 5 h before being lysed with the lysis buffer (50 mM Tris-HCl, 150 mM NaCl, 1% (v/v) Nonidet P-40, pH 8.0) supplemented with 1 × protease inhibitor cocktail (Sigma).

For co-IP assays, the protein lysates were incubated with ANTI-

FLAG® M2 Affinity Gel (Sigma) overnight at 4 °C with head-over-tail rotation, followed by stringent washing. The co-IP complexes were resolved through a reducing 12% SDS-PAGE gel before being subjected to an immunoblot assay. The V5-tagged fusion proteins were detected with rabbit anti-V5 antibody (Sigma), whereas the FLAG-tagged fusion proteins were detected with mouse anti-FLAG antibody (Sigma). Horseradish peroxidase-conjugated anti-rabbit or anti-mouse IgG served as secondary antibodies (Life Technologies). Antibody binding complexes were visualized with Clarity™ Western ECL Substrate (Bio-Rad) on X-ray films.

2.7. RNA interference (RNAi) of WSSV164

A 387-bp DNA fragment of the WSSV164 gene was amplified using the primers WSSV164-F and WSSV164-R (Table 1) and cloned into the pDrive vector (QIAGEN). The recombinant plasmids with the opposite orientation of WSSV164 fragments as verified by DNA sequencing were linearized and used as templates for the generation of the corresponding dsRNA by *in vitro* transcription using a T7 RiboMAX™ Express Large Scale RNA Production System (Promega) following the manufacturer's protocol. A negative dsRNA control (GFP dsRNA) was prepared as previously described (Amparyup et al., 2009). For the RNAi experiment, shrimp *P. monodon* (5 g, wet body weight) was intramuscularly injected with a saline solution containing WSSV164 dsRNA (3 μg/g shrimp), whereas the two control groups were shrimp injected with GFP dsRNA (3 μg/g shrimp) and 150 mM NaCl, respectively. At 24 h after injection, the dsRNA-injected groups were challenged with WSSV, while the negative NaCl-injected control was injected with 150 mM NaCl. Shrimp were reared for 48 h before subjected to further analysis.

2.8. RT-PCR analysis

Semi-quantitative RT-PCR analysis was employed to evaluate the gene silencing efficiency of WSSV164 dsRNA. Hemolymph was withdrawn from the shrimp ventral sinus 48 h after WSSV injection. Total RNA was extracted from shrimp hemocytes, and cDNA was then synthesized. The suppression efficiency of the WSSV164 gene transcripts was then determined by semi-quantitative RT-PCR using the specific primers WSSV164-F and WSSV164-R (Table 1). RT-PCR reactions were composed of 1 μl cDNA template, 0.2 μM of each forward and reverse primer, 200 μM of dNTP mix, 1.25 U of Taq DNA polymerase (RBC Bioscience) and 1 × reaction buffer. The PCR amplification was performed at 94 °C for 3 min, followed by 30 cycles of 94 °C for 30 s, 55 °C for 30 s, 72 °C for 30 s and final extension at 72 °C for 5 min. Amplification of the EF1α fragment (25 cycles) served as an internal control. Quantification of WSSV164 gene silencing effect on WSSV replication in shrimp was carried out using the gene-specific primer pairs for ICP11 and WSSV453 (Table 1). RT-PCR products were analyzed through a TBE-1.8% agarose gel followed by ethidium bromide staining.

2.9. PO activity assay of WSSV164 silenced shrimp

PO activity in the hemolymph of WSSV164 silenced shrimp was measured as described previously (Amparyup et al., 2009). In brief, hemolymph was withdrawn from the shrimp ventral sinus without any anticoagulant solution at 48 h after the WSSV challenge, and total protein concentration was determined by a Bradford protein assay kit (Bio-Rad). For the PO activity assay, 0.4 mg of total hemolymph protein was mixed with 26 μl of 3 mg/ml L-3,4-dihydroxyphenylalanine (L-DOPA; Fluka). After incubation at room temperature for 30 min, PO activity was determined by measuring the absorbance at 490 nm. Hemolymph PO activity was defined as ΔA_{490}/mg total protein/min. The experiment was performed three times and the results from three independent experiments were analyzed using one-way analysis of variance (ANOVA) followed by Tukey's test.

2.10. Recombinant protein expression of PmproPO1 and PmproPO2

The recombinant proteins of *Pm*proPO1 and *Pm*proPO2 were produced using the Sf-9 cell expression system. *Pm*proPO1/FLAG and *Pm*proPO2/FLAG constructs were separately transfected into Sf-9 cells using Cellfectin® II reagent (Life Technologies) according to the manufacturer's instructions. At 16 h post-transfection, the cell culture medium was replaced with fresh media supplemented with 500 μM $CuCl_2$ (Sigma). Cells were subsequently induced by heat shock at 42 °C for 30 min. After incubation at 27 °C for 5 h, cells were lysed in lysis buffer (50 mM Tris-HCl, pH 8.0, 150 mM NaCl, 1% Nonidet P-40). The expressed proteins were then analyzed by a 12% reducing SDS-PAGE followed by an immunoblot assay using the anti-FLAG antibody. For the enzyme activity assay, 0.4 mg of whole cell lysate was preincubated with 1 μM trypsin (Sigma) for 5 min at room temperature. For each sample, L-DOPA (Fluka) was added and the reaction mixtures were further incubated at room temperature for 30 min. PO activity was analyzed by monitoring the absorbance at 490 nm and defined as ΔA_{490}/mg total protein/min. The obtained whole cell lysates were kept at −80 °C for further assays.

2.11. Effect of recombinant WSSV164 on proPO activation in shrimp HLS

The hemocyte lysate supernatant (HLS) was prepared as previously described (Charoensapsri et al., 2014). The effect of WSSV164 on the interference of proPO activation in shrimp was determined by incubating 0.3 mg of whole cell lysate of r*Pm*proPO1 or r*Pm*proPO2 with 0.06 mg or 0.6 mg of whole cell lysate of rWSSV164, 60 μg of HLS and 50 μg of lipopolysaccharide (LPS) from *E. coli* 0111:B4 (Sigma) for 5 min at room temperature. The whole cell lysate obtained from the empty pDHsp/FLAG transfected cells served as a control to substitute the r*Pm*proPOs. L-DOPA was then added to the reaction mixture (Fluka). PO activity was monitored at 490 nm after the reaction mixture was incubated at room temperature for 30 min.

3. Results

3.1. Identification of differentially expressed transcripts from hemocytes of PmproPO1/2 silenced shrimp challenged with WSSV

Melanization is crucial for the immune response against major pathogens in shrimp (Amparyup et al., 2013a; Tassanakajon et al., 2013, 2018). Our previous finding demonstrated that WSSV overcomes the shrimp melanization cascade by suppressing the host proPO-activating system (Sutthangkul et al., 2015, 2017). Two proPO isoforms, *Pm*proPO1 and *Pm*proPO2, are the key components of the proPO cascade of shrimp *P. monodon* (Amparyup et al., 2009, 2013a; Charoensapsri et al., 2014; Sutthangkul et al., 2015). To gain insights into the molecular mechanism of WSSV-host interactions in the shrimp melanization cascade, in the present study, we initially conducted suppression subtractive hybridization (SSH) to identify the potential differentially expressed cDNAs from the hemocytes of the shrimp *P. monodon* after the *Pm*proPO1 and 2 gene transcripts were suppressed and challenged with WSSV. Interestingly, a highly redundant SSH clone, which showed 100% amino acid sequence identity to the WSSV164 gene of the WSSV Taiwan isolate (GenBank accession number: AAL89032), was obtained. WSSV164 was previously identified as a viral immediate-early (IE) gene (Li et al., 2009). However, the exact role of the WSSV164

protein remains unclear. Sequence analysis revealed that WSSV164 (Fig. 1) contains an open reading frame (ORF) of 1221 bp, encoding a polypeptide of 406 amino acid residues with a calculated molecular mass and an estimated isoelectric point of 43.45 kDa and 9.02, respectively. Domain searches based on the SMART and Prosite programs indicated that WSSV164 contains no putative specific domain or important functional motif. Nonetheless, four low-complexity regions and seven *N*-glycosylation sites were observed throughout the WSSV164 polypeptide chain. To understand the interplay between shrimp *Pm*proPOs and the WSSV protein, WSSV164 was thus selected for further characterization.

3.2. Interaction of WSSV proteins with shrimp PmproPOs using yeast two-hybrid system and co-IP assay

Yeast two-hybrid assays were conducted to screen whether *Pm*proPO1 and *Pm*proPO2 proteins could interact with WSSV164. Each *Pm*proPO1/BD, *Pm*proPO2/BD and p53/BD (as a negative control) bait plasmid was co-transformed with the WSSV164/AD prey plasmid into the yeast AH109 strain. The readout for the interaction of two proteins was the growth of yeast with a blue colony on the selective high stringency media (-A/-H/-L/-W) supplemented with X-α-gal. The results showed that *Pm*proPO2 was capable of interacting with WSSV164 (Fig. 2). However, *Pm*proPO1 did not show binding with WSSV164 in the yeast two-hybrid system (Fig. 2). In addition, the prey WSSV164/AD had no positive interaction with the bait control p53/BD and no self-activation occurred when *Pm*proPO1/BD and *Pm*proPO2/BD were co-transformed with an empty AD plasmid (Fig. 2). Data suggests that the interaction derived from the yeast two-hybrid assay is a genuine interaction.

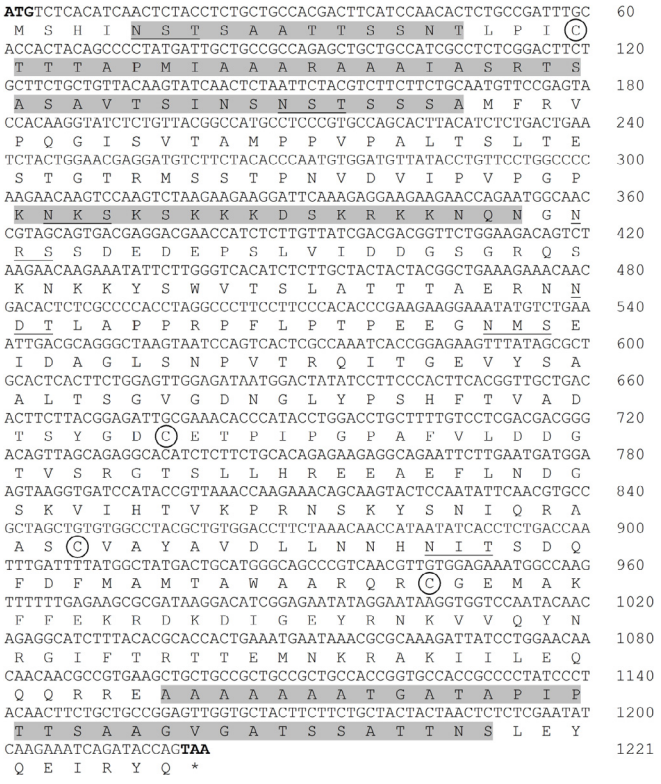


Fig. 1. Nucleotide and deduced amino acid sequences of WSSV164. Numbers at right margin indicate positions of last nucleotide on each line. Proposed start and stop codons are in bold. Low-complexity regions are shaded in gray. Predicted *N*-glycosylation sites are underlined. Circle indicates cysteine residues.

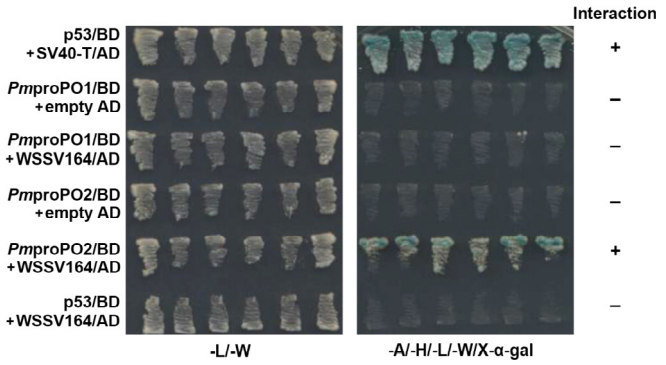


Fig. 2. Yeast two-hybrid analysis of *Pm*proPO1 and *Pm*proPO2 with WSSV164. *Pm*proPO1 and *Pm*proPO2 were constructed in-frame with the BD domain and WSSV164 with the AD domain. Indicated pairwise interactions were tested by co-transformation of BD and AD constructs into yeast AH109 and grown on -L/-W plates. Putative interactions are indicated by growth and blue color in six independent transformants on -A/-H/-L/-W/X-α-gal plate. The positive control comprised interactions between murine p53 (p53/BD) and SV40 large T-antigen (SV40-T/AD). Negative controls comprised yeast cells containing *Pm*proPO1/BD or *Pm*proPO2/BD with empty AD vector and p53/BD with WSSV164/AD.

To further access the interactions between *Pm*proPO proteins and other WSSV proteins, *Pm*proPO1/BD and *Pm*proPO2/BD were used as bait plasmids to screen for interacting partners from WSSV DNA library. After interaction screening, a putative clone was identified from the *Pm*proPO2 bait protein, while *Pm*proPO1 did not show any interaction in the yeast two-hybrid system. Sequence analysis and a homology search using the BLAST program revealed that this putative clone is WSSV164 (GenBank accession number: AAL89032). The result is consistent with data from direct binding (Fig. 2) and thus confirmed that *Pm*proPO2 but not *Pm*proPO1 interacted with WSSV164 via the yeast two-hybrid system.

Protein-protein interaction acquired from yeast two-hybrid analysis was further confirmed by co-IP assay. A pair of tested plasmids, *Pm*proPO1/FLAG + WSSV164/V5 and *Pm*proPO2/FLAG + WSSV164/V5, were co-transfected into Sf-9 cells, and the expression of recombinant proteins was induced by the heated shock method. Sf-9 cells co-transfected with WSSV164/V5 + empty pDHsp/FLAG plasmid or WSSV164/V5 + *Pm*HtrA2/FLAG (an apoptosis-related protein) were included as negative controls. Proteins from the crude Sf-9 cell lysates designated “input proteins” were first analyzed by SDS-PAGE and immunoblot analysis. As shown in Fig. 3, three protein bands of approximately 85 kDa, 85 kDa and 43 kDa corresponding to the calculated molecular mass of the r*Pm*proPO1, r*Pm*proPO2 and r*Pm*HtrA2, respectively, were detected by antibody targeting to the FLAG-epitope. When using antibody targeting to the V5-epitope, an approximately 65-kDa protein band of rWSSV164 protein was also detected in all input fractions (Fig. 3). These results indicated that r*Pm*proPO1, r*Pm*proPO2, r*Pm*HtrA2 (as a control) and rWSSV164 were successfully produced. All input proteins were subsequently subjected to the co-IP assay using an anti-FLAG M2 affinity gel, and protein complexes were subsequently subjected to SDS-PAGE and immunoblotting using the anti-V5 antibody. As shown in Fig. 3, WSSV164/V5 was specifically immunoprecipitated in the presence of *Pm*proPO1-FLAG or *Pm*proPO2/FLAG (IP, lane 1 and 2) while WSSV164/V5 alone or with the *Pm*HtrA2/FLAG was not (IP, lane 3 and 4). Taken together with the biological yeast two-hybrid test, WSSV164 could interact with *Pm*proPO2, and with the physical co-IP assay the data strongly indicated that WSSV164 is the potential interacting protein of both *Pm*proPO1 and *Pm*proPO2.

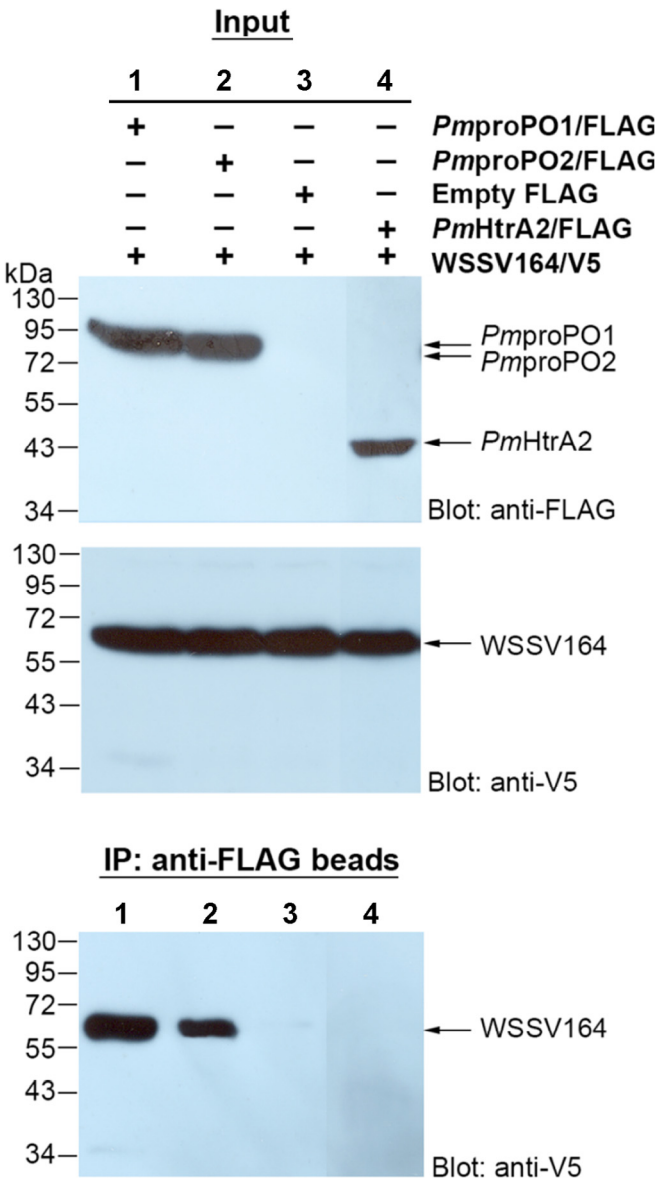


Fig. 3. Co-immunoprecipitation of *Pm*proPO1 and *Pm*proPO2 with WSSV164 in Sf-9 cells. *Pm*proPO1 and *Pm*proPO2 were constructed in-frame with FLAG tag and WSSV164 with V5 tag. Each pair of indicated constructs was transiently co-expressed in Sf-9 cells. At 5 h after heat shock, cell lysates (input) were examined for the presence of expressed proteins by immunoblot assay probing with anti-V5 and anti-FLAG antibodies. The remaining cell lysates were subjected to immunoprecipitation with anti-FLAG M2 resins. The immunoprecipitated complexes (IP) were analyzed by immunoblot assay probing with anti-V5 antibody. Co-immunoprecipitation of the FLAG vector or *Pm*HtrA2 with WSSV164 served as the negative control interaction.

3.3. *Effect of WSSV164 gene silencing on shrimp phenoloxidase (PO) activity*

The functional role of WSSV164 involved in the regulation of the proPO system was subsequently investigated using RNAi-mediated gene silencing and the determination of PO activity. *In vivo* gene silencing assays in shrimp were conducted in three groups; (I) injection of WSSV164 dsRNA, (II) injection of GFP dsRNA and (III) injection of NaCl buffer as negative control. After dsRNA treatment for 24 h, shrimp in group I and II were then challenged with WSSV, whereas group III was injected with saline buffer. To examine the efficacy of viral gene knockdown, hemolymph samples were collected at 48 h post-WSSV challenge and subjected to semi-quantitative RT-PCR analysis of the WSSV164 transcript. The result revealed the effective suppression of WSSV164 transcript in shrimp-derived WSSV164 dsRNA but not GFP dsRNA (Fig. 4A). Furthermore, RT-PCR analysis of the effect of WSSV164 gene knockdown on the viral replication also revealed no significant difference of the expression levels of ICP11 and WSSV453 gene transcripts (Fig. 4A), suggesting that suppression of WSSV164 had no effect on viral replication. The total hemolymph PO activity was then determined in all three groups using L-DOPA as the substrate. Interestingly, compared with the control GFP-silenced shrimp, WSSV164-silenced shrimp revealed a highly significant increase in PO activity (Fig. 4B). In addition, this high PO activity level was not significantly different from the non-WSSV-infected shrimp (i.e., injection of NaCl buffer). With respect to the binding capability of WSSV164 to *Pm*proPOs and the gene silencing of WSSV164 to restore hemolymph PO activity, it was therefore suggested that WSSV164 might directly control the proPO system via binding and suppressing of *Pm*proPOs function.

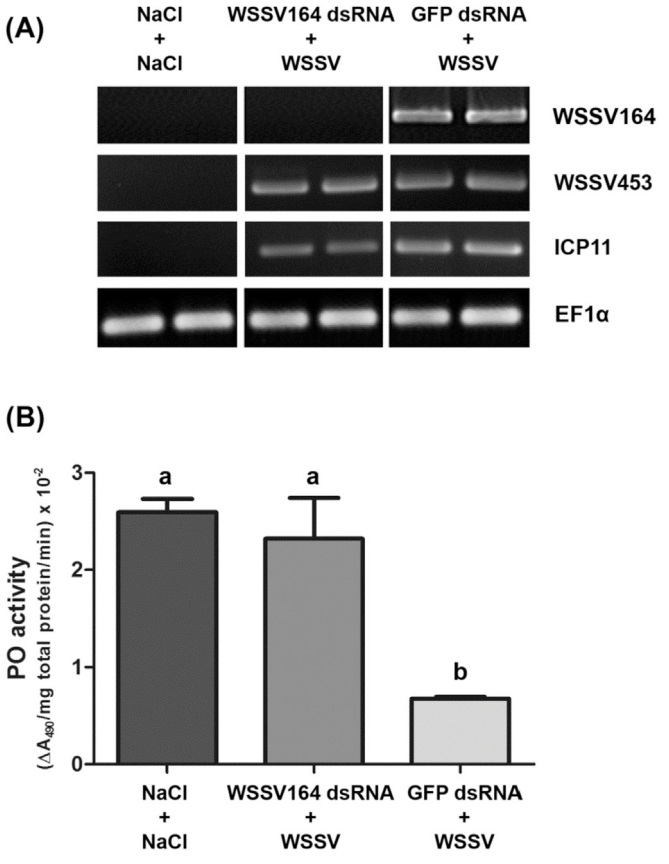


Fig. 4. Effect of WSSV164 gene silencing on hemolymph phenoloxidase (PO) activity. Shrimp were injected with WSSV164 dsRNA (3 μg/g shrimp) and control was injected with GFP dsRNA. At 24 h after dsRNA injection, shrimp in the same groups were challenged with WSSV at a LD_{50} dose. Negative control of WSSV infection was injected with NaCl solution. At 48 h after WSSV challenge, hemolymph was collected and subjected to gene knockdown efficiency and PO activity measurements. (A) RT-PCR analysis of WSSV164 transcript in knocked-down shrimp compared with WSSV453, ICP11, and internal control EF1α. Each lane represents RT-PCR products from individual shrimp. (B) Hemolymph PO activity from WSSV164 silenced shrimp was determined using L-DOPA as substrate and defined as ΔA_{490}/mg total protein/min. Data are derived from three independently replicated experiments and shown as mean ± SD (error bars). Significantly different between means ($P < 0.05$) are indicated by lower case letters above each bar.

3.4. In vitro activation of recombinant PmproPO1 and PmproPO2

Although the mechanism of WSSV164 in the suppression of *Pm*proPOs is unknown, the *in vivo* gene silencing described above clearly indicated the relevance of WSSV164 in the regulation of the proPO system. To further investigate this inhibitory mechanism, the proPO activation assay of the recombinant *Pm*proPOs generated in Sf-9 cells was then observed before being tested with the viral protein. As in the immunoblot assay (Fig. 5A), each of r*Pm*proPO1/FLAG or r*Pm*proPO2/FLAG was successfully expressed in Sf-9 cells. The cell lysate containing r*Pm*proPO1 or r*Pm*proPO2 was then subjected for proPO activation using an exogenous proteinase trypsin as an elicitor to convert zymogen *Pm*proPOs to active POs. The empty pDHsp/FLAG transfected cells were also included as control. The capability of r*Pm*proPOs activation is defined as the increase in PO activity measured spectrophotometrically by absorbance at 490 nm. As shown in Fig. 5B, the r*Pm*proPO1 and r*Pm*proPO2 can be activated by trypsin. In summary, the r*Pm*proPOs produced in Sf-9 cells were appropriate for further biochemical assays with the WSSV164 protein.

3.5. Direct inhibition of prophenoloxidases by WSSV164

Previous studies have revealed a significant reduction of PO activity caused by WSSV infection (Mathew et al., 2007; Yeh et al., 2009). It was later proved that suppression of the proPO system occurred through inhibition of serine proteinase *Pm*PPAE2 by the WSSV453 protein (Sutthangkul et al., 2015, 2017). In addition to WSSV453, in this study, WSSV demonstrated its ability to encode the WSSV164 protein to target both the *Pm*proPO1 and *Pm*proPO2 proteins. To investigate whether WSSV164 can regulate the proPO system, the recombinant WSSV164, *Pm*proPO1 and *Pm*proPO2 were generated in insect cells and employed for the inhibitory PO activity assay. The HLS added with the elicitor LPS was used as endogenous shrimp proteinases to activate *Pm*proPO1 and *Pm*proPO2. Compared with the control empty FLAG vector, simultaneous incubation of HLS plus LPS with r*Pm*proPO1 or r*Pm*proPO2 showed a highly significant increase in PO activity (i.e., 1.63-fold for r*Pm*proPO1 and 1.88-fold for r*Pm*proPO2) (Fig. 6). This indicated that r*Pm*proPO1 and 2 can be converted to active PO by both endogenous shrimp proteinases and exogenous proteinase (above result). However, the PO activity derived from r*Pm*PO1 or r*Pm*PO2 was significantly reduced (i.e., 0.64-fold for r*Pm*proPO1 and 0.68-fold for r*Pm*proPO2) when rWSSV164 was incubated in the reactions. This suppression was dose-dependent, since more reduction of PO activity was observed when the dosage of WSSV164 protein increase (Fig. 6). There was a slight but significant difference in the basal PO activity when high dosages of WSSV164 were mixed in the control empty FLAG vector (Fig. 6). Therefore, it was concluded that the reduced PO activity was due to direct inhibition of *Pm*proPO1 and *Pm*proPO2 by the viral protein WSSV164.

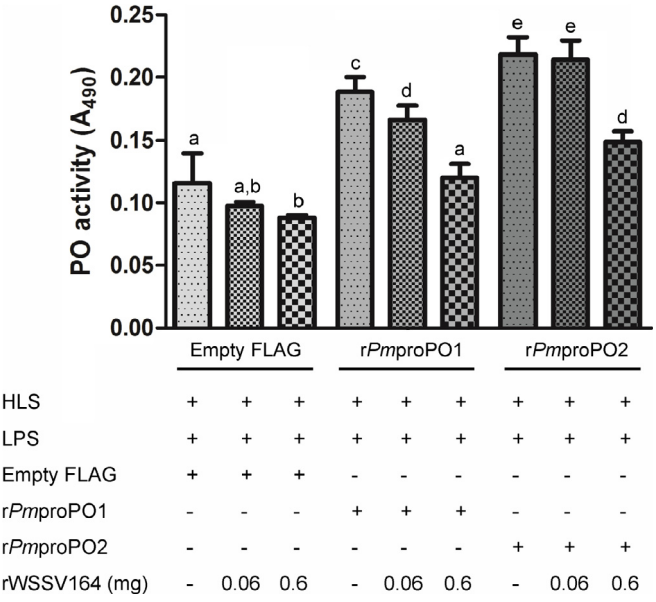


Fig. 6. Suppression of phenoloxidase (PO) activity from *Pm*proPO1 and *Pm*proPO2 by WSSV164. Shrimp hemocyte lysate supernatant (HLS) with the elicitor LPS was used as endogenous proteinase to activate r*Pm*proPO1 and 2. Sf-9 cell lysate expressing either r*Pm*proPO1 or r*Pm*proPO2 (0.3 mg) was incubated with cell lysates containing a low dose of rWSSV164 (0.06 mg of whole cell lysate of rWSSV164) or high dose of rWSSV164 (0.6 mg of whole cell lysate of rWSSV164) for 5 min at room temperature, followed by further incubation with the substrate L-DOPA for 30 min. Empty FLAG vector-transfected cell lysates were used as control to substitute the r*Pm*proPOs. PO activity was determined by measuring the absorbance at 490 nm. Each bar represents PO activity as mean ± SD from three replicates. Significantly different between means ($P < 0.05$) are indicated by lower case letters above each bar.

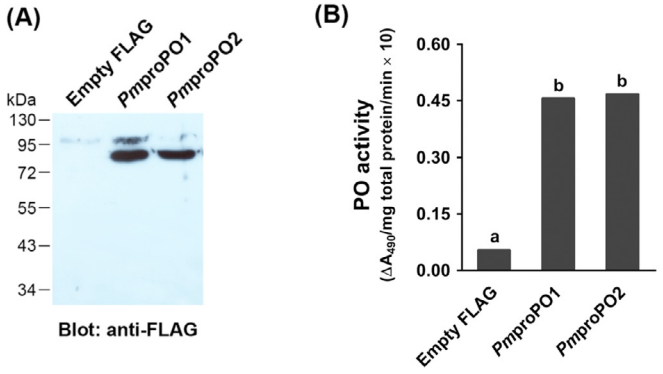


Fig. 5. Phenoloxidase (PO) activity of r*Pm*proPO1 and r*Pm*proPO2 expressing in Sf-9 cells. Transfected Sf-9 cells with either *Pm*proPO1/FLAG or *Pm*proPO2/FLAG were examined for recombinant protein expression and PO activity was measured *in vitro*. (A) An immunoblot assay of cell lysates containing expressed r*Pm*proPO1 or r*Pm*proPO2 probed with anti-FLAG antibody. (B) PO activity of r*Pm*proPO1 and r*Pm*proPO2. Cell lysates containing either r*Pm*proPO1 or r*Pm*proPO2 were simultaneously mixed with the elicitor trypsin and substrate L-DOPA for 30 min at room temperature. PO activity was defined as ΔA_{490}/mg total protein/min. Significantly different between means ($P < 0.05$) are indicated by lower case letters above each bar. The empty pDHsp/FLAG transfected cells were comparatively analyzed as a control.

4. Discussion

Melanization is one of the most important in humoral immunity because it rapidly produces melanin as well as intermediate toxic substances to encapsulate and kill invading pathogens (Cerenius and Söderhäll, 2004; Cerenius et al., 2008). Several studies in insects and crustaceans have revealed the prominent role of melanization in defense against microbial infection, including bacteria, fungi and parasites (Kanost et al., 2004; Cerenius et al., 2008; Amparyup et al., 2013a).

Regarding viral pathogens, the importance of melanization/proPO systems in antiviral response has been discovered in insects (Beck and Strand, 2007; Lu et al., 2008, 2010) and crustaceans (Sutthangkul et al., 2015, 2017; Guo et al., 2017). In the insect *Manduca sexta*, it was found that the virulence factors encoded by MdBV are the epidermal growth factor-like motif (Egf) proteins Egf1.0 and Egf1.5, also known as small serine proteinase inhibitor homologues, which inhibit melanization by interfering with the proPO-activating proteinases (PAPs) (Beck and Strand, 2007; Lu et al., 2008, 2010).

In this study, we focused on the interaction between phenoloxidase (PO), the key enzyme of the proPO cascade, and the devastating WSSV pathogen. We initially used suppression subtractive hybridization (SSH) to identify the differentially expressed genes from the hemocytes of *Pm*proPO1/2 co-silenced shrimp challenged with WSSV. Interestingly, a viral gene, namely, WSSV164, was discovered. We further assessed the implication of WSSV164 in the regulation of the shrimp proPO system and the convincing evidence of WSSV controlling proPO system was demonstrated herein. Based on yeast two-hybrid and co-IP assays, *Pm*proPO1 and *Pm*proPO2 were revealed to interact with the new virulence WSSV164 protein. Previously, WSSV164 (also known as WSV108) was identified as a viral immediate-early (IE) gene with no identifiable domains except low-complexity regions (LCRs) in the protein sequence (Li et al., 2009). The LCRs represent the repeated number of a single amino acid or short amino acids that are found in many proteins (DePristo et al., 2006) and may allow LCR-containing proteins to interact with the different binding partners (Coletta et al., 2010). However, the functional role of the LCRs found in WSSV164 in *Pm*proPO interactions awaits further studies.

In crustaceans, specifically the shrimp *P. monodon*, our previous findings provided evidence that the shrimp proPO system plays significant roles in immune defense against the major shrimp viral pathogen WSSV (Sutthangkul et al., 2015). We demonstrated that the melanization reaction of the shrimp *P. monodon* could neutralize WSSV infection and enhance shrimp survival rate. On the other hand, suppression of melanization led to increased WSSV susceptibility (Sutthangkul et al., 2015). At the same time, we also proved that the virus reciprocally produced WSSV453 protein to negatively regulate the activation of the shrimp proPO system through the interaction with *Pm*PPAE2, a crustacean proPO-activating enzyme (Sutthangkul et al., 2015, 2017). Similarly, it has been shown that in the crayfish *Pacifastacus leniusculus*, a clip-domain serine protease (*Plc*SP) that interacts with WSSV structural protein VP28 has been reported (Guo et al., 2017). Moreover, *in vitro* gene silencing of *Plc*SP decreased the WSSV copy number in hematopoietic stem (HPT) cells, suggesting that this proteinase may be of importance for WSSV infection into crayfish HPT cells (Guo et al., 2017). These reports in shrimp and crayfish lead to a hypothesis for whether melanization/proPO in crustaceans is negatively controlled upon WSSV infection.

The involvement of WSSV164 in the regulation of shrimp melanization function was next examined using the RNAi assay, and it was found that knockdown of WSSV164 can fully restored the hemolymph PO activity in WSSV-infected shrimp. In contrast to the *Pm*PPAE2-interacting protein, knockdown of WSSV453 could partially improve PO activity after WSSV infection (Sutthangkul et al., 2015). Therefore, it can be concluded that WSSV164 is a negative regulator of the shrimp proPO system, although the mode of interaction and suppression between proPOs and WSSV164 in shrimp requires further investigation. It is known that the viral IE genes have an essential role for the viral life cycle and evasion of the host immune responses (Stinski and Meier, 2007). For example, Kaposi's sarcoma-associated herpesvirus (KSHV) encodes the IE genes K.42 and K5 to interfere with immunoglobulin assembly and downregulate the histocompatibility complex class I, respectively (Ishido et al., 2000; Wong et al., 2013). Therefore, the IE gene encoding WSSV164 may be responsible for suppressing the shrimp immune response by targeting the proPO system.

To examine the functional role of *Pm*proPO1 and *Pm*proPO2 in the host-viral interaction, r*Pm*proPO1 (an inactive form) and r*Pm*proPO2 (an inactive form) were successfully expressed in insect Sf-9 cells. Accordingly, it was clear that rWSSV164 dose-dependently controlled PO activity from r*Pm*proPO1 and r*Pm*proPO2. Further, a slight but significant decrease of PO activity was also detected after incubated high dose of rWSSV164 protein with the Empty FLAG control group. This finding presumably suggested that WSSV164 acts as the negative regulator by interfering with the activation of the proPO system in shrimp. However, the biological functions either WSSV164 hampered the activation of proPO system via inhibition of proPO activation or direct suppression of active *Pm*PO1 and *Pm*PO2 still need further investigation.

In conclusion, this study has demonstrated the significant role of the proPO system in response to WSSV infection in *P. monodon* and that WSSV has evolved ways to escape from this antiviral immunity. WSSV can control the gene expression of *Pm*proPO1 and *Pm*proPO2 and reduce PO activity in shrimp plasma. WSSV164 was then discovered as the novel virulence factor that can interact with both *Pm*proPO1 and *Pm*proPO2 and suppress PO activity. Because the melanization activated by the proPO system is complicated, more WSSV proteins involved in the regulation of shrimp melanization are currently being investigated by our research group to provide a greater understanding in the area of shrimp-virus interactions. This knowledge will be essential for developing antiviral strategies based on shrimp immunity.

Acknowledgments

This work was supported by research grants from the Thailand Research Fund to A.T. (TRF Senior Scholar No. RTA5880004) and the Thailand Research Fund and Thailand National Center for Genetic Engineering and Biotechnology (BIOTEC) to P.A. (Grant No. BRG5880016). Financial support for the training program to W.C. from the Japan Science and Technology Agency (JST)/the Japan International Cooperation Agency (JICA), Science and Technology Research Partnership for Sustainable Development (SATREPS) is acknowledged. J.S. is the recipient of a student fellowship from the Royal Golden Jubilee Ph.D. Program, Joint Funding of the Thailand Research Fund and Chulalongkorn University.

References

Amparyup, P., Jitvaropas, R., Pulsook, N., Tassanakajon, A., 2007. Molecular cloning, characterization and expression of a masquerade-like serine proteinase homologue from black tiger shrimp *Penaeus monodon*. Fish Shellfish Immunol. 22, 535–546.

Amparyup, P., Charoensapsri, W., Tassanakajon, A., 2009. Two prophenoloxidases are important for the survival of *Vibrio harveyi* challenged shrimp *Penaeus monodon*. Dev. Comp. Immunol. 33, 247–256.

Amparyup, P., Sutthangkul, J., Charoensapsri, W., Tassanakajon, A., 2012. Pattern recognition protein binds to lipopolysaccharide and β-1,3-glucan and activates shrimp prophenoloxidase system. J. Biol. Chem. 287, 10060–10069.

Amparyup, P., Charoensapsri, W., Tassanakajon, A., 2013a. Prophenoloxidase system and its role in shrimp immune responses against major pathogens. Fish Shellfish Immunol. 34, 990–1001.

Amparyup, P., Promrungreang, K., Charoensapsri, W., Sutthangkul, J., Tassanakajon, A., 2013b. A serine proteinase *Pm*ClipSP2 contributes to prophenoloxidase system and plays a protective role in shrimp defense by scavenging lipopolysaccharide. Dev. Comp. Immunol. 41, 597–607.

Beck, M.H., Strand, M.R., 2007. A novel polydnavirus protein inhibits the insect prophenoloxidase activation pathway. Proc. Natl. Acad. Sci. U. S. A 104, 19267–19272.

Cerenius, L., Söderhäll, K., 2004. The prophenoloxidase-activating system in invertebrates. Immunol. Rev. 198, 116–126.

Cerenius, L., Lee, B.L., Söderhäll, K., 2008. The proPO-system: pros and cons for its role in invertebrate immunity. Trends Immunol. 29, 263–271.

Cerenius, L., Babu, R., Söderhäll, K., Jiravanichpaisal, P., 2010. *In vitro* effects on bacterial growth of phenoloxidase reaction products. J. Invertebr. Pathol. 103, 21–23.

Charoensapsri, W., Amparyup, P., Hirono, I., Aoki, T., Tassanakajon, A., 2009. Gene silencing of a prophenoloxidase activating enzyme in the shrimp, *Penaeus monodon*, increases susceptibility to *Vibrio harveyi* infection. Dev. Comp. Immunol. 33, 811–820.

Charoensapsri, W., Amparyup, P., Hirono, I., Aoki, T., Tassanakajon, A., 2011. *Pm*PPAE2, a new class of crustacean prophenoloxidase (proPO)-activating enzyme and its role in PO activation. Dev. Comp. Immunol. 35, 115–124.

Charoensapsri, W., Amparyup, P., Suriyachan, C., Tassanakajon, A., 2014.

Melanization reaction products of shrimp display antimicrobial properties against their major bacterial and fungal pathogens. Dev. Comp. Immunol. 47, 150–159.
Coletta, A., Pinney, J.W., Solís, D.Y.W., Marsh, J., Pettifer, S.R., Attwood, T.K., 2010. Low-complexity regions within protein sequences have position-dependent roles. BMC Syst. Biol. 4, 43.
DePristo, M.A., Zilversmit, M.M., Hartl, D.L., 2006. On the abundance, amino acid composition, and evolutionary dynamics of low-complexity regions in proteins. Gene 378, 19–30.
Gietz, R.D., Schiestl, R.H., Willems, A.R., Woods, R.A., 1995. Studies on the transformation of intact yeast cells by the LiAc/SS-DNA/PEG procedure. Yeast 11, 355–360.
Guo, E., Korkut, G.G., Jaree, P., Söderhäll, I., Söderhäll, K., 2017. A *Pacifastacus leniusculus* serine protease interacts with WSSV. Fish Shellfish Immunol. 68, 211–219.
Ishido, S., Wang, C., Lee, B.S., Cohen, G.B., Jung, J.U., 2000. Downregulation of major histocompatibility complex class I molecules by Kaposi's sarcoma-associated herpesvirus K3 and K5 proteins. J. Virol. 74, 5300–5309.
Jearaphunt, M., Amparyup, P., Sangsuriya, P., Charoensapsri, W., Senapin, S., Tassanakajon, A., 2015. Shrimp serine proteinase homologues *Pm*MasSPH-1 and -2 play a role in the activation of the prophenoloxidase system. PLoS One 10 e0121073.
Jitvaropas, R., Amparyup, P., Gross, P.S., Tassanakajon, A., 2009. Functional characterization of a masquerade-like serine proteinase homologue from the black tiger shrimp *Penaeus monodon*. Comp. Biochem. Physiol. B Biochem. Mol. Biol. 153, 236–243.
Kanost, M.R., Gorman, M.J., 2008. Phenoloxidases in insect immunity. In: Beckage, N.E. (Ed.), Insect Immunology. Academic Press, San Diego, CA, pp. 69–96.
Kanost, M.R., Jiang, H., Yu, X.Q., 2004. Innate immune responses of a lepidopteran insect, *Manduca sexta*. Immunol. Rev. 198, 97–105.
Khorattanakulchai, N., Amparyup, P., Tassanakajon, A., 2017. Binding of *Pm*ClipSP2 to microbial cell wall components and activation of the proPO-activating system in the black tiger shrimp *Penaeus monodon*. Dev. Comp. Immunol. 77, 38–45.
Leu, J.H., Kuo, Y.C., Kou, G.H., Lo, C.F., 2008. Molecular cloning and characterization of an inhibitor of apoptosis protein (IAP) from the tiger shrimp. Penaeus monodon. Dev. Comp. Immunol 32, 121–133.
Leu, J.H., Yang, F., Zhang, X., Xu, X., Kou, G.H., Lo, C.F., 2009. Whispovirus. Curr. Top. Microbiol. Immunol 328, 197–227.
Li, F., Li, M., Ke, W., Ji, Y., Bian, X., Yan, X., 2009. Identification of the immediate-early genes of white spot syndrome virus. Virology 385, 267–274.
Lu, Z., Beck, M.H., Wang, Y., Jiang, H., Strand, M.R., 2008. The viral protein Egf1.0 is a dual activity inhibitor of prophenoloxidase-activating proteinases 1 and 3 from *Manduca sexta*. J. Biol. Chem. 283, 21325–21333.
Lu, Z., Beck, M.H., Strand, M.R., 2010. Egf1.5 is a second phenoloxidase cascade inhibitor encoded by *Microplitis demolitor* bracovirus. Insect Biochem. Mol. Biol. 40, 497–505.
Mathew, S., Kumar, K.A., Anandan, R., Viswanathan Nair, P.G., Devadasan, K., 2007. Changes in tissue defence system in white spot syndrome virus (WSSV) infected *Penaeus monodon*. Comp. Biochem. Physiol. C Toxicol. Pharmacol. 145, 315–320.
Monwan, W., Amparyup, P., Tassanakajon, A., 2017. A snake-like serine proteinase (*Pm*Snake) activates prophenoloxidase-activating system in black tiger shrimp *Penaeus monodon*. Dev. Comp. Immunol. 67, 229–238.
Nappi, A.J., Christensen, B.M., 2005. Melanogenesis and associated cytotoxic reactions: applications to insect innate immunity. Insect Biochem. Mol. Biol. 35, 443–459.
Noothuan, N., Amparyup, P., Tassanakajon, A., 2017. Melanization inhibition protein of *Penaeus monodon* acts as a negative regulator of the prophenoloxidase-activating system. Dev. Comp. Immunol. 72, 97–102.
Sánchez-Paz, A., 2010. White spot syndrome virus: an overview on an emergent concern. Vet. Res. 41, 43.
Sangsuriya, P., Huang, J.Y., Chu, Y.F., Phiwsaiya, K., Leekitcharoenphon, P., Meemetta, W., Senapin, S., Huang, W.P., Withyachumnarnkul, B., Flegel, T.W., Lo, C.F., 2014. Construction and application of a protein interaction map for white spot syndrome virus (WSSV). Mol. Cell. Proteomics 13, 269–282.
Sangsuriya, P., Charoensapsri, W., Chomwong, S., Senapin, S., Tassanakajon, A., Amparyup, P., 2016. A shrimp pacifastin light chain-like inhibitor: molecular identification and role in the control of the prophenoloxidase system. Dev. Comp. Immunol. 54, 32–45.
Stinski, M.F., Meier, J.L., 2007. Immediate-early viral gene regulation and function. In: Arvin, A., Campadelli-Fiume, G., Mocarski, E., Moore, P.S., Roizman, B., Whitley, R., Yamanishi, K. (Eds.), Human Herpesviruses: Biology, Therapy, and Immunoprophylaxis. Cambridge University Press, Cambridge, pp. 241–263.
Sutthangkul, J., Amparyup, P., Charoensapsri, W., Senapin, S., Phiwsaiya, K., Tassanakajon, A., 2015. Suppression of shrimp melanization during white spot syndrome virus infection. J. Biol. Chem. 290, 6470–6481.
Sutthangkul, J., Amparyup, P., Eum, J.H., Strand, M.R., Tassanakajon, A., 2017. Anti-melanization mechanism of the white spot syndrome viral protein, WSSV453, via interaction with shrimp proPO-activating enzyme, *Pm*proPPAE2. J. Gen. Virol. 98, 769–778.
Suwannaboon, R., Phiwsaiya, K., Senapin, S., Khunrae, P., Rattanarojpong, T., 2013. The identification and expression of the full-length HtrA2 gene from *Penaeus monodon* (black tiger shrimp). Protein Expr. Purif. 92, 183–189.
Tassanakajon, A., Somboonwiwat, K., Supungul, P., Tang, S., 2013. Discovery of immune molecules and their crucial functions in shrimp immunity. Fish Shellfish Immunol. 34, 954–967.
Tassanakajon, A., Rimphanitchayakit, V., Visetnan, S., Amparyup, P., Somboonwiwat, K., Charoensapsri, W., Tang, S., 2018. Shrimp humoral responses against pathogens: antimicrobial peptides and melanization. Dev. Comp. Immunol. 80, 81–93.
Verbruggen, B., Bickley, L., van Aerle, R., Bateman, K., Stentiford, G., Santos, E., Tyler, C., 2016. Molecular mechanisms of white spot syndrome virus infection and perspectives on treatments. Viruses 8, 23.
Wong, L.Y., Brulois, K., Toth, Z., Inn, K.S., Lee, S.H., O'Brien, K., Lee, H., Gao, S.J., Cesarman, E., Ensser, A., Jung, J.U., 2013. The product of Kaposi's sarcoma-associated herpesvirus immediate early gene K4.2 regulates immunoglobulin secretion and calcium homeostasis by interacting with and inhibiting pERP1. J. Virol. 87, 12069–12079.
Yeh, S.P., Chen, Y.N., Hsieh, S.L., Cheng, W., Liu, C.H., 2009. Immune response of white shrimp, *Litopenaeus vannamei*, after a concurrent infection with white spot syndrome virus and infectious hypodermal and hematopoietic necrosis virus. Fish Shellfish Immunol. 26, 582–588.
Zhao, P., Li, J., Wang, Y., Jiang, H., 2007. Broad-spectrum antimicrobial activity of the reactive compounds generated *in vitro* by *Manduca sexta* phenoloxidase. Insect Biochem. Mol. Biol. 37, 952–959.
Zhao, P., Lu, Z., Strand, M.R., Jiang, H., 2011. Antiviral, antiparasitic, and cytotoxic effects of 5,6-dihydroxyindole (DHI), a reactive compound generated by phenoloxidase during insect immune response. Insect Biochem. Mol. Biol. 41, 645–652.

Developmental and Comparative Immunology 81 (2018) 291–302

Contents lists available at ScienceDirect

Developmental and Comparative Immunology

journal homepage: www.elsevier.com/locate/dci

A cytosolic sensor, *Pm*DDX41, mediates antiviral immune response in black tiger shrimp *Penaeus monodon*

Suthinee Soponpong [a], Piti Amparyup [b], Anchalee Tassanakajon [a, *]

[a] Center of Excellence for Molecular Biology and Genomics of Shrimp, Department of Biochemistry, Faculty of Science, Chulalongkorn University, Bangkok 10330, Thailand

[b] National Center for Genetic Engineering and Biotechnology (BIOTEC), National Science and Technology Development Agency (NSTDA), Pathumthani 12120, Thailand

ARTICLE INFO

Article history:
Received 21 November 2017
Received in revised form
13 December 2017
Accepted 13 December 2017
Available online 14 December 2017

Keywords:
DDX41
DNA-sensing pathway
Shrimp immunity
Antiviral response
White spot syndrome virus

ABSTRACT

DEAD (Asp-Glu-Ala-Asp)-box polypeptide 41 (DDX41), a receptor belonging to the DExD family, has recently been identified as an intracellular DNA sensor in vertebrates. Here, we report on the identification and functional characterization of *Pm*DDX41, the first cytosolic DNA sensor in shrimp. By searching a *Penaeus monodon* expressed sequence tag (EST) database (http://pmonodon.biotec.or.th), three cDNA fragments exhibiting similarity to DDX41 in various species were identified and assembled, resulting in a complete open reading frame of *Pm*DDX41 that contains 1863-bp and encodes a putative protein of 620 amino acids. *Pm*DDX41 shares 83% and 79% similarity to DDX41 homolog from the bee *Apis florea* and fruit fly *Drosophila melanogaster*, respectively and contains three conserved domains in the protein: DEADc domain, HELICc domain, and zinc finger domain. The transcript of *Pm*DDX41 was detected in all tested tissues and was up-regulated upon infection with a DNA virus, white spot syndrome virus (WSSV). However, *Pm*DDX41 mRNA expression was not significantly changed and down-regulated in response to a bacterium, *Vibrio harveyi*, or an RNA virus, yellow head virus (YHV), respectively, compared with the control phosphate-buffered saline-injected shrimp. Furthermore, the suppression of *Pm*DDX41 by dsRNA-mediated gene silencing resulted in more rapid death of WSSV-infected shrimp and a significant decrease in the mRNA expression levels of several immune-related genes (*Pm*IKKβ, *Pm*IKKε, *Pm*Relish, *Pm*Cactus, *Pm*Dorsal, *Pm*PEN3, *Pm*PEN5, and ALF*Pm*6). These results suggest that *Pm*DDX41 is involved in the antiviral response, probably via a DNA-sensing pathway that is triggered through the IκB kinase complex and leads to the activation of several immune-related genes.

© 2017 Elsevier Ltd. All rights reserved.

1. Introduction

The innate immune system is conserved across both vertebrates and invertebrates. It plays a key role in the defense against pathogens mediated by pattern recognition receptors (PRRs) which binds to pathogen-associated molecule patterns (PAMPs) and leads to the activation of the cellular and humoral immune response (Tassanakajon et al., 2013). In shrimp *Penaeus monodon*, the important PRR of the prophenoloxidase (proPO) system is the lipopolysaccharide and β-1,3-glucan binding protein (*Pm*LGBP) that recognizes the lipopolysaccharide (LPS) from Gram-negative bacteria and β-glucans from fungi and subsequently activates the proPO system (Amparyup et al., 2012). Moreover, *Pm*MasSPH1, *Pm*QM and C-type lectin (*Pm*Lec) were identified in *P. monodon* as putative peptidoglycan recognition proteins (PGRPs). These can bind to peptidoglycan (PGN) from Gram-positive bacteria (Jearaphunt et al., 2015; Udompetcharaporn et al., 2014).

In vertebrates, the recognition of PAMPs by specific receptors can activate the NF-κB pathway, which plays a central role in coordinating the expression of pro-inflammatory cytokines, chemokines, and type I interferons (IFNs) to eliminate viral and bacterial infections by triggering inflammation and recruiting innate and acquired immune cells (Takeuchi and Akira, 2010). PRRs can be divided into several classes depending on the adaptor usage, including Toll-like receptors (TLRs), retinoic acid-inducible gene I (RIG-I)-like receptors (RLRs), NOD-like receptors (NLRs), C-type lectin receptors (CLRs), and cytosolic DNA sensors (Pandey et al., 2014). In mice, TLR4 has been found to activate the innate

* Corresponding author.
E-mail address: anchalee.k@chula.ac.th (A. Tassanakajon).

https://doi.org/10.1016/j.dci.2017.12.013
0145-305X/© 2017 Elsevier Ltd. All rights reserved.

immune response to the LPS from bacterial cell walls (Hoshino et al., 1999). Moreover, TLR3, 7, 8, and 9 have been characterized as nucleic acid sensors (Pandey et al., 2014). Nevertheless, type I IFN production in response to virus infection has been reported even in the absence of TLRs, leading to the synthesis of intracellular RNA sensors, the RLRs (Hornung et al., 2004; Yoneyama et al., 2004). In addition, the initial antiviral response is dominated by the recognition of nucleic acids, and several sensors of cytosolic DNA have been identified, including DNA-dependent activator of IFN-regulatory factors (DAI), RNA polymerase III, cyclic GMP-AMP (cGAMP) synthase (cGAS), and gamma-inducible protein 16 (IFI16). Recently, it has been reported that several DExD/H-box helicases contribute to antiviral immunity, either by acting as sensors for viral nucleic acids or by facilitating downstream signaling pathways (Chiu et al., 2009; Sun et al., 2013).

The DExD/H-box protein family comprises RNA and DNA helicases that all contain a DExD/H-box domain (Yoneyama et al., 2004). DEAD (Asp-Glu-Ala-Asp)-box (DDX) proteins have been implicated in the regulation of gene induction and are involved in other processes including signal transduction, gene promoter regulation, mRNA splicing, and translation regulation (Schroder et al., 2008). Several DDX proteins have been reported to play a role in innate immunity by functioning as RNA sensors, such as RIG-I and melanoma differentiation-associated gene 5 (MDA5) (Schmidt et al., 2012). Some of these proteins, such as DDX3, function as signaling molecules. In the cytoplasm, RIG-I and MDA5 are classified in a class of PRRs for viral PAMPs (Oshiumi et al., 2010). These specific structures perform crucial roles in inducing the synthesis of type I interferon in response to viral infection (Schroder et al., 2008). In mammals, there is a three-helicase complex, DDX1–DDX21–DHX36, in myeloid dendritic cells (mDCs) that functions as a sensor for synthetic cytosolic RNA duplex poly(I:C) and triggers the IFN-I innate immune response in the host (Zhang et al., 2011a). Recently, a new molecular cytosolic sensor named DDX41 has been reported that induces the synthesis of type I interferon (Parvatiyar et al., 2012). Normally, IFNs are found only in vertebrates. These are polypeptides that are secreted by infected cells in response to pathogens and exhibit a protective effect against acute viral and bacterial infections. However, in recent studies, IFN-like molecules, named Vago, have been identified in the fruit fly *Drosophila melanogaster* (Deddouche et al., 2008) and Pacific white shrimp *Litopenaeus vannamei* (Wang et al., 2013a). It was also found that the shrimp *Lv*Vago promoter could be activated by IκB kinase, *Lv*IKKε. It is possible that Vago may play a role as a cytokine-like IFN in nucleic-acid-induced antiviral immunity of shrimp, indicating that shrimp possess nucleic-acid-induced antiviral immunity similar to the vertebrate IFN antiviral system (Wang et al., 2013b).

Recently, DDX41 was first identified in chicken cells and its function in IFN-β production was investigated. The knockdown of chDDX41 expression by shRNA reduced the IFN-β promoter activity after dsDNA analogue poly(dA:dT) stimulation and found to interact with chicken stimulator of interferon genes (chSTING) (Cheng et al., 2017). In the Japanese flounder, *Paralichthys olivaceus*, the DDX41 gene was identified and found that the activity of the IFN-I promoter was increased in DDX41-overexpressing HINAE cells treated with C-di-GMP. The Japanese flounder DDX41 has been reported to function as a cytosolic DNA sensor that is capable of inducing the expression of antiviral and inflammatory cytokines in the presence of cyclic di-GMP (Quynh et al., 2015). In pigs, porcine DDX41 (poDDX41) was found and investigated in porcine kidney (PK-15). The overexpression of poDDX41 in PK-15 cells induced IFN-β by activating transcription factor 3 (IRF3) and NF-κB (Zhu et al., 2014). In *Drosophila*, a homolog of DDX41 named Abstrakt was found to share 66% identity and 80% similarity at the amino acid-level to vertebrate DDX41. Abstrakt is essential for survival at all stages throughout the life cycle of the fruit fly and plays a role in controlling cell polarity and asymmetric cell division in multiple cell types (Schmucker et al., 1997).

In shrimp, the viral DNA-sensing molecules have not been studied and DDX41 has not been reported to date. The aim of this study was to identify and characterize the *Pm*DDX41 gene and investigate its involvement in the DNA-sensing cascade in the immune response of the black tiger shrimp *Penaeus monodon*. Gene expression analysis of *Pm*DDX41 was performed for various tissues and in response to white spot syndrome virus (WSSV) infection. Furthermore, the function of *Pm*DDX41, particularly in terms of antiviral innate immunity, was characterized using RNA-mediated gene silencing.

2. Materials and methods

2.1. Shrimp and sample preparation

Healthy black tiger shrimp *Penaeus monodon* (10–15 g body weight) were kindly provided by Charoen Pokphand Foods in Chanthaburi province, Thailand. The shrimp were maintained in aerated seawater (20 ppt) at 28 °C for a week prior to the experiment. To determine the tissue expression pattern of the *Pm*DDX41 transcripts, eight different tissues (hemocytes, intestine, hepatopancreas, lymphoid organ, gill, heart, muscle, and eye stalk) from three shrimp were separately collected as described previously (Amparyup et al., 2010). All samples were then stored at −80 °C until used for RNA extraction.

2.2. Total RNA extraction and reverse transcription

Hemocytes and tissue samples were homogenized in GENEzol (Geneaid, Taiwan). The total RNA was isolated according to the manufacturer's protocol and treated with DNaseI (NEB, USA) to destroy the contaminating DNA. First-strand cDNA synthesis was carried out using a RevertAid First Strand cDNA Synthesis Kit (Thermo Fisher Scientific, USA) and the cDNA was stored at −20 °C until required for the real-time (RT)-PCR analysis.

2.3. Cloning and sequencing of open reading frame (ORF) cDNA of PmDDX41

A cDNA sequence of a putative *Pm*DDX41 was retrieved from the *P. monodon* expressed sequence tag (EST) database (http://pmonodon.biotec.or.th) (Tassanakajon et al., 2006). Gene-specific primers, ORF-*Pm*DDX41-F and ORF-*Pm*DDX41-R (Table 1), were designed from the EST sequences to amplify the ORF cDNA of *Pm*DDX41. PCR amplification was performed under the following cycling conditions: 94 °C for 1 min, followed by 35 cycles of 94 °C for 30 s, 65 °C for 30 s, and 72 °C for 30 s, with an extension step at 72 °C for 10 min. The PCR products were separated by agarose gel electrophoresis, and the bands with the expected size were then excised and purified using a FavorPrep GEL/PCR Purification Kit (FAVORGEN Biotech Corp., Taiwan). The purified DNA fragments were cloned into the RBC TA Cloning Vector Kit (RBC Bioscience, Taiwan) and sequenced.

2.4. Sequence analysis

The cDNA and deduced amino acid sequences of *Pm*DDX41 were analyzed using the programs GENETYX 7.0.3 (GENETYX Corporation, Japan) and BLAST (http://www.ncbi.nlm.nih.gov/blast). Protein domains were analyzed using the SMART 4.0 program (http://smart.embl-heidelberg.de/). A multiple sequence alignment was

Table 1
Primers used in this study.

Primer name	Sequence (5′ to 3′)	Purpose
ORF-*Pm*DDX41-F	CGACCATGGACAGCCCGAAGA	ORF cDNA
ORF-*Pm*DDX41-R	GAGTTTAGTAATCAGCTGCATTAGC	ORF cDNA
*Pm*DDX41i-F1	CGAGCCATACATTCCGGTTAAGGA	RNAi
*Pm*DDX41i-R1	GTCTCCATGCTGTAACTACAGAATC	RNAi
*Pm*DDX41i-T7F1	GGATCCTAATACGACTCACTATAGG CGAGCCATACATTCCGGTTAAGGA	RNAi
*Pm*DDX41i-T7R1	GGATCCTAATACGACTCACTATAGG GTCTCCATGCTGTAACTACAGAATC	RNAi
*Pm*DDX41-F	AGCCCTTCAAGGACGTGACATGA	Transcription study
*Pm*DDX41-R	GCATATCTATGAGGCGTCCTGGA	Transcription study
EF1-α-F	GGTGCTGGACAAGCTGAAGGC	Transcription study
EF1-α-R	CGTTCCGGTGATCATGTTCTTGATG	Transcription study
*Pm*IKKβ-F	CTGAGGGCATGACGCGACCAC	Transcription study
*Pm*IKKβ-R	GCCTGCTCATCATAGTAGTCGAG	Transcription study
*Pm*IKKε-F	ACCGTCTCGAGAAAAGGGTCCTA	Transcription study
*Pm*IKKε-R	CGGATCGTCCAGAATGTTGAAGAG	Transcription study
*Pm*Vago1-F	GAACACACCCCAGTGCACTGGT	Transcription study
*Pm*Vago1-R	ATGGAGCTTGTTCCCCTTCTGTG	Transcription study
*Pm*Vago4-F	ACTCCTCTCCCTTCAGGGCATC	Transcription study
*Pm*Vago4-R	TGGCAGGAACTTCTCTCGCTGC	Transcription study
*Pm*Vago5-F	AGAAGCATTTAGGCTCAGGGCAG	Transcription study
*Pm*Vago5-R	GATGGCCAGAGTTATTGTGACGC	Transcription study
*Pm*Dorsal-F	TCACTGTTGACCCACCTTAC	Transcription study
*Pm*Dorsal-R	GGAAAGGGTCCACTCTAATC	Transcription study
*Pm*Cactus-F	ACGGCAGTAGGATCGGGGTTTGCCT	Transcription study
*Pm*Cactus-R	ATGCCCCACAGAGGTGATGCCCTGA	Transcription study
Crustin*Pm*1-F	CTGCTGCGAGTCAAGGTATG	Transcription study
Crustin*Pm*1-R	AGGTACTGGCTGCTCTACTG	Transcription study
Crustin*Pm*7-F	GGCATGGTGGCGTTGTTCCT	Transcription study
Crustin*Pm*7-R	TGTCGGAGCCGAAGCAGTCA	Transcription study
ALF*Pm6*-F	AGTCAGCGTTTAGAGAGGTT	Transcription study
ALF*Pm6*-R	GCTCGAACTCTCCACTCTC	Transcription study
*Pm*Relish-F	TCTCCAGGTGAGCACTCAGTTGGC	Transcription study
*Pm*Relish-R	GCTGTAGCTGTTGCTGTTGTTGAG	Transcription study
*Pm*PEN5-F	ATCCCGACCTATTAGTACTC	Transcription study
*Pm*PEN5-R	TTATCCTTTCAATGCAGAACAA	Transcription study
ALF*Pm3*-F	CCCACAGTGCCAGGCTCAA	Transcription study
ALF*Pm3*-R	TGCTGGCTTCTCCTCTGATG	Transcription study
*Pm*PEN3-F	GGTCTTCCTGGCCTCCTTCG	Transcription study
*Pm*PEN3-R	TTTGCATCACAACAACGTCCTA	Transcription study

created with the ClustalX 2.1 program. An unrooted tree was constructed by the neighbor-joining method based on the amino acid sequences using ClustalX 2.1 and MEGA 6 software (Tamura et al., 2013). Bootstrap sampling was reiterated 1000 times.

2.5. Tissue distribution analysis

The tissue-specific expression of the *Pm*DDX41 transcripts was determined by semi-quantitative RT-PCR using the specific primers *Pm*DDX41-F and *Pm*DDX41-R (Table 1). A partial fragment (150 bp) of the elongation factor 1-α (EF1-α) gene was also amplified using the EF1-α-F and EF1-α-R primers (Table 1) to serve as an internal reference control for normalization. The PCR conditions were 94 °C for 1 min, followed by 30 cycles of 94 °C for 30 s, 55 °C for 30 s, and 72 °C for 30 s, followed by a final extension step at 72 °C for 5 min. The PCR products were analyzed by 2.0% (w/v) agarose gel electrophoresis and visualized by UV-transillumination.

2.6. Gene expression analysis in response to pathogen infection

Quantitative RT-PCR (qRT-PCR) was used to measure the changes in *Pm*DDX41 transcript levels in *P. monodon* hemocytes after injection with the following shrimp pathogens: bacteria *Vibrio harveyi*, WSSV, and YHV. For the microorganism challenge, the shrimp were divided into triplicate groups of three shrimp each. The animals were then injected with either *V. harveyi* suspension ($OD_{600} = 1.9$, approximately 3.2×10^5 CFU/mL in PBS), WSSV suspension (2.64×10^5 copies/mL of WSSV in PBS), or YHV suspension (3.25×10^6 copies/mL of YHV in PBS) in the second abdominal segment (50 μL for each shrimp). The control group was injected with phosphate-buffered saline pH 7.4 (PBS; 137 mM NaCl, 2.7 mM KCl, 4.3 mM Na_2HPO_4, 1.4 mM KH_2PO_4). The experimental shrimp were reared in seawater tanks, and hemocyte cell pellets were randomly collected at 0, 6, 12, 24, and 48 h post-injection (hpi) for the RNA extraction. The total RNA extraction and first-strand cDNA synthesis were performed following the methods described in Section 2.2. The extracted total RNAs from three shrimps per treatment at each time point were pooled. The qRT-PCR analysis was performed as described by Amparyup et al. (2007) using the *Pm*DDX41-F and *Pm*DDX41-R primer pair (Table 1). EF1-α was amplified as the internal control and reference standard to verify the qRT-PCR reaction. Three replicates were performed for each template, and three independent replicates were utilized for each data point. The Ct values of the infected hemocyte samples at each time point were normalized using the PBS-injected samples. The mathematical model described by Pfaffl (2001) was used to determine the relative expression ratio.

2.7. Double-stranded RNA preparation

Large quantities of dsRNA were prepared as described previously (Amparyup et al., 2009). The DNA fragment of 344 bp was amplified by PCR from the recombinant plasmid containing the *Pm*DDX41 gene using the gene-specific primers *Pm*DDX41i-F1 and

*Pm*DDX41i-R1 for *Pm*DDX41 (Table 1). The primers for the dsRNA synthesis consisted of the same primer sequences but flanked at the 5′ end by a T7 promoter recognition site (5′-GGATCCTAATACGACTCACTATAGG-3′, Table 1). A DNA fragment (740 bp) corresponding to the green fluorescent protein (GFP) sequence was amplified as a negative control as described previously (Amparyup et al., 2009). The PCR products were purified using a FavorPrep GEL/PCR Purification Kit (FAVORGEN Biotech Corp., Taiwan) and used to construct the dsRNA with a T7 RNA polymerase (T7 RiboMAX Express Large Scale RNA Production System, Promega, USA), according to the manufacturer's protocols. The formation of dsRNAs was monitored by determining the product size of the reactants using TBE-1.8% (w/v) agarose gel electrophoresis. The synthesized dsRNAs were dissolved in nuclease-free water and quantified by spectrophotometry.

2.8. RNA interference (RNAi) treatment of shrimp

Shrimp (3–5 g) were injected with either *Pm*DDX41 or GFP (control) dsRNA as described previously (Amparyup et al., 2009). Briefly, approximately 2 μg of *Pm*DDX41 dsRNA in 150 mM NaCl per 1 g body weight was injected intramuscularly into shrimp in the lateral area of the fourth abdominal segment using a 0.5-mL syringe with a 29-gauge needle, to assess the sequence-specific knockdown effect of dsRNA. The injection of 150 mM NaCl alone was performed as an additional control for handling- and injection-induced mortality. After 24 h, shrimp hemolymph were collected for total RNA extraction using a FavorPrep Tissue Total RNA Purification Mini Kit (FAVORGEN Biotech Corp., Taiwan) according to the manufacturer's instructions. First-strand cDNA was synthesized from the total RNA (200 ng) using a RevertAid First Strand cDNA Synthesis Kit (Thermo Fisher Scientific, USA) and oligo$(dT)_{15}$ primer, according to the manufacturer's instructions.

2.9. Semi-quantitative RT-PCR analysis

The efficiency of the *Pm*DDX41 knockdown was analyzed by semi-quantitative RT-PCR analysis using gene-specific primers *Pm*DDX41-F and *Pm*DDX41-R (Table 1). A fragment of the EF1-α gene was amplified in a separate tube and served as an internal control for normalization. The PCR reactions and thermal cycling conditions were carried out as described above (Section 2.3 and 2.5). After amplification, the RT-PCR products were separated using TBE-2% (w/v) agarose gel electrophoresis and visualized as stated above.

2.10. Effect of PmDDX41 gene silencing on the expression of other immune genes

The effects of the dsRNA-mediated *Pm*DDX41 gene silencing on the transcript expression levels of the other immune genes were determined by RT-PCR amplification and the expression levels were confirmed using quantitative real-time RT-PCR with specific primers for the *P. monodon* shrimp signal transduction pathways (*Pm*IKKβ, *Pm*IKKε, *Pm*Relish, *Pm*Cactus, and *Pm*Dorsal), antimicrobial peptides (*Pm*PEN3, *Pm*PEN5, ALF*Pm*3, ALF*Pm*6, Crustin*Pm*1, and Crustin*Pm*7), and IFN-like molecules (*Pm*Vago1, *Pm*Vago4, and *Pm*Vago5) (Table 1). Amplification of the EF1-α fragment served as the internal control for cDNA template normalization.

2.11. Cumulative mortality assay

Cumulative mortality experiments for the *Pm*DDX41-knockdown shrimp were performed using three groups of shrimps (3–5 g) that were intramuscularly injected with either *Pm*DDX41 dsRNA (2 μg), GFP dsRNA (2 μg), or 150 mM NaCl (25 μL volume). Twenty-four hours after the first dsRNA injection, the shrimp were injected with 2.64×10^3 copies/mL of WSSV in PBS. The shrimp injected with GFP dsRNA or NaCl were used as the controls. The numbers of dead shrimp were recorded daily for five days post-WSSV infection. Each experiment was performed in triplicate, with each group consisting of 9–10 healthy shrimp. Statistical analysis of the cumulative mortality was performed using one-way analysis of variance (ANOVA).

3. Results

3.1. Sequence characterization of PmDDX41 transcript

To identify a DNA sensor in *P. monodon*, the *P. monodon* EST database (http://pmonodon.biotec.or.th) was searched for the cDNA sequence of DDX41. A DNA sequence from three ESTs, namely, NODE_45370, NODE_133992, and NODE_285756, was assembled and identified as DDX41. The primers ORF-*Pm*DDX41-F/-R (Table 1) were designed to amplify the ORF of *Pm*DDX41 cDNA from shrimp hemocytes. The ORF of *Pm*DDX41 consists of 1863 bp encoding a protein with 620 amino acid residues (GenBank accession number: KY608746; Fig. 1A). The protein has a predicted molecular mass and isoelectric point (p*I*) of 70 kDa and 6.84, respectively. Analysis of the conserved domain using the SMART program revealed that *Pm*DDX41 contains a DEAD-like helicase superfamily domain (DEADc, 193–411 aa), one helicase superfamily C-terminal domain (HELICc, 439–520 aa), and one zinc finger domain (ZnF, 579–595 aa) (Fig. 1B). A database search using the BLASTX algorithm revealed that *Pm*DDX41 shared high similarity to Abstrakt in invertebrates (*Ha*Abstrakt in *Hyalella azteca* (88% similarity), *Mr*Abstrakt in *Megachile rotundata* (83% similarity), *Af*Abstrakt in *Apis florea* (83% similarity), and *Dm*Abstrakt in *Drosophila melanogaster* (79% similarity)) and DDX41 in vertebrates (*Lo*DDX41 in *Lepisosteus oculatus* (80% similarity), *Bt*DDX41 in *Bos taurus* (81% similarity), *Ss*DDX41 in *Sus scrofa* (80% similarity), and *Hs*DDX41 in *Homo sapiens* (80% similarity)).

3.2. Multiple sequence alignment and phylogenetic analysis

The multiple sequence alignment of the deduced amino acid sequences of *Pm*DDX41 with other species using ClustalX 2.1 revealed that the protein contains three conserved domains, namely, the DEADc domain, the HELICc domain, and the zinc finger domain (Fig. 2A). To examine the relationship of *Pm*DDX41 with its analogues from other species of vertebrates and invertebrates, an unrooted neighbor-joining phylogenetic tree was drawn based on the predicted DEADc and HELICc domains from various species. The results showed that these DDX41 proteins could be divided into two groups (Fig. 2B). Group 1 contains DDX41 proteins from vertebrates, whereas group 2 contains Abstrakt proteins from invertebrates. *Pm*DDX41 clustered together with Abstrakt from amphipod crustaceans and invertebrates.

3.3. Tissue-specific expression of PmDDX41

The transcript levels of *Pm*DDX41 in various shrimp tissues were determined by semi-quantitative RT-PCR using EF1-α as an internal control gene. The results showed that the *Pm*DDX41 transcript was expressed in all of the tested tissues, including the hemocytes, intestine, hepatopancreas, lymphoid organ, gill, heart, muscle, and eye stalk (Fig. 3A). However, particularly high mRNA expression levels of *Pm*DDX41 were found in the hemocytes, intestine,

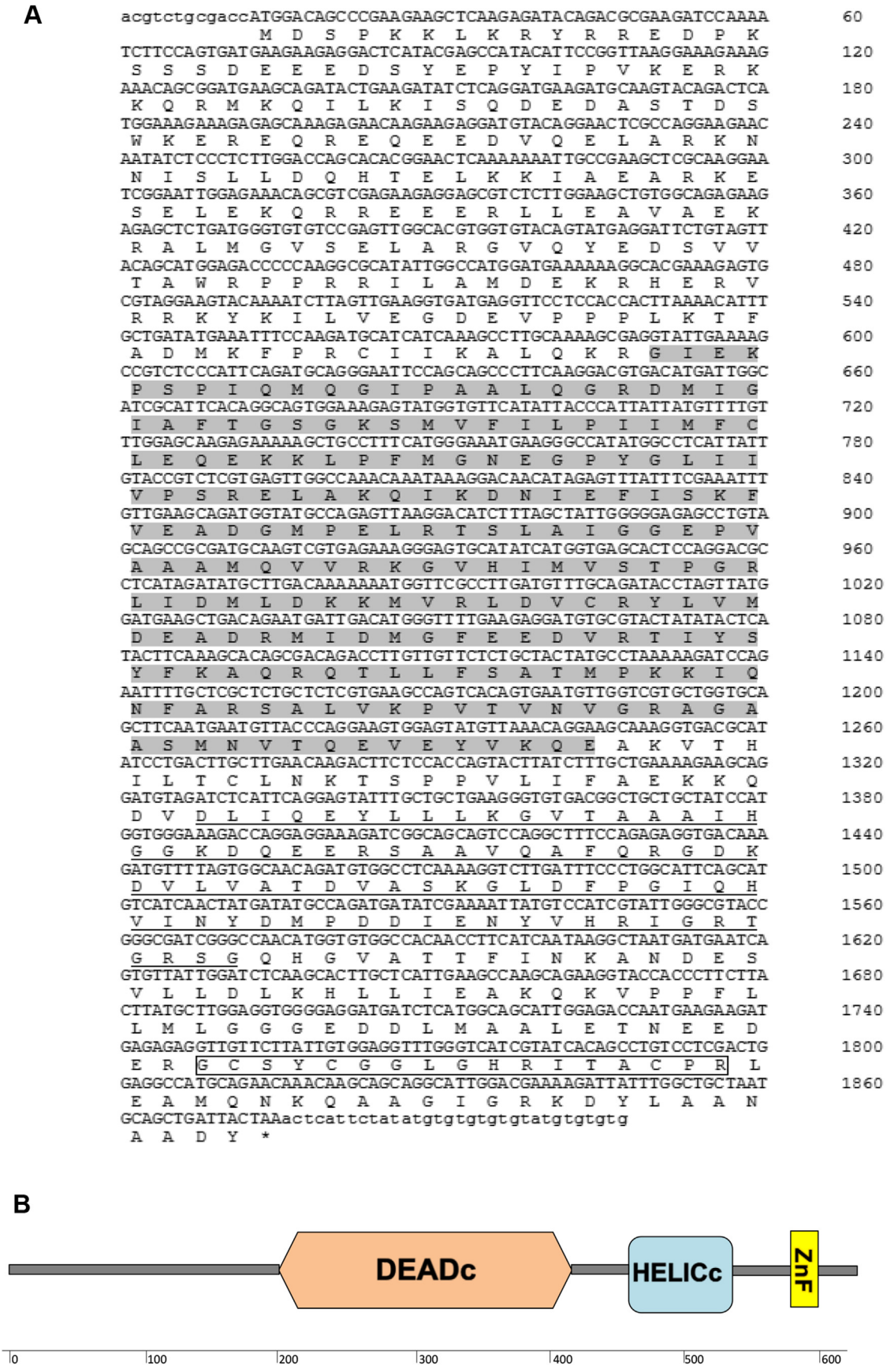


Fig. 1. Sequence and domain analysis of *Pm*DDX41. (A) Nucleotide and deduced amino acid sequences of *Pm*DDX41 cDNA. The DEADc domain is boxed with a gray background. The HELICc domain is underlined. The zinc finger domain is boxed. The stop codon TAA is indicated with an asterisk. (B) A schematic representation of the structural domains of *Pm*DDX41 analyzed using the SMART program.

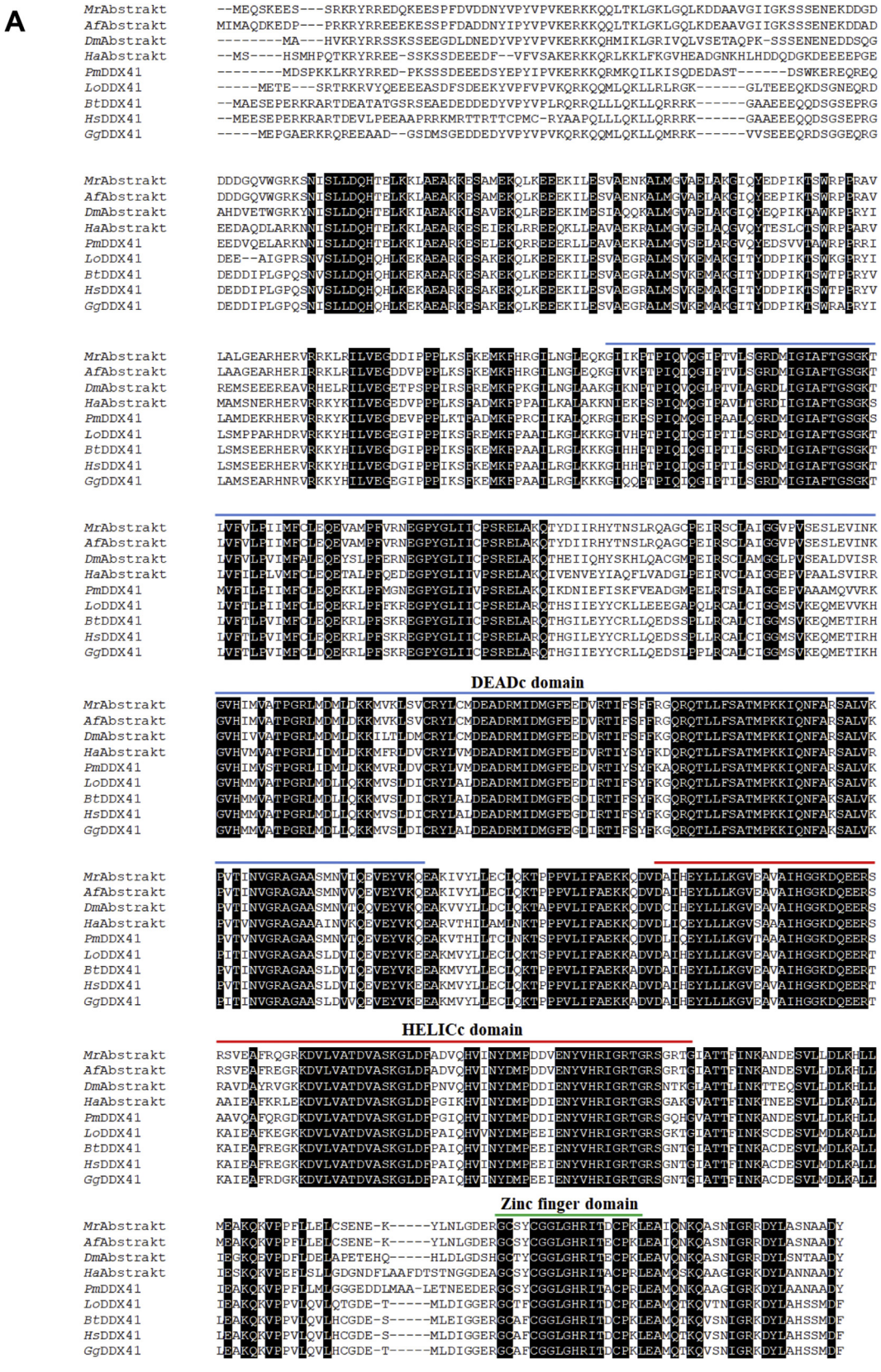


Fig. 2. Sequence analysis of *Pm*DDX41 gene. (A) Multiple alignment of the deduced amino acid sequence of *Pm*DDX41 cDNA with various species. The conserved residues are shaded in black. (B) Bootstrapped unrooted neighbor-joining tree of the DEADc and HELICc domains of DDX41 from various species of vertebrates and invertebrates using the MEGA 6.0 program based on the multiple sequence alignment by ClustalX 2.1. The *Pm*DDX41 protein is underlined in red. *Penaeus monodon* DDX41 (*Pm*DDX41); *Hyalella azteca* (XP_018015918.1); *Megachile rotundata* (XP_003704771.1); *Eufriesea mexicana* (XP_017758091.1); *Apis florea* (XP_012345472.1); *Apis mellifera* (XP_006563505.1); *Bombus terrestris* (XP_003401085.1); *Apis cerana* (XP_016919394.1); *Melipona quadrifasciata* (KOX72336.1); *Athalia rosae* (XP_012260261.1); *Tribolium castaneum* (XP_008199686.2); *Copidosoma floridanum* (XP_014212020.1); *Zootermopsis nevadensis* (KDR18857.1); *Microplitis demolitor* (XP_008554237.1); *Halyomorpha halys* (XP_014290780.1); *Cimex lectularius*

hepatopancreas, gill, heart and muscle.

3.4. Temporal expression of PmDDX41 mRNA after pathogen challenges

To investigate the effects of bacterial and viral infections on *Pm*DDX41 gene expression, *V. harveyi*, WSSV, and YHV were used. The qRT-PCR results showed induction of the *Pm*DDX41 transcript by WSSV but not YHV or *V. harveyi* infection. In brief, *Pm*DDX41 expression had increased by 1.57- and 1.36-fold, respectively, at 6 and 48 h after infection with WSSV ($p < 0.05$) (Fig. 3B). In the YHV-challenged group, *Pm*DDX41 was slightly down-regulated by 0.33-fold at 6 h after infection (Fig. 3C). In contrast, after infection with *V. harveyi*, *Pm*DDX41 mRNA expression was not significantly changed at any of the time points when compared with the control PBS-injected shrimp ($p > 0.05$) (Fig. 3D).

3.5. Effect of silencing the PmDDX41 gene on the expression of shrimp immune-related genes

To characterize the important role of *Pm*DDX41 in the innate immunity of shrimp, we used the RNA interference (RNAi) technique to knockdown the *Pm*DDX41 gene. Shrimp (3–5 g) were injected with *Pm*DDX41 dsRNA (2 μg/g shrimp), GFP dsRNA, or 150 mM NaCl, where the latter two groups were used as controls. Semi-quantitative RT-PCR was used to analyze the efficacy of the gene silencing of the targeted gene after systemic dsRNA treatment. The results revealed that the *Pm*DDX41 gene was suppressed by the *Pm*DDX41 dsRNA, while GFP dsRNA or NaCl injection had no effect on *Pm*DDX41 expression (Fig. 4A).

Furthermore, the effects of *Pm*DDX41 gene silencing on the expression of other immune-related genes were investigated by semi-quantitative RT-PCR. The expression levels of genes in the signal transduction pathways (*Pm*IKKβ, *Pm*IKKε, *Pm*Relish, *Pm*Cactus, and *Pm*Dorsal), antimicrobial peptides (*Pm*PEN3, *Pm*PEN5, ALF*Pm*3, ALF*Pm*6, Crustin*Pm*1, and Crustin*Pm*7), and IFN-like molecules (*Pm*Vago1, *Pm*Vago4, and *Pm*Vago5) were analyzed. The results revealed that the expression levels of the *Pm*IKKβ, *Pm*IKKε, *Pm*Relish, *Pm*Cactus, *Pm*Dorsal, *Pm*PEN3, *Pm*PEN5, and ALF*Pm*6 genes were decreased compared with the control groups, whereas the expression levels of the other genes (*Pm*Vago1, *Pm*Vago4, *Pm*Vago5, ALF*Pm*3, Crustin*Pm*1, and Crustin*Pm*7) were unchanged.

To confirm the effects of silencing the *Pm*DDX41 gene on the expression of immune-related genes, qRT-PCR was performed. The expression levels of the signal transduction pathway genes *Pm*IKKβ, *Pm*IKKε, *Pm*Relish, *Pm*Cactus, and *Pm*Dorsal were decreased to 0.26, 0.09, 0.07, 0.03, and 0.45-fold, respectively, relative to the control group. Moreover, the expression levels of the antimicrobial peptide genes *Pm*PEN3, *Pm*PEN5, and ALF*Pm*6 were decreased to 0.42, 0.72, and 0.20-fold, respectively (Fig. 4B).

3.6. Survival rate of PmDDX41-knockdown shrimp after WSSV infection

To further address the potential role of *Pm*DDX41 in the shrimp defense against viral infection, the *Pm*DDX41-knockdown shrimp were systemically challenged with WSSV. The shrimp were injected with 2 μg/g shrimp of *Pm*DDX41 dsRNA, GFP dsRNA, or 150 mM NaCl. Twenty-four hours after the first dsRNA injection, the shrimp were injected with 2.64×10^3 copies/mL of WSSV in PBS. The survival rate was recorded over a period of five days after the challenge. For the *Pm*DDX41-knockdown shrimp, all of the shrimp had died within three days of WSSV infection, whereas in the controls injected with 150 mM NaCl or GFP dsRNA, 100% death was only observed by five days after WSSV infection. Therefore, the *Pm*DDX41-knockdown shrimp exhibited a more rapid death after WSSV infection compared with the controls, which suggests that *Pm*DDX41 is likely involved in the antiviral response and plays an important role in protecting shrimp from WSSV infection (Fig. 5).

4. Discussion

Upon PAMP engagement, PRRs trigger intracellular signaling cascades ultimately leading to the expression of antiviral and antimicrobial molecules (Medzhitov and Janeway, 2000). In recent years, it has been reported that several DExD/H-box helicases contribute to antiviral immunity in vertebrates, either by acting as sensors for viral nucleic acids or by facilitating downstream signaling events (Ahmad and Hur, 2015).

In this study, the first DDX41 from the shrimp *Penaeus monodon* (*Pm*DDX41) was identified and characterized according to its role in innate immunity against viral infection. The ORF of the *Pm*DDX41 cDNA was composed of 1863 bp encoding a polypeptide of 620 amino acid residues. According to the SMART program, *Pm*DDX41 contains three important domains, namely, the DEADc, HELICc, and zinc finger domains. In a previous study, it was shown that DDX41 binds to DNA via the DEADc domain (Zhang et al., 2011b). From the phylogenetic tree, *Pm*DDX41 clustered together with invertebrate Abstrakt genes, with the closest similarity to the amphipod Abstrakt. Abstrakt in *Drosophila* is the homolog of DDX41, which shares 65% identity and 79% similarity at the amino acid level. The gene was initially identified by a very specific phenotype, the failure of the Bolwig nerve to fasciculate and project normally (Schmucker et al., 1997). The Abstrakt gene is essential for survival at all stages throughout the life cycle of the fruit fly (Irion and Leptin, 1999).

Tissue distribution analysis revealed that the *Pm*DDX41 transcript was expressed in various shrimp tissues, including hemocytes, intestine, hepatopancreas, lymphoid organ, gill, heart, muscle, and eye stalk. However, particularly high mRNA expression levels of *Pm*DDX41 were found in immune-related tissues including the hepatopancreas, gill, and hemocytes. These tissues play an important role in metabolism and immunity in crustaceans (He

(XP_014251014.1); *Limulus polyphemus* (XP_013786635.1); *Trachymyrmex septentrionalis* (XP_018355138.1); *Acromyrmex echinatior* (XP_011055156.1); *Diuraphis noxia* (XP_015375005.1); *Bactrocera latifrons* (XP_018799159.1); *Linepithema humile* (XP_012223009.1); *Aethina tumida* (XP_019876402.1); *Anoplophora glabripennis* (XP_018573118.1); *Diachasma alloeum* (XP_015112885.1); *Dinoponera quadriceps* (XP_014485147.1); *Monomorium pharaonis* (XP_012522153.1); *Ceratitis capitata* (XP_004533592.1); *Cerapachys biroi* (XP_011329703.1); *Ceratosolen solmsi marchali* (XP_011504405.1); *Pogonomyrmex barbatus* (XP_011646631.1); *Aedes albopictus* (XP_019536629.1); *Drosophila kikkawai* (XP_017036024.1); *Ixodes scapularis* (XP_002404560.1); *Trichogramma pretiosum* (XP_014223294.1); *Octopus bimaculoides* (XP_014777272.1); *Musca domestica* (XP_005190431.1); *Drosophila takahashii* (XP_016992688.1); *Drosophila melanogaster* (NP_524220.1); *Papilio polytes* (XP_013139917.1); *Culex quinquefasciatus* (XP_001865238.1); *Aplysia californica* (XP_005090184.1); *Lingula anatina* (XP_013383180.1); *Lepisosteus oculatus* (XP_006631993.1); *Melopsittacus undulatus* (XP_005147385.1); *Zonotrichia* albicollis (XP_005483802.1); *Latimeria chalumnae* (XP_005992418.1); *Serinus canaria* (XP_009089776.1); *Nipponia nippon* (XP_009470434.1); *Coturnix japonica* (XP_015731521.1); *Haliaeetus leucocephalus* (XP_010577335.1); *Picoides pubescens* (XP_009902922.1); *Oryzias latipes* (XP_004073424.1); *Kryptolebias marmoratus* (XP_017282102.1); *Danio rerio* (XP_017209912.1); *Pygocentrus nattereri* (XP_017561740.1); *Ovis aries* (XP_004008770.1); *Pantholops hodgsonii* (XP_005971040.1); *Python bivittatus* (XP_007420367.1); *Monodelphis domestica* (XP_001381058.2); *Gekko japonicus* (XP_015268030.1); *Clupea harengus* (XP_012687658.1); *Myotis brandtii* (XP_005865545.1); *Hippocampus comes* (XP_019725479.1); *Tupaia chinensis* (*Tc*DDX41; XP_006158984.2); *Scleropages formosus* (XP_018597371.1); *Dasypus novemcinctus* (XP_004456590.1); *Vicugna pacos* (XP_006198995.1); *Camelus ferus* (XP_006175810.1); *Homo sapiens* (NP_057306.2); *Mus musculus* (NP_598820.2); *Rattus norvegicus* (NP_001101516.1); *Sus scrofa* (AGK93040.1); *Bos taurus* (NP_001076071.1); *Bactrocera dorsalis* (JAC51753.1); *Crassostrea gigas* (EKC40522.1). (For interpretation of the references to colour in this figure legend, the reader is referred to the Web version of this article.)

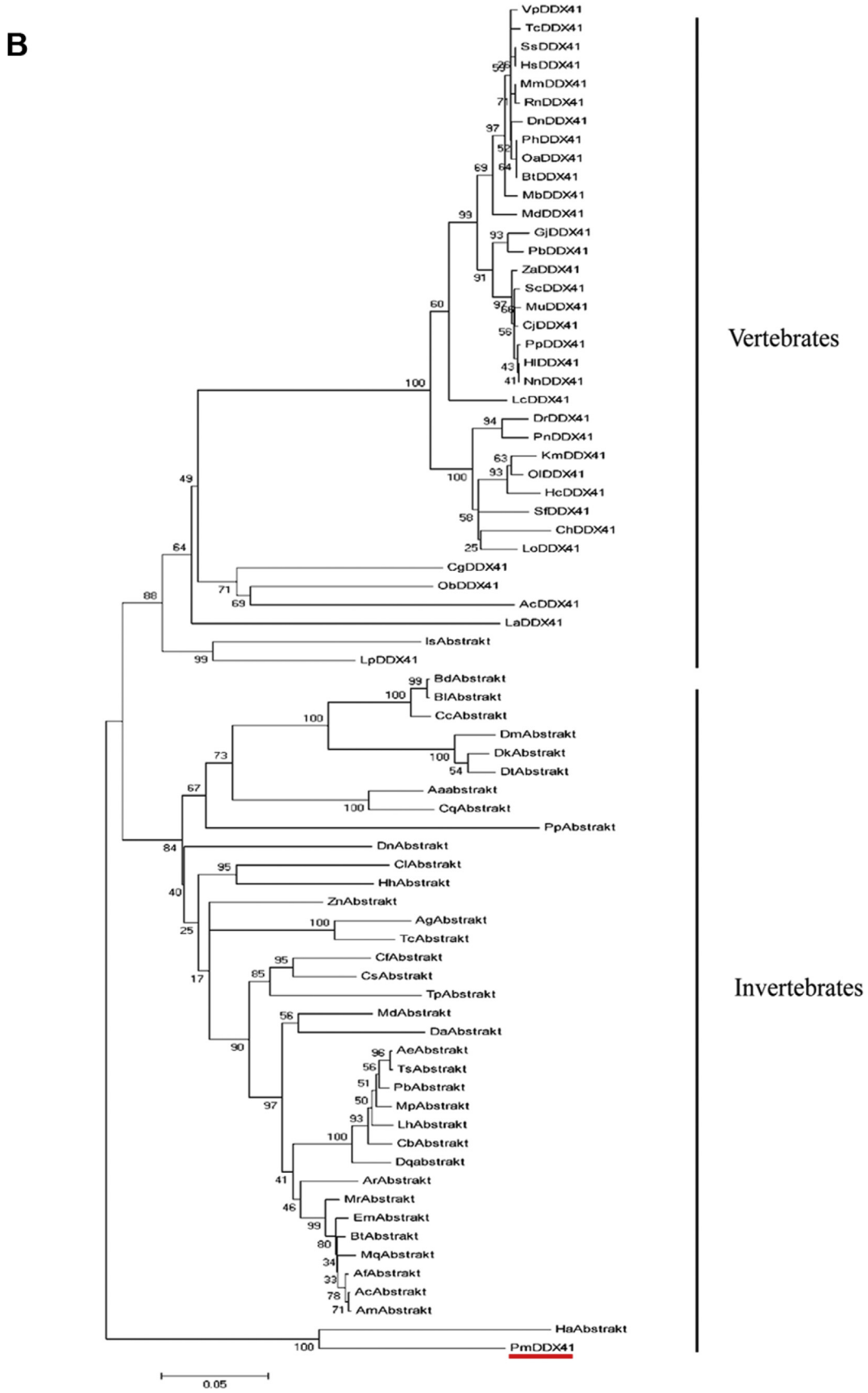


Fig. 2. (*continued*).

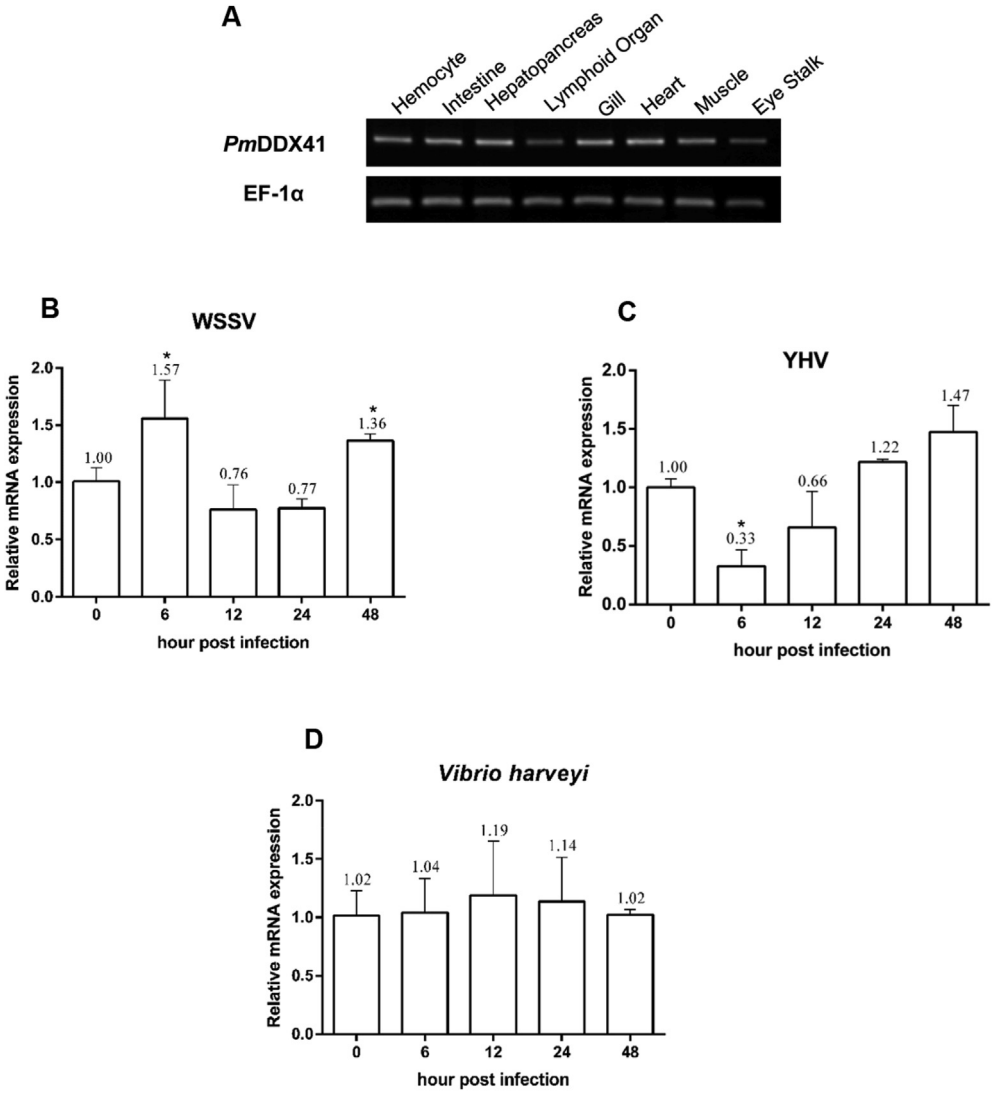


Fig. 3. Gene expression analysis of *Pm*DDX41. (A) The tissue distribution of *Pm*DDX41 was analyzed by semi-quantitative RT-PCR in the following shrimp tissues: hemocyte, intestine, hepatopancreas, lymphoid organ, gill, heart, muscle, and eye stalk. The real-time RT-PCR analysis of the *Pm*DDX41 transcript in the shrimp hemocytes challenged with (B) WSSV, (C) YHV, and (D) *Vibrio harveyi* at various time points. The expression levels were normalized against those from PBS-injected *P. monodon*. The relative expression levels were calculated according to the method of Pfaffl (2001) using EF1-α as an internal reference gene. The data were derived from three independently replicated experiments and are shown as the mean ± 1 SD (error bars). The asterisks above each bar indicate significantly different mean values ($p < 0.05$).

et al., 2015). DDX41 in chickens was found to be expressed in various tissues and most expressed in the digestive crop (Cheng et al., 2017). The porcine DDX41 was expressed in all of the tested tissues, especially the stomach and liver (Zhu et al., 2014). The porcine DDX41 has been reported to be involved in the dsDNA- and dsDNA-virus-mediated type I IFN signaling pathway in porcine kidney cells (Zhu et al., 2014). DDX41 was identified as a PRR in mouse dendritic cells (DCs) that sensed the dsDNA, cyclic di-GMP, and cyclic di-AMP. DDX41 was reported to form a complex with STING and activate type I interferon via interferon regulatory factors (IRF3 and IRF7) (Parvatiyar et al., 2012; Zhang et al., 2011b). More recently, an interferon regulatory factors (IRF) has been characterized in the Pacific white shrimp and found to be involved in the IFN-like system in shrimp (Li et al., 2015).

To further investigate the role of *Pm*DDX41 in the shrimp immune response, the shrimp were challenged with three major pathogens (WSSV, *V. harveyi*, and YHV) and analyzed for hemocyte *Pm*DDX41 expression patterns. The results revealed that *Pm*DDX41 was up-regulated after challenge with the dsDNA virus WSSV but down-regulated after challenge with the ssRNA virus YHV, and no significant change was observed after challenge with the bacterium *V. harveyi*. In chickens, the chDDX41 transcript was slightly up-regulated by the dsDNA analogue poly(dA:dT) but not by the dsRNA analogue poly(I:C) or RNA virus (Cheng et al., 2017). In terms of vertebrates, DDX41 expression was induced in the olive flounder by Ranavirus stimulation in monocyte-like cells (Quynh et al., 2015). DDX41 was found to recognize a dsDNA virus in innate immunity in vertebrates. It functions through the STING-TBK1-IRF3 pathway and directly binds DNA and STING via its DEAD domain (Zhang et al., 2011b). Our results suggest that *Pm*DDX41 might be involved in the immune response to the dsDNA virus WSSV.

WSSV is one of the most common and destructive pathogens in shrimp aquaculture, and shrimp mortality can reach 100% within 3–10 days after infection (Wang et al., 1999). To evaluate the role of *Pm*DDX41 in the shrimp immune response to WSSV, we knocked down *Pm*DDX41 prior to WSSV infection and determined the survival rate of the knockdown shrimp compared to the control shrimp. The results showed that 100% death was observed within

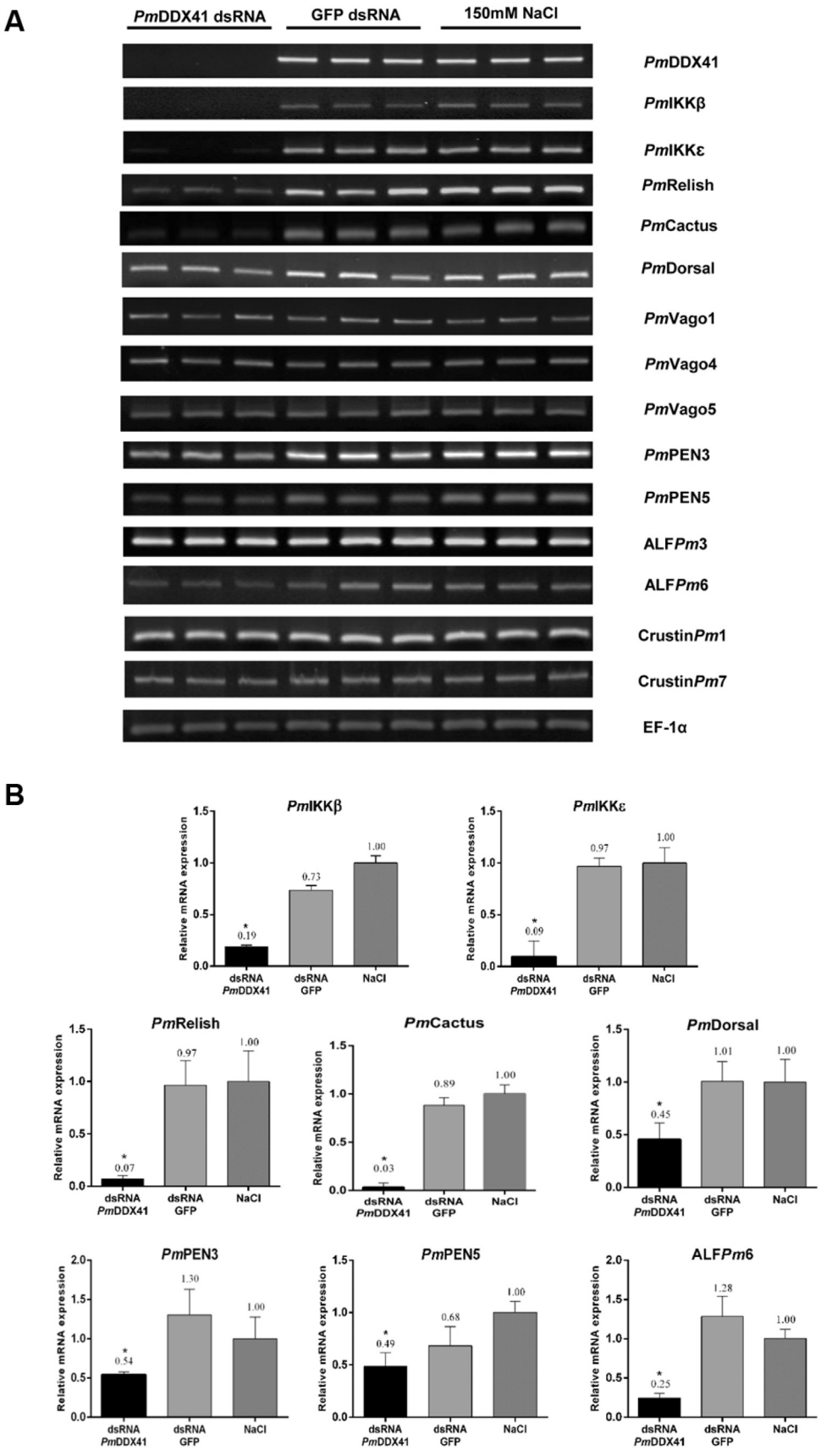


Fig. 4. Effect of gene silencing of *Pm*DDX41 on the expression levels of the antiviral and antimicrobial peptide associated genes. The shrimp were injected with *Pm*DDX41 dsRNA, GFP dsRNA, or 150 mM NaCl. After 24 h, hemolymph were collected for (A) semi-quantitative RT-PCR analysis and (B) quantitative RT-PCR analysis. EF1-α was used as an internal control. The expression levels of genes involved in the signal transduction pathway (*Pm*IKKβ, *Pm*IKKε, *Pm*Relish, *Pm*Cactus, and *Pm*Dorsal), antimicrobial peptides (*Pm*PEN3, *Pm*PEN5, ALF*Pm*3, ALF*Pm*6, Crustin*Pm*1, and Crustin*Pm*7), and IFN-like molecules (*Pm*Vago1, *Pm*Vago4, and *Pm*Vago5) were evaluated by semi-quantitative RT-PCR using gene-specific primers for each gene (Table 1). The data were derived from three independently replicated experiments and are shown as the mean ± 1 SD (error bars). The asterisks above each bar indicate significantly different mean values ($p < 0.05$).

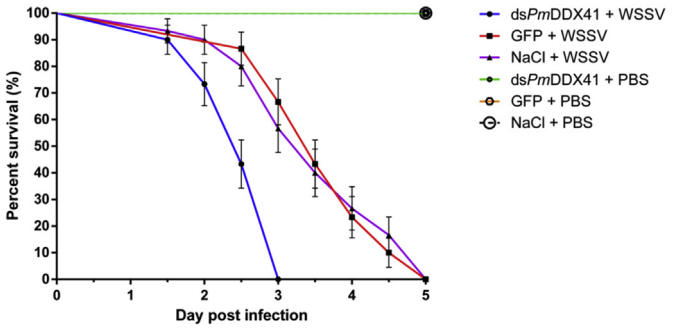


Fig. 5. Percent survival of *Pm*DDX41-silenced shrimp challenged with WSSV. Shrimp were injected with WSSV (2.64×10^3 copies/mL of WSSV in PBS) 24 h after the injection of *Pm*DDX41 dsRNA, GFP dsRNA, or 150 mM NaCl. Shrimp mortality was recorded daily for five days. Each group contained 9–10shrimp. The data were derived from three independently replicated experiments and are shown as the mean ± 1 SE (error bars).

three days for the *Pm*DDX41-silenced shrimp, compared with five days for the control shrimp, which indicates that *Pm*DDX41 plays an important role in the shrimp antiviral response to WSSV infection.

To further investigate the effects of *Pm*DDX41 knockdown in the shrimp immune response, we observed the expression levels of genes involved in signal transduction pathways, antimicrobial peptides, and IFN-like molecules. It was found that the expression levels of genes involved in the signal transduction pathways (*Pm*IKKβ, *Pm*IKKε, *Pm*Relish, and *Pm*Dorsal) and antimicrobial peptides (*Pm*PEN3, *Pm*PEN5, and ALF*Pm*6) were reduced in the *Pm*DDX41-knockdown shrimp. In vertebrates, the knockdown of DDX41 via short-hairpin RNA inhibited the immune response to cyclic di-GMP and resulted in defective activation of the DNA-sensing pathway by decreasing IFN-β (Parvatiyar et al., 2012). In the Pacific white shrimp *Litopenaeus vannamei*, IKKβ and IKKε are the central regulators of the NF-κB signaling pathway and represent a point of convergence for most of the signal transduction pathways that lead to NF-κB activation (Vallabhapurapu and Karin, 2009). In addition, the levels of the shrimp antimicrobial peptides (*Lv*PEN2, *Lv*PEN3, and *Lv*PEN4) were significantly decreased in *Lv*IKKβ- and *Lv*IKKε-silenced *L. vannamei*. Recently, ALF*Pm*6 transcript was up-regulated after challenged with WSSV and was decreased in MyD88-silenced shrimp, suggested that ALF*Pm*6 was controlled by the Toll/Dorsal pathway (Kamsaeng et al., 2017). In Chinese shrimp *Fenneropenaeus chinensis,* the expression of *Fc*Dorsal was up-regulated in WSSV-infected shrimp and *Vibrio anguillarium*-infected shrimp. In addition, transcript of *Fc*Penaeidin 5 in dsRNA-*Fc*Dorsal silencing group was decreased suggested that the expression of *Fc*Penaeidin 5 was regulated by Toll pathway (Li et al., 2010). The IMD pathway, which is involved in the sensing of RNA viruses and Gram-negative bacteria and mediated by the IKK complex to activate the NF-κB transcription factor Relish, has been studied in shrimp (Wang and Wang, 2013). The activated Relish is translocated into the nucleus to induce the expression of shrimp antimicrobial peptides (penaeidins, crustins, and anti-lipopolysaccharide factor) (Tassanakajon et al., 2013). After knockdown of the *Pm*Relish gene in shrimp, it was found that the *Pm*PEN5 transcript was suppressed, while *Pm*PEN3 was slightly upregulated. These results indicate that *Pm*PEN5 and *Pm*PEN3 are regulated by *Pm*Relish (Visetnan et al., 2015).

It is well known that DEAD-box helicases are essential in various cellular processes including mRNA export, transcriptional and translational regulation, and ribosome biogenesis (Rocak and Linder, 2004). More recent studies have suggested that vertebrate DDX41 could recognize the bacterial secondary messengers cyclic di-GMP or cyclic di-AMP to activate the type I IFN immune response, and that DDX41 senses intracellular DNA mediated by the adaptor STING in dendritic cells (Bowie, 2012; Miyabe et al., 2014; Parvatiyar et al., 2012). Interestingly, another recently identified DNA sensor, cGAS, also recognizes microbial DNA to generate the second messenger cGAMP to initiate the STING pathway and subsequent IFN production (Ablasser et al., 2013; Diner and Vance, 2014; Sun et al., 2013). In arthropods, the Vago, a virally activated secreted peptide, is considered to be a cytokine functionally similar to IFN. Recently, it has been reported that the shrimp Vago might function as an IFN-like molecule and shrimp might possess an antiviral mechanism similar to the IFN system (Li et al., 2015). In this study, the expression of *Pm*Vagos was not changed in the *Pm*DDX41-knockdown shrimp. Thus, it is interesting to speculate whether shrimp DDX41 functions in concert with or engages directly with the STING innate immune-sensing pathway to induce the production of antiviral molecules, which will be a topic for further investigation.

In conclusion, we have identified the first DDX41 from shrimp and demonstrated that it shares high sequence identity with DDX41 from various organisms and contains the conserved domains of DEADc, HELICc, and zinc finger. The transcript of *Pm*DDX41 was up-regulated after infection with the dsDNA virus WSSV, suggesting that *Pm*DDX41 plays a role in the immune response to DNA viruses. Gene silencing of *Pm*DDX41 resulted in the more rapid death of WSSV-infected shrimp and a reduction in the levels of several immune transcripts related to the signaling pathway and antimicrobial peptides. These results suggest that *Pm*DDX41 is likely involved in the antiviral response via a DNA-sensing pathway.

Acknowledgments

This work was supported by research grants from the Thailand Research Fund (TRF) to A.T. (TRF Senior Scholar No. RTA5880004) and from the TRF and the Thailand National Center for Genetic Engineering and Biotechnology (BIOTEC) to P.A. (Grant No. BRG5880016). Additional support from the TRF (Grant No. IRG5780008) to the Department of Biochemistry, Faculty of Science, Chulalongkorn University, is gratefully acknowledged. S.S. is the recipient of a student fellowship from the 100th Anniversary Chulalongkorn University Fund for Doctoral Scholarship, the 90th Anniversary of Chulalongkorn University Fund (Ratchadaphiseksomphot Endowment Fund), and the Overseas Research Experience Scholarship for Graduate Student from the Graduate School, Chulalongkorn University.

Appendix A. Supplementary data

Supplementary data related to this article can be found at https://doi.org/10.1016/j.dci.2017.12.013.

References

Ablasser, A., Goldeck, M., Cavlar, T., Deimling, T., Witte, G., Rohl, I., Hopfner, K.P., Ludwig, J., Hornung, V., 2013. cGAS produces a 2'-5'-linked cyclic dinucleotide second messenger that activates STING. Nature 498, 380–384.

Ahmad, S., Hur, S., 2015. Helicases in antiviral immunity: dual properties as sensors and effectors. Trends Biochem. Sci. 40, 576–585.

Amparyup, P., Charoensapsri, W., Tassanakajon, A., 2009. Two prophenoloxidases are important for the survival of *Vibrio harveyi* challenged shrimp *Penaeus monodon*. Dev. Comp. Immunol. 33, 247–256.

Amparyup, P., Jitvaropas, R., Pulsook, N., Tassanakajon, A., 2007. Molecular cloning, characterization and expression of a masquerade-like serine proteinase homologue from black tiger shrimp *Penaeus monodon*. Fish Shellfish Immunol. 22, 535–546.

Amparyup, P., Sutthangkul, J., Charoensapsri, W., Tassanakajon, A., 2012. Pattern recognition protein binds to lipopolysaccharide and beta-1,3-glucan and

activates shrimp prophenoloxidase system. J. Biol. Chem. 287, 10060–10069.
Amparyup, P., Wiriyaukaradecha, K., Charoensapsri, W., Tassanakajon, A., 2010. A clip domain serine proteinase plays a role in antibacterial defense but is not required for prophenoloxidase activation in shrimp. Dev. Comp. Immunol. 34, 168–176.
Bowie, A.G., 2012. Innate sensing of bacterial cyclic dinucleotides: more than just STING. Nat. Immunol. 13, 1137–1139.
Cheng, Y., Liu, Y., Wang, Y., Niu, Q., Gao, Q., Fu, Q., Ma, J., Wang, H., Yan, Y., Ding, C., Sun, J., 2017. Chicken DNA virus sensor DDX41 activates IFN-beta signaling pathway dependent on STING. Dev. Comp. Immunol. 76, 334–342.
Chiu, Y.H., Macmillan, J.B., Chen, Z.J., 2009. RNA polymerase III detects cytosolic DNA and induces type I interferons through the RIG-I pathway. Cell 138, 576–591.
Deddouche, S., Matt, N., Budd, A., Mueller, S., Kemp, C., Galiana-Arnoux, D., Dostert, C., Antoniewski, C., Hoffmann, J.A., Imler, J.L., 2008. The DExD/H-box helicase Dicer-2 mediates the induction of antiviral activity in *drosophila*. Nat. Immunol. 9, 1425–1432.
Diner, E.J., Vance, R.E., 2014. Taking the STING out of cytosolic DNA sensing. Trends Immunol. 35, 1–2.
He, Y., Ju, C., Zhang, X., 2015. Roles of small RNAs in the immune defense mechanisms of crustaceans. Mol. Immunol. 68, 399–403.
Hornung, V., Schlender, J., Guenthner-Biller, M., Rothenfusser, S., Endres, S., Conzelmann, K.K., Hartmann, G., 2004. Replication-dependent potent IFN-alpha induction in human plasmacytoid dendritic cells by a single-stranded RNA virus. J. Immunol. 173, 5935–5943.
Hoshino, K., Takeuchi, O., Kawai, T., Sanjo, H., Ogawa, T., Takeda, Y., Takeda, K., Akira, S., 1999. Cutting edge: Toll-like receptor 4 (TLR4)-deficient mice are hyporesponsive to lipopolysaccharide: evidence for TLR4 as the Lps gene product. J. Immunol. 162, 3749–3752.
Irion, U., Leptin, M., 1999. Developmental and cell biological functions of the *Drosophila* DEAD-box protein abstrakt. Curr. Biol. 9, 1373–1381.
Jearaphunt, M., Amparyup, P., Sangsuriya, P., Charoensapsri, W., Senapin, S., Tassanakajon, A., 2015. Shrimp serine proteinase homologues *Pm*MasSPH-1 and -2 play a role in the activation of the prophenoloxidase system. PLoS One 10, e0121073.
Kamsaeng, P., Tassanakajon, A., Somboonwiwat, K., 2017. Regulation of anti-lipopolysaccharide factors, ALF*Pm*3 and ALF*Pm*6. In: Penaeus monodon, vol. 7, p. 12694. Sci. Rep.
Li, C., Li, H., Chen, Y., Chen, Y., Wang, S., Weng, S.P., Xu, X., He, J., 2015. Activation of Vago by interferon regulatory factor (IRF) suggests an interferon system-like antiviral mechanism in shrimp. Sci. Rep. 5, 15078.
Li, F., Wang, D., Li, S., Yan, H., Zhang, J., Wang, B., Zhang, J., Xiang, J., 2010. A Dorsal homolog (*Fc*Dorsal) in the Chinese shrimp *Fenneropenaeus chinensis* is responsive to both bacteria and WSSV challenge. Dev. Comp. Immunol. 34, 874–883.
Medzhitov, R., Janeway Jr., C., 2000. Innate immune recognition: mechanisms and pathways. Immunol. Rev. 173, 89–97.
Miyabe, H., Hyodo, M., Nakamura, T., Sato, Y., Hayakawa, Y., Harashima, H., 2014. A new adjuvant delivery system 'cyclic di-GMP/YSK05 liposome' for cancer immunotherapy. J. Contr. Release 184, 20–27.
Oshiumi, H., Sakai, K., Matsumoto, M., Seya, T., 2010. DEAD/H BOX 3 (DDX3) helicase binds the RIG-I adaptor IPS-1 to up-regulate IFN-beta-inducing potential. Eur. J. Immunol. 40, 940–948.
Pandey, S., Kawai, T., Akira, S., 2014. Microbial sensing by Toll-like receptors and intracellular nucleic acid sensors. Cold Spring Harb Perspect Biol 7, a016246.
Parvatiyar, K., Zhang, Z., Teles, R.M., Ouyang, S., Jiang, Y., Iyer, S.S., Zaver, S.A., Schenk, M., Zeng, S., Zhong, W., Liu, Z.J., Modlin, R.L., Liu, Y.J., Cheng, G., 2012. The helicase DDX41 recognizes the bacterial secondary messengers cyclic di-GMP and cyclic di-AMP to activate a type I interferon immune response. Nat. Immunol. 13, 1155–1161.
Quynh, N.T., Hikima, J., Kim, Y.R., Fagutao, F.F., Kim, M.S., Aoki, T., Jung, T.S., 2015. The cytosolic sensor, DDX41, activates antiviral and inflammatory immunity in response to stimulation with double-stranded DNA adherent cells of the olive flounder, *Paralichthys olivaceus*. Fish Shellfish Immunol. 44, 576–583.
Rocak, S., Linder, P., 2004. DEAD-box proteins: the driving forces behind RNA metabolism. Nat. Rev. Mol. Cell Biol. 5, 232–241.
Schmidt, A., Rothenfusser, S., Hopfner, K.P., 2012. Sensing of viral nucleic acids by RIG-I: from translocation to translation. Eur. J. Cell Biol. 91, 78–85.
Schmucker, D., Jackle, H., Gaul, U., 1997. Genetic analysis of the larval optic nerve projection in *Drosophila*. Development 124, 937–948.
Schroder, M., Baran, M., Bowie, A.G., 2008. Viral targeting of DEAD box protein 3 reveals its role in TBK1/IKKepsilon-mediated IRF activation. EMBO J. 27, 2147–2157.
Sun, L., Wu, J., Du, F., Chen, X., Chen, Z.J., 2013. Cyclic GMP-AMP synthase is a cytosolic DNA sensor that activates the type I interferon pathway. Science 339, 786–791.
Takeuchi, O., Akira, S., 2010. Pattern recognition receptors and inflammation. Cell 140, 805–820.
Tamura, K., Stecher, G., Peterson, D., Filipski, A., Kumar, S., 2013. MEGA6: molecular evolutionary genetics analysis version 6.0. Mol. Biol. Evol. 30, 2725–2729.
Tassanakajon, A., Klinbunga, S., Paunglarp, N., Rimphanitchayakit, V., Udomkit, A., Jitrapakdee, S., Sritunyalucksana, K., Phongdara, A., Pongsomboon, S., Supungul, P., Tang, S., Kuphanumart, K., Pichyangkura, R., Lursinsap, C., 2006. *Penaeus monodon* gene discovery project: the generation of an EST collection and establishment of a database. Gene 384, 104–112.
Tassanakajon, A., Somboonwiwat, K., Supungul, P., Tang, S., 2013. Discovery of immune molecules and their crucial functions in shrimp immunity. Fish Shellfish Immunol. 34, 954–967.
Udompetcharaporn, A., Junkunlo, K., Senapin, S., Roytrakul, S., Flegel, T.W., Sritunyalucksana, K., 2014. Identification and characterization of a QM protein as a possible peptidoglycan recognition protein (PGRP) from the giant tiger shrimp *Penaeus monodon*. Dev. Comp. Immunol. 46, 146–154.
Vallabhapurapu, S., Karin, M., 2009. Regulation and function of NF-kappaB transcription factors in the immune system. Annu. Rev. Immunol. 27, 693–733.
Visetnan, S., Supungul, P., Hirono, I., Tassanakajon, A., Rimphanitchayakit, V., 2015. Activation of PmRelish from *Penaeus monodon* by yellow head virus. Fish Shellfish Immunol. 42, 335–344.
Wang, P.H., Gu, Z.H., Wan, D.H., Liu, B.D., Huang, X.D., Weng, S.P., Yu, X.Q., He, J.G., 2013a. The shrimp IKK-NF-kappaB signaling pathway regulates antimicrobial peptide expression and may be subverted by white spot syndrome virus to facilitate viral gene expression. Cell. Mol. Immunol. 10, 423–436.
Wang, P.H., Yang, L.S., Gu, Z.H., Weng, S.P., Yu, X.Q., He, J.G., 2013b. Nucleic acid-induced antiviral immunity in shrimp. Antivir. Res. 99, 270–280.
Wang, X.W., Wang, J.X., 2013. Pattern recognition receptors acting in innate immune system of shrimp against pathogen infections. Fish Shellfish Immunol. 34, 981–989.
Wang, Y.G., Hassan, M.D., Shariff, M., Zamri, S.M., Chen, X., 1999. Histopathology and cytopathology of white spot syndrome virus (WSSV) in cultured *Penaeus monodon* from peninsular Malaysia with emphasis on pathogenesis and the mechanism of white spot formation. Dis. Aquat. Org. 39, 1–11.
Yoneyama, M., Kikuchi, M., Natsukawa, T., Shinobu, N., Imaizumi, T., Miyagishi, M., Taira, K., Akira, S., Fujita, T., 2004. The RNA helicase RIG-I has an essential function in double-stranded RNA-induced innate antiviral responses. Nat. Immunol. 5, 730–737.
Zhang, Z., Kim, T., Bao, M., Facchinetti, V., Jung, S.Y., Ghaffari, A.A., Qin, J., Cheng, G., Liu, Y.J., 2011a. DDX1, DDX21, and DHX36 helicases form a complex with the adaptor molecule TRIF to sense dsRNA in dendritic cells. Immunity 34, 866–878.
Zhang, Z., Yuan, B., Bao, M., Lu, N., Kim, T., Liu, Y.J., 2011b. The helicase DDX41 senses intracellular DNA mediated by the adaptor STING in dendritic cells. Nat. Immunol. 12, 959–965.
Zhu, X., Wang, D., Zhang, H., Zhou, Y., Luo, R., Chen, H., Xiao, S., Fang, L., 2014. Molecular cloning and functional characterization of porcine DEAD (Asp-Glu-Ala-Asp) box polypeptide 41 (DDX41). Dev. Comp. Immunol. 47, 191–196.

Developmental and Comparative Immunology 88 (2018) 19–27

Contents lists available at ScienceDirect

Developmental and Comparative Immunology

journal homepage: www.elsevier.com/locate/devcompimm

Heat shock factor 1 regulates heat shock proteins and immune-related genes in *Penaeus monodon* under thermal stress

Phornphan Sornchuer[a,1], Wisarut Junprung[a], Warumporn Yingsunthonwattana[a], Anchalee Tassanakajon[a,b,*]

[a] Center of Excellence for Molecular Biology and Genomics of Shrimp, Department of Biochemistry, Faculty of Science, Chulalongkorn University, Bangkok, 10330, Thailand

[b] Omics Science and Bioinformatics Center, Faculty of Science, Chulalongkorn University, Bangkok, 10330, Thailand

ARTICLE INFO

Keywords:
Heat shock factor
Heat shock protein
Penaeus monodon
Thermal stress
Shrimp immunity

ABSTRACT

Heat shock factors (HSFs) participate in the response to environmental stressors and regulate heat shock protein (Hsp) expression. This study describes the molecular characterization and expression of *Pm*HSF1 in black tiger shrimp *Penaeus monodon* under heat stress. *Pm*HSF1 expression was detected in several shrimp tissues: the highest in the lymphoid organ and the lowest in the eyestalk. Significant up-regulation of *Pm*HSF1 expression was observed in hemocytes ($p < 0.05$) following thermal stress. The expression of several *Pm*Hsps was rapidly induced following heat stress. Endogenous *Pm*HSF1 protein was expressed in all three types of shrimp hemocyte and strongly induced under heat stress. The suppression of *Pm*HSF1 expression by dsRNA-mediated gene silencing altered the expression of *Pm*Hsps, several antimicrobial genes, genes involved in the melanization process, and an antioxidant gene (*Pm*SOD). *Pm*HSF1 plays an important role in the thermal stress response, regulating the expression of Hsps and immune-related genes in *P. monodon*.

1. Introduction

Aquatic organisms encounter various environmental stressors such as heat, chemicals toxicants, and viral and bacterial pathogens. These stressors induce multiple changes in a cell that ultimately affect protein structure and function. An important mechanism that protects cells from damage caused by these stressors is the activation of the heat shock response. This response is predominantly regulated by various heat shock factors (HSFs), which bind to heat shock elements (HSEs) in the promoters of heat shock genes to induce their expression (Morimoto, 1998).

HSFs were first characterized in *Saccharomyces cerevisiae* (Sorger and Pelham, 1988; Wiederrecht et al., 1988) and *Drosophila melanogaster* (Clos et al., 1990). The mammalian HSF family consists of four members [HSF1, HSF2, HSF3, and HSF4 (Akerfelt et al., 2010a)]. Distinct HSFs possess unique and overlapping functions, exhibit tissue-specific patterns of expression and multiple post-translational modifications, and have several interacting protein partners (Akerfelt et al., 2007, 2010b; Anckar and Sistonen, 2007; Fujimoto et al., 2010). HSF1 and HSF2 are the well-studied factors because of their co-expression in most tissues and cell lines (Ostling et al., 2007; Pirkkala et al., 2001). HSF3 has only been identified in avian species, while HSF4 has been identified in mammals and is expressed predominantly in the lens and brain (Hu and Mivechi, 2006; Inouye et al., 2003; Min et al., 2004; Nakai, 1999; Nakai et al., 1997; Somasundaram and Bhat, 2004). Mammalian HSF1 corresponds to the single HSF in yeast, nematodes, and fruit flies (Clos et al., 1990; Hilgarth et al., 2004; Sorger and Pelham, 1988; Wiederrecht et al., 1988) and is considered the *bona fide* stress-activated transcription factor. HSF members are characterized by their conserved structure of the DNA binding domain (DBD) and hydrophobic heptad repeat (HR-A/B). The DBD, which is the best preserved domain throughout evolution, belongs to the family of winged helix-turn-helix DBDs (Damberger et al., 1994; Harrison et al., 1994; Vuister et al., 1994). The common activation process in all eukaryotic HSFs begins with the conversion of the inactive monomeric HSF1 to high-affinity DNA-binding trimers (Baler et al., 1993; Sarge et al., 1993). The trimerization of HSFs is mediated by arrays of HR-A and HR-B via the formation of a coil; this process is dependent on intermolecular hydrophobic non-covalent interactions (Lu et al., 2009; Sarge et al., 1993).

* Corresponding author. Center of Excellence for Molecular Biology and Genomics of Shrimp, Department of Biochemistry, Faculty of Science, Chulalongkorn University, Bangkok, 10330, Thailand.
E-mail address: anchalee.k@chula.ac.th (A. Tassanakajon).
[1] Current address: Microbiology and Immunology, Department of Preclinical Science, Faculty of Medicine, Thammasat University (Rangsit Campus), Klongluang, Pathum Thani 12120, Thailand.

https://doi.org/10.1016/j.dci.2018.06.013
Received 8 May 2018; Accepted 29 June 2018
Available online 02 July 2018
0145-305X/ © 2018 Elsevier Ltd. All rights reserved.

Table 1
Summary of primers used in this study.

Primer name	Sequence (5′ → 3′)	Purpose
PmHSF1fl-F	GGACCAAAACGTGTGTAAACAAA	cDNA cloning
PmHSF1fl-R	TCAGGCCAAGCATTCACTTC	cDNA cloning
PmHSF1fm-F	TGGGAATGTCCCGGCGTTTT	RT-PCR, qRT-PCR
PmHSF1fm-R	ACATGTTCAGCTGTCTCACA	RT-PCR, qRT-PCR
PmHsp10-F	TCGACCGTGTGCTGGTCCAA	qRT-PCR
PmHsp10-R	GTGGTGCCAGCATCAGTTCT	qRT-PCR
PmHsp21-F	CACGAGGAGAAGTCTGACAAC	qRT-PCR
PmHsp21-R	GAGAGCGAGGACTTGATGAG	qRT-PCR
PmHsp60-F	CCCCAAGGGTCGAAATGTAA	qRT-PCR
PmHsp60-R	GGCAACATCTTGGACCAACT	qRT-PCR
PmHsp70-F	CTTCGACAACCGCATGGTGA	qRT-PCR
PmHsp70-R	GAAGAGGGAGCCGATCTCCA	qRT-PCR
PmHsc70-F	TGTCGGTATTGATCTGGGAA	qRT-PCR
PmHsc70-R	TTGGCGTCGAATACAGTGTT	qRT-PCR
PmHsp90-F	CGTCGAGAAGGAGAGGGACA	qRT-PCR
PmHsp90-R	TCAGCTCTTCGTCCTCCGTG	qRT-PCR
PmPEN3-F	ATGCGTCTCGTGGTCTGCCT	qRT-PCR
PmPEN3-R	CCTGTGAATACACGAGGA	qRT-PCR
PmPEN5-F	TTGGTCTATGCTTTGCAAGG	qRT-PCR
PmPEN5-R	ACAGATAGTTAAAGTGAAAGAC	qRT-PCR
PmALF3-F	ATACTAGAATTCCAAGGGTGGGAGGCTGTGGCA	qRT-PCR
PmALF3-R	TATTATGGATCCCTATGAGCTGAGCCACTGGTTGGCCT	qRT-PCR
CrustinPm1-F	CTGCTGCGAGTCAAGGTATG	qRT-PCR
CrustinPm1-R	AGGTACTGGCTGCTCTACTG	qRT-PCR
CrustinPm7-F	GGCATGGTGGCGTTGTTCCT	qRT-PCR
CrustinPm7-R	TGTCGGAGCCGAAGCAGTCA	qRT-PCR
PmproPO1-F	GGTCTTCCCCTCCCGCTTCG	qRT-PCR
PmproPO1-R	GCCGCAGGTCCTTTGGCAGC	qRT-PCR
PmproPO2-F	GCCAAGGGGAACGGGTGATG	qRT-PCR
PmproPO2-R	TCCCTCATGGCGGTCGAGGT	qRT-PCR
PmPPAE1-F	CGTCTGCTTCATTGAGGGAGTG	qRT-PCR
PmPPAE1-R	GTAGTAGATGGTGCCCCAGCCT	qRT-PCR
PmPPAE2-F	GCGGCGGTCACGCTCCTTGTTC	qRT-PCR
PmPPAE2-R	ACTCTCGGGGGCACGCTTGTTG	qRT-PCR
PmSOD-F	GCTGCTACAAAGAAGTTGGT	qRT-PCR
PmSOD-R	GGACTGGAATGATCCAAAGC	qRT-PCR
PmPrx-F	GTTCAGGCCTTCCAGTTCAC	qRT-PCR
PmPrx-R	CTTCAAGGCTTCCCTTTGCT	qRT-PCR
EF1-α-F	GGTGCTGGACAAGCTGAAGGC	RT-PCR, qRT-PCR
EF1-α-R	CGTTCCGGTGATCATGTTCTTGATG	RT-PCR, qRT-PCR
siRNA_HSF1F1	GGATCCTAATACGACTCACTATAGGAAGGACCTGCAATGGATGT	RNAi
siRNA_HSF1R1	AATGACTGGGTTACAGCACTT	RNAi
siRNA_HSF1F2	AAGGACCTGCAATGGATGT	RNAi
siRNA_HSF1R2	GGATCCTAATACGACTCACTATAGGAATGACTGGGTTACAGCACTT	RNAi
siRNA_GFPF1	GGATCCTAATACGACTCACTATAGGATGGTGAGCAAGGGCGAGGA	RNAi
siRNA_GFPR1	TTACTTGTACAGCTCGTCCA	RNAi
siRNA_GFPF2	ATGGTGAGCAAGGGCGAGGA	RNAi
siRNA_GFPR2	GGATCCTAATACGACTCACTATAGGTTACTTGTACAGCTCGTCCA	RNAi

HSFs have been reported to play diverse functions in response to a variety of physiological and environmental stimuli (Pirkkala et al., 2001; Shabtay and Arad, 2006). In mammals, HSF1 acts as a classical stress-responsive factor that regulates the expression of heat shock proteins (Hsps). During stress, HSF1 triggers the expression of a broad range of heat-responsive genes in *Drosophila*, including Hsp90 (Westwood et al., 1991). In small abalone, the expression level of HSF1 is up-regulated under thermal and hypoxia stresses; this protects cells from damage (Huang et al., 2014). Moreover, alterations in HSF1 mRNA levels following heavy metal exposure have also been reported in goldfish; cadmium exposure has been shown to induce strong expression of HSF1 mRNA in several tissues (Kim et al., 2015). In the Pacific white shrimp *Litopenaeus vannamei*, *Lv*HSF1 is up-regulated in response to infection by *Vibrio alginolyticus* and *Staphylococcus aureus* (Yan et al., 2014); however, the genes that regulate *Lv*HSF1 have not been identified to date.

In this study, the cDNA encoding *Pm*HSF1 was cloned and characterized from hemocytes of the black tiger shrimp *Penaeus monodon*. The temporal expression of *Pm*HSF1, as well as that of other *Pm*Hsps transcripts, was determined under conditions of heat stress. The effect of *Pm*HSF1 gene knockdown on the expression of several *Pm*Hsps and immune-related genes was also investigated. Our results provide novel insights into the molecular mechanisms underlying the role of HSF1 against heat stress in the black tiger shrimp.

2. Materials and methods

2.1. Shrimp samples

Juvenile *Penaeus monodon* shrimp (wet weight: 2–5 g) were kindly provided by the Shrimp Biotech Center I, Charoen Pokphand Foods Philippines Corporation in Chantaburi province, Thailand. The animals were acclimatized in laboratory tanks at ambient temperature (28 ± 4 °C), and maintained in aerated water with a salinity of 15 ppt for at least one week before use in the experiments. Each container was stocked with maximum density of 40 shrimp in 40 L of water.

2.2. Cloning of PmHSF1 from P. monodon

A 1925-bp cDNA fragment of *Pm*HSF1 was obtained by polymerase

chain reaction (PCR) using the cDNA template and the primers *Pm*HSF1fl-F and *Pm*HSF1fl-R (Table 1). The primers used for PCR were designed based on the 5′-untranslated region retrieved from cDNA sequence of *Lv*HSF1 from *L. vannamei* (GenBank accession number: KC782836). PCR reactions were performed using the Advantage 2 PCR kit (Clontech, USA). After agarose gel electrophoresis, PCR products were removed from the gel and cloned into the TA cloning vector (RBC Bioscience, Taiwan). The recombinant plasmid was then sequenced in both directions.

2.3. Sequence characterization and phylogenetic analysis

The deduced amino acid sequence of *Pm*HSF1 was analyzed using the simple modular architecture research tool (SMART) (http://smart.embl-heidelberg.de). Multiple-sequence alignment was performed using the ClustalX 2.1 program. HSFs amino acid sequences from different species were aligned and used to construct phylogenetic trees. A neighbor-joining phylogenetic tree was constructed by MEGA 6 software based on the deduced amino acid sequences of the related genes in typical species. Bootstrap sampling was reiterated 1000 times. Molecular weight prediction was carried out using the EXPASY database (http://web.expasy.org/compute_pi/).

2.4. Exposure of shrimp to heat stress

Healthy *P. monodon* shrimp were maintained at 29 ± 1 °C with 15 ppt salinity for one week prior to heat shock treatment. Shrimp were then transferred from the seawater tank at 29 ± 1 °C to 38 °C for 30 min of heat stress and then returned to 29 ± 1 °C to recover prior to sampling for RNA, immunofluorescence detection, and a gene-specific knockdown experiment.

2.5. mRNA expression analysis of PmHSF1 in response to heat stress

To determine the effect of heat stress on the expression of *Pm*HSF1 and *Pm*Hsps in shrimp, hemolymph was collected with anticoagulant (10% (w/v) sodium citrate) at 0, 1, 3, 6, 12, 24, and 48 h after recovery. Three pooled samples were collected at different time points, with each pooled sample harvested from three individual shrimp. The hemocytes were separated by centrifugation at 800 × *g* for 10 min at 4 °C. Total RNA was then isolated using GeneZol (Geneaid, Taiwan) reagent in accordance with the manufacturer's protocol. The samples were then incubated with RQ1 RNase-free DNase I (Promega, USA) to remove contaminating genomic DNA before being reverse-transcribed into cDNA using oligo $(dT)_{18}$ primers with the RevertAid RT Reverse Transcription Kit (Thermo Fisher Scientific, USA) according to the manufacturer's protocol. The synthesized cDNA was then stored at −20 °C until further use.

The expression level of the heat shock-responsive genes in hemocytes was analyzed by quantitative real-time RT- PCR (qRT-PCR). EF-1α was used as an internal control and reference standard to verify the qRT-PCR reaction. Primers were designed using Clone Manager Pro9.2, which specified an expected PCR product of 150–200 bp; primer annealing temperatures were in the range of 55–60 °C. PCR was carried out in a 10-μl reaction volume containing 1 μl of cDNA, 5 μl of 2 × QPCR Green Master Mix Fluorescein (Biotechrabbit, Germany), and 0.2 μM of each primer. Reactions were analyzed in a Mini Opticon™ Real-Time PCR System using CFX Manager™ Software. The reaction conditions were as follows: 95 °C for 2 min, followed by 40 cycles of 95 °C for 5 s, 55 °C for 20 s, and then 72 °C for 30 s. The comparative CT method for the relative quantification of gene expression was used for assessing the normalized expression value of each gene (Pfaffl, 2001). All values are expressed the mean ± SD of three replicates. Statistical analysis was performed using SPSS (Version 10.0). Group means were compared using one-way analysis of variance (ANOVA) followed by Duncan's test for multiple comparisons. A p value < 0.05 indicated a statistically significant difference.

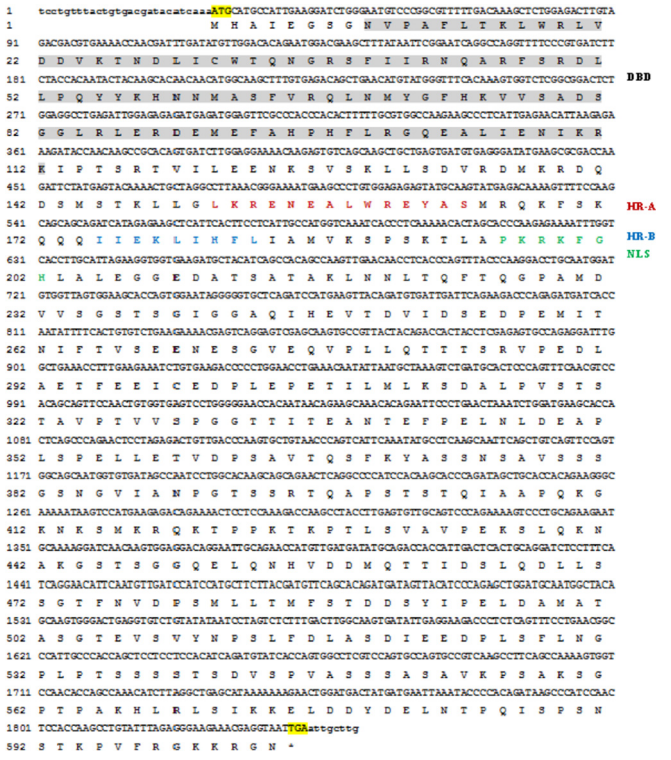


Fig. 1. Nucleotide and deduced amino acid sequence of *Pm*HSF1 from *Penaeus monodon*. The nucleotide (upper row) and deduced amino acid (lower row) sequences are shown and numbered on the left. The initiation codon (ATG) and stop codon (TGA) are in boldface with yellow shading. The putative conserved domains of DBD are shaded, whereas the HR-A/B domains are shown in red and blue, respectively. The putative nuclear localization signal (NLS) is shown in green. (For interpretation of the references to colour in this figure legend, the reader is referred to the web version of this article.)

2.6. mRNA expression analysis of PmHSF1 in shrimp tissues

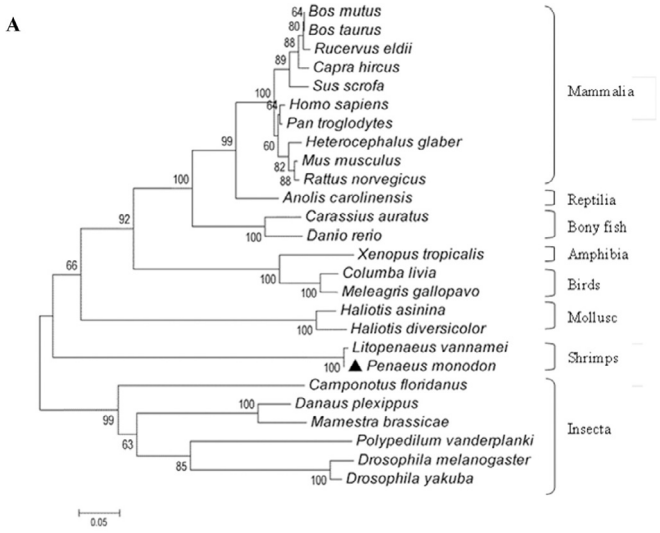
To investigate the tissue-specific expression of the *Pm*HSF1 transcript, various tissues of healthy shrimp (heart, gill, lymphoid organ, hepatopancreas, intestine, eyestalk, and hemocyte) were dissected and snap-frozen in liquid nitrogen. Hemocytes were prepared as described above and stored in liquid nitrogen. *Pm*HSF1 transcript expression levels in different tissues were qualitatively assayed by semi-quantitative reverse transcription-PCR (RT-PCR) with PmHSF1fm-F/R primers (Table 1). PCR was performed in a 12.5-μl reaction containing 1 μl of cDNA template and 0.4 μM of each primer under the following conditions: denaturation at 94 °C for 1 min, followed by 30 cycles of amplification (denaturing for 20 s at 94 °C, annealing for 20 s at 55 °C, and extension for 30 s at 72 °C). The final extension was performed at 72 °C for 5 min. The EF-1α gene fragment was amplified using EF1-α-F/R primers (Table 1) as an internal control. The PCR product was resolved by 1.8% (w/v) agarose-TBE gel electrophoresis and visualized by UV-transillumination followed by ethidium bromide staining.

2.7. Preparation of hemocyte lysate

Hemolymph was collected from healthy shrimp to investigate the expression of *Pm*HSF1 protein. Hemocytes were separated from plasma by centrifugation at 800 × *g* for 10 min at 4 °C. The cells were washed twice with cold 1× phosphate buffered saline pH 7.4 (PBS; 137 mM NaCl, 2.7 mM KCl, 4.3 mM Na_2HPO_4, 1.4 mM KH_2PO_4)) solution before resuspending in 200 μl of 1× PBS pH 7.4. Then, hemocytes were lysed by sonication. The total protein concentrations of plasma and hemocyte lysate were determined by the Bradford assay.



Fig. 2. Multiple amino acid sequence alignment of the conserved domains of *Penaeus monodon* HSF1 with that of other HSFs (using the ClustalX 2.1 program). Identical amino acid residues are shown with grey shading. The DBD and HR-A/B are indicated in boxes. Species of HSF: *Lv*HSF1 (*L. vannamei* HSF1); *Xl*HSF (*Xenopus laevis* heat shock factor protein); *Dr*HSF1 (*Danio rerio* HSF1 protein); *Ha*HSF (*Haliotis asinina* HSF).



B

Species	GenBank Accession number	Species	GenBank Accession number
Bos mutus	ELR54887	*Xenopus tropicalis*	XP002937220
Bos taurus	NP_001070727	*Columba livia*	EMC89380
Rucervus eldi	ACJ06400	*Meleagris gallopavo*	XP003209686
Capra hircus	AFN69446	*Haliotis asinina*	ABR15461
Sus scrofa	NP_001230748	*Haliotis diversicolor*	AGN53400
Homo sapiens	BAD96217	*Litopenaeus vannamei*	AHI13794
Pan troglodytes	BAK63583	*Camponotus floridanus*	EFN73771
Heterocephalus glaber	EHB16894	*Danaus plexippus*	EHJ73660
Mus musculus	EDL29570	*Mamestra brassicae*	BAG07219
Rattus norvegicus	NP_077369	*Polypedilum vanderplanki*	ADM13379
Anolis carolinensis	XP003228941	*Drosophila melanogaster*	NP_476575
Carassius auratus	AFM77715	*Drosophila yakuba*	XP_002091977
Danio rerio	AAB34899		

Fig. 3. Phylogenetic tree of *Pm*HSF1 compared with HSF1 from other species (A) Phylogenetic tree analysis of the full-length amino acid sequences of HSF proteins was performed by the neighbor-joining method and was bootstrapped 1000 times using MEGA 6 software. (B) Species and GenBank Accession numbers of HSF1.

2.8. SDS-PAGE and Western blot analysis

The total protein content of hemocyte lysate (50 μg) and plasma (200 μg) were separated by 12.5% SDS-PAGE. Separated proteins were then transferred to a polyvinylidene difluoride (PVDF) membrane and *Pm*HSF1 protein was detected using a specific antibody. In brief, membranes were incubated in blocking buffer (5% skimmed milk in 1X PBS-0.05% Tween 20) at 4 °C overnight before incubation with polyclonal rabbit anti-HSF1 antibody (Thermo Fisher Scientific, USA) (1: 5000 dilution in 5% skimmed milk in 1× PBS-T). After incubation at room temperature for 1 h, membranes were washed three times with washing buffer (1× PBS-T) to remove non-specific binding reaction. The membrane was then incubated with goat anti-rabbit IgG-AP conjugate (1: 10000). Positive bands were then detected by 5-bromo-4-chloro-3-indolyphosphate/nitro blue tetrazolium (BCIP/NBT) solution.

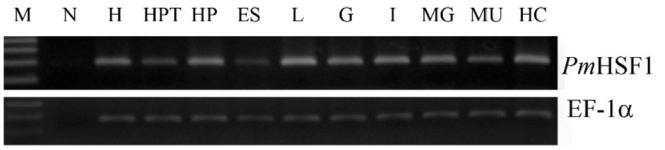


Fig. 4. *Pm*HSF1 transcript expression analysis in various *P. monodon* tissues by RT-PCR. The tissues examined were heart (H), hematopoietic tissue (HPT), hepatopancreas (HP), eye stalk (ES), lymphoid (L), gill (G), intestine (I), midgut (MG), muscle (MU), and hemocyte (HC). EF-1α was used as an internal reference and PCR control; M, 100-bp marker; N, negative control.

2.9. Immunofluorescence detection of PmHSF1 protein in shrimp hemocytes

The expression of *Pm*HSF1 in hemocytes was analyzed using a polyclonal rabbit anti-HSF1 antibody. Hemolymph was collected from heat-treated (described in Section 2.4) or untreated shrimp and fixed in 4% paraformaldehyde in a 1:1 ratio. Immunofluorescence detection method was modified from the method previously described (Chaikeeratisak et al., 2012). Hemocytes were then separated by centrifugation and resuspended in 1× PBS pH 7.4 before counting with a hemocytometer. Cells were then coated onto poly-L-lysine slides (Thermo Fisher Scientific, USA) at a concentration of 110 cells/slide, by centrifugation at 1000 × *g* at 4 °C for 10 min. The cells were washed with PBS three times, permeabilized by 1% Triton X-100 in PBS for 5 min at room temperature and washed again. The cells were then blocked with 10% fetal bovine serum (FBS) in PBS at room temperature for 1 h, and then probed with a 1: 100 dilution of polyclonal rabbit anti-HSF1 antibody at room temperature for 2 h. The negative control was incubated with 1% FBS in PBS. The slides were then washed and probed

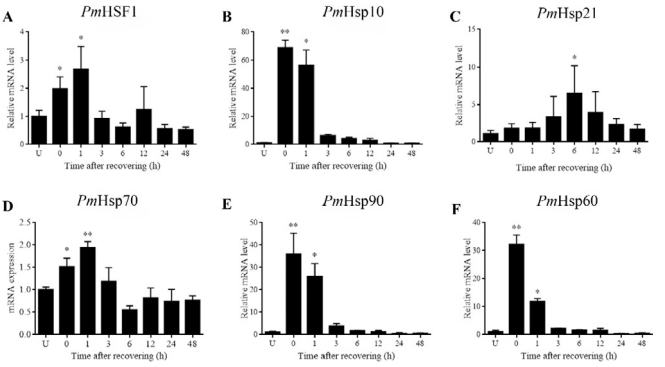


Fig. 5. Time-course gene expression data for *Pm*HSF1 (A), *Pm*Hsp10 (B), *Pm*Hsp21 (C), *Pm*Hsp70 (D), *Pm*Hsp90 (E), and *Pm*Hsp60 (F) under heat shock conditions in the hemocytes of *P. monodon*. RNA was isolated from the hemocytes of untreated shrimp (U) and heat-shocked shrimp at 38 °C for 30 min followed by 0, 1, 3, 6, 12, 24, and 48 h of recovery. The untreated group was considered as control. EF-1α RNA was used as an internal control and the relative expression levels of each gene were obtained relative to untreated expression. Each bar represents the mean ± standard deviation (SD) (n = 3); * and ** indicate significant differences compared with the untreated group (one-way analysis of variance, ANOVA, $p < 0.05$).

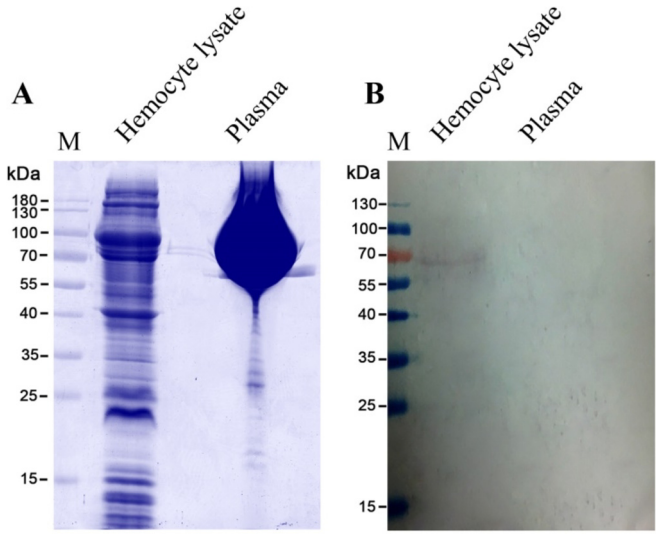


Fig. 6. SDS-PAGE and Western blot analysis of the *Pm*HSF1 protein. (A) Total proteins from hemocyte lysate (50 μg) and plasma (200 μg) of healthy shrimp *P. monodon* were resolved by 12.5% SDS-PAGE. (B) Immunoblotting using anti-HSF1 as a primary antibody; M represents molecular mass standards in kDa.

with a secondary antibody, 1: 1000 dilution of goat anti-rabbit antibody conjugated with Alexa Fluor 488 (Thermo Fisher Scientific, USA) in 1% FBS in PBS at room temperature for 1 h. Cells were also stained for nuclear DNA by incubating with 1: 1500 TO-PRO®-3 iodide (Thermo Fisher Scientific, USA) before mounting with Prolong Gold Anti-fade reagent (Thermo Fisher Scientific, USA). Fluorescence staining was then evaluated using a FV1000 confocal laser scanning microscope (Olympus, Japan).

2.10. In vivo gene knockdown of PmHSF1

To investigate the role of the *Pm*HSF1 gene in the response to acute heat stress, gene silencing was performed by using RNA interference. Double-stranded RNAs (dsRNAs) specifically targeted to *Pm*HSF1 were synthesized using the T7 RiboMAX™ Express Large Scale RNA Production System (Promega, USA). DNA fragments of the *Pm*HSF1 gene were amplified by PCR using specific primers: siRNA_HSF1F1/R1 (sense strand template) and siRNA_HSF1F2/R2 primers (anti-sense strand template) (Table 1). For a negative dsRNA control, DNA template amplification was performed using the green fluorescent protein (GFP) gene of the pEGFP-1 vector (Clontech, USA) with siRNA_GFPF1/R1 (Table 1) for the sense strand template and siRNA_GFPF2/R2 (Table 1) for the anti-sense strand template. The size of *Pm*HSF1 dsRNA was 430 nucleotides, covering the region of nucleotides 677–1106. Sense and anti-sense DNA templates, containing the T7 promoter sequence at the 5′-end on each different strand, were generated by PCR using oligonucleotide primers containing the T7 promoter RNA polymerase recognition sequence at the 5′-end. *In vitro* transcription using T7 RNA polymerase was performed to produce sense and anti-sense RNA strands according to the manufacturer's protocol. In brief, 1.5 μg of purified PCR product was incubated with ribonucleotides and RNA polymerase enzyme at 37 °C overnight. An equal amount of single stranded RNAs was annealed to produce dsRNA. The quality of dsRNAs was verified by 1.2% agarose gel electrophoresis and quantified using UV spectrophotometer.

Shrimp were exposed to heat treatment as described in Section 2.4. Immediately after heat treatment (0 h recovery time), shrimp were divided into three groups of three individuals each. The dsRNAs were then injected into shrimp using 0.5-ml insulin syringes with 29-guage needles. *Pm*HSF1 or GFP dsRNAs (10 μg of dsRNA dissolved in 150 mM NaCl per g of a shrimp in 30 μl) were injected intramuscularly into the third abdominal segment of shrimp. Twenty four hours after the first injection, dsRNAs were re-injected to ensure that knockdown had been successfully achieved.

Shrimp hemocytes were collected at various time points (0, 3, 6, 12, 24, and 48 h post-injection). Total RNAs and cDNAs were prepared as described above. The differential gene expression of immune-related genes was evaluated by qRT-PCR using specific primers (Table 1). The relative expression was calculated by normalizing to the expression in the group of shrimp injected with GFP dsRNAs.

3. Results

3.1. Cloning and sequence analysis of PmHSF1

The cDNA sequence of *Pm*HSF1 was successfully amplified using PmHSF1fl-F and PmHSF1fl-R primers (Table 1) which were designed based on the sequence of *Lv*HFS1 (accession number KC782836). The obtained DNA fragment was then cloned and sequenced. The open reading frame (ORF) of *Pm*HSF1 was 1815 bp in length, spanning from the ATG translation start site to the stop codon and encoding a predicted polypeptide of 604 amino acids (Fig. 1) with a calculated molecular weight of 65.8 kDa. The cDNA was submitted to NCBI GenBank under Accession Number MH105755. The SMART program (http://smart.embl-heidelberg.de/) revealed that *Pm*HSF1 contains a DBD (9–112 aa) and HR-A/B domains (151–164 and 175–183 aa).

BLASTX further revealed that the deduced amino acid sequence of *Pm*HSF1 exhibited 96.67% sequence identity with *Lv*HSF1 from *L. vannamei*. Sequence alignment showed that the conserved domains of DBD and HR-A/B were located at the N-terminus, while the C-terminus showed high variation. Multiple amino acid sequence alignments of conserved domains of *Pm*HSF1 with those of other HSFs are shown in Fig. 2. The conserved domains of *Pm*HSF1 showed 98.25%, 55.74%, 56.89%, and 54.59% sequence identity with those of *Lv*HSF1 in *L. vannamei*, *Xl*HSF in *Xenopus laevis*, *Dr*HSF1 in *Danio rerio*, and *Ha*HSF in *Haliotis asinina*, respectively.

3.2. Phylogenetic analysis of PmHSF1 and other HSFs

To determine the relationship between *Pm*HSF1 and other known HSFs, phylogenetic tree analysis of the conserved domain of HSFs was generated using the MEGA 6 neighbor-joining method. The phylogenetic tree of HSFs was divided into two clusters, one comprising mammalian, reptile, bony fish, amphibian, bird, mollusc and shrimp proteins, and the other containing insect HSF proteins. Of these, *Pm*HSF1 was grouped into the shrimp cluster and positioned closely to *L. vannamei* (Fig. 3).

3.3. Expression analysis of PmHSF1 mRNA in different tissues

RNA was extracted from heart, hematopoietic tissue, hepatopancreas, eye stalk, lymphoid, gill, intestine, midgut, muscle, and hemocytes from healthy shrimp, and the level of *Pm*HSF1 transcripts was assessed using semi-quantitative RT-PCR. EF-1α was used as an internal control. The amplification reaction yielded a single amplicon of 191 bp of gene-specific cDNA fragment. The transcript of *Pm*HSF1 was detected in all of the tissues examined (Fig. 4) with the highest expression in lymphoid and the lowest level in eyestalk; all other tissues showed moderate levels of expression.

3.4. Expression of PmHSF1 and PmHsp genes in hemocytes after heat shock stress

The expression of *Pm*HSF1 and *Pm*Hsp genes was analyzed using reverse transcription and real-time quantitative PCR. An elevated temperature of 38 °C for 30 min was selected for application of heat shock: at this temperature, the heat shock stress response may be induced but with only a minor effect on shrimp survival rates (Junprung et al., 2017). The transcript expression of *Pm*HSF1 and *Pm*Hsps in *P. monodon* hemocytes was investigated at 0, 1, 3, 6, 12, 24, and 48 h after

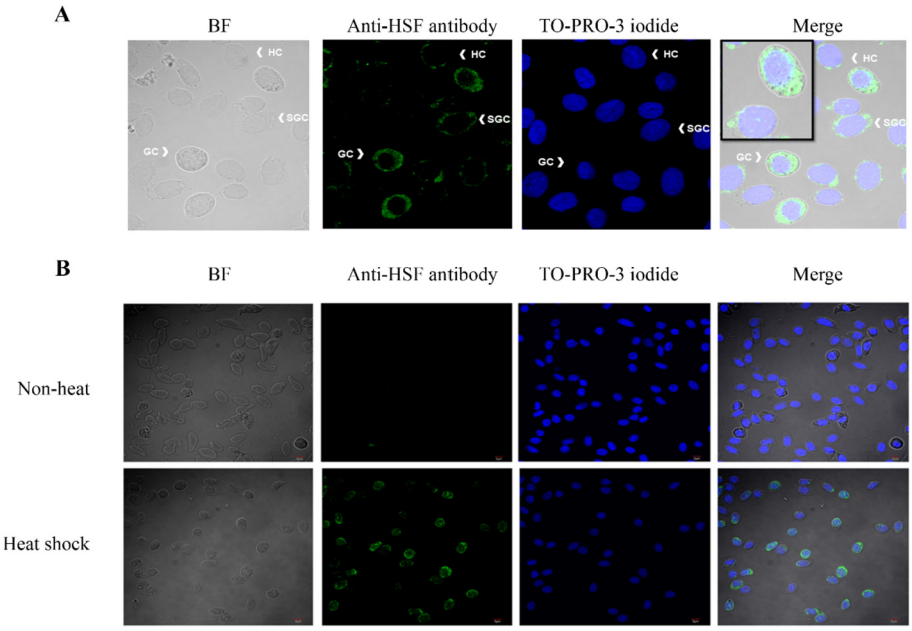


Fig. 7. Immunofluorescence detection of *Pm*HSF1-producing hemocytes. (A) The *Pm*HSF1 protein was expressed in different types of hemocytes (hyaline: HC, granular: GC, and semigranular: SGC). Shrimp were exposed to heat stress and tested for the expression of *Pm*HSF1 in the hemocytes immediately after recovery. *Pm*HSF1 is shown in green and the nucleus in blue. BF represents bright field. (B) The *Pm*HSF1 protein was expressed under non-heat and heat shock conditions.

heat shock stress, using the untreated condition as a baseline control. The expression level of *Pm*HSF1 increased at 0 (immediately after recovery at 29 °C) and 1 h post treatment, with levels 2.0- and 2.7-fold higher than that of non-heated shrimp, respectively ($p < 0.05$) (Fig. 5A). Under the heat shock condition, the expression of *Pm*Hsp10 was highly induced at 0 h (by 68.3-fold) and 1 h (by 56.0-fold) post-treatment (Fig. 5B). Thereafter, the *Pm*Hsp10 expression level dramatically reduced to baseline levels. Similarly, the expression levels of *Pm*Hsp90 and *Pm*Hsp60 were up-regulated at 0 and 1 h after heat shock stress compared with those of the non-heated control (Fig. 5E and F, respectively). The expression level of *Pm*Hsp70 after heat shock treatment showed a slight increase at 0 h (by 1.5-fold) and 1 h (by 1.9-fold) after heat stress ($p < 0.05$) but then returned to basal levels thereafter (Fig. 5D). The expression of *Pm*Hsp21 was significantly induced 6 h after treatment (by 6.0-fold) but then dropped to baseline levels (Fig. 5C).

3.5. Localization of PmHSF1 protein in P. monodon hemocytes

To determine whether *Pm*HSF1 protein was present in shrimp hemocytes or plasma, 50 µg of *P. monodon* hemocyte lysate supernatant and 200 µg of cell-free plasma were separated by 12.5% SDS-PAGE and detected by Western blot analysis. The results showed that *Pm*HSF1 protein was detected in the hemocyte lysate supernatant but not in the plasma, and that the protein size corresponded to the predicted molecular weight (Fig. 6A and B). In addition, we used immunofluorescence and confocal microscopy to investigate which type of hemocyte expressed these proteins. Hemocytes were processed for the detection of endogenous *Pm*HSF1, as described earlier. The nucleus was stained blue with TO-PRO-3 iodide dye and *Pm*HSF1 was visualized in green using Alexa Fluor 488 dye. The results revealed that the *Pm*HSF1 protein was expressed in all three types of shrimp hemocytes; hyaline cells, granular cells and semigranular cells, after challenging the shrimp with heat stress (Fig. 7A). The expression of *Pm*HSF1 was strongly induced under heat stress compared with that in shrimp that did not experience heat stress (Fig. 7B).

3.6. The effect of PmHSF1 gene silencing on the expression of immune-related genes

To investigate the functions of *Pm*HSF1, RNAi-mediated gene silencing was performed to knockdown *Pm*HSF1 transcripts in the shrimp. Total RNA was extracted from hemocytes of the knockdown and control shrimp at various time points after injection of dsRNA and then subjected to semi-quantitative RT-PCR and qRT-PCR. The relative expression ratio was calculated as the ratio between the gene expression level in *Pm*HSF1 dsRNA-injected shrimp and that in the GFP dsRNA-injected group. At 0 and 3 h post-injection (hpi), the relative expression ratio of *Pm*HSF1 was approximately 1; however, this value reduced dramatically at 6 h post-dsRNA injection, until 48 hpi (Fig. 8A and B).

The expression of six *Pm*Hsp genes in the hemocytes of *Pm*HSF1-silenced shrimp is shown in Fig. 8C. Down-regulation of *Pm*Hsp10, *Pm*Hsp21, and *Pm*Hsp60 was observed at 6 h post-dsRNA injection (hpi) followed by a subsequent return to basal levels. The expression of *Pm*Hsp90 was down-regulated at 6 hpi until 48 hpi. Similarly, the relative expression ratio of *Pm*Hsp70 and *Pm*Hsc70 was decreased from 12 hpi until 48 hpi.

The effects of *Pm*HSF1 gene silencing on the expression of several immune-related genes were also observed. The expression of *P. monodon* penaeidin3 (*Pm*PEN3), *P. monodon* penaeidin5 (*Pm*PEN5), crustin*Pm*1, and crustin*Pm*7 were significantly down-regulated at 6 hpi ($p < 0.05$) (Fig. 8D). However, the expression of crustin*Pm*7 returned to basal level at 12 hpi while the expression of all other genes remained suppressed. Interestingly, dramatic up-regulation of *P. monodon* anti-lipopolysaccharide factor 3 (*Pm*ALF3) was observed at 12 hpi followed by a reduction thereafter.

Gene silencing of *Pm*HSF1 also affected the expression of genes involved in the melanization process. The effect of *Pm*HSF1 down-regulation on the expression of *P. monodon* prophenoloxidase 1 (*Pm*proPO1) at 12 hpi, which showed down-regulation, was clearly observed (Fig. 9A). In contrast, the expression of *Pm*proPO2 was up-regulated at 6 and 12 hpi before returning to baseline levels. The expression of *P. monodon* proPO-activating enzyme 1 (*Pm*PPAE1) was significantly decreased at 24 hpi followed by a return to baseline level at 48 hpi. Moreover, the expression of *Pm*PPAE2 was dramatically reduced at 6 hpi and thereafter.

The expression of two antioxidant genes, *P. monodon* superoxide dismutase (*Pm*SOD) and *P. monodon* peroxiredoxin (*Pm*Prx), was determined in *Pm*HSF1-knockdown shrimp. Gene silencing of *Pm*HSF1 led to a down-regulation in the expression of *Pm*SOD at 24 hpi ($p < 0.05$) but had no effect on the expression of *Pm*Prx ($p > 0.05$) (Fig. 9B).

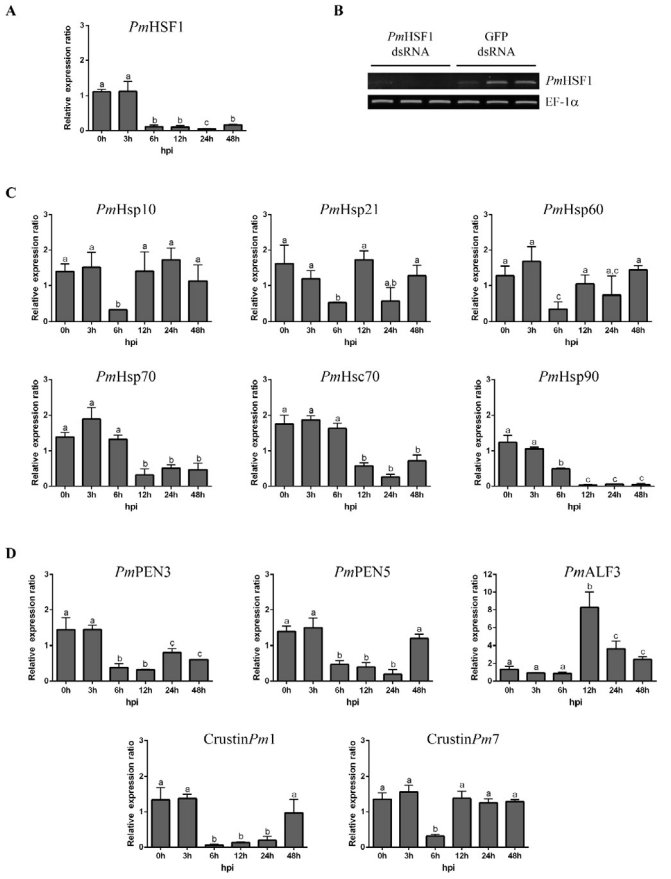


Fig. 8. Gene-silencing of *Pm*HSF1 in *P. monodon* shrimp and the effects of *Pm*HSF1 knockdown on the expression of immune-related genes. Shrimp were exposed to heat stress prior to the double injection of 10 μg/g shrimp of GFP dsRNA or 10 μg/g shrimp of *Pm*HSF1 dsRNA. The gene silencing efficiency of *Pm*HSF1 was analyzed by (A) qRT-PCR and (B) semi-quantitative RT-PCR at various time points after the second dsRNA injection (0, 3, 6, 12, 24, and 48 hpi). Semi-quantitative RT-PCR was performed at 24 hpi. The expression of (C) *Pm*Hsp genes and (D) immune-related genes was assessed in *Pm*HSF1-silenced shrimp. EF-1α was used as an internal control. The relative expression ratio was calculated from the ratio between the gene expression level in *Pm*HSF1 dsRNA-injected shrimp and GFP dsRNA-injected shrimp. Data from three independently replicated experiments are shown as the mean ± SD. Different lower case letters indicate significance at $p < 0.05$.

4. Discussion

HSF1 is a major transcriptional regulator in eukaryotic cells that is induced in response to a variety of cellular stressors, including elevated temperatures, oxidative stress, and pathogenic infections (Pirkkala et al., 2001; Shabtay and Arad, 2006). HSF1 binds to heat shock factor elements in the promoter region and regulates the expression of several target genes, many of which are HSPs. HSF1 also participates in a large network of protein homeostasis or proteostasis. HSF members are characterized by their conserved domain structures: the DBD and the hydrophobic heptad repeat, HR-A/B. In the present study, the ORF of HSF1 sequence from *P. monodon* was successfully cloned. *Pm*HSF1 contains a heat shock factor domain at amino acid residues 9–112. Sequence homology analysis showed that *Pm*HSF1 proteins contain a highly conserved DNA-binding domain similar to *Lv*HSF, which indicated that they possess a similar function. Comparison of amino acid sequences indicated that the conserved domains of *Pm*HSF1 have moderate similarities with the corresponding domains of other species (African clawed frog, zebra fish, and tropical abalone), therefore reflecting cross-species variation in evolution. This implies that the HSF1 of shrimps binds specifically to the same, or very similar, HSE consensus sequence.

Tissue distribution analyses showed that *Pm*HSF1 was observed in all tissues examined, suggesting the function of this transcription factor in gene regulation in a variety of tissues. *Lv*HSF1 was highly expressed in heart, intestine, and gill tissue but expressed at low levels in the seminal vesicle, hepatopancreas, and epithelium (Yan et al., 2014). It may be assumed that *Lv*HSF1 is sensitive to environmental stress and pathogens, as the intestine and gills often encounter various pathogens (Yan et al., 2014). The mRNA expression levels of the *Pm*HSF1 and several *Pm*Hsps in hemocytes in *P. monodon* under thermal stress were rapidly up-regulated. Heat shock treatment has been known to cause numerous types of damage to cells, including the denaturation and aggregation of proteins, disruption of the integrity of essential organelles, and the inhibition of transcription and mRNA translation processes (Richardson et al., 2011). In response to this stress, Hsps are synthesized to assist misfolded proteins by acting as molecular chaperones. Transcription activation of the Hsp genes is regulated by HSF, in which the binding of HSF to heat shock elements mediates the transcription of heat shock genes. Accordingly, the expression level of *Pm*HSF1 and *Pm*Hsps in black tiger shrimp was immediately up-regulated under thermal stress in order to protect cells from damage. The internal body temperature of shrimp varies with environmental temperature; further, these marine animals encounter fluctuations in water temperatures in the environment, suggesting that they possess regulatory systems that readily respond to variations in temperature.

Shrimp rely on the innate immune system for defense against a range of microbes by recognizing and destroying them through cellular and humoral immune responses. The two humoral immune responses, antimicrobial peptides (AMPs) and melanization, have been intensively characterized in penaeid shrimp as they play a crucial role in defense against shrimp pathogens, especially *Vibrio* species and white spot syndrome virus (WSSV) infections (Tassanakajon et al., 2018). Various types of antimicrobial peptides have been identified in penaeid shrimp, including Penaeidin (Destoumieux et al., 1997), Crustin (Gross et al., 2001), and anti-lipopolysaccharide factor (ALF) (Supungul et al., 2002). These AMPs play important roles in the innate immunity of shrimp to defense against the infection of various microbes (Tassanakajon et al., 2010). Melanization, which is regulated by the prophenoloxidase activating cascade, also plays a crucial role in the killing and sequestration of invading pathogens. The two proPO genes (*Pm*proPO1 and *Pm*proPO2) are important for the survival of shrimp during bacterial (*V. harveyi*), fungal (*Fusarium solani*), and viral (WSSV) infections (Amparyup et al., 2009, 2013; Charoensapsri et al., 2014; Sutthangkul et al., 2015).

HSFs regulate the expression of Hsps by binding specifically to the heat shock element in the promoters of heat shock genes. Several transcription factor-binding sites have been predicted in the 5′-upstream regulatory region of shrimp immune-related genes. The upstream sequence of crustin*Pm*5 contains a putative promoter with two potential binding sites for NF-κB and one complete heat-shock regulatory element (Vatanavicharn et al., 2009). Moreover, expression analysis revealed that the transcript levels of crustin*Pm*5, crustin*Pm*1, and crustin-like*Pm* in epipodite tissue were up-regulated upon heat treatment. HSEs were also found in the 5′- upstream region of the cytosolic manganese superoxide dismutase (*Lvc*MnSOD2) gene in *L. vannamei* (Sookruksawong et al., 2013). In addition, *Lvc*MnSOD2 expression levels were significantly modulated by thermal stress. The study in *P. vannamei* indicate that *Lv*HSF1 is involved in the expression of several immune-related genes, including shrimp antimicrobial peptides (AMPs) such as Atta, Mtk, and PEN4 (Yan et al., 2014). *Lv*HSF1 regulates AMPs via the NF-κB signal transduction pathway since it could enhance the role of the IκB homolog *Lv*Cactus on AMP regulation. Correspondingly, analysis of the Cactus promoter region revealed several HSF binding sites (Wang et al., 2013). Gene silencing of *Pm*HSF1 affects the transcription pattern of several genes including Hsps, AMP genes, genes involved in the melanization process, and antioxidant

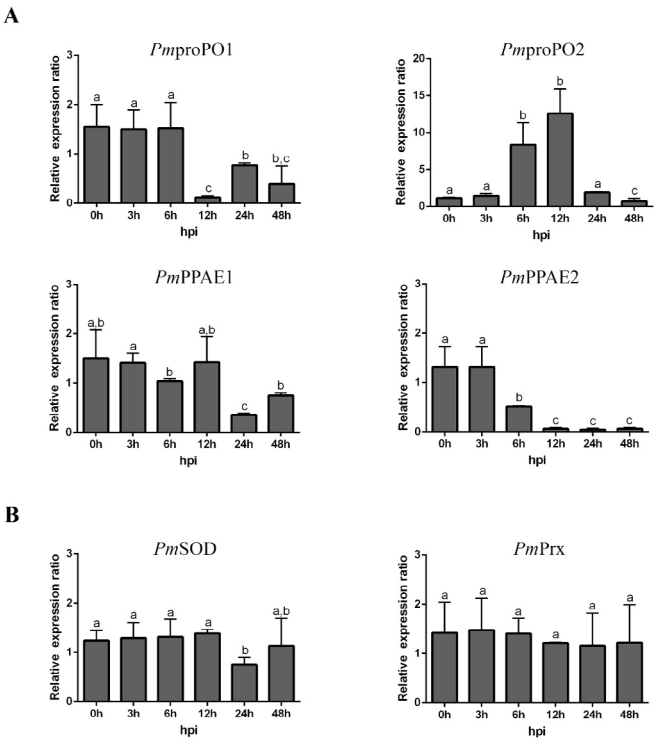


Fig. 9. Effects of *Pm*HSF1 knockdown on the expression of genes involved in the melanization process and antioxidant genes. Shrimp were exposed to heat stress before double injection with 10 μg/g shrimp of GFP dsRNA or 10 μg/g shrimp of *Pm*HSF1 dsRNA. The expression of (A) genes involved in the melanization process and (B) antioxidant genes, was assessed in *Pm*HSF1-silenced shrimp. EF-1α was used as an internal control. The relative expression ratio was calculated from the ratio between the gene expression level in *Pm*HSF1 dsRNA-injected shrimp and the GFP dsRNA-injected group. Data from three independently replicated experiments are shown as the mean ± SD. Different lower case letters indicate significance at $p < 0.05$.

genes in *P. monodon*, suggesting that *Pm*HSF1 might regulate the expression of these genes through several pathways. To date, little is known regarding the presence of HSE in the promoter region of these genes; consequently, the regulatory mechanisms involved remain unclear and require further investigation. However, significantly reduced levels of hemolymph PO activity in shrimp, in which *Lv*Hsp70 and *Lv*Hsp90 were silenced, have been reported (Junprung et al., 2017). HSFs regulate the expression of several Hsps, including Hsp70 and Hsp90; therefore, it may therefore be assumed that HSFs indirectly affect other immune-related genes.

HSF is known to be crucial for several processes, including the regulation of Hsp expression, and is also involved regulating the immune response in a wide range of organisms. The present study revealed that *Pm*HSF1 is involved in the regulation of several Hsps and immune-related genes in black tiger shrimp. Finally, this study also identified potential target genes of *Pm*HSF1 in several pathways. The present findings provide the basis for future investigation of the mechanisms underlying immune regulation in shrimp.

Declarations of interest

None.

Acknowledgements

The authors acknowledge the Shrimp Biotech Center I, Charoen Pokphand Foods Philippines Corporation for providing the experimental animals. This research was supported by the Thailand Research Fund to A.T. (TRF Senior Scholar No. RTA5880004). Postdoctoral fellowship to P.S. was supported by the Rachadapisek Sompote Endowment Fund, Chulalongkorn University. The authors would also like to thank the support from Chulalongkorn University under the Ratchadaphisek Somphot Endowment to the Center of Excellence for Molecular Biology and Genomics of Shrimp and Outstanding Research Performance Program: Chulalongkorn Academic Advancement into Its 2nd Century Project (CUAASC).

References

Akerfelt, M., Morimoto, R.I., Sistonen, L., 2010a. Heat shock factors: integrators of cell stress, development and lifespan. Nat. Rev. Mol. Cell Biol. 11, 545–555.
Akerfelt, M., Trouillet, D., Mezger, V., Sistonen, L., 2007. Heat shock factors at a crossroad between stress and development. Ann. N. Y. Acad. Sci. 1113, 15–27.
Akerfelt, M., Vihervaara, A., Laiho, A., Conter, A., Christians, E.S., Sistonen, L., Henriksson, E., 2010b. Heat shock transcription factor 1 localizes to sex chromatin during meiotic repression. J. Biol. Chem. 285, 34469–34476.
Amparyup, P., Charoensapsri, W., Tassanakajon, A., 2009. Two prophenoloxidases are important for the survival of Vibrio harveyi challenged shrimp Penaeus monodon. Dev. Comp. Immunol. 33, 247–256.
Amparyup, P., Charoensapsri, W., Tassanakajon, A., 2013. Prophenoloxidase system and its role in shrimp immune responses against major pathogens. Fish Shellfish Immunol. 34, 990–1001.
Anckar, J., Sistonen, L., 2007. Heat shock factor 1 as a coordinator of stress and developmental pathways. Adv. Exp. Med. Biol. 594, 78–88.
Baler, R., Dahl, G., Voellmy, R., 1993. Activation of human heat shock genes is accompanied by oligomerization, modification, and rapid translocation of heat shock transcription factor HSF1. Mol. Cell Biol. 13, 2486–2496.
Chaikeeratisak, V., Somboonwiwat, K., Tassanakajon, A., 2012. Shrimp alpha-2-macroglobulin prevents the bacterial escape by inhibiting fibrinolysis of blood clots. PLoS One 7, e47384.
Charoensapsri, W., Amparyup, P., Suriyachan, C., Tassanakajon, A., 2014. Melanization reaction products of shrimp display antimicrobial properties against their major bacterial and fungal pathogens. Dev. Comp. Immunol. 47, 150–159.
Clos, J., Westwood, J.T., Becker, P.B., Wilson, S., Lambert, K., Wu, C., 1990. Molecular cloning and expression of a hexameric Drosophila heat shock factor subject to negative regulation. Cell 63, 1085–1097.
Damberger, F.F., Pelton, J.G., Harrison, C.J., Nelson, H.C., Wemmer, D.E., 1994. Solution structure of the DNA-binding domain of the heat shock transcription factor determined by multidimensional heteronuclear magnetic resonance spectroscopy. Protein Sci. 3, 1806–1821.
Destoumieux, D., Bulet, P., Loew, D., Van Dorsselaer, A., Rodriguez, J., Bachere, E., 1997. Penaeidins, a new family of antimicrobial peptides isolated from the shrimp Penaeus vannamei (Decapoda). J. Biol. Chem. 272, 28398–28406.
Fujimoto, M., Hayashida, N., Katoh, T., Oshima, K., Shinkawa, T., Prakasam, R., Tan, K., Inouye, S., Takii, R., Nakai, A., 2010. A novel mouse HSF3 has the potential to activate nonclassical heat-shock genes during heat shock. Mol. Biol. Cell 21, 106–116.
Gross, P.S., Bartlett, T.C., Browdy, C.L., Chapman, R.W., Warr, G.W., 2001. Immune gene discovery by expressed sequence tag analysis of hemocytes and hepatopancreas in the Pacific White Shrimp, Litopenaeus vannamei, and the Atlantic White Shrimp, L. setiferus. Dev. Comp. Immunol. 25, 565–577.
Harrison, C.J., Bohm, A.A., Nelson, H.C., 1994. Crystal structure of the DNA binding domain of the heat shock transcription factor. Science 263, 224–227.
Hilgarth, R.S., Murphy, L.A., O'Connor, C.M., Clark, J.A., Park-Sarge, O.K., Sarge, K.D., 2004. Identification of Xenopus heat shock transcription factor-2: conserved role of sumoylation in regulating deoxyribonucleic acid-binding activity of heat shock transcription factor-2 proteins. Cell Stress Chaperones 9, 214–220.
Hu, Y., Mivechi, N.F., 2006. Association and regulation of heat shock transcription factor 4b with both extracellular signal-regulated kinase mitogen-activated protein kinase and dual-specificity tyrosine phosphatase DUSP26. Mol. Cell Biol. 26, 3282–3294.
Huang, Y., Cai, X., Zou, Z., Wang, S., Wang, G., Wang, Y., Zhang, Z., 2014. Molecular cloning, characterization and expression analysis of three heat shock responsive genes from Haliotis diversicolor. Fish Shellfish Immunol. 36, 590–599.
Inouye, S., Katsuki, K., Izu, H., Fujimoto, M., Sugahara, K., Yamada, S., Shinkai, Y., Oka, Y., Katoh, Y., Nakai, A., 2003. Activation of heat shock genes is not necessary for protection by heat shock transcription factor 1 against cell death due to a single exposure to high temperatures. Mol. Cell Biol. 23, 5882–5895.
Junprung, W., Supungul, P., Tassanakajon, A., 2017. HSP70 and HSP90 are involved in shrimp Penaeus vannamei tolerance to AHPND-causing strain of Vibrio parahaemolyticus after non-lethal heat shock. Fish Shellfish Immunol. 60, 237–246.
Kim, S.S., Chang, Z., Park, J.S., 2015. Identification, tissue distribution and characterization of two heat shock factors (HSFs) in goldfish (Carassius auratus). Fish Shellfish Immunol. 43, 375–386.
Lu, M., Sohn, K.J., Kim, S.W., Li, C.R., Kim, S., Kim, D.K., Park, J.S., 2009. Alpha-helix 1 in the DNA-binding domain of heat shock factor 1 regulates its heat-induced trimerization and DNA-binding. Biochem. Biophys. Res. Commun. 385, 612–617.
Min, J.N., Zhang, Y., Moskophidis, D., Mivechi, N.F., 2004. Unique contribution of heat shock transcription factor 4 in ocular lens development and fiber cell differentiation. Genesis 40, 205–217.
Morimoto, R.I., 1998. Regulation of the heat shock transcriptional response: cross talk between a family of heat shock factors, molecular chaperones, and negative

regulators. Genes Dev. 12, 3788–3796.
Nakai, A., 1999. New aspects in the vertebrate heat shock factor system: Hsf3 and Hsf4. Cell Stress Chaperones 4, 86–93.
Nakai, A., Tanabe, M., Kawazoe, Y., Inazawa, J., Morimoto, R.I., Nagata, K., 1997. HSF4, a new member of the human heat shock factor family which lacks properties of a transcriptional activator. Mol. Cell Biol. 17, 469–481.
Ostling, P., Bjork, J.K., Roos-Mattjus, P., Mezger, V., Sistonen, L., 2007. Heat shock factor 2 (HSF2) contributes to inducible expression of hsp genes through interplay with HSF1. J. Biol. Chem. 282, 7077–7086.
Pfaffl, M.W., 2001. A new mathematical model for relative quantification in real-time RT-PCR. Nucleic Acids Res. 29, e45.
Pirkkala, L., Nykanen, P., Sistonen, L., 2001. Roles of the heat shock transcription factors in regulation of the heat shock response and beyond. Faseb. J. 15, 1118–1131.
Richardson, P.G., Mitsiades, C.S., Laubach, J.P., Lonial, S., Chanan-Khan, A.A., Anderson, K.C., 2011. Inhibition of heat shock protein 90 (HSP90) as a therapeutic strategy for the treatment of myeloma and other cancers. Br. J. Haematol. 152, 367–379.
Sarge, K.D., Murphy, S.P., Morimoto, R.I., 1993. Activation of heat shock gene transcription by heat shock factor 1 involves oligomerization, acquisition of DNA-binding activity, and nuclear localization and can occur in the absence of stress. Mol. Cell Biol. 13, 1392–1407.
Shabtay, A., Arad, Z., 2006. Reciprocal activation of HSF1 and HSF3 in brain and blood tissues: is redundancy developmentally related? Am. J. Physiol. Regul. Integr. Comp. Physiol. 291, R566–R572.
Somasundaram, T., Bhat, S.P., 2004. Developmentally dictated expression of heat shock factors: exclusive expression of HSF4 in the postnatal lens and its specific interaction with alphaB-crystallin heat shock promoter. J. Biol. Chem. 279, 44497–44503.
Sookruksawong, S., Pongsomboon, S., Tassanakajon, A., 2013. Genomic organization of the cytosolic manganese superoxide dismutase gene from the Pacific white shrimp, Litopenaeus vannamei, and its response to thermal stress. Fish Shellfish Immunol. 35, 1395–1405.
Sorger, P.K., Pelham, H.R., 1988. Yeast heat shock factor is an essential DNA-binding protein that exhibits temperature-dependent phosphorylation. Cell 54, 855–864.
Supungul, P., Klinbunga, S., Pichyangkura, R., Jitrapakdee, S., Hirono, I., Aoki, T., Tassanakajon, A., 2002. Identification of immune-related genes in hemocytes of black tiger shrimp (Penaeus monodon). Mar. Biotechnol. 4, 487–494.
Sutthangkul, J., Amparyup, P., Charoensapsri, W., Senapin, S., Phiwsaiya, K., Tassanakajon, A., 2015. Suppression of shrimp melanization during white spot syndrome virus infection. J. Biol. Chem. 290, 6470–6481.
Tassanakajon, A., Amparyup, P., Somboonwiwat, K., Supungul, P., 2010. Cationic antimicrobial peptides in penaeid shrimp. Mar. Biotechnol. 12, 487–505.
Tassanakajon, A., Rimphanitchayakit, V., Visetnan, S., Amparyup, P., Somboonwiwat, K., Charoensapsri, W., Tang, S., 2018. Shrimp humoral responses against pathogens: antimicrobial peptides and melanization. Dev. Comp. Immunol. 80, 81–93.
Vatanavicharn, T., Supungul, P., Puanglarp, N., Yingvilasprasert, W., Tassanakajon, A., 2009. Genomic structure, expression pattern and functional characterization of crustinPm5, a unique isoform of crustin from Penaeus monodon. Comp. Biochem. Physiol. B Biochem. Mol. Biol. 153, 244–252.
Vuister, G.W., Kim, S.J., Wu, C., Bax, A., 1994. NMR evidence for similarities between the DNA-binding regions of Drosophila melanogaster heat shock factor and the helix-turn-helix and HNF-3/forkhead families of transcription factors. Biochemistry 33, 10–16.
Wang, D., Li, F., Li, S., Chi, Y., Wen, R., Feng, N., Xiang, J., 2013. An IkappaB homologue (FcCactus) in Chinese shrimp Fenneropenaeus chinensis. Dev. Comp. Immunol. 39, 352–362.
Westwood, J.T., Clos, J., Wu, C., 1991. Stress-induced oligomerization and chromosomal relocalization of heat-shock factor. Nature 353, 822–827.
Wiederrecht, G., Seto, D., Parker, C.S., 1988. Isolation of the gene encoding the S. cerevisiae heat shock transcription factor. Cell 54, 841–853.
Yan, H., Zhang, S., Li, X.Y., Yuan, F.H., Qiu, W., Chen, Y.G., Weng, S.P., He, J.G., Chen, Y.H., 2014. Identification and functional characterization of heat shock transcription factor1 in Litopenaeus vannamei. Fish Shellfish Immunol. 37, 184–192.

Developmental and Comparative Immunology 80 (2018) 81–93

Contents lists available at ScienceDirect

Developmental and Comparative Immunology

journal homepage: www.elsevier.com/locate/dci

Shrimp humoral responses against pathogens: antimicrobial peptides and melanization

Anchalee Tassanakajon [a, *], Vichien Rimphanitchayakit [a], Suwattana Visetnan [a], Piti Amparyup [b], Kunlaya Somboonwiwat [a], Walaiporn Charoensapsri [b], Sureerat Tang [b]

[a] Center of Excellence for Molecular Biology and Genomics of Shrimp, Department of Biochemistry, Faculty of Science, Chulalongkorn University, Phyathai Road, Bangkok 10330, Thailand
[b] National Center for Genetic Engineering and Biotechnology (BIOTEC), National Science and Technology Development Agency (NSTDA), 113 Paholyothin Road, Klong1, Klong Luang, Pathumthani 12120, Thailand

ARTICLE INFO

Article history:
Received 29 March 2017
Received in revised form
10 May 2017
Accepted 10 May 2017
Available online 10 May 2017

Keywords:
Shrimp innate immunity
Humoral immune responses
Signal transduction pathways
Antimicrobial peptides
Melanization
Prophenoloxidase system

ABSTRACT

Diseases have caused tremendous economic losses and become the major problem threatening the sustainable development of shrimp aquaculture. The knowledge of host defense mechanisms against invading pathogens is essential for the implementation of efficient strategies to prevent disease outbreaks. Like other invertebrates, shrimp rely on the innate immune system to defend themselves against a range of microbes by recognizing and destroying them through cellular and humoral immune responses. Detection of microbial pathogens triggers the signal transduction pathways including the NF-κB signaling, Toll and Imd pathways, resulting in the activation of genes involved in host defense responses. In this review, we update the discovery of components of the Toll and Imd pathways in shrimp and their participation in the regulation of shrimp antimicrobial peptide (AMP) synthesis. We also focus on a recent progress on the two most powerful and the best-studied shrimp humoral responses: AMPs and melanization. Shrimp AMPs are mainly cationic peptides with sequence diversity which endues them the broad range of activities against microorganisms. Melanization, regulated by the prophenoloxidase activating cascade, also plays a crucial role in killing and sequestration of invading pathogens. The progress and emerging research on mechanisms and functional characterization of components of these two indispensable humoral responses in shrimp immunity are summarized and discussed. Interestingly, the pattern recognition protein (PRP) crosstalk is evidenced between the proPO activating cascade and the AMP synthesis pathways in shrimp, which enables the innate immune system to build up efficient immune responses.

© 2017 Elsevier Ltd. All rights reserved.

1. Introduction

Shrimp aquaculture industry has suffered serious infectious diseases which has caused huge economic losses and impeded the sustainable development of the industry worldwide. Viruses and bacteria are major pathogens contributing over 80% of disease outbreaks in shrimp (Flegel, 2012) while fungi and parasites have much lesser impact. Vibrio species are the most important bacterial pathogens while white spot syndrome virus (WSSV), the causative agent of white spot disease (WSD), has consistently affected and caused serious economic consequences to the shrimp farming (Lo et al., 2012). Recently, there have been several reports on large economic impact of the new emerging disease known as early mortality syndrome (EMS), officially named acute hepatopancreatic necrosis disease (AHPND) (Tran et al., 2013; see also a review by Thitamadee et al., 2016). The causative agent of AHPND is found to be unique isolates of *Vibrio parahaemolyticus* (VP_{AHPND}) that contains a 69 kb plasmid carrying binary Pir-like toxin genes, $Pir^{vp}A$ and $Pir^{vp}B$ (Yang et al., 2014). Moreover, a high prevalence of the pathogen *Enterocytozoon hepatopenaei* (EHP) detected in cultivated black tiger shrimp (*Penaeus monodon*) and Pacific white shrimp (*Litopenaeus vannamei*), has been reported in several Asian countries including China, Vietnam, Thailand and India (Tangprasittipap et al., 2013; Tourtip et al., 2009). Therefore, prevention of disease outbreaks is a major concern in shrimp farming and it requires a better knowledge on shrimp immunity against invading pathogens.

* Corresponding author.
E-mail address: anchalee.k@chula.ac.th (A. Tassanakajon).

http://dx.doi.org/10.1016/j.dci.2017.05.009
0145-305X/© 2017 Elsevier Ltd. All rights reserved.

2. Innate immunity in shrimp

Similar to other invertebrates, shrimp cells can innately recognize the invading microbes by the engagement of host pattern recognition proteins (PRPs) with pathogen-associated molecular patterns (PAMPs). Innate immune cells rapidly respond to this engagement through intracellular signaling cascades which lead to the activation of cellular and humoral immune responses (Tassanakajon et al., 2013). The humoral responses are mediated by macromolecules in hemolymph. The important humoral responses are the melanin synthesis by the prophenoloxidase (proPO) system, the blood clotting system and the generation of circulating antimicrobial peptides (AMPs). On the other hand, the activities of cells, particularly those in the circulating system are involved in the cellular responses whose activities are apoptosis, phagocytosis, nodule formation and encapsulation of the intruders (Flegel and Sritunyalucksana, 2011). Therefore, the majorities of the defense mechanisms are carried out in the hemolymph and the cells that are involved called “hemocytes”. There are three types of hemocytes in the shrimp which are hyaline (agranular), semigranular (small granular) and granular (large granular) hemocytes (Johansson et al., 2000; Tsing et al., 1989). Although the hemocytes are the effectors of cellular immune responses, they are involved in the synthesis of the majorities of humoral effectors.

The cellular and humoral immune responses in shrimp immunity have been previously reviewed (Tassanakajon et al., 2013; Xu et al., 2014). Here, we focus on the recent progress of the two humoral immune responses: the antimicrobial peptides and melanization, which have been intensively characterized in penaeid shrimp as they play a crucial role in defense against shrimp pathogens especially *Vibrio* species and WSSV infections.

3. Humoral responses

Similar to Drosophila, the humoral responses of shrimp are the important part of shrimp immune defense system for they are a first line of defense against pathogens. The responses to microbial infections are rapid and very strong involving the secretion of immune proteins from the granular hemocytes into the circulating system and, then, the re-synthesis of said proteins in the immune cells. The humoral responses arise when the extracellular signal molecules from pathogens, such as the pathogen-associated molecular patterns (PAMPs) or the viral protein antigens, are detected by the cell-surface receptors or pattern recognition proteins (PRPs) resulting in the activation of NF-κB signaling pathways (Janeway, 1989; Li and Xiang, 2013a; Shaukat et al., 2015). The activation triggers the secretion of circulating antimicrobial peptides and other immune proteins to eradicate the infection. Two major signaling immune pathways are directly involved in these responses, known as Toll and Imd (immune deficiency) pathways. These two distinct signaling pathways regulate the expression of different sets of AMPs (Leclerc and Reichhart, 2004; Naitza and Ligoxygakis, 2004; Tanji and Ip, 2005). They may also act in parallel in response to different kinds of microorganisms (Li and Xiang, 2013b).

3.1. Immune signaling pathways in shrimp

Immediately after pathogens are detected by the recognition proteins in the animals, the infection is signaled through either one or both of the two immune signaling pathways, Toll and Imd pathways (Fig. 1). Each pathway is composed of a series of signaling chains starting with the PRPs that specifically bind to cell wall polysaccharides of the foreign invaders. The binding of cell wall components by the receptors initiates the signal transduction leading to the synthesis of appropriate AMPs or other immune proteins in the shrimp hemocytes (Chen et al., 2014; Dionne, 2014; Li and Xiang, 2013a; Valenzuela-Muñoz and Gallardo-Escárate, 2014). There are other signaling pathways of shrimp that respond indirectly to the infections such as JAK-STAT and JNK pathways.

3.1.1. Toll pathway

The Toll pathway plays a key role in the response to Gram-positive bacteria with Lys-type peptidoglycans (PNGs), possibly fungi and some viruses. The pathogens are recognized by PRPs (Amparyup et al., 2012; Jearaphunt et al., 2015; Udompetcharaporn et al., 2014; Wang and Wang, 2013). As in insects, a protease cascade is probably induced to finally cleaved ProSpätzle into active Spätzle (Shi et al., 2009; Wang et al., 2012). The Spätzle binds to the Toll receptor sending the infection signal into the cell (Arts et al., 2007; Wang et al., 2012). A series of signaling proteins comprising of Myeloid differentiation factor 88 (MyD88) (Wen et al., 2013; Zhang et al., 2012), Tube (Li et al., 2014a; Wang et al., 2011), Pelle (Li et al., 2014b; Wang et al., 2011) and tumor necrosis factor receptor (TNFR)-associated factor 6 (TRAF6) (Deepika et al., 2014) relay the signal to the Dorsal-Cactus complex (Huang et al., 2010; Li et al., 2010, 2012; Wang et al., 2013a). Cactus is phosphorylated, then dissociates from Dorsal, after which it is degraded, while the unmasked NF-κB transcription factor Dorsal migrates into the nucleus to regulate the synthesis of cognate AMPs.

The Toll pathway regulates the expression of a large set of genes including AMPs, many small peptides with unknown functions, components of melanization and components of clotting system (De Gregorio et al., 2002). There are PRPs in shrimp that are able to sense the presence of infection and stimulate the immune response processes. The microbial components that induce the Toll pathway are cell wall components such as peptidoglycans from Gram-positive bacteria and β-1,3-glucan from fungi. Viral protein antigens from several viruses can also activate the pathway. The microbial inducers are recognized by the circulating PRPs. The complexes are, then, recognized by the receptor of PRPs (Amparyup et al., 2012; Jearaphunt et al., 2015; Udompetcharaporn et al., 2014; Wang and Wang, 2013). A number of PRPs have been functionally studied and found to have different binding specificities and immune functions (Amparyup et al., 2012; Wang and Wang, 2013). The binding of microbial inducer to these proteins leads to the initiation of Toll pathway presumably by activating a proteolytic cascade. The end result of the cascade is the active Spätzle-processing enzyme that cleaves an inactive pro-Spätzle in the circulating system into an active form. The active Spätzle binds to the Toll receptor in the cell membrane to initiate the consequential intracellular signaling.

Besides innate immune response, the Drosophila Toll system is also involved in developmental system. This system has not been studied in shrimp. So, the Tolls, Spätzles and other proteins in the Toll pathway described herein have been studied for its functions in shrimp innate immune response. Several orthologs of Spätzles have been identified in shrimp. The *Fc*Spätzle from the hemocytes of Chinese shrimp, *Fenneropenaeus chinensis* is the first Spätzle to be reported. Its recombinant active form, *Fc*Spätzle C-114, can trigger the expression of crustin 2 in crayfish (Shi et al., 2009). Multiple Spätzles, *Lv*Spätzle 1–4, are identified in *L. vannamei*. The activation of *Lv*Spätzle 1 and 4 possibly leads to the synthesis of penaeidin 4 (Wang et al., 2012; Yuan et al., 2017).

The Toll receptors in shrimp and related species have also been identified, for example the *Mj*Toll from *Marsupenaeus japonicus*, *Fc*Toll from *F. chinensis*, *Lv*Toll from *L. vannamei* and *Mr*Toll from *Macrobrachium rosenbergii*, *Pc*Toll from *Procambarus clarkii*, and *Pm*Toll from *P. monodon* (Arts et al., 2007; Mekata et al., 2008; Shi

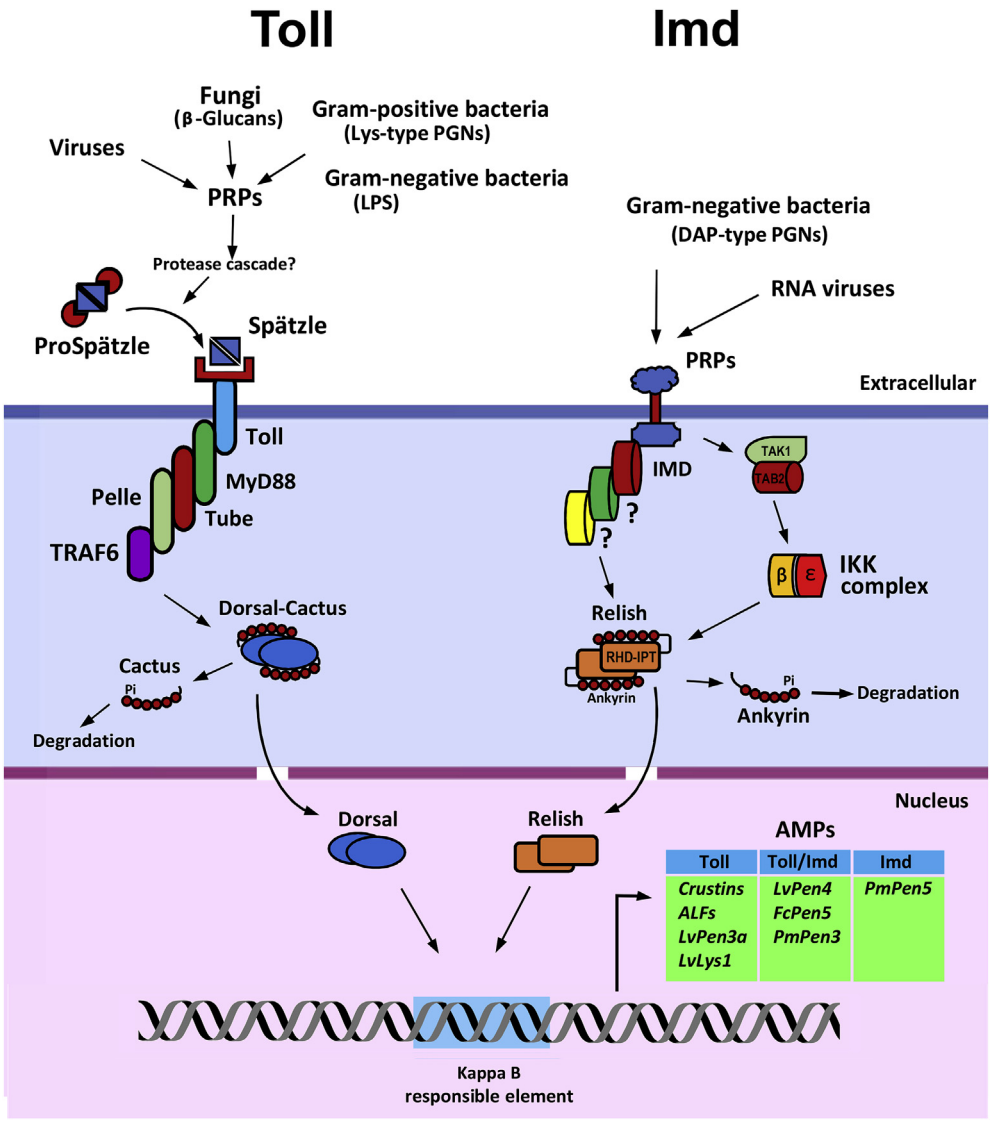


Fig. 1. Penaeid shrimp Toll and Imd signaling pathways. The Toll pathway is stimulated by fungi and Gram-positive bacteria while the Imd pathway is triggered by Gram-negative bacteria. The activation of signaling pathways in the shrimp hemocytes induces the expression of appropriate AMPs that are directed against the invading bacteria, fungi or viruses. The question marked icons are the extrapolation data from Drosophila.

et al., 2009; Srisuk et al., 2014; Wang et al., 2010; Yang et al., 2007). Multiple types of Toll are found in *L. vannamei* and shown to have different specificities in recognizing pathogens possibly via different Spätzles. The activation of Toll pathway leads to the synthesis of antimicrobial proteins, i.e. the *Lv*Toll from *L. vannamei* regulates the transcription of penaeidin3a and anti-lipopolysaccharide factor (ALF) but not crustinP (Hou et al., 2014), and the *Pc*Toll from *P. clarkii* regulates the transcription of crustin 1, crustin 2, anti-lipopolysaccharide factor 2 (ALF 2) and lysozyme 1 (Wang et al., 2015a).

Activation of Toll leads to the recruitment of three cytoplasmic proteins, which are MyD88, Tube and Pelle, forming the sensing complex in the cytoplasm underneath the cell membrane. The heterotrimeric complex is formed through their death domains which interacts with the cytoplasmic Toll/interleukin-1 receptor (TIR) domain of the activated Toll receptor through the TIR domain of MyD88 (Huang et al., 2014; Wen et al., 2013; Zhang et al., 2012). Besides interacting with MyD88, the Tube also interacts with the death domain of Pelle, a homologue of interleukin-1 receptor-associated kinase-1 (IRAK1) in *Drosophila melanogaster* (Li et al., 2014a; Wang et al., 2015a). The tumor necrosis factor receptor (TNFR)-associated factor 6 (TRAF 6) is a signaling adaptor protein that associates with Pelle during Toll signal transduction (Wang et al., 2011).

Two accessory proteins are required for the Toll signaling, the leucine-rich repeat flightless-I-interacting protein 2 (LRRFIP2), a myeloid differentiation factor 88-interacting protein (Zhang et al., 2013) and the Pellino. The Pellino binds to Pelle which leads to the activation of Dorsal and subsequent expression of AMPs (Li et al., 2014b). The Pelle or IRAK-1 homoloque is an adapter protein that links downstream of MyD88 to TRAF6 to activate Dorsal (Xu et al., 2017).

The activated Pelle acts on the cytoplasmic Dorsal-Cactus complex. In this step, the Cactus is phosphorylated by unidentified kinase (Hetru and Hoffmann, 2009). Normally, the cytoplasmic Dorsal is retained in the cytoplasm by interacting with the Cactus, an inhibitor kappa B-light domain (IκB). After phosphorylation, the IκB dissociates allowing the NF-κB transcription factor, Dorsal,

translocates into the nucleus where it binds to the κB-response elements and up-regulates the expression of AMP genes. The Cactus is probably degraded afterwards (Hoffmann, 2003; Tanji and Ip, 2005; Towb et al., 2001). The *Lv*Dorsal from *L. vannamei* regulates the transcription of shrimp penaeidin 4 gene while the *Fc*Dorsal from *F. chinensis* regulates the transcription of penaeidin 5 gene (Huang et al., 2010; Li et al., 2010). The Dorsal also activates the transcription of other immune related genes besides the antimicrobial proteins. The *Lv*Cactus from *L. vannamei* is the first report of IκB homologue in crustacean. It is activated in response to bacterial, LPS and poly (I:C) challenges, but down regulated upon WSSV infection. The *Lv*Cactus are localized in cytoplasm and interacts with *Lv*Dorsal. The expression of *Lv*Cactus is activated by *Lv*Dorsal but is inhibited by the *Lv*Cactus itself, indicating a feedback regulatory pathway between *Lv*Cactus and *Lv*Dorsal (Li et al., 2012).

Recently, the negatively regulators of Toll signaling pathway in shrimp *M. japonicus*, the β-arrestins, have been repoted. The β-arrestins act in two different ways. First, the N-terminal domain of β-arrestin interacts with the C-terminal PEST domain of Cactus while the Cactus interacts with the RHD domain of Dorsal via the ankyrin repeats, forming a heterotrimeric complex of β-arrestin-Cactus-Dorsal, with the Cactus as a bridge. Second, the β-arrestins also interact with a non-phosphorylated extracellular signal-regulated protein kinase (ERK) through the arrestin-C domain to inhibit ERK phosphorylation. The forming of β-arrestin-ERK complex prevents the phosphorylation of Cactus leading to the prohibition of Dorsal translocation into the nucleus and, thus, inhibiting the activation of Toll signaling pathway (Sun et al., 2016).

3.1.2. Imd pathway

In contrast to the activation of Toll pathway that requires the interaction of microbial ligands with circulating recognition proteins such as PRPs, the Imd pathway is initiated on direct interaction of the Gram-negative bacterial PNGs to the transmembrane receptors. The Imd pathway is preferentially triggered by Gram-negative bacteria and some Gram-positive *Bacilli* with the meso-diaminopimelic acid-type (DAP-type) PNGs. The bacteria and some RNA viruses are recognized by the membrane-bound PRPs (Jearaphunt et al., 2015; Udompetcharaporn et al., 2014; Wang and Wang, 2013). The infection signal is sent into the cells and relays via 2 routes to activate a NF-κB transcription factor Relish. The first route is through the IMD (Feng et al., 2014; Lan et al., 2013) and probably a few signaling proteins whereas the second route is through the transforming growth factor β-activated kinase 1 (TAK1)/TGF-β activated kinase 1/MAP3K7 binding protein 2 (TAB2) complex and IκB kinase (IKK) complex (Wang et al., 2013b, 2015b, 2016). The ankyrin repeat of Relish, analogous to Cactus, is cleaved off and the activated Relish migrates into the nucleus to regulate the synthesis of AMPs under this pathway (Feng et al., 2014; Huang et al., 2009; Li et al., 2009; Shi et al., 2015; Visetnan et al., 2015).

In shrimp, different types of PRPs are reported, including lipopolysaccharide and β-1,3-glucan binding protein (LGBP) and C-type lectins (CTLs). The *Ps*EST-289 from *P. stylirostris*, *Fc*LGBP/*Fc*βGBP-HDL from *F. chinensis*, *Pm*LGBP from *P. monodon*, *Lv*LGBP from *L. vannamei*, *Fp*βGBP from *F. paulensis* and *Ls*βGBP from *L. schmitti* are identified. The binding of LGBP to LPS and β-1,3-glucan leads to the expression of AMPs and immune proteins to defense against infection. Interestingly, four types of LGBPs: *Ps*EST-289, *Fp*βGBP, *Ls*βGBP and *Pm*LGBP, are able to enhance the activation of proPO system (Amparyup et al., 2012; Chen et al., 2016; Dalmo and Bogwald, 2008; Goncalves et al., 2012; Lai et al., 2011; Liu et al., 2009; Roux et al., 2002).

Binding of microbial ligands, DAP-type PGNs from Gram-negative bacteria, to the cognate transmembrane receptors induces the dimerization or oligomerization of the receptors and the initiation of intracellular immune signaling. For the shrimp, the cytoplasmic cascade begins by recruitment of several proteins including the IMD, TAK1, TAB2, IKK signalosome and the transcription factor Relish (Huang et al., 2009; Wang et al., 2009, 2013b, 2015b, 2016). A few signaling proteins in the pathway as compared to that of insects have not been identified.

The immune deficiency (IMD) protein is a death domain protein for it contains a C-terminal death domain similar to that of *Drosophila* IMD and human receptor interacting protein 1 (RIP 1) of the tumor necrosis factor receptor (TNFR) pathway in mammal. The *Lv*IMD from *L. vannamei* is the first IMD to be reported in shrimp. The *Lv*IMD is able to induce the expression of penaeidin 4 (Wang et al., 2009). Other shrimp IMD is from *F. chinensis* (*Fc*IMD). They are induced by Gram-negative bacteria and WSSV suggesting the presence of Imd pathway in shrimp (Hou et al., 2014; Lan et al., 2013; Liu et al., 2016a). The IMD protein further associates with other signaling proteins for the activation of Relish via two branched signaling pathways. The first branch goes through the IKK complex to phosphorylate the Relish. The second branch cleaves the phosphorylated Relish by a caspase. The mechanisms in shrimp are not fully understood at present but the activated IMD induces the interaction of TAK1 to TAB2 resulting in the phosphorylation and activation of the IKK (IκB kinase) complex. The TAK1, a member of transforming growth factor β-activated kinase 1 families, has been identified from *L. vannamei* called *Lv*TAK1 and can interact with its binding protein *Lv*TAB2 (Wang et al., 2016). There are also two IKK homologs, *Lv*IKKβ and *Lv*IKKε, in Pacific white shrimp that participate in the regulation of shrimp AMP synthesis (Wang et al., 2013b).

Similar to Dorsal, the NF-κB/Rel transcription factor Relish is a key signal mediator and a regulatory factor for the synthesis of cognate AMPs. The Relish is able to move into the nucleus and activates the synthesis of AMPs providing that it is activated. Normally, the full length Relish consists of a Rel homology domain (RHD), a nucleus localization signal, an IκB-like domain containing six ankyrin repeats and a death domain. The Relish is activated by cleaving away its C-terminal half, ankyrin repeats and a death domain, with a caspase enzyme (Dushay et al., 1996; Kim et al., 2014). Recently, several NF-κB transcription factor Relish from shrimp are reported. The activated *Lv*Relish from *L. vannamei* controls the expression of penaeidin 4 (Huang et al., 2009). The *Fc*Relish from *F. chinensis* regulates the expression of penaeidin 5 (Li et al., 2009). The *Pm*Relish which is up-regulated upon *V. harveyi*, WSSV and YHV challenge also regulates the expression of penaeidin 5 (Visetnan et al., 2015).

3.2. Antimicrobial proteins

Inhabiting an aquatic environment, shrimp are constantly under an enormous microbial challenge. A first-line defense is thus needed. The AMPs play a key role in this defense by killing/controlling the microorganisms and the secondary roles in modulating other immune responses. Therefore, the AMPs are considered as major humoral immune effectors. The shrimp AMPs are gene-encoded peptides and the cleaved peptides derived from larger proteins. The gene-encoded AMPs are produced as precursor proteins, stored in granule-containing hemocytes, and released upon induction. Like other organisms, a number of families of gene-encoded AMPs in shrimp have been reported. They are penaeidins, crustins, antilipopolysaccharide factors (ALFs), and stylicins (Liu et al., 2015a; Tassanakajon et al., 2013). For the cleaved peptides, the precursor proteins, hemocyanin and histones, undergo proteolysis in response to infection releasing the active cleaved-AMPs (Destoumieux-Garzón et al., 2001). According to the net

charge, the shrimp AMPs can be classified as cationic and anionic AMPs. The cationic AMPs are commonly found whereas the anionic AMPs in shrimp are fewer; only stylicin, hemocyanin derived peptide and some ALFs are anionic AMPs.

3.2.1. Penaeidins

Penaeidins are considered a unique AMP family specifically identified in penaeid shrimp (Destoumieux et al., 1997; Tassanakajon et al., 2013) and play an important role in the host defense system of shrimp. The penaeidins are highly cationic molecules having the major characteristics of an N-terminal proline-rich region (PRR) with the following signature (Y,F)T(R,G)P(X)2(R,K)P and a C-terminal cysteine-rich region (CRR) containing six cysteine residues forming three disulfide bridges with the following signature $C(X)_{2\text{-}3}C(X)_7RXCC(X)_5CC$ (Vaseeharan et al., 2012).

Based on the amino acid sequence similarities, the penaeidins have been identified in many species of penaeid shrimp including *L. vannamei*, *L. setiferus*, *F chinensis* and *P. monodon* (Cuthbertson et al., 2008; Gueguen et al., 2006; Kang et al., 2007; Li and Song, 2010; Tassanakajon et al., 2013). Recently, penaeidins have been also discovered in *M. japonicus*, *F. indicus* and *Metapenaeus monoceros* (Afsal et al., 2016; An et al., 2016). From the recent finding in *M. japonicus*, a MjPen-II sequence is identified from the hemocyte transcriptomic analysis that has an additional N-terminal serine-rich region (SRR) when compared to previously identified penaeidins. Based on this recent finding, the penaeidins can be divided into two subfamilies. A penaeidin subfamily I which includes Pen1-Pen5 possesses the two PRR and CRR domains and represents the majority of penaeidins reported to date; and a penaeidin subfamily II, which contains all three SRR, PRR and CRR domains (An et al., 2016).

The penaeidins in subfamily I are antimicrobial peptides normally active against Gram-positive bacteria and filamentous fungi (Tassanakajon et al., 2013). Note that their chitin-binding activity is thought to account for their antifungal properties (Destoumieux et al., 2000). The possible role in antiviral immunity of Pen5 from *P. monodon* has also been reported (Woramongkolchai et al., 2011). The proline-rich region provides additional function as autocrine-acting cytokine (Li and Song, 2010). For the penaeidin subfamily II, the MjPen-II exhibits an antibacterial activity against Gram-negative and Gram-positive bacteria. The domain analysis reveals that the SRR, PRR, and CRR are required for its antibacterial activity. A single domain assay indicates that the SRR exhibits antibacterial activity but not bacterial agglutination activity. The PRR and CRR have antibacterial activity and can promote bacterial agglutination but are not able to kill the bacteria. Moreover, the MjPen-II has secondary role in promoting phagocytosis (An et al., 2016).

3.2.2. Crustins

Besides their signal sequences, the cationic crustins contain glycine-rich, proline-rich, cysteine-rich, or aromatic amino acid-rich regions at the N-termini with usually 1, or sometimes 2, whey acidic protein (WAP) domains at the C-termini. The WAP domain contains 50–60 amino acid residues in length with a four-disulfide core structure. The WAP domain containing proteins have diverse functions but mostly protease inhibition and/or antimicrobial activities (Smith et al., 2008; Tassanakajon et al., 2015). Crustins and crustin-like sequences have been found in many shrimp species. They can be divided into type I-type V according to the domain structures. Type I crustin including carcinins possesses a Cys-rich region at its N-terminus and a WAP domain at the C-terminus. Type II crustin, the most abundant crustin, contains a glycine-rich region, a cysteine-rich region and a single WAP domain. Type III crustin has a short N-terminal proline/arginine-rich sequence and a C-terminal WAP domain. The protein containing two WAP domains is the type IV crustin. Unlike other types, type V crustin has an extra aromatic amino acid-rich region located between the cysteine-rich region and WAP domain. The latter crustin type is found in ant and several species of Hymenoptera but not in crustaceans and other invertebrate species (Tassanakajon et al., 2015).

The shrimp crustins have a very diverse mixture of isoforms of type I–IV (Donpudsa et al., 2014; Kim et al., 2012; Smith et al., 2008; Tassanakajon et al., 2015). In the morotoge shrimp, *Pandalopsis japonica*, type I and II crustins are identified. However, their antibacterial activity has not been reported (Kim et al., 2012). A type I crustin, MrCrs, is found in a freshwater prawn *M. rosenbergii*. It is expressed in response to IHHNV, WSSV and Gram-positive and Gram-negative bacteria. It possesses bacterial agglutination activity on Gram-positive bacteria except *Lactococcus lactis* and Gram-negative bacteria. Only bactericidal activity against a Gram-negative bacterium *Edwardsiella* sp. has been reported (Arockiaraj et al., 2013).

In *P. monodon*, several isoforms of crustin type I-IV have been identified from the EST database (Donpudsa et al., 2014; Tassanakajon et al., 2013, 2015). Type I crustin (carcinin*Pm*1 and carcinin*Pm*2), type II crustin (crustin*Pm*1-10), and type III crustin (SWD*Pm*1-3) have been identified (Amparyup et al., 2008; Donpudsa et al., 2014). Most crustins studied exhibit antimicrobial activity towards Gram-positive bacteria and less active against Gram-negative bacteria (Donpudsa et al., 2014; Tassanakajon et al., 2013) whereas the type III crustin has both antimicrobial activity against Gram-positive bacteria and proteinase inhibition activity (Amparyup et al., 2008). The protein expression profiles of hyaline and granule-containing hemocytes of unchallenged *P. monodon* show that the type II crustin, crustin*Pm*1, expresses exclusively in granule-containing hemocytes. The crustin*Pm*1 protein is secreted into the plasma upon YHV infection resulting in the elevation of crutin*Pm*1 plasma level in early periods of infection (Havanapan et al., 2016). Other crustin type II, crustin*Pm*4-1, is capable of inhibiting the WSSV infectivity (Donpudsa et al., 2014). The *Pm*DWD, the type IV crustin, has no antibacterial activity but can inhibit the proteinase activity of crude extracts from shrimp lymphoid organs and bacterial proteinases (Suthianthong et al., 2011). Binding assay of crustins against various lipids and cell wall components indicates that the bacterial agglutination activity and membrane-disrupting properties of crustins probably involve in the binding of crustins to phosphatidic acid, lipoteichoic acid (LTA) and lipopolysaccharide (LPS), with a 2:1 stoichiometry in a positive cooperative manner (Arayamethakorn et al., 2017; Krusong et al., 2012).

In *F. chinensis*, type II-IV crustins, are discovered. A type II crustin, Crus-likeFc1, shows antimicrobial activity against Gram-positive bacteria (Zhang et al., 2007). Activity analysis of FcDWD, the type IV crustin, indicates that the N-terminal WAP domain binds to the Gram-positive bacteria and exhibits proteinase inhibitory activity against secretory bacterial proteinases. In contrast, the C-terminal WAP domain of FcDWD exhibits neither antibacterial activity nor proteinase inhibitory activity (Du et al., 2009).

In *M. japonicus*, five type I crustins, *Mj*Crus I-1 to 5, have been identified according to their domain architecture from transcriptome sequencing (Jiang et al., 2015a; Liu et al., 2015b). The *Mj*Crus I-1 to 5 differ in their expression levels in different tissues, experimental pathogenic challenge conditions, binding properties on various bacteria, and a range of protease inhibitory activity. The WAP domain of *Mj*Crus I-1 but not the cysteine-rich domain has antibacterial and agglutination activities. Apart from bactericidal activity, the *Mj*Crus I-1 can promote phagocytosis activities against *V. anguillarum* and *S. aureus* (Liu et al., 2015b). Unlike the *Mj*Crus I-2

and 3 that can inhibit the activities of secreted bacterial proteases, the *Mj*Crus I-4 that contains an atypical WAP domain lacking two cysteine residues does not exhibit protease inhibitory activity. Even though most crustins are normally expressed at high level in haemocytes, an up-regulation of expression after WSSV stimulation is noticed for *Mj*Crus I-2 indicating its importance in shrimp antiviral response (Jiang et al., 2015a). An atypical type III crustin, MjSWD, that contains only a single WAP domain without the proline/arginine-rich region exhibits only the proteinase inhibitory activity (Jiang et al., 2013). The Mj-DWD, a type IV crustin, can inhibit bacterial proteinases. Interestingly, the expression of Mj-DWD can be induced by WSSV infection and is kept at high level in the virus-resistant shrimp after WSSV injection indicating its role in antiviral defense (Chen et al., 2008).

3.2.3. Antilipopolysaccharide factors

Antilipopolysaccharide factors (ALFs) have been discovered and characterized not only in the horseshoe crab or shrimp but also in several crustaceans (Tassanakajon et al., 2015). Recently, the powerful deep sequencing technique provides insight into the diversity of ALF in shrimp. The primary structure of ALF contains key features of hydrophobic N-terminal region and a LPS-binding domain (LPS-BD). The LPS-BD flanked by two conserved cysteine residues that help stabilize the molecule via disulfide loop, holds a cluster of positively charged amino acid residues for cationic ALFs and of negatively charged amino acid residues for anionic ALFs. According to the 3D structure of ALF, it is believed that the LPS-BD is solely responsible for the biological activity of ALF. Experimentally, the LPS-BD has been recognized as a functional domain with antimicrobial and antiviral activities (Jiang et al., 2015b; Li et al., 2015; Somboonwiwat et al., 2005). Also, it is shown that the modification of LPS-BD sequence of ALFFc has affected the strength of antibacterial activity and the specificity of antiviral activity (Guo et al., 2014). The crucial role of conserved disulfide bond, lysine and arginine residues inside the LPS-BD in antibacterial activity as well as of specific lysine residues inside the LPS-BD in displaying anti-WSSV activity have been revealed (Li et al., 2015).

The ALFs in penaeid shrimp can be classified based on their sequence diversity of the full-length ALF sequences and the LPS-BD sequences into 5 groups (groups A-E). It has been proven that all the ALF groups are expressed simultaneously in a single shrimp (Jiang et al., 2015b; Li et al., 2013; Li et al., 2015; Rosa et al., 2013). The LPS-BD sequence is highly conserved within each group. The ALFs with net positively charged LPS-BDs (Group A, B, C, and E) exhibit antimicrobial activity (Jiang et al., 2015b; Tassanakajon et al., 2013). The ALFs with impaired-LPS binding sites belonging to group D have been identified in *L. vannamei*, *L. stylirostris*, *M. japonicus* (Jiang et al., 2015a,b; Rosa et al., 2013). They are defective in binding the LPS and devoid of antimicrobial activity (Rosa et al., 2013). In group E, the 2 newly identified members from *M. japonicus* are highly varied in their sequences (Jiang et al., 2015b) and probably belong to different groups. If more group E members are discovered in other species, the ALFs should be re-classified.

The diversity in the full-length sequences and LPS-BD sequences of ALFs as well as variations in tissue distribution patterns allow them to response to stimuli differently and perform different functions in shrimp immunity (Li et al., 2015; Liu et al., 2005; Ponprateep et al., 2009). In kuruma shrimp, *M. japonicus*, the expression of three ALF isoforms is modulated by the C-type lectin. The Alf4 and Alf6 are mostly responsible for the bacterial inhibition whereas the Alf5 has a moderate level of activity against bacteria tested (Wang et al., 2014). The ALFs in group E from *M. japonicus*, MjALF-E1 and 2, mainly inhibit the growth of Gram-negative bacteria and show binding activity to LPS and PGN. The MjALF-E2 is involved in the clearance activity against *V. anguillarum* and *S. aureus* in vivo (Jiang et al., 2015b).

Among the shrimp ALFs identified, the ALFs from *P. monodon* (ALF*Pm*s) have been well-studied. Although six cationic ALF isoforms have been identified, only the major isoforms of ALF*Pm*2 (group A), ALF*Pm*3 (group B) and ALF*Pm*6 (group C) have been characterized in terms of the expression patterns upon pathogen challenges, range of activity against various microorganisms and the molecular mechanisms against major bacterial and viral pathogens of shrimp. These major ALF*Pm* isoforms are up-regulated upon bacterial and viral infections with different expression profiles.

The recombinant ALF*Pm*3 (rALF*Pm*3) has a wide-range of antimicrobial activities against filamentous fungi, Gram-positive and Gram-negative bacteria including the disastrous bacterial pathogens, *V. harveyi* causing a vibriosis and VP_{AHPND} causing an early mortality syndrome (Somboonwiwat et al., 2005; Supungul et al., 2017). The rALF*Pm*3 can bind to LPS and LTA, components of bacterial cell membrane, and induces the membrane permeabilization and cell lysis of *V. harveyi* and VP_{AHPND} (Jaree et al., 2012; Somboonwiwat et al., 2008; Supungul et al., 2017). The anti-WSSV activity of rALF*Pm*3 is evidenced for the rALF*Pm*3 can inhibit WSSV propagation in crayfish hematopoietic cell culture and in shrimp (Tharntada et al., 2009). Recently, the interaction between ALF*Pm*3 and five WSSV structural proteins has been experimentally confirmed (Methatham et al., 2017; Suraprasit et al., 2014). Transmission electron micrographs reveal that the rALF*Pm*3 incubation leads to the instability of envelope and nucleocapsid structures and the breaking up of the WSSV virions (Methatham et al., 2017).

Recently, the potential use of ALF*Pm*3 in shrimp aquaculture disease control has been reported. Administration of dietary rALF*Pm*3 as a potential immunostimulant enhances the transcription level of immune-related genes and increases the shrimp survival following the WSSV challenge (Supungul et al., 2017). Besides the ALF*Pm*3, the ALF*Pm*6 gene has been shown to be up-regulated in *P. monodon* hemocytes in response to the yellow head virus infection (Prapavorarat et al., 2010) and is important to shrimp immune response against *V. harveyi* and WSSV infections (Ponprateep et al., 2012). Our recent study suggests that the LPS-BD of ALF*Pm*6 has bactericidal activity against Gram-negative and Gram-positive bacteria mediated by the bacterial agglutination (unpublished data).

Seven ALF isoforms, FcALF1-6 and ALFFc, are also identified in the Chinese shrimp *F. chinensis*. They have different expression patterns in the tissues of shrimp (Guo et al., 2014; Li et al., 2013; Liu et al., 2005). The recombinant protein ALFFc (group B) strongly inhibits the growth of Gram-positive and Gram-negative bacteria and the propagation of WSSV through the activity of a synthetic peptide of ALFFc LPS-BD (Guo et al., 2014). The rFcALF5 exhibits antibacterial activity and also inhibits the infectivity of WSSV in shrimp. Similar to what observed for rALF*Pm*3, the rFcALF5 and the synthetic peptide corresponding to its LPS-BD have direct interaction with the envelope protein VP24 of WSSV (Yang et al., 2015). Analysis of the antibacterial and antiviral activities of the LPS-BDs of different ALFs shows that the different ALFs have distinct antibacterial and antiviral activities (Li et al., 2013, 2015; Liu et al., 2005). A peptide corresponding to the LPS-BD of FcALF2 possesses strong antibacterial activity against Gram-positive bacteria and the inhibition activity against WSSV. The LPS-BD peptides of four FcALFs, FcALF1 (group C), FcALF2 (group C), FcALF5 and ALFFc, inhibit the WSSV replication in experimental animals. Sequence analysis coupled with experiment data indicates that a conserved lysine residue at specific site on LPS-BD is required for anti-WSSV activity (Li et al., 2015).

3.2.4. Stylicins

A stylicin family is the only family of anionic AMPs identified in shrimp and bivalve. Members of stylicin family are limited as compared to other AMP families. In shrimp, stylicins are identified in *L. stylirostris*, *L vannamei*, *P. monodon* and *M. japonicus* (Rolland et al., 2010). A stylicin has a N-terminal proline-rich region and a C-terminal portion that contains 13 cysteine residues. Only the stylicins from *L. stylirostris* (Ls-Stylicin1) and *M. japonicus* (Mj-sty) have been characterized (Liu et al., 2015a; Rolland et al., 2010). The Mj-sty with a theoretical pI of 4.79 is rather negatively charged compared with the Ls-Stylicin1 with a theoretical pI of 5.0. The Mj-sty has been expressed since early developmental stages from fertilized eggs to post-larvae of 17 days (PL17). In sub-adult shrimp, the Mj-sty gene is mainly transcribed in gills and hemocytes. The Ls-Stylicin1 is produced in both hyaline and granular haemocytes of sub-adult shrimp. The recombinant Ls-Stylicin1 (rLs-Stylicin1) in either monomeric or dimeric form exhibits poor antimicrobial activity against *V. penaeicidae* but has bacteriostatic effect through the interaction with *V. penaeicidae* LPS. Strong activity of Ls-Stylicin1 against the filamentous fungus pathogenic to the shrimp, *Fusarium oxysporum*, has been shown (Rolland et al., 2010). Therefore, the stylicin is considered as an antifungal peptide but its molecular mechanism is still mysterious.

3.2.5. Haemocyanin-derived peptides

Although most of the known shrimp AMPs are gene-encoded cationic peptides, a significant number of cleaved peptides with antimicrobial activity have been reported. The shrimp haemocyanin is a major haemolymph protein consisting of various subunits and functions as an oxygen transporter. Sequence heterogeneity in hemocyanin transcripts has been described (Johnson et al., 2016; Zhao et al., 2016). The hemocyanin subunits can be classified into three distinct immunological classes: Hcα, Hcβ, and Hcγ in decapod crustaceans, only Hcβ, and Hcγ types have been identified in shrimp so far (Johnson et al., 2016). Furthermore, the haemocyanin is considered as multifunctional protein because it exhibits the phenoloxidase, antimicrobial, and bacterial agglutination activities (Decker and Jaenicke, 2004; Sivakamavalli and Vaseeharan, 2015; Zhang et al., 2004). Moreover, it is involved in regulating the ERK1/2 signaling pathway during the Taura syndrome virus (TSV) infection (Havanapan et al., 2009).

The antimicrobial peptides generated by cleavage of haemocyanin C-terminus can be detected in the hemolymph of shrimp such as *L. vannamei* (PvHCt), *P. stylirostris* (PsHCt1 and PsHCt2), *P. monodon, P. japonicus, F. chinensis* (Destoumieux-Garzón et al., 2001; Lei et al., 2008; Qiu et al., 2014; Zhang et al., 2004). They have fungicidal activity, antibacterial activity, and antiviral activity. The well-characterized truncated hemocyanin with antimicrobial activity is the PvHCt. The PvHCt is an anionic peptide corresponding to 23 C-terminal amino acid residues of *L. vannamei* hemocyanin that contains 5 histidine and another 3 anionic residues with the theoretical pI of 6.16. The PvHCt is cleaved within the primary structure of precursor protein and released by proteolysis in response to infection (Destoumieux-Garzón et al., 2001). It inhibits hypha growth and spore germination (Petit et al., 2016). The PvHCt exhibits fungicidal activity by inducing membrane damage on a fungal *F. oxysporum* spores and hyphae in dose-dependent manner. Recently, an 18.4 kDa truncated haemocyanin small subunit identified from *V. parahaemolyticus*-challenged *L. vannamei* has been shown to possess agglutinating activity against the virulent *V. parahaemolyticus* (Wen et al., 2016).

3.3. Melanization

Melanization pathway activated by the prophenoloxidase (proPO) system is a principal innate immune response in shrimp (Amparyup et al., 2013a; Tassanakajon et al., 2013). Upon pathogen invasion, the binding of PRPs to corresponding microbial cell wall components activates the serine proteinase cascade which subsequently activates the final proteinases, called proPO-activating enzymes (PPAEs). The PPAEs, then, cleave the inactive proPOs to active POs which lead to initiation of the melanin formation. Inevitably, the activation of melanization cascade needs to be tightly regulated and locally restricted to prevent damage to the host by controlling the proteinases and inhibiting the proPO system (Amparyup et al., 2013a; Charoensapsri et al., 2014).

Melanization pathway consists of three major processes: the pathogen recognition, the proteolytic cascade and the activation of proPO enzymes (Amparyup et al., 2013a). Currently, several melanization/proPO system-related genes have been identified and functional characterized in shrimp, whose studies contribute to the knowledge of shrimp innate immunity. Here, we review all relevant articles and summarized the important roles of melanization in shrimp.

3.3.1. Pattern recognition proteins

The specificity of the proPO cascade relies on the PRPs, which is the first step in initiating the immune activation of proPO system. Upon microbial invasion, the proPO system uses specific molecules, PRPs, to recognize and bind the conserved structures of microbial cell wall components, such as the β-glucan, LPS, and PGN, leading to subsequent activation of the melanization process (Amparyup et al., 2013a).

In shrimp, the lipopolysaccharide and β-1,3-glucan binding protein (LGBP), which is one of the most important receptor families of the proPO system, is a gene encoded protein molecule that recognizes the conserved microbial patterns of β-glucan from fungi and LPS from Gram-negative bacteria. However, it has been shown that the LGBP does not bind PGN (Amparyup et al., 2012, 2013a). The domain organization of the shrimp LGBPs are composed of a potential polysaccharide-binding, glucanase- and β-glucan-recognition motifs and two putative Arg-Gly-Asp (RGD) cell adhesion sites (Amparyup et al., 2012). Nonetheless, the binding specificity of these domains of LGBP in the proPO activating system is still somewhat elusive and poorly elucidated. Suppressing the *Pm*LGBP in shrimp hemocytes by using RNAi leads to significantly decrease of *Pm*LGBP mRNA and protein levels and also the PO activity suggesting that the *Pm*LGBP functions as a PRP in the shrimp proPO system (Amparyup et al., 2012, 2013a). Moreover, several PRP genes have been cloned and preliminary functional characterized in shrimp including β-glucan-binding proteins (βGBPs and βGBP-HDLs) and C-type lectins (reviewed in Amparyup et al., 2013a). However, no functional characterization has been demonstrated on the role of these PRPs in the proPO activation, even though some C-type lectins and QM proteins can enhance the PO activity or melanization in shrimp (Junkunlo et al., 2012; Udompetcharaporn et al., 2014). Other PRPs of the shrimp proPO system remain to be discovered.

3.3.2. Proteolytic cascade

Activation of proteolytic cascade by the clip domain serine proteinases (clip-SPs) is an important step in the regulation of proPO system in invertebrates. Upon recognition of microbial polysaccharides by specific PRPs, the clip-SPs as inactive zymogens become sequentially activated by cleavage at a specific site located at the N-terminus of the SP domain (Charoensapsri et al., 2009, 2011). After their functions, the active clip-SPs are inactivated by serine proteinase inhibitors (Amparyup et al., 2013a).

To date, more than seven clip-SPs have been identified and characterized in *P. monodon* and *L. vannamei* (Amparyup et al.,

2013a). The RNAi experiments have demonstrated that several clip-SPs including the *Pm*PPAE1 (Charoensapsri et al., 2009), *Pm*PPAE2 (Charoensapsri et al., 2011), *Pm*ClipSP2 (Amparyup et al., 2013b) and *Pm*Snake-like proteinase (Monwan et al., 2017) from *P. monodon* and the *Lv*PPAE1 (Jang et al., 2011) and *Lv*PPAE2 (Pang et al., 2014) from *L. vannamei* play roles in the activation of the proPO pathway, but the substrates of these proteinases have not been identified. Nevertheless, these studies have led to more detailed understanding of the proteinase activation of the proPO cascade in shrimp.

In insects, the initiation proteinase (*Manduca* HP14, *Tenebrio* MSP or *Drosophila* ModSP) of the proPO pathway is autoactivated after the PRP binding complex of microbial polysaccharides have been recognized (Ryu et al., 2010; Wang and Jiang, 2010). The domain organization of the insect initiation proteinases is generally composed of 4–5 domains of low-density lipoprotein receptor domain class A (LDLa) domains and a complement control protein (CCP) domain at its N-terminus and a SP domain at its C-terminus (Takahashi et al., 2015). In shrimp *P. monodon*, a clip-SP, named *Pm*ClipSP2, has been demonstrated to act as a PRP by binding to LPS and β-glucan and also activates the shrimp proPO system. Thus, it is probably an initial proteinase of the proteolytic cascade in the shrimp proPO cascade (Amparyup et al., 2013b). However, the *Pm*ClipSP2 is a clip-SP which does not contain the LDLa or CCP domains but can bind to LPS and β-1,3-glucan and activates the PO activity. In insect, the binding of microbial cell wall components to the PRP complex induces auto-activation of the initiation proteinase in the melanization cascade (Ryu et al., 2010). However, the mechanism of shrimp *Pm*ClipSP2 in the PRP complex formation in the proPO activating system still remains to be elucidated.

More recently, a *Pm*Snake-like proteinase (*Pm*Snake) has been discovered by suppression subtractive hybridization of the cDNA library of proPO dsRNA-treated hemocytes and shown to be homologous to the insect snake proteinase *Ms*HP21 of *Manduca sexta* with 52% similarity (Monwan et al., 2017). However, sequence analysis reveals that the *Pm*Snake is quite relatively distant from other *Pm*ClipSPs from *P. monodon* including the *Pm*PPAE1, *Pm*PPAE2, *Pm*ClipSP1 and *Pm*ClipSP2 (Amparyup et al., 2010, 2013a, 2013b; Charoensapsri et al., 2009, 2011). *In vivo* gene silencing of *Pm*Snake and the affect of recombinant *Pm*Snake protein on *in vitro* PO activity indicate that the *Pm*Snake functions as a clip-SP in the shrimp proPO system (Monwan et al., 2017). In *M. sexta*, the *Ms*HP21, which is a downstream clip-SP of initial proteinase HP14, is found to be involved in the proPO activating cascade (Gorman et al., 2007; Wang and Jiang, 2007). Although the *Pm*Snake exhibits high similarity to the insect *Ms*HP21, the mechanism of proPO activation by which this protein activates the *P. monodon* proPO system remains unknown and needs further investigation.

Only 4 terminal proteinases, PPAEs, have been reported and proposed as the proteinase activators of the shrimp proPO enzymes. Based on amino acid sequence similarity, the shrimp *Pm*PPAE1 and *Lv*PPAE1 show high similarity to the crustacean PPAE (>60%) and the shrimp *Pm*PPAE2 and *Lv*PPAE2 show high similarity to the insect PPAE (>50%). More recently, it was demonstrated *in vitro* that a recombinant *Pm*PPAE2 can cleave both *Pm*proPO1 and *Pm*proPO2 and also activates the PO activity (Sutthangkul et al., 2017).

The clip-domain serine proteinase homologues (clip-SPHs), lacking proteolytic activity and functioning as protein regulators of other clip-SPs in the melanization cascade, have been reported in shrimp (Amparyup et al., 2013a; Jearaphunt et al., 2015; Ma et al., 2014). The role of shrimp clip-SPHs is still largely unexplored, although the insect clip-SPHs may act as cofactors of active PPAEs or clip-SPs. Recently, two clip-SPHs (*Pm*MasSPH1 and *Pm*MasSPH2) have been characterized in shrimp (Jearaphunt et al., 2015). The *Pm*MasSPH1 is a multifunctional immune protein based on its antimicrobial and binding activities against Gram-negative bacteria *Vibrio harveyi* (Amparyup et al., 2013a). Additional studies indicate that the *Pm*MasSPH-1 and 2 play a role in binding to the PGN of Gram-positive bacteria and in activation of the PGN-induced proPO system. Moreover, the *Pm*MasSPH1 also shows a specific interaction with the *Pm*PPAE2, the final proteinase of shrimp proPO cascade. The *Pm*MasSPH1 knockdown suppresses the gene expression of *Pm*PPAE2 and antimicrobial peptides suggesting that this gene may also be involved in the cross-talk regulation of the melanization cascade and antimicrobial peptide synthesis in shrimp (Jearaphunt et al., 2015).

3.3.3. Activation of proPO enzymes

Phenoloxidase (PO) is a type of tyrosinase that is a copper-containing enzyme. The PO is mainly involved in the catalytic oxidation of mono- or *o*-diphenols to the corresponding *o*-quinone. The quinones, which crosslink together to form melanin, may be involved in the production of superoxides and hydroxyl radicals to kill the invading pathogens (Amparyup et al., 2013a; Charoensapsri et al., 2014).

To date, three proPO genes have been reported in shrimp, proPO1, proPO2 (Amparyup et al., 2013a) and proPO3 (or named as proPOβ) (Kuyama et al., 2013; Masuda et al., 2012). Based on the amino acid sequences, the *Pm*proPO1 from *P. monodon* exhibits high similarity to *Pm*proPO2 with approximately 80% similarity and low similarity with approximately 55% similarity to *Mj*proPO3 from *M. japonicus*. The *Pm*proPO1 and *Pm*proPO2 have the characteristic features of proPO members, which are composed of two highly conserved tyrosinase copper-binding motifs with six histidine residues and a thiol ester-like motif (Amparyup et al., 2009, 2013a). The *Mj*proPO3 also contains two putative copper-binding sites, copper A and copper B, but the different characteristics between *Mj*proPO3 and *Pm*proPO1 (or *Pm*proPO2) are observed including a putative signal peptide sequence and a substitution of the highly conserved thiol ester motif (Masuda et al., 2012). In addition, tissue distribution analysis indicates that the proPO1 and proPO2 transcripts are hemocyte-type transcripts (Amparyup et al., 2009) while the proPO3 transcripts is a hepatopancreas-type transcript, which was resemble to those of arthropod hemocyanins (Masuda et al., 2012). However, the primary structure and enzymatic properties suggested that *Mj*proPO3 belongs to the family of crustacean proPO protein (Masuda et al., 2012). Recently, the structure of *Mj*proPO3 has been solved by X-ray crystallography (Masuda et al., 2014), which enables us to better understand the structure-function relationship of this protein family.

The crucial role of melanization in defense against pathogen invasion in shrimp has been demonstrated. It is clearly shown that the two proPO genes (*Pm*proPO1 and *Pm*proPO2) are important for the survival of shrimp upon bacterial (*V. harveyi*), fungal (*Fusarium solani*) and viral (WSSV) infections (Amparyup et al., 2009, 2013a; Charoensapsri et al., 2014; Sutthangkul et al., 2015). However, the important role and the molecular mechanism of *Mj*proPO3 in the immune defense remains to be further elucidated.

3.3.4. Negative regulators of proPO activating system

The melanization reaction unavoidably generates highly toxic molecules, which are involved in pathogen killing but they can also damage the host cells (Amparyup et al., 2013a; Charoensapsri et al., 2014). Thus, the activation mechanism of melanization cascade is needed to be tightly regulated (Amparyup et al., 2013a). To date, several negative regulators of melanization cascade have been reported in shrimp including the melanization inhibition protein (MIP) (Angthong et al., 2010; Noothuan et al., 2017), serine proteinase inhibitors (serpins) (Liu et al., 2014, 2015c, 2016b, 2017;

Somnuk et al., 2012; Wetsaphan et al., 2013), alpha-2-macroglobulin (A2M) (Ponprateep et al., 2017) and pacifastin inhibitor (Sangsuriya et al., 2016).

Based on the reports of the inhibition of proPO activation using recombinant proteins and/or RNAi assays, it is suggested that a MIP (*Pm*MIP) (Noothuan et al., 2017) and two serpins (*Pm*SERPIN3 and *Pm*SERPIN8) from *P. monodon* (Somnuk et al., 2012; Wetsaphan et al., 2013) and four serpins (*Lv*serpin, *Lv*serpin3, *Lv*serpin7 and *Lv*serpin8) (Liu et al., 2014, 2015c, 2016b, 2017) and an A2M (*Lv*A2M) (Ponprateep et al., 2017) from *L. vannamei* function as the negative regulators of shrimp proPO system. In addition, a shrimp pacifastin light chain-like inhibitor (*Pm*Pacifastin-like) from *P. monodon*, identified from a reverse suppression subtractive hybridization cDNA library created from hemocytes of the *Pm*proPO1/2 co-silenced shrimp, has been functional characterized (Sangsuriya et al., 2016). The pacifastin is a class of proteinase inhibitors that act as a negative regulator of the proPO cascade in crayfish *Pacifastacus leniusculus* (Liang et al., 1997). Supression of the *Pm*Pacifastin-like function leads to a strong increase in PO activity in shrimp hemolymph and also down regulation of *Pm*PPAE2 suggesting that the *Pm*Pacifastin-like protein participates in the negative regulation of shrimp proPO cascade (Sangsuriya et al., 2016). Although several shrimp proteinase inhibitors are shown to decrease the PO activity, little is known about their target proteinases and further studies are required.

It is widely known that many molecules produced from the pathogens are involved in the suppression of proPO activation in insects (Beck and Strand, 2007; Lu et al., 2008, 2010). More recently, a viral protein of WSSV has been found to negatively regulate the melanization cascade of host cells (Sutthangkul et al., 2015). Upon infection, the WSSV produces a WSSV453 protein that has the ability to interfere with the shrimp proPO activation through the interaction with *Pm*PPAE2 (Sutthangkul et al., 2015). This report provides novel insights into the molecular mechanism of viral-host interactions in shrimp melanization cascade. From the studies of the shrimp proPO system, the proposed model of the proPO cascade in shrimp *P. monodon* is shown schematically in Fig. 2. Although the identification of proteins or enzymes in shrimp proPO pathway have been determined by molecular biology approaches, for example the RNAi, recombinant protein and biochemical assays, the detailed functions of most proteins and enzymes in shrimp melanization cascade are largely unknown. Thus, it is very likely that additional proteins and enzymes acting in shrimp proPO system remain to be discovered and functionally characterized.

4. Concluding remarks

The Toll and Imd pathways recognize the invading microbes and subsequently relay the infection signals to activate the synthesis of AMPs and other immune effectors to eradicate the pathogens. The shrimp AMPs which are stored in hemocytes, are released upon induction to directly kill the microorganisms and also activate the

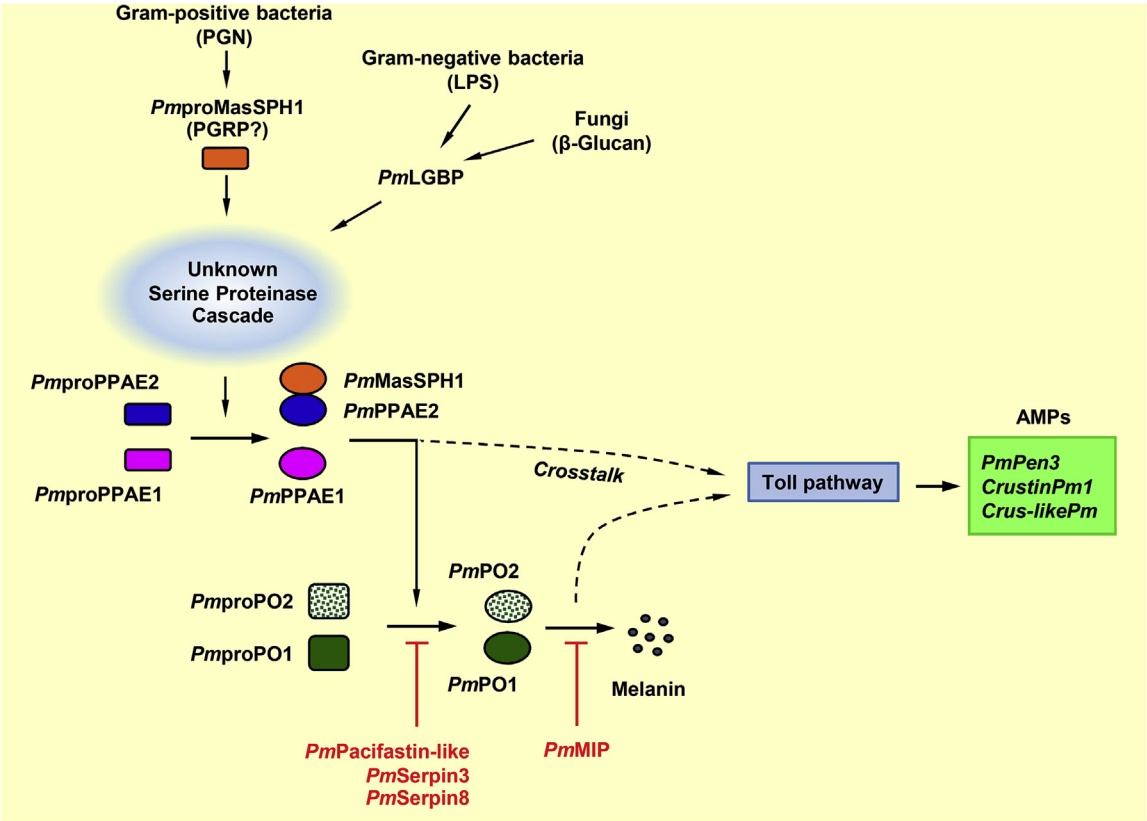


Fig. 2. Activation of the proPO cascade and crosstalk with antimicrobial peptide (AMP) gene synthesis pathway in shrimp *Penaeus monodon*. Upon microbial recognition, certain PRPs, including *Pm*LGBP and *Pm*MasSPH1, bind with the conserved microbial patterns, such as LPS produced by Gram-negative bacteria, PGN produced by Gram-positive bacteria and β-glucan produced by fungi, and trigger the sequential activation of the unknown serine proteinases (SPs), leading to the processing of final clip-domain serine proteinase (clip-SP) designated as proPO-activating enzyme (PPAE). Activated PPAEs, including *Pm*PPAE1 and *Pm*PPAE2, subsequently cleave proPO zymogens, including *Pm*proPO1 and *Pm*proPO2, to generate active POs (*Pm*PO1 and *Pm*PO2), which function as key enzyme in the melanin synthesis for killing of invading microbes. The serine proteinase inhibitors, including *Pm*Pacifastin-like, *Pm*SERPIN3 and *Pm*SERPIN8, and a melanization inhibition protein (*Pm*MIP) are presumed to contribute as the negative regulators of this cascade through inhibiting or interfering with the clip-SP activities. POs and *Pm*MasSPH1 are the proPO pathway components that likely involved in the crosstalk regulation of melanization cascade and antimicrobial peptide (AMP) gene synthesis in shrimp, although the exact roles of these molecules have not yet been fully characterized.

immune responses. Several shrimp AMPs have been characterized for their antimicrobial actions against various strains of bacteria, fungi and viruses. The potential use of ALF*Pm*3 to control AHPND and WSD in shrimp farming has been demonstrated. Despite the report that the deathly virus, WSSV, has an ability to suppress host melanization by interfering with the serine proteinase cascade, the importance of melanization in defense against bacterial, fungal and viral infections have been shown. Many components participate in the shrimp proPO system have been functionally characterized and, perhaps, many more remain to be discovered. The molecular mechanism regulating the activation steps by the proPO components is largely unknow and requires further investigation. Interestingly, the RNAi-mediated gene silencing of the proPO components suggests the PRP crosstalk between the proPO activating system and the AMP synthesis pathways which enables the innate immune system to enhance the magnitude of the immune response.

Acknowledgments

The research on shrimp immunity is supported by Thailand Research Fund to A.T. (TRF Senior Scholar No. RTA5880004), Thailand Research Fund and Thailand National Center for Genetic Engineering and Biotechnology (BIOTEC) to P.A. (Grant No. BRG5880016). Additional support from TRF (Grant No. IRG5780008) to the Department of Biochemistry, Faculty of Science, Chulalongkorn University is acknowledged. We also would like to thank Chulalongkorn University for the support to the Center of Excellence for Molecular Biology and Genomics of Shrimp and a postdoctoral fellowship to S.V. under the Ratchadaphisek Somphot Endowment Fund. Equipment for research is supported by the JST/JICA, Science and Technology Research Partnership for Sustainable Development (SATREPS).

References

Afsal, V.V., Antony, S.P., Philip, R., Bright Singh, I.S., 2016. Molecular characterization of a newly identified subfamily member of penaeidin from two penaeid shrimps, *Fenneropenaeus indicus* and *Metapenaeus monoceros*. Probiotics Antimicrob. Proteins 8, 46–52.

Amparyup, P., Charoensapsri, W., Tassanakajon, A., 2009. Two prophenoloxidases are important for the survival of *Vibrio harveyi* challenged shrimp *Penaeus monodon*. Dev. Comp. Immunol. 33, 247–256.

Amparyup, P., Charoensapsri, W., Tassanakajon, A., 2013a. Prophenoloxidase system and its role in shrimp immune responses against major pathogens. Fish. Shellfish Immunol. 34, 990–1001.

Amparyup, P., Donpudsa, S., Tassanakajon, A., 2008. Shrimp single WAP domain (SWD)-containing protein exhibits proteinase inhibitory and antimicrobial activities. Dev. Comp. Immunol. 32, 1497–1509.

Amparyup, P., Promrungreang, K., Charoensapsri, W., Sutthangkul, J., Tassanakajon, A., 2013b. A serine proteinase *Pm*ClipSP2 contributes to prophenoloxidase system and plays a protective role in shrimp defense by scavenging lipopolysaccharide. Dev. Comp. Immunol. 41, 597–607.

Amparyup, P., Sutthangkul, J., Charoensapsri, W., Tassanakajon, A., 2012. Pattern recognition protein binds to lipopolysaccharide and β-1,3-glucan and activates shrimp prophenoloxidase system. J. Biol. Chem. 287, 10060–10069.

Amparyup, P., Wiriyaukaradecha, K., Charoensapsri, W., Tassanakajon, A., 2010. A clip domain serine proteinase plays a role in antibacterial defense but is not required for prophenoloxidase activation in shrimp. Dev. Comp. Immunol. 34, 168–176.

An, M.Y., Gao, J., Zhao, X.F., Wang, J.X., 2016. A new subfamily of penaeidin with an additional serine-rich region from kuruma shrimp (*Marsupenaeus japonicus*) contributes to antimicrobial and phagocytic activities. Dev. Comp. Immunol. 59, 186–198.

Angthong, P., Watthanasurorot, A., Klinbunga, S., Ruangdej, U., Söderhäll, I., Jiravanichpaisal, P., 2010. Cloning and characterization of a melanization inhibition protein (*Pm*MIP) of the black tiger shrimp, *Penaeus monodon*. Fish. Shellfish Immunol. 29, 464–468.

Arayamethakorn, S., Supungul, P., Tassanakajon, A., Krusong, K., 2017. Characterization of molecular properties and regulatory pathways of Crustin*Pm*1 and Crustin*Pm*7 from the black tiger shrimp *Penaeus monodon*. Dev. Comp. Immunol. 67, 18–29.

Arockiaraj, J., Gnanam, A.J., Muthukrishnan, D., Gudimella, R., Milton, J., Singh, A., Muthupandian, S., Kasi, M., Bhassu, S., 2013. Crustin, a WAP domain containing antimicrobial peptide from freshwater prawn *Macrobrachium rosenbergii*: immune characterization. Fish. Shellfish Immunol. 34, 109–118.

Arts, J.A., Cornelissen, F.H., Cijsouw, T., Hermsen, T., Savelkoul, H.F., Stet, R.J., 2007. Molecular cloning and expression of a Toll receptor in the giant tiger shrimp, *Penaeus monodon*. Fish. Shellfish Immunol. 23, 504–513.

Beck, M.H., Strand, M.R., 2007. A novel polydnavirus protein inhibits the insect prophenoloxidase activation pathway. Proc. Natl. Acad. Sci. U. S. A. 104, 19267–19272.

Charoensapsri, W., Amparyup, P., Hirono, I., Aoki, T., Tassanakajon, A., 2009. Gene silencing of a prophenoloxidase activating enzyme in the shrimp, *Penaeus monodon*, increases susceptibility to *Vibrio harveyi* infection. Dev. Comp. Immunol. 33, 811–820.

Charoensapsri, W., Amparyup, P., Hirono, I., Aoki, T., Tassanakajon, A., 2011. *Pm*PPAE2, a new class of crustacean prophenoloxidase (proPO)–activating enzyme and its role in PO activation. Dev. Comp. Immunol. 35, 115–124.

Charoensapsri, W., Amparyup, P., Suriyachan, C., Tassanakajon, A., 2014. Melanization reaction products of shrimp display antimicrobial properties against their major bacterial and fungal pathogens. Dev. Comp. Immunol. 47, 150–159.

Chen, D., He, N., Xu, X., 2008. *Mj*-DWD, a double WAP domain-containing protein with antiviral relevance in *Marsupenaeus japonicus*. Fish. Shellfish Immunol. 25, 775–781.

Chen, Y., Li, X., He, J., 2014. Recent advances in researches on shrimp immune pathway involved in white spot syndrome virus genes regulation. J. Aquac. Res. Dev. 5, 1000228.

Chen, Y.Y., Chen, J.C., Kuo, Y.H., Lin, Y.C., Chang, Y.H., Gong, H.Y., Huang, C.L., 2016. Lipopolysaccharide and β-1,3-glucan-binding protein (LGBP) bind to seaweed polysaccharides and activate the prophenoloxidase system in white shrimp *Litopenaeus vannamei*. Dev. Comp. Immunol. 55, 144–151.

Cuthbertson, B.J., Deterding, L.J., Williams, J.G., Tomer, K.B., Etienne, K., Blackshear, P.J., Büllesbach, E.E., Gross, P.S., 2008. Diversity in penaeidin antimicrobial peptide form and function. Dev. Comp. Immunol. 32, 167–181.

Dalmo, R.A., Bøgwald, J., 2008. Beta-glucans as conductors of immune symphonies. Fish. Shellfish Immunol. 25, 384–396.

De Gregorio, E., Han, S.J., Lee, W.J., Baek, M.J., Osaki, T., Kawabata, S., Lee, B.L., Iwanaga, S., Lemaitre, B., Brey, P.T., 2002. An immune-responsive Serpin regulates the melanization cascade in *Drosophila*. Dev. Cell. 3, 581–592.

Decker, H., Jaenicke, E., 2004. Recent findings on phenoloxidase activity and antimicrobial activity of hemocyanins. Dev. Comp. Immunol. 28, 673–687.

Deepika, A., Sreedharan, K., Paria, A., Makesh, M., Rajendran, K.V., 2014. Toll-pathway in tiger shrimp (*Penaeus monodon*) responds to white spot syndrome virus infection: evidence through molecular characterisation and expression profiles of MyD88, TRAF6 and TLR genes. Fish. Shellfish Immunol. 41, 441–454.

Destoumieux, D., Bulet, P., Loew, D., Van Dorsselaer, A., Rodriguez, J., Bachère, E., 1997. Penaeidins, a new family of antimicrobial peptides isolated from the shrimp *Penaeus vannamei* (Decapoda). J. Biol. Chem. 272, 28398–28406.

Destoumieux, D., Munoz, M., Bulet, P., Bachère, E., 2000. Penaeidins, a family of antimicrobial peptides from penaeid shrimp (Crustacea, Decapoda). Cell Mol. Life Sci. 57, 1260–12671.

Destoumieux-Garzón, D., Saulnier, D., Garnier, J., Jouffrey, C., Bulet, P., Bachère, E., 2001. Crustacean immunity. Antifungal peptides are generated from the C terminus of shrimp hemocyanin in response to microbial challenge. J. Biol. Chem. 276, 47070–47077.

Dionne, M., 2014. Immune-metabolic interaction in *Drosophila*. Fly 8, 75–79.

Donpudsa, S., Visetnan, S., Supungul, P., Tang, S., Tassanakajon, A., Rimphanitchayakit, V., 2014. Type I and type II crustins from *Penaeus monodon*, genetic variation and antimicrobial activity of the most abundant crustin*Pm*4. Dev. Comp. Immunol. 47, 95–103.

Du, Z.Q., Ren, Q., Zhao, X.F., Wang, J.X., 2009. A double WAP domain (DWD)-containing protein with proteinase inhibitory activity in Chinese white shrimp, *Fenneropenaeus chinensis*. Comp. Biochem. Physiol. B Biochem. Mol. Biol. 154, 203–210.

Dushay, M.S., Asling, B., Hultmark, D., 1996. Origins of immunity: relish, a compound Rel-like gene in the antibacterial defense of *Drosophila*. Proc. Natl. Acad. Sci. U. S. A. 93, 10343–10347.

Feng, N., Wang, D., Wen, R., Li, F., 2014. Functional analysis on immune deficiency (IMD) homolog gene in Chinese shrimp *Fenneropenaeus chinensis*. Mol. Biol. Rep. 41, 1437–1444.

Flegel, T.W., 2012. Historic emergence, impact and current status of shrimp pathogens in Asia. J. Invert. Pathol. 110, 166–173.

Flegel, T.W., Sritunyalucksana, K., 2011. Shrimp molecular responses to viral pathogens. Mar. Biotechnol. 13, 587–607.

Goncalves, P., Vernal, J., Rosa, R.D., Yepiz-Plascencia, G., de Souza, C.R., Barracco, M.A., Perazzolo, L.M., 2012. Evidence for a novel biological role for the multifunctional β-1,3-glucan binding protein in shrimp. Mol. Immunol. 51, 363–367.

Gorman, M.J., Wang, Y., Jiang, H., Kanost, M.R., 2007. *Manduca sexta* hemolymph proteinase 21 activates prophenoloxidase-activating proteinase 3 in an insect innate immune response proteinase cascade. J. Biol. Chem. 282, 11742–11749.

Gueguen, Y., Garnier, J., Robert, L., Lefranc, M.P., Mougenot, I., de Lorgeril, J., Janech, M., Gross, P.S., Warr, G.W., Cuthbertson, B., Barracco, M.A., Bulet, P., Aumelas, A., Yang, Y., Bo, D., Xiang, J., Tassanakajon, A., Piquemal, D., Bachère, E., 2006. PenBase, the shrimp antimicrobial peptide penaeidin database: sequence-based classification and recommended nomenclature. Dev. Comp. Immunol. 30, 283–288.

Guo, S., Li, S., Li, F., Zhang, X., Xiang, J., 2014. Modification of a synthetic LPS-binding

domain of anti-lipopolysaccharide factor from shrimp reveals strong structure-activity relationship in their antimicrobial characteristics. Dev. Comp. Immunol. 45, 227–232.
Havanapan, P.O., Kanlaya, R., Bourchookarn, A., Krittanai, C., Thongboonkerd, V., 2009. C-terminal hemocyanin from hemocytes of *Penaeus vannamei* interacts with ERK1/2 and undergoes serine phosphorylation. J. Proteome Res. 8, 2476–2483.
Havanapan, P.O., Taengchaiyaphum, S., Ketterman, A.J., Krittanai, C., 2016. Yellow head virus infection in black tiger shrimp reveals specific interaction with granule-containing hemocytes and crustin*Pm*1 as a responsive protein. Dev. Comp. Immunol. 54, 126–136.
Hetru, C., Hoffmann, J.A., 2009. NF-κB in the immune response of Drosophila. Cold Spring Harb. Perspect. Biol. 1, a000232.
Hoffmann, J.A., 2003. The immune response of *Drosophila*. Nature 426, 33–38.
Hou, F., He, S., Liu, Y., Zhu, X., Sun, C., Liu, X., 2014. RNAi knock-down of shrimp *Litopenaeus vannamei* Toll gene and immune deficiency gene reveals their difference in regulating antimicrobial peptides transcription. Dev. Comp. Immunol. 44, 255–260.
Huang, X.D., Yin, Z.X., Jia, X.T., Liang, J.P., Ai, H.S., Yang, L.S., Liu, X., Wang, P.H., Li, S.D., Weng, S.P., Yu, X.Q., He, J.G., 2010. Identification and functional study of a shrimp Dorsal homologue. Dev. Comp. Immunol. 34, 107–113.
Huang, X.D., Yin, Z.X., Liao, J.X., Wang, P.H., Yang, L.S., Ai, H.S., Gu, Z.H., Jia, X.T., Weng, S.P., Yu, X.Q., He, J.G., 2009. Identification and functional study of a shrimp Relish homologue. Fish. Shellfish Immunol. 27, 230–238.
Huang, Y., Chen, Y.H., Wang, Z., Wang, W., Ren, Q., 2014. Novel myeloid differentiation factor 88, *Es*MyD88, exhibits *Es*Tube-binding activity in Chinese mitten crab *Eriocheir sinensis*. Dev. Comp. Immunol. 47, 298–308.
Janeway Jr., C.A., 1989. Approaching the asymptote? Evolution and revolution in immunology. Cold Spring Harbor Symp. Quant. Biol. 54, 1–13.
Jang, I.K., Pang, Z., Yu, J., Kim, S.K., Seo, H.C., Cho, Y.R., 2011. Selectively enhanced expression of prophenoloxidase activating enzyme 1 (PPAE1) at a bacteria clearance site in the white shrimp, *Litopenaeus vannamei*. BMC Immunol. 12, 70.
Jaree, P., Tassanakajon, A., Somboonwiwat, K., 2012. Effect of the anti-lipopolysaccharide factor isoform 3 (ALF*Pm*3) from *Penaeus monodon* on *Vibrio harveyi* cells. Dev. Comp. Immunol. 38, 554–560.
Jearaphunt, M., Amparyup, P., Sangsuriya, P., Charoensapsri, W., Senapin, S., Tassanakajon, A., 2015. Shrimp serine proteinase homologues *Pm*MasSPH-1 and -2 play a role in the activation of the prophenoloxidase system. PLoS One 24, e0121073.
Jiang, H.S., Jia, W.M., Zhao, X.F., Wang, J.X., 2015a. Four crustins involved in antibacterial responses in *Marsupenaeus japonicus*. Fish. Shellfish Immunol. 43, 387–395.
Jiang, H.S., Sun, C., Wang, T., Zhao, X.F., Wang, J.X., 2013. A single whey acidic protein domain containing protein (SWD) inhibits bacteria invasion and dissemination in shrimp *Marsupenaeus japonicus*. Fish. Shellfish Immunol. 35, 310–318.
Jiang, H.S., Zhang, Q., Zhao, Y.R., Jia, W.M., Zhao, X.F., Wang, J.X., 2015b. A new group of anti-lipopolysaccharide factors from *Marsupenaeus japonicus* functions in antibacterial response. Dev. Comp. Immunol. 48, 33–42.
Johansson, M.W., Keyser, P., Sritunyalucksana, K., Söderhäll, K., 2000. Crustacean haemocytes and haematopoiesis. Aquaculture 191, 45–52.
Johnson, J.G., Burnett, L.E., Burnett, K.G., 2016. Uncovering hemocyanin subunit heterogeneity in penaeid shrimp using RNA-seq. Integr. Comp. Biol. 56, 1080–1091.
Junkunlo, K., Prachumwat, A., Tangprasittipap, A., Senapin, S., Bavornphinyo, S., Flegel, T.W., 2012. A novel lectin domain-containing protein (*Lv*CTLD) associated with response of the whiteleg shrimp *Penaeus (Litopenaeus) vannamei* to yellow head virus (YHV). Dev. Comp. Immunol. 37, 334–341.
Kang, C.J., Xue, J.F., Liu, N., Zhao, X.F., Wang, J.X., 2007. Characterization and expression of a new subfamily member of penaeidin antimicrobial peptides (penaeidin 5) from *Fenneropenaeus chinensis*. Mol. Immunol. 44, 1535–1543.
Kim, C.H., Paik, D., Rus, F., Silverman, N., 2014. The caspase-8 homolog Dredd cleaves Imd and Relish but is not inhibited by p35. J. Biol. Chem. 289, 20092–20101.
Kim, M., Jeon, J.M., Oh, C.W., Kim, Y.M., Lee, D.S., Kang, C.K., Kim, H.W., 2012. Molecular characterization of three crustin genes in the morotoge shrimp, *Pandalopsis japonica*. Comp. Biochem. Physiol. B Biochem. Mol. Biol. 163, 161–171.
Krusong, K., Poolpipat, P., Supungul, P., Tassanakajon, A., 2012. A comparative study of antimicrobial properties of crustin*Pm*1 and crustin*Pm*7 from the black tiger shrimp *Penaeus monodon*. Dev. Comp. Immunol. 36, 208–215.
Kuyama, H., Masuda, T., Nakajima, C., Momoji, K., Sugawara, T., Nishimura, O., Hirata, T., 2013. Mass spectrometry based N- and C-terminal sequence determination of a hepatopancreas-type prophenoloxidase from the kuruma prawn, *Marsupenaeus japonicus*. Anal. Bioanal. Chem. 405, 2333–2340.
Lai, X., Kong, J., Wang, Q., Wang, W., Meng, X., 2011. Cloning and characterization of a β-1,3-glucan-binding protein from shrimp *Fenneropenaeus chinensis*. Mol. Biol. Rep. 38, 4527–4535.
Lan, J.F., Zhou, J., Zhang, X.W., Wang, Z.H., Zhao, X.F., Ren, Q., Wang, J.X., 2013. Characterization of an immune deficiency homolog (IMD) in shrimp (*Fenneropenaeus chinensis*) and crayfish (*Procambarus clarkii*). Dev. Comp. Immunol. 41, 608–617.
Leclerc, V., Reichhart, J.M., 2004. The immune response of *Drosophila melanogaster*. Immunol. Rev. 198, 59–71.
Lei, K., Li, F., Zhang, M., Yang, H., Luo, T., Xu, X., 2008. Difference between hemocyanin subunits from shrimp *Penaeus japonicus* in anti-WSSV defense. Dev. Comp. Immunol. 32, 808–813.
Li, C., Chai, J., Li, H., Zuo, H., Wang, S., Qiu, W., Weng, S., He, J., Xu, X., 2014b. Pellino protein from pacific white shrimp *Litopenaeus vannamei* positively regulates NF-κB activation. Dev. Comp. Immunol. 44, 341–350.
Li, C., Chen, Y., Weng, S., Lid, S., Zuo, H., Yu, X., Li, H., He, J., Xu, X., 2014a. Presence of Tube isoforms in *Litopenaeus vannamei* suggests various regulatory patterns of signal transduction in invertebrate NF-κB pathway. Dev. Comp. Immunol. 42, 174–185.
Li, C., Chen, Y.X., Zhang, S., Lü, L., Chen, Y.H., Chai, J., Weng, S., Chen, Y.G., He, J., Xu, X., 2012. Identification, characterization, and function analysis of the Cactus gene from *Litopenaeus vannamei*. PLoS ONE 7, e49711.
Li, C.Y., Song, Y.L., 2010. Proline-rich domain of penaeidin molecule exhibits autocrine feature by attracting penaeidin-positive granulocytes toward the wound-induced inflammatory site. Fish. Shellfish Immunol. 29, 1044–1052.
Li, F., Wang, D., Li, S., Yan, H., Zhang, J., Wang, B., Zhang, J., Xiang, J., 2010. A Dorsal homolog (*Fc*Dorsal) in the Chinese shrimp *Fenneropenaeus chinensis* is responsive to both bacteria and WSSV challenge. Dev. Comp. Immunol. 34, 874–883.
Li, F., Xiang, J., 2013a. Recent advances in researches on the innate immunity of shrimp in China. Dev. Comp. Immunol. 39, 11–26.
Li, F., Xiang, J., 2013b. Signaling pathways regulating innate immune responses in shrimp. Fish. Shellfish Immunol. 34, 973–980.
Li, F., Yan, H., Wang, D., Priya, T.A., Li, S., Wang, B., Zhang, J., Xiang, J., 2009. Identification of a novel relish homolog in Chinese shrimp *Fenneropenaeus chinensis* and its function in regulating the transcription of antimicrobial peptides. Dev. Comp. Immunol. 33, 1093–1101.
Li, S., Guo, S., Li, F., Xiang, J., 2015. Functional diversity of anti-lipopolysaccharide factor isoforms in shrimp and their characters related to antiviral activity. Mar. Drugs 13, 2602–2616.
Li, S.H., Zhang, X.J., Sun, Z., Li, F.H., Xiang, J.H., 2013. Transcriptome analysis on Chinese shrimp *Fenneropenaeus chinensis* during WSSV acute infection. Plos One 8, e58627.
Liang, Z., Sottrup-Jensen, L., Aspán, A., Hall, M., Söderhäll, K., 1997. Pacifastin, a novel 155-kDa heterodimeric proteinase inhibitor containing a unique transferring chain. Proc. Natl. Acad. Sci. U. S. A. 94, 6682–6687.
Liu, F., Li, F., Dong, B., Wang, X., Xiang, J., 2009. Molecular cloning and characterisation of a pattern recognition protein, lipopolysaccharide and beta-1,3-glucan binding protein (LGBP) from Chinese shrimp *Fenneropenaeus chinensis*. Mol. Biol. Rep. 36, 471–477.
Liu, F.S., Liu, Y.C., Li, F.H., Dong, B., Xiang, J.H., 2005. Molecular cloning and expression profile of putative antilipopolysaccharide factor in Chinese shrimp (*Fenneropenaeus chinensis*). Mar. Biotechnol. 7, 600–608.
Liu, H.T., Wang, J., Mao, Y., Liu, M., Niu, S.F., Qiao, Y., Su, Y.Q., Wang, C.Z., Zheng, Z.P., 2015a. Identification and expression analysis of a novel stylicin antimicrobial peptide from kuruma shrimp (*Marsupenaeus japonicus*). Fish. Shellfish Immunol. 47, 817–823.
Liu, N., Lan, J.F., Sun, J.J., Jia, W.M., Zhao, X.F., Wang, J.X., 2015b. A novel crustin from *Marsupenaeus japonicus* promotes hemocyte phagocytosis. Dev. Comp. Immunol. 49, 313–322.
Liu, Y., Hou, F., He, S., Qian, Z., Wang, X., Mao, A., Sun, C., Liu, X., 2014. Identification, characterization and functional analysis of a serine protease inhibitor (*Lv*serpin) from the Pacific white shrimp, *Litopenaeus vannamei*. Dev. Comp. Immunol. 43, 35–46.
Liu, Y., Hou, F., Wang, X., Liu, X., 2015c. Recombinant expression and characterization of a serine protease inhibitor (*Lv*serpin7) from the Pacific white shrimp, *Litopenaeus vannamei*. Fish. Shellfish Immunol. 42, 256–263.
Liu, Y., Liu, T., Hou, F., Wang, X., Liu, X., 2016b. *Lv*serpin3 is involved in shrimp innate immunity via the inhibition of bacterial proteases and proteases involved in prophenoloxidase system. Fish. Shellfish Immunol. 48, 128–135.
Liu, Y., Song, L., Sun, Y., Liu, T., Hou, F., Liu, X., 2016a. Comparison of immune response in Pacific white shrimp, *Litopenaeus vannamei*, after knock down of Toll and IMD gene in vivo. Dev. Comp. Immunol. 60, 41–52.
Liu, Y., Sun, Y., Wang, Q., Hou, F., Liu, X., 2017. Identification and functional characterizations of serpin8, a potential prophenoloxidase-activating protease inhibitor in Pacific white shrimp, *Litopenaeus vannamei*. Fish. Shellfish Immunol. 60, 492–501.
Lo, C.F., Aoki, T., Bonami, J.R., Flegel, T.W., Leu, J.H., Lightner, D.V., Stentiford, G., Söderhäll, K., Walker, P.J., Wang, H.C., Xun, X., Yang, F., Vlak, J.M., 2012. Nimaviridae. In: King, A.M.Q., Adams, M.J., Carstens, E.B., Lefkowitz, E.J. (Eds.), Virus Taxonomy: Ninth Report of the International Committee on Taxonomy of Viruses. Elsevier, New York, pp. 229–234.
Lu, Z., Beck, M.H., Strand, M.R., 2010. Egf1.5 is a second phenoloxidase cascade inhibitor encoded by *Microplitis demolitor* bracovirus. Insect Biochem. Mol. Biol. 40, 497–505.
Lu, Z., Beck, M.H., Wang, Y., Jiang, H., Strand, M.R., 2008. The viral protein Egf1.0 is a dual activity inhibitor of prophenoloxidase activating proteinases 1 and 3 from *Manduca sexta*. J. Biol. Chem. 283, 21325–21333.
Ma, T.H., Benzie, J.A., He, J.G., Sun, C.B., Chan, S.F., 2014. *Pm*PPAF is a prophenoloxidase activating factor involved in innate immunity response of the shrimp *Penaeus monodon*. Dev. Comp. Immunol. 44, 163–172.
Masuda, T., Momoji, K., Hirata, T., Mikami, B., 2014. The crystal structure of a crustacean prophenoloxidase provides a clue to understanding the functionality of the type 3 copper proteins. FEBS J. 281, 2659–2673.
Masuda, T., Otomo, R., Kuyama, H., Momoji, K., Tonomoto, M., Sakai, S., Nishimura, O., Sugawara, T., Hirata, T., 2012. A novel type of prophenoloxidase from the kuruma prawn *Marsupenaeus japonicus* contributes to the

melanization of plasma in crustaceans. Fish. Shellfish Immunol. 32, 61–68.
Mekata, T., Kono, T., Yoshida, T., Sakai, M., Itami, T., 2008. Identification of cDNA encoding Toll receptor, *Mj*Toll gene from kuruma shrimp, *Marsupenaeus japonicus*. Fish. Shellfish Immunol. 24, 122–133.
Methatham, T., Boonchuen, P., Jaree, P., Tassanakajon, A., Somboonwiwat, K., 2017. Antiviral action of the antimicrobial peptide ALF*Pm*3 from *Penaeus monodon* against white spot syndrome virus. Dev. Comp. Immunol. 69, 23–32.
Monwan, W., Amparyup, P., Tassanakajon, A., 2017. A snake-like serine proteinase (*Pm*Snake) activates prophenoloxidase-activating system in black tiger shrimp *Penaeus monodon*. Dev. Comp. Immunol. 67, 229–238.
Naitza, S., Ligoxygakis, P., 2004. Antimicrobial defences in *Drosophila*: the story so far. Mol. Immunol. 40, 887–896.
Noothuan, N., Amparyup, P., Tassanakajon, A., 2017. Melanization inhibition protein of *Penaeus monodon* acts as a negative regulator of the prophenoloxidase-activating system. Dev. Comp. Immunol. 72, 97–102.
Pang, Z., Kim, S.K., Yu, J., Jang, I.K., 2014. Distinct regulation patterns of the two prophenoloxidase activating enzymes corresponding to bacteria challenge and their compensatory over expression feature in white shrimp (*Litopenaeus vannamei*). Fish. Shellfish Immunol. 39, 158–167.
Petit, V.W., Rolland, J.L., Blond, A., Cazevieille, C., Djediat, C., Peduzzi, J., Goulard, C., Bachère, E., Dupont, J., Destoumieux-Garzón, D., Rebuffat, S., 2016. A hemocyanin-derived antimicrobial peptide from the penaeid shrimp adopts an alpha-helical structure that specifically permeabilizes fungal membranes. Biochim. Biophys. Acta 1860, 557–568.
Ponprateep, S., Somboonwiwat, K., Tassanakajon, A., 2009. Recombinant anti-lipopolysaccharide factor isoform 3 and the prevention of vibriosis in the black tiger shrimp, *Penaeus monodon*. Aquaculture 289, 219–224.
Ponprateep, S., Tharntada, S., Somboonwiwat, K., Tassanakajon, 2012. Gene silencing reveals a crucial role for anti-lipopolysaccharide factors from *Penaeus monodon* in the protection against microbial infections. Fish. Shellfish Immunol. 32, 29–34.
Ponprateep, S., Vatanavicharn, T., Lo, C.F., Tassanakajon, A., Rimphanitchayakit, V., 2017. Alpha-2-macroglobulin is a modulator of prophenoloxidase system in pacific white shrimp *Litopenaeus vannamai*. Fish. Shellfish Immunol. 62, 68–74.
Prapavorarat, A., Pongsomboon, S., Tassanakajon, A., 2010. Identification of genes expressed in response to yellow head virus infection in the black tiger shrimp, *Penaeus monodon*, by suppression subtractive hybridization. Dev. Comp. Immunol. 34, 611–617.
Qiu, C., Sun, J., Liu, M., Wang, B., Jiang, K., Sun, S., Meng, X., Luo, Z., Wang, L., 2014. Molecular cloning of hemocyanin cDNA from *Fenneropenaeus chinensis* and antimicrobial analysis of two C-terminal fragments. Mar. Biotechnol. 16, 46–53 (NY).
Rolland, J.L., Abdelouahab, M., Dupont, J., Lefevre, F., Bachère, E., Romestand, B., 2010. Stylicins, a new family of antimicrobial peptides from the Pacific blue shrimp *Litopenaeus stylirostris*. Mol. Immunol. 47, 1269–1277.
Rosa, R.D., Vergnes, A., de Lorgeril, J., Goncalves, P., Perazzolo, L.M., Sauné, L., Romestand, B., Fievet, J., Gueguen, Y., Bachère, E., Destoumieux-Garzón, D., 2013. Functional divergence in shrimp anti-lipopolysaccharide factors (ALFs): from recognition of cell wall components to antimicrobial activity. PLoS One 8, e67937.
Roux, M.M., Pain, A., Klimpel, K.R., Dhar, A.K., 2002. The lipopolysaccharide and beta-1,3-glucan binding protein gene is upregulated in white spot virus-infected shrimp (*Penaeus stylirostris*). J. Virol. 76, 7140–7149.
Ryu, K.H., Park, J.W., Kurokawa, K., Matsushita, M., Lee, B.L., 2010. The molecular activation and regulation mechanisms of proteolytic Toll signaling cascade in insect innate immunity. Invert. Surviv. J. 7, 181–191.
Sangsuriya, P., Charoensapsri, W., Chomwong, S., Senapin, S., Tassanakajon, A., Amparyup, P., 2016. A shrimp pacifastin light chain-like inhibitor: molecular identification and role in the control of the prophenoloxidase system. Dev. Comp. Immunol. 54, 32–45.
Shaukat, Z., Liu, D., Gregory, S., 2015. Sterile inflammation in *Drosophila*. Mediat. Inflamm. 2015, 369286.
Shi, X.Z., Zhang, R.R., Jia, Y.P., Zhao, X.F., Yu, X.Q., Wang, J.X., 2009. Identification and molecular characterization of a Spätzle-like protein from Chinese shrimp (*Fenneropenaeus chinensis*). Fish. Shellfish Immunol. 27, 610–617.
Shi, Y.R., Jin, M., Ma, F.T., Huang, Y., Huang, X., Feng, J.L., Zhao, L.L., Chen, Y.H., Ren, Q., 2015. Involvement of Relish gene from *Macrobrachium rosenbergii* in the expression of anti-microbial peptides. Dev. Comp. Immunol. 52, 236–244.
Sivakamavalli, J., Vaseeharan, B., 2015. Enzymatic elucidation of haemocyanin from kuruma shrimp *Marsupenaeus japonicus* and its molecular recognition mechanism towards pathogens. J. Biomol. Struct. Dyn. 33, 1302–1314.
Smith, V.J., Fernandes, J.M., Kemp, G.D., Hauton, C., 2008. Crustins: enigmatic WAP domain-containing antibacterial proteins from crustaceans. Dev. Comp. Immunol. 32, 758–772.
Somboonwiwat, K., Bachère, E., Rimphanitchayakit, V., Tassanakajon, A., 2008. Localization of anti-lipopolysaccharide factor (ALF*Pm*3) in tissues of the black tiger shrimp, *Penaeus monodon*, and characterization of its binding properties. Dev. Comp. Immunol. 32, 1170–1176.
Somboonwiwat, K., Marcos, M., Tassanakajon, A., Klinbunga, S., Aumelas, A., Romestand, B., Gueguen, Y., Boze, H., Moulin, G., Bachère, E., 2005. Recombinant expression and anti-microbial activity of anti-lipopolysaccharide factor (ALF) from the black tiger shrimp *Penaeus monodon*. Dev. Comp. Immunol. 29, 841–851.
Somnuk, S., Tassanakajon, A., Rimphanitchayakit, V., 2012. Gene expression and characterization of a serine proteinase inhibitor *Pm*SERPIN8 from the black tiger shrimp *Penaeus monodon*. Fish. Shellfish Immunol. 33, 332–341.
Srisuk, C., Longyant, S., Senapin, S., Sithigorngul, P., Chaivisuthangkura, P., 2014. Molecular cloning and characterization of a Toll receptor gene from *Macrobrachium rosenbergii*. Fish. Shellfish Immunol. 36, 552–562.
Sun, J.J., Lan, J.F., Shi, X.Z., Yang, M.C., Niu, G.J., Ding, D., Zhao, X.F., Yu, X.Q., Wang, J.X., 2016. β-Arrestins negatively regulate the Toll pathway in shrimp by preventing dorsal translocation and inhibiting dorsal transcriptional activity. J. Biol. Chem. 291, 7488–7504.
Supungul, P., Jaree, P., Somboonwiwat, K., Junprung, W., Proespraiwong, P., Mavichak, R., Tassanakajon, A., 2017. A potential application of shrimp anti-lipopolysaccharide factor in disease control in aquaculture. Aquacult. Res. 48, 809–821.
Suraprasit, S., Methatham, T., Jaree, P., Phiwsaiya, K., Senapin, S., Hirono, I., Lo, C.F., Tassanakajon, A., Somboonwiwat, K., 2014. Anti-lipopolysaccharide factor isoform 3 from *Penaeus monodon* (ALF*Pm*3) exhibits antiviral activity by interacting with WSSV structural proteins. Antivir. Res. 110, 142–150.
Suthianthong, P., Pulsook, N., Supungul, P., Tassanakajon, A., Rimphanitchayakit, V., 2011. A double WAP domain-containing protein *Pm*DWD from the black tiger shrimp *Penaeus monodon* is involved in the controlling of proteinase activities in lymphoid organ. Fish. Shellfish Immunol. 30, 783–790.
Sutthangkul, J., Amparyup, P., Charoensapsri, W., Senapin, S., Phiwsaiya, K., Tassanakajon, A., 2015. Suppression of shrimp melanization during white spot syndrome virus infection. J. Biol. Chem. 290, 6470–6481.
Sutthangkul, J., Amparyup, P., Eum, J.H., Strand, M.R., Tassanakajon, A., 2017. Anti-melanization mechanism of the white spot syndrome viral protein, WSSV453, via interaction with shrimp proPO-activating enzyme, PmproPPAE2. J. Gen. Virol. http://dx.doi.org/10.1099/jgv.0.000729 ([Epub ahead of print]).
Takahashi, D., Garcia, B.L., Kanost, M.R., 2015. Initiating protease with modular domains interacts with β-glucan recognition protein to trigger innate immune response in insects. Proc. Natl. Acad. Sci. U. S. A. 112, 13856–13861.
Tangprasittipap, A., Srisala, J., Chouwdee, S., Somboon, M., Chuchird, N., Limsuwan, C., Srisuvan, T., Flegel, T.W., Sritunyalucksana, K., 2013. The microsporidian *Enterocytozoon hepatopenaei* is not the cause of white feces syndrome in whiteleg shrimp *Penaeus (Litopenaeus) vannamei*. BMC Vet. Res. 9, 139.
Tanji, T., Ip, Y.T., 2005. Regulators of the Toll and Imd pathways in the *Drosophila* innate immune response. Trends Immunol. 26, 193–198.
Tassanakajon, A., Somboonwiwat, K., Amparyup, P., 2015. Sequence diversity and evolution of antimicrobial peptides in invertebrates. Dev. Comp. Immunol. 48, 324–341.
Tassanakajon, A., Somboonwiwat, K., Supungul, P., Tang, S., 2013. Discovery of immune molecules and their crucial functions in shrimp immunity. Fish. Shellfish Immunol. 34, 954–967.
Tharntada, S., Ponprateep, S., Somboonwiwat, K., Liu, H., Söderhäll, I., Söderhäll, K., Tassanakajon, A., 2009. Role of anti-lipopolysaccharide factor from the black tiger shrimp, *Penaeus monodon*, in protection from white spot syndrome virus infection. J. Gen. Virol. 90, 1491–1498.
Thitamadee, S., Prachumwat, A., Srisala, J., Jaroenlak, P., Salachan, P.V., Sritunyalucksana, K., Flegel, T.W., Itsathitphaisarn, O., 2016. Review of current disease threats for cultivated penaeid shrimp in Asia. Aquaculture 452, 69–87.
Tourtip, S., Wongtripop, S., Stentiford, G.D., Bateman, K.S., Sriurairatana, S., Chavadej, J., Sritunyalucksana, K., Withyachumnarnkul, B., 2009. *Enterocytozoon hepatopenaei* sp. nov. (Microsporida: enterocytozoonidae), a parasite of the black tiger shrimp *Penaeus monodon* (Decapoda: Penaeidae): fine structure and phylogenetic relationships. J. Invert. Pathol. 102, 21–29.
Towb, P., Bergmann, A., Wasserman, S.A., 2001. The protein kinase Pelle mediates feedback regulation in the *Drosophila* Toll signaling pathway. Development 128, 4729–4736.
Tran, L., Nunan, L., Redman, R.M., Mohney, L.L., Pantoja, C.R., Fitzsimmons, K., Lightner, D.V., 2013. Determination of the infectious nature of the agent of acute hepatopancreatic necrosis syndrome affecting penaeid shrimp. Dis. Aquat. Org. 105, 45–55.
Tsing, A., Arcier, J.M., Brehélin, M., 1989. Hemocytes of penaeid and palaemonid shrimps: morphology, cytochemistry, and hemograms. J. Invert. Pathol. 53, 64–77.
Udompetcharaporn, A., Junkunlo, K., Senapin, S., Roytrakul, S., Flegel, T.W., Sritunyalucksana, K., 2014. Identification and characterization of a QM protein as a possible peptidoglycan recognition protein (PGRP) from the giant tiger shrimp *Penaeus monodon*. Dev. Comp. Immunol. 46, 146–154.
Valenzuela-Muñoz, V., Gallardo-Escárate, C., 2014. TLR and IMD signaling pathways from Caligus rogercresseyi (Crustacea: Copepoda): in silico gene expression and SNPs discovery. Fish. Shellfish Immunol. 36, 428–434.
Vaseeharan, B., Shanthi, S., Chen, J.C., Espiñeira, M., 2012. Molecular cloning, sequence analysis and expression of Fein-Penaeidin from the haemocytes of Indian white shrimp *Fenneropenaeus indicus*. Results Immunol. 14, 35–43.
Visetnan, S., Supungul, P., Hirono, I., Tassanakajon, A., Rimphanitchayakit, V., 2015. Activation of *Pm*Relish from *Penaeus monodon* by yellow head virus. Fish. Shellfish Immunol. 42, 335–344.
Wang, H.C., Tseng, C.W., Lin, H.Y., Chen, I.T., Chen, Y.H., Chen, Y.M., Chen, T.Y., Yang, H.L., 2010. RNAi knock-down of the *Litopenaeus vannamei* Toll gene (*Lv*Toll) significantly increases mortality and reduces bacterial clearance after challenge with *Vibrio harveyi*. Dev. Comp. Immunol. 34, 49–58.
Wang, P.H., Gu, Z.H., Huang, X.D., Liu, B.D., Deng, X.X., Ai, H.S., Wang, J., Yin, Z.X., Weng, S.P., Yu, X.Q., He, J.G., 2009. An immune deficiency homolog from the white shrimp, *Litopenaeus vannamei*, activates antimicrobial peptide genes. Mol. Immunol. 46, 1897–1904.

Wang, P.H., Gu, Z.H., Wan, D.H., Zhang, M.Y., Weng, S.P., Yu, X.Q., He, J.G., 2011. The Shrimp NF-κB pathway is activated by white spot syndrome virus (WSSV) 449 to facilitate the expression of WSSV069 (ie1), WSSV303 and WSSV371. PloS One 6, e24773.

Wang, P.H., Liang, J.P., Gu, Z.H., Wan, D.H., Weng, S.P., Yu, X.Q., He, J.G., 2012. Molecular cloning, characterization and expression analysis of two novel Tolls (*Lv*Toll2 and *Lv*Toll3) and three putative Spätzle-like Toll ligands (*Lv*Spz1–3) from *Litopenaeus vannamei*. Dev. Comp. Immunol. 36, 359–371.

Wang, D., Li, F., Li, S., Chi, Y., Wen, R., Feng, N., Xiang, J., 2013a. An IκB homologue (*Fc*Cactus) in Chinese shrimp *Fenneropenaeus chinensis*. Dev. Comp. Immunol. 39, 352–362.

Wang, P.H., Gu, Z.H., Wan, D.H., Liu, B.D., Huang, X.D., Weng, S.P., Yu, X.Q., He, J.G., 2013b. The shrimp IKK-NF-κB signaling pathway regulates antimicrobial peptide expression and may be subverted by white spot syndrome virus to facilitate viral gene expression. Cell Mol. Immunol. 10, 423–436.

Wang, X.W., Xu, J.D., Zhao, X.F., Vasta, G.R., Wang, J.X., 2014. A shrimp C-type lectin inhibits proliferation of the hemolymph microbiota by maintaining the expression of antimicrobial peptides. J. Biol. Chem. 289, 11779–11790.

Wang, Z., Chen, Y.H., Dai, Y.J., Tan, J.M., Huang, Y., Lan, J.F., Ren, Q., 2015a. A novel vertebrates Toll-like receptor counterpart regulating the anti-microbial peptides expression in the freshwater crayfish, *Procambarus clarkii*. Fish. Shellfish Immunol. 43, 219–229.

Wang, S., Li, H., Qian, Z., Song, X., Zhang, Z., Zuo, H., Xu, X., Weng, S., He, J., Li, C., 2015b. Identification and functional characterization of the TAB2 gene from *Litopenaeus vannamei*. Fish. Shellfish Immunol. 46, 206–216.

Wang, S., Li, H., Lǔ, K., Qian, Z., Weng, S., He, J., Li, C., 2016. Identification and characterization of transforming growth factor β-activated kinase 1 from *Litopenaeus vannamei* involved in anti-bacterial host defense. Fish. Shellfish Immunol. 52, 278–288.

Wang, X.W., Wang, J.X., 2013. Pattern recognition receptors acting in innate immune system of shrimp against pathogen infections. Fish. Shellfish Immunol. 34, 981–989.

Wang, Y., Jiang, H., 2007. Reconstitution of a branch of the *Manduca sexta* prophenoloxidase activation cascade in vitro: snake-like hemolymph proteinase 21 (HP21) cleaved by HP14 activates prophenoloxidase-activating proteinase-2 precursor. Insect Biochem. Mol. Biol. 37, 1015–1025.

Wang, Y., Jiang, H., 2010. Binding properties of the regulatory domains in *Manduca sexta* hemolymph proteinase-14, an initiation enzyme of the prophenoloxidase activation system. Dev. Comp. Immunol. 34, 316–322.

Wen, R., Li, F., Sun, Z., Li, S., Xiang, J., 2013. Shrimp MyD88 responsive to bacteria and white spot syndrome virus. Fish. Shellfish Immunol. 34, 574–581.

Wen, Y., Zhan, S., Huang, H., Zhong, M., Chen, J., You, C., Wang, F., Zhang, Y., 2016. Identification and characterization of an 18.4 kDa antimicrobial truncation from shrimp *Litopenaeus vannamei* hemocyanin upon *Vibrio parahaemolyticus* infection. Fish. Shellfish Immunol. 56, 450–458.

Wetsaphan, N., Rimphanitchayakit, V., Tassanakajon, A., Somboonwiwat, K., 2013. *Pm*SERPIN3 from black tiger shrimp *Penaeus monodon* is capable of controlling the proPO system. Dev. Comp. Immunol. 41, 110–119.

Woramongkolchai, N., Supungul, P., Tassanakajon, A., 2011. The possible role of penaeidin5 from the black tiger shrimp, *Penaeus monodon*, in protection against viral infection. Dev. Comp. Immunol. 35, 530–536.

Xu, D., Liu, W., Alvarez, A., Huang, T., 2014. Cellular immune responses against viral pathogens in shrimp. Dev. Comp. Immunol. 47, 287–297.

Xu, Y., Huang, Y., Cai, S., 2017. Characterization and function analysis of interleukin-1 receptor-associated kinase-1 (IRAK-1) from *Fenneropenaeus penicillatus*. Fish. Shellfish Immunol. 61, 111–119.

Yang, H., Li, S., Li, F., Lv, X., Xiang, J., 2015. Recombinant expression and functional analysis of an isoform of anti-lipopolysaccharide factors (*Fc*ALF5) from Chinese shrimp *Fenneropenaeus chinensis*. Dev. Comp. Immunol. 53, 47–54.

Yang, L.S., Yin, Z.X., Liao, J.X., Huang, X.D., Guo, C.J., Weng, S.P., Chan, S.M., Yu, X.Q., He, J.G., 2007. A Toll receptor in shrimp. Mol. Immunol. 44, 1999–2008.

Yang, Y.T., Chen, I.T., Lee, C.T., Chen, C.Y., Lin, S.S., Hor, L.I., Tseng, T.C., Huang, Y.T., Sritunyalucksana, K., Thitamadee, S., Wang, H.C., Lo, C.F., 2014. Draft genome sequences of four strains of *Vibrio parahaemolyticus*, three of which cause early mortality syndrome/acute hepatopancreatic necrosis disease in shrimp in China and Thailand. Genome Announc 2 e00816–14.

Yuan, K., Yuan, F.H., Weng, S.P., He, J.G., Chen, Y.H., 2017. Identification and functional characterization of a novel Spätzle gene in *Litopenaeus vannamei*. Dev. Comp. Immunol. 68, 46–57.

Zhang, J., Li, F., Wang, Z., Xiang, J., 2007. Expression, purification, and characterization of recombinant Chinese shrimp crustin-like protein (Cru*Fc*) in *Pichia pastoris*. Biotechnol. Lett. 29, 813–817.

Zhang, S., Li, C.Z., Yan, H., Qiu, W., Chen, Y.G., Wang, P.H., Weng, S.P., He, J.G., 2012. Identification and function of myeloid differentiation factor 88 (MyD88) in *Litopenaeus vannamei*. PloS One 7, e47038.

Zhang, S., Yan, H., Li, C.Z., Chen, Y.H., Yuan, F.H., Chen, Y.G., Weng, S.P., He, J.G., 2013. Identification and function of leucine-rich repeat flightless-I-interacting protein 2 (LRRFIP2) in *Litopenaeus vannamei*. PLoS One 8, e57456.

Zhang, X.B., Huang, C.H., Qin, Q.W., 2004. Antiviral properties of hemocyanin isolated from shrimp *Penaeus monodon*. Antivir. Res. 61, 93–99.

Zhao, X., Guo, L., Lu, X., Lu, H., Wang, F., Zhong, M., Chen, J., Zhang, Y., 2016. Evidences of abundant hemocyanin variants in shrimp *Litopenaeus vannamei*. Mol. Immunol. 77, 103–112.

Fish and Shellfish Immunology 72 (2018) 86–94

Contents lists available at ScienceDirect

Fish and Shellfish Immunology

journal homepage: www.elsevier.com/locate/fsi

Short communication

WSSV-responsive gene expression under the influence of *Pm*VRP15 suppression

Phawida Tummamunkong, Phattarunda Jaree, Anchalee Tassanakajon, Kunlaya Somboonwiwat*

Center of Excellence for Molecular Biology and Genomics of Shrimp, Department of Biochemistry, Faculty of Science, Chulalongkorn University, Phayathai Road, Bangkok 10330, Thailand

ARTICLE INFO

Keywords:
Penaeus monodon
*Pm*VRP15
Suppression subtractive hybridization
Hemocyte homeostasis

ABSTRACT

The viral responsive protein 15 from black tiger shrimp *Penaeus monodon* (*Pm*VRP15), is highly up-regulated and produced in the hemocytes of shrimp with white spot syndrome virus (WSSV) infection. To investigate the differential expression of genes from *P. monodon* hemocytes that are involved in WSSV infection under the influence of *Pm*VRP15 expression, suppression subtractive hybridization (SSH) of *Pm*VRP15-silenced shrimp infected with WSSV was performed. The 189 cDNA clones of the forward library were generated by subtracting the cDNAs from WSSV-infected and *Pm*VRP15 knockdown shrimp with cDNAs from WSSV-infected and GFP knockdown shrimp. For the opposite subtraction, the 176 cDNA clones in the reverse library was an alternative set of genes in WSSV-infected shrimp hemocytes in the presence of *Pm*VRP15 expression. The abundant genes in forward SSH library had a defense/homeostasis of 26%, energy/metabolism of 23% and in the reverse SSH library a hypothetical protein with unknown function was found (30%). The differential expressed immune-related genes from each library were selected for expression analysis using qRT-PCR. All selected genes from the forward library showed high up-regulation in the WSSV-challenged *Pm*VRP15 knockdown group as expected. Interestingly, *Pm*HHAP, a hemocyte homeostasis associated protein, and granulin-like protein, a conserved growth factor, are extremely up-regulated in the absence of *Pm*VRP15 expression in WSSV-infected shrimp. Only transcript level of transglutaminase II, that functions in regulating hematopoietic tissue differentiation and inhibits mature hemocyte production in shrimp, was obviously down-regulated as observed from SSH results. Taken together, our results suggest that *Pm*VRP15 might have a function relevant to hemocyte homeostasis during WSSV infection.

1. Introduction

Shrimp disease outbreaks affect shrimp aquaculture worldwide. The major disease problems come from viral, bacterial and fungal pathogens. White spot syndrome virus (WSSV) is the most virulent viral pathogen causing a cumulative mortality of up to 100% within 3–10 days [1,2]. Shrimp lack true adaptive immunity but rely solely on innate immunity. Shrimp's innate immunity functions according to two main mechanisms including cellular and humoral responses. Cellular responses include phagocytosis, encapsulation, and lysis of foreign cells. The humoral responses are the prophenoloxidase (proPO) system, the clotting cascade and the synthesis of a wide array of antimicrobial peptides [3,4]. During WSSV infection, shrimp respond through several mechanisms. In the innate immune system, several immune-related genes/proteins are regulated either by the host, or WSSV. Whereas WSSV tries to infect host cells by annexing host mechinery. shrimp fight against infection with several immune reactions and active molecules [3].

Shrimp hemocytes are an important immune cell which can be classified as hyaline, semigranular, and granular cells. Each cell type is responsible for several defense reactions; for example, hyaline cells are involved in phagocytosis and the function of granular cells is associated with apoptosis, melanization, encapsulation, and nodulation [5]. The number of circulating hemocytes is dramatically changed during viral infection [6]. However, shrimp also respond to infection by maintaining hemocyte homeostasis in the circulation during infection [7–9].

Although several immune-related genes have been characterized so far, still many more uncharacterized proteins are highly expressed in response to WSSV infection and might play crucial roles in antiviral immunity. The viral responsive proteins that are highly up-regulated in *Penaeus monodon* upon WSSV infection have been previously identified. Interestingly, the functions of these proteins in the shrimp immune system were revealed but not fully characterized. Hemocyte homeostasis-associated protein (*Pm*HHAP) from *P. monodon* is highly up-

* Corresponding author.
E-mail address: kunlaya.s@chula.ac.th (K. Somboonwiwat).

http://dx.doi.org/10.1016/j.fsi.2017.10.006
Received 25 July 2017; Received in revised form 2 October 2017; Accepted 6 October 2017
Available online 07 October 2017
1050-4648/ © 2017 Elsevier Ltd. All rights reserved.

regulated after WSSV infection [7] and performs an essential role in hemocyte homeostasis by preventing apoptosis via caspase inactivation during WSSV infection [9]. In 2014, the viral responsive protein 15 (*Pm*VRP15) from *P. monodon* was first shown to be highly up-regulated at both transcript and protein levels during WSSV infection [10]. Later on, Leu et al. (2015) identified the protein called *Pm*ERP15 as an endoplasmic reticulum (ER) stress-induced protein. ER stress triggered by WSSV infection induced *Pm*ERP15 gene expression in shrimp. Sequence analysis revealed that *Pm*VRP15 and *Pm*ERP15 are the same gene which will henceforth be referred to as "*Pm*VRP15" according to our first report [10,11]. The effect of *Pm*VRP15 gene knockdown reduced viral gene expression and also the cumulative mortality of WSSV-infected shrimp. Moreover, it has been shown that the *Pm*VRP15 protein can interact with the viral tegument protein, WSV399, and is probably involved in WSSV trafficking and assembly during infection [12]. However, the molecular function of the *Pm*VRP15 protein in shrimp immunity against WSSV infection needs further investigation.

In the current study, suppression subtractive hybridization (SSH) was used to look for genes that are differentially expressed in WSSV-infected shrimp when the *Pm*VRP15 gene was silenced to further investigate the possible functions of *Pm*VRP15 in the antiviral response. The expression of differentially expressed genes identified from the SSH libraries was confirmed by quantitative real time RT-PCR.

2. Materials and methods

2.1. Shrimp and the WSSV challenge

The healthy black tiger shrimp, *Penaeus monodon*, with a body weight of 3–5 g used in this study were purchased from a local farm in the Chachoengsao province, Thailand. The shrimp were reared in laboratory tanks at 28 ± 1 °C and maintained in aerated water with a salinity of 15 ppt for at least 7 days before use.

White spot syndrome virus (WSSV) was prepared as described by Vatanavicharn et al. (2014) [10]. WSSV copy number of the virus stock was calculated as described by Zhu et al. (2007) [13]. WSSV stock (7×10^8 virions/μl) was diluted with 0.85% NaCl (normal saline) to 10^{-7}-fold dilution and 50 μl of diluted virus containing 3×10^3 virions (causing 100% mortality of shrimp in 4 days after injection) was injected into shrimp at the abdominal muscle.

2.2. Production of double stranded RNAs (dsRNA) of PmVRP15 and GFP genes

The dsRNA of *Pm*VRP15 and GFP genes were generated using the T7 RiboMAX™ Express Large Scale RNA Production System (Promega). The *Pm*VRP15 dsRNA and GFP dsRNA used as a control dsRNA were prepared as described in the authors' previous study [10]. Briefly, the specific primers of *Pm*VRP15-T7-F/*Pm*VRP15-R and *Pm*VRP15-F/*Pm*VRP15-T7-R (Table 1) were used for the synthesis of sense and antisense strands of *Pm*VRP15 dsRNA, respectively. The GFP dsRNA sense and antisense strands were generated using primers GFP-T7-F/GFP-R and GFP -F/GFP -T7R, respectively (Table 1), using plasmid clones containing either *Pm*VRP15 or GFP genes as a DNA template. Then, 1 μg of each PCR product was used as a template for *in vitro* transcription using the T7 RiboMAX™ Express Large Scale RNA Production System (Promega). Equal amounts of the complementary RNA strands were annealed. The quality and amount of dsRNA were analyzed with 1.5% (w/v) agarose gel electrophoresis and measured spectrophotometrically, respectively.

2.3. Construction of suppression subtractive hybridization (SSH)

To investigate the response of shrimp under the *Pm*VRP15 knockdown with WSSV infection by SSH, the shrimp were divided into two groups of six shrimp each including WSSV-challenged GFP knockdown (GFP dsRNA-WSSV group) and WSSV-challenged *Pm*VRP15 knockdown (*Pm*VRP15 dsRNA-WSSV group). Shrimp were injected with 0.85% NaCl plus WSSV containing *Pm*VRP15 dsRNA (20 μg/g shrimp) or GFP dsRNA (20 μg/g shrimp), respectively. The hemocytes were collected at 24 h after injection. Total RNA was extracted using TRI Reagent® (Molecular Research Center) followed by RQ1 RNase-free DNase (Promega) treatment. The RNase-free total RNA was purified using NucleoSpin® RNA II Kit (Maccherey-Nagel) and kept at −80 °C until used.

Prior to perform SSH, the efficiency of gene knockdown and WSSV infection was verified by semi-quantitative RT-PCR analysis. RNase-free total RNA was used for cDNA synthesis using the RevertAid First Strand cDNA Synthesis kit (Thermo Scientific) according to the manufacturer's instruction. The cDNA of 5-fold dilution was then used as a template. *Pm*VRP15 transcript was amplified using 10 μM of *Pm*VRP15-RTF/RTR primers (Table 1). The EF-1α gene, an internal control, was amplified using 10 μM of the primer pair EF-1-F/R (Table 1). To confirm WSSV infection in the shrimp, the WSSV marker gene for the late stage of infection,VP28 gene, was amplified using 10 μM of the primer pair *vp28* -F/R (Table 1). The PCR conditions maintained 94 °C for 1 min followed by 27 cycles at 95 °C for 30 s, 58 °C for *Pm*VRP15 and EF-1α genes or 60 °C for VP28 gene for 30 s, and 72 °C for 30 s, with a final extension at 72 °C for 5 min. The PCR products were analyzed with 2.5% (w/v) agarose gel electrophoresis.

In order to identify differentially expressed genes from *Pm*VRP15 knockdown shrimp, the SSH cDNA libraries were constructed in two directions, forward and reverse, using the PCRSelect™ cDNA Subtraction Kit (Clontech), according to the manufacturer's instructions. For *Pm*VRP15 dsRNA-WSSV and GFP dsRNA-WSSV groups, an equal amount of RNase-free total RNA from two shrimps was pooled and used for SSH library construction. For the forward subtraction, the driver cDNA of the *Pm*VRP15 dsRNA-WSSV group was used to subtract from those of the tester, cDNA of GFP dsRNA-WSSV group. For the reverse subtraction, the driver cDNA of GFP dsRNA-WSSV group was used to subtract from those of the tester, cDNA of *Pm*VRP15 dsRNA-WSSV group. The efficiency of SSH was confirmed by checking the absence of EF-1α gene expression. The subtracted mixture was nested PCR-amplified and cloned into a pGEM-T easy vector (Promega), then transformed into *Escherichia coli* TOP10 competent cells (Invitrogen). The positive clones were randomly selected using blue/white screening and extracted with a FavorPrep Plasmid DNA Extraction Mini Kit (Flavogen). The recombinant plasmids were sequenced using the T7 forward primer by Macrogen Inc., South Korea.

2.4. Bioinformatics analysis of genes derived from the SSH libraries

From forward and reverse SSH libraries, the nucleotide sequences of genes removed the unwanted vector and adaptor sequences using NCBI vecscreen tools (https://www.ncbi.nlm.nih.gov/tools/vecscreen/). The gene sequences were analyzed for sequence homology against the NCBI GenBank database with the BLASTN and BLASTX programs (https://blast.ncbi.nlm.nih.gov/Blast.cgi). Significant matches were accepted at *E*-values lower than 1×10^{-4}. The genes were categorized according to their functions into these groups including defense and homeostasis, cell cycle and DNA synthesis, gene expression, energy and metabolism, transport, miscellaneous function, hypothetical proteins and unknown proteins. The number of genes was recorded.

2.5. Validation of gene expression in response to WSSV infection under the PmVRP15 knockdown and non-knockdown conditions

The shrimp were divided into four groups of fifteen shrimp each including normal saline (NaCl control group), WSSV-challenged normal saline (WSSV group), WSSV-challenged GFP knockdown (GFP dsRNA-WSSV group) and WSSV-challenged *Pm*VRP15 knockdown (*Pm*VRP15 dsRNA-WSSV group). Shrimp in the NaCl control group were injected

Table 1
DNA sequences of the PCR primers used in this study.

Primer name	Sequence (5′- 3′)	Usage
*Pm*VRP15- T7-F	GGATCCTAATACGACTCACTATAGGCGCGACCGAGCCAAGAG	Preparation of *Pm*VRP15 dsRNA
*Pm*VRP15- T7-R	GGATCCTAATACGACTCACTATAGGTGAGCTGACGGAAGGCC	
*Pm*VRP15-F	TCACTCTTTCGGTCGTGTCG	
*Pm*VRP15-R	CCACACACAAAGGTGCCAAC	
GFP-F	ATGGTGAGCAAGGGGGAGGA	Preparation of GFP dsRNA
GFP-R	TTACTTGTACAGCTCGTCCA	
GFP-FT7	GGATCCTAATACGACTCACTATAGGATGGTGAGCAAGGGGGAGGA	
GFP-RT7	GGATCCTAATACGACTCACTATAGGTTACTTGTACAGCTCGTCCA	
*Pm*VRP15-RTF	CGTCCTTCAGTGCGCTTCCATA	RT-PCR
*Pm*VRP15-RTR	ACAGCGACTCCAAGGTCTACGA	
VP28 -F	GGGAACATTCAAGGTGTGGA	
VP28 -R	GGTGAAGGAGGAGGTGTTGG	
EF-1α-F	GGTGCTGGACAAGCTGAAGGC	
EF-1α-R	CGTTCCGGTGATCATGTTCTTGATG	
*Pm*HHAP-qrt-F	GCAACAGGAGAACCTGTGGATA	Expression analyses of selected genes from forward SSH library
*Pm*HHAP-qrt-R	GGTTCCAGAATCGCCTCCTATA	
CathepsinL-qrt-F	CGAGTACGTCAAGGAGAATG	
CathepsinL-qrt-R	GCATCAATAGCCACAGACAC	
Thioredoxin-qrt -F	ATCGACTTCTACGCCACCTG	
Thioredoxin-qrt -R	GCACCAGACAAGCTGTCAAG	
Tetraspanin-qrt -F	GGAGGAGCTAGTCAAGAAGA	
Tetraspanin-qrt -R	CAGGTACTCCAGTCACATTC	
Granulin like-qrt -F	ACTGCTGCCCTCAGGATATGC	
Granulin like-qrt -R	TTCGCGCAGATGATTACTCTCCTC	
ALF*Pm*3-qrt-F	CCCACAGTGCCAGGCTCAA	Expression analyses of selected genes from reverse SSH library
ALF*Pm*3-qrt-R	TGCTGGCTTCTCCTCTGATG	
Cytochrome C oxidase III qrt-F	CGGTCTTCGATGAGGTATAATCTTG	
Cytochrome C oxidase III qrt-R	GAGGCAAGAAGGATTGCTGTATTAAG	
Fortilin-qrt-F	TACTTCGCCTCCAGGACCTT	
Fortilin-qrt-R	ATGGACATGGAGGGCATACG	
Transglutaminase-qrt-F	TGGCATTCGTGACTCCATCT	
Transglutaminase-qrt-R	GGCACGTCGTACTTCAGGTC	

with 0.85% NaCl while shrimp in the WSSV group were injected with 0.85% NaCl plus WSSV. Shrimp in the *Pm*VRP15 dsRNA-WSSV group and GFP dsRNA-WSSV group were prepared as described above. Total RNA was extracted using TRI Reagent® (Molecular Research Center) and treated. An equal amount of RNase-free total RNA from three shrimps was pooled and total RNA was used for cDNA synthesis.

To verify whether the expression of selected genes in WSSV-challenged shrimp was affected by *Pm*VRP15 gene knockdown, the selected genes from both SSH libraries were analyzed using quantitative real time RT-PCR. Five up-regulated genes were selected from the forward SSH library: HHAP (hemocyte homeostasis associated protein), thioredoxin, tetraspanin, cathepsin L and granulin-like, and four down-regulated genes were selected from the reverse SSH library: TGSII (transglutaminase type II), ALF*Pm*3 (antilipopolysaccharide factor isoform 3), fortilin and cytochrome *c* oxidase subunit III. The EF-1α was used as an internal reference control. The cDNAs from NaCl control, WSSV, GFP dsRNA-WSSV and *Pm*VRP15 dsRNA-WSSV groups were used to evaluate the expression of selected genes. The 5-fold diluted cDNA was used to amplify selected genes using specific primers (Table 1). Real-time PCR was performed using the SsoFast EvaGreen Supermix on a CFX96 touch real-time PCR detection system (Bio-Rad) under the following conditions: 95 °C for 5 min, 40 cycles of 95 °C for 30 s, 60 °C for 30 s and 72 °C for 45 s. Each qRT-PCR reaction was done in triplicate. The standard curve for nine selected genes and EF-1α was generated by running triplicate reactions of five different cDNA concentrations. The cDNA was prepared in 5-fold serial dilution. Cycle threshold (Ct) values were recorded and gene expression levels of the interesting mRNA relative to the EF-1α gene were calculated using the $2^{-\Delta\Delta Ct}$ method (Pfaffl, 2001). Data was analyzed for statistical significance using a one-way ANOVA followed by a Duncan's multiple ranges test and presented as means ± standard deviations. Different letters indicate significant differences between groups accepted at $P \leq 0.05$.

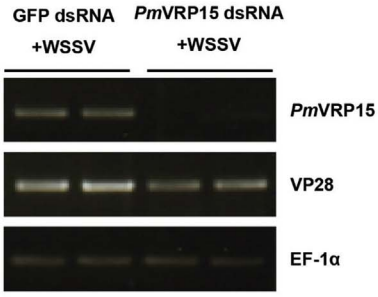
3. Results and discussion

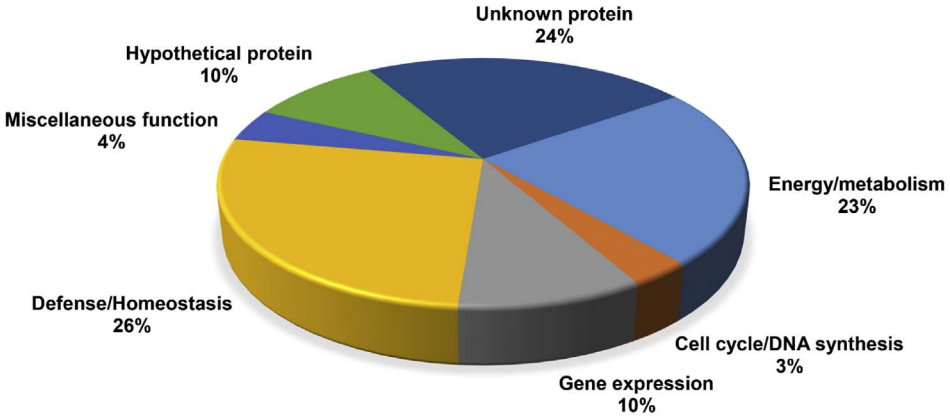
3.1. Suppression subtractive hybridization

SSH techniques has been widely used to identify differentially expressed genes under stress conditions in order to study shrimp immunity [3,5,14]. The high level of expression of genes coding for apoptotic-related proteins and antioxidant enzymes was found in the hepatopancreas of resistant WSSV-challenged *L. vannamei* [15]. Visetnan et al. (2015) identified defense responsive genes (kunitz, penaeidin3, penaeidin5, transglutaminase and SWD*Pm*2) under the influence of *Pm*Relish regulation in yellow head virus (YHV)-infected shrimp. Also, ALF*Pm*3, crustin*Pm*1, penaeidin3 and penaeidin5 were expressed in response to *Vibrio harveyi* infection [14,16]. From our previous report, Prapavorarat et al. (2010) used SSH and cDNA microarray to identify viral responsive gene expression in WSSV-challenged *P. monodon* hemocytes [7]. In the current study, SSH and the dsRNA-mediated gene knockdown techniques were used to study the possible functions of *Pm*VRP15 in WSSV-infected shrimp hemocytes.

The cDNAs were prepared from *Pm*VRP15 and GFP knockdown shrimp after WSSV infection. The *Pm*VRP15 transcript was tested for efficacy on gene knockdown using RT-PCR (Fig. 1A). PCR analysis of the subtraction efficiency after subtractive hybridization showed that the abundance of the housekeeping gene EF-1α was effectively reduced (data not shown). As compared to the cDNAs isolated from GFP knockdown and WSSV-infected shrimp, it was found that *Pm*VRP15 gene expression was completely suppressed in *Pm*VRP15 dsRNA-WSSV shrimp.

There were two directions of subtraction. The forward library subtracted the cDNA of the *Pm*VRP15 dsRNA-WSSV shrimp from those of the GFP dsRNA-WSSV shrimp. The remaining cloneable cDNAs were the WSSV-responsive genes under *Pm*VRP15 gene knockdown. Thus, the cloneable genes in the forward library were expressed within the





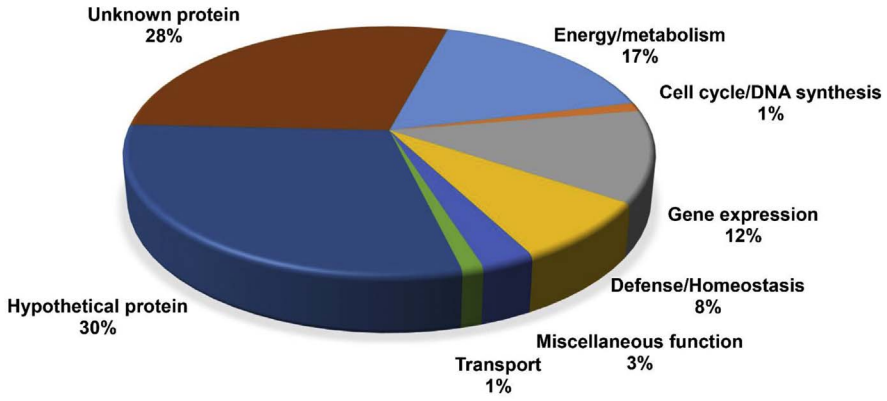


Fig. 1. Percentages of gene groups identified from forward and reverse SSH libraries. The data was annotated and categorized into 7 and 8 functional groups, respectively. (A) Expression levels of *Pm*VRP15 and EF-1α genes in WSSV-infected and *Pm*VRP15 knockdown shrimp hemocytes were analyzed with RT-PCR. (B) A total of 148 sequences of clones were up-regulated genes in the forward library. (C) A total of 145 sequences of clones were down-regulated genes in the reverse library.

loss of *Pm*VRP15 activity in WSSV-infected shrimp while reverse subtraction did the opposite.

The cloneable cDNAs remaining after subtraction were cloned into plasmid vector and sequencing. Then, 189 clones in total were found from the forward library and 176 clones were from the reverse library. The sequences were blast searched for sequence homology against the NCBI GenBank database with the BLASTN and BLASTX programs. Significant matches (*E*-value $< 1 \times 10^{-4}$) were used to identify the homolog genes. The annotatable known genes represented 126 (66.67%) clones of the forward library and 74 (42.05%) clones of the reverse library. The remaining 63 (33.33%) and 102 (57.95%) clones were hypothetical protein and unknown genes in the forward and reverse libraries, respectively (Tables 2 and 3, Fig. 1B and C).

The differentially expressed genes were categorized according to their functions into six groups including defense/homeostasis, cell cycle/DNA synthesis, gene expression, energy/metabolism, transport and miscellaneous function (Fig. 1B and C). In the forward library, the 50 (26.46%) and 44 (23.28%) clones revealed that these genes were mainly involved in defense/homeostasis and energy/metabolism, respectively. In contrast, the 52 (29.55%) clones of the hypothetical protein were plentifully found in the reverse library. We selected these genes which were highly abundant or from interesting proteins, for further validation the SSH technique. The up-regulated genes from the forward library included *Pm*HHAP, granulin-like, cathepsin L, thioredoxin, tetraspanin, of which *Pm*HHAP was predominant. Four down-regulated genes in the reverse library were TGSII, cytochrome *c* oxidase subunit III, ALF*Pm*3, fortilin of which TGSII was the most abundant clone.

3.2. Differential expression of genes from SSH libraries

WSSV infection leads to the altered expression of several immune

Table 2
Up-regulated genes identified from forward SSH library.

Highest homology	Accession number	*E* value	Closet species	No. of clones
Defense & Homeostasis				
Hemocyte homeostasis-associated protein	ADN43412	7.00E-21	*Penaeus monodon*	48
Leukocyte receptor cluster member 9	ACO10547	1.00E-14	*Caligus rogercresseyi*	1
WD repeat-containing protein 92	XP_011143511	3.00E-141	*Harpegnathos saltator*	1
Cell cycle & DNA synthesis				
Granulins-like	XP_004225530	7.00E-20	*Ciona intestinalis*	3
RNA pseudouridylate synthase domain containing 3-like protein	ACY66491	4.00E-14	*Scylla paramamosain*	2
Malignant T cell amplified sequence 1	EFN72640	2.00E-88	*Camponotus floridanus*	1
Helicase SKI2W-like	XP_006813031	2.00E-77	*Saccoglossus kowalevskii*	1
20S proteasome alpha subunit	ACY66486	1.00E-50	*Scylla paramamosain*	1
Ras homolog enriched in brain	ADV76255	8.00E-37	*Homarus americanus*	1
Gene expression, regulation & protein synthesis				
28S ribosomal protein	EZA55913	7.00E-42	*Cerapachys biroi*	2
40S ribosomal protein S17- like isoform X1	XP_004558071	1.00E-59	*Maylandia zebra*	2
39S ribosomal protein L9 mitochondrial-like	XP_004924514	5.00E-37	*Bombyx mori*	2
CCAAT/enhancer-binding protein gamma-like isoform 1	XP_001606194	2.00E-16	*Nasonia vitripennis*	1
RNA binding protein	XP_002407514	3.00E-26	*Ixodes scapularis*	1
U5 small nuclear ribonucleoprotein component-like	XP_796586	2.00E-101	*Strongylocentrotus purpuratus*	1
Speckle targeted PIP5K1A-regulated poly(A) polymerase-like	XP_003702379	5.00E-15	*Megachile rotundata*	1
Ribosomal protein	ACU52718	7.00E-127	*Fenneropenaeus merguiensis*	1
Ribosome maturation protein SBDS-like	XP_004569637	5.00E-40	*Maylandia zebra*	1
39S ribosomal protein L21	XP_004518974	1.00E-40	*Ceratitis capitata*	1
Putative regulator of ribosome biosynthesis	EHJ66162	2.00E-49	*Danaus plexippus*	1
Tripeptidyl-peptidase 2	EFN68015	3.00E-71	*Camponotus floridanus*	1
PiggyBac transposable element-derived protein 2-like	XP_004083158	2.00E-38	*Oryzias latipes*	1
Nascent polypeptide-associated complex alpha	ACJ47904	3.00E-85	*Penaeus monodon*	1
Flotillin-1	ACY66412	2.00E-43	*Scylla paramamosain*	1
Energy & metabolism				
Thioredoxin	ADV36299	4.00E-08	*Penaeus monodon*	8
NADH dehydrogenase subunit 1	NP_038300	8.00E-41	*Penaeus monodon*	4
Cytochrome *c* oxidase subunit II	AEO12678	3.00E-149	*Fenneropenaeus merguiensis*	3
Cytochrome *c* oxidase subunit I	NP_038289	3.00E-134	*Penaeus monodon*	3
Pyruvate kinase	ABY66598	5.00E-43	*Litopenaeus vannamei*	2
Methyltransferase-like protein 6-like	XP_005929566	8.00E-87	*Haplochromis burtoni*	2
Protein disulfide isomerase 2	AEE36486	5.00E-97	*Fenneropenaeus chinensis*	2
Regulatory particle non-ATPase 3, Dox-A2	BAM18273	6.00E-91	*Papilio xuthus*	2
Cathepsin L	ABQ10739	5E- 113	*Penaeus monodon*	2
Cytochrome oxidase subunit I	AGH32567	1.00E-59	*Penaeus monodon*	1
Cytochrome oxidase subunit I	AEJ90009	2E- 125	*Aegla rostrata*	1
Mitochondrial cytochrome *c* oxidase subunit IV	AFY10818	1.00E-84	*Litopenaeus vannamei*	1
NADH dehydrogenase subunit 1	YP_002587085	2.00E-23	*Litopenaeus stylirostris*	1
Peroxisome biogenesis factor 2-like	XP_006557309	4.00E-04	*Apis mellifera*	1
Serine hydroxymethyltransferase, cytosolic-like	XP_003708127	3.00E-74	*Megachile rotundata*	1
Dehydrogenase/reductase SDR family member 11-like	XP_004076655	2.00E-95	*Oryzias latipes*	1
Retinol dehydrogenase 12	NP_001134576	3.00E-41	*Salmo salar*	1
O-acetyl-ADP-ribose deacetylase 1-like	XP_002734397	5.00E-15	*Saccoglossus kowalevskii*	1
O-acetyl-ADP-ribose deacetylase 1-like deacetylase 1	XP_005059547	9.00E-49	*Ficedula albicollis*	1
N-acylsphingosine amidohydrolase (acid ceramidase), putative	XP_002405171	7.00E-79	*Ixodes scapularis*	1
Rab GTPase	AFK08607	8E- 134	*Litopenaeus vannamei*	1
Epoxide hydrolase 4-like isoform X2	XP_006006058	7.00E-27	*Latimeria chalumnae*	1
Vacuolar-H-ATPase H	AKC35142	4.00E-28	*Cherax quadricarinatusnis*	1
Protein disulfide isomerase 2	AEE36486	3.00E-97	*Fenneropenaeus chinensis*	1
THO complex subunit 3 isoform X1	XP_002938105	2.00E-51	*Xenopus (Silurana) tropicalis*	1
Miscellaneous function				
Tetraspanins-like protein	AHM10345	2.00E-97	*Penaeus monodon*	2
Signal recognition particle receptor	XP_002416464	3.00E-48	*Ixodes scapularis*	1
Single VWC domain protein 5	AEB54795	8.00E-05	*Litopenaeus vannamei*	1
EH domain-containing protein 3	NP_001133614	6.00E-10	*Salmo salar*	1
Hypothetical protein				
Hypothetical protein	BAN20797	2.00E-04	*Riptortus pedestris*	3
Hypothetical protein	XP_002607098	1.00E-30	*Branchiostoma floridae*	1
Hypothetical protein	XP_002610266	2.00E-58	*Branchiostoma floridae*	1
Hypothetical protein	EKC25831	3.00E-50	*Crassostrea gigas*	1
Hypothetical protein	EFX78817	9.00E-165	*Daphnia pulex*	1
Hypothetical protein	EFX72757	7.00E-43	*Daphnia pulex*	1
Hypothetical protein	EFX65492	4.00E-26	*Daphnia pulex*	1
Hypothetical protein	EFX73836	2.00E-24	*Daphnia pulex*	1
Hypothetical protein	EFX84930	3.00E- 122	*Daphnia pulex*	1
Hypothetical protein	EFX79856	7.00E-19	*Daphnia pulex*	1
Hypothetical protein	EFX72994	3.00E-39	*Daphnia pulex*	1
Hypothetical protein	EFX79445	6.00E-69	*Daphnia pulex*	1
Hypothetical protein	ENN79977	1.00E-74	*Dendroctonus ponderosae*	1
Hypothetical protein	EFN87317	2.00E-08	*Harpegnathos saltator*	1
Hypothetical protein	XP_002410968	2.00E-30	*Ixodes scapularis*	1

(*continued on next page*)

Table 2 (*continued*)

Highest homology	Accession number	*E* value	Closet species	No. of clones
Hypothetical protein	ESO85742	4.00E-116	*Lottia gigantea*	1
Unknown proteins				45
Total				189

Table 3
Down-regulated genes identified from reverse SSH library.

Highest homology	Accession number	*E* value	Closet species	No. of clones
Defense & Homeostasis				
Transglutaminase type II	AAL78166	1.00E-05	*Penaeus monodon*	8
Anti-lipopolysaccharide factor isoform 3 (ALF*Pm*3)	ABP73289	4.00E-30	*Penaeus monodon*	2
Fortilin binding protein 1	ACB87923	3.00E-10	*Penaeus monodon*	2
Viral responsive protein (*Pm*VRP15)	AHN10846	5.00E-29	*Penaeus monodon*	2
Cell cycle & DNA synthesis				
Putative myosin regulatory light chain 2 smooth muscle	ACY66440	2.00E-83	*Scylla paramamosain*	1
Putative DNA polymerase	AFX59875	7.00E-61	*White spot syndrome virus*	1
Gene expression, regulation & protein synthesis				
tail muscle elongation factor 1 gamma	ABG11961	2.00E-18	*Procambarus clarkii*	5
40S ribosomal protein S15-like	XP_002735558	5.00E-13	*Saccoglossus kowalevskii*	4
ribosomal protein S6	AEB54649	1.00E-105	*Procambarus clarkii*	3
Elongation factor 1-alpha	AAM90311	4.00E-39	*Litopenaeus stylirostris*	1
60S ribosomal protein L35Ae-like protein	ABV60321	4.00E-28	*Lutzomyia longipalpis*	1
translationally controlled tumor protein	ABY55541	3.00E-106	*Litopenaeus vannamei*	1
Eukaryotic initiation factor 4A	AGZ89665	6.00E-49	*Litopenaeus vannamei*	1
60S ribosomal protein L7a	EKC37537	1.00E-17	*Crassostrea gigas*	1
60S ribosomal protein L5-like	XP_001177830	3.00E-21	*Strongylocentrotus purpuratus*	1
Proteasome subunit alpha type	XP_001651498	3.00E-43	*Aedes aegypti*	1
Eukaryotic translation initiation factor 3 subunit C-like	XP_002005987	7.00E-44	*Ceratitis capitata*	1
tRNA-splicing ligase RtcB homolog	XP_003706516	9.00E-51	*Megachile rotundata*	1
Energy & metabolism				
Cytochrome *c* oxidase subunit III	NP_038293	2.00E-79	*Penaeus monodon*	7
ATP synthase	NP_038292	2.00E-20	*Penaeus monodon*	4
Cytochrome *b*	AAF36100	2.00E-96	*Penaeus monodon*	2
Cytochrome oxidase subunit II	AAL31589	5.00E-47	*Lepidopa californica*	2
Engulfment and cell motility protein 1	XP_003700803	1.00E-50	*Megachile rotundata*	2
Gelsolin	CCI71879	3.00E-72	*Homarus americanus*	2
Malate dehydrogenase	ACY66481	3.00E-98	*Scylla paramamosain*	1
Beta-thymosin 3	AFV39709	5.00E-77	*Pacifastacus leniusculus*	1
Beta-thymosin 5	AGI98173	6.00E-46	*Pacifastacus leniusculus*	1
Fructose-bisphosphate aldolase	BAM17865	6.00E-68	*Papilio xuthus*	1
CKLF-like MARVEL transmembrane domain-containing protein 4	EGI61226	3.00E-20	*Acromyrmex echinatior*	1
Arginase	EHJ70423	2.00E-05	*Danaus plexippus*	1
NADH dehydrogenase subunit 1	NP_038300	3.00E-80	*Penaeus monodon*	1
Lipoamide acyltransferase	XP_007250754	2.00E-61	*Astyanax mexicanus*	1
Cytochrome *c* oxidase subunit I	YP_001315033	9.00E-135	*Litopenaeus vannamei*	1
ATP synthase F0 subunit 6	YP_001315036	4.00E-28	*Litopenaeus vannamei*	1
ATP synthase F0 subunit 7	YP_001315036	4.00E-57	*Litopenaeus vannamei*	1
Transport				
Translocon-associated protein	EZA56351	1.00E-06	*Cerapachys biroi*	1
Tubulin alpha-1B chain-like, partial	XP_005139885	4.00E-60	*Melopsittacus undulatus*	1
Miscellaneous function				
Receptor accessory protein 5	AEB54634	1.00E-68	*Procambarus clarkii*	1
Putative myosin regulatory light chain 2 smooth muscle	ACY66440	2.00E-84	*Scylla paramamosain*	1
Pacifastin heavy chain	AFQ98270	1.00E-63	*Macrobrachium rosenbergii*	1
Hematological and neurological expressed 1 protein-like	XP_006635521	3.00E-05	*Lepisosteus oculatus*	1
Nucleosome assembly protein 1-like 1-like isoform X5	XP_005101976	1.00E-60	*Aplysia californica*	1
Hypothetical protein				
Hypothetical protein	CAM36311	2.00E-11	*Thermobia domestica*	37
Hypothetical protein	EFX75021	7.00E-15	*Daphnia pulex*	4
Hypothetical protein	EFZ19168	2.00E-06	*Solenopsis invicta*	2
Hypothetical protein	XP_002593268	5.00E-64	*Branchiostoma floridae*	1
Hypothetical protein	ELT90787	6.00E-23	*Capitella teleta*	1
Hypothetical protein	EFX68294	6.00E-111	*Daphnia pulex*	1
Hypothetical protein	EFX80903	1.00E-14	*Daphnia pulex*	1
Hypothetical protein	ENN75064	7.00E-20	*Dendroctonus ponderosae*	1
Hypothetical protein	ERL86130	1.00E-21	*Dendroctonus ponderosae*	1
Hypothetical protein	ESN92117	7.00E-169	*Helobdella robusta*	1
Hypothetical protein	ESO86545	2.00E-28	*Lottia gigantea*	1
Hypothetical protein	WP_004989554	9.00E-21	*Streptomyces ghanaensis*	1
Unknown proteins				50
Total				176

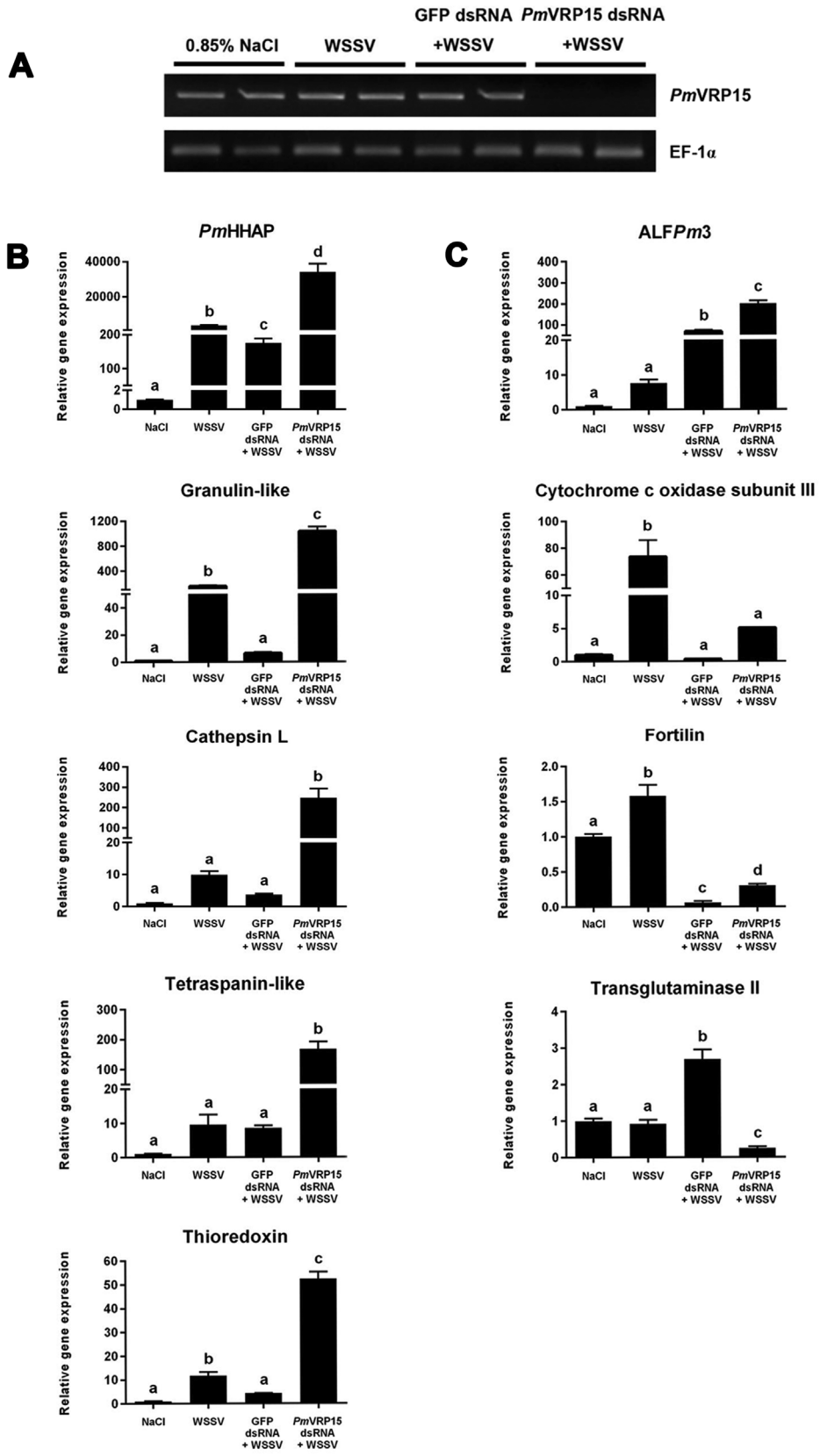


Fig. 2. Relative expression of selected genes from the forward and reverse libraries in hemocytes of NaCl control, WSSV-infected, GFP dsRNA-WSSV and *Pm*VRP15 dsRNA-WSSV groups by quantitative real-time RT-PCR. (A) Expression level of *Pm*VRP15, VP28 and EF-1α genes in WSSV-infected and *Pm*VRP15 knockdown shrimp hemocytes were analyzed with RT-PCR at 24 h post infection. (B) The selected up-regulated genes from the forward library are *Pm*HHAP, granulin-like, cathepsin L, tetraspanin-like and thioredoxin. (C) The selected down-regulated genes from the reverse library are antilipopolysaccharide factor isoform 3 (ALF*Pm*3), cytochrome c oxidase subunit III, (TGSII), fortilin and transglutaminase II (TGSII). The gene expression levels of selected genes relative to an internal reference control, EF-1α gene were analyzed in shrimp hemocytes using the $2^{-\Delta\Delta Ct}$ method (Pfaffl, 2001). The experiment was done in triplicate. Data is presented as means ± standard deviations. Different letters indicate significant differences between groups accepted at $P \leq 0.05$.

genes/proteins. In this study, SSH identified up- and down-regulated genes in *Pm*VRP15-silenced and WSSV-infected shrimp. Although SSH has proven successful in isolating differentially expressed genes, some false positive clones were still present [17]. Herein, the expression of selected genes was verified using qRT-PCR in an uninfected (0.85% NaCl challenged) control group and WSSV-challenged groups under the influence of *Pm*VRP15 suppression (WSSV alone or with GFP dsRNA and *Pm*VRP15 dsRNA). The efficiency of *Pm*VRP15 gene knockdown of

the sample was evaluated using RT-PCR analysis (Fig. 2A). Up-regulation under *Pm*VRP15 knockdown and WSSV infection of five genes from the forward library including cathepsin L, tetraspanins-like, thioredoxin, granulin-like and *Pm*HHAP was verified (Fig. 2B).

The crustaceans cathepsin L was firstly investigated in the American lobster, *Homarus americanus*, later also found in shrimp hepatopancreas, *P. vannamei* and *Metapenaeus ensis* [18–20]. The shrimp cathepsin plays roles in food digestion and regulation of cell morphology [21]. Moreover, cathepsin L is involved in shrimp antiviral immune defense by over-expressing after WSSV infection as in *L. vannamei* which has been reported [15]. According to our result, *P. monodon* cathepsin L was also highly up-regulated after WSSV infection under *Pm*VRP15 knockdown conditions. This result suggests that cathepsin L might be involved in the antiviral immune response.

Tetraspanins belong to the transmembrane 4 superfamily consisting of four transmembrane domains suggesting their major role in membrane biology [22]. Several tetraspanins were found early during evolution in *Drosophila melanogaster* and *Caenorhabditis elegans* [23,24]. Different tetraspanins from *Fenneropenaeus chinensis* were up-regulated in WSSV-challenged shrimp tissues [25]. An important role in response to WSSV infection of *Fc*Tetraspanin-3 has been revealed by dsRNA mediated gene silencing [26]. A sensible decrease of the viral copy number in the tetraspanin knockdown shrimp was found. Blocking a large extracellular loop of the tetraspanin domain of *Fc*Tetraspanin-3 with a specific antibody could inhibit WSSV infection. Likewise, our study showed that a tetraspanin-like gene was up-regulated upon WSSV infection and even higher in *Pm*VRP15 knockdown shrimp. This implies that in the decrease of *Pm*VRP15, tetraspanin-like gene should be expressed more and likely plays a role in antiviral defense.

Generally, thioredoxin is a key component of the redox homeostasis machinery in the cell after ROS production generated by oxidative stress [5]. In shrimp, especially in *L. vannamei* and *F. chinensis*, the thioredoxin gene is expressed in response to WSSV infection. Moreover, the function of *Fc*thioredoxin was involved in antiviral immunity [27-29]. Although, the mechanism involved in antiviral activity of shrimp thioredoxin is limited but it was evidenced that in mammals thioredoxin is an inhibitor of apoptosis and induces cell growth [30]. From our result, it was found that in *Pm*VRP15 knockdown shrimp, thioredoxin was highly up-regulated after WSSV infection. It can be surmised that thioredoxin helps shrimp lacking *Pm*VRP15 to fight against WSSV infection.

Granulin-like proteins have been identified in invertebrates including locusts [31], scallops [32], and leeches [33] and involved in the regulation of cell growth [34]. Granulin is a growth factor that induces a proliferative response in goldfish macrophages. It conduces to innate immune system as a critical soluble cofactor for Toll-like Receptor 9 signaling [35]. Extremely high up-regulation of the granulin-like gene in *Pm*VRP15 knockdown *P. monodon* infected with WSSV revealed that granulin-like expression is somehow under the influence of *Pm*VRP15 expression.

Interestingly, the greatest expression of *Pm*HHAP in WSSV-challenged shrimp under *Pm*VRP15 suppression was shown in the SSH forward library and qRT-PCR results. Furthermore, *Pm*VRP15 and *Pm*HHAP have been reported as WSSV-responsive genes [7]. Previously, Prapavorarat et al. (2010) reported that *Pm*HHAP gene knockdown resulted in a significant decrease of circulating hemocyte numbers indicating *Pm*HHAP's role in the regulation of hemocyte homeostasis [7]. There is evidence showing that *Pm*HHAP regulates hemocyte homeostasis by preventing apoptosis via caspase activation during viral infection [9]. In this study, *Pm*VRP15 suppression was found to lead to *Pm*HHAP gene up-regulation after WSSV infection suggesting that *Pm*VRP15 expression is probably involved in hemocyte homeostasis and/or apoptosis.

In contrast, it was expected that ALF*Pm*3, fortilin, cytochrome *c* oxidase subunit III and TGSII in the reverse SSH library were down-regulated under *Pm*VRP15 knockdown and WSSV infection. It was hypothesized that the function of down-regulated genes can probably also provide clues about the function of *Pm*VRP15. The expression of 3 out of 4 selected genes determined by qRT-PCR was different from expectations (Fig. 2C). The results showed that ALF*Pm*3, fortilin and cytochrome *c* oxidase subunit III were up-regulated upon WSSV infection as reported previously [15,16] but did not respond to *Pm*VRP15 knockdown in WSSV-infected shrimp.

The expression of TGSII identified from the reverse library agreed with findings from the significant down-regulated gene under *Pm*VRP15 suppression and WSSV infection analyzed with qRT-PCR. TGSII regulates circulating hemocytes in shrimp. The depletion of TGSII in *M. japonicas* led to a decrease in the total hemocyte count (THC) [36]. Similarly, Lin et al. (2008) reported that TGSII is involved in hemocyte homeostasis by preventing hematopoietic tissue differentiation or mature hemocyte production [37]. The very low expression of TGSII in *Pm*VRP15 knockdown and WSSV infection suggests that *Pm*VRP15 might function to promote TGSII expression to inhibit hemocyte production during WSSV infection.

As reported previously, *Pm*VRP15 might facilitate viral trafficking during WSSV infection via binding to WSV399 [12]. Our SSH results identified genes that have relevant functions in hemocyte homeostasis such as *Pm*HHAP and granulin-like and TGSII. The influence of *Pm*VRP15 on the expression of these genes was revealed by dsRNA mediated RNA interference. During WSSV infection *Pm*VRP15 over-expression resulted in reduction of *Pm*HHAP and granulin-like genes and an upsurge of TGSII genes suggesting the role of *Pm*VPP15 in negative regulation of hemocyte differentiation. Moreover, the homolog of C19 orf 12 shared some similarity (35–38%) with *Pm*VRP15. C19 orf 12 protein located in mitochondria and also exclusively present in the ER (endoplasmic reticulum) and MAM (mitochondria associated membrane). The putative function of C19 orf 12 protein involved in the induction of oxidative stress, inhibition of apoptosis and stimulation of autophagy, which are essential for the maintenance of cellular homeostasis and for determination of cell fate under pathogen invasion [38]. Taken together, it is proposed that *Pm*VRP15 is a key host protein that promotes WSSV infectivity by binding to viral tegument protein WSV399 to facilitate virus trafficking as well as inhibiting hemocyte differentiation. However, all the above-mentioned speculations still require confirmation.

Acknowledgments

This research is supported by the 90th Anniversary of Chulalongkorn University Fund (Ratchadaphiseksomphot Endowment Fund) to P.T. and by the Thailand Research Fund to the Department of Biochemistry, Faculty of Science, Chulalongkorn University (Grant No. IRG5780008). Partial support by the TRF Senior Research Scholar to A.T. (RTA5880004) is acknowledged. We also would like to thank Chulalongkorn University for the support to the Center of Excellence for Molecular Biology and Genomics of Shrimp and a postdoctoral fellowship to P.J. under the Ratchadaphisek Somphot Endowment Fund.

References

[1] S. Durand, D.V. Lightner, R.M. Redman, J.R. Bonami, Ultrastructure and morphogenesis of white spot syndrome baculovirus (WSSV), Dis. Aquat. Org. 29 (3) (1997) 205–211.

[2] M.C. van Hulten, J. Witteveldt, S. Peters, N. Kloosterboer, R. Tarchini, M. Fiers, H. Sandbrink, R.K. Lankhorst, J.M. Vlak, The white spot syndrome virus DNA genome sequence, Virology 286 (1) (2001) 7–22.

[3] A. Tassanakajon, K. Somboonwiwat, P. Supungul, S. Tang, Discovery of immune molecules and their crucial functions in shrimp immunity, Fish. Shellfish. Immunol. 34 (4) (2013) 954–967.

[4] A. Tassanakajon, V. Rimphanitchayakit, S. Visetnan, P. Amparyup, K. Somboonwiwat, W. Charoensapsri, S. Tang, Shrimp humoral responses against pathogens: antimicrobial peptides and melanization, Dev. Comp. Immunol. (2017), http://dx.doi.org/10.1016/j.dci.2017.05.009 (in press).

[5] F. Li, J. Xiang, Recent advances in researches on the innate immunity of shrimp in China, Dev. Comp. Immunol. 39 (1) (2013) 11–26.

[6] M.W. Johansson, P. Keyser, K. Sritunyalucksana, K. Söderhäll, Crustacean haemocytes and haematopoiesis, Aquaculture 191 (1) (2000) 45–52.
[7] A. Prapavorarat, T. Vatanavicharn, K. Söderhäll, A. Tassanakajon, A novel viral responsive protein is involved in hemocyte homeostasis in the black tiger shrimp, *Penaeus monodon*, J. Biol. Chem. 285 (28) (2010) 21467–21477.
[8] W.L. Xia, L.H. Kang, C.-B. Liu, C.-J. Kang, Death associated protein 1 (DAP 1) positively regulates virus replication and apoptosis of hemocytes in shrimp *Marsupenaeus japonicus*, Fish. Shellfish. Immunol. 63 (2017) 304–313.
[9] K. Apitanyasai, P. Amparyup, W. Charoensapsri, S. Senapin, A. Tassanakajon, Role of *Penaeus monodon* hemocyte homeostasis associated protein (*Pm*HHAP) in regulation of caspase-mediated apoptosis, Dev. Comp. Immunol. 53 (1) (2015) 234–243.
[10] T. Vatanavicharn, A. Prapavorarat, P. Jaree, K. Somboonwiwat, A. Tassanakajon, *Pm*VRP15, a novel viral responsive protein from the black tiger shrimp, *Penaeus monodon*, promoted white spot syndrome virus replication, PLoS. One 9 (3) (2014) e91930.
[11] J.H. Leu, K.F. Liu, K.Y. Chen, S.H. Chen, Y.B. Wang, C.Y. Lin, C.F. Lo, The novel white spot syndrome virus-induced gene, *Pm*ERP15, encodes an ER stress-responsive protein in black tiger shrimp, *Penaeus monodon*, Dev. Comp. Immunol. 49 (2) (2015) 239–248.
[12] P. Jaree, S. Senapin, I. Hirono, C.-F. Lo, A. Tassanakajon, K. Somboonwiwat, WSV399, a viral tegument protein, interacts with the shrimp protein *Pm*VRP15 to facilitate viral trafficking and assembly, Dev. Comp. Immunol. 59 (2016) 177–185.
[13] Q. Zhou, Y.-P. Qi, F. Yang, Application of spectrophotometry to evaluate the concentration of purified white spot syndrome virus, J. Virol. Methods 146 (1) (2007) 288–292.
[14] A. Prapavorarat, S. Pongsomboon, A. Tassanakajon, Identification of genes expressed in response to yellow head virus infection in the black tiger shrimp, *Penaeus monodon*, by suppression subtractive hybridization, Dev. Comp. Immunol. 34 (6) (2010) 611–617.
[15] Z.Y. Zhao, Z.X. Yin, S.P. Weng, H.J. Guan, S.D. Li, K. Xing, S.M. Chan, J.G. He, Profiling of differentially expressed genes in hepatopancreas of white spot syndrome virus-resistant shrimp (*Litopenaeus vannamei*) by suppression subtractive hybridisation, Fish. Shellfish. Immunol. 22 (5) (2007) 520–534.
[16] S. Visetnan, P. Supungul, S. Tang, I. Hirono, A. Tassanakajon, V. Rimphanitchayakit, YHV-responsive gene expression under the influence of *Pm*Relish regulation, Fish. Shellfish. Immunol. 47 (1) (2015) 572–581.
[17] L. Diatchenko, Y. Lau, A.P. Campbell, A. Chenchik, F. Moqadam, B. Huang, S. Lukyanov, K. Lukyanov, N. Gurskaya, E.D. Sverdlov, Suppression subtractive hybridization: a method for generating differentially regulated or tissue-specific cDNA probes and libraries, Proc. Natl. Acad. Sci. U.S.A. 93 (12) (1996) 6025–6030.
[18] M.V. Laycock, R.M. MacKay, M. Di Fruscio, J.W. Gallant, Molecular cloning of three cDNAs that encode cysteine proteinases in the digestive gland of the American lobster (*Homarus americanus*), Febs. Lett. 292 (1–2) (1991) 115–120.
[19] C. Le Boulay, D. Sellos, A. Van Wormhoudt, Cathepsin L gene organization in crustaceans, Gene 218 (1) (1998) 77–84.
[20] K.J. Hu, P.C. Leung, Shrimp cathepsin L encoded by an intronless gene has predominant expression in hepatopancreas, and occurs in the nucleus of oocyte, Comp. Biochem. Phys. B 137 (1) (2004) 21–33.
[21] K.J. Hu, P.C. Leung, Food digestion by cathepsin L and digestion-related rapid cell differentiation in shrimp hepatopancreas, Comp. Biochem. Phys. B 146 (1) (2007) 69–80.
[22] C. Boucheix, E. Rubinstein, Tetraspanins, Cell. Mol. Life Sci. 58 (9) (2001) 1189–1205.
[23] E. Todres, J. Nardi, H. Robertson, The tetraspanin superfamily in insects, Insect. Mol. Biol. 9 (6) (2000) 581–590.
[24] M.G. Tomlinson, M.D. Wright, A new transmembrane 4 superfamily molecule in the nematode, *Caenorhabditis elegans*, J. Mol. Evol. 43 (3) (1996) 312–314.
[25] B. Wang, F. Li, J. Xiang, L. Gui, Z. Luo, H. Yan, Three tetraspanins from Chinese shrimp, *Fenneropenaeus chinensis*, may play important roles in WSSV infection, J. Fish. Dis. 33 (1) (2010) 15–29.
[26] L. Gui, B. Wang, F.-H. Li, Y.-M. Sun, Z. Luo, J.-H. Xiang, Blocking the large extracellular loop (LEL) domain of *Fc*Tetraspanin-3 could inhibit the infection of white spot syndrome virus (WSSV) in Chinese shrimp, *Fenneropenaeus chinensis*, Fish. Shellfish. Immunol. 32 (6) (2012) 1008–1015.
[27] E. Aispuro-Hernandez, K.D. Garcia-Orozco, A. Muhlia-Almazan, L. del-Toro-Sanchez, R.M. Robles-Sanchez, J. Hernandez, G. Gonzalez-Aguilar, G. Yepiz-Plascencia, R.R. Sotelo-Mundo, Shrimp thioredoxin is a potent antioxidant protein, Comp. Biochem. Phys. C 148 (1) (2008) 94–99.
[28] K.D. Garcia-Orozco, A. Sanchez-Paz, E. Aispuro-Hernandez, S. Gomez-Jimenez, A. Lopez-Zavala, S. Araujo-Bernal, A. Muhlia-Almazan, Gene expression and protein levels of thioredoxin in the gills from the whiteleg shrimp (*Litopenaeus vannamei*) infected with two different viruses: the WSSV or IHHNV, Fish. Shellfish. Immunol. 32 (6) (2012) 1141–1147.
[29] Q. Ren, R.-R. Zhang, X.-F. Zhao, J.-X. Wang, A thioredoxin response to the WSSV challenge on the Chinese white shrimp, *Fenneropenaeus chinensis*, Comp. Biochem. Phys. C 151 (1) (2010) 92–98.
[30] G. Powis, W.R. Montfort, Properties and biological activities of thioredoxins, Annu. Rev. Biophys. Biomol. Struct. 30 (1) (2001) 421–455.
[31] N. Nakakura, H. Hietter, A. Dorsselaer, B. Luu, Isolation and structural determination of three peptides from the insect *Locusta migratoria*, Febs. J. 204 (1) (1992) 147–153.
[32] K. Nara, H. Matsue, T. Naraoka, Granulin-like peptide in the mid-gut gland of the bivalve mollusk, *Patinopecten yessoensis*, Biochim. Biophys. Acta 1675 (1) (2004) 147–154.
[33] S.J. Hong, K.W. Kang, Purification of granulin-like polypeptide from the blood-sucking leech, *Hirudo nipponia*, Protein. Expr. Purif. 16 (2) (1999) 340–346.
[34] A. Bateman, H. Bennett, Granulins: the structure and function of an emerging family of growth factors, J. Endocrinol. 158 (2) (1998) 145–151.
[35] B. Park, L. Buti, S. Lee, T. Matsuwaki, E. Spooner, M.M. Brinkmann, M. Nishihara, H.L. Ploegh, Granulin is a soluble cofactor for toll-like receptor 9 signaling, Immunity 34 (4) (2011) 505–513.
[36] L. Lorand, R.M. Graham, Transglutaminases: crosslinking enzymes with pleiotropic functions, Nat. Rev. Mol. Cell Biol. 4 (2) (2003) 140.
[37] X. Lin, K. Söderhäll, I. Söderhäll, Transglutaminase activity in the hematopoietic tissue of a crustacean, *Pacifastacus leniusculus*, importance in hemocyte homeostasis, Bmc. Immunol. 9 (1) (2008) 58.
[38] P. Venco, M. Bonora, C. Giorgi, E. Papaleo, A. Iuso, H. Prokisch, P. Pinton, V. Tiranti, Mutations of C19orf12, coding for a transmembrane glycine zipper containing mitochondrial protein, cause mis-localization of the protein, inability to respond to oxidative stress and increased mitochondrial Ca^{2+}, Front. Genet. 6 (2015).

Fish and Shellfish Immunology 79 (2018) 18–27

Contents lists available at ScienceDirect

Fish and Shellfish Immunology

journal homepage: www.elsevier.com/locate/fsi

Full length article

Silencing of a Kazal-type serine proteinase inhibitor *SPIPm2* from *Penaeus monodon* affects YHV susceptibility and hemocyte homeostasis

Suwattana Visetnan[a], Suchao Donpudsa[b,**], Anchalee Tassanakajon[a], Vichien Rimphanitchayakit[a,*]

[a] Center of Excellence for Molecular Biology and Genomics of Shrimp, Department of Biochemistry, Faculty of Science, Chulalongkorn University, Phyathai Road, Bangkok 10330, Thailand
[b] Department of Chemistry, Faculty of Science, Srinakharinwirot University, Bangkok 10110, Thailand

ARTICLE INFO

Keywords:
Kazal-type serine proteinase inhibitor
SPI*Pm2*
Penaeus monodon
YHV
Homeostasis

ABSTRACT

In shrimp, the Kazal-type serine proteinase inhibitors (KPIs) are involved in host innate immune defense system against pathogenic microorganisms. A five-Kazal-domain SPI*Pm2* is the most abundant KPIs in the black tiger shrimp *Penaeus monodon* and up-regulated in response to yellow head virus (YHV) infection. In this study, the role of SPI*Pm2* in YHV infection was investigated. The expression of SPI*Pm2* in hemocytes, gill and heart from 48-h YHV-infected shrimp was increased. The expression of SPI*Pm2* in hemocytes was significantly increased after 12 h of infection and gradually increased higher afterwards. Silencing of *SPIPm2* by dsRNA interference resulted in the increased expression of different apoptosis-related genes, the increased expression of transcriptional factors of antimicrobial synthesis pathways, the reduction of circulating hemocytes in the shrimp hemolymph, and the increased susceptibility of the silenced shrimp to YHV infection. The activities of caspase-3 and caspase-7 in the hemocytes of *SPIPm2*-silenced shrimp was also increased by 5.32-fold as compared with those of the control shrimp. The results suggested that the SPI*Pm2* was involved in the hemocyte homeostasis.

1. Introduction

Serine proteinase inhibitors (SPIs) are widely distributed in living organisms and play crucial roles in many proteinase-mediated biological processes, such as the complement system, blood coagulation, melanization, innate immune system, apoptosis pathway, etc., by regulating the proteinase activity spatially and temporally [1–4].

In shrimp, several SPIs linked to the innate immune system have been identified [5]. Based on structures, topological similarities and inhibition mechanisms, the SPIs are classified into several families such as Kunitz-type, serpin, alpha-2-macroglobulin, pacifastin and Kazal-type [6]. The Kazal-type SPIs (KPIs) have been extensively studies in shrimp [1]. They usually are multi-domain proteins consisting of more than one Kazal domain. Each Kazal domain is about 50–60 amino acid residues in length with six conserved cysteine residues forming three intra-molecular disulfide bridges [1,7]. A typical or canonical Kazal domain has a three-conserved disulfide-bond pattern: Cys1→Cys5, Cys2→Cys4 and Cys3→Cys6, that the first cysteine residue forms bridges with the fifth cysteine residue and so on [8,9]. The inhibitory specificity of each domain is determined mainly by the P1 amino acid residue which is the second amino acid residue after the second cysteine. The interaction of the side chain of P1 amino acid residue is the key to different inhibitory activity [8,10].

Previously, at least 9 types of KPIs, named SPI*Pm*1-SPI*Pm*9, have been identified from the *Penaeus monodon* EST database [11,12]. The SPI*Pm2* is the most abundant KPI in the EST libraries. It consists of five Kazal domains and is capable of inhibiting subtilisin and elastase but does not inhibit chymotrypsin [13]. It also has bacteriostatic activity against *Bacillus subtilis* [14]. The SPI*Pm2* is stored in the granules of granular and semi-granular hemocytes and released into the hemolymph upon white spot syndrome virus (WSSV) infection [15]. The expression of *SPIPm2* gene is increased in response to viral infection by WSSV and yellow head virus (YHV). For WSSV infection, the SPI*Pm2* restricts the propagation of WSSV and neutralizes the WSSV infectivity [15–18].

In this study, we are also interested in a KPI, SPI*Pm2*, from the black tiger shrimp *P. monodon* and would like to know how it works in shrimp. Herein, we report the possible function of SPI*Pm2* in shrimp and its activity against YHV infection.

* Corresponding author.
** Corresponding author.
E-mail addresses: dsuchao@gmail.com (S. Donpudsa), kpvr2@yahoo.com (V. Rimphanitchayakit).

https://doi.org/10.1016/j.fsi.2018.05.004
Received 17 January 2018; Received in revised form 20 March 2018; Accepted 2 May 2018
Available online 04 May 2018
1050-4648/ © 2018 Published by Elsevier Ltd.

2. Materials and methods

2.1. Animals and YHV

The healthy shrimp, *P. monodon*, weighting 5–15 g (approximately 5 g for gene silencing and 10–15 g for other experiments) were obtained from a farm of Charoen Pokphand (CP), Chanthaburi Province, Thailand. The shrimp were cultured temporarily and acclimatized in aquaria at an ambient temperature of about 28 ± 1 °C for 1 week before processing.

The YHV suspension was the hemolymph drawn with anticoagulant from the moribund YHV-infected *P. monodon* according to Pongsomboon et al. (2008) [19]. In this study, the YHV suspension used induced accumulative mortality of 50% within 60 h post injection [20].

2.2. Tissue distribution of SPIPm2

The expression of *SPIPm2* was determined by RT-PCR in six shrimp tissues: heart, hepatopancreas, hemocytes, gill, lymphoid organ and intestine. The shrimp tissues were collected from normal and YHV-infected shrimp. Shrimp were injected with 50 μL of YHV suspension in 0.85% (w/v) NaCl for experimental group and 50 μL of 0.85% (w/v) NaCl for the control group. The various tissues were collected at 48 h post injection. These tissues were extracted for total RNA using a FavorPrep™ Blood/Cultured Cell Total RNA Purification Mini Kit (Favorgen). The cDNA template for RT-PCR was prepared from 1 μg of total RNA using a cDNA First-strand Synthesis Kit (Fermentas) according to the manufacturer's instruction.

The specific primers for *SPIPm2*, *SPIPm2*-F and *SPIPm2*-R, were used in the PCR analysis of *SPIPm2* expression following a protocol by Visetnan et al., 2009 [12] (Table 1). The PCR amplification was performed in 25 μL reaction volume containing appropriate amount of first-strand cDNA, 500 mM KCl, 15 mM $MgCl_2$, 100 mM Tris–HCl pH 8.3, 1 mg/ml BSA, 100 mM $(NH_4)_2SO_4$, 0.2 mM each dNTP, 0.4 mM each primer and 1.5 units Tag DNA polymerase (RBC Bioscience). The reaction was denaturation at 94 °C for 2 min followed by 32 cycles for *SPIPm2* or 25 cycles for the elongation factor 1-α gene (*EF-1α*) of 94 °C for 30 s, annealing at 60 °C for SPI*Pm2* or 52 °C for *EF-1α* for 30 s and extension at 72 °C for 30 s, and the final extension step at 72 °C for 10 min. The *EF-1α* was used as an internal control. Amplified products of 250 bp for *SPIPm2* and 150 bp for *EF-1α* were analyzed with 2.5% agarose gel electrophoresis.

2.3. Expression of SPIPm2 in YHV-challenged shrimp

To study the expression of *SPIPm2* in the hemocytes of YHV-infected shrimp, the shrimp were injected with 50 μL of YHV suspension in 0.85% (w/v) NaCl. The control shrimp were injected with 50 μL of 0.85% (w/v) NaCl. The shrimp hemocytes were collected from 5 shrimp each at 3, 6, 12, 24, 48 and 72 h post infection (hpi). The total RNA was prepared and subjected to cDNA synthesis. The transcription levels of *SPIPm2* were analyzed by real-time PCR using specific primers (Table 1). The expression of *EF-1α* was used as an internal control. Three replicates of qRT-PCR were performed.

The 10 μL of real-time PCR master mix containing 5 μL of an iCycleriQ™ Real-Time Detection system using iQ™ SYBR Green Supermix (Bio-Rad), 1 μL of 10 μM of forward and reverse primer mix, an appropriate amount of cDNA for each gene and distilled water to 10 μL. The real-time PCR condition was 95 °C for 2 min, 40 cycles of 95 °C for 30 s, 60 °C for 30 s and 72 °C for 45 s. The real-time PCR efficiencies for *SPIPm2* and *EF-1α* were 101.6 and 99.8%, respectively. Relative expression was calculated using a mathematic model of Pfaffl (2001) [21]. The data were calculated for statistically significant using one-way ANOVA followed by Duncan's new multiple ranges test and presented as means ± SDs. The significant differences were considered at $P < 0.05$.

2.4. SPIPm2 gene silencing mediated by double-stranded RNA (dsRNA) interference

To explore the function of SPI*Pm2* in the shrimp immune system, the dsRNA-mediated gene knockdown of *SPIPm2* was performed. The dsRNA corresponding to part of *SPIPm2* gene was synthesized by using the T7 RiboMAX™ Express RNAi System (Promega). Primers KD-*SPIPm2*-T7_F/KD-*SPIPm2*_R and KD-*SPIPm2*_F/KD-*SPIPm2*_T7R (Table 1) for the synthesis of upper and lower RNA strands, respectively, were designed from the specific *SPIPm2* gene region (nucleotides 351–691 of the openreading frame of *SPIPm2* [13]). The *GFP* dsRNA as a control for dsRNA treatment was produced using primers KD_*GFP*_T7F/KD_*GFP*_R and KD_*GFP*_F/KD_*GFP*_T7R (Table 1). Briefly, a recombinant plasmid containing either *SPIPm2* gene or *GFP* gene was used as a template in the PCR reaction using *Taq* DNA polymerase (RBC Bioscience) as described above. One microgram of each PCR product was used as a template for *in vitro* transcription using the T7 RiboMAX™ Express Large Scale RNA Production System (Promega) according to the manufacturer's protocol. The quality and amount of dsRNAs were verified by 1.5% agarose gel electrophoresis and measured spectrophotometrically, respectively.

The dsRNA silencing was conducted in three groups of shrimp by the injection of 10 or 15 μg/g shrimp of *SPIPm2* dsRNA or 15 μg/g shrimp of *GFP* dsRNA into nine shrimp per group. After 12 h, the shrimp in each group were randomly selected and collected the hemolymph from three individual shrimp for total RNA extraction and first strand cDNA synthesis as described above. The RT-PCR with the primers *SPIPm2*-F and *SPIPm2*-R (Table 1) was used to detect the efficiency of dsRNA silencing. The experiment was repeated three times. The expression of *EF-1α* was used as an internal control.

To prepare the samples for qRT-PCR analysis of the expression of immune genes (see below), the shrimp were given double injection of dsRNA to ensure the silencing as much as possible of the *SPIPm2* expression. The two groups of ten shrimp were given double injection with 20 μL of *SPIPm2* dsRNA (15 μg/g shrimp) and *GFP* dsRNA (15 μg/g shrimp). After 12 h, the shrimp were given the second injection with the same amounts of dsRNA solutions. After 12 h of second injection, the hemolymph was collected from each group (5 shrimp/group).

2.5. Effect of SPIPm2 silencing on the transcription of immune-related genes

After testing the efficiency of dsRNA interference, we investigated the effect of *SPIPm2* silencing on the expression of 20 immune genes: *ALFPm3*, *crustinPm1*, *crustinPm7*, *SWDPm2*, *penaeidin3*, *penaeidin5*, *cyclophilin A*, *PmKunitz*, *SPIPm5*, *PmIAP*, *PmHHAP*, *Pmcaspase3* and *Pmcaspase3c*, *PmToll*, *PmDorsal*, *PmRelish*, *PmPO1*, *PmPO2*, *PmPPAE1* and *PmPPAE2*, using real-time RT-PCR.

The qRT-PCR was performed using an appropriated amount of cDNA for each gene in an iCycleriQ™ Real-Time Detection System using PerffeCTa® SYBR®Green FastMix® (Quanta, Biosciences™) with the following condition: 95 °C for 1 min, 40 cycles of 95 °C for 30 s, 57 °C for 30 s and 72 °C for 45 s. The real-time PCR reaction was done in triplicate. The standard curve for 20 genes and *EF-1α* was generated by running triplicate reactions of 5 different cDNA concentrations prepared by 2-fold serial dilution as described above. The real time PCR efficiencies for the immune genes are in the range 97%–102%. The data were presented as means ± standard deviations. The statistical significance of the data was determined by one-way ANOVA followed by post hoc test (Dancan's new multiple range test). The values were considered significant at $P < 0.05$.

2.6. Circulating hemocytes in SPIPm2-knockdown shrimp

In order to examine the number of shrimp circulating hemocytes after *SPIPm2* gene knockdown, the 3 groups of 5 shrimp each were injected with 20 μL of 0.85% (w/v) NaCl, 20 μL of *GFP* dsRNA and 20 μL

Table 1
Primers used in this study.

Primer Names	Sequences (5′–3′)	Usage	Analysis of gene(s)
SPIPm2-F	ATGCAACCACGTCTGTACTG	RT-PCR of *SPIPm2*	SPI*Pm2*
SPIPm2-R	CTGCAAGGTTCCACATCT		
EF-1a_F	GGTGCTGGACAAGCTGAAGGC	Internal control gene	
EF-1a_R	CGTTCCGGTGATCATGTTCTTGA		
ALFPm3_F	CCCACAGTGCCAGGCTCAA	RT-PCR and real-time PCR	Antimicrobial peptides
ALFPm3_R	TGCTGGCTTCTCCTCTGATG		
CrustinPm1_F	CTGCTGCGAGTCAAGGTATG		
CrustinPm1_R	AGGTACTGGCTGCTCTACTG		
CrustinPm7_F	CGGCAGGTGTCCACAGATTCG		
CrustinPm7_R	AATTGATGAGTCGAACATGCAGGCCTAT		
SWDPm2_F	CGGCATCATCACCACGTGCGAG		
SWDPm2_R	TCAGTAACCTTTCCAGGGAGAC		
Penaeidin3_F	GGCTTAGCCCCTTACA		
Penaeidin3_R	GACCCATACCTACAAATAAC		
Penaeidin5_F	ATCCCGACCTATTAGTACTC		
Penaeidin5_R	TTATCCTTTCAATGCAGAACAA		
CyclophilinA_F	ATCGCATATGGGCAACCCCAAG		Cytosolic binding protein
CyclophilinA_R	ATCGCTCGAGCAGCTGGCCGCAGTT		
PmKunitz_F	GCCATGGGCCTACTCCGCCCA		Serine proteinase inhibitors
PmKunitz_R	GCTCGAGTCGGCCGCAGAC		
SPIPm5_F	TGGAACGGACGGCAAGACAT		
SPIPm5_R	GTCGTGACAGTCTTGAGTCC		
PmIAP_F	ACAGATGGGACACTGAGTAAGAGCG		Apoptosis-related proteins
PmIAP_R	AAGCCAAGGAGATGACGAGGCAATG		
PmHHAP_F	GCAACAGGAGAACCTGTGGATA		
PmHHAP_R	GGTTCCAGAATCGCCTCCTATA		
Pmcaspase3_F	GGAGGAACCTGCGAAGAACG		
Pmcaspase3_R	AGAACACCTCAGGCTGGAAC		
Pmcaspase3b_F	TTGGACGCTATGACCTGCTA		
Pmcaspase3b_R	ACAAGTCTGTCAGCCTCTTC		
PmToll_F	GAATGCTTCCTCGGGTCTGC		Toll receptor
PmToll_R	GCTCAGCCATGACGAGATTC		
PmDorsal_F	GAGCCACACGAGTACCATCT		Transcription factors
PmDorsal_R	GGACATAGCTGGACCTTGTG		
PmRelish_F	TCTCCAGGTGAGCACTCAGTTGGC		
PmRelish_R	GCTGTAGCTGTTGCTGTTGTTGAG		
PmPO1_F	GGTCTTCCCCTCCCGCTTCG		Enzymes in proPO activating system
PmPO1_R	GCCGCAGGTCCTTTGGCAGC		
PmPO2_F	GCCAAGGGGAACGGGTGATG		
PmPO2_R	TCCCTCATGGCGGTCGAGGT		
PmPPAE1_F	ATGAAGGGCGTGACGGTGGTTCTATG		
PmPPAE1_R	CTCTTCTTCAAGCTCACCACTTCTATCT		
PmPPAE2_F	ATGCACTACCGGGTTCCCACGATC		
PmPPAE2_R	CTAAGGTTTGAGATTCTGCACG		
KD_SPIPm2_F	CGATGGACGTTGTGGTT	Preparation of dsRNA for gene silencing	SPI*Pm2* and GFP
KD_SPIPm2_R	TTCCGCACACGGGGTAA		
KD_SPIPm2_T7F	GGATCCTAATACGACTCACTATAGGCGATGGACGTTGTGGTT		
KD_SPIPm2_T7R	GGATCCTAATACGACTCACTATAGGTTCCGCACACGGGGTAA		
KD_GFP_F	ATGGTGAGCAAGGGCGAGGA		
KD_GFP_R	TTACTTGTACAGCTCGTCCA		
KD_GFP_T7F	GGATCCTAATACGACTCACTATAGGATGGTGAGCAAGGGGGAGGA		
KD_GFP_T7R	GGATCCTAATACGACTCACTATAGGTTACTTGTACAGCTCGTCCA		

of *SPIPm2* dsRNA for control group, *GFP* dsRNA control group and *SPIPm2* dsRNA silencing group, respectively, as described above. The total hemocytes were collected and washed once with 1 × PBS and re-suspended in 200 μL of 2 × L15 medium supplemented with 20% fetal bovine serum (GIBCO). The total hemocyte suspensions were counted with a hemocytometer under a light microscope. The numbers of total hemocytes in each group were recorded. The experiment was done in triplicate. The data were calculated, and analyzed by one-way ANOVA followed by post hoc test (Dancan's new multiple range test). The significant difference was accepted at $P < 0.05$.

2.7. Effect of SPIPm2 knockdown on the caspase activity in shrimp hemocytes

The activities of caspase-3 and caspase-7 were investigated in the hemocytes of *SPIPm2*-knockdown shrimp to determine whether the caspase proteins were also increased. The shrimp with an average weight of 10–15 g were used for dsRNA silencing as described above. After 12 h post second injection, the hemolymph was collected and the hemocytes were separated and washed three 3 times with 1 × PBS by centrifugation. The hemocytes were resuspended with 1 × PBS. The total protein concentration of hemocyte preparation was measured using Bradford Reagent (Bio-Rad) [22]. The shrimp hemocytes from three shrimps per group were pooled and assayed for the caspase-3 and caspase-7 activities using the Caspase-Glo 3/7 Assay Kit (Promega) following the manufacturer's protocol.

Briefly, 100 μL (200 μg of total protein) of the pooled hemocytes was added into the 96-well white plate. Then, 100 μL of Caspase-Glo reagents was added and mixed. The plate was incubated at room temperature for 15 min. The luminescence was determined from each well in a plate-reading luminometer (Molecular devices). The caspase activity assay was performed three times. The data were analyzed and reported using GraphPad Prism.

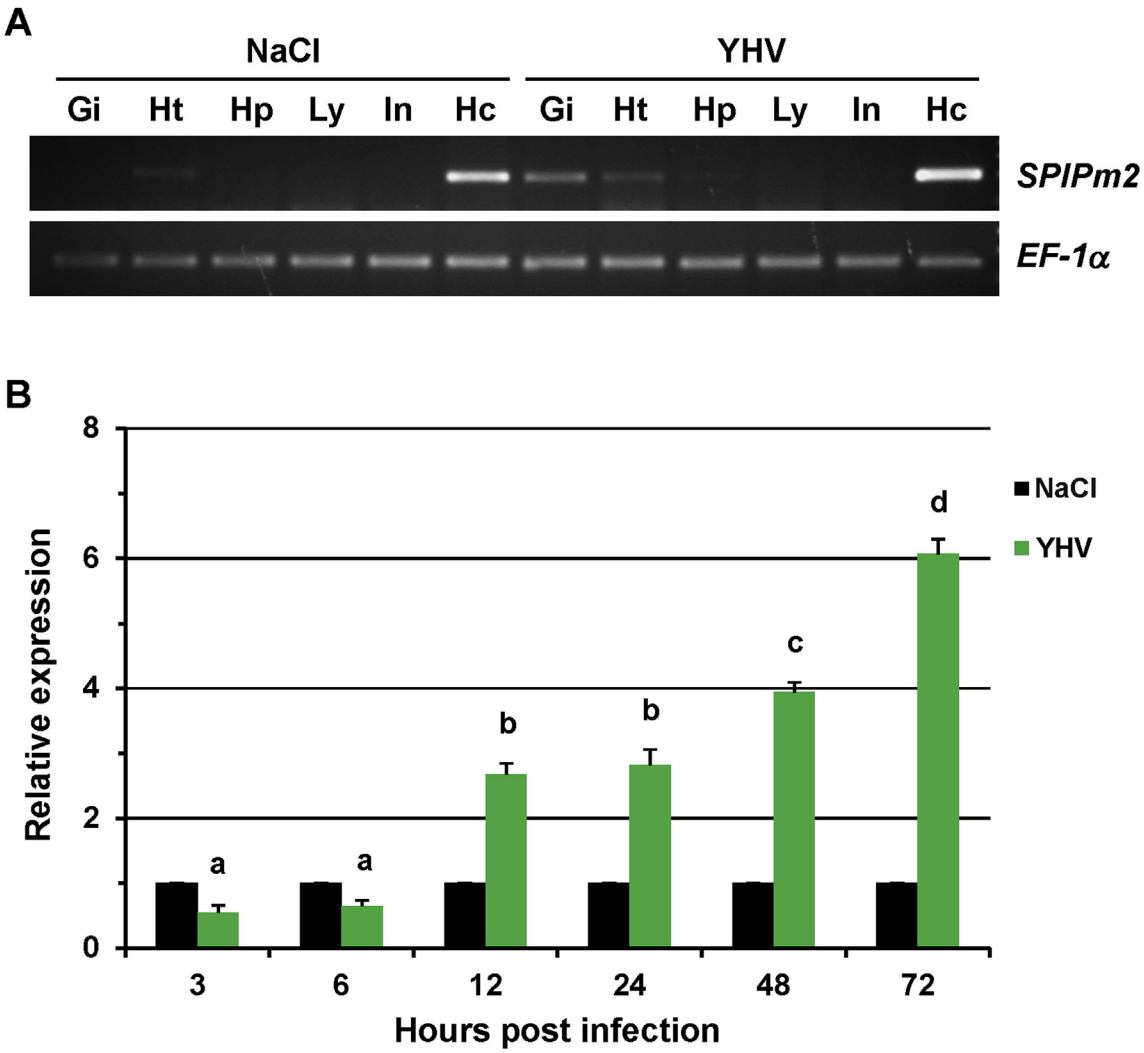


Fig. 1. The expression of *SPIPm*2 in shrimp tissues in response to YHV infection. (A) Six tissues: gill (Gi), heart (Ht), hepatopancreas (Hp), lymphoid organ (Ly), intestine (In) and hemocytes (Hc) were collected from normal and 48-h YHV-infected shrimp for RT-PCR analysis of *SPIPm*2 gene expression. (B) The real-time RT-PCR analysis of *SPIPm*2 gene expression in hemocytes at various time points after YHV infection relative to normal saline control. The data are means ± standard deviations. Different letters indicate significant differences accepted at $P < 0.05$. In both cases, the expression of *EF-1α* was used as an internal control.

2.8. Mortality assay of SPIPm2-silenced and SPIPm2-injected shrimp against YHV

To determine the importance of *SPIPm2* in the shrimp immune defense against YHV, the Juvenile shrimp (5 g) were divided into six groups of ten shrimp. They were injected with 20 μL of 0.85% NaCl, YHV suspension, *GFP* dsRNA, *SPIPm2* dsRNA, *GFP* dsRNA plus YHV and *SPIPm2* dsRNA plus YHV. The YHV preparation used caused 100% mortality in 3–4 days. The shrimp mortality rate was observed and recorded every 6 h up to 84 h.

In another experiment using an opposite approach, the recombinant SPI*Pm*2 (rSPI*Pm*2) was over-expressed in an *E. coli* system using a protocol from Somprasong et al. (2006) [13]. The rSPI*Pm*2 was injected into the shrimp to determine whether it had any effect on the YHV infection. The shrimp were divided into four groups of ten shrimp and each injected with carbonate buffer as a control, 1.8 nmol rSPI*Pm*2, 1.8 nmol SPI*Pm*2 plus YHV and YHV. The YHV suspension used had an LD_{50} of about 48 h. The shrimp mortality rate was observed every 12 h up to 172 h.

The above experiments were repeated three times. The data were plotted and analyzed using GraphPad Prism.

3. Results

The KPI, called SPI*Pm*2, has been studied for some time. It was identified from the hemocyte EST libraries of *P. monodon* [23]. It is highly abundant in shrimp hemolymph and its expression is responsive to viral-infection [12,16,18,19]. It has been shown to negatively affect the WSSV infection and help the shrimp defend against the virus. Besides the WSSV, the expression of SPI*Pm*2 is also up-regulated in response to YHV infection [16]. The effect of SPI*Pm*2 on YHV infection in shrimp were, then, investigated.

3.1. Expression of SPIPm2 in shrimp in response to YHV-infection

The *SPIPm2* transcript is expressed abundantly in shrimp hemocytes [17,24]. The tissue distribution of *SPIPm2* expression from six tissues of YHV-infected shrimp: gill, heart, hepatopancreas, lymphoid organ, intestine and hemocytes, were examined by RT-PCR compared with that of normal shrimp. The results showed that the *SPIPm2* was mainly synthesized in hemocytes and the YHV infection could up-regulate the expression of *SPIPm2* in gill, heart and hemocytes but not in hepatopancreas, lymphoid organ and intestine (Fig. 1 A).

The expression of *SPIPm*2 in response to YHV infection was explored further in hemocytes using real-time PCR to see the expression

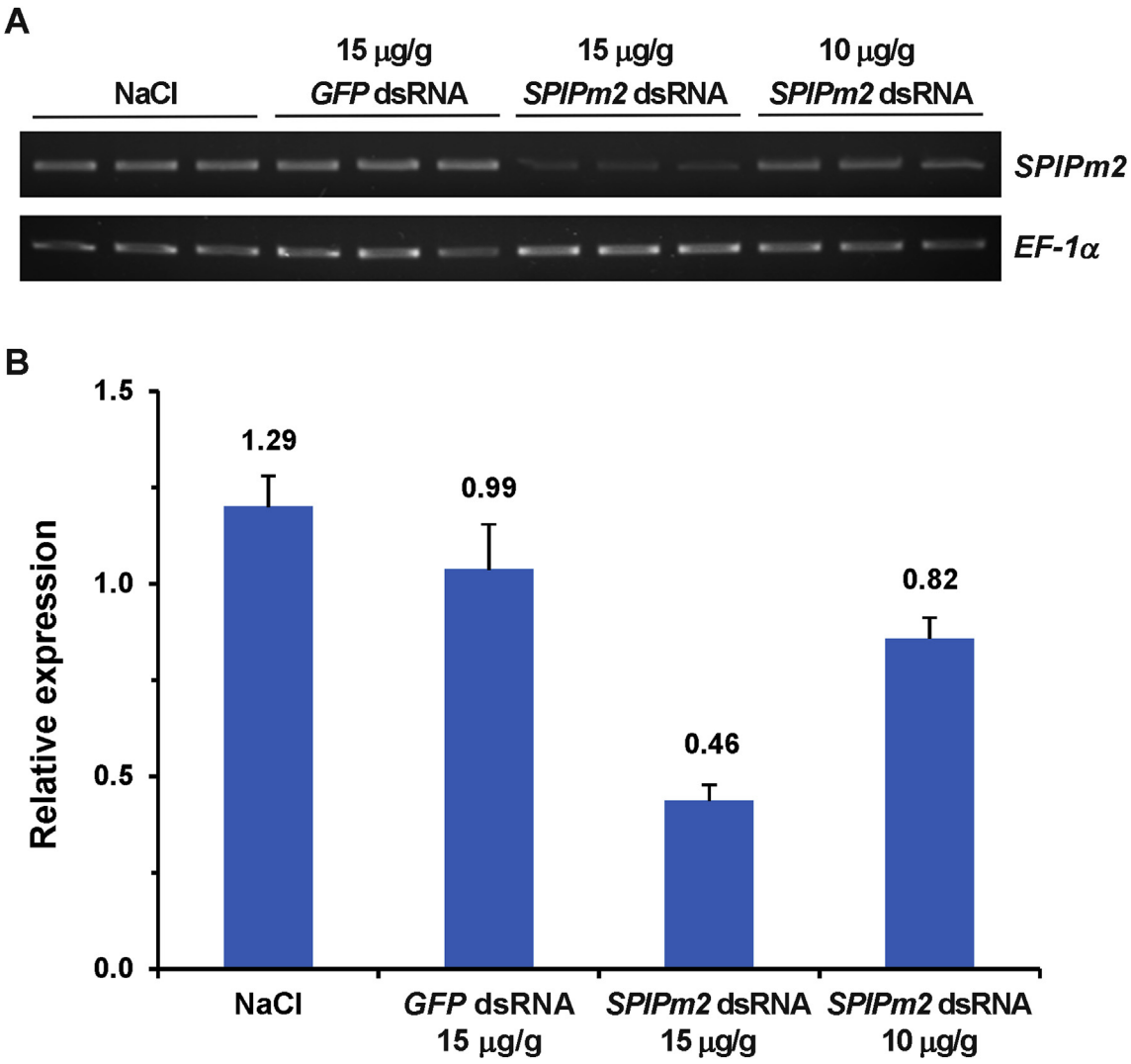


Fig. 2. Silencing of *SPIPm2*. The normal shrimp was injected with 0.85% (w/v) NaCl, *GFP* dsRNA and *SPIPm2* dsRNA. At 12 h after injection, the expression of *SPIPm2* was analyzed by RT-PCR. The *EF-1α* was used as a control. (A) Agarose gel electrophoresis analysis of the RT-PCR products. (B) The graph of relative expression of *SPIPm2*. The data are means ± standard deviations of the band intensities normalized by those of *EF-1α* of the four shrimp groups. The mean values are shown above the bars. The statistical analysis indicates significant differences accepted at $P < 0.05$.

timewise. Upon YHV infection, the expression of *SPIPm2* was increased gradually from 3-fold at 12 hpi to 6-fold at 72 hpi (Fig. 1 B). Interestingly, the transcription of *SPIPm2* was down-regulated in early hours of YHV infection. Therefore, the YHV infection, indeed, increased the expression of the *SPIPm2* gene.

3.2. Silencing of SPIPm2 by dsRNA interference

The above results indicated that the SPI*Pm2* may be somehow involved in YHV defense. To investigate the function of *SPIPm2* in YHV infection, the dsRNA interference was employed to silence the expression of *SPIPm2* gene. Preliminary testing was done by injecting 10 μg/g and 15 μg/g shrimp of *SPIPm2* dsRNA into the shrimp and the interference was checked by RT-PCR at 12 h after injection (Fig. 2 A). It was found that the expression of *SPIPm2* was reduced by 36% and 65% when 10 μg/g and 15 μg/g shrimp were used, respectively, compared with that in control group (0.85% (w/v) NaCl) (Fig. 2 B). Subsequently, the two consecutive doses of 15 μg/g shrimp were used for silencing the expression of *SPIPm2*. The percentage of gene silencing of the latter protocol remained more or less the same (data not shown).

3.3. Effect of SPIPm2 silencing on the transcription of immune related-genes

Upon infection, the expression of *SPIPm2* is up-regulated and the protein product may perform its function to help the shrimp defense against YHV. The presence of SPI*Pm2* protein might influence the functions of other immune proteins as well as their expression in the defense mechanism. On the other hand, the lack of SPI*Pm2* might also influence the function of the same set of immune genes. Therefore, we explored the effect of *SPIPm2* knockdown on the transcription of twenty shrimp immune-related genes: *ALFPm3*, *crustinPm1*, *crustinPm7*, *SWDPm2*, *penaeidin3*, *penaeidin5*, *cyclophilinA*, *PmKunitz*, *SPIPm5*, *PmIAP*, *PmHHAP*, *Pmcaspase3*, *Pmcaspase3c*, *PmToll*, *PmDorsal*, *PmRelish*, *PmPO1*, *PmPO2*, *PmPPAE1* and *PmPPAE2*.

The shrimp were given two consecutive injections of dsRNA to ensure that the expression of *SPIPm2* was suppressed. The hemolymph was collected afterwards at 12 h for real-time RT-PCR analysis. The results showed that the expressions of antimicrobial peptide genes: *crustinPm1*, *crustinPm7*, *SWDPm2*, *penaeidin3* and *penaeidin5*, were significantly decreased except that of *ALFPm3*. The expressions of *ALFPm3* was up-regulated about 4-fold compared with that in *GFP* dsRNA-injecting shrimp. The same down-regulation was observed in the genes of proPO activating system, *PmPPAE1* and *PmPPAE2*. The expression of

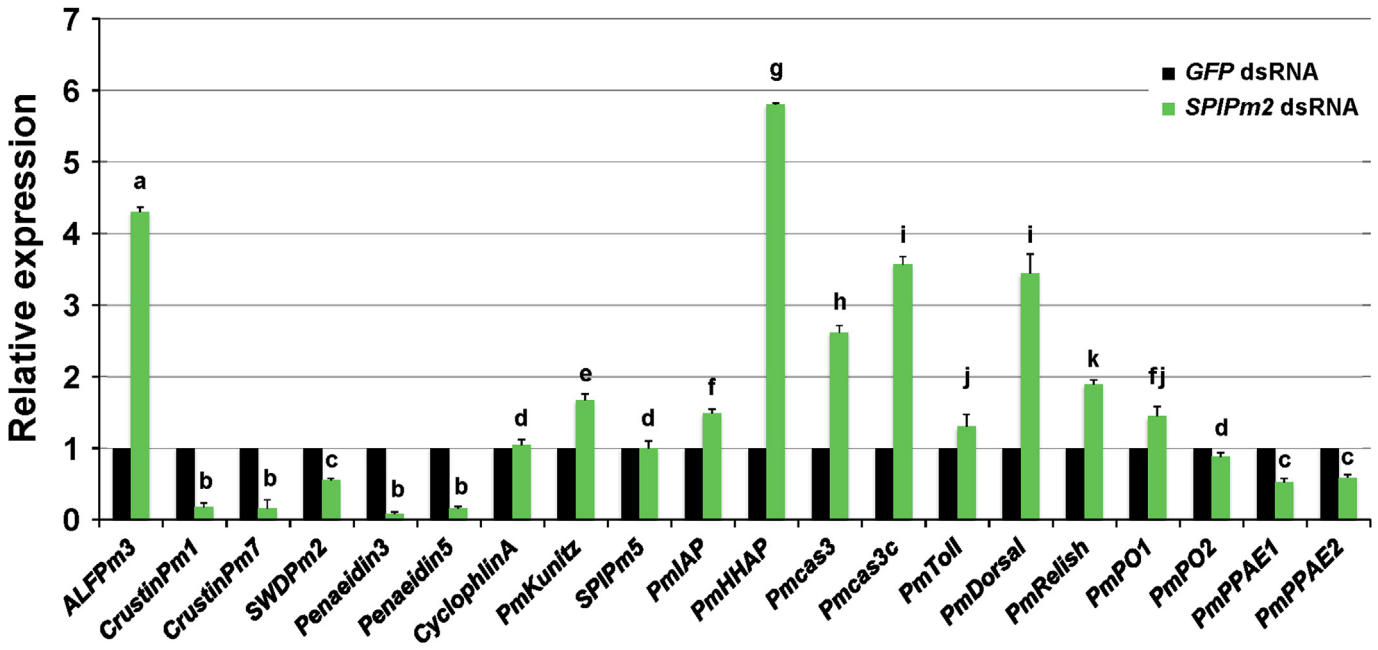


Fig. 3. Expression of twenty immune genes in *SPIPm2*-silencing shrimp. The expression was analyzed by qRT-PCR. The expression of *EF-1α* was used as a control. The expression was normalized with that of control GFP dsRNA-injecting shrimp. The data are means ± standard deviations. Letters indicate significant differences accepted at $P < 0.05$.

PmPO1 was slightly up-regulated whereas that of *PmPO2* remained unchanged (Fig. 3).

For the transcription of SPIs: *PmKunitz* and *SPIPm*5, and SPI-related gene *cyclophilinA*, the expression of *PmKunitz* was slightly up-regulated but that of *SPIPm*5 and *cyclophilinA* was not induced. Surprisingly, the expression of apoptosis-related genes: *PmIAP*, *PmHHAP*, *Pmcaspase3* and *Pmcaspase3c*, the transcription factor genes: *PmDorsal* and *PmRelish*, and the immune-related receptor gene, *PmToll*, were increased by 1.5-fold–6-fold (Fig. 3). The results suggested that the SPI*Pm*2 might be involved in shrimp innate immune response.

3.4. The shrimp circulating hemocytes in SPIPm2 knockdown shrimp

During the preparation of hemocytes by centrifugation, it was noticeable that the volumes of packed hemocytes from the *SPIPm2*-silenced shrimp were much less than those from the normal shrimp. It was suspected that the number of circulating hemocytes was reduced due to the silencing of *SPIPm2* gene. The amount of circulating hemocytes was investigated. In this experiment, the shrimp with the same size were specifically selected, the equal volume of hemolymph was drawn from each shrimp and the equal volume of hemocytes was used in cell counting. Our observation indicated that the shrimp circulating hemocytes were actually reduced in *SPIPm2*-silenced shrimp compared with those of *GFP* dsRNA-injected shrimp (Fig. 4A and B). It also indicated that the SPI*Pm*2 might be involved in homeostasis of the shrimp hemocytes.

3.5. Caspase activity in SPIPm2-silenced shrimp hemocytes

Our results on the up-regulation of caspase expression and the reduced number of hemocytes in *SPIPm2*-silenced shrimp revealed that the SPI*Pm*2 might be involved in hemocyte homeostasis. The reduction of hemocyte number might be the result of apoptosis. To prove this scenario, the activities of caspase-3 and caspase-7 were assayed in *SPIPm2*-silenced shrimp for they were key members of the apoptosis pathway.

Indeed, the activities of caspase-3 and caspase-7 in hemocytes of the *SPIPm2*-silenced shrimp were increased by 5.32-fold after 12 h of gene silencing compared with that in the control shrimp (Fig. 4 C). Therefore, the hemocyte apoptosis was significantly induced by the *SPIPm2* silencing. This result indicated that the reduction of SPI*Pm*2 activated the hemocyte apoptosis pathway.

3.6. Reduction of SPIPm2 expression rendered the shrimp more susceptible to YHV infection

The above results suggested that the SPI*Pm*2 played an essential role in homeostasis regarding the apoptosis process. With YHV infection, it was predicted that the gene silenced shrimp were more vulnerable to YHV virulence. To test this possibility, the *SPIPm2*-silenced shrimp were also injected with YHV and the mortality was observed every 6 h. It was found that the *SPIPm2*-silenced shrimp died faster with YHV infection with 50% cumulative mortality rate from 60 h to 36 h. The control groups injecting with 0.85% (w/v) NaCl, *SPIPm2* dsRNA and *GFP* dsRNA endured through the end of experiment (Fig. 5 A). These results also suggested that the SPI*Pm*2 might be important for the shrimp to defense against YHV.

If the SPI*Pm*2 was important for the defense against YHV, the addition of rSPI*Pm*2 should be able to prolong the mortality rate of YHV-infected shrimp. To test this hypothesis, the rSPI*Pm*2 protein was over-produced and injected into the shrimp along with YHV. The mortality rate was observed. We found, in the contrary, that the rSPI*Pm*2 did not have any positive effect on the mortality of YHV-infected shrimp for the LD_{50} was the same as the YHV-infected shrimp control (Fig. 5 B). It was concluded that the rSPI*Pm*2 could not help the shrimp withstand the severity of YHV infection but the shrimp were more sensitive to YHV infection when the rSPI*Pm*2 was depleted. We also checked the YHV replication by RT-PCR of *gp64* gene in 24-h YHV-infected shrimp and saw no effect on the YHV replication (data not shown).

4. Discussion

All multicellular organisms possess protease-mediated biological processes such as food digestion, blood coagulation, melanization and other innate immune pathways, to maintain homeostasis of life. These processes are regulated by serine proteinase inhibitors (SPIs). A Kazal-

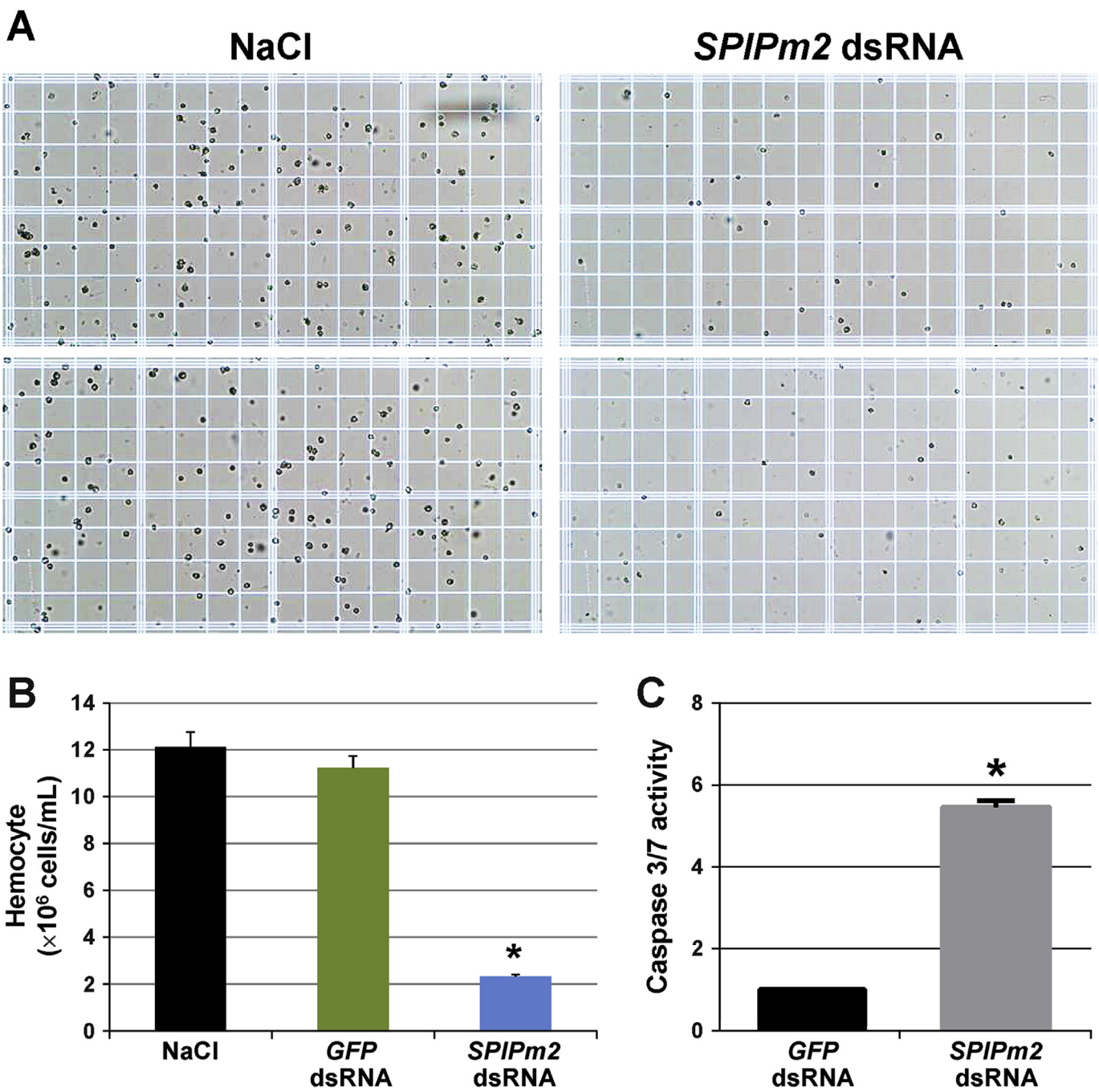


Fig. 4. Reduction of *P. monodon* hemocyte number after *SPIPm2* silencing and the increase in caspase-3/caspase-7 activities. The shrimp were injected with 0.85% (w/v) NaCl, *SPIPm2* dsRNA and *GFP* dsRNA. After 12 hpi, the hemolymph was collected for hemocyte counting using the hemocytometer. (A) Hemocyte density in hemolymph as observed under light microscope. Photographs are representatives of at least five such fields of view per sample and three different samples. Only the photographs from NaCl- and *SPIPm2* dsRNA-injected shrimp are shown. (B) The number of hemocytes in the shrimp hemolymph. The data are reported as means ± standard deviations derived from three independent trials. An asterisk indicates significant difference at $P < 0.05$ analyzed by one-way ANOVA and Scheffe *post hoc* test. (C) Assay of caspase-3 and caspase-7 activities in hemocytes of *SPIPm2*-silenced shrimp. The hemocytes were collected from the *SPIPm2* dsRNA- and *GFP* dsRNA-injected shrimp for the assay. The caspase activity was normalized by that of GFP dsRNA-injected shrimp. The data obtained from three replicates are shown as means ± standard deviations. An asterisk indicates a statistical significant difference accepted at $P < 0.05$.

type serine proteinase inhibitor from *P. monodon*, SPI*Pm*2, is believed to have important roles in regulating the serine proteinase-mediated cascades in shrimp and defending against pathogenic bacteria and WSSV in shrimp [14,15,17]. Microarray analysis and suppression subtractive hybridization indicate that the expression of *SPIPm2* is increased against WSSV and YHV infections [16,20,25]. Moreover, the SPI*Pm*2 has been shown to inhibit the replication of WSSV in WSSV-infected hemocytes [17]. It is, then, interesting to see how the SPI*Pm*2 reacts to YHV. In this study, the function of SPI*Pm*2 upon YHV infection was investigated.

In 48-h YHV-infected shrimp, the expression of *SPIPm2* was up-regulated in hemocytes, gill and heart. The main expression site was still in hemocytes. The time course expression of *SPIPm2* in hemocytes in response to YHV infection revealed that the expression was down-regulated in the early hours of infection. The expression was later increased after 12 h of infection and continued to rise by several fold

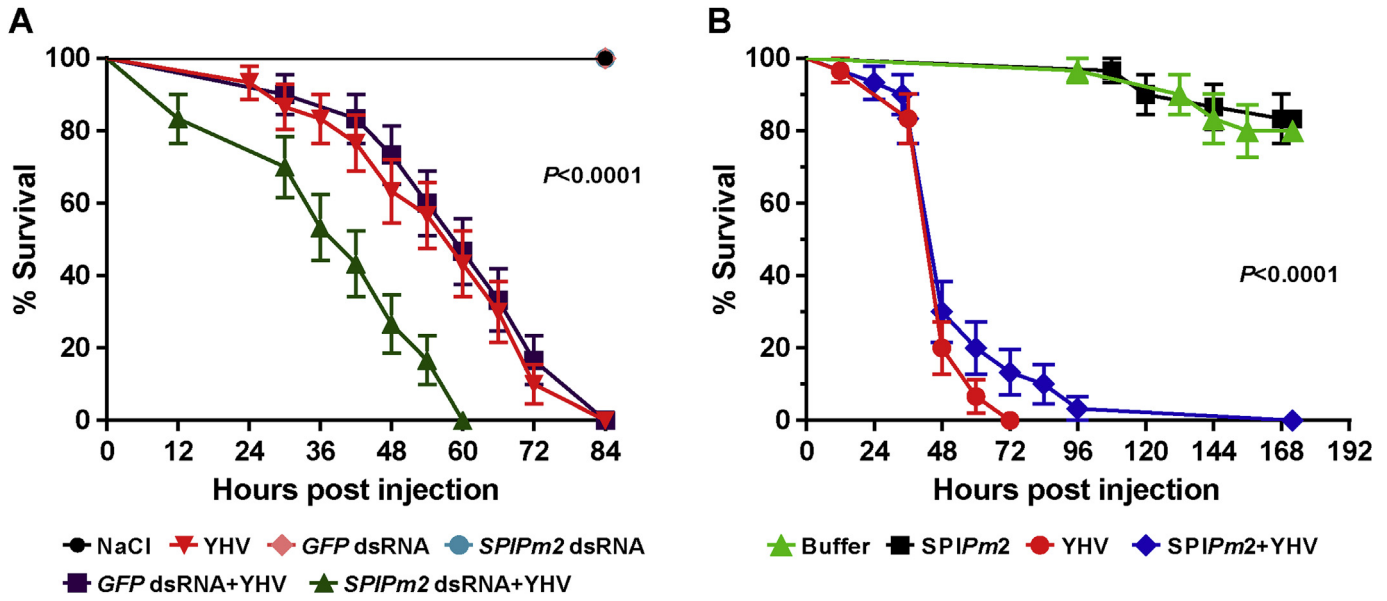


Fig. 5. Mortality of *SPIPm2*-silenced and SPI*Pm2*-injected shrimp. (A) Mortality of *SPIPm2*-silenced shrimp upon YHV infection. The shrimp were injected with 0.85% (w/v) NaCl, *GFP* dsRNA, *SPIPm2* dsRNA, YHV, *GFP* dsRNA + YHV and *SPIPm2* dsRNA + YHV. The mortality was observed every 6 h for 84 h. (B) Mortality of SPI*Pm2*-injected shrimp upon YHV infection. The shrimp were injected with carbonate buffer, 1.8 nmol rSPI*Pm2*, 1.8 nmol SPI*Pm2* plus YHV and YHV. The shrimp mortality rate was recorded every 12 h. The experiments were repeated three times. The data were plotted using GraphPad Prism as means ± standard deviations. The *P* values indicated were calculated by log-rank test in the GraphPad Sigma Plot.

afterwards. The results were consistent with those previously reported that the *SPIPm2* transcript was significantly decreased in an early stage of infection and increased afterwards [16,20]. Normally, the SPI*Pm2* is produced and stored in secretory granules within the shrimp hemocytes readily to be secreted. In an early or eclipse phase of infection, the SPI*Pm2* is secreted into the hemolymph [15] and the expression of *SPIPm2* may not yet be activated. The expression of *SPIPm2* is induced later in the infection probably at the infectious period, a period that the virus spreads.

While the SPI*Pm2* has been shown to restrain the replication of WSSV and inhibit the regulatory function of WSV477 [15,18], the role of SPI*Pm2* in YHV infection has not been elucidated. In this study, the function of SPI*Pm2* in YHV infection was examined using RNA interference technique to see if the depletion of SPI*Pm2* had any effect on the expression of twenty immune related genes. The *SPIPm2* dsRNA was created and tested for its silencing efficiency by RT-PCR. It was found that the expression of *SPIPm2* was not completely silenced but significantly reduced by about 65% at 12 h post injection compared with the control groups. Two consecutive injections of *SPIPm2* dsRNA gave similar result and was used in our study. The 20 immune-related genes were selected from several systems in innate immunity of shrimp such as genes of antimicrobial peptides (*ALFPm3*, *crustinPm1*, *crustinPm7*, *SWDPm2*, *penaeidin3*, *penaeidin5*), cytosolic binding protein (*cyclophilinA*), serine proteinase inhibitors (*PmKunitz*, *SPIPm5*), apoptosis-related proteins (*PmIAP*, *PmHHAP*, *Pmcaspase3*, *Pmcaspase3c*, transcription factors (*PmDorsal*, *PmRelish*), immune receptor protein (*PmToll*) and enzymes in proPO-activating system (*PmPO1*, *PmPO2*, *PmPPAE1*, *PmPPAE2*). Their expression was analyzed by real-time PCR.

When the *SPIPm2* was silenced, the expression of shrimp AMPs: *crustinPm1*, *crustinPm7*, *SWDPm2*, *penaeidin3* and *penaeidin5*, was significantly down-regulated. Only the *ALFPm3* transcript was highly up-regulated. Similar expression profiles of AMPs are obtained in *LvIAP2*-silenced shrimp in which the expression of *LvPENs*, *Lvcrustins*, *LvVICPs* (*Vibrio penaeicidae-induced cysteine and proline-rich peptides*) and *LvLysozyme* from *Litopenaeus vannamei* is decreased in contrast to the increased expression of *LvALFs* [26]. Different themes of AMP expression profiles are observed in *FcCactus*-silenced Chinese shrimp, *Fenneropenaeus chinensis*, where the expression of *FcPen3* and *FcPen5* but not *FcALF* is up-regulated [27]. Variation in the expression of *Lv*Pen is observed in *LvTollip*-silenced shrimp, *L. vannamei* [28]. The expression of AMPs tested is down-regulated in *Lv*Pellino-silenced shrimp and *Es*MyD88-silenced Chinese mitten crab, *E. sinensis* [29,30]. Thus, there are different regulation mechanisms for the expression of various AMPs. The silencing of *SPIPm2* might affect different regulation mechanisms of AMP synthesis that increased the expression of *ALFPm3* but not those of *crustinPm1*, *crustinPm7*, *SWDPm2*, *penaeidin3* and *penaeidin5*.

The Toll and Imd pathways are the immune pathways known to regulate the synthesis of AMP in response to stresses [31,32]. Silencing of *SPIPm2* did not affect the expression of immune receptor of the Toll pathway, *PmToll*, but significantly increased the expression levels of transcription factors, *PmDorsal* of Toll pathway and *PmRelish* of Imd pathway. The increase in the two transcription factors did not result in the expression of most AMPs. This was probably due to the fact that there was no infection signal. The transcription factors might be deterred to take effect by some factors, such as a positive nuclear factor in insects and mammals, *Lv*Akirin, that when forms complex with 14-3-3 and Relish acts as a negative regulator of AMP synthesis in Imd pathway [33,34], a Fas-binding protein, *Lv*Daxx, from *L. vannamei*, that controls the activation of NF-κB transcription factors [35] and the *Drosophila* casper that blocks the translocation of Relish into the nucleus [36].

The silencing of *SPIPm2* did not affect the expression of serine proteinase inhibitors (*PmKunitz* and *SPIPm5*), cytosolic binding protein (*cyclophilinA*) and enzymes in proPO cascade (*PmPO1*, *PmPO2*, *PmPPAE1* and *PmPPAE2*) although some genes: *PmKunitz* and *PmPO1*, were slightly up-regulated. In fact, the expression of *PmPPAE1* and *PmPPAE2* was suppressed.

To our surprise, the expression of apoptosis-related genes, *PmHHAP*, *Pmcaspase3* and *Pmcaspase3c*, except *PmIAP* was highly increased in the *SPIPm2*-silenced shrimp. That of *PmIAP* was slightly increased. It was even more surprising when we observed the decrease in circulating hemocytes in the *SPIPm2*-silenced shrimp. These two observations were likely to be related to each other, that the depletion of SPI*Pm2* caused the cell death possibly by apoptosis.

Apoptosis is a cell suicide process that is initiated through a pathway executed by caspases [42]. The caspases are synthesized as

inactive zymogens and undergo activation at the onset of apoptosis [43]. Since the caspases were key factors in the mediation of apoptosis, the caspase-3 and caspase-7 activities were measured in the *SPIPm2*-silenced shrimp in addition to the qRT-PCR of *Pmcapases3* and *Pmcaspase3c*. As expected, the activities of caspase-3 and caspase-7 were increased in *SPIPm2*-knockdown hemocytes suggesting that the SPI*Pm*2 was likely to be involved in the apoptosis process and the hemocyte homeostasis in shrimp.

The *Pm*HHAP, a hemocyte homeostasis-associated protein, from *P. monodon* has been shown to regulate the hemocyte homeostasis by inhibiting the caspase-dependent apoptotic pathway through caspase inhibition [44]. Similar to that of *SPIPm2*, the *PmHHAP* knockdown increases the number of apoptotic cells and the activities of caspase-3 and -7. However, the knockdown of *SPIPm2* in this study also increased the expression of *Pm*HHAP. We speculated that the SPI*Pm*2 might participate in apoptosis different from the *Pm*HHAP.

The SPI*Pm*2 is likely to control the proteases involved in apoptotic process. For example, the SPI*Pm*2 protects the hemocytes by inhibiting the proteinases and/or caspases involved in apoptotic process similar to a serine proteinase inhibitor 2 (SPI-2) from vaccinia virus that is shown to inhibit apoptotic process [37–39]. The SPI-2 and its orthologue, CPXV cytokine response modifier A (*CrmA*), from cowpox virus inhibit extrinsic apoptosis and host inflammatory response. The target of these two proteins are caspase-1 and the virus-infected cells are protected from the TNF- and Fas-mediated apoptosis or the proteolysis activation from interferon, interleukin-1β, a cytokine from host cells [38–41]. With the depletion of SPI*Pm*2 in our study, the shrimp needed to produce more *Pm*HHAP to help control the apoptotic process. Although the *Pm*HHAP could inhibit the caspase-dependent apoptotic pathway, it was not enough to protect the decrease in circulating hemocytes affecting from the lacking of SPI*Pm*2. Nevertheless, this hypothesis is awaiting for further study.

With the reduction of hemocytes in the *SPIPm2*-silenced shrimp, the shrimp was supposedly more sensitive to YHV infection. Upon YHV challenging, the *SPIPm2*-silenced shrimp died faster than the control shrimp. In the reverse situation, the injection of rSPI*Pm*2 along with YHV into the normal shrimp did not help the shrimp survive any longer. This might be because the SPI*Pm*2 was normally abundant in the normal shrimp. Adding more SPI*Pm*2 did not help the shrimp anymore. In conclusion, our results suggested that the SPI*Pm*2 might have an important role in hemocyte homeostasis providing necessary protection to the hemocytes as an innate immune defense against pathogenic invaders and self-destruction processes.

Acknowledgements

This project was supported by the RachadapisekSompote Fund for Postdoctoral Fellowship Chulalongkorn University to S. Visetnan, and the research grant from the Srinakharinwirot University (B.E. 2560) to S. Donpudsa (Grant No. 523/2560). We thank the TRF Senior Research Scholar (No. RTA5880004), Thailand Research Fund to A. Tassanakajon and the support under the Ratchadapisek Somphot Endowment to the Center of Excellence for Molecular Biology and Genomics of Shrimp. We appreciate the support of equipment used in this study under JST-JICA joint program “Science and Technology Research Partnership for Sustainable Development, SATREPS”.

References

[1] V. Rimphanitchayakit, A. Tassanakajon, Structure and function of invertebrate Kazal-type serine proteinase inhibitors, Dev. Comp. Immunol. 34 (2010) 377–386.
[2] P. Jiravanichpaisal, B.L. Lee, K. Söderhäll, Cell-mediated immunity in arthropods: hematopoiesis, coagulation, melanization and opsonization, Immunobiology 211 (2006) 213–236.
[3] S. Iwanaga, B.L. Lee, Recent advances in the innate immunity of invertebrate animals, J. Biochem. Mol. Biol. 38 (2005) 128–150.
[4] M.R. Kanost, Serine proteinase inhibitors in arthropod immunity, Dev. Comp. Immunol. 23 (1999) 291–301.
[5] A. Tassanakajon, K. Somboonwiwat, P. Supungul, S. Tang, Discovery of immune molecules and their crucial functions in shrimp immunity, Fish Shellfish Immunol. 34 (2013) 954–967.
[6] M. Laskowski Jr., M.A. Qasim, What can the structures of enzyme-inhibitor complexes tell us about the structures of enzyme substrate complexes? Biochim. Biophys. Acta 1477 (2000) 324–337.
[7] W. Bode, R. Huber, Natural protein proteinase inhibitors and their interaction with proteinases, Eur. J. Biochem. 204 (1992) 433–451.
[8] M. Laskowski Jr., I. Kato, Protein inhibitors of proteinases, Annu. Rev. Biochem. 49 (1980) 593–626.
[9] H.J. Mägert, L. Ständker, P. Kreutzmann, H.D. Zucht, M. Reinecke, C.P. Sommerhoff, H. Fritz, W.G. Forssmann, LEKTI, a novel 15-domain type of human serine proteinase inhibitor, J. Biol. Chem. 274 (1999) 21499–21502.
[10] P. Kreutzmann, A. Schulz, L. Ständker, W.G. Forssmann, H.J. Mägert, Recombinant production, purification and biochemical characterization of domain 6 of LEKTI: a temporary Kazal-type-related serine proteinase inhibitor, J. Chromatogr. B Anal. Technol. Biomed. Life Sci. 803 (2004) 75–81.
[11] A. Tassanakajon, S. Klinbunga, N. Paunglarp, V. Rimphanitchayakit, A. Udomkit, S. Jitrapakdee, K. Sritunyalucksana, A. Phongdara, S. Pongsomboon, P. Supungul, S. Tang, K. Kuphanumart, R. Pichyangkura, C. Lursinsap, *Penaeus monodon* gene discovery project: the generation of an EST collection and establishment of a database, Gene 384 (2006) 104–112.
[12] S. Visetnan, S. Donpudsa, P. Supungul, A. Tassanakajon, V. Rimphanitchayakit, Kazal-type serine proteinase inhibitors from the black tiger shrimp *Penaeus monodon* and the inhibitory activities of SPI*Pm*4 and 5, Fish Shellfish Immunol. 27 (2009) 266–274.
[13] N. Somprasong, V. Rimphanitchayakit, A. Tassanakajon, A five-domain Kazal-type serine proteinase inhibitor from black tiger shrimp *Penaeus monodon* and its inhibitory activities, Dev. Comp. Immunol. 30 (2006) 998–1008.
[14] S. Donpudsa, A. Tassanakajon, V. Rimphanitchayakit, Domain inhibitory and bacteriostatic activities of the five-domain Kazal-type serine proteinase inhibitor from black tiger shrimp *Penaeus monodon*, Dev. Comp. Immunol. 33 (2009) 481–488.
[15] S. Ponprateep, K. Phiwsaiya, A. Tassanakajon, V. Rimphanitchayakit, Interaction between Kazal serine proteinase inhibitor SPI*Pm*2 and viral protein WSV477 reduces the replication of white spot syndrome virus, Fish Shellfish Immunol. 35 (2013) 957–964.
[16] A. Prapavorarat, S. Pongsomboon, A. Tassanakajon, Identification of genes expressed in response to yellow head virus infection in the black tiger shrimp, *Penaeus monodon*, by suppression subtractive hybridization, Dev. Comp. Immunol. 34 (2010) 611–617.
[17] S. Donpudsa, S. Ponprateep, A. Prapavorarat, S. Visetnan, A. Tassanakajon, V. Rimphanitchayakit, A Kazal-type serine proteinase inhibitor SPI*Pm*2 from the black tiger shrimp *Penaeus monodon* is involved in antiviral responses, Dev. Comp. Immunol. 34 (2010) 1101–1108.
[18] S. Visetnan, S. Donpudsa, P. Supungul, A. Tassanakajon, V. Rimphanitchayakit, Domain 2 of a Kazal serine proteinase inhibitor SPI*Pm*2 from *Penaeus monodon* possesses antiviral activity against WSSV, Fish Shellfish Immunol. 41 (2014) 526–530.
[19] S. Pongsomboon, S. Tang, S. Boonda, T. Aoki, I. Hirono, M. Yasuike, A. Tassanakajon, Differentially expressed genes in *Penaeus monodon* hemocytes following infection with yellow head virus, BMB Rep. 41 (2008) 670–677.
[20] S. Visetnan, P. Supungul, I. Hirono, A. Tassanakajon, V. Rimphanitchayakit, Activation of *Pm*Relish from *Penaeus monodon* by yellow head virus, Fish Shellfish Immunol. 42 (2015) 335–344.
[21] M.W. Pfaffl, A new mathematical model for relative quantification in real-time RT-PCR, Nucleic Acids Res. 29 (2001) e45.
[22] M.M. Bradford, A rapid and sensitive method for the quantitation of microgram quantities of protein utilizing the principle of protein-dye binding, Anal. Biochem. 72 (1976) 248–254.
[23] P. Supungul, S. Klinbunga, R. Pichyangkura, S. Jitrapakdee, I. Hirono, T. Aoki, A. Tassanakajon, Identification of immune-related genes in hemocytes of black tiger shrimp (*Penaeus monodon*), Mar. Biotechnol. 4 (2002) 487–494.
[24] B. Jarasrassamee, P. Supungul, S. Panyim, S. Klinbunga, V. Rimphanichayakit, A. Tassanakajon, Recombinant expression and characterization of five-domain Kazal-type serine proteinase inhibitor of black tiger shrimp (*Penaeus monodon*), Mar. Biotechnol. 7 (2005) 46–52.
[25] S. Pongsomboon, S. Tang, S. Boonda, T. Aoki, I. Hirono, A. Tassanakajon, A cDNA microarray approach for analyzing transcriptional changes in *Penaeus monodon* after infection by pathogens, Fish Shellfish Immunol. 30 (2011) 439–446.
[26] P.H. Wang, D.H. Wan, Z.H. Gu, W. Qiu, Y.G. Chen, S.P. Weng, X.Q. Yu, J.G. He, Analysis of expression, cellular localization, and function of three inhibitors of apoptosis (IAPs) from *Litopenaeus vannamei* during WSSV infection and in regulation of antimicrobial peptide genes (AMPs), PLoS One 8 (2013) e72592.
[27] D. Wang, F. Li, S. Li, Y. Chi, R. Wen, N. Feng, J. Xiang, An IκB homologue (*Fc*Cactus) in Chinese shrimp *Fenneropenaeus chinensis*, Dev. Comp. Immunol. 39 (2013) 352–362.
[28] P.H. Wang, Z.H. Gu, D.H. Wan, W.B. Zhu, W. Qiu, Y.G. Chen, S.P. Weng, X.Q. Yu, J.G. He, *Litopenaeus vannamei* Toll-interacting protein (*Lv*Tollip) is a potential negative regulator of the shrimp Toll pathway involved in the regulation of the shrimp antimicrobial peptide gene penaeidin-4 (PEN4), Dev. Comp. Immunol. 40 (2013) 266–277.
[29] C. Li, J. Chai, H. Li, H. Zuo, S. Wang, W. Qiu, S. Weng, J. He, X. Xu, Pellino protein from pacific white shrimp *Litopenaeus vannamei* positively regulates NF-κB activation, Dev. Comp. Immunol. 44 (2014) 341–350.
[30] Y. Huang, Y.H. Chen, Z. Wang, W. Wang, Q. Ren, Novel myeloid differentiation

factor 88, *Es*MyD88, exhibits *Es*Tube-binding activity in Chinese mitten crab *Eriocheir sinensis*, Dev. Comp. Immunol. 47 (2014) 298–308.
[31] E. De Gregorio, P.T. Spellman, P. Tzou, G.M. Rubin, B. Lemaitre, The Toll and Imd pathways are the major regulators of the immune response in *Drosophila*, EMBO J. 21 (2002) 2568–2579.
[32] T. Tanji, Y.T. Ip, Regulators of the Toll and Imd pathways in the *Drosophila* innate immune response, Trends Immunol. 26 (2005) 193–198.
[33] F. Hou, X. Wang, Z. Qian, Q. Liu, Y. Liu, S. He, X. Mi, C. Bai, C. Sun, X. Liu, Identification and functional studies of Akirin, a potential positive nuclear factor of NF-κB signaling pathways in the Pacific white shrimp, *Litopenaeus vannamei*, Dev. Comp. Immunol. 41 (2013) 703–714.
[34] N. Liu, X.W. Wang, J.J. Sun, L. Wang, H.W. Zhang, X.F. Zhao, J.X. Wang, Akirin interacts with Bap60 and 14-3-3 proteins to regulate the expression of antimicrobial peptides in the kuruma shrimp (*Marsupenaeus japonicus*), Dev. Comp. Immunol. 55 (2016) 80–89.
[35] M. Yan, J. Tang, Q. Liang, G. Zhu, H. Li, C. Li, S. Weng, J. He, X. Xu, Daxx from Pacific white shrimp *Litopenaeus vannamei* is involved in activation of NF-κB pathway, Fish Shellfish Immunol. 45 (2015) 443–453.
[36] M. Kim, J.H. Lee, S.Y. Lee, E. Kim, J. Chung, Caspar, a suppressor of antibacterial immunity in Drosophila, Proc. Natl. Acad. Sci. U.S.A. 103 (2006) 16358–16363.
[37] M. Dobbelstein, T. Shenk, Protection against apoptosis by the vaccinia virus SPI-2 (B13R) gene product, J. Virol. 70 (1996) 6479–6485.
[38] S. Kettle, A. Alcamí, A. Khanna, R. Ehret, C. Jassoy, G.L. Smith, Vaccinia virus serpin B13R (SPI-2) inhibits interleukin-1beta-converting enzyme and protects virus-infected cells from TNF- and Fas-mediated apoptosis, but does not prevent IL-1beta-induced fever, J. Gen. Virol. 78 (1997) 677–685.
[39] Y. Qin, M. Li, S.L. Zhou, W. Yin, Z. Bian, H.B. Shu, SPI-2/CrmA inhibits IFN-β induction by targeting TBK1/IKKε, Sci. Rep. 7 (2017) 10495.
[40] T. Komiyama, C.A. Ray, D.J. Pickup, A.D. Howard, N.A. Thornberry, E.P. Peterson, G. Salvesen, Inhibition of interleukin-1 beta converting enzyme by the cowpox virus serpin CrmA, an example of cross-class inhibition, J. Biol. Chem. 269 (1994) 19331–19337.
[41] M. Dobbelstein, T. Shenk, Protection against apoptosis by the vaccinia virus SPI-2 (B13R) gene product, J. Virol. 70 (1996) 6479–6485.
[42] L. Galluzzi, I. Vitale, J.M. Abrams, E.S. Alnemri, E.H. Baehrecke, M.V. Blagosklonny, T.M. Dawson, V.L. Dawson, W.S. El-Deiry, S. Fulda, E. Gottlieb, D.R. Green, M.O. Hengartner, O. Kepp, R.A. Knight, S. Kumar, S.A. Lipton, X. Lu, F. Madeo, W. Malorni, P. Mehlen, G. Nuñez, M.E. Peter, M. Piacentini, D.C. Rubinsztein, Y. Shi, H.U. Simon, P. Vandenabeele, E. White, J. Yuan, B. Zhivotovsky, G. Melino, G. Kroemer, Molecular definitions of cell death subroutines: recommendations of the Nomenclature Committee on Cell Death 2012, Cell Death Differ. 19 (2012) 107–120.
[43] Y. Shi, Caspase activation, inhibition, and reactivation: a mechanistic view, Protein Sci. 13 (2004) 1979–1987.
[44] K. Apitanyasai, P. Amparyup, W. Charoensapsri, S. Senapin, A. Tassanakajon, Role of Penaeus monodon hemocyte homeostasis associated protein (*Pm*HHAP) in regulation of caspase-mediated apoptosis, Dev. Comp. Immunol. 53 (2015) 234–243.

Manuscript Details

Manuscript number	DCI_2018_272
Title	Two host gut-derived lactic acid bacteria activate the proPO system and increase resistance to an AHPND-causing strain of Vibrio parahaemolyticus in the shrimp Litopenaeus vannamei
Article type	Full Length Article

Abstract

Lactic acid bacteria (LAB) are group of beneficial bacteria that have been proposed as relevant probiotics with immunomodulatory functions. In this study, we initially isolated and identified host-derived LAB from the gut of the Pacific white shrimp Litopenaeus vannamei. Analysis of the bacterial 16S rRNA gene sequence revealed two candidate LAB, the Lactobacillus plantarum strain SGLAB01 and the Lactococcus lactis strain SGLAB02, which exhibited 99% identity to the L. plantarum strain LB1-2 and the L. lactis strain R-53658, which were isolated from bee gut, respectively. The two LAB displayed antimicrobial activities against gram-positive and gram-negative bacteria, including the virulent acute hepatopancreatic necrosis disease (AHPND)-causing strain of Vibrio parahaemolyticus (VPAHPND). Viable colony count and SEM analysis showed that the two candidate LAB, administered via oral route as feed supplement, could reside and adhere in the shrimp gut. Double-stranded RNA-mediated gene silencing of LvproPO1 and LvproPO2 revealed a significant role of two LvproPOs in the proPO system as well as in the immune response against VPAHPND infection in L. vannamei shrimp. The effect of LAB supplementation on modulation of the shrimp proPO system was investigated in vivo, and the results showed that administration of the two candidate LAB significantly increased hemolymph PO activity, the relative mRNA expression of LvproPO1 and LvproPO2, and resistance to VPAHPND infection. These findings suggest that administration of L. plantarum and L. lactis could modulate the immune system and increase shrimp resistance to VPAHPND infection presumably via upregulation of the two LvproPO transcripts.

Keywords	Probiotic, Lactic Acid Bacteria, Shrimp, Vibrio parahaemolyticus, Immunity, proPO system
Manuscript category	Invertebrate

Corresponding Author	Piti Amparyup
Corresponding Author's Institution	National Science and Technology Development Agency (NSTDA)
Order of Authors	Sudarat Chomwong, Walaiporn Charoensapsri, Piti Amparyup, Anchalee Tassanakajon

Submission Files Included in this PDF

File Name [File Type]

Cover Letter.docx [Cover Letter]

Highlights_PA21062018.doc [Highlights]

Abstract.docx [Abstract]

MS_Probiotic_PA21062018.docx [Manuscript File]

Fig1.docx [Figure]

Fig2.docx [Figure]

Fig3.docx [Figure]

Fig4.docx [Figure]

Fig5.docx [Figure]

Fig6.docx [Figure]

Table 1.docx [Table]

Table 2.docx [Table]

To view all the submission files, including those not included in the PDF, click on the manuscript title on your EVISE Homepage, then click 'Download zip file'.

June 21, 2018

To: Professor Kenneth Söderhall

Editors-in-chief, *Developmental & Comparative Immunology*

Dear Sir,

Please find the manuscript entitled "**Two host gut-derived lactic acid bacteria activate the proPO system and increase resistance to an AHPND-causing strain of *Vibrio parahaemolyticus* in the shrimp *Litopenaeus vannamei***" submitted for your consideration to be published in *Developmental & Comparative Immunology*.

Sincerely Yours,

Piti Amparyup, Ph.D.

National Center for Genetic Engineering and Biotechnology (BIOTEC),
National Science and Technology Development Agency (NSTDA),
Pathumthani 12120, THAILAND
E-mail: piti.amp@biotec.or.th
Tel. (66-2) 644 8150 ext. 81826

Highlights

- Two host-derived LAB were isolated from the gut of the shrimp *Litopenaeus vannamei.*
- The two host-derived LAB displayed antimicrobial activity against VP_{AHPND}.
- The two host-derived LAB modulated shrimp immunity by activating the proPO system.
- The two host-derived LAB increased resistance to VP_{AHPND} infection in shrimp.

Abstract

Lactic acid bacteria (LAB) are group of beneficial bacteria that have been proposed as relevant probiotics with immunomodulatory functions. In this study, we initially isolated and identified host-derived LAB from the gut of the Pacific white shrimp *Litopenaeus vannamei*. Analysis of the bacterial 16S rRNA gene sequence revealed two candidate LAB, the *Lactobacillus plantarum* strain SGLAB01 and the *Lactococcus lactis* strain SGLAB02, which exhibited 99% identity to the *L. plantarum* strain LB1-2 and the *L. lactis* strain R-53658, which were isolated from bee gut, respectively. The two LAB displayed antimicrobial activities against gram-positive and gram-negative bacteria, including the virulent acute hepatopancreatic necrosis disease (AHPND)-causing strain of *Vibrio parahaemolyticus* (VP_{AHPND}). Viable colony count and SEM analysis showed that the two candidate LAB, administered via oral route as feed supplement, could reside and adhere in the shrimp gut. Double-stranded RNA-mediated gene silencing of *Lv*proPO1 and *Lv*proPO2 revealed a significant role of two *Lv*proPOs in the proPO system as well as in the immune response against VP_{AHPND} infection in *L. vannamei* shrimp. The effect of LAB supplementation on modulation of the shrimp proPO system was investigated *in vivo,* and the results showed that administration of the two candidate LAB significantly increased hemolymph PO activity, the relative mRNA expression of *Lv*proPO1 and *Lv*proPO2, and resistance to VP_{AHPND} infection. These findings suggest that administration of *L. plantarum* and *L. lactis* could modulate the immune system and increase shrimp resistance to VP_{AHPND} infection presumably via upregulation of the two *Lv*proPO transcripts.

Two host gut-derived lactic acid bacteria activate the proPO system and increase resistance to an AHPND-causing strain of *Vibrio parahaemolyticus* in the shrimp *Litopenaeus vannamei*

Sudarat Chomwong[a,b,c], Walaiporn Charoensapsri[c,d], Piti Amparyup[c,*], and Anchalee Tassanakajon[a,*]

[a]*Center of Excellence for Molecular Biology and Genomics of Shrimp, Department of Biochemistry, Faculty of Science, Chulalongkorn University, 254 Phayathai Road, Bangkok 10330, Thailand*

[b]*Program of Biotechnology, Faculty of Science, Chulalongkorn University, 254 Phayathai Road, Bangkok 10330, Thailand*

[c]*National Center for Genetic Engineering and Biotechnology (BIOTEC), National Science and Technology Development Agency (NSTDA), 113 Paholyothin Road, Klong 1, Klong Luang, Pathumthani 12120, Thailand*

[d]*Center of Excellence for Shrimp Molecular Biology and Biotechnology (Centex Shrimp), Faculty of Science, Mahidol University, Rama VI Road, Bangkok 10400, Thailand*

Keywords: Probiotic, Lactic Acid Bacteria, Shrimp, *Vibrio parahaemolyticus*, Immunity, proPO system

[*]Corresponding author.

E–mail address: piti.amp@biotec.or.th (P. Amparyup).

[*]Corresponding author.

E–mail address: anchalee.k@chula.ac.th (A. Tassanakajon).

Abstract

Lactic acid bacteria (LAB) are group of beneficial bacteria that have been proposed as relevant probiotics with immunomodulatory functions. In this study, we initially isolated and identified host-derived LAB from the gut of the Pacific white shrimp *Litopenaeus vannamei*. Analysis of the bacterial 16S rRNA gene sequence revealed two candidate LAB, the *Lactobacillus plantarum* strain SGLAB01 and the *Lactococcus lactis* strain SGLAB02, which exhibited 99% identity to the *L. plantarum* strain LB1-2 and the *L. lactis* strain R-53658, which were isolated from bee gut, respectively. The two LAB displayed antimicrobial activities against gram-positive and gram-negative bacteria, including the virulent acute hepatopancreatic necrosis disease (AHPND)-causing strain of *Vibrio parahaemolyticus* (VP_{AHPND}). Viable colony count and SEM analysis showed that the two candidate LAB, administered via oral route as feed supplement, could reside and adhere in the shrimp gut. Double-stranded RNA-mediated gene silencing of *Lv*proPO1 and *Lv*proPO2 revealed a significant role of two *Lv*proPOs in the proPO system as well as in the immune response against VP_{AHPND} infection in *L. vannamei* shrimp. The effect of LAB supplementation on modulation of the shrimp proPO system was investigated *in vivo,* and the results showed that administration of the two candidate LAB significantly increased hemolymph PO activity, the relative mRNA expression of *Lv*proPO1 and *Lv*proPO2, and resistance to VP_{AHPND} infection. These findings suggest that administration of *L. plantarum* and *L. lactis* could modulate the immune system and increase shrimp resistance to VP_{AHPND} infection presumably via upregulation of the two *Lv*proPO transcripts.

1. Introduction

Intensive shrimp farming has suffered from many troublesome problems that have led to an increase in incidences of viral and bacterial diseases. So far, conventional approaches for disease control have relied on the use of antimicrobial drugs. However, indiscriminate use of antibiotics has led to many adverse effects, especially the evolution of antimicrobial resistance among bacterial pathogens (Moriarty, 1997). Thus, a novel solution that is safe and environmentally friendly and that can efficiently control disease outbreaks or eliminate the use of antibiotics is necessary. Administration of beneficial microorganisms, called probiotics, is regarded as a promising alternative strategy for the control of microbial-derived diseases in aquaculture. During the last two decades, several beneficial microbes have been identified, characterized and applied as probiotics that compete with pathogens and that promote the growth and immunity of cultured shrimp (Farzanfar, 2006; Lakshmi et al., 2013; Ninawe and Selvin, 2009).

Lactic acid bacteria (LAB) are a group of nonsporulating, nonrespiring but aerotolerant, coccus or rod-shaped, gram-positive polyphyletic bacteria with the ability to produce lactic acid and different antimicrobial agents, such as bacteriocins (Ouwehand and Vesterlund, 2004; von Wright and Axelsson, 2011). LAB are among a group of favorable microbes that are often identified as components of the gut microbiota and that have been suggested to be relevant candidates for use as probiotics in aquaculture (Farzanfar, 2006; Merrifield et al., 2014; Ringø and Gatesoupe, 1998). Applications of LAB and their metabolic products have been reported to promote survival, growth, and immune responses and to increase resistance to pathogens in shrimp (Adel et al., 2017; Castex et al., 2008, 2009, 2010; Chiu et al., 2007; Kongnum

74 and Hongpattarakere, 2012; Leyva-Madrigal et al., 2011; Lv et al., 2017; Maeda et al.,
75 2014; Peraza-Gómez et al., 2009; Vieira et al., 2007, 2008, 2010). In recent years,
76 host-associated microorganisms have gained popularity, and their potential as a source
77 of probiotics with immunomodulatory functions has been emphasized (Lazado et al.,
78 2015). Several indigenous LAB from the digestive tract of penaeid shrimp have been
79 isolated and identified (Adel et al., 2017; Kongnum and Hongpattarakere, 2012; Kosin
80 and Rakshit, 2010; Leyva-Madrigal et al., 2011; Liu et al., 2011; Maeda et al., 2014;
81 Merrifield et al., 2014; Vieira et al., 2007). However, the successful use of host-derived
82 LAB as probiotics in shrimp is relatively rare.

83 The melanization cascade, controlled by the prophenoloxidase-activating
84 system (proPO system), is one of the main defense pathways that plays a significant
85 role in the innate immune system of invertebrates, allowing a rapid response in the
86 killing and sequestration of invading pathogens (Amparyup et al., 2013a; Cerenius and
87 Söderhäll, 2004; Cerenius et al., 2008; Kanost and Gorman, 2008; Tassanakajon et al.,
88 2018). Several studies have reported that administration of diets containing probiotics,
89 including LAB, significantly increased phenoloxidase (PO) activity, proPO mRNA
90 transcription levels and the survival rate of shrimp after challenge with pathogenic
91 bacteria (Chiu et al., 2007). However, the immunostimulatory effects conferred by
92 host-derived LAB administration on the proPO system in the shrimp gut remains
93 barely investigated.

94 Acute hepatopancreatic necrosis disease (AHPND), initially referred to as
95 early mortality syndrome (EMS), is caused by a specific set of virulent strains of *Vibrio*
96 *parahaemolyticus*, including AHPND-causing *V. parahaemolyticus* (VP_{AHPND}), that
97 become virulent after acquiring the pVA1 plasmid, which encodes the deadly

Photorhabdus insect-related (Pir) binary toxins pirA^{vp} and pirB^{vp} (de la Pena et al., 2015; Flegel, 2012; Han et al., 2015; Joshi et al., 2014; Kondo et al., 2014; Lee et al., 2015; Lightner et al., 2012; Nunan et al., 2014; Soto-Rodriguez et al., 2015; Tran et al., 2013; Yang et al., 2014). This disease causes a high mortality rate (40-100%) accompanied by massive sloughing of hepatopancreatic epithelial cells within the first ~35 days post-stocking of ponds with post larvae (Flegel, 2012; Leano and Mohan, 2012; Lightner et al., 2012; Tran et al., 2013). Although several attempts have been carried out to minimize AHPND outbreaks, many shrimp-producing areas remain uncontrolled.

In this study, we initially isolated host-derived LAB from the gut of the shrimp *L. vannamei*. Two candidate probiotic LAB, *Lactobacillus plantarum* and *Lactococcus lactis*, were chosen, and their antimicrobial activities against various pathogenic bacteria, including the toxic strain of *V. parahaemolyticus* (VP_{AHPND}), was determined *in vitro*. The potential roles of two proPOs (*Lv*proPO1 and *Lv*proPO2) in the defense against VP_{AHPND} infection were investigated using a double-stranded (dsRNA)-mediated RNA interference (RNAi) approach. Thereafter, evaluation of the effect of the candidate LAB on activation of the shrimp proPO system and on improvement of resistance to VP_{AHPND} infection was performed.

2. Materials and methods

2.1. Isolation of the host-derived lactic acid bacteria (LAB) from the shrimp gut

The healthy cultured Pacific white shrimp *L. vannamei* with an average weight of 10 ± 2 g were collected from a shrimp farm in Samut Prakan province, Thailand. The entire shrimp digestive tracts were initially dissected out and homogenized in

0.85% (w/v) NaCl. The homogenates were used as inoculums for lactic acid bacteria (LAB) isolation using de Man, Rogosa and Sharpe (MRS) agar. The plates were incubated under aerobic and anaerobic conditions at 30 °C for 48 h to 72 h. Single colony was then picked and re-streaked on MRS agar plate to obtain the pure isolates for further analysis.

2.2. 16S rRNA sequence analysis

A bacterial 16S ribosomal RNA (16S rRNA) gene was PCR-amplified using the universal primers UFUL and URUL (Table 1). DNA templates were prepared from the LAB isolates by resuspended the bacterial cells in lysozyme solution (20 µg/ml lysozyme in 10 mM Tris-HCl, pH 8.0; Sigma-Aldrich), incubated at room temperature for 15 min followed by boiling at 100 °C for 30 min. The PCR was carried out at 94 °C for 3 min, followed by 35 cycles of 94 °C for 1 min, 55 °C for 1 min and 72 °C for 1 min plus a final extension at 72 °C for 5 min. The PCR product was verified by TBE-1.5% agarose gel electrophoresis with UV visualization following ethidium bromide staining. The PCR amplicons with an expected molecular size of approximately 500 bp were gel purified and directly sequenced (Macrogen Inc., Korea).

The two candidate LAB with high homology to the probiotics (*L. plantarum* and *L. lactis*), were selected for long sequence analysis of the bacterial 16S rRNA gene. Primers UFUL and LpLl_16sR (Table 1) and the genomic DNA of the candidate LAB were subjected to PCR amplification as described above. The amplified product was analyzed by agarose gel electrophoresis. The products with an expected molecular size of approximately 1,300 bp were gel purified, cloned and commercially sequenced on both strands (Macrogen Inc., Korea). The obtained sequences were analyzed using

146 the blastn program (https://blast.ncbi.nlm.nih.gov/Blast.cgi). Multiple sequence
147 alignment was carried out using the ClustalW2 program
148 (http://www.ebi.ac.uk/Tools/clustalw2/). The phylogenetic tree was created using the
149 Molecular Evolutionary Genetics Analysis (MEGA) software version 10.0.
150
151 **2.3. Antimicrobial activity assay**
152 *In vitro* antimicrobial activity assays were performed as previously described
153 by Kongnum and Hongpattarakere (2012), with a slight modification. The
154 antimicrobial activity of the candidate LAB, *L. plantarum* and *L. lactis*, was tested
155 against four gram-positive bacteria (*Staphylococcus aureus*, *Aerococcus viridans*,
156 *Bacillus megaterium*, and *B. subtilis*) and three gram-negative bacteria (VP_{AHPND}, *V.*
157 *harveyi*, and *Escherichia coli*). Two candidate LAB were grown in MRS medium at
158 30 °C for 24 h. Cells were centrifuged at 11,000 × g for 10 min at 4 °C. Supernatants
159 were collected and passed through a 0.45-μm pore size filter. The obtained cell-free
160 culture supernatants were used to detect the antimicrobial activity according to
161 Imjongjirak et al. (2007) with some modifications. Briefly, 20 μl of each two-fold
162 serially diluted cell-free culture supernatants in MRS medium was added to each well
163 of a 96-well microplate. Wells were then inoculated with 80 μl of a mid-log phase
164 bacteria (10^5 cfu/ml) in Poor Broth (1% (w/v) tryptone, 0.5% (w/v) NaCl, pH 7.5).
165 Cultures were grown at 30 °C with constant shaking for 24 h. The bacterial growth
166 was evaluated by measuring the optical density at 600 nm (OD_{600}) using a microplate
167 reader. The negative controls were performed as above using 20 μl of MRS medium.
168 All tests were carried out in triplicate. The antimicrobial activity was determined as
169 the minimal inhibitory concentration (MIC), which was taken as the interval of

concentration [a]-[b], where [a] is the highest concentration tested at which microbial growth can be observed and [b] is the lowest concentration at which microbial growth was inhibited after 24 h of an incubation at 30 °C.

2.4. Experimental feeding

The LAB-supplemented feed was prepared from a mixture of two candidate LAB (*L. plantarum* and *L. lactis*; 1:1 ratio). The LAB were separately grown in MRS medium at 30 °C until the culture reached an OD_{600} of 1.6. The cells were harvested by centrifugation, washed twice and resuspended in 0.85% (w/v) NaCl. The viable bacterial number was determined as cfu/ml of a bacterial suspension using the plate count method. The obtained *L. plantarum* and *L. lactis* cells were mixed with shrimp commercial feed, yielding a final concentration of 2-4 × 10^8 cfu/g feed using 1% (v/v) fish oil as an adhesive and feed attractant. The control feed was commercial feed mixed with 0.85% (w/v) NaCl and coated with 1% (v/v) fish oil. The feed was stored at 4 °C for use within 3 days.

The juvenile *L. vannamei* (average wet weight of 2 g) obtained from a shrimp farm in Chachoengsao Province, Thailand, were maintained in 20 ppt continuously aerated seawater at 25 ± 2 °C. The shrimp were allowed to acclimatize for one week. For the feeding experiment, the shrimp were divided into two groups with three replicates in each. The first group was shrimp fed *L. plantarum*- and *L. lactis*-supplemented feed. The second group was shrimp fed the control feed and used as the control group. The shrimp were fed three times a day (09:00, 12:00 and 18:00) for a period of 16 days, and each shrimp sample was subjected to PO activity assay and gene

193 expression analysis. For viable colony count and SEM analysis, the shrimp were
194 further fed the commercial feed for a period of 5 days.
195
196 **2.5. Microbiological determination**
197 The presence of candidate LAB in the shrimp gut was evaluated using the
198 viable plate count method followed by 16S rRNA sequence analysis. At 5 days post-
199 LAB feeding, three individual shrimp were randomly collected from the LAB-
200 supplemented and control groups, and the tissues of foregut, midgut, and hindgut were
201 separately dissected out. Each gut sample was homogenized in 0.85% (w/v) NaCl and
202 plated onto MRS agar in triplicate. The plates were incubated at 30 °C for 48 h to 72
203 h. LAB colonies were counted and recorded as cfu/g of fresh guts. Strains of viable
204 bacteria were confirmed by 16S rRNA sequence analysis followed by the method
205 described above.
206
207 **2.6. Scanning electron microscopy (SEM)**
208 Scanning electron microscopic (SEM) analysis was performed to evaluate
209 whether the supplemented *L. plantarum* and *L. lactis* could survive in the shrimp gut.
210 At 5 days post feeding, the LAB-supplemented shrimp were randomly collected, and
211 their midguts were dissected out and fixed with 2.5% (w/v) glutaraldehyde in 0.1 M
212 phosphate buffer (pH 7.4). Preparation of the samples for SEM analysis was carried
213 out as previously described (Amparyup et al., 2013b). The samples were observed
214 under a JEOL scanning electron microscope (model JSM-5410LV) at an accelerating
215 voltage of 15 kV.
216

2.7. Total RNA isolation and cDNA synthesis

Total RNA was extracted using Tri Reagent® (Molecular Research Center) according to the manufacturer's instructions followed by DNase I (Promega) treatment. One microgram of the DNA free-total RNA was reverse-transcribed to the first-strand cDNA using RevertAid First Strand cDNA Synthesis Kit (Thermo Fisher Scientific) according to the manufacturer's protocol. The cDNAs were stored at -80 °C until used.

2.8. Tissue distribution analysis of *Lv*proPOs

Tissue distribution analysis of two *Lv*proPO (*Lv*proPO1 and *Lv*proPO2) gene transcripts was performed using semiquantitative RT-PCR. The tissues of hemocytes, hapatopancreas, foregut, midgut and hindgut were individually collected from three healthy shrimp *L. vannamei*. Total RNA extraction and cDNA synthesis were performed as described above. Semiquantitative RT-PCR was carried out as previously described (Amparyup et al., 2009) using the gene specific primers designed from *Lv*proPO1 (EF115296) and *Lv*proPO2 (EF565469) (Table 1). A fragment of an elongation factor 1-α (EF1-α) gene was amplified as used as an internal reference control gene (Table 1).

2.9. Preparation of double-stranded RNA (dsRNA) and *in vivo* gene silencing of *Lv*proPO1 and *Lv*proPO2 transcripts

Double-stranded RNAs (dsRNAs) of *Lv*proPO1, *Lv*proPO2 and green fluorescent protein (GFP) (control) were generated by *in vitro* transcription using the T7 RiboMAX™ Express Large Scale RNA Production System (Promega) with the

gene-specific primers listed in Table 1 and were further purified as previously described (Amparyup et al., 2009). *In vivo* gene silencing was achieved by intramuscularly injecting *L. vannamei* shrimp (~3 g, fresh weight) with 25 µl of 150 mM NaCl containing *Lv*proPO1 and *Lv*proPO2 dsRNAs (2 µg/g shrimp). Shrimp injected with GFP dsRNA at the same concentration was used as the sequence-independent dsRNA control group, and shrimp injected with 25 µl of 150 mM NaCl were included as the handling control group. A second injection of dsRNA (2 µg/g shrimp) or 150 mM NaCl was repeated at 24 h after the first dsRNA injection. The *Lv*proPO1- and *Lv*proPO2-cosilenced and control shrimp were reared for an additional 48 h after the second dsRNA injection, and hemolymph was then collected for further analysis.

2.10. Semiquantitative RT-PCR analysis of *Lv*proPO1- and *Lv*proPO2-cosilenced shrimp

Hemolymph collected from each individual *Lv*proPO1- and *Lv*proPO2-cosilenced and control shrimp was subjected to total RNA isolation using an Illustra™ RNAspin mini kit (GE Healthcare). First-strand cDNA was synthesized as described above. Semiquantitative RT-PCR analysis of the gene silencing efficiency was performed as described previously (Amparyup et al., 2009) using gene specific primers (*Lv*PO1-F/-R for *Lv*proPO1 and *Lv*PO2-F/-R for *Lv*proPO2) (Table 1). Amplification of EF1-α gene fragment served as an internal reference control (Table 1).

2.11. PO activity assay of *Lv*proPO1- and *Lv*proPO2-cosilenced shrimp

PO activity was assayed according to the method used by Amparyup et al. (2009). Briefly, hemolymph was withdrawn from the *Lv*proPO1- and *Lv*proPO2-cosilenced and control shrimp at 48 h after the second dsRNA injection (or 150 mM NaCl only for the control). Protein concentration was determined using a Bradford assay kit (Bio-Rad). Total hemolymph protein (2 mg) was incubated with PO substrate (L-3,4-dihydroxyphenylalanine; L-DOPA) at room temperature for 30 min. The absorbance was measured at 490 nm. PO activity was defined as the ΔA_{490}/mg total protein/min. The experiment was performed three times with three samples from the three pooled shrimp groups. Statistical analysis was carried out using one-way analysis of variance (ANOVA) followed by Duncan's test. Statistical significance was accepted at $P< 0.05$.

To assay for PO activity in the shrimp gut, the *Lv*proPO1- and *Lv*proPO2-cosilenced and control shrimp were collected at 48 h after the second dsRNA injection. The whole gut was dissected out and washed with PBS (pH 7.4). Shrimp guts were then submerged in a saturated solution of dopamine, a PO substrate, and incubated in the dark for 2 h at room temperature before experimental observation. Shrimp guts incubated with dopamine in the presence of the PO inhibitor phenylthiourea (PTU) were included as controls.

2.12. Cumulative mortality assay of *Lv*proPO1- and *Lv*proPO2-cosilenced shrimp after VP_{AHPND} challenge

To assess the potential function of *Lv*proPO1 and *Lv*proPO2 in the defense against pathogenic VP_{AHPND} infection, *L. vannamei* shrimp (~3 g, fresh weight) were intramuscularly injected with *Lv*proPO1 and *Lv*proPO2 dsRNAs (2 μg/g shrimp).

Control shrimp were injected with GFP dsRNA or 150 mM NaCl. At 24 h after the first dsRNA injection, the shrimp were injected again with the same concentration of dsRNAs or 150 mM NaCl and then immediately challenged with VP_{AHPND}.

For the challenge experiment, a single colony of VP_{AHPND} was cultured in tryptic soy broth (TSB) containing 1.5% (w/v) NaCl (TSB medium) at 30 °C for 1 h with constant shaking. The culture was subsequently diluted 1:100 with fresh TSB medium and further cultured until the bacterial density reached an OD_{600} of 0.6. The bacterial suspension was poured into the culture tanks to give a final bacterial density of ~1×10^4 cfu/ml. The *Lv*proPO1- and *Lv*proPO2-cosilenced and control shrimp were then immersed, and the cumulative mortality was recorded daily. All experiments were performed in triplicate, with 9–10 shrimp/replicate/group. Statistical analysis was performed by one-way ANOVA followed by Duncan's test.

2.13. Assay of PO activity in the LAB-supplemented shrimp

To investigate whether the administration of the LAB-supplemented feed could modulate PO activity in the hemolymph of the shrimp *L. vannamei*, the shrimp were divided into 2 groups and fed *L. plantarum* and *L. lactis*-supplemented and control feed for 16 days as described above. Afterward, hemolymph was collected, and PO activity was assayed according to the method used by Amparyup et al. (2009) as described above. PO activity was recorded as ΔA_{490}/mg total protein/min. The experimental test was carried out in triplicate, with three samples from three pooled shrimp/group. Statistical analysis was performed using one-way ANOVA followed by Duncan's test. Statistical significance was accepted at $P < 0.05$.

312 **2.14. Expression analysis of *Lv*proPO genes in the LAB-supplemented shrimp**

313 To analyze the effect of LAB supplementation on the expression of two proPO
314 transcripts (*Lv*proPO1 and *Lv*proPO2), the shrimp were divided into two groups and
315 fed (i) *L. plantarum* and *L. lactis*-supplemented feed or (ii) control feed for 16 days as
316 described above. Midguts were individually collected from three individual shrimp at
317 days 0, 1, and 16 post feeding. Total RNA was extracted and reverse transcribed into
318 first-strand cDNA as described above. Quantitative real-time RT-PCR was then
319 carried out according to the protocol used by Amparyup et al. (2007) using the gene-
320 specific primers listed in Table 1. Amplification of the gene EF1-α served as an
321 internal reference control (Table 1). The Ct values of each sample at each time point
322 was normalized with the control sample. The relative mRNA expression was
323 determined according to a mathematical model described by Pfaffl (2001). The relative
324 expression level between each time point was statistically tested using one-way
325 ANOVA followed by Duncan's test. P values of less than 0.05 ($P< 0.05$) were
326 considered significant.

327

328 **2.15. Immersion challenge test of the LAB-supplemented shrimp**

329 Commercial feed supplemented with *L. plantarum*, *L. lactis*, and a mixture of
330 *L. plantarum* and *L. lactis* (1:1 ratio) were prepared as described above. Healthy *L.*
331 *vannamei* shrimp (average wet weight of 2 g) were divided into four groups and fed
332 (i) *L. plantarum*-supplemented feed, (ii) *L. lactis*-supplemented feed, (iii) *L. plantarum*
333 and *L. lactis*-supplemented feed, and (iv) control feed. Shrimp were fed three times a
334 day (09:00, 12:00 and 18:00) for a period of 16 days. Thereafter, the immersion
335 challenge test with VP_{AHPND} was carried out as described above. Cumulative mortality

was recorded daily over a 10-day period of immersion. The experiment was performed in triplicate, with 9–10 shrimp/replicate/group. Statistical analysis was performed using one-way ANOVA followed by Duncan's test.

3. Results

3.1. Isolation and identification of host-associated LAB from the gut of the shrimp *L. vannamei*

To isolate host-derived LAB for use as potential probiotics in shrimp, LAB strains were screened from the whole gut of the cultured Pacific white shrimp *L. vannamei* using MRS as the selective media. A total of 100 presumptive LAB clones that appeared as single colonies on the MRS agar plate were randomly selected for verification of the bacterial strains. Genomic DNA was extracted from each LAB isolate and then used as a template for amplification of partial DNA fragments of the bacterial 16S rRNA gene (approximately 500 bp) using the universal primers UFUL and URUL. Sequence analysis revealed that the obtained isolates consisted of rod-shaped (i.e., *Lactobacillus*) and cocci-shaped (i.e., *Lactococcus* and *Vagococcus*) LAB. Then, two candidate species (*L. plantarum* strain SGLAB01 and *L. lactis* strain SGLAB02) were chosen for long sequence analysis of the bacterial 16S rRNA (approximately 1300 bp) using the primers UFUL and LpLl_16sR. After Blast analysis against the 16S rRNA sequence in the GenBank database, the results revealed that these isolates were closest to *L. plantarum* subsp. *plantarum* strain LB1-2, isolated from the hindgut of the European honeybee *Apis mellifera* (99% identity; GenBank accession number CP025991.1), and *L. lactis* strain R-53658 isolate H78-17, isolated

359 from the bumble bee gut (99% identity; GenBank accession number LT631749.1),
360 respectively.

361 A phylogenetic tree constructed using the neighbor-joining method was then
362 carried out, and the results showed that the *L. plantarum* strain SGLAB01 was
363 clustered in the group of the genus *Lactobacillus* and grouped with the *L. plantarum*
364 strain LB1-2 in a 100% bootstrap cluster (Fig. 1). Meanwhile, the *L. lactis* strain
365 SGLAB02 was placed in the cluster of *Lactococcus* and grouped with the *L. lactis*
366 strain R-53658 with a bootstrap of 100% (Fig. 1). This finding clearly demonstrated
367 that the LAB candidates are ascribed to the species *L. plantarum* and *L. lactis*,
368 respectively (Fig. 1).

369

370 **3.2. Antimicrobial activity of the candidate LAB against microbial pathogens**

371 The antimicrobial activity of the candidate LAB (*L. plantarum* strain
372 SGLAB01 and *L. lactis* strain SGLAB02) were tested against four gram-positive
373 bacteria (*S. aureus*, *A. viridans*, *B. megaterium*, and *B. subtilis*) and three gram-
374 negative bacteria (VP_{AHPND}, *V. harveyi*, and *E. coli*). As shown in Table 2, the *L.*
375 *plantarum* strain SGLAB01 displayed antimicrobial activity against *A. viridans*, with
376 a MIC value of 3.125-6.25 μg/ml; against *V. harveyi*, with a MIC value of 6.25-12.5
377 μg/ml; and against *S. aureus*, *B. megaterium*, *B. subtilis*, *E. coli* and VP_{AHPND}, with a
378 MIC value of 12.5-25 μg/ml. The *L. lactis* strain SGLAB02 was found to display
379 antimicrobial activity against *A. viridans*, with a MIC value of 6.25-12.5 μg/ml;
380 against VP_{AHPND}, with a MIC value of 12.5-25 μg/ml; and against *S. aureus*, *B.*
381 *megaterium*, *B. subtilis*, *V. harveyi* and *E. coli*, with a MIC value of 25-50 μg/ml (Table
382 2). These results indicated that the LAB candidates exhibited antimicrobial activity

against both gram-positive and gram-negative bacteria, including the virulent, pathogenic strain of *V. parahaemolyticus* (VP_{AHPND}) that causes AHPND outbreaks in shrimp (Table 2).

3.3. Detection of the candidate LAB in the gut of the LAB-supplemented *L. vannamei* shrimp

To further assess whether the candidate LAB (*L. plantarum* strain SGLAB01 and *L. lactis* strain SGLAB02) could survive in the GI tract of *L. vannamei* shrimp, shrimp were fed the candidate LAB-supplemented feed for 16 days, and the viable LAB colonies in different gut parts were determined using MRS agar plates. As shown in Fig. 2A, significantly higher numbers of viable LAB were observed in the foregut, midgut and hindgut of the LAB-supplemented shrimp at 5 days post probiotic feeding than in the guts of the control group fed control feed ($P< 0.05$). Moreover, it was found that the number of viable LAB in the midgut was 2.0- and 9.1-fold higher than those in the foregut and hindgut, respectively (Fig. 2A).

The strains of the viable LAB isolates in different gut parts were then confirmed by using 16S rRNA sequence analysis. The viable bacterial isolates were randomly collected from each specimen of shrimp guts and subjected to PCR amplification using universal primers for the bacterial 16S rRNA gene, followed by DNA sequencing. The results demonstrated that viable isolates obtained from the GI tract of *L. vannamei* shrimp were LAB and showed 100% sequence identify with the 16S rRNA sequence of the *L. plantarum* strain SGLAB01 and the *L. lactis* strain SGLAB02 (data not shown).

406 To further confirm the existence of the administered LAB in the shrimp GI
407 tract, scanning electron microscope (SEM)-based analysis of microbial attachment in
408 the inner surface of the shrimp GI tract was carried out (Fig. 2B). Several rod- and
409 cocci-shaped bacterial cells were found to adhere to the GI tract of the LAB-
410 supplemented shrimp (Fig. 2B; e-h). In contrast, no bacterial cells were observed in
411 the GI tract of the control shrimp (Fig. 2B; c-d).
412
413 **3.4. Expression analysis of *Lv*proPO1 and *Lv*proPO2 mRNA in different shrimp**
414 **tissues**
415 To assess the mRNA expression levels of *Lv*proPO1 and *Lv*proPO2 in different
416 shrimp tissues, total RNA extracted from the tissues of hemocytes, hepatopancreas,
417 foregut, midgut and hindgut was reversed transcribed into cDNA and subjected to
418 semiquantitative RT-PCR analysis. As shown in Fig. 3A, the RT-PCR results
419 demonstrated that the expression level of *Lv*proPO1 mRNA was highest in hemocytes,
420 followed by the midgut, foregut, hindgut and hepatopancreas. A similar expression
421 pattern was also observed for *Lv*proPO2 mRNA transcripts. The result showed that
422 *Lv*proPO2 mRNA was highly expressed in hemocytes, followed by the midgut,
423 foregut, and hindgut, with a relatively low expression level in the hepatopancreas (Fig.
424 3A).
425
426 **3.5. Effect of RNAi-mediated cosilencing of *Lv*proPO1 and *Lv*proPO2 on PO**
427 **activity**
428 To ascertain the potential function of two *Lv*proPOs in the *L. vannamei* proPO
429 system, *in vivo* cosilencing of *Lv*proPO1 and *Lv*proPO2 transcripts was then employed.

RT-PCR analysis showed that injection of *Lv*proPO1 and *Lv*proPO2 dsRNAs significantly decreased the expression levels of the respective *Lv*proPO1 and *Lv*proPO2 transcripts in shrimp hemocytes compared with their expression levels in control groups injected with GFP dsRNA (Fig. 3B). This finding suggests that *Lv*proPO1 and *Lv*proPO2 dsRNAs efficiently suppressed the transcript levels of *Lv*proPO1 and *Lv*proPO2, respectively (Fig. 3B). The effect of *Lv*proPO1 and *Lv*proPO2 cosilencing on the reduction in PO activity was then determined. Hemolymph from *Lv*proPO1- and *Lv*proPO2-cosilenced and control shrimp was collected at 48 h after the second dsRNA injection and subjected to a PO activity assay using L-DOPA as a substrate. As shown in Fig. 3C, the hemolymph PO activity of *Lv*proPO1- and *Lv*proPO2-cosilenced shrimp was decreased significantly, by 66% compared with the control groups ($P< 0.05$). To further test whether the melanization in the shrimp gut is due to the activity of *Lv*proPO1 and *Lv*proPO2, *ex vivo* assaying of the PO activity in the whole gut of the *Lv*proPO1- and *Lv*proPO2-cosilenced shrimp was carried out. After 2 h of incubation with the PO substrate, melanization in the guts of the *Lv*proPO1- and *Lv*proPO2-cosilenced shrimp was abolished such that it was comparable with melanization in the guts of the GFP dsRNA-injected and NaCl control shrimp and the PO inhibitor (PTU) control group, indicating that *Lv*proPO1 and *Lv*proPO2 contributed to gut PO activity (Fig. 3D). This result indicates that these two *Lv*proPOs function in the proPO system of *L. vannamei* shrimp.

3.6. *Lv*proPO1 and *Lv*proPO2 are required for the defense response against VP_{AHPND} infection in the shrimp *L. vannamei*

453 DsRNA-mediated *in vivo* gene-silencing experiments were employed to
454 investigate the roles of *Lv*proPOs in the defense response against VP_{AHPND} infection.
455 Shrimp were double-injected with dsRNAs corresponding to *Lv*proPO1 and *Lv*proPO2
456 dsRNA, followed by VP_{AHPND} challenge. As shown in Fig. 4, significant increases in
457 cumulative mortality, at 93% and 100% was observed in the *Lv*proPO1 and *Lv*proPO2
458 cosilenced shrimp after challenged with VP_{AHPND} for 2 and 3 days, respectively,
459 compared with cumulative mortality values of 53% and 80%, respectively, for the GFP
460 dsRNA-injected control shrimp and cumulative mortality values of 47% and 63%,
461 respectively, for the NaCl-injected control shrimp, suggesting that these two *Lv*proPOs
462 play significant roles in the defense response against VP_{AHPND} infection in the shrimp
463 *L. vannamei*.
464
465 **3.7. Effect of LAB supplementation on the modulation of shrimp PO activity**
466 To evaluate the effect of LAB supplementation on modulation of the shrimp
467 proPO system, *L. vannamei* shrimp were fed a diet supplemented with two candidate
468 LAB (*L. plantarum* strain SGLAB01 and *L. lactis* strain SGLAB02) for 16 days, and
469 hemolymph was then collected for the PO activity assay. Interestingly, a significant
470 increase in PO activity was observed in the LAB-supplemented shrimp compared with
471 the control group fed control feed (Fig. 5A). The enzymatic PO activity of shrimp fed
472 the two candidate LAB was approximately 1.7-fold higher than that of control shrimp
473 (Fig. 5A). This finding suggests that the candidate LAB, *L. plantarum* strain
474 SGLAB01 and *L. lactis* strain SGLAB02, play roles in modulation of the host proPO
475 system.
476

3.8. Effect of LAB supplementation on the expression of *Lv*proPO1 and *Lv*proPO2 transcripts

The effect of LAB supplementation on the transcriptional expression of the *Lv*proPO1 and *Lv*proPO2 genes was then examined using quantitative real-time RT-PCR analysis. Total RNA was isolated from the midgut tissue collected from experimental and control shrimp at days 0, 1, and 16 post probiotic feeding. As shown in Fig. 5B, feeding shrimp with the diet supplemented with the two probiotic LAB (*L. plantarum* strain SGLAB01 and *L. lactis* strain SGLAB02) significantly increased the expression levels of *Lv*proPO1 and *Lv*proPO2 mRNA transcripts. The expression level of *Lv*proPO1 mRNA in the midgut was dramatically increased by 6.3-fold at day 1 and 14.3-fold at day 16 compared with that at day 0 post feeding (Fig. 5B). Likewise, the expression level of *Lv*proPO2 mRNA in the midgut was shown to be slightly increased by 1.7-fold at day 1 and dramatically increased by 9.9-fold at day 16 compared with that at day 0 post feeding (Fig. 5B). This finding suggests that feeding the shrimp the candidate probiotics *L. plantarum* and *L. lactis* transiently upregulated the expression levels of *Lv*proPO1 and *Lv*proPO2 transcripts in the midgut of *L. vannamei* shrimp.

3.9. Effect of LAB supplementation on the survival of *L. vannamei* shrimp after VP_{AHPND} challenge

Prior to the experimental challenge, the toxicity of each LAB strain was evaluated *in vivo*. Shrimp were fed the *L. plantarum* strain SGLAB01 and *L. lactis* strain SGLAB02 inoculums at 10^7 cfu/shrimp, and no shrimp death was observed (data not shown). This finding demonstrated that both candidate strains are nonpathogenic LAB to *L. vannamei* shrimp. To evaluate whether supplementation of the two probiotic

LAB (*L. plantarum* strain SGLAB01 and *L. lactis* strain SGLAB02) could prevent or increase shrimp resistance to infection with the pathogenic bacteria VP_{AHPND}, *L. vannamei* were fed the LAB-supplemented diet for 16 days prior to challenge with 10^4 cfu/ml VP_{AHPND}. As shown in Fig. 6, shrimp fed separately with *L. plantarum* strain SGLAB01 and *L. lactis* strain SGLAB02 at a concentration of 2-4 × 10^8 cfu/g feed displayed respective cumulative mortality percentages of 50% and 40% at 10 days postinfection (dpi). Interestingly, it was found that feeding the shrimp a combination of the *L. plantarum* strain SGLAB01 and *L. lactis* strain SGLAB02 at a concentration of 2-4 × 10^8 cfu/g feed resulted in the lowest cumulative mortality, 36.7% at 10 dpi. For control shrimp that were fed the control feed, a cumulative mortality of 90% at 10 dpi was observed (Fig. 6). The obtained results indicate that administration of the two candidate LAB as probiotics could protect shrimp from VP_{AHPND} infection, thus increasing shrimp resistance to VP_{AHPND} infection.

4. Discussion

LAB are generally considered a major group of health-promoting (probiotic) bacteria that are often identified as components of the gut microbiota and play a beneficial role in promoting growth performance, modulating the host immune response and increasing disease resistance to pathogens (Gillor et al., 2008; Merrifield et al., 2014; Ouwehand and Vesterlund, 2004). In shrimp aquaculture, applications of LAB as probiotics have been reported (Adel et al., 2017; Castex et al., 2008, 2009, 2010; Kongnum and Hongpattarakere, 2012; Leyva-Madrigal et al., 2011; Lv et al., 2017; Maeda et al., 2014; Peraza-Gómez et al., 2009; Vieira et al., 2007, 2008, 2010).

524 However, data on the utilization of host-derived LAB as probiotics with
525 immunomodulatory functions is still limited.

526 In the present study, we initially screened for host-derived LAB strains from
527 the whole GI tracts of the shrimp *L. vannamei.* Then, we identified two major strains,
528 the *L. plantarum* strain SGLAB01 (rod shaped) and *L. lactis* strain SGLAB02 (cocci
529 shaped), as candidate probiotic species in the shrimp gut based on long 16S rRNA
530 (~1300 bp) sequencing and phylogenetic tree analysis. This result is consistent with
531 previous reports on the isolation of LAB from the shrimp gut, which showed that most
532 of the LAB strains were cocci- and rod-shaped strains (Kongnum and
533 Hongpattarakere, 2012; Maeda et al., 2014). For LAB isolated from wild and
534 cultivated shrimp guts, cocci-shaped LAB accounted for 78.23–79.49% of total LAB
535 isolates and appeared as the most common isolates in the shrimp gut (Kongnum and
536 Hongpattarakere, 2012). Maeda et al. (2014) also showed that 67.75% of the LAB
537 isolated from kuruma shrimp *M. japonicus* intestines were coccoid shaped, whereas
538 rod shaped LAB accounted for 32.25% of the total isolates.

539 Previously, the LAB *L. plantarum* strain MRO3.12, which was isolated from
540 the digestive tracts of wild shrimp, was shown to exhibit a strong inhibitory effect
541 against *V. harveyi*, while complete reduction of *V. harveyi* was observed after
542 cocultivation of *V. harveyi* and the *L. plantarum* strain MRO3.12 for 24 h under both
543 aerobic and anaerobic conditions (Kongnum and Hongpattarakere, 2012). The LAB *L.*
544 *lactis* strain D1813, which was isolated from the digestive tract of kuruma shrimp, was
545 also shown to exhibit an antibacterial effect against the pathogenic bacteria *V.*
546 *penaeicida* (Maeda et al., 2014). In this study, the antimicrobial activity of two
547 candidate LAB was tested against four gram-positive bacteria and three gram-negative

548 bacteria. Our result demonstrated that the two candidate LAB, the *L. plantarum* strain
549 SGLAB01 and *L. lactis* strain SGLAB02, exhibited antimicrobial activity against both
550 gram-positive and gram-negative bacteria. Both LAB candidates acted as efficient
551 bacteriostatic agents against *A. viridans*. More importantly, our LAB candidates also
552 displayed antibacterial activity against the virulent pathogenic strains *V. harveyi* and
553 VP_{AHPND}, which cause serious disease outbreaks in shrimp.

554 In an attempt to apply the host-derived LAB as potential probiotics with
555 immunomodulatory functions in the shrimp *L. vannamei*, we first determined whether
556 the two candidate LAB could survive in the shrimp gut after feeding the shrimp the
557 LAB-supplemented diet. Significantly, we observed a high number of viable LAB in
558 the entire gut, including the foregut, midgut and hindgut, of the LAB-supplemented
559 shrimp. This result is in agreement with previous reports that showed that the presence
560 of LAB in digestive tracts of LAB-fed shrimp *L. vannamei* challenged with *V. harveyi*
561 was obviously increased at the end of the feeding trial (Kongnum and
562 Hongpattarakere, 2012). Using 16S rRNA sequence analysis, the obtain data
563 confirmed that the viable cells in the shrimp gut were the candidate *L. plantarum* strain
564 SGLAB01 and *L. lactis* strain SGLAB02. SEM analysis also revealed several
565 adherences of rod-shaped and cocci-shaped bacterial cells to the inner surface of GI
566 tract of the LAB-fed shrimp compared with the control group shrimp. Taken together,
567 these findings suggest that *L. plantarum* strain SGLAB01 and *L. lactis* strain
568 SGLAB02 that are prepared as feed supplement and applied via oral route could reside
569 and adhere in the GI tract of the LAB-fed shrimp *L. vannamei*.

570 Melanization, mediated by the activation of the proPO system, is a potent rapid
571 innate defense mechanism that plays crucial roles in pathogen sequestration in

572 invertebrates (Amparyup et al., 2013a; Cerenius and Söderhäll, 2004; Cerenius et al.,
573 2008; Kanost and Gorman, 2008; Tassanakajon et al., 2018). The proPO system is an
574 enzymatic cascade system that is triggered upon recognition of pathogen-associated
575 molecular patterns (PAMPs) by host pattern-recognition receptors (PRPs) (Hoffmann
576 et al., 1999; Ishii et al., 2008; Janeway and Medzhitov, 2002; Medzhitov, 2007). PO
577 is a key enzyme of the proPO system that oxidizes monophenols and diphenols into
578 quinone precursors, which are required for melanin biosynthesis (Cerenius and
579 Söderhäll, 2004; Nappi and Christensen, 2005). Indeed, the subsequent intermediates
580 produced during the proPO system activation, such as quinone-like substances,
581 reactive oxygen (ROI) or nitrogen (RNI) intermediates, also exhibit cytotoxic activity
582 and are involved in the restriction and/or killing of the invading pathogens (Cerenius
583 et al., 2008, 2010; Charoensapsri et al., 2014; Nappi and Christensen, 2005;
584 Sutthangkul et al., 2015; Zhao et al., 2007, 2011). Because of the important function
585 of the proPO-activating cascade, in this study, we were interested in evaluating
586 whether LAB supplementation could modulate the activation of the proPO system in
587 the LAB-fed shrimp *L. vannamei*.

588 In penaeid shrimp, several proPO genes have been identified, including one
589 proPO gene from *P. semisulcatus* and two proPO genes from *P. monodon*
590 (Sritunyalucksana et al., 1999; Amparyup et al., 2009), *M. japonicus* (Adachi et al.,
591 2004; Masuda et al., 2012), and *F. chinensis* (Gao et al., 2009). In *L. vannamei*, two
592 proPO genes (*Lv*proPO1 and *Lv*proPO2) have been reported (Ai et al., 2008, 2009; Lai
593 et al., 2005; Wang et al., 2007). However, data on the function of these two *Lv*proPO
594 genes in the shrimp gut remain elusive. In this study, we first determined the tissue
595 distribution of *Lv*proPO1 and *Lv*proPO2 mRNA transcripts in different tissues,

596 including the shrimp gut. Interestingly, in addition to the high level of mRNA
597 expression that was detected in shrimp hemocytes, moderate to low levels of
598 *Lv*proPO1 and *Lv*proPO2 were detected in the entire guts of normal shrimp, including
599 the midgut, foregut and hindgut, and in the hepatopancreas. Previous findings have
600 demonstrated that the proPOs of *L. vannamei* were localized only in shrimp hemocytes
601 (Ai et al., 2009; Lai et al., 2005). The proPO transcripts of shrimp *P. monodon* and *F.*
602 *chinensis* have also been shown to be mainly expressed in hemocytes (Amparyup et
603 al., 2009; Gao et al., 2009; Sritunyalucksana et al., 1999). Nevertheless, the proPO
604 transcripts were also detected in other tissues, such as in the hepatopancreas of *M.*
605 *japonicus* (Masuda et al., 2012). Although the proPO system plays a major role in the
606 immune defense of hemocytes in invertebrates, several studies have reported a positive
607 role of melanization in the regulation of bacterial pathogens and detoxification in the
608 gut system (Shao et al., 2012; Wu et al., 2015). Additionally, our preliminary analysis
609 of PO activity in the gut of normal shrimp and proPO-knockdown shrimp suggested
610 the existence of proPO in shrimp guts. By staining shrimp guts using dopamine as a
611 substrate in the presence or absence of the PO inhibitor phenylthiourea (PTU), our
612 results demonstrated that PO activity could be detected in the gut of normal shrimp
613 and that the activity was abolished in the guts of proPO-knockdown shrimp and PTU-
614 treated shrimp. In accordance with this study, low levels of *Lv*proPOs in shrimp guts
615 may be related to the functions of PO in gut immunity. However, the exact functions
616 remain to be elucidated and will require further study.

617 To further confirm the involvement of the two *Lv*proPOs in the proPO system
618 as well as in defense against VP_{AHPND} infection, *in vivo* gene silencing of *Lv*proPO1
619 and *Lv*proPO2 transcripts was employed. A PO activity assay of hemolymph samples

620 collected from the *Lv*proPO1- and *Lv*proPO2-cosilenced shrimp revealed that both
621 *Lv*proPO1 and *Lv*proPO2 function in the *L. vannamei* shrimp proPO system. A
622 significance increase in the cumulative mortality of the *Lv*proPO1- and *Lv*proPO2-
623 cosilenced shrimp was also demonstrated after VP_{AHPND} challenge. The significant role
624 of PO against infectious pathogens has been reported in many insects and crustacean
625 species (Amparyup et al., 2009, 2013a, Binggeli et al., 2014; Cerenius et al., 2008,
626 2010; Charoensapsri et al., 2014; Fagutao et al., 2009; Liu et al., 2007). In shrimp, the
627 important function of proPOs in host defenses has also reported. In *P. monodon*,
628 RNAi-mediated suppression of two *Pm*proPOs (*Pm*proPO1 and *Pm*proPO2), followed
629 by pathogen challenges, suggested the important role of *Pm*proPOs in shrimp defenses
630 against the pathogenic bacteria *V. harveyi*, the fungus *Fusarium solani*, and white spot
631 syndrome virus infections (Amparyup et al., 2009, 2013a; Charoensapsri et al., 2014;
632 Sutthangkul et al., 2015). In *M. japonicus*, silencing of the proPO gene resulted in an
633 increase in bacterial load in the knockdown shrimp hemolymph and an increase in
634 shrimp mortality (Fagutao et al., 2009). However, the role of the two *Lv*proPOs in *L.*
635 *vannamei* shrimp in pathogen defense has yet to be verified. Here, dsRNA-mediated
636 gene silencing followed by bacterial challenge experiments was employed to evaluate
637 the potential functions of two *Lv*proPO transcripts in shrimp immunity. Our findings
638 suggest that these two *Lv*proPOs play significant roles in the defense against VP_{AHPND}
639 infection in the shrimp *L. vannamei*.
640 To further evaluate whether supplementation of the candidate LAB could
641 modulation the activation of the shrimp proPO system, *L. vannamei* shrimp were fed
642 a diet supplemented with the two candidate LAB (*L. plantarum* strain SGLAB01 and
643 *L. lactis* strain SGLAB02) for a period of 16 days. Interestingly, analysis of the

644 hemolymph PO activity revealed a significant increase in enzymatic PO activity in the
645 two candidate LAB-fed shrimp. Moreover, we further examined the expression of the
646 two *Lv*proPO genes in the LAB-fed shrimp, and the results showed that feeding shrimp
647 the two candidate LAB transiently upregulated the expression levels of *Lv*proPO1 and
648 *Lv*proPO2 transcripts in the midgut of *L. vannamei* shrimp. Previously, LAB were
649 shown to display high immune-stimulating activity in human and animals (Ichikawa
650 et al., 2012; Kawashima et al., 2013). Multiple studies have demonstrated the ability
651 of probiotics to activate innate immunity in several crustacean species (Gullian et al.,
652 2004; Hai et al., 2009; Li et al., 2009). However, the ability of LAB to stimulate the
653 proPO system in shrimp is still limited. In this study, our findings revealed a significant
654 increase in PO activity when shrimp were fed a diet supplemented with the two
655 candidate LAB, indicating an increase in shrimp immunity. This finding is in
656 agreement with those of previous reports that showed that a significant improvement
657 of PO was observed when animals are fed a probiotic-supplemented diet (Chiu et al.,
658 2007). This finding suggests that the two candidate LAB, the *L. plantarum* strain
659 SGLAB01 and *L. lactis* strain SGLAB02, are potential probiotics that display an
660 immunomodulatory function in the activation of the proPO system in the shrimp *L.*
661 *vannamei*.

662 Feed-incorporated probiotics have been reported to improve resistance to
663 pathogens in aquaculture (Verschuere et al., 2000). Here, the potential function of two
664 candidate LAB, *L. plantarum* and *L. lactis*, as probiotics in shrimp was tested against
665 the pathogenic bacterium VP_{AHPND}. We found that feeding shrimp feed containing the
666 *L. plantarum* strain SGLAB01 and *L. lactis* strain SGLAB02 significantly increased
667 tolerance to the lethality of VP_{AHPND} infections. In the kuruma shrimp *M. japonicus*, a

668 significant increase in resistance to *V. penaeicida* infection was observed in shrimp
669 fed a probiotic-supplemented diet when compared with the control group (Maeda et
670 al., 2014).

671 In summary, two candidate LAB, *L. plantarum* and *L. lactis*, were isolated from
672 the digestive tract of healthy cultured Pacific white shrimp *L. vannamei*. These two
673 candidate LAB displayed antimicrobial activity against gram-positive and gram-
674 negative bacteria. The immunomodulatory function of the two LAB on two *Lv*proPO
675 genes as well as on the activation of the shrimp proPO system were evaluated, and the
676 results demonstrated that administration of a diet supplemented with the two candidate
677 LAB significantly enhanced PO activity, increased the expression levels of two
678 *Lv*proPO transcripts and promoted disease resistance to VP_{AHPND} infection in the LAB-
679 fed shrimp *L. vannamei*. These findings suggest the potential application of the two
680 LAB candidates, *L. plantarum* and *L. lactis*, as feed supplement that activates the host
681 immune response and likely increases disease resistance to VP_{AHPND}, probably via the
682 upregulation of the two *Lv*proPO transcripts.

683

684 **Acknowledgments**

685 This work was supported by research grants from the Thailand Research Fund
686 to AT (TRF Senior Scholar No. RTA5880004), and from the Thailand Research Fund
687 and Thailand National Center for Genetic Engineering and Biotechnology (BIOTEC)
688 to PA (Grant No. BRG5880016). SC is the recipient of a student fellowship from the
689 Thailand Graduate Institute of Science and Technology (TGIST) program of National
690 Science and Technology Development Agency (NSTDA) and the 90th Anniversary of
691 Chulalongkorn University Fund (Ratchadaphiseksomphot Endowment Fund).

692 **References**

693 Adachi, K., Hirata, T., Nagai, K., Fujio, A., Sakaguchi, M., 2004. Hemocyanin-related
694 reactions induce blackening of freeze-thawed prawn during storage, in:
695 Sakaguchi, M., (Ed.), More efficient utilization of fish and fisheries products.
696 Elsevier, Amsterdam, pp. 317–330.

697 Adel, M., El-Sayed, A.M., Yeganeh, S., Dadar, M., Giri, S.S., 2017. Effect of potential
698 probiotic *Lactococcus lactis* subsp. *lactis* on growth performance, intestinal
699 microbiota, digestive Enzyme activities, and disease resistance of *Litopenaeus*
700 *vannamei*. Probiotics Antimicrob. Proteins. 9, 150–156.

701 Ai, H.S., Huang, Y.C., Li, S.D., Weng, S.P., Yu, X.Q., He, J.G., 2008. Characterization
702 of a prophenoloxidase from hemocytes of the shrimp *Litopenaeus vannamei* that
703 is down-regulated by white spot syndrome virus. Fish Shellfish Immunol. 25,
704 28–39.

705 Ai, H.S., Liao, J.X., Huang, X.D., Yin, Z.X., Weng, S.P., Zhao, Z.Y., Li, S.D., Yu,
706 X.Q., He, J.G., 2009. A novel prophenoloxidase 2 exists in shrimp hemocytes.
707 Dev. Comp. Immunol. 33, 59–68.

708 Amparyup, P., Jitvaropas, R., Pulsook, N., Tassanakajon, A., 2007. Molecular cloning,
709 characterization and expression of a masquerade-like serine proteinase
710 homologue from black tiger shrimp *Penaeus monodon*. Fish Shellfish Immunol.
711 22, 535–546.

712 Amparyup, P., Charoensapsri, W., Tassanakajon, A., 2009. Two prophenoloxidases
713 are important for the survival of *Vibrio harveyi* challenged shrimp *Penaeus*
714 *monodon*. Dev. Comp. Immunol. 33, 247–256.

715 Amparyup, P., Charoensapsri, W., Tassanakajon, A., 2013a. Prophenoloxidase system
716 and its role in shrimp immune responses against major pathogens. Fish Shellfish
717 Immunol. 34, 990–1001.
718 Amparyup, P., Promrungreang, K., Charoensapsri, W., Sutthangkul, J., Tassanakajon,
719 A., 2013b. A serine proteinase *Pm*ClipSP2 contributes to prophenoloxidase
720 system and plays a protective role in shrimp defense by scavenging
721 lipopolysaccharide. Dev. Comp. Immunol. 41, 597–607.
722 Binggeli, O., Neyen, C., Poidevin, M., Lemaitre, B., 2014. Prophenoloxidase
723 activation is required for survival to microbial infections in *Drosophila*. PLoS
724 Pathog. 10, e1004067.
725 Castex, M., Chim, L,. Pham, D., Lemaire, P., Wabete, N., Nicolas, J.L., Schmidely,
726 P., Mariojouls, C., 2008. Probiotic *P. acidilactici* application in shrimp
727 *Litopenaeus stylirostris* culture subject to vibriosis in New Caledonia.
728 Aquaculture. 275: 182–193.
729 Castex, M., Lemaire, P., Wabete, N., Chim, L., 2009. Effect of dietary probiotic
730 *Pediococcus acidilactici* on antioxidant defences and oxidative stress status of
731 shrimp *Litopenaeus stylirostris*. Aquaculture. 294, 306–331.
732 Castex, M., Lemaire, P., Wabete, N., Chim, L., 2010. Effect of probiotic *Pediococcus*
733 *acidilactici* on antioxidant defences and oxidative stress of *Litopenaeus*
734 *stylirostris* under *Vibrio nigripulchritudo* challenge. Fish Shellfish Immunol. 28,
735 622–631.
736 Cerenius, L., Söderhäll, K., 2004. The prophenoloxidase-activating system in
737 invertebrates. Immunol. Rev. 198, 116–126.

738 Cerenius, L., Lee, B.L., Söderhäll, K., 2008. The proPO-system: pros and cons for its
739 role in invertebrate immunity. Trends Immunol. 29, 263–271.
740 Cerenius, L., Babu, R., Söderhäll, K., Jiravanichpaisal, P., 2010. *In vitro* effects on
741 bacterial growth of phenoloxidase reaction products. J. Invertebr. Pathol. 103,
742 21–23.
743 Charoensapsri, W., Amparyup, P., Suriyachan, C., Tassanakajon, A., 2014.
744 Melanization reaction products of shrimp display antimicrobial properties
745 against their major bacterial and fungal pathogens. Dev. Comp. Immunol. 47,
746 150–159.
747 Chiu, C.H., Guu, Y.K., Liu, C.H., Pan, T.M., Cheng, W., 2007. Immune responses and
748 gene expression in white shrimp, *Litopenaeus vannamei*, induced by
749 *Lactobacillus plantarum*. Fish Shellfish Immunol. 23, 364–377.
750 de la Peña, L.D., Cabillon, N.A., Catedral, D.D., Amar, E.C., Usero, R.C., Monotilla,
751 W.D., Calpe, A.T., Fernandez, D.D., Saloma, C.P., 2015. Acute
752 hepatopancreatic necrosis disease (AHPND) outbreaks in *Penaeus vannamei*
753 and *P. monodon* cultured in the Philippines. Dis. Aquat. Organ. 116, 251–254.
754 Fagutao, F.F., Koyama, T., Kaizu, A., Saito-Taki, T., Kondo, H., Aoki, T., Hirono, I.,
755 2009. Increased bacterial load in shrimp hemolymph in the absence of
756 prophenoloxidase. FEBS J. 276, 5298–5306.
757 Farzanfar A., 2006. The use of probiotics in shrimp aquaculture. FEMS Immunol.
758 Med. Microbiol. 48, 149–158.
759 Flegel, T.W., 2012. Historic emergence, impact and current status of shrimp pathogens
760 in Asia. J. Invertebr. Pathol. 110, 166–173.

761 Gao, H., Li, F., Dong, B., Zhang, Q., Xiang, J., 2009. Molecular cloning and
762 characterisation of prophenoloxidase (ProPO) cDNA from *Fenneropenaeus*
763 *chinensis* and its transcription injected by *Vibrio anguillarum*. Mol. Biol. Rep.
764 36, 1159–1166.
765 Gillor, O., Etzion, A., Riley, M.A., 2008. The dual role of bacteriocins as anti- and
766 probiotics. Appl. Microbiol. Biotechnol. 81, 591–606.
767 Gullian, M., Thompson, F., Rodriguez, J., 2004. Selection of probiotic bacteria and
768 study of their immunostimulatory effect in *Penaeus vannamei* Aquaculture. 233,
769 1–14.
770 Hai, N.V., Buller, N., Fotedar, R., 2009. Effects of probiotics (*Pseudomonas*
771 *synxantha* and *Pseudomonas aeruginosa*) on the growth, survival and immune
772 parameters of juvenile western king prawns (*Penaeus latisulcatus* Kishinouye,
773 1896). Aquaculture Res. 40, 590–602.
774 Han, J.E., Tang, K.F., Tran, L.H., Lightner, D.V., 2015. Photorhabdus insect-related
775 (Pir) toxin-like genes in a plasmid of *Vibrio parahaemolyticus*, the causative
776 agent of acute hepatopancreatic necrosis disease (AHPND) of shrimp. Dis.
777 Aquat. Organ. 113, 33–40.
778 Hoffmann, J.A., Kafatos, F.C., Janeway, C.A., Ezekowitz, R.A., 1999. Phylogenetic
779 perspectives in innate immunity. Science. 284, 1313–1318.
780 Ichikawa, S., Miyake, M., Fujii, R., Konishi, Y., 2012. MyD88 associated ROS
781 generation is crucial for *Lactobacillus* induced IL-12 production in macrophage.
782 PLoS One. 7, e35880.
783 Imjongjirak, C., Amparyup, P., Tassanakajon, A., Sittipraneed, S., 2007.
784 Antilipopolysaccharide factor (ALF) of mud crab *Scylla paramamosain*:

785 molecular cloning, genomic organization and the antimicrobial activity of its
786 synthetic LPS binding domain. Mol. Immunol. 44, 3195–3203.
787 Ishii, K.J., Koyama, S., Nakagawa, A., Coban, C., Akira, S., 2008. Host innate immune
788 receptors and beyond: making sense of microbial infections. Cell Host Microbe.
789 3, 352–363.
790 Janeway, C.A. Jr, Medzhitov, R., 2002. Innate immune recognition. Annu. Rev.
791 Immunol. 20, 197–216.
792 Joshi, J., Srisala, J., Truong, V.H., Chen, I.T., Nuangsaeng, B., Suthienkul, O., Lo,
793 C.F., Flegel, T.W., Sritunyalucksana, K., Thitamadee, S., 2014. Variation in
794 *Vibrio parahaemolyticus* isolates from a single Thai shrimp farm experiencing
795 an outbreak of acute hepatopancreatic necrosis disease (AHPND). Aquaculture.
796 428-429:297–302.
797 Kanost, M.R., Gorman, M.J., 2008. Phenoloxidases in insect immunity, in: Beckage,
798 N.E. (Ed.), Insect Immunology. Academic Press, San Diego, pp. 69–96.
799 Kawashima, T., Kosaka, A., Yan, H., Guo, Z., Uchiyama, R., Fukui, R., Kaneko, D.,
800 Kumagai, Y., You, D.J., Carreras, J., Uematsu, S., Jang, M.H., Takeuchi, O.,
801 Kaisho, T., Akira, S., Miyake, K., Tsutsui, H., Saito, T., Nishimura, I., Tsuji,
802 N.M., 2013. Double-stranded RNA of intestinal commensal but not pathogenic
803 bacteria triggers production of protective interferon-β. Immunity. 38, 1187–
804 1197.
805 Kondo, H., Tinwongger, S., Proespraiwong, P., Mavichak, R., Unajak, S., Nozaki, R.,
806 Hirono, I., 2014. Draft genome sequences of six strains of *Vibrio*
807 *parahaemolyticus* isolated from early mortality syndrome/acute

808 hepatopancreatic necrosis disease shrimp in Thailand. Genome Announc. 2,
809 e00221–14.
810 Kongnum, K., Hongpattarakere, T., 2012. Effect of *Lactobacillus plantarum* isolated
811 from digestive tract of wild shrimp on growth and survival of white shrimp
812 (*Litopenaeus vannamei*) challenged with *Vibrio harveyi*. Fish Shellfish
813 Immunol. 32, 170–177.
814 Kosin, B., Rakshit, S.K., 2010. Induction of heat tolerance in autochthonous and
815 allochthonous thermotolerant probiotics for application to white shrimp feed.
816 Aquaculture. 306, 302–309.
817 Lai, C.Y., Cheng, W., Kuo, C.M., 2005. Molecular cloning and characterisation of
818 prophenoloxidase from haemocytes of the white shrimp, *Litopenaeus vannamei*.
819 Fish Shellfish Immunol. 18, 417–430.
820 Lakshmi, B., Viswanath, B., Sai Gopal, D.V., 2013. Probiotics as antiviral agents in
821 shrimp aquaculture. J. Pathog. 424123.
822 Lazado, C.C., Caipang, C.M., Estante, E.G. 2015. Prospects of host-associated
823 microorganisms in fish and penaeids as probiotics with immunomodulatory
824 functions. Fish Shellfish Immunol. 45, 2–12.
825 Leaño, E.M., Mohan, C.V., 2012. Early mortality syndrome threatens Asia's shrimp
826 farms. Global Aquaculture Advocate 15, 38–39.
827 Lee, C.T., Chen, I.T., Yang, Y.T., Ko, T.P., Huang, Y.T., Huang, J.Y., Huang, M.F.,
828 Lin, S.J., Chen, C.Y., Lin, S.S., Lightner, D.V., Wang, H.C., Wang, A.H., Wang,
829 H.C., Hor, L.I., Lo, C.F., 2015. The opportunistic marine pathogen *Vibrio*
830 *parahaemolyticus* becomes virulent by acquiring a plasmid that expresses a
831 deadly toxin. Proc. Natl. Acad. Sci. U S A. 112, 10798–10803.

832 Leyva-Madrigal, K.Y., Luna-Gonzalez, A., Escobedo-Bonilla, C.M., Fierro-
833 Coronado, J.A., Maldonado-Mendoza, I.E., 2011. Screening for potential
834 probiotic bacteria to reduce prevalence of WSSV and IHHNV in whiteleg shrimp
835 (*Litopenaeus vannamei*) under experimental conditions. Aquaculture. 322–323,
836 16–22.
837 Li, J., Tan, B., Mai, K., 2009. Dietary probiotic *Bacillus* OJ and
838 isomaltooligosaccharides influence the intestine microbial populations, immune
839 responses and resistance to white spot syndrome virus in shrimp (*Litopenaeus*
840 *vannamei*). Aquaculture. 291, 35–40.
841 Lightner, D.V., Redman, R.M., Pantoja, C.R., Noble, B.L., Tran, L., 2012. Early
842 mortality syndrome affects shrimp in Asia. Global Aquaculture Advocate. 15:40.
843 Liu, H., Jiravanichpaisal, P., Cerenius, L., Lee, B.L., Söderhäll, I., Söderhäll, K., 2007.
844 Phenoloxidase is an important component of the defense against *Aeromonas*
845 *hydrophila* Infection in a crustacean, *Pacifastacus leniusculus*. J. Biol. Chem.
846 282, 33593–33598.
847 Liu, H., Wang, L., Liu, M., Wang, B., Jiang, K., Ma, S., Li, Q., 2011. The intestinal
848 microbial diversity in Chinese shrimp (*Fenneropenaeus chinensis*) as
849 determined by PCR-DGGE and clone library analyses. Aquaculture. 317, 32–
850 36.
851 Lv, X., Du, J., Jie, Y., Zhang, B., Bai, F., Zhao, H., Li, J., 2017. Purification and
852 antibacterial mechanism of fish-borne bacteriocin and its application in shrimp
853 (*Penaeus vannamei*) for inhibiting *Vibrio parahaemolyticus*. World J.
854 Microbiol. Biotechnol. 33, 156.

855 Maeda, M., Shibata, A., Biswas, G., Korenaga, H., Kono, T., Itami, T., Sakai, M.,
856 2014. Isolation of lactic acid bacteria from kuruma shrimp (*Marsupenaeus*
857 *japonicus*) intestine and assessment of immunomodulatory role of a selected
858 strain as probiotic. Mar Biotechnol. 16, 181–192.
859 Masuda, T., Otomo, R., Kuyama, H., Momoji, K., Tonomoto, M., Sakai, S.,
860 Nishimura, O., Sugawara, T., Hirata, T., 2012. A novel type of prophenoloxidase
861 from the kuruma prawn *Marsupenaeus japonicus* contributes to the melanization
862 of plasma in crustaceans. Fish Shellfish Immunol. 32, 61–68.
863 Medzhitov, R., 2007. Recognition of microorganisms and activation of the immune
864 response. Nature. 449, 819–826.
865 Merrifield, D.L., Balcázar, J.L., Daniels, C., Zhou, Z., Carnevali, O., Sun, Y.Z.,
866 Hoseinifar, H.S., Ringø, E., 2014. Indigenous Lactic Acid Bacteria in Fish and
867 Crustaceans, in: Ringø, E., Merrifield, D.L. (Eds.), Aquaculture Nutrition: Gut
868 Health, Probiotics and Prebiotics. John Wiley & Sons, Ltd., pp. 128–168.
869 Moriarty, D.J.W., 1997. The role of microorganisms in aquaculture ponds.
870 Aquaculture. 151, 333–349.
871 Nappi, A.J., Christensen, B.M., 2005. Melanogenesis and associated cytotoxic
872 reactions: applications to insect innate immunity. Insect Biochem. Mol. Biol. 35,
873 443–459.
874 Ninawe, A.S., Selvin, J., 2009. Probiotics in shrimp aquaculture: avenues and
875 challenges. Crit. Rev. Microbiol. 35, 43–66.
876 Nunan, L., Lightner, D., Pantoja, C., Gomez-Jimenez, S., 2014. Detection of acute
877 hepatopancreatic necrosis disease (AHPND) in Mexico. Dis. Aquat. Organ. 111,
878 81–86.

879 Ouwehand, A.C., Vesterlund, S., 2004. Antimicrobial components from lactic acid
880 bacteria, in: Salminen, S., von Wright, A., Ouwehand, A.C. (Eds.), Lactic Acid
881 Bacteria: Microbiological and Functional Aspects. Marcel Dekker, Inc., New
882 York, pp. 375–395.
883 Peraza-Gómez, V., Luna-González, A., Campa-Córdova, Á.I., López-Meyer, M.,
884 Fierro-Coronado, J.A., Álvarez-Ruiz, P., 2009. Probiotic microorganisms and
885 antiviral plants reduce mortality and prevalence of WSSV in shrimp
886 (*Litopenaeus vannamei*) cultured under laboratory conditions. Aquaculture Res.
887 40, 1481–1489.
888 Pfaffl, M.W., 2001. A new mathematical model for relative quantification in real-time
889 RT-PCR. Nucleic Acids Res. 29, e45.
890 Ringø, E., Gatesoupe, F.J., 1998, Lactic acid bacteria in fish: a review. Aquaculture.
891 160, 177–203.
892 Shao, Q., Yang, B., Xu, Q., Li, X., Lu, Z., Wang, C., Huang, Y., Söderhäll, K., Ling,
893 E., 2012. Hindgut innate immunity and regulation of fecal microbiota through
894 melanization in insects. J. Biol. Chem. 287, 14270–14279.
895 Soto-Rodriguez, S.A., Gomez-Gil, B., Lozano-Olvera, R., Betancourt-Lozano, M.,
896 Morales-Covarrubias, M.S., 2015. Field and experimental evidence of *Vibrio*
897 *parahaemolyticus* as the causative agent of acute hepatopancreatic necrosis
898 disease of cultured shrimp (*Litopenaeus vannamei*) in Northwestern Mexico.
899 Appl. Environ. Microbiol. 81, 1689–1699.
900 Sritunyalucksana, K., Cerenius, L., Söderhäll, K., 1999. Molecular cloning and
901 characterization of prophenoloxidase in the black tiger shrimp, *Penaeus*
902 *monodon*. Dev. Comp. Immunol. 23, 179–186.

903 Sutthangkul, J., Amparyup, P., Charoensapsri, W., Senapin, S., Phiwsaiya, K.,
904 Tassanakajon, A., 2015. Suppression of shrimp melanization during white spot
905 syndrome virus infection. J. Biol. Chem. 290, 6470–6481.
906 Tassanakajon, A., Rimphanitchayakit, V., Visetnan, S., Amparyup, P.,
907 Somboonwiwat, K., Charoensapsri, W., Tang, S., 2018. Shrimp humoral
908 responses against pathogens: antimicrobial peptides and melanization. Dev.
909 Comp. Immunol. 80, 81–93.
910 Tran, L., Nunan, L., Redman, R.M., Mohney, L.L., Pantoja, C.R., Fitzsimmons, K.,
911 Lightner, D.V., 2013. Determination of the infectious nature of the agent of acute
912 hepatopancreatic necrosis syndrome affecting penaeid shrimp. Dis. Aquat.
913 Organ. 105, 45–55.
914 Verschuere, L., Rombaut, G., Sorgeloos, P., Verstraete, W., 2000. Probiotic bacteria
915 as biological control agents in aquaculture. Microbiol. Mol. Biol. Rev. 64, 655–
916 671.
917 Vieira, F.N., Pedrotti, F.S., Neto, C.C.B., Mouriño, J.L.P., Beltrame, E., Martins,
918 M.L., Ramirez, C., Arana, L.A.V., 2007. Lactic-acid bacteria increase the
919 survival of marine shrimp, *Litopenaeus vannamei*, after infection with *Vibrio*
920 *harveyi*. Braz. J. Oceanogr. 55, 251–255.
921 Vieira, F.N., Neto, C.C.B., Mouriño, J.L.P., Jatobá, A., Ramirez, C., Martins, M.L.,
922 Barracco, M.A.A.M., Vinatea, L.A., 2008. Time-related action of *Lactobacillus*
923 *plantarum* in the bacterial microbiota of shrimp digestive tract and its action as
924 immunostimulants. Pesq. Agropec. Bras. 43, 763–767.
925 Vieira, F.N., Buglione, C.C., Mouriño, J.L.P., Jatobá, A., Martins, M.L., Schleder,
926 D.D., Andreatta, E.R., Barraco, M.A., Vinatea, L.M., 2010. Effect of probiotic

supplemented diet on marine shrimp survival after challenge with *Vibrio harveyi*. Arq. Bras. Med. Vet. Zootec. 62, 631–638.

von Wright, A., Axelsson, L., 2011. Lactic Acid Bacteria: An Introduction, in: Lahtinen, S., Ouwehand, A.C., Salminen, S., von Wright, A. (Eds.), Lactic Acid Bacteria: Microbiological and Functional Aspects. CRC Press, Boca Raton, pp. 1–16.

Wang, Y.C., Chang, P.S., Chen, H.Y., 2007. Tissue expressions of nine genes important to immune defence of the Pacific white shrimp *Litopenaeus vannamei*. Fish Shellfish Immunol. 23, 1161–1177.

Wu, K., Zhang, J., Zhang, Q., Zhu, S., Shao, Q., Clark, K.D., Liu, Y., Ling, E., 2015. Plant phenolics are detoxified by prophenoloxidase in the insect gut. Sci. Rep. 5, 16823.

Yang, Y.T., Chen, I.T., Lee, C.T., Chen, C.Y., Lin, S.S., Hor, L.I., Tseng, T.C., Huang, Y.T., Sritunyalucksana, K., Thitamadee, S., Wang, H.C., Lo, C.F., 2014. Draft genome sequences of four strains of *Vibrio parahaemolyticus*, three of which cause early mortality syndrome/acute hepatopancreatic necrosis disease in shrimp in China and Thailand. Genome Announc. 2, e00816–14.

Zhao, P., Li, J., Wang, Y., Jiang, H., 2007. Broad-spectrum antimicrobial activity of the reactive compounds generated in vitro by *Manduca sexta* phenoloxidase. Insect Biochem. Mol. Biol. 37, 952–959.

Zhao, P., Lu, Z., Strand, M.R., Jiang, H., 2011. Antiviral, anti-parasitic, and cytotoxic effects of 5,6-dihydroxyindole (DHI), a reactive compound generated by phenoloxidase during insect immune response. Insect Biochem. Mol. Biol. 41, 645–652.

951 **Figure Legends**

952 **Fig. 1. Phylogenetic tree of the host gut-derived probiotic LABs, the *Lactobacillus***
953 ***plantarum* SGLAB01 and the *Lactococcus lactis* SGLAB02, with the related LABs**
954 **based on 16S rRNA gene sequences (1300 bp).** A phylogenetic tree was built with
955 the neighbor-joining method using MEGA software program. The accession numbers
956 are shown to the left of the strain name. Sequences from *L. plantarum* SGLAB01 and
957 *L. lactis* SGLAB02 are indicated in bold. The 16S rRNA gene sequences of *Bacillus*
958 *pumilus* and *B. subtilis* were used as the outgroup. Numbers on each node represent
959 the bootstrap value from 1,000 replicates.

960

961 **Fig. 2. Viable LABs in the gut of the probiotic LAB-supplemented *L. vannamei*.**
962 Shrimp were fed with *L. plantarum* SGLAB01 and *L. lactis* SGLAB02-supplemented-
963 feed for a period of 16 days. Control shrimp was fed with control feed. The tissues of
964 foregut, midgut, and hindgut were dissected out at 5 days postprobiotic feeding. (A)
965 The viable LAB number in each shrimp gut was evaluated using plate count method.
966 Data shown as the mean ± S.D. (error bars) are derived from the triplicate experiments.
967 Asterisks (above each bar) indicate a significant difference between mean of the two
968 samples ($P< 0.05$). (B) Representative SEM images showing the morphology of the
969 candidate probiotic LABs; the *L. plantarum* SGLAB01 (a), and the *L. lactis* SGLAB02
970 (b); and the microbial attachments in the inner surface of the control (c, d) and LAB-
971 supplemented (e-h) shrimp gut.

972

973 **Fig. 3. RNAi-mediated functional analysis of *Lv*proPO1 and *Lv*proPO2**
974 **transcripts in shrimp *L. vannamei*.** (A) Tissue distribution analysis of *Lv*proPO1 and

975 *Lv*proPO2 transcripts by semiquantitative RT-PCR. Total RNA was extracted from the
976 tissues of hemocytes, hepatopancreas, foregut, midgut and hindgut and RT-PCR
977 amplification was carried out using the specific primers for *Lv*proPO1 and *Lv*proPO2.
978 EF1-α was amplified and used as an internal control. Gel images shown are
979 representative of three independent experiments. (B) Semiquantitative RT-PCR
980 analysis of the gene silencing efficiency of *Lv*proPO1 and *Lv*proPO2 dsRNAs in
981 shrimp hemocytes. Total RNA was extracted from hemocytes of the *Lv*proPOs-
982 cosilenced and control shrimp at 48 h after the second dsRNA injection and subjected
983 to analyze by semiquantitative RT-PCR. Amplification of EF1-α was used as an
984 internal reference gene control. (C) PO activity assay of *Lv*proPO1- and *Lv*proPO2-
985 cosilenced shrimp. Hemolymph was withdrawn from *Lv*proPOs-cosilenced and
986 control shrimp at 48 h after the second dsRNA injection. PO activity was assay using
987 L-DOPA as substrate and defined as the ΔA_{490}/mg total protein/min. Data are shown
988 as the mean ± S.D. (error bars) derived from three independently replicated
989 experiments. Different letters (above each bar) indicate a significant difference
990 between mean of each samples ($P< 0.05$). (D) Melanization in the gut of *Lv*proPO1-
991 and *Lv*proPO2-cosilenced shrimp. The whole guts collected from *Lv*proPOs-
992 cosilenced and control shrimp was soaked in the PO substrate, dopamine. Shrimp gut
993 soaked in dopamine containing PTU was included as control.
994
995 **Fig. 4. Cumulative mortality assay of *Lv*proPO1 and *Lv*proPO2-cosilenced**
996 **shrimp *L. vannamei* after VP_{AHPND} challenge.** Shrimp were double injected with
997 *Lv*proPO1 and *Lv*proPO2 dsRNAs followed by VP_{AHPND} challenge. The shrimp
998 injected with GFP dsRNA or 150 mM NaCl were included as the control groups.

999 Shrimp mortality was recorded daily. Data are shown as the mean ± S.D. (error bars)
1000 derived from three independently replicated experiments.
1001
1002 **Fig. 5. Effect of probiotic LAB-supplementation on the modulation of the**
1003 **immunity of shrimp *L. vannamei*.** (A) Effect of probiotic LAB-supplementation on
1004 the modulation of PO activity in shrimp hemolymph. Shrimp were fed with *L.*
1005 *plantarum* SGLAB01 and *L. lactis* SGLAB02-supplemented and control feed for 16
1006 days and hemolymph was then collected. PO activity was assayed using L-DOPA as
1007 substrate and recorded as ΔA_{490}/mg total protein/min. (B) Effect of probiotic LAB-
1008 supplement on modulation of the expression of *Lv*proPO1 and *Lv*proPO2 transcripts.
1009 Midgut was collected from the LAB-supplement and control shrimp at day 0, 1, and
1010 16 postfeeding and further subjected to total RNA extraction. The relative expression
1011 of *Lv*proPO1 and *Lv*proPO2 transcripts was evaluated using real-time RT-PCR
1012 analysis and calculated according to Pfaffl (2001) using EF1-α as internal reference
1013 gene. The experiment was performed triplicates. Data are shown as the mean ± S.D.
1014 (error bars). Different letters (above each bar) indicate a significant difference between
1015 mean of each samples ($P< 0.05$).
1016
1017 **Fig. 6. Effect of probiotic LAB-supplementation on the modulation of the**
1018 **resistance to VP_{AHPND} infection in shrimp *L. vannamei*.** Shrimp were fed (i) *L.*
1019 *plantarum* SGLAB01-supplemented-feed, (ii) *L. lactis* SGLAB02-supplemented-feed,
1020 (iii) *L. plantarum* SGLAB01 and *L. lactis* SGLAB02-supplemented-feed, and (iv)
1021 control feed for 16 days. The immersion challenge test with VP_{AHPND} was carried out
1022 by immersed shrimp in the cultured water containing VP_{AHPND} suspension $\sim 1 \times 10^4$

1023 cfu/ml. Cumulative mortality was recorded daily. The experiment was performed in
1024 triplicates. Data are shown as the mean ± S.D. (error bars).

Fig. 1.

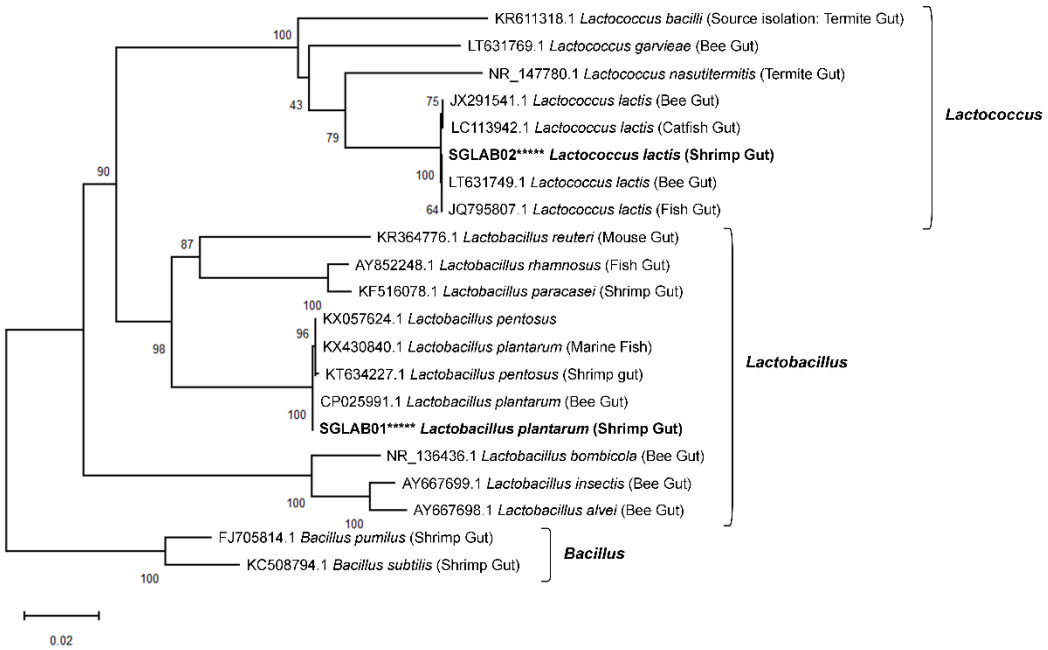

KR611318.1 Lactococcus bacilli (Source isolation: Termite Gut)
LT631769.1 Lactococcus garvieae (Bee Gut)
NR_147780.1 Lactococcus nasutitermitis (Termite Gut)
JX291541.1 Lactococcus lactis (Bee Gut)
LC113942.1 Lactococcus lactis (Catfish Gut)
SGLAB02***** Lactococcus lactis (Shrimp Gut)
LT631749.1 Lactococcus lactis (Bee Gut)
JQ795807.1 Lactococcus lactis (Fish Gut)
Lactococcus
KR364776.1 Lactobacillus reuteri (Mouse Gut)
AY852248.1 Lactobacillus rhamnosus (Fish Gut)
KF516078.1 Lactobacillus paracasei (Shrimp Gut)
KX057624.1 Lactobacillus pentosus
KX430840.1 Lactobacillus plantarum (Marine Fish)
KT634227.1 Lactobacillus pentosus (Shrimp gut)
CP025991.1 Lactobacillus plantarum (Bee Gut)
SGLAB01***** Lactobacillus plantarum (Shrimp Gut)
NR_136436.1 Lactobacillus bombicola (Bee Gut)
AY667699.1 Lactobacillus insectis (Bee Gut)
AY667698.1 Lactobacillus alvei (Bee Gut)
Lactobacillus
FJ705814.1 Bacillus pumilus (Shrimp Gut)
KC508794.1 Bacillus subtilis (Shrimp Gut)
Bacillus
100
43
75
79
100
64
90
87
100
96
98
100
100
100
100
100
0.02

Fig. 2.

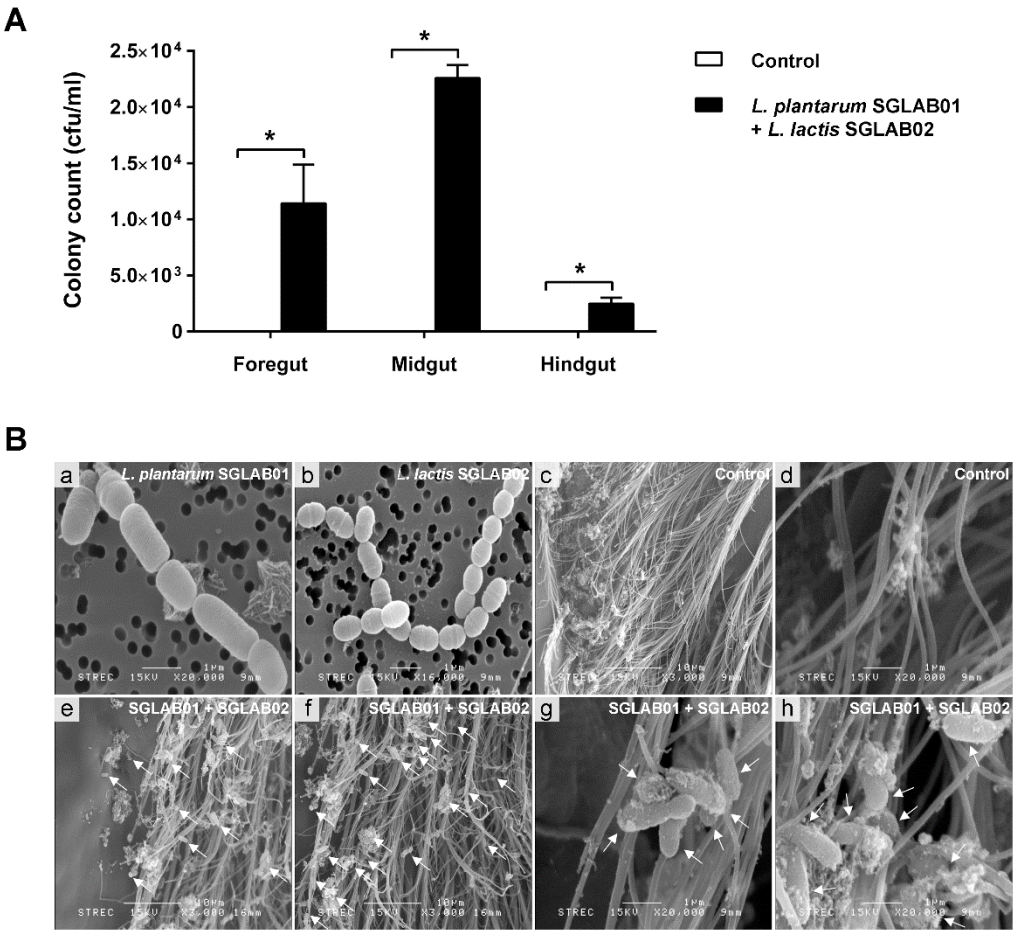

A
Colony count (cfu/ml)
2.5×10⁴
2.0×10⁴
1.5×10⁴
1.0×10⁴
5.0×10³
0
*
*
*
Foregut
Midgut
Hindgut
Control
L. plantarum SGLAB01
+ L. lactis SGLAB02
B
a L. plantarum SGLAB01
b L. lactis SGLAB02
c Control
d Control
e SGLAB01 + SGLAB02
f SGLAB01 + SGLAB02
g SGLAB01 + SGLAB02
h SGLAB01 + SGLAB02

Fig. 3.

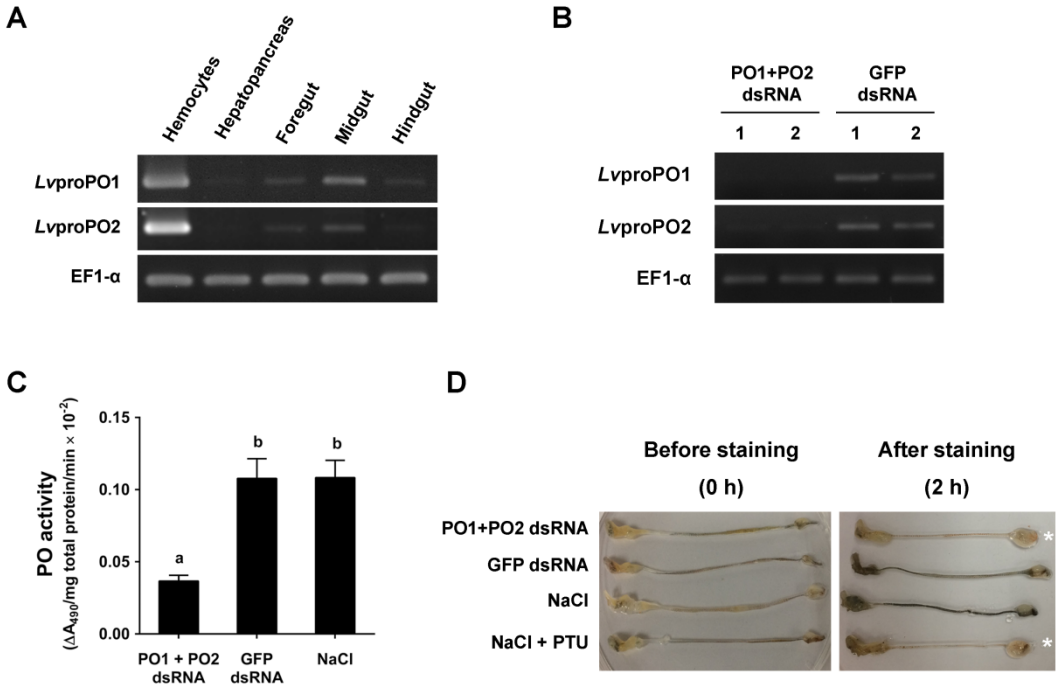

A
Hemocytes
Hepatopancreas
Foregut
Midgut
Hindgut
LvproPO1
LvproPO2
EF1-α
B
PO1+PO2 dsRNA
GFP dsRNA
1
2
1
2
LvproPO1
LvproPO2
EF1-α
C
PO activity
(ΔA490/mg total protein/min × 10-2)
0.15
0.10
0.05
0.00
a
b
b
PO1 + PO2 dsRNA
GFP dsRNA
NaCl
D
Before staining
(0 h)
After staining
(2 h)
PO1+PO2 dsRNA
GFP dsRNA
NaCl
NaCl + PTU

Fig. 4.

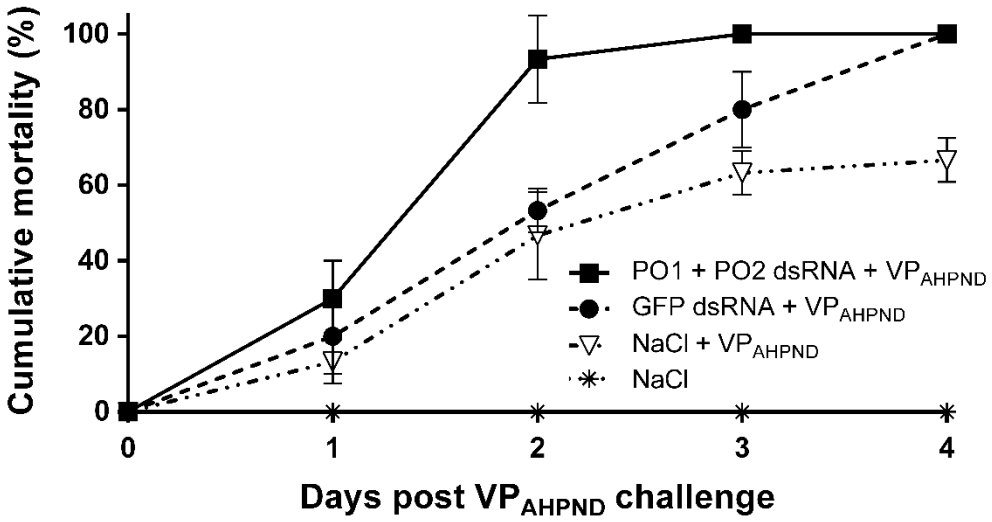

Cumulative mortality (%)
100
80
60
40
20
0
0
1
2
3
4
Days post VP$_{AHPND}$ challenge
PO1 + PO2 dsRNA + VP$_{AHPND}$
GFP dsRNA + VP$_{AHPND}$
NaCl + VP$_{AHPND}$
NaCl

Fig. 5.

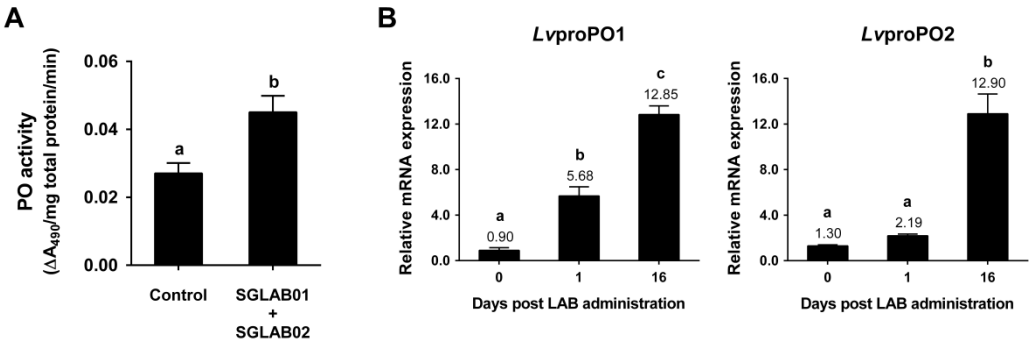

A
PO activity
(ΔA490/mg total protein/min)
0.06
0.04
0.02
0.00
a
b
Control
SGLAB01
+
SGLAB02
B
LvproPO1
Relative mRNA expression
16.0
12.0
8.0
4.0
0.0
a
0.90
b
5.68
c
12.85
0
1
16
Days post LAB administration
LvproPO2
Relative mRNA expression
16.0
12.0
8.0
4.0
0.0
a
1.30
a
2.19
b
12.90
0
1
16
Days post LAB administration

Fig. 6.

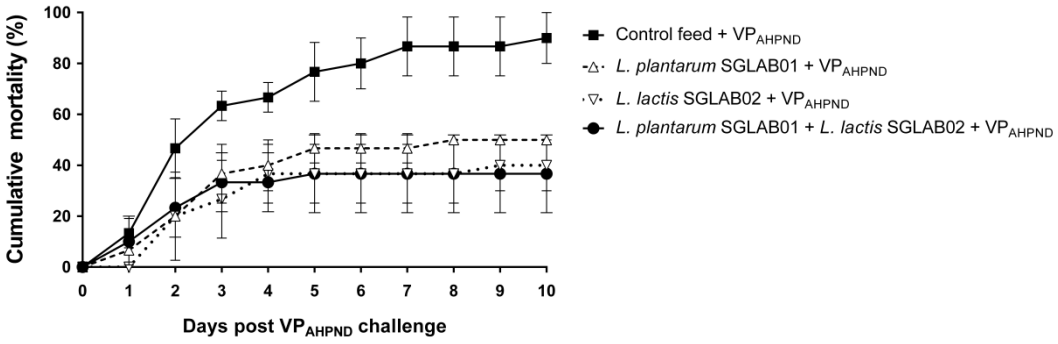

Cumulative mortality (%)
100
80
60
40
20
0
0
1
2
3
4
5
6
7
8
9
10
Days post VP$_{AHPND}$ challenge
Control feed + VP$_{AHPND}$
L. plantarum SGLAB01 + VP$_{AHPND}$
L. lactis SGLAB02 + VP$_{AHPND}$
L. plantarum SGLAB01 + L. lactis SGLAB02 + VP$_{AHPND}$

Table 1

Nucleotide sequences of the primers used.

Primer	Sequence (5'-3')	GenBank accession number
16S rRNA sequence analysis		
UFUL	GCCTAACACATGCAAGTCGA	-
URUL	CGTATTACCGCGGCTGCTGG	-
LpLl_16sR	TGGTGTGACGGGCGGTGTGTACA	-
Gene silencing		
LvPO1i-F	CGCCGCGGGCGCTCCTCTTT	EF115296
LvPO1i-R	CAGATCCTGCAGCGCCACGT	EF115296
LvPO1T7-F	GGATCCTAATACGACTCACTATAGGCGCCGCGGG CGCTCCTCTTT	EF115296
LvPO1T7-R	GGATCCTAATACGACTCACTATAGGCAGATCCTG CAGCGCCACGT	EF115296
LvPO2i-F	CGTCCTCCGTGGCCGCTCCT	EF565469
LvPO2i-R	CCACGGGGACGCCGCCACCA	EF565469
LvPO2T7-F	GGATCCTAATACGACTCACTATAGGCGTCCTCCGT GGCCGCTCCT	EF565469
LvPO2T7-R	GGATCCTAATACGACTCACTATAGGCCACGGGGA CGCCGCCACCA	EF565469
GFP-F	ATGGTGAGCAAGGGCGAGGA	U55761
GFP-R	TTACTTGTACAGCTCGTCCA	U55761
GFPT7-F	TAATACGACTCACTATAGGATGGTGAGCAAGGGC GAGGA	U55761
GFPT7-R	TAATACGACTCACTATAGGTTACTTGTACAGCTCG TCCA	U55761
Semi-quantitative RT-PCR analysis		
LvPO1-F	CATTCCGTCCGTCTGCCGA	EF115296
LvPO1-R	CAGGCGGGTAGATCAGGTGC	EF115296
LvPO2-F	TCTCAGCGTGAACTCGCCTTAC	EF565469
LvPO2-R	GATCCTGCTCGGTGTACGGTCT	EF565469
EF1α-F	GGTGCTGGACAAGCTGAAGGC	-
EF1α-R	CGTTCCGGTGATCATGTTCTTGATG	-

Table 2

Antibacterial activity of the LAB candidates.

Microorganism	MIC value (µg/ml)[a]	
	***L. plantarum* SGLAB01**	***L. lactis* SGLAB02**
Gram-positive bacteria		
Staphylococcus aureus	12.5-25	25-50
Aerococcus viridans	3.125-6.25	6.25-12.5
Bacillus megaterium	12.5-25	25-50
Bacillus subtilis	12.5-25	25-50
Gram-negative bacteria		
Vibrio parahaemolyticus (VP_{AHPND})	12.5-25	12.5-25
Vibrio harveyi	6.25-12.5	25-50
Escherichia coli	12.5-25	25-50

[a]MIC values are expressed as the interval of concentration [a]–[b], where [a] is the highest concentration tested at which microbial growth can be observed and [b] is the lowest concentration that causes 100% growth inhibition. Experiments were performed in triplicate.